TEXTS AND READINGS IN THE PHYSICAL SCIENCES - 22

Classical Mechanics

From Particles to Continua and Regularity to Chaos

Govind S. Krishnaswami

HINDUSTAN
BOOK AGENCY

TEXTS AND READINGS IN PHYSICAL SCIENCES - 22

Classical Mechanics

From Particles to Continua and Regularity to Chaos

Texts and Readings in Physical Sciences

Managing Editors
Ram Ramaswamy, Indian Institute of Technology, New Delhi
(ramakrishna.ramaswamy@gmail.com)

Debashis Ghoshal, Jawaharlal Nehru University, New Delhi
(dghoshal@jnu.ac.in)

Editors

Kedar Damle, Tata Institute of Fundamental Research, Mumbai (kedar@theory.tifr.res.in)
Ashok Das, University of Rochester, New York (das@pas.rochester.edu)
Gautam Menon, Ashoka University, Sonepat (gautam.menon@ashoka.edu.in)

Volumes published so far

1. Field Theories in Condensed Matter Physics, *Sumathi Rao* (Ed.)
2. Numerical Methods for Scientists and Engineers (3/E), *H. M. Antia*
3. Lectures on Quantum Mechanics (2/E), *Ashok Das*
4. Lectures on Electromagnetism (2/E), *Ashok Das*
5. Current Perspectives in High Energy Physics, *Debashis Ghoshal* (Ed.)
6. Linear Algebra and Group Theory for Physicists (2/E), *K. N. Srinivasa Rao*
7. Nonlinear Dynamics: Near and Far from Equilibrium, *J. K. Bhattacharjee and S. Bhattacharyya*
8. Spacetime, Geometry and Gravitation, *Pankaj Sharan*
9. Lectures on Advanced Mathematical Methods for Physicists, *Sunil Mukhi and N. Mukunda*
10. Computational Statistical Physics, *Sitangshu Bikas Santra and Purusattam Ray* (Eds.)
11. The Physics of Disordered Systems, *Gautam I. Menon and Purusattam Ray* (Eds.)
12. Surveys in Theoretical High Energy Physics 1, *P. Ramadevi* (Ed.)
13. Fragility of Glass Forming Liquids, *A. Lindsay Greer, Kenneth Kelton and Srikanth Sastry* (Eds.)
14. Lie Groups and Lie Algebras for Physicists, *Ashok Das and Susumu Okubo*
15. Surveys in Theoretical High Energy Physics 2, *Raghavan Rangarajan and M. Sivakumar* (Eds.)
16. N = 2 Supersymmetric Dynamics for Pedestrians, *Yuji Tachikawa*
17. Classical Dynamics: A Modern Perspective, *E.C.G. Sudershan and N. Mukunda*
18. Intermediate Statistical Mechanics: A Handbook, *Jayanta K. Bhattacharjee and Dhruba Banerjee*
19. Topology and Condensed Matter Physics, *Somendra M. Bhattacharjee, Mahan Mj. and Abhijit Bandyopadhyay (Eds.)*
20. Open Quantum Systems: Dynamics of Nonclassical Evolution, *Subhashish Banerjee*
21. Classical Theory of Electricity and Magnetism: A Course of Lectures, *A. K. Raychaudhuri*

Classical Mechanics
From Particles to Continua and Regularity to Chaos

Govind S. Krishnaswami
Chennai Mathematical Institute

HINDUSTAN
BOOK AGENCY

Published in India by

Hindustan Book Agency (India)
P 19 Green Park Extension
New Delhi 110 016
India

Email: info@hindbook.com
www.hindbook.com

Copyright © 2024, Hindustan Book Agency (India)

No part of the material protected by this copyright notice may be reproduced or utilized in any form or by any means, electronic or mechanical, including photocopying, recording or by any information storage and retrieval system, without written permission from the copyright owner, who has also the sole right to grant licences for translation into other languages and publication thereof.

ISBN 978-81-957829-9-4

Texts and Readings in Physical Sciences

The Texts and Readings in Physical Sciences (TRiPS) series of books aims to provide a forum for physical scientists to describe their fields of research interest. Each book is intended to cover a subject in a detailed manner and from a personal viewpoint, so as to give students in the field a unique exposure to the subject that is at once accessible, pedagogic, and contemporary. The monographs and texts that have appeared so far, as well as the volumes that we plan to bring out in the coming years, will cover a range of areas at the core as well as at the frontiers of physics.

In addition to texts on a specific topic, the TRiPS series includes lecture notes from a thematic School or Workshop and topical volumes of contributed articles focusing on a currently active area of research. Further, we also reissue and revive selected classic texts that have gone out of print but which remain relevant and contemporary. Through these various forms of exposition, we hope that the series will be valuable for researchers at all stages of their careers.

Ram Ramaswamy
New Delhi

Debashis Ghoshal
New Delhi

Classical Mechanics

From Particles to Continua and Regularity to Chaos

Govind S. Krishnaswami

Chennai Mathematical Institute

Texts and Readings in Physical Sciences - 22

Draft updated: July 20, 2024

This well-rounded and self-contained treatment of classical mechanics strikes a balance between examples, concepts, phenomena and formalism. While addressed to graduate students and their teachers, the minimal prerequisites and ground covered should make it useful also to undergraduates and researchers. Starting with conceptual context, physical principles guide the development. Chapters are modular and the presentation is precise yet accessible, with numerous remarks, footnotes and problems enriching the learning experience. Essentials such as Galilean and Newtonian mechanics, the Kepler problem, Lagrangian and Hamiltonian mechanics, oscillations, rigid bodies and motion in noninertial frames lead up to discussions of canonical transformations, angle-action variables, Hamilton-Jacobi and linear stability theory. Bifurcations, nonlinear and chaotic dynamics as well as the wave, heat and fluid equations receive substantial coverage. Techniques from linear algebra, differential equations, manifolds, vector and tensor calculus, groups, Lie and Poisson algebras and symplectic and Riemannian geometry are gently introduced. A dynamical systems viewpoint pervades the presentation. A salient feature is that classical mechanics is viewed as part of the wider fabric of physics with connections to quantum, thermal, electromagnetic, optical and relativistic physics highlighted. Thus, this book will also be useful in allied areas and serve as a stepping stone for embarking on research.

About the author: Govind Krishnaswami is a Professor of Physics at the Chennai Mathematical Institute, India, and is a recipient of the Apker Award and Marie Curie, EPSRC and Ramanujan Fellowships. His research in areas such as particle physics, nonlinear dynamics and fluid mechanics has often exploited ideas and tools from classical mechanics. He has taught a wide variety of subjects and is known for the clarity of his lectures and pedagogical articles in Resonance, a journal of science education.

Contents

Preface ix

1 Mechanical systems with one degree of freedom **1**

1.1 Newton's laws and qualitative characterization of motion on a line 1
1.2 Time period of conservative oscillations between turning points 7
1.3* Inverse problem: determination of potential from time period 8
1.4* Time delay in unbounded 'scattering' trajectories 10
1.5 Simple pendulum: basic properties and small oscillations 13
1.6 Problems 17

2 Kepler's gravitational two-body problem **21**

2.1 Inverse problem: universal law of gravity from Kepler's laws 22
2.2 Direct problem: center of mass & relative vectors and conservation laws . . 26
2.3 Planetary orbits 29
2.4 Time period of elliptical orbits 33
2.5* LRL vector and relations among conserved quantities 34
2.6* Collision of two gravitating point masses 38
2.7* Rutherford scattering cross section 42
2.8* The three-body problem: Euler and Lagrange solutions 49
2.9 Problems 51

3 Newtonian to Lagrangian and Hamiltonian mechanics **55**

3.1 Time, space, light, simultaneity, causality, homogeneity and isotropy 55
3.2 Degrees of freedom and instantaneous configurations 56
3.3 Newton's laws and Galileo's relativity and equivalence principles 57
3.4 Phase space, dynamical variables, conserved quantities, collisions 65
3.5 Principle of extremal action and Euler-Lagrange equations 68
3.6 Nonuniqueness of Lagrangian 74
3.7 Conjugate momenta, their geometric meaning and cyclic coordinates 74
3.8 Coordinate invariance of the form of Lagrange's equations 76
3.9 Hamiltonian and its conservation 77
3.10 Symmetries to conserved quantities: Noether's theorem 79
3.11* Noether's theorem when Lagrangian changes by a time derivative 83
3.12 Inertial frames of reference and Galilean invariance 84
3.13* Polar vectors, axial vectors, true scalars and pseudoscalars 89
3.14 Hamilton's equations 91
3.15 Legendre transform: Hamiltonian from Lagrangian 93
3.16* Lagrange multipliers and constrained extremization 96
3.17* Singular Lagrangians and constraints 98
3.18* Action as a function along a trajectory 100
3.19 Variational principles for Hamilton's equations 102
3.20* Coordinate invariance of Lagrange and Hamilton equations 104
3.21 Canonical Poisson brackets 105

3.22 Properties of the Poisson bracket 107
3.23* Canonical formulation of charged particle in electromagnetic field 111
3.24* Poisson algebra of conserved quantities in the Kepler problem 113
3.25* Functional independence of conserved quantities 116
3.26* Noncanonical Poisson brackets, Poisson and symplectic manifolds 121
3.27* Free particle trajectories as geodesics on configuration space 127
3.28* Euler-Maupertuis principle and the Jacobi-Maupertuis metric 131
3.29 Problems 134

4 Introduction to special relativistic mechanics 149
4.1 Difficulties with Newtonian mechanics 149
4.2 Postulates of special relativity 150
4.3 Synchronization of clocks and simultaneity 151
4.4 Lorentz transformations 153
4.5 Time dilation, length contraction, proper length and time 156
4.6 Space-like, time-like and light-like intervals and causality 158
4.7 Relativistic addition of velocities 159
4.8 Relativistic momentum from two particle collision 160
4.9 Relativistic energy and energy-momentum dispersion relation 162
4.10* Minkowski space-time and relativistic dynamics 163
4.11 Problems 169

5 Dynamics viewed as a vector field on state space 171
5.1 Vector fields from Newtonian and Hamiltonian dynamics 171
5.2* Vector fields in one dimension 175
5.3 Existence and uniqueness of solutions 180
5.4* Vector fields on the phase plane 184
5.5 Problems 192

6 Small oscillations for one degree of freedom 195
6.1 Linear harmonic oscillator in 1d and neutral stability 195
6.2 Linear vector fields on the phase plane 197
6.3 Phase portrait from spectrum of coefficient matrix 199
6.4 Damped harmonic oscillator: view from the phase plane 201
6.5 Critically damped oscillator: deficient coefficient matrix 205
6.6* Trace-determinant classification of linear fixed points 207
6.7* Robustness of the linear theory 209
6.8 Driven or forced oscillations 210
6.9* Driven damped oscillations 217
6.10 Parametric oscillations and resonant amplification 218
6.11 Problems 219

7 Nonlinear oscillations: pendulum and anharmonic oscillator 225
7.1 Simple pendulum: view from phase space 225
7.2* Introduction to Jacobi elliptic functions 229
7.3* Time-dependence of pendulum in terms of elliptic functions 232
7.4 Anharmonic oscillations: quartic double-well potential 234

7.5* Quartic oscillator: exact solution and Lindstedt-Poincaré method 236
7.6 Problems 240

8 Rigid body mechanics **243**
8.1 Lab and comoving frames 245
8.2 Configuration space and degrees of freedom 245
8.3 Infinitesimal displacement and angular velocity of rigid body 246
8.4 Kinetic energy and inertia tensor 249
8.5 Types of rigid bodies 251
8.6 Angular momentum of a rigid body 253
8.7 Equations of motion of a rigid body 254
8.8 Force-free motion of rigid bodies 257
8.9 Euler angles and rotations 261
8.10 Angular velocity and kinetic energy in terms of Euler angles 264
8.11 Euler equations for a rigid body in body-fixed frame 267
8.12 Ellipsoid of inertia and qualitative description of free motion 270
8.13* Solution of force-free Euler equations via elliptic functions 275
8.14* Poisson bracket formulation of Euler's equations 277
8.15 Motion of a heavy symmetrical (Lagrange) top 280
8.16 Problems 283

9 Motion in noninertial frames of reference **289**
9.1 Uniformly accelerating frames and the equivalence principle 290
9.2 Nonuniformly accelerated frames: Lagrangian approach 291
9.3 Uniform rotation: Hamiltonian formulation and magnetic analog 294
9.4 Precession of Foucault's pendulum 295
9.5* Circular restricted three-body problem 296
9.6 Problems 298

10 Canonical transformations **301**
10.1 From point transformations to canonical transformations 303
10.2 Preservation of Hamilton's equations and Poisson brackets 305
10.3* Comparison of classical and quantum mechanical formalisms 308
10.4 Canonical transformations and area-preserving maps 311
10.5 Canonical transformations preserve Poisson tensor 314
10.6 Generating function for infinitesimal canonical transformations 316
10.7 Symmetries & Noether's theorem in the Hamiltonian framework 319
10.8 Liouville's theorem 321
10.9* Poincaré recurrence 324
10.10 Generating functions for finite canonical transformations 329
10.11 Problems 335

11 Angle-action variables **341**
11.1 Angle-action variables for the harmonic oscillator 342
11.2 Generator of CT to angle-action variables: Hamilton-Jacobi equation 344
11.3 Generating function for oscillator angle-action variables 346
11.4 Angle-action variables for systems with one degree of freedom 347

11.5* Angle-action variables for libration of the simple pendulum 348
11.6* Bohr-Sommerfeld quantization rule 349
11.7* Liouville integrability and KAM tori 351
11.8* Liouville-Arnold theorem 353
11.9* Conserved quantities from a Lax pair 357
    11.9.1* Harmonic oscillator Lax pair 357
    11.9.2* Isospectral evolution and conserved quantities 358
    11.9.3* Toda chain: Flaschka's variables and a Lax pair 359
    11.9.4* Euler-Poinsot top Lax pair: spectral parameter 361
11.10 Problems 362

12 Hamilton-Jacobi equation 365
12.1 Time-dependent Hamilton-Jacobi evolution equation 367
12.2* Connection of Hamilton-Jacobi to Schrödinger and eikonal equations 370
12.3 Separation of variables in the Hamilton-Jacobi equation 372
12.4 Hamilton's principal function as action along a trajectory 376
12.5* Geometric interpretation of Hamilton-Jacobi equation 377
12.6 Problems 380

13 Normal modes of oscillation and linear stability 383
13.1 Elementary examples of coupled small oscillations 384
    13.1.1 Normal modes of two weakly coupled pendula 384
    13.1.2 Normal modes of a diatomic molecule 386
13.2 Double pendulum: formulation and small oscillations 387
    13.2.1 Energy, Lagrangian and equations of motion 388
    13.2.2 Normal modes of a double pendulum 390
13.3* Normal modes around a static equilibrium: general framework 396
13.4 Small perturbations around a periodic solution 401
    13.4.1 Formulation as a system of first order equations 403
    13.4.2* Time evolution matrix 404
    13.4.3* Monodromy matrix 408
    13.4.4* Stability of a periodic solution 408
    13.4.5* Kapitza pendulum with oscillating support: Mathieu equation . . . 410
13.5 Problems 413

14 Bifurcations: qualitative changes in dynamics 417
14.1 Bifurcations of vector fields on the real line 417
    14.1.1* Saddle-node bifurcation 418
    14.1.2* Transcritical bifurcation 419
    14.1.3* Pitchfork bifurcations 420
        14.1.3.1* Supercritical pitchfork bifurcation 421
        14.1.3.2* Subcritical pitchfork bifurcation 422
14.2 Bifurcations in two dimensions 425
    14.2.1* Saddle-node, transcritical and pitchfork bifurcations 425
    14.2.2* Hopf bifurcations 427
14.3 Problems 430

15 From regular to chaotic motion 431
- 15.1 Chaos in iterations of a map 432
  - 15.1.1 Lyapunov exponent and sensitivity to initial conditions 433
  - 15.1.2 Chirikov-Taylor standard map: a kicked rotor 434
  - 15.1.3 Logistic map: period doubling, Cantor dust and Lyapunov exponent 438
- 15.2* Lyapunov exponents for continuous-time dynamical systems 446
- 15.3* Poincaré return map and Homoclinic tangle 452
- 15.4 Hamiltonian chaos: order-chaos-order transition in a double pendulum . . . 454
  - 15.4.1* Poincaré sections and onset of chaos 457
  - 15.4.2* Return to regularity at high energies 466
  - 15.4.3* Understanding the zero gravity double pendulum 468
- 15.5* Chaos in Lorenz's model for convection 472
- 15.6 Problems 478

16 Dynamics of continuous deformable media 483

17 Vibrations of a stretched string and the wave equation 485
- 17.1 Wave equation for transverse vibrations of a stretched string 486
- 17.2 Finite differences: wave equation as a system of ODEs 490
- 17.3 Normal modes and solution by Fourier series 491
- 17.4 Right- and left-moving waves and d'Alembert's solution 495
- 17.5 Conserved energy of small oscillations of a stretched string 498
- 17.6 Three local conservation laws for the wave equation 499
- 17.7 Lagrangian and Hamiltonian for stretched string 501
- 17.8 Conserved quantities from Noether's theorem 504
- 17.9 Dispersion relation, phase and group velocities 505
- 17.10* Lax pair for the first order wave equation 507
- 17.11 Problems 509

18 Heat diffusion equation and Brownian motion 513
- 18.1 Obtaining the heat equation and its basic properties 514
- 18.2 Solution of initial value problem on an interval by Fourier's series 517
- 18.3* Heat kernel: time evolution operator for heat equation 518
- 18.4 From Brownian motion to the diffusion equation 523
  - 18.4.1 Brownian motion and the atomic hypothesis 523
  - 18.4.2* Random walk model and the diffusion equation 526
- 18.5 Problems 529

19 Introduction to fluid mechanics 531
- 19.1 Fluid element, local thermal equilibrium and dynamical fields 532
- 19.2 Fluid statics: aero- or hydrostatics 533
- 19.3 Flow visualization: streamlines, streaklines and pathlines 535
- 19.4 Material derivative 537
- 19.5 Compressibility, incompressibility and divergence of velocity field 537
- 19.6 Local conservation of mass: continuity equation 540
- 19.7 Euler equation for inviscid flow 541
- 19.8 Ideal adiabatic flow: entropy advection and equation of state 544

19.9 Bernoulli's equation . . . 546
19.10 Sound waves in homentropic flow . . . 548
19.11 Vorticity and its evolution . . . 550
19.12 Vortex tubes: Kelvin and Helmholtz theorems . . . 552
19.13 Conservation of energy, (angular) momentum and helicity . . . 555
19.14* Hamiltonian and Poisson brackets for inviscid flow . . . 558
19.15* Clebsch variables and Lagrangian for ideal flow . . . 563
19.16 Navier-Stokes equation for incompressible viscous flow . . . 566
19.17 Problems . . . 573

A Mathematical and kinematical background 581

A.1 Vectors in Euclidean space . . . 582
A.2 Position coordinates and velocity and acceleration vectors . . . 586
A.3 Circular motion: uniform and nonuniform . . . 587
A.4 Integration of kinematical equations: uniform acceleration . . . 590
A.5 Plane polar coordinates . . . 590
A.6 Spherical polar coordinates . . . 593
A.7 Taylor series . . . 594
A.8 Some vector calculus: grad, div and curl . . . 596
A.9 Stokes', Green's and Gauss' integral theorems . . . 600
A.10 Vector spaces, matrices and eigenvalue problems . . . 601
A.11* Fourier transform . . . 607
A.12 Problems . . . 609

B Primer on manifolds, tensors and groups 613

B.1 The concept of a manifold . . . 613
B.2* Submanifolds, connected and simply connected manifolds . . . 618
B.3* Smooth functions or scalar fields . . . 620
B.4* Vector fields . . . 620
B.5* Covector fields or 1-forms . . . 624
B.6* Tensors of rank two and 2-forms . . . 626
B.7* Higher rank tensor fields and forms . . . 631
B.8* Pushforward and pullback of tensors . . . 632
B.9* Exterior algebra, exterior derivative and Bianchi's identity . . . 634
B.10* Integration on manifolds and Stokes' theorem . . . 637
B.11* Covariant derivative . . . 641
B.12* Curvature on a Riemannian manifold . . . 643
  B.12.1* Riemann-Christoffel curvature tensor . . . 644
  B.12.2* Geodesic deviation and Riemannian curvature . . . 647
B.13* Groups, Lie groups and their Lie algebras . . . 649
B.14* Quaternions and the axis-angle representation of rotations . . . 662
B.15 Problems . . . 665

Supplementary reading 671

References 672

Index 679

Preface

Why classical mechanics?

Classical[1] mechanics traces its origins to the study of the motion of bodies. It is an old subject whose basic principles were formulated in Galileo's and Newton's time (1600s). However, the subject remains alive and continues to thrive. This is because (a) it is the basis for the formulation of most physical systems and remains the predictive framework in which we try to understand and control the vast majority of physical phenomena despite the advent of the quantum theory[2], (b) the theoretical edifice of mechanics has undergone repeated rejuvenation allowing it to be understood in increasingly deep ways (Lagrangians, Hamiltonians, Poisson brackets, symplectic forms, canonical transformations, Hamilton-Jacobi equation, perturbation theory, Dirac-Bergmann constraints, Lax pairs, Kolmogorov-Arnold-Moser (KAM) theory, symbolic dynamics, renormalization and so forth) and (c) old classical phenomena like turbulence are yet to be satisfactorily understood and new phenomena such as those surrounding integrable, chaotic, mixed and open systems pose fresh challenges. The history of classical mechanics also reveals that the theoretical and computational schemes developed to understand and solve Newton's equations of mechanics (such as conservation laws, variational principles, constraints, the Hamiltonian formulation or that in terms of geodesics or Hamilton-Jacobi wavefronts) have a utility beyond the validity of Newton's laws. They have even been used to discover and formulate other or more accurate laws of nature (such as those governing electromagnetism or the quantum dynamics of relativistic particles and fields) as well as to set up effective or statistical frameworks to deal with unexpected 'emergent' phenomena that arise in the presence of nonlinearities or when many degrees of freedom interact. Furthermore, developments in classical mechanics have been inspired by and used in numerous practical problems of science and engineering such as projectile motion, timekeeping, construction of roads, bridges, dams, musical instruments and gyroscopes, flight of airplanes, launching and placement of satellites and weather prediction. If we add to this the beauty of the mathematical form of classical dynamics, we begin to see why it remains a central part of physics research and education.

Scope of this book.

This book is meant primarily for postgraduate students of physics and their teachers. However, it should also be of use to undergraduates, researchers and others interested in mechanics, especially when viewed as a part of the larger fabric of theoretical physics. An attempt has been made to keep the book reasonably self-contained by developing topics from basic principles and by providing physical context, intuition and reasoning. Topics are presented in a manner that elucidates the thought process behind calculations. Mathematical constructions and terms are motivated and explained alongside physical developments. Readers should find them useful in thinking about physics and communicating effectively. It is hoped that these features will make the book suitable both for use in taught courses and self-study. Many details and subtle issues are clarified, which should enable teachers to explain ideas effectively. The process of learning mechanics is not linear: a novice is not expected to follow, at the first instance, every concept that is presented. Things tend to become clearer on subsequent readings. Footnotes are an integral part of this book and are used to avoid interrupting the flow. They contain qualifications, explanations, additional material, etc. While some of them are meant for instructors and advanced readers, many should be helpful even to first-time readers. Starred sections, on the other hand, contain topics that may be skipped on a first reading without affecting the continuity of the material. It is hoped that the reader will acquire a working knowledge of, affinity and appreciation for mechanics, its challenges and its connections to other areas of physics, as well as a degree of theoretical sophistication by working through this book.

---

[1] The adjective *classical* conveys that it is the oldest and best established branch of mechanics. Technically, the term *classical* is used to distinguish it from *quantum* mechanics.

[2] Even phenomena or systems that require a quantum mechanical treatment are often fruitfully first understood in some classical limit.

Genesis of this book.

The specific suggestion to write this book for the Texts and Readings in Physical Sciences (TRiPS) series came from D K Jain of Hindustan Book Agency on 19 January, 2018, although he had mentioned it more casually earlier as well. He followed this up with periodic exhortations to start writing. The fact that both my guru S G Rajeev and my mama (maternal uncle) N Mukunda (with E C G Sudarshan) had written advanced books on mechanics [106, 124] was a source of inspiration, but also made it a daunting task. Encouragement and feedback from students who took my courses, my colleagues H S Mani, K P N Murthy, A Laddha and K G Arun (who had seen my lecture notes) and D Ghoshal helped convince me that it was all right to attempt yet another book on mechanics. Although my lecture notes had been with me for a few years, it was not until the day after new year's day, 15 April, 2020 that I started preparing the manuscript. The lock-down due to the COVID-19 pandemic played an important role in helping me get started and sustaining the effort. I soon realized how inadequate my rough lecture notes were, but it took longer for me to recognize just how much effort was needed to write this book! The process itself has been fun and rewarding and I hope readers will enjoy this book.

Acknowledgements.

The classic text by Landau and Lifshitz [83] remains a good place to learn mechanics. I have occasionally relied on their exposition. My interest in mechanics and the viewpoint in this book owe a lot to what I learned from S G Rajeev. His work and writings continue to inspire me. I have also benefited from my collaboration with A Thyagaraja, who has helped shape my viewpoint on fluid mechanics. Over the past decade, I have given lectures at several places in India (Chennai Mathematical Institute (CMI), Science Academy Refresher Courses and Workshops, etc.). The questions and comments from those who attended my lectures were useful in the preparation of my notes. I thank V V Sreedhar, G Rajasekaran, H S Mani, M Lakshmanan, C Rao, A N Kumara, S Ananth, K Indulekha, N V Suryanarayana, D Jatkar, M Ashefas and others for asking me to deliver these lectures. Comments and suggestions from R Jagannathan, R Parthasarathy, G Date, T R Ramadas, R Nityananda, A V Khare, M V N Murthy, J K Bhattacharjee, A Das, A Arul and anonymous reviewers have enriched the book, as have those of the Editors R Ramaswamy and D Ghoshal of TRiPS. Advice and suggestions from the publishers D K Jain and J K Jain of Hindustan Book Agency and S Ahmad of Springer Nature have helped me prepare this book for publication. I am also grateful to my colleagues and the staff at CMI for the pleasant working environment.

Special thanks go to PhD students Sachin Phatak, Sonakshi Sachdev, Himalaya Senapati, T R Vishnu, Ankit Yadav and Pritish Sinha as well as summer student Shivangi Dhiman with whom I have discussed many of the topics and exercises in this book. Shivangi helped prepare several of the figures and parts of the Index for the first three chapters. Her detailed study of the first drafts of these chapters helped iron out some obscurities. Ankit too helped with many figures, numerical calculations in Chap. 8, 13 and 15 and gave much useful feedback on a majority of the chapters. Himalaya's critical comments on practically all chapters has significantly improved the exposition. He also helped with getting the LaTeX typesetting software package to do useful things! Sections 2.8* and 9.5* on the three-body problem are based on the article [72] written with Himalaya. Pritish's questions upon reading portions of Chap. 1, 2, 3, 4, 19 and Appendix B, have helped clarify some subtle concepts. The introduction to quaternions in Appendix B.14* is based on the article [71] coauthored with Sonakshi. The discussion of Lax pairs in Chap. 11 and Chap. 17 is based on expository articles [76, 77] written with Vishnu, who also made useful comments on Chap. 7.

I would like to acknowledge generous financial support in the form of a Ramanujan Fellowship, a Core Research Grant and a MATRICS grant from the Science and Engineering Research Board (SERB) of the Department of Science and Technology, Government of India at various stages in the preparation of this book.

Finally, this book was made possible by the support I have received from my family, especially Krishnaswami, Leela and Maithreyi. It is written for Shraddha and dedicated to my parents and to Professors C S Seshadri and G Rajasekaran who unfortunately passed away while I was writing it.

Prerequisites.

Although most mathematical methods are developed along the way, we assume some familiarity with calculus, vectors and matrices. Some of this background is in Appendix A while more may be found in [8, 24, 49, 69, 114, 120, 121, 130]. Connections to electromagnetism, optics, thermodynamics, relativity, quantum and statistical mechanics are occasionally pointed out. For those unfamiliar with these subjects, such remarks may simply be ignored. Finally, it is hoped that a reader can begin reading several of the chapters without having studied many of the preceding ones.

Arrangement of material

The order of presentation is based on certain guiding principles. (1) Increasing number of degrees of freedom: point particles (1d to 3d), rigid bodies and then continuous media. (2) A historical path through the development of the formalism of classical mechanics, progressing from the ideas of Galileo and Newton through the Bernoullis, d'Alembert, Maupertuis, Euler, Lagrange, Hamilton, Poisson, Jacobi, Lie, Hill, Poincaré, Lyapunov, etc. (3) Small oscillations to large oscillations: linear to nonlinear equations of motion. (4) The idea that the study of concrete examples often leads to general principles/formalisms which then inform on the behavior of other model systems. (5) Configuration and phase spaces that are topologically trivial (e.g., Euclidean spaces) followed by those that are not (e.g., circles, spheres, cylinders). (6) Increasing mathematical sophistication. (7) Regular dynamics to chaotic dynamics.

Outline of chapters.

For those who would like to begin with some mathematical and kinematical preliminaries, Appendix A deals with vectors in Euclidean space, kinematics, circular motion, polar coordinates, Taylor series, vector calculus, linear algebra and the Fourier transform. We begin our study of mechanics in Chap. 1 with the Newtonian formulation of the motion of a particle on a line and discuss some of the general phenomena that arise. The harmonic oscillator and pendulum are introduced as important examples of systems with one degree of freedom. The notions of oscillatory time period, time delay and inverse problems are introduced. Chap. 2 is devoted to Kepler's two-body central force problem which is used to motivate and illustrate the consequences of Newton's laws of mechanics and gravity in the context of planetary orbits. Replacing the gravitational force with the Coulomb force between charged particles, we derive Rutherford's differential cross section for the scattering of alpha particles by gold nuclei. The utility of Keplerian orbits goes beyond the two-body problem: we show how they turn up in the Euler and Lagrange solutions of the three-body problem! With this background at hand, we move (in Chap. 3) to the conceptual and formal development from Galileo's principle of relativity to the Newtonian, Euler-Lagrangian, Hamiltonian, Poisson bracket and Euler-Maupertuis formalisms of mechanics. Chap. 3 has been placed after Chapters 1 and 2 in keeping with the adage that physics tends to be developed through the study of examples or model systems. General principles often emerge from the study of specific systems. A reader may of course go straight to Chap. 3 and return to the previous chapters when necessary. In Chap. 4, we point out the shortcomings of Newtonian mechanics in treating phenomena where speeds of particles or frames relative to an inertial frame are comparable to that of light, and give a brief introduction to special relativistic mechanics. In Chap. 5, we return to nonrelativistic mechanics and adopt a dynamical systems viewpoint where we think of mechanical systems in terms of their associated vector fields on the state space. We then turn to a variety of examples in Chapters 6, 7, 8 and 9:

small oscillations for one degree of freedom, (not necessarily small) oscillations of a simple pendulum and quartic anharmonic oscillator, rigid bodies and motion in noninertial frames (with applications to Foucault's pendulum and the restricted three-body problem). The formalisms developed in earlier chapters are put to use here, while new techniques (both exact and approximate) are also introduced. We then return to general structural aspects by discussing canonical transformations, angle-action variables and the Hamilton-Jacobi equation in Chapters 10, 11 and 12, where we also meet Poincaré recurrence, Liouville integrability, KAM tori and Lax pairs. In Chap. 13, we go back to the study of small oscillations, this time around static and periodic solutions of systems with two or more degrees of freedom. Pendula coupled by a spring, a diatomic molecule and the double pendulum are used to illustrate normal modes, while the Kapitza pendulum provides a context to examine the stability of oscillations. In Chap. 14, we discuss several simple examples of bifurcations of vector fields, which illustrate how the qualitative behavior of a system can change as a control parameter is varied. This is followed in Chap. 15, by examples of discrete-time and continuous-time dynamical systems (standard and logistic maps, double pendulum and Lorenz oscillator) illustrating the passage from regular to chaotic motion. The next four chapters (16, 17, 18 and 19) provide an introduction to continuum mechanics via d'Alembert's wave equation for vibrations of a stretched string, Fourier's equation for heat diffusion and Brownian motion and finally fluid mechanics. Appendix A discusses mathematical and kinematical preliminaries while Appendix B contains an informal introduction to concepts from the theory of manifolds, tensors, differential geometry, groups and Lie algebras that we use in our treatment of mechanical systems. We end with a list of books that treat related topics, cited references to the literature and a detailed index. Readers are encouraged to attempt the end-of-chapter problems, which are an integral part of the book. Each chapter begins with an introductory section providing conceptual context, outlining topics to be treated and mentioning further developments.

Planning a course.

A first course on mechanics for undergraduates has been taught by starting with background on vectors, kinematics, polar coordinates and vector calculus (Appendix A) followed by the framework of Newtonian mechanics (Sect. 3.1, 3.2), Galileo's relativity principle and Newton's laws (Sect. 3.3), concepts of phase space, conservation laws and their illustration via collisions (Sect. 3.4), motion in one dimension (Sect. 1.1, 1.2), Kepler's laws and Newton's law of gravity (Sect. 2.1), an introduction to the harmonic oscillator and simple pendulum (Sect. 1.1, 6.1, 1.5), uniformly accelerated frames (Sect. 9.1) and the elements of special relativity (Sect. 4.1, 4.2, 4.3, 4.4, 4.5, 4.6). A second course on mechanics could cover Lagrangian mechanics (Sect. 3.5, 3.6, 3.7, 3.8, 3.9, 3.10), Hamiltonian mechanics (Sect. 3.14, 3.15), Poisson brackets (Sect. 3.21), canonical transformations (Sect. 10.1,10.4, time permitting), the gravitational 2-body problem (Sect. 2.2, 2.3), small oscillations and normal modes (Sect. 13.1), damped harmonic oscillations (Sect. 6.4, time permitting), rigid bodies (Sect. 8.1, 8.2, 8.3, 8.4, 8.5) and noninertial frames of reference (Sect. 9.2). The content of a Master's course would depend on student background. It may be based on a selection from the following topics, with some being assigned as reading projects:

motion in one dimension (Sect. 1.1, 1.2, 1.5), the Kepler problem (Sect. 2.1, 2.2, 2.3, 2.4, 2.5*), the formalism of Newtonian, Lagrangian and Hamiltonian mechanics (Sect. 3.1, 3.2, 3.3, 3.4, 3.5, 3.6, 3.7, 3.8, 3.9, 3.10, 3.12, 3.14, 3.15, 3.18*, 3.19, 3.21, 3.22), driven oscillations (Sect. 6.8) or anharmonic oscillations (Sect. 7.1), rigid body dynamics (Sect. 8.6, 8.7, 8.9, 8.10, 8.11, 8.12), canonical transformations (Sect. 10.1, 10.2, 10.4, 10.5, 10.6, 10.7, 10.8, 10.10), angle-action variables (Sect. 11.1, 11.2, 11.3, 11.4) and the Hamilton-Jacobi equation (Sect. 12.1, 12.3, 12.4). A course on nonlinear dynamics could treat vector fields in one and two dimensions (Sect. 5.1, 5.2*, 5.3, 5.4*), planar vector fields arising from small oscillations (Sect. 6.1, 6.2, 6.3, 6.4, 6.5, 6.6*, 6.7*), the pendulum (Sect. 7.1) or anharmonic oscillator (Sect. 7.4, 7.5*), infinitesimal canonical transformations (Sect. 10.6), Liouville's theorem (Sect. 10.8), Poincaré recurrence (Sect. 10.9*), angle-action variables (Sect. 11.1, 11.2, 11.3, 11.4), Liouville integrability and KAM tori (Sect. 11.7*), normal modes (Sect. 13.2), stability of periodic solutions (Sect. 13.4), bifurcations of vector fields (Sect. 14.1, 14.2) and chaos (Sect. 15.1, 15.4). An introductory continuum mechanics course (sans elasticity) may be based on the unstarred sections in Chapters 16, 17, 18 and 19. Mathematical supplements from Appendix B may be introduced when the need arises or in a course on mathematical methods of physics. In planning courses, instructors should feel free to omit passages based on student background and time available. Many chapters are self-contained, so teachers may treat topics in an order they are comfortable with. For instance, motion in noninertial frames could be discussed before rigid bodies, although the corotating frame of a rigid body is a nice example of a noninertial frame. Finally, I hope to maintain a list of errata and additional resources at the web address:

http://www.cmi.ac.in/∼govind.

Govind S Krishnaswami
Chennai, 20 May, 2024.

Chapter 1

Mechanical systems with one degree of freedom

As one might suspect, it is easier to deal with systems with fewer particles and with lesser room to move. We begin with the simplest of mechanical systems, where a single nonrelativistic[1] particle moves along a line or a circle. In Chap. 2, we will graduate to two interacting particles moving in three dimensions. The lessons learned from the examples in these two chapters will then motivate the general concepts and formalisms developed in Chap. 3. Despite its apparent simplicity, motion in one dimension is physically realistic (as in a pendulum) and several of its features apply more generally. What is more, motion in higher dimensions, especially in the presence of symmetries, can sometimes be reduced to effectively one-dimensional (1d) motion. In some other cases, an approximate one-dimensional treatment may be possible if the effects of all the other variables can be encoded in an effective external influence or force. Thus, one-dimensional motion is a very instructive context in which to begin our study of mechanics.

The primary question we would like to address in this chapter is that of determining features of the trajectory of a particle, given how it begins and given the external influences it is subject to. Subsequently, we will also address the inverse problem of trying to deduce the external forces, given that a particle is experimentally observed to move in a particular way. We will begin by focusing on conservative systems which, for the present, means that the force is derived from a potential function ensuring that there is a conserved 'energy' that restricts the nature of the motion. Subsequently, we will allow for dissipation and comment on how it modifies the dynamics.

1.1 Newton's laws and qualitative characterization of motion on a line

Consider a point particle of fixed mass[2] $m > 0$ that can move along a straight line[3] (which we will call the real line $\mathbb{R}$) that is, say, fixed relative to the Earth and viewed by an observer who is also fixed relative to the Earth. Its position at time t is denoted $x(t)$. The particle is said to possess one degree of freedom since precisely one real coordinate (x) is needed to specify its instantaneous location. In his book titled

---

[1] Nonrelativistic means moving at speeds much less than that of light. The 'special relativistic' framework of Chap. 4 deals with particles approaching the speed of light.

[2] Mass is a measure of the particle's inertia: a more massive particle is more reluctant to move when subjected to the same external influence (force). We will say more on the properties of mass and assignment of masses to particles in Sect. 3.1, Sect. 3.3 and Footnote 10 of Chap. 2.

[3] We do this for simplicity, though many of the features we discuss are valid more generally. A particle moving on a circle or other curve also has one degree of freedom. See Sect. 3.5 for an example and a framework to handle such problems.

PhilosophiæNaturalis Principia Mathematica (1687), Isaac Newton formulated laws[4] governing the motion of such a particle. It is called a free particle if it is isolated (far from physical interactions with other bodies; for this it may have to be far from the Earth!). In this case, Newton's 1st law implies that it must either be at rest or moving at a constant velocity $v = \dot{x} = \frac{dx}{dt}$ (or equivalently constant momentum $p = m\dot{x}$) to the right or left. The trajectory of a free particle is therefore given by $x(t) = x(0) + vt$ where $x(0)$ and $v = \dot{x}(0)$ are its position and velocity at $t = 0$. More generally, if the particle is not necessarily free and if its interactions can be described by an 'external' force F acting on it, Newton's 2nd law says that the particle accelerates according to the *equation of motion* (EOM) mass $\times$ acceleration $=$ force or $m\ddot{x} = F$. To find the trajectory $x(t)$ of the particle, we need to solve this second order ordinary differential equation subject to a pair of initial conditions (ICs), which could be the initial location and velocity $(x(0), \dot{x}(0))$ [one may replace $\dot{x}(0)$ with $p(0) = m\dot{x}(0)$]. If the force depends only on location[5] $F = F(x)$, then in 1 dimension[6], we may define a potential function such that $F(x) = -V'(x)$. The latter is a negative[7] antiderivative or primitive of F:

$$V(x) = V(0) - \int_0^x F(x')\, dx'. \tag{1.1}$$

In 1d, a force that is the negative derivative of a potential is called a conservative force. The potential (or potential energy) $V(x)$ is of course defined only up to an additive constant ($V(0)$) that cancels out in $V'(x)$. The quantity $F(x')dx'$ has the physical meaning of the infinitesimal work done by the force F (assumed positive if rightward directed) as the particle is moved from x' to $x' + dx'$. Evidently, the potential energy (1.1) decreases as the particle moves in the direction of the force (as from x_2 to its right in Fig. 1.2). The integral $\int_0^x F(x')dx'$ is the total work done by the force in moving the particle from 0 to x. It does not depend on the manner (speed, whether back and forth, etc.) in which the particle is moved from 0 to x. This is a special feature of 1d motion subject to forces that depend only on location. For a velocity-dependent force such as friction in (1.4), the work done generally depends on the manner of motion and not just on the initial and final locations.

For a conservative force, Newton's equation becomes $m\ddot{x} + V'(x) = 0$. Multiplying by the 'integrating factor' $\dot{x}$ we get

$$m\ddot{x}\dot{x} + V'(x)\dot{x} = 0 \quad \text{or} \quad \frac{d}{dt}\left(\frac{1}{2}m\dot{x}^2 + V(x(t))\right) = 0. \tag{1.2}$$

---

[4] Newton's laws will be stated more precisely and discussed more extensively in Sect. 3.3.

[5] In other words, the force $F = F(x(t))$ does not depend explicitly on time (as the external driving force $F = f \cos \nu t$ of Sect. 6.8 does) or on the velocity $\dot{x}$, like the magnetic Lorentz force $q\dot{\boldsymbol{x}} \times \boldsymbol{B}$ of Sect. 3.23*. We *will* consider a velocity-dependent damping force later in this section.

[6] In two or more dimensions, a force that depends only on location need not be a derivative (precisely, 'gradient') of a potential energy function.

[7] The minus sign is conventional. It ensures that the potential $\frac{1}{2}kx^2$ for a stabilizing linear restoring force (Hooke's law) $-kx$ for $k > 0$ is bounded below rather than above.

Thus, the total energy $E = \frac{1}{2}m\dot{x}^2 + V(x)$ is conserved[8]. This energy is the sum of a kinetic energy $\frac{1}{2}m\dot{x}^2$ (which accrues from the particle's motion) and the previously introduced potential energy $V(x)$. The physical inspiration for the use of this integrating factor comes from calculating the rate of work done by the force. Indeed, the first term in (1.2) is the rate of increase in kinetic energy of the particle while the second is the (negative of) the rate of work done by the force: $-F(x)dx/dt$.

Linear or simple harmonic oscillator. Perhaps the simplest one-dimensional mechanical system after the free particle is the linear or simple harmonic oscillator. Here, a particle of mass m is subject to Robert Hooke's linear force law $F(x) = -kx$ for a force constant $k > 0$. There is no force at $x = 0$, which is therefore called a point of equilibrium. The real variable x may be viewed as the displacement of the particle from equilibrium. Hooke's law (1676) is said to represent a *restoring force* since it tends to restore the particle to its equilibrium position: it is negative (leftward) when $x > 0$ and positive (rightward) when $x < 0$. Ignoring friction, for small[9] x, $F(x)$ is an approximation to the force felt by a particle of mass m attached to one end of a horizontal spring, with x measuring the expansion/compression of the spring whose other end is held fixed (see Fig. 1.1a). The qualifier simple in the name refers to the presence of a single rather than multiple springs. Such a particle is observed to perform oscillatory motion, with x varying periodically between 'turning points' where x is maximal and minimal. The potential for Hooke's force law may be taken as $V(x) = \frac{1}{2}kx^2$ so as to ensure that there is no potential energy at the equilibrium point $x = 0$. As the particle oscillates, potential energy $V(x)$ stored in the stretched/compressed spring is continually converted into kinetic energy of the particle's motion ($\frac{1}{2}m\dot{x}^2$) and vice versa while ensuring that the total energy $E = \frac{1}{2}m\dot{x}^2 + \frac{1}{2}kx^2$ is conserved. Evidently, $E = 0$ if the particle is at rest at equilibrium. Since the kinetic energy is nonnegative, for any $E > 0$, the particle is confined to the interval $|x| \le a$ where $a = \sqrt{2E/k}$ is called the oscillation amplitude. At the turning points $x = \pm a$, the particle comes momentarily to rest as its speed vanishes. These features of the motion can be understood by examining the graph of $V(x)$ shown in Fig. 1.1b. The motion is called 'harmonic' since the solution (see Prob. 1.6 and 1.7) of Newton's equation $m\ddot{x} = -kx$ is a sinusoidal[10] function of time: $x(t) = a\cos(\omega t + \phi)$ where the amplitude a and 'initial phase' ϕ are constants of integration and $\omega = \sqrt{k/m}$. We will have more to say about the harmonic oscillator in Sect. 1.2 and Sect. 6.1. □

---

[8] The idea of a conserved energy appeared in *Institutions de Physique* (1756), a translation and commentary on Newton's Principia by Émilie du Châtelet.

[9] Small means $|x| \ll \ell$ where ℓ is the equilibrium length of the spring. For larger $|x|$, the force ceases to be linear. 'Anharmonic' restoring forces such as $F(x) = -kx - gx^3$ for positive constants k and g are used to model the resulting motion, see Sect. 7.5*.

[10] Sinusoids are sines and cosines. The name harmonic oscillator is reasonable since sinusoids are also used to model the 'harmonics' observed in the shape of a vibrating string (see Fig. 17.2).

[11] There is another way of visualizing the motion with the aid of phase portraits, that applies to both conservative and nonconservative systems. See Fig. 3.2 and Chap. 5

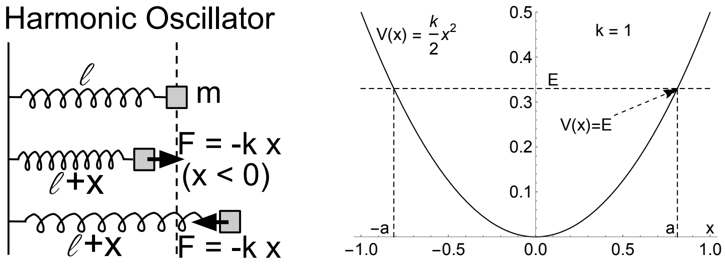

(a) (b)

Figure 1.1: (a) Hooke's linear restoring force for a mass attached to a spring. (b) Parabolic potential for a harmonic oscillator. Turning points $\pm a$ for a fixed energy are indicated.

Pictorial characterization of motion[11]**.** Having a conserved energy is helpful in understanding the dynamics[12]. Indeed, for a given energy E, the nature of the motion can be deduced from a graph of the potential[13] $V(x)$. On account of the positivity of kinetic energy $\frac{1}{2}m\dot{x}^2$, the motion is confined to the region where $E \geq V(x)$. This region, when nonempty, may be a union of several intervals/points (see Fig 1.2). However, due to 'potential barriers', a particle cannot jump between two disconnected intervals[14], so we may discuss each in isolation[15]. The points x where the energy-E horizontal line intersects the graph of $V(x)$ are the places where $\dot{x}$ vanishes momentarily and the energy is purely potential. They are called 'turning points' since the particle turns around at such a point if reached in finite time [this happens if $V' \neq 0$ at a turning point, see Sect. 1.2]. It is possible for V to have finite or infinite discontinuities such as at the edge of a step potential (e.g., $V(x) = V_0 \operatorname{sgn}(x)$) or infinite potential well (e.g., $V(x) = 0$ for $|x| < a$ and $V(x) = \infty$ for $|x| \geq a > 0$) where the force becomes infinite. When the potential presents a wall-like barrier at a turning point, the particle's velocity is simply reversed upon reaching the turning point.

For the potential in Fig. 1.2, the classically allowed region corresponding to the

---

[12] Dynamics refers to the evolution of a system in time, the motion of a system due to the forces in operation. Statics refers to situations where a system does not change with time. In a somewhat different direction, kinematics (or phoronomy) refers to those aspects of the system and its motion that do not depend on the specific forces that act, but on other features like the number of degrees of freedom, the range of values that physical variables can take, how these values change in different frames of reference, etc. The problem of finding the trajectory from the acceleration is kinematical while finding the trajectory from the forces involves dynamics.

[13] Without such a conservation law, one cannot say as much, simply by looking at the potential. Having an inequality such as (1.5) for damped motion does allow a partial pictorial understanding based on the potential. However, one needs more information to distinguish between, say, overdamped, underdamped and critically damped motion for a harmonic restoring force, see Sect. 6.4.

[14] In Fig. 1.2, the closed interval $[x_2, x_3]$ (the square brackets mean the endpoints are included) is a connected set, any two points in it can be joined by a curve lying in it. On the other hand, the disjoint union $[x_2, x_3] \cup \{x_4\}$ is disconnected.

[15] In the quantum theory, a particle may be able to 'tunnel' between disconnected classically allowed regions.

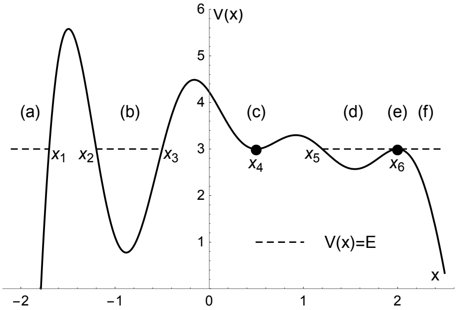

Figure 1.2: Qualitative characterization of motion of a particle in a 1d potential.

indicated energy is a union of six connected sets, with initial conditions determining in which one the motion takes place. From left to right, try to argue that the qualitative motion is of the following sorts:

(a) $(-\infty, x_1]$: The particle can come in from any point to the left of x_1, 'collide' against the potential barrier at x_1, turn around and escape/scatter to $-\infty$. In this process, the particle reaches x_1 in a finite time. This is indicated via the square bracket, which means the interval is closed at the x_1 end.

(b) $[x_2, x_3]$: The particle oscillates with finite time period between the turning points at x_2 and x_3.

(c) x_4: The particle remains at rest at the stable equilibrium point x_4.

(d) $[x_5, x_6)$: For instance, a particle starting at x_5 accelerates and moves rightward but then slows down and takes infinitely long to reach x_6. Consequently, x_6 is not part of the interval, and this is indicated via the round bracket. By contrast, the turning point at x_5 is reached in finite time, at which the particle comes instantaneously to rest and reverses direction. $[x_5, x_6)$ is a 'closed-open' interval.

(e) x_6: The particle remains at rest at the unstable equilibrium point x_6.

(f) (x_6, ∞): The particle can come leftwards from large x, but slows down and takes infinitely long to reach x_6. Starting from $x > x_6$ with rightward velocity, the particle speeds up and escapes to infinity.

(g) (x_1, x_2), (x_3, x_4) and (x_4, x_5) are forbidden intervals. The particle cannot be found in any of these intervals since its kinetic energy would have to be negative.

While in (b)-(e) the particle is 'bound' or 'confined', in (a) and (f) the motion can be unbounded. The foregoing statements about the finite or infinite time taken to reach turning points will be established in Sect. 1.2.

Time-reversal invariance. Newton's equation $m\ddot{x} = -V'(x)$ is time-reversal invariant in the sense that if $x(t)$ is a solution[16], then so is $x(-t)$. To see this, let $\tilde{t} = -t$.

---

[16] Here, we assumed that the solution $x(t)$ exists for all time t. If it exists for $t_{\min} \le t \le t_{\max}$, then the assertion is that $x(t_{\max} - t)$ is also a solution for $0 \le t \le t_{\max} - t_{\min}$.

Then $\frac{d}{d\tilde{t}} = -\frac{d}{dt}$ and $\frac{d^2}{d\tilde{t}^2} = \frac{d^2}{dt^2}$. So Newton's equation $m\frac{d^2}{dt^2}x(t) = -V'(x(t))$ implies that

$$m\frac{d^2}{d\tilde{t}^2}x(-\tilde{t}) = -V'(x(-\tilde{t})). \tag{1.3}$$

We see that $x(-\tilde{t})$ satisfies the same equation as $x(\tilde{t})$ satisfied [$\tilde{t}$ is just a dummy variable, it could be renamed t]. In other words, a movie of a solution played backwards is also an admissible motion. Note that the initial velocity for the reversed motion is the negative of the final velocity of the forward motion. Under time-reversal ($t \to -t$, $x(t) \to x(-t)$), show that $\ddot{x}(t) \to \ddot{x}(-t), F(x(t)) \to F(x(-t)), V(x(t)) \to V(x(-t))$ while $\dot{x}(t) \to -\dot{x}(-t)$. Thus, motion subject to any conservative force is time-reversible.

Damped motion without time-reversal invariance. Of course, not every system is conservative. In fact, most real-world systems are *not* conservative due to interaction with the environment: dissipation, external driving, noise, etc. For instance, suppose a particle moves under the influence of both a conservative force as well as a *frictional* or *damping* force proportional to its speed and directed opposite to its velocity:

$$m\ddot{x} = -V'(x) - \gamma\dot{x} \quad \text{with damping coefficient} \quad \gamma > 0. \tag{1.4}$$

The frictional force $-\gamma\dot{x}$, being dependent on $\dot{x}$, cannot be written as the derivative (with respect to x) of some function of x. Thus this frictional force is not conservative. Furthermore, the friction term breaks the time-reversal invariance of this equation: it reverses sign under $t \to -t$ while all other terms do not change sign. In this case, we may show that the above-defined energy is monotonically decreasing. Multiplying (1.4) by $\dot{x}$, we get

$$\frac{d}{dt}\left(\frac{1}{2}m\dot{x}^2 + V(x)\right) = -\gamma\dot{x}^2 \leq 0. \tag{1.5}$$

From (1.4), the steady-state or static solutions (time-independent solutions $\dot{x} \equiv 0, \ddot{x} \equiv 0$) are at extrema $x = x_s$ of the potential where $V'(x_s) = 0$. For most initial conditions (other than, for example, starting at rest at a local maximum of V) the particle will execute damped oscillations and settle down at a local minimum of the potential.

Dimensional analysis. Physical quantities like the position x of a particle moving on a line, a time interval or a force, can each be assigned a dimension. It turns out that the dimensions of all mechanical quantities may be expressed in terms of three basic dimensions: length L, mass M and time T [whose values are specified in units of meters (or centimeters), kilograms (or grams) and seconds in the International System (SI) (or CGS system) of units]. More precisely, any physical quantity f can be assigned a dimension $[f] = M^a L^b T^c$ for some real numbers a, b, c (which are typically rational numbers). If $a = b = c = 0$, then f is dimensionless. Consistency requires that all terms in an equation (or inequality) have the same dimensions. For example, some of the quantities introduced in this section have the dimensions $[x] = L$, $[m] = M$, $[t] = T$, $[\dot{x}] = LT^{-1}$, $[\ddot{x}] = LT^{-2}$, $[p] = MLT^{-1}$, $[F] = MLT^{-2}$ and $[E] = [V] = ML^2T^{-2}$. What are the dimensions of an angle and of the damping coefficient γ? □

1.2 Time period of conservative oscillations between turning points

Consider conservative motion of a particle along a line subject to the differentiable potential $V(x)$. For a given energy E, suppose $x_1 < x_2$ are a pair of finite adjacent turning points that are not extrema of the potential: $V(x_1) = V(x_2) = 0$ while $V'(x_1), V'(x_2) \neq 0$ [we will soon see what happens if a turning point is an extremum]. Moreover, if $V(x) < E$ for $x_1 < x < x_2$, then $[x_1, x_2]$ is a classically allowed interval for the motion and the particle oscillates between these turning points. The conservation of energy (1.2) allows us to write

$$\frac{dx}{dt} = \pm \left[\frac{2}{m} (E - V(x)) \right]^{1/2}. \tag{1.6}$$

Separating variables[17] and integrating subject to the initial condition $x(t_0) = x_0$ gives

$$t - t_0 = \pm \sqrt{\frac{m}{2}} \int_{x(t_0)}^{x(t)} \frac{dx}{\sqrt{E - V(x)}}. \tag{1.7}$$

The ± signs correspond to an initial velocity that is right/leftward directed. The time to go from turning point x_1 to x_2 and from x_2 to x_1 are equal (by time-reversal invariance of Newton's equation or by comparing the integrals below)

$$T_{x_1 \to x_2} = \sqrt{\frac{m}{2}} \int_{x_1}^{x_2} \frac{dx}{\sqrt{E - V(x)}} \quad = \quad T_{x_2 \to x_1} = -\sqrt{\frac{m}{2}} \int_{x_2}^{x_1} \frac{dx}{\sqrt{E - V(x)}}. \tag{1.8}$$

Let us check that this time is finite. The range of integration is finite and the integrand is finite as long as $x \neq x_{1,2}$ since we are dividing by the square-root of the nonzero kinetic energy. The integrand diverges only at the turning points. So it suffices to check that the integral receives finite contributions from the vicinity of the turning points. Near the left turning point x_1, $V'(x_1) < 0$ so

$$V(x) = V(x_1) + V'(x_1)(x - x_1) + \cdots = E - |V'(x_1)|(x - x_1) + \cdots . \tag{1.9}$$

Thus, when $x_1 < x < x_1 + \epsilon$, the integral behaves as

$$\sqrt{\frac{m}{2|V'(x_1)|}} \int_{x_1}^{x_1+\epsilon} (x - x_1)^{-1/2} dx \tag{1.10}$$

which is finite for any fixed $\epsilon > 0$. We say that the integrand has an integrable singularity or integrable divergence at $x = x_1$ (see Prob. 1.8). The same applies to the right turning point x_2. Thus, the period of oscillation between x_1 and x_2 is finite and equal to

$$T_{x_1 \leftrightarrow x_2}(E) = T_{x_1 \to x_2} + T_{x_2 \to x_1} = \sqrt{2m} \int_{x_1}^{x_2} \frac{dx}{\sqrt{E - V(x)}}. \tag{1.11}$$

---

[17] The technique of separating variables in ordinary differential equations goes back to Leibniz (1691).

Notice from (1.10) that when $V'(x_1)$ or $V'(x_2) \to 0$, the time period diverges (see Prob. 1.9). Thus, if a turning point is also an extremum of the potential, the particle takes infinitely long to reach it.

Putting things together, a potential $V(x)$ determines the time period function $T(E)$ for any energy $E \geq \min_x V(x)$. $T(E)$ may be a multivalued function for some energies since there may be more than one classically allowed interval at that energy, as in the example of Fig. 1.2. A direct problem is to find $T(E)$ given $V(x)$. Above, this problem has been reduced to quadrature[18]. $T(E)$ may be evaluated explicitly for some potentials (see Prob. 1.10 and Prob. 1.11). The simple harmonic oscillator [with $V(x) = \frac{1}{2}m\omega^2 x^2$ for constant ω, see Sect. 1.1 and Sect. 6.1] is isochronous in the sense that $T(E) = \frac{2\pi}{\omega}$ (for $E \geq 0$) is independent of E. This means a particle subject to the linear restoring force $-m\omega^2 x$ oscillates with the same time period irrespective of what its energy may be. See [83] for more examples.

1.3* Inverse problem: determination of potential from time period

The inverse problem of deducing a potential with a given time period of oscillations[19] as a function of energy $(T(E))$ is much harder[20]. The potential $V(x)$ may not be unique. For instance, $V(x - x_0)$ has the same $T(E)$ as $V(x)$. But V could be nonunique in more nontrivial ways as we will observe below. Besides, we have seen that $T(E)$ is not even singlevalued if the potential supports more than one type of oscillation for a fixed energy (a double-well potential[21] $V(x) = 0.6 + (x+1)^2(x-1)^4$ for instance, see Fig. 1.3). For simplicity, suppose we seek only those potentials $V(x)$ which are convex ($V'' > 0$), have a single minimum, say $V(0) = 0$ and satisfy $V(x) \to \infty$ for $x \to \pm\infty$. Then $T(E)$ is singlevalued and related to $V(x)$ via energy conservation for all $E > 0$:

$$T(E) = \sqrt{2m} \int_{x_1}^{x_2} \frac{dx}{\sqrt{E - V(x)}}, \tag{1.12}$$

where $x_1 < x_2$ are adjacent turning points. We may regard this as a nonlinear integral equation for the unknown function $V(x)$, given $T(E)$.

For simplicity, suppose we look for a potential that is even[22] $V(x) = V(-x)$. In this case

$$T(E) = 2\sqrt{2m} \int_0^{x_0} \frac{dx}{\sqrt{E - V(x)}}, \quad \text{where} \quad V(x_0) = E \quad \text{and} \quad x_0 > 0. \tag{1.13}$$

---

[18] Quadrature refers to evaluating integrals. The name comes from the estimation of areas of 2d regions by approximately covering them by quadrilaterals (rectangles).

[19] We are given the function $T(E)$ and asked to find a potential $V(x)$ in which the oscillation time period as a function of energy is $T(E)$. We are not given the turning points.

[20] A similar problem is solved in going from Kepler's 3rd law to Newton's law of gravitation, see Sect. 2.1. Inverse scattering theory deals with more such questions.

[21] For an even double-well potential like $(x^2 - 1)^2$, $T(E)$ is singlevalued.

[22] It turns out that with this condition, $V(x)$ is unique, though there are infinitely many nonsymmetric convex $V(x)$ with the same $T(E)$, see [83]. Intuitively, one may imagine deforming the potential to speed up the particle in some places and slow it down elsewhere in such a way that the time period for any given energy is unchanged.

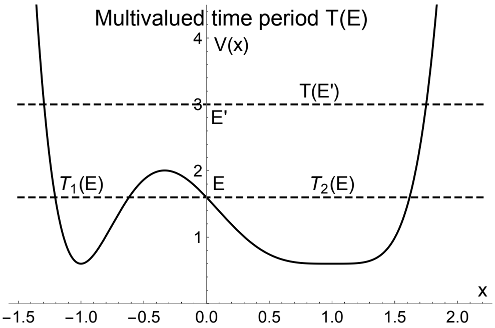

Figure 1.3: Asymmetric double-well potential $V(x) = 0.6 + (x+1)^2(x-1)^4$ with double- and singlevalued time period $T(E)$ for low and high energies.

Interestingly, the above nonlinear integral equation can be turned into a linear integral equation for $x'(V) = dx/dV$ if we regard x as a function[23] of V. Indeed, $dx = x'(V)\,dV$ and $x = 0 \Rightarrow V = 0$ while $x = x_0$ implies $V = E$. Hence,

$$T(E) = 2\sqrt{2m}\int_0^E \frac{x'(V)\,dV}{\sqrt{E-V}}. \tag{1.14}$$

This is now an inhomogeneous linear integral equation[24] for $x'(V)$[25]. If we are able to solve this equation, then we may integrate to find $x(V) = \int_0^V x'(W)dW$. The nonlinear part of the problem is then to invert $x(V)$ to find $V(x)$. This could be done graphically, if not otherwise.

Remarkably, the above linear integral equation can be solved for $x'(V)$. The idea[26] to extract $x'(V)$ is to multiply either side by a suitable power of $(W-E)$ and integrate

---

[23] In general, $V(x)$ is not one-to-one. In fact, under our hypotheses, it is two-to-one so that $x(V)$ is double-valued.

[24] An integral equation is one where the unknown function appears under the integral sign (as well as possibly elsewhere). For example, $\int k(t,t')y(t')dt' = f(t)$ is an integral equation for the function $y(t)$ if $f(t)$ and $k(t,t')$ are prescribed functions. It is linear since only y^1 and y^0 appear. It is inhomogeneous since $y \to \lambda y$ is not a symmetry (consequently, $y \equiv 0$ is generally not a solution). It would be homogeneous if f were the zero function. Viewed somewhat differently, we say that f is an integral transform of y and that $y(t) \mapsto \int k(t,t')y(t')dt'$ is a linear integral transform or a linear integral operator. $k(t,t')$ is called the *integral kernel* of the integral operator. It plays the role of the matrix elements of a linear transformation, as we see by comparing with $\sum_{1\le j\le n} K_{ij}Y_j = F_i$ where F and Y are $n\times 1$ column vectors and K is an $n\times n$ matrix. The summation over the discrete index j is replaced by integration over the continuous variable t'. See Sect. 18.3* for more on integral kernels.

[25] The *integral kernel* $K(E,V) = (E-V)^{-1/2}$ is translation-invariant, depending only on the difference $E-V$:

$$2\sqrt{2m}\int_0^E K(E-V)x'(V)\,dV = T(E). \tag{1.15}$$

[26] Compare with how we invert the Fourier transform (Appendix A.11*), where the kernel is

over E. We try $(W-E)^{-1/2}$,

$$2\sqrt{2m}\int_0^W dE\int_0^E dV\frac{x'(V)}{\sqrt{(E-V)(W-E)}}=\int_0^W dE\frac{T(E)}{\sqrt{W-E}}. \tag{1.17}$$

Changing the order of integrals, noting that $V \leq E \leq W$ and that $V \geq 0$ and $V \leq W$, we get

$$2\sqrt{2m}\int_0^W dV\, x'(V)\int_V^W \frac{dE}{\sqrt{(E-V)(W-E)}}=\int_0^W dE\frac{T(E)}{\sqrt{W-E}}. \tag{1.18}$$

The inner integral is just π, independent of W and V! [see Prob. 1.14]. Thus,

$$x(V)=\frac{1}{2\pi\sqrt{2m}}\int_0^V \frac{T(E)\, dE}{\sqrt{V-E}}. \tag{1.19}$$

So the determination of $x(V)$ has been reduced to calculating a certain integral transform of the period function $T(E)$. Finally, we must invert $x(V)$ to find $V(x)$.

As a simple illustration, let us 'discover' the harmonic oscillator potential from its isochronous property, namely $T(E)$ is independent of E. Suppose $T(E)=2\pi/\omega$ for some constant angular frequency ω. Assuming V is even and taking $x>0$,

$$x(V)=\frac{1}{\omega\sqrt{2m}}\int_0^V\frac{dE}{\sqrt{V-E}}=\frac{\sqrt{2V}}{\omega\sqrt{m}} \quad\Rightarrow\quad V(x)=\frac{1}{2}m\omega^2x^2. \tag{1.20}$$

1.4* Time delay in unbounded 'scattering' trajectories

In Sect. 1.2 and Sect. 1.3*, we considered bound trajectories where the particle is confined to a finite interval on the real line. Let us briefly consider a case where the particle can escape to infinity, i.e., a 'scattering' or 'unbound' trajectory. For simplicity, consider a potential that tends to zero as $x\to\pm\infty$ and which does not have any infinite barriers at finite values of x. Many physically occurring conservative forces arise from such potentials: there are no forces far from the region of interest. Particularly simple special cases are (1) a 'repulsive' potential $V(x)>0$, shaped like a speed breaker on a road and (2) an 'attractive' potential $V(x)<0$, shaped like a depression/trough on a road (see Fig. 1.4). A famous example [32] of such a potential is $V(x)=\pm V_o\,\mathrm{sech}^2(x/l)$ for $V_o>0$ and $l>0$. The term 'repulsive potential' is meant to convey that the potential is like a barrier, it repels particles that try to approach it from either side (see Prob. 1.12). We will be interested in situations where the particle comes in from $x=-\infty$ and escapes to $x=\infty$. Of course, energy

---

$K(x,k)=e^{ikx}$:

$$f(x)=\int_{-\infty}^{\infty}\tilde f(k)e^{ikx}\frac{dk}{2\pi}\quad\Rightarrow\int_{-\infty}^{\infty}f(x)e^{-ilx}dx=\int_{-\infty}^{\infty}\frac{dk}{2\pi}\tilde f(k)\int_{-\infty}^{\infty}dx\, e^{i(k-l)x}=\tilde f(l). \tag{1.16}$$

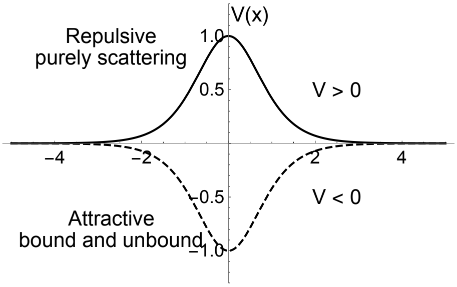

Figure 1.4: Repulsive and attractive $V(x) = \operatorname{sech}^2(x)$ potentials. The former admits only unbound trajectories while the latter admits both bound and unbound trajectories.

$E = \frac{1}{2}m\dot{x}^2 + V(x)$ is conserved. So we must have $E > 0$. In fact, we will assume $E > \max_x V$, so that it does not encounter a potential barrier and rebound. For lower energies, the potential may also support oscillations in some local minima, as discussed in Sect. 1.2.

For scattering trajectories, a possible notion that replaces the time period of oscillations is the time it takes[27] for the particle to go from $-\infty$ to $+\infty$. But typically, this is infinite. In fact, even a free particle with any finite velocity takes infinitely long to go from $-\infty$ to $+\infty$. A more useful concept is the time delay, the excess time it takes the particle to traverse this distance relative to a free particle. However, this needs to be defined carefully since, on the face of it, it is the difference between two infinite quantities. To make sense of the time delay, we will enclose the system in a long pipe of length $2a$ and think of the time it takes the particle to traverse the length of the pipe in the presence/absence of the potential. Here, a is called a *regulator*, it will eventually be taken to ∞ leaving us with a finite time delay, as long as the potential falls off sufficiently fast at $\pm\infty$. Thus, let us first consider the time taken to go from $-a$ to $+a$ (for $a > 0$) with and without a potential[28]:

$$T_V(a) = \sqrt{\frac{m}{2}} \int_{-a}^{a} \frac{dx}{\sqrt{E - V(x)}} \quad \text{and} \quad T_0(a) = \sqrt{\frac{m}{2}} \int_{-a}^{a} \frac{dx}{\sqrt{E}}. \tag{1.21}$$

Define the *regularized* time delay by

$$\Delta T(a) = T_V(a) - T_0(a) = \sqrt{\frac{m}{2}} \int_{-a}^{a} \left(\frac{1}{\sqrt{E - V(x)}} - \frac{1}{\sqrt{E}} \right) dx. \tag{1.22}$$

---

[27] An alternate setup is to have an infinite barrier, say at $x = 0$ and consider the time taken for the particle to come in from $+\infty$, interact with a potential and return to $+\infty$.

[28] More generally, we could use asymmetric limits, $a_1 < a_2$. However, we will soon see that the integral from $-\infty$ to ∞ is absolutely convergent for a wide class of potentials that decay at $\pm\infty$. For these potentials, the manner of taking the limit does not matter. If the manner of taking the limit matters, then we would need additional physical input (e.g., on how the experiment is performed) to decide what to do.

The time delay ΔT is then defined as the limit of the regularized time delay as $a \to \infty$:

$$\Delta T = \lim_{a\to\infty} \Delta T(a) = \sqrt{\frac{m}{2}} \int_{-\infty}^{\infty} \left(\frac{1}{\sqrt{E - V(x)}} - \frac{1}{\sqrt{E}} \right) dx. \tag{1.23}$$

Though the individual times are both infinite, we will show that the difference is finite if for large $|x|$, the particle in potential V behaves nearly like a free particle. Let us examine the behavior of the integrand for large $|x|$ using the fact that $V \to 0$ as $|x| \to \infty$. Since $E > 0$, $|V/E| < 1$ for sufficiently large $|x|$, and

$$\frac{1}{\sqrt{E-V}} - \frac{1}{\sqrt{E}} = \frac{1}{\sqrt{E}} \left(1 + \frac{V}{2E} + \cdots \right) - \frac{1}{\sqrt{E}} \to \frac{V}{2E^{3/2}} + \cdots \tag{1.24}$$

as $|x| \to \infty$. In other words, for large $|x|$, the integrand is simply proportional to V. So the time delay will be finite if $V(x)$ is absolutely integrable, i.e., if $\int_{-\infty}^{\infty} |V| \, dx < \infty$. This will be the case for instance if $V(x)$ is bounded and decays exponentially fast as $|x| \to \infty$. In fact, it is sufficient that the potential decay as a power-law $1/|x|^{1+\epsilon}$ for some $\epsilon > 0$. A potential that falls off as the reciprocal of the distance ($\epsilon = 0$) is on the borderline and would have a divergent time delay. An example is provided by the Coulomb/Newtonian potential $V(r) \propto -1/r$ where r is the radial coordinate in three dimensions (see Chap. 2). The Coulomb potential is called a long-range potential, colloquially, its effects are felt even far away.

Notice that the time delay is positive for a purely repulsive potential ($V(x) > 0$). Suppose the particle comes in from $-\infty$ with speed v_∞. Then its speed at x is

$$v(x) = \sqrt{\frac{2}{m}(E - V)} = \sqrt{v_\infty^2 - \frac{2V(x)}{m}}. \tag{1.25}$$

So in a purely positive potential, $v(x) \le v_\infty$. Under the influence of the potential, the particle slows down compared to a free particle. So it will take longer to reach $x = a$. On the other hand, in a purely attractive potential $V(x) < 0$, the time delay is negative. The particle speeds up compared to the free particle and arrives in advance.

As in Sect. 1.3*, one may study the inverse problem of determining the scattering potential $V(x)$ from a knowledge of the time delay $\Delta T(E)$. This too is a problem of solving an analogous nonlinear integral equation, though we do not pursue it here.

Relation of time delay to EM action shift. A quantity of some importance in mechanics [it appears in the Euler-Maupertuis (EM) principle (Sect. 3.27*, Sect. 3.28*) and in the Bohr-Sommerfeld semiclassical quantization condition] is the EM action[29] $\mathscr{S}$, which may be evaluated for a trajectory of energy E between x_1 and x_2:

$$\mathscr{S}(E; x_1, x_2) = \int_{x_1}^{x_2} p(x)\, dx = \int_{x_1}^{x_2} \sqrt{2m(E - V(x))}\, dx. \tag{1.26}$$

---

[29] The EM action is called the *abbreviated action* in [83]. However, it is not accurate to think of it as a truncated version of the 'phase space' action $S = \int_{t_1}^{t_2} [p\dot{x} - H(x,p)] dt$ of Sect. 3.19. The quantity pdx is the Liouville 1-form that we will meet again in Appendix B.5*, Sect. 3.28* and elsewhere.

As before, we assume $E > \max_x V$. Holding x_1, x_2 fixed, it is evident that the derivative of $\mathscr{S}$ is equal to the time it takes the particle to go from x_1 to x_2:

$$\frac{d\mathscr{S}}{dE} = \sqrt{\frac{m}{2}} \int_{x_1}^{x_2} \frac{dx}{\sqrt{E - V(x)}} = T_{x_1 \to x_2}. \tag{1.27}$$

This relation between the Euler-Maupertuis action and duration of trajectory also holds for bound motion. As with the total time, $\mathscr{S}$ is infinite for a 'full' trajectory between $x = \pm\infty$. So it makes sense to consider the EM action shift

$$\Delta\mathscr{S} = \int_{-\infty}^{\infty} \left(\sqrt{2m(E-V)} - \sqrt{2mE}\right)\, dx. \tag{1.28}$$

Then the time delay is the derivative $\Delta T = d(\Delta\mathscr{S})/dE$. See Prob. 1.16 for an example. The 'Wigner' time delay is an analogous concept in quantum mechanics and is of particular interest in the context of near-resonant scattering. ☐

1.5 Simple pendulum: basic properties and small oscillations

The (plane) simple pendulum is a practically and conceptually important physical system with one degree of freedom. Unlike the real coordinate $x(t)$ of the particle in Sect. 1.1 that moves on a line, the degree of freedom of a simple pendulum is an angular one that we will denote $\theta(t)$. To set things up, consider a bob of mass m suspended from a rigid rod of length ℓ clamped at a pivot, as shown in Fig. 1.5. The bob is free to move in a fixed vertical plane subject to Earth's constant downward acceleration due to gravity $g > 0$, as in a 'grandfather' clock. A heavy pendulum bob (wrecking ball) may be used to demolish buildings! If the bob is treated as a point mass and the rod is massless, the system is called a simple pendulum. A 'compound pendulum' is one where the mass is not point-like but distributed, for instance, over the rod and bob. A simple pendulum can be used to illustrate many basic concepts of mechanics. Here, we will introduce the pendulum, derive Newton's equation of motion for it, deduce a conserved energy and discuss its small oscillations. We will revisit the pendulum in Chap. 7 after developing more of the formalism of mechanics in Chap. 3.

Observations tell us that the pendulum is in equilibrium when hanging vertically downward, the downward gravitational force being balanced by the upward tension in the rod. This equilibrium is stable since an arbitrarily small push away from equilibrium results in a force that tends to restore the bob to its original position. The pendulum is also in equilibrium when it is balanced vertically upwards. But this is unstable equilibrium: a small push in either direction takes the bob far from equilibrium.

A spherical pendulum. A spherical pendulum is one whose motion is not confined to a vertical plane. The bob's initial displacement vector (relative to the point of stable equilibrium) and the downward directed acceleration due to gravity, together define a plane. If the initial velocity vector (which must be tangent to the sphere of radius ℓ) does not lie in this plane, then the resulting motion is that of a spherical pendulum: it is not confined to a vertical plane. On the other hand, if the initial velocity lies in the aforementioned plane, the motion is that of a simple pendulum, confined to that plane. Henceforth, the term 'pendulum' shall mean a simple plane pendulum. ☐

Libration and Rotation. A pendulum displays two distinct types of motion (see Fig. 1.6). (1) Libration is oscillation between a pair of turning points on either side of the vertical. In a sense, the bob is *bound* or *trapped* around its point of stable equilibrium. (2) Intuitively, rotation ensues if the energy or initial speed of the bob is large enough. The bob then rotates around the pivot, in general at a nonuniform rate: slower at the top and faster at the bottom. The bob is not trapped near its point of stable equilibrium and the motion does not have any turning points. This is in a sense an unbound orbit: the deflection angle can become arbitrarily large in magnitude though the bob cannot escape to infinity since the length of the rod is held fixed.

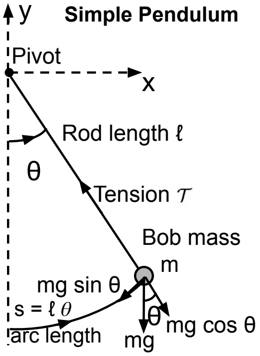

Figure 1.5: Simple pendulum suspended from a fixed support with massless rod and free to oscillate in a vertical plane.

Newton's equation of motion. The pendulum has one degree of freedom, the (counterclockwise) angle of deflection θ from its stable equilibrium position (see Fig. 1.5). The downward gravitational force $-mg\hat{y}$ is resolved into a radially outward component $mg\cos\theta$ and a tangential component $-mg\sin\theta\hat{\theta}$. Here $\hat{\theta}$ is the unit vector in the direction of increasing θ tangent to the circle of radius ℓ. The tangential component of the gravitational force tends to reduce the magnitude of the angle of deflection and causes the bob to accelerate towards its equilibrium position. Suppose $s = \ell\theta$ is the arc length corresponding to a counterclockwise deflection angle θ. Then the tangential velocity of the bob is $\dot{s}\hat{\theta} = \ell\dot{\theta}\hat{\theta}$ and its acceleration is $\ell\ddot{\theta}\hat{\theta}$ since ℓ is constant. Newton's second law in the tangential direction[30] then says that $m\ell\ddot{\theta} = -mg\sin\theta$. Thus, we arrive at the 2nd order equation of motion[31]

$$\ddot{\theta} = -(g/\ell)\ \sin\theta = -\omega^2\sin\theta \quad \text{where} \quad \omega = \sqrt{g/\ell}. \tag{1.29}$$

---

[30] Newton's second law in the radial direction is $\mathcal{T} - mg\cos\theta = m\ell\dot{\theta}^2$. The quantity on the right is the mass × the centripetal acceleration (see Prob. 2.1) while $\mathcal{T}$ is the radially inward tension in the rod. $\mathcal{T}$ must vary with angle and is greatest when $\theta = 0$ since the angular speed $\dot{\theta}$ is largest at the bottom and $mg\cos\theta$ is also maximal when $\theta = 0$. Since there is no radial motion, the radial Newton equation simply fixes $\mathcal{T}$ once the angular motion is determined.

[31] The same EOM will be reobtained in Sect. 3.5 by considering a bead constrained to move on a vertical circular hoop and in Sect. 3.16* by imposing the constraint using Lagrange multipliers.

The constant ω has dimensions of a frequency (inverse time). The mass of the bob cancelled out. So the time-dependence of θ and the motion of the pendulum are independent of m. They can depend only on ω and initial conditions.

Empirically, the motion of the pendulum is found to be periodic. Assuming this is the case, the time period of oscillation must be independent of the mass as a consequence of (1.29). This was discovered experimentally by Galileo around 1602. As discussed above, this time period can depend only on ω and the initial conditions $\theta(0)$ and $\dot\theta(0)$. Since ω has dimensions of inverse time, we may always write the time period as $T = \frac{1}{\omega} f(\theta(0), \dot\theta(0)/\omega)$ where f is a function of its dimensionless arguments. We will determine f by integrating (1.29) in Sect. 7.3*. It generally depends on the amplitude of oscillations though the ICs. In other words, unlike oscillations due to a linear restoring force studied in Sect. 1.2 (where the time period was independent of amplitude), the simple pendulum is generally not isochronous. This is because the $\sin\theta$ in (1.29) makes it a very nonlinear equation for the dependent variable θ.

Conserved energy of a simple pendulum. Despite its nonlinearity, the simple pendulum is a conservative system. It admits a conserved energy that may be obtained by multiplying Newton's equation of motion $m\ell\ddot\theta = -mg\sin\theta$ (1.29) by the integrating factor $\dot s = \ell\dot\theta$ (tangential component of velocity) to get

$$m\ell^2\ddot\theta\dot\theta = -mg\ell\sin\theta\,\dot\theta \quad \text{or} \quad \frac{d}{dt}\left(\frac{1}{2}m\ell^2\dot\theta^2 - mg\ell\cos\theta\right) = 0. \tag{1.30}$$

The RHS of the first equation is the rate at which the gravitational force does work on the bob. Choosing the integration constant as $mg\ell$, we arrive at a conserved energy

$$E = \frac{1}{2}m\ell^2\dot\theta^2 + mg\ell(1-\cos\theta). \tag{1.31}$$

The first term in E is the kinetic energy. It is simply $\frac{1}{2}mv^2 = \frac{1}{2}m\dot s^2$. The quantity $m\ell^2\ddot\theta\dot\theta$ on the LHS of (1.30) represents the rate of increase in kinetic energy of the bob. The potential energy is $V(\theta) = mg\ell(1-\cos\theta)$. Here, we have chosen $V = 0$ when the bob hangs down ($\theta = 0$). The extrema of V correspond to equilibria where the pendulum is stationary. Now $V'(\theta) = mg\ell\sin\theta = 0$ when $\theta = 0$ or π (modulo 2π), corresponding to the bob pointing vertically downwards or upwards. As Fig. 1.6 shows, the former is a local minimum of V (stable equilibrium) while the latter is a maximum (unstable equilibrium).

Small oscillations. Let us now specialize to oscillations of small amplitude ($|\theta| \ll \pi/2$) or equivalently low energy $E \gtrsim 0$. In this case, the bob always remains close to its point of stable equilibrium and we may take $\sin\theta \approx \theta$. The EOM $\ddot\theta = -\omega^2\sin\theta$ (1.29) may be approximated by the linear equation for simple harmonic motion due to a linear restoring force encountered in Sect. 1.2: $\ddot\theta = -\omega^2\theta$. The general solution is $\theta(t) = A\cos\omega t + B\sin\omega t$ with A and B dimensionless constants of integration. They are related to the initial angle and initial angular velocity by $\theta(0) = A$ and $\dot\theta(0) = B\omega$. It is physically revealing to replace A and B with two new constants of

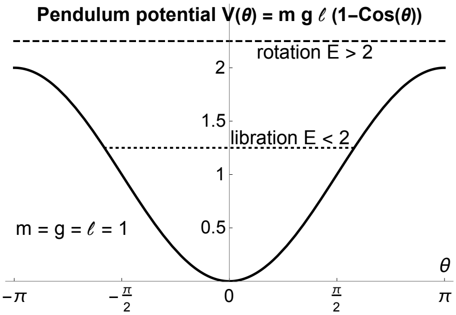

Figure 1.6: Potential $V(\theta)$ (for $m = g = \ell = 1$) showing stable equilibrium at $\theta = 0$ and unstable one at $\theta = \pm\pi$ as well as examples of librational and rotational energies.

integration $A = \theta_{\max}\sin\phi$ and $B = \theta_{\max}\cos\phi$, in terms of which the solution is

$$\theta(t) = \theta_{\max}\sin(\omega t + \phi) \quad \text{with} \quad \theta(0) = \theta_{\max}\sin\phi \quad \text{and} \quad \dot{\theta}(0) = \omega\theta_{\max}\cos\phi. \tag{1.32}$$

It is clear that the deflection angle is a sinusoidally varying function of time, with a maximum angle of deflection $\theta_{\max}$ (the 'amplitude'). Of course, for the small angle approximation to hold, $\theta_{\max}$ must be small[32] compared to $\pi/2$. The time period of these small oscillations $T = 2\pi/\omega = 2\pi\sqrt{\ell/g}$ is not just independent of the bob's mass, but also independent of the energy or amplitude $\theta_{\max}$. A pendulum executing small oscillations is isochronous, as discovered experimentally by Galileo. This is a feature that allowed pendula to be used as the most accurate clocks ('chronometers') from the mid 1600s (Christiaan Huygens, 1656) to the early 20th century. The best pendulum clocks had an accuracy of about a second per day. They were replaced by clocks based on quartz crystal oscillators and subsequently by atomic clocks based on the frequency of electromagnetic waves emitted in atomic transitions.

Pendula were also used as gravimeters, to measure the variation of the acceleration due to gravity g over the surface of the Earth. Indeed, it was found that pendula of the same length lose time (the pendulum clock 'runs slow') near the equator and gain time ('runs fast') at high latitudes, so g is smaller near the equator and grows with latitude. This is explained by the fact that the Earth bulges out near the equator and is flattened at the poles. It may be modeled as an ellipsoid of revolution called an oblate spheroid or oblate ellipsoid. The difference between the equatorial (6378km) and polar (6357km) semiaxes is about 21 km.

Large amplitude oscillations. It was also found empirically that even if the oscillations are not small, the motion is still periodic, though the time period grows with amplitude $\theta_{\max}$. This is also evident from the graph of the potential in Fig. 1.6. For $E < 2mgl$ we have oscillatory motion between two turning points $\pm\theta_{\max}$ where $E = V(\pm\theta_{\max})$. For $E > 2mgl$, there are no turning points but the bob rotates around the pivot in a periodic manner since $V(\theta)$ is 2π periodic. What is more, as argued in Sect. 1.2, we should expect the time period to diverge as $E \to 2mg\ell$ since the potential has a local maximum at the 'turning points' $\theta = \pm\pi$. However, the nonlinear EOM (1.29) cannot be solved in general using elementary functions like trigonometric functions of time: we need elliptic functions, which we shall introduce in Sect. 7.2*. In Sect. 7.3*, they will be used to find explicit expressions for $\theta(t)$ and the time period.

---

[32] How small depends on the accuracy desired.

1.6 Problems

1. **Dimensional analysis.** Find the dimensions ($M^\alpha L^\beta T^\gamma$) of (a) Newton's gravitational constant G (2.5), (b) Planck's constant h from the formula $E = h\nu$ where E and ν are the energy and frequency of a photon, (c) GM_e/c^2 where M_e is the mass of the Earth and c the speed of light and (d) the probability amplitude $\psi(x)$ for finding an electron within dx of x, given that the total probability $\int_{-\infty}^{\infty} |\psi(x)|^2 dx$ for finding the electron somewhere on the real line is one.
2. **Taylor-Sedov-von Neumann blast wave problem.** In a nuclear explosion, a spherically symmetric expanding blast wave is produced. It may be argued that to first approximation, the radius of this blast wave R can only depend on the total energy E of the explosion, the ambient mass density ρ of the gas into which the blast wave propagates and on time. Use dimensional analysis to show that $R(t)$ must be of the form $R(t) = (Et^2/A\rho)^{1/5}$ where A is a dimensionless constant. G. I. Taylor used **dimensional analysis** to estimate the energy in the Trinity nuclear test of 1945 using photographs (with time stamps and a length scale displayed) of the expanding blast wave.
3. Use a suitable '**integrating factor**' to derive a conserved energy for Newton's equation $m\ddot{x}_i = f_i$ for a particle moving in 3d subject to a potential V so that it experiences a force with Cartesian components $f_i = -\frac{\partial V}{\partial x_i}$ for $i = 1, 2, 3$.
4. **Time reversal.** Show that if $x(t)$ solves Newton's equation $m\ddot{x} = -V'(x)$, then so does $x(-t)$. What happens to the initial conditions for position and velocity?
5. **Time reversal.** Suppose a particle of mass m and charge q moves in $\mathbb{R}^3$ subject to the force $q\boldsymbol{v} \times \boldsymbol{B}(\boldsymbol{r})$ where $\boldsymbol{r}(t)$ is the position of the particle and $\boldsymbol{v}(t) = \dot{\boldsymbol{r}}$. $\boldsymbol{B}(\boldsymbol{r})$ is a *fixed* vector field called the **magnetic field**. (a) Write Newton's equation of motion for this particle. (b) Explain whether the motion of this particle is time-reversal invariant or not. (c) Physically interpret the equation that $\boldsymbol{r}(-t)$ satisfies.
6. Look for solutions to the **simple harmonic oscillator** equation of motion $\ddot{x} = -\omega^2 x$ for constant $\omega > 0$ by making the guess $x = Ne^{rt}$ where N, r are constants. Find the most general solution of this sort and show that it may be expressed as $A\cos(\omega t + \phi)$ for suitable constants A and ϕ.
7. **Harmonic oscillator solution by quadrature.** Recall from (1.7) that for motion of a particle of mass m on a line, finding solutions $x(t)$ of Newton's equation with energy E and initial position x_0 was reduced to evaluating the integral

$$t - t_0 = \pm \int_{x_0}^{x} [(2/m)(E - V(y))]^{-1/2} dy. \tag{1.33}$$

Consider the harmonic oscillator potential $V(x) = \frac{1}{2}kx^2$ for which $E \geq 0$ and let $\omega = \sqrt{k/m}$. (a) Evaluate the integral and solve for the trajectories with given

E, x_0. Show that you get

$$x(t) = \pm\sqrt{2E/k}\sin\left(\omega(t-t_0) \pm \arcsin\left(\sqrt{k/2E}\, x_0\right)\right). \qquad (1.34)$$

The upper signs correspond to one solution and the lower signs to another solution. Hint: $\int du/\sqrt{1-u^2} = \arcsin u$. (b) Specialize to the case where the particle starts from the equilibrium position at $t_0 = 0$ and simplify the formula for $x(t)$. Also find the momentum $p(t)$. (c) Show that $x(t)$ satisfies the 'initial conditions' $x(0) = 0$ and $\frac{1}{2}(m\dot{x}^2 + kx^2) = E$. (d) For $E > 0$, indicate pictorially (on the space of locations x) how the two solutions obtained above differ.

8. Consider the integral $\int_0^1 dx/x^a$. Show that the integrand $1/x^a$ has an **integrable divergence** (integrand diverges but integral is finite) at $x = 0$ for $0 < a < 1$ and a nonintegrable divergence for $a \geq 1$. What is the integral when it is finite?
9. Suppose $V'(x_*) = 0$ but $V''(x_*) < 0$ at a turning point x_* for 1d motion with energy $E = V(x_*)$ (x_* is a local maximum of the potential). Show using a Taylor approximation that the **time to reach the turning point** from sufficiently nearby is logarithmically divergent in the distance from the turning point.
10. Find the time period T of oscillations of energy E in the **harmonic oscillator** potential $\frac{1}{2}m\omega^2x^2$. Show that it is **isochronous** (i.e., T is independent of energy).
11. Find an integral expression for the time period $T(E)$ of energy-E oscillations in the **anharmonic oscillator** potential $V = \frac{1}{2}kx^2 + gx^4$ for $k, g > 0$.
12. Calculate the **force** corresponding to the $V(x) = V_o \operatorname{sech}^2(x/l)$ for a fixed length $l > 0$. Show that for $V_o > 0$, it **repels particles** coming in from $\pm\infty$. Plot $V(x)$.
13. **A** sech^2 **potential.** Consider a particle in the 1d potential $V(x) = -V_o \operatorname{sech}^2(x/l)$ where $V_o > 0$ and $l > 0$ is a length scale.

    a. Roughly plot the potential, label the axes, mark l and V_o. Indicate an energy for which there is oscillatory motion.
    b. For $0 > E \geq -V_o$, find the turning points $\pm x_0$ ($x_0 \geq 0$) of the motion.
    c. Show that the period of oscillations in this potential is given by

    $$T(E) = 2\sqrt{2m/V_o}\int_0^{x_0}(1 - f\cosh^2(x/l))^{-1/2}\cosh(x/l)\,dx \qquad (1.35)$$

    where f is the energy fraction $f = |E|/V_o$, satisfying $0 < f \leq 1$.
    d. Obtain a very simple formula for $T(E)$. Hint: Change variables to $y = f\cosh^2(x/l)$. It also helps to use (see Prob. 1.14)

    $$\pi = \int_V^W \frac{dE}{\sqrt{(E-V)(W-E)}} = \int_f^1 \frac{dy}{\sqrt{(1-y)(y-f)}}. \qquad (1.36)$$

    e. How does the time period $T(E)$ depend on the depth of the potential V_o? Qualitatively indicate why the behavior of $T(E)$ as $E \to 0^-$ is physically expected.

14. **Definite integral.** For $W > V > 0$, evaluate the integral

$$\Pi = \int_V^W dE/\sqrt{(E-V)(W-E)}. \tag{1.37}$$

Hint: Complete the square in the denominator or put $x = \sqrt{(E-V)/(W-E)}$.

$*$15. **Isochronous potentials.** Recall that for a particle of mass m moving on the real line subject to a linear restoring force $-m\omega^2 x$ (harmonic oscillator potential $V(x) = (1/2)m\omega^2 x^2$), the oscillation time period ($T(E) = 2\pi/\omega$ for $E \geq 0$) is independent of energy. Try to find a 1-parameter family of potentials $V_a(x)$ that share the same time period function $T(E)$. We suppose that these potentials are convex, go to ∞ as $|x| \to \infty$ and have a single minimum $V = 0$ at $x = 0$. With the exception of the harmonic oscillator, these potentials cannot be even.

16. **Time delay.** We consider the EM action shift at energy $E > 0$ for the attractive potential $-V_o \operatorname{sech}^2(x/l)$ of Prob. 1.13. (a) Show that

$$\Delta\mathscr{S} = 2l\sqrt{2mE}\int_0^\infty \left(\sqrt{1 + (V_o/E)\operatorname{sech}^2 y} - 1\right) dy \equiv 2l\sqrt{2mE}\,\mathcal{I}, \tag{1.38}$$

where $y = x/l$. (b) The integral $\mathcal{I}$ is a function of the dimensionless ratio E/V_o. It can be evaluated in closed form. Show that

$$\Delta\mathscr{S} = 2l\sqrt{2mE}\left[\sqrt{V_o/E}\arctan(\sqrt{V_o/E}) - (1/2)\log(1 + V_o/E)\right]. \tag{1.39}$$

Hint: Differentiate $\mathcal{I}$ with respect to the dimensionless variable $v = V_0/E$ and make the substitution $z = \sqrt{1 + v\operatorname{sech}^2 y}$. Show that $\mathcal{I}'(v) = (\arctan\sqrt{v})/2\sqrt{v}$. Then integrate with respect to v and determine the constant of integration. (c) Use this to derive a simple formula for the time delay $\Delta T(E)$ for the scattering of a particle of energy E against this potential. (d) Does the particle arrive earlier or later than a free particle? (e) What is the asymptotic behavior of the time delay as $E \to 0^+$ and $E \to \infty$. Physically interpret these limiting behaviors and comment on why they are reasonable. (f) Show that the time delay can also be expressed as

$$\Delta T = \sqrt{2ml^2/E}\int_0^\infty [(1 + v\operatorname{sech}^2 y)^{-1/2} - 1]dy. \tag{1.40}$$

Evaluate this integral and compare with ΔT calculated using the shift in the Euler-Maupertuis action.

$*$17. **Potential scattering in quantum mechanics.** Identify a quantum mechanical quantity that one encounters in the scattering of a particle against a potential, which is defined in a manner similar to the classical time delay. Hint: Consider the expression for the scattering amplitude in the partial wave expansion [114].

18. **Linearization of pendulum equation.** Linearize the equation of motion $\ddot{\theta} = -\omega^2 \sin\theta$ for a simple pendulum around $\theta = \pi$. Here $\omega = \sqrt{g/\ell}$. (a) Find the linear equation satisfied by $\phi = \theta - \pi$. (b) Use a suitable guess to find two

linearly independent solutions of the equation for ϕ and the general solution of the equation for given $\phi(0)$ and $\dot{\phi}(0)$. (c) Physically interpret the consequences of the solution of the linear differential equation for ϕ for typical (nonexceptional) initial conditions and comment on what it means for the stability of the static solution $\theta = \pi$. (d) Comment on any exceptional ICs and the resulting time evolution.

$*$19. **Simple pendulum: angular momentum and torque.** Consider a simple pendulum with bob of mass m and rod of length l subject to Earth's acceleration due to gravity with magnitude g. Denote the counterclockwise deflection angle θ and use the coordinate frame of Fig. 1.5 (a) Find an expression (in terms of θ) for the torque $\boldsymbol{\tau} = \boldsymbol{r} \times \boldsymbol{F}$ on the bob about the pivot. Which forces do/do not contribute to $\boldsymbol{\tau}$? (b) Write an expression (in terms of θ) for the angular momentum $\boldsymbol{L} = \boldsymbol{r} \times \boldsymbol{p}$ of the bob about the pivot. (c) Use the evolution equation $\dot{\boldsymbol{L}} = \boldsymbol{\tau}$ to derive a differential equation for $\theta(t)$. How does it compare with the EOM for θ derived from Newton's second law? (d) Propose a limit holding m, l, g fixed in which the angular momentum is asymptotically conserved. Specify the limit through a suitable comparison of physical quantities. Comment on the nature of motion in this limit.

$*$20. **Triangular system of equations.** Explain a sense in which the radial and tangential equations of motion for a simple pendulum can be considered as a triangular system for the deflection angle θ and tension $\mathcal{T}$. Explain by a suitable comparison with an upper triangular matrix.

Chapter 2

Kepler's gravitational two-body problem

In this chapter, we move to motion in more than one dimension by considering the problem of two gravitating point masses: the so-called Kepler problem of celestial mechanics. This problem historically arose in the context of planetary orbits around the Sun. It may be regarded as a first step towards understanding the dynamics of the solar system[1]. Observations from antiquity, suitably interpreted, indicated that planets move in a periodic manner around the Sun and that the orbits hardly change for hundreds of years (a time long compared to the orbital periods). This suggested that dissipative effects[2] must be negligibly small and that the motion of a planet around the Sun may be describable via a conservative force between masses that is derivable from a potential. Kepler's empirical laws of planetary motion around the Sun made precise and quantitative the observed regularities in planetary motion. We begin with Kepler's laws and sketch how they led to Newton's inverse square law for the gravitational force, using Newton's second law. We will in effect be solving an *inverse* problem[3], as in Sect. 1.3*. We will then address the *direct* problem of two gravitating point masses, based on Newton's laws of motion and gravity. We will use the conservation of momentum to reduce the two-body problem to an effective one-body problem and then use the conservation of energy and angular momentum to determine the elliptical shapes of planetary orbits and their time periods of revolution. We then discuss a novel conserved quantity, the eccentricity or Laplace-Runge-Lenz vector, whose existence is related to the fact that all noncollisional bound orbits are periodic. It is somewhat special to two bodies interacting via a force that falls off as the square of the distance of separation. An elegant picture emerges of how all the conserved quantities fit together and determine the orbits. As a bonus, we will use this to describe Pauli's approach to finding the quantum energy spectrum of hydrogen. Having dealt with elliptical orbits in Sect. 2.1 - Sect. 2.5*, the next two sections deal with the two other possibilities: straight-line trajectories and head-on collisions in Sect. 2.6* and hyperbolic orbits in Sect. 2.7*. The latter will be applied to derive the celebrated Rutherford cross section for Coulomb scattering. Finally, in Sect. 2.8* we introduce the gravitational 3-body problem and sketch how 2-body Keplerian orbits can be used to construct certain special solutions of the 3-body problem: those of Euler and Lagrange.

---

[1] For the purpose of determining the orbit of the Earth around the Sun (or the Sun around the Earth), it is a reasonable first approximation to ignore the gravitational effects of all the other planets since the Sun is so much heavier. To improve on this, one would have to include the effect of, say, Jupiter on the Sun-Earth system, turning the 2-body problem into a 3-body problem. By contrast, to determine the motion of the Sun about the center of mass of the solar system (as opposed to relative to the Earth), one cannot simply consider the effect of the Earth but would have to first consider the effects of the heavier planets such as Jupiter and Saturn. Fortunately, since the Sun is so massive (a 1000 times more massive than Jupiter), it hardly moves relative to the CM of the solar system and can essentially be taken to be at rest relative to the CM.

[2] There are of course dissipative processes in the solar system, such as the passage of meteors through the Earth's atmosphere or the collision of comet Shoemaker-Levy 9 with Jupiter.

[3] In solving the inverse problem, we will only apply Kepler's laws to circular orbits to deduce the inverse square gravitational force law as the simplest possibility. It will remain to check whether this law also leads to elliptical planetary orbits as well as other phenomena observed in celestial mechanics. For this, we will need to study the direct problem.

2.1 Inverse problem: universal law of gravity from Kepler's laws

Based on the Danish astronomer Tycho Brahe's naked eye observations of planetary positions (accurate to better than 0.01°), the German mathematical astronomer Johannes Kepler formulated (1609-1619) three laws of planetary motion around the Sun [35]:

1. Planetary orbits are ellipses with the Sun at a focus. In particular, each orbit lies on a plane, the ecliptic plane[4] of the planet.
2. The radius vector connecting the Sun to a planet sweeps out equal areas in equal times.
3. The square of the period of revolution is proportional to the cube of the semimajor axis, with a proportionality constant that is approximately the same for all planets

$$R^3 = KT^2 \quad \text{where} \quad K \approx 365^{-2} \approx 7.5 \times 10^{-6}\ (\text{AU})^3/(\text{day})^2 \approx 3.4 \times 10^{18}\ \text{m}^3/\text{s}^2 \tag{2.1}$$

   is 'Kepler's constant'. An astronomical unit AU is roughly the mean Sun-Earth distance, approximately 150 million kilometers.

In this section, we will address the inverse problem of deducing Newton's universal inverse-square force law of gravitation from Kepler's laws and Newton's second law $\boldsymbol{F} = m\boldsymbol{a}$. This is somewhat similar to the inverse problem (of Sect. 1.3*) of determining a 1d potential $V(x)$ from a knowledge of the time period $T(E)$ of oscillations it supports. Loosely, Kepler's third law for the planetary period as a function of semimajor axis is like knowing $T(E)$. However, as we have seen in Sect. 1.3*, the potential $V(x)$ may not be unique. Moreover, the general problem of deducing a 3d potential $V(\boldsymbol{r})$ for the force between Sun and planet is harder than in 1d. We will nevertheless find a solution to this problem by considering special cases (circular orbits), making some physically justified simplifying assumptions (that the force is central, just as we assumed the potential in Sect. 1.3* was even) and using some general features of Newtonian mechanics (angular momentum conservation in a central potential).

To begin with, we set up a coordinate frame. In view of Kepler's first law, the planet's orbit lies on a plane (the ecliptic plane), which we take to be the x-y plane.

---

[4] The ecliptic plane gets its name from the possibility of eclipses when the Moon crosses the ecliptic plane of the Earth.

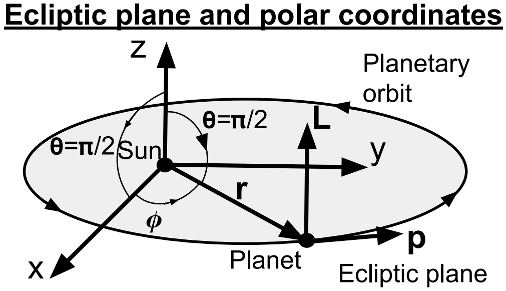

Figure 2.1: Spherical polar coordinates with the Sun at the origin and the planet moving on the x-y ecliptic plane.

We will find it useful to define the z axis so that xyz becomes a right-handed system. The z-direction will be helpful to discuss angular momentum. We use spherical polar coordinates (r, θ, ϕ) for the planet's location $\boldsymbol{r} = (x, y, z)$ with the Sun at the origin (see Fig. 2.1):

$$z = r\cos\theta, \quad x = r\sin\theta\cos\phi \quad \text{and} \quad y = r\sin\theta\sin\phi. \tag{2.2}$$

Both bodies are treated as point particles as they are small compared to the observed sizes of orbits[5]. Since the planet moves on the x-y plane, $z = 0$ and $\theta \equiv \pi/2$ and both the position and momentum vectors $\boldsymbol{r}, \boldsymbol{p}$ of the planet lie in the x-y plane. It follows that the angular momentum about the origin $\boldsymbol{L} = \boldsymbol{r} \times \boldsymbol{p}$ must point in the $\hat{z}$ or $-\hat{z}$ direction. Since planets are observed to go around the Sun without switching direction, the direction of angular momentum cannot change, it must point along $\hat{z}$ or $-\hat{z}$ at all times. In spherical polar coordinates, the z-component of angular momentum[6] can be expressed as $l_z = xp_y - yp_x = mr^2\sin^2\theta\,\dot{\phi}$ with $\theta = \pi/2$ (see Prob. 2.2). Now, Kepler's second law may be used to deduce that the magnitude of angular momentum is constant in time. Indeed, as shown in Fig. 2.2, the infinitesimal area $(d\mathrm{Ar})$ swept out[7] by the line joining the Sun to the planet in a small time dt while the planet's angular position changes $d\phi$ is $d\mathrm{Ar} \approx \frac{1}{2}r\; rd\phi$. Dividing by dt and taking the limit, the constancy of the areal speed

$$\frac{d\mathrm{Ar}}{dt} = \frac{1}{2}r^2\dot{\phi} = \frac{l_z}{2m} \tag{2.3}$$

implies l_z and hence angular momentum $\boldsymbol{L}$ is conserved. It is an independent mathematical fact of Newtonian dynamics (following from Newton's second law) that angular momentum is conserved in a central force field[8] (see Eq. 2.16). This suggests that

---

[5] The Sun's radius is 7×10^8m while the mean Sun-Earth distance is 1.5×10^{11}m.

[6] In this chapter, we denote the magnitude of angular momentum by l, $\sqrt{\boldsymbol{L}\cdot\boldsymbol{L}} = l$ and its z-component by $\boldsymbol{L}\cdot\hat{z} = l_z$.

[7] We ignore here the small change in area that results from a change in r, for this area, given approximately by the shaded triangle in Fig. 2.2 is 2nd order in infinitesimals, $\propto d\phi\; dr$. When this is divided by dt and we let $dr, d\phi, dt \to 0$, this term vanishes, unlike the leading term given in (2.3).

[8] A force field $\boldsymbol{F}(\boldsymbol{r})$ where $\boldsymbol{r}$ is the radius vector from the Sun to the planet is called central if

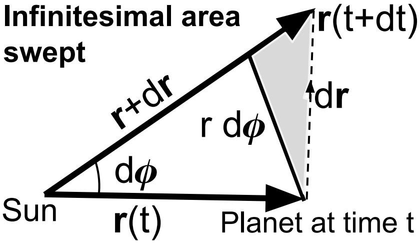

Figure 2.2: Infinitesimal area swept out by a planet. Roughly, we ignore the shaded region whose area is second order in the infinitesimals $d\phi$ and dr.

the gravitational force is central $\boldsymbol{F} = -f(r)\hat{r}$ (with the negative sign for attraction). The inverse-square nature of the force is guessed from Kepler's third law $T^2 = r^3/K$. To see this, we first note that the eccentricity (defined in Sect. 2.3) of several planetary orbits is fairly small ($\epsilon = .02$ for the Earth) and they approximately describe (by virtue of the constancy of areal speed) uniform circular motion around the Sun. Kepler's 3rd law certainly applies to these planets, so let us see what it implies.

Consider a planet such as the Earth moving uniformly around a circle of radius r at constant angular speed ω. It takes a time $T = 2\pi/\omega$ to go round once. Its linear speed is $v = 2\pi r/T = r\omega$. To find its acceleration we write its position vector in the x-y plane as $\boldsymbol{r} = (r\cos\omega t, r\sin\omega t)$, from which we find its velocity $\boldsymbol{v} = \dot{\boldsymbol{r}} = \omega r(-\sin\omega t, \cos\omega t)$. Its acceleration is $\boldsymbol{a} = \ddot{\boldsymbol{r}} = -\omega^2 r(\cos\omega t, \sin\omega t)$. We see that $\boldsymbol{a} = -\omega^2\boldsymbol{r} = -(v^2/r)\hat{r}$: the acceleration is directed radially inwards, and therefore called centripetal[9]. Newton's 2nd law requires the (radially inward) centripetal acceleration to equal the inward gravitational force per unit mass of the Earth. This gives

$$-m_e\frac{v^2}{r}\hat{r} = -f(r)\hat{r} \quad \text{with} \quad v^2 = \frac{(2\pi r)^2}{T^2} = \frac{K(2\pi r)^2}{r^3} \quad \Rightarrow \quad f(r) = \frac{4\pi^2 K m_e}{r^2}. \tag{2.4}$$

Besides its inverse-square nature, the above gravitational force on the Earth due to the Sun is proportional to the Earth's mass m_e (since K is approximately the same for all planets) so that the Earth's acceleration is *independent* of its mass[10]. Newton postulated that this must be true also of the force felt by the Sun due to the Earth (his

---

it is invariant under rotations (and reflections) of $\boldsymbol{r}$. Such a field is called spherically symmetric. It points radially everywhere and has a magnitude that depends only on the radial distance r. It is evident that the torque about the origin $\boldsymbol{\tau} = \boldsymbol{r} \times \boldsymbol{F} = 0$ for a central force. This implies that the angular momentum $\boldsymbol{L} = \boldsymbol{r} \times \boldsymbol{p}$ is conserved, since Newton's second law $\dot{\boldsymbol{p}} = \boldsymbol{F}$ implies that $\dot{\boldsymbol{L}} = \boldsymbol{\tau}$. It is a tribute to the richness of Newtonian mechanics that a central force can support, with suitable initial conditions, orbits that are not circular.

[9] Centripetal is Latin for towards or seeking the center. In Sect. 9.2, we will learn of the *centrifugal* force, which arises when such motion is observed from a frame that rotates with the planet. This force points radially outward and is also felt by a person on a merry-go-round.

[10] Here, m_e is called the *inertial mass* of the Earth, as it came from the inertia term in Newton's 2nd law. So m_s would have to be the inertial mass of the Sun. Readers who may have heard of gravitational masses and the equivalence principle (see Sect. 3.3) may wonder how gravitational masses that could be distinct from inertial masses may enter Newton's law

3^{rd} law, see Sect. 3.3) and concluded that $K \propto m_s$. Thus, we guess the universal (both terrestrial and celestial) law of gravitation

$$\boldsymbol{F} = -\frac{G m_s m_e}{r^2}\hat{r} \quad \text{where} \quad G = \frac{4\pi^2 K}{m_s} \approx 6.67 \times 10^{-11}\ \mathrm{Nm}^2/\mathrm{kg}^2. \tag{2.5}$$

We will often use the abbreviation $\alpha = G m_e m_s$. Note that $m_e \approx 6 \times 10^{24}$ kg and $m_s \approx 2 \times 10^{30}$ kg. Kepler's first law on elliptical orbits may now be derived as a consequence of Newton's second law and the universal law of gravitation. An important feature of the gravitational force is that it is derivable[11] from the gravitational potential $V(r) = -\alpha/r$ (see Prob. 2.7):

$$\boldsymbol{F} = -\frac{\alpha}{r^2}\hat{r} = -\boldsymbol{\nabla}_{\boldsymbol{r}}\left(-\frac{\alpha}{r}\right) = -\boldsymbol{\nabla}_{\boldsymbol{r}} V(r). \tag{2.6}$$

Here $\boldsymbol{\nabla}_{\boldsymbol{r}}$ is the vector gradient (see Appendix A.8 and [49] for an introduction to vector calculus). If $\boldsymbol{r} = (x, y, z)$ are the Cartesian components of the position vector, then $\boldsymbol{\nabla}_{\boldsymbol{r}} = (\frac{\partial}{\partial x}, \frac{\partial}{\partial y}, \frac{\partial}{\partial z})$. The gravitational force is called central since it points radially and has a magnitude that depends only on the radial distance. The corresponding potential $V(r)$ depends only on the distance from the origin and is called a central or spherically symmetric potential. In obtaining the $1/r$ potential from Kepler's laws, we have in effect solved an *inverse problem*, i.e., of deducing a potential from features of trajectories. More specifically, we deduced a potential from the period of oscillations that it supports (see Sect. 1.3* for the 1d version). To solve such a problem in general is very difficult, and Isaac Newton and his contemporaries like Edmond Halley and Robert Hooke are lucky to have succeeded in this case of central importance. In the next section, we address the *direct problem* of finding the orbits given the Newtonian gravitational potential. The approach we will follow combines methods from differential equations and some geometry. Newton's approach in his Principia (1687) [98] was much more geometric, partly because that was the language familiar to his contemporaries. The use of differential equations became more prevalent with the work of Johann and Daniel Bernoulli and Leonhard Euler in the 1700s.

The lunar perigee problem. It took time for Newton's inverse-square law of gravitational force to be tested and widely accepted. Newton (1643-1727) showed that it did give the observed elliptical orbits of some planets and comets. However, a difficulty

---

of gravity. This apparent lack of room for gravitational masses is because we took Kepler's constant K to be independent of the planet. This is analogous to Galileo's assertion that all bodies fall the same way when dropped from the same height above the Earth's surface. In fact, K is not quite the same for all planets. To incorporate this dependence on the planet, we could write $K m_e = k m_e^g$ where k is independent of the planet and m_e^g is a property of the planet which we choose to call its gravitational mass. Then, by Newton's third law we would write $k = k' m_s^g$ where m_s^g is the gravitational mass of the Sun and k' is a constant independent of both bodies. Finally, denoting $4\pi^2 k'$ by the symbol G, we get Newton's law for the gravitational force of the Sun on the Earth, with magnitude $G m_s^g m_e^g / r^2$. As it turns out, the dependence of K on planet is not due to a difference between gravitational and inertial masses and can be explained by other effects that we have ignored (e.g., see Sect. 2.4).

[11] Any central force field is conservative, expressible as the (negative) gradient of a potential.

arose in applying it to lunar motion. The Moon's approximately elliptical orbit around the Earth was observed to precess. The lunar perigee (closest approach to the Earth) rotates by 40° of arc per annum (see Fig. 2.6a). This was believed to be due to the Sun's effect on the Earth-Moon system. This leads to the famous three-body problem of celestial mechanics (see Sect. 2.8* and [72] for an introduction). Newton tried to estimate the motion of the lunar perigee (using his laws of motion and gravity) due to the Sun's effect. However, his approximate calculations suggested that the lunar perigee could rotate by only about 20° per annum. It was unclear whether the discrepancy was due to the approximations he made or due to deficiencies in the laws. In fact, Euler had doubts on the veracity of Newton's $1/r^2$ force law and Alexis Clairaut even proposed a small $1/r^3$ correction to it. A lively competition ensued among Euler, Clairaut and d'Alembert [13] to develop a theory of solar perturbations to the Moon's orbit. Eventually, Clairaut (1759) was able to use the purely inverse-square force law to account for 85% of the motion of the lunar perigee using a third order perturbative treatment of the Sun's effect. This indicated that more accurate treatments of the Earth-Moon-Sun problem had the potential to bring the predictions of Newtonian mechanics closer to observations. Subsequent work (such as that of Pierre-Simon Laplace) on a variety of solar system trajectories led to widespread acceptance of Newton's laws of motion and gravity. In fact, by the time of Simon Newcomb's work on orbital data in the late 1800s, calculations based on Newtonian mechanics could account for practically all solar system trajectories within errors. There was, however, one mismatch: Newtonian mechanics could not account for 42 of the 566 seconds of arc in the centennial precession of Mercury's perihelion. This discrepancy was eventually explained by Einstein's general relativity. □

2.2 Direct problem: center of mass and relative vectors and conservation laws

We now turn to the direct problem: we wish to solve Newton's equations of motion for a pair of point masses, say $m_1 = m_s$ and $m_2 = m_e$, that interact via the inverse-square gravitational force to find the trajectories[12] of the Sun and Earth. Let $\boldsymbol{r}_1(t)$ and $\boldsymbol{r}_2(t)$ denote the position vectors of the Sun and Earth relative to the origin of an inertial frame. The Sun-Earth system has 6 degrees of freedom, say, the Cartesian components of $\boldsymbol{r}_1$ and $\boldsymbol{r}_2$. If we put $\alpha = G m_1 m_2$, then Newton's equations are

$$m_1 \ddot{\boldsymbol{r}}_1 = \frac{\alpha}{|\boldsymbol{r}_2 - \boldsymbol{r}_1|^3}(\boldsymbol{r}_2 - \boldsymbol{r}_1) \quad \text{and} \quad m_2 \ddot{\boldsymbol{r}}_2 = -\frac{\alpha}{|\boldsymbol{r}_2 - \boldsymbol{r}_1|^3}(\boldsymbol{r}_2 - \boldsymbol{r}_1). \tag{2.7}$$

This is a system of six 2^{nd} order nonlinear ordinary differential equations (ODEs). We wish to solve these equations given the initial values $\boldsymbol{r}_1(0), \boldsymbol{r}_2(0), \dot{\boldsymbol{r}}_1(0)$ and $\dot{\boldsymbol{r}}_2(0)$. To complicate matters, the evolution of $\boldsymbol{r}_1$ and $\boldsymbol{r}_2$ are coupled since the RHS of (2.7) involves $\boldsymbol{r} = \boldsymbol{r}_2 - \boldsymbol{r}_1$: the Sun affects the motion of the Earth and vice versa. It would be helpful to find new variables in terms of which the dynamics decouples. It is clear from (2.7) that the relative vector $\boldsymbol{r} = \boldsymbol{r}_2 - \boldsymbol{r}_1$ that points from the Sun to the Earth (see Fig. 2.3) is a natural variable in which to express the gravitational forces. In fact, if we introduce the potential $V(r) = -\alpha/r$, then from (2.6), the EOM become

---

[12] A trajectory may be viewed as having two pieces of information. First, there is the shape of the planetary orbit around the Sun and second there is the manner in which the planet traverses this orbit: moving slower in some places and faster in others. Kepler's 3rd law provides information on the latter. An equation for the shape of the orbit without regard to the rate of motion is called an orbit equation (e.g., (2.26)) to distinguish it from the more complete equation of motion for the position as a function of time.

$$m_1 \ddot{\boldsymbol{r}}_1 = \frac{\alpha}{r^2}\hat{r} = \boldsymbol{\nabla}_{\boldsymbol{r}} V(r) \quad \text{and} \quad m_2 \ddot{\boldsymbol{r}}_2 = -\frac{\alpha}{r^2}\hat{r} = -\boldsymbol{\nabla}_{\boldsymbol{r}} V(r). \tag{2.8}$$

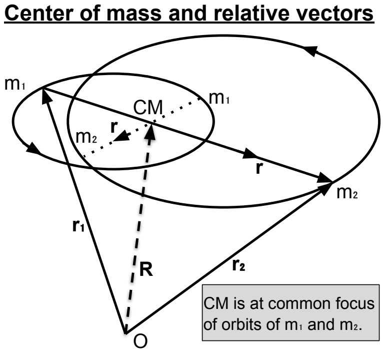
Center of mass and relative vectors
m₁
CM
m₁
m₂
r
r
m₂
r₁
R
r₂
CM is at common focus of orbits of m₁ and m₂.
O

Figure 2.3: Center of mass (CM) and relative vectors $\boldsymbol{R}$ and $\boldsymbol{r}$ as well as position vectors $\boldsymbol{r}_1$ and $\boldsymbol{r}_2$ of the two masses. For $E < 0$, the ellipses traversed by m_1 and m_2 are indicated, they have a common focus at the CM, which is assumed to be at rest. The ellipse traversed by $\boldsymbol{r}$ is not indicated since in this figure $\boldsymbol{r}$ emanates from the moving location of m_1. To draw the corresponding ellipse, we could parallel translate $\boldsymbol{r}$ to emanate from the CM and trace its tip.

What is more, if we add the two equations, the forces cancel and we find that $m_1\ddot{\boldsymbol{r}}_1 + m_2\ddot{\boldsymbol{r}}_2 = 0$. In other words, if we introduce the center of mass vector $\boldsymbol{R} = (m_1\boldsymbol{r}_1 + m_2\boldsymbol{r}_2)/M$ where $M = m_1 + m_2$ is the total mass, then $M\ddot{\boldsymbol{R}} = 0$. Thus, the center of mass (CM) of the system may be viewed as moving like a free particle of mass M along a straight line: $\boldsymbol{R}(t) = \boldsymbol{R}(0) + \dot{\boldsymbol{R}}(0)t$. Its dynamics has decoupled from the relative motion of m_1 and m_2. Henceforth, wherever convenient, we will choose the origin of the inertial frame to lie at the CM so that the CM is stationary.

On the other hand, subtracting the first from the second in (2.8) gives us an evolution equation for the relative vector $\boldsymbol{r}$:

$$\ddot{\boldsymbol{r}} = \ddot{\boldsymbol{r}}_2 - \ddot{\boldsymbol{r}}_1 = -\left(\frac{1}{m_1} + \frac{1}{m_2}\right)\boldsymbol{\nabla} V \quad \Rightarrow \quad m\ddot{\boldsymbol{r}} \equiv \dot{\boldsymbol{p}} = -\boldsymbol{\nabla} V. \tag{2.9}$$

We abbreviated $\boldsymbol{\nabla}_{\boldsymbol{r}} = \boldsymbol{\nabla}$ and defined the relative momentum $\boldsymbol{p} = m\dot{\boldsymbol{r}}$ where $m = m_1 m_2/(m_1 + m_2)$ is called the reduced mass[13]. Thus, the relative vector $\boldsymbol{r}$ evolves independently of the CM vector $\boldsymbol{R}$. So by switching from $\boldsymbol{r}_1, \boldsymbol{r}_2$ to $\boldsymbol{R}, \boldsymbol{r}$, via the transformation (see also Prob. 2.8)

---

[13] There is no particle with mass m. But if $m_1 \gg m_2$, as is the case for the Sun and a planet, then the total mass $M = m_1 + m_2 \approx m_1$ is approximately that of the Sun and the reduced mass that of the planet $m \approx m_2$. We will soon see that there is a fictitious particle with mass m whose motion decouples from that of the center of mass.

$$\boldsymbol{R} = \frac{m_1\boldsymbol{r}_1 + m_2\boldsymbol{r}_2}{M} \quad \text{and} \quad \boldsymbol{r} = \boldsymbol{r}_2 - \boldsymbol{r}_1 \quad \text{with} \quad \boldsymbol{r}_{1,2} = \boldsymbol{R} \mp \frac{m_{2,1}}{M}\boldsymbol{r}, \tag{2.10}$$

we have decoupled the equations of motion. We may view the dynamics of $\boldsymbol{r}$ as a self-contained mechanical system with just three degrees of freedom. The latter system is a one-body problem concerning the motion of a fictitious particle[14] of mass m located at $\boldsymbol{r}$ and subject to the central force $-\boldsymbol{\nabla}_{\boldsymbol{r}} V(r)$.

Our aim is to solve the EOM for $\boldsymbol{r}$ and then work our way back using (2.10) to find out how $\boldsymbol{r}_1$ and $\boldsymbol{r}_2$ vary with time. However, (2.9) remains a nonlinear coupled system of equations for the three Cartesian components of $\boldsymbol{r} = (x, y, z)$. To find the corresponding trajectories (see Sect. 2.3), we will exploit certain conservation laws.

Momentum. The simplest one to consider is that of momentum. Since $\dot{\boldsymbol{p}} = -\boldsymbol{\nabla} V \neq 0$, the relative momentum is *not* conserved[15]. However, the total momentum $\boldsymbol{P} = \boldsymbol{p}_1 + \boldsymbol{p}_2 = m_1\dot{\boldsymbol{r}}_1 + m_2\dot{\boldsymbol{r}}_2 = M\dot{\boldsymbol{R}}$ *is* conserved, indeed

$$\dot{\boldsymbol{P}} = \dot{\boldsymbol{p}}_1 + \dot{\boldsymbol{p}}_2 = \boldsymbol{\nabla} V - \boldsymbol{\nabla} V = 0. \tag{2.11}$$

Energy. To obtain a conserved energy, we dot the first equation in (2.8) by the integrating factor $\dot{\boldsymbol{r}}_1$ and the second by $\dot{\boldsymbol{r}}_2$ to get (compare with (1.2))

$$m_1\ddot{\boldsymbol{r}}_1 \cdot \dot{\boldsymbol{r}}_1 = \dot{\boldsymbol{r}}_1 \cdot \boldsymbol{\nabla}_{\boldsymbol{r}} V(r) \quad \text{and} \quad m_2\ddot{\boldsymbol{r}}_2 \cdot \dot{\boldsymbol{r}}_2 = -\dot{\boldsymbol{r}}_2 \cdot \boldsymbol{\nabla}_{\boldsymbol{r}} V(r). \tag{2.12}$$

Adding these two equations, we get

$$\frac{d}{dt}\left(\frac{1}{2}m_1\dot{\boldsymbol{r}}_1^2 + \frac{1}{2}m_2\dot{\boldsymbol{r}}_2^2\right) = -\dot{\boldsymbol{r}} \cdot \boldsymbol{\nabla}_{\boldsymbol{r}} V(r) = -\frac{dV(r)}{dt}. \tag{2.13}$$

Hence, energy is conserved:

$$E_{\text{tot}} = \frac{1}{2}m_1\dot{\boldsymbol{r}}_1^2 + \frac{1}{2}m_2\dot{\boldsymbol{r}}_2^2 + V(r) \quad \text{where} \quad V(r) = -\frac{\alpha}{r}. \tag{2.14}$$

It is revealing to write this in terms of the center of mass and relative coordinates. One finds (see Prob. 2.10)

$$E_{\text{tot}} = E_{\text{cm}} + E \quad \text{where} \quad E_{\text{cm}} = \frac{1}{2}M\dot{\boldsymbol{R}}^2 \quad \text{and} \quad E = \frac{1}{2}m\dot{\boldsymbol{r}}^2 + V(r). \tag{2.15}$$

Since $\dot{\boldsymbol{R}}(t) = \dot{\boldsymbol{R}}(0)$, E_{cm} is separately conserved. It follows that the energy E of relative motion is also conserved.

---

[14] For the Sun-Earth system, since $m_1 \gg m_2$, the Sun is located nearly at the CM (which is taken to be the origin) and $\boldsymbol{r}$ is nearly the position vector of the Earth, whose mass m_2 almost coincides with the reduced mass m.

[15] We will learn from Noether's theorem in Sect. 3.10 that this is related to the lack of translation invariance with respect to the relative coordinate. When we focus exclusively on relative motion, the center of mass is fixed at the origin and this breaks translation invariance.

Angular momentum. Using (2.9), one checks that the relative angular momentum $\boldsymbol{L} = \boldsymbol{r} \times \boldsymbol{p}$ is conserved, since the force is central ($\boldsymbol{\nabla}_{\boldsymbol{r}} V(r) = V'(r)\,\hat{r}$)

$$\dot{\boldsymbol{L}} = \dot{\boldsymbol{r}} \times \boldsymbol{p} + \boldsymbol{r} \times \dot{\boldsymbol{p}} = \frac{1}{m}\boldsymbol{p} \times \boldsymbol{p} - \boldsymbol{r} \times \boldsymbol{\nabla}_{\boldsymbol{r}} V(r) = 0. \tag{2.16}$$

The total angular momentum $\boldsymbol{L}_{\rm tot} = \boldsymbol{r}_1 \times \boldsymbol{p}_1 + \boldsymbol{r}_2 \times \boldsymbol{p}_2$ is of course also conserved

$$\dot{\boldsymbol{L}}_{\rm tot} = \boldsymbol{r}_1 \times \dot{\boldsymbol{p}}_1 + \boldsymbol{r}_2 \times \dot{\boldsymbol{p}}_2 = -(\boldsymbol{r}_2 - \boldsymbol{r}_1) \times \boldsymbol{\nabla} V(r) = -\boldsymbol{r} \times \boldsymbol{\nabla} V(r) = 0, \tag{2.17}$$

where we used $\dot{\boldsymbol{r}}_1 \times \boldsymbol{p}_1 = \dot{\boldsymbol{r}}_2 \times \boldsymbol{p}_2 = 0$. We will learn in Sect. 3.10 that the conservation of total and relative angular momenta is related to a symmetry of the EOM under simultaneous rigid rotations of $\boldsymbol{r}_1, \boldsymbol{r}_2$ and $\boldsymbol{r}$. Furthermore, in Prob. 2.11 we verify that $\boldsymbol{L}_{\rm tot} = \boldsymbol{L}_{\rm cm} + \boldsymbol{L}$ so that $\boldsymbol{L}_{\rm cm} = \boldsymbol{R} \times \boldsymbol{P}$ is also conserved.

Laplace-Runge-Lenz vector. There is one more conserved quantity, the Laplace-Runge-Lenz vector, which we will study in Sect. 2.5*.

2.3 Planetary orbits

In this section, we will use the conservation of relative angular momentum and energy to deduce the shapes of planetary orbits from Newton's laws of motion and gravity. Since the relative angular momentum $\boldsymbol{L} = \boldsymbol{r} \times \boldsymbol{p}$ is a conserved vector (2.16), we may choose $\hat{z}$ along $\boldsymbol{L}$, assuming it is nonzero[16]. Once $\hat{z}$ is fixed, $\hat{x}$ and $\hat{y}$ may be chosen so that $\hat{x} \times \hat{y} = \hat{z}$ and xyz form a right-handed system. From $\boldsymbol{L} = \boldsymbol{r} \times \boldsymbol{p}$, both the relative vector $\boldsymbol{r}$ and momentum $\boldsymbol{p}$ must lie on the (x-y) plane perpendicular to $\boldsymbol{L}$. By the right-hand rule for cross products, orbits must have a 'counterclockwise' sense on the x-y plane. We will show that planetary orbits are ellipses with the center of mass at a focus. However, in order to do this, we need to be able to recognize the formula for an ellipse when we encounter it. Thus, we begin with a quick primer on the equation for an ellipse in plane polar coordinates, since that is the way it will arise.

Equation for an ellipse in polar form. An ellipse centered at the origin of the x-y plane with axes along the x and y axes is defined as the set of points satisfying $x^2/a^2 + y^2/b^2 = 1$. For definiteness, we may take $a \geq b > 0$, they are the lengths of the semiaxes. The eccentricity $\epsilon = \sqrt{1 - b^2/a^2}$, which lies between 0 and 1 is a measure of the departure from a circle, which results when $a = b$ and $\epsilon = 0$. The points $(\pm\sqrt{a^2 - b^2}, 0)$ are called the foci of the ellipse. One verifies that the sum of the distances of any point on the ellipse from the foci is the constant $2a$. For application to planetary orbits, it is clear from Kepler's second law that it is more convenient to place the origin (roughly the Sun) at a focus rather than at the center of the ellipse. Furthermore, just as in circular motion, it is more convenient to use polar coordinates in place of Cartesian coordinates. We will soon show that the equation for

---

[16] If $\boldsymbol{L} = 0$, it means the planet is heading radially inwards or away from the Sun. Since planetary orbits are not of this sort, it is safe to assume $\boldsymbol{L} \neq 0$. If $\boldsymbol{L} = 0$, then the angular momentum vector does not define a direction. The case $\boldsymbol{L} = 0$ is the subject of Sect. 2.6*.

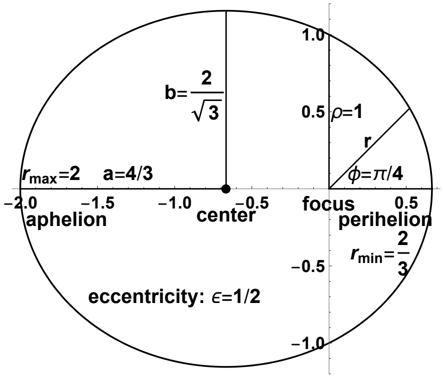

Figure 2.4: Ellipse $r = \rho/(1+\epsilon\cos\phi)$ for semilatus rectum $\rho = 1$ and eccentricity $\epsilon = 1/2$ showing the lengths a and b of the semimajor and semiminor axes marked in bold. Note that the origin lies at the right focus rather than at the center, to make formulae simpler.

an ellipse with the left focus on the x axis and the right focus at the origin of plane polar coordinates [22] is

$$r = \frac{\rho}{(1+\epsilon\cos\phi)}, \quad \text{where} \quad \rho > 0 \tag{2.18}$$

is a constant length (the semilatus rectum) that sets the scale and $0 < \epsilon < 1$ is the eccentricity[17] (see Fig. 2.4 which shows the semilatus rectum extending from the focus upwards). Why is this an ellipse? When $\epsilon = 0$, it is obviously a circle of radius ρ. Using Cartesian coordinates $x = r\cos\phi$ and $y = r\sin\phi$, (2.18) becomes $r = \rho - \epsilon x$. Upon squaring and completing the square, we get

$$(1-\epsilon^2)x^2 + 2\rho\epsilon x + y^2 - \rho^2 = 0 \quad \text{or} \quad \frac{(1-\epsilon^2)^2}{\rho^2}\left(x + \frac{\rho\epsilon}{1-\epsilon^2}\right)^2 + \frac{(1-\epsilon^2)}{\rho^2}y^2 = 1. \tag{2.19}$$

This is now in the standard Cartesian form $\frac{(x-x_0)^2}{a^2} + \frac{y^2}{b^2} = 1$ of an ellipse centered at the point $(-\rho\epsilon/(1-\epsilon^2), 0)$. The semilatus rectum ρ is related to the length a of the semimajor axis via $\rho = a(1-\epsilon^2)$ while $b = \rho/\sqrt{1-\epsilon^2}$ is the semiminor axis and $\epsilon^2 = 1 - b^2/a^2$ (see Fig. 2.4 for the semiaxes, they are measured from the center). When $\epsilon > 1$, the coefficients of x^2 and y^2 have opposite signs and we get a hyperbola. For $\epsilon = 1$ we get the parabola $y^2 = \rho^2 - 2\rho x$ opening out to the left. A nice feature of (2.18) is that it applies not just to ellipses but also to parabolae and hyperbolae simply by extending the range of ϵ. □

Elliptical orbits from conservation laws and orbit equation. Conservation of relative energy and angular momentum allow us to establish the elliptical shape of planetary orbits. More precisely, we will first show that the relative vector $\boldsymbol{r}$ traverses an ellipse and then deduce that the planet $\boldsymbol{r}_2$ and the Sun $\boldsymbol{r}_1$ also follow elliptical paths in a frame where the CM is at rest (see Fig. 2.3). To begin with, the relative kinetic energy in (2.15) may be expressed as a sum of radial and angular kinetic energies and the latter absorbed into an 'effective' potential energy[18]. If $m = m_1 m_2/(m_1 + m_2)$ denotes the reduced mass, then

---

[17] Closest approach to the Sun (perihelion) occurs at $r = r_{\min} = \frac{\rho}{1+\epsilon}$ when $\phi = 0$ and aphelion (farthest point from Sun) at $r = r_{\max} = \frac{\rho}{1-\epsilon}$ when $\phi = \pi$. We have oriented and positioned the axes to ensure the semimajor axis is along $\hat{x}$ and there is a $y \to -y$ symmetry. The origin $x = y = 0$ is at the right focus. A rotated ellipse results if we take $\frac{\rho}{r} = 1 + \epsilon\cos(\phi - \phi_0)$. By choosing $\phi_0 = \pi$ we may move the origin to the left focus.

$$E = \frac{1}{2} m \dot{r}^2 + V_{\text{eff}} \quad \text{where} \quad V_{\text{eff}} = \frac{l^2}{2mr^2} - \frac{\alpha}{r} \quad \text{and} \quad \alpha = G m_1 m_2. \tag{2.20}$$

We get this from the square of relative angular momentum[19] $\boldsymbol{L} = \boldsymbol{r} \times \boldsymbol{p}$,

$$\boldsymbol{L}^2 = l^2 = (\boldsymbol{r} \times \boldsymbol{p})^2 = r^2 p^2 - (\boldsymbol{r} \cdot \boldsymbol{p})^2 \quad \Rightarrow \quad \frac{\boldsymbol{p}^2}{2m} = \frac{(\hat{r} \cdot \boldsymbol{p})^2}{2m} + \frac{l^2}{2mr^2}. \tag{2.21}$$

The latter is the promised splitting of kinetic energy into radial and angular contributions. In spherical polar coordinates, $l^2 = (mr^2)^2(\dot{\theta}^2 + \sin^2\theta\, \dot{\phi}^2)$ (see Prob. 2.3) and for motion on the $\theta = \pi/2$ plane, $l = mr^2\dot{\phi}$. However, despite the appearance of all these derivatives of angles, l^2 is a constant and the angular kinetic energy may be viewed as a function of r alone. It appears as a repulsive angular momentum barrier (sometimes referred to as a centrifugal barrier) $l^2/2mr^2$ in the effective potential V_{eff}, which also includes the attractive gravitational potential $-\alpha/r$. As Fig. 2.5 indicates, for any fixed E and $l^2 > 0$ the angular momentum term prevents the radial distance from becoming arbitrarily small.

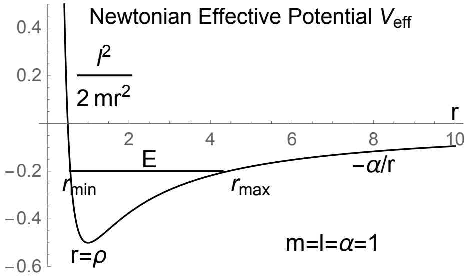

Figure 2.5: Effective potential $V_{\text{eff}} = l^2/2mr^2 - \alpha/r$ showing radial turning points for an energy $E < 0$.

Let us now use the methods of Sect. 1.1 to determine the possible types of radial motion using the graph (Fig. 2.5) of $V_{\text{eff}}(r)$. For fixed angular momentum $l \neq 0$, the minimum energy orbit is a circle of radius $r = \rho = l^2/m\alpha$ which is the location of the minimum: $V'_{\text{eff}}(\rho) = 0$. The planet executes uniform circular motion $\dot{r} = 0$ and $\dot{\phi} = l/m\rho^2$ with energy $E = -\frac{\alpha}{2\rho}$. On the other hand, if $-\frac{\alpha}{2\rho} < E < 0$, from Fig. 2.5, we expect the radial distance to oscillate about $r = \rho$ with radial turning points at perihelion $r_{\rm min}$ and aphelion $r_{\rm max}$ which are the roots of the quadratic equation

---

[18] The potential is typically the part of the energy that does not depend explicitly on velocities. The name effective potential is used because it differs from the Newtonian gravitational potential $V(r) = -\alpha/r$ by the term $l^2/2mr^2$. This latter term comes from the angular part of the kinetic energy, but is expressible in a manner independent of velocities due to the conservation of angular momentum.

[19] We used $\hat{r} \cdot \boldsymbol{p} = m\dot{r}$. To see this, recall that $\hat{r} = (x, y, z)/r$ and $\boldsymbol{p} = m(\dot{x}, \dot{y}, \dot{z})$. Thus, $\hat{r} \cdot \boldsymbol{p} = (m/r)(x\dot{x} + y\dot{y} + z\dot{z}) = (m/2r)dr^2/dt = m\dot{r}$.

$$V_{\rm eff}(r) = E \quad \text{or} \quad 2mEr^2 + 2m\alpha r - l^2 = 0. \tag{2.22}$$

For $E \geq 0$, the orbit is unbounded, though it has a radial turning point at perihelion[20], resulting in parabolic and hyperbolic orbits. These could be used to model an aperiodic (single apparition) comet which comes in from far away, reaches a point of closest approach to the Sun and then escapes from the solar system. Finally, if $l = 0$, there is no angular momentum barrier and we get straight-line orbits where the reduced mass moves radially towards or away from the center of mass (see Sect. 2.6*). In what follows, we obtain the shapes of orbits for $E < 0$.

Energy conservation ($E = \frac{1}{2}m\dot{r}^2 + V_{\rm eff}(r)$) gives a 1st order equation. We could integrate it to find $t(r)$ (see Prob. 2.13 and [83])

$$\pm\,(t - t_0) = \sqrt{\frac{m}{2}} \int_{r_0}^{r} \frac{ds}{\sqrt{E - V_{\rm eff}(s)}} \tag{2.23}$$

and invert to find $r(t)$. Then we may use conservation of $l = mr^2\dot{\phi}$ to find $\phi(t)$

$$\phi(t) - \phi_0 = \int_{t_0}^{t} \frac{l\, dt'}{mr^2(t')} = \pm\frac{l}{\sqrt{2m}} \int_{r_0}^{r(t)} \frac{ds}{s^2\sqrt{E - V_{\rm eff}(s)}}. \tag{2.24}$$

In the second equality, we used $dt^2 = (m/2)dr^2/(E - V_{\rm eff})$ from (2.20) and renamed r as s. So, at least for $l \neq 0$, the solution of the EOM has been reduced to quadrature.

However, if we are primarily interested in the shape of the orbit (rather than the time-dependence), it is simpler to think of r as a function[21] of ϕ. Then

$$\dot{r} = r'(\phi)\dot{\phi} = r'(\phi)(l/mr^2). \tag{2.25}$$

A 1st order *orbit equation* is obtained by using energy conservation:

$$E = \frac{l^2}{2mr^4}r'^2 + \frac{l^2}{2mr^2} - \frac{\alpha}{r}. \tag{2.26}$$

However, this equation is rather nonlinear and difficult to solve directly. The appearance of r'/r^2 suggests the substitution $u = 1/r$ in terms of which the energy becomes

$$E = (l^2/2m)\left(u^2 + u'(\phi)^2\right) - \alpha u. \tag{2.27}$$

However, this is still a nonlinear equation! Fortunately, differentiating in ϕ allows us to eliminate E and leaves us with an inhomogeneous *linear* 2nd order differential equation for the orbit parametrized by ϕ:

$$u'' + u = \frac{m\alpha}{l^2} \equiv \frac{1}{\rho} \quad \text{where } \rho \text{ is the radius of the circular orbit for that } l. \tag{2.28}$$

---

[20] The $l^2/2mr^2$ angular momentum barrier in $V_{\rm eff}$ prevents the reduced mass from getting too close, the point of closest approach is perihelion. There is no aphelion as it can escape to infinity.

[21] This is permitted since conservation of $\boldsymbol{L}$ prevents retrograde motion.

This is the equation for a harmonic oscillator encountered in Sect. 1.2 (with angular frequency $\omega = 1$ and with u playing the role of the displacement from equilibrium and ϕ that of time) with constant driving force (see Sect. 6.8). A particular solution is the constant $u_p = 1/\rho$ and the general solution of the homogeneous equation $u'' + u = 0$ is $u_h = \kappa \cos(\phi - \phi_o)$ where κ may be taken positive (a $-$ sign can be eliminated by advancing ϕ_o by π). In fact, the phase ϕ_o, simply rotates the orbit and will be omitted. The second integration constant κ has dimensions of inverse length and will be related to the energy. Thus, the equation for the orbit reduces to that of a conic section (2.18) with the origin at a focus if we identify the dimensionless constant $\kappa\rho$ with the eccentricity:

$$\frac{1}{r} = \kappa \cos\phi + \frac{1}{\rho} \quad \text{or} \quad \frac{\rho}{r} = 1 + \epsilon \cos\phi. \tag{2.29}$$

If $0 \le \epsilon < 1$, we conclude that the tip of the relative vector $\boldsymbol{r}$ (from Sun to planet) traces an ellipse with focus at the origin (Sun). By substituting in (2.27) we express the energy in terms of the parameters of the ellipse (ϵ, ρ or semimajor axis a)

$$E = -\frac{\alpha}{2\rho}\left(1 - \epsilon^2\right) = -\frac{\alpha}{2a} \quad \text{where} \quad \rho = \frac{l^2}{m\alpha}. \tag{2.30}$$

The semilatus rectum ρ for given l is physically interpreted as the radius of the circular orbit for that l. The condition $0 \le \epsilon < 1$ implies $E < 0$, which ensures the motion is bounded. It is clear that for $E = -\alpha/2\rho$ the eccentricity vanishes and we get a circular orbit. For $-\alpha/2\rho < E < 0$ we have $0 < \epsilon < 1$ and we get elliptical orbits. For $E = 0$, the eccentricity $\epsilon = 1$ and we have an unbound parabolic orbit $y^2 = \rho^2 - 2\rho x$. For $\epsilon > 1$, $E > 0$ and we have unbound hyperbolic orbits which will play an important role in Sect. 2.7* on scattering.

Finally, we may revert to the position vectors of the Sun and Earth via (2.10):

$$\boldsymbol{r}_1 = \boldsymbol{R} - \frac{m_2}{M}\boldsymbol{r} \quad \text{and} \quad \boldsymbol{r}_2 = \boldsymbol{R} + \frac{m_1}{M}\boldsymbol{r}. \tag{2.31}$$

We see that in a frame where the CM $\boldsymbol{R}$ is at rest, $\boldsymbol{r}_1$ and $\boldsymbol{r}_2$ trace out rescaled conic sections with the CM as a focus (see Fig. 2.3). For the Sun-Earth system, $m_2/M \ll 1$, so the Sun's orbit is a tiny ellipse around the center of mass (see Prob. 2.12). On the other hand, $m_1/M \approx 1$, so the Earth's orbit relative to the CM is nearly congruent to the ellipse traced by the relative vector $\boldsymbol{r}$.

2.4 Time period of elliptical orbits

For $E < 0$, since orbits are closed curves (ellipses), the motion is periodic in the sense that position and velocity return to their initial values after a time T. Why? Suppose after time T, $\boldsymbol{r}$ returns to its initial position $\boldsymbol{r}(0)$. Energy is unchanged throughout and so the potential energy must return to its initial value (since it depends only on $|\boldsymbol{r}|$). Thus the kinetic energy and speed must also be unchanged. The direction of velocity is tangent to the same ellipse and is also unchanged. So both the relative position and velocity return to their original values. From (2.31), the Sun's and Earth's elliptical trajectories also have the same period T. We now wish to find an expression for T in terms of the semimajor axis a and compare with Kepler's 3rd law.

There is a simple way to find the period T of elliptical orbits without evaluating the integral in (2.23). By the conservation of angular momentum, the areal speed (2.3) is a constant $\frac{d\mathrm{Ar}}{dt} = \frac{l}{2m}$ (Kepler's second law). Integrating over one period, the area of the ellipse is $\mathrm{Ar} = lT/2m$. On the other hand, the area is also given by $\mathrm{Ar} = \pi ab = \pi a\sqrt{a\rho}$ from (2.19). Using $\rho = l^2/m\alpha$ (2.30) to eliminate l and $m = m_1 m_2/M$ we get

$$T^2 = \frac{4m^2}{l^2}(\mathrm{Ar})^2 = \frac{4\pi^2 m}{\alpha}a^3 = \frac{4\pi^2}{GM}a^3 = \frac{a^3}{\tilde{K}}. \tag{2.32}$$

We have expressed the period in terms of the semimajor axis and $\tilde{K} = GM/4\pi^2$. We also recover Kepler's 3^{rd} law (not just for circular orbits). Since $M = m_1 + m_2$, $\tilde{K}$ depends on the *sum* of solar and planetary masses. But since all planets are at least a 1000 times lighter than the Sun, $M \approx m_s$. Hence, $\tilde{K} \approx Gm_s/4\pi^2 = K$ reduces to Kepler's constant (2.5) and is approximately the same for all planets. The time period can also be expressed in terms of the energy of the orbit, see Prob. 2.17.

2.5* LRL eccentricity vector and relations among conserved quantities

The $V(r) = -\alpha/r$ Newtonian potential has the special feature that all noncollisional bound trajectories are closed, leading to periodic motion. This is not generally true of central potentials. For instance[22], the central potential $\tilde{V}(r) = -\frac{\alpha}{r} - \frac{\alpha'}{r^2}$ for small[23] α' does have a closed trajectory, the circular one at the minimum of the effective potential. But not every bound trajectory is closed as shown in Fig. 2.6a, for reasons we now try to make plausible. For energy more than the minimal value of the effective potential, a typical trajectory fails to close and looks like a rosette or 'precessing ellipse' as illustrated in Fig. 2.6a. It is clear from the effective potential $\tilde{V}_{\text{eff}} = l^2/2mr^2 + \tilde{V}(r)$ that for fixed E and l, $r(t)$ is a periodic function of time, oscillating between turning points determined by $E = \tilde{V}_{\text{eff}}(r_{\min}) = \tilde{V}_{\text{eff}}(r_{\max})$ (as for the Newtonian effective potential in Fig. 2.5). In particular, the perihelion and aphelion distances do not change with time. However, the problem is that the period of $r(t)$ is not (in general) rationally related[24] to the time it takes for the angle ϕ to go from zero to 2π. From (2.26), the change in ϕ as r goes from $r_{\min}$ (when $\phi = \phi_o$) to

---

[22] Recall Clairaut's proposal (from the end of Sect. 2.1), to modify Newton's $1/r$ potential with an additional $1/r^2$ term to accommodate the lunar perihelion precession illustrated in Fig. 2.6a.

[23] We assume that $l^2 > 2m\alpha'$ so that there is an angular momentum barrier in the effective potential $\tilde{V}_{\text{eff}} = \frac{l^2}{2mr^2} - \frac{\alpha}{r} - \frac{\alpha'}{r^2}$.

[24] Consider a motion that is the superposition of two periodic motions $x(t) = \cos t + \cos(2t/3)$ with individual periods 2π and 3π. The combined motion is also periodic, with a period given by their least common (integer) multiple, 6π. On the other hand, $y(t) = \cos t + \cos\sqrt{2}t$ is aperiodic (more precisely quasiperiodic or conditionally periodic) as it is a superposition of 2π and $\sqrt{2}\pi$ periodic motions which have no common (integer) multiple since their ratio is irrational.

$r_{\max}$ and returns to $r_{\min}$ is

$$\phi - \phi_o = 2 \times \frac{l}{\sqrt{2m}} \int_{r_{\min}}^{r_{\max}} \frac{dr}{r^2 \sqrt{E - \tilde{V}_{\text{eff}}(r)}}. \tag{2.33}$$

But $\phi - \phi_o$ need not be an integer (or even a rational) multiple of 2π. As a consequence, the orbit is not closed. For such a rosette-shaped orbit, the vector from the origin to perihelion is not fixed, but rotates (see Fig. 2.6a). Of course, in such cases, this vector is only defined at discrete times when the planet is at perihelion, though its length does not change since the distance to perihelion is fixed by the turning point $r_{\min}$ in $\tilde{V}_{\text{eff}}$.

Remark. Joseph Bertrand's theorem (1873) implies that the only central force fields in 3d in which *all* (noncollisional) bounded orbits are closed, correspond to the attractive Newtonian $(-\alpha/r)$ potential and the isotropic harmonic oscillator potential $\frac{1}{2}m\omega^2 r^2$ (see Prob. 2.18, Sect. 3.6 of [46], Sect. 2.8.D of [2] and [63]). □

For the closed elliptical trajectories of the Newtonian $-\alpha/r$ potential, since the ellipse does not precess, the vector from the origin (focus) to perihelion is independent of time. This feature explains[25] why we might expect there to be a new conserved vector in the problem, the so-called Laplace-Runge-Lenz (LRL) vector. One could try to discover a formula for this vector by taking a linear combination of $\boldsymbol{r}, \boldsymbol{p}$ and $\boldsymbol{p} \times \boldsymbol{L}$ that lie in the plane of the orbit and requiring that it be independent of time. A combination that works is the LRL vector $\boldsymbol{A}$ (see Fig. 2.6b)

$$\boldsymbol{A} = \boldsymbol{p} \times \boldsymbol{L} - m\alpha\hat{r}. \tag{2.34}$$

Notice that $\boldsymbol{A} \cdot \boldsymbol{L} = 0$, so $\boldsymbol{A}$ lies in the orbital plane and must be expressible as a linear combination of $\boldsymbol{r}$ and $\boldsymbol{p}$. We show in Prob. 2.19 that $\boldsymbol{A}$ can also be written as

$$\boldsymbol{A} = 2m\left(H + \frac{\alpha}{2r}\right)\boldsymbol{r} - (\boldsymbol{r} \cdot \boldsymbol{p})\boldsymbol{p}. \tag{2.35}$$

The LRL vector can be thought of as a measure of the eccentricity of the orbit. Indeed, suppose we divide it by $m\alpha$ and define the *eccentricity vector*

$$\boldsymbol{\epsilon} = \frac{\boldsymbol{A}}{m\alpha} = \frac{\boldsymbol{v} \times \boldsymbol{L}}{\alpha} - \hat{r}. \tag{2.36}$$

We will see that $\boldsymbol{\epsilon}$ has a length equal to the eccentricity[26] of the orbit: $|\boldsymbol{\epsilon}| = \epsilon$. Let us first check that the LRL vector is conserved. Using $\dot{\boldsymbol{L}} = 0$ and $\dot{\boldsymbol{p}} = -\alpha\boldsymbol{r}/r^3$ (2.9),

$$\begin{aligned} \dot{\boldsymbol{A}} &= \dot{\boldsymbol{p}} \times \boldsymbol{L} - m\alpha\frac{\dot{\boldsymbol{r}}}{r} + \frac{m\alpha\,\dot{r}\,\boldsymbol{r}}{r^2} = \dot{\boldsymbol{p}} \times (\boldsymbol{r} \times \boldsymbol{p}) - \frac{\alpha\boldsymbol{p}}{r} + \frac{\alpha(\boldsymbol{r}\cdot\boldsymbol{p})\boldsymbol{r}}{r^3} \\ &= \boldsymbol{r}(\dot{\boldsymbol{p}} \cdot \boldsymbol{p}) - \boldsymbol{p}(\dot{\boldsymbol{p}} \cdot \boldsymbol{r}) - \frac{\alpha\boldsymbol{p}}{r} + \frac{\alpha(\boldsymbol{r}\cdot\boldsymbol{p})\boldsymbol{r}}{r^3} = 0. \end{aligned} \tag{2.37}$$

---

[25] See Prob. 2.18 for an analog of the LRL vector in the isotropic 2d harmonic oscillator.

[26] In particular $\boldsymbol{A}$ and $\boldsymbol{\epsilon}$ will vanish for a circular orbit, which is reasonable since every point on a circular orbit can be taken as perihelion and there is no preferred direction.

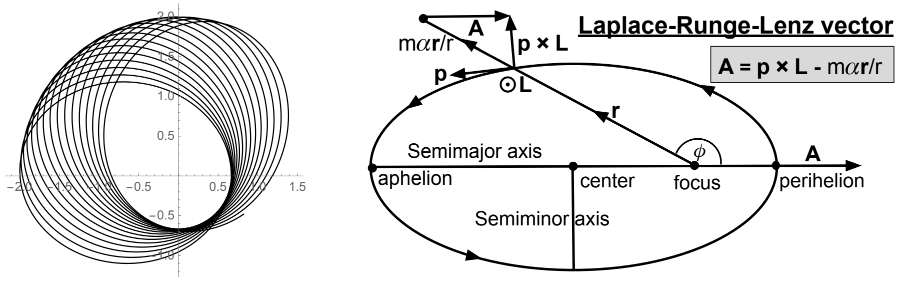

(a) (b)

Figure 2.6: (a) Rosette-shaped trajectory showing an approximately precessing elliptical orbit. (b) Relative momentum, angular momentum and LRL vectors for an elliptical orbit.

Being a conserved vector, we may find its direction at any time, say at perihelion. Now, $\frac{\rho}{r} = 1 + \epsilon \cos\phi$. Since $\boldsymbol{L}$ is in the $\hat{z}$ direction, the motion is counterclockwise and perihelion occurs at $\phi = 0, r_{\min} = \rho/(1+\epsilon)$. At perihelion, $\boldsymbol{r} = r_{\min}\hat{x}$ and by the $y \to -y$ symmetry of the orbit, the tangent to the curve is in the $\hat{y}$ direction, $\boldsymbol{p} = p\hat{y}$ with $p > 0$. To find p at perihelion we write

$$\frac{\boldsymbol{p}^2}{2m} = E + \frac{\alpha}{r_{\min}} = -\frac{\alpha}{2\rho}(1-\epsilon^2) + \frac{\alpha(1+\epsilon)}{\rho} = \frac{\alpha}{2\rho}(1+\epsilon)^2. \tag{2.38}$$

Thus, using (2.30)

$$p = \sqrt{\frac{m\alpha}{\rho}}(1+\epsilon) = \frac{m\alpha}{l}(1+\epsilon). \tag{2.39}$$

It follows that at perihelion

$$\boldsymbol{A} = (lp - m\alpha)\hat{x} = m\alpha\epsilon\,\hat{x}. \tag{2.40}$$

Hence $\boldsymbol{A}$ points towards perihelion and has a magnitude $m\alpha\epsilon$. Thus, the eccentricity vector $\boldsymbol{\epsilon} = \boldsymbol{A}/m\alpha$ has a length equal to the eccentricity. Both $\boldsymbol{A}$ and $\boldsymbol{\epsilon}$ vanish for circular orbits.

Thus, for motion in the potential $V(r) = -\alpha/r$ we have found 7 conserved quantities: E and the components of $\boldsymbol{L}$ and $\boldsymbol{A}$. However, this relative motion system has only three degrees of freedom and requires 6 real numbers as initial data $(\boldsymbol{r}(0), \boldsymbol{v}(0))$ to determine time evolution. We may view conserved quantities as functions of the initial conditions, simply by evaluating them at $t = 0$, e.g., $l_z = m(x(0)\dot{y}(0) - y(0)\dot{x}(0))$. To begin with, let us assume that the conserved quantities are independent[27]. Suppose we are given the (numerical) values of all the conserved quantities. Each one imposes one relation among the initial data. Thus we would have 7 equations among 6 ICs and there would in general not be any way of satisfying them. If only 6 of the conserved quantities were independent, then we would generally find a discrete set of admissible ICs $[(\boldsymbol{r}_1(0), \boldsymbol{v}_1(0)), (\boldsymbol{r}_2(0), \boldsymbol{v}_2(0)), \ldots]$. However, such a circumstance would not permit nonstatic trajectories with continuous time evolution, since every point on a trajectory is a possible choice of ICs with the same values for conserved quantities. Thus, for a system with 3 degrees of freedom to admit nontrivial trajectories, one can have at most 5 independent conserved quantities. More generally, we can have at most $2n-1$ independent conserved quantities for a system with n degrees of freedom[28]. If there is such a maximal set of conserved quantities, and their values are specified, then they determine a curve in the space of positions and velocities: the trajectory $(\boldsymbol{r}(t), \boldsymbol{v}(t))$ parametrized by time. If there was another independent conserved quantity, it would force the trajectory to be a point (i.e., a static solution).

---

[27] For instance, l_z and l_z^2 are not independent of each other, nor are the energy $p^2/2m$ and momentum p of a free particle moving on a line.

This implies that there must be at least 2 relations among $E, \boldsymbol{L}$ and $\boldsymbol{A}$. One is obvious: $\boldsymbol{A}\cdot\boldsymbol{L}=0$. For simplicity and to get started, we next look for another scalar relation among the conserved quantities[29]. The only scalars available to us are A^2 and l^2 so the relation must be of the form $f(E, A^2, l^2; m, \alpha) = 0$. To get an idea of what this relation may be, we recall the expressions for A, l and E for the orbits determined so far (i.e., for $l \neq 0$):

$$E = -\frac{\alpha}{2\rho}(1-\epsilon^2), \quad A^2 = m^2\alpha^2\epsilon^2 \quad \text{and} \quad l^2 = m\alpha\rho. \tag{2.41}$$

Substituting for ρ and ϵ^2 in terms of l^2 and A^2 in E we arrive at the relation $A^2 = 2mEl^2 + m^2\alpha^2$. If a relation among conserved quantities holds for every solution of the equations of motion, then it must be generally true.

To be sure, we may also obtain this scalar relation from the definition of $\boldsymbol{A}, \boldsymbol{L}$ and E (without using the solution of the Kepler problem) simply by computing the square of $\boldsymbol{A} = \boldsymbol{p}\times\boldsymbol{L} - m\alpha\hat{r}$ and using $p^2 = 2m(E+\alpha/r)$ and $\boldsymbol{p}\cdot\boldsymbol{L}=0$,

$$\begin{aligned} \boldsymbol{A}^2 &= (\boldsymbol{p}\times\boldsymbol{L})^2 - 2m\alpha\hat{r}\cdot(\boldsymbol{p}\times\boldsymbol{L}) + m^2\alpha^2 \\ &= p^2l^2 - (\boldsymbol{p}\cdot\boldsymbol{L})^2 - \frac{2m\alpha}{r}\boldsymbol{L}\cdot(\boldsymbol{r}\times\boldsymbol{p}) + m^2\alpha^2 \\ &= 2mEl^2 + \frac{2m\alpha l^2}{r} - \frac{2m\alpha l^2}{r} + m^2\alpha^2 = 2mEl^2 + m^2\alpha^2. \end{aligned} \tag{2.42}$$

Evidently, this relation is special to a central potential $\propto 1/r$. We may also view it as expressing the energy in terms of the squares of the conserved vectors $\boldsymbol{A}$ and $\boldsymbol{L}$:

$$E = \frac{A^2 - m^2\alpha^2}{2ml^2}. \tag{2.43}$$

Spectrum of hydrogen atom. Interestingly, as discovered by Wolfgang Pauli, (2.43) provides a simple way of obtaining the Bohr energy spectrum of the hydrogen atom whose energy is $E = \frac{\boldsymbol{p}^2}{2m} - \frac{e^2}{(4\pi\epsilon_o)r}$. Here $-e^2$ is the product of proton and electron charges in SI units, ϵ_0 is a constant (the permittivity of free space) and we may identify $\alpha = \frac{e^2}{4\pi\epsilon_o}$. For circular orbits, $A^2 = 0$ but $l \neq 0$. Bohr's postulate of quantization of angular momentum $l = n\hbar$ for $n = 1, 2, 3, \ldots$ along with (2.43) then gives:

---

[28] An n degree of freedom system with $2n-1$ conserved quantities is called superintegrable.

[29] If we do not find a scalar relation, we could look for a vector relation, which would entail three relations. See Sect. 3.25* for more on the independence of Keplerian conserved quantities.

$$E_n = -\frac{me^4}{(4\pi\epsilon_o)^2 2n^2\hbar^2} \quad \text{where} \quad n = 1, 2, 3, \ldots. \tag{2.44}$$

Pauli found the Bohr spectrum by this use of the relation among conserved quantities before the Schrödinger wave equation of quantum mechanics was formulated! □

2.6* Collision of two gravitating point masses: collision time and universality

In finding the orbits for the Kepler problem, we avoided the case where the magnitude of the relative angular momentum vanishes ($l = 0$), so that there is no angular momentum barrier in V_{eff} (2.20). We discuss this case now. Consider two point masses m_1 and m_2, subject only to their mutual gravitational force. Their center of mass moves uniformly in a straight line and we will go to a frame that moves uniformly so that the CM is at rest. The energy of relative motion is

$$E = \frac{1}{2}m\dot{\boldsymbol{r}}^2 - \frac{\alpha}{r} = \frac{1}{2}m\dot{r}^2 + \frac{l^2}{2mr^2} - \frac{\alpha}{r} \quad \text{where} \quad r \geq 0 \tag{2.45}$$

and m is the reduced mass. For a collision to occur (i.e., $\boldsymbol{r} = 0$), we need the relative angular momentum $\boldsymbol{L} = \boldsymbol{r} \times \boldsymbol{p}$ to be zero since it is conserved and is zero at the time of collision. So $\boldsymbol{p}$ must be either along or in the direction opposite to $\boldsymbol{r}$ and the motion is purely radial[30] and $E = \frac{1}{2}m\dot{r}^2 - \frac{\alpha}{r}$. In this case the effective potential (2.20) is just $V_{\text{eff}} = -\alpha/r$. For $E < 0$, there is only one radial turning point at $r_{\max} = -\alpha/E$. For $E \geq 0$ there are no turning points and the motion can be unbounded.

Suppose the particle is at a radial distance $r = r_0$ at $t = 0$. There are two possibilities: (a) it is given a radially outward initial velocity or (b) it is given a radially inward initial velocity. In case (a), the particle will escape to $r = \infty$ if $E \geq 0$ or go out, return and collide if $E < 0$. In case (b) the particle will collide irrespective of its initial radially inward velocity. In case (a) with $E < 0$ the particle will return to r_0 with radially inward velocity and may be treated from thereon as in case (b). So to study collisions, we restrict to case (b) with radially inward initial velocity. In this case, we know that $E \geq -\frac{\alpha}{r_0} \geq -\frac{\alpha}{r(t)}$ since kinetic energy is nonnegative and $r(t) \leq r_0$. Conservation of energy tells us that

$$\dot{r}^2 = (2/m)\left(E + \alpha/r\right). \tag{2.46}$$

As the particle is falling inward, $\dot{r} \leq 0$. Thus we take the negative square-root and get

$$\dot{r} = -\sqrt{\frac{2}{m}}\sqrt{E + \frac{\alpha}{r}} \quad \Rightarrow \quad -\int_0^t dt' = \sqrt{\frac{m}{2}}\int_{r_0}^{r} \frac{dr'}{\sqrt{E + \frac{\alpha}{r'}}}. \tag{2.47}$$

Since the particle has to cover a finite distance and is speeding up, we expect a collision to happen in a finite time t_c when r reduces to zero:

$$t_c = \sqrt{m/2}\int_0^{r_0} \frac{dr}{\sqrt{E + \alpha/r}}. \tag{2.48}$$

---

[30] An example of such motion is zero *impact parameter* ($b = 0$) scattering, see Fig. 2.8.

We assume the bodies are point-like, otherwise the collision will happen a little earlier than t_c. Since the kinetic energy $E + \frac{\alpha}{r} > 0$ for $0 \leq r < r_0$, the integrand is finite for all $0 \leq r < r_0$. At $r = r_0$ the integrand is finite as long as the particle has nonzero initial velocity. If its initial velocity is zero (so that $E = -\alpha/r_0$), the integrand diverges at $r = r_0$ but only in a mild way $(\sim 1/\sqrt{r_0 - r})$. Thus, even if its initial velocity is zero, the integrand has an integrable divergence at $r = r_0$, just as in (1.10). So the collision time is finite. We will find an expression for t_c shortly.

It is also interesting to find the radial distance as a function of time, especially as the collision time is approached. For this we integrate (2.47) from t to t_c

$$t_c - t = \sqrt{m/2} \int_0^r \frac{dr'}{\sqrt{E + \alpha/r'}}. \tag{2.49}$$

For $t \to t_c^-$, $r \to 0^+$ and the $\frac{\alpha}{r'}$ term dominates,

$$t_c - t \approx \sqrt{\frac{m}{2\alpha}} \int_0^r \sqrt{r'}\, dr' = \frac{2}{3}\sqrt{\frac{m}{2\alpha}} r^{3/2} \quad \Rightarrow \quad r(t) \approx \left(\frac{9\alpha}{2m}\right)^{1/3} (t_c - t)^{2/3} \tag{2.50}$$

as $t \to t_c$. We see that the behavior of the radial distance just before the collision is independent of the energy E as well as the initial distance r_0. The power-law $(t_c - t)^{2/3}$ is universal in this sense and $2/3$ is like a critical exponent. In fact, even if we had a third gravitating mass, it would not affect this result. This is because the effects of the third mass are negligible when the other two bodies are close to a collision[31]. This power-law may be viewed as a collisional version[32] of Kepler's 3rd law (2.1) which relates the length of the semimajor axis to the time period of elliptic trajectories: $R = K^{1/3}T^{2/3}$. Both these power-laws are a reflection of the $1/r$ potential. They are related to a scaling symmetry (also known as *mechanical similarity*) of the $1/r$ potential, valid for any angular momentum.

Scaling symmetry. If $\boldsymbol{r}(t)$ is a solution of Newton's equation $m\ddot{\boldsymbol{r}} = -\frac{\alpha}{r^2}\hat{r}$, then so is $\boldsymbol{s}(t) = \lambda^{-2/3}\boldsymbol{r}(\lambda t)$, for any $\lambda > 0$, as one checks. In other words,

$$t \to t/\lambda, \quad \boldsymbol{r} \to \lambda^{-2/3}\boldsymbol{r} \quad (\text{or} \quad r \to \lambda^{-2/3} r, \quad \phi \to \phi, \quad \theta \to \theta) \tag{2.51}$$

is a symmetry of the EOM. To discover this symmetry, consider the transformation[33] $t \to t/\lambda, \boldsymbol{r} \to \lambda^\gamma \boldsymbol{r}$, so that

$$\dot{\boldsymbol{r}} \to \lambda^{\gamma+1}\dot{\boldsymbol{r}}, \quad \text{and} \quad \ddot{\boldsymbol{r}} \to \lambda^{\gamma+2}\ddot{\boldsymbol{r}} \quad \text{and} \quad r^{-2} \to \lambda^{-2\gamma} r^{-2} \quad \text{while} \quad \hat{r} \to \hat{r}. \tag{2.52}$$

Invariance of Newton's equation tells us that $\lambda^{\gamma+2} = \lambda^{-2\gamma}$ or $\gamma = -2/3$. ☐

---

[31] In the absence of triple collisions, Karl Sundman developed a very slowly converging series solution to the three-body problem in powers of $(t_c - t)^{1/3}$ [72, 116, 133].

[32] This power law is valid only in the vicinity of a collision. Kepler's 3rd law too has its limitations: it only deals with the time period and not the detailed time-dependence of a trajectory.

[33] With the exception of the limiting case where time is not rescaled at all, any rescaling of $\boldsymbol{r}$ and t can be reduced to this for some λ and γ.

Finally, we find the collision time t_c (2.48) for purely downward motion. There are two cases.
1. If $E \geq 0$ we get

$$t_c = \sqrt{\frac{m}{2\alpha}} \int_0^{r_0} \sqrt{\frac{r}{1+\frac{Er}{\alpha}}}\, dr = \sqrt{\frac{m\alpha^2}{2E^3}} \tau_+ \left(\frac{Er_0}{\alpha}\right) \tag{2.53}$$

where we defined the function (see Prob. 2.20 and Prob. 2.21)

$$\tau_+(s) = \int_0^s \sqrt{\frac{\sigma}{1+\sigma}}\, d\sigma = \sqrt{s(1+s)} - \operatorname{arcsinh}\sqrt{s} \quad \text{for} \quad s \geq 0. \tag{2.54}$$

2. For[34] $-\frac{\alpha}{r_0} \leq E \leq 0$, by putting $\sigma = -\frac{Er}{\alpha} > 0$ we get for $0 \leq s = -\frac{Er_0}{\alpha} \leq 1$:

$$t_c = \sqrt{\frac{m\alpha^2}{2|E|^3}}\, \tau_- \left(-\frac{Er_0}{\alpha}\right) \quad \text{where} \quad \tau_-(s) = \int_0^s \sqrt{\frac{\sigma}{1-\sigma}}\, d\sigma = \arcsin\sqrt{s} - \sqrt{s(1-s)}. \tag{2.55}$$

Using the identity $\arcsin x = -i \operatorname{arcsinh}(ix)$ we may combine the two cases (see Prob. 2.22) and express the time to collision as

$$t_c = \operatorname{sgn}(E) \sqrt{\frac{m\alpha^2}{2E^3}} \left[\sqrt{\frac{Er_0}{\alpha}\left(1+\frac{Er_0}{\alpha}\right)} - \operatorname{arcsinh}\sqrt{\frac{Er_0}{\alpha}}\right] \quad \text{for} \quad -\frac{\alpha}{r_0} \leq E, \tag{2.56}$$

where r_0 is the initial radial distance and E the relative energy. See Fig. 2.7 where we plot t_c as a function of energy.

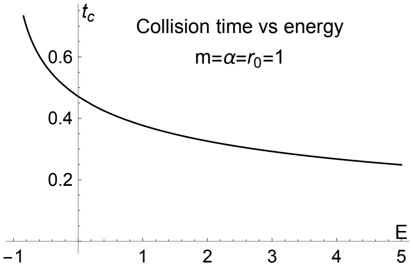

Figure 2.7: Time to collision t_c (in units where $m = \alpha = r_0 = 1$) for purely downward motion from initial separation r_0 decreases monotonically with energy starting from free fall ($E = -\alpha/r_0 = -1$). t_c falls off as $\sim 1/\sqrt{2E}$ for large E as shown in (2.59).

Galileo's observation and Newton's third law: If the body falls freely (zero initial speed, minimal energy $E = -\alpha/r_0$), then the collision time is maximal. Replacing

$$\alpha = Gm_1m_2 \ \text{ and } \ m = m_1m_2/M, \quad \text{we get} \quad t_c = (\pi/2)\sqrt{r_0^3/2GM}. \tag{2.57}$$

It is reasonable that the time to impact increases with initial separation r_0 and decreases with increasing gravitational coupling and *total* mass. Imagine a ball falling onto the Earth. In this case, the reduced mass is approximately the ball's mass and the total mass is approximately the Earth's mass. Then we find that the time of descent from a fixed height is *universal*, i.e., approximately independent of the ball's mass. It follows that all bodies, irrespective of their mass and size (assumed small compared to those of the Earth) take nearly the same time to fall if we ignore friction. An experimental deduction of this is popularly attributed to Galileo (1564-1642)[35]. Note that the collision time cannot be *exactly* independent of the mass of the ball. For, the collision time would then have to be independent of the mass of the Earth as well. This is because the process could also be viewed as the Earth rising up and colliding with the ball, in which case the roles of the two masses are reversed, but t_c must be the same by Newton's third law, which posits that the forces in the two cases are equal in magnitude and oppositely directed. But measurements show that objects would fall slower on a lighter planet. This means the collision time has to depend on both masses. The above formula for t_c keeps its peace with Galileo's observation as well as the reciprocity requirement of Newton's 3^{rd} law by depending on the total mass rather than the individual masses separately. A closely related empirical deduction of Galileo concerns the universality of the acceleration felt by all bodies falling from a common distance r_0 from the Earth. This is encoded in Newton's law of gravity and his second law which together imply that all bodies, irrespective of their mass m_b feel the same acceleration towards the Earth (mass m_e):

---

[34] The lower bound on E follows from the positivity of the radial kinetic energy in (2.46).

$$-\frac{Gm_e m_b}{r_0^2}\hat{r} = m_b \boldsymbol{a} \quad \Rightarrow \quad \boldsymbol{a} = -\frac{Gm_e}{r_0^2}\hat{r}. \tag{2.58}$$

This universality is called the equivalence principle. The cancellation of m_b happened since the *gravitational mass* of the body that enters Newton's law of gravity is postulated to be the same as the *inertial mass* of the body which multiplies acceleration in Newton's second law (see Sect. 3.3 for more on this). This postulate has been empirically checked to high accuracy and is called the principle of equivalence of inertial and gravitational masses. It suggests that gravitation is in some sense equivalent to acceleration, an idea that lies at the foundation of Einstein's theory of gravity. □

Remark: As the energy grows, t_c (2.56) monotonically drops to zero as in Fig. 2.7. If $E = 0$, then $t_c = (2/3)\sqrt{r_0^3/2GM}$. For high energies, the collision time goes to zero in a manner independent of α, as we'd expect. In fact, as $E \to \infty$, gravity may be ignored and so the dependence of energy on $\alpha = GMm$ drops out, $E \approx \frac{1}{2}m\dot{r}^2$, and the particle covers a distance r_0 at the roughly uniform speed $v = r_0/t_c$ giving

$$t_c \to \sqrt{mr_0^2/2E} \quad \text{as} \quad E \to \infty. \tag{2.59}$$

This result is verified by taking $E \to \infty$ in (2.48) or in (2.56). One may worry that sufficiently close to collision, the gravitational potential energy grows without bound and may not be ignored. However, for large E, its effect on t_c is suppressed since the particle spends very little time close to collision as its speed is very large. □

---

[35] Though he asserted this universality on empirical grounds, it is unclear whether Galileo conducted the experiment of dropping objects from the leaning tower of Pisa. Such an experiment was performed in 1586 by Simon Stevin and Jan Cornets de Groot from a tower in Delft and possibly by others even earlier [5].

2.7* Rutherford scattering cross section

So far, in this chapter, we have dealt with the two-body problem of gravitating masses that interact via an attractive Newtonian $1/r$ potential. In addition to the elliptic and straight line orbits discussed in Sect. 2.3 and Sect. 2.6*, there are unbounded hyperbolic (and parabolic) orbits with nonnegative relative energy E. Interestingly, it has been known from the time of Coulomb (1785) that point-like charged particles also interact via a $1/r$ 'Coulomb' potential, though the force can be either attractive or repulsive according as the charges have the same or opposite sign. In either case, the same sort of hyperbolic trajectories arise when the relative energy is positive. Such a situation arises in Rutherford scattering. Thus, in this section, we apply to atomic physics the principles of classical dynamics we have learned in the context of celestial mechanics.

Gold foil experiment. Geiger, Marsden and Rutherford (1909-1911) scattered positively charged alpha particles (Helium nuclei in our current understanding) against a thin gold foil. At the time, the structure of the atom was not known, with J J Thomson suggesting (in 1904) that atoms were made of point-like electrons embedded (like plums) in a background of positive charge that was smeared (like pudding) over the atom. This experiment was instrumental in deducing the microscopic structure of (gold) atoms. They found that a majority of the α particles passed undeflected or suffered slight deflections, suggesting that most of the atom is empty. A small but significant fraction were scattered through wide angles while some were even back-scattered towards the source. The angular distribution of scattered α-particles was measured using a detector. The observation of wide-angle scattering and recoil suggested that the positive charge could not be smeared over the atom but was probably concentrated in a tiny heavy nucleus. Since the gold foil was very thin and the atom supposedly largely empty, multiple scattering was unlikely and it was supposed that alpha particles were essentially scattering against a single highly charged gold nucleus[36]. To examine this hypothesis, Rutherford used classical mechanics to calculate the expected angular distribution (or differential scattering cross section) of alpha particles scattering against the Coulomb field of a single point-like nucleus. The calculated distribution was similar to the measured one, allowing them to rule out Thomson's plum pudding model and leading Rutherford to propose the nuclear model of the atom.

We give here a brief classical treatment[37] of this 'Coulomb scattering' problem and obtain Rutherford's celebrated differential scattering cross section, which encodes the angular distribution of particles scattered by the Coulomb field of a nucleus. Fortuitously, this formula agrees with the leading order quantum mechanical result. This is significant since in some parts of atomic physics, such as the spectrum and structure of bound states, the naive classical treatment is misleading and a poor approximation to the quantum theory. Thus, we are fortunate that Rutherford could use classical physics to interpret his experiment and correctly deduce the nuclear model of the atom, well before quantum mechanics was formulated (around 1926).

---

[36] The individual (much lighter) electrons in a gold atom have a much smaller charge ($1/79$ the nuclear charge) and were presumed to be spread out over the vast expanse of the atom

[37] See also Sect. 3.4 and [83] for more on the classical treatment of collisions.

Coulomb scattering cross section. Suppose the beam of incoming particles (say from the left along $\hat{z}$) has an intensity or flux of $\mathcal{F}$, which is the number of incoming particles per unit time per unit area normal to the beam as shown in Fig. 2.8. After scattering, we want to find dN, the number of particles entering solid angle[38] $d\Omega$ per unit time. dN is the rate at which particles should be detected by a detector covering solid angle $d\Omega$. This should be proportional to the incoming flux, so $dN = \mathcal{F} d\sigma$ where $d\sigma$ is an area. $d\sigma$ may be interpreted as the area normal to the beam through which the particles must pass so that they are scattered into $d\Omega$. The ratio $\frac{d\sigma}{d\Omega}$ is called the differential scattering cross section. It is a function of spherical polar coordinates[39] θ and ϕ. The total cross section is defined as the integral over all directions

$$\sigma_{\text{tot}} = \int_0^{\pi} \sin\theta \, d\theta \int_0^{2\pi} d\phi \, \frac{d\sigma}{d\Omega}. \tag{2.60}$$

The total cross section may be interpreted as the total effective area (normal to the beam) presented by the scatterer.

Suppose a projectile of charge q_2, mass m and energy E scatters from the repulsive Coulomb potential of a point charge q_1 assumed infinitely massive and fixed at the origin[40]. The potential energy of interaction is given by $V = \frac{q_1 q_2}{4\pi r}$. The projectile follows a hyperbolic orbit[41] with q_1 at a focus, as shown in Fig. 2.8. At early and late times, the trajectory approaches a straight line given by the asymptotes to the

---

[38] The rate at which particles are detected by the detector depends on the size of the detector and how far away it is. In an idealized treatment, we imagine the detector to be placed at an infinite distance from the origin and to cover a certain angular patch or solid angle. If we use spherical polar coordinates, the polar and azimuthal angles (θ, ϕ) determine a direction from the origin. The solid angle corresponding to directions lying within $d\theta$ and $d\phi$ of (θ, ϕ) is the area of the corresponding patch on the unit sphere: $d\Omega = \sin\theta \, d\theta \, d\phi$. In general, the solid angle subtended (in steradians) by a cone of directions from the origin is the area enclosed by the cone on the unit sphere. This generalizes the concept of angle (in radians) subtended by a cone of directions from the origin on a plane: an angle in radians is the length of the arc on the unit circle enclosed by the cone of directions.

[39] Spherical (as opposed to cylindrical) coordinates are appropriate for treating Rutherford scattering since (a) the Coulomb potential is spherically symmetric and (b) the scattering depends strongly on the polar angle θ with respect to the beam direction, which allows us to distinguish among forward, wide-angle and back-scattering. The angular distribution is independent of the angle ϕ about the beam axis due the spherical symmetry of the Coulomb potential.

[40] In this section, we use Heaviside-Lorentz (HL) units for electric charge. In SI units there would be an additional ϵ_0 multiplying 4π in the denominator of Coulomb's potential. HL units differ from SI units mainly through the absence of ϵ_0 and μ_0 in the Coulomb and Biot-Savart laws, and the appearance of the speed of light c in Maxwell's equations (multiplying time and dividing the electric current density) and the Lorentz force (dividing the velocity). Unlike in Gaussian units, factors of 4π do not appear in Maxwell's equations. HL units are commonly used in quantum field theory and high energy physics.

[41] This problem is very similar to the gravitational two-body problem in the attractive Newto-

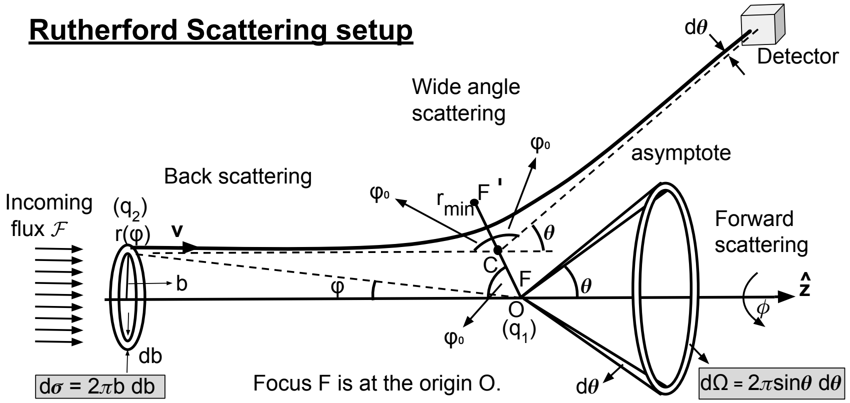

Figure 2.8: Schematic diagram of Coulomb scattering of incident charge q_2 against fixed charge q_1 located at the origin O, which is also the focus F of the hyperbolic trajectory of q_2. The source and detector are both located far from O so that the charge q_2 behaves like a free particle in those asymptotic regions. The line from q_1 to the point of closest approach (where $r = r_{\min}$) is the axis of symmetry. The asymptotes intersect at the center C of the hyperbola. The angle of deflection from straight-line motion is the scattering angle θ while ϕ is the azimuthal angle around the beam axis. The scattering goes from forward ($\theta = 0$) through wide angles and finally to back scattering ($\theta = \pi$). The angular region of width $d\theta$ around θ and for any ϕ into which scattering occurs has been parallel-translated for all the hyperbolic orbits with impact parameters lying in $[b, b + db]$ to form a cone with apex at the origin.

hyperbola which intersect at the center C. The latter lies on the symmetry axis of the hyperbola: the line through the origin and the point of closest approach (periapsis). The deflection angle θ between the past and future asymptotes is called the scattering angle. Forward and back scattering thus correspond to $\theta = 0$ and $\theta = \pi$. Due to rotation invariance about the beam axis, the scattering is azimuthally symmetric and Rutherford's differential cross section depends only on the (polar) scattering angle θ:

$$\frac{d\sigma}{d\Omega} = \left(\frac{q_1 q_2}{16\pi E \sin^2(\theta/2)} \right)^2 . \tag{2.61}$$

Aided by Fig 2.8, let us see how this formula is obtained. Consider particles coming in through an annulus with impact parameters[42] between b and $b + db$ and any azimuthal angle ϕ. Suppose they are deflected by angles between θ and $\theta + d\theta$ and therefore enter a solid angle $d\Omega = 2\pi \sin\theta d\theta$. The number of particles entering this solid angle per unit time is the product of the area of the annulus and the incident flux

$$dN = 2\pi\, b\, db\, \mathcal{F}. \tag{2.62}$$

---

nian $1/r$ potential. In the latter case, we have an unbounded positive relative energy hyperbolic orbit that bends towards the center of mass. In fact, the trajectory of the reduced mass is the same hyperbola as in Fig. 2.8 provided the CM is placed at the other focus.

[42] The impact parameter is the perpendicular distance between the scattering center O (location of q_1) and the straight line along which the projectile came in from afar.

Now we divide by $\mathcal{F}$ to get $d\sigma$ and divide by $d\Omega$ to get the differential cross section:

$$\frac{d\sigma}{d\Omega} = -\frac{b}{\sin\theta}\frac{db}{d\theta}. \tag{2.63}$$

The minus sign is because larger impact parameters imply smaller scattering angles. By integrating Newton's equation of motion in a repulsive Coulomb potential we will obtain the following relation between impact parameter and scattering angle:

$$1 + \frac{4b^2}{a^2} = \operatorname{cosec}^2(\theta/2). \tag{2.64}$$

We differentiate this to get Rutherford's differential cross section (2.61):

$$\frac{8b}{a^2}db = -2\frac{\cos(\theta/2)}{\sin^3(\theta/2)}\frac{1}{2}d\theta \quad \Rightarrow \quad -\frac{db}{d\theta} = \frac{\cos(\theta/2)}{\sin^3(\theta/2)}\frac{a^2}{8b}. \tag{2.65}$$

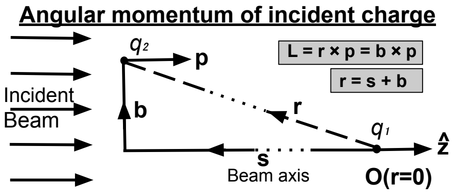

Figure 2.9: Equality of angular momenta of q_2 about origin O and a point far to the left on the beam axis.

To derive the relation (2.64) between b and θ, we use Newton's 2nd law. In fact, we only need to integrate once if we use conservation of energy $E = \frac{1}{2}m\dot{r}^2 + \frac{l^2}{2mr^2} + \frac{q_1 q_2}{4\pi r}$ (2.20). If v is the initial speed of the projectile (say coming in from the left as in Fig. 2.8 and Fig. 2.9), then its (conserved) angular momentum[43] and energy evaluated at early times are $l = mvb$ and $E = \frac{1}{2}mv^2$. Eliminating v we express the angular momentum as $l^2 = 2mEb^2$. Since we are interested in the angular deviation of the orbit rather than its time-dependence, we view the orbit (see Fig. 2.8) as the curve $r(\varphi)$ where φ (not to be confused with the azimuthal angle ϕ) is the polar angle of the projectile in the plane of the trajectory measured with respect to the direction of the beam source. As in (2.27), the orbit equation simplifies if we use $u = 1/r$ in place of r. Thus $\dot{r} = r'(\varphi)\dot{\varphi}$ with $r' = -r^2 u'$ and $l = mr^2\dot{\varphi}$ give

$$\dot{r} = -u'(\varphi)\frac{l}{m} \quad \Rightarrow \quad \frac{1}{2}m\dot{r}^2 = \frac{l^2}{2m}u'(\varphi)^2 = Eb^2u'(\varphi)^2. \tag{2.66}$$

---

[43] Angular momentum is defined relative to an origin. We have been using the location of q_2 as the origin. However, the angular momentum of the projectile is more easily evaluated relative to a point ($\boldsymbol{s}$ in the $-\hat{z}$ direction) far to the left along the beam pipe, since there, the momentum is known to be in the $\hat{z}$ direction (see Fig. 2.9). It turns out that the angular momenta defined relative to these two different origins are equal! Suppose the incoming particle far to the left has momentum $\boldsymbol{p}$ directed along $\hat{z}$ at a point $\boldsymbol{r}$. We write $\boldsymbol{r} = \boldsymbol{s} + \boldsymbol{b}$ where $\boldsymbol{b}$ is a 'vertical' vector with magnitude equal to the impact parameter. Thus $\boldsymbol{L}_{\text{origin}} = \boldsymbol{r}\times\boldsymbol{p} = \boldsymbol{s}\times\boldsymbol{p}+\boldsymbol{b}\times\boldsymbol{p} = \boldsymbol{b}\times\boldsymbol{p}$ as $\boldsymbol{p}$ and $\boldsymbol{s}$ are antiparallel.

Thus, conservation of energy becomes

$$Eb^2u'(\varphi)^2 = E - Eb^2u^2 - \frac{q_1q_2}{4\pi}u. \tag{2.67}$$

Defining the length $a = q_1q_2/4\pi E$ which is the (hypothetical) radial distance at which the Coulomb potential energy equals the total projectile energy[44] we get

$$d\varphi = \frac{bdu}{\sqrt{1 - b^2u^2 - au}}. \tag{2.68}$$

Now, as shown in Fig. 2.8, the projectile comes in from $r = \infty$ with $\varphi = 0$, reaches a point of closest approach where $r = r_{\min} = 1/u_{\max}$ [$\dot r = 0$, the mid-point of the trajectory, with $\varphi = \varphi_0$. $u_{\max}$ is the positive root of the quadratic in (2.68), $u_{\max} = \left(\sqrt{a^2 + 4b^2} - a\right)/2b^2$] and eventually scatters off to $r = \infty$ reaching an asymptotic $\varphi = 2\varphi_0$. The scattering angle is $\theta = \pi - 2\varphi_0$. The integral can be done by completing the square and a trigonometric substitution using $\int \frac{dx}{\sqrt{1-x^2}} = \arcsin x$,

$$\varphi_0 = \int_0^{u_{\max}} \frac{b\,du}{\sqrt{1 - au - b^2u^2}} = \frac{\pi}{2} - \arcsin\frac{1}{\sqrt{1 + 4b^2/a^2}} \quad\Rightarrow\quad \operatorname{cosec}^2\frac{\theta}{2} = 1 + 4\frac{b^2}{a^2}. \tag{2.69}$$

This is the advertised relation (2.64) between impact parameter and scattering angle for Coulomb scattering. It leads to the Rutherford differential cross section (2.61) upon use of (2.63). We conclude with a few remarks on the Rutherford formula.

1. As observed in Sect. 1.4*, the Coulomb potential $V(r) \propto 1/r$ has a long range. Thus, though the scattering charge q_1 is point-like, its electrostatic force is felt even far from the origin. Incoming charges q_2 with larger impact parameters b suffer smaller deflections θ. Nevertheless, the long-range nature of the potential implies that small scattering angles θ contribute significantly to the total cross section $\sigma = \int(d\sigma/d\Omega)2\pi\sin\theta d\theta$ (see Fig. 2.10). In fact, the total cross section for Coulomb scattering is infinite (see Prob. 2.27) due to a divergence at $\theta = 0$.

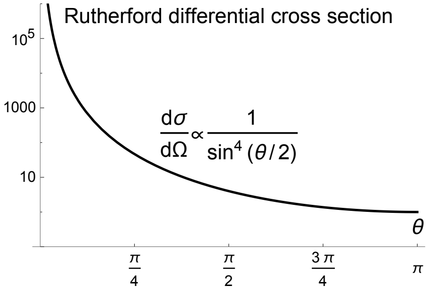

Figure 2.10: Rutherford differential cross section (2.61) in units where $q_1q_2/16\pi E = 1$, as a function of scattering angle showing large contributions from small θ.

---

[44] Except in the case of zero impact parameter, the projectile does not actually get as close as a since it never comes to rest if the conserved angular momentum is nonzero.

2. The cross section (2.61) only depends on the square of each of the charges, so the charges need not have the same sign and an attractive Coulomb potential would give the same differential cross section. The same hyperbolic trajectory applies with q_1 now located at the other focus F' of the hyperbola in Fig. 2.8.
3. As Fig. 2.10 shows, the Rutherford scattering cross section depends strongly on the scattering angle θ, it is *not* isotropic[45]. Moreover, there is nontrivial scattering for large impact parameters b or large angular momenta $l = mvb$. This is to be contrasted with a very short-range potential such as the Yukawa potential $\propto e^{-r/\xi}/r$ with $\xi \ll b$. For such short-range potentials, projectiles with large impact parameters or angular momenta barely feel the force and hardly contribute to the cross section. In a wave mechanical context (as in quantum mechanics or wave optics), in the limit of a very short range potential ($\xi \to 0$), incoming waves with only the lowest angular momentum ($\boldsymbol{L} = 0$) contribute to scattering. A wave with zero angular momentum is termed an S-wave, it is spherically symmetric, i.e., independent of θ and ϕ. When S-wave scattering dominates, the outgoing waves are spherically symmetric, and the cross section $d\sigma/d\Omega$ becomes isotropic.
4. Though the differential cross section decays monotonically as θ goes from 0 to π (decreasing from forward to back scatter), there is still significant scattering through wide angles. The fall-off would be much faster if the repulsive charge were not concentrated at a point-like[46] nucleus but spread out over the atom. This was the experimental signal favoring Rutherford's nuclear model of the atom over Thomson's 'plum pudding' model. Let us indicate why this is the case. The incoming alpha particle (now recognized as a Helium nucleus) is much smaller than the atom. Suppose the positive charge was smeared all over the atom, then its density would be greatly reduced unlike when concentrated in the nucleus. It would also be partly neutralized[47] by the oppositely charged electrons which were thought to be like plums embedded in the pudding of positive charge. Now imagine an α particle passing through this plum pudding atom. Besides being of significantly smaller magnitude, the forces exerted on the α particle by the charges in different parts of this atom would be in different directions and partly cancel out, resulting in far less wide-angle scattering compared to the nuclear model.

*5. The same Rutherford formula arises in nonrelativistic quantum mechanics in the first Born approximation (which is valid at high (nonrelativistic) energies). If $E = \hbar^2 k^2/2m$ is the initial and final kinetic energy (in elastic scattering, the incoming charge just changes direction), then from Fig. 2.11 the magnitude of transferred momentum $\boldsymbol{q} = \boldsymbol{k}_f - \boldsymbol{k}_i = k\hat{r} - k\hat{z}$ is $q = 2k\sin(\theta/2)$ since

$$q^2 = (k\hat{r} - k\hat{z})^2 = 2k^2(1 - \cos\theta) = 4k^2 \sin^2(\theta/2). \qquad (2.70)$$

---

[45] Isotropic means independent of direction, which here would mean independent of θ and ϕ.

[46] The nucleus has a size of 10^{-15}m, which is much smaller than that of the atom $\sim 10^{-10}$m.

[47] The neutralizing electrons are present in the nuclear model too. However, they are spread over the vast expanse of the atom and hardly affect the motion of the α particle when it comes close to the nucleus, just as Pluto has a negligible effect on a comet that is approaching the Sun.

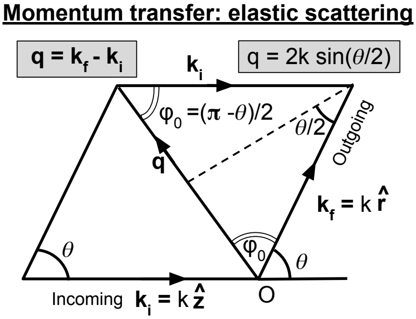

Figure 2.11: Initial and final wave vectors $\boldsymbol{k}_i = \boldsymbol{p}_i/\hbar$ and $\boldsymbol{k}_f = \boldsymbol{p}_f/\hbar$ (directed along $\hat{z}$ and radially outwards) and *momentum transfer* $\boldsymbol{q} = \boldsymbol{k}_f - \boldsymbol{k}_i$ for elastic scattering against a potential in wave mechanics.

The leading order Born scattering amplitude $f(\theta, \phi)$ is proportional to the Fourier transform (see Appendix A.11*) of the potential,

$$f(\theta, \phi) \approx -\frac{2m}{4\pi\hbar^2}\tilde{V}(q) = -\frac{2m}{4\pi\hbar^2}\frac{q_1 q_2}{q^2} = -\frac{q_1 q_2}{16\pi E}\frac{1}{\sin^2(\theta/2)}. \tag{2.71}$$

Here, the Fourier transform[48] is isotropic on account of spherical symmetry

$$\tilde{V}(\boldsymbol{q}) = \int V(\boldsymbol{r}) e^{-i\boldsymbol{q}\cdot\boldsymbol{r}} d\boldsymbol{r} \quad \text{and} \quad V(r) = \frac{q_1 q_2}{4\pi r} \quad \Rightarrow \quad \tilde{V}(q) = \frac{q_1 q_2}{q^2}. \tag{2.72}$$

Finally, the cross section is the absolute square of the scattering amplitude

$$\frac{d\sigma}{d\Omega} = |f|^2 \approx \left(\frac{q_1 q_2}{16\pi E \sin^2(\theta/2)}\right)^2. \tag{2.73}$$

*6. In a relativistic treatment using Feynman diagrams in Quantum Electrodynamics, scattering between a pair of charges is (at leading order) due to exchange of a virtual photon. For example, one may consider electron-muon scattering or electron-proton scattering (so that one of the particles is much heavier than the other and we may ignore its recoil, just as in the α-gold nucleus case.) The calculation is more intricate, but the answer, Mott's cross section (see p.255 of [50]), resembles Rutherford's formula (and reduces to it in the nonrelativistic limit $p \ll mc$ where c is the speed of light). Assuming both particles have a charge of magnitude e,

$$\left[\frac{d\sigma}{d\Omega}\right]_{\text{Mott}} = \left(\frac{e^2}{16\pi(p^2/2m)\sin^2(\theta/2)}\right)^2 \left[1 + \frac{p^2}{m^2c^2}\cos^2(\theta/2)\right]. \tag{2.74}$$

---

[48] The Fourier transform can be got from the knowledge that the electrostatic potential for a point charge e, $\phi = e/4\pi r$ satisfies Poisson's equation $-\boldsymbol{\nabla}^2\phi = \rho = e\delta^3(\boldsymbol{r})$ since $E = -\boldsymbol{\nabla}\phi$ and $\boldsymbol{\nabla}\cdot E = \rho$. Fourier expanding $\phi(r) = \int \tilde{\phi}(q) e^{i\boldsymbol{q}\cdot\boldsymbol{r}}[dq]$ and $\boldsymbol{\nabla}^2\phi(r) = -\int q^2 \tilde{\phi}(q) e^{i\boldsymbol{q}\cdot\boldsymbol{r}}[dq]$ and using $\delta^3(\boldsymbol{r}) = \int e^{i\boldsymbol{q}\cdot\boldsymbol{r}}[dq]$, Poisson's equation gives $\tilde{\phi}(q) = e/q^2$. Here we abbreviated $dq/2\pi = [dq]$.

Here, p is the magnitude of the lab frame momentum of the electron, m its mass and θ the scattering angle. In the nonrelativistic approximation, $p^2/2m$ is simply the kinetic energy E of the incoming electron.

$*7.$ The cross section (2.61) falls off as $1/E^2$ with increase in energy. We could have guessed this from dimensional analysis. The Coulomb potential energy is $q_1 q_2/4\pi r$. Thus, the quantity $q_1 q_2/E$ has dimensions of length and its square has dimensions of area giving the Rutherford cross section its $1/E^2$ behavior. This is a characteristic feature of scattering of point charges at high energies, since the energy is the only dimensional parameter in the problem[49] with which to construct a quantity with dimensions of area (particle masses can be ignored at sufficiently large E and there is no length scale from the dimensions of the point particles). For instance, the cross section for e^+e^- annihilation to any final state has been measured from millions of electron volts to 100s of giga electron volts center of mass energies (see Fig. 5.3, p.145 of [101]). It shows an overall $1/E^2$ fall off with localized peaks at resonant energies where new particles are produced.

2.8* The three-body problem: Euler and Lagrange solutions

Having studied the two-body problem, we now briefly consider the problem of 3 point masses m_1, m_2, m_3 with position vectors $\boldsymbol{r}_a$ $(a = 1, 2, 3)$ moving subject to their mutual gravitational attraction[50]. As mentioned at the end of Sect. 2.1, this is relevant to the Sun-Moon-Earth or Sun-Jupiter-Trojan asteroid systems. Newton's equations of motion are the coupled system of nine 2^{nd} order ODEs:

$$m_a \frac{d^2\boldsymbol{r}_a}{dt^2} = \sum\nolimits_{b\neq a} G m_a m_b \frac{\boldsymbol{r}_b - \boldsymbol{r}_a}{|\boldsymbol{r}_b - \boldsymbol{r}_a|^3} \quad \text{for} \quad a = 1, 2 \text{ and } 3. \tag{2.75}$$

As in the 2-body problem, the total momentum $\boldsymbol{P} = \sum_a m_a \dot{\boldsymbol{r}}_a$, angular momentum $\boldsymbol{L} = \sum_a \boldsymbol{r}_a \times \boldsymbol{p}_a$ and energy

$$E = \frac{1}{2} \sum\nolimits_{a=1}^{3} m_a \dot{\boldsymbol{r}}_a^2 - \sum\nolimits_{a<b} \frac{G m_a m_b}{|\boldsymbol{r}_a - \boldsymbol{r}_b|} \equiv T + V \tag{2.76}$$

are conserved. As a consequence of the conservation of $\boldsymbol{P}$, if $M = m_1 + m_2 + m_3$ is the total mass, the tip of the center of mass vector[51] $\boldsymbol{r}_{\text{CM}} = M^{-1} \sum_a m_a \boldsymbol{r}_a$ must move uniformly along a straight line. At any instant of time, the positions of the three bodies defines a triangle with masses at its vertices. The 'moment of inertia' about the center of mass $I_{\text{CM}} = \sum_a m_a (\boldsymbol{r}_a - \boldsymbol{r}_{\text{CM}})^2$ determines the size of the triangle, which

---

[49] A 'scale invariant' potential [e.g., the Coulomb potential $q_1 q_2/4\pi r$] does not have any length scale of its own. Other potentials may have an associated length scale ξ, in which case the cross section could depend on both E and ξ. An example of non-point-like particle scattering is hadron-hadron scattering. Hadrons such as protons, neutrons and pions have a size (radius) a of order a Fermi and at high energies, the cross section approaches a constant, roughly the classically expected value of $\pi(2a)^2$ where $2a$ is the minimal distance between their centers.

[50] This section is based on [72], which contains additional background and references.

[51] Jacobi vectors [72] generalize the CM and relative vectors to the 3-body problem.

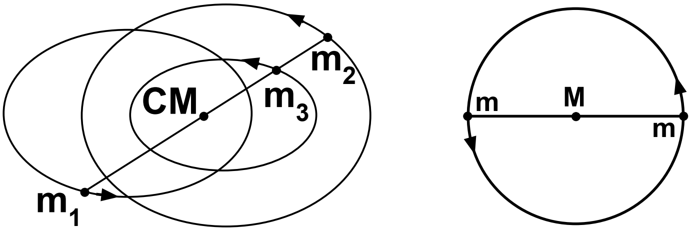

Figure 2.12: Euler collinear periodic solutions of the 3-body problem in frame where the center of mass is at rest. (a) Masses traverse fixed Keplerian ellipses with one focus at the CM. (b) Two equal masses m in a circular orbit centered at a third mass M that lies at their CM.

could change with time. For instance, $I_{\rm CM} \to \infty$ when at least one of the bodies flies off to infinity. The particles suffer a triple collision if $I_{\rm CM} \to 0$.

Unlike in the Kepler problem, the constants of motion are insufficient to integrate the equations of motion in general. Nevertheless, several exact solutions of the 3-body problem are known[52]. The most well-known are those of Euler (1767) and Lagrange (1772), which concern planar motion and are built from Keplerian orbits.

Euler and Lagrange solutions. In the planar 3-body problem, the masses always lie on a fixed plane in a frame that moves with their CM. In Euler's solutions, the masses are collinear, each traversing a Keplerian orbit about their common CM (Fig. 2.12). The line through the masses rotates about the CM with the ratio of interparticle separations remaining constant. The Euler solutions are periodic if the Keplerian orbits are ellipses. In Lagrange's solutions, the masses lie at the vertices of equilateral triangles whose size and angular orientation may vary with time (see Fig. 2.13). In the limiting case of zero angular momentum about the CM, we get Lagrange homotheties: implosion/explosion solutions with 3 masses moving toward/away from their CM along straight lines. Remarkably, in both cases, the force on each mass is always toward the common center of mass and proportional to the distance from it. To see this, consider for instance, the force on m_1 in a proposed Lagrange equilateral solution:

$$\begin{aligned} \boldsymbol{F}_1 &= G m_1 m_2 \frac{\boldsymbol{r}_2 - \boldsymbol{r}_1}{|\boldsymbol{r}_2 - \boldsymbol{r}_1|^3} + G m_1 m_3 \frac{\boldsymbol{r}_3 - \boldsymbol{r}_1}{|\boldsymbol{r}_3 - \boldsymbol{r}_1|^3} \\ &= \frac{G m_1}{d^3} \left(m_1 \boldsymbol{r}_1 + m_2 \boldsymbol{r}_2 + m_3 \boldsymbol{r}_3 - M \boldsymbol{r}_1 \right) \end{aligned} \tag{2.77}$$

where $d = |\boldsymbol{r}_2 - \boldsymbol{r}_1| = |\boldsymbol{r}_3 - \boldsymbol{r}_1|$ is the instantaneous length of the sides of the equilateral triangle. Recalling that $\boldsymbol{r}_{\rm CM} = (m_1 \boldsymbol{r}_1 + m_2 \boldsymbol{r}_2 + m_3 \boldsymbol{r}_3)/M$, we get

$$\boldsymbol{F}_1 = \frac{G m_1}{d^3} M \left(\boldsymbol{r}_{\rm CM} - \boldsymbol{r}_1 \right) \equiv G m_1 \delta_1 \frac{\boldsymbol{r}_{\rm CM} - \boldsymbol{r}_1}{|\boldsymbol{r}_{\rm CM} - \boldsymbol{r}_1|^3} \tag{2.78}$$

---

[52] For instance, the figure-8 'choreography' solution discovered numerically by Chris Moore (1993) is a stable zero angular momentum orbit where three equal masses traverse an ∞-shaped trajectory equally spaced in time. A periodic solution is called a choreography if all masses traverse the same orbit separated equally in time.

where $\delta_1 = M|\boldsymbol{r}_{\rm CM} - \boldsymbol{r}_1|^3/d^3$ is a function of the masses alone[53]. Thus, the equation of motion for m_1,

$$m_1 \ddot{\boldsymbol{r}}_1 = G m_1 \delta_1 \frac{\boldsymbol{r}_{\rm CM} - \boldsymbol{r}_1}{|\boldsymbol{r}_{\rm CM} - \boldsymbol{r}_1|^3}, \tag{2.79}$$

takes the same form as in the two-body Kepler problem. The same applies to m_2 and m_3. A similar analysis applies to the Euler collinear solutions as well.

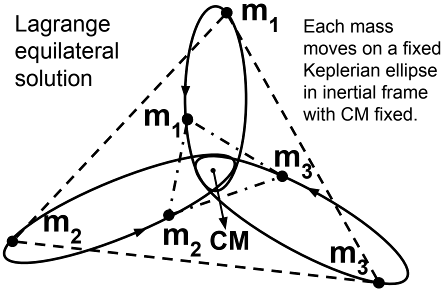

Figure 2.13: Rough sketch of Lagrange's periodic solution with three masses at vertices of equilateral triangles that shrink/expand and rotate. The CM is fixed and lies at a focus of each ellipse. The ratios of interparticle separations are functions of the mass ratios alone.

There is a convenient way of specifying the Euler and Lagrange solutions by identifying the plane of motion with the complex plane $\mathbb{C}$. Let the three complex numbers $z_{a=1,2,3}(t)$ denote the positions of the three masses at time t. For instance, $x_1 = \Re z_1$ and $y_1 = \Im z_1$ are the Cartesian components of the position vector $\boldsymbol{r}_1$ of the first mass. In Lagrange's solutions, $z_a(t)$ lie at vertices of an equilateral triangle while they are collinear in Euler's solutions. We may now summarize what we have found. Suppose $z_a(0)$ denote the initial positions of the masses. Then the curves $z_a(t) = z(t) z_a(0)$ are solutions of Newton's equations for three bodies provided $z(t)$ is a Keplerian orbit for an appropriate two-body problem. In other words, each mass traverses a rescaled Keplerian orbit about the common centre of mass.

We will have more to say about the 3-body problem in Sect. 9.5*, where we consider the special case where one of the bodies is very light compared to the other two (primaries) as happens in the case of the Sun, Jupiter and a Trojan asteroid.

2.9 Problems

1. **Plane polar coordinates.** Consider polar coordinates (r, θ) defined in terms of Cartesian coordinates (x, y) on the plane via $x = r\cos\theta$ and $y = r\sin\theta$. (a) If $\hat{x}$ and $\hat{y}$ are unit vectors in the x and y directions, argue that the unit vectors in the direction of increasing r and θ holding the other fixed are given by $\hat{r} = \cos\theta\,\hat{x} + \sin\theta\,\hat{y}$ and $\hat{\theta} = -\sin\theta\,\hat{x} + \cos\theta\,\hat{y}$. (b) Check that $\hat{r}$ and $\hat{\theta}$ are orthonormal: $\hat{r}\cdot\hat{\theta} = 0$ and $\hat{r}\cdot\hat{r} = \hat{\theta}\cdot\hat{\theta} = 1$. (c) Express $\hat{x}$ and $\hat{y}$ as linear combinations of $\hat{r}$ and $\hat{\theta}$. (d) Unlike $\hat{x}$ and $\hat{y}$ which point in the same direction everywhere, the directions

---

[53] Indeed, $\boldsymbol{r}_{\rm CM} - \boldsymbol{r}_1 = (m_2(\boldsymbol{r}_2 - \boldsymbol{r}_1) + m_3(\boldsymbol{r}_3 - \boldsymbol{r}_1))/M \equiv (m_2 \boldsymbol{b} + m_3 \boldsymbol{c})/M$ where $\boldsymbol{b}$ and $\boldsymbol{c}$ are two of the sides of the equilateral triangle of length d. Using the cosine formula, this leads to $|(\boldsymbol{r}_{\rm CM} - \boldsymbol{r}_1)/d| = \sqrt{m_2^2 + m_3^2 + m_2 m_3}/M$, which is a function of masses alone.

of $\hat r$ and $\hat\theta$ change with location. Suppose a particle has the trajectory given by the position vector $\boldsymbol{r} = x(t)\hat x + y(t)\hat y = r(t)\hat r(t)$. Show that $\dot{\hat r} = \dot\theta\hat\theta$ and $\dot{\hat\theta} = -\dot\theta\hat r$. (e) Show that the velocity of the particle is given by $\boldsymbol{v} = \dot{\boldsymbol{r}}(t) = \dot r\,\hat r + r\,\dot\theta\,\hat\theta$, a sum of radial and azimuthal velocities. (f) Show that the acceleration is given by $\boldsymbol{a} = \dot{\boldsymbol{v}} = (\ddot r - r\dot\theta^2)\hat r + (r\ddot\theta + 2\dot r\dot\theta)\hat\theta$. Interpret the terms in $\boldsymbol{a}$.

2. Suppose $p_x = m\dot x$ and $p_y = m\dot y$ are the Cartesian components of linear momentum of a particle moving on the plane. If $x = r\cos\phi$ and $y = r\sin\phi$, show that the z-component of **angular momentum** $l_z = xp_y - yp_x$ is given by $l_z = mr^2\dot\phi$.
3. Suppose $p_x = m\dot x$, $p_y = m\dot y$ and $p_z = m\dot z$ are the Cartesian components of linear momentum. If $z = r\cos\theta$, $x = r\sin\theta\cos\phi$ and $y = r\sin\theta\sin\phi$, show that the square of **angular momentum** $l^2 = l_x^2 + l_y^2 + l_z^2$ is given by $l^2 = (mr^2)^2(\dot\theta^2 + \sin^2\theta\dot\phi^2)$. Show also that the radial component of linear momentum $\hat r \cdot \boldsymbol{p} = m\dot r$.
4. In **spherical polar coordinates**, (a) show that the angular momentum $\boldsymbol{L}$ of a point particle of mass m can be expressed as $\boldsymbol{L} = mr^2(\dot\theta\hat\phi - \dot\phi\sin\theta\,\hat\theta)$. (b) Show that the z component of its **angular momentum** is $L_z = mr^2\sin^2\theta\,\dot\phi$.
5. **Angular momentum components.** Show that the components of the angular momentum of a particle of mass m can be expressed in spherical coordinates as

$$\begin{aligned} L_z &= mr^2\sin^2\theta\,\dot\phi, \quad L_x = -mr^2\left(\sin\phi\,\dot\theta + \cos\theta\sin\theta\cos\phi\,\dot\phi\right) \quad \text{and} \\ L_y &= mr^2\left(\cos\phi\,\dot\theta - \cos\theta\sin\theta\sin\phi\,\dot\phi\right). \end{aligned} \tag{2.80}$$

6. State the **law of Kepler** that (a) is valid for any central potential and (b) leads most directly to the inverse-square form of the gravitational force. Give brief reasons.
7. **Gradient.** Find the gradient of the scalar field $\phi = 1/\sqrt{x^2 + y^2 + z^2}$ in Cartesian coordinates. Re-express the answer in spherical polar coordinates.
8. Consider the transformation to **CM and relative coordinates** $\boldsymbol{R} = (\mu_1\boldsymbol{r}_1 + \mu_2\boldsymbol{r}_2)$ and $\boldsymbol{r} = \boldsymbol{r}_2 - \boldsymbol{r}_1$. Here, m_1, m_2 are masses of two particles located at $\boldsymbol{r}_1, \boldsymbol{r}_2$, $M = m_1 + m_2$ and $\mu_{1,2} = m_{1,2}/M$. (a) Express the derivatives with respect to $\boldsymbol{r}_1$ and $\boldsymbol{r}_2$ in terms of derivatives with respect to $\boldsymbol{r}$ and $\boldsymbol{R}$. Abbreviating $\boldsymbol{\nabla}_1 = \boldsymbol{\nabla}_{\boldsymbol{r}_1}$, etc., show that $\boldsymbol{\nabla}_1 = -\boldsymbol{\nabla}_{\boldsymbol{r}} + \mu_1\boldsymbol{\nabla}_{\boldsymbol{R}}$ and $\boldsymbol{\nabla}_2 = \boldsymbol{\nabla}_{\boldsymbol{r}} + \mu_2\boldsymbol{\nabla}_{\boldsymbol{R}}$. Hint: Use the chain rule. The fact that these are 3d vectors is not essential. For practice, you could treat them as one dimensional and replace vector gradients by partial derivatives. (b) Show that when acting on functions of $r = |\boldsymbol{r}|$, $\boldsymbol{\nabla}_1 V(r) = -\boldsymbol{\nabla}_{\boldsymbol{r}} V(r)$ and $\boldsymbol{\nabla}_2 V(r) = +\boldsymbol{\nabla}_{\boldsymbol{r}} V(r)$. (c) Newton's 2^{nd} law for masses m_1, m_2 in their mutual gravitational potential are

$$m_1\ddot{\boldsymbol{r}}_1 = -\boldsymbol{\nabla}_1 V(r) \quad \text{and} \quad m_2\ddot{\boldsymbol{r}}_2 = -\boldsymbol{\nabla}_2 V(r) \quad \text{where} \quad V(r) = -\frac{\alpha}{r}. \tag{2.81}$$

   Using integrating factors and previous results, derive a conserved total energy $E = \frac{1}{2}(m_1\dot{\boldsymbol{r}}_1^2 + m_2\dot{\boldsymbol{r}}_2^2) + V(r)$. (d) Find $\boldsymbol{r}_1$ and $\boldsymbol{r}_2$ in terms of $\boldsymbol{R}$ and $\boldsymbol{r}$.
9. **CM and relative variables.** Show that the transformation to CM and relative variables in the problem of two point masses may be expressed as ($\mu_{1,2} = m_{1,2}/M$)

$$\begin{aligned} &\boldsymbol{R} = \mu_1\boldsymbol{r}_1 + \mu_2\boldsymbol{r}_2, \quad \boldsymbol{r} = \boldsymbol{r}_2 - \boldsymbol{r}_1, \qquad \boldsymbol{P} = \boldsymbol{p}_1 + \boldsymbol{p}_2 \quad \boldsymbol{p} = \boldsymbol{p}_2/\mu_2 - \boldsymbol{p}_1/\mu_1 \quad \text{and} \\ &\boldsymbol{r}_1 = \boldsymbol{R} - \mu_2\boldsymbol{r}, \quad \boldsymbol{r}_2 = \boldsymbol{R} + \mu_1\boldsymbol{r}, \qquad \boldsymbol{p}_1 = \mu_1\boldsymbol{P} - \boldsymbol{p}, \quad \boldsymbol{p}_2 = \mu_2\boldsymbol{P} + \boldsymbol{p}. \end{aligned} \tag{2.82}$$

10. **Total energy.** Express the total energy (2.14) of the two-body central force problem as a sum of center of mass and relative energies as in (2.15).

11. **Total and relative angular momenta.** Show that the total angular momentum of a pair of point masses may be expressed as a sum of center of mass and relative angular momenta: $\boldsymbol{r}_1 \times \boldsymbol{p}_1 + \boldsymbol{r}_2 \times \boldsymbol{p}_2 = \boldsymbol{R} \times \boldsymbol{P} + \boldsymbol{r} \times \boldsymbol{p}$.

12. Given that the radius of the Sun is $r_s \approx 7 \times 10^5$ km, make order of magnitude estimates to find whether the CM of the **Sun-Earth system** and the orbit of the Sun lie within the solar interior. Recall that 1 AU $\approx 1.5 \times 10^8$ km, $m_e \approx 6 \times 10^{24}$ kg and $m_s \approx 2 \times 10^{30}$ kg. Hint: The eccentricity of the orbit is very small.

13. **Time-dependence of relative vector.** Evaluate the integral appearing in (2.23) to determine t as a function of radial distance r. Try to invert the expression to find $r(t)$. From this, how would we, in principle, find the azimuthal angle $\phi(t)$?

14. Consider **three point masses** m_e, m_m, m_s with positions $\boldsymbol{r}_e, \boldsymbol{r}_m, \boldsymbol{r}_s$ (relative to a fixed origin of coordinates) that move in 3d space subject to their pairwise gravitational forces. (a) Write Newton's 2nd law equations of motion for $\boldsymbol{r}_e(t), \boldsymbol{r}_m(t)$ and $\boldsymbol{r}_s(t)$. (b) Show that the total linear momentum of the system is conserved.

15. Look for a **scaling symmetry** of the equations of motion of a particle moving in 3d in a $V(r) = -\frac{\alpha}{r^n}$ potential for $n > 0$, similar to the one for the Newtonian potential discussed in (2.51). What we mean is that if $\boldsymbol{r}(t)$ is a solution, then so must $\boldsymbol{s}(t) = \lambda^\gamma \boldsymbol{r}(\lambda t)$ for some γ and for any $\lambda > 0$. Can you find a γ that does the job? Hint: Unit vectors remain unit vectors under rescaling.

16. **Collision trajectories.** Consider a particle of mass m in a $V(r) = -\alpha/r^n$ potential for $n > 0$. It starts at $t = 0$ at a radial distance r_0 with a radially inward directed velocity (≥ 0). Will a collision occur in finite time t_c? Why? If so, find the asymptotic behavior of the radial distance $r(t)$ near the collision time $t \lesssim t_c$.

17. For the **Kepler problem**, find the **time period** $T(E)$ as a function of energy $E < 0$ for the bound elliptical orbits. Show that $T(E)$ diverges as $E \to 0^-$ and find the manner in which it diverges. (a) Proceed without evaluating any integrals, use Kepler's laws and the formulae we have derived. (b) As a second approach, find $T(E)$ by evaluating the integral in (2.23) between suitable limits.

18. Consider the **2-dimensional isotropic harmonic oscillator** with Hamiltonian $H = \frac{1}{2m}(p_x^2 + p_y^2) + \frac{1}{2}m\omega^2(x^2 + y^2)$. (a) Why is it called isotropic? What symmetry does it possess? (b) Write the decoupled equations of motion for x and y. (c) Show that by a suitable choice of origin of time, the general solution to the EOM can be written as $x(t) = A\cos(\omega t)$ and $y(t) = B\cos(\omega t + \varphi)$ where A, B and φ are constants of integration. (d) What is the shape of the trajectory on the x-y configuration plane for $\varphi = 0$? (e) For $\varphi \neq 0$, show that the trajectory lies along an ellipse. Find the equation of the ellipse. (f) Find the principal axes of the ellipse and argue that the trajectory generally defines a fixed direction on the plane and relate it to the phase difference φ. (g) Find the eccentricity of the ellipse. (h) Propose an analog of the LRL vector for the isotropic oscillator. Show that it is conserved. Express the vector in the Cartesian $(\hat{x}, \hat{y})$ as well as in the $(\boldsymbol{r}, \boldsymbol{p})$ basis.

19. Show that the **Laplace-Runge-Lenz vector** $\boldsymbol{A} = \boldsymbol{p} \times \boldsymbol{L} - m\alpha\hat{r}$ may be expressed as a linear combination of $\boldsymbol{r}$ and $\boldsymbol{p}$: $\boldsymbol{A} = 2m\,(H + \alpha/2r)\,\boldsymbol{r} - (\boldsymbol{r} \cdot \boldsymbol{p})\boldsymbol{p}$. Hint: Use the vector identity $\boldsymbol{a} \times (\boldsymbol{b} \times \boldsymbol{c}) = \boldsymbol{b}(\boldsymbol{a} \cdot \boldsymbol{c}) - \boldsymbol{c}(\boldsymbol{a} \cdot \boldsymbol{b})$.
20. **Time to collision.** Evaluate the integrals $\tau_\pm(s) = \int_0^s \sqrt{\sigma/(1 \pm \sigma)}\, d\sigma$ appearing in the time to collision for zero angular momentum (2.54) and (2.55). Hint: Use the substitutions $\sigma = \sinh^2\alpha$ and $\sigma = \sin^2\alpha$.
21. Suppose $y = f(x)$, then $\frac{dx}{dy} = 1/\frac{dy}{dx} = 1/f'(x) = 1/f'(f^{-1}(y))$. Use this to show that $(\operatorname{arcsinh} x)' = 1/\sqrt{1+x^2}$ and deduce [as asserted in (2.54)] that

$$\left(\sqrt{s(1+s)} - \operatorname{arcsinh}\sqrt{s}\right)' = \sqrt{s/(1+s)}. \tag{2.83}$$

22. **Collision time.** Verify the common formula (2.56) for the collision time $t_c(E)$ for head-on collision by using the identity $\arcsin x = -i \operatorname{arcsinh}(ix)$ to combine (2.53) and (2.55). The identity itself may be checked by applying the sine function to either side and using $\sin ix = i \sinh x$.

$*$23. **Hohmann transfer orbit.** A problem of spaceflight is to find ways to launch a spacecraft from the Earth and maneuver it so as to make it reach another planet in an efficient way. The first thing to bear in mind is that any rocket is already in an orbit (the Earth's orbit) around the Sun. One proceeds to adjust this orbit by applying suitable forces to the rocket. Look up the idea of the Hohmann transfer orbit to understand some of the issues involved and how launch windows are determined.

$*$24. **Gravity assist maneuvers.** Look up the principles and techniques involved in gravity assist maneuvers (or gravitational slingshots) that are used in planning the trajectory of a spacecraft on interplanetary missions.

$*$25. **Dissipative process.** Roughly estimate the fractional change in the speed of Jupiter in a head-on inelastic collision with a comet like Shoemaker-Levy 9.

26. Plot the **Rutherford differential cross section** (2.61) as a function of the scattering angle θ in the appropriate range. Give both (a) a Cartesian plot of $d\sigma/d\Omega$ vs θ and (b) a polar plot where the radial distance from the origin is $r(\theta) = d\sigma/d\Omega$. (c) If $x = r\cos\theta$ and $y = r\sin\theta$, then show that the differential cross section can be expressed as the following implicit algebraic relation:

$$y^4 = 16\varsigma(x+\varsigma)(x^2+y^2) \quad \text{where} \quad \varsigma = (q_1 q_2/16\pi E)^2. \tag{2.84}$$

    Plot this curve on the x-y plane and compare with the polar plot of $d\sigma/d\Omega$.

27. Show that the **total cross section** $\sigma = \int_0^\pi (d\sigma/d\Omega)\, 2\pi \sin\theta\, d\theta$ for **Coulomb scattering** diverges due to a nonintegrable singularity in the Rutherford differential cross section at $\theta = 0$.

Chapter 3

Newtonian to Lagrangian and Hamiltonian mechanics

We begin this chapter with some comments on the nature of space and time: simultaneity, causality, homogeneity and isotropy. Bearing in mind the examples from Chap. 1 and Chap. 2, we then introduce the concepts of instantaneous configurations and the number of degrees of freedom of a mechanical system. We then develop several formulations[1] of mechanics starting from Galileo's principle of relativity and Newton's laws. The subsequent formulations are associated with the names of d'Alembert, Maupertuis, Euler, Lagrange, Hamilton, Jacobi and Poisson among others. These different formulations are often equivalent for the simplest of systems, but each affords distinct advantages for special classes of systems. Along the way (and in Appendix B), we will pick up some of the necessary mathematical tools: differential and integral calculus of several variables, ordinary differential equations, the calculus of variations, Lagrange multipliers, differentiable manifolds, vector fields, tensor calculus, some symplectic, Poisson and Riemannian geometry and group theory.

3.1 Time, space, light, simultaneity, causality, homogeneity and isotropy

To describe the dynamics of mechanical systems, observers find it helpful to have a notion of time (measured with a clock) to index a sequence of events. In Newtonian mechanics, one assumes that if there is a flash of light somewhere, then all observers (irrespective of their locations and states of motion) receive the flash instantaneously. In effect, light is assumed to travel infinitely fast. Using such flashes of light, all observers can synchronize their clocks and assign the same time for a given event. Another consequence is that two events (possibly at different locations) that occur at the same time for one observer occur simultaneously for any other observer: we say that simultaneity is absolute rather than relative. These assumptions about light, time and simultaneity were in line with common human experience in Newton's time (as well as today!). In Newtonian mechanics, one also assumes that masses of particles[2], scales of length and time are the same for all observers. In other words, distances (like the length of a meter stick) and time intervals (like that between two ticks on a clock) are the same for all observers.

Our experience with physical systems indicates that they respect the principle of *causality*: cause precedes effect. For example, a stone that is stationary is seen to move only when a force is applied to it. The principle of causality postulates that it is not possible to send a signal from an event to its past. Given our Newtonian concept of time, all observers have a common notion of the past and future of an event. The future of an event that occurs at time t_0 consists of all events that occur at $t > t_0$ and the past consists of events that occurred at $t < t_0$.

---

[1] By the formulation of a mechanical system we primarily mean obtaining the equations of motion and understanding some of their structural features as opposed to *solving* the EOM. Of course, a formulation of a system may also suggest a method of solution.

[2] In Sect. 3.3, we will indicate how masses can be assigned to bodies.

These notions of time, simultaneity and universality of masses, space and time intervals had to be replaced with more accurate concepts (see Chap. 4) in the special theory of relativity, where speeds of bodies or observers could be comparable to that of light, which is a large but finite constant in vacuum ($c \approx 3 \times 10^8$ m/s). Nonrelativistic mechanics is a limiting case where the speed of light is very large compared to other speeds. The principle of causality continues to apply in special relativity, though the notions of past and future needed to be revised.

From observing and experimenting with mechanical phenomena in nature, we deduce that space and time possess some symmetries. Space is *homogeneous*, which means that given identical external conditions, the results of mechanical experiments do not depend on where they are performed. In addition, *space is isotropic* in the sense that there is no distinguished direction at any given location. In other words, rotating an experimental apparatus does not change the results of experiments, provided external conditions are identical. Finally, we have the *homogeneity of time*: for the same external conditions, results of mechanical experiments do not depend on when they are performed. In this sense, results of experiments are found to be reproducible. The laws/principles/equations of mechanics that we will introduce in Sect. 3.3 will have to incorporate these observations of homogeneity and isotropy.

3.2 Degrees of freedom and instantaneous configurations

A point particle moving in a central force field in three-dimensional space has three *degrees of freedom*, we need three coordinates to specify the location of the particle at any instant of time (and in particular at the initial time, say $t = 0$). The number of degrees of freedom is the dimension of the space of possible instantaneous locations of the particle. The number of degrees of freedom does not depend on the nature of forces. So a free particle moving in three-dimensional space also has three degrees of freedom. On the other hand, a bead that is constrained to move along a fixed wire (say, because the wire passes through the bead) has only one degree of freedom if it is not allowed to spin. A particle constrained to move on a fixed spherical surface (such as a bob at the end of a rigid rod whose other end is attached to a pivot) has only two degrees of freedom. These two are examples of so-called holonomic constraints: for a particle moving in 3d Euclidean space, a constraint of the form $C(x, y, z, t) = 0$ is called a holonomic constraint (see Footnote 30 for more on this). We see that each such constraint reduces the number of degrees of freedom by one. Two point masses moving in three dimensional space (e.g., the Sun and the Earth[3]) have six degrees of freedom (see Sect. 2.2). One does not need to know about the nature of trajectories to count the number of degrees of freedom. A fluid consisting of $N \sim 10^{24}$ molecules in a bucket has a very large number[4] of degrees of freedom, which can be taken to be the $3N$ Cartesian coordinates needed to specify the locations of the N molecules, treated as point masses. An *instantaneous configuration* of a system of two point particles is any possible location of the two particles. The set of all instantaneous configurations of a mechanical system is called its configuration space $\mathcal{Q}$. For a pair of point particles moving in three dimensions ($\mathbb{R}^3$), $\mathcal{Q}$ is the space (more accurately, *manifold*, see Appendix B.1) $\mathbb{R}^6$ with coordinates given, for instance, by the Cartesian components of the positions of each of the particles x_1^i, x_2^j for $i, j = 1, 2, 3$. Conventionally, the component indices on coordinates on $\mathcal{Q}$ are denoted by superscripts. The number of degrees of freedom is the dimension of the configuration space. It is important to bear in mind that $\mathcal{Q}$ is in general *not* a linear space and typically cannot be given the structure of a vector space[5]. For a particle constrained to move on the surface of a sphere embedded in three-dimensional Euclidean space, the configuration space is the so-called two-sphere, denoted S^2 (see Fig. 3.1). The latter is not a vector space, we do not have a notion of 'adding' points on the sphere to get points on the sphere.

---

[3] Here we do not restrict to a particular orbit of the Earth around the Sun (treated as point masses) but ask how many coordinates are needed to specify all possible initial locations of the Sun and the Earth *prior* to solving Newton's equations of motion.

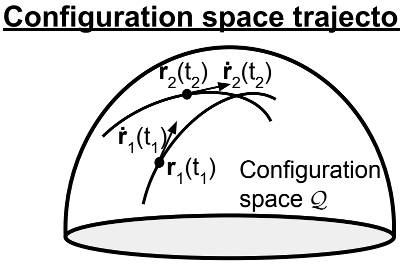
Configuration space trajectories
$\mathbf{r}_2(t_2)$
$\dot{\mathbf{r}}_2(t_2)$
$\dot{\mathbf{r}}_1(t_1)$
$\mathbf{r}_1(t_1)$
Configuration space $\mathcal{Q}$

Figure 3.1: Configuration space $\mathcal{Q}$ with two trajectories $\boldsymbol{r}_1(t)$ and $\boldsymbol{r}_2(t)$ indicated. A velocity vector such as $\dot{\boldsymbol{r}}_1(t_1)$ is a tangent vector to the trajectory and lives in the tangent space (plane) to $\mathcal{Q}$ at the point $\boldsymbol{r}_1(t_1)$. Trajectories on $\mathcal{Q}$ *can* intersect. The configuration space is generally not a linear space, we cannot add configurations. However, we *can* add two tangent vectors lying in the *same* tangent space, such as at an intersection of trajectories.

3.3 Newton's laws and Galileo's relativity and equivalence principles

Zeroth law of classical mechanics. The *zeroth law of mechanics* can be regarded as saying that the trajectory $\boldsymbol{r}(t)$ of a particle is a (twice) differentiable function of time. This not an assumption but rather an assertion about natural phenomena, deduced by observing the motion of terrestrial and celestial bodies. This assertion applies to the motion of planets, pendulum bobs, golf balls, etc. However, it fails for Brownian motion (movement of pollen grains in water, which are observed to follow very jagged paths due to frequent collisions with water molecules, so that it is not useful to try to model the trajectory of a pollen grain via a twice differentiable function $\boldsymbol{r}(t)$, see

---

[4] A fluid is often treated as a *field*, i.e., as a system with infinitely many degrees of freedom. Scalar and vector fields are introduced in Appendix B while some physical fields are studied in Chap. 16 - Chap. 19.

[5] A real vector space is a set of vectors $\boldsymbol{v}, \boldsymbol{w}, \ldots$ that is closed under linear combinations, i.e., $\alpha\boldsymbol{v} + \beta\boldsymbol{w}$ is also a vector for any real numbers α, β. In other words, we may add vectors and multiply them by real scalars.

Sect. 18.4.1). It also fails for electrons in an atom, which require a quantum mechanical treatment. The quantum mechanical analog of this zeroth law may be viewed as saying that the wave function or propagator (time evolution operator) is a (once) differentiable function of time.

Isaac Newton proposed three laws[6] of classical mechanics in his Principia (1687).

Newton's 1^{st} law. Newton's 1^{st} law, or the law of inertia, says that "Every body continues in its state of rest, or of uniform motion in a straight line, unless it is compelled to change that state by a force impressed upon it" [92,98]. In other words, the velocity $\boldsymbol{v} = \dot{\boldsymbol{r}}$ or momentum $\boldsymbol{p} = m\boldsymbol{v} = m\dot{\boldsymbol{r}}$ of a particle that is free[7] (isolated or far from physical interactions) does not change with time. The mass $m > 0$ of a particle is an intrinsic[8] attribute of the particle (like its charge) and is postulated to be independent of time and the frame of reference (we will say more on frames of reference shortly). It is customary to use subscripts for the components of momentum $\boldsymbol{p} = (p_1, p_2, p_3)$ for reasons that will be explained in Sect. 3.7.

$*$ **Quantum version of Newton's 1^{st} law.** The quantum mechanical analog of Newton's first law is that the propagator (time evolution operator) of a free particle is a Gaussian. Gaussian propagators replace straight lines in the quantum theory:

$$U(\boldsymbol{r}', t'; \boldsymbol{r}, t) = \left(\frac{m}{ih(t-t')} \right)^{3/2} \exp\left[\frac{im|\boldsymbol{r} - \boldsymbol{r}'|^2}{2\hbar(t-t')} \right]. \tag{3.1}$$

Briefly, U gives the probability amplitude (its absolute square is the probability) for a free particle of mass m to go from location $\boldsymbol{r}$ at time t to $\boldsymbol{r}'$ at time t'. Here $h = 2\pi\hbar$ is Planck's constant. □

We have been a bit imprecise in our discussion of Newton's first law. Newton's first law as well as its quantum version hold only in certain coordinate frames. To specify the components of the position and velocity vectors, we need a frame of reference, i.e., an origin and coordinate axes. It is found that a particle that is not subject to any forces (i.e., an isolated body) could fail to follow a constant velocity trajectory in certain reference frames. A frame in which Newton's first law holds is said to be an inertial frame. To a reasonable approximation (if one ignores some effects of the rotation of the Earth), a frame that is fixed in a tennis court on Earth is an inertial frame for the motion of tennis balls and racquets. In particular, if the effects of gravity and friction may be neglected, then tennis balls in this frame would always move uniformly in a straight line[9]. However, it is found that Newton's first law for tennis balls fails to hold in a frame that is attached to a swinging pendulum or a rotating merry-go-round beside the tennis court. Such frames are called accelerated or noninertial. For instance, a frame which rotates and whose origin moves around irregularly in a faraway spaceship is not inertial, since a free particle at rest in the same spaceship would appear to move in a nonuniform manner. Similarly, a frame that is attached to and participates in the rotational motion of a top that spins on the floor of the spaceship is noninertial (more on this in Sect. 8.11). We will remark upon motion in inertial and noninertial frames in more detail in Sect. 3.12 and Chap. 9. Henceforth, unless otherwise stated, all quantities will be specified with respect to an inertial frame of reference. To summarize, Newton's first law is the assertion that there is a frame of reference (called an inertial frame) in which all isolated bodies (far from physical interactions) move at constant velocity. As we will see shortly, the principle of relativity enunciated by Galileo implies that an inertial frame is not unique.

---

[6] It is noteworthy that Newton had more than three laws in his manuscript *De motu corporum in mediis regulariter cedentibus* that he wrote a couple of years before his *PhilosophiæNaturalis Principia Mathematica*. Some postulates/laws, such as a version of the principle of relativity were later demoted to corollaries of what we now call his three laws of motion.

[7] It is found that macroscopic physical interactions (gravitational, electric, magnetic) tend to decrease with separation, so it is possible to isolate a particle by taking it far from other bodies.

[8] By intrinsic attribute, we mean a property that does not depend on its state of motion, unlike the speed or position of a particle.

[9] It is possible to (essentially arbitrarily) reduce the effects of gravity and friction in some

Newton's 2^{nd} law. The departure from rest or uniform motion along a straight line (in an inertial frame) is caused by forces. For example, tugging at a string that is attached to a ball exerts a force on the ball and makes it accelerate. Forces typically arise from interactions between objects. The Earth exerts a force on a ball that is released from rest, making it accelerate downwards. Newton's 2^{nd} law says that in an inertial frame, the rate of change of momentum is equal to the impressed force. For a single particle, the acceleration $\ddot{\boldsymbol{r}}$ that results from a force $\boldsymbol{F}$ that causes the particle to move along the trajectory $\boldsymbol{r}(t)$ is determined by the equation

$$m\ddot{\boldsymbol{r}} = \boldsymbol{F} \quad \text{or} \quad \dot{\boldsymbol{p}} = \boldsymbol{F}. \tag{3.2}$$

The trajectory is a directed curve on configuration space, parametrized by increasing time (see Fig. 3.1). Velocities such as $\boldsymbol{v}(t) = \dot{\boldsymbol{r}}$ are tangent vectors to the trajectory and at a given time t, lie in the tangent space to the configuration space at $\boldsymbol{r}(t)$.

Assignment of masses. The time-independent positive real number m is a property of each body called its inertial mass or mass for short. Newton's 2^{nd} law gives a way of assigning inertial masses to bodies. We begin by selecting a reference body A and choose units in which its mass is assigned the value 1. We apply a force to A (e.g., let a compressed spring push it), and record its acceleration $\boldsymbol{a}_A$. Given body B whose mass we wish to determine, we apply the same force to it, and measure its acceleration $\boldsymbol{a}_B$. Then we assign the mass $m_B = |\boldsymbol{a}_A|/|\boldsymbol{a}_B|$. □

In *Cartesian coordinates*, the trajectory is given by $\boldsymbol{r}(t) = (x^1, x^2, x^3) = (x, y, z)$ and Newton's second law becomes $m\ddot{x}^i = F^i$. This component form of Newton's equation changes in curvilinear coordinates, such as spherical polar coordinates (i.e.,

---

cases. Consider the horizontal motion of a ball on a ping-pong table placed in the tennis court. A ball that starts out at rest on the table is seen to remain at rest. A ping-pong ball that starts out rolling on the table continues to roll in the same direction though it is seen to slow down. We attribute this to friction with the surface. The magnitude of this frictional force depends on the weight of the ball, but by polishing the surface and ball we may reduce the effect of friction and find that the ball maintains its velocity for a long time. In this way, we arrive at a body that is essentially free in so far as its horizontal motion is concerned. Its uniform motion is evidence in favor of the inertial nature of a frame fixed to the Earth.

it does not simply say $m\ddot{r} = \boldsymbol{F} \cdot \hat{r}$, etc.). For instance, there could be terms involving products of first derivatives of coordinates in addition to naive second derivative 'acceleration' terms, as is the case in plane polar coordinates (see Prob. 2.1):

$$m(\ddot{r} - r\dot{\theta}^2) = \boldsymbol{F} \cdot \hat{r} \quad \text{and} \quad m(r\ddot{\theta} + 2\dot{r}\dot{\theta}) = \boldsymbol{F} \cdot \hat{\theta}. \tag{3.3}$$

One may transform the equation from Cartesian coordinates to the desired system to find the form it takes. We will say more about this in Sect. 3.8.

The force is generally a vector field $\boldsymbol{F}(\boldsymbol{r})$, it could depend on the location of the particle. To begin with, $\boldsymbol{F}(\boldsymbol{r})$ may not be known to us. So we measure accelerations of particles and deduce what $\boldsymbol{F}(\boldsymbol{r})$ might be. This is called the inverse problem. Having done this to our satisfaction, we make predictions for what a given particle may do when subjected to this force field, by solving Newton's equation with prescribed initial conditions. This is the direct problem of finding trajectories given a force field. We then compare these predicted trajectories with new observations to validate our understanding of the force field. If discrepancies are found, we may need to revise our formula for the force field (or incorporate ignored effects like relativistic or quantum ones). Thus, one goes back and forth between the inverse and direct problems.

Linear superposition of forces. Suppose a particle is acted upon by two forces $\boldsymbol{F}_1$ and $\boldsymbol{F}_2$ (say gravitational and frictional). Then according to the *superposition principle*[10], the total force $\boldsymbol{F}$ on the particle or *resultant* of the two forces is the vector sum $\boldsymbol{F} = \boldsymbol{F}_1 + \boldsymbol{F}_2$. This is to be expected from Newton's 2nd law: acceleration is a vector so force too must be a vector subject to the parallelogram law of addition. Though we state the superposition principle separately, as it is very useful and has been empirically tested, Newton deduced the parallelogram law for forces as Corollary 1 to his laws. On the other hand, suppose a composite body is made up of several constituent parts (e.g., a rigid body made of several point masses). Then the total force on the composite body is the vector sum of the forces on its constituents. □

Galileo's relativity principle. Notice that Newton's 2nd law relates the force to the *second derivative* of position along a trajectory, as opposed to the first, third or other derivative. This is in part to incorporate Galileo's relativity principle [42] which says roughly that there is no dynamical way of telling if a frame is at rest or moving uniformly relative to an inertial frame. In 1632, Galileo Galilei observed that it was not possible to detect the uniform motion (constant velocity motion without rocking) of a ship relative to the shore by performing mechanical experiments[11] under the deck of the ship (i.e., without referring to forces external to the ship or looking out, for instance). This is elevated to the principle of Galilean relativity, which states that the laws of mechanics[12] must hold in one inertial frame iff (if and only if) they hold in any other, or equivalently, that they take the same mathematical form in a frame that moves uniformly relative to an inertial frame (see Sect. 3.12 for more on this). In Galilean relativity, it is assumed that (a) the mass of a particle is the same in two frames that are in uniform relative motion, (b) both observers use the same scale for measuring distances and (c) both observers agree on the time interval between any pair of events. In other words, uniformly moving measuring sticks have the same length as when they are observed at rest and a clock that is moving at a constant velocity neither slows down nor speeds up relative to a clock at rest.

---

[10] We do not have a linear superposition principle for *solutions* of Newton's equation. For example, suppose $m\ddot{\boldsymbol{r}}_1 = \boldsymbol{f}_1(\boldsymbol{r}_1)$ and $m\ddot{\boldsymbol{r}}_2 = \boldsymbol{f}_2(\boldsymbol{r}_2)$ are trajectories in the presence of individual forces. Then putting $\boldsymbol{r} = \boldsymbol{r}_1 + \boldsymbol{r}_2$, we get $m\ddot{\boldsymbol{r}} = \boldsymbol{f}_1(\boldsymbol{r}_1) + \boldsymbol{f}_2(\boldsymbol{r}_2)$. However, the latter is generally *not* equal to the vector field $\boldsymbol{f}_1 + \boldsymbol{f}_2$ evaluated at $\boldsymbol{r}_1 + \boldsymbol{r}_2$. So we cannot in general 'add' trajectories in the presence of separate forces to get a trajectory when both forces are present. Bonnet's theorem [72] gives an interesting alternative: a curve that is a trajectory in two separate force fields, is also a trajectory in the presence of both. However, argue that we cannot, generally, linearly superpose solutions to Newton's equation in a given force field to get other solutions in the same force field (see Prob. 3.7). Weaker superposition principles do apply in special cases: one may asymptotically superpose soliton solutions in certain one-dimensional integrable systems [32].

With these assumptions, the appearance of acceleration $\ddot{\boldsymbol{r}}$ (rather than velocity $\dot{\boldsymbol{r}}$) in Newton's 2^{nd} law can be motivated. It ensures that when referred to a frame K' moving at constant velocity $\boldsymbol{u}$ relative to an inertial frame K, Newton's 2^{nd} law takes the same form for a system of (possibly interacting) bodies. For example, suppose the frames coincide at $t = 0$ so that $\boldsymbol{r}' = \boldsymbol{r} - \boldsymbol{u}t$. Then $\ddot{\boldsymbol{r}} = \ddot{\boldsymbol{r}}'$ and the equation for a free particle is the same in both frames: $m\ddot{\boldsymbol{r}} = 0$ and $m\ddot{\boldsymbol{r}}' = 0$. So a particle is free in one frame iff it is free in the other. Similarly, Newton's second law for a pair of particles subject to forces that depend on their separation,

$$m\ddot{\boldsymbol{r}}_1 = \boldsymbol{F}_{2\text{ on }1}(|\boldsymbol{r}_1 - \boldsymbol{r}_2|) \quad \text{and} \quad m\ddot{\boldsymbol{r}}_2 = \boldsymbol{F}_{1\text{ on }2}(|\boldsymbol{r}_2 - \boldsymbol{r}_1|) \tag{3.4}$$

takes the same form in frame K' with $\boldsymbol{r}_{1,2}$ replaced with $\boldsymbol{r}'_{1,2}$ since

$$\boldsymbol{r}_1 - \boldsymbol{r}_2 = \boldsymbol{r}'_1 + \boldsymbol{u}t - \boldsymbol{r}'_2 - \boldsymbol{u}t = \boldsymbol{r}'_1 - \boldsymbol{r}'_2. \tag{3.5}$$

The velocity $\boldsymbol{u}$ cancels out from the difference in position vectors and makes no appearance in the equation of motion in K'. It also cancels out from the difference in velocity vectors $\dot{\boldsymbol{r}}_1 - \dot{\boldsymbol{r}}_2$, so the same conclusion also applies to interparticle forces, such as friction, that depend on relative velocities. Thus, Newton's second law implies that (a) projectiles move in exactly the same way when observed in two frames in uniform relative motion (ignoring a possible variation of the external gravitational acceleration) and (b) a brick sliding on a plank subject to friction displays the same dynamics irrespective of whether the experiment is performed below the deck of a docked ship or a uniformly moving ship.

On the other hand, Newton's 2^{nd} law for a particle subject to an *external* force $m\ddot{\boldsymbol{r}} = \boldsymbol{F}(\boldsymbol{r})$ is *not* the same in the two frames. It becomes $m\ddot{\boldsymbol{r}}' = \boldsymbol{F}(\boldsymbol{r}' + \boldsymbol{u}t)$ in K'. The appearance of $\boldsymbol{u}$ in this frame would mean that one could find out which frame corresponds to the moving ship and which to the docked ship. For instance, variation in the acceleration due to gravity at different locations could be used to determine that the experiment was performed in a moving ship rather than at a fixed location on the shore. This does not violate Galileo's principle of relativity since the latter is not concerned with forces external to the lab on the ship.

---

[11] These experiments could include observing the motion of projectiles (e.g., how long it takes for a ball thrown horizontally at a given speed to reach a wall), the manner in which water drips from a jug, how flies and fish move and so on. Thus, the relative motion of bodies is the same whether observed on a docked ship or on a uniformly moving ship.

[12] Galileo's principle of relativity continues to hold in special relativity, see Sect. 4.2. To accommodate the constancy of the speed of light, Einstein modified the transformation rule that relates coordinates in two frames that are in uniform motion relative to each other, see Sect. 4.4.

Furthermore, if Newton's 2^{nd} law for a particle involved velocity instead of acceleration, say $\nu\dot{\boldsymbol{r}} = \boldsymbol{G}$ for some constant ν, then in a frame moving at velocity $\boldsymbol{u}$, the equation for a free particle would become $\nu(\dot{\boldsymbol{r}}' + \boldsymbol{u}) = 0$. The appearance of $\boldsymbol{u}$ gives this equation a different form from the one in K ($\nu\dot{\boldsymbol{r}} = 0$) and would allow us to determine the velocity $\boldsymbol{u}$ of the frame relative to K and thereby tell the frames apart, in violation of Galileo's principle. Relating the force to the second derivative of position [as opposed to, say, the third derivative of $\boldsymbol{r}(t)$] is the simplest way of incorporating Galileo's principle. This appeal to simplicity is referred to as the principle of parsimony or Occam's razor. Fortunately, experiments and observations confirm that Newton's 2^{nd} law accurately describes both terrestrial and celestial mechanical phenomena (motion of projectiles, planets and so forth). Moreover, inclusion of higher time derivatives in Newton's equation would generally lead to violations of Newton's 1^{st} law: force-free motion of particles would not necessarily be at constant velocity (see Prob. 3.6). Thus, we do not include higher time derivatives in Newton's 2^{nd} law, although they would not violate Galileo's principle.

Note that the left member of Newton's equation $m\ddot{\boldsymbol{r}} = \boldsymbol{F}$ cannot include a term that depends explicitly on the particle's position, such as $\lambda\boldsymbol{r}$ for some constant λ. This would violate Newton's 1^{st} law: free particles would not always follow straight line trajectories with constant speed. It would also violate the *homogeneity of space* (see Sect. 3.1), which states that given identical external conditions, the results of mechanical experiments do not depend on where they are performed. In fact, the laws of mechanics must also respect the *isotropy of space* (the angular orientation of a frame of reference has no dynamical significance) and *homogeneity of time* (for the same external conditions, results of mechanical experiments do not depend on when they are performed). Taken together, we postulate that the laws of mechanics must be Galilean invariant (invariant under space-time translations, rotations and 'boosts' to frames in uniform motion, see Sect. 3.12).

Work done by a force. As in one dimension (see Sect. 1.1), we have the notion of the work done by a force. Suppose the particle is moved from $\boldsymbol{a}$ to $\boldsymbol{b}$ along a configuration space path $\gamma(s) : [0,1] \to \mathcal{Q}$, then the work done by the force $\boldsymbol{F}(\boldsymbol{r})$ is defined as the line integral [see (B.51)]

$$W(\gamma) = \int_\gamma \boldsymbol{F}\cdot\, d\gamma = \int_0^1 \boldsymbol{F}\cdot\dot{\gamma}\, ds. \tag{3.6}$$

Note that γ need not be a trajectory and s is simply a parameter along the curve, it need not be time (the special case of a trajectory is, of course, interesting). In general, this work depends on the path γ and not just on the endpoints $\gamma(0) = \boldsymbol{a}$ and $\gamma(1) = \boldsymbol{b}$. However, there is a special class of forces where this work depends only on the endpoints. In fact, suppose the force field is given by the negative gradient of a potential function $\boldsymbol{F}(\boldsymbol{r}) = -\boldsymbol{\nabla} V(\boldsymbol{r})$. Then the work done by such a 'conservative' force is

$$W(\gamma) = -\int_0^1 \boldsymbol{\nabla} V \cdot \frac{d\gamma}{ds} ds = -\int_0^1 \frac{dV(\gamma(s))}{ds} ds = V(\boldsymbol{a}) - V(\boldsymbol{b}), \qquad (3.7)$$

which is seen to be the drop in the potential. Notice that we did not use Newton's equation of motion, so γ need not be a trajectory. Many interesting forces such as the gravitational force, the electrostatic force and the simple harmonic restoring force (but not friction, see (1.4)) are conservative. For such conservative forces, the sum of kinetic and potential energies, $E = \frac{1}{2}m\dot{\boldsymbol{r}}^2 + V(\boldsymbol{r})$ is conserved along trajectories ($\dot{E} = 0$), as shown in (1.2) and in Prob. 1.3. This total energy may also be expressed in terms of momentum rather than velocity: $E = \boldsymbol{p}^2/2m + V(\boldsymbol{r})$. In the latter form, the energy is also called the Hamiltonian.

Work in terms of kinetic energy. Interestingly, even if the force is not conservative, the work done by the force *along a trajectory* can be expressed as the increase in kinetic energy $\frac{1}{2}m\boldsymbol{v}^2$. Indeed, suppose $\boldsymbol{\gamma} = \boldsymbol{r}(t)$ for $t_a \leq t \leq t_b$ is a trajectory from $\boldsymbol{a}$ to $\boldsymbol{b}$, then using Newton's second law,

$$\begin{aligned} W(\gamma) &= \int_{t_a}^{t_b} \boldsymbol{F} \cdot \frac{d\boldsymbol{r}}{dt}\, dt = \int \frac{d\boldsymbol{p}}{dt} \cdot \boldsymbol{v}\, dt = \int \frac{d(m\boldsymbol{v})}{dt} \cdot \boldsymbol{v}\, dt \\ &= \int m\boldsymbol{v} \cdot d\boldsymbol{v} = \int \frac{1}{2} m d(\boldsymbol{v}^2) = \frac{1}{2} m \boldsymbol{v}_{\boldsymbol{b}}^2 - \frac{1}{2} m \boldsymbol{v}_{\boldsymbol{a}}^2. \qquad (3.8) \end{aligned}$$

This result is called the *work-energy theorem or principle*[13]. When applied to a conservative force, it may be used to deduce the conservation of energy. Indeed, equating (3.7) and (3.8), we find that $\frac{1}{2}m\boldsymbol{v}_{\boldsymbol{a}}^2 + V(\boldsymbol{a}) = \frac{1}{2}m\boldsymbol{v}_{\boldsymbol{b}}^2 + V(\boldsymbol{b})$. Since $\boldsymbol{a}$ and $\boldsymbol{b}$ are arbitrary points along a trajectory, we conclude that the sum of kinetic and potential energies must be a constant of the motion.

d'Alembert's principle. This consequence of Newton's 2nd law was formulated by Jean d'Alembert (1758) [81, 117]. Consider a system of particles labelled by $a = 1, \ldots, N$, with positions $\boldsymbol{r}_a$, masses m_a and subject to forces $\boldsymbol{F}_a$. Then $\boldsymbol{F}_a - m_a\ddot{\boldsymbol{r}}_a = 0$ for each a. By analogy with the true forces $\boldsymbol{F}_a$, the mass × acceleration terms on the left are called inertial forces. Suppose the particles are infinitesimally displaced by $\delta\boldsymbol{r}_a$. Dotting with these 'virtual displacements' and adding, we get

$$\sum\nolimits_a \boldsymbol{F}_a \cdot \delta\boldsymbol{r}_a - \sum\nolimits_a m_a \ddot{\boldsymbol{r}}_a \cdot \delta\boldsymbol{r}_a = 0. \qquad (3.9)$$

The two terms may be interpreted as the work done by true and inertial forces. If the particles are subject to some constraints, (e.g., that the bob of a pendulum must be at a fixed distance from the support), then the forces may be written as a sum of 'applied' and constraint forces: $\boldsymbol{F}_a = \boldsymbol{F}_a^{\text{applied}} + \boldsymbol{F}_a^{\text{constraint}}$. However, as d'Alembert noticed, if the virtual displacements respect the constraints, then $\boldsymbol{F}_a^{\text{constraint}} \cdot \delta \boldsymbol{r}_a = 0$ for each a. Thus, we arrive at d'Alembert's principle, which says that along a trajectory, the difference between the 'virtual work' done by applied and inertial forces must vanish:

---

[13] Let us contrast this with formula (3.7) for the work done by a conservative force, which depends only on the difference in potential energies at the endpoints of a trajectory. Despite appearances, the RHS of (3.8), (where we make no assumption about the force being conservative) generally depends on the trajectory and not just the endpoints $\boldsymbol{a}$ and $\boldsymbol{b}$. In fact, the kinetic energies at $\boldsymbol{a}$ and $\boldsymbol{b}$ depend on the *velocities* at $\boldsymbol{a}$ and $\boldsymbol{b}$. As we will soon learn, the specification of initial position and velocity is enough to determine an entire trajectory.

$$\sum_a \boldsymbol{F}_a^{\text{applied}} \cdot \delta \boldsymbol{r}_a - \sum_a m_a \ddot{\boldsymbol{r}}_a \cdot \delta \boldsymbol{r}_a = 0, \tag{3.10}$$

provided the virtual displacements are in harmony with the constraints. d'Alembert's principle is a generalization of the so-called *principle of virtual work*: in static equilibrium, the virtual work done by applied forces must vanish. By viewing the acceleration term as another 'inertial' force, problems of dynamics are made to look like problems of static equilibrium. Notably, the applied forces need not be conservative. Nevertheless, when they are conservative, d'Alembert's principle can be used to obtain Hamilton's principle of extremal action. We shall do this in Sect. 3.5. Applications of the principle of virtual work and d'Alembert's principle may be found in [117].

$*$ **Schrödinger's equation.** A quantum counterpart of Newton's evolution equation is Schrödinger's equation[14] for the time evolution of the propagator $U(t,t')$, which is a linear operator on the linear space of quantum states (see Sect. 10.3*). Forces enter through the potential in the Hamiltonian, e.g., $H = \frac{\boldsymbol{p}^2}{2m} + V(\boldsymbol{r})$ with $\boldsymbol{p} = -i\hbar\boldsymbol{\nabla}$:

$$i\hbar \frac{\partial U(t,t')}{\partial t} = HU(t,t') \quad \text{with} \quad U(t',t') = I. \tag{3.11}$$

The propagator evolves the state vector forward in time from t' to t: $U(t,t')|\psi(t')\rangle = |\psi(t)\rangle$. For a free particle, V is a constant and the solution for the propagator reduces to the Gaussian (3.1). □

Equivalence principle. Unlike the inertial mass m_i in Newton's 2^{nd} law $\boldsymbol{F} = m_i \boldsymbol{a}$, the masses that appear in Newton's law of gravity $\boldsymbol{F}_{2 \text{ on } 1} = G m_{1g} m_{2g} (\boldsymbol{r}_2 - \boldsymbol{r}_1)/|\boldsymbol{r}_2 - \boldsymbol{r}_1|^3$ (2.5) are called the gravitational masses. Let us focus on the gravitational force of the Earth on small bodies near its surface. At the surface of the Earth, the force on a gravitational mass m_g is $\boldsymbol{F} = -G M_e m_g \hat{r}/R_e^2$ where M_e is the gravitational mass of the Earth and R_e its radius. The acceleration due to gravity of the body is then $\boldsymbol{g} = \boldsymbol{F}/m_i = -G M_e (m_g/m_i)\hat{r}/R_e^2$. On the face of it, $\boldsymbol{g}$ depends on the body through its inertial and gravitational masses. However, experiments show that the acceleration due to gravity is the same for all bodies and has a magnitude $g \approx 9.8 m/s^2$. The story of different objects falling in unison from the leaning tower of Pisa is a way to remember this. Thus, the ratio m_g/m_i must be the same for all bodies. By absorbing this constant ratio into G, we arrive at the equality $m_i = m_g$. This is called the principle of equivalence of inertial and gravitational masses. Henceforth, we will not make a distinction between inertial and gravitational masses. □

---

[14] Schrödinger's equation for the quantum mechanical wave function is $i\hbar \frac{\partial \psi}{\partial t} = H\psi$.

Newton's 3^{rd} law. Newton's 3^{rd} law says that 'for every action there is always opposed an equal reaction'. In other words, if body A exerts a force $\boldsymbol{F}$ on body B, then B exerts a force $-\boldsymbol{F}$ on A. These two forces are called the *impressed* and *expressed* forces. A cubical block of concrete of mass m that lies on the floor exerts a downward force on the floor equal to $m\boldsymbol{g}$ where $\boldsymbol{g}$ is the acceleration due to gravity. On the other hand, the floor exerts an upward force $-m\boldsymbol{g}$ of the same magnitude on the block. Both these forces are called 'normal reaction' forces. Similarly, small neighboring volumes of fluid exert equal and opposite pressure forces on each other, that act normal to the surface that separates them. We have already met some other examples of the third law in (2.5) and (2.57). While the third law is *not* needed to understand the motion of a particle subject to given external forces, it *is* needed to understand the motion of particles subject to interparticle forces. An important consequence of the third law (and Newton's second law) is that in an inertial frame, the total momentum of an isolated system of particles is conserved (see Prob. 3.8). The third law also helps distinguish between real and fictitious forces in noninertial reference frames (see Sect. 9.2). Unlike a fictitious force, an acceleration due to a real force felt by a body is distinguished by the presence of an equal and opposite reaction force on some other body.

3.4 Phase space, dynamical variables, conserved quantities and collisions

Phase space. Being 2^{nd} order in time, Newton's equation (3.2) requires both the initial position $\boldsymbol{r}$ *and* velocity $\dot{\boldsymbol{r}}$ (or momentum $\boldsymbol{p}$) as initial conditions. Knowledge of current position and momentum determines[15] the subsequent trajectory via Newton's 2^{nd} law[16]. We say that the *state* of the particle is specified by giving its instantaneous position *and* momentum. The set M of possible instantaneous states of the particle is called its state space or *phase space*. For a particle moving in 3d space, its configuration space is $Q = \mathbb{R}^3$ and its phase space is $M = \mathbb{R}^6$ (locations and momenta).

Phase portrait. The path of the particle $\boldsymbol{r}(t)$ (satisfying Newton's equation and initial conditions) in configuration space is called its trajectory. A trajectory is a directed curve, the direction being that of increasing time. Also of interest is the trajectory in phase space $(\boldsymbol{x}(t), \boldsymbol{p}(t))$. Consider the phase plane trajectories for a free particle moving on the real line $(m\ddot{x} = \dot{p} = 0)$ displayed in Fig. 3.2. Since energy is conserved, these trajectories must lie inside level sets[17] of energy $E = p^2/2m$. But in general, an energy level set may be a union of several trajectories. For $E > 0$, the energy level sets of a free particle consist of precisely two trajectories: the horizontal lines of fixed $p = \pm\sqrt{2mE}$. Trajectories are directed toward increasing x for $p > 0$ and vice versa. In general, we will extend trajectories as far forward (and backward) in time as possible. See Fig. 3.2 for the *phase portrait* of a free particle. Notice that the $E = 0$ level set is a union of infinitely many static solutions $(x = x(0), p = 0)$.

---

[15] See Sect. 5.3 for some remarks on the uniqueness of solutions to ordinary differential equations with specified initial conditions.

[16] Thus, mere specification of a point on Q does *not* determine the trajectory. Interestingly, in the quantum theory (see Sect. 10.3*), for reasons having to do with the Heisenberg uncertainty principle, the Schrödinger wave function $\psi(q)$ is a function on the classical configuration space rather than the phase space!

[17] By a level set of energy we mean the set of points in phase space where the energy takes a specific numerical value.

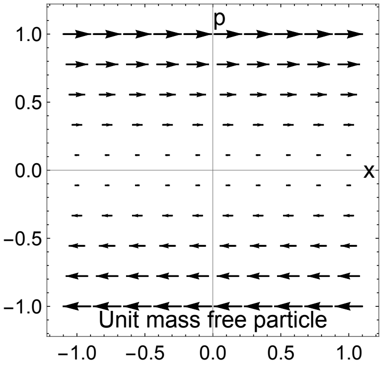

Figure 3.2: Phase portrait of particle subject to no forces, free to move on the real line. Every point on the x axis is a static solution with $p = 0$; together, they form the zero energy level set. The lengths of the arrows are proportional to the speed of the particle.

Dynamical variables and conserved quantities. Angular momentum $\boldsymbol{L} = \boldsymbol{r} \times \boldsymbol{p}$ is called the moment of linear momentum[18]. Its evolution is governed by the moment of the force or torque $\boldsymbol{\tau} = \boldsymbol{r} \times \boldsymbol{F}$:

$$\dot{\boldsymbol{L}} = \dot{\boldsymbol{r}} \times \boldsymbol{p} + \boldsymbol{r} \times \dot{\boldsymbol{p}} = m\cancel{\dot{\boldsymbol{r}} \times \dot{\boldsymbol{r}}} + \boldsymbol{r} \times \boldsymbol{F} = \boldsymbol{\tau}. \tag{3.12}$$

Notably, both $\boldsymbol{L}$ and $\boldsymbol{\tau}$ depend on the chosen origin for the radius vector $\boldsymbol{r}$.

The components of position, momentum, angular momentum and total energy $E = \boldsymbol{p}^2/2m + V(\boldsymbol{r})$ are interesting physical quantities associated with the dynamics of a particle. They are examples of *dynamical variables* or *observables*. In general, a dynamical variable is a smooth (infinitely differentiable, denoted C^∞) or at least sufficiently differentiable real-valued function on phase space. For a single particle, dynamical variables may be regarded as functions $f(\boldsymbol{r}, \boldsymbol{p})$. The potential $V(\boldsymbol{r})$ is a function on configuration space and so also a function on phase space independent of momenta. While x^i are called coordinate functions on configuration space, the components of position and momentum x^i and p_j are called coordinate functions on phase space. *Conserved quantities* are dynamical variables that are constant along *every* trajectory. Of course, the value of a conserved quantity may differ[19] from trajectory to trajectory. Conserved quantities are also called constants or integrals of motion.

Conservation of mass, momentum and energy in collisions. We will now illustrate the use of conserved quantities in the context of collisions. By a collision of point particles, we shall mean an interaction among particles[20] that behave as free particles in the asymptotic past and future so that each of them has a constant velocity as $t \to \pm\infty$. Such a situation arises if the forces between particles are sufficiently short-ranged and particles are separated by distances large compared to the range of forces as $t \to \pm\infty$. For example (a) two particles may 'scatter' (without necessarily coming into contact), each suffering a deflection in asymptotic direction of motion, (b) a particle may disintegrate/decay into two or more particles, (c) two or more particles may coalesce, etc. Evidently, the number of incoming and outgoing particles in a collision need not be equal. Though particle number need not be conserved, collisions may be fruitfully treated using the conservation laws of mass, momentum and energy even without a detailed knowledge of the forces of interaction. Inertial mass, regarded intuitively as the amount of matter, is conserved in nonrelativistic mechanical processes: it is neither created nor destroyed. The conservation of momentum and energy should not come as a surprise, we derived them for the problem of two gravitating point masses in Sect. 2.2. If external forces may be neglected, the total momentum of a system is conserved. For a system of particles, this is a consequence of Newton's 2nd and 3rd laws, with the latter allowing cancellation of interparticle forces in computing the rate of change of total momentum. The total energy of an isolated system is also conserved. However, kinetic energy could arise from or be transformed into other types of energy (e.g., potential energy in a spring, chemical bond energy) and we must account for this.

---

[18] The word moment has a different meaning in probability theory: the n^{th} moment of the real random variable ξ with probability density $p_\xi(x)$ is $\langle \xi^n \rangle = \int x^n p(x)\, dx$.

[19] The value of a conserved quantity must vary smoothly or continuously (rather than discontinuously) from one trajectory to a neighboring trajectory. If we dropped this condition, we could concoct a limitless supply of conserved quantities for any system simply by assigning a randomly chosen real number to each trajectory on phase space.

Suppose we have a collision among p ('past') incoming particles resulting in f ('future') outgoing particles. Let the masses and velocities (as $t \to \mp\infty$) of the particles be denoted $(m_i, \boldsymbol{v}_i)$ for $i = 1, \ldots, p, p+1, \ldots, p+f$. Then the law of conservation of mass states that

$$m_1 + \cdots + m_p = m_{p+1} + \cdots + m_{p+f}. \tag{3.13}$$

The conservation of linear momentum in a collision is the statement that

$$m_1\boldsymbol{v}_1 + \cdots + m_p\boldsymbol{v}_p = m_{p+1}\boldsymbol{v}_{p+1} + \cdots + m_{p+f}\boldsymbol{v}_{p+f}. \tag{3.14}$$

The conservation of energy (kinetic + potential + other forms) implies that

$$\sum_{i=1}^{p} \frac{1}{2} m_i \boldsymbol{v}_i^2 = \sum_{i=p+1}^{p+f} \frac{1}{2} m_i \boldsymbol{v}_i^2 + Q. \tag{3.15}$$

The difference Q between initial and final kinetic energies is positive if, say, kinetic energy is stored in a compressed spring or released as heat. It is negative if, say, internal potential energy is converted into kinetic energy, for instance in the decay of a particle that was initially at rest. If $Q = 0$, the collision is called elastic: kinetic energy is conserved but may be redistributed among the particles.

An example of a collision is the elastic '2 → 2' scattering of two particles which retain their identities (including their masses). In this case, conservation of mass is automatic and we have effectively 4 conservation laws (for energy and the three components of momentum). Given the initial velocities $\boldsymbol{v}_1, \boldsymbol{v}_2$, these 4 equations are insufficient to determine the final velocities $\boldsymbol{v}_3, \boldsymbol{v}_4$, which comprise 6 unknowns. Although conservation laws place restrictions on the final velocities, one needs information on the nature of forces to determine the latter. However, in 1d, we have 2 conservation laws and 2 unknown final velocity components and the system of equations is even-determined (rather than under-determined). If the lab frame initial and final velocities are v_1, v_2 and v_1', v_2', then the conservation laws for elastic scattering become

---

[20] A collision does not necessarily mean that the particles come into contact.

$$\begin{aligned} m_1 v_2 + m_2 v_2 &= m_1 v_1' + m_2 v_2' \equiv p \quad \text{and} \\ \frac{1}{2} m_1 v_1^2 + \frac{1}{2} m_2 v_2^2 &= \frac{1}{2} m_1 v_1'^2 + \frac{1}{2} m_2 v_2'^2 \equiv T. \end{aligned} \tag{3.16}$$

Eliminating $v_1' = (p - m_2 v_2')/m_1$ and writing $M = m_1 + m_2$, we get

$$\begin{aligned} v_2' &= M^{-1} \left[p \pm \sqrt{p^2 - M(m_1/m_2)(p^2/m_1 - 2T)} \right] \\ &= (2m_1 v_1 + (m_2 - m_1) v_2)/M \quad \text{or} \quad v_2. \end{aligned} \tag{3.17}$$

The second solution is the trivial one, where the particles retain their velocities $v_1' = v_1, v_2' = v_2$. In the first, the scattering is nontrivial. For instance, suppose the particles had equal and opposite initial velocities, then show that the heavier particle comes to rest after the collision if it is thrice as massive as the lighter one (see Prob. 3.10).

3.5 Principle of extremal action and Euler-Lagrange equations

Hamilton's variational principle of extremal action (1835) provides a powerful reformulation of Newton's equations of motion, especially for systems with conservative forces. In this case, it leads to Lagrange's equations of motion, which are equivalent to Newton's equations. One advantage of Lagrange's equations is that unlike Newton's equations, they retain the same form in all systems of coordinates on configuration space (see Sect. 3.8). What is more (for conservative systems), a single real-valued function (the Lagrangian) can be used to generate all the equations of motion simply by differentiating it with respect to the various coordinates and velocities. This also makes it easier to change from one coordinate system to another since one only needs to transform one function rather than each component of the vector forces. Constraints among the various coordinates (such as those that force a particle to move on a curve or surface) can also be accounted for without worrying about the forces that are responsible for enforcing the constraints. However, all this is not free of cost: (a) the Lagrangian formulation does not directly apply to dissipative systems, unlike the Newtonian formulation where a frictional force can easily be added and (b) the principle of extremal action relies on the calculus of infinitely many variables, called the variational calculus of paths[21] on configuration space, unlike Newton's equation that is based on the calculus of finitely many variables parameterizing points on configuration space. Nevertheless, once one learns the methods of the calculus of variations, it can be applied to other optimization problems like Plateau's problem on finding the shapes of soap films or the Brachistochrone problem (Prob. 3.19). A still deeper benefit is that the concept of the action plays a central role in the formulation of the quantum theory via Feynman's path integral.

---

[21] Hamilton's is an integral variational principle. Interestingly, there are also differential variational principles, such as Gauss' *principle of least constraint* and Hertz's *principle of least curvature* that do not require the calculus of variations for their formulation [117].

Extremal action principle. The idea of the action or variational principle is as follows[22]. A static solution (time-independent trajectory) of Newton's equation for a particle in a potential ($m\ddot{x} = -V'(x)$) occurs when the particle is located at an extremum of the potential. The action principle gives a way of identifying (possibly) time-dependent trajectories as extrema of an action function. However, unlike the potential, the relevant action is not a function on configuration space but a function on the *space of differentiable paths* on configuration space[23]. This is quite natural since instead of identifying one (or more) among the points of $\mathcal{Q}$ as a static solution, we wish to select one (or more) among the paths on $\mathcal{Q}$ as a trajectory. Suppose $q^i(t)$ for $t_1 \leq t \leq t_2$ is a differentiable path on $\mathcal{Q}$ between specified initial and final times[24]. Then the action[25] is typically a functional[26] of the form

$$S[q] = \int_{t_1}^{t_2} L(q^i, \dot{q}^i)\, dt. \tag{3.19}$$

Here, $L(q^i, \dot{q}^i)$ is called the Lagrangian of the system, a function of coordinates and velocities. For a suitable L (invariably the difference between kinetic and potential energies, $L = T - V$), we will see that Newtonian trajectories are extrema of S.

In other words, we consider the problem of determining the trajectory that a particle might take if it is at q_1 at t_1 and at q_2 at t_2. Instead of specifying the initial position and velocity (as in an initial value problem), we give the initial and final positions at these times. Which among all the paths that connect these points solves Newton's

---

[22] The action principle may be obtained from d'Alembert's principle, see (3.23) and (3.24).

[23] The space of differentiable paths on configuration space is an infinite-dimensional space. This is already the case for a system with just one degree of freedom, where a path between q_1 at t_1 and q_2 at t_2 is simply a differentiable function of time $q(t)$ with these initial and final values. If we imagine expanding $q(t)$ in a Fourier series, the Fourier coefficients are freely specifiable as long as the series converges. These infinitely many coefficients furnish coordinates on the space of such paths. For example, a Fourier series for $q(t)$ for $t_1 \leq t \leq t_2$ with $q(t_1) = q_1$ and $q(t_2) = q_2$ is given by

$$q(t) = q_1 + (q_2 - q_1)\frac{t - t_1}{t_2 - t_1} + \sum\nolimits_{n=1}^{\infty} a_n \sin(n\pi(t - t_1)/(t_2 - t_1)), \tag{3.18}$$

where $a_1, a_2, \ldots$ are the Fourier coefficients.

[24] It is common to use the symbol q^i (instead of x^i) for coordinates on configuration space. They are called *generalized* coordinates: q^i need not be Cartesian coordinates of particles and need not have dimensions of length, any system of coordinates (with appropriate dimensions) for the degrees of freedom of the system will work.

[25] The times $t_{1,2}$ are held fixed in this 'Hamilton-Lagrange' action while the energy will be held fixed in the 'Euler-Maupertuis' action to be introduced in Sect. 3.28*.

[26] The action S is a function of the function $q(t)$. Such objects are called functionals. However, S does not depend on t, since it is integrated.

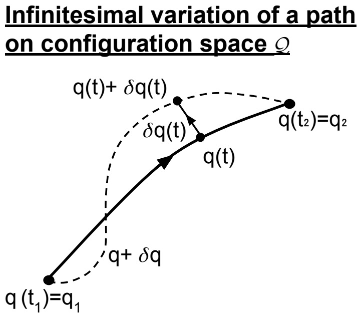
Infinitesimal variation of a path
on configuration space $\mathcal{Q}$
q(t)+ δq(t)
δq(t)
q(t₂)=q₂
q(t)
q+ δq
q (t₁)=q₁

Figure 3.3: Infinitesimal variation of a path while holding the initial and final configurations $q(t_1) = q_1$ and $q(t_2) = q_2$ fixed.

equation? The action principle says that classical trajectories are extrema of S. Note that unlike the initial value problem where $q^j(t_1), \dot{q}^j(t_1)$ are specified, this initial-final value problem (where $q^j(t_1)$ and $q^j(t_2)$ are specified), may not have a unique solution. The action may have more than one extremum (see Prob. 3.16).

Euler-Lagrange equations. To understand this idea, we need to determine the conditions [called Euler-Lagrange equations] for S to be extremal. For the case of static or time-independent solutions discussed above, the condition for $V(x)$ to be extremal is that its change under an infinitesimal shift δx of x must vanish to first order in δx, this turns out to be the condition $V'(x) = 0$. The Euler-Lagrange equations are got by computing the infinitesimal change δS in action, under a small change in path[27] $q^i(t) \to q^i(t) + \delta q^i(t)$ while holding the initial and final locations $q^i(t_1), q^i(t_2)$ unchanged ($\delta q^i(t_1) = \delta q^i(t_2) = 0$, see Fig. 3.3). Assuming the variation (this is what gives the principle its name) in the path is such that $\frac{d\delta q(t)}{dt} = \delta\dot{q}$, we get

$$\begin{aligned}\delta S &= \textstyle\sum_{i=1}^{n} \displaystyle\int_{t_1}^{t_2} dt' \left\{ \frac{\partial L}{\partial q^i}\delta q^i(t') + \frac{\partial L}{\partial \dot{q}^i}\delta\dot{q}^i(t') \right\} + \mathcal{O}(\delta q)^2 \\ &= \int_{t_1}^{t_2} \delta q^i(t') \left(\frac{\partial L}{\partial q^i} - \frac{d}{dt'}\frac{\partial L}{\partial \dot{q}^i} \right) dt' \\ &\quad + \delta q^i(t_2)\frac{\partial L}{\partial \dot{q}^i(t_2)} - \delta q^i(t_1)\frac{\partial L}{\partial \dot{q}^i(t_1)} + \mathcal{O}(\delta q)^2, \end{aligned} \tag{3.20}$$

where a sum over the repeated index i is implied. We integrated by parts to isolate the coefficient of δq. The last two 'boundary terms' are zero due to the initial and final conditions. For δS to vanish to first order in infinitesimals, the integral must vanish. Now $\delta q^i(t')$ is an arbitrary function for $t_1 < t < t_2$. So the only way the integral can vanish is for the quantity in parenthesis to be identically zero at all such times[28].

---

[27] Arbitrary infinitesimal shifts in locations of particles (or generalized coordinates subject to any constraints on the system) are also called virtual displacements since they do not have to be tangent to a trajectory. Such virtual displacements arose in the principle of virtual work and d'Alembert's principle [81] which were precursors to the principle of extremal action.

[28] $\int_a^b f(t)g(t)dt = 0$ for all $f(t)$ implies that $g(t) = 0$ for $a < t < b$. Intuitively, this says that g is orthogonal (with respect to the L^2 inner product) to all functions f and therefore

Thus, we get the *Euler-Lagrange* (EL) (or just Lagrange's) equations

$$\frac{\partial L}{\partial q^i(t)} - \frac{d}{dt}\frac{\partial L}{\partial \dot{q}^i(t)} = 0 \quad \text{for} \quad i = 1, 2, \ldots, n. \tag{3.21}$$

Now, let us see how the principle of extremal action (for a suitable choice of L) implies Newton's equation of motion in Cartesian coordinates for a particle in a potential. Comparing $m\ddot{q} = -V'(q)$ with the EL equation $\frac{d}{dt}\frac{\partial L}{\partial \dot{q}} = \frac{\partial L}{\partial q}$ we notice that if we choose[29] $L = \frac{1}{2}m\dot{q}^2 - V(q)$, then

$$\frac{\partial L}{\partial \dot{q}} = m\dot{q} \quad \text{and} \quad \frac{\partial L}{\partial q} = -V'(q) \tag{3.22}$$

and the EL equation reduces to Newton's equation. This is easily generalized to a particle moving in three dimensions: $L = \frac{1}{2}m(\dot{x}^2 + \dot{y}^2 + \dot{z}^2) - V(x, y, z)$.

Explicitly time-dependent Lagrangian. Notice that the same EL equations (3.21) are obtained even if the Lagrangian $L(q, \dot{q}, t)$ depended explicitly on time. The computation of the first variation of S in (3.20) under an infinitesimal change in path $q \to q + \delta q$ is unaltered. □

Hamilton's principle from d'Alembert's principle. One may arrive at the principle of extremal action from d'Alembert's principle applied to a system subject to conservative forces. Recall from (3.10) that along a trajectory, the difference between the virtual work done by applied and inertial forces must vanish, provided the virtual displacements are orthogonal to any constraint forces. Restricting attention (for simplicity) to a single particle of mass m subject to the applied force $\boldsymbol{F}^{\text{applied}}(\boldsymbol{r}) = -\boldsymbol{\nabla} V(\boldsymbol{r})$, we have:

$$\boldsymbol{\nabla} V \cdot \delta \boldsymbol{r} + m\ddot{\boldsymbol{r}} \cdot \delta \boldsymbol{r} = 0 \quad \text{or} \quad \delta V + \frac{d}{dt}(m\dot{\boldsymbol{r}} \cdot \delta \boldsymbol{r}) - m\dot{\boldsymbol{r}}\delta\dot{\boldsymbol{r}} = 0. \tag{3.23}$$

As before, we have assumed that $d(\delta \boldsymbol{r})/dt = \delta \dot{\boldsymbol{r}}$. Now, we notice that the last term is the infinitesimal variation of the kinetic energy: $m\dot{\boldsymbol{r}}\delta\dot{\boldsymbol{r}} = \delta T$ where $T = (1/2)m\dot{\boldsymbol{r}}^2$. Writing $L = T - V$ and integrating with respect to t from t_1 to t_2, we have

$$\delta L = \frac{d}{dt}(m\dot{\boldsymbol{r}} \cdot \delta \boldsymbol{r}) \quad \text{or} \quad \delta \int_{t_1}^{t_2} L\, dt = m(\dot{\boldsymbol{r}}(t_2)\delta \boldsymbol{r}(t_2) - \dot{\boldsymbol{r}}(t_2)\delta \boldsymbol{r}(t_2)) = 0 \tag{3.24}$$

---

must vanish. One way to see this is to suppose that $f(t)$ is zero everywhere except in a small neighborhood of t' of width ϵ where it takes the value $1/\epsilon$. Then the value of the integral approaches $g(t')$ as $\epsilon \to 0$. Thus, $g(t') = 0$ for any $t' \in (a, b)$.

[29] Lagrangians of physical systems typically do not involve second or higher time derivatives of displacements as they would lead to EOM that are third or higher order in time derivatives. If present in the EOM for a free particle (e.g., $\alpha \dddot{q} = 0$), they would alter Newton's first law by allowing the particle to have a parabolic rather than straight line trajectory. They would also alter the usual interpretation of Newton's second law which implies that we need only two ICs for time evolution. The Abraham-Lorentz radiation damping force on a charged particle in classical electrodynamics involves the third derivative of its displacement. However, a straightforward treatment of this force is problematic as it can lead to a violation of causality and runaway solutions in the Lorentz-Dirac [28] equation. When treated more carefully [79, 108, 109], one ends up with a second order equation called the Landau-Lifshitz equation (Sect. 76 of [84]).

where we assumed that the variations vanish at the end points. Thus, we arrive at the principle of extremal action: trajectories extremize the action: $\delta S = 0$.

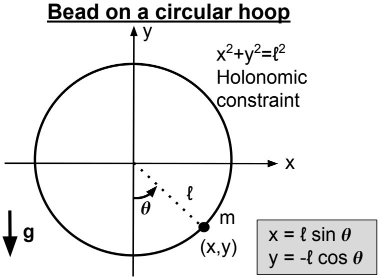

Figure 3.4: Bead of mass m constrained to move on a circular hoop subject to gravity. A 'holonomic' constraint is a relation among coordinates (and possibly time).

Particle moving on a vertical hoop. The Lagrangian approach to obtaining equations of motion is particularly convenient when there are constraints which make identifying forces to write down Newton's equations somewhat tricky. Let us illustrate the use of the Lagrangian with the example of a bead of mass m free to move frictionlessly on a fixed vertical circular hoop (see Fig. 3.4) of radius l under the influence of a constant acceleration due to gravity g. This problem is physically important: it is equivalent to the simple pendulum which we introduced in Sect. 1.5 and will study in more detail in Chap. 7. The length of the massless pendulum shaft is l and m is the mass of the bob. Let us use the horizontal and vertical Cartesian coordinates x and y on the plane of the hoop with the origin at its center. The bead is constrained[30] to move on the circle $x^2 + y^2 = l^2$. As above, the kinetic energy is given by $T = \frac{1}{2}m(\dot{x}^2 + \dot{y}^2)$ while the potential energy is $V = mgy + mgl$ leading to the Lagrangian

$$L = \frac{1}{2}m(\dot{x}^2 + \dot{y}^2) - mg(l + y). \tag{3.25}$$

We have added the constant mgl to V so that it vanishes at the bottom of the hoop where $y = -l$. The constraint ensures that the bead has only one degree of freedom.

---

[30] Such a constraint is called holonomic: a relation among the generalized coordinates and possibly time, of the form $C(q^1, q^2, \ldots, q^n, t) = 0$. Associated to a holonomic constraint, we have the differential relation $\phi \equiv dC = 0$ or $\phi = \frac{\partial C}{\partial q^1} dq^1 + \ldots + \frac{\partial C}{\partial q^n} dq^n + \frac{\partial C}{\partial t} dt = 0$. $\phi = dC$ is called an exact differential since it arises as the differential of some function $C(q, t)$. It is also called integrable, since ϕ may be integrated to obtain C. One can imagine more general differential relations of the form $\psi = \sum_k \psi_k(q, t) dq^k + \psi_{n+1}(q, t) dt = 0$, where ψ is not exact, i.e., $\psi \neq dC$ for some function $C(q, t)$ and not even integrable after multiplication by an integrating factor (i.e., there is no function $\tau(q, t)$ such that $\tau\psi$ is exact). A differential constraint that is not integrable was called nonholonomic by Heinrich Hertz. The word *holos* means whole (or integer) in Greek. More generally, a constraint that cannot be expressed as $C(q, t) = 0$ (for instance, one that involves generalized velocities, momenta or an inequality) is called a nonholonomic constraint. See Sect. 3.17* for an example.

We may use the constraint $x^2 + y^2 = l^2$ to eliminate $\dot{x}$ from the Lagrangian[31]. Indeed,

$$2x\dot{x} + 2y\dot{y} = 0 \quad \Rightarrow \quad \dot{x}^2 = \frac{y^2\dot{y}^2}{x^2} = \frac{y^2\dot{y}^2}{l^2 - y^2} \tag{3.26}$$

so that

$$L(y, \dot{y}) = \frac{1}{2}m\dot{y}^2\left(1 + \frac{y^2}{l^2 - y^2}\right) - mg(l + y). \tag{3.27}$$

One finds

$$\frac{\partial L}{\partial y} = \frac{ml^2 y\dot{y}^2}{(l^2 - y^2)^2} - mg \quad \text{and} \quad \frac{d}{dt}\frac{\partial L}{\partial \dot{y}} = \frac{ml^2(l^2 - y^2)\ddot{y} + 2ml^2 y\dot{y}^2}{(l^2 - y^2)^2}. \tag{3.28}$$

The resulting equation of motion

$$l^2(l^2 - y^2)\ddot{y} + l^2 y\dot{y}^2 + g(l^2 - y^2)^2 = 0 \tag{3.29}$$

looks somewhat formidable. However, it can be simplified by expressing it as an equation for the angle θ that the bead makes with the negative y-axis by putting $y = -l\cos\theta$. We get $\dot{y} = l\sin\theta\dot{\theta}$ and $\ddot{y} = l\cos\theta\dot{\theta}^2 + l\sin\theta\ddot{\theta}$ leading to the elegantly simple equation

$$\ddot{\theta} = -\frac{g}{l}\sin\theta, \tag{3.30}$$

which we recognize as being identical to that of the simple pendulum (1.29). The simplicity of the final equation for θ suggests it may have been easier to eliminate the constraint by expressing the Lagrangian in polar coordinates before deriving the EOM. In fact, putting $x = l\sin\theta$ and $y = -l\cos\theta$ the constraint is identically satisfied and we get

$$L = \frac{1}{2}ml^2\dot{\theta}^2 - mgl(1 - \cos\theta), \quad \frac{d}{dt}\frac{\partial L}{\partial \dot{\theta}} = ml^2\ddot{\theta} \quad \text{and} \quad \frac{\partial L}{\partial \theta} = -mgl\sin\theta \tag{3.31}$$

which leads to the same equation (3.30). This nonlinear equation will be studied in more detail and solved in Chap. 7. Thus, aside from rederiving the equation of motion for a pendulum, we have verified that Lagrange's equations (3.21) give the same result whether we use rectilinear ($q = y$) or polar ($q = \theta$) coordinates. This freedom to choose generalized coordinates will be further clarified in Sect. 3.8. □

Remark: Given equations of motion for a system, there is no deductive procedure to find a Lagrangian for them. One relies on trial and error and past experience in searching for a Lagrangian. In fact, there are cases (such as the damped motion of a particle in Eq. (1.4)) where the equations may not admit any Lagrangian formulation. On the other hand, if a Lagrangian exists, it is not unique, as we shall see in Sect. 3.6. □

---

[31] In fact, if we wanted, we could have taken $T = \frac{1}{2}m(\dot{x}^2 + \dot{y}^2 + \dot{z}^2)$ and imposed a second constraint $z = 0$ and used its derivative $\dot{z} = 0$ to eliminate $\dot{z}$.

3.6 Nonuniqueness of Lagrangian

A Lagrangian for a given system of equations is not uniquely defined. For instance, we may add a constant to $L(q, \dot{q}, t)$ or multiply it by a nonzero real constant without affecting the Euler-Lagrange equations (3.21). Another source of nonuniqueness arises from the freedom to add the 'total' time derivative of any (differentiable) function $F(q, t)$ to the Lagrangian: $L \mapsto L' = L + \dot{F}$. The resulting change in the action (3.19) is

$$S \mapsto S' \quad \text{where} \quad S' - S = \int_{t_1}^{t_2} \frac{dF}{dt} dt = F(q(t_2), t_2) - F(q(t_1), t_1). \tag{3.32}$$

When inserted in Hamilton's variational principle (3.20), $S' - S$ has zero variation since t_1, t_2, $q(t_1)$, $q(t_2)$ are all held fixed as the path is varied. So the addition of $\dot{F}$ to L does not affect the EL equations. Thus, a strange-looking Lagrangian may give an equivalent description of a familiar system, as Prob. 3.11 illustrates. This freedom to ignore or add time-derivative terms to L can be useful, as we will see in the context of motion in boosted or accelerated frames in Sect. 3.12 and Sect. 9.2. Moreover, we will exploit this freedom to find generating functions for canonical transformations in Sect. 10.10.

On the other hand, there is no restriction on the initial and final velocities of the perturbed paths ($\delta \dot{q}_1 \equiv \delta \dot{q}(t_1), \delta \dot{q}_2 \equiv \delta \dot{q}(t_2)$ are not required to vanish) in Hamilton's variational principle. Suppose $F(q, \dot{q}, t)$ depended on velocities. Then the difference between actions would be $S' - S = F(q_2, \dot{q}_2, t_2) - F(q_1, \dot{q}_1, t_1)$ and its variation is

$$\delta(S' - S) = \frac{\partial F}{\partial q_2}\cancel{\delta q_2} + \frac{\partial F}{\partial \dot{q}_2}\delta \dot{q}_2 + \frac{\partial F}{\partial t_2}\cancel{\delta t_2} - \frac{\partial F}{\partial q_1}\cancel{\delta q_1} - \frac{\partial F}{\partial \dot{q}_1}\delta \dot{q}_1 - \frac{\partial F}{\partial t_1}\cancel{\delta t_1}. \tag{3.33}$$

Since $\delta \dot{q}_1$ and $\delta \dot{q}_2$ are arbitrary and independent, the only way for the extrema of S' and S to coincide would be for $\frac{\partial F}{\partial \dot{q}_1}$ and $\frac{\partial F}{\partial \dot{q}_2}$ to vanish. This must happen for any initial and final times t_1 and t_2, so $\frac{\partial F}{\partial \dot{q}}$ must vanish. In other words, for S and S' to lead to the same equations of motion, F must be independent of velocities.

3.7 Conjugate momenta, their geometric meaning and cyclic coordinates

Given a Lagrangian $L(q^i, \dot{q}^i)$, the momentum p_i conjugate to the coordinate q^i is defined as[32]

$$p_i = \frac{\partial L}{\partial \dot{q}^i}. \tag{3.34}$$

In general, conjugate momenta do not have the dimensions of `mass × velocity`, just as generalized coordinates q^i do not necessarily have dimensions of length. However, since L has dimensions of energy, the product of a coordinate and its conjugate momentum always has dimensions of `energy` × `time` or action. Conjugate momentum is a useful concept. If a coordinate q^j does not appear in the Lagrangian, then its conjugate momentum is automatically conserved in view of (3.21):

---

[32] An (unsummed or free) index such as i in a so-called tensorial equation like $p_i = \frac{\partial L}{\partial \dot{q}^i}$ is said to be consistently placed if it appears in all terms as a subscript (or as a superscript throughout). For this purpose, a superscript in the denominator plays the same role as a subscript in the numerator and vice versa. In (3.34), this ensures that both the LHS and RHS are covariant vectors. See Appendix B.5* for more on these matters.

$$\frac{dp_j}{dt} = \frac{d}{dt}\frac{\partial L}{\partial \dot{q}^j} = \frac{\partial L}{\partial q^j} = 0. \tag{3.35}$$

Such a coordinate is called a *cyclic coordinate*[33]. For a free particle moving on a line, $L = \frac{1}{2}m\dot{x}^2$ has the cyclic coordinate x leading to the conservation of the conjugate momentum $p_x = m\dot{x}$, $\dot{p}_x = 0$. See Prob. 3.14 and Prob. 3.17 for more examples.

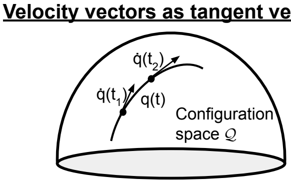
Velocity vectors as tangent vectors
q̇(t₂)
q̇(t₁)
q(t)
Configuration space $\mathcal{Q}$

Figure 3.5: Velocity vector as a tangent vector to a trajectory and to the configuration space. Note that velocity vectors at distinct points along a trajectory live in different tangent spaces and cannot simply be 'added'.

$*$ **Geometrical interpretation of generalized velocity and momentum.** Geometrically, the trajectory $q^i(t)$ is a curve on configuration space $\mathcal{Q}$. At any instant of time, $\dot{q}^i(t)$ are the components of the tangent vector to this curve (see Fig. 3.5). Thus, generalized velocities are components of tangent vectors to the configuration space. Tangent vectors are *contravariant* vectors (see Appendix B.4*) and their components are denoted with upper indices. On the other hand, the generalized momenta p_i are components of cotangent vectors (covectors or *covariant* vectors, denoted with lower indices). They are elements of the vector space dual[34] to the tangent space. Tangent and cotangent vectors *at the same point of the configuration space* may be *contracted* via the pairing between a vector space and its dual to get a number. For instance[35]

---

[33] The name *cyclic* comes from simple examples where the cyclic coordinate is an angle and is associated with the presence of periodic orbits (cycles). For example, in the harmonic oscillator treated in angle-action variables (see Sect. 11.1), the angle variable θ is cyclic and trajectories lie along the closed level curves of the action variable I.

[34] Given a real vector space V, its dual V^* is the space of real-valued linear functions on V. $\phi : V \to \mathbb{R}$ is a linear function if $\phi(au + bv) = a\phi(u) + b\phi(v)$ for all $u, v \in V$ and all scalars $a, b \in \mathbb{R}$. A momentum covector p (at the point $q \in \mathcal{Q}$) defines a linear function on the tangent space of velocities of curves passing through q. Its value on a velocity vector $\dot{q}$ is $p(\dot{q}) = \sum_i p_i \dot{q}^i$ which is evidently linear in the components of $\dot{q}$. Thus, momenta live in the space dual to velocities, called the cotangent space. A finite dimensional vector space and its dual are isomorphic, but in general there is no distinguished isomorphism between them. The formula $p_i = \frac{\partial L}{\partial \dot{q}^i}$ provides a canonical isomorphism between tangent and cotangent spaces by associating a specific momentum covector to any given velocity tangent vector.

[35] The repeated index i appearing once as an upper and once as a lower index in a term is summed from 1 to the number of degrees of freedom. A repeated index is called a dummy index and can be replaced with any other repeated symbol $p_i\dot{q}^i = p_j\dot{q}^j$.

$p_i(t)\dot{q}^i(t)$ is a real number at each point $q^i(t)$ along the curve. This number is independent of what coordinate system we use on configuration space and defines the scalar function $p_i\dot{q}^i$ along the curve. For fixed energy, its integral along the curve is the EM action of (1.26). □

Not every conserved quantity may arise as the momentum conjugate to a cyclic coordinate. For example, if we use Cartesian coordinates for the particle in a central potential on a plane, $L = \frac{1}{2}m(\dot{x}^2 + \dot{y}^2) - V(\sqrt{x^2+y^2})$, then neither x nor y is cyclic and neither of the momenta ($p_x = m\dot{x}, p_y = m\dot{y}$) is conserved. But as we might suspect from the Kepler problem (and as we will see below), the momentum conjugate to the cyclic angular coordinate $\phi = \arccos(x/\sqrt{x^2+y^2})$ is conserved. So some physical insight/cleverness/luck may be needed in choosing coordinate systems in which one or more coordinates are cyclic.

3.8 Coordinate invariance of the form of Lagrange's equations

One of the important advantages of Lagrange's equations over Newton's second law is that unlike the latter, they are valid in any system of coordinates on configuration space. Here, we illustrate this through an example and indicate the reason, while a proof is given in Sect. 3.20*.

Let us begin with an example to show that Newton's equations in Cartesian coordinates $m\ddot{x}^i = f^i$ change their form if we switch to a different coordinate system on configuration space. Consider a free particle moving on the x-y plane. Newton's equations are $m\ddot{x} = 0$ and $m\ddot{y} = 0$ since there is no force. Now let us transform to polar coordinates via $x = r\cos\phi$ and $y = r\sin\phi$. Upon calculating the derivatives, the equations of motion for r and ϕ are found to be

$$m\ddot{r} = mr\dot{\phi}^2 \quad \text{and} \quad mr\ddot{\phi} = -2m\dot{r}\dot{\phi}. \tag{3.36}$$

There is no force in the $\hat{r}$ or $\hat{\phi}$ directions. Yet, the naive radial and angular 'accelerations' $\ddot{r}$ and $\ddot{\phi}$ are nonzero! Thus, in polar coordinates, Newton's equations do not take the same '$m\ddot{q}^i = f^i$' form[36] that they did in Cartesian coordinates (Nb. by f^θ we mean $\boldsymbol{f}\cdot\hat{\theta}$ and so on).

Let us now contrast this with Lagrange's equations $\frac{d}{dt}\frac{\partial L}{\partial \dot{q}^i} = \frac{\partial L}{\partial q^i}$ (3.21) for the same system. In Cartesian coordinates ($q^1 = x, q^2 = y$), $L = \frac{1}{2}m(\dot{x}^2+\dot{y}^2)$ leads to the familiar equations $m\ddot{x} = 0$ and $m\ddot{y} = 0$. Upon transforming to plane polar coordinates[37] (see Prob. 3.3), the Lagrangian becomes

$$L = \frac{m}{2}(\dot{r}^2 + r^2\dot{\phi}^2). \tag{3.37}$$

The momenta conjugate to r and ϕ are

$$p_r = \frac{\partial L}{\partial \dot{r}} = m\dot{r} \quad \text{and} \quad p_\phi = \frac{\partial L}{\partial \dot{\phi}} = mr^2\dot{\phi}. \tag{3.38}$$

---

[36] All is not lost: the equations $m\boldsymbol{a}\cdot\hat{\phi} = \boldsymbol{f}\cdot\hat{\phi}$ and $m\boldsymbol{a}\cdot\hat{r} = \boldsymbol{f}\cdot\hat{r}$ do hold.

[37] This Lagrangian also follows from the square of the Euclidean line element $ds^2 = dr^2 + r^2 d\phi^2$, which implies that the square of velocity is $\dot{\boldsymbol{r}}^2 = (ds/dt)^2 = \dot{r}^2 + r^2\dot{\phi}^2$.

They coincide with the radial component of linear momentum ($\boldsymbol{p} \cdot \hat{\boldsymbol{r}}$) and the z-component of angular momentum (2.2). The first of Lagrange's equations is

$$\dot{p}_r = m\ddot{r} = \frac{\partial L}{\partial r} = mr\dot{\phi}^2. \tag{3.39}$$

This is the balance of mass × radial acceleration and the 'centripetal acceleration'. On the other hand, ϕ is a cyclic coordinate and so p_ϕ is conserved:

$$\dot{p}_\phi = \frac{d}{dt}(mr^2\dot{\phi}) = \frac{\partial L}{\partial \phi} = 0 \quad \Rightarrow \quad mr\ddot{\phi} = -2m\dot{r}\dot{\phi}. \tag{3.40}$$

This states the conservation of angular momentum, and involves the Coriolis acceleration term[38] on the RHS when written out. We see that these equations agree with Newton's equations transformed to polar coordinates (3.36). Thus, Lagrange's equations in the form $\frac{d}{dt}\frac{\partial L}{\partial \dot{q}^i} = \frac{\partial L}{\partial q^i}$ are valid in both Cartesian and polar coordinates, while Newton's equations in the form $m\ddot{q}^i = f^i$ are valid in Cartesian but not polar coordinates.

More generally, as we will see in Sect. 3.20*, Lagrange's equations (3.21) are valid in any system of coordinates on configuration space. The reason is easy to see: we obtained the EL equations by extremizing the action (3.19) without making any assumption about what the q^i are. So q^i could be Cartesian or polar or any other coordinates.

Aside from conceptual elegance, the above feature of Lagrange's equations is of significant practical value. We are often interested in studying a system with n degrees of freedom in a particular coordinate system (e.g., for reasons of symmetry) and need to transform the equations from, say, Cartesian coordinates. To transform Newton's equations we need to transform n equations and in each case, calculate second derivatives of the equations of transformation, as we did in arriving at (3.36). On the other hand, in the Lagrangian approach, it is enough to transform a single Lagrange function (which typically involves only first derivatives in time) and use it to generate the equations in the new coordinate system. Both approaches lead to the same EOM. We may say that the diagram in Fig. 3.6 commutes.

$$\begin{tikzcd}
\text{Cartesian Lagrangian} \arrow[r, "\text{change}", "\text{variables}"'] \arrow[d, "\text{EL eqn}"] & \text{Polar Lagrangian} \arrow[d, "\text{EL eqn}"] \\
\text{Cartesian EOM} \arrow[r, "\text{change}", "\text{variables}"'] & \text{Polar EOM}
\end{tikzcd}$$

Figure 3.6: Commutative diagram showing change from Cartesian to polar variables.

3.9 Hamiltonian and its conservation

Besides the momenta conjugate to cyclic coordinates, the Lagrangian formulation leads automatically to another conserved quantity, the Hamiltonian. For a moment, suppose the Lagrangian depends explicitly[39] on time $L = L(q(t), \dot q(t), t)$. Then

---

[38] The Coriolis *acceleration* is to be contrasted with the Coriolis *force* of Sect. 9.2, which is a fictitious force that appears to act in a rotating frame of reference. The Coriolis acceleration is present in an inertial frame when the particle's r and θ coordinates both vary with time.

$$\frac{dL}{dt} = \frac{\partial L}{\partial q}\dot q + \frac{\partial L}{\partial \dot q}\ddot q + \frac{\partial L}{\partial t} = \dot p \dot q + p \ddot q + \frac{\partial L}{\partial t} = \frac{d(p\dot q)}{dt} + \frac{\partial L}{\partial t} \tag{3.41}$$

which implies $\frac{d(p\dot q - L)}{dt} = -\frac{\partial L}{\partial t}$. So, if we define the Hamiltonian $H = p\dot q - L$, then $\dot H = -\frac{\partial L}{\partial t}$. Thus, if the Lagrangian does not depend explicitly on time, H would be conserved[40]. For example, suppose $L = \frac{1}{2}m\dot q^2 - V(q)$ for a particle moving along a line. Then $p = m\dot q$ and $H = m\dot q^2 - \frac{1}{2}m\dot q^2 + V(q) = \frac{1}{2}m\dot q^2 + V(q)$ coincides with the total energy. Thus, the Lagrangian approach gives us a new way of discovering a conserved energy that complements the approach of using an integrating factor (1.2) in Newton's equation.

Explicitly time-dependent Lagrangian. To see what could happen when L depends explicitly on time, consider $L = \frac{1}{2}m\dot q^2 - \frac{1}{2}k(t)q^2$. This models a particle that is subject to a linear restoring force $-k(t)q$ whose 'spring constant' k varies with time. This could happen, for instance, if the spring 'loses' elasticity with time in a prescribed manner. In this case, the EL equation of motion $m\ddot q = -k(t)q$ implies that the Hamiltonian $H = \frac{1}{2}m\dot q^2 + \frac{1}{2}k(t)q^2$ evolves according to $\dot H = \frac{1}{2}\dot k q^2$. Thus, this Hamiltonian ('energy') is not conserved. Another example is an oscillating pendulum that is pushed every time it reaches one of the turning points. In this case, the usual energy of oscillatory motion would be expected to grow with time due to the external driving. □

For many of the systems we study (with $\frac{\partial L}{\partial t} = 0$), the Hamiltonian coincides with the sum of kinetic and potential energies. Suppose we consider a system with kinetic energy $T = (1/2)m_{ij}(q)\dot q^i \dot q^j$, potential energy $V(q)$ and total energy $E = T + V$. Here $m_{ij} = m_{ji}$ may be taken to be the components of a symmetric matrix or tensor[41], it is a sort of position-dependent mass matrix, usually a positive-definite matrix (i.e., real symmetric matrix with positive eigenvalues). For example, for a free particle on the plane in polar coordinates (r, ϕ), we find from (3.37) that $m_{ij} = m\left(\begin{smallmatrix} 1 & 0 \\ 0 & r^2 \end{smallmatrix}\right)$ is a position-dependent matrix. Such a *positive-definite matrix*[42] $m_{ij}(q)$ is called a

---

[39] We say that the Lagrangian $L(q(t), \dot q(t))$, does not depend explicitly on time, but only implicitly through $q(t)$ and $\dot q(t)$. An example of an explicitly time-dependent Lagrangian is $L = \frac{1}{2}m(t)\dot q^2$ where $m(t)$ is a time-dependent mass parameter.

[40] Note that the Lagrangian is in general not a conserved quantity even if it does not depend explicitly on time: $\dot L = \frac{d(p\dot q)}{dt}$. For a particle moving in a 1d potential, $\dot L = -2pV'(q)/m$ which is not identically zero if there is a force.

[41] Any real matrix with entries m_{ij} can be written uniquely as a sum of a symmetric and an antisymmetric matrix $m_{ij} = s_{ij} + a_{ij}$. The antisymmetric part does not contribute to the kinetic energy $a_{ij}\dot q^i \dot q^j = 0$ (see Prob. 3.22).

[42] We will often gloss over the difference between a tensor and its components, the latter are defined once a basis is chosen, see Appendix B.6*

Riemannian metric[43] on configuration space. Suppose the Lagrangian is

$$L = T - V = \frac{1}{2} m_{ij}(q) \dot{q}^i \dot{q}^j - V(q), \tag{3.42}$$

where, as before, lower and upper repeated indices are summed. Then, one finds that the conjugate momenta are

$$p_k = \frac{\partial L}{\partial \dot{q}^k} = \frac{1}{2} m_{ij} \delta^i_k \dot{q}^j + \frac{1}{2} m_{ij} \dot{q}^i \delta^j_k = m_{ki} \dot{q}^i. \tag{3.43}$$

Here, δ^i_k is the Kronecker symbol, 1 if $i = k$ and 0 otherwise. The formula $p_k = m_{ki}\dot{q}^i$ further justifies the use of lower indices for the components of the conjugate momentum. Here, the repeated index i is summed (see Footnote 35) leaving the lower index k as the only free index. Moreover, the Hamiltonian coincides with energy

$$H = p_k \dot{q}^k - L = m_{ki} \dot{q}^i \dot{q}^k - \frac{1}{2} m_{ij} \dot{q}^i \dot{q}^j + V = \frac{1}{2} m_{ij}(q) \dot{q}^i \dot{q}^j + V(q) = E. \tag{3.44}$$

Here, we regard the Hamiltonian as a function of generalized coordinates and velocities. In Sect. 3.14, when we discuss the Hamiltonian formulation of mechanics, we will eliminate $\dot{q}^i$ in favor of momenta and regard the Hamiltonian as a function of coordinates and momenta.

If the Lagrangian is not quadratic (bilinear) in velocities, then the Hamiltonian may not coincide with $T + V$. For example, consider a Lagrangian $L = T - V$ with cubic kinetic term $T = \frac{1}{2} m \dot{q}^2 + \frac{1}{3} g \dot{q}^3$ and some smooth potential V. Then the conjugate momentum is

$$p = \frac{\partial L}{\partial \dot{q}} = m\dot{q} + g\dot{q}^2. \tag{3.45}$$

The Hamiltonian is seen not to coincide with $T + V$:

$$H = p\dot{q} - L = (m\dot{q} + g\dot{q}^2)\dot{q} - \frac{1}{2} m \dot{q}^2 - \frac{g}{3} \dot{q}^3 + V = \frac{1}{2} m \dot{q}^2 + \frac{2}{3} g \dot{q}^3 + V \neq T + V. \tag{3.46}$$

While the Hamiltonian is always conserved (provided $\frac{\partial L}{\partial t} = 0$), $T + V$ may not be conserved (see Prob. 3.20) and may not be a particularly interesting physical quantity. In fact, henceforth, we will use the word energy for the conserved quantity $p_k \dot{q}^k - L$, rather than for $T + V$, if they are distinct.

3.10 Symmetries to conserved quantities: Noether's theorem

Lagrange's (and Newton's) equations of classical mechanics have been formulated as conditions for the action $S = \int L \, dt$ to be extremal. Many concepts (such as symmetries) may be formulated more simply in terms of the action or Lagrangian than in terms of the equations of motion.

---

[43] A Riemannian metric allows one to define the inner product of a pair of tangent vectors at a point. If $\dot{q}$ and $\dot{\tilde{q}}$ are velocity vectors to a pair of curves passing through a point of $\mathcal{Q}$, then their inner product is defined as $(\dot{q}, \dot{\tilde{q}}) = m_{ij} \dot{q}^i \dot{\tilde{q}}^j$. The inner product may then be used to define angles between tangent vectors and lengths of tangent vectors.

If a coordinate q^j is cyclic (absent from the Lagrangian), then its conjugate momentum $p_j = \frac{\partial L}{\partial \dot{q}^j}$ is conserved as a consequence of Lagrange's equation $\dot{p}_j = \frac{\partial L}{\partial q^j} = 0$. If the Lagrangian is independent of a coordinate, then it is unchanged when this coordinate is shifted by a constant: $\delta L = 0$ under $q^j \to q^j + \delta q^j$. We say that translations of a cyclic coordinate q^j are a symmetry of the Lagrangian. This relation between symmetries and conserved quantities is deeper, it goes beyond mere translations of a cyclic coordinate.

A transformation of coordinates $q^i \to \tilde{q}^i$ is a symmetry of the equations of motion (EOM) if it leaves them unaltered: i.e., the EOM for $\tilde{q}$ is the same as that for q. Symmetries usually allow us to produce new solutions from known ones. For example, the free particle equation $m\ddot{q} = 0$ is left unchanged by a translation of the coordinate $q \to \tilde{q} = q + a$ for any constant length a. Now $q = 0$ is one static solution. We may use the symmetry under translations to produce other static solutions, namely $q = a$ for any $a \in \mathbb{R}$, i.e., the particle is at rest at the location with coordinate a rather than at the origin. Incidentally, the momentum of a free particle is conserved in time. We will see that such symmetries are associated with conserved quantities. On the other hand, the equation of motion of a particle attached to a spring $m\ddot{q} = -kq$ is nontrivially modified by a translation of the coordinate $q \to \tilde{q} = q + a$ since $\tilde{q}$ satisfies a different equation $m\ddot{\tilde{q}} = -k\tilde{q} + ka$. Moreover, $p = m\dot{q}$ is not (in general) conserved for a particle executing simple harmonic motion: the momentum is zero at the turning points and maximally nonvanishing at the point of equilibrium (see Sect. 6.1).

Remark. It is important to note that not every transformation of q qualifies as a symmetry of the equations of motion. We have already argued in Sect. 3.8 that every transformation of coordinates leaves the form of Lagrange's equations invariant. So here, when we say 'leaves the EOM invariant', we are not referring to the form of Lagrange's equations, i.e., $\frac{\partial}{\partial t}\frac{\partial L}{\partial \dot{q}} = \frac{\partial L}{\partial q}$ but to the differential equations written out explicitly without any Lagrange function present. □

A symmetry of the Lagrangian is a transformation that leaves L unchanged (i.e., L remains invariant). E.g., for the free particle, $L = \frac{1}{2}m\dot{q}^2$ is unchanged under the shift $q \to q + a$. It follows that the action $S[q] = \int_{t_1}^{t_2} \frac{1}{2}m\dot{q}^2 \, dt$ is also unchanged under the shift $q \to q+a$. Since the EOM are the conditions for S to be stationary, a symmetry of the Lagrangian must also be a symmetry of Lagrange's equations. Noether's theorem constructs a conserved quantity associated to each *infinitesimal* continuous symmetry of the Lagrangian[44]. Let us see how. Suppose the infinitesimal change[45] $q^i \to q^i + \delta q^i$ leaves the Lagrangian unchanged to linear order in δq. Then it is automatically an infinitesimal symmetry of the action. Let us explicitly calculate the first variation of the action for paths between the (arbitrary) times t_1 and t_2, $S[q + \delta q] = S[q] + \delta S$. Up to terms of order $(\delta q)^2$ we get

$$\delta S = \int_{t_1}^{t_2} \left[\delta q^i \frac{\partial L}{\partial q^i} + \delta \dot{q}^i \frac{\partial L}{\partial \dot{q}^i} \right] dt = \int_{t_1}^{t_2} \left[\delta q^i \frac{\partial L}{\partial q^i} + \frac{d}{dt}\left(\delta q^i \frac{\partial L}{\partial \dot{q}^i} \right) - \delta q^i \frac{d}{dt}\frac{\partial L}{\partial \dot{q}^i} \right] dt$$

---

[44] There is a generalization to the case where L changes by a time derivative, see Sect. 3.11*.

[45] Here, δq^i could be functions of all the coordinates.

$$= \quad \delta q^i(t_2)\frac{\partial L}{\partial \dot{q}^i}(t_2) - \delta q^i(t_1)\frac{\partial L}{\partial \dot{q}^i}(t_1) + \int_{t_1}^{t_2} \delta q^i \left[\frac{\partial L}{\partial q^i} - \frac{d}{dt}\frac{\partial L}{\partial \dot{q}^i}\right] dt. \tag{3.47}$$

So far, this is true for any path and for any infinitesimal change[46] δq^i. Let us now specialize to infinitesimal changes about a trajectory, so that $q^i(t)$ satisfies Lagrange's equations and the last term vanishes. Furthermore, let us suppose that the transformation is an infinitesimal symmetry of the Lagrangian, so that $\delta S = 0$:

$$0 = \delta S = \delta q^i(t_2)\frac{\partial L}{\partial \dot{q}^i}(t_2) - \delta q^i(t_1)\frac{\partial L}{\partial \dot{q}^i}(t_1). \tag{3.48}$$

Since t_1, t_2 are arbitrary, the quantity $\delta q^i \, \frac{\partial L}{\partial \dot{q}^i}$ must be constant along a trajectory. In other words, an infinitesimal symmetry $q \to q + \delta q$ of the Lagrangian implies that

$$Q = p_i(t)\delta q^i(t) = \boldsymbol{p} \cdot \delta \boldsymbol{q} \tag{3.49}$$

is a constant of the motion, i.e., the dynamical variable Q has the same value at all points along a trajectory. Q is called the conserved Noether 'charge', in loose analogy with the conservation of electric charge.

Example 1: We already saw that the free particle Lagrangian is translation invariant with $\delta q^i = a^i$ where a^i are the components of an arbitrary infinitesimal vector. It follows that $Q = a^i p_i = \boldsymbol{p} \cdot \boldsymbol{a}$ is a conserved quantity. In other words, the component of momentum in *any* direction is conserved. $\square$

Example 2: Now consider a particle in a central potential $V(\boldsymbol{q}^2)$ so that the Lagrangian is

$$L(\boldsymbol{q}, \dot{\boldsymbol{q}}) = \frac{1}{2} m \dot{\boldsymbol{q}} \cdot \dot{\boldsymbol{q}} - V(\boldsymbol{q} \cdot \boldsymbol{q}). \tag{3.50}$$

Let us first show that L is invariant under rotations of 3d Euclidean space $\boldsymbol{q} \to R\boldsymbol{q}$ where R is any rotation matrix[47] ($R^t R = I, \det R = 1$ where ^{t} denotes the transpose). Recall that the dot product is defined as $\boldsymbol{a} \cdot \boldsymbol{b} = \boldsymbol{a}^t \boldsymbol{b}$ for any column vectors $\boldsymbol{a}, \boldsymbol{b}$ and that $(R\boldsymbol{a})^t = \boldsymbol{a}^t R^t$ for any matrix R. Thus,

$$L(R\boldsymbol{q}, R\dot{\boldsymbol{q}}) = \frac{1}{2} m \dot{\boldsymbol{q}} R^t R \dot{\boldsymbol{q}} - V(\boldsymbol{q}^t R^t R \boldsymbol{q}) = \frac{1}{2} m \dot{\boldsymbol{q}}^t \dot{\boldsymbol{q}} - V(\boldsymbol{q}^t \boldsymbol{q}) = L(\boldsymbol{q}, \dot{\boldsymbol{q}}). \tag{3.51}$$

---

[46] We do not require that δq vanish at the initial and final times. A symmetry transformation would not know about these arbitrarily chosen times. For instance, if the symmetry were a translation, $\delta q = a$ would not vanish anywhere!

[47] Rotations (or proper rotations) are orientation-preserving linear transformations of $\mathbb{R}^3$ that preserve the lengths of vectors and angles between vectors. Lengths and angles are preserved if inner products are preserved: $(\boldsymbol{u}, \boldsymbol{v}) = (R\boldsymbol{u}, R\boldsymbol{v})$, which is the condition $\boldsymbol{u}^t \boldsymbol{v} = \boldsymbol{u}^t R^t R \boldsymbol{v}$ for all $\boldsymbol{u}, \boldsymbol{v} \in \mathbb{R}^3$. Thus, we must have $R^t R = I$, the 3×3 identity matrix. Such matrices form the orthogonal group $O(3)$ (see Sect. 3.13* and Appendix B.13*) and have determinant ± 1. Those with $\det R = -1$ are orientation-reversing and involve reflections in an essential way (see Prob. 3.24). Excluding them leaves the group of proper rotations $SO(3)$ of special orthogonal matrices. Composition of rotations is given by matrix multiplication.

So the Lagrangian is invariant under rotations. Noether's theorem, however, refers to infinitesimal transformations, rotations in this case. So let us find a formula for an infinitesimal rotation.

Suppose we make an infinitesimal counterclockwise rotation of the vector $\boldsymbol{q}$ about the axis $\hat{\boldsymbol{n}}$ by a small angle θ, as shown in Fig. 3.7. Then the vector $\boldsymbol{q}$ sweeps out a sector of a cone. Suppose $\boldsymbol{q}$ makes an angle ϕ with respect to $\hat{\boldsymbol{n}}$, so that the opening angle of the cone is ϕ. Then the rotated vector $\tilde{\boldsymbol{q}}$ also makes an angle ϕ with respect to the axis $\hat{\boldsymbol{n}}$. Let $\delta\boldsymbol{q} = \tilde{\boldsymbol{q}} - \boldsymbol{q}$ be the infinitesimal change in $\boldsymbol{q}$. By looking at the base of this cone, we find that it is a sector of a circle with radius $q\sin\phi$ and opening angle $\theta \ll 1$. So we find that $|\delta\boldsymbol{q}| \approx \theta q \sin\phi$. Moreover δq points in the direction of $\hat{\boldsymbol{n}} \times \boldsymbol{q}$. Thus, under a counterclockwise rotation about the axis $\hat{\boldsymbol{n}}$ by a small angle θ, the change in $\boldsymbol{q}$ is

$$\delta\boldsymbol{q} = \theta\, \hat{\boldsymbol{n}} \times \boldsymbol{q} \qquad \text{and} \qquad \delta\dot{\boldsymbol{q}} = \theta\, \hat{\boldsymbol{n}} \times \dot{\boldsymbol{q}}. \tag{3.52}$$

In particular, we see that $\delta\boldsymbol{q}$ and $\delta\dot{\boldsymbol{q}}$ are orthogonal to $\boldsymbol{q}$ and $\dot{\boldsymbol{q}}$ respectively.

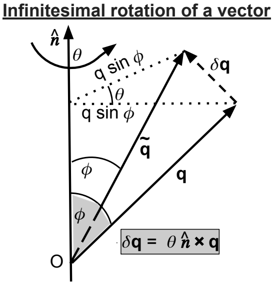
Infinitesimal rotation of a vector

Figure 3.7: Infinitesimal counterclockwise rotation of vector $\boldsymbol{q}$ about axis $\hat{\boldsymbol{n}}$ by small angle θ.

Now we check that the Lagrangian (3.50) is invariant under infinitesimal rotations:

$$L(\boldsymbol{q}+\delta\boldsymbol{q}, \dot{\boldsymbol{q}}+\delta\dot{\boldsymbol{q}}) \approx \frac{1}{2}m\dot{\boldsymbol{q}}^2 + \frac{1}{2}m\dot{\boldsymbol{q}}\cdot\delta\dot{\boldsymbol{q}} + \frac{1}{2}m\delta\dot{\boldsymbol{q}}\cdot\dot{\boldsymbol{q}} - V(\boldsymbol{q}^2 + \boldsymbol{q}\cdot\delta\boldsymbol{q} + \delta\boldsymbol{q}\cdot\boldsymbol{q}) = L(\boldsymbol{q}, \dot{\boldsymbol{q}}). \tag{3.53}$$

The last equality follows on account of the orthogonality properties just mentioned. Thus the Lagrangian (and action) are invariant under infinitesimal rotations. The resulting conserved quantity from Noether's theorem is

$$Q = \boldsymbol{p}\cdot\theta\ (\hat{\boldsymbol{n}} \times \boldsymbol{q}) = \theta\, \hat{\boldsymbol{n}} \cdot (\boldsymbol{q} \times \boldsymbol{p}) = \theta\, \boldsymbol{L}\cdot\hat{\boldsymbol{n}}. \tag{3.54}$$

Since Q is conserved for any small angle θ and for any axis of rotation $\hat{\boldsymbol{n}}$, we conclude that the component of angular momentum in *any* direction is conserved. So the angular momentum vector is a constant of motion $\frac{d\boldsymbol{L}}{dt} = 0$, a fact we are familiar with from the Kepler problem for the $1/r$ central potential (2.16). We also knew this since the torque $\boldsymbol{r} \times \boldsymbol{F}$ on such a particle about the force center vanishes: the moment arm and force both point radially. □

Remark. One may wonder whether all conserved quantities arise from the application of Noether's theorem to symmetries. This is not the case. To begin with, it only applies to continuous symmetry transformations that depart infinitesimally from the identity transformation. There are discrete symmetries outside its purview (like parity) that can lead to conserved quantities. What is more, there are systems (especially integrable systems with infinitely many degrees of freedom) where some conserved quantities arise from the application of Noether's theorem to space-time or internal symmetries while the remaining conserved quantities do not, in any straightforward sense. In addition, in our treatment of Noether's theorem, we have only considered transformations of the configuration space variables that leave the Lagrangian invariant. There are more general transformations that either do not leave the Lagrangian invariant or which are defined on the phase (rather than configuration) space, but that could still count as symmetries and lead to conservation laws. We will see this in Sect. 3.11* and in Sect. 10.7, where we take a phase space approach to Noether's theorem. □

3.11* Noether's theorem when Lagrangian changes by a time derivative

As before, consider an infinitesimal transformation $q^i \to q^i + \delta q^i$ which is a symmetry of the equations of motion. In other words, if $q^i(t)$ is a solution of the EOM, then so is $q^i + \delta q^i$ where δq^i is treated to first order. Interestingly, even if the Lagrangian is *not* invariant under this infinitesimal transformation, but changes by a time derivative $\delta L = \frac{dK}{dt}$, we still have a conserved quantity:

$$Q = p_i \, \delta q^i - K. \tag{3.55}$$

Here $K(q(t), t)$ can be a function of coordinates and time as in Sect. 3.6. Let us see why this is the case. Consider the action for a path between times t_1 and t_2. As before, we compute the change in action due to an infinitesimal variation of path $\delta q^i(t)$

$$\delta S = \int_{t_1}^{t_2} \left[\frac{\partial L}{\partial q^i} \delta q^i + \frac{\partial L}{\partial \dot{q}^i} \delta \dot{q}^i \right] dt = \int_{t_1}^{t_2} \left[\left(\frac{\partial L}{\partial q^i} - \frac{d}{dt} \frac{\partial L}{\partial \dot{q}^i} \right) \delta q^i + \frac{d}{dt} \left(\frac{\partial L}{\partial \dot{q}^i} \delta q^i \right) \right] dt. \tag{3.56}$$

Now suppose the path happened to be a trajectory satisfying Lagrange's equations, then the first term vanishes and the change in action under the above transformation is

$$\delta S = (p_i \, \delta q^i)(t_2) - (p_i \, \delta q^i)(t_1). \tag{3.57}$$

Note that in general, the action will not be invariant under this transformation. As mentioned in Footnote 46, it is important to bear in mind that the variation δq need not vanish at t_1 and t_2. The infinitesimal change δq knows nothing about t_1, t_2, it is not the type of variation we considered while deriving the EL equations in Sect. 3.5.

Now we have another way of computing the infinitesimal change in action around a trajectory, due to the above transformation,

$$\delta S = \int_{t_1}^{t_2} \delta L \, dt = \int_{t_1}^{t_2} \frac{dK}{dt} dt = K(t_2) - K(t_1). \tag{3.58}$$

Equating these two expressions for δS we find

$$p_i(t_2) \, \delta q^i(t_2) - K(t_2) = p_i(t_1) \, \delta q^i(t_1) - K(t_1). \tag{3.59}$$

Since t_1, t_2 are arbitrary, we conclude that the quantity $Q(t) = p_i \delta q^i - K$ is a constant of motion, $\dot{Q} = 0$.

Example: Let us illustrate with the example of a Galilean boost for a free particle moving on a line with Lagrangian $L = \frac{1}{2} m\dot{x}^2$ and equation of motion $m\ddot{x} = 0$. Define the infinitesimal Galilean boost by a small velocity c:

$$x \to \tilde{x} = x + \delta x = x + ct. \tag{3.60}$$

Note: c is not to be confused with the speed of light! It corresponds to changing from one inertial reference frame to another that is moving at velocity c (see Sect. 3.12). Then

$$\delta x = ct, \quad \delta\dot{x} = c \quad \text{and} \quad \delta\ddot{x} = 0. \tag{3.61}$$

It follows that the transformation leaves the equation of motion unchanged since $m\ddot{\tilde{x}} = m\ddot{x} = 0$. So a Galilean boost is a symmetry of the EOM. The corresponding change in the Lagrangian is a time derivative:

$$\delta L = m\dot{x}\,\delta\dot{x} = mc\dot{x} = \frac{d}{dt}(mcx). \tag{3.62}$$

So we may take $K = mcx$ (K is defined up to an additive constant). The above theorem asserts that

$$Q = p\,\delta x - K = c(pt - mx) \tag{3.63}$$

is a constant of motion. Since c is an arbitrary small constant, we drop it and take $Q = pt - mx$. We check using the equation of motion ($\dot{p} = 0$) that Q is indeed conserved:

$$\dot{Q} = \dot{p}t + p - m\dot{x} = p - p = 0. \tag{3.64}$$

A Galilean boost is a symmetry also for a particle subject to a constant external force, where $V(x) = V_0 x$ is linear. But it is not a symmetry of the equation of motion $m\ddot{x} + V'(x) = 0$ for a particle in a more general potential. Though $\delta\ddot{x} = 0$, $\delta V'(x) = V''(x)ct \neq 0$ in general. A simple harmonic oscillator potential, for instance, breaks Galilean invariance, just as it breaks translation invariance. □

3.12 Inertial frames of reference and Galilean invariance

Recall from Sect. 3.3 that an inertial frame of reference is one in which Newton's first law holds. The name inertial derives from the fact that Newton's first law is also called the law of inertia. In general, Newton's second law is valid only in inertial frames of reference. To find out whether a frame is inertial, one needs to perform experiments or make observations to check whether a particle believed to be free (isolated) travels uniformly along a straight-line trajectory to the desired accuracy[48]. For most practical purposes concerning the motion of projectiles and billiard balls, a frame fixed in a lab on the Earth can be considered inertial, though there are situations where the rotation of the Earth can produce noninertial effects (as in Foucault's pendulum, see Sect. 9.4). For the motion of the Sun, planets and satellites, the frame of the faraway 'fixed stars' can serve as an inertial frame to a reasonable accuracy.

---

[48] There are indirect ways to check whether a frame is inertial even if one cannot isolate particles. One option is to try to cancel out forces, e.g., (i) the upward normal reaction force cancels the gravitational force on a body moving on a horizontal table or (ii) introducing an electric field can counterbalance a gravitational force on massive charged particles. Another

Given an inertial frame K (with an origin and, say, Cartesian coordinate axes and a clock for time-keeping), consider a frame K' (equipped with its Cartesian coordinates and clock) that differs from K at most by a combination of (a) a translation of time, (b) a spatial translation by a fixed vector, (c) a Galilean boost[49] resulting from K' moving at a fixed velocity relative to K and (d) a fixed rotation (proper or improper). We will show that Newton's equations of motion take the same form[50] in K' as they did in K, so that K' may also be regarded as inertial. The advantage of inertial frames is that the laws governing motion take a simple form in them: free particles remain at rest if they began that way. All possible locations and orientations of a system as a whole in space and all possible 'starting' instants of time to describe the dynamics in an inertial frame lead to the same form for the equations of motion. We say that space and time are homogeneous ('no preferred location or time') and that space is isotropic ('no preferred direction') in an inertial frame. That the laws of mechanics[51] take the same form in two inertial frames that are in uniform motion relative to each other was postulated by Galileo Galilei [42] and is called the principle of Galilean relativity[52]. This is encoded in the invariance of the form of Newton's second law under Galilean transformations between inertial frames of reference.

Examples of noninertial frames include those that are rotating (uniformly or otherwise) relative to K or, more generally, are accelerating relative to K. We will see in Chap. 9, that Newton's equations generally *do not* retain their $m\ddot{\boldsymbol{r}} = \boldsymbol{F}$ form when one goes from an inertial frame to a noninertial one. In particular, free particles can be subject to 'fictitious' forces in a noninertial frame, so that the law of inertia does not hold in its simple form.

---

possibility is to make use of Newton's second law, which is a statement about inertial frames. Suppose we assume a frame is inertial, deduce consequences using Newton's second law and find that they are experimentally violated. Then, a possible reason for the discrepancy can be that the frame was not inertial to begin with. The Foucault pendulum of Sect. 9.4 gives a concrete realization of this idea and strongly suggests that a frame fixed in a lab on the Earth is not quite an inertial frame, due to the Earth's rotation on its axis.

[49] The name Galilean boost is used to distinguish it from Lorentz boosts (4.7) encountered in the special theory of relativity.

[50] To show this, we will postulate that the mass of a particle is the same in both frames, i.e., that it is a Galilean invariant.

[51] In other words, Newton's laws are valid in one inertial frame iff they are valid in another inertial frame. In particular, mechanical phenomena cannot be used to pick out any one inertial frame as being 'stationary'.

[52] An early precursor is Āryabhaṭa's principle of relativity of motion (circa 500 CE). For instance, in the 9th verse of the *Gola Pada* (spherical trigonometry and celestial mechanics) section of his Āryabhaṭīya [115], he says: *Just as a person traveling on a boat sees fixed objects moving in the opposite direction, fixed stars likewise appear to move westwards when viewed from Lanka.* In the next verse, he says: *Driven by the pravaaha wind, the cage of asterisms together with planets constantly move westwards of Lanka resulting in their rising and setting.*

To be concrete, let us consider a system of N particles with positions $\boldsymbol{r}_a$ and masses m_a for $a = 1, 2, \ldots, N$, interacting via interparticle central forces derived from a potential V. Newton's equations referred to the inertial frame K are

$$m_a \ddot{\boldsymbol{r}}_a = -\boldsymbol{\nabla}_a \sum_{b \neq a} V(|\boldsymbol{r}_a - \boldsymbol{r}_b|) = -\sum_{b \neq a} V'(|\boldsymbol{r}_a - \boldsymbol{r}_b|) \frac{\boldsymbol{r}_a - \boldsymbol{r}_b}{|\boldsymbol{r}_a - \boldsymbol{r}_b|} \tag{3.65}$$

for $a = 1, \ldots, N$. The gradients are evaluated as in Sect. 2.2. These equations follow from the Lagrangian

$$L = \sum\nolimits_a \frac{1}{2} m_a \dot{\boldsymbol{r}}_a^2 - \frac{1}{2} \sum\nolimits_{a \neq b} V(|\boldsymbol{r}_a - \boldsymbol{r}_b|). \tag{3.66}$$

The factor of $1/2$ in the second term is to avoid counting the potential energy between particles a and b twice. The gravitational two-body problem of Chap. 2 is the special case with $N = 2$ and $V(|\boldsymbol{r}_1 - \boldsymbol{r}_2|) = -G m_1 m_2 / |\boldsymbol{r}_1 - \boldsymbol{r}_2|$.

Let us now examine how (3.65) and (3.66) transform under translations, rotations and boosts assuming the masses m_a remain unchanged. The variables measured with respect to frame K' will be denoted by primes.

Time-translation. Under a time-translation, the time as kept by an observer in K' is $t' = t + \tau$ where t is the time with respect to K. Since $\frac{d}{dt'} = \frac{d}{dt}$ and the potential is not explicitly time-dependent, both (3.65) and (3.66) are invariant under time-translations.

Space-translation. Suppose the origin of K' is located at the point[53] $-\boldsymbol{s}$ with respect to the origin of K while the axes of both frames are parallel. As shown in Fig. 3.8a, under such a translation, all position vectors are shifted by the common vector $\boldsymbol{s}$:

$$\boldsymbol{r}_a \mapsto \boldsymbol{r}'_a = \boldsymbol{r}_a + \boldsymbol{s} \quad \text{for all} \quad a = 1, 2 \ldots, N. \tag{3.67}$$

Consequently, velocities and accelerations do not change under a translation: $\dot{\boldsymbol{r}}'_a = \dot{\boldsymbol{r}}_a$ and $\ddot{\boldsymbol{r}}'_a = \ddot{\boldsymbol{r}}_a$. Gradients and relative vectors also remain unchanged $\boldsymbol{\nabla}'_a = \boldsymbol{\nabla}_a$ and $\boldsymbol{r}'_a - \boldsymbol{r}'_b = \boldsymbol{r}_a - \boldsymbol{r}_b$. It follows that the EOM (3.65) as well as the Lagrangian (3.66) are invariant under space-translations.

Galilean boost. Here, the origin of K' moves at a constant velocity $-\boldsymbol{v}$ relative to the origin of K while keeping the axes parallel, as shown in Fig. 3.8b. Through a suitable choice of origin of their common time, we will suppose that the frames coincide at $t = 0$. Under such a boost,

$$\boldsymbol{r}_a \mapsto \boldsymbol{r}'_a = \boldsymbol{r}_a + \boldsymbol{v}t \quad \text{while} \quad \dot{\boldsymbol{r}}'_a = \dot{\boldsymbol{r}}_a + \boldsymbol{v}, \quad \ddot{\boldsymbol{r}}'_a = \ddot{\boldsymbol{r}}_a \quad \text{and} \quad \boldsymbol{\nabla}'_a = \boldsymbol{\nabla}_a. \tag{3.68}$$

As with translations, relative vectors are unchanged. Thus, the EOM (3.65) are invariant under Galilean boosts. The transformed Lagrangian on the other hand is

$$L' = L + \sum_a \left[\frac{1}{2} m_a \boldsymbol{v}^2 + m_a \dot{\boldsymbol{r}}_a \cdot \boldsymbol{v} \right] = L + \frac{d}{dt} \sum_a \left[\frac{1}{2} m_a \boldsymbol{v}^2 t + m_a \boldsymbol{r}_a \cdot \boldsymbol{v} \right]. \tag{3.69}$$

---

[53] We choose the shift $-\boldsymbol{s}$ to avoid some negative signs in the formula (3.74) for composing Galilean transformations.

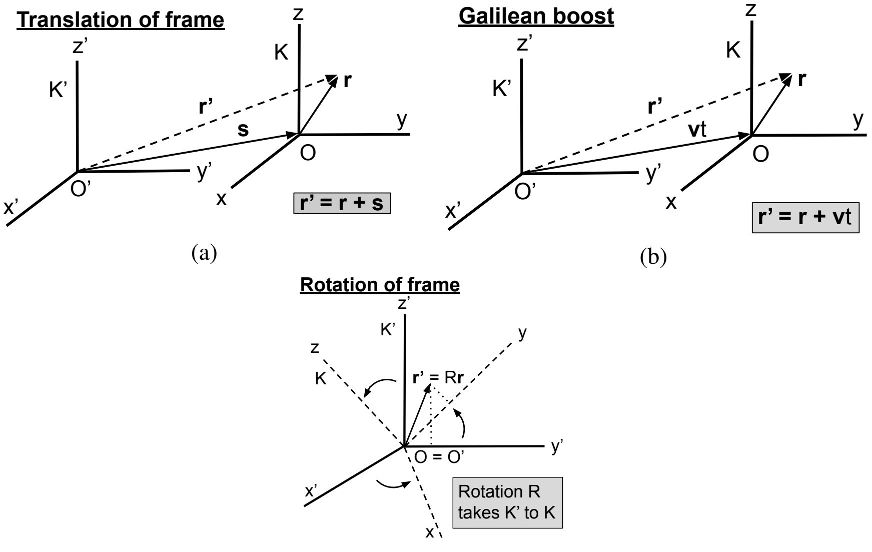

(a) (b) (c)

Figure 3.8: Reference frames K and K' for (a) a space translation (b) a boost and (c) a rotation. For the rotation of frames, though $\boldsymbol{r}$ and $\boldsymbol{r}'$ refer to the same radius vector, their components (with respect to K and K') are different, as indicated by the dotted lines.

Since the Lagrangian L' in the boosted frame differs from that in the original frame by the time derivative of a function of positions and time, it leads to the same EOM, as shown in Sect. 3.6.

Rigid rotation (proper or improper). Suppose the axes of the frame K' are obtained from those of K via the orthogonal rotation matrix R^{-1} (see Fig. 3.8c). In particular, K and K' have a common origin. As with translations, the frame and components of vectors in the frame transform oppositely. Thus,

$$\boldsymbol{r}_a \mapsto \boldsymbol{r}'_a = R\boldsymbol{r}_a \quad \text{or} \quad x'_{ai} = R_{ij}x_{aj} \quad \text{where} \quad R^t R = I. \tag{3.70}$$

Here, we used $i, j = 1, 2, 3$ to label Cartesian components. A sum over repeated indices is implied. Evidently, velocities and accelerations transform in the same way as position vectors do, since R is independent of time: $\dot{\boldsymbol{r}}'_a = R\dot{\boldsymbol{r}}_a$ and $\ddot{\boldsymbol{r}}'_a = R\ddot{\boldsymbol{r}}_a$. Moreover, lengths of velocity vectors and relative vectors are unchanged under rotations (as well as reflections). Thus, the LHS and RHS of (3.65) both transform in the same way (as vectors) so that the EOM for $\boldsymbol{r}'_a$ and $\boldsymbol{r}_a$ are the same. Similarly, the Lagrangian is unchanged under a rotation or a reflection.

Combining all four, a Galilean transformation, which acts as an affine transformation on position vectors and time:

$$(t, \boldsymbol{r}_a) \mapsto (t', \boldsymbol{r}'_a) = (t + \tau, R\,\boldsymbol{r}_a + \boldsymbol{v}t + \boldsymbol{s}) \tag{3.71}$$

is a symmetry of Newton's equations for a system of particles subject to conservative central forces. Thus, the equations take the same form in any two inertial frames of reference.

External forces and their lack of Galilean invariance. It is important to bear in mind that Newton's equations are *not* Galilean invariant for certain external or time-dependent forces. For instance, the external gravitational force on a particle in a lab on the Earth always points downwards and breaks the isotropy of space within the lab. To recover isotropy, one needs to consider the combined particle-Earth system. Newton's equation for a single particle subject to an *external* harmonic potential $m\ddot{x} = -kx$ is neither translation-invariant nor boost-invariant: $V(x) = \frac{1}{2}kx^2$ explicitly breaks translation-invariance (the point $x = 0$ is special) and a nonzero V'' implies the harmonic potential is *not* boost-invariant either (see Sect. 3.11*). Similarly, Newton's equation (2.9) for the Keplerian one-body problem concerning the motion of the reduced mass in a central potential is not translation-invariant. Focusing on the relative motion and ignoring the motion of the center of mass breaks the homogeneity of space: the point $\boldsymbol{r} = 0$ is special as it is the center of the 'external' gravitational force. Similarly, an explicitly time-dependent force breaks the homogeneity of time. Analogously, Newton's equation for a particle subject to an external damping force dependent on its velocity is *not* invariant under a Galilean boost (though it is invariant under space and time translations). In fact, under the boost $x' = x + vt, t' = t$, the equation $m\ddot{x} = -\gamma\dot{x}$ for constant damping coefficient γ becomes $m\ddot{x}' = -\gamma(\dot{x}' - v)$. These examples do not contradict Galileo's principle of relativity or the Galilean invariance of Newton's laws, since the principle applies to interparticle forces rather than to external forces.

$*$ **Galilean transformations form a group**[54]**.** A Galilean transformation g acts on space-time by taking a point (or event) with coordinates $(t, \boldsymbol{r})$ in an inertial frame to a transformed point $(t', \boldsymbol{r}') = (t + \tau, R\boldsymbol{r} + \boldsymbol{v}t + \boldsymbol{s})$. This is an affine transformation[55] and may be expressed in matrix form:

$$\begin{pmatrix} t' \\ x' \\ y' \\ z' \end{pmatrix} = \begin{pmatrix} 1 & 0 & 0 & 0 \\ v_1 & R_{11} & R_{12} & R_{13} \\ v_2 & R_{21} & R_{22} & R_{23} \\ v_3 & R_{31} & R_{32} & R_{33} \end{pmatrix} \begin{pmatrix} t \\ x \\ y \\ z \end{pmatrix} + \begin{pmatrix} \tau \\ s_1 \\ s_2 \\ s_3 \end{pmatrix}. \tag{3.72}$$

We will label this Galilean transformation by the ordered 4-tuple $g = (\tau, \boldsymbol{s}, \boldsymbol{v}, R)$. When Galilean transformation g' acts after g, we get their composition $g' \circ g$ taking $(t, \boldsymbol{r}) \to (t', \boldsymbol{r}') \to (t'', \boldsymbol{r}'')$. What is more, a Galilean transformation g can be undone or inverted to take $(t', \boldsymbol{r}')$ back to $(t, \boldsymbol{r})$ so that the composition of g followed by its inverse is the identity transformation. We say that the set of Galilean transformations acts as a group of affine transformations of space-time. We now briefly comment on the structure of this Galilean group and the nature of its action on space-time. To begin with, the identity transformation which takes space-time points back to themselves is $(0, \boldsymbol{0}, \boldsymbol{0}, I)$ where I is the 3×3 identity matrix. While space-time translations

---

[54] For a brief introduction to the concept of a group, see Appendix B.13*

[55] An affine transformation is a linear transformation plus a shift. Galilean transformations preserve time intervals and the distance between simultaneous events. They may be characterized as affine transformations with these two properties.

$\boldsymbol{r}' = \boldsymbol{r} + \boldsymbol{s}, t' = t + \tau$ are inhomogeneous, rotations $\boldsymbol{r}' = R\boldsymbol{r}$ and boosts $\boldsymbol{r}' = \boldsymbol{r} + \boldsymbol{v}t$ are homogeneous as they preserve the origin $(t = 0, \boldsymbol{r} = \boldsymbol{0})$. Given another Galilean transformation $g' = (\tau', \boldsymbol{s}', \boldsymbol{v}', R')$, the effect of applying g' after g is

$$t'' = t + \tau + \tau' \quad \text{and} \quad \begin{aligned} \boldsymbol{r}'' &= R'(R\boldsymbol{r} + \boldsymbol{v}t + \boldsymbol{s}) + \boldsymbol{v}'(t + \tau) + \boldsymbol{s}' \\ &= R'R\boldsymbol{r} + (R'\boldsymbol{v} + \boldsymbol{v}')t + (R'\boldsymbol{s} + \boldsymbol{s}' + \boldsymbol{v}'\tau). \end{aligned} \tag{3.73}$$

Thus, the group composition law is

$$g' \circ g = (\tau', \boldsymbol{s}', \boldsymbol{v}', R') \circ (\tau, \boldsymbol{s}, \boldsymbol{v}, R) = (\tau + \tau', R'\boldsymbol{s} + \boldsymbol{s}' + \boldsymbol{v}'\tau, R'\boldsymbol{v} + \boldsymbol{v}', R'R). \tag{3.74}$$

In particular, the inverse is obtained by requiring that $g' \circ g = (0, \boldsymbol{0}, \boldsymbol{0}, I)$:

$$(\tau, \boldsymbol{s}, \boldsymbol{v}, R)^{-1} = (-\tau, -R^t\boldsymbol{s} + R^t\boldsymbol{v}\tau, -R^t\boldsymbol{v}, R^t). \tag{3.75}$$

The Galilei group is a 10 dimensional 'Lie' group. Indeed, to specify a Galilean transformation, one needs 10 real parameters: a time shift τ (1 parameter), a shift vector $\boldsymbol{s}$ (3 parameters), a boost velocity $\boldsymbol{v}$ (3 parameters) and finally an axis (say a unit vector) (2 parameters) and an angle of rotation (1 parameter) to specify R (up to a reflection). Special cases of the composition law (3.74) are easy to understand: successive rotations (R followed by R') are composed by matrix multiplication: $R'R$ which is in general a nonabelian (noncommutative) composition law in the sense that the order of composition matters: $R'R \neq RR'$. Successive temporal or spatial translations or boosts are composed additively and in an abelian (commutative) fashion where the order does not matter: $\tau'' = \tau + \tau'$, $\boldsymbol{s}'' = \boldsymbol{s} + \boldsymbol{s}'$ and $\boldsymbol{v}'' = \boldsymbol{v} + \boldsymbol{v}'$. More generally, it can be shown (see Appendix B.13* and [124]) that (3.74) gives the Galilei group the structure of a 'semidirect product' of the subgroup of rotations and boosts acting on the abelian normal subgroup of time and space translations. The former subgroup is called the homogeneous Galilei group.

3.13* Polar vectors, axial vectors, true scalars and pseudoscalars

By this point, we have met several scalars and vectors associated to the motion of a particle in 3d Euclidean space $\mathbb{R}^3$. Starting with the position vector $\boldsymbol{r}$ (relative to a fixed origin) at any point along a trajectory, we have met the velocity $\boldsymbol{v} = \dot{\boldsymbol{r}}$, momentum $\boldsymbol{p} = m\boldsymbol{v}$, angular momentum $\boldsymbol{L} = \boldsymbol{r} \times \boldsymbol{p}$, torque $\boldsymbol{r} \times \boldsymbol{F}$, square of radial distance $\boldsymbol{r} \cdot \boldsymbol{r}$, kinetic energy $\boldsymbol{p}^2/2m$, etc. We have also met rotations and reflections in $\mathbb{R}^3$ (relative to the same origin), especially in the context of symmetries. As noted in Footnote 47, rotations (proper and improper) are linear transformations[56] of $\mathbb{R}^3$ that preserve the lengths of vectors and angles between vectors. This is ensured if inner products are preserved: $(\boldsymbol{u}, \boldsymbol{v}) = (R\boldsymbol{u}, R\boldsymbol{v})$, which is the condition $\boldsymbol{u}^t\boldsymbol{v} = \boldsymbol{u}^t R^t R\boldsymbol{v}$ for all $\boldsymbol{u}, \boldsymbol{v} \in \mathbb{R}^3$. Thus, we must have $R^t R = I$, the 3×3 identity matrix. Such matrices form the orthogonal group $O(3)$ (see Appendix B.13*) and have determinant ± 1. Those with $\det R = -1$ are called improper rotations. They reverse the orientation of a right-handed orthogonal coordinate system. They involve reflections in an essential way. An example is a reflection in the y-z plane ($R = \text{diag}(-1, 1, 1)$), see Prob. 3.24. Excluding them leaves the subgroup of proper rotations $SO(3)$ of special orthogonal matrices. They preserve the orientation of a right-handed orthogonal coordinate system. For example, a counterclockwise rotation by angle θ about the z-axis is represented by the (proper) rotation matrix $R = (c, -s, 0|s, c, 0|0, 0, 1)$ where $c = \cos\theta$, $s = \sin\theta$ and $|$ indicates the start of a new row.

---

[56] Linear transformations $\boldsymbol{u} \mapsto A\boldsymbol{u}$ take the origin $\boldsymbol{u} = 0$ to itself and therefore do not include translations. An affine transformation $\boldsymbol{u} \mapsto A\boldsymbol{u} + \boldsymbol{v}$ is a translation if $A = I$.

We have already discussed the transformation of a vector under a proper rotation in the context of rotation invariance and Noether's theorem in Sect. 3.10. Here we ask how scalars and vectors transform under a reflection or more generally an improper rotation. In fact, in 3d Euclidean space, we may classify vectors and scalars according to their behavior under (improper) rotations. This leads to the useful concept of polar vectors and axial or pseudovectors as well as true scalars and pseudoscalars.

Suppose R is an orthogonal transformation of 3d Euclidean space $\mathbb{R}^3$, taking $x_i \to R_{ij} x_j$ for $i = 1, 2, 3$. A polar or true vector is one that transforms according to $\boldsymbol{v} \to R\boldsymbol{v}$. A pseudovector or axial vector $\boldsymbol{w}$ is one that transforms according to $\boldsymbol{w} \to \det(R) R\boldsymbol{w}$. Since any improper rotation may be obtained by composing an appropriate proper rotation with a reflection[57] through the origin ($R = -I$ with $\det R = -1$, taking $\boldsymbol{r} \to -\boldsymbol{r}$ and called the parity transformation), it is enough to examine the behavior of a vector under such reflections to determine whether it is polar or axial. It is polar if it reverses sign under the reflection through the origin while it is axial if it does not reverse sign. The position vector $\boldsymbol{r}$ may be regarded as the basic polar vector. Velocity $\dot{\boldsymbol{r}}$, momentum $\boldsymbol{p} = m\dot{\boldsymbol{r}}$ and acceleration $\ddot{\boldsymbol{r}}$, are similarly polar vectors: they reverse sign under a reflection through the origin. The central gravitational force due to a mass is $\propto \boldsymbol{r}$ and is polar. On the other hand, angular momentum $\boldsymbol{L} = \boldsymbol{r} \times \boldsymbol{p}$ is a pseudovector: the changes in sign of $\boldsymbol{r}$ and $\boldsymbol{p}$ cancel out. In general, the cross product of two polar vectors is an axial vector while that of a polar and an axial vector is polar. Torque $\boldsymbol{\tau} = \boldsymbol{r} \times \boldsymbol{F}$ and angular velocity $\boldsymbol{\omega}$ are axial vectors. This is consistent with the formula $\boldsymbol{v} = \boldsymbol{\omega} \times \boldsymbol{r}$; both sides transform as polar vectors.

Moving to vector fields that we will encounter in Chap. 19, the velocity vector field $\boldsymbol{v}$ of a fluid is a polar vector field as it is obtained from the time derivative of the position vector of the fluid element. It reverses sign $\boldsymbol{v} \to -\boldsymbol{v}$ under $\boldsymbol{r} \to -\boldsymbol{r}$ (more precisely, $\boldsymbol{v}(\boldsymbol{r}) \to -\boldsymbol{v}(-\boldsymbol{r})$). On the other hand, the curl of a polar vector field is an axial vector field since $\boldsymbol{\nabla} \to -\boldsymbol{\nabla}$ under the same reflection. Thus, vorticity $\boldsymbol{w} = \boldsymbol{\nabla} \times \boldsymbol{v}$ is an axial vector field. In magnetism, the vector potential $\boldsymbol{A}$ is a polar vector, while the magnetic field $\boldsymbol{B} = \boldsymbol{\nabla} \times \boldsymbol{A}$ is an axial vector.

The classification into 'true' and 'pseudo' may also be applied to scalars. A pseudoscalar changes sign under a reflection through the origin while a true scalar does not. While the dot product of any vector with itself is a true scalar, the dot product of a polar and axial vector is a pseudoscalar. In particular, kinetic energy $\frac{1}{2} m v^2$ is a true scalar, while a particle's helicity $\boldsymbol{p} \cdot \boldsymbol{L}$ and a fluid's helicity density $\boldsymbol{v} \cdot \boldsymbol{w}$ are pseudoscalars.

---

[57] This is related to the fact that the orthogonal group $O(3)$ has only two connected components corresponding to $\det R = \pm 1$, see Appendix B.13*.

Equations in physics typically[58] relate quantities of the same sort (scalars, polar vectors, axial vectors, etc.) so that all terms in the equation transform in the same way. This is the case, for instance, in Newton's second law ($m\ddot{\boldsymbol{a}} = \boldsymbol{F}$) in a gravitational force field, the Lorentz force law ($\boldsymbol{F} = q(\boldsymbol{E} + \boldsymbol{v} \times \boldsymbol{B})$) and the Euler equations (8.54) for a rigid body ($\dot{\boldsymbol{L}} + \boldsymbol{\Omega} \times \boldsymbol{L} = \boldsymbol{\tau}$ and $\dot{\boldsymbol{P}} + \boldsymbol{\Omega} \times \boldsymbol{P} = \boldsymbol{F}$). We say that the motion of a planet, a charged particle and a rigid body are parity or reflection symmetric: a reflected trajectory is also a valid trajectory.

Levi-Civita symbol. The Levi-Civita symbol ϵ_{ijk} introduced in Prob. 3.48 has been defined to have the same components in any coordinate system. In particular, under a reflection in $\mathbb{R}^3$, ϵ_{ijk} do not change sign. Based on this behavior under reflections, we say that ϵ_{ijk} are the components of a pseudotensor. It follows that the cross product of two polar vectors $\sum_{j,k} \epsilon_{ijk} a_j b_k$ does not change sign under a reflection, and is therefore a pseudovector, as noted above.

3.14 Hamilton's equations

In Sect. 3.9, we introduced the Hamiltonian $H = p_i \dot{q}^i - L(q, \dot{q})$ as an interesting conserved quantity implied by Lagrange's equations for a Lagrangian that is not explicitly dependent on time. Here $p_i = \frac{\partial L}{\partial \dot{q}^i}$ is the momentum conjugate to q^i. To understand H better, let us compute its differential using Lagrange's equations

$$dH = p_i d\dot{q}^i + \dot{q}^i dp_i - \frac{\partial L}{\partial q^i} dq^i - \frac{\partial L}{\partial \dot{q}^i} d\dot{q}^i = \cancel{p_i d\dot{q}^i} + \dot{q}^i dp_i - \dot{p}_i dq^i - \cancel{p_i d\dot{q}^i} = -\dot{p}_i dq^i + \dot{q}^i dp_i. \tag{3.76}$$

This reveals that the independent variables in H are the generalized coordinates q^i and the generalized momenta p_i, the terms involving the differentials of velocities cancelled out. So we should think of H as $H(q,p)$. On the other hand, by the definition of partial derivatives,

$$dH(q,p) = \frac{\partial H}{\partial q^i} dq^i + \frac{\partial H}{\partial p_i} dp_i. \tag{3.77}$$

Comparing (3.76) and (3.77), we find that the time derivatives of coordinates and momenta may be expressed in terms of partial derivatives of the Hamiltonian

$$\dot{q}^i = \frac{\partial H}{\partial p_i} \quad \text{and} \quad \dot{p}_i = -\frac{\partial H}{\partial q^i}. \tag{3.78}$$

These first order ODEs are called Hamilton's equations. They give us yet another way of expressing the equations of time evolution. To make sense of these equations we are first supposed to express $H = p_i \dot{q}^i - L(q^i, \dot{q}^i)$ as a function of the coordinates q and momenta p. This is done by eliminating $\dot{q}^i$ in favor of q, p using the definition of conjugate momenta $p_j = \frac{\partial L}{\partial \dot{q}^j}$.

As in the Lagrangian framework, we have the notion of cyclic coordinates. A cyclic coordinate q^j is one that does not appear in $H(q,p)$. A moment's thought will reveal that if q^j does not appear in L, it cannot appear in any of the relations $p_j = \frac{\partial L}{\partial \dot{q}^j}$ and therefore cannot appear in H. The momentum p_j conjugate to a cyclic coordinate q^j is conserved as a consequence of (3.78).

---

[58] There are exceptions when a physical interaction violates reflection or parity symmetry, as with the weak nuclear force.

Example: Particle in a 1d potential. Here $L = \frac{1}{2}m\dot{q}^2 - V(q)$ and $p = m\dot{q}$ so $\dot{q} = p/m$. Then $H = p\dot{q} - L = pp/m - p^2/2m + V(q) = p^2/2m + V(q)$. Hamilton's equations are $\dot{q} = \frac{\partial H}{\partial p} = p/m$ which recovers the definition of conjugate momentum and $\dot{p} = -\frac{\partial H}{\partial q} = -V'(q)$ which is Newton's second law. □

Remark: Time-dependent Hamiltonian. If L depends explicitly on time, then H too will do so. Proceeding as in (3.76), the differential of H admits two expressions:

$$dH = \dot{q}dp - \dot{p}dq - \frac{\partial L}{\partial t}dt \quad \text{and} \quad dH = \frac{\partial H}{\partial q}dq + \frac{\partial H}{\partial p}dp + \frac{\partial H}{\partial t}dt. \tag{3.79}$$

Comparing, we get

$$\dot{q} = \frac{\partial H}{\partial p}, \quad \dot{p} = -\frac{\partial H}{\partial q} \quad \text{and} \quad \frac{\partial H}{\partial t} = -\frac{\partial L}{\partial t}. \tag{3.80}$$

So even for a time-dependent H, Hamilton's equations for coordinates and momenta take the same form as in (3.78). □

Significance of the Hamiltonian formulation. The idea of the Hamiltonian $H(q, p)$ and the associated formulation of dynamics has far-reaching consequences. To begin with, the point of the Hamiltonian formulation is not so much as a technical tool for solving the equations of motion[59] but as an alternate way of obtaining them and thinking about them. It reveals structural features, especially of conservative systems, that are not obvious in the Newtonian formulation. Just like the Lagrangian, a single Hamilton function can generate all the equations of motion which take the same form in all systems of coordinates on configuration space, as we will show in Sect. 3.20*. However, unlike Newton's or Lagrange's equations which are typically second order in time, Hamilton's equations (3.78) are first order in time, admit a formulation in terms of vector fields (see Chap. 5) and reveal a certain hidden symmetry between generalized coordinates and momenta. This observation eventually leads to the recognition that Hamilton's equations retain their form under a larger class of changes of variables called canonical transformations (or symplectic transformations), discussed in Chap. 10. Symmetries of the equations of motion, like translations and rotations, can be economically formulated as properties of the Hamiltonian (see Sect. 3.21 and Sect. 3.22). The Hamiltonian is also used in Sect. 12.1 to give yet another formulation of the equations of dynamics in terms of the Hamilton-Jacobi partial differential equation. This form turns out to be closely related to the equations of wave optics and the idea of a wavefront. It may also be regarded as the 'point of closest approach' of classical dynamics to the Schrödinger equation (see Footnote 14 of Chap. 3) of quantum mechanics, which too is formulated in terms of a (quantum) Hamiltonian. On the other hand, Hamilton's ordinary differential equations (3.78) for trajectories are the mechanical analog of the equations of ray optics. They are also the point of closest approach of classical dynamics to the Heisenberg equations of quantum mechanics. They may also be used to describe magnetic field lines in a plasma and the mixing of fluids. The Hamiltonian also plays a central role in equilibrium statistical mechanics. In the canonical ensemble at absolute temperature T, the state (q,p) on phase space occurs with relative probability $e^{-H(q,p)/k_bT}$ where k_b is Boltzmann's constant. □

---

[59] The Hamiltonian formulation *does* lead to new ways of (approximately) solving the equations of motion. For instance, classical perturbation theory is based on the idea of making a succession of 'canonical transformations' to bring the Hamiltonian to a 'normal' form so that the EOM can be solved more easily at each order in perturbation theory. On the other hand, the first order formulation brings to bear techniques from the theory of vector fields and dynamical systems. Accurate schemes to numerically integrate the equations of motion (such as symplectic integrators) are also based on the Hamiltonian formulation.

3.15 Legendre transform: Hamiltonian from Lagrangian

The Legendre transform summarizes the passage[60] from Lagrangian $L(q,\dot{q})$ to Hamiltonian $H(q,p)$. It is a way of swapping one independent variable for another: momentum replaces velocity in going from L to H. We begin by observing that the formula for the conjugate momenta $p_j = \frac{\partial L}{\partial \dot{q}^j}$ is the condition for the quantity $p_i\dot{q}^i - L(q,\dot{q})$ to be extremal with respect to small variations in $\dot{q}^j$. Indeed, differentiating in $\dot{q}^j$ and equating to zero,

$$\frac{\partial}{\partial \dot{q}^j}(p_i\dot{q}^i - L(q,\dot{q})) = p_i\delta^i_j - \frac{\partial L}{\partial \dot{q}^j} = 0 \quad \text{we get} \quad p_j = \frac{\partial L(q,\dot{q})}{\partial \dot{q}^j}. \qquad (3.81)$$

In finding the condition for an extremum, p is regarded as an independent variable, not as a function of q and $\dot{q}$. It is only at the extremum that p becomes a specific function of q and $\dot{q}$, as determined by the Lagrangian.

Moreover, the extremal value of the quantity $p\dot{q} - L$ is the Hamiltonian $H(q,p)$. Thus, we may write

$$H(q,p) = \text{ext}_{\dot{q}}\left[p_i\dot{q}^i - L(q,\dot{q})\right]. \qquad (3.82)$$

The extremization is carried out with respect to *all* the generalized velocities. Equation (3.82) is the definition of the Legendre transform and we say that H is the Legendre transform of L.

Changing independent variables. It is noteworthy that q plays a passive role in the Legendre transform from $L(q,\dot{q})$ to $H(q,p)$. The Legendre transform allows us to use p as an independent variable[61] in place of $\dot{q}$. We may regard $\dot{q}$ and p as living in dual vector spaces, the tangent and cotangent spaces at the point q on the configuration manifold (see Footnote 34). Consequently, the Legendre transform may be viewed as a recipe for transforming a function on a vector space to a function on the dual vector space. Thus, though we introduced the Legendre transform to systematize the passage from Lagrangian to Hamiltonian, it can be used more generally to change independent variables in functions. Good examples are furnished by the transformations among internal energy, Helmholtz free energy, enthalpy and Gibbs free energy in thermodynamics where we switch between the conjugate variables temperature and entropy or pressure and volume, see Prob. 3.29.

---

[60] The Legendre transform as a way of obtaining the Hamiltonian is relevant to Lagrangians that are quadratic (or of higher degree) in the generalized velocities $\dot{q}^i$. To obtain the Hamiltonian corresponding to a Lagrangian linear in velocities see Prob. 3.39 and Prob. 3.40 as well as the example in Sect. 19.15*.

[61] This is similar to how the Fourier transform $\tilde{f}(\omega) = \int_{-\infty}^{\infty} f(t)e^{-i\omega t}dt$ allows us to change independent variables from time t to angular frequency ω or from position to momentum. In fact, the two transforms are related, see Prob. 3.36.

Existence and singlevaluedness of Legendre transform. The key step in the Legendre transform is to solve for the (real) velocities $\dot{q}$ in terms of the momenta and coordinates using $p_i = \frac{\partial L(q,\dot{q})}{\partial \dot{q}^i}$. This is not always possible. For a quadratic $L = \frac{1}{2}m\dot{q}^2$ with $m \neq 0$, this is easily done since (3.81) gives us a linear equation for $\dot{q}$: $p = m\dot{q}$. This allows us to eliminate $\dot{q} = p/m$ in favor of p giving $H(q,p) = pp/m - \frac{1}{2}m(p/m)^2 = \frac{p^2}{2m}$. However, more generally, it could happen that there is none or more than one real solution $\dot{q}$ to (3.81) for given q, p. If so, H may not exist[62] or may be a multivalued function of coordinates and momenta. Conditions that guarantee that the Legendre transform exists as a singlevalued function is convexity[63] (or concavity) of the Lagrangian as a twice differentiable function of $\dot{q}$ for all $q, \dot{q}$ along with the requirement that $|\frac{\partial L}{\partial \dot{q}}| \to \infty$ as $\dot{q} \to \pm\infty$ for any fixed q. The convexity and growth conditions are seen to be satisfied by $L = \frac{1}{2}m\dot{q}^2$ if $m > 0$[64]. Let us see how these conditions help. L is convex provided the 2nd derivative or Hessian $\frac{\partial^2 L}{\partial \dot{q}^2} > 0$ for all $q, \dot{q}$. Suppose this is the case, then $\Pi(q,\dot{q}) = \frac{\partial L}{\partial \dot{q}}$ must be a strictly monotonically increasing function of $\dot{q}$ for any q. The growth condition implies that $\Pi(q,\dot{q}) \to \pm\infty$ as $\dot{q} \to \pm\infty$. Thus the horizontal line at height p (for any real p) cuts the graph of $\Pi(q,\dot{q})$ as a function of $\dot{q}$ at precisely one point. It follows that the equation $p = \frac{\partial L}{\partial \dot{q}}$ has a unique solution $\dot{q}$ for any given values of q, p. In other words, under the given hypotheses, the Legendre transform of H exists for all q, p and is singlevalued.

If the growth condition is violated, $\Pi(q,\dot{q})$ could asymptote to a finite value as $\dot{q} \to \pm\infty$ resulting in no solution to $\frac{\partial L}{\partial \dot{q}} = p$ for sufficiently large p or $-p$. For instance, $L(q,\dot{q}) = e^{\dot{q}}$ is convex but violates the growth condition as $\dot{q} \to -\infty$. In this case, there is no real solution to $e^{\dot{q}} = p$ for $p < 0$. In other words, the Hamiltonian $H = p \log p - p$ is defined only for positive momentum. In circumstances where this is acceptable, *the growth condition can be dropped.*

To see what can go wrong when convexity fails, let us attempt to compute the Legendre transform of $L = \frac{1}{4}\dot{q}^4 - \frac{1}{2}\dot{q}^2$. The Hessian $L''(\dot{q})$ is $3\dot{q}^2 - 1$. It is negative for $|\dot{q}| < 1/\sqrt{3}$ and positive for $|\dot{q}| > 1/\sqrt{3}$ so L is neither convex nor concave everywhere. It is shaped like a double-well and we expect to run into trouble. Indeed, if we try to solve for $\dot{q}$ in $p = \frac{\partial L}{\partial \dot{q}} = \dot{q}^3 - \dot{q}$, there are three real solutions for any given $|p| < 2/3\sqrt{3}$. In this case, the Legendre transform H is not singlevalued. It is worth noting that we are concerned with real velocities, so nonreal complex roots of this cubic equation are inadmissible. For instance, reversing the sign of $\dot{q}^2$ leads to the Lagrangian $L = \frac{1}{4}\dot{q}^4 + \frac{1}{2}\dot{q}^2$ which is convex everywhere and satisfies the growth condition. What is more, as is seen from the graph, the equation $p = \frac{\partial L}{\partial \dot{q}} = \dot{q}^3 + \dot{q}$ has a unique real solution $\dot{q}$ for any given p, and the Legendre transform is defined as a singlevalued function.

---

[62] When we cannot solve for the velocities in terms of coordinates and momenta, we say that the Lagrangian is singular. In Sect. 3.17* we will indicate how to define a Hamiltonian for singular Lagrangians in such a way that Hamilton's equations agree with Lagrange's equations.

[63] A function $f(x)$ of one real variable x is convex if the graph of f for $x_1 < x < x_2$ lies below the chord joining $f(x_1)$ to $f(x_2)$ for any $x_1 < x_2$. It is concave if the graph lies above the chord. Viewed from below, a sagging clothesline is convex while an arch is concave.

[64] If $m < 0$, L is concave and if $m = 0$ it is neither and the equation $p = 0$ cannot be used to solve for $\dot{q}$ in terms of p.

Legendre transform for more degrees of freedom. For several[65] degrees of freedom, the Legendre transform is defined if L is convex (or concave) and satisfies a growth condition: $|\frac{\partial L}{\partial \dot{q}^i}| \to \infty$ as $|\dot{q}^j| \to \infty$ for each i, j. Note that L is convex provided the 2nd derivative (Hessian) matrix with entries $\frac{\partial^2 L}{\partial \dot{q}^i \partial \dot{q}^j}$ is a positive-definite matrix for all $\dot{q}^i$ and $q \in \mathcal{Q}$. For example, if $L = \frac{1}{2} m_{ij}(q) \dot{q}^i \dot{q}^j - V(q)$, then the Hessian is just the kinetic metric tensor $m_{ij}(q)$ (see (3.42) and Sect. 3.27*). So positive-definiteness of the kinetic metric on $\mathcal{Q}$ ensures convexity of the Lagrangian as a function of velocities. In this case, $p_i = m_{ij}\dot{q}^j$. Inverting, $\dot{q}^j = m^{jk} p_k$ where m^{jk} are the entries of the inverse of the mass matrix $m^{jk} m_{kl} = \delta^j_l$. Putting this in (3.82), the Hamiltonian may be obtained as a singlevalued function of coordinates and momenta: $H = \frac{1}{2} m^{ij} p_i p_j + V(q)$.

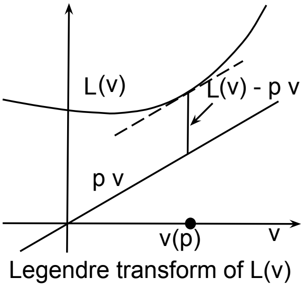

Figure 3.9: Legendre transform $H(p) = pv(p) - L(v(p))$. We find $v(p)$ by extremizing the vertical distance between $L(v)$ and the straight line through the origin with slope p. The extremum occurs when the slope $L'(v) = p$. In this example, we chose a positive value of p.

Graphical interpretation. Suppose $L(v)$ is a convex (or concave) function of a velocity and $H(p) = \text{ext}_v\,[pv - L(v)]$ is its Legendre transform, a function of momentum. The Legendre transform may be obtained by a graphical construction, which is a recipe for finding H given a value of p. Consider the graph of L as a function of v (see Fig. 3.9). Given a value of p we draw the line pv through the origin with slope p. The vertical distance between the graph of $L(v)$ and this straight line is $pv - L(v)$ (or its negative). Given p, we find the point(s) $v(p)$ at which this distance is an extremum.

---

[65] For more than 1 degree of freedom, one may choose to perform a partial Legendre transform, replacing some velocities in the Lagrangian by their conjugate momenta and retaining other velocities. The resulting function that replaces the Hamiltonian is called the Routhian.

There is precisely one such point if L is convex and satisfies the growth condition[66]. Evidently, $(v(p), L(v(p)))$ is the point on the graph where the tangent to the graph is parallel to the straight line pv. Then we define the value of the Legendre transform as $H(p) = p\, v(p) - L(v(p))$.

Inverse Legendre transform and involutive property. Finally, when the Legendre transform is defined, the Lagrangian can be re-obtained from $H(q,p)$ by another Legendre transform

$$L(q, \dot{q}) = \text{ext}_p \left[p_i \dot{q}^i - H(q,p) \right] . \tag{3.83}$$

For example, taking $H = p^2/2m$ one finds $L = \frac{1}{2} m \dot{q}^2$ while if $H = p \log p - p$ for $p > 0$ then $L = e^{\dot{q}}$. Thus, applying the Legendre transform twice to a convex function produces the identity transformation. The Legendre transform is its own inverse and we say that it is an involution.

3.16* Lagrange multipliers and constrained extremization

Constrained extremization via Lagrange multipliers. Here, we introduce the technique of Lagrange multipliers for constrained extremization problems. This will be used to obtain a Lagrangian formulation for certain systems with constraints (such as a pendulum) and also in our discussion of singular Lagrangians in Sect. 3.17*. Consider the problem of extremizing a real-valued function $F(\boldsymbol{x})$ subject to a constraint $\mathcal{C}(\boldsymbol{x}) = 0$, where $\boldsymbol{x} \in \Omega$. Ω could be $\mathbb{R}^n$ or some connected open region in $\mathbb{R}^n$. We may think of $\mathcal{C}(\boldsymbol{x}) = 0$ as defining a constraint hypersurface $\Sigma \subset \Omega$ (see Fig. 3.10). Our task is to find the points on Σ where F is stationary subject to infinitesimal changes in $\boldsymbol{x}$ tangent to Σ. The method of Lagrange multipliers says that to extremize F subject to the constraint $\mathcal{C}$ is the same as the unconstrained extremization of $F - \lambda\mathcal{C}$ on Ω. Here, the real number λ is called a *Lagrange multiplier*. The value of λ is not known in advance. There are typically several allowed values of λ corresponding to several local extrema of F subject to the constraint $\mathcal{C}$ (see Prob. 3.37 for an example). Let us see why this prescription works. The condition for extrema of $F - \lambda\mathcal{C}$ is $\boldsymbol{\nabla} F = \lambda \boldsymbol{\nabla}\mathcal{C}$. Geometrically, this says that the gradient $\boldsymbol{\nabla} F$ must point along/opposite to $\boldsymbol{\nabla}\mathcal{C}$. Since $\boldsymbol{\nabla}\mathcal{C}$ points normal to the constraint hypersurface Σ, this would ensure that $\boldsymbol{\nabla} F$ is also normal to Σ. In other words, F would be stationary on the constraint hypersurface, as desired! If $\boldsymbol{\nabla} F$ and $\boldsymbol{\nabla}\mathcal{C}$ were not collinear at a point $\boldsymbol{x} \in \Sigma$, then one could move along the constraint hypersurface (along/opposite to the projection of $\boldsymbol{\nabla} F$) to an infinitesimally nearby point where F takes a larger/smaller value.

The method of Lagrange multipliers may be extended to the problem of extremizing a function F subject to several constraints $\mathcal{C}_1 = 0, \mathcal{C}_2 = 0, \ldots$. Argue that this problem is equivalent to the unconstrained extremization of $F - \lambda_1\mathcal{C}_1 - \lambda_2\mathcal{C}_2 - \cdots$.

Lagrangian for a plane pendulum: tension as a Lagrange multiplier. Recall from Sect. 1.5 that Newton's equations for a plane pendulum are given by the $\hat{r}$ and $\hat{\theta}$ components of $m\boldsymbol{a} = \boldsymbol{F}$:

$$- m\ell\dot{\theta}^2 = mg\cos\theta - \mathcal{T} \quad \text{and} \quad m\ell\ddot{\theta} = -mg\sin\theta. \tag{3.84}$$

---

[66] If the growth condition is violated but L is convex, there can either be zero or one such v.

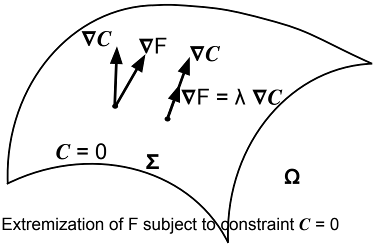

Figure 3.10: Constrained extremization via Lagrange multipliers. While $\boldsymbol{\nabla}\mathcal{C}$ is always normal to the constraint surface $\mathcal{C} = 0$, $\boldsymbol{\nabla}F$ is generally not. At an extremum of F subject to the constraint, $\boldsymbol{\nabla}F$ is normal to the surface and is a multiple of $\boldsymbol{\nabla}\mathcal{C}$.

Here $\mathcal{T}$ is the radially inward tension in the rod while m and ℓ are the bob mass and length of rod. We seek a Lagrangian for these EOM. The Lagrangian in (3.31) leads to the angular equation but not the radial one, which involves the tension as a new dynamical variable. To account for radial forces and the centripetal acceleration, it is natural to regard $r(t)$ as a dynamical variable that is, however, subject to the constraint $r(t) - \ell = 0$. In the absence of the constraint, we have a particle (bob) moving in a vertical plane subject to the downward gravitational force. The corresponding equations of motion are the stationarity conditions for the action

$$S = \int_{t_i}^{t_f} L\, dt \quad \text{where} \quad L = \frac{1}{2}m(\dot{r}^2 + r^2\dot{\theta}^2) - mgr(1-\cos\theta). \tag{3.85}$$

Now, we have one constraint $r(t) - \ell = 0$ for each instant of time. To deal with these (infinitely many) constraints, let us first define the sequence of intermediate times $t_j = t_i + j\Delta$ for $j = 1, \ldots, n$, where $\Delta = (t_f - t_i)/n$. The constraint at time t_j may be written as $(r(t_j) - \ell)\Delta = 0$ and may be imposed via the Lagrange multiplier $\lambda(t_j)$. In the limit $n \to \infty$, $\Delta \to 0$ and

$$\lim_{n\to\infty} \sum\nolimits_{j=1}^{n} \lambda(t_j)(r(t_j) - \ell)\Delta = \int_{t_i}^{t_f} \lambda(t)(r(t) - \ell)dt. \tag{3.86}$$

Hence, the extremization of S subject to these constraints is equivalent to the unconstrained extremization of the 'effective' action

$$S_{\text{eff}} = \int_{t_i}^{t_f} L_{\text{eff}} \quad \text{where} \quad L_{\text{eff}} = L - \lambda(t)(r - \ell). \tag{3.87}$$

Thus, we arrive at an effective Lagrangian for the plane pendulum:

$$L_{\text{eff}}(r, \dot{r}, \theta, \dot{\theta}, \lambda) = \frac{1}{2}m(\dot{r}^2 + r^2\dot{\theta}^2) - mgr(1-\cos\theta) - \lambda(r - \ell). \tag{3.88}$$

It remains to verify that L_{eff} leads to the EOM (3.84) and to identify the physical meaning of the Lagrange multipliers $\lambda(t)$. The EL equations for r, θ and λ are

$$m\ddot{r} = mr\dot{\theta}^2 - mg(1-\cos\theta) - \lambda, \quad mr^2\ddot{\theta} + 2mr\dot{r}\dot{\theta} = -mgr\sin\theta \quad \text{and} \quad r = \ell. \tag{3.89}$$

We use the third equation to eliminate r and arrive at the pair of equations

$$-m\ell\dot{\theta}^2 = mg\cos\theta - mg - \lambda \quad \text{and} \quad m\ell\ddot{\theta} = -mg\sin\theta. \tag{3.90}$$

Comparing with (3.84), we see that these equations agree with the radial and tangential Newton equations if we interpret $\lambda + mg$ as the tension. So up to an additive constant, the Lagrange multiplier function is the tension $\mathcal{T}$ in the rod. □

3.17* Singular Lagrangians and constraints

When the Hessian of the Lagrangian with respect to generalized velocities $\frac{\partial^2 L}{\partial \dot{q}^i \dot{q}^j}$ is not invertible, we cannot solve $p_i = \frac{\partial L}{\partial \dot{q}^i}$ to express all the velocities in terms of momenta and coordinates. Such a Lagrangian is called singular and does not admit a standard Hamiltonian formulation via a Legendre transform.

Example of primary constraints. Working in units where a mass parameter $m = 1$, $L = (1/2)(\dot{x}^2 + \dot{y}^2 + 2\dot{x}\dot{y})$ is singular, since $p_x = \dot{x} + \dot{y}$ and $p_y = \dot{x} + \dot{y}$. Singular Lagrangians are associated to constraints (see Footnote 30). In this case, the 'primary' constraint is $\mathcal{C} = p_y - p_x = 0$, a relation among phase space variables. It is an example of a nonholonomic constraint. Dirac developed a method (see Chap. 1 of [29] and Sect. 7.6 of [131]) to deal with such constraints and set up a Hamiltonian formulation[67]. We shall not attempt an exposition of Dirac's theory here but instead briefly illustrate the procedure in this toy example. To begin with, a naive Hamiltonian $H_0 = p_x\dot{x} + p_y\dot{y} - L$ may be defined and expressed as $H_0 = \frac{1}{2}p_x^2$ upon use of the primary constraint. However, the EOM following from H_0, viz., $\dot{p}_x = 0$, $\dot{p}_y = 0$, $\dot{x} = p_x$ and $\dot{y} = 0$, which may be written as $\ddot{x} = \ddot{y} = 0$, are *not* equivalent to Lagrange's equation: $\ddot{x} + \ddot{y} = 0$. To remedy this, we introduce an auxiliary variable[68] $\lambda(t)$ that will play the role of a 'Lagrange multiplier' to enforce the constraint $\mathcal{C} = 0$. Thus, we define a new Hamiltonian

$$H = H_0 + \lambda\mathcal{C} = (1/2)p_x^2 + \lambda(p_y - p_x). \tag{3.91}$$

Hamilton's equations now become

$$\dot{p}_x = 0, \quad \dot{p}_y = 0, \quad \dot{x} = p_x - \lambda \quad \text{and} \quad \dot{y} = \lambda. \tag{3.92}$$

They reduce to the 2^{nd} order equations $\ddot{x} = -\dot{\lambda}$ and $\ddot{y} = \dot{\lambda}$. Pleasantly, these are equivalent to the Lagrange equation $\ddot{x} + \ddot{y} = 0$ for an arbitrary function $\lambda(t)$. Thus, we have found a Hamiltonian formulation for our singular Lagrangian! □

---

[67] This is significant since the standard Lagrangian for the electromagnetic field as well as those for the gauge fields of the strong and weak interactions and general relativity are all singular. See [7, 124] for more on the Dirac-Bergmann theory of constraints.

[68] The Lagrange multiplier λ is not an independent dynamical variable with an equation of motion but an arbitrary function of time. It will either remain unspecified (and appear as such in solutions) or be determined in terms of other phase space variables.

Example with primary and secondary constraints. As a second example, we consider the same singular Lagrangian augmented by a quadratic potential (other potentials may also be considered). In this case, the Lagrange multiplier will be determined in terms of other dynamical variables. Suppose $L = (1/2)(\dot{x}^2 + \dot{y}^2 + 2\dot{x}\dot{y}) - (k/2)(x^2 + y^2)$. The momenta $p_x = p_y = \dot{x} + \dot{y}$ continue to satisfy the primary constraint $\mathcal{C} = p_y - p_x = 0$. The naive Hamiltonian is $H_0 = (1/2)p_x^2 + (k/2)(x^2 + y^2)$. The EOM following from H_0 are $\dot{p}_x = -kx$, $\dot{p}_y = -ky$, $\dot{x} = p_x$ and $\dot{y} = 0$. These reduce to $\ddot{x} = -kx$ and $\ddot{y} = 0$, which are not equivalent to Lagrange's equations

$$\ddot{x} + \ddot{y} = -kx \quad \text{and} \quad \ddot{x} + \ddot{y} = -ky. \tag{3.93}$$

In passing, we notice that consistency of Lagrange's equations requires that $x = y$. As before, we introduce a Lagrange multiplier λ and a new Hamiltonian

$$H = H_0 + \lambda\mathcal{C} = (1/2)p_x^2 + (k/2)(x^2 + y^2) + \lambda(p_y - p_x), \tag{3.94}$$

with new Hamilton equations of motion

$$\dot{p}_x = -kx, \quad \dot{p}_y = -ky, \quad \dot{x} = p_x - \lambda \quad \text{and} \quad \dot{y} = \lambda. \tag{3.95}$$

These equations ($\ddot{x} = -kx - \dot{\lambda}$ and $\ddot{y} = \dot{\lambda}$) are not equivalent to Lagrange's equations. However, we have not made full use of the constraints. In fact, differentiating the primary constraint $\mathcal{C} = p_y - p_x = 0$ in time, we get $\dot{\mathcal{C}} = \dot{p}_y - \dot{p}_x = 0$. Simplifying this using the new Hamilton equations leads us to the (holonomic) 'secondary' constraint[69] $-k(y - x) = 0$. Differentiating the secondary constraint in time, we get $\dot{x} = \dot{y}$. Aided by Hamilton's equations, this allows us to eliminate the Lagrange multiplier: $\lambda = (1/2)p_x$. Substituting in the new Hamiltonian, we get $H = (1/2)p_x p_y + (k/2)(x^2 + y^2)$. The resulting EOM $\dot{p}_x = -kx$, $\dot{p}_y = -ky$, $\dot{x} = p_y/2$ and $\dot{y} = p_x/2$ may be written as $\ddot{x} = -(k/2)y$ and $\ddot{y} = -(k/2)x$. These are seen to be equivalent to Lagrange's equations $\ddot{x} + \ddot{y} = -kx$ and $\ddot{x} + \ddot{y} = -ky$ upon use of the secondary constraint! When supplemented by the primary and secondary constraints, Hamilton's equations (after the possible elimination of Lagrange multipliers) are equivalent to the original Lagrange equations. □

Plane curves of minimal Euclidean arc length. As a third example, we consider the action $S = \int_{t_1}^{t_2} \sqrt{\dot{x}^2 + \dot{y}^2}\,dt$ which represents the Euclidean arc length of the parametrized plane curve $(x(t), y(t))$ joining the points (x_1, y_1) and (x_2, y_2) between the times $t_1 \le t \le t_2$. Taking $L = \sqrt{\dot{x}^2 + \dot{y}^2}$, we see that both coordinates x and y on the configuration space $\mathcal{Q} = \mathbb{R}^2$ are cyclic. As a consequence, the conjugate momenta $p_x = \dot{x}/\sqrt{\dot{x}^2 + \dot{y}^2}$ and $p_y = \dot{y}/\sqrt{\dot{x}^2 + \dot{y}^2}$ are both conserved. However, these equations of motion imply that the constants of motion p_x and p_y must satisfy the (nonholonomic) primary constraint $\mathcal{C} = p_x^2 + p_y^2 - 1 = 0$. Thus, the conjugate momentum vector $\boldsymbol{p} = (p_x, p_y)$ is a unit vector; geometrically it is the unit tangent vector to the curve. Bearing in mind that $\dot{x}$ and $\dot{y}$ have the same signs as p_x and p_y, we square the EOM to arrive at the equations of motion

---

[69] In general, secondary constraints arise from differentiating primary constraints in time and using the new Hamilton equations to express them as constraints among phase space variables. Here, the secondary constraint generally depends on the potential that we included in L.

$$(1-p_x^2)\dot{x}^2 - p_x^2\dot{y}^2 = 0 \quad \text{and} \quad p_y^2\dot{x}^2 - (1-p_y^2)\dot{y}^2 = 0. \qquad (3.96)$$

However, in view of the primary constraint, these equations are identical. Thus, it is not possible to solve for velocities uniquely in terms of momenta. Thus the Lagrangian is singular. There is only one independent equation of motion, which can be taken as the constancy of the ratio $\dot{y}/\dot{x} = p_y/p_x$. This simply states that the direction of the velocity (tangent) vector to the trajectory ($\theta = \arctan(\dot{y}/\dot{x})$) is independent of time. In other words, trajectories are straight lines. However, they are generally not free particle trajectories since $\ddot{x}$ and $\ddot{y}$ are not necessarily zero. What is more, the naive Hamiltonian

$$H_0 = p_x\dot{x} + p_y\dot{y} - L = p_x^2\sqrt{\dot{x}^2+\dot{y}^2} + p_y^2\sqrt{\dot{x}^2+\dot{y}^2} - \sqrt{\dot{x}^2+\dot{y}^2} = 0 \qquad (3.97)$$

vanishes identically on account of the primary constraint. In particular, Hamilton's equations based on H_0 cannot reproduce the original EL equations. But all is not lost. Following our recipe, we introduce a Lagrange multiplier λ and a new Hamiltonian

$$H = H_0 + \lambda\mathcal{C} = \lambda(p_x^2 + p_y^2 - 1), \qquad (3.98)$$

which is a 'pure constraint' since $H_0 = 0$. However, we notice that there is no secondary constraint: the time derivative of the primary constraint function $\mathcal{C}$ is $p_x\dot{p}_x + p_y\dot{p}_y$, which is identically zero on account of the conservation of p_x and p_y. We next examine Hamilton's equations following from H. They are

$$\dot{x} = 2\lambda p_x, \quad \dot{y} = 2\lambda p_y, \quad \dot{p}_x = 0 \quad \text{and} \quad \dot{p}_y = 0. \qquad (3.99)$$

The last pair of equations recover the conservation of momenta. Eliminating λ from the first pair of equations leads to $\dot{y}/\dot{x} = p_y/p_x$, which we recognize as the same as the one independent equation following from the original Lagrangian. Thus, we see that the new Hamiltonian allows us to give a canonical formulation of the EOM with x, p_x and y, p_y two pairs of canonically conjugate phase space variables. The Lagrange multiplier λ is undetermined. It can be an arbitrary function of time. Comparing the new Hamilton equations (3.99) with the EL equations, we observe that $\lambda = \frac{1}{2}\sqrt{\dot{x}^2+\dot{y}^2}$ may be interpreted as one-half the speed at which the straight-line trajectory is traversed. However, this speed is not determined by the EOM, it can be an arbitrary (positive) function of time. In fact, this reflects the invariance of S under a reparametrization of time $t \to \tau(t)$ with $\dot{\tau} > 0$. The Jacobian $d\tau/dt$ cancels out when transforming the product: $\sqrt{\dot{x}^2+\dot{y}^2}dt = \sqrt{x'(\tau)^2+y'(\tau)^2}d\tau$. The arbitrariness of the local speed of traversal of the straight-line trajectories is responsible for the singular nature of the original Lagrangian (see also Prob. 3.14). □

3.18* Action as a function along a trajectory

The action $S[q] = \int_{t_1}^{t_2} L(q,\dot{q})\,dt$ was defined in (3.19) as a functional of any path (not necessarily one that satisfies Lagrange's equations) from q_1 at t_1 to q_2 at t_2.

Here, we will view the action along a trajectory, now as a function of one or more of the initial and final configurations and times. The resulting formulae will be useful in deducing a phase space variational principle for Hamilton's equations in Sect. 3.19, the Euler-Maupertuis variational principle in Sect. 3.28* as well as in relating the action to Hamilton's principal function, whose evolution is governed by the Hamilton-Jacobi equation (see Sect. 12.4). They will also allow us to draw an analogy with the first and second laws of thermodynamics.

To begin with, we recall from (3.20) that the first variation of the action is

$$\delta S = \int_{t_1}^{t_2} \delta q^i(t') \left(\frac{\partial L}{\partial q^i} - \dot{p}_i(t') \right) dt' + \delta q^i(t_2) p_i(t_2) - \delta q^i(t_1) p_i(t_1) + \mathcal{O}(\delta q)^2. \tag{3.100}$$

Let us specialize to trajectories (so that the EL equations are satisfied) while holding q_1, t_1 and t_2 fixed and consider S as a function of the final configuration $q_2 = q(t_2)$ that such a trajectory could reach at time t_2. The infinitesimal change in S is

$$\delta S = p_i(t_2)\, \delta q^i(t_2) \quad \text{so that} \quad \frac{\partial S}{\partial q_2^i} = p_i(t_2). \tag{3.101}$$

Thus, the partial derivatives of the action (evaluated along a trajectory) with respect to the generalized coordinates at the end of the trajectory are the corresponding conjugate momenta.

Similarly, we may regard the action as a function of the final time $t_2 = t$ by evaluating it along trajectories that begin at q_1 at t_1 and pass through a fixed final configuration[70] q_2 at various possible times t. Interestingly, we will now show that

$$\delta S = -H \delta t \quad \text{so that} \quad \frac{\partial S}{\partial t} = -H. \tag{3.102}$$

To see this, we view $S = \int_{t_1}^{t} L(q(t'), \dot{q}(t')) dt'$ as a function of the final coordinate $q_2 = q$ and time $t_2 = t$. The fundamental theorem of calculus (Prob. 6.27) says that the derivative of S with respect to the upper limit of integration is the integrand. Thus, $\frac{dS}{dt} = L = p_i \dot{q}^i - H$. We may compute the same quantity in another way:

$$\frac{dS}{dt} = \frac{\partial S}{\partial t} + \frac{\partial S}{\partial q^i} \dot{q}^i = \frac{\partial S}{\partial t} + p_i \dot{q}^i \tag{3.103}$$

where we used (3.101). Comparing the two expressions for $\frac{dS}{dt}$, we obtain (3.102) on the partial derivative of S with respect to the arrival time.

Combining (3.101) and (3.102), we get the differential of the action along a trajectory, regarded as a function of the final coordinates and time:

$$dS = p_i dq^i - H dt. \tag{3.104}$$

---

[70] For instance, for a free particle moving on a line, there are many trajectories that start at q_1 at t_1 and arrive at a specified q_2 at some later time. The times of arrival are $t_2 = t_1 + (q_2 - q_1)/v$ where v is the velocity of the particle.

The same formula with opposite signs holds for S viewed as a function of the initial time and coordinates. Combining the two, and regarding the action as a function of the initial and final times and configurations along a trajectory, we also have

$$dS = p_2 dq_2 - H(q_2, p_2) dt_2 - p_1 dq_1 + H(q_1, p_1) dt_1, \tag{3.105}$$

where the sum over the indices labelling degrees of freedom has been suppressed.

Remark. Equation (3.104) resembles the first law of thermodynamics combined with the second law for an infinitesimal reversible transformation of a gas:

$$dU = T d\mathtt{S} + p dV. \tag{3.106}$$

Here U is the internal energy while $T, \mathtt{S}, p$ and V are the absolute temperature, entropy, pressure and volume. When evaluated on an infinitesimal process, Eq. (3.106) says that the infinitesimal heat $T d\mathtt{S}$ added and work done pdV on the gas, though not exact differentials themselves, must sum to an exact differential, namely that of the internal energy. This condition must hold irrespective of the nature of the gas, i.e., whether it is hydrogen, helium, ideal, polytropic, van der Waals, etc. In a similar vein, the infinitesimal evolution of a mechanical system along a trajectory must be such that the generally imperfect differentials $p_i dq^i$ and $-H dt$ must sum to give an exact differential, namely that of the action regarded as a function of the final point on the trajectory. Again, this must hold irrespective of the nature of the mechanical system (i.e., what the constituents are and the forces they are subject to). Said differently, the final state of the system must be related to the initial state in such a way that the RHS of (3.105) is an exact differential. □

3.19 Variational principles for Hamilton's equations

We seek a variational principle for Hamilton's equations (3.78), just as we had one in Sect. 3.5 for Lagrange's equations: $S[q] = \int L \, dt$ with the infinitesimal variation $\delta S = 0$. Integrating (3.104) with respect to t, we obtain a functional that we call the (phase space) action[71]:

$$S[q, p] = \int_{t_1}^{t_2} \left[p_i \dot{q}^i - H(q, p) \right] \, dt. \tag{3.107}$$

The phase space action is a functional of a path $(q(t), p(t))$ on *phase space*, unlike $S[q] = \int L(q, \dot{q}) \, dt$ which is a functional of a path on *configuration space*[72]. We are forced to view it as a functional of a path on phase space since $H(q, p)$ is a function on phase space and $p\dot{q}$ involves both the position and momentum along the path. Along such a path, $\dot{q}$ is not an independent quantity, it is obtained simply by differentiating

---

[71] Those who have not read Sect. 3.18* may view $S[q, p]$ as a phase space analog of $\int L \, dt$ with L formally replaced by $p\dot{q} - H$.

[72] As always, $\dot{q}(t)$ is simply the time derivative of $q(t)$ and is not an independent quantity. This is why $S[q] = \int L(q, \dot{q}) dt$ is a functional of a path on configuration space and it would *not* make sense to write it as $S[q, \dot{q}]$.

$q(t)$. To obtain Hamilton's equations, we ask that $S[q,p]$ be stationary with respect to small variations in the phase path $(q^i(t), p_j(t)) \to (q^i(t) + \delta q^i(t), p_j(t) + \delta p_j(t))$ while holding the initial and final configurations and times fixed: $\delta q(t_1) = 0$ and $\delta q(t_2) = 0$ (see Fig. 3.11). Note that we do not constrain $\delta p(t_1)$ or $\delta p(t_2)$. That would be an overspecification[73].

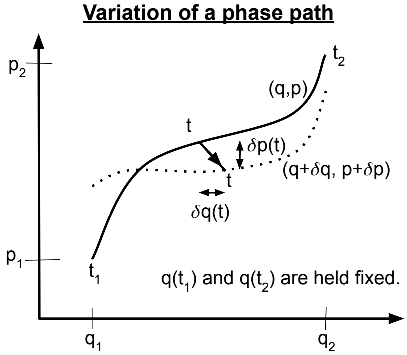

Figure 3.11: Infinitesimal variation of a phase path. Note that $p(t_1)$ and $p(t_2)$ are *not* held fixed.

Now,

$$\delta S = \int_{t_1}^{t_2} \left[\delta p_i \, \dot{q}^i + p_i \delta \dot{q}^i - \frac{\partial H}{\partial q^i} \delta q^i - \frac{\partial H}{\partial p_i} \delta p_i \right] dt + \dots . \tag{3.108}$$

We find upon integrating by parts in the second term and using $\delta q(t_{1,2}) = 0$,

$$S[q + \delta q, p + \delta p] = S[q,p] + \int_{t_1}^{t_2} \left[\dot{q}^i \delta p_i - \dot{p}_i \delta q^i - \frac{\partial H}{\partial q^i} \delta q^i - \frac{\partial H}{\partial p_i} \delta p_i \right] dt + \dots . \tag{3.109}$$

The action must be stationary with respect to arbitrary infinitesimal independent variations δp, δq subject to $\delta q(t_1) = \delta q(t_2) = 0$. So the coefficients of δp and δq must individually vanish. Thus we recover Hamilton's equations (3.78) at all times $t_1 < t < t_2$:

$$\dot{q}^i = \frac{\partial H}{\partial p_i} \quad \text{and} \quad \dot{p}_i = -\frac{\partial H}{\partial q^i}. \tag{3.110}$$

Hamilton's equations treat position and momentum on an equal footing except for a sign. But the above boundary conditions treat them asymmetrically since we fix q at t_1 and t_2 but allow p to vary at these times. Could we do the opposite, i.e., fix the initial and final momenta but allow the positions to vary? This is a clue that there is *another* variational principle for Hamilton's equations. Consider the functional of a path on phase space[74]

$$\tilde{S}[q,p] = \int_{t_1}^{t_2} \left[-q^j \dot{p}_j - H(q,p) \right] dt \tag{3.111}$$

---

[73] In general, there would not be *any* trajectory joining specified values of q *and* p at *both* t_1 and t_2 (see Prob. 3.13).

[74] A way to remember $\tilde{S}$ is that it is obtained from S through integration by parts while ignoring the boundary terms.

which we extremize with respect to small variations $\delta q, \delta p$ while holding $\delta p_j(t_1) = \delta p_j(t_2) = 0$. Then integrating by parts,

$$\begin{aligned} \delta\tilde{S} &= \int_{t_1}^{t_2} \left[-\dot{p}_j \delta q^j - q^j \delta\dot{p}_j - \frac{\partial H}{\partial q^j}\delta q^j - \frac{\partial H}{\partial p_j}\delta p_j \right] dt \\ &= \int_{t_1}^{t_2} \left[-\left(\dot{p}_j + \frac{\partial H}{\partial q^j} \right) \delta q^j + \left(\dot{q}^j - \frac{\partial H}{\partial p_j} \right) \delta p_j \right] dt. \qquad (3.112) \end{aligned}$$

So $\delta\tilde{S} = 0$ also implies Hamilton's equations. We will exploit both these variational principles while studying canonical transformations in Sect. 10.10.

3.20* Coordinate invariance of Lagrange and Hamilton equations

One of the advantages of having a variational principle is that it allows us to show that the equations of motion *expressed in terms of the Hamiltonian*, take the same form in any system of coordinates on configuration space[75] $\mathcal{Q}$. We first explain why this is the case for Lagrange's equations, as observed in Sect. 3.8.

We begin by noting that the condition for a function to be stationary is independent of choice of coordinates, as long as we make nonsingular changes of coordinates[76]. Consider $f(x)$, a function of one real variable. It is extremal when $f'(x) = 0$. Now change to a new coordinate $X(x)$ (e.g., $X(x) = 2x$). Then $f(x) = f(x(X)) \equiv F(X)$. Moreover, by the chain rule, $f'(x) = F'(X)\frac{dX}{dx}$. If the change of variables is nonsingular, $\frac{dX}{dx} \neq 0$. It follows that $f'(x) = 0 \Leftrightarrow F'(X) = 0$. For several variables, a real-valued function $f(x)$ is extremal at a point if $\frac{\partial f}{\partial x^i} = 0$ for all i. Under a change of coordinates

$$x^i \mapsto X^i(x), \quad \frac{\partial f}{\partial x^i} = \frac{\partial F}{\partial X^j} J_i^j \quad \text{where the Jacobian matrix} \quad J_i^j = \frac{\partial X^j}{\partial x^i}. \qquad (3.113)$$

It follows that the condition for f to be extremal is independent of coordinates provided the Jacobian matrix has a trivial kernel or null space, which is the same as being nonsingular (nonzero determinant) or invertible at the relevant point.

Recall that Lagrange's equations (3.21) are the conditions for stationarity of the action $S[q] = \int L(q, \dot{q}) dt$. Now suppose we make a nonsingular change of coordinates $q \to Q(q)$ on $\mathcal{Q}$. We work with 1 degree of freedom though the same applies to several degrees of freedom. We define a new Lagrange function by expressing the old coordinates and velocities in terms of the new ones[77]

---

[75] The question of changes of variables on phase space that leave Hamilton's equations unchanged will be addressed in Chap. 10.

[76] A change of variables $q^i \to Q^i$ is said to be nonsingular if it is a differentiable and invertible change of variables (*with differentiable inverse*). The change is nonsingular in some neighborhood of the point q_0 if the matrix of first partials (Jacobian matrix) $J_j^i = \frac{\partial Q^i}{\partial q^j}$ is a nonsingular matrix (i.e., has nonzero determinant) at $q = q_0$.

$$S[q] = \int L(q,\dot q)\,dt = \int \tilde L(Q,\dot Q)\,dt \equiv \tilde S[Q] \;\text{ where }\; L(q,\dot q) = \tilde L(Q(q),\dot Q(q,\dot q)). \tag{3.114}$$

As before, the conditions for stationarity under infinitesimal variations are the same: $\delta S[q] = 0$ iff $\delta\tilde S[Q] = 0$. Thus, Lagrange's equations must take the same form in the q and Q coordinates:

$$\frac{d}{dt}\frac{\partial L}{\partial \dot q} = \frac{\partial L}{\partial q} \quad \Leftrightarrow \quad \frac{d}{dt}\frac{\partial \tilde L}{\partial \dot Q} = \frac{\partial \tilde L}{\partial Q}. \tag{3.115}$$

We apply the same sort of reasoning to argue that Hamilton's equations (3.78) take the same form in all systems of coordinates on $\mathcal{Q}$. Suppose we change from $q \to Q$. Then we get a new Lagrange function $\tilde L(Q,\dot Q)$. We also get a new conjugate momentum $P = \frac{\partial \tilde L}{\partial \dot Q}$ while $p = \frac{\partial L}{\partial \dot q}$. In general, $Q = Q(q)$ but P will be a function of both q and p. Hamilton's equations are the conditions for the action functional $S[q,p] = \int [p\dot q - H(q,p)]\,dt$ (3.107) to be extremal with respect to infinitesimal variations in the phase path, $\delta S = 0$. We also have a new Hamiltonian $\tilde H(Q,P) = H(q(Q), p(Q,P))$ and new action functional

$$\tilde S[Q,P] = \int [P\dot Q - \tilde H(Q,P)]\,dt \quad \text{while} \quad S[q,p] = \int [p\dot q - H(q,p)]\,dt. \tag{3.116}$$

As before, the conditions $\delta S = 0$ imply the conditions $\delta\tilde S = 0$ so that Hamilton's equations take the same form in both systems of coordinates on configuration space.

Though we changed coordinates on $\mathcal{Q}$, we did not change the momenta in an arbitrary way. The change in momenta was 'induced' by the change in coordinates via the formula $P = \frac{\partial \tilde L}{\partial \dot Q}$ where $\tilde L(Q,\dot Q)$ is the Lagrangian expressed in terms of the new coordinates and velocities. So far, we used the Lagrangian as a 'walking stick' to define the momenta. But Hamilton's equations treat coordinates and momenta on a fairly equal footing. Leaving behind the walking stick of the Lagrange function, one wonders if Hamilton's equations take the same form in a larger class of coordinate systems on *phase space* as opposed to just *configuration space*. Remarkably, Hamilton's equations *do* take the same form in a slightly larger class of coordinate systems on phase space, namely those that are *canonically* related to q,p. This brings us to the topic of canonical transformations, which we will take up in Chap. 10. It is possible to deduce this using the variational principle of Sect. 3.19, as well as using Poisson brackets, which we introduce in the next section.

3.21 Canonical Poisson brackets

In Sect. 3.15, we defined the Hamiltonian as the Legendre transform of the Lagrangian and used it to express the equations of motion as 1st order ODEs (3.78).

---

[77] Though we use the same symbol $\tilde S$ here and in Sect. 3.19, they represent different quantities.

Now, we introduce another way of obtaining and thinking about Hamilton's equations: via Poisson brackets. We will see that when expressed in terms of Poisson brackets, Hamilton's equations take the same form for any observable and for any choice of coordinates on phase space. Poisson brackets endow Hamiltonian mechanics with an elegant algebraic and geometric structure which has been hidden from view thus far. They turn out to be a very useful conceptual and technical tool (e.g., to study conserved quantities, symmetries, discuss solvability of equations and so on.) and played a central role in Dirac's formulation of quantum mechanics via their quantum counterpart: the commutator of matrices/operators[78].

Consider a particle (or system of particles) with configuration space $\mathbb{R}^n$, generalized coordinates q^i and generalized momenta $p_i = \frac{\partial L}{\partial \dot{q}^i}$. To motivate the idea of Poisson brackets (PBs), let us use Hamilton's equations ($\dot{q}^i = \frac{\partial H}{\partial p_i}$ and $\dot{p}_i = -\frac{\partial H}{\partial q^i}$) to find the time evolution of any dynamical variable $f(q, p; t)$. In general, f is a function on phase space, which could depend explicitly on time. By the chain rule, we get

$$\begin{aligned} \frac{df}{dt} &= \frac{\partial f}{\partial t} + \sum\nolimits_{i=1}^{n} \left(\frac{\partial f}{\partial q^i(t)} \frac{dq^i}{dt} + \frac{\partial f}{\partial p_i(t)} \frac{dp_i}{dt} \right) \\ &= \frac{\partial f}{\partial t} + \sum\nolimits_{i=1}^{n} \left(\frac{\partial f}{\partial q^i(t)} \frac{\partial H}{\partial p_i(t)} - \frac{\partial f}{\partial p_i(t)} \frac{\partial H}{\partial q^i(t)} \right) = \frac{\partial f}{\partial t} + \{f, H\}. \end{aligned} \tag{3.117}$$

Here, we introduced Poisson's bracket $\{\cdot, \cdot\}$ of f with the Hamiltonian (in the expression $\{\cdot, \cdot\}$, the dots are 'placeholders' for any pair of functions). More generally, the canonical PB of 2 dynamical variables[79] gives another dynamical variable defined as[80]

$$\{f, g\} = \sum\nolimits_{i=1}^{n} \left(\frac{\partial f}{\partial q^i} \frac{\partial g}{\partial p_i} - \frac{\partial f}{\partial p_i} \frac{\partial g}{\partial q^i} \right). \tag{3.118}$$

This is called an *equal-time* PB since f and g are evaluated at the same time t. Unequal-time PBs are explored in Prob. 3.47 and commented upon in Sect. 10.2. In $\{f, g\}$, we refer to f as the function in the first slot or entry and g as occupying the second. So the time derivative of any observable is given by its PB with the Hamiltonian (aside from any explicit time-dependence). From here on, we will restrict to observables that are not explicitly time-dependent (i.e., depend on time only via $q(t)$

---

[78] Dirac recalls thinking about this "$(uv - vu)$" one Sunday in October 1925. In words that nearly match those of Dirac [30], he noticed that there seemed to be a close similarity between the Poisson bracket and the quantum commutator. He did not remember very well the precise formula for a Poisson bracket and only had some vague recollections. He thought he might be getting to some big idea. However, he could not find any reference to Poisson brackets in the notes he had taken at various lectures or in the textbooks he had at home. There was nothing he could do, because it was Sunday evening and the libraries were all closed. He had to wait impatiently through that night. The next morning, he hurried along to one of the libraries as soon as it was open, and then looked up Poisson brackets in Whittaker's *Analytical Dynamics* [133]. He found that they were just what he needed!

[79] The Poisson bracket $\{f, g\}$ has dimensions of $[fg/\mathtt{action}]$.

[80] Some authors (e.g., Landau & Lifshitz [83]) define the PB with an overall minus sign relative to our definition. When this is done, the equation of motion becomes $\dot{f} = \{H, f\}$.

and $p(t)$), unless otherwise stated. Hamilton's equations for time evolution may now be written

$$\dot{q}^i = \{q^i, H\} \quad \text{and} \quad \dot{p}_j = \{p_j, H\}. \tag{3.119}$$

Verify that upon use of (3.118), these equations reduce to Hamilton's equations (3.78). If H is not explicitly dependent on time, then time does not appear explicitly on the RHS of Hamilton's equations. In this case, we say that the ODEs for q and p are an autonomous system.

One advantage of Poisson brackets is that the time evolution of *any* observable $f(q,p)$ is given by an equation of the same sort $\dot{f} = \{f, H\}$. We will see later that this holds irrespective of our choice of coordinates on phase space as long as a PB is defined. We say that the Hamiltonian generates infinitesimal time evolution via the Poisson bracket (for more on such infinitesimal transformations see Chap. 10):

$$f(q(t+\delta t), p(t+\delta t)) = f(q(t), p(t)) + (\delta t)\ \{f, H\} + \mathcal{O}((\delta t)^2). \tag{3.120}$$

If $\{f, g\} = 0$, we say that f 'Poisson commutes' with g. In particular, f is a constant of motion iff it Poisson commutes with the Hamiltonian, $\dot{f} = 0 \Leftrightarrow \{f, H\} = 0$. We begin to see the utility of the Poisson bracket in the study of conserved quantities.

$*$ **Explicitly time-dependent conserved quantities.** Suppose $F(q(t), p(t), t)$ is a conserved quantity that depends explicitly on time. Then from (3.117),

$$0 = \frac{dF}{dt} = \frac{\partial F}{\partial t} + \{F, H\}. \tag{3.121}$$

This formula holds even if H depends explicitly on time. Now let us specialize to the case where H is not explicitly time-dependent. Then we may use F to generate additional conserved quantities (see Prob. 3.38). Indeed, $\frac{\partial^p F}{\partial t^p}$ are conserved for $p = 0, 1, 2, \ldots$. To see this, we take the partial time derivative of (3.121):

$$0 = \frac{\partial}{\partial t}\frac{dF}{dt} = \frac{\partial^2 F}{\partial t^2} + \{\frac{\partial F}{\partial t}, H\} = \frac{d}{dt}\frac{\partial F}{\partial t}. \tag{3.122}$$

Thus we have shown that $\frac{\partial F}{\partial t}$ is conserved! Proceeding this way we conclude that the higher order partial time derivatives of a conserved quantity are also conserved. □

3.22 Properties of the Poisson bracket

From definition (3.118), the Poisson bracket of any dynamical variable with a constant is zero. In fact, it has several other notable properties.

Linearity. The Poisson bracket is *linear* in each entry. Verify that $\{f, \mu g\} = \mu\{f, g\}$ and $\{f, g+h\} = \{f, g\} + \{f, h\}$, where μ is a real constant. More generally, $\{f, \lambda g + \mu h\} = \lambda\{f, g\} + \mu\{f, h\}$ for $\lambda, \mu \in \mathbb{R}$ and and any 3 dynamical variables f, g and h.

Antisymmetry. The Poisson bracket (3.118) is *antisymmetric* in the dynamical variables $\{f, g\} = -\{g, f\}$. In particular, the PB of any observable with itself vanishes $\{h, h\} = 0$. A special case of this encodes the conservation of energy. Assuming H is not explicitly dependent on time,

$$\frac{dH}{dt} = \{H, H\} = 0. \tag{3.123}$$

Leibniz rule. Since (3.118) involves only first derivatives of f, the PB satisfies the *Leibniz* or *product rule* of differentiation. In fact, one verifies that

$$\{fg,h\} = f\{g,h\} + \{f,h\}g \quad \text{and} \quad \{f,gh\} = \{f,g\}h + g\{f,h\}. \qquad (3.124)$$

Antisymmetry ensures that the Leibniz rule applies to the second entry once it holds for the first entry. We say that the PB is a *derivation*[81] in either entry. The space of functions of position and momentum equipped with the Poisson bracket is called the *Poisson algebra*[82] of observables.

Canonical PB relations. The basic Poisson brackets are between coordinates and momenta. For one degree of freedom we have

$$\{q,p\} = 1 \quad \text{or} \quad \{p,q\} = -1, \quad \text{while} \quad \{q,q\} = 0 \quad \text{and} \quad \{p,p\} = 0. \qquad (3.125)$$

The last 3 equations are consequences of the antisymmetry of the PB. For n-degrees of freedom, the basic PB among coordinates and momenta follow from (3.118):

$$\{q^i,p_j\} = \delta^i_j \quad \text{and} \quad \{q^i,q^j\} = \{p_i,p_j\} = 0 \quad \text{for } 1 \le i,j \le n. \qquad (3.126)$$

These are called the canonical ('standard') PB relations between coordinates and conjugate momenta. The noun *canon* and the adjective *canonical* refer to something that is standard or conventional. For the Cartesian coordinates and momenta of a particle moving in 3d, the nonvanishing canonical PBs (up to antisymmetry) are

$$\{x,p_x\} = \{y,p_y\} = \{z,p_z\} = 1. \qquad (3.127)$$

Poisson's theorem. A remarkable feature of the Poisson bracket is that it can be used to produce new conserved quantities from a pair of existing ones. Poisson's theorem states that if f and g are conserved, then so is $\{f,g\}$. Let us first illustrate this with a couple of examples. For a free particle moving on a plane we know that p_x and p_y are both conserved. Their Poisson bracket is $\{p_x,p_y\} = 0$, which is of course trivially a conserved quantity. As a second example, consider a particle moving in three dimensions under the influence of a central potential. We know that $L_x = yp_z - zp_y$ and $L_y = zp_x - xp_z$ are both conserved. We compute $\{L_x,L_y\}$ by using bilinearity, the Leibniz rule and the basic PBs (3.127) and find $\{L_x,L_y\} = L_z$:

$$\{L_x,L_y\} \quad = \quad \{yp_z - zp_y, zp_x - xp_z\}$$

---

[81] A derivation of an algebra is a linear operation that takes an element of an algebra and produces another such element while satisfying the product rule. Differentiation in calculus is the original example of a derivation. It is a derivation of the commutative algebra of real-valued functions of one real variable: $(fg)' = f'g + fg'$. The commutator with a fixed matrix C: $[A,C] = AC - CA$ is another example of a derivation, here of the (associative) algebra of $n \times n$ matrices: $[AB,C] = [A,C]B + A[B,C]$. The PB with a particular function h, $\{f,h\}$ is a derivation of the algebra of functions of position and momentum: $\{fg,h\} = \{f,h\}g + f\{g,h\}$.

[82] An algebra is a vector space with a binary operation (product) that is bilinear. Real functions $f(q,p)$ form a vector space under real linear combinations $\alpha f + \beta g$ and a (commutative) algebra with the binary operation of pointwise product $(fg)(x) = f(x)g(x) = g(x)f(x)$, which is evidently linear in both f and g.

$$\begin{aligned} &= \{yp_z, zp_x\} - \cancel{\{yp_z, xp_z\}} - \cancel{\{zp_y, zp_x\}} + \{zp_y, xp_z\} \\ &= y\{p_z, z\}p_x + p_y\{z, p_z\}x = -yp_x + xp_y = L_z. \end{aligned} \qquad (3.128)$$

And indeed, we know that L_z is also a conserved quantity. Similarly we check that (see Prob. 3.49)

$$\{L_x, L_y\} = L_z, \quad \{L_y, L_z\} = L_x \quad \text{and} \quad \{L_z, L_x\} = L_y. \qquad (3.129)$$

This is called the angular momentum Poisson algebra (see Footnote 82). The quantities on the RHS are linear in the components of angular momentum. When this happens, the Poisson algebra defines a Lie algebra, see Appendix B.13* for more on this.

Jacobi's identity: More generally, Poisson's theorem is a consequence of the Jacobi identity. For any three dynamical variables f, g and h, the following cyclic sum of twice-iterated Poisson brackets vanishes:

$$\{f, \{g, h\}\} + \{h, \{f, g\}\} + \{g, \{h, f\}\} = 0. \qquad (3.130)$$

Using antisymmetry, we could rewrite the Jacobi identity as

$$\{\{f, g\}, h\} + \{\{g, h\}, f\} + \{\{h, f\}, g\} = 0. \qquad (3.131)$$

Before we prove the Jacobi identity, let us use it to establish Poisson's theorem. Suppose f, g are conserved so that each of them Poisson commutes with the Hamiltonian $h = H$, i.e., $\{f, H\} = \{g, H\} = 0$. Then the Jacobi identity implies that

$$\{\{f, g\}, H\} = 0 \quad \Rightarrow \quad \frac{d}{dt}\{f, g\} = 0. \qquad (3.132)$$

So the PB of two conserved quantities is again a conserved quantity.

$*$ **Poisson's tensor:** To prove the Jacobi identity, it is convenient to introduce a compact notation. Let us combine the positions and momenta into a $2n$-component 'grand' coordinate $\boldsymbol{\xi}$ on phase space and write its components with upper indices:

$$\boldsymbol{\xi} = (\xi^1, \xi^2, \ldots, \xi^n, \xi^{n+1}, \ldots, \xi^{2n}) = (\boldsymbol{q}, \boldsymbol{p}) = (q^1, \ldots, q^n, p_1, \ldots, p_n). \quad (3.133)$$

Then check that the basic Poisson bracket relations may be expressed in terms of ξ^i

$$\{\xi^i, \xi^j\} = r^{ij} \quad \text{where} \quad r^{\text{row, column}} = \left(\begin{smallmatrix} 0 & I \\ -I & 0 \end{smallmatrix}\right). \qquad (3.134)$$

Here, r is a $2n \times 2n$ block matrix with $n \times n$ blocks proportional to the identity and zero matrices as indicated. The constant matrix with components r^{ij} is called the Poisson tensor (see Appendix B.6* for more on such tensors) of the canonical PB relations. At present, r^{ij} may simply be regarded as a short-form for $\{\xi^i, \xi^j\}$. We will soon understand its properties (see Sect. 3.26*) and begin to appreciate its utility, for instance in proving the Jacobi identity in (3.141).

The PB of any pair of observables may now be written in terms of the ‘basic’ PB between coordinates and momenta. Beginning with $n = 1$, show that

$$\{f, g\} = \sum_{i=1}^{n} \left(\frac{\partial f}{\partial q^i} \frac{\partial g}{\partial p_i} - \frac{\partial f}{\partial p_i} \frac{\partial g}{\partial q^i} \right) = \sum_{i,j=1}^{2n} \frac{\partial f}{\partial \xi^i} \frac{\partial g}{\partial \xi^j} \{\xi^i, \xi^j\} = \sum_{i,j=1}^{2n} r^{ij} \partial_i f \partial_j g. \tag{3.135}$$

Here, we denote partial differentiation by $\partial_i f = \frac{\partial f}{\partial \xi^i}$. Henceforth, we will suppress the summation symbol with a sum over repeated indices being implied. Several properties of the canonical Poisson brackets are encoded in the Poisson tensor[83]. Of particular importance to us is the antisymmetry of r^{ij} (equivalent to antisymmetry of the PB) and the constancy of the components r^{ij}. □

$*$ **Remarks on Leibniz rule and derivation property.** Equation (3.135) leads to some useful formulae for PBs. For instance, taking $f = \xi^k$,

$$\{\xi^k, g(\xi)\} = \frac{\partial \xi^k}{\partial \xi^i} \frac{\partial g}{\partial \xi^j} \{\xi^i, \xi^j\} = \frac{\partial g}{\partial \xi^j} \{\xi^k, \xi^j\}. \tag{3.136}$$

In particular, taking the PB of a function of position with a momentum coordinate produces the corresponding partial derivative:

$$\{p_k, g(q)\} = \frac{\partial g}{\partial q^j} \{p_k, q_j\} + \frac{\partial g}{\partial p_j} \{p_k, p_j\} = -\frac{\partial g}{\partial q^k}. \tag{3.137}$$

This is again a reflection of the Leibniz rule: the PB acts as a ‘derivation’. In fact, a useful way of expressing this derivation property is

$$\{f, g\} = \frac{\partial f}{\partial \xi^i} \{\xi^i, g\}. \tag{3.138}$$

The proof follows by noticing that both sides are equal to (3.135). On the other hand, suppose f depends on ξ^i only through some function $h(\xi)$, then

$$\{f(h(\xi)), g\} = f'(h) \frac{\partial h}{\partial \xi^i} \{\xi^i, g\} = f'(h) \{h, g\}. \tag{3.139}$$

$*$ **Proof of Jacobi’s identity.** We wish to evaluate the cyclic sum

$$J = \{\{f, g\}, h\} + \{\{g, h\}, f\} + \{\{h, f\}, g\}. \tag{3.140}$$

We use the Poisson tensor and the Leibniz rule to write the first term of J as

$$\{\{f, g\}, h\} = \left(f_i g_j r^{ij} \right)_k h_l r^{kl} = \left[f_{ik} g_j h_l + f_i g_{jk} h_l \right] r^{ij} r^{kl}. \tag{3.141}$$

---

[83] As we will explain in Appendix B.6*, the Poisson tensor $r = r^{ij} \partial_i \otimes \partial_j$ is an antisymmetric contravariant tensor field on the phase space. It is also called the Poisson bivector field, as it has two upper indices. In general, its components could vary with location, as is the case for the angular momentum algebra (3.129). More on this in Sect. 3.26*.

Here, $f_i = \frac{\partial f}{\partial \xi^i}$ denotes the partial derivative. In expressions such as these, r^{ij} are entries of a real matrix and h_l are real-valued functions, so they can be written in any order. Adding its cyclic permutations,

$$J = \left[f_{ik} g_j h_l + f_i g_{jk} h_l + g_{ik} h_j f_l + g_i h_{jk} f_l + h_{ik} f_j g_l + h_i f_{jk} g_l \right] r^{ij} r^{kl}. \quad (3.142)$$

If J has to vanish for any sufficiently smooth functions f, g, h on phase space, then the terms involving 2^{nd} derivatives of f must mutually cancel as must those involving 2^{nd} derivatives of g or h. So let us consider the two terms involving second derivatives of f, and call their sum J_f. We find

$$\begin{aligned} J_f &= f_{ik} g_j h_l r^{ij} r^{kl} + f_{jk} g_l h_i r^{ij} r^{kl} = f_{ik} g_j h_l r^{ij} r^{kl} + f_{ik} g_l h_j r^{ji} r^{kl} \\ &= f_{ik} g_j h_l r^{ij} r^{kl} + f_{ik} g_j h_l r^{li} r^{kj} = f_{ik} g_j h_l r^{ij} r^{kl} + f_{ki} g_j h_l r^{lk} r^{ij} \\ &= f_{ik} g_j h_l r^{ij} r^{kl} - f_{ik} g_j h_l r^{ij} r^{kl} = 0. \end{aligned} \quad (3.143)$$

We relabelled indices of summation $i \leftrightarrow j$, $j \leftrightarrow l$ and $i \leftrightarrow k$ in the three successive equalities and finally used the equality of mixed partial derivatives $\frac{\partial^2 f}{\partial \xi^i \xi^k} = \frac{\partial^2 f}{\partial \xi^k \xi^i}$ and antisymmetry of the Poisson tensor $r^{kl} = -r^{lk}$. Thus, we have shown that $J_f = 0$. By cyclic symmetry, $J_g = J_h = 0$. Thus, $J = J_f + J_g + J_h = 0$ and the Jacobi identity has been established. As a corollary, we obtain Poisson's theorem on the conservation of the PB of any two conserved quantities. □

$*$ **Symplectic form.** The canonical Poisson tensor is a $2n \times 2n$ invertible matrix with entries r^{ij}. Its inverse $\omega = r^{-1}$ is called the canonical symplectic tensor or form, a concept that will be explained in Appendix B.6*. Its components are determined by

$$\omega_{ij} r^{jk} = \delta_i^k \quad \text{where} \quad \delta_i^k \text{ is the Kronecker symbol.} \quad (3.144)$$

Antisymmetry of r implies that ω too is antisymmetric (see Prob. 3.53). As a matrix,

$$\omega = \begin{pmatrix} 0 & -I \\ I & 0 \end{pmatrix}_{2n \times 2n}. \quad (3.145)$$

The symplectic form is a covariant 2^{nd} rank antisymmetric tensor[84]. □

3.23* Canonical formulation of charged particle in electromagnetic field

As an illustration of the use of Poisson brackets, we discuss a canonical formulation for the motion of a charged particle subject to electric and magnetic fields. This is an important physical system that finds applications from the motion of electrons in an atom to protons in the ionosphere. It will also give us an opportunity to introduce the principle of minimal coupling that we will use to find a Hamiltonian for a charged particle. The dynamics of a nonrelativistic particle of charge e and mass m moving in an electromagnetic field ($\boldsymbol{E}(\boldsymbol{r},t)$ and $\boldsymbol{B}(\boldsymbol{r},t)$) in 3d is governed by the Newton-Lorentz equation of motion given here in Cartesian coordinates in an inertial frame in CGS-Gaussian units:

---

[84] The symplectic form is not to be confused with what are unfortunately referred to as symplectic matrices. The latter are matrix representations (M) of linear transformations that preserve the symplectic form: $M^t \omega M = \omega$. Physically, M represent linear canonical transformations, which we will encounter in Chap. 10.

$$m\ddot{x}_i = eE_i + \frac{e}{c}\left(\boldsymbol{v}\times\boldsymbol{B}\right)_i \quad \text{where} \quad \boldsymbol{v} = \dot{\boldsymbol{r}} \quad \text{and} \quad \boldsymbol{r} = (x_1, x_2, x_3). \tag{3.146}$$

Nonrelativistic means the particle's speed is much less than that of light $|\boldsymbol{v}| \ll c$. In this equation, the basic dynamical variables are $x_i(t)$, the coordinates of the particle. The electric and magnetic fields, though they may depend on time, are assumed given to us. We are not concerned with their dynamics, which is governed by Maxwell's equations. The Newton-Lorentz equation admits a Hamiltonian formulation in terms of the vector and scalar potentials $\boldsymbol{A}(\boldsymbol{r},t)$ and $\phi(\boldsymbol{r},t)$, in terms of which the electric and magnetic fields[85] are given by [49, 104]

$$\boldsymbol{E} = -\boldsymbol{\nabla}\phi - \frac{1}{c}\frac{\partial\boldsymbol{A}}{\partial t} \quad \text{and} \quad \boldsymbol{B} = \boldsymbol{\nabla}\times\boldsymbol{A}. \tag{3.147}$$

We will show that the Hamiltonian

$$H = \frac{1}{2m}\left(\boldsymbol{p} - \frac{e}{c}\boldsymbol{A}\right)^2 + e\phi \tag{3.148}$$

leads to the Newton-Lorentz EOM if we postulate canonical PBs between x_i and p_j[86]:

$$\{x_i, p_j\} = \delta_{ij}, \quad \{x_i, x_j\} = 0 \quad \text{and} \quad \{p_i, p_j\} = 0. \tag{3.149}$$

It is instructive to compare the Hamiltonian (3.148) with that of an uncharged particle. The first term is obtained by replacing the momentum $\boldsymbol{p}$ by $\boldsymbol{p} - e\boldsymbol{A}/c$. Similarly, the second term, which is the electric potential energy may be obtained by replacing H by $H - e\phi$. This procedure for writing the Hamiltonian for a charged particle interacting with an EM field is called 'minimal coupling'. It turns out to be at the heart of one of the most successful principles in physics: the gauge principle.

Expanding out (3.148),

$$H = \frac{p_j p_j}{2m} + \frac{e^2}{2mc^2}A_j(\boldsymbol{r})A_j(\boldsymbol{r}) - \frac{e}{mc}p_j A_j(\boldsymbol{r}) + e\phi(\boldsymbol{r}), \tag{3.150}$$

---

[85] These expressions for $\boldsymbol{E}$ and $\boldsymbol{B}$ are chosen so that the homogeneous (source-free) Maxwell equations $\boldsymbol{\nabla}\cdot\boldsymbol{B} = 0$ and $\boldsymbol{\nabla}\times\boldsymbol{E} = -\frac{1}{c}\frac{\partial\boldsymbol{B}}{\partial t}$ are identically satisfied upon use of the vector identities $\boldsymbol{\nabla}\times(\boldsymbol{\nabla}\phi) = 0$ and $\boldsymbol{\nabla}\cdot(\boldsymbol{\nabla}\times\boldsymbol{A}) = 0$ for all ϕ and $\boldsymbol{A}$.

[86] In this section, all indices are placed as subscripts and repeated indices summed from 1 to 3. There is a reason for this: the kinetic energy $\frac{1}{2}m\dot{\boldsymbol{r}}^2 = \frac{1}{2}m\delta_{ij}\dot{x}^i\dot{x}^j$ that appears in the Lagrangian (3.153) defines the Euclidean metric on $\mathbb{R}^3$ whose components are given by the Kronecker symbol δ_{ij} (with inverse δ^{ij}). Since these are the components of the identity matrix, the vector with components v^i and the corresponding covector with components $\delta_{ij}v^j$ have numerically the same components though they reside in dual spaces. With this understanding, vectors and covectors may be identified with each other. One says that all upper indices have been lowered by use of the Kronecker delta. For instance, $p_j p_j$ really means $p_i p_j \delta^{ij}$. In contexts where the relevant metric components differ from those of the identity matrix (for instance, if we use curvilinear coordinates such as spherical polars on $\mathbb{R}^3$) we will need to be more careful with the placement of indices.

we find that Hamilton's equations are

$$\begin{aligned} \dot{x}_i &= v_i = \{x_i, H\} = \frac{\partial H}{\partial p_i} = \frac{p_i}{m} - \frac{eA_i}{mc} \quad \text{and} \\ \dot{p}_i &= \{p_i, H\} = -\frac{\partial H}{\partial x_i} = -\frac{e^2}{mc^2} A_j \frac{\partial A_j}{\partial x_i} + \frac{ep_j}{mc}\frac{\partial A_j}{\partial x_i} - e\frac{\partial \phi}{\partial x_i}. \end{aligned} \tag{3.151}$$

Combining them, we get the Newton-Lorentz equation:

$$\begin{aligned} m\ddot{x}_i &= \dot{p}_i - \frac{e\dot{A}_i}{c} = -e\frac{\partial \phi}{\partial x_i} - \frac{e^2}{mc^2} A_j \frac{\partial A_j}{\partial x_i} + \frac{ep_j}{mc}\frac{\partial A_j}{\partial x_i} - \frac{e}{c}\frac{\partial A_i}{\partial t} - \frac{e}{c}\frac{\partial A_i}{\partial x_j}\frac{dx_j}{dt} \\ &= eE_i + \frac{e}{c} v_j \frac{\partial A_j}{\partial x_i} - \frac{e}{c} v_j \frac{\partial A_i}{\partial x_j} = eE_i + \frac{e}{c} v_j (\partial_i A_j - \partial_j A_i) \\ &= eE_i + \frac{e}{c}\epsilon_{ijk} v_j B_k = \left(e\boldsymbol{E} + \frac{e}{c}\boldsymbol{v} \times \boldsymbol{B}\right)_i . \end{aligned} \tag{3.152}$$

Here ϵ_{ijk} is the totally antisymmetric Levi-Civita symbol introduced in Prob. 3.48. A Lagrangian for this charged particle may be obtained from H via an inverse Legendre transform (see Prob. 3.32):

$$L(\boldsymbol{r}, \dot{\boldsymbol{r}}) = \text{ext}_{\boldsymbol{p}}(\boldsymbol{p} \cdot \dot{\boldsymbol{r}} - H) = \frac{1}{2} m\dot{\boldsymbol{r}}^2 + \frac{e}{c}\boldsymbol{A} \cdot \dot{\boldsymbol{r}} - e\phi. \tag{3.153}$$

The momentum conjugate to $\boldsymbol{r}$ is seen to be the *canonical* momentum $\boldsymbol{p} = m\dot{\boldsymbol{r}} + e\boldsymbol{A}/c$ rather than the *mechanical* momentum $\boldsymbol{\pi} = m\dot{\boldsymbol{r}}$. In fact, $\boldsymbol{\pi} = \boldsymbol{p} - e\boldsymbol{A}/c$ does *not* satisfy canonical PBs: its components do not even commute with each other:

$$\begin{aligned} \{\pi_i, \pi_j\} &= \{p_i - \frac{e}{c}A_i, p_j - \frac{e}{c}A_j\} = -\frac{e}{c}\left(\{p_i, A_j\} + \{A_i, p_j\}\right) \\ &= -\frac{e}{c}\left[\frac{\partial A_j}{\partial x_k}\{p_i, x_k\} + \frac{\partial A_i}{\partial x_k}\{x_k, p_j\}\right] \\ &= \frac{e}{c}\left(\partial_i A_j - \partial_j A_i\right) = \frac{e}{c}\epsilon_{ijk} B_k. \end{aligned} \tag{3.154}$$

We used the fact that $\{A_i(\boldsymbol{r}), A_j(\boldsymbol{r})\} = 0$ since positions commute, as well as the Leibniz rule in the form given in (3.137). This feature and its quantum counterpart are relevant, for instance, in describing electrons moving on a plane subject to an orthogonal magnetic field as happens in the Hall effect.

Remark. We note that when acting on the wave function $\psi(\boldsymbol{r})$ in the quantum theory, $p_j = -i\hbar\frac{\partial}{\partial x^j}$ are proportional to the *partial derivatives* with respect to the components of position [114]. On the other hand, the components of $\boldsymbol{\pi}$ are given by those of the *covariant derivative* $\pi_j = -i\hbar\partial_j - (e/c)A_j$, which plays an important role in differential geometry. See Appendix B.11* for another example of a covariant derivative. □

3.24* Poisson algebra of conserved quantities in the Kepler problem

As a second example of Poisson brackets at work, we determine the Poisson algebra of conserved quantities of the Kepler problem, thereby verifying Poisson's theorem of Sect. 3.22. In the process we are led to the concept of a Lie algebra and get a glimpse of a hidden symmetry of the Kepler problem.

In Sect. 2.5*, we learned that the relative energy, angular momentum and LRL vectors

$$H = \frac{\boldsymbol{p}^2}{2m} - \frac{\alpha}{r}, \quad \boldsymbol{L} = \boldsymbol{r} \times \boldsymbol{p} \text{ and } \boldsymbol{A} = \boldsymbol{p} \times \boldsymbol{L} - m\alpha\hat{r} = 2m\left(H + \frac{\alpha}{2r}\right)\boldsymbol{r} - (\boldsymbol{p}\cdot\boldsymbol{r})\boldsymbol{p} \tag{3.155}$$

are conserved[87]. We denote the components of the relative vector $\boldsymbol{r}$ by x_i and its length by $r = |\boldsymbol{r}|$. To find the PBs among these seven conserved quantities, we begin with the canonical PBs $\{x_i, p_j\} = \delta_{ij}$, $\{x_i, x_j\} = \{p_i, p_j\} = 0$ and work our way up by repeated use of linearity, antisymmetry and the Leibniz rule. For instance, one finds that the nontrivial PBs among position, momentum and angular momentum are

$$\{x_i, p_j\} = \delta_{ij}, \quad \{L_i, x_j\} = \epsilon_{ijk}x_k, \quad \{L_i, p_j\} = \epsilon_{ijk}p_k \quad \text{and} \quad \{L_i, L_j\} = \epsilon_{ijk}L_k. \tag{3.156}$$

The last three PBs have a common form since $\boldsymbol{r}, \boldsymbol{p}$ and $\boldsymbol{L}$ all transform as vectors under rotations (the significance of this statement will be clarified when we study canonical transformations in Sect. 10.6). On the other hand, $\boldsymbol{p}\cdot\boldsymbol{r}$ is a scalar (i.e., invariant) under rotations and one finds that $\{L_i, \boldsymbol{p}\cdot\boldsymbol{r}\} = 0$.

Next, using (3.137), the radial distance r (or any function of it $f(r)$) has the following PBs with linear and angular momentum:

$$\{r, p_i\} = \partial_i r = \frac{x_i}{r}, \quad \{f(r), p_i\} = f'(r)\frac{x_i}{r} \quad \text{and} \quad \{L_i, f(r)\} = 0. \tag{3.157}$$

The latter PB reflects the fact that r is a scalar, i.e., invariant under rotations. To obtain it we proceed as follows:

$$\{L_i, f(r)\} = \epsilon_{ijk}\{x_j p_k, f(r)\} = \epsilon_{ijk}x_j\{p_k, f(r)\} = -\epsilon_{ijk}x_j x_k \frac{f'(r)}{r} = 0. \tag{3.158}$$

The final equality is because ϵ_{ijk} is antisymmetric in j and k while $x_j x_k$ is symmetric. The other PBs in this section can be obtained similarly and are left as exercises.

The PBs of the Hamiltonian merely reproduce the corresponding equations of time evolution:

$$\begin{aligned} \{x_i, H\} &= \frac{p_i}{m}, \quad \{f(r), H\} = f'(r)\frac{\boldsymbol{p}\cdot\hat{r}}{m}, \\ \{p_i, H\} &= -\frac{\alpha}{r^3}x_i \quad \text{and} \quad \{L_i, H\} = \{A_i, H\} = 0. \end{aligned} \tag{3.159}$$

To obtain $\{A_i, H\}$, we made use of the previous PBs with H. Next, to find $\{L_i, A_j\}$ we combine

$$\{x_i, A_j\} = x_j p_i - (\boldsymbol{r}\cdot\boldsymbol{p})\delta_{ij} - \epsilon_{ijk}L_k$$

---

[87] A conserved quantity can be characterized as an observable f that Poisson commutes with the Hamiltonian: $\{f, H\} = 0$. The set of observables that commute with H form its *commutant*. The commutant of H is a subalgebra of the Poisson algebra of all observables. In the Kepler problem, it consists of all smooth functions of H and the components of $\boldsymbol{L}$ and $\boldsymbol{A}$.

$$\text{and} \quad \{p_i, A_j\} \;=\; p_i p_j - 2m\delta_{ij}\left(H + \frac{\alpha}{2r}\right) - \frac{m\alpha}{r^3} x_i x_j \qquad (3.160)$$

to arrive at $\{L_i, A_j\} = \epsilon_{ijk} A_k$. We recognize this as having the same form as (3.156). Finally, we make use of the pleasantly simple results

$$\{r, A_i\} = \frac{1}{r}\epsilon_{ijk} x_j L_k \quad \text{and} \quad \{f(r), A_i\} = \frac{f'(r)}{r}\epsilon_{ijk} x_j L_k \qquad (3.161)$$

to obtain the last remaining PB $\{A_i, A_j\} = -2mH\epsilon_{ijk} L_k$. We may now summarize the Poisson algebra of conserved quantities of the Kepler problem:

$$\begin{aligned} \{L_i, H\} &= \{A_i, H\} = 0, \quad \{L_i, L_j\} = \epsilon_{ijk} L_k, \\ \{L_i, A_j\} &= \epsilon_{ijk} A_k \quad \text{and} \quad \{A_i, A_j\} = -2mH\epsilon_{ijk} L_k. \end{aligned} \qquad (3.162)$$

The first two formulae simply state the conservation of $\boldsymbol{L}$ and $\boldsymbol{A}$. The next two state that $\boldsymbol{L}$ and $\boldsymbol{A}$ transform as vectors under rotations, which are generated by angular momentum (more on this when we discuss canonical transformations in Sect. 10.6). The last one ensures that the algebra is *closed*. The PB of any two conserved quantities is again a conserved quantity built from $H, \boldsymbol{L}$ and $\boldsymbol{A}$. In particular, we cannot use Poisson's theorem to generate any additional independent conserved quantities beyond these seven. Interestingly, aside from $\{A_i, A_j\}$, the RHS of each of the PBs in (3.162) is linear in the components of $\boldsymbol{L}$ and $\boldsymbol{A}$. This last PB too can be made linear by rescaling the LRL vector by the Hamiltonian, which Poisson commutes with $\boldsymbol{L}$ and $\boldsymbol{A}$ and therefore behaves like a constant. For definiteness, let us restrict attention to bound trajectories, so that $H < 0$. If we define $\boldsymbol{K} = \boldsymbol{A}/\sqrt{-2mH}$, then (3.162) becomes

$$\begin{aligned} \{L_i, H\} = \{K_i, H\} = 0, &\qquad \{L_i, L_j\} = \epsilon_{ijk} L_k, \\ \{L_i, K_j\} = \epsilon_{ijk} K_k &\qquad \text{and} \quad \{K_i, K_j\} = \epsilon_{ijk} L_k. \end{aligned} \qquad (3.163)$$

The RHS in each of these PBs is a linear combination of the components of $\boldsymbol{L}$ and $\boldsymbol{K}$. So this is a *linear* Poisson algebra. Linear Poisson algebras are particularly simple and special: they are called *Lie algebras*[88]. They are associated to infinitesimal symmetries which can be extended to 'Lie groups' of finite symmetry transformations (see Appendix B.13*). In the case at hand, $\boldsymbol{L}$ and $\boldsymbol{K}$ generate a Lie algebra isomorphic to the $\mathfrak{so}(4)$ Lie algebra of infinitesimal rotations of 4d Euclidean space[89]. Thus, the somewhat laborious task of calculating these Poisson brackets has allowed us to discover a hidden symmetry of the Kepler problem [9, 123] that goes beyond the rotation invariance of its spherically symmetric potential. The latter spatial rotation symmetry is encoded in the $\mathfrak{so}(3)$ Lie algebra $\{L_i, L_j\} = \epsilon_{ijk} L_k$ of the components of relative angular momentum and forms a subalgebra of $\mathfrak{so}(4)$. From the standpoint of Noether's theorem, this larger symmetry should not come as a surprise, it is associated to the conservation of the LRL vector.

---

[88] Thus, a Lie algebra (introduced in Appendix B.13*) is a vector space (here the 7d real vector space spanned by H, L_i and K_j) that is equipped with a bilinear antisymmetric bracket operation that satisfies the Jacobi identity. Since the basic space is a linear vector space, we do not consider products such as $L_1 K_2$ as elements of the Lie algebra. It is for this reason that we do not include the Leibniz product rule as one of the axioms of a Lie algebra. Evidently, the concept of a Lie algebra is a very special case of that of a Poisson algebra.

[89] In $\mathbb{R}^4$, there are $\binom{4}{2} = 6$ coordinate planes in which we may define basic independent rotations. Thus, there are 6 generators as opposed to just three in $\mathbb{R}^3$. This $\mathbb{R}^4$ is not to be confused with Minkowski space-time.

Conserved quantities in involution. Having found the Poisson algebra of conserved quantities of the Kepler problem, it is of interest to identify conserved quantities that are in involution, i.e., that commute not just with the Hamiltonian but pairwise with each other. As we will learn in Sect. 11.7*, a system with n degrees of freedom is Liouville integrable if it possesses n conserved quantities in involution. Moreover, in the quantum theory, conserved quantities that commute with each other are said to be compatible and may be simultaneously measured. The Kepler problem is Liouville integrable, it has three conserved quantities in involution. These may be chosen, for instance, as H, L_i, A_i for $i = 1, 2$ or 3 or $H, L_j, \boldsymbol{L}^2$ for $j = 1, 2$ or 3. □

3.25* Functional independence of conserved quantities

Suppose a system with an n-dimensional phase space M has several conserved quantities $f_1, \ldots, f_s$. Here, we explain what it means for them to be *functionally* independent and give a way of testing for independence. For instance, for a particle free to move on a line, the Hamiltonian H and momentum p are both conserved. However, they are not independent since they satisfy the functional relation $H = p^2/2m$. More generally, identifying a relation between conserved quantities (if one exists) may not be straightforward. For instance, in the Kepler problem of Sect. 2.5*, the Hamiltonian and the 3 components of relative angular momentum $\boldsymbol{L}$ and the LRL vector $\boldsymbol{A}$ are all conserved. However, there is no relation between any two of these conserved quantities: the simplest involves six of them $L_1 A_1 + L_2 A_2 + L_3 A_3 = 0$ and required some understanding of the dynamics to deduce. The other relation (2.43) involves all 7 conserved quantities and was far less obvious. Thus, it would be useful to have a calculational method to test for functional independence.

To begin with, we say that the smooth dynamical variables $f_1, \ldots, f_s$ on an n-dimensional manifold[90] M are functionally independent if the only functional relation $R(f_1, \ldots, f_s) = 0$ that they satisfy at all points of M is the one where R is the zero function[91]. This in particular means that if they are independent, we cannot express any one observable as a (possibly nonlinear) function of the others. Sometimes, observables may not satisfy any relation on the whole of the phase space, but may do so on some smaller portion (a 'submanifold') where special circumstances prevail. Thus, it is often useful to talk about local dependence/independence at a point p. By local independence at p, we mean there is a neighborhood of p where the dynamical variables do not satisfy any nontrivial functional relation.

---

[90] An introduction to manifolds may be found in Appendix B.

[91] We suppose R is a sufficiently smooth function of its arguments. Notice the similarity with the definition of linear independence of vectors. Vectors $\boldsymbol{u}, \boldsymbol{v}, \boldsymbol{w}$ are linearly independent if the only linear relation $a\boldsymbol{u} + b\boldsymbol{v} + c\boldsymbol{w} = 0$ they satisfy is the one where the scalars $a = b = c = 0$.

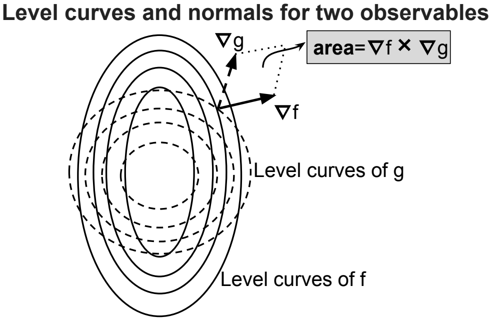

Figure 3.12: Normals $\boldsymbol{\nabla} f$ and $\boldsymbol{\nabla} g$ to levels curves of a pair of independent functions f and g are linearly independent almost everywhere and define a parallelogram with nonzero area $\boldsymbol{\nabla} f \times \boldsymbol{\nabla} g$. Their level curves intersect at isolated points.

It pays to understand functional independence geometrically. A dynamical variable f has an associated family of level sets on each of which the function takes a constant value (see Fig. 3.12). These are typically hypersurfaces[92] in M of dimension $n-1$, as they involve one condition among n variables: $f(\xi^1, \ldots, \xi^n) = c$. For example, the level sets[93] of the harmonic oscillator Hamiltonian $H = p^2/2m + m\omega^2 x^2/2$ on its 2d phase plane are typically one dimensional curves: they are concentric ellipses and an exceptional single-point zero-energy level set at the origin (see Fig. 6.1a). If f is a dynamical variable that is a function of H, e.g., $f = H/\omega$ or $f = H^3$, then f too is constant on any level set of H. In fact, if the level sets of f and H coincide, then they must be functionally related[94]. On the other hand, if f and g are independent, their level hypersurfaces are distinct and generally intersect along $n-2$ dimensional submanifolds. For example, on the 2d x-y phase plane, the level curves of the independent functions $f = 2x^2 + y^2$ and $g = 3x^2 + 4y^2$ are 'tall' and 'broad' concentric ellipses that intersect at isolated points which may be regarded as zero dimensional manifolds (see Fig. 3.12).

More generally, let S_{c_i} be the level hypersurface $f_i = c_i$ where $c_1, \ldots, c_s$ are real numbers. Then the intersection

$$S = S_{c_1} \cap S_{c_2} \cap \cdots \cap S_{c_s} \qquad (3.164)$$

is called a common level set of the s dynamical variables. By the foregoing, $f_1, \ldots, f_s$ are functionally independent if S is an $n-s$ dimensional space nearly everywhere. When this happens, we also say that S has codimension[95] s.

---

[92] A hypersurface is an $n-1$ dimensional submanifold of an n dimensional manifold.

[93] A level set of a function $f : M \to \mathbb{R}$ is the set of points in M where f takes a specified numerical value, say c; thus it is the inverse image of a point: $f^{-1}(c)$.

[94] Even if f and H are functionally related, their level sets may not quite coincide. For $\mathcal{E}$ a constant with dimensions of energy, the example $f = \sin(H/\mathcal{E})$ shows why: the $f = 0$ level set is a union of the $H = n\pi\mathcal{E}$ level sets. However, even when this happens, the level sets of f and H coincide in any sufficiently small region of phase space.

[95] A p-dimensional submanifold of an n-dimensional manifold has codimension $n-p$.

We may now combine this geometric viewpoint with calculus to arrive at a linear algebraic local criterion for functional independence. Given dynamical variables $f_1, \ldots, f_s$, at each point $p \in M$, we have the normal vectors $\boldsymbol{\nabla} f_1, \boldsymbol{\nabla} f_2, \ldots, \boldsymbol{\nabla} f_s$ to the corresponding levels sets (generally level hypersurfaces) passing through p. Recall that $\boldsymbol{\nabla} f$ is the vector that points in the direction in which the function f increases most rapidly. This means $\boldsymbol{\nabla} f$ is normal[96] to the level surfaces of f. We see that if $f_1, \ldots, f_s$ are functionally independent at p, then $\boldsymbol{\nabla} f_i$ are linearly independent. Stated differently, if the volume of the s-dimensional parallelepiped defined by the normal vectors is zero, then they are functionally dependent.

Formulation in terms of differential forms. An alternative formulation that does not require M to be Euclidean is in terms of differential forms, to be introduced more formally in Appendix B.5*. Suppose f and g satisfy a nontrivial relation $R(f, g) = 0$ on M. Taking its differential we get $R_f df + R_g dg = 0$ where subscripts denote partial derivatives. Thus, at points where R_f and R_g are not both zero[97], df and dg are linearly dependent. Thus, if f and g satisfy a relation, then df and dg are linearly dependent at most points of M. This linear dependence of 1-forms can also be expressed in terms of wedge products. Taking the wedge product[98] with dg and df, we get $R_f df \wedge dg = 0$ and $R_g df \wedge dg = 0$. So at points where the partial derivatives of the relation are not both zero, we have $df \wedge dg = 0$. Thus, if there is a relation, then $df \wedge dg$ must vanish at most places. This gives a way of detecting or ruling out relations among dynamical variables. We may of course extend the argument to several conserved quantities: if $f_1, \ldots, f_s$ satisfy a relation, then the wedge product of their differentials is an s-form that must vanish almost everywhere:

$$df_1 \wedge df_2 \wedge \cdots \wedge df_s = 0. \tag{3.166}$$

If this wedge product is nonzero almost everywhere, then it would indicate that f_i are generally functionally independent. For example, if we have three functions that satisfy the relation $R(f, g, h) = 0$, then evaluating the exterior derivative and taking wedge products with any two of df, dg and dh gives us three equations $R_f df \wedge dg \wedge dh = 0$, $R_g dg \wedge dh \wedge df = 0$ and $R_h dh \wedge df \wedge dg = 0$. As long as one of the partial derivatives is nonzero, we must have $df \wedge dg \wedge dh = 0$.

Example. Suppose $M = \mathbb{R}^2$ with the origin omitted and we are given 2 observables

$$f = x/\sqrt{x^2 + y^2} \quad \text{and} \quad g = y/\sqrt{x^2 + y^2}. \tag{3.167}$$

---

[96] Let us recall why $\boldsymbol{\nabla} f(\boldsymbol{r})$ is normal to the level surface S_c of f passing through $\boldsymbol{r}$, where $f(\boldsymbol{r}) = c$. A tangent vector $\boldsymbol{t}$ to S_c at $\boldsymbol{r}$ is defined by the condition that $f(\boldsymbol{r} + \epsilon \boldsymbol{t}) = c$ to first order in ϵ. In other words, $f(\boldsymbol{r}) + \epsilon \boldsymbol{t} \cdot \boldsymbol{\nabla} f = c$ or $\boldsymbol{t} \cdot \boldsymbol{\nabla} f = 0$. Thus, $\boldsymbol{\nabla} f$ is orthogonal to all tangent vectors and is therefore normal to the surface S_c at $\boldsymbol{r}$.

[97] This can only happen on a lower dimensional submanifold of the phase space. This is because we need to impose two conditions $R_f = 0$ and $R_g = 0$.

[98] The appearance of the wedge product is to be expected: for functions on $\mathbb{R}^3$,

$$df \wedge dg = (f_x g_y - f_y g_x) dx \wedge dy + (f_y g_z - f_z g_y) dy \wedge dz + (f_z g_x - f_x g_z) dz \wedge dx \tag{3.165}$$

has the same components as the cross product $\boldsymbol{\nabla} f \times \boldsymbol{\nabla} g$ in Cartesian coordinates. The magnitude of the latter measures the area of the parallelogram defined by $\boldsymbol{\nabla} f$ and $\boldsymbol{\nabla} g$.

Evaluating the exterior derivatives, we get with $r = \sqrt{x^2+y^2}$,

$$df = \frac{1}{r}\left(1 - \frac{x^2}{r^2}\right)dx - \frac{xy}{r^3}dy \quad \text{and} \quad dg = -\frac{xy}{r^3}dx + \frac{1}{r}\left(1 - \frac{y^2}{r^2}\right)dy. \tag{3.168}$$

Thus, the wedge product is

$$df \wedge dg = \frac{1}{r^2}\left(1 - \frac{x^2}{r^2}\right)\left(1 - \frac{y^2}{r^2}\right)dx \wedge dy + \frac{x^2y^2}{r^6}dy \wedge dx = 0. \tag{3.169}$$

We used $dx \wedge dy = -dy \wedge dx$. Since $df \wedge dg \equiv 0$, df and dg must be linearly dependent everywhere and we infer that f and g must satisfy a relation. In this example, the relation is easily identified: $R(f,g) = f^2 + g^2 - 1 = 0$. Identifying such a relation is in general not easy. While calculating the wedge products by hand can be laborious, it is a process that can be automated using symbolic computation. On the other hand, there is no such algorithm to find a relation among conserved quantities. □

Independence of Keplerian conserved quantities. As a second example, we examine the independence of Keplerian conserved quantities (3.155):

$$H = \frac{p^2}{2m} - \frac{\alpha}{r}, \quad L_i = \epsilon_{ijk}x_j p_k \quad \text{and} \quad A_i = 2m\left(H + \frac{\alpha}{2r}\right)x_i - (\boldsymbol{p}\cdot\boldsymbol{r})p_i \tag{3.170}$$

on the $\mathbb{R}^6$ phase space (with coordinates $x_1, x_2, x_3, p_1, p_2, p_3$) for relative motion. It is clear that $\boldsymbol{L}\cdot\boldsymbol{A} = 0$. Thus, we would expect to find that $dL_1 \wedge dL_2 \wedge dL_3 \wedge dA_1 \wedge dA_2 \wedge dA_3 = 0$ almost everywhere on phase space. On the other hand, the scalar relation (2.43) among H, L^2 and A^2 is less obvious. Suppose we were not aware of it. To test for a possible relation among these three scalars, we will calculate the 3-fold wedge product $dH \wedge dA^2 \wedge dL^2$ and show that it is identically zero on the phase space. This will imply that they are functionally related. The rest of this section is devoted to this somewhat challenging calculation and the techniques used to simplify it.

To begin with, we find the differentials of the conserved quantities:

$$\begin{aligned}
dL_i &= \epsilon_{ijk}(x_j dp_k + p_k dx_j), \quad dH = \frac{1}{m}p_i dp_i + \frac{\alpha}{r^2}dr = \frac{1}{m}p_i dp_i + \frac{\alpha}{r^3}x_i dx_i, \\
dL^2 &= 2\epsilon_{ijk}L_i(x_j dp_k + p_k dx_j) = 2(\boldsymbol{L}\times\boldsymbol{r})_k dp_k + 2(\boldsymbol{p}\times\boldsymbol{L})_k dx_k, \\
dA_i &= 2mx_i\left[dH - \frac{\alpha}{2r^2}dr\right] + 2m\left[H + \frac{\alpha}{2r}\right]dx_i - (\boldsymbol{p}\cdot\boldsymbol{r})dp_i - p_i(p_j dx_j + x_j dp_j) \\
&= 2mx_i\left[dH - \frac{\alpha dr}{2r^2}\right] + \left[2m\left[H + \frac{\alpha}{2r}\right]\delta_{ij} - p_i p_j\right]dx_j - (p_i x_j + \boldsymbol{p}\cdot\boldsymbol{r}\delta_{ij})dp_j, \\
\frac{dA^2}{2} &= A_i dA_i = 2m(\boldsymbol{A}\cdot\boldsymbol{r})\left(dH - \frac{\alpha}{2r^2}dr\right) + \left(2m\left(H + \frac{\alpha}{2r}\right)A_i - \boldsymbol{A}\cdot\boldsymbol{p}\,p_i\right)dx_i \\
&\quad -(\boldsymbol{A}\cdot\boldsymbol{p}\,x_i + \boldsymbol{p}\cdot\boldsymbol{r}\,A_i)dp_i.
\end{aligned} \tag{3.171}$$

Next, we find the two-fold wedge product

$$\begin{aligned}
\frac{1}{2}dH \wedge dA^2 \quad &= \quad -\frac{\alpha}{r^3}(\boldsymbol{A}\cdot\boldsymbol{r})p_i x_j dp_i \wedge dx_j \\
&\quad + (2m(H + \alpha/2r)A_j - \boldsymbol{A}\cdot\boldsymbol{p}\,p_j)\left(\frac{1}{m}p_i dp_i \wedge dx_j + \frac{\alpha}{r^3}x_i dx_i \wedge dx_j\right)
\end{aligned}$$

$$\begin{aligned} & -(\boldsymbol{A}\cdot\boldsymbol{p}\, x_j + \boldsymbol{p}\cdot\boldsymbol{r}\, A_j)\left(\frac{1}{m}p_i dp_i \wedge dp_j + \frac{\alpha}{r^3}x_i dx_i \wedge dp_j\right) \\ = \;& R_{ij}dp_i\wedge dp_j + S_{ij}dx_i \wedge dx_j + T_{ij}dp_i\wedge dx_j \qquad (3.172)\end{aligned}$$

where we have defined three second-rank tensors

$$\begin{aligned} R_{ij} &= -\frac{p_i}{m}[\boldsymbol{A}\cdot\boldsymbol{p}\, x_j + \boldsymbol{p}\cdot\boldsymbol{r}\, A_j], \quad S_{ij} = \frac{\alpha}{r^3}\left[2m\left(H+\frac{\alpha}{2r}\right)x_i A_j - \boldsymbol{A}\cdot\boldsymbol{p}\, x_i p_j\right] \\ \text{and} \quad T_{ij} &= -\frac{\alpha}{r^3}\boldsymbol{A}\cdot\boldsymbol{r}\, p_i x_j + 2\left(H+\frac{\alpha}{2r}\right)p_i A_j \\ & -\frac{\boldsymbol{A}\cdot\boldsymbol{p}}{m}\, p_i p_j + \frac{\alpha}{r^3}(\boldsymbol{A}\cdot\boldsymbol{p}\, x_i x_j + \boldsymbol{p}\cdot\boldsymbol{r}\, A_i x_j). \qquad (3.173)\end{aligned}$$

To proceed further, it is convenient to introduce the symbols $\boldsymbol{Q} = \boldsymbol{r}\times\boldsymbol{L}$ and $\boldsymbol{M} = \boldsymbol{p}\times\boldsymbol{L}$ so that $dL^2 = -2Q_k dp_k + 2M_k dx_k$. We thus get the three-fold wedge product:

$$\begin{aligned} \frac{dH\wedge dA^2 \wedge dL^2}{4} &= (T_{ik}Q_j + R_{ij}M_k)\, dp_i\wedge dp_j \wedge dx_k \\ & -(S_{ij}Q_k + T_{kj}M_i)\, dx_i \wedge dx_j \wedge dp_k \\ & + S_{ij}M_k\, dx_i\wedge dx_j \wedge dx_k - R_{ij}Q_k\, dp_i \wedge dp_j \wedge dp_k \\ &= \gamma_1 - \gamma_2 + \gamma_3 - \gamma_0. \qquad (3.174)\end{aligned}$$

The subscript on γ encodes the number of dx factors. For this to vanish, each of the four terms must vanish. The latter two coordinate 3-forms $dx_i\wedge dx_j\wedge dx_k$ and $dp_i\wedge dp_j\wedge dp_k$ are totally antisymmetric in the indices i, j, k. Thus, their coefficients must vanish when totally antisymmetrized.

For instance, proceeding as in (B.34),

$$\begin{aligned} \gamma_0 &= R_{ij}Q_k dp_i\wedge dp_j \wedge dp_k = \omega_{ijk}dp_i \wedge dp_j \wedge dp_k \quad \text{where} \\ 6\omega_{ijk} &= (R_{ij} - R_{ji})Q_k + \text{cyclic permutations.} \qquad (3.175)\end{aligned}$$

On account of its total antisymmetry, ω_{ijk} (like ϵ_{ijk}) can have at most one linearly independent component, which can be taken as ω_{123}. So to show that $\gamma_0 = 0$, it suffices to show that $\omega_{123} = 0$. We find

$$\begin{aligned} R_{ij} - R_{ji} &= \frac{\boldsymbol{A}\cdot\boldsymbol{p}}{m}(x_i p_j - x_j p_i) + \frac{\boldsymbol{p}\cdot\boldsymbol{r}}{m}(A_i p_j - A_j p_i) \\ &= \frac{\boldsymbol{A}\cdot\boldsymbol{p}}{m}\epsilon_{ijl}L_l + \frac{\boldsymbol{p}\cdot\boldsymbol{r}}{m}\epsilon_{ijl}(\boldsymbol{A}\times\boldsymbol{p})_l \qquad (3.176)\end{aligned}$$

and consequently,

$$\begin{aligned} 6\omega_{123} &= \frac{\boldsymbol{A}\cdot\boldsymbol{p}}{m}\epsilon_{123}L_3 Q_3 + \frac{\boldsymbol{p}\cdot\boldsymbol{r}}{m}\epsilon_{123}(\boldsymbol{A}\times\boldsymbol{p})_3 Q_3 + \text{cyclic perm.} \\ &= \frac{\boldsymbol{A}\cdot\boldsymbol{p}}{m}\boldsymbol{L}\cdot(\boldsymbol{r}\times\boldsymbol{L}) + \frac{\boldsymbol{p}\cdot\boldsymbol{r}}{m}(\boldsymbol{A}\times\boldsymbol{p})\cdot(\boldsymbol{r}\times\boldsymbol{L}) = 0 \qquad (3.177)\end{aligned}$$

as $\boldsymbol{r}\times\boldsymbol{L}$ lies in the orbital plane while $\boldsymbol{A}\times\boldsymbol{p}$ is perpendicular to it. Thus $\gamma_0 = 0$. A very similar calculation shows that $\gamma_3 = 0$. In this case,

$$\gamma_3 = \phi_{ijk}dx_i\wedge dx_j \wedge dx_k \quad \text{where} \quad 6\phi_{ijk} = (S_{ij} - S_{ji})M_k + \text{cyclic perm.} \qquad (3.178)$$

is again totally antisymmetric. One finds

$$6\phi_{123} = \frac{2m\alpha}{r^3}\left(H + \frac{\alpha}{2r}\right)(\boldsymbol{r}\times\boldsymbol{A})\cdot(\boldsymbol{p}\times\boldsymbol{L}) - \frac{\alpha}{r^3}(\boldsymbol{A}\cdot\boldsymbol{p})\,\boldsymbol{L}\cdot(\boldsymbol{p}\times\boldsymbol{L}) = 0, \quad (3.179)$$

so that $\gamma_3 = 0$.

By contrast, γ_1 and γ_2 are more involved since the 3-forms $dp_i \wedge dp_j \wedge dx_k$ and $dx_i \wedge dx_j \wedge dp_k$ are antisymmetric only in i and j. Thus, we may write

$$\begin{aligned}\gamma_1 &= \frac{1}{2}\psi_{ijk} dp_i \wedge dp_j \wedge dx_k \quad \text{where} \quad \psi_{ijk} = T_{ik}Q_j - T_{jk}Q_i + (R_{ij} - R_{ji})M_k \ \text{ and}\\ \gamma_2 &= \frac{\theta_{ijk}}{2} dx_i \wedge dx_j \wedge dp_k \ \text{ where } \ \theta_{ijk} = (S_{ij} - S_{ji})Q_k + T_{kj}M_i - T_{ki}M_j. \quad (3.180)\end{aligned}$$

Here ψ and θ are antisymmetric in i and j. To simplify things, we choose the axes so that $\boldsymbol{L} \propto \hat{z}$, $\boldsymbol{A} \propto \hat{x}$ (which are known to be independent of time) and $\hat{y} = \hat{z} \times \hat{x}$. Then $A_2 = A_3 = L_1 = L_2 = p_3 = x_3 = 0$ and it follows from (3.173) that

$$R_{ij} = S_{ij} = T_{ij} = 0 \quad \text{and} \quad Q_i = M_i = 0 \quad \text{if} \quad i \ \text{or} \ j = 3. \qquad (3.181)$$

Then by inspection, ψ_{ijk} and θ_{ijk} vanish if any one of $i, j, k = 3$. Accounting for antisymmetry, it only remains to check whether $\psi_{121}, \psi_{122}, \theta_{121}$ and θ_{122} vanish. We find (see Prob. 3.57) $\psi_{121} = -A_1L_3p_2A_2/m$, $\psi_{122} = A_1L_3p_1A_2/m$, $\theta_{121} = -\alpha A_1L_3x_2A_2/r^3$ and $\theta_{122} = \alpha A_1L_3x_1A_2/r^3$, all of which vanish since $A_2 = 0$ in our coordinate system. Thus $\gamma_1 = \gamma_2 = 0$. Putting this in (3.174) we therefore reach the happy conclusion that $dH \wedge dA^2 \wedge dL^2 = 0$ throughout the phase space. Thus, H, A^2 and L^2 must satisfy a relation. Fortunately, we have already found such a relation in (2.43)!

3.26* Noncanonical Poisson brackets, Poisson and symplectic manifolds

The Poisson brackets (3.126) for the canonical coordinates and momenta q^i and p_j can be generalized to so-called noncanonical[99] PBs which arise naturally in many physical contexts. In fact, the angular momentum PBs (3.129) furnish such an example. The 3d manifold $\mathbb{R}^3$ with Cartesian coordinates $L^1 = L_x, L^2 = L_y, L^3 = L_z$ equipped with the Poisson brackets

$$\{L_x, L_y\} = L_z \quad \text{and cyclic permutations, or} \quad \{L^i, L^j\} = \epsilon^{ij}{}_k L^k = r^{ij}(L) \qquad (3.182)$$

leads to a Poisson tensor[100] r whose components define a 3 × 3 nonconstant antisymmetric matrix. Here $\epsilon^{ij}{}_k$ are numerically equal[101] to the components of the Levi-Civita symbol ϵ_{ijk} defined in Prob. 3.48, leading to

---

[99] When we say canonical PBs among coordinates on a manifold, we mean that the coordinates on the manifold are split into n position-like variables q^i and n momentum-like variables p_j with the PBs $\{q^i, p_j\} = \delta^i_j$, $\{q^i, q^j\} = 0$ and $\{p_i, p_j\} = 0$. Anything other than this is noncanonical. When q^i and p_j satisfy canonical PBs, we will say that q^i is canonically conjugate to p_i and that they furnish Darboux coordinates on the manifold.

[100] See Appendix B.6* and Appendix B.9* for an introduction to tensor and differential forms on a manifold.

[101] The Euclidean metric has been used to raise indices $\epsilon^{ij}{}_k = \delta^{il}\delta^{jm}\epsilon_{lmk}$.

$$r^{ij} = \begin{pmatrix} 0 & L_z & -L_y \\ -L_z & 0 & L_x \\ L_y & -L_x & 0 \end{pmatrix}. \tag{3.183}$$

This Poisson bracket was derived in (3.129) from the canonical PBs among the position and momentum coordinates of a particle moving in 3d, with $L_x = yp_z - zp_y$, etc. However, here we restrict attention from the 6d phase space with coordinates x^i and p_j and focus on the 3d angular momentum phase space. In particular, we are only concerned with observables that can be expressed in terms of L^i and not more general functions of x, y, z and p_x, p_y, p_z. The above Poisson algebra will be studied in more detail in Sect. 8.14* in the context of rigid body dynamics. Here, we notice that the angular momentum PBs (among the coordinates L_x, L_y, L_z) are antisymmetric and satisfy the Jacobi identity (see Prob. 3.49). So far, we have only defined 'basic' PBs among the coordinates L^i. General observables are smooth real-valued functions of L_x, L_y and L_z (such as $L_x^2 + L_y^2 + L_z^2$), and we would like to define PBs among them. Inspired by (3.135), we define the bracket between any two functions as

$$\{f(L), g(L)\} = \sum_{i,j} \frac{\partial f}{\partial L^i}\frac{\partial g}{\partial L^j} r^{ij} = \sum_{i,j,k} \frac{\partial f}{\partial L^i}\frac{\partial g}{\partial L^j} \epsilon^{ij}{}_k L^k = (\boldsymbol{\nabla} f \times \boldsymbol{\nabla} g)\cdot \boldsymbol{L}. \tag{3.184}$$

This definition is nice: antisymmetry is manifest and so is linearity, while the appearance of only first order derivatives of f and g guarantees the Leibniz rule. For instance, $\{L_x, 2L_y + 3L_z\} = 2\{L_x, L_y\} + 3\{L_x, L_z\}$,

$$\{L_x L_y, L_z\} = L_x\{L_y, L_z\} + \{L_x, L_z\}L_y \quad \text{and} \quad \{L_x, g(L)\} = \sum_{i=1}^{3} \frac{\partial g}{\partial L^i}\{L_x, L^i\}. \tag{3.185}$$

The Jacobi identity may also be verified by expressing it as a condition on the Poisson tensor (see Prob. 3.54 and 3.58). Thus, we have defined a Poisson bracket among observables on the angular momentum phase space $\mathbb{R}^3$. This PB is far from canonical, $\mathbb{R}^3$ is odd-dimensional and there is no splitting of L^i into positions and momenta!

Poisson manifold. Based on the examples of the position-momentum and angular momentum PBs, we now define the notion of a Poisson manifold M. This is a useful concept since the phase space of a classical mechanical system is typically a Poisson manifold. To begin with, the latter is a differentiable (or smooth) manifold (see Appendix B.1 for an introduction to manifolds) M whose points are the states of the system. Dynamical variables $f, g, h, \ldots$ are (sufficiently smooth) real-valued functions on M. M is equipped with a Poisson structure, by which we mean a bilinear antisymmetric bracket operation $\{f, g\}$ which associates a function to any ordered pair of functions. This bracket is required to satisfy two additional properties: the Leibniz rule (3.124) and the Jacobi identity (3.130). $\mathbb{R}^{2n}$ with the canonical PB (3.118) is our primary example of a Poisson manifold. $\mathbb{R}^3$ with the angular momentum PBs (3.184) provides another example[102]. In particular, a Poisson manifold need not be even-dimensional and there may not be any obvious splitting of coordinates on M into 'positions' and 'momenta'. Given coordinates ξ^i for $i = 1, \ldots, n$, where n is the dimension of M, we may express the Poisson structure in terms of a Poisson tensor:

---

[102] Other examples of Poisson manifolds include (a) the cotangent bundle of any manifold (regarded as a configuration space), (b) $\mathbb{C}^n$, (c) the vector space dual to a Lie algebra (d) Riemann surfaces like a sphere, torus and higher handlebodies and (e) Kähler manifolds.

$$r^{ij}(\xi) = \{\xi^i, \xi^j\} \quad \text{with} \quad \{f, g\}(\xi) = \sum\nolimits_{i,j=1}^{n} (\partial_i f)(\partial_j g) r^{ij}(\xi). \tag{3.186}$$

In general, the components r^{ij} can depend on ξ in a nonlinear fashion: they were constant for the position-momentum example (3.134) and linear for the angular momentum example (3.182). Antisymmetry of the PBs implies r is antisymmetric $r^{ij} = -r^{ji}$. Though the components depend on the coordinates chosen, we will show (using the Leibniz rule) that r^{ij} transforms as a contravariant tensor field (see Appendix B.6*) of 2nd rank (2 upper indices) on M. Indeed, suppose $\eta^i = \eta^i(\xi)$ is a new system of coordinates on an overlapping coordinate patch. Then the new Poisson tensor is

$$\tilde{r}^{ij} = \{\eta^i, \eta^j\} = \frac{\partial \eta^i}{\partial \xi^k} \frac{\partial \eta^j}{\partial \xi^l} \{\xi^k, \xi^l\} = J^i_k J^j_l r^{kl}. \tag{3.187}$$

The appearance of two Jacobian matrices as in (B.14), implies that r is a contravariant 2nd rank tensor field. Interestingly, the Jacobi identity (3.130) can be expressed as a quadratic condition on r and its partial derivatives (see Prob. 3.54):

$$r^{il} \partial_l r^{jk} + r^{kl} \partial_l r^{ij} + r^{jl} \partial_l r^{ki} = 0. \tag{3.188}$$

This is a quadratically nonlinear first order partial differential equation (PDE) for the Poisson tensor r. It is obviously satisfied by the canonical q-p Poisson tensor (3.134) whose components are constants. We verify in Prob. 3.58 that it is also satisfied by the angular momentum Poisson tensor (3.182).

Symplectic manifold. In general, the Poisson tensor r^{ij} may not be an invertible matrix. The angular momentum PBs furnish an example where (3.183) implies that $\det r = 0$ (see Sect. 8.14* for more on this). However, when $\det r \neq 0$ we say that the Poisson structure is nondegenerate and may be inverted to define a symplectic structure on M. This is the case for the canonical q-p Poisson tensor (3.134). A necessary condition for invertibility of the Poisson tensor is that M be even-dimensional[103]. As in (3.144), the symplectic tensor or form is given by the inverse of r, $\omega_{ij} r^{jk} = \delta^k_i$. The symplectic tensor is an antisymmetric covariant tensor field of rank two on M. One of the nice features of ω is that, as shown in Prob. 3.60, the quadratically nonlinear Jacobi relation (3.188) becomes a linear equation for ω called the Bianchi identity:

$$\omega_{ij,k} + \omega_{ki,j} + \omega_{jk,i} = 0 \quad \text{where} \quad \omega_{ij,k} = \partial_k \omega_{ij} \quad \text{etc.} \tag{3.189}$$

The terms in the Bianchi identity are obtained via cyclic permutations of i, j, k. In the language of differential forms of Appendix B.9*, the Bianchi identity says that the symplectic form $\omega = \frac{1}{2} \omega_{ij} d\xi^i \wedge d\xi^j$ is a closed two-form: $d\omega = 0$. Based on this observation, one defines a symplectic manifold M as an even-dimensional manifold equipped with a nondegenerate closed two-from[104]. In local coordinates, nondegenerate means that the components ω_{ij} define an invertible matrix at every point of M. If M has dimension n, this is equivalent to the condition that ω^n is nowhere zero on M (i.e., it defines a so-called volume form on M) and also to the property that at each point $p \in M$, $\omega(u, v) = 0$ for all tangent vectors u at p implies that $v = 0$.

---

[103] Indeed, show that an odd-dimensional antisymmetric matrix has zero determinant.

Casimir invariants and symplectic leaves. Poisson manifolds other than the $\mathbb{R}^{2n}$ position-momentum phase space can exhibit some new features. For instance, there could be dynamical variables that Poisson commute with all other dynamical variables[105]. The angular momentum Poisson manifold $\mathbb{R}^3$ is a case in point where one verifies (see Prob. 3.51) that $L^2 = L_x^2 + L_y^2 + L_z^2$ commutes with L_x, L_y and L_z and therefore with all observables (by the Leibniz rule). Such an observable is called a Casimir invariant (or simply a Casimir) and is said to lie in the center of the Poisson algebra of functions. Any function of Casimirs is also a Casimir (see Prob. 3.61). Constant functions of course commute with anything, so they automatically lie in the center and we usually do not designate them Casimirs. Casimir invariants are conserved quantities since they would commute with any Hamiltonian function. A Poisson algebra with Casimirs (i.e., a nontrivial center) is called a degenerate Poisson algebra. This is reasonable since it turns out that the Poisson tensor is invertible if and only if the center of the Poisson algebra is trivial. The angular momentum phase space $\mathbb{R}^3$ is a degenerate Poisson manifold: L^2 is a Casimir and (3.183) has zero determinant. Since L^2 is conserved, a trajectory must lie on the part of phase space where L^2 takes a constant value. In other words, trajectories are confined to level sets of a Casimir (in this case, constant L^2 hypersurfaces shown in Fig. 3.13). If there are several Casimirs, then the dynamics is restricted to the intersection of their level sets. Thus, we may assign numerical values to the Casimirs and restrict the dynamics to the intersection of their level hypersurfaces. In the angular momentum example, L^2 is the only independent Casimir and its level sets are concentric spheres which foliate the Poisson manifold $\mathbb{R}^3$ like the layers of an onion. These common level sets of Casimirs are called symplectic leaves. Moreover, one may show (see Sect. 8.14*) that the Poisson tensor r, when restricted to any one such leaf is invertible and therefore defines a symplectic form ω. Thus, the symplectic leaves of a Poisson manifold must be even-dimensional and nondegenerate and therefore define symplectic manifolds. By a fundamental result of Darboux, every symplectic manifold can be covered by local coordinate patches in which the coordinates are canonical (split into position and conjugate momentum variables). Such canonical local coordinates are called Darboux coordinates. The sphere S^2 discussed in the example below is a simple example of a symplectic manifold.

---

[104] Examples of symplectic manifolds include $\mathbb{R}^{2n}$, $\mathbb{C}^n$, the cotangent bundle of any (configuration) manifold, Riemann surfaces and Kähler manifolds.

[105] On the canonical position-momentum phase space $\mathbb{R}^{2n}$, there is no nonconstant function that commutes with all other functions of x^i and p_j. Indeed if $\{x^i, f\} = 0$ then $\partial f/\partial p_i = 0$ while if $\{f, p_j\} = 0$ then $\partial f/\partial x^j = 0$. So the only functions that commute with all positions and momenta are constant functions.

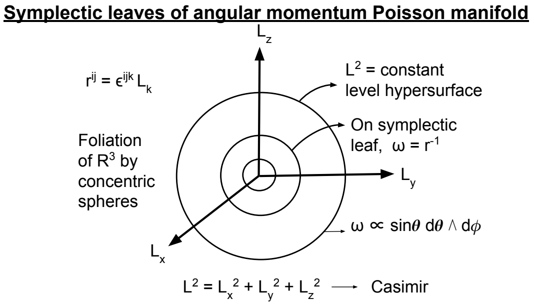
Symplectic leaves of angular momentum Poisson manifold
L_z
r^ij = ε^ijk L_k
L² = constant level hypersurface
On symplectic leaf, ω = r⁻¹
Foliation of R³ by concentric spheres
L_y
ω ∝ sinθ dθ ∧ dφ
L_x
L² = L_x² + L_y² + L_z² ⟶ Casimir

Figure 3.13: The Casimir $L^2 = L_x^2 + L_y^2 + L_z^2$ is conserved, it commutes with all observables. So trajectories must remain on a constant L^2 surface. Level sets of L^2 are symplectic leaves of the angular momentum phase space: they are concentric spheres and the point at the origin.

Hamiltonian dynamical system. It is important to notice that the notion of a Poisson bracket (or Poisson manifold and Poisson algebra of observables) is kinematical. It has information on the degrees of freedom, phase space and possible dynamical variables but does not contain information on the forces in operation. In particular, it does not *by itself* determine the dynamics (time evolution). For that we also need a Hamiltonian. In fact, we may define a Hamiltonian dynamical system as a Poisson manifold equipped with a smooth (or at least differentiable) real-valued Hamiltonian function H. Time evolution of any observable f is then given by

$$\dot{f} = \{f, H\} = r^{ij}\partial_i f \partial_j H. \tag{3.190}$$

In particular, taking $f = \xi^k$ to be one of the coordinates, we have[106] $\dot{\xi}^k = r^{kj}\frac{\partial H}{\partial \xi^j}$. Here $V_H^k = r^{kj}\partial_j H$ are the components of a vector field (see Appendix B.4* and (5.6)) on phase space called the Hamiltonian vector field. Verify that the equations $\dot{\xi}^k = V_H^k$ reduce to Hamilton's canonical equations on the phase plane if $(\xi^1, \xi^2) = (x, p)$ and $r^{ij} = \left(\begin{smallmatrix} 0 & 1 \\ -1 & 0 \end{smallmatrix}\right)$.

Example: The unit sphere $S^2 \subset \mathbb{R}^3$ with spherical polar coordinates θ and ϕ can be given the structure of a Poisson manifold (see Fig. 3.13) with PBs given by[107]

$$\{\phi, \cos\theta\} = 1/\ell \tag{3.191}$$

where ℓ is a constant parameter with dimensions of action. The Leibniz rule implies that $\{\theta, \phi\} = \ell^{-1}\csc\theta$. Thus, though θ and ϕ are not canonically conjugate, ϕ and $l\cos\theta$ are Darboux coordinates: $\{\phi, \ell\cos\theta\} = 1$. In the θ, ϕ coordinate system, show that the Poisson and symplectic tensors are

$$r^{ij} = \begin{pmatrix} \{\theta,\theta\} & \{\theta,\phi\} \\ \{\phi,\theta\} & \{\phi,\phi\} \end{pmatrix} = \ell^{-1}\begin{pmatrix} 0 & \csc\theta \\ -\csc\theta & 0 \end{pmatrix} \quad \& \quad \omega_{ij} = \ell\begin{pmatrix} 0 & -\sin\theta \\ \sin\theta & 0 \end{pmatrix}. \tag{3.192}$$

---

[106] When the Poisson tensor is invertible, with $r^{-1} = \omega$, we may of course write Hamilton's equations as $\dot{\xi}^k = (\omega^{-1})^{kj}\partial_j H$.

[107] θ and ϕ are not global coordinates on the sphere. They are valid on a patch that excludes one longitude such as the prime meridian: $0 < \theta < \pi$ and $0 < \phi < 2\pi$. One needs a minimum of two coordinate patches to cover S^2.

Now, suppose we take the Hamiltonian to be the 'height' function $H = \mathcal{E}\cos\theta$ where $\mathcal{E}$ is a constant with dimensions of energy. Then the equations of motion are

$$\dot{\phi} = \{\phi, H\} = \mathcal{E}/\ell \quad \text{and} \quad \dot{\theta} = \{\theta, \cos\theta\} = 0. \tag{3.193}$$

Thus, ϕ is cyclic (it does not appear in H) and its conjugate momentum $\ell\cos\theta$ is conserved. Trajectories are the latitude circles: $\theta(t) = \theta(0)$ (see Fig. B.5b) with the longitude varying linearly in time $\phi(t) = \phi(0) + \mathcal{E}t/\ell$. □

$*$ **Canonical vector fields.** The idea of the Hamiltonian vector field may be generalized to dynamical variables other than the Hamiltonian. Given any observable (sufficiently smooth real-valued function $f(\xi)$ on phase space), we define the associated canonical vector field via its components $V_f^i = r^{ij}\partial_j f$. Now, suppose f and g are two observables, then it may be shown (see Prob. 3.59) using the Jacobi identity that the canonical vector field associated to the PB $\{f, g\}$ is the (negative of) the commutator of canonical vector fields

$$V_{\{f,g\}} = -[V_f, V_g]. \tag{3.194}$$

Here, the commutator of vector fields $[v, w]^i = v^j\partial_j w^i - w^j\partial_j v^i$ is defined in (B.8). It follows that if two observables f and g Poisson commute ($\{f, g\} = 0$), then the corresponding canonical vector fields commute $[V_f, V_g] = 0$. In particular, if f is a conserved quantity (i.e., $\dot{f} = \{f, H\} = 0$), then $[V_f, V_H] = 0$. Suppose f and g are both conserved, then $[V_f, V_H] = [V_g, V_H] = 0$. It follows that $[V_{\{f,g\}}, V_H] = 0$ since $\{f, g\}$ is also conserved by Poisson's Theorem. Thus, $[[V_f, V_g], V_H] = 0$. Consequently, the space of canonical vector fields that commute with the Hamiltonian is closed under the operation of taking the commutator of vector fields. We say that conserved quantities or canonical vector fields associated to conserved quantities form a Lie algebra[108]. We will learn in Sect. 10.7 that conserved quantities generate infinitesimal symmetry transformations on phase space. They generate flows (see Sect. 5.1) on phase space that commute with time evolution, which is the flow generated by the Hamiltonian. The above Lie algebra is typically the infinitesimal version of a Lie group of symmetries of the Hamiltonian system. See Appendix B.13* for a brief introduction to the concept of a Lie group and its Lie algebra. □

Solution of Hamilton's equations via iterated PBs. A sometimes useful feature of PBs is that they give us a way of formally solving Hamilton's equations (3.190). Let us consider an observable f that is not explicitly dependent on time and suppose H is time independent. We wish to express $f(\xi(t))$ in terms of $f(\xi(0))$ (henceforth, for brevity we will write $f(t)$ for $f(\xi(t))$). Assuming that $f(\xi(t))$ admits a convergent Taylor expansion (i.e., that it is real analytic) at least up to time t, we may write

$$f(t) = f(0) + \frac{t}{1!}\dot{f}(0) + \frac{t^2}{2!}\ddot{f}(0) + \frac{t^3}{3!}\dddot{f}(0) + \cdots . \tag{3.195}$$

Now, by Hamilton's equations at $t = 0$, we have

$$\dot{f}(0) \;=\; \{f(0), H\}, \quad \ddot{f}(0) = \{\dot{f}(0), H\} = \{\{f(0), H\}, H\},$$

---

[108] A similar result holds in Riemannian geometry, where the commutator of Killing vector fields is again a Killing vector field. Killing vector fields are symmetries of a metric tensor.

$$\dddot{f}(0) = \{\ddot{f}(0), H\} = \{\{\{f(0), H\}, H\}, H\}, \quad \text{etc.} \tag{3.196}$$

Putting these in the Taylor series, we get an infinite series for $f(\xi(t))$:

$$f(t) = f(0) + t\{f(0), H\} + \frac{t^2}{2}\{\{f(0), H\}, H\} + \frac{t^3}{3!}\{\{\{f(0), H\}, H\}, H\} + \cdots . \tag{3.197}$$

Successive terms involve repeated (or iterated) PBs with the Hamiltonian. In favorable cases (such as the free particle, harmonic oscillator and some other integrable systems (see Sect. 11.7*)), the series can be summed to obtain an explicit solution of the equations of motion (see Prob. 3.62) or at least used to get solutions that are as accurate as one wishes. By truncating this series, one may also get an approximate solution to Hamilton's equations for relatively short times. However, the formula has its limitations. For a given Hamiltonian, there is no guarantee that the series converges. In other words, the solution $\xi^i(t)$ need not be real analytic in time. Even if the series converges, the radius of convergence may be too small for it to be useful for moderate or long times without resorting to analytic continuation. In fact, for a majority of Hamiltonian systems (such as the chaotic ones of Chap. 15), the series is generally divergent. Nevertheless, it can often be used to obtain approximate or asymptotic series solutions for short times. The formula is also of theoretical importance. It is a precursor to similar series solutions of the Heisenberg equations of motion (see Sect. 10.3* and Prob. B.52) in quantum mechanics in terms of iterated commutators. Such 'Lie series' are useful in many areas: classical and quantum optics, differential equations (Magnus series), Lie groups and algebras (Baker-Campbell-Hausdorff formula), etc. We will see similar infinite series solutions (that apply even when the analog of the Hamiltonian is explicitly time-dependent) via 'time-ordered' exponentials in Sect. 13.4.2*. □

3.27* Free particle trajectories as geodesics on configuration space

Newton's first law tells us that in an inertial frame, the trajectory of a free particle (i.e., subject to no forces) moving on a plane or in 3d space is a straight line, the shortest path between two points. Similarly, trajectories of a free particle moving on the surface of a sphere are great circles (see Prob. 3.17). More generally, for a system with n degrees of freedom, suppose the Lagrangian is quadratic in velocities:

$$L = (1/2)m_{ij}(q)\dot{q}^i\dot{q}^j \quad \text{where} \quad m_{ij} \text{ is a Riemannian metric on } \mathcal{Q}. \tag{3.198}$$

A Riemannian metric[109] is a real symmetric positive-definite[110] (and hence invertible) matrix field[111] on the configuration space $\mathcal{Q}$. We will call m_{ij} the mass or kinetic metric on $\mathcal{Q}$. The components m_{ij} could be constant, as in the case of a free particle in Cartesian coordinates, where $m_{ij} = m\delta_{ij}$ is proportional to the Kronecker symbol[112]. However, they need not be. For instance, for a free particle moving on a plane, the kinetic metric in polar coordinates has the components $m_{rr} = m$, $m_{\theta\theta} = mr^2$ and $m_{r\theta} = m_{\theta r} = 0$, which we deduce from the Lagrangian $L = \frac{1}{2}m(\dot{r}^2 + r^2\dot{\theta}^2)$. In general, the Lagrangian (3.198) describes a free particle moving on the (possibly curved) manifold $\mathcal{Q}$. On a curved manifold, geodesics play the role of straight lines: curves of shortest or extremal length (with respect to infinitesimal variations) between two points. We will show that Lagrange's equations (and therefore Hamilton's equations, see Prob. 3.33) following from (3.198) are equivalent to the geodesic equations (derived at the end of this section) with respect to the metric m_{ij} on $\mathcal{Q}$:

$$m_{ij}\,\ddot{q}^j(t) = -(1/2)\,(m_{ji,k} + m_{ki,j} - m_{jk,i})\,\dot{q}^j(t)\,\dot{q}^k(t) \quad \text{where} \quad m_{ij,k} = \partial_{q^k} m_{ij}. \tag{3.199}$$

Here, it is important to note that (up to a possible constant shift or constant rescaling) t is the arc length parameter[113] (3.205) along the geodesic. The geodesic equations are often written in terms of the Christoffel symbols ${\Gamma^l}_{ij}$:

$$\ddot{q}^l + \Gamma^l_{ij}\dot{q}^i\dot{q}^j = 0 \quad \text{where} \quad {\Gamma^l}_{ij} = (1/2)m^{lk}\left[m_{ki,j} + m_{kj,i} - m_{ij,k}\right] \tag{3.200}$$

and m^{ij} is the inverse of the metric, $m_{ij}m^{jk} = \delta_i^k$. The geodesic equations are a generalization of the zero force straight line conditions $\ddot{q}^i = 0$ in Cartesian coordinates, to which they reduce if m_{ij} are constant. However, even for a free particle moving in Euclidean space, m_{ij} need not be constant if we use curvilinear coordinates, as in the polar coordinate example above. Nevertheless, for the particle on the plane in polar coordinates, the geodesic equations reduce (see Prob. 3.63) to Lagrange's equations of motion $\ddot{r} = r\dot{\theta}^2$ and $d(mr^2\dot{\theta})/dt = 0$.

To relate the EOM to the geodesic equations, we begin with Lagrange's equations which are second order in time, just like (3.199):

---

[109] A Riemannian metric gives a way of assigning lengths to tangent vectors to $\mathcal{Q}$. For example, the length of a velocity vector $\dot{q}$ at a point q is $(m_{ij}(q)\dot{q}^i\dot{q}^j)^{1/2}$. By integrating the lengths of velocity vectors along a curve, one can define the length of the curve. If q has dimensions of length, then what we call the length of $\dot{q}$ has dimensions of speed × the square-root of mass. The latter factor can be removed by expressing m_{ij} in units of some mass.

[110] A symmetric matrix has real eigenvalues, it is positive-definite if its eigenvalues are strictly positive. Being a field, the matrix entries m_{ij} could depend on q. We do not allow them to depend on $\dot{q}$ as that would mean the Lagrangian is not quadratic in velocities and the geometric interpretation of this section would not be applicable.

[111] A matrix field is a smoothly varying matrix assigned to each point of $\mathcal{Q}$.

[112] $\delta_{ij} = 1$ if $i = j$ and vanishes otherwise.

[113] An affine transformation is a linear transformation plus a shift. Parameters t' that are related to arc length via $t' = at + b$ are said to be affine parameters. The geodesic equation takes the same form for any affine parameter. The geodesic equation would look more complicated if we used parametrizations that are not affine.

$$\frac{d}{dt}\frac{\partial L}{\partial \dot{q}^k} = \frac{\partial L}{\partial q^k} \quad \text{or} \quad \frac{d}{dt}\left(m_{kj}\dot{q}^j\right) = \frac{1}{2}m_{ij,k}\dot{q}^i\dot{q}^j \quad \text{which implies}$$

$$m_{kj,i}\dot{q}^i\dot{q}^j + m_{kj}\ddot{q}^j = \frac{1}{2}m_{ij,k}\dot{q}^i\dot{q}^j \quad \text{or} \quad m_{kj}\ddot{q}^j = \left[\frac{1}{2}m_{ij,k} - m_{kj,i}\right]\dot{q}^i\dot{q}^j. \qquad (3.201)$$

Contracting with the inverse metric m^{lk} we get

$$\ddot{q}^l = m^{lk}\left[(1/2)m_{ij,k} - m_{kj,i}\right]\dot{q}^i\dot{q}^j. \qquad (3.202)$$

To see the emergence of the Christoffel symbols Γ^l_{ij} (3.200) which are symmetric in the lower indices, we use the symmetry of $\dot{q}^i\dot{q}^j$ to observe that only the symmetric part of $m_{kj,i}$, i.e., $\frac{1}{2}(m_{kj,i} + m_{ki,j})$ can contribute when contracted with $\dot{q}^i\dot{q}^j$ (the antisymmetric part would give zero):

$$\ddot{q}^l = (1/2)m^{lk}\left[m_{ij,k} - m_{kj,i} - m_{ki,j}\right]\dot{q}^i\dot{q}^j. \qquad (3.203)$$

Thus, Lagrange's equations for (3.198) reduce to the geodesic equations (3.200). Thus, we have related two apparently disparate concepts: the EL equations of a Lagrangian quadratic in velocities (sans a potential) and the geodesic equations for the associated mass metric on configuration space! It remains to show that the geodesic equation (3.199) describes curves that extremize the length as defined by this metric.

Geodesic equation from extremizing length of curve. Geodesics generalize the concept of straight lines on the Euclidean plane and are governed by equations that generalize those for a straight line ($\ddot{x}^i = 0$). More precisely, a geodesic is a curve of extremal length joining two points on a Riemannian manifold M (see Appendix B for more on manifolds and tensors). Suppose x^i are coordinates on a patch where the metric tensor (positive-definite symmetric matrix depending on location) has components $m_{ij}(x)$. Let γ be a sufficiently smooth curve lying in this patch, given by $x^i(\tau)$ for some parameter $0 \leq \tau \leq 1$. Its length is defined as[114]

$$\ell(\gamma) = \int_0^1 \sqrt{m_{ij}\dot{x}^i\dot{x}^j}\, d\tau. \qquad (3.204)$$

The arc length $s(\tau)$ is defined as the length of the curve up to parameter value τ:

$$s(\tau) = \int_0^\tau \sqrt{m_{ij}\dot{x}^i\dot{x}^j}\, d\tau'. \qquad (3.205)$$

Evidently, $\ell(\gamma) = s(1)$. Since the parametrization that appears in the simplest form of the geodesic equation (3.200) is the arc length, we will change parametrizations from τ to s. This is facilitated by introducing a symbol for the speed

$$c(x(\tau), \dot{x}(\tau)) = \sqrt{m_{ij}\dot{x}^i\dot{x}^j}, \qquad (3.206)$$

---

[114] The length of the curve is independent of the choice of parametrization τ. An invertible reparametrization $\tau \to \sigma(\tau)$ (with $\sigma'(\tau) > 0$) does not alter the form of the integrand: $\sqrt{m_{ij}\dot{x}^i(\tau)\dot{x}^j(\tau)}\, d\tau = \sqrt{m_{ij}\dot{x}^i(\sigma)\dot{x}^j(\sigma)}\, d\sigma$ since the Jacobian factor $d\sigma/d\tau$ cancels out.

which loosely plays the role of a Lagrangian in the length functional (3.204). By the fundamental theorem of calculus,

$$\frac{ds}{d\tau} = c \quad \text{or} \quad \frac{d}{d\tau} = c\frac{d}{ds}. \tag{3.207}$$

Now, the Euler-Lagrange condition (3.21) for $\ell(\gamma)$ to be stationary to first order in variations $x \to x + \delta x$ holding the endpoints at $\tau = 0, 1$ fixed is

$$\frac{d}{d\tau}\frac{\partial c}{\partial \dot{x}^k} = \frac{\partial c}{\partial x^k}. \tag{3.208}$$

The RHS is

$$\frac{\partial c}{\partial x^k} = \frac{1}{2c} m_{ij,k}\dot{x}^i\dot{x}^j = \frac{c}{2} m_{ij,k}\frac{dx^i}{ds}\frac{dx^j}{ds}. \tag{3.209}$$

Similarly,

$$\frac{\partial c}{\partial \dot{x}^k} = \frac{1}{c} m_{kj}\dot{x}^j = m_{kj}\frac{dx^j}{ds}. \tag{3.210}$$

So the LHS of (3.208) is[115]

$$\frac{d}{d\tau}\frac{\partial c}{\partial \dot{x}^k} = c\frac{d}{ds}\left(m_{kj}\frac{dx^j}{ds}\right) = c\left[m_{kj,i}\frac{dx^i}{ds}\frac{dx^j}{ds} + m_{kj}\frac{d^2x^j}{ds^2}\right]. \tag{3.211}$$

Equating the two, we get the condition for $\ell(\gamma)$ to be extremal:

$$m_{kj}\frac{d^2x^j}{ds^2} = \frac{1}{2}\left(m_{ij,k} - 2m_{kj,i}\right)\frac{dx^i}{ds}\frac{dx^j}{ds}. \tag{3.212}$$

Symmetrizing the second term on the right under $i \leftrightarrow j$ and contracting with the inverse metric, we get the geodesic equation (3.200) in terms of the Christoffel symbols and arc length parametrization:

$$\ddot{x}^l + \Gamma^l_{ij}\dot{x}^i\dot{x}^j = 0 \quad \text{where} \quad \Gamma^l_{ij} = (1/2)m^{lk}\left[m_{ki,j} + m_{kj,i} - m_{ij,k}\right]. \tag{3.213}$$

We notice that the Christoffel symbols vanish if the metric components are constant. In particular, in Cartesian coordinates on Euclidean space (where $m_{ij} = \delta_{ij}$), the geodesic equation reduces to that for a straight line: $\ddot{x}^l = 0$.

$*$ **Geodesic equation in terms of covariant derivative.** It is possible to rewrite the geodesic equation in a nice way if we introduce the so-called covariant derivative. The covariant derivative $\boldsymbol{\nabla}_u v$ of a vector v along the vector u is a generalization of the directional derivative in vector calculus. In addition to the partial derivative, it includes a ‘correction’ term involving the Christoffel symbols (3.200):

$$(\boldsymbol{\nabla}_u v)^i = u^j \boldsymbol{\nabla}_j v^i = u^j \partial_j v^i + u^j \Gamma^i_{jk} v^k. \tag{3.214}$$

---

[115] Notice that if we did not use arc length parametrization (or one that is affinely related to it), the resulting formulae would be more complicated. In fact, if we try to work with τ instead of s, to calculate the τ derivative of the ‘momentum’ conjugate to $\dot{x}^k$ in (3.210), we would need to calculate $\frac{d(1/c)}{d\tau}$. This would produce additional terms in the condition for ℓ to be extremal. Thus, the geodesic equation takes the simple form (3.200) only for affine parameters.

We will show in Appendix B.11* that this correction term ensures that $\boldsymbol{\nabla}_u v$ behaves like a vector field just as v itself does. By contrast, $u^j \partial_j v^i$ does not. Now taking $u = v = \dot{x}$ and using the chain rule $\frac{d}{ds} = \frac{dx^j}{ds}\frac{\partial}{\partial x^j} = \dot{x}^j \frac{\partial}{\partial x^j}$ we get

$$(\boldsymbol{\nabla}_{\dot{x}} \dot{x})^i = \dot{x}^j \partial_j \dot{x}^i + \dot{x}^j \Gamma^i_{jk} \dot{x}^k. \tag{3.215}$$

Thus, the geodesic equation is simply the statement that $\boldsymbol{\nabla}_{\dot{x}} \dot{x} = 0$, where dots denote derivatives with respect to s. This means the covariant derivative of the tangent vector along the tangent to a geodesic is zero. We say that the tangent vector to a geodesic is covariantly constant along the geodesic. Thus, a geodesic may also be viewed as a curve parametrized by arc length that 'parallel transports' its own tangent vector. □

3.28* Euler-Maupertuis principle and the Jacobi-Maupertuis metric

Remarkably, the correspondence of Sect. 3.27* between trajectories and geodesics on configuration space continues to hold even in the presence of conservative forces derived from a potential V. This follows from the Euler-Maupertuis (1744) principle and a subsequent reformulation due to Jacobi. To set the stage, recall that in optics, Fermat's principle [15] states that light rays extremize the optical path length[116]. The Euler-Maupertuis (EM) variational principle [2, 81, 83] is a mechanical counterpart of Fermat's principle. It states that the energy-E configuration orbits from q_1 to q_2 are curves that extremize[117] the EM action $\mathscr{S} = \int_{q_1}^{q_2} p_i dq^i$ encountered in Sect. 1.4*. The momenta p_i conjugate to q^i are to be determined from the constancy of energy. Notably, the principle does not directly involve the parametrization of orbits by Newtonian time. In what follows, we first sketch how the EM principle is related to Hamilton's principle of extremal action (Sect. 3.5) and then connect it to geodesics.

Let us assume that the system in question has a Lagrangian that is not explicitly dependent on time and therefore admits a conserved Hamiltonian $H(q,p)$. We have seen that Hamilton's equations follow from extremizing the action (3.107):

$$S = \int_{q_1}^{q_2} p_j \, dq^j - \int_{t_1}^{t_2} H \, dt' \tag{3.216}$$

while holding the initial and final configurations fixed at times which we will denote t_1 and $t_2 = t$. Now, let us restrict to variations of the path that conserve energy, so that $H = E$ is a constant and we may write

$$S = \mathscr{S} - E(t - t_1) \quad \text{where} \quad \mathscr{S} = \int_{q_1}^{q_2} p_j \, dq^j \tag{3.217}$$

---

[116] The optical path length of a curve $\boldsymbol{r}(s)$ in a medium of variable refractive index $n(\boldsymbol{r})$ (ratio of speed of light c in vacuum to speed of light $c(\boldsymbol{r})$ in the medium) is $\int n(\boldsymbol{r}(s)) \, ds$ where s is the arc length parameter along the path. The optical path length is $c\times$ the time $\int ds/c(\boldsymbol{r}(s))$ taken to traverse the path. In Fermat's original formulation, light rays minimized this time. If ν is the frequency (which remains constant even as the refractive index varies), then the optical path length is proportional to the geometric length of the path $[\int ds/\lambda(\boldsymbol{r}(s))]$ in units of the local wavelength $\lambda(\boldsymbol{r}) = c/n(\boldsymbol{r})\nu$.

[117] Contrast this with Hamilton's principle of extremal action of Sect. 3.5 where the initial and final times, rather than the energy, are held fixed.

is the EM action that appears in the Euler-Maupertuis principle. Thus, along trajectories of energy E, the variation of S holding q_1, q_2 and t_1 fixed is

$$\delta S = \delta \mathscr{S} - E\delta t = 0. \tag{3.218}$$

On the other hand, from (3.102), the variation of S (holding t_1, q_1 and q_2 fixed) is also given by $\delta S = -H\delta t$, which reduces to $\delta S = -E\delta t$ if $H = E$. Equating these, we find that the EM action $\mathscr{S}$ has an extremum along any trajectory of energy E that goes from q_1 at t_1 to q_2 at any time t. Since the time elapsed $t - t_1$ is not fixed, the Euler-Maupertuis principle determines the shape of the trajectory from q_1 to q_2 without regard to its parametrization by Newtonian time. We will now make this more concrete by specializing to a convenient class of Lagrangians and interpreting the extrema of $\mathscr{S}$ geometrically in terms of geodesics. This will also allow us to explain how Newtonian time is related to the affine parameter along geodesics.

Remark. It is important to bear in mind that Hamilton's principle of extremal action and the Euler-Maupertuis principle are both valid variational formulations of classical dynamics. While the time elapsed is fixed in the former, the energy of the orbit is fixed in the latter. While the energy of the trajectory has to be separately calculated in the former, the same applies to the time elapsed in the latter. In a sense, energy and time elapsed are conjugate variables, they cannot both be fixed independently. ☐

To relate the Euler-Maupertuis principle to geodesics on configuration space, we consider a Lagrangian quadratic in velocities (as in Sect. 3.27*) with a potential V:

$$L = (1/2)m_{ij}(q)\dot{q}^i\dot{q}^j - V(q) \quad \text{where } \; m_{ij} \; \text{ is a Riemannian metric on } \mathcal{Q}. \tag{3.219}$$

Recall that a Riemannian metric is a nondegenerate positive-definite symmetric matrix that could vary with location. For any given constant parameter E (which we will soon interpret as energy $\frac{1}{2}m_{ij}\dot{q}^i\dot{q}^j + V$), we restrict attention to the submanifold of the configuration space $\mathcal{Q}_E$ where $V(q) \leq E$ (once we interpret E as energy, this may be interpreted as the classically allowed portion or so-called Hill region of the configuration space). On $\mathcal{Q}_E$, we define the Jacobi-Maupertuis (JM) metric[118]

$$g^E_{ij} = (E - V(q))m_{ij} \quad \text{corresponding to the line element} \quad ds^2_{\scriptscriptstyle E} = g^E_{ij}dq^i dq^j. \tag{3.220}$$

This metric (parametrically dependent on the constant E) is a rescaled version of the mass or kinetic metric and is said to be conformally related to it via the nonnegative conformal factor $T \equiv E - V \geq 0$. Conformally related metrics give generally different notions of distance, but assign the same opening angle[119] to a pair of tangent vectors at a point. Of course, while m_{ij} is a single metric on $\mathcal{Q}$, g^E_{ij} is a family of metrics parametrized by E, one on each Hill region $\mathcal{Q}_E \subset \mathcal{Q}$.

---

[118] The formula for the inverse JM metric $g^{ij} = m^{ij}/(E - V)$ may also be read off from the time-independent Hamilton-Jacobi (HJ) equation $(m^{ij}/2(E - V))\ \partial_i W \partial_j W = 1$ by analogy with the rescaled kinetic metric $m^{ij}/2E$ appearing in the free particle HJ equation $(m^{ij}/2E)\partial_i W \partial_j W = 1$ (see Sect. 12.3 and p.74 of [106]).

[119] The angle between a pair of tangent vectors u, v is $\arccos[(u,v)/\sqrt{(u,u)(v,v)}]$ where the inner product $(u,v) = g_{ij}u^i v^j$.

Now, the remarkable fact is that trajectories of energy E (up to a reparametrization of time) and geodesics of the JM metric[120] g^E_{ij} coincide[121]. Precisely, Lagrange's equations following from (3.219),

$$m_{ki}\ddot{q}^i(t) + \frac{1}{2}\left(m_{ik,j} + m_{jk,i} - m_{ij,k}\right)\dot{q}^i(t)\,\dot{q}^j(t) = -\partial_k V \tag{3.221}$$

may be regarded as reparametrized geodesic equations for the JM metric. This would be a generalization of our results in Sect. 3.27* where we did not allow for a potential.

To establish this connection, we note from Sect. 3.27* that geodesics of the JM metric are extrema of the length functional $\ell = \int ds_{E}$. On the other hand, by the Euler-Maupertuis principle, trajectories are extrema of $\int p\,dq$ holding energy fixed. Thus, we now aim to relate the integral of the JM line element ds_{E} to the Euler-Maupertuis action. From (3.220), notice that

$$ds_{E} = \sqrt{(E-V)m_{ij}dq^i dq^j} = \sqrt{T}\sqrt{m_{ij}dq^i dq^j} \quad \text{where} \quad T = \frac{1}{2}m_{ij}\dot{q}^i\dot{q}^j. \tag{3.222}$$

Thus, the length of a curve γ becomes

$$\begin{aligned}\ell(\gamma) = \int ds_{E} &= \int \frac{ds_{E}}{dt}\,dt = \int \sqrt{T}\sqrt{m_{ij}\dot{q}^i\dot{q}^j}\,dt = \sqrt{2}\int T dt \\ &= \sqrt{2}\int \frac{1}{2}p_i\dot{q}^i dt = \frac{1}{\sqrt{2}}\int p dq = \frac{\mathscr{S}}{\sqrt{2}},\end{aligned} \tag{3.223}$$

where we used the formula for the conjugate momentum $p_i = m_{ij}\dot{q}^j$ following from (3.219). This means the length of a curve with respect to the JM metric on $\mathcal{Q}_E$ is $(1/\sqrt{2})$ times the Euler-Maupertuis action of that curve. It follows that the two functionals have the same extrema. The extrema of $\int ds_{E}$ are the geodesics of the JM metric, while by the Euler-Maupertuis principle, the extrema of $\int p\,dq$ are curves whose shapes coincide with trajectories of energy E. Thus, the curves followed by Newtonian trajectories are geodesics of the JM metric! This geometric formulation can be exploited: ideas from Riemannian geometry such as geodesic deviation and curvature (see Appendix B.12*) may be used to examine the stability of trajectories.

Remark on reparametrization of time: Newtonian time t along trajectories is generally (i.e., for nonzero V) not the same as the arc length s (or other affine parameter) along geodesics. Rather, the geodesic equations for the JM metric

$$\ddot{q}^l(s) = -\frac{1}{2}g^{lk}\left(g_{ki,j} + g_{kj,i} - g_{ij,k}\right)\dot{q}^i(s)\dot{q}^j(s) \tag{3.224}$$

reduce to (3.221) under the reparametrization

$$\frac{d}{ds} = \frac{1}{\sigma}\frac{d}{dt} \quad \text{where} \quad \sigma = \frac{(E-V)}{\sqrt{T}}. \tag{3.225}$$

---

[120] See [72] for an application of the JM metric in the study of the three-body problem.

[121] Once this is established, we may interpret the parameter E in the JM metric as energy.

This may be checked explicitly, as we invite the reader to do in Prob. 3.64. It is to be expected, as we have shown that ℓ and $\mathscr{S}$ have the same extrema. Here, $\mathcal{T} = \frac{1}{2} g_{ij} \dot{q}^i \dot{q}^j$ (with dots denoting s derivatives) is the conserved 'kinetic energy' along geodesics and $\mathcal{T} = 1/2$ for arc-length parametrization[122]. To obtain σ, suppose $y^i(t)$ is a trajectory and $q^i(s)$ the corresponding geodesic. Then at a point $q^i(s) = y^i(t)$, the velocities are related by $\sigma \dot{q}^i(s) = \dot{y}^i(t)$ leading to

$$\mathcal{T} = \frac{1}{2} g_{ij} \dot{q}^i \dot{q}^j = \frac{E-V}{2} m_{ij} \dot{q}^i \dot{q}^j = \frac{E-V}{2\sigma^2} m_{ij} \dot{y}^i \dot{y}^j = \left(\frac{E-V}{\sigma}\right)^2 . \quad (3.226)$$

3.29 Problems

1. **Events and simultaneity.** (a) Suppose events A and B occur at the same location $\boldsymbol{r}_0$ but at distinct times $t_A < t_B$, as observed in an inertial frame K. Do they occur at the same location in all other inertial frames? (b) Suppose events A and B occur simultaneously a distance d apart as observed in an inertial frame K. Do A and B occur simultaneously a distance d apart in all other inertial frames of reference?
2. Consider an idealized straight rigid wire of zero thickness and fixed length ℓ (essentially a line segment) that is free to move in a room. How many degrees of freedom does this system possess? Explain by enumerating the **degrees of freedom**.
3. **Practice with polar coordinates.** Consider a particle moving on the x-y plane ($z = 0$) in a central potential $V(r)$. The Lagrangian is $L = \frac{1}{2} m(\dot{x}^2 + \dot{y}^2) - V(r)$. Define plane polar coordinates for the particle's location via $x = r\cos\phi, y = r\sin\phi$. Abbreviate $\sin\phi = s, \cos\phi = c$. Recall that the unit vector in the radial direction is $\hat{r} = c\hat{x} + s\hat{y}$ and that linear momentum is $\boldsymbol{p} = m\dot{x}\hat{x} + m\dot{y}\hat{y}$. The Euler-Lagrange equations in polar coordinates were found (in Sect. 3.8) to be $m\ddot{r} = mr\dot{\phi}^2 - V'(r)$ and $mr\ddot{\phi} = -2m\dot{r}\dot{\phi}$.

   a. Show that $\dot{r} = c\dot{x} + s\dot{y}$.
   b. Show that $\dot{\phi} = (1/r^2)\,(x\dot{y} - y\dot{x})$.
   c. Show that the momentum $p_r = m\dot{r}$ conjugate to r is just the radial component of linear momentum $\boldsymbol{p} \cdot \hat{r}$.
   d. Show that the momentum $p_\phi = mr^2\dot{\phi}$ conjugate to ϕ is the z-component of $\boldsymbol{L} = \boldsymbol{r} \times \boldsymbol{p}$. Proceed by explicitly calculating the cross product.
   e. Draw the unit vector in the direction of increasing ϕ, called $\hat{\phi}$, in a diagram. Using an appropriate triangle, express $\hat{\phi}$ as a linear combination of $\hat{x}$ and $\hat{y}$. Choose $0 < \phi < \pi/2$. Check that $\hat{r} \cdot \hat{\phi} = 0$.
   f. Suppose we define the angular velocity as $\boldsymbol{\omega} = \dot{\phi}\hat{z}$. Show that the RHS of the Euler-Lagrange equation $mr\ddot{\phi} = -2m\dot{r}\dot{\phi}$ is the $\hat{\phi}$ component of $-2\boldsymbol{\omega} \times \boldsymbol{p}$.

---

[122] Arc length parametrization of a curve is the one for which the speed along the curve is unity. So it is also called unit speed parametrization. For such a parametrization, the length of the velocity vector must be one: $(g_{ij}\dot{q}^i\dot{q}^j)^{1/2} = 1$. If $s_1 \leq s \leq s_2$ is the arc length parameter for a curve $q(s)$, then the length of the curve $\int (g_{ij}\dot{q}^i\dot{q}^j)^{1/2} ds$ is simply $s_2 - s_1$.

g. $\hat{x}, \hat{y}$ are constant unit vectors, in the sense that they point in the same direction everywhere on configuration space and also at every point along a trajectory: $\frac{d\hat{x}}{dt} = \frac{d\hat{y}}{dt} = 0$. But $\hat{r}, \hat{\phi}$ change direction from place to place. Show that

$$\frac{d\hat{\phi}}{dt} = -\dot{\phi}\hat{r} \quad \text{and} \quad \frac{d\hat{r}}{dt} = \dot{\phi}\hat{\phi}. \tag{3.227}$$

4. **Acceleration without a force.** A particle is not subject to any force but observer A finds that it executes accelerated motion with respect to A's frame of reference. On the basis of Newton's 1^{st} law, explain whether A's frame is inertial or not.
5. **Force without acceleration.** Suppose a particle is known to be subject to a net force but an observer finds that it does not move. (a) Based on Newton's 1^{st} law, what can be deduced about whether the observer's frame is inertial or noninertial? (b) What can be said using Newton's 2^{nd} law?
6. Suppose **Newton's second law** for a particle moving along a line had a 3^{rd} derivative term: $m\ddot{x} + \nu\dddot{x} = f$, for some constant $\nu \neq 0$, where f is the force. Deduce that Newton's first law could in general be violated.
7. Suppose $\boldsymbol{r}_1(t)$ and $\boldsymbol{r}_2(t)$ are solutions of Newton's equation for a force field $\boldsymbol{f}$. Argue that generally, the **superposition** $\boldsymbol{r} = \boldsymbol{r}_1 + \boldsymbol{r}_2$ does not satisfy $m\ddot{\boldsymbol{r}} = \boldsymbol{f}(\boldsymbol{r})$.
8. **Conservation of momentum.** Consider a system of two point particles A and B of masses m_a and m_b. A exerts a force $\boldsymbol{F}_b$ on B and B exerts a force $\boldsymbol{F}_a$ on A. Write Newton's 2^{nd} law equations of motion for this system in an inertial frame where the position vectors of the particles are $\boldsymbol{r}_a$ and $\boldsymbol{r}_b$. Use Newton's laws to show that the total momentum of the system is independent of time.
9. **Work done by a force.** Suppose a particle is subject to a force $\boldsymbol{F} = \boldsymbol{v} \times \boldsymbol{h}$ where $\boldsymbol{v}$ is its velocity and $\boldsymbol{h}$ some vector. What is the work done by $\boldsymbol{F}$ in displacing the particle infinitesimally? Find physical examples of such forces.
10. Consider an **elastic collision** of 2 particles of masses m_1 and m_2 in one dimension with incoming velocities v_1 and v_2 in the lab frame. Using conservation laws, obtain formulae (3.17) for the final velocity v_2'. Show that the formula for v_1' is obtained by $1 \leftrightarrow 2$ exchange. Suppose the particles had equal and opposite velocities as $t \to -\infty$, then assuming nontrivial scattering, show that the heavier particle comes to rest after the collision if it is thrice as massive as the lighter one. What is the velocity of the lighter particle as $t \to \infty$?
11. **Nonuniqueness of Lagrangian.** Consider a particle whose dynamics is specified by the Lagrangian $L(q, \dot{q}) = \frac{1}{2}m\dot{q}^2 + b(q)\dot{q}$ where $b(q)$ is some differentiable function of the real coordinate q. (a) Find the momentum conjugate to q and the equation of motion. What sort of motion does the Lagrangian describe? Find all trajectories. (b) Explain the role played by the $b(q)\dot{q}$ term in extremizing the action $S = \int_{t_1}^{t_2} L\, dt$ among paths with fixed end points $q(t_{1,2}) = q_{1,2}$.
12. Consider the Lagrangian $L(q, \dot{q}) = \frac{1}{2}\, \mu(q)\, \dot{q}^2$, where $\mu(q) > 0$ is a differentiable function, a sort of **position-dependent mass**.

a. Find Lagrange's equation of motion. It is a somewhat complicated looking nonlinear ODE. We seek a change of *dependent* variable to simplify it.
b. Find a change of variable from $q(t) \to x(q(t))$ that makes the Lagrangian that of a free particle of mass m and coordinate x.
c. Apply the above-discovered change of variable to the equation of motion for q to reduce it to the equation of motion of a free particle.

13. **No trajectory joining given states.** Show through an example [involving a free particle] that if both q and $p = m\dot{q}$ at initial and final times are specified, there may be no trajectory joining these states.
14. Consider **planar motion** of a particle governed by $S = \int_{t_1}^{t_2} \sqrt{\dot{x}^2 + \dot{y}^2}\, dt$. (a) Give a geometric interpretation of the action S. (b) Identify any cyclic coordinates. (c) Write down the Euler-Lagrange equations for S to be extremal with respect to small variations in the path $(x(t), y(t))$ holding the endpoints fixed at $x(t_j) = x_j, y(t_j) = y_j$ for $j = 1, 2$. Express them as a pair of ODEs (no need to expand out derivatives of quotients). (d) Interpret the EOM. Hint: They state that some geometric quantity is conserved, what quantity? (e) Find the conjugate momenta p_x, p_y. (f) Try to solve for the velocities (or their squares) in terms of momenta. Is there a unique solution, no solution or several solutions? Indicate why based on convexity/concavity properties of $L = \sqrt{\dot{x}^2 + \dot{y}^2}$.
15. **Lagrangian involving 2^{nd} derivatives.** Suppose the Lagrangian for a system with configuration space $\mathcal{Q} = \mathbb{R}$ is $L = L(q, \dot{q}, \ddot{q})$. Consider the action S for paths $q(t)$ with $t_1 \le t \le t_2$ between points q_1 and q_2 on $\mathcal{Q}$. We ask that S be extremal with respect to infinitesimal variations of path holding the initial and final positions and velocities fixed. (a) Find the EL equation for the stationarity of S. (b) Taking $L = \frac{1}{2}m\dot{q}^2 - V(q) + \frac{1}{2}\alpha\ddot{q}^2$ find the EL equation and mention its order.
16. **Multiple trajectories between configurations.** Give an example from the Kepler problem to illustrate the fact that there may be more than one trajectory joining given initial and final locations at specified times. Illustrate with a figure showing $\boldsymbol{r}(t_i), \boldsymbol{r}(t_f)$ and more than one trajectory connecting them. Try to come up with more examples to show that the extremum of action need not be unique.
17. Suppose a **particle of mass** m **moves on a sphere** of radius a and its Lagrangian is given by $L = \boldsymbol{L}^2/2ma^2$ where $\boldsymbol{L}^2$ is the square of its angular momentum. (a) Express L as a function of spherical polar angles and velocities and show that the conjugate momenta are $p_\theta = ma^2\dot{\theta}$ and $p_\phi = ma^2 \sin^2\theta\, \dot{\phi}$. (b) Express the Hamiltonian in terms of spherical polar angles and momenta. (c) Find any cyclic coordinates and derive Lagrange's and Hamilton's equations. (d) What curves do you expect the trajectories to define? (e) Show that $\frac{1}{2}\dot{\theta}^2 + \frac{1}{2}\omega^2 \operatorname{cosec}^2\theta$ is conserved, where $\omega = p_\phi/ma^2$. Use this to integrate the equations. Hint: See Prob. 2.3.
18. Consider a free particle of mass m moving in 3d. Express the Cartesian components of **angular momentum** in terms of the momenta conjugate to spherical polar coordinates. Use Prob. 2.5 to show that

$$L_z \quad = \quad p_\phi, \quad L_x = -\sin\phi\, p_\theta - \cot\theta \cos\phi\, p_\phi \quad \text{and}$$

$$L_y = \cos\phi\, p_\theta - \cot\theta \sin\phi\, p_\phi. \tag{3.228}$$

19. **Brachistochrone problem**[123]**.** This problem played a key role in the early development of variational calculus. Consider a point particle of mass m sliding down a frictionless wire (curve) in a vertical plane subject to Earth's vertically downward gravitational acceleration g. The x axis is chosen horizontal and rightwards and the y axis vertically *downwards*. The particle starts *from rest* at point A: $(x, y) = (0, 0)$ (see Fig. 3.14). The potential energy is defined to vanish when $y = 0$. The wire ends at a fixed point B below (starting from rest, the particle cannot climb higher than its initial height, so $y \geq 0$) and to the right of A. We wish to find the shape $y(x)$ of the wire which minimizes the time taken to reach B: (x_f, y_f).

    a. Draw a diagram of this situation indicating the axes and the points mentioned and a proposed curve of shortest time (we will see that it is not a straight line).
    b. What is the numerical value of the conserved energy of the particle?
    c. Show that the time taken to go from A to B along a curve $y(x)$ is

    $$T_{\text{AB}} = \int_0^{x_f} \sqrt{(1 + y'(x)^2)/(2gy)}\, dx. \tag{3.229}$$

    d. Define the 'Lagrange' function $L(y, y') = \sqrt{(1 + y'(x)^2)/(2gy)}$ and obtain the Euler-Lagrange equation for extremization of T_{AB}. Show that you get

    $$2yy'' + y'^2 + 1 = 0. \tag{3.230}$$

    e. We will treat this as a sort of Newton equation and try to integrate it to find $y(x)$. Find an integrating factor (like for Newton's equation) and integrate this equation once. Show that you get (here R is a constant length of integration)

    $$y(1 + y'^2) = 2R. \tag{3.231}$$

    f. Reduce this 1st order ODE to quadrature and integrate it using the trigonometric substitution $y = 2R \sin^2\theta$ from $(x, y) = (0, 0)$ to (x, y). Show that you get

    $$x/2R = \arcsin\sqrt{y/2R} - \sqrt{(y/2R)\,(1 - y/2R)}. \tag{3.232}$$

    g. Show that the equation for the curve of shortest time is not a straight line, but in parametric form is the equation for a cycloid

    $$x = R(\phi - \sin\phi) \quad \text{and} \quad y = R(1 - \cos\phi). \tag{3.233}$$

    How is ϕ related to the variable θ introduced above? Plot the cycloid on a graph, showing R, bearing in mind that y increases downwards. The values of ϕ and θ corresponding to (x_f, y_f) will be denoted ϕ_f and θ_f.

---

[123] *Brachistochrone* means 'shortest time' in Greek. The problem was posed by Johann Bernoulli in 1696 and solved by him as well as Jakob Bernoulli, l'Hôpital, Newton, Leibniz and Tschirnhaus. Johann used Fermat's principle (see [15] and Footnote 116) via a clever analogy with light passing through a medium whose refractive index decreases with depth. His elder brother Jakob used a method we now associate with the calculus of variations.

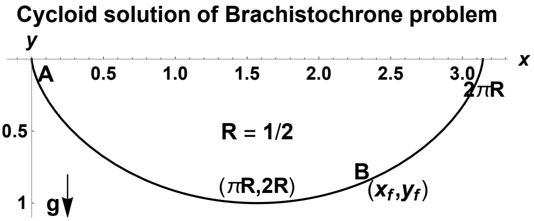

Figure 3.14: Cycloid-shaped wire for $R = 1/2$, giving the curve of shortest time for a particle to slide frictionlessly from rest at A to B under the influence of a constant acceleration due to gravity. $\phi = \pi$ at the bottom of the cycloid while it is $0, 2\pi$ at the top.

h. Show that a cycloid is the locus of a point on the rim of a circular hoop of radius R that rolls on a horizontal straight line.

i. What are the coordinates of the bottom of the cycloid, and what is the time taken to go from $(0, 0)$ to the bottom of the cycloid?

j. Show that the minimal time T_{AB}^{cyc} may be expressed as,

$$T_{AB}^{\text{cyc}} = \sqrt{4R/g}\,\arcsin\sqrt{y_f/2R} = \sqrt{R/g}\;\phi_f. \tag{3.234}$$

k. (a) Give an implicit formula relating R to x_f and y_f. (b) For small ϕ_f (or small x_f/y_f), obtain the following explicit formulae for ϕ_f and R:

$$\phi_f \approx 3x_f/y_f \quad \text{and} \quad 2R \approx y_f\,\mathrm{cosec}^2(3x_f/2y_f) \approx 4y_f^3/9x_f^2. \tag{3.235}$$

l. Given A $(0, 0)$ and B (x_f, y_f), show that if $x_f/y_f > \pi/2$ then the bottom of the cycloid lies to the left of B. In other words, if $x_f/y_f < \pi/2$, the particle does not have to travel upwards in its journey.

m. Suppose the wire is a straight line from A to B and the particle stars from rest and slides frictionlessly from A to B under the influence of a constant downward acceleration due to gravity. Show that the time taken to reach B is

$$T_{AB}^{\text{st-line}} = \sqrt{2(x_f^2 + y_f^2)/gy_f} = \sqrt{2y_f\sec^2\psi_f/g} \quad \text{where} \quad \tan\psi_f = x_f/y_f. \tag{3.236}$$

n. Compare the time taken to go from A to B along a straight wire to that taken to go along the cycloid. Give some physical intuition as to why the particle may need to go upwards in some portion of the path to reach B in the shortest possible time. Write a program to numerically compute the fractional difference $(T_{AB}^{\text{st-line}} - T_{AB}^{\text{cyc}})/T_{AB}^{\text{cyc}}$ for a convenient array of values of (x_f, y_f). Validate the program by considering small ϕ_f where one can find $R(x_f, y_f)$ more explicitly. Where does the straight line provide a good/bad approximation to the cycloid in so far as minimizing the time is concerned? Show analytically that the fractional time difference depends on x_f and y_f only through the ratio x_f/y_f. Verify that the numerical results obey this condition.

o. How does the speed of the particle vary with height y? Draw an analogy with the passage of light through a stratified medium of variable refractive index to argue that the brachistochrone curve must be convex from below.

20. **Lagrangian cubic in velocities.** Consider the Lagrangian $L = T - V$ for a system with 1 real degree of freedom q. Suppose $T = \frac{1}{2}m\dot{q}^2 + \frac{1}{3}g\dot{q}^3$ and $V(q)$ is some smooth nonconstant potential function and m, g are nonzero real constants. (a) Find the momentum p conjugate to q. (b) Find the EL EOM as a 2^{nd} order ODE. (c) Express the Hamiltonian as a function of q and $\dot{q}$ and comment on whether it is equal to $J = T + V$. (d) Use the EL equation to check whether H and $J = T + V$ are conserved. (e) Briefly comment on what you may infer from this example.

21. **Nature of extremum of action.** Consider a particle of mass m in the potential $V(x) = \frac{1}{2}m\omega^2 x^2$. Suppose $x(t)$ is a trajectory between $x(t_i) = x_i$ and $x(t_f) = x_f$ and let $x(t) + \delta x(t)$ be a neighboring path with $\delta x(t_i) = \delta x(t_f) = 0$.

    a. Write the action of the path $x + \delta x$ for small δx as a quadratic Taylor polynomial in δx. Show that you get the following expression. What is S_1?

    $$\begin{aligned} S[x+\delta x] \quad &\approx \quad S_0 + S_1 + S_2 = S[x] - \int_{t_i}^{t_f} (m\ddot{x} + m\omega^2 x)\, \delta x \, dt \\ &+ \int_{t_i}^{t_f} \left[\frac{1}{2}m(\delta\dot{x})^2 - \frac{1}{2}m\omega^2(\delta x)^2 \right] dt. \end{aligned} \tag{3.237}$$

    b. For what κ is $x(t) + \delta x(t)$ a legitimate neighboring path for the variation $\delta x(t) = \epsilon \, \sin \kappa(t - t_i)$?
    c. Evaluate $S_2[\delta x]$ for all the allowed values of κ.
    d. Take $\Delta t = t_f - t_i = 10\text{s}$ and $\omega = 1$ Hz. Find a path that can be made arbitrarily close to the trajectory $x(t)$, whose action is *less* than that of $x(t)$. [Ignore corrections to the quadratic Taylor approximation here and below.]
    e. Take $\Delta t = t_f - t_i = 10\text{s}$ and $\omega = 1$ Hz. Find a path that can be made arbitrarily close to the trajectory $x(t)$, whose action is *more* than that of $x(t)$.
    f. What sort of an extremum of action is the classical trajectory?

22. Suppose m_{ij} is an $n \times n$ real matrix (or rank 2 tensor). (a) Find **symmetric and antisymmetric matrices** $s_{ij} = s_{ji}$ and $a_{ij} = -a_{ji}$ such that $m_{ij} = s_{ij} + a_{ij}$. (b) Suppose $t^{ij} = t^{ji}$ is a symmetric tensor. Show that its contraction with any antisymmetric tensor vanishes: $a_{ij}t^{ij} = 0$.

23. Show that an infinitesimal change $q \to q + \tilde{\delta} q$ that is a **symmetry of the Lagrangian** L (leaves it unchanged to linear order in infinitesimals), is automatically a symmetry of the equations of motion (to linear order in infinitesimals) and so takes solutions to solutions. Rather than performing a detailed calculation, try to explain via careful reasoning and a diagram. Hints: Consider the action of a path from $q_1 = q(t_1)$ to $q_2 = q(t_2)$. Under what circumstances is the path a trajectory? Explain in words and draw a picture. Then consider the effect of the symmetry transformation $\tilde{\delta} q$ on the original path. You must distinguish between the variations of a path δq that are considered in deriving the EOM and the transformation $q \to q + \tilde{\delta} q$ that is a symmetry of L. In what respects are they different?

24. Suppose R is a 3×3 **orthogonal matrix** $R^t R = I$. (a) Show that $\det R = \pm 1$. (b) Show that the columns of R are three orthonormal vectors. (c) Suppose $x' =$

$-x, y' = y, z' = z$ is a linear transformation of 3d Euclidean space. Express the transformation via a 3×3 orthogonal matrix R and show that it has determinant -1. Interpret it as a reflection in an appropriate plane. (d) Suppose $\hat{x}, \hat{y}, \hat{z}$ is the usual right-handed orthonormal frame ($\hat{x} \times \hat{y} = \hat{z}$). Show that the transformed frame $\hat{x}', \hat{y}', \hat{z}'$ is left-handed, so that the reflection is orientation-reversing.

25. Consider the **Sun-Earth system** treated as a pair of point particles with masses m_s, m_e moving in 3d with position vectors $\boldsymbol{r}_s = (x_s, y_s, z_s), \boldsymbol{r}_e = (x_e, y_e, z_e)$ relative to some fixed origin in an inertial frame. Newton's gravitational constant is G. (a) What are the configuration and phase spaces of this system? (b) $\langle \mathbf{4} \rangle$ Write down the standard Lagrangian for this system. (c) Identify three infinitesimal translation symmetries of this Lagrangian. (d) Use **Noether's theorem** to deduce corresponding conserved quantities.
26. Show that a **Galilean transformation** (3.71) between inertial frames preserves time intervals and the spatial distance between simultaneous events.
27. On the x-p plane, draw **energy level curves** for the oscillator whose Hamiltonian is $H = p^2/2m + \frac{1}{2}m\omega^2 x^2$. Indicate the arrow of time and at least 2 qualitatively different trajectories (extended indefinitely forward and backward in time).
28. Consider a particle in the 1d potential $V(x) = g(x^2 - a^2)^2$ with $g, a > 0$.

    a. What are the dimensions of a and g? Find a conserved energy. Find all equilibrium points (classify them as stable and unstable) and their energies.
    b. Roughly sketch the potential as a function of x, indicating the point a and the value of energy at the unstable equilibrium point.
    c. Give a suitable name for this potential.
    d. Draw a **phase portrait** for this system, i.e., indicate the phase space trajectories for a few values of energy/initial conditions. Do this without solving the EOM, but using conservation of energy, previous results and physical reasoning. You must draw at least 8 qualitatively distinct trajectories (with arrows showing direction of motion) and mention the nature of the motion along each of them. Hint: An energy level curve could be a union of trajectories.

29. **Legendre transform in thermodynamics.** The 1^{st} law of thermodynamics [38] says that the increase in internal energy of a gas is equal to the heat transferred to the gas minus the work done by the gas. Using the 2^{nd} law, for infinitesimal reversible changes, $dU = TdS - pdV$. Here, dU, dV, dS are the increase in internal energy, volume and entropy, p is the pressure and T the absolute temperature.

    a. What are the independent variables that U depends on?
    b. Write formulae to determine T and p from the internal energy.
    c. The Helmholtz free energy F may be introduced via $F = U - TS$. Find the independent variables that F depends on.
    d. Express the pressure p and entropy S in terms of the Helmholtz free energy.
    e. Write a formula for F as a Legendre transform (see Sect. 3.15) of U. Indicate which variable to extremize in and give the condition for an extremum.

30. Suppose we wish to extremize the internal energy U among thermodynamic states with a fixed value of entropy S_0. Formulate this problem via a **Lagrange multiplier** and suggest a possible physical interpretation of the Lagrange multiplier.

31. **Charged particle.** A particle of charge e moving in $\mathbb{R}^3$ subject to a magnetic field $\boldsymbol{B} = \boldsymbol{\nabla} \times \boldsymbol{A}$ is governed by the Lagrangian $L = (1/2)m\dot{\boldsymbol{q}}^2 + \frac{e}{c}\boldsymbol{A} \cdot \dot{\boldsymbol{q}}$. Here, $\boldsymbol{A}(\boldsymbol{q})$ is a *vector potential* with components A_i and c the speed of light. (a) Find the momenta conjugate to the position coordinates q^i. (b) What is the dimension of the quantity $e\boldsymbol{A}$? (c) Derive the Euler-Lagrange equations (see Sect. 3.23*) and relate them to the Newton-Lorentz equation for a charged particle.

32. The Lagrangian of a particle of charge e subject to a vector potential $\boldsymbol{A}(\boldsymbol{q})$ is

$$L = (1/2)m\dot{\boldsymbol{q}}^2 + (e/c)\boldsymbol{A} \cdot \dot{\boldsymbol{q}}. \tag{3.238}$$

(a) Find the momentum $\boldsymbol{p}$ conjugate to $\boldsymbol{q}$. (b) Find the Hamiltonian $H(\boldsymbol{q}, \boldsymbol{p})$ via a Legendre transform. (c) For a free particle, $2mH = \boldsymbol{p} \cdot \boldsymbol{p}$ is the dot product of the momentum with itself. Here, we seek a generalization of this formula to a **charged particle interacting with a magnetic field**. Express $2mH$ as the dot product of a vector with itself. How does this vector differ from the canonical momentum $\boldsymbol{p}$?

33. Suppose we consider a system with generalized coordinates q^i, potential energy $V(q)$, kinetic energy $T = \frac{1}{2}m_{ij}(q)\dot{q}^i\dot{q}^j$ and total energy $E = T + V$.

    a. Argue that the **mass matrix** $m_{ij}(q)$ may be taken symmetric.
    b. Suppose the Lagrangian is $L = T - V = (1/2)m_{ij}(q)\dot{q}^i\dot{q}^j - V(q)$. Find a simple formula for the momenta p_k conjugate to q^k.
    c. Find the Hamiltonian $H = p_k\dot{q}^k - L$ and relate it to the energy E. At this stage, we regard H as a function of q and $\dot{q}$, rather than of q and p.
    d. What linear-algebraic property of the matrix field $m_{ij}(q)$ would ensure that the kinetic energy is nonnegative in *any* state of the system? Define the linear algebraic property and explain using Dirac bra-ket notation. Hint: Think in terms of expectation values in a state or in terms of eigenvalues.
    e. Solve for the velocities $\dot{q}^i$ and express the Hamiltonian in terms of coordinates and momenta. Show that $H = \frac{1}{2}m^{ij}p_ip_j + V(q)$, where $m^{ij}m_{jk} = \delta^i_k$. We recognize this as a generalization of $p^2/2m + V$.
    f. Show that Hamilton's equations can be expressed as

$$\dot{q}^i = \frac{\partial H}{\partial p_i} = m^{ij}p_j \quad \text{and} \quad \dot{p}_i = -\frac{\partial H}{\partial q^i} = -\frac{1}{2}p_kp_l\frac{\partial m^{kl}}{\partial q^i} - \partial_i V(q). \tag{3.239}$$

34. **Legendre self-conjugate function.** Find a smooth convex function $L(v)$ of a real variable v whose Legendre transform $H(p) = \text{ext}_v(pv - L(v))$ is the same function as L. In other words, $H(\cdot) = L(\cdot)$ for any real argument (i.e., they are the same function of their respective arguments). You may first try to guess such a function using physical knowledge. But you must also formulate the above condition as an equation and try to solve it to determine such a function. Hint: Formulate the condition for convexity using differential calculus.

35. **Legendre transform.** Suppose the kinetic energy and Lagrangian are given by $T = L(q, \dot{q}) = \frac{1}{4}\dot{q}^4 - \frac{1}{2}\dot{q}^2$. (a) Plot T as a function of $\dot{q}$. (b) Find the momentum p conjugate to q. (c) Plot p as a function of $\dot{q}$. (d) To go from L to the Hamiltonian we need to express $\dot{q}$ in terms of p. Indicate on the p versus $\dot{q}$ graph whether and where one may solve for $\dot{q}$ in terms of a given p uniquely/nonuniquely. An explicit formula for $\dot{q}(p)$ is not required. (e) Does $H = p\dot{q} - L$ with $p = \frac{\partial L}{\partial \dot{q}}$ define H as a singlevalued function of q and p? Where do we run into trouble? Comment on the connection between the uniqueness of $\dot{q}$ for a given q and p, the singlevaluedness of the Legendre transform and the convexity/concavity of L in the foregoing example.

∗36. **Classical limit of the Fourier transform.** In the quantum theory of fields [62] [and in statistical mechanics and probability], we are often interested in the generating function of connected correlations $W(J)$, which is defined in terms of the action $S(\phi)$ via a functional integral. J is called a source. As a caricature, consider a real field ϕ on a space-time with just one point, so that the functional integral is just an ordinary integral over one real variable ϕ:

$$e^{\frac{iW(J)}{\hbar}} = \int_{-\infty}^{\infty} e^{\frac{i}{\hbar}(S(\phi) - J\phi)} d\phi. \tag{3.240}$$

Here $\hbar = h/2\pi$ where h is Planck's constant.(a) Why may we regard this integral as a Fourier transform? What is it the Fourier transform of? If we think of ϕ as 'position', then what is the Fourier conjugate 'momentum'? (b) In the classical limit $\hbar \to 0$, express $W(J)$ in terms of $S(\phi)$, state the result in words and try to relate it to the Legendre transform. Hint: Evaluate the integral in the stationary phase approximation. When $\hbar \to 0$, the dominant contribution to the integral comes from the point ϕ (assumed unique for simplicity) where the phase is stationary. (c) Look up the Feynman path integral formulation of quantum mechanics [114]. A quantum analog of the classical Legendre transform from Hamiltonian to Lagrangian is encountered in going from the phase space Feynman path integral to the configuration space path integral. Fourier transforms play a role in this process.

∗37. Use **Lagrange multipliers** to find the local extrema of $E(\boldsymbol{x}) = \boldsymbol{x}^t H \boldsymbol{x}$ subject to $\boldsymbol{x}^t\boldsymbol{x} = 1$, where $\boldsymbol{x} \in \mathbb{R}^3$ and H is a 3×3 symmetric positive-definite real matrix with eigenvalues $0 < \lambda_1 < \lambda_2 < \lambda_3$. Interpret the problem and solution geometrically, linear algebraically and in terms of the Euler top of Sect. 8.12.

38. **Explicitly time-dependent conserved quantity.** Consider the harmonic oscillator with Hamiltonian $H = p^2/2m + m\omega^2 x^2/2$. (a) Find Hamilton's equations. (b) Show that $F = x\cos\omega t - (p/m\omega)\sin\omega t$ is conserved. (c) Find $\frac{\partial F}{\partial t}$ and show that it too is conserved. (d) Express F and $\frac{\partial F}{\partial t}$ in terms of the ICs $x(0)$ and $p(0)$.

39. With reference to Footnote 60, consider the **Lagrangian linear in velocities** $L = A_j(q)\dot{q}^j - V(q)$. Here, A_j, V are differentiable functions of the n coordinates $q^1, \ldots, q^n$ for $j = 1, \ldots, n$. Obtain the Euler-Lagrange equations of motion and observe that they are first order in time (i.e., they do not contain any 'acceleration' terms). Show that they may be expressed in the form $\eta_{ij}\dot{q}^j = \frac{\partial V}{\partial q^i}$. Find the antisymmetric matrix $\eta_{ij}(q)$. Observe that it looks like the electromagnetic field strength tensor if A_i are the components of the vector potential.

$*$40. **Hamiltonian and PB for Lagrangian linear in velocities.** As in Prob. 3.39 and following the treatment of [124], consider the Lagrangian $L = A_j(q)\dot{q}^j - V(q)$ linear in the n generalized velocities $\dot{q}^j$. The Euler-Lagrange equations are expressible as $\eta_{ij}\dot{q}^j = \frac{\partial V}{\partial q^i}$ and are first order in time. Assuming the matrix η_{ij} is nonsingular, denote its inverse by η^{ij} (argue that it must be antisymmetric). Then the EOM become $\dot{q}^i = \eta^{ij}(q)\frac{\partial V}{\partial q^j}$. These equations can be given a Hamiltonian-Poisson bracket formulation by defining $H = V$ and taking η^{ij} to be a Poisson tensor. In other words, declare q^j to be coordinates on phase space and define the Poisson bracket between functions of q to be

$$\{f(q), g(q)\} = \eta^{ij}\frac{\partial f}{\partial q^i}\frac{\partial g}{\partial q^j}. \tag{3.241}$$

(a) Use associativity to show that if a square matrix M has both a left and a right inverse (L, R), then they must be the same. (b) A square matrix M is called invertible if there is a matrix W with $WM = MW = I$. Show that when an inverse exists, it is unique. (c) Show that the inverse of an invertible antisymmetric matrix must be antisymmetric. (d) What are $\{q^i, q^j\}$ and $\{q^i, A_j\}$? (e) Show that the PB $\{q^i, q^j\}$ following from (3.241) satisfies the Jacobi identity for $\eta_{ij} = \frac{\partial A_j}{\partial q^i} - \frac{\partial A_i}{\partial q^j}$. Hint: Check whether the provisional Poisson tensor satisfies the relevant quadratically nonlinear differential equation. (f) Verify that Hamilton's equations $\dot{q}^i = \{q^i, H\}$ reduce to the Euler-Lagrange EOM. Notice that there is no canonical splitting of the q^j into positions and momenta. This is an effect of Lagrange's equations being first order in time. (g) Define the 'conjugate momenta' p_j as we do for Lagrangians quadratic in velocities. Comment on the result and on whether p_i and q^j can be taken as independent variables. (h) Try to obtain a Hamiltonian via a Legendre transform of L. Observe what goes wrong but proceed formally to obtain a proposed H and compare with the proposal $H = V$. (i) What is the $\{q^i, A_j\}$ PB that results from postulating that the momenta p_j are canonically conjugate to the q^i, i.e., $\{q^i, p_j\} = \delta^i_j$? is this consistent with the result obtained from (3.241)?

$*$41. **Vibrations of a stretched string.** Consider a string stretched between $x = 0$ and $x = l$ and free to vibrate in a vertical plane. The instantaneous height of the string relative to equilibrium is $u(x,t)$. The tension in the string is τ (tangential stretching force exerted on any segment of the string to either side) and ρ is its mass per unit length. A Lagrangian for small transverse vibrations is

$$L = \int_0^l \frac{1}{2}\rho\left[(u_t)^2 - c^2(u_x)^2\right]\,dx \equiv \int_0^l \mathcal{L}\,dx. \tag{3.242}$$

$\mathcal{L}$ is the Lagrangian density and $c^2 = \tau/\rho$, where τ and ρ are assumed constant.

a. How many degrees of freedom does this system have? What are they?
b. Recall a typical point particle Lagrangian $L_p = \sum_i \frac{1}{2}m\dot{q}_i^2 - V(q)$. Provide a dictionary relating quantities from particle mechanics to appropriate ones for a vibrating string: (i) index i, (ii) coordinate q_i, (iii) particle mass m, (iv) $\sum_i$.

c. What is the momentum $\pi(x)$ conjugate to the coordinate $u(x)$?
d. Obtain the Euler-Lagrange EOM. Show that it is the 1d wave equation: $u_{tt} = c^2 u_{xx}$.
e. Find the Hamiltonian $H[u, \pi] = \int \mathcal{H}\, dx$ via a Legendre transform.
f. Find Hamilton's equations and check that they give the wave equation.
g. Show that $\dot{H} = 0$, assuming the string is clamped at $x = 0, l$.
h. State the main result of Noether's theorem for a symmetry $q^i \to q^i + \delta q^i$ of the point particle Lagrangian L_p. If $u(x) \to u(x) + \delta u(x)$ is a symmetry of the string Lagrangian, what is the formula for the conserved quantity?
i. Show that a constant shift $u(x,t) \to u(x,t) + \alpha$ is a symmetry of the Lagrangian subject to free boundary conditions ($u_x = 0$ at endpoints).
j. Find the Noether conserved quantity Q following from the above symmetry. Check by differentiating under the integral sign that $\dot{Q} = 0$.

42. Try to generalize the **variational principles** for Lagrange's and Hamilton's equations [(3.19) and (3.107)] to ones where the initial position and initial velocity or momentum are held fixed.

43. Suppose $f(q(t), p(t))$ is a dynamical variable in a 1 degree of freedom system with Hamiltonian $H(q,p)$. (a) Use Hamilton's equations to derive a formula for df/dt and express it in terms of **Poisson brackets**. (b) Express the condition for conservation of f in terms of PBs and also state the condition in words.

44. **Composition and PBs.** Suppose ξ are coordinates on phase space and that f and g are observables with the property that $f = f(h(\xi), k(\xi))$. Then show that

$$\{f(h(\xi), k(\xi)), g(\xi)\} = \frac{\partial f}{\partial h}\{h, g\} + \frac{\partial f}{\partial k}\{k, g\}. \tag{3.243}$$

45. Consider a **particle moving on the plane**: $L = \frac{1}{2}m(\dot{x}^2 + \dot{y}^2) - V(x,y)$ with x, y, p_x, p_y the old coordinates and momenta. Define new polar coordinates $x = r\cos\theta$ and $y = r\sin\theta$. We wish to compare the PBs among the new coordinates and momenta to those among the old coordinates and momenta.

a. Find the partial derivatives (denoted by subscripts) $r_x, r_y, \theta_x, \theta_y$. Show that

$$r_x = x/r, \quad r_y = y/r, \quad \theta_x = -y/r^2, \quad \theta_y = x/r^2. \tag{3.244}$$

b. Show that the new velocities may be expressed in terms of the old velocities and coordinates (here we use $r = \sqrt{x^2 + y^2}$ for brevity)

$$\dot{r} = (x\dot{x} + y\dot{y})/r \quad \text{and} \quad \dot{\theta} = (x\dot{y} - y\dot{x})/r^2. \tag{3.245}$$

c. Verify that the new Lagrangian is (what is $\tilde{V}(r,\theta)$?)

$$\tilde{L}(r, \theta, \dot{r}, \dot{\theta}) = (1/2)m(\dot{r}^2 + r^2\dot{\theta}^2) - \tilde{V}(r,\theta). \tag{3.246}$$

d. Find the new momenta from the Lagrangian in the new variables and express them in terms of the old coordinates and momenta. Show that you get

$$p_r = \frac{x}{r} p_x + \frac{y}{r} p_y \quad \text{and} \quad p_\theta = x p_y - y p_x. \tag{3.247}$$

e. Find the partial derivatives $r_{p_x}, r_{p_y}, \theta_{p_x}, \theta_{p_y}$.

f. Find the derivatives of the new momenta with respect to the old coordinates and momenta. You must give 8 formulae, two of which must be shown to be

$$(p_r)_x = \frac{p_x}{r} - \frac{x^2}{r^3} p_x - \frac{xy}{r^3} p_y \quad \text{and} \quad (p_r)_y = \frac{p_y}{r} - \frac{y^2}{r^3} p_y - \frac{xy}{r^3} p_x. \tag{3.248}$$

g. From the definition $\{f, g\} = f_x g_{p_x} - f_{p_x} g_x + f_y g_{p_y} - f_{p_y} g_y$, find the 6 (after accounting for antisymmetry) PBs among the new coordinates and momenta (a) $\{r, \theta\}$, (b) $\{r, p_r\}$, (c) $\{r, p_\theta\}$, (d) $\{\theta, p_\theta\}$, (e) $\{\theta, p_r\}$ and (f) $\{p_r, p_\theta\}$.

h. Compare the PBs among the old variables to those among the new variables.

46. Suppose q^i, p_j are canonical coordinates on phase space and suppose time evolution is generated by $H(q, p)$. Show that **infinitesimal time evolution preserves the Poisson brackets** among q, p, i.e., show that $\{q^i(t+\delta t), p_j(t+\delta t)\} = \delta^i_j$, etc., for small δt. An upshot of this result is that we often suppress the time at which an (equal-time) PB is evaluated. Hint: One may regard $q(t+\delta t)$ and $p(t+\delta t)$ as functions of $q(t)$ and $p(t)$ using infinitesimal time evolution and then use the original PBs at time t. Note that the proof makes essential use of the Jacobi identity.

47. Find the **unequal-time Poisson brackets** $\{q(0), q(t)\}$ for a free particle of mass m moving on a line. For more on unequal-time PBs see Sect. 10.2.

48. **Levi-Civita symbol.** Define the Levi-Civita symbol ϵ_{ijk} for $1 \leq i, j, k \leq 3$ by the condition that it is antisymmetric under interchange of any pair of *neighboring* indices along with the condition $\epsilon_{123} = 1$.

a. What are ϵ_{121} and ϵ_{112} and ϵ_{321}?

b. Verify that the condition of being antisymmetric under interchange of neighboring indices is consistent: ϵ_{321} may be got from ϵ_{123} in more than one way.

c. Show that it is antisymmetric under interchange of *any* pair of indices.

d. Verify that $\epsilon_{ijk} = \pm 1$ according as ijk is an even or odd permutation of 123 and zero otherwise. We will define the Levi-Civita symbol to have the same components in any coordinate system.

e. Find all components of the ϵ symbol. How many components are there in all?

f. From $\boldsymbol{L} = \boldsymbol{r} \times \boldsymbol{p}$, write the 3 components of angular momentum L_x, L_y, L_z in terms of x, y, z, p_x, p_y, p_z and show that they may be summarized by the formula $L_i = \epsilon_{ijk} r_j p_k$. Repeated indices are summed.

g. Establish this identity for $1 \leq j, k, l, m \leq 3$ (a sum over $i = 1, 2, 3$ is implied)

$$\epsilon_{ijk}\epsilon_{ilm} = \delta_{jl}\delta_{km} - \delta_{jm}\delta_{kl}. \tag{3.249}$$

h. Try to generalize the definition of the Levi-Civita symbol to one with four indices: ϵ_{ijkl}, where $1 \leq i, j, k, l \leq 4$.

49. **Angular momentum Poisson brackets** from $\{r_i, p_j\} = \delta_{ij}$ for $1 \leq i, j \leq 3$. Recall from Prob. 3.48 that the Cartesian components of angular momentum may be expressed as $L_i = \epsilon_{ijk} r_j p_k$. For simplicity of notation, we place all indices 'down-stairs' in this problem, and sum repeated indices from 1 to 3.

    a. Use properties of the PB and the identity (3.249) to show that $\{L_i, L_j\} = r_i p_j - r_j p_i$. Begin by taking $L_i = \epsilon_{ikl} r_k p_l$ and $L_j = \epsilon_{jmn} r_m p_n$.
    b. Use the above formula for L_i to show that $\epsilon_{ijk} L_k = r_i p_j - r_j p_i$. Thus, we conclude that $\{L_i, L_j\} = \epsilon_{ijk} L_k$.
    c. Use the above results to show that $\{\{L_i, L_j\}, L_k\} = \delta_{ik} L_j - \delta_{jk} L_i$.
    d. Show that the components of angular momentum satisfy the Jacobi identity

$$\{\{L_i, L_j\}, L_k\} + \{\{L_j, L_k\}, L_i\} + \{\{L_k, L_i\}, L_j\} = 0. \tag{3.250}$$

50. Consider the PB among functions on $\mathbb{R}^3$ given by $\{f, g\}(\boldsymbol{r}) = \boldsymbol{r} \cdot (\boldsymbol{\nabla} f \times \boldsymbol{\nabla} g)$. Relate this Poisson structure to a familiar one.

51. Show that $L^2 = L_x^2 + L_y^2 + L_z^2$ is a **Casimir invariant** of the angular momentum Poisson algebra by showing that (a) $\{L^2, L_i\} = 0$ for $i = 1, 2, 3$ and (b) use this to show that $\{L^2, f(\boldsymbol{L})\} = 0$ for any function $f(L_1, L_2, L_3)$ of angular momenta. In general, to show that an observable is a Casimir of a Poisson algebra, it suffices to show that it commutes with all the coordinates on phase space, see Prob. 3.61.

52. Consider a system whose phase space is $\mathbb{R}^3$ with coordinates L_1, L_2, L_3 satisfying the angular momentum PB. Recall that in the case of $\mathbb{R}^2$ phase space with coordinates $\xi^i = (x, p)$, we had the Poisson tensor $\{\xi^i, \xi^j\} = r^{ij}(\xi) = (0, 1| - 1, 0)$, in terms of which the PB of any pair of observables is $\{f, g\} = \frac{\partial f}{\partial \xi^i} \frac{\partial g}{\partial \xi^j} r^{ij}$. (a) Write down the **angular momentum Poisson brackets** $\{L_i, L_j\}$ and identify the Poisson tensor $r_{ij}(L)$. Are its components constant? We use lower indices for L_i, although the convention is to use superscripts for coordinates on phase space. (b) Show that L^2 is conserved under evolution by *any* differentiable Hamiltonian $H(L_i)$. Hint: Use the formula for PB $\{f, g\}$ in terms of $r_{ij}(L)$.

53. Show that the inverse of an **invertible antisymmetric matrix** is antisymmetric, i.e., if $r\omega = I$ and $r^t = -r$ then $\omega^t = -\omega$.

$*$54. Show that the **Jacobi identity** (3.130) for any three functions f, g and h may be written as the quadratic condition (3.188) on the Poisson tensor. Hint: Use $\{f, g\} = r^{ij} \partial_i f \partial_j g$ repeatedly. Relabel summed indices to collect terms. All terms with 2$^{\text{nd}}$ derivatives of f, g and h should cancel due to antisymmetry of r.

$*$55. **Levi-Civita identity.** Verify that the Levi-Civita symbol satisfies the quadratic identity $\epsilon_{ilm}\epsilon_{jkl} + \epsilon_{klm}\epsilon_{ijl} + \epsilon_{jlm}\epsilon_{kil} = 0$. Explain its origin.

$*$56. **Independence of angular momentum and LRL vector components.** Consider the components of relative angular momentum L_i and the LRL vector A_j in the

Kepler problem. (a) Express dL_i and dA_j as linear combinations of the coordinate basis 1-forms $dx_{1,2,3}$ and $dp_{1,2,3}$ on the 6d $\boldsymbol{r}$-$\boldsymbol{p}$ phase space. (b) Evaluate the 3-form $dL_1 \wedge dL_2 \wedge dL_3$. Does it vanish anywhere and what does this imply for the independence of the components of angular momentum? (c) Do the same for $dA_1 \wedge dA_2 \wedge dA_3$. (d) Find the 6-form $dL_1 \wedge dL_2 \wedge dL_3 \wedge dA_1 \wedge dA_2 \wedge dA_3$. Do you expect it to vanish almost everywhere and why?

$*$57. **Relations among Keplerian conserved quantities** H, A^2, L^2. In Sect. 3.25*, we had reduced the task of showing that the three-fold wedge product $dH \wedge dA^2 \wedge dL^2$ vanishes, to showing that two tensors antisymmetric in i and j,

$$\begin{aligned}\psi_{ijk} &= T_{ik}Q_j - T_{jk}Q_i + (R_{ij} - R_{ji})M_k \quad \text{and} \\ \theta_{ijk} &= (S_{ij} - S_{ji})Q_k + T_{kj}M_i - T_{ki}M_j\end{aligned} \tag{3.251}$$

vanish. Here, R, S, T are defined in (3.173), $\boldsymbol{Q} = \boldsymbol{r} \times \boldsymbol{L}$ and $\boldsymbol{M} = \boldsymbol{p} \times \boldsymbol{L}$. Now let us write $\psi = \psi^s + \psi^l$ and $\theta = \theta^s + \theta^l$ where

$$\begin{aligned}\psi^s_{ijk} = (R_{ij} - R_{ji})M_k \quad &\text{and} \quad \psi^l_{ijk} = T_{ik}Q_j - T_{jk}Q_i \quad \text{and} \\ \theta^s_{ijk} = (S_{ij} - S_{ji})Q_k \quad &\text{and} \quad \theta^l_{ijk} = T_{kj}M_i - T_{ki}M_j\end{aligned} \tag{3.252}$$

and choose coordinate axes such that $\hat{x}$ is along $\boldsymbol{A}$ and $\hat{z}$ is along $\boldsymbol{L}$. Then $A_2 = A_3 = L_1 = L_2 = p_3 = x_3 = 0$.

a. Show that $\psi_{ijk} = 0 = \theta_{ijk}$ if any one of i, j or k is 3.
b. Argue that up to antisymmetry, it only remains to show that $\psi_{121}, \psi_{122}, \theta_{121}$ and θ_{122} vanish.
c. Show that $M_1 = p_2 L_3$, $M_2 = -p_1 L_3$, $Q_1 = x_2 L_3$ and $Q_2 = -x_1 L_3$ while,

$$\begin{aligned}T_{21} &= A_1\left(\frac{p_1 p_2^2}{m} - \frac{\alpha}{r}p_2 - \frac{\alpha}{r^3}x_1 L_3\right), \quad T_{22} = -A_1\left(\frac{\alpha}{r^3}x_2 L_3 + \frac{1}{m}p_1 p_2^2\right), \\ T_{12} &= A_1\left(\frac{\alpha}{r^3}x_2(p_1 x_1 + p_2 x_2) - \frac{1}{m}p_1^2 p_2\right) \quad \text{and} \\ T_{11} &= A_1\left(\frac{p_1 p_2^2}{m} - \frac{\alpha}{r}p_1 + \frac{\alpha}{r^3}x_1(p_1 x_1 + p_2 x_2)\right).\end{aligned} \tag{3.253}$$

d. Show that

$$\theta^s_{121} = -\frac{\alpha x_2 L_3 A_1}{r^3}\left[p_1 L_3 + 2m\left[H + \frac{\alpha}{2r}\right]x_2\right] \;\; \& \;\; \theta^l_{121} = \frac{\alpha}{r^3}A_1 L_3\left[r^2 p_2^2 - L_3^2\right]. \tag{3.254}$$

Combine these to show that $\theta_{121} = -\alpha x_2 L_3 A_1 A_2 / r^3 = 0$.

e. Similarly, show that

$$\begin{aligned}\theta^s_{122} &= \frac{\alpha}{r^3}x_1 L_3 A_1\left[p_1 L_3 + 2m(H + \alpha/2r)x_2\right] \quad \text{and} \\ \theta^l_{122} &= -\frac{\alpha}{r^3}A_1 L_3\left[(x_1 p_1 + x_2 p_2)L_3 + r^2 p_1 p_2\right].\end{aligned} \tag{3.255}$$

Combine these to show that $\theta_{122} = \alpha x_1 L_3 A_1 A_2 / r^3 = 0$.

f. Proceed in a similar manner to show that $\psi_{121} = -p_2 L_3 A_1 A_2 / m$ and $\psi_{122} = p_1 L_3 A_1 A_2 / m$ so that both vanish as $A_2 = 0$ in our coordinate frame.

58. Show that the angular momentum Poisson tensor $r^{ij} = \epsilon^{ij}{}_{k} L^k$ satisfies the quadratically nonlinear **Jacobi condition** (3.188) where ϵ is the Levi-Civita symbol.

59. Suppose f and g are 2 dynamical variables on phase space. Use the Jacobi identity (3.188) to show that the **canonical vector field** associated to the PB $\{f, g\}$ is the negative of the commutator of canonical vector fields $V_{\{f,g\}} = -[V_f, V_g]$ (3.194).

$*$60. **Bianchi identity.** Suppose the Poisson tensor r^{ij} is invertible with inverse ω_{ij} (the symplectic form, see Sect. 3.26*). (a) Using $r\omega = I$ show that $\partial_l r = -r(\partial_l \omega) r$. Here $\partial_l = \frac{\partial}{\partial \xi^l}$ is the derivative with respect to the l^{th} coordinate on phase space. (b) Use this to show that the first term in the Jacobi expression (3.188) is

$$r^{il}\partial_l r^{jk} = -r^{il} r^{jm} \partial_l \omega_{mn} r^{nk}. \tag{3.256}$$

(c) Adding the cyclic permutations and contracting with the invertible matrices $\omega_{jp}\omega_{kq}\omega_{is}$ show that (3.188) reduces to the Bianchi identity

$$\omega_{pq,s} + \omega_{qs,p} + \omega_{sp,q} = 0 \quad \text{where} \quad \omega_{pq,s} = \partial_s \omega_{pq}. \tag{3.257}$$

61. Suppose ξ^i for $i = 1, \ldots, n$ are coordinates on a Poisson manifold, generalizing Prob. 3.51 on angular momenta. (a) Suppose the function $c(\xi)$ commutes with all the coordinates: $\{c(\xi), \xi^i\} = 0$ for all i. Then show that $c(\xi)$ is a **Casimir invariant** by establishing that it commutes with any observable $f(\xi)$. (b) Show that any function $g(c)$ of a Casimir is also a Casimir. (c) Use the Leibniz rule to show that any function $h(c, \tilde{c})$ of a pair of Casimirs is also a Casimir.

62. Use the solution of Hamilton's equations in terms of **iterated Poisson brackets** (3.197) to express $x(t)$ and $p(t)$ in terms of $x(0)$ and $p(0)$ for (a) a free particle, $[H = p^2/2m]$ and (b) the harmonic oscillator, where $H = p^2/2m + m\omega^2 x^2/2$.

63. Show that Lagrange's equations in polar coordinates for a free particle moving on the plane ($L = \frac{1}{2}m(\dot{r}^2 + r^2\dot{\theta}^2)$) are the same as the **geodesic equations** (3.199) for the mass metric. Hint: Find the Christoffel symbols (3.200) in polar coordinates.

$*$64. Verify that the geodesic equations (3.224) for the **Jacobi-Maupertuis metric** reduce to Lagrange's equations (3.221) under the reparametrization

$$\frac{d}{ds} = \frac{1}{\sigma}\frac{d}{dt} \quad \text{where} \quad \sigma = \frac{(E - V)}{\sqrt{\mathcal{T}}} \quad \text{and} \quad \mathcal{T} = \frac{1}{2} g_{ij} \dot{q}^i(s) \dot{q}^j(s). \tag{3.258}$$

65. **2d isotropic oscillator, Hill region and JM metric.** Consider the 2d isotropic harmonic oscillator with Hamiltonian $H = (p_x^2 + p_y^2)/2m + m\omega^2(x^2 + y^2)/2$. (a) What is the Hill region of the configuration space for energy $H = E$? (b) What are the equations of motion? (c) Argue that the solutions of the EOM may be written as $x(t) = a\cos(\omega t + \phi)$ and $y(t) = b\cos(\omega t + \psi)$ for some initial phases ϕ and ψ and amplitudes $a, b \geq 0$. (d) How are a and b constrained by the energy E? (e) Discuss the shapes of the trajectories in the Hill region. Under what circumstances do the trajectories reach the boundary of the Hill region? (f) Give the expression for the JM metric for this system. (g) Try to solve the geodesic equations for the JM metric. (h) Examine whether the geodesics have the same shapes as the trajectories.

Chapter 4

Introduction to special relativistic mechanics

In Chap. 3, we introduced the principles of nonrelativistic mechanics. The current chapter is devoted to the principles of special relativity and relativistic mechanics. We begin by pointing out the inadequacies with the Newtonian concepts of space and time when speeds approach that of light. An elementary introduction to special relativity and relativistic kinematics follows. In Sect. 4.10*, we introduce the Minkowski geometry of space-time and use it to formulate relativistic kinematics and dynamics.

4.1 Difficulties with Newtonian mechanics

Newton, in his formulation of mechanics, postulated that all observers, irrespective of their state of relative motion could synchronize their clocks to a common time and could agree about the simultaneity of a pair of events. In the late 1800s, Ernst Mach criticized this postulate as it was not backed by an examination of the physical processes involved in measuring times using clocks carried by various observers. Nevertheless, Newton's assumption about time remained at the foundation of mechanics for nearly 200 years, since its consequences were largely in agreement with empirical observations. With the benefit of hindsight, we may say that the Newtonian assumption is a good approximation as long as speeds (of particles or of observers relative to an inertial frame) are much less than that of light (see Prob. 4.1). In effect, Newton had assumed that light traveled infinitely fast.

It is perhaps not a surprise that difficulties in the application of Newtonian mechanics first arose in matters concerning light. First, by the 1800s there was strong empirical evidence that light traveled at a large but finite speed $\approx 3 \times 10^8$ m/s in vacuum. Next, Maxwell's equations that had been hugely successful in understanding electricity and magnetism predicted that electromagnetic waves (which included light) must travel at the same fixed speed c in vacuum without regard to the motion of the source or observer. Other types of waves known at that time, such as sound waves, waves in a string and surface water waves were traveling disturbances in a medium like air or water. Moreover, the observed speed of sound depended on the motion of the observer through the medium. Based on the analogy with sound, it was assumed that light waves too must travel in an as yet unobserved medium, which was called ether. It was thought that Maxwell's equations were valid in the frame of the ether. Ether had to have some peculiar properties: (a) to allow light to travel very fast, it had to be minimally deformable [i.e., very stiff/rigid, since sound travels faster in a solid than in a gas (see (19.44))] but (b) it had to be very rare (not dense) to have evaded detection through its effect on the motion of celestial or terrestrial bodies.

Albert Michelson set out to detect the effect of the motion of an observer (relative to the proposed ether medium) on the observed speed of light. Using an interferometer, he (in 1881) and later he along with Edward Morley (in 1887), obtained a null result: the speed of light was the same for a variety of observers moving differently through the ether (the orientation of the arms of the interferometer and rotation of the Earth altered the velocity of motion through the proposed ether). This seemed to be at odds with expectations based on Newtonian mechanics. Attempts were made to explain this null result. Though ingenious, they often seemed unsatisfactory. For instance, George FitzGerald and Hendrik Lorentz proposed that motion through the ether produced just the right contraction of one arm of the interferometer to cancel the effect of the change in speed of light due to the relative motion. Henri Poincaré, by analogy with Newton's third law, proposed the principle that though the ether was real, it could not be detected by any experiment since the effect of motion through the ether would be cancelled by an equal and opposite compensating effect!

4.2 Postulates of special relativity

In 1905, Albert Einstein brought clarity to this confusing situation when he introduced his special theory of relativity[1]. Though Einstein appears not to have been influenced by the null result[2] of Michelson and Morley, Mach's critique of Newtonian mechanics and Maxwell's electrodynamics significantly influenced Einstein's thinking. Einstein's insight was that the principles of Newtonian mechanics had to be revised so as to make mechanics compatible with Maxwell's electrodynamics and avoid the contradictions in interpreting phenomena involving light. Special relativity is based on a pair of postulates: the principle of relativity and the constancy of the speed of light.

The principle of relativity goes back to Galileo, who had proposed it in the context of mechanics (see Sect. 3.3). Galileo had pointed out that there is no mechanical way of determining whether an inertial frame is at rest or in uniform motion[3]. Einstein argued that this principle must apply to all the laws of physics[4]: *if a law holds in one inertial frame, it must also hold in any other frame moving at a constant velocity relative to it.* Accepting the principle of relativity meant discarding the ether hypothesis since the latter would mean that there is a distinguished inertial frame in which Maxwell's equations are valid, namely the one in which the ether is at rest. The failure to detect motion relative to the ether suggested that it was more economical to discard the ether concept while retaining the principle of relativity. Moreover, Maxwell's equations predicted a universal speed for light, without reference to any medium, so there was no role for ether in electromagnetism (though Maxwell erroneously believed in it). This brings us to the 2^{nd} postulate of special relativity, which concerns the **constancy of the speed of light**: *the speed of light in vacuum is the same constant c in all inertial frames*[5]. Since Maxwell's theory seemed to predict a constant speed of light independent of the motion of the source or observer and without reference to any medium, Einstein postulated that the speed of light must be the same for all inertial observers. In other words, the analogy with sound waves, which are disturbances in a medium and whose speed depends on the motion of the observer and source, has its limitations.

---

[1] The qualifier 'special' is meant to convey that the theory deals with physical phenomena observed from inertial (rather than more general) frames of reference. Relativity refers to the fact that certain concepts such as simultaneity of events or lengths of rods, which were considered absolute in Newtonian mechanics, are defined relative to an observer.

[2] Einstein appears to have come to a similar conclusion based on Hippolyte Fizeau's 1851 experiments that attempted to detect the effect of a moving medium (water and air) on the speed of light. Fizeau found an unexpectedly small effect in water and no effect in air. See [14] for a discussion of the experimental basis of special relativity.

[3] When we speak of Galileo's principle of relativity, we are not referring to the Galilean transformation (3.68), which is a rule for transforming quantities between inertial frames. As we will see in Sect. 4.4, this rule needed to be revised in special relativity to make it consistent with the constancy of the speed of light.

[4] The same suggestion was also made by Poincaré in 1905.

These postulates seemed to be the simplest way to accommodate the available theoretical knowledge (constancy of speed of light in Maxwell theory, absence of distinguished frame in Galilean relativity) and experimental/observational data (observer independence of speed of light, ether going undetected).

In addition to these two postulates, Einstein was guided by what one might call the **correspondence principle**[6]: *the relativistic generalization of the laws of mechanics and rules for transforming physical quantities between inertial frames must reduce to those of Newton and Galileo when speeds are small compared to that of light.*

The predictions of the special theory of relativity have been extensively tested; they are in agreement with a wide variety of experiments. A survey of some of these experiments may be found in [138].

4.3 Synchronization of clocks and simultaneity

Synchronization of clocks. In Newtonian mechanics, if a flash of light goes off somewhere, then it arrives instantaneously at the locations of all observers, who can then synchronize their clocks so that any event has a common time of occurrence according to all the observers.

Synchronizing clocks by the radar method. In special relativity, the speed of light is finite. Einstein proposed a 'radar' scheme by which all inertial observers (at rest relative to one another) would assign the same time to any given event. Such a system of clocks is said to be synchronized and is of practical value, for instance in coordinating times across the internet. Suppose A and B are a pair of observers with identical clocks. Suppose A sends a light signal[7] at time t_A (according to his clock) towards

---

[5] In particular, the speed of light in vacuum must be the same in all directions.

[6] The name *correspondence principle* was introduced by Niels Bohr in postulating that the laws of quantum mechanics must reduce to those of classical mechanics in the semiclassical limit of large quantum numbers, where appropriate quantities with dimensions of action are large compared to Planck's constant.

[7] When we speak of light, we do not restrict to visible light. We may use electromagnetic waves of any frequency (X-rays, microwaves, etc.) as they all travel at the speed of light. We use light instead of electrons or protons since light signals have a common speed for all inertial observers, which simplifies the discussion. Electrons of different kinetic energies have different speeds and their speed depends on the observer.

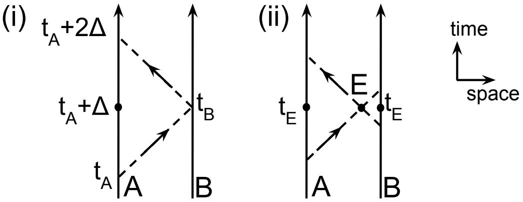

Figure 4.1: Space-time diagrams of two inertial observers A and B who are at rest relative to each other. Time increases upwards while the horizontal direction is space. The trajectories of A and B ('world lines') are upward-directed solid straight lines. World lines of light signals are indicated by dashed lines inclined at 45° since we work in units where $c = 1$. (i) A synchronizes his clock with that of B by sending and receiving a light signal and calibrating his clock to read t_B at the time $t_A + \Delta$. (ii) Having synchronized their clocks, both observers assign the same time to any event E.

B. Suppose B receives this light signal at a time t_B on her clock. To synchronize A's clock with that of B, B immediately sends a light pulse back (with a message giving the time t_B), which is received by A at a time $t_A + 2\Delta$. Now, the clocks are synchronized if A shifts the time displayed by his clock in such a way that $t_B = t_A + \Delta$ (see Fig. 4.1(i)). Having synchronized them, both clocks will assign the same time to any event E, as shown in Fig. 4.1(ii). By contrast, as we will soon see, observers in relative motion cannot have their clocks remain in synchrony in this manner.

Inertial coordinates. The radar method can also be used by an inertial observer O (equipped with a clock and the ability to send and receive light signals) to set up an 'inertial' coordinate system for events, as proposed by E A Milne. Consider one spatial dimension for simplicity. O sends out a light signal at time t_1 along the (arbitrarily chosen) positive direction of the line. This signal is received at an event E and a light signal is immediately sent back towards O, arriving at time t_2 on the local clock, as shown in Fig. 4.2. Since the speed of the outgoing and returning light signals are the same and they had to cover the same distance (in O's rest frame), O would declare that the event E' at time $(t_1 + t_2)/2$ at O's location is simultaneous with E. For the same reason, O assigns a distance $c(t_2 - t_1)/2$ to E from E' [we only define distances between simultaneous events]. Thus, the inertial coordinates of E are $(t, x) = ((t_1 + t_2)/2, c(t_2 - t_1)/2)$. Events that occur on the other side of the line are given negative spatial coordinates and O lies at $x = 0$ in this coordinate system.

Relativity of simultaneity. Two events E_1 and E_2 occur simultaneously for observer A if they occur at the same time on A's clock. The above radar method of synchronization ensures that if B is at rest relative to A, then E_1 and E_2 are simultaneous for B as well. However, the space-time diagram of Fig. 4.3 and the example that follows show that observers in relative motion need not agree on the simultaneity of events[8].

A guard stands in the middle of an empty railway wagon of length $2L$ and switches on a lantern sending out a light pulse in all directions propagating at speed c. In the

---

[8] Less surprisingly, as this is already the case in Galilean relativity, it can be shown that events that occur at the same location (but at different times) in one system, may not appear to occur at the same location in a different frame of reference (see Prob. 3.1).

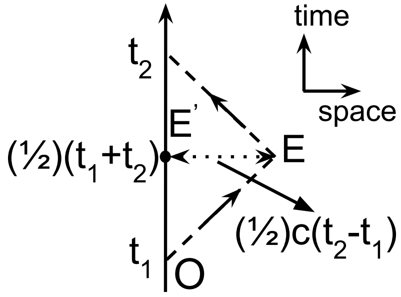

Figure 4.2: Inertial coordinates of event E assigned by inertial observer O. E' is the event on O's world line that is simultaneous with E. As before, time increases upwards and the horizontal direction represents space. We work in units where $c = 1$.

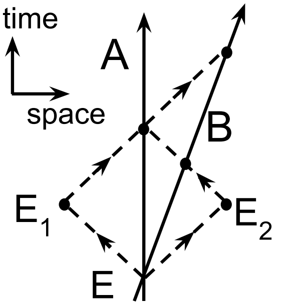

Figure 4.3: *Simultaneity is relative.* In this figure, we work in units where $c = 1$, so light rays travel along straight lines inclined at 45°. Observer B moves at a uniform velocity of magnitude $< c$ relative to inertial observer A, so their world lines (solid) are inclined at an angle less than 45°. Time, as measured on their clocks increases upwards along their world lines. They meet at the event E, when both send light signals (dashed) to events E_1 and E_2, which are then sent back. Events E_1 and E_2 are simultaneous according to A (as he receives the returned signals at the same time on his clock) but not as reckoned by B. B says that E_2 precedes E_1 as she receives the reflected light signal from E_2 before the one from E_1.

rest frame of the wagon, the light pulse arrives simultaneously at the left and right ends A and B of the wagon after a time L/c. Now let us view these events from a frame that is moving to the right at speed v relative to the railway wagon. In this frame, the wagon moves to the left with speed v. Though the light pulse travels at the same speed c in this frame, it has to cover a distance shorter than L to reach the right end and a distance longer than L to reach the left end. Thus, in this frame, the pulse does not arrive simultaneously at the two ends of the wagon!

4.4 Lorentz transformations

More generally, we wish to relate coordinates of an event as observed in two inertial frames in uniform relative motion. Galilean transformations do not work as:

Galilean boosts violate the constancy of the speed of light. To see this, consider a pair of inertial frames $S(t, x, y, z)$ and $S'(t', x', y', z')$ that coincide at $t = 0$, with S'

moving at speed v along the x direction, as shown in Fig. 4.4. The coordinates of the event at (t,x,y,z) when viewed from S' are given by the Galilean boost:

$$t' = t, \quad x' = x - vt, \quad y' = y, \quad z' = z. \tag{4.1}$$

We suppose that at $t = 0$, a pulse of light is emitted from the origin of S and travels along the x-axis at speed c. Then, at time t, the light pulse is located at $x = ct$. When viewed from frame S', the location of the light pulse at time t is given by $x' = (c-v)t$. Thus, in frame S', the light pulse moves at speed $\frac{dx'}{dt'} = c - v$. This is inconsistent with the postulate that the speed of light is the same for all inertial observers.

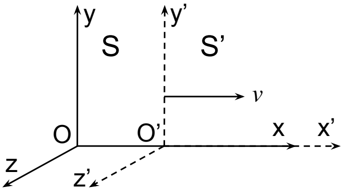

Figure 4.4: A boost from frame S to frame S' that moves along x at speed v.

Lorentz transformation. Einstein found a new transformation that ensures the speed of light is the same in both frames. It is called the Lorentz transformation[9] since a similar transformation had been introduced by Hendrik Lorentz in an attempt to explain the Michelson-Morley null result. As before, suppose we have two inertial frames $S(t,x,y,z)$ and $S'(t',x',y',z')$ that coincide at $t = t' = 0$ with S' moving with speed $v \leq c$ along the positive x axis as shown in Fig. 4.4. The simplest possibility is to take the transformation to be linear, like the Galilean transformation (4.1). A nonlinear transformation could lead to an acceleration of a particle in S' even if its velocity were constant in S. Here, we try to retain, to the extent possible, the basic idea of Newton's first law.

Since the motion is only along the x direction, we begin with the most general linear transformation that does not affect (nor is affected by) the y and z coordinates[10]

$$x' = Ax + Bt, \quad y' = y, \quad z' = z \quad \text{and} \quad t' = Cx + Dt. \tag{4.2}$$

---

[9] Lorentz transformations are a symmetry of Maxwell's equations. However, this was not recognized till after the advent of special relativity.

[10] Here is a 'thought experiment' to justify the assumption that y and z are not affected by motion in the x direction. Suppose there is an arch of height h (in the y direction) on a railway track that runs along the x axis. A stick of height h fits exactly into the arch when placed there at rest. Now suppose the stick approaches the arch along the track at speed v. Suppose the y coordinate is affected by a boost along x. Then relative to the arch, the top of the moving stick would be at a height say, $h' > h$ (a similar argument applies if $h' < h$). Then from the rest frame of the arch, the moving stick cannot pass through. However, viewed from the frame of the stick, the arch would approach it at speed v and consequently appear to have a height h' greater than that of the stick, allowing it to pass through. These two conclusions contradict each other. Thus, we must have $h' = h$. In other words, dimensions perpendicular to the direction of motion are not affected by the Lorentz transformation.

We assume that $D > 0$ so that for fixed x, t' increases with t. This will ensure that the transformation is orthochronous, i.e., the arrow of time (past to future with increasing time) is the same for both observers. We will now attempt to fix the constants A, B, C and D (which could depend on v) by (i) comparing the coordinates of certain distinguished events viewed from the two frames and (ii) requiring that the speed of light is c in both frames.

1. The origin of $S(x = 0, t)$ viewed from S' at time t' has coordinates $(x' = -vt', t')$. Then $-vt' = Bt$ and $t' = Dt$ or $B = -vD$.
2. The origin of $S'(x' = 0, t')$ viewed from S at time t has coordinates $(x = vt, t)$. Then $Avt + Bt = 0$ or $B = -vA$. Combining, we must have $A = D$.
3. A pulse of light emitted from $x = x' = 0$ at $t = t' = 0$ is later observed in S at $(x = ct, t)$. By the constancy of the speed of light, the same event has coordinates $(x' = ct', t')$ in S'. Thus, $ct' = Act + Bt$ and $t' = Cct + Dt$. Combining with $A = D$ we get $B/C = c^2$ and using $B = -vA$ we get $C = -(v/c^2)A$.
4. A pulse of light emitted from $x = x' = 0$ at $t = t' = 0$ is observed later along the y axis in S at $(x = 0, y = ct, t)$. In S' this event occurs at time t', at $x' = -vt'$ and at a height y' determined by the constancy of the speed of light: $y'^2 + (vt')^2 = (ct')^2$, *assuming*[11] $v \leq c$. Thus, $y' = \sqrt{(ct')^2 - (vt')^2}$. Equation (4.2) then implies $t' = Dt$ and $y = ct = y' = \sqrt{(ct')^2 - (vt')^2}$. Combining these, we get
$$D = \gamma \equiv (1 - v^2/c^2)^{-1/2} \geq 1. \tag{4.3}$$

The appearance of the factor γ ensures that the speed of light is the same in S and S'. In terms of γ,

$$A = D = \gamma, \quad B = -vD = -v\gamma \quad \text{and} \quad C = -(v/c^2)A = -\gamma v/c^2. \tag{4.4}$$

Thus, the Lorentz transformation from S to S' moving at speed $v < c$ along x is

$$x' = \gamma(x - vt), \quad y' = y, \quad z' = z, \quad t' = \gamma(t - vx/c^2). \tag{4.5}$$

The inverse transformation from S' to S is obtained by reversing the sign of v:

$$x = \gamma(x' + vt'), \quad y = y', \quad z = z', \quad t = \gamma(t' + vx'/c^2). \tag{4.6}$$

As expected, in the nonrelativistic limit $v/c \to 0$, the Lorentz transformation reduces to a Galilean boost. In fact, in this limit, $\gamma \to 1$ and we recover (4.1).

More generally, if S' coincides with S at $t = t' = 0$, but moves at the constant velocity $\boldsymbol{v}$ relative to S, then the Lorentz transformation is given by

$$\boldsymbol{r}'_{||} = \gamma(\boldsymbol{r}_{||} - \boldsymbol{v}t), \quad \boldsymbol{r}'_{\perp} = \boldsymbol{r}_{\perp} \quad \text{and} \quad t' = \gamma(t - \boldsymbol{r} \cdot \boldsymbol{v}/c^2). \tag{4.7}$$

---

[11] A frame S' moving at speed c relative to S could be viewed as traveling with a light pulse, so that the latter would have zero speed. However, according to the 2nd postulate of special relativity, the speed of light is the same (c) in all inertial frames. So such an S' may not be regarded as an inertial frame. A symptom of this is that as $v \to c$, $\gamma \to \infty$ and the formulae (4.5) for the Lorentz transformation become ill-defined.

Here we resolve $\boldsymbol{r} = \boldsymbol{r}_{||} + \boldsymbol{r}_{\perp}$ and $\boldsymbol{r}' = \boldsymbol{r}'_{||} + \boldsymbol{r}'_{\perp}$ into vectors along and orthogonal to $\boldsymbol{v}$: $\boldsymbol{r}_{\perp} \cdot \boldsymbol{v} = 0$ and $\boldsymbol{r}_{||} = (\boldsymbol{r} \cdot \boldsymbol{v})\boldsymbol{v}/v^2$, etc., and $\gamma = 1/\sqrt{1 - \boldsymbol{v}^2/c^2}$. Spatial coordinates perpendicular to the boost velocity $\boldsymbol{v}$ are unaffected and do not affect the other coordinates. Furthermore, if $E_1(t_1, \boldsymbol{r}_1)$ and $E_2(t_2, \boldsymbol{r}_2)$ are a pair of events with $\boldsymbol{r}_{1,2} = (x_{1,2}, y_{1,2}, z_{1,2})$, then we show in Prob. 4.5 that the square of the space-time 'distance' between them

$$c^2(t_2 - t_1)^2 - (x_2 - x_1)^2 - (y_2 - y_1)^2 - (z_2 - z_1)^2, \tag{4.8}$$

is unchanged under Lorentz transformations.

Interpretation of null result of Michelson-Morley experiment. Suppose S and S' are as above and at $t = t' = 0$, a light pulse is emitted at the origin $x = y = z = x' = y' = z' = 0$ and spreads spherically outwards. At time t, the wavefront in S is the spherical surface $x^2 + y^2 + z^2 = (ct)^2$. Using (4.5) and $\gamma^2 = c^2/(c^2 - v^2)$ we find that $x'^2 - c^2t'^2 = x^2 - c^2t^2$ (see Prob. 4.6). So the wavefront in S' lies on the surface $x'^2 + y'^2 + z'^2 = (ct')^2$. Thus, both observers see a spherical wavefront that expands at the speed c, independent of the relative velocity v. The Michelson-Morley experiment looked for a difference in the speed of light in directions parallel to and perpendicular to the Earth's motion. That no such difference was found ('null result'), is consistent with the constancy of the speed of light for all observers, a feature that is built into the formula for a Lorentz transformation.

4.5 Time dilation, length contraction, proper length and time

Time dilation. A consequence of the Lorentz transformation of time intervals is that moving clocks run slow. This is called the phenomenon of time dilation. Consider a clock at rest at location x in frame S. Suppose τ is the time interval between successive clock ticks at time t and $t + \tau$, as observed in S. We wish to find the interval between successive ticks τ' as observed from S', which is moving to the right with velocity v. The times of the two ticks, as viewed from S' are

$$t' = \gamma(t - xv/c^2) \quad \text{and} \quad t' + \tau' = \gamma(t + \tau - xv/c^2). \tag{4.9}$$

Subtracting, $\tau' = \gamma\tau$. Since $\gamma > 1$, we see that the time interval between successive ticks as observed from the moving frame are longer than in the clock's rest frame. Now suppose the observer in S' has a clock identical to the one in S. This observer would say that the moving clock in S runs slow and loses time when compared to the clock at rest in S'. In fact, there is a reciprocity here: when two inertial observers are in uniform relative motion, each perceives the other's clock to run slow[12].

---

[12] The twin 'paradox' is a scenario inspired by the idea of time dilation. Suppose A and B are twins, each carrying an identical clock. B stays at home, which is an inertial frame. A goes on a journey, traveling at constant velocity $\boldsymbol{v}$ while outbound and at $-\boldsymbol{v}$ while returning home. B perceives A's clock to run slow during these two legs of the journey. By a simple-minded application of time dilation, when A returns home, B says that A is younger than B. On the other hand, according to A, B's clock has been running slow, so A believes that B is

Length contraction. Another consequence of the Lorentz transformation is that moving sticks appear to contract in the direction of motion. Suppose a stick at rest in S has length ℓ. We wish to find its length, as observed from frame S' that moves along the negative x-axis with speed v. To measure the length of the stick in S, we note the coordinates of the ends a and b at the same[13] time t. Thus, we have the two events (x_a, t) and (x_b, t) with $x_b - x_a = \ell$. To measure the length of the stick as seen from S', we must determine the coordinates (x'_b and x'_a) of the ends of the stick simultaneously[14] (at a common time t') in S'. Now, from (4.6),

$$x_b = \gamma(x'_b - vt') \quad \text{and} \quad x_a = \gamma(x'_a - vt'). \tag{4.10}$$

Subtracting, $x_b - x_a = \ell = \gamma(x'_b - x'_a) = \gamma\ell'$. Thus, the length observed in S' is $\ell' = \ell/\gamma < \ell$ and the moving stick appears shorter. Again, there is a reciprocity: when two inertial observers are in uniform relative motion at speed v, each perceives a meter stick carried by the other (and lying along the direction of relative motion) to have length $1/\gamma$ meters.

Proper length. Given a stick, it has a distinguished frame, the one in which it is at rest. The length of a stick in its rest frame is called its proper length ℓ. What we have shown above is that the length of the stick ℓ' measured in a frame in which the stick moves uniformly (along its length) is always less than its proper length: $\ell' = \ell/\gamma$.

Proper time. Similarly, given a clock, a time interval measured by an observer who moves with the clock in its rest frame is called a proper time interval τ. We have shown that the corresponding time interval τ' measured in a frame in which the clock is moving, is always larger than the proper time interval: $\tau' = \gamma\tau$.

Broomstick and barn 'paradox'. In this thought experiment, there is a barn with entrance and exit doors a distance ℓ apart, through which a horizontal broomstick of proper length $L > \ell$ can pass (with doors open). The broomstick flies horizontally along its length at a suitable constant speed v through the barn so that $L/\gamma(v) = \ell$. According to farmers at rest in the barn, due to length contraction, there is an instant of time when the whole broomstick fits exactly inside the barn. On the other hand, according to a witch who is seated on the broom as it flies, the length of the barn is contracted to ℓ/γ. The witch therefore concludes that the broom cannot possibly fit inside the barn. There is no paradox: both the farmers and the witch are correct. The point is that simultaneity is relative. The events when the front and rear ends of the

---

younger! The difficulty lies in the fact that we have not accounted for the initial, middle and final portions of A's journey, where A must (i) accelerate from rest to velocity $\boldsymbol{v}$, (ii) decelerate from $\boldsymbol{v}$ to $-\boldsymbol{v}$ and finally (iii) accelerate from $-\boldsymbol{v}$ to rest. The reciprocity between A and B is broken during this accelerated motion where A's frame is noninertial, unlike B's. The behavior of clocks during accelerated motion [68] lies outside the purview of special relativity.

[13] Since the stick is at rest in S, $x_b - x_a = \ell$ even if the ends were observed at distinct times.

[14] An incorrect approach would be to use (4.5) to find the coordinates of (x_a, t) and (x_b, t) in the S' frame and subtract the positions. This would suggest $\ell' = \gamma\ell$. This is incorrect since in S', the locations of the ends of the stick would not be determined simultaneously. To measure the length of an object, we need to find the locations of its extremes at the *same* time in the frame considered.

broom were at the exit and entrance doors are simultaneous according to the farmers. According to the witch, these events are not simultaneous: the front of the broom reaches the exit somewhat before the tail end of the broom crosses the entrance.

Muon lifetime: time dilation and length contraction. Muons ($\mu^{\pm}$) are unstable particles produced in the upper atmosphere through collisions with cosmic ray protons. The negatively charged muon decays to an electron and a pair of neutrinos ($\mu^- \to e^- + \nu_\mu + \bar{\nu}_e$). The decay of muons is a random process, but if we start with a large number $N(0)$ of muons at rest at $t = 0$, then after time t, the number of muons that survive is found to be given by $N(t) \approx N(0)e^{-t/\tau}$. Here, $\tau \approx 2.2\mu s$ is the mean lifetime of muons. If muons travel at speed v, then on average, they may be expected to cover a distance $\langle L \rangle \approx v\tau$ before decaying (assuming the same lifetime τ). High energy muons in the atmosphere travel at close to the speed of light, so we may take $v \approx c$. So on average, muons can cover a distance $\langle L \rangle \approx 660m$ before decaying. Suppose muons are monitored at a reference location on a hill and at a lake $L \approx 1624$ meters below. Muons take about $t = L/c$ seconds to cover this distance. So the expected fraction of muons that survive this journey is

$$\frac{N(L)}{N(0)} = \frac{N(t)}{N(0)} = e^{-L/c\tau} \approx e^{-1624/660} \approx 0.09. \tag{4.11}$$

However, measurements performed by Bruno Rossi and David Hall in Denver, Colorado in 1940 showed that a much larger fraction of muons survived. This was explained by time dilation. In a reference frame fixed to the Earth, the clock traveling with the muon appears to run slow. So for an observer on the Earth, the mean lifetime of the muon is not τ but $\gamma\tau$. For the case studied, $\gamma \approx 3$. Taking this into account, the expected fraction of surviving muons is approximately

$$\frac{N(L)}{N(0)} \approx e^{-L/c\gamma\tau} \approx e^{-1624/3\times 660} \approx 0.4. \tag{4.12}$$

The situation may also be viewed from the rest frame of the muons, in which they live on average a lifetime of $\tau = 2.2\ \mu s$. However, the distance they have to cover is Lorentz contracted to L/γ. So more of them cover this distance before decaying, explaining the larger number of muons observed at the lake.

4.6 Space-like, time-like and light-like intervals and causality

Suppose events A and B have coordinates (x_A, t_A) and (x_B, t_B) in inertial frame S. The spatial separation between them is $L = x_B - x_A$ while they are $T = t_B - t_A$ apart in time (we assume that $L, T \geq 0$, an argument similar to the one below applies when either of them is negative, see Prob. 4.7).

Now suppose $L > cT$, so that a particle would have to travel at a speed $> c$ to go from A to B. Suppose frame S' moves with speed $v < c$ along the x-axis of S. The Lorentz transformation (4.5) determines the coordinates (x'_A, t'_A) and (x'_B, t'_B) of the events in S'. The corresponding spatial and temporal separations between the events as viewed from S' are

$$L' = x'_B - x'_A = \gamma(L - vT) \quad \text{and} \quad T' = t'_B - t'_A = \gamma(T - Lv/c^2). \tag{4.13}$$

Since we have assumed $L > cT$ and $c > v$, L' is positive while T' could have either sign or even vanish. We say that A and B are *space-like separated*. There is no frame in which they occur at the same location, though there is one (with $v = c^2T/L$) in which they occur simultaneously.

On the other hand, suppose $L < cT$ so that a particle could go from A to B traveling at a speed less than c. Then T' is always positive while L' can have either sign. In this case, we say that the events are *time-like separated*, since there is no frame in which they occur at the same time, though there is a frame (with $v = L/T$) in which they occur at the same location.

Finally, if $L = cT$, then we say that the events are *light-like separated*, as a light signal can be sent from A to B.

Causality. Based on this, we postulate the *principle of causality*. It encodes the idea that signals cannot be transmitted at speeds exceeding c. The principle states that in an inertial frame, the event $B(t', x', y', z')$ lies to the future of $A(t, x, y, z)$ if $t' \geq t$ and the two events are either time-like or light-like separated. This will ensure that a massive particle or light (see Sect. 4.10*) can travel from A to B and thereby convey a signal. We will say that A and B are causally connected. Space-like separated events are not causally connected. Moreover, if A is in the future of B in one inertial frame, then the same holds in any other inertial frame.

4.7 Relativistic addition of velocities

As before, let S and S' be two frames with S' moving along x at velocity $\boldsymbol{v} = v\hat{x}$. Suppose a particle has velocity with components $\boldsymbol{u}' = (u'_x, u'_y, u'_z)$ in the frame S'. What is its velocity $\boldsymbol{u}$ as viewed from frame S? Based on Galilean transformations, the answer is $\boldsymbol{u} = \boldsymbol{v} + \boldsymbol{u}'$. For instance, if $v = c/2$ and $\boldsymbol{u}' = (3c/4, 0, 0)$ then the particle would appear to have a speed $5c/4 > c$ in S. In light of our discussion of causality in Sect. 4.6, this is problematic as it would allow signals to be transmitted faster than the speed of light. We now seek a 'velocity addition formula' in special relativity, where Galilean transformations are replaced by Lorentz transformations. To begin with, the velocity components in S and S' are defined as $u_x = \lim_{\Delta t \to 0} \frac{\Delta x}{\Delta t}$, $u'_x = \lim_{\Delta t' \to 0} \frac{\Delta x'}{\Delta t'}$, etc. To relate these velocity components, we first use the Lorentz transformation (4.6) to relate the displacement and time intervals in S' and S. If x'_1, t'_1 and x'_2, t'_2 are coordinates of two events, then

$$x_i = \gamma(x'_i + vt'_i) \quad \text{and} \quad t_i = \gamma(t'_i + x'_i v/c^2) \quad \text{for} \quad i = 1, 2. \tag{4.14}$$

Writing $\Delta x = x_2 - x_1$, $\Delta x' = x'_2 - x'_1$, $\Delta t' = t'_2 - t'_1$ and so on, we get

$$\Delta x = \gamma(\Delta x' + v\Delta t') \quad \text{and} \quad \Delta t = \gamma(\Delta t' + (v/c^2)\Delta x'), \tag{4.15}$$

while $\Delta y = \Delta y', \;\; \Delta z = \Delta z'$. Thus,

$$\begin{aligned} u_x &= \lim_{\Delta t \to 0} \frac{\Delta x}{\Delta t} = \lim_{\Delta t \to 0} \frac{\gamma(\Delta x' + v\Delta t')}{\gamma[\Delta t' + (v/c^2)\Delta x']} = \frac{u'_x + v}{1 + vu'_x/c^2}, \\ u_y &= \frac{u'_y}{\gamma(1 + vu'_x/c^2)} \quad \text{and} \quad u_z = \frac{u'_z}{\gamma(1 + vu'_x/c^2)}. \end{aligned} \tag{4.16}$$

Conversely,

$$u_x' = \frac{u_x - v}{1 - vu_x/c^2}, \quad u_y' = \frac{u_y}{\gamma(1 - vu_x/c^2)}, \quad u_z' = \frac{u_z}{\gamma(1 - vu_x/c^2)}. \tag{4.17}$$

These are Einstein's relativistic velocity addition formulae[15]. Though the boost is along the x direction, $u_y \neq u_y'$ since t and t' are not the same. In the limiting case where the particle is a light pulse, $u_x' = c$ and we find $u_x = c$, independent of the relative speed v of the two frames, confirming that the speed of light is the same for both observers.

Let us apply (4.16) to the above example, taking $u_x' = 3c/4$ and $v = c/2$. Then, as viewed from S, the particle travels at $u_x = 10c/11$ rather than at $5c/4$, as the Galilean velocity addition formula suggested. Can we accelerate a massive particle to a speed c? We will see in Sect. 4.8 that this would require us to transfer an infinite amount of momentum to the particle, costing an infinite amount of energy. However, it is possible in principle to accelerate a massive particle to any desired speed less than c.

4.8 Relativistic momentum from two particle collision

We will propose a formula for the relativistic momentum of a particle by (i) requiring that it be conserved in a collision of two particles and (ii) reduce to the Newtonian expression $\boldsymbol{p} = m\boldsymbol{v}$ when $\boldsymbol{v}^2/c^2 \ll 1$. To begin with, we show that the Newtonian momentum $m\boldsymbol{v}$ is generally *not* conserved in collisions of relativistic particles. For this purpose, consider an elastic collision of two identical particles A and B of mass m that move in the x-y plane. In a frame S where the center of mass is at rest, we suppose that in the far past and future, the particles have equal and oppositely directed horizontal and vertical velocities, as shown in Fig. 4.5. In this frame, the collision is such that it reverses the y-components of the particle velocities:

$$A(-v_x, -v_y) + B(v_x, v_y) \to A(-v_x, v_y) + B(v_x, -v_y). \tag{4.18}$$

In this frame, it is clear that the total Newtonian momentum $m\boldsymbol{v}_a + m\boldsymbol{v}_b$ is zero both before and after the collision and is therefore conserved.

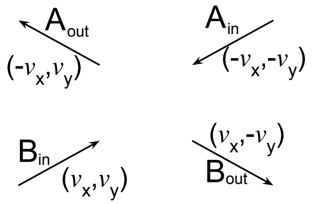

Figure 4.5: Elastic scattering of two identical particles of mass m resulting in reversal of their vertical velocities in the center of mass frame.

---

[15] See Prob. 4.9 for a formulation in terms of rapidities (4.30). In the nonrelativistic limit $v \ll c$, the denominators are approximately 1 and we recover the nonrelativistic formula $u_x = u_x' + v$ along with $u_y = u_y'$ and $u_z = u_z'$.

Suppose we view this collision from a frame S' that moves along the x-axis with velocity $\boldsymbol{u} = v_x\hat{x}$ relative to S. The x-components of the velocities of both particles, when viewed from S, are unchanged as a result of the collision and therefore remain unchanged in S'. So the x-component of Newtonian momentum is conserved in S'.

On the other hand, the y-component of momentum turns out not to be conserved. From the velocity addition formula (4.17), when viewed from S', the y-components of the velocities of the particles before the collision are

$$-v'_{ay} = \frac{-v_y}{\gamma(1-u(-v_x)/c^2)} \quad \text{and} \quad v'_{by} = \frac{v_y}{\gamma(1-uv_x/c^2)}, \tag{4.19}$$

where $u = v_x$ and $\gamma = 1/\sqrt{1-v_x^2/c^2}$. We notice that the magnitudes of these y-components are unequal. So initially $p_y^{\text{in}} = -mv'_{ay} + mv'_{by} \neq 0$. After the collision, the y-components of the velocities reverse their signs to v'_{ay} and $-v'_{by}$, so that $p_y^{\text{out}} = -p_y^{\text{in}} \neq 0$. Thus, the Newtonian momentum $m\boldsymbol{v}$ is *not* conserved in frame S'.

We may trace the difficulty to the fact that the y-component of the Newtonian momentum of the particle depends on the x-component of the velocity of the frame in which the particle is observed.

We now seek a new definition of momentum whose y-component does not change when we transform to a frame moving in the x-direction. Now, although Δy is unchanged under a Lorentz boost in the x-direction, Δt does change, making $v_y = \lim_{\Delta t\to 0} \Delta y/\Delta t$ depend on the frame. This may be avoided by using the proper time interval $\Delta\tau$, which is the time elapsed in the rest frame of the particle, in place of Δt. From its definition, $\Delta\tau$ is the same in all inertial frames. From Sect. 4.5, we know that

$$\Delta t = \gamma\Delta\tau \quad \text{so that} \quad \frac{\Delta y}{\Delta\tau} = \gamma\frac{\Delta y}{\Delta t}, \quad \text{where} \quad \gamma = 1/\sqrt{1-\boldsymbol{v}^2/c^2} \tag{4.20}$$

with $\boldsymbol{v}$ the Newtonian velocity of the particle (note that this γ is different from the one in (4.19)). Thus, taking the limit $\Delta t \to 0$, if we define the relativistic momentum $\boldsymbol{p} = \gamma m\boldsymbol{v}$, then its y component will be unaltered by a boost in the x-direction. So the total y-momentum will be conserved in S' if it is conserved in S. In the above collision, there was no change in the x-component of the velocity of either particle, so $p_x^{\text{in}} = \gamma m v_{ax} + \gamma m v_{bx}$ is automatically conserved.

In the nonrelativistic limit $\gamma \to 1$, so $\boldsymbol{p} = \gamma m\boldsymbol{v}$ approaches the Newtonian expression $m\boldsymbol{v}$, in accordance with the correspondence principle. On the other hand, as the particle's speed approaches that of light, $\gamma \to \infty$ and the magnitude of the relativistic momentum grows without bound. Crucially, the proposed formula $\boldsymbol{p} = \gamma m\boldsymbol{v}$ has been experimentally verified to lead to a conserved momentum in a wide variety of collisions and has therefore gained acceptance as the correct expression for the momentum of a relativistic particle whose Newtonian velocity is $\boldsymbol{v}$:

$$\boldsymbol{p} = \gamma m\boldsymbol{v} = \frac{m\boldsymbol{v}}{\sqrt{1-\boldsymbol{v}^2/c^2}}. \tag{4.21}$$

Relativistic mass and its dependence on speed. The quantity $M = \gamma m$ appearing in the relativistic momentum formula (4.21) is called the relativistic mass of the particle.

It reduces to the Newtonian mass m in the rest frame of the particle, where $\boldsymbol{v} = 0$. Thus, m is also called the rest mass. Unlike the speed of a particle, which (by the causality principle of Sect. 4.6) is bounded above by c, there is no upper bound on the magnitude of the momentum of a particle. In particle accelerators, charged particles rapidly reach speeds close to that of light. Most of the remaining effort goes into increasing M so as to increase the momentum.

Massless particles must travel at the speed of light. Relativistic mechanics allows us to introduce the concept of a particle with zero mass that nevertheless has nonvanishing momentum. In (4.21), notice that it is possible to take a limit where $m \to 0$ and $\boldsymbol{v}^2 \to c^2$ in such a way that $\boldsymbol{p}$ remains finite (and possibly nonzero). Thus, a massless particle (such as a photon) must travel at the speed of light in order that it possess a finite momentum. This is in contrast with the nonrelativistic formula $\boldsymbol{p} = m\boldsymbol{v}$, where taking $m \to 0$ results in vanishing momentum for any finite $\boldsymbol{v}$.

4.9 Relativistic energy and energy-momentum dispersion relation

What is the relativistic analog of the nonrelativistic kinetic energy $\frac{1}{2}m\boldsymbol{v}^2$ of a particle? To obtain it, we first recall that by the work-energy principle (3.8), the (increase in) kinetic energy may be deduced from the work done by a force along a trajectory. As in the nonrelativistic theory, the work done in moving the particle from $\boldsymbol{a}$ to $\boldsymbol{b}$ along a trajectory is

$$W = \int \boldsymbol{F} \cdot \frac{d\boldsymbol{r}}{dt}\, dt = \int \dot{\boldsymbol{p}} \cdot \boldsymbol{v}\, dt = \int_{\boldsymbol{a}}^{\boldsymbol{b}} \boldsymbol{v} \cdot d\boldsymbol{p}. \tag{4.22}$$

Integrating by parts (see Prob. 4.10),

$$\begin{aligned} W &= \int_{\boldsymbol{a}}^{\boldsymbol{b}} d(\boldsymbol{v}\cdot\boldsymbol{p}) - \int_{\boldsymbol{a}}^{\boldsymbol{b}} \boldsymbol{p}\cdot d\boldsymbol{v} = [m(\gamma\boldsymbol{v}^2)]_a^b - \int_a^b \frac{m\boldsymbol{v}\cdot d\boldsymbol{v}}{\sqrt{1-\boldsymbol{v}^2/c^2}} \\ &= \left[m\gamma\boldsymbol{v}^2 + mc^2\sqrt{1-\boldsymbol{v}^2/c^2}\right]_a^b. \end{aligned} \tag{4.23}$$

Assuming the particle was at rest at $\boldsymbol{r} = \boldsymbol{a}$ and denoting $\boldsymbol{v}_b = \boldsymbol{v}$, the increase in kinetic energy due to the work done is (see Prob. 4.11)

$$K = m\gamma\boldsymbol{v}^2 + \frac{mc^2}{\gamma} - mc^2 = \gamma mc^2 - mc^2. \tag{4.24}$$

If we write $M = \gamma m$ for the relativistic mass, then $Mc^2 = K + mc^2$. Einstein interpreted mc^2 as the rest energy of the particle accruing by virtue of its (rest) mass and present even if it is at rest. He then suggested that

$$E = Mc^2 = \gamma mc^2 = K + mc^2, \tag{4.25}$$

be interpreted as the total energy of a free particle, being the sum of its kinetic and rest energies[16]. This interpretation means that when an energy ΔE is supplied to a particle, its relativistic mass increases by $\Delta E/c^2$.

---

[16] In the nonrelativistic limit $\gamma = (1-\boldsymbol{v}^2/c^2)^{-1/2} \approx 1 + \boldsymbol{v}^2/2c^2$ and K reduces to $\frac{1}{2}m\boldsymbol{v}^2$ while the rest energy mc^2 is an additive constant in the total energy E, that we usually omit.

Relativistic energy-momentum dispersion relation. In nonrelativistic mechanics, the total energy of a free particle (i.e., kinetic energy) is related to its momentum via the 'dispersion relation' $E = \boldsymbol{p}^2/2m$. What is the relativistic analog of this? The relativistic momentum of a particle with velocity $\boldsymbol{v}$ is $\boldsymbol{p} = \gamma m \boldsymbol{v}$ where $\gamma = 1/\sqrt{1 - \boldsymbol{v}^2/c^2}$. On the other hand, its total energy (kinetic + rest energy) is $E = \gamma mc^2$. To find a relation between $\boldsymbol{p}$ and E, we note that E is a scalar in 3d (rotation-invariant) while $\boldsymbol{p}$ is a 3d vector. To relate the two we consider the 3d scalar $\boldsymbol{p}^2 = \gamma^2 m^2 \boldsymbol{v}^2$. It is then natural to consider $E^2 = \gamma^2 m^2 c^4$. In fact, $\boldsymbol{p}^2$ does not have the same dimensions as E^2; but $\boldsymbol{p}^2 c^2$ does. So we consider

$$\boldsymbol{p}^2 c^2 = c^2 \gamma^2 m^2 \boldsymbol{v}^2 = \frac{c^2 \boldsymbol{v}^2 m^2}{1 - \boldsymbol{v}^2/c^2} \quad \text{and} \quad E^2 = \frac{m^2 c^4}{1 - \boldsymbol{v}^2/c^2}. \tag{4.26}$$

Thus, we arrive at the relativistic energy-momentum dispersion relation for a particle of rest mass m:

$$E^2 - \boldsymbol{p}^2 c^2 = (mc^2)^2. \tag{4.27}$$

Massless particles. Just as a massless particle can have a nonzero momentum, it can also possess energy. Indeed, taking $m \to 0$ in the dispersion relation (4.27), we get $E^2 = \boldsymbol{p}^2 c^2$ or $E = |\boldsymbol{p}|c$ since $E = \gamma mc^2$ was positive to begin with. In Newtonian mechanics, when particles are combined to form a composite system, the mass is the sum of (necessarily nonzero) particle masses. Due to this conservation of mass, particles cannot be created nor destroyed in nonrelativistic mechanics. In relativistic mechanics, mass is not separately conserved though total energy and momentum are. This allows for particle production and destruction. Massless particles such as photons can be created particularly easily since unlike massive particles, their energy does not include any contribution from rest mass and can be arbitrary low. Photons are copiously emitted when charged particles are accelerated. On the other hand, atoms can absorb photons and get excited, resulting in the destruction of photons.

4.10* Minkowski space-time and relativistic dynamics

In 1908, Hermann Minkowski presented a geometric formulation of special relativity in terms of the geometry of the space of 4-vectors[17]. He proposed that space and time be combined into a 4-dimensional (or '3+1' dimensional) space-time manifold (see Appendix B for an introduction to manifolds) which we call Minkowski space. The points of Minkowski space are events. Given a choice of inertial frame S with Cartesian coordinates (x, y, z), events are given by 4-tuples $(x^0, x^1, x^2, x^3) = (ct, x, y, z)$. We multiply t by c to ensure that it has the same dimensions as the spatial coordinates. Greek indices $\mu, \nu, \ldots = 0, 1, 2, 3$ are used to label the space-time coordinates $x^\mu = (x^0, x^1, x^2, x^3)$, while Latin indices $i, j, \ldots = 1, 2, 3$ label spatial coordinates $x^i = (x, y, z)$. Upon transforming to a frame S' that coincides with S at $t = 0$ and moves uniformly relative to S, the coordinates of Minkowski space transform via a Lorentz transformation $x'^\mu = \Lambda^\mu_\nu x^\nu$ (with repeated indices being summed) or $x' = \Lambda x$ for short. To ensure that the sense of time is preserved, we assume $\Lambda^0_0 > 0$: such transformations are called orthochronous. E.g., if S' moves at speed v in the positive x direction, then from (4.5),

---

[17] A precursor to Minkowski's work was Poincaré's observation in 1905-06 that Lorentz transformations could be regarded as rotations in a 4d space with coordinates (x, y, z) and an imaginary coordinate ict. Minkowski's geometry uses a real time coordinate and an indefinite metric so that Lorentz boosts may be viewed as 'hyperbolic' rather than 'trigonometric' rotations.

$$ct' = \gamma(ct - \beta x), \quad x' = \gamma(-\beta ct + x), \quad y' = y \quad \text{and} \quad z' = z. \tag{4.28}$$

In this case, the entries of the 4×4 matrix Λ are given by

$$\Lambda^\mu_\nu = \begin{pmatrix} \gamma & -\beta\gamma & 0 & 0 \\ -\beta\gamma & \gamma & 0 & 0 \\ 0 & 0 & 1 & 0 \\ 0 & 0 & 0 & 1 \end{pmatrix} \quad \text{where} \quad \beta = v/c \quad \text{and} \quad \gamma = (1 - \beta^2)^{-1/2}. \tag{4.29}$$

The Lorentz boost (4.28) may be viewed as a hyperbolic rotation if we introduce the 'rapidity' $\zeta = \operatorname{arctanh} \beta$ which plays the role of a hyperbolic angle of rotation. Then using $\gamma = \cosh\zeta$ and $\beta\gamma = \sinh\zeta$, (4.28) becomes

$$ct' = (\cosh\zeta)ct - (\sinh\zeta)x, \quad x' = -(\sinh\zeta)ct + (\cosh\zeta)x. \tag{4.30}$$

A nice feature of rapidity is that the composition of Lorentz boosts in the x direction with rapidities ζ_1 and ζ_2 is a boost in x with rapidity $\zeta_1 + \zeta_2$ (see Prob. 4.15). Notice that $\det \Lambda = 1$; this ensures that the integration element $cdtd\boldsymbol{r} = cdt'd\boldsymbol{r'}$ is unchanged. By contrast, a rescaling of time or space coordinates would correspond to a transformation matrix with determinant different from unity.

Minkowski metric. Minkowski postulated that space-time in an inertial frame be endowed with a metric[18] η with components $\eta_{\mu\nu} = \operatorname{diag}(1, -1, -1, -1)$. If $u^\mu = (u^0, \boldsymbol{u})$ and $v^\mu = (v^0, \boldsymbol{v})$ are tangent vectors at a point of Minkowski space, their inner product $u \cdot v = \eta(u, v)$ is given by

$$\eta(u, v) = u^t \eta v = \eta_{\mu\nu} u^\mu v^\nu = u^0 v^0 - u^1 v^1 - u^2 v^2 - u^3 v^3 = u^0 v^0 - \boldsymbol{u} \cdot \boldsymbol{v}. \tag{4.31}$$

The quantity $u \cdot u = \eta(u, u) \equiv u^2$ is called the squared-norm (or square of the length) of the vector u.

Lorentz transformations are *isometries* of this metric[19], i.e., they leave the inner product invariant: $\eta(\Lambda u, \Lambda v) = \eta(u, v)$ for all u, v. In other words, $\Lambda^\mu_\nu \eta_{\mu\sigma} \Lambda^\sigma_\kappa = \eta_{\nu\kappa}$ or $\Lambda^t \eta \Lambda = \eta$ (see Prob. 4.14). In particular, $\eta(u, u) = u^0 u^0 - \boldsymbol{u} \cdot \boldsymbol{u}$ takes the same value in all inertial frames: it is invariant under Lorentz transformations and is therefore called a Lorentz scalar. A 4-tuple (v^0, v^1, v^2, v^3) is called a 4-vector if under Lorentz transformations its components transform according to $v'^{\mu} = \Lambda^{\mu}_{\nu} v^{\nu}$. The product of a scalar with a 4-vector is again a 4-vector. The metric and its inverse provide isomorphisms between the spaces of 4-vectors and 4-covectors. If v^μ is a 4-vector and A_μ a 4-covector, then $v_\mu = \eta_{\mu\nu} v^\nu$ is a 4-covector while $A^\mu = \eta^{\mu\nu} A_\nu$ is a 4-vector.

---

[18] The inverse of the metric has entries denoted by $\eta^{\mu\nu}$ and is defined via $\eta^{\mu\nu}\eta_{\nu\sigma} = \delta^\mu_\sigma$.

[19] Lorentz transformations may be composed and inverted via matrix multiplication and inversion. Along with (proper) spatial rotations (which too are isometries of η), they form a 6 dimensional connected Lie group called the proper orthochronous Lorentz group, $SO(3, 1)$. Its Lie algebra is generated by rotations about and boosts along the x, y and z axes. Upon including the other isometries of η consisting of space-time translations, one obtains the 10 dimensional proper orthochronous Poincaré group. See Appendix B.13* for a brief introduction to Lie groups.

The Minkowski metric is not Riemannian since it is not positive-definite. It is said to be an indefinite metric[20] as there are vectors u (e.g., (1,0,0,0), (1,1,0,0) or (0,1,0,0)) with positive, zero or even negative squared length $\eta(u,u)$. In fact, a tangent vector u is said to be space-like if $\eta(u,u) < 0$, time-like if $\eta(u,u) > 0$ and null or light-like if $\eta(u,u) = 0$. Similarly, if x and y are a pair of events with coordinates x^μ and y^μ, they are said to be space-like, time-like or null separated if $\eta(x-y, x-y)$ is strictly negative, strictly positive or zero (see Sect. 4.6).

Causality. Causality (introduced in Sect. 4.6) may also be formulated in terms of the Minkowski metric. Given two events x and y as before, y lies in the future of x if the difference vector $y - x$ is time-like or null: $\eta(y-x, y-x) \geq 0$ and $y^0 > x^0$. In particular, space-like separated events are not causally connected: they cannot communicate. Thus, no signal can travel faster than the speed of light. The properties of being space-like, time-like or null separated or of lying in the future are invariant under orthochronous Lorentz transformations since $\eta(u,u)$ is a Lorentz scalar.

Events and their causal relationships in an inertial frame are conveniently visualized on a space-time diagram as in Fig. 4.6. For simplicity, consider 2+1 dimensional Minkowski space with the time axis running vertically upwards and the spatial x and y axes lying in a horizontal plane. Consider the event $(0,0,0)$ at the origin O of space-time. Events $E = (ct, x, y)$ that are light-like separated from O must lie on the surface $c^2t^2 = x^2 + y^2$. This surface is called the light cone with apex at the origin: the upper and lower halves ($t \geq 0$ and $t \leq 0$) are called the future and past light cones at O. Events lying inside the light cone ($c^2t^2 > x^2 + y^2$) are time-like separated from O while events outside ($c^2t^2 < x^2 + y^2$) are space-like separated from O. Events lying on or inside the light cone are causally connected to O and among those, the ones with $t > 0$ ($t < 0$) lie in the future (past) of O. Events lying on the horizontal plane $t = 0$ are simultaneous with O in the frame considered.

World line. The events along the trajectory of a particle can be described by a directed curve in space-time called its world line (see Fig. 4.1 and Fig. 4.3). A light signal emitted from O, by virtue of traveling at the speed c, must have a world line that lies on the future light cone at O (see Fig. 4.6). Massive particles travel at speeds less than c. Thus, the world line of a massive particle that begins at O must lie within the future light cone[21]. For instance, a particle at rest at the origin of the frame has a world line that rises vertically upwards along the positive ct axis.

---

[20] The Minkowski metric has 1 positive and 3 negative eigenvalues. Such a metric is called a Lorentzian metric with signature (+,-,-,-). Some treatments use $\eta_{\mu\nu} = \text{diag}(-1,1,1,1)$.

[21] Not every curve that lies within the future light cone can arise as the world line of a massive particle. For instance, its slope must be such that its speed is less than c, see (4.43).

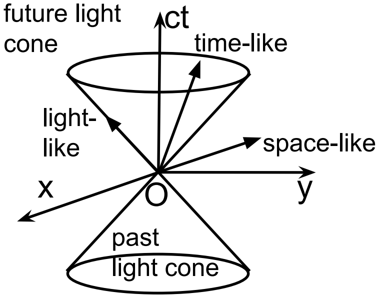

Figure 4.6: Light cone with apex at the origin.

4-velocity and world line of a massive particle. The velocity of a massive particle can be encoded in a 4-vector. Suppose events on its world line are given by the position coordinate $x^\mu = (ct, x, y, z)$. An infinitesimal difference in Δx^μ transforms as a 4-vector, so if it is divided by a Lorentz invariant time interval, we will get another 4-vector. The time elapsed during a displacement of the particle generally depends on the frame chosen to observe the motion. However, all inertial observers would agree on the proper time elapsed as this is the time interval $\Delta\tau$ measured by a clock that travels with the particle. Thus, we define the 4-velocity of a massive particle:

$$u^\mu = \lim_{\Delta\tau\to 0} \frac{\Delta x^\mu}{\Delta\tau} = \frac{dx^\mu}{d\tau} = \left(\frac{d(ct)}{d\tau}, \frac{d\boldsymbol{r}}{d\tau}\right). \tag{4.32}$$

To relate this to the Newtonian notion of velocity $\boldsymbol{v} = d\boldsymbol{r}/dt$, we recall that $dt = \gamma d\tau$ where $\gamma = (1 - \boldsymbol{v}^2/c^2)^{-1/2}$. Then

$$u^\mu = (c\gamma, \gamma\boldsymbol{v}) = \gamma(c, \boldsymbol{v}). \tag{4.33}$$

We see that the 4-velocity of a massive particle is a time-like vector with constant length-squared:

$$\eta(u, u) = \gamma^2(c^2 - \boldsymbol{v}^2) = c^2. \tag{4.34}$$

Thus, the world line of a massive particle is a curve $x^\mu(\tau)$ that is parametrized by the proper time τ and possesses a time-like tangent vector of constant length-squared. More generally, we will call a curve time-like if its tangent vector is time-like everywhere. In terms of the time t measured by an inertial observer, the proper time along a curve $x^\mu(t) = (ct, \boldsymbol{r}(t))$ that begins at $t = t_0$ is the length of the curve measured with respect to the Minkowski metric. To see this, we integrate the expression $d\tau = (1/\gamma)dt$ to obtain:

$$\tau(t) = \frac{1}{c}\int_{t_0}^{t} \sqrt{c^2 - \boldsymbol{v}(t')^2}\, dt' = \frac{1}{c}\int_{t_0}^{t} \sqrt{\eta\left(\frac{dx}{dt'}, \frac{dx}{dt'}\right)} dt'. \tag{4.35}$$

Energy-momentum 4-vector. Having defined the 4-velocity u^μ of a massive particle, we proceed to define its 4-momentum by multiplying by its rest mass:

$$p^\mu = m u^\mu = \gamma m(c, \boldsymbol{v}) = M(\boldsymbol{v})(c, \boldsymbol{v}). \tag{4.36}$$

Here $M(\boldsymbol{v}) = \gamma m$ is the relativistic mass of the particle. Since m is a Lorentz scalar, p^μ must transform as a 4-vector. Its time and space components are familiar to us:

$$p^0 = \gamma mc = E/c \quad \text{and} \quad (p^1, p^2, p^3) = \gamma m\boldsymbol{v} = \boldsymbol{p}. \tag{4.37}$$

Here, E is the relativistic energy (4.25) and $\boldsymbol{p}$ the relativistic momentum (4.21) of a particle moving at velocity $\boldsymbol{v}$. Thus, p^μ is also called the energy-momentum 4-vector. As a consequence, we have discovered that under Lorentz transformations, E/c and $\boldsymbol{p}$ transform as the time and space components of a 4-vector. In particular, the squared norm of p^μ is a Lorentz scalar:

$$p^2 = \eta(p,p) = m^2 u \cdot u = m^2 c^2. \tag{4.38}$$

We see that the 4-momentum of a massive particle[22] is time-like. Noting that $p^2 = E^2/c^2 - \boldsymbol{p}^2$, we recover the relativistic energy-momentum dispersion relation $E^2 = \boldsymbol{p}^2 c^2 + m^2 c^4$ (4.27). This relation is also called the mass-shell condition since it defines a 2 sheeted hyperboloid (‘shells’) in the 4d space of 4-momenta. The upper sheet with $E > 0$ is the physical one.

Gradient, divergence and d’Alembertian. The partial derivatives $\partial_\mu = (c^{-1}\partial_t, \boldsymbol{\nabla})$ of a scalar function on space-time are the components of a covector field:

$$\frac{\partial f}{\partial x^\mu} = \partial_\mu f = \left(c^{-1}\partial_t f, \partial_x f, \partial_y f, \partial_z f\right). \tag{4.39}$$

To get a 4-vector field, we contract with the inverse metric $\eta^{\mu\nu}$ to get the **4-gradient**

$$(\text{grad } f)^\mu = \partial^\mu f = \eta^{\mu\nu}\partial_\nu f = (c^{-1}\partial_t f, -\partial_x f, -\partial_y f, -\partial_z f). \tag{4.40}$$

The 4-gradient ∂^μ is a vector operator, it transforms like a 4-vector under Lorentz transformations. We may take the inner product of the 4-gradient ∂^μ with a vector field $v^\mu(x)$ to obtain a scalar field on space time, called the **4-divergence** of v:

$$\text{div } v = \eta_{\mu\nu}\partial^\mu v^\nu = \partial_\nu v^\nu = \frac{1}{c}\partial_t v^0 + \partial_x v^1 + \partial_y v^2 + \partial_z v^3. \tag{4.41}$$

The d’Alembertian is the analog of the Laplacian: it is a 2nd order operator, taking scalar fields to scalar fields, obtained via the composition $\Box = \text{div grad}$:

$$\Box f = \partial_\mu \partial^\mu f = \left(c^{-2}\partial_t^2 - \partial_x^2 - \partial_y^2 - \partial_z^2\right) f. \tag{4.42}$$

It is also called the *wave operator* as it appears in the wave equation for the propagation of sound (19.48), light or disturbances in a stretched string (17.6).

The concepts of Lorentz scalars and vectors help us reformulate the **principle of relativity**. All terms in the equations expressing laws of physics must transform in the same way (i.e., as Lorentz scalars, 4-vectors or tensors, etc.) under Lorentz transformations between inertial frames. Such an equation is said to be *Lorentz covariant*. This will ensure that the equations take the same form in all such frames.

---

[22] The 4-momentum of a massless particle is a null vector of the form $p^\mu = (\sqrt{\boldsymbol{p}\cdot\boldsymbol{p}}, \boldsymbol{p})$ since $E = |\boldsymbol{p}|c$ for a massless particle with positive energy.

Newton's 1^{st} **law** continues to hold in special relativity. In an inertial frame, a massive free particle travels in a straight line at constant speed. For example, the world lines of massive free particles that pass through the origin O at $t = 0$ are straight lines that lie within the future light cone with apex at O. This law may be given a variational formulation just like for a nonrelativistic free particle (see Prob. 3.14). Consider a curve in Minkowski space $x^\mu(\sigma)$ where $\sigma \in [a, b]$ is any parameter along the curve. It is called a time-like curve if the tangent vector $\frac{dx^\mu}{d\sigma}$ is a time-like vector for $a \le \sigma \le b$. Let us define the action of a time-like curve as its length, given by

$$S[x] = \frac{1}{c}\int_a^b \left[\eta\left(\frac{dx}{d\sigma}, \frac{dx}{d\sigma}\right)\right]^{1/2} d\sigma = \frac{1}{c}\int_a^b \left[c^2\left(\frac{dt}{d\sigma}\right)^2 - \left(\frac{d\boldsymbol{r}}{d\sigma}\right)^2\right]^{1/2} d\sigma. \tag{4.43}$$

This action is invariant under reparametrization of the curve: $S[x] = S[\tilde{x}]$ if $\tilde{x}(\sigma) = x(f(\sigma))$ where $f : [a, b] \to [a, b]$ is a monotonic differentiable function. Comparing with (4.35), we see that $S[x]$ is the total proper time elapsed on a clock carried by an observer moving along the curve. The world line of a massive free particle that travels from $x(a)$ to $x(b)$ is a curve that extremizes the length S. Such a curve is a time-like geodesic (see Sect. 3.27*): a straight line in a space-time diagram with slope exceeding one (see Fig. 4.6 and Prob. 4.16). Massless particles travel along null geodesics: solutions of the geodesic equation with respect to the Minkowski metric with null tangent vectors[23]. These are simply straight lines with unit slope in a space-time diagram.

Newton's 2^{nd} **law.** The acceleration 4-vector $a^\mu = du^\mu/d\tau$ helps us formulate a Lorentz-covariant generalization of Newton's 2^{nd} law (3.2) for a particle of rest mass m:

$$\frac{dp^\mu}{d\tau} = m\frac{du^\mu}{d\tau} = (\text{force})^\mu. \tag{4.44}$$

For example, a particle of charge e in an electromagnetic field feels the Lorentz force

$$\frac{dp^\mu}{d\tau} = eF^{\mu\nu}\frac{u_\nu}{c}, \quad \text{where} \quad F_{\mu\nu} = \partial_\mu A_\nu - \partial_\nu A_\mu \tag{4.45}$$

is the covariant electromagnetic field strength tensor and $F^{\mu\nu} = \eta^{\mu\rho}\eta^{\nu\sigma}F_{\rho\sigma}$. The gauge potential $A^\mu = (\phi, \boldsymbol{A})$ includes the scalar and vector potentials (introduced in Sect. 3.23*) for the electric and magnetic fields $\boldsymbol{E} = -c^{-1}\partial_t\boldsymbol{A} - \boldsymbol{\nabla}\phi$ and $\boldsymbol{B} = \boldsymbol{\nabla}\times\boldsymbol{A}$ (see Prob. 4.17 and Prob. 4.18).

Remark. Newton's third law [which states that if body A exerts a force on body B then B must exert an equal and opposite force on A, see Sect. 3.3] does not have a straightforward generalization to special relativity. Among other things, signals cannot be transmitted instantaneously, so we cannot consistently speak of instantaneous and simultaneous forces between bodies that are space-like separated. On the other hand, one of the main consequences of Newton's third law, which is that the total momentum of an isolated system is conserved (see Prob. 3.8) does continue to hold in special relativistic mechanics, with the relativistic definition of momentum (4.21). ☐

---

[23] Unlike for time-like curves, arc length cannot be used to parametrize curves with null tangents, such as null geodesics. If t is a parameter along a curve $x^\mu(t)$ with null tangents, then $\eta(\dot{x}, \dot{x}) = 0$ and as a consequence, the arc length (4.35) vanishes.

4.11 Problems

1. Estimate the **magnitude of relativistic effects** by evaluating v^2/c^2 for (a) a tennis ball served at the speed $v = 100$ km/h and (b) the Earth's motion at a speed of 30 km/s around the Sun.
2. Recall the **space-time diagram** in Fig. 4.3 showing the world lines of two inertial observers A and B in relative motion, along with light signals to and from events E_1 and E_2. It was drawn in a frame in which A is at rest and in units where $c = 1$. Redraw the diagram in a frame in which B is at rest.
3. Try to give an example to illustrate that if **Lorentz transformations** were nonlinear, then a free particle in one inertial frame could appear not to be free in another inertial frame, in violation of **Newton's first law**.
4. Try to suggest a reason why x' and t' must not depend on y and z in the proposed formula for a **Lorentz transformation** (4.2) to a frame S' moving along the x direction relative to the inertial frame S.
5. Suppose $E_1(t_1, \boldsymbol{r}_1)$ and $E_2(t_2, \boldsymbol{r}_2)$ are a pair of events in frame S. Show that the **square of the space-time interval** between them

$$c^2(t_2 - t_1)^2 - (x_2 - x_1)^2 - (y_2 - y_1)^2 - (z_2 - z_1)^2, \tag{4.46}$$

is unchanged under the Lorentz transformation (4.7) to frame S'.

6. Suppose at time t in inertial frame S, a light **wavefront** lies on the sphere $x^2 + y^2 + z^2 = (ct)^2$. Show using the Lorentz boost to frame S' that $x'^2 + y'^2 + z'^2 = (ct')^2$.
7. Two events A, B have coordinates (x_A, t_A) and (x_B, t_B) in inertial frame S with $L = x_B - x_A$ and $T = t_B - t_A$. Suppose one or both of L and T is negative. Formulate the concepts of **space-like, time-like and light-like separation** in this case, as done in Sect. 4.6.
8. In Einstein's **velocity addition formula** (4.16), suppose $u'_x < c$ and $v < c$. then show that $u_x < c$. Interpret the result.
9. **Rapidity.** Einstein's velocity addition formula (4.16) simplifies when expressed in terms of rapidities. Suppose we write $u_x/c = \tanh \zeta''$, $u'_x/c = \tanh \zeta'$ and $v/c = \tanh \zeta$. Then show that $\tanh \zeta'' = \tanh(\zeta + \zeta')$.
10. Show that

$$\int \frac{m\boldsymbol{v} \cdot d\boldsymbol{v}}{\sqrt{1 - \boldsymbol{v}^2/c^2}} = -mc^2\sqrt{1 - \boldsymbol{v}^2/c^2} + \text{constant}. \tag{4.47}$$

11. Show that $1 + \gamma^2 \boldsymbol{v}^2/c^2 = \gamma^2$ where $\gamma = (1 - \boldsymbol{v}^2/c^2)^{-1/2}$.
12. Show that the relativistic **energy-momentum dispersion relation** $E^2 - \boldsymbol{p}^2c^2 = (mc^2)^2$ (4.27) reduces to $E = \boldsymbol{p}^2/2m$ in the nonrelativistic limit.

13. Assuming space is 2-dimensional, draw the surface in the $E - p_1 - p_2$ space defined by the relativistic **energy-momentum dispersion relation** $E^2 - \boldsymbol{p}^2 c^2 = (mc^2)^2$ and describe it. The dispersion relation is also called the mass-shell condition or hyperboloid. Why?

14. Verify that the **Lorentz boost** by speed v along x represented by the matrix Λ in (4.29) is an **isometry of the Minkowski metric** η.

15. Show that the **composition of two Lorentz boosts** along x with rapidities ζ_1 and ζ_2 (4.30) is a boost along x with rapidity $\zeta_1 + \zeta_2$.

16. Show that the Euler-Lagrange variational equations following from the massive free particle action $S[x^\mu]$ (4.43) are $\ddot{x}^\mu(\sigma) = 0$. Use $t = x^0/c$ to parametrize these geodesics and demonstrate that they are straight lines parametrized by time in 3d space. What restriction does the condition of being a **time-like geodesic** impose?

17. Show that the **electric and magnetic fields** $\boldsymbol{E} = -c^{-1}\partial_t \boldsymbol{A} - \boldsymbol{\nabla}\phi$ and $\boldsymbol{B} = \boldsymbol{\nabla} \times \boldsymbol{A}$ with Cartesian components $E^i, B^i = \epsilon^{ijk}\partial_j A^k$ can be expressed in terms of the **field strength** $F_{\mu\nu} = \partial_\mu A_\nu - \partial_\nu A_\mu$ (here $A^\mu = (\phi, \boldsymbol{A})$):

$$F^{0i} = \partial^0 A^i - \partial^i A^0 = -E^i \quad \text{and} \quad F^{ij} = \partial^i A^j - \partial^j A^i = \partial_j A^i - \partial_i A^j = -\epsilon^{ijk} B^k. \tag{4.48}$$

Use $F_{\mu\nu} = \eta_{\mu\rho}\eta_{\nu\sigma}F^{\rho\sigma}$ to show that $F_{0i} = -F^{0i}$ and $F_{ij} = F^{ij}$ and

$$F^{\mu\nu} = \begin{pmatrix} 0 & -E^1 & -E^2 & -E^3 \\ E^1 & 0 & -B^3 & B^2 \\ E^2 & B^3 & 0 & -B^1 \\ E^3 & -B^2 & B^1 & 0 \end{pmatrix} \quad \text{and} \quad F_{\mu\nu} = \begin{pmatrix} 0 & E^1 & E^2 & E^3 \\ -E^1 & 0 & -B^3 & B^2 \\ -E^2 & B^3 & 0 & -B^1 \\ -E^3 & -B^2 & B^1 & 0 \end{pmatrix}. \tag{4.49}$$

18. **Nonrelativistic limit.** For a charged particle that moves slowly compared to light $\boldsymbol{v}^2/c^2 \ll 1$, show that the spatial components of (4.45) reduce to the nonrelativistic **Lorentz force** equation in the lab frame: $\dot{\boldsymbol{p}} = e(\boldsymbol{E} + (\boldsymbol{v}/c) \times \boldsymbol{B})$. Show that the time component of (4.45) reduces to the **energy evolution equation**: $\frac{dE}{dt} = e\boldsymbol{E} \cdot \boldsymbol{v}$. This is the rate at which the Lorentz force does work on the particle; the magnetic field does not contribute.

Chapter 5

Dynamics viewed as a vector field on state space

We have already encountered the Newtonian, Euler-Lagrange, Hamiltonian and Poisson bracket formulations of (nonrelativistic) mechanics. In this chapter, we place mechanical systems in the framework of dynamical systems by viewing them in terms of vector fields[1] on the state space, a viewpoint that Henri Poincaré emphasized. This allows us to view a mechanical system as defining a flow on its state space in a manner similar to the flow of a fluid in a container. The essential idea (Sect. 5.1) is to write the equations of motion as first order equations by introducing enough additional variables (like momenta). Hamilton's equations are particularly well suited for such an interpretation as they are first order in time. The interpretation in terms of vector fields allows us to obtain qualitative information on the dynamics even if explicit analytic solutions of the equations of motion (EOM) are not available. Here, tools such as phase portraits and the study of static (fixed points) or periodic solutions and their stability and basins of attraction/repulsion can provide valuable insight into the short as well as long-time behavior of solutions. We first study vector fields on one-dimensional state spaces (such as the real line and circle, in Sect. 5.2*). Questions of existence and uniqueness of solutions as well as the possibility of solutions blowing up in finite time are addressed in Sect. 5.3 and illustrated with simple examples. We then proceed in Sect. 5.4* to examine vector fields on the plane, where new types of fixed points and time-dependent solutions (limit cycles, homoclinic orbits) can arise. The viewpoint in terms of vector fields is very general and applies both to conservative and dissipative systems as well as those that are subject to external driving. We end the chapter with a discussion of the Poincaré-Bendixon theorem which restricts what a (time-independent) vector field on the plane can do, essentially ruling out chaotic behavior. Examples of chaotic behavior in systems with three-dimensional and four-dimensional phase spaces will be discussed in Chap. 15.

5.1 Vector fields from Newtonian and Hamiltonian dynamics

Vector fields and their integral curves. We are familiar with the concept of a vector field on the x-y plane: it is a vector-valued function with Cartesian components $\boldsymbol{v}(x,y) = (u(x,y), v(x,y))$ which defines a vector[2] (or arrow) at each point on the plane (see Fig. 5.1). Given such a vector field, we may profitably view it as the velocity field of a steadily flowing fluid. Then we may imagine placing a tiny 'test particle' at a point on the plane and recording its trajectory as it is carried along by the fluid flow. Such a trajectory is called an integral curve or 'field line' of the vector field. More accurately, *integral curves* are curves $(x(t), y(t))$ on the plane that are everywhere tangent to $\boldsymbol{v}$ (see Fig. 5.1 and Prob. 5.1):

---

[1] Vector fields in the differential geometric setting of manifolds and tensor fields and their behavior under changes of coordinates are discussed in Appendix B.

[2] It is important that these vectors be tangent to the plane or 'lie on the plane'. Similarly, a smooth vector field on a sphere consists of a smoothly varying distribution of tangent vectors at each point on the sphere.

$$(\dot{x}, \dot{y}) = (u(x, y), v(x, y)). \tag{5.1}$$

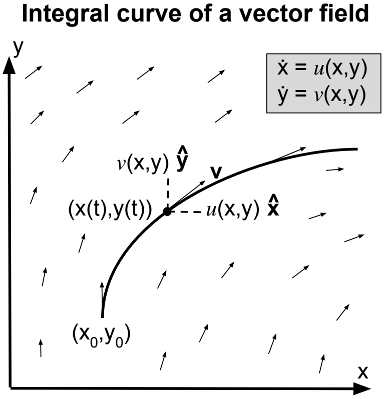

Figure 5.1: Integral curve through the point (x_0, y_0) of a vector field on the x-y plane.

The integral curve that passes through (x_0, y_0) at $t = 0$ is the solution of this pair of ordinary differential equations (ODEs) subject to the initial condition $x(0) = x_0$ and $y(0) = y_0$. Provided this initial value problem (IVP) admits unique solutions (see Fig. 5.2 and Sect. 5.3), we would have an integral curve passing through every point of the phase plane.

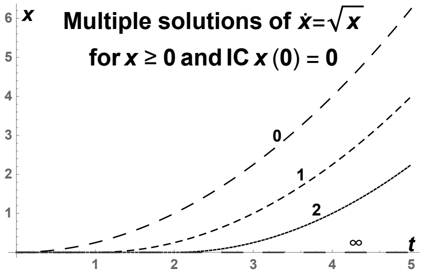

Figure 5.2: Nonunique solutions of the initial value problem for the 1d vector field $\dot{x} = \sqrt{x}$ for $x \geq 0$ with $x(0) = 0$. The four curves display $x(t) = (t - t_0)^2/4$ for $t \geq t_0$ and $x(t) = 0$ for $0 \leq t \leq t_0$ with $t_0 = 0, 1, 2, \infty$.

Vector fields arise in other physical contexts as well: the electric or magnetic field around charges, currents and magnets as well as the gravitational field around a massive object. The field lines of an electric or magnetic or gravitational field are defined in a similar way, via the above pair of 1st order ODEs. However, it is important to bear in mind that an integral curve of the electric, magnetic or gravitational field is *not* the trajectory of a test charge or mass in such a field, since the Newton-Lorentz equation for a charge ($m\ddot{\boldsymbol{r}} = q(\boldsymbol{E} + \dot{\boldsymbol{r}} \times \boldsymbol{B})$) or Newton's equation for a massive particle ($m\ddot{\boldsymbol{r}} = F_{\text{gravity}}$) are second order and relate these force fields to acceleration rather than velocity.

More generally, a vector field $v^i(\xi)$ on an n-dimensional state space with coordinates $\xi = (\xi^1, \ldots, \xi^n)$, is associated with a system of n first order ODEs

$$\dot{\xi}^i(t) = v^i(\xi) \quad \text{for} \quad i = 1, 2, \ldots, n. \tag{5.2}$$

While time t is the only independent variable, the dynamical variables ξ^i are called dependent variables. A state space along with a vector field to specify time evolution via (5.2) defines for us a dynamical system.

Newtonian and Hamiltonian vector fields. Though dynamical systems arise in various areas of science and engineering [122] we will primarily be concerned with mechanical ones. For instance, Newton's second law ($m\ddot{\boldsymbol{r}} = \boldsymbol{F}$) defines[3] a vector field on the 6-dimensional position-momentum state space:

$$\dot{\boldsymbol{r}} = \frac{\boldsymbol{p}}{m} \quad \text{and} \quad \dot{\boldsymbol{p}} = \boldsymbol{F}. \tag{5.3}$$

Similarly, Hamilton's equations may be viewed as defining a vector field on the state space of positions and momenta, usually referred to as the phase space of the mechanical system. For one degree of freedom, if we consider q and p as coordinates on the phase plane, then Hamilton's equations (3.78) define the Hamiltonian vector field

$$(\dot{q}, \dot{p}) = v_H = \left(\frac{\partial H}{\partial p}, -\frac{\partial H}{\partial q}\right), \tag{5.4}$$

for a differentiable Hamiltonian function H. Due to the minus sign and the reversed order of q and p, we call v_H the symplectic-gradient of H. For n degrees of freedom, if we use $(q^1, \ldots, q^n, p_1 \ldots, p_n)$ as coordinates on phase space, the components of the Hamiltonian vector field are

$$v_H = \left(\frac{\partial H}{\partial p_1}, \cdots, \frac{\partial H}{\partial p_n}, -\frac{\partial H}{\partial q^1}, \cdots, -\frac{\partial H}{\partial q^n}\right). \tag{5.5}$$

The components of the Hamiltonian vector field can be expressed succinctly in terms of the antisymmetric $2n \times 2n$ Poisson tensor r^{ij} introduced in (3.134). Suppose $\xi^1, \ldots, \xi^{2n}$ are coordinates on phase space, consisting of the coordinates and momenta as in (3.133), then verify that

$$v_H^i = r^{ij} \frac{\partial H}{\partial \xi^j} \equiv r^{ij} \partial_j H \quad \text{for} \quad i = 1, \cdots, 2n. \tag{5.6}$$

When invertible, the inverse of r^{ij} is the symplectic form (3.144), justifying the name symplectic gradient for $r^{ij}\partial_j H$. The integral curves of the Hamiltonian vector field[4] are simply the trajectories of the mechanical system. Thus, Hamiltonian mechanics is the study of a special class of vector fields on phase space. Vector fields arise in other ways as well. For instance, the velocity field of a steadily flowing fluid defines a vector field in the container. In fact, given any vector field on a manifold, it is conventional to speak of the flow that it generates via (5.2); we thus have *Hamiltonian flow* $\dot{\xi}^i = r^{ij}\partial_j H$ on phase space.

---

[3] The force $\boldsymbol{F}$ here could depend on position, velocity and time, it need not be conservative.

[4] In fact, given any observable (function on phase space $f(\xi)$), we may define the associated canonical vector field via its components $v_f^i = r^{ij}\partial_j f$, see Sect. 3.26*

Phase portraits, fixed points and basin of attraction. Now we introduce some basic notions concerning vector fields. A sketch of the pattern of integral curves of a vector field (with arrows indicating the direction of time) is called a *phase portrait* of the vector field (see Fig. 5.3). The *zeros* of a vector field are the points ξ_* on phase space where all components of the vector field vanish: $v^i(\xi_*) = 0$ for $i = 1, 2, \cdots, n$. A zero ξ_* of a vector field is also called a *fixed point*, it is a static or time-independent solution of (5.2). If the vector field is the velocity field of a steadily flowing fluid, then a fixed point is a stagnation point: one where the fluid is at rest.

A fixed point ξ_* is an attractor if all trajectories that begin in a sufficiently small neighborhood approach ξ_* as $t \to \infty$. A fixed point may be called a *repeller* if all trajectories that begin in a sufficiently small neighborhood, when evolved backward in time approach ξ_* as $t \to -\infty$ (see Fig. 5.3). The *basin of attraction* of a fixed point ξ_* is the set of ICs ξ_0 for which $\xi(t) \to \xi_*$ as $t \to \infty$ (sometimes, one defines the basin of attraction as the closure of this set). If the basin of attraction is the whole phase space, we say that ξ_* is a global attractor. In addition, there are various notions of stability of a fixed point. We will encounter some of these in Sect. 5.2*, Sect. 6.1 and Sect. 6.2.

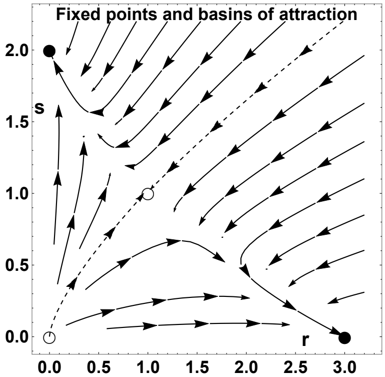

Figure 5.3: Phase portrait of the competitive Lotka-Volterra vector field $\dot{r} = r(3 - r - 2s)$ and $\dot{s} = s(2 - s - r)$ in the first quadrant of the r-s plane. The nonnegative variables r and s may be regarded as the populations of rabbits and sheep (in suitable units) that compete for resources in a common plot of land. There is a repelling fixed point at (0,0) and attractors at (0,2) and (3,0). The basins of attraction of (3,0) and (0,2) consist of points below and above the dashed integral curves (separatrices) that lead to (1,1). The fixed point at (1,1) where rabbits and sheep coexist is neither an attractor nor a repeller. Trajectories that start close to the fixed point (0,0) flow to one of the other three fixed points as $t \to \infty$. They are called heteroclinic trajectories, a concept to be defined in Sect. 5.4*.

Autonomous & nonautonomous systems. The system $\dot{\xi}^i = v^i$ is *autonomous* if the RHS does not depend explicitly on time, $v^i = v^i(\xi, \not{t})$. A Hamiltonian system is autonomous if the Hamiltonian does not depend explicitly on time. A *steadily flowing* fluid (i.e., one for which the velocity field is independent of time) defines an autonomous system of equations $\dot{\xi}^i = v^i(\xi)$. The integral curves of the velocity field of a steadily flowing fluid are its streamlines (see Sect. 19.3): they may be regarded as trajectories of test particles (specks of dust) released into and carried by the flow.

A nonautonomous system of n ODEs $\dot{\xi}^i = v^i(\boldsymbol{\xi}, t)$ can be turned into an autonomous one by introducing an extra dependent variable $\xi^{n+1} = t$, so that

$$\begin{pmatrix} (\dot{\xi}^i)_{1 \le i \le n} \\ \dot{\xi}^{n+1} \end{pmatrix} = \begin{pmatrix} (v^i(\boldsymbol{\xi}, \xi^{n+1}))_{1 \le i \le n} \\ 1 \end{pmatrix}. \tag{5.7}$$

Hence, a time-dependent vector field on $\mathbb{R}^n$ may be viewed as a time-independent vector field on $\mathbb{R}^{n+1}$. For this reason, we will often restrict attention to autonomous systems. While this trick of rewriting a time-dependent vector field as a time-independent one can provide an alternate viewpoint, it comes at a cost: it increases the dimension of the state space by one and can convert a linear system into a nonlinear one (see below). Moreover, it hardly makes a dent in the problem of solving the ODEs.

Linear and nonlinear vector fields. If the components $v^i(\xi)$ of the vector field are nonlinear functions of the coordinates ξ, then the vector field and associated system (5.2) are said to be *nonlinear*. In particle mechanics, the Newtonian or Hamiltonian vector field in Cartesian coordinates is linear if the force is linear or the potential is quadratic, as in a harmonic oscillator, where

$$\dot{x} = p/m \quad \text{and} \quad \dot{p} = -kx. \tag{5.8}$$

Evidently, whether a vector field is linear or nonlinear depends on the coordinates used. A change of coordinates can convert a linear vector field into a nonlinear one (though the opposite cannot always be done[5]). Most vector fields are nonlinear in the coordinates in which they naturally arise and can display remarkably rich phenomena.

5.2* Vector fields in one dimension

Perhaps the simplest vector fields are those in one dimension[6], such as on the real line $\mathbb{R}$ ($\dot{x} = v(x)$) or on the circle S^1 ($\dot{\theta} = v(\theta)$). However, such vector fields do not arise directly from Newton's equation since a particle with one degree of freedom has a 2d state space on account of the second order nature of Newton's 2nd law. Interestingly, one *does* get a vector field in 1d in an inertialess limit of a Newtonian particle subject to a frictional force, $m\ddot{x} = F(x,t) - \gamma\dot{x}$ (1.4). In fact, suppose the effects of the damping and external forces $-\gamma\dot{x}$ and F are so large that we may ignore the inertial term $m\ddot{x}$. Then we arrive at the *first order* equation[7]

---

[5] The desired linearizing transformation may not exist or may not be nice enough (e.g., smooth). For instance, if one tries to construct it using a series, the series may not converge.

[6] Flows in 1d can sometimes capture some essential features of higher dimensional flows. Due to dissipation, higher dimensional flows can sometimes undergo a 'dimensional reduction' after transients die out and behave in effect like 1d flows.

$$\dot{x} = v(x,t) \equiv (1/\gamma)F(x,t). \tag{5.9}$$

If we further assume that the external force F is independent of time, then we arrive at the autonomous equation

$$\dot{x} = v(x) \quad \text{with} \quad x(0) = x_0. \tag{5.10}$$

Another physical interpretation of this equation is that v represents the velocity field of a fluid flowing steadily on the line and $x(t)$ is the trajectory of an infinitesimal test particle that is released into the flow at x_0. Such an equation can be reduced to quadrature (evaluation of an integral)

$$\int_0^t dt' = t = \int_{x_0}^{x} \frac{dx'}{v(x')}. \tag{5.11}$$

In favorable cases, the integral can be evaluated in closed form to give t as a function of x. The result would have to be inverted to find $x(t)$. This is rarely feasible (see Prob. 5.4).

Qualitative behavior of 1d vector fields. Even without an explicit expression for $x(t)$, much qualitative insight may be gained by studying the geometric nature of $v(x)$, as emphasized by Poincaré. To begin with, we have a static solution $x(t) \equiv x_*$ for all t at each zero (or fixed point) of v. On the other hand, if $v(x) \neq 0$, then the particle moves to the right or left at x depending on whether $v(x)$ is positive or negative respectively. Moreover, the 'acceleration' is given by $\ddot{x} = v'(x)\dot{x} = vv'$. So if $v > 0$ and $v' > 0$, then the phase point speeds up as it moves to the right. If $v > 0$ and $v' < 0$, then the phase point slows down as it moves to the right (see Fig. 5.5). This means the graph of x as a function of t is convex from below if $v > 0$ and $v' > 0$ and concave from below if $v > 0$ and $v' < 0$. Similarly, if $v < 0$ and $v' > 0$ then the particle speeds up as it moves to the left and the graph of x vs t is concave from below. Finally, if $v, v' < 0$, $\ddot{x} > 0$ and the particle slows down as it moves to the left: $x(t)$ is a convex from below. Given a graph of $v(x)$, these observations, are enough to get a qualitative understanding of trajectories. The following examples serve to illustrate these features.

---

[7] The character of Newton's equation changes significantly when we ignore the inertia term and arrive at a first order equation. The inertia term is said to be a singular perturbation of the inertialess damped equation as it increases the order by one and requires an additional initial condition. Some of our intuition about particle mechanics, such as the ubiquity of oscillations, no longer applies. The ways in which a singular perturbation can alter the nature of an equation is loosely captured in an amusing analogy mentioned by Michael Berry, which is paraphrased here. If you bite into an apple and swallow a piece of it but see $3/4^{\text{ths}}$ of a worm (maggot) in the remainder, then it is bad. If you see half a worm leftover, it is worse. This is like a nonsingular perturbation. Taking things a step further, if you bite into an apple and see no worm leftover you think you are safe, but that may not be the case! This is akin to a singular perturbation!

Inertialess damped spring. For instance, consider $\dot{x} = v(x) = -kx$, where x may be thought of as the extension of an inertialess ($m = 0$) spring governed by a linear restoring force with force constant (per unit damping coefficient) $k > 0$. There is only one fixed point ($x_* = 0$) corresponding to zero extension of the spring. As shown in Fig. 5.4, the flow is towards the fixed point from either side since $v(x) > 0$ for $x < 0$ and vice versa. The spring monotonically returns (without any oscillation) to its unextended length when stretched or compressed. It is as though the massless spring moves through a very viscous medium preventing oscillations.

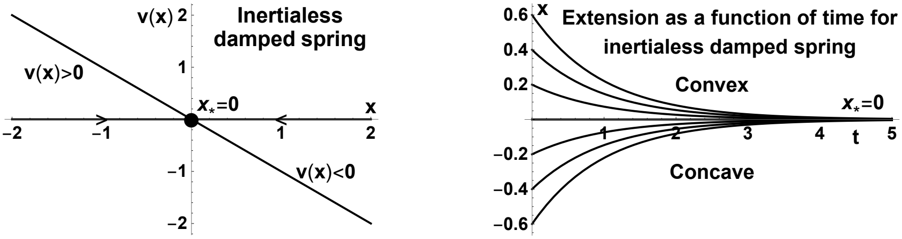

(a) (b)

Figure 5.4: (a) Phase portrait for the extension x of an inertialess damped spring $\dot{x} = -kx$ with $k = 1$. The flow is directed towards the stable fixed point $x_* = 0$. (b) Graph of $x(t)$ showing monotonic approach of x to fixed point value 0 from various initial extensions $x(0)$. Notice that the graph is convex from below if $x(0) > 0$ and concave from below if $x(0) < 0$.

RC circuit. In an RC circuit, the dynamical variable is the charge $Q(t)$ that builds up on a capacitor of capacitance C, when connected in series at $t = 0$ to a resistance R and a DC battery with constant voltage V. The battery voltage V is then the sum of the voltage drops IR and Q/C across the resistor and capacitor where $I = \dot{Q}$ is the current. The resulting evolution equation is

$$\dot{Q} = \frac{V}{R} - \frac{Q}{RC} = v(Q). \tag{5.12}$$

There is a unique fixed point $Q_* = CV$ with the flow being towards it both from $Q > Q_*$ and $Q < Q_*$. The charge Q monotonically approaches Q_* (see Fig. 5.5), though we will see that it takes infinitely long to do so (see Prob. 5.3).

Stability of fixed points. Fixed points may be classified by their stability. In the above examples, $x_* = 0$ and $Q_* = CV$ are both stable fixed points[8] as the flow is directed towards them in both directions. A third possibility is provided by the half-stable fixed point at the origin for the vector field $v(x) = \alpha x^2$ with $\alpha > 0$. Notice from Fig. 5.6 that trajectories either go off to ∞ or approach the fixed point $x = 0$ in a monotonic fashion.

---

[8] In fact, they are globally stable. For instance, the charge on the capacitor always tends asymptotically to $Q_* = CV$ irrespective of the initial charge.

[9] As the name 'linear stability' suggests, nonlinear effects can alter/reinforce conclusions of a linear stability analysis. This is especially so if the linearization vanishes. Nonlinear effects typically cannot render a linearly stable fixed point unstable to sufficiently small perturbations. On the other hand, nonlinear effects can prevent a linear instability from growing without bound. For more on the robustness of the linear approximation, see Sect. 6.7*

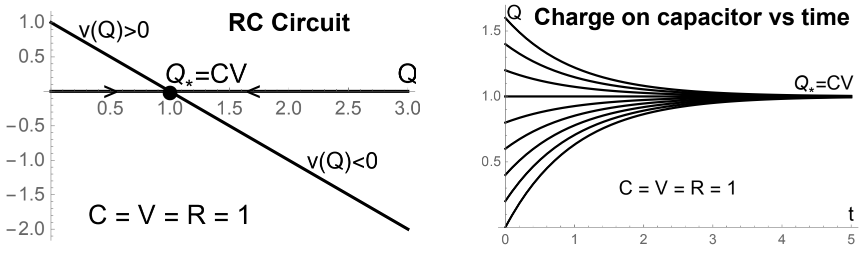

(a) (b)

Figure 5.5: (a) Obtaining the phase portrait for the charge in an RC circuit. The flow is directed towards the stable fixed point Q_*. (b) Exponentially fast approach of charge to fixed point value CV from various initial charges $Q(0)$.

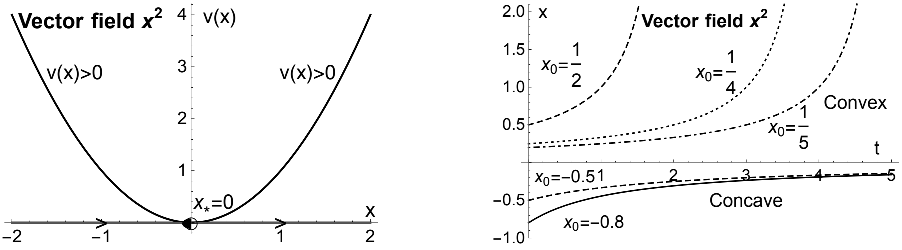

(a) (b)

Figure 5.6: (a) Phase portrait for $\dot{x} = \alpha x^2$ with $\alpha = 1$ showing rightward flow and the half-stable fixed point at $x_* = 0$. (b) Graph of solutions $x(t) = x_0/(1 - x_0 t)$ showing they are concave from below for $x(0) = x_0 < 0$ and convex from below for $x_0 > 0$. Solutions with $x_0 > 0$ blow up at $t = 1/x_0$.

Linear stability[9]**.** The stability/instability of a fixed point x_* may be quantified by a decay/growth rate that controls how fast the phase point approaches or leaves the fixed point from its immediate vicinity. It is obtained by linearizing the vector field in the neighborhood of the fixed point x_*:

$$\dot{x} = v(x) = \cancel{v(x_*)} + v'(x_*)(x - x_*) + \ldots \approx v'(x_*)(x - x_*), \qquad (5.13)$$

where we dropped higher order terms assuming $v'(x_*) \neq 0$. The vector field has now become a linear function of x. The solution with IC $x(0) = x_0 \approx x_*$ is

$$x(t) = x_* + (x_0 - x_*)e^{v'(x_*)t} \quad \text{for small} \quad |x - x_*|. \qquad (5.14)$$

We see that the trajectory moves away or towards x_* according as $v'(x_*)$ is positive or negative. We say the fixed point x_* is linearly unstable or stable in these two cases. In the RC circuit, $v'(Q_*) = -1/RC < 0$ so that the fixed point is linearly stable. When $v'(x_*) < 0$, (5.14) can be trusted for all $t > 0$ and in fact becomes increasingly accurate with $x \to x_*$ as $t \to \infty$. This explains why it took infinitely long for the nonconstant solutions in the above examples to approach the stable fixed points (see Fig. 5.4b). On the other hand, when $v'(x_*) > 0$, the exponentially growing solution cannot always be trusted for very long, as $|x - x_*|$ would become large. Ignored nonlinear effects, if any, would become important. In the example of Prob. 5.4, this exponential growth away from the unstable fixed points is soon superseded by *nonlinear saturation* effects as $x(t)$ approaches a stable fixed point value as $t \to \infty$.

When $v'(x_*) \neq 0$, the characteristic time $\tau(x_*) = 1/|v'(x_*)|$ is the exponential growth or decay time scale. It controls how quickly a trajectory leaves or approaches x_*. For instance, if x_* is linearly stable, a smaller τ would indicate a more rapid approach to equilibrium and greater stability. For a linearly unstable fixed point, a shorter τ would mean greater instability. When $v'(x_*)$ vanishes, this linear stability analysis is inconclusive and the fixed point is said to be of neutral or marginal stability. One could include higher order terms in (5.13) to try to understand its stability in a nonlinear sense.

Flows on $\mathbb{R}$ as gradient flows. We have seen that fixed points of flows on the real line tend to have large basins of attraction or repulsion (intervals, rays, etc). Since the whole basin of attraction/repulsion evolves to the fixed point as $t \to \pm\infty$, the flow does not preserve lengths of intervals on the line (see also Liouville's theorem in Sect. 10.8) and suggests that they are not conservative. The monotonic approach to equilibrium and lack of any oscillations also indicates that they describe dissipative processes where some 'potential energy' is monotonically decreasing along the flow. Can we find such a monotonically decreasing function? Yes! In fact, suppose $-\phi$ is an antiderivative for v, i.e., $v(x) = -\phi'(x)$. ϕ may be viewed as a potential energy (or velocity potential in fluid mechanics, see Footnote 30 in Sect. 19.11). Then the flow equation becomes

$$\dot{x} = -\phi'(x). \tag{5.15}$$

In other words, we have expressed the vector field as the gradient of a potential: this is always possible for vector fields on the real line since the potential can be taken as

$$\phi(x) = -\int_0^x v(x')dx' \tag{5.16}$$

Replacing 0 with a different lower limit would add an inconsequential constant to ϕ. Such a flow is called a gradient flow. Now consider

$$\frac{d\phi}{dt} = \phi'(x)\frac{dx}{dt} = -\phi'(x)^2 \leq 0. \tag{5.17}$$

Thus we see that the potential ϕ is monotonically decreasing (nonincreasing) along the flow. Such a function ϕ is sometimes called a *Lyapunov* function. In particular, x cannot return to its initial value or oscillate since then ϕ too would have to return to its initial value. Thus, there can be no nonconstant periodic solutions. The phase point, if it does not start at a fixed point, must approach a fixed point or $\pm\infty$ monotonically as in the examples above (see Fig. 5.6a). We may view $\dot{x} = -\phi'(x)$ as an inertialess limit ($m \to 0$) of Newton's equation $m\ddot{x} = -\gamma\dot{x} - \phi'(x)$ for a particle moving in the potential $\phi(x)$ subject to a damping force of strength $\gamma = 1$. Roughly, by ignoring the inertia term, we have exaggerated the effect of damping, thereby eliminating the possibility of oscillations.

Vector fields on a circle. These provide the simplest examples of dynamical systems that can display oscillations. The integral curves of a vector field $v(\theta)$ on a circle are solutions of $\dot\theta = v(\theta)$. Here, the angular coordinate θ (considered modulo 2π) parametrizes points on a circle, with θ increasing counterclockwise. In particular, $v(\theta)$ must be 2π-periodic so that the vector field is singlevalued. Let us consider a couple of simple examples. (a) The *constant vector field* $v(\theta) = \omega \neq 0$ describes uniform oscillations with time period $T = 2\pi/|\omega|$. Indeed, $\theta = \theta_0 + \omega t$ describes a phase point rotating uniformly (counterclockwise if $\omega > 0$) at angular velocity ω. This vector field has no fixed points (see Fig. 5.7a)! (b) *Inertialess damped pendulum.* In suitable units, $\dot\theta = -\sin\theta$ describes a damped simple pendulum subject to downward gravity (see Chap. 7) with the inertial acceleration term ignored. The fixed points $\theta = 0, \pi$ (mod 2π) lie at the bottom and top of the circle as shown in Fig. 5.7b. The flow is clockwise on the right semicircle and counterclockwise on the left. Thus $\theta = 0$ (bob hanging down) is stable while $\theta = \pm\pi$ (bob pointing up) is unstable. All trajectories other than the constant one at $\theta = \pi$ eventually end up at the attractive fixed point $\theta = 0$. See Prob. 5.6 for a combination of these two examples.

Unlike on $\mathbb{R}$, most vector fields on the circle are not gradient vector fields. As before, one is tempted to define the potential $\phi(\theta) = -\int_0^\theta v(\theta')d\theta'$ which satisfies $\phi'(\theta) = -v(\theta)$. However, ϕ is typically not a singlevalued function on the circle. Indeed, $\phi(0) = 0$ while $\phi(2\pi) = \int_0^{2\pi} v(\theta)d\theta$ is nonzero unless v happens to have zero average. Thus ϕ is generally *not* a 2π-periodic function of θ and the argument leading to (5.17) does not hold. In other words, a phase point on a circle *can* return to its initial state, as for the constant vector field above.

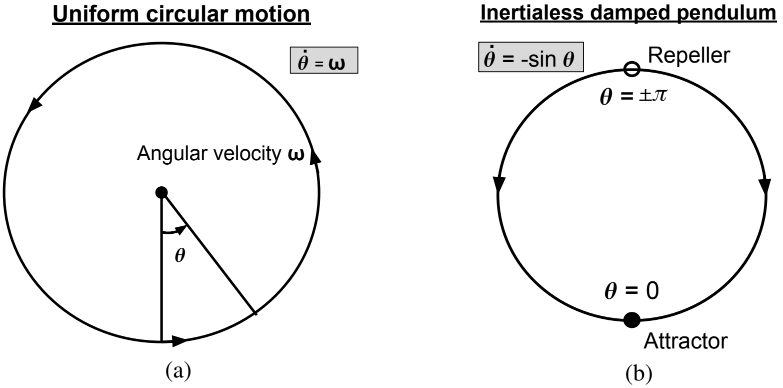

(a) (b)

Figure 5.7: Vector fields on the circle. (a) Constant vector field with no fixed points. (b) Inertialess damped pendulum with an attractor and a repeller. All nonconstant integral curves are heteroclinic trajectories (see Sect. 5.4*) that approach the two fixed points as $t \to \pm\infty$.

5.3 Existence and uniqueness of solutions

Given the 1d vector field $v(x)$, when can we guarantee that the initial value problem (IVP) $\dot x = v(x)$, $x(0) = x_0$ has a unique solution that exists for some time t? We begin with examples that illustrate how existence and/or uniqueness can fail.

Failure of existence: Let us consider the vector field

$$v(x)=\begin{cases}-c & \text{if} \quad x>0\\ +c & \text{if} \quad x\le 0 \quad \text{where} \quad c>0 \quad \text{is a constant speed,}\end{cases} \tag{5.18}$$

and the corresponding IVP $\dot{x}=v(x)$ with $x(0)=0$. We notice that $x=0$ is not a fixed point, so x cannot stay there. Since $v(0)=c$, the phase point wants to move to the right. However, for arbitrarily small positive x, $v(x)=-c$, so that the phase point must move to the left. These two tendencies cannot both be satisfied: there is no solution for this IC. In other words, the trajectory does not know what to do at $x=0$. On the other hand, if we start from a nonzero IC, say $x(0)=x_0>0$, then there *is* a solution $x(t)=x_0-ct$. However, this solution ceases to exist at $t=x_0/c$ when the phase point approaches the origin. In this case, we may trace the lack of existence to the discontinuity of v at $x=0$. The vector field v points in different directions as one approaches $x=0$ from above or below. This would be fine if $v\to 0$ as $x\to 0$ so that $x=0$ is a fixed point, but that is not the case here.

Interestingly, discontinuous vector fields do not always fail to admit solutions to an IVP. The problem in the above example is that the flow was ‘attracted’ to $x=0$, but once it got there, it did not know what to do, due to the discontinuity in v. By contrast, the equation $\dot{x}=v(x)$ for the discontinuous vector field of Fig. 5.8:

$$v(x)=c\,\operatorname{sgn} x=\begin{cases}+c & \text{if} \quad x>0\\ 0 & \text{if} \quad x=0\\ -c & \text{if} \quad x<0 \quad \text{where} \quad c>0 \quad \text{is a constant speed,}\end{cases} \tag{5.19}$$

has solutions ($x(t)=x_0+(\operatorname{sgn} x_0)\,ct$) for any IC $x(0)=x_0$ that exist for all time! $x_*=0$ here is an unstable fixed point, a repeller, so that trajectories are not troubled by the discontinuity at $x=0$. Thus, while continuity may help, it is not necessary for the existence of solutions. See Prob. 5.5 for another example.

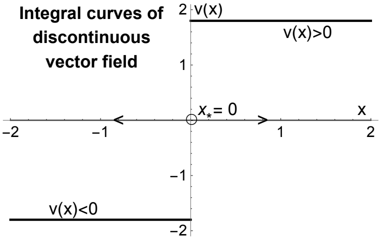

Figure 5.8: Discontinuous vector field with solutions to IVP that exist for all time.

Failure of uniqueness: Consider $\dot{x}=\sqrt{x}$ for $x\ge 0$ subject to the IC $x(0)=0$. Unlike in all the cases encountered before[10], we will show that this IVP has multiple distinct solutions. If true, this would mean that despite being first order, specification of the initial state $x(0)=0$ *does not* uniquely determine the future evolution of this system. Let us examine how this counterintuitive situation emerges. $x_* = 0$ is clearly a fixed point. Thus, we have the obvious constant solution to the IVP $x_{\rm const}(t) = 0$ for all $t \geq 0$. However, this is *not* the only possible solution for the initial condition $x(0) = 0$. Indeed, integrating, we find $2\sqrt{x} = t + \text{constant}$. Imposing the IC $x(0) = 0$ we arrive at the *nonconstant solution* $x(t) = t^2/4$ for $t \geq 0$. In other words, a phase point starting at $x = 0$ can either stay there for ever or move out quadratically with time! We say that the IVP does not have a unique solution[11]. In fact, the nonuniqueness is more severe. There are infinitely many distinct solutions to the above IVP. Indeed, we verify that the following is a solution[12] for any $t_0 \geq 0$ (see Fig. 5.2):

---

[10] For instance, the ODE $\dot{x}=-x$ has the general solution $x(t)=x_0e^{-t}$ and imposing the IC $x(0)=0$ picks out the constant solution $x(t)=0$ for all $t\ge 0$.

$$x(t) = \begin{cases} 0 & \text{for } \; 0 \leq t \leq t_0 \\ (t - t_0)^2/4 & \text{for } \; t \geq t_0. \end{cases} \tag{5.20}$$

In other words, a phase point that begins at $x(0) = 0$ can 'choose' to remain there for a time $t_0 \geq 0$ and then suddenly wake up and run away. The constant and $t^2/4$ solutions we found earlier are clearly limiting cases of this more general family of solutions, corresponding to $t_0 \to \infty$ and $t_0 = 0$ respectively.

It is possible to avoid this nonuniqueness if v is sufficiently regular. There are various sufficient conditions that guarantee existence and uniqueness of solutions. One of these[13] is given in the theorem below (see [20] for more on this).

Existence-Uniqueness theorem: Suppose $v(x)$ and $v'(x)$ are continuous on an open interval containing x_0. We say that v is continuously differentiable[14] or C^1. Then the ODE $\dot{x} = v(x)$ with $x(0) = x_0$ has a unique solution for some time interval $|t| < \tau > 0$. Moreover, if v and the IC depend continuously on some parameters (like masses or coupling constants), then (assuming Lipschitz continuity and uniform boundedness of v) the solution depends continuously on the parameters and ICs.

This theorem is not special to one dimension. More generally, consider the IVP $\dot{\boldsymbol{r}} = \boldsymbol{v}$ with $\boldsymbol{r}(0) = \boldsymbol{r}_0$ on an n-dimensional manifold and suppose the components of $\boldsymbol{v}$ are differentiable with continuous first partial derivatives in some open connected region containing $\boldsymbol{r}_0$. Then a unique solution to the above IVP exists for some time $|t| < \tau > 0$. *Uniqueness means trajectories cannot cross on the state space.* This does not prevent two trajectories from approaching each other asymptotically, as they can do at a fixed point.

---

[11] Why did this happen? Notice that $v = \sqrt{x}$ is not differentiable at $x = 0$, its derivative $v'(x) = 1/2\sqrt{x}$ diverges there. As a consequence, linear stability analysis would say that the fixed point $x_* = 0$ is infinitely unstable: the characteristic time scale $\tau = 1/v'(0)$ has gone to zero, so points that begin nearby are driven away very rapidly.

[12] Though these are legitimate solutions to the IVP, for $t_0 > 0$ we notice that they have a discontinuous second derivative at $t = t_0$.

[13] A slightly weaker sufficient condition is 'Lipschitz continuity' of v in the interval. v is Lipschitz continuous if $|v(x) - v(y)| \leq K|x - y|$ for some Lipschitz constant K and for all x, y in the interval.

[14] A C^0 function is one that is continuous. A C^2 function is one for which the first two derivatives exist and are continuous. A C^∞ function is one for which all derivatives exist and are continuous, such a function is called smooth.

Picard iteration is a method to construct a solution to the IVP $\dot{x} = v(x)$, $x(0) = x_0$ and to prove the existence-uniqueness theorem when v is continuously differentiable. It proceeds by defining a sequence of functions $x_k(t)$ for $k = 0, 1, 2, \ldots$ inductively via

$$x_0(t) = x_0 \quad \text{and} \quad x_{k+1}(t) = x_0 + \int_0^t v(x_k(t'))\, dt' \tag{5.21}$$

which are then shown to converge to the solution using a fixed point theorem. The idea behind this scheme is to first convert the ODE into an integral equation by integrating from 0 to t:

$$x(t) - x(0) = \int_0^t v(x(t'))\, dt' \quad \Rightarrow \quad x(t) = x_0 + \int_0^t v(x(t'))\, dt'. \tag{5.22}$$

This integral equation is a compact form of the IVP: it encodes both the differential equation and the IC. However, $x(t)$ appears both on the left and the right. The idea is to begin with the zeroth approximant $x_0(t) = x_0$ and use it to generate the next approximant by replacing $x(t)$ by $x_0(t)$ on the RHS. Thus $x_1(t) = x_0 + \int_0^t v(x_0(t'))dt'$. Repeating this we obtain the Picard iterates (5.21). See Prob. 5.9 for some simple examples. Picard iteration can be used to solve the time-dependent and time-independent Schrödinger equation in quantum mechanics via the Born series. A similar procedure is employed in quantum field theory and goes by the name Dyson series. Truncating the series after a few terms gives a reasonable approximation in several physically interesting problems. In fact, truncating after the first nontrivial term led to the Rutherford cross section in Eq. (2.71) of Sect. 2.7*.

Can a trajectory $x(t)$ reach or emerge from a fixed point x_* in a finite time? In the examples $v(x) = -x$ and the RC circuit of Sect. 5.2*, we saw that it takes infinitely long for a solution to either reach or emerge[15] from a fixed point. This is typically the case for many of the systems we encounter. However, there are exceptions. Given a fixed point x_*, we always have the trivial or constant solution $x(t) = x_*$ for all t. Additionally, if a solution emerges from (or reaches) x_* in finite time, then the IVP through x_* would have at least two solutions and thus would not admit unique solutions. For instance, if $v = \sqrt{x}$ (5.20), in addition to the constant solution $x(t) \equiv 0$ we have the nonconstant solution $x(t) = t^2/4$ that emerges from the fixed point $x_* = 0$ in finite time. Alternatively, the time-reversed flow $\dot{x} = -\sqrt{x}$ with IC $x(0) = x_0 \geq 0$ has a fixed point at $x_* = 0$, which is reached by the solution $x(t) = (\sqrt{x_0} - t/2)^2$ in finite time $t_* = 2\sqrt{x_0}$. In both these cases, uniqueness of solutions to an IVP fails. On the other hand, if the conditions of the Existence-Uniqueness theorem are met in a neighborhood of a fixed point, then trajectories cannot reach or emerge from the fixed point in finite time. □

Finite-time blowups. Though the theorem guarantees the existence of a solution for some time, the solution need not exist for all time, it could blow up at a singularity. For example, consider the smooth vector field $v(x) = 1 + x^2$. It has no zeros and the above theorem guarantees existence and uniqueness of solutions for any initial state x_0. However, the solution $x(t) = \tan(t + \arctan x_0)$ diverges as $t + \arctan x_0$ approaches the nearest odd multiple of $\pi/2$ from below (see Fig. 5.6b for a closely related example). This is an example of a finite time blowup. Roughly, the reason this happened is that the vector field $v(x) = 1 + x^2$ grows without bound rather quickly [see Prob. 5.11]. Notice that this does not happen for a bounded vector field like $v(x) = -\sin x$ [see Prob. 5.4] or one that grows linearly $v(x) = x$. In the latter case, the solution $x(t) = x_0 e^t$ grows but diverges only as $t \to \infty$.

---

[15] We say that a nonconstant $x(t)$ takes infinitely long to emerge from the fixed point x_* if $x(t) \neq x_*$ at any finite time t but $x(t) \to x_*$ as $t \to -\infty$.

5.4* Vector fields on the phase plane

An autonomous vector field on the x-y plane is given in Cartesian coordinates by $\boldsymbol{v} = (f(\boldsymbol{r}), g(\boldsymbol{r}))$ where $\boldsymbol{r} = (x, y)$. The integral curves of such a vector field are solutions of the pair of ODEs

$$\dot{\boldsymbol{r}} = \boldsymbol{v}(\boldsymbol{r}) \quad \text{or} \quad \dot{x} = f(x,y) \quad \text{and} \quad \dot{y} = g(x,y) \quad \text{with} \quad \boldsymbol{r}(0) = \boldsymbol{r}_0 = (x_0, y_0). \tag{5.23}$$

Here x and y could be the position and momentum of a particle and $\boldsymbol{v}$ the Hamiltonian vector field (5.4). The corresponding trajectory is now a plane curve (see Fig. 5.1). As discussed in Sect. 5.3, if the components f and g are continuously differentiable in some open connected region $R \subset \mathbb{R}^2$ containing $\boldsymbol{r}_0$, then a unique solution to the above initial value problem exists for some time $|t| < \tau > 0$. Uniqueness means trajectories cannot cross. This does not prevent two trajectories from approaching each other asymptotically, as they can at a fixed point.

There is a larger variety of fixed points of 2d vector fields than we encountered in 1d. In this section, we will present some examples and get a taste for some of the possibilities. In Sect. 6.3 and Sect. 6.6* we will classify fixed points of 2d vector fields by considering the linearization around such fixed points and place them in the physical context of small oscillations. A useful distinction is the one between isolated and nonisolated fixed points. The former include centers, nodes, spirals and saddles, which we introduce below. Nonisolated fixed points are continuous families of fixed points which could lie along a line/curve (e.g., the free particle example in Fig. 3.2) or fill an entire 2d region. As on $\mathbb{R}$, we have the possibility of *heteroclinic trajectories*. A heteroclinic trajectory approaches a pair of distinct fixed points as $t \to \pm\infty$. We have met examples of heteroclinic trajectories in the inertialess damped pendulum of Fig. 5.7b and in the competitive Lotka-Volterra model of Fig. 5.3. A new possibility is that of *homoclinic trajectories*, those which approach the *same* fixed point as $t \to \pm\infty$. Examples are to be found in the dipole field of Fig. 5.9c. Yet another new phenomenon is that of a limit cycle, which we will introduce shortly.

Example: Centers and spirals. Some vector fields are more easily presented in coordinates other than Cartesian. Consider the system

$$\dot{\theta} = 1 \quad \text{and} \quad \dot{r} = -ar^n \tag{5.24}$$

in plane polar coordinates $r = (x^2 + y^2)^{1/2} \geq 0$ and $\theta = \arccos(x/r)$. For $a = 0$, it is clear that trajectories are concentric circles ($r =$ constant) traversed counterclockwise.

The fixed point at the origin is called a *center*. More generally, suppose $a > 0$ and let $n \geq 1$ be an integer. It is clear that r decreases monotonically to zero (see Prob. 5.12) while θ grows linearly:

$$\theta = \theta_0 + t \quad \text{and} \quad r = [r_0^{1-n} + (n-1)at]^{-1/(n-1)}. \tag{5.25}$$

Hence, as shown in Fig. 5.9a, the phase point spirals counterclockwise towards the origin, which is a *spiral sink* (or *spiral source* for $a < 0$). ☐

Unlike on the real line, on the phase plane, there is the possibility of periodic trajectories (cycles or closed orbits) which can model oscillations. A special topological feature of dynamics on a plane is that a periodic trajectory (a closed curve with no self-intersections) separates the phase plane into an 'inside' and an 'outside'. Trajectories that begin inside cannot wander outside while those that begin outside cannot come in. A novel possibility is that of a *limit cycle*: an isolated periodic trajectory[16] as shown in Fig. 5.9b. Since a limit cycle is isolated, trajectories that begin in a sufficiently small ribbon-shaped neighborhood cannot be periodic and must spiral either toward or away from the limit cycle. This leads to stable, unstable and half-stable limit cycles. Stable limit cycles, when they exist, represent dynamically generated (self-sustained, i.e., without external driving) oscillations of a nonlinear system with a dynamically determined asymptotic $(t \to \infty)$ period and waveform, including amplitude[17]. By contrast, periodic trajectories of a linear system can have any amplitude by a suitable choice of initial conditions, due to the freedom to rescale a periodic trajectory. There are several examples of periodic motions that may be modeled as limit cycles: oscillations in electric circuits and chemical reactions such as the van der Pol oscillator and Brusselator, airplane wing flutter, certain vibrations in bridges and so on.

Example: Limit cycle in plane polar coordinates: It is easy to come up with a limit cycle on the plane using polar coordinates. In fact, consider the system

$$\dot{r} = r(1-r) \quad \text{and} \quad \dot{\theta} = 1. \tag{5.26}$$

The angular motion is uniform counterclockwise rotation and decouples from the radial motion which has a repulsive fixed point at $r = 0$ and an attractive one at $r = 1$. Thus, the circle $r = 1$ is a stable limit cycle with trajectories spiraling towards it from either side as shown in Fig. 5.9b. The limit cycle is the circular orbit $(x, y) = (\cos t, \sin t)$. To see how the trajectories spiral towards the limit cycle, we may solve the Riccati-type radial equation $\dot{r} + r^2 - r = 0$ via the linearizing transformation $r = \dot{f}/f$. On finds that $\ddot{f} - \dot{f} = 0$, with the solution $f = ae^t + b$. Thus, the solution of the system is $r(t) = 1/(1 + c_1 e^{-t})$ and $\theta(t) = t + c_2$. It shows that as $t \to \infty$, $r \to 1$ exponentially fast. See Prob. 5.13 for the corresponding vector field in Cartesian variables. ☐

---

[16] Linear systems do not admit limit cycles. Suppose $\boldsymbol{r}(t)$ is a periodic orbit of a linear system $\dot{\boldsymbol{r}} = \boldsymbol{v}(\boldsymbol{r})$. Since $\boldsymbol{v}(\lambda \boldsymbol{r}) = \lambda \boldsymbol{v}(\boldsymbol{r})$, a slightly rescaled periodic orbit ($\lambda \boldsymbol{r}(t)$ for $\lambda \approx 1$) must also be a periodic orbit of the linear system. In other words, there are periodic orbits arbitrarily close to a given periodic orbit of a linear system. Thus, $\boldsymbol{r}(t)$ cannot be isolated.

[17] For ICs in the basin of attraction of a stable limit cycle, the trajectory eventually approaches the limit cycle which has a definite period and shape. In Fig. 5.9b the shape happened to be circular. The waveform refers to the 'shape' of a trajectory.

van der Pol oscillator: Balthasar van der Pol (1920) introduced the equation $m\ddot{x} + \mu(x^2 - 1)\dot{x} + kx = 0$ to describe triode oscillations in a certain electrical circuit while working at Phillips, in the Netherlands. For m, k and μ positive, this oscillator turns out to have a limit cycle (which resulted in oscillations that he called relaxation oscillations). To make this plausible (see also Prob. 6.19 and [122]), we notice that for large $x^2 > 1$, the first derivative term $\mu(x^2 - 1)\dot{x}$ has a dissipative effect, drawing the phase point $(x, m\dot{x})$ inward, while for small $x^2 < 1$, it has an antidamping effect, expelling the phase point away form the origin. These competing effects help to create a stable limit cycle at an intermediate distance from the origin. □

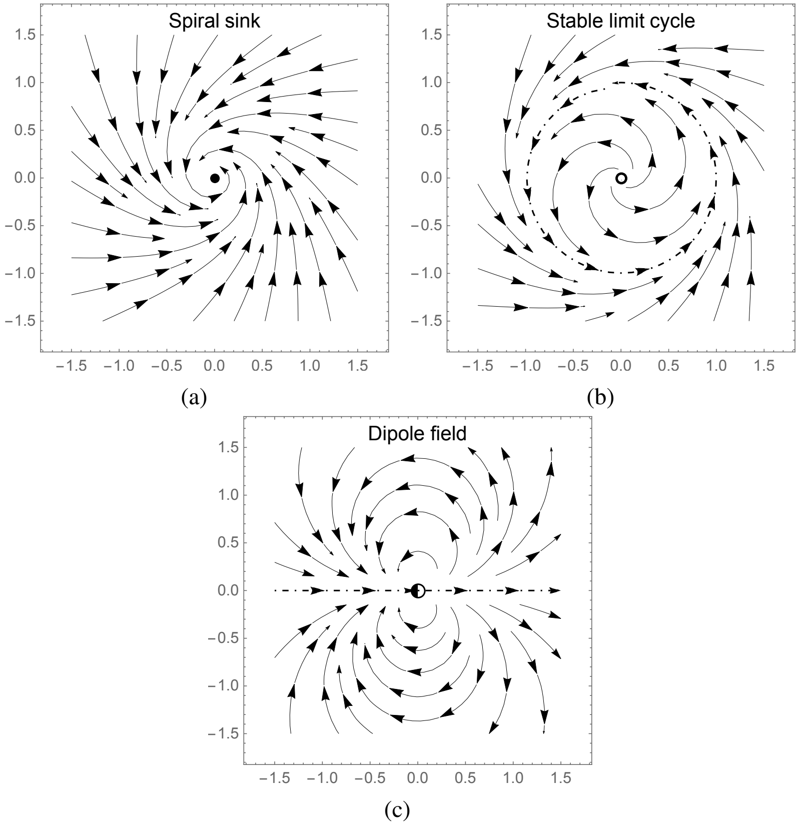

Figure 5.9: Integral curves of (a) the spiral sink of (5.24) with $a = 1, n = 2$, (b) the stable limit cycle $r = 1$ of (5.26) along with a spiral source at (0,0) and (c) the dipole field of (5.28). Aside from the trajectories along the positive and negative horizontal axes, all integral curves of the dipole field are homoclinic. Note that the solution to the IVP is unique: the homoclinic trajectories take infinitely long to reach or emanate from the fixed point at the origin. The stable, unstable and half-stable fixed points at the origin are indicated in the three phase portraits.

Unlike with 1d vector fields (5.11) the coupled equations (5.23) for integral curves of 2d vector fields cannot always be reduced to quadrature. One special case where the equations *can* be integrated is if the vector field is linear. $\dot{x} = f(x, y) = ax + by$

and $\dot{y} = g(x, y) = cx + dy$. Such linear vector fields arise in the study of small oscillations of a mechanical system with one degree of freedom. In Chap. 6 we will investigate such linear vector fields and classify their fixed points and phase portraits.

More generally, as in 1d, the linearization of a nonlinear vector field around a fixed point $\boldsymbol{r}_* = (x_*, y_*)$ can provide a useful approximation. The derivative $v'(x_*)$ is now replaced by a 2 × 2 matrix. Writing $x = x_* + \delta x$ and $y = y_* + \delta y$ for small $(\delta x, \delta y)$ and expanding in a Taylor series, the linearization of the ODEs (5.23) reads [18]

$$\frac{d}{dt}\begin{pmatrix} \delta x \\ \delta y \end{pmatrix} = \begin{pmatrix} \frac{\partial f}{\partial x} & \frac{\partial f}{\partial y} \\ \frac{\partial g}{\partial x} & \frac{\partial g}{\partial y} \end{pmatrix}_{\boldsymbol{r}_*} \begin{pmatrix} \delta x \\ \delta y \end{pmatrix}. \tag{5.27}$$

The coefficient matrix of this linear system is the Jacobian matrix of first partial derivatives, evaluated at the fixed point. We will employ this linearization in Sect. 7.1 and elsewhere to study the behavior of nonlinear vector fields near fixed points. However, the linearization cannot always be trusted, as the following example of a dipole field illustrates.

A dipole field. This describes the magnetic field around a point magnetic dipole on a plane that contains the axis of the dipole. In suitable units, the equations for the field lines (of a dipole at the origin and pointing along x) are given by the system

$$\dot{x} = x^2 - y^2 \quad \text{and} \quad \dot{y} = 2xy. \tag{5.28}$$

These equations are the real and imaginary parts of $\dot{z} = z^2$ where $z = x + iy$. The origin $(0, 0)$ is the only fixed point. However, we verify that the linearization around it leads to a Jacobian matrix (5.27) that is identically zero. Thus the linear approximation (5.27) to this vector field is the zero vector field, which would wrongly suggest that every point on the plane is a fixed point! This happens because the origin is a 'double zero' of the vector field z^2 (similar things happen for vector fields with higher order zeros). To understand the dipole field, let us sketch its phase portrait (see Fig. 5.9c). For this, it sometimes helps to draw the *nullclines*. Nullclines are curves along which the flow is either horizontal ($\dot{y} = 0$) or vertical ($\dot{x} = 0$). For instance, the flow is horizontal when $\dot{y} = 2xy = 0$, which consists of the coordinate axes. The flow is to the right on the x-axis and to the left on the y-axis. On the other hand, the flow is vertical when $\dot{x} = x^2 - y^2 = 0$. The flow is upwards on $y = x$ and downwards on $y = -x$. In general, nullclines intersect at the fixed points, in this case there is just one fixed point, the origin, which lies at the intersection of the coordinate axes and the lines $y = \pm x$. What is more, the nullclines divide the phase plane into open regions where $\dot{x}$ and $\dot{y}$ have a fixed sign (since they cannot vanish). Here there are eight such regions: the octants. For instance, in the lower octant of the first quadrant, $\dot{x}$ and $\dot{y}$ are positive and the flow is roughly to the north-east while it is roughly to the north-west in the upper octant of the first quadrant. Needless to say, nullclines are in general not trajectories[19]. Trajectories can cross nullclines as long as the latter are not trajectories

---

[18] We use the two-variable Taylor expansion $f(x_* + \delta x, y_* + \delta y) = f(x_*, y_*) + \frac{\partial f}{\partial x}\delta x + \frac{\partial f}{\partial y}\delta y + \cdots$, etc., where derivatives are evaluated at the fixed point.

[19] A $\dot{y} = 0$ nullcline is a union of trajectories provided it is horizontal and an $\dot{x} = 0$ nullcline is a union of trajectories if it is vertical.

(in our example, the nullcline $y = 0$ happens to be the union of two trajectories and a fixed point). We can now sketch the phase portrait, which should be familiar from the field lines of an electric or magnetic dipole. In the upper half-plane, all trajectories begin and end at the origin and proceed counterclockwise: they are homoclinic orbits. The lower half-plane is a mirror image, it consists of clockwise homoclinic orbits. This phase portrait does not resemble that of any linear 2d system (see Sect. 6.3): an attempt at a linear approximation does a poor job by producing a plane of fixed points. Homoclinic orbits are an essentially nonlinear phenomenon. ☐

Conservative systems. Conservative systems[20] are autonomous dynamical systems $\dot{\boldsymbol{r}} = \boldsymbol{v}(\boldsymbol{r})$ that admit a conserved quantity: a nontrivial dynamical variable that is constant along trajectories. This generalizes the notion of a conservative mechanical system introduced in Chap. 1. In fact, the Hamiltonian vector field for a particle moving in a 1d potential ($\dot{x} = p/m$, $\dot{p} = -V'(x)$) is conservative: the energy $E = p^2/2m + V(x)$ is conserved. More generally, we say that a system $\dot{\boldsymbol{r}} = \boldsymbol{v}(\boldsymbol{r})$ (on a phase space of any dimension) is conservative if it admits a continuous real-valued function $E(\boldsymbol{r})$ that is not constant on any open subset of phase space and which satisfies $\dot{E} = 0$ along every trajectory. A function that is constant on phase space is always trivially conserved, so we must exclude it to ensure that our definition does not classify every dynamical system as conservative!

It is relatively easy to see that nontrivial flows on the real line $\dot{x} = v(x)$ (with v not identically zero) cannot be conservative. In fact, suppose $E(x)$ were conserved and not constant on any open subset of $\mathbb{R}$. Then trajectories must be confined to level sets of E. However, every level set of E must be a discrete set of points (zero dimensional). It follows that continuous time evolution is not possible (every trajectory must be a fixed point) and the vector field $v(x)$ must be trivial. In fact, we should not be surprised: vector fields on the real line are always gradient vector fields (see (5.15)) and describe inertialess damped (dissipative) motion. By contrast, conservative vector fields are plentiful in phase spaces of dimension higher than one: every Hamiltonian system furnishes an example.

A simple consequence of the definition is that a conservative system cannot have an attracting or repelling fixed point (such as the node in Fig. 6.2b or the spiral in Fig. 5.9a). A fixed point $\boldsymbol{r}_*$ is attracting if all trajectories $\boldsymbol{r}(t)$ starting from points in a sufficiently small neighborhood approach $\boldsymbol{r}_*$ as $t \to \infty$. Replacing the condition with $t \to -\infty$ defines a repeller. Now, if a conservative system had an attracting fixed point $\boldsymbol{r}_*$, then the conserved quantity would be constant throughout its basin of attraction[21]. Since the basin of attraction includes an open set containing $\boldsymbol{r}_*$, the conserved quantity would be inadmissible[22]. A similar argument applies to repelling fixed points. In the same vein, one may argue that conservative systems cannot admit limit cycles: a limit cycle would imply that the conserved quantity is constant on a narrow ribbon-like open neighborhood of the isolated periodic trajectory. On the other hand, conservative systems *can* display centers (as in the harmonic oscillator of Fig. 6.1a), saddles (as in the pendulum of Fig. 7.3 and the anharmonic oscillator of Fig. 7.6) as well as nonisolated fixed points (as in the free particle of Fig. 3.2). For instance, as we argue in Sect. 6.7*, if $\boldsymbol{r}_*$ is an isolated fixed point of $\boldsymbol{v}$ that lies at a minimum or maximum of the conserved quantity $E(\boldsymbol{r})$, then $\boldsymbol{r}_*$ is a center. In this case, all trajectories that start sufficiently close to $\boldsymbol{r}_*$ are closed and continuously deformable into circles.

---

[20] Some authors define a conservative system as one that admits a volume element in phase space such that the volume of any region is conserved in time. We call such a vector field volume preserving. A volume preserving vector field $\boldsymbol{v}$ is one whose divergence $\boldsymbol{\nabla} \cdot \boldsymbol{v}$ (with respect to the relevant volume form) vanishes. A flow is called dissipative if $\boldsymbol{\nabla} \cdot \boldsymbol{v} \leq 0$, and strictly negative in some portion of the phase space. On the other hand, $\boldsymbol{\nabla} \cdot \boldsymbol{v} > 0$ usually corresponds to the presence of a source or some ‘driving force’. However, to avoid runaway solutions, a driven system needs to have some dissipation.

[21] Consider a trajectory $\boldsymbol{r}(t)$ that approaches $\boldsymbol{r}_*$ as $t \to \infty$. Since E is conserved, it must

Gradient Flows. Unlike on the real line, not every vector field on the phase plane is a gradient vector field. Nevertheless, gradient vector fields are a particularly simple and interesting class of vector fields. By a gradient flow in a planar or 3d region (the same definition applies to flows on a phase space M of any dimension) we mean one where $\dot{\boldsymbol{r}} = \boldsymbol{v} = -\boldsymbol{\nabla} W$ where W is a singlevalued scalar 'potential' function. Fixed points of a gradient flow are seen to lie at local extrema of the potential W. Since the curl of a gradient vanishes, a necessary condition[23] for a flow to be a gradient flow is that $\boldsymbol{v}$ be curl-free $\boldsymbol{\nabla} \times \boldsymbol{v} = 0$. When a potential exists, $W(\boldsymbol{r})$ can be expressed as a line integral [as in (5.16)] from a reference point $\boldsymbol{r}_0 \in M$ to $\boldsymbol{r}$:

$$W(\boldsymbol{r}) = -\int_\gamma \boldsymbol{v}(\boldsymbol{r}') \cdot d\boldsymbol{r}' \text{ where } \gamma : [0,1] \to M \quad \text{with} \quad \gamma(0) = \boldsymbol{r}_0 \text{ and } \gamma(1) = \boldsymbol{r}. \tag{5.29}$$

The line integral does not depend on the choice of path γ since $\boldsymbol{v}$ is curl-free[24]. Trajectories in a gradient flow point along the direction of steepest decrease of W and can model some dissipative processes. In fact, the potential is monotonically decreasing (or at least nonincreasing) along the flow

$$\frac{dW}{dt} = \boldsymbol{\nabla} W \cdot \frac{d\boldsymbol{r}}{dt} = -|\boldsymbol{\nabla} W|^2 \leq 0. \tag{5.30}$$

As a consequence, gradient flows do not admit periodic(oscillatory) motions. In fact, suppose $\boldsymbol{r}(t)$ for $t \in [0,T]$ is a closed trajectory (that is not a ring of fixed points). The change in W as we go once round the closed trajectory

$$\Delta W = \int_0^T \frac{dW}{dt}\, dt = \int_0^T \boldsymbol{\nabla} W \cdot \dot{\boldsymbol{r}}\, dt = -\int_0^T |\boldsymbol{\nabla} W|^2 dt \tag{5.31}$$

---

have the same value all along $\boldsymbol{r}(t)$ and by continuity, this value must coincide with $E(\boldsymbol{r}_*)$. The same applies to every trajectory in the basin of attraction of $\boldsymbol{r}_*$. Consequently $E = E(\boldsymbol{r}_*)$ throughout the basin.

[22] We may use reasoning along these lines to argue that the vector field of the competitive Lotka-Volterra model of Fig. 5.3 cannot be conservative since it has attractors and a repeller.

[23] It is also sufficient if the region is simply connected, i.e., every closed curve can be shrunk to a point while remaining in it. In 2d, a disk is simply connected while an annulus is not.

[24] In three dimensions, this is a consequence of Stokes' theorem (see Appendix B.10*). The difference of line integrals along two different paths γ and γ' joining $\boldsymbol{r}_0$ and $\boldsymbol{r}$ is the line integral around a closed loop $\oint \boldsymbol{v} \cdot d\boldsymbol{r} = \int_S (\boldsymbol{\nabla} \times \boldsymbol{v}) \cdot d\boldsymbol{S} = 0$ where S is a surface whose boundary is the closed curve $\gamma \cup \bar{\gamma}'$ where $\bar{\gamma}'$ is the path γ' traversed in the opposite direction.

is strictly negative. On the other hand, ΔW must vanish, since W is singlevalued and must return to its original value when we go round the closed trajectory. Thus we arrive at a contradiction: we cannot have periodic trajectories in a gradient flow.

Lyapunov functions. Even if a flow is not a gradient flow, it may display similar features if it admits a *Lyapunov function* on phase space that decreases along the flow. More precisely, the (continuously differentiable) real-valued function $L(\boldsymbol{r})$ is said to be a Lyapunov function for the flow $\dot{\boldsymbol{r}} = \boldsymbol{v}(\boldsymbol{r})$ if (a) L is nonnegative on the phase space (b) L vanishes only at fixed points and (c) $\dot{L}(\boldsymbol{r}) < 0$ along the flow as long as $\boldsymbol{r}$ is not a fixed point. For instance, the existence of a Lyapunov function rules out closed orbits (see Prob. 5.15). An example of a Lyapunov function is the potential function W of a gradient flow that has only one fixed point $\boldsymbol{r}_*$ which is located at the global minimum of W; we may add a constant to W to ensure that $W(\boldsymbol{r}_*) = 0$.

Poincaré-Bendixon theorem. Though 2d flows arising from autonomous systems are quite rich, they are still relatively regular. If trajectories are confined to a compact (closed and bounded) region of the plane so that they cannot escape to infinity, then the Poincaré-Bendixon theorem restricts what they can do. Looked at more positively, the theorem gives sufficient conditions for the existence of closed orbits including limit cycles, which can be used to model oscillations. The statement is as follows[25]. Suppose the C^1 vector field $\dot{\boldsymbol{r}} = \boldsymbol{v}(\boldsymbol{r})$ is defined in an open subset D of the phase plane and let $K \subset D$ be a compact subset that contains no fixed points. Let γ be a 'trapped' trajectory that begins in K (at some time) and remains in K at all subsequent times (see Fig. 5.10a). Then γ is either a closed orbit or approaches (spirals towards) a closed orbit as $t \to \infty$. Since K contains all its limit points, the limiting closed orbit in the latter case must lie within K. Either way, K contains a closed trajectory.

It can be shown [using index theory (Sect. 6.8 of [122]) or by drawing phase portraits] that a closed orbit on the plane must enclose a fixed point. Since the theorem requires that the compact region K be fixed point free, K must be chosen to exclude the fixed points that lie within the closed orbit that the theorem guarantees. Thus, in applications of the Poincaré-Bendixon theorem, K is typically chosen to be shaped like an annulus (Fig. 5.10a). In practice, it may be tricky to identify a trajectory that remains in K. A way to ensure there is one, is to pick K to be a *trapping region*: a connected compact subset of D on whose boundary the vector field points inward. All trajectories that begin in a trapping region are confined to it. If a trapping region does not contain any fixed points, then the Poincaré-Bendixon theorem guarantees that it has a closed trajectory and that all trapped orbits are either periodic or approach a closed orbit.

Example. Let us apply the Poincaré-Bendixon theorem to show that the vector field in plane polar coordinates

$$\dot{r} = r(1-r) + \alpha r \sin\theta \quad \text{and} \quad \dot{\theta} = 1 \tag{5.32}$$

admits a closed trajectory for any sufficiently small $\alpha > 0$. On the face of it, (5.32) is a nonlinear system of equations. After eliminating $\theta = t +$ constant, we are left

---

[25] For more on the Poincaré-Bendixon theorem, see [57, 122]

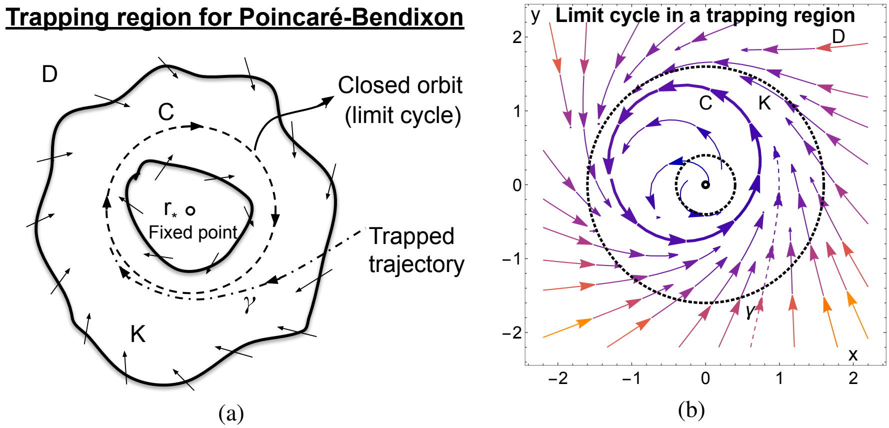

Figure 5.10: (a) Poincaré-Bendixon theorem: annular fixed point free trapping region K with trapped trajectory γ and closed orbit C. (b) Vector field of (5.32) for $\alpha = 0.6$ showing annular trapping region (with dark dashed boundary) $K : 1 - \alpha < r < 1 + \alpha$, trapped trajectory γ (thin dashed) and closed orbit (limit cycle C, dark). There is a spiral source at the origin.

with a nonlinear ODE for $r(t)$ with variable coefficients. Even without having any idea of how such an equation may be solved analytically, we may use the Poincaré-Bendixon theorem to infer the existence of a closed trajectory. In fact, we may choose the trapping region to be the annulus $r_{\text{min}} = 1 - \alpha \le r \le r_{\text{max}} = 1 + \alpha$ for any $0 < \alpha < 1$. We need to ensure that $\dot{r} = r(1-r) + \alpha r \sin\theta > 0$ for $r = r_{\text{min}}$ and $\dot{r} < 0$ for $r = r_{\text{max}}$. Use the fact that $-1 \le \sin\theta \le 1$ to check that this is satisfied. See Fig. 5.10b for a sketch of the trapping region and closed trajectory. ☐

Absence of chaos on the phase plane. The Poincaré-Bendixon theorem restricts the possible behavior of trajectories on the phase plane. If a trajectory is confined to a compact region without fixed points, the trajectory must either be periodic or approach a periodic orbit[26]. In other words, the trajectory cannot wander around endlessly in a bounded region without approaching a fixed point or a limit cycle or being periodic. In all three cases, there is no sensitivity to initial conditions as the asymptotic behavior is known[27]. Sensitivity to initial conditions is a hallmark of chaos. There is no chaos in autonomous systems on the plane essentially because trajectories do not have enough room to maneuver.

In three and higher dimensions, phase trajectories confined to a bounded region can be chaotic: they can wander around endlessly without approaching a fixed point or a periodic orbit and display extreme sensitivity to initial conditions. In addition to fixed points, periodic orbits and limit cycles, one encounters 'strange attractors' that are fractals: this happens for instance in Lorenz's 1963 toy model for atmospheric convection, which has a 3d phase space (see Sect. 15.5*). For certain classes of initial conditions, the motion is irregular or chaotic: sensitive to initial conditions, remaining bounded and never settling down to periodic motion, as illustrated in Fig. 15.22.

---

[26] Irrational windings on a torus (Fig. 10.1) do not approach a fixed point or a periodic trajectory on the torus, but also do not display sensitive dependence on initial conditions: neighboring trajectories are parallel lines at constant separation.

[27] In unbounded regions, trajectories that begin nearby can grow far apart, but then they may fly off to infinity in a regular fashion, as in the Kepler problem.

5.5 Problems

1. Sketch **phase portraits** (arrows indicating the direction and magnitude) for the vector fields on the plane given in Cartesian coordinates by $\boldsymbol{v} =$ (a) $(1,0)$, (b) $(0,1)$, (c) $(1,1)$, (d) $(1,-1)$, (e) (x,y), (f) $(-y,x)$, (g) $(y,0)$. Describe each vector field qualitatively and find any fixed points.

2. Consider the **forced damped oscillator** equation $m\ddot{x} + \gamma\dot{x} + kx = f\cos t$, for positive constants m, γ, k and real constant f. Is it linear or nonlinear, of what order and homogeneous/inhomogeneous? Write it as an **autonomous system** of first order ODEs as in (5.7). Is the autonomous system linear or nonlinear?

3. **Charging a capacitor.** For positive constants V, R and C, solve the IVP for the charge on a capacitor $\dot{Q} = \frac{V}{R} - \frac{Q}{RC}$ given that $Q(0) = Q_0$. How long does it take for the charge to reach its asymptotic value? Compare your answer with Fig. 5.5b.

4. Draw a **phase portrait** for the system $\dot{x} = v(x) = -\sin x$ on the real line. Use it to roughly plot several representative trajectories (x as a function of time t) on the t-x plane. Extend the trajectories to $t \to \pm\infty$. The trajectories should include at least 2 static and 4 nonstatic solutions each of a different qualitative nature. Comment on the nonlinear saturation (in the sense of Sect. 5.2*) of exponentially growing solutions. Integrate the equation to express t as a function of x.

5. **Sliding friction vector field.** Consider the sliding motion of a block of mass m along a horizontal line (x-axis) subject to a constant downward acceleration due to gravity g and sliding friction. It is empirically observed that the frictional force is directed opposite to velocity and increases with the weight of the block. A simple model for sliding friction is that it produces a force of magnitude μN where $N = mg$ is the upward directed *normal reaction* and μ is a constant coefficient of sliding friction. If the instantaneous location of the center of the block is denoted $x(t)$, then Newton's second law reads $m\ddot{x} = -\mu mg\,\mathrm{sgn}(\dot{x})$ with the understanding that $\mathrm{sgn}(0) = 0$ since there is no sliding frictional force on a stationary block. (a) Taking $p = m\dot{x}$ write the EOM as a first order system and identify the corresponding vector field $v(x,p)$ on the phase plane. We will now understand the phase portrait of v (note that v is not the velocity of the block!). (b) What are the zeros of v? (c) Where is v (dis)continuous? (d) Solve the EOM for ICs $x(0)$ and both positive and negative $\dot{x}(0)$. What transformation permits you to go from one to the other? (e) Unlike a damped oscillator, the block comes to rest in finite time; find that time t_{rest} and $x(t_{\text{rest}})$. (f) Plot $x(t)$ for some representative ICs. (g) Mention one discrete and one continuous symmetry of v. Plot a phase portrait of v. (h) Observe that all integral curves reach a fixed point in finite time and stay there. The solution of the IVP is unique and exists for all time despite the discontinuity in v (see Sect. 5.3). Backward time evolution is also unique, except if we begin at a fixed point, in which case there are three possible solutions backwards in time,

what do they correspond to physically? (i) Find the eigenvalues and eigenvectors of the Jacobian matrix of v at the fixed points. What does linear stability analysis (formally) suggest about the stability of these fixed points?

6. **Inertialess damped pendulum subject to constant torque:** Consider the vector field on the circle

$$\dot{\theta} = \omega - a\sin\theta \quad \text{with} \quad \omega \geq 0 \quad \text{and} \quad a \geq 0. \tag{5.33}$$

This first order equation is obtained by ignoring the inertial acceleration term in the equation for a pendulum subject to damping and a constant torque

$$ml^2\ddot{\theta} = -mgl\sin\theta - \gamma\dot{\theta} + \tau. \tag{5.34}$$

We think of $\omega = \tau/\gamma$ as a measure of the counterclockwise torque and $a = mgl/\gamma$ as a measure of the downward acceleration due to gravity, which tries to make the bob come down to $\theta = 0$. On the other hand, ω drives the bob uniformly counterclockwise. For definiteness, we will hold $\omega > 0$ fixed and imagine increasing the control parameter a.

   a. What is the nature of the motion when the gravitational force is absent?
   b. For $0 < a < \omega$ what is the nature of the motion? Does the particle go around the circle? Draw a phase portrait and plot $v(\theta)$. What are the fixed points?
   c. For $0 < a < \omega$, where does the bob move the slowest and the fastest and why?
   d. Draw the phase portrait and comment on the fixed points and their nature for $a = a_c = \omega$.
   e. Calculate the time period $T(a;\omega)$ for oscillatory motion (when $a < \omega$) by evaluating the appropriate integral in closed form and comment on its behavior as $a \to \omega^-$.
   f. Estimate the time $T_{\text{bottleneck}}(r)$ spent near the bottleneck around $x = 0$ for trajectories of the canonical vector field displaying a 'saddle-node bifurcation' (see Sect. 14.1.1*) $v(x) = r + x^2$ as $r \to 0^+$. Give reasons for any approximation made. Compare the behavior of $T_{\text{bottleneck}}(r)$ with the above time period $T(a;\omega)$ in the appropriate limits.
   g. When $a > \omega > 0$, how many fixed points are there and where are they located? Find the growth/decay time scales by linearizing the vector field in the neighborhood of the fixed points.
   h. For $a > \omega$, what are the basins of attraction of the various fixed points. Is oscillatory motion possible?

7. Give examples of **fixed points** x_* of vector fields $v(x)$ on $\mathbb{R}$ with $v'(x_*) = 0$ (so that linear stability analysis is inconclusive) but for which x_* is (a) stable (b) unstable and (c) half-stable. Illustrate with suitable phase portraits as in Sect. 5.2*.

8. If x_* is a **fixed point** of $\dot{x} = v(x)$ with $v'(x_*) \neq 0$, we have seen that the trajectory approaches/emerges from x_* exponentially in time. The **rate of approach** to a fixed point can be different if $v'(x_*) = 0$. Take the examples from Prob. 5.7, solve

the ODE for an IC in the neighborhood of x_* (or a general IC) and comment on the rate of approach to (or emergence from) equilibrium.

9. **Picard iteration** is a method to solve the IVP $\dot{x} = v(x)$, $x(0) = x_0$. It proceeds by defining a sequence of functions $x_k(t)$ for $k = 0, 1, 2, \ldots$ inductively via

$$x_0(t) = x_0 \quad \text{and} \quad x_{k+1}(t) = x_0 + \int_0^t v(x_k(t'))\, dt', \tag{5.35}$$

which, in favorable cases, converges to the solution. Let us illustrate the method with two simple examples. (a) Obtain the Picard iterates $x_k(t)$ for $\dot{x} = ax$ with constant a, subject to the IC $x(0) = x_0$. To which function do they converge as $k \to \infty$? (b) Obtain the Picard iterates $\boldsymbol{x}_k(t)$ for $\dot{\boldsymbol{x}} = A\boldsymbol{x}$ where $A = \sigma_1 = (0, 1|1, 0)$ is the first Pauli matrix with IC $\boldsymbol{x}(0) = (1, 0)^t$ (superscript t denotes transpose). To which $\boldsymbol{x}(t)$ do they converge as $k \to \infty$?

10. Consider the vector field on the Euclidean plane $\boldsymbol{v}(x, y) = (f(x, y), g(x, y))$. (a) What would it mean for v to be a **gradient vector field**? Derive a general monotonicity property for the system $\dot{\boldsymbol{r}} = \boldsymbol{v}$ where $\boldsymbol{v}$ is a gradient vector field. (b) Consider $\boldsymbol{v}(x, y) = (y, -x - x^3)$ on the x-y plane. Express $\boldsymbol{v}$ as a gradient vector field or show why it cannot be one. What physical system does $(\dot{x}, \dot{y}) = \boldsymbol{v}$ describe? Give its name and the meanings of x, y and the terms in $\boldsymbol{v}$.

11. **Finite time blowup.** Consider the vector field on the positive real line $v(x) = x^{1+\epsilon}$ (with $x > 0$) for some $\epsilon > 0$. Find the solution with IC $x(0) = x_0 > 0$. Show that the solution blows up in finite time for any $\epsilon > 0$. Find the blowup time.

12. **Center and spiral.** Verify that the solution to the IVP (5.24) proposed in (5.25) is valid for any integer $n > 1$ and also for $n = 1$ in a limiting sense.

13. Express the **plane polar coordinate** vector field $\dot{r} = r(1 - r), \dot{\theta} = 1$ of (5.26) in Cartesian coordinates. Show that you get

$$\dot{x} = -y + x(1 - r) \quad \text{and} \quad \dot{y} = x + y(1 - r) \quad \text{where} \quad r = (x^2 + y^2)^{1/2}. \tag{5.36}$$

In Cartesian coordinates, it is less clear that $r = 1$ is an invariant curve.

14. Consider the system on the x-y plane defined by $\dot{x} = x - x(x^2 + y^2)$ and $\dot{y} = y - y(x^2 + y^2)$. Show that it has no periodic trajectories by expressing it as a **gradient flow** for a suitable potential function $W(x, y)$. Plot a graph of W and describe its shape. What is the circle $x^2 + y^2 = 1$ in this system?

15. Show that the existence of a **Lyapunov function** (positive function on phase space that decreases along the flow and vanishes only at fixed points) for the flow $\dot{\boldsymbol{r}} = \boldsymbol{v}(\boldsymbol{r})$ forbids closed trajectories.

Chapter 6

Small oscillations for one degree of freedom

Oscillations are ubiquitous in physics. For instance, in mechanics, we encounter them in compressed springs, pendula and elastic solids. Small oscillations give us a window into the types of phenomena that can occur in more general oscillations and also a first approximation to describing them. In this chapter, we discuss small oscillations (or vibrations) of a system with one degree of freedom around a static stable equilibrium. This includes free simple harmonic oscillations, damped oscillations, forced or driven oscillations as well as parametric resonance. Some extensions to nonlinear oscillations and to systems with more degrees of freedom and oscillations around time-dependent states are discussed in Chap. 7, 13 and 15.

6.1 Linear harmonic oscillator in 1d and neutral stability

A conservative system in the vicinity of a stable equilibrium configuration generically executes linear or simple harmonic motion. Consider a system with one degree of freedom subject to the potential $V(q)$ with a local minimum at q_0. Consequently $V'(q_0) = 0$ and $q = q_0$ is a static equilibrium. Away from q_0, the system feels a force $-V'(q)$ that, for sufficiently small departures from q_0, tends to restore it to the equilibrium configuration. For definiteness, suppose we have a particle of mass m and Lagrangian $\frac{1}{2}m\dot{q}^2 - V(q)$ [more general possibilities are considered in Sect. 13.3*]. For sufficiently small displacements from equilibrium, we approximate V by its quadratic Taylor polynomial and write

$$L = \frac{1}{2}m\dot{q}^2 - V(q_0) - V'(q_0)(q - q_0) - \frac{1}{2}V''(q_0)(q - q_0)^2 - \cdots . \tag{6.1}$$

Changing variables to the displacement $x = q - q_0$ from stable equilibrium, omitting the constant $V(q_0)$ from L and denoting $k = V''(q_0) > 0$, we get the simple harmonic approximation[1] and corresponding linear equation of motion

$$L_{\text{quadratic}} = \frac{1}{2}m\dot{x}^2 - \frac{1}{2}kx^2 \quad \text{and} \quad m\ddot{x} = -kx. \tag{6.2}$$

This linear differential equation could describe small free (as opposed to driven) oscillations of the extension x of a spring of force constant k with mass m attached. It is customary to define the parameter $\omega = \sqrt{k/m}$ so that (6.2) becomes $\ddot{x} = -\omega^2 x$. The solution may be obtained by reduction to quadrature through an integrating factor as discussed in Prob. 1.7. The same solution may also be obtained by putting the guess $x = Ne^{rt}$ for suitable constants N, r in (6.2) and deducing that $r = \pm i\omega$. Linearity allows us to write the general solution of this sort as $x(t) = \tilde{a}e^{i\omega t} + \tilde{b}e^{-i\omega t}$. Reality of $x(t)$ implies that $\tilde{a} = \tilde{b}^*$ so that we may write $\tilde{a} = \tilde{A} + i\tilde{B}$ and $\tilde{b} = \tilde{A} - i\tilde{B}$ for real constants $\tilde{A}$ and $\tilde{B}$. Putting $c_1 = 2\tilde{A}$ and $c_2 = -2\tilde{B}$, we obtain $x(t) = c_1 \cos\omega t + c_2 \sin\omega t$ where c_1 and c_2 are the two real constants of integration expected of a 2^{nd} order equation. The solution may also be expressed as[2]

---

[1] We assume $V''(q_0) \neq 0$. If it vanishes, we could use a higher degree Taylor polynomial.

$$x(t) = a\cos(\omega t + \alpha). \tag{6.3}$$

Evidently, the particle displays sinusoidal or harmonic oscillations with amplitude $a = \sqrt{c_1^2 + c_2^2}$ and initial phase $\alpha = \arccos(c_1/a)$, which are determined by initial conditions. The material constant ω is called the angular frequency and determines the time period $T = 2\pi/\omega$ of the small oscillations, which is independent of amplitude. As we observed in Sect. 1.2, this isochronous nature of harmonic oscillations is special to a linear restoring force.

Energy and Hamiltonian. The conserved energy of the linear oscillator (6.2) is $E = \frac{1}{2}m\dot{x}^2 + \frac{1}{2}m\omega^2 x^2$. Introducing the conjugate momentum $p = \frac{\partial L}{\partial \dot{x}} = m\dot{x}$, we get the Hamiltonian $H = \frac{1}{2m}p^2 + \frac{1}{2}m\omega^2 x^2$. Hamilton's equations are the first order pair of coupled homogeneous[3] linear equations

$$\dot{x} = \frac{\partial H}{\partial p} = \frac{p}{m} \quad \text{and} \quad \dot{p} = -\frac{\partial H}{\partial x} = -kx \quad \text{or} \quad \begin{pmatrix} \dot{x} \\ \dot{p} \end{pmatrix} = \begin{pmatrix} 0 & 1/m \\ -k & 0 \end{pmatrix} \begin{pmatrix} x \\ p \end{pmatrix}. \tag{6.4}$$

They define a linear vector field (see Sect. 5.1) on the x-p phase plane. Notice that the coefficient matrix $A = (0, 1/m| - k, 0)$ on the right is *not* symmetric. In fact, this formulation can be used to solve the initial value problem via the matrix exponential: $(x(t) \;\; p(t))^t = e^{At}(x(0) \;\; p(0))^t$, as we do in Prob. 6.1.

Phase portrait. It is instructive to plot a phase portrait of the linear oscillator (see Fig. 6.1a). In fact, the trajectories (given by (6.3)) coincide with the level curves of H, which are the ellipses $H = \frac{1}{2m}p^2 + \frac{1}{2}m\omega^2 x^2 = E$ with the phase point (x, p) moving clockwise (see Prob. 6.6). For $E = 0$, the ellipse degenerates to the point at the origin, which is a fixed point ($\dot{x} = \dot{p} = 0$) of the vector field.

Stability of fixed point. What is the nature of the fixed point at the origin? It is called a center, an elliptic fixed point or an O-point. It is neither an attractive fixed point nor a repulsive one: trajectories that begin nearby do not approach it as $t \to \pm\infty$. However, a trajectory that begins nearby remains nearby: this is called Lyapunov stability, after the Russian mathematical physicist Aleksandr Lyapunov (1857-1918). Furthermore, we say that the fixed point at the origin is neutrally stable since it is Lyapunov stable but not attracting. Coincidentally, the coefficient matrix in (6.4) is not diagonalizable over the reals: it has purely imaginary eigenvalues ($\pm i\omega$) (see Prob. 6.4). We will see in Sect. 6.2 how this is related to the stability of the fixed point at the origin.

---

[2] Alternatively, one may write $x(t) = \Re\left[Ae^{i\omega t}\right]$ where the complex amplitude $A = ae^{i\alpha}$.

[3] Homogeneous linear implies there is no external force $f_{\text{ext}}(t)$ contributing to $\dot{p}$ in (6.4).

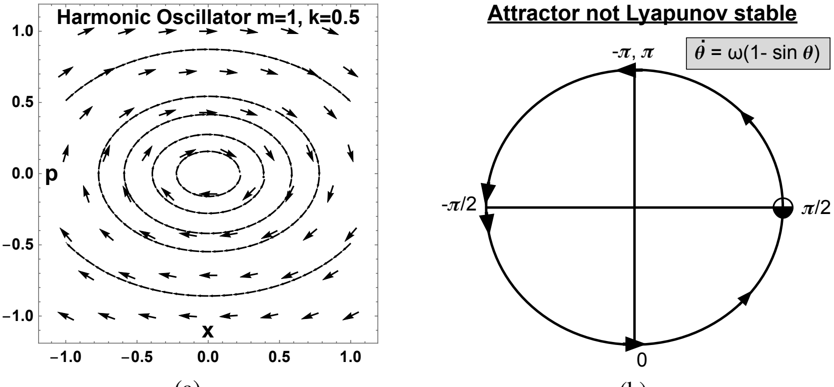

(a) (b)

Figure 6.1: (a) Phase portrait of the harmonic oscillator showing concentric ellipse integral curves around the center at the origin which is a Lyapunov stable fixed point. (b) Attracting but not Lyapunov stable fixed point at $\theta_* = \pi/2$ of the vector field on the circle: $\dot{\theta} = \omega(1 - \sin\theta)$ for $\omega > 0$. Note that $\theta_* = \pi/2$ is also a repeller.

Asymptotic and Lyapunov stability. We have introduced two notions of stability here. The first concerns asymptotic behavior: a fixed point $\boldsymbol{r}_*$ is said to be attractive if trajectories that begin sufficiently close to $\boldsymbol{r}_*$ approach $\boldsymbol{r}_*$ as $t \to \infty$. On the other hand, Lyapunov stability concerns behavior at all times: $\boldsymbol{r}_*$ is Lyapunov stable if trajectories that begin sufficiently close to $\boldsymbol{r}_*$ remain close to $\boldsymbol{r}_*$ at all subsequent times[4]. A fixed point that is both attracting and Lyapunov stable is called asymptotically stable. Although the two often occur together, they need not. The origin in the harmonic oscillator is Lyapunov stable but not attracting. On the contrary, a fixed point may be attracting but not Lyapunov stable, if trajectories that begin nearby go far away before eventually reaching $\boldsymbol{r}_*$. An example is given by the half-stable fixed point $\theta_* = \pi/2$ of the vector field $\dot{\theta} = v(\theta) = \omega(1 - \sin\theta)$ on the circle examined in Prob. 5.6 and displayed in Fig. 6.1b. It is attracting, since all trajectories eventually approach $\theta = \pi/2$. However, it is not Lyapunov stable as the trajectories have to go 'round the circle' before eventually arriving at the fixed point.

6.2 Linear vector fields on the phase plane

The harmonic oscillator led us to a system of homogeneous linear ODEs or an autonomous linear vector field (6.4) on the phase plane. Here, we will consider the most general such linear vector field on the plane and classify the possible types of fixed points and phase portraits[5]. We will then apply our results to the damped harmonic oscillator in Sect. 6.4. Thus, we consider the linear system with real coefficients

---

[4] More precisely, $\boldsymbol{r}_*$ is Lyapunov stable if given any tolerance $\epsilon > 0$ there exists a $\delta > 0$ so that we can guarantee that $|\boldsymbol{r}(t) - \boldsymbol{r}_*| < \epsilon$ for all $t > 0$ provided we start close enough ($|\boldsymbol{r}(0) - \boldsymbol{r}_*| < \delta$). If we do not have notions of distance but only the topological notion of open sets, this condition can be formulated in terms of open neighborhoods. $\boldsymbol{r}_*$ is Lyapunov stable if given any nonempty neighborhood N of $\boldsymbol{r}_*$, there exists a nonempty neighborhood V of $\boldsymbol{r}_*$ such that if the initial condition lies within V then $\boldsymbol{r}(t)$ is guaranteed to lie within N for all $t \geq 0$.

$$\left(\begin{smallmatrix} \dot{x} \\ \dot{y} \end{smallmatrix}\right) = A \left(\begin{smallmatrix} x \\ y \end{smallmatrix}\right) \quad \text{or} \quad \dot{\boldsymbol{r}} = \boldsymbol{v} = A\boldsymbol{r} \quad \text{where} \quad \boldsymbol{r} = \left(\begin{smallmatrix} x \\ y \end{smallmatrix}\right) \quad \text{and} \quad A = \left(\begin{smallmatrix} a & b \\ c & d \end{smallmatrix}\right) \tag{6.5}$$

subject to the initial conditions $x(0) = x_0$ and $y(0) = y_0$. In mechanical applications, x and y are typically position and momentum. It is clear that the origin $\boldsymbol{r}_* = 0$ is always a zero of the vector field (i.e., fixed point or static solution). There could be nontrivial fixed points $\boldsymbol{r}_* \neq 0$ with $A\boldsymbol{r}_* = 0$, if A is singular (i.e., if $\det A = 0$ or equivalently if it has a nontrivial null space or kernel). More precisely, (i) the origin is the only fixed point if $\det A \neq 0$, (ii) we have a line of fixed points along the null space if A has a one-dimensional kernel and (iii) we have a plane of fixed points if A has a two-dimensional null space (in which case $A = 0$). The trajectories or integral curves of the vector field are directed parametrized curves $(x(t), y(t))$ on the x-y plane with tangent vector $\boldsymbol{v}$.

Remark. The time-dependent Schrödinger equation of quantum mechanics (QM) $i\hbar\dot{\psi} = H\psi$ is a linear equation of the above sort, with the Hamiltonian operator H defining a linear vector field on the state space. However, the state space in QM is generally a *complex* vector space (with Hermitian inner product) whose dimension could be finite or infinite and H is invariably Hermitian (see Sect. 10.3*). □

Examples. Before treating the general case, let us consider four examples that illustrate some of the possibilities. Consider the coefficient matrices A given by

$$\text{(i)} \left(\begin{smallmatrix} -1 & 0 \\ 0 & -1 \end{smallmatrix}\right), \quad \text{(ii)} \left(\begin{smallmatrix} -2 & 0 \\ 0 & -1 \end{smallmatrix}\right), \quad \text{(iii)} \left(\begin{smallmatrix} 2 & 0 \\ 0 & -1 \end{smallmatrix}\right) \quad \text{and} \quad \text{(iv)} \left(\begin{smallmatrix} -2 & 0 \\ 0 & 0 \end{smallmatrix}\right). \tag{6.6}$$

In the first three cases, A is invertible and the origin is the only fixed point. In all cases, the equations for x and y decouple. Let us consider them one by one (see Fig. 6.2).

(i) Here $\dot{x} = -x$ and $\dot{y} = -y$ so that $x(t) = x_0 e^{-t}$ and $y(t) = y_0 e^{-t}$ approach zero at the same rate and all nonconstant trajectories are straight lines that approach the origin as $t \to \infty$. The origin is a *symmetrical node* or *star*. It is both Lyapunov stable and attracting and therefore asymptotically stable.

(ii) $x(t) = x_0 e^{-2t}$ and $y(t) = y_0 e^{-t}$: all nonconstant trajectories approach the origin while becoming asymptotically tangent to the y-axis, as x decays faster than y. The fixed point at the origin is called a *stable node*, it is asymptotically stable.

(iii) $x(t) = x_0 e^{2t}$ and $y(t) = y_0 e^{-t}$. The fixed point at the origin is a *saddle point*, also called an X-point. It is an example of a hyperbolic fixed point[6]. Trajectories with $x_0 = 0$ approach it along the y axis. But all other nonconstant trajectories asymptotically approach either $(\infty, 0)$ or $(-\infty, 0)$. Thus, the saddle point is neither

---

[5] Such an analysis was performed by Poincaré as preparation for his work on the three-body problem of celestial mechanics.

[6] Somewhat confusingly, the name hyperbolic fixed point (see Sect. 6.7*) is used for a wider class of fixed points that includes saddles, nodes and spirals.

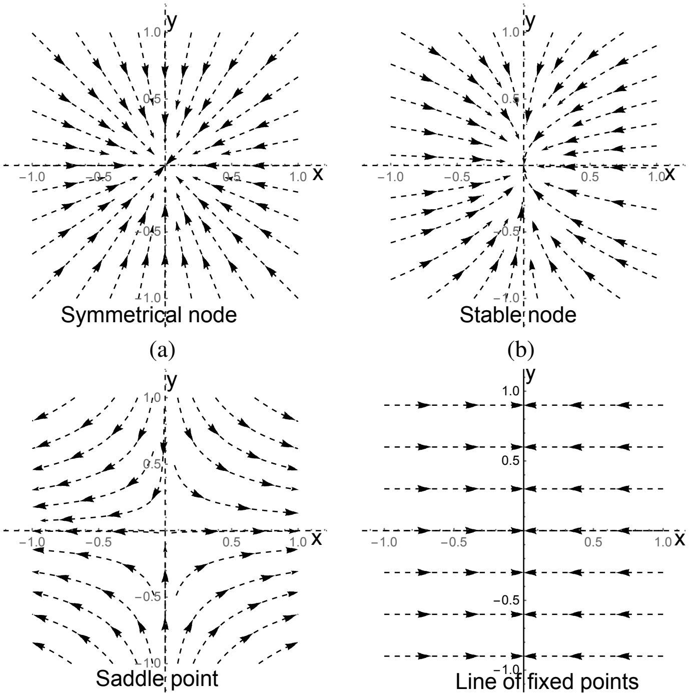

(a) (b) (c) (d)

Figure 6.2: Phase portraits of the star, node, saddle and line of fixed points (along the y-axis) corresponding to the coefficient matrices in (6.6).

Lyapunov stable nor attractive[7]. The phase portrait consists of a family of curves on which xy^2 is constant.

(iv) $x(t) = x_0 e^{-2t}$ while $y = y_0$ is independent of time. We have a *line of fixed points* along the y axis. Nonconstant trajectories are horizontal rays approaching one of these fixed points either from the right or left half-plane. Each of these fixed points is neutrally stable (Lyapunov stable but not attracting), as trajectories that begin nearby remain nearby but may not approach the fixed point as $t \to \infty$.

6.3 Phase portrait from spectrum of coefficient matrix

It was easy to analyze the examples in Eq. (6.6) since A was diagonal and the equations for x and y decoupled. The horizontal and vertical directions were eigendirections[8] of A. In this section, we consider coefficient matrices A that are not necessarily diagonal. In general, an initial condition in an eigendirection of A leads to simple evolution. Let us see why. Suppose $\boldsymbol{w}$ is a (real) eigenvector of A with (real) eigenvalue λ, $A\boldsymbol{w} = \lambda\boldsymbol{w}$. If the initial state $\boldsymbol{r}(0) = r_0\boldsymbol{w}$ is in this eigendirection, then the trajectory remains along $\boldsymbol{w}$ at all times. Indeed, we see that the solution is given by $\boldsymbol{r}(t) = e^{\lambda t} r_0 \boldsymbol{w}$ since $\dot{\boldsymbol{r}} = \lambda\boldsymbol{r}(t)$ is the same as $A\boldsymbol{r}(t)$. Clearly, it is beneficial to try to decompose the initial state as a linear combination of eigenvectors of A. In the rest of this section, we will assume that A has two linearly independent eigenvectors, so that this spectral decomposition is possible [see Sect. 6.5 for what to do if this fails].

---

[7] For a saddle point (and more generally for any fixed point), one defines the notions of stable and unstable manifolds. The stable manifold W_s of a fixed point $\boldsymbol{r}_*$ is defined as the set of ICs (x_0, y_0) (points on phase space) for which the trajectory tends to $\boldsymbol{r}_*$ as $t \to \infty$ (the basin of 'attraction'). The unstable manifold W_u is similarly the set of ICs for which the trajectory tends to $\boldsymbol{r}_*$ as $t \to -\infty$ (basin of 'repulsion'). For the saddle point of Fig. 6.2c, W_s is the y-axis while W_u is the x-axis. We observe that a typical trajectory (in this case, every trajectory) approaches the unstable/stable manifold as $t \to \pm\infty$.

Suppose the real coefficient matrix $A = (a, b|c, d)$ (6.5) has 2 distinct eigenvalues

$$\lambda_\pm = \frac{1}{2}\left[(a+d) \pm \sqrt{(a+d)^2 - 4(ad-bc)}\right] \tag{6.7}$$

which must either be real or complex conjugates. Then we are guaranteed[9] that the corresponding eigenvectors $\boldsymbol{w}_\pm$ are linearly independent. Thus, if we expand the initial state as $\boldsymbol{r}(0) = r_-\boldsymbol{w}_- + r_+\boldsymbol{w}_+$, then we can immediately write down the solution to the initial value problem (IVP):

$$\boldsymbol{r}(t) = r_- e^{\lambda_- t}\boldsymbol{w}_- + r_+ e^{\lambda_+ t}\boldsymbol{w}_+. \tag{6.8}$$

Notably, this formula works even if the eigenvalues and eigenvectors are not real! However, $\boldsymbol{r}(0)$ must be real; a convenient way of ensuring this is to exploit the fact that $\lambda_\pm$ must be complex conjugates to take $\boldsymbol{w}_\pm$ to also be complex conjugates and $r_+ = r_-^*$. An immediate consequence is that if the real parts of the eigenvalues $\lambda_\pm$ are negative, then the origin is an attractor while it is unstable[10] if $\Re\lambda_+ > 0$ or $\Re\lambda_- > 0$. However, when the eigenvalues are not real, the eigenvectors are also not real and the corresponding eigenspaces are not lines through the origin on the plane; they cannot be interpreted as invariant subspaces for the dynamics on the plane. On the other hand, if the eigenvalues are real, then the eigenvectors can be taken real and define invariant subspaces for the dynamics. They are unstable/stable depending on whether the corresponding eigenvalue is positive/negative. We list the possibilities below.

a. If $\lambda_+ = \lambda_- \neq 0$, and they nevertheless have linearly independent eigenvectors, then $A = \lambda_+ I$ and we have a stable or unstable *star* (also known as a symmetrical node) depending on whether the eigenvalues are negative or positive (see Fig. 6.2a).

---

[8] An eigendirection or more precisely an eigenspace corresponding to a given eigenvalue is an invariant subspace for the dynamics. If the initial condition lies in it, time evolution cannot take it outside.

[9] Suppose $A\boldsymbol{v} = \lambda\boldsymbol{v}$ and $A\boldsymbol{w} = \mu\boldsymbol{w}$ are two (nonzero) eigenvectors corresponding to distinct eigenvalues $\lambda \neq \mu$. Suppose $\boldsymbol{v} = \alpha\boldsymbol{w}$ are linearly dependent. Then $A\boldsymbol{v} = \lambda\boldsymbol{v}$ and also $A\boldsymbol{v} = A\alpha\boldsymbol{w} = \alpha\mu\boldsymbol{w} = \mu\boldsymbol{v}$ so that $(\lambda - \mu)\boldsymbol{v} = 0$ or $\lambda = \mu$, contradicting the hypothesis.

[10] The Routh-Hurwitz criterion [80] is a necessary and sufficient condition for all the eigenvalues (roots of the characteristic polynomial) of the Jacobian matrix to have negative real parts. It is applicable to phase spaces of any dimension and can be used to study the linear stability of fixed points.

b. If $\lambda_\pm$ are real nonzero and of the same sign, then as is Fig. 6.2b, the origin is either a stable or unstable *node* depending on whether $\lambda_\pm$ are negative or positive.

c. The origin is a *saddle point* if λ_+ and λ_- have opposite signs as in Fig. 6.2c.

d. If one eigenvalue, say λ_-, is zero and the other is nonzero, then we have a *line of fixed points* along the 0-eigenspace. The fixed points are stable (as in Fig. 6.2d) if $\lambda_+ < 0$ and unstable if $\lambda_+ > 0$.

e. If $\lambda_- = \lambda_+ = 0$ but A has 2 linearly independent eigenvectors, then A must be the zero matrix and *every point on the plane is a neutrally stable fixed point*.

f. On the other hand, if the eigenvalues are purely imaginary $\lambda_\pm = \pm i\omega$, then the trajectory

$$\boldsymbol{r}(t) = r_- e^{-i\omega t}\boldsymbol{w}_- + r_+ e^{i\omega t}\boldsymbol{w}_+ \tag{6.9}$$

is periodic with period $2\pi/\omega$, as in the case of the harmonic oscillator of Sect. 6.1 and the origin is a *neutrally stable center* (see Fig. 6.1a and Prob. 6.4).

g. *Spiral sink or source:* A center is not structurally stable. What this means is that a center is generally not preserved under a perturbation of system parameters a, b, c and d. Typical perturbations (that preserve the reality of A) would cause the pure imaginary eigenvalues to move off the imaginary axis and become truly complex and conjugate to each other. In fact, if the eigenvalues are not real or imaginary, they must be of the form $\lambda_\pm = \gamma \pm i\omega$ (with $\gamma, \omega \neq 0$). The solution is then

$$\boldsymbol{r}(t) = e^{\gamma t}\left(r_- e^{-i\omega t}\boldsymbol{w}_- + r_+ e^{i\omega t}\boldsymbol{w}_+\right). \tag{6.10}$$

In this case, we have a stable or unstable spiral (spiral sink or source, sometimes called a *focus*) according as γ is negative or positive; see Fig. 6.3c. Here, γ is called the decay or growth rate. Physically, the motion is like that of an (underdamped) oscillator, to which we turn next.

6.4 Damped harmonic oscillator: view from the phase plane

In the simplest model of a damped harmonic oscillator, the particle is subject to a damping force proportional to velocity, in addition to a linear restoring force proportional to the displacement x from equilibrium:

$$m\ddot{x} = -kx - \gamma\dot{x} \quad \text{with} \quad m, k, \gamma \geq 0. \tag{6.11}$$

The damping coefficient γ must be positive to ensure that the damping force acts in a direction opposite to the instantaneous velocity, thereby slowing the particle down. As noted in Sect. 1.1, this is not a conservative system, it does not admit a Lagrangian of the usual sort nor a conserved energy for $\gamma \neq 0$. Nevertheless, it is convenient to introduce the linear momentum $p = m\dot{x}$ and write (6.11) as a first order system on the x-p phase plane

$$\begin{pmatrix}\dot{x}\\ \dot{p}\end{pmatrix} = \begin{pmatrix}0 & 1/m\\ -k & -\gamma/m\end{pmatrix}\begin{pmatrix}x\\ p\end{pmatrix}. \tag{6.12}$$

The eigenvalues of the coefficient matrix A are

$$\lambda_\pm = (1/2m)(-\gamma \pm \sqrt{\gamma^2 - 4m^2\omega^2}) \quad \text{where} \quad \omega = \sqrt{k/m}. \tag{6.13}$$

It is useful to note that $\det A = \lambda_+\lambda_- = \omega^2$. Since $\Re\lambda_\pm = -\gamma/2m < 0$, the origin is an attractor: the particle eventually comes to rest at the equilibrium point $x = 0$. There are three qualitatively different parameter regimes.

1. If $\gamma < 2m\omega$ (weak damping), then $\lambda_\pm$ are complex and the origin is a spiral sink. The motion is said to be *underdamped*: As shown in Fig. 6.3a, x oscillates infinitely often (with 'time period' $2\pi/|\Im\lambda_\pm| = 2\pi/\sqrt{\omega^2 - \gamma^2/4m^2}$) with exponentially decreasing amplitude as it settles down to $x = 0$. The phase trajectory winds clockwise around the origin as in Fig. 6.3b. These features are also reflected in the formula for the solution

$$x(t) = a e^{-\gamma t/2m} \cos\left(t\sqrt{\omega^2 - \gamma^2/4m^2} + \alpha \right) \tag{6.14}$$

   where a and α are constants of integration.

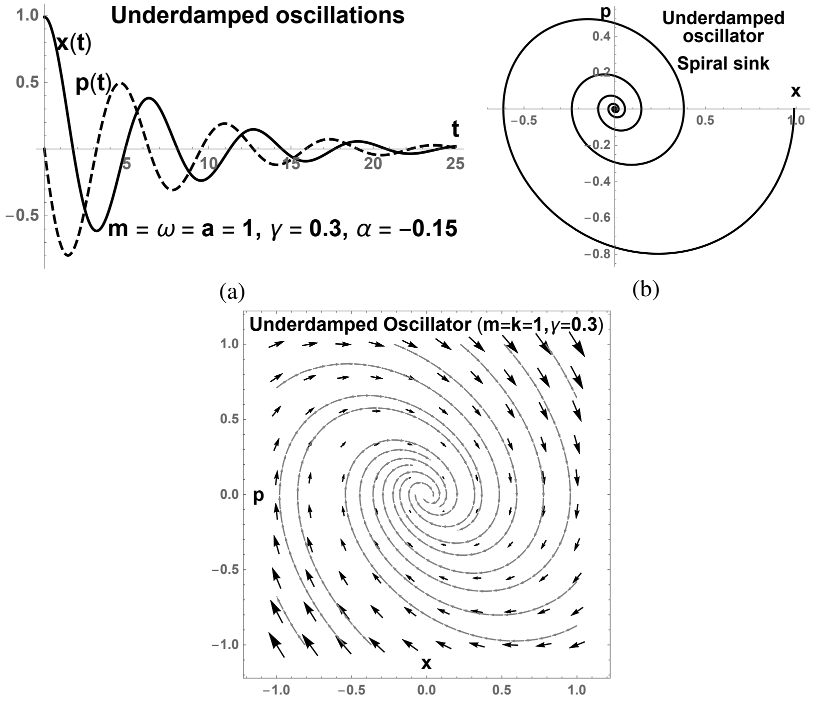

(a) (b)

(c)

Figure 6.3: (a) $x(t)$ and $p(t)$ for underdamped oscillations ($m = \omega = 1, \gamma = 0.3$) from rest at $x = 1$. (b) Corresponding spiral trajectory and (c) phase portrait of the same oscillator.

2. When $\gamma = 2m\omega$, the eigenvalues coincide $\lambda_\pm = -\gamma/2m = -\omega$. However, in this case A is not proportional to the identity and there is only one linearly independent eigenvector, which can be taken as $(1, -m\omega)^t$. The motion is said to be *critically damped* and the origin is a *degenerate node*, as shown in Fig. 6.4. The solution to

the IVP is given by (6.31):

$$x(t) = e^{-\omega t}\left[x_0(1+\omega t) + \frac{p_0 t}{m}\right]. \tag{6.15}$$

We will look at this case in more detail in Sect. 6.5.

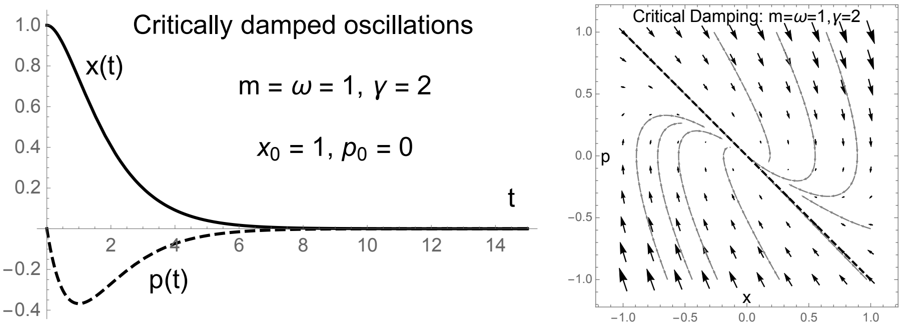

(a) (b)

Figure 6.4: (a) Critically damped oscillations starting from rest at $x = 1$. (b) Phase portrait showing stable degenerate node with only one invariant direction along $(1, -m\omega)$.

3. If $\gamma > 2m\omega$ (strong damping), then $\lambda_\pm$ are real, distinct and negative ($\lambda_- < \lambda_+ < 0$). The origin is an asymptotically stable node. The motion is said to be *overdamped* or *aperiodically damped*: the particle performs less than one full oscillation before coming to rest at $x = 0$. In fact, the eigenvectors corresponding to $\lambda_\pm$ can be taken as

$$\boldsymbol{w}_\pm = \begin{pmatrix} \lambda_\mp \\ m\omega^2 \end{pmatrix}. \tag{6.16}$$

Since $\lambda_- < \lambda_+ < 0$, $\boldsymbol{w}_+$ points roughly towards west-north-west while $\boldsymbol{w}_-$ points in a north-north-westerly direction (see Fig. 6.5b). They enclose a 'small' wedge in the 2^{nd} quadrant with acute opening angle while $-\boldsymbol{w}_-$ and $-\boldsymbol{w}_+$ do so in the 4^{th} quadrant. Similarly, $\boldsymbol{w}_-$ and $-\boldsymbol{w}_+$ (or $-\boldsymbol{w}_-$ and $\boldsymbol{w}_+$) enclose a 'large' wedge with obtuse opening angle. The trajectory $\boldsymbol{r}(t) = r_+ e^{\lambda_+ t}\boldsymbol{w}_+ + r_- e^{\lambda_- t}\boldsymbol{w}_-$ approaches the origin along $\boldsymbol{w}_+$ as $t \to \infty$. As $t \to -\infty$ both components of $\boldsymbol{r}$ become unbounded, but the $\boldsymbol{w}_-$ component grows faster, so $\boldsymbol{r}$ points along $\pm\boldsymbol{w}_-$ as $t \to -\infty$. We see that x either monotonically approaches 0 or changes sign once (i.e., passes through the equilibrium point once) before eventually reaching 0 as $t \to \infty$. The first case occurs if the IC is in one of the two small wedges and the latter possibility occurs if the IC lies in one of the two large wedges. The general solution in the overdamped case is a linear combination of two damped exponentials:

$$x(t) = a\, e^{-\left(\gamma/2m + \sqrt{\gamma^2/4m^2 - \omega^2}\right)t} + b\, e^{-\left(\gamma/2m - \sqrt{\gamma^2/4m^2 - \omega^2}\right)t}. \tag{6.17}$$

$*$ **Comparison of decay rates and a note of caution.** It is interesting to compare the rates of decay of $x(t)$ in the under- (u), over- (o) and critically (c) damped cases for

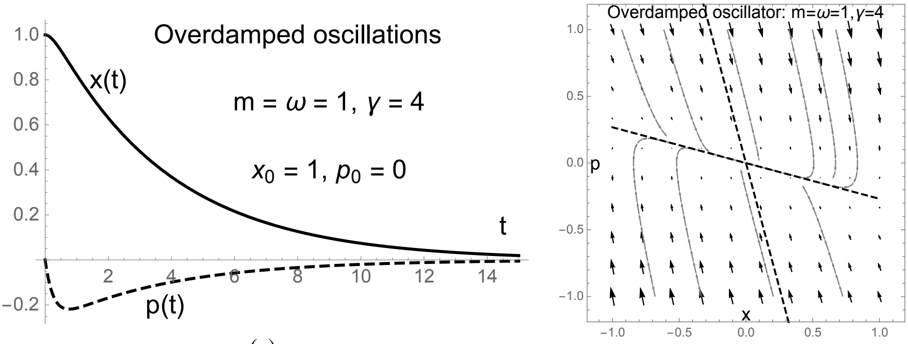

(a)

(b)

Figure 6.5: (a) $x(t)$ and $p(t)$ for an overdamped oscillator starting from rest. (b) Phase portrait showing corresponding stable node and eigenspaces spanned by $\boldsymbol{w}_\pm$ which point towards west-north-west and north-north-west.

common values of m and ω. From (6.14), (6.15) and (6.17) we read off the exponential decay constants in $x(t) \sim e^{-\mu t}$ for large t:

$$\mu_{\rm u} = \frac{\gamma_u}{2m}, \quad \mu_{\rm o} = \frac{\gamma_o}{2m} - \sqrt{\frac{\gamma_o^2}{4m^2} - \omega^2} \quad \text{and} \quad \mu_{\rm c} = \frac{\gamma_c}{2m} = \omega \tag{6.18}$$

which are valid for $\gamma_u < 2m\omega$, $\gamma_o > 2m\omega$ and $\gamma_c = 2m\omega$. It may be shown (see Prob. 6.16) that for fixed m and ω,

$$\mu_{\rm o}, \mu_{\rm u} < \mu_{\rm c} = \omega. \tag{6.19}$$

Thus, $x(t)$ decays fastest in the critically damped case, even though the damping coefficient γ is larger for an overdamped oscillator. This is seen in Figs. 6.3a, 6.4a and 6.5a. On the other hand, no such inequality holds between $\mu_{\rm o}$ and $\mu_{\rm u}$. In fact, for any given $\gamma_{\rm o}$, there are values of $\gamma_{\rm u}$ such that the corresponding underdamped oscillations decay faster and slower than those of the given overdamped oscillator. The same holds with the roles of $\gamma_{\rm o}$, and $\gamma_{\rm u}$ reversed (see Prob. 6.16). Thus, the possible naive expectation that an overdamped oscillation would decay faster than any underdamped oscillation with the same values of m and ω is incorrect. ☐

$*$ **Energy loss and dissipation function.** Recall from (1.4) that damped motion in a potential governed by

$$m\ddot{x} = -V'(x) - \gamma\dot{x} \quad \text{for} \quad \gamma > 0 \tag{6.20}$$

leads to a loss of mechanical energy at the rate $\dot{E} = -\gamma\dot{x}^2$. It is sometimes convenient to introduce the *dissipation function* $F = \frac{1}{2}\gamma\dot{x}^2$ so that $\dot{E} = -2F$. Although (6.20) does not follow from a Lagrangian $L(x, \dot{x}, t)$, it is possible to augment Lagrange's equations by the frictional forces on the RHS to get (6.20). In fact, if $L = \frac{1}{2}m\dot{x}^2 - V(x)$, then

$$\frac{d}{dt}\frac{\partial L}{\partial \dot{x}} = \frac{\partial L}{\partial x} - \frac{\partial F}{\partial \dot{x}} \tag{6.21}$$

gives (6.20). These formulae generalize (see Prob. 6.17) to damped systems with several degrees of freedom

$$m_{ij}\ddot{x}^j = -\partial_i V - \gamma_{ij}\dot{x}^j \tag{6.22}$$

if we define the dissipation function $F = \frac{1}{2}\gamma_{ij}\dot{x}^i\dot{x}^j$ where γ_{ij} is a *symmetric* dissipation tensor. □

6.5 Critically damped oscillator: deficient coefficient matrix

The example of the critically damped oscillator encourages us to consider the special case where the two eigenvalues of A are equal but there is only one linearly independent eigenvector. This degenerate case is somewhat exceptional (nongeneric), as a small perturbation of matrix elements would make the eigenvalues distinct. Nevertheless, it is an interesting case since the eigenvectors do not furnish a basis in which to expand a general initial state and the matrix A may be said to be deficient.

Upper triangular toy. For instance, consider the 'strictly upper triangular' system

$$\dot{x} = y, \quad \dot{y} = 0 \quad \text{corresponding to} \quad A = \left(\begin{smallmatrix} 0 & 1 \\ 0 & 0 \end{smallmatrix}\right). \tag{6.23}$$

A has only one eigenvalue 0, with algebraic multiplicity two. The corresponding null space is spanned by the one linearly independent eigenvector, say $\hat{x} = (1,0)^t$. Thus, the horizontal axis is a line of fixed points. The solution to the IVP is $y = y_0$ and $x = x_0 + y_0 t$. The flow is horizontal and to the right in the upper half-plane and to the left in the lower half-plane. Draw the phase portrait (see Prob. 6.14). None of the fixed points is stable, as a small perturbation either upwards or downwards would go off to $x = \pm\infty$. More generally, consider the upper triangular system

$$\dot{x} = \lambda x + y, \quad \dot{y} = \lambda y \quad \text{corresponding to} \quad A = \left(\begin{smallmatrix} \lambda & 1 \\ 0 & \lambda \end{smallmatrix}\right) \quad \text{with} \quad \lambda < 0. \tag{6.24}$$

As A is invertible, the origin is the only fixed point. λ is a doubly degenerate eigenvalue with only one linearly independent eigenvector, say $(1,0)^t$, so that the x axis is an invariant subspace with points driven towards the origin: $(x(0),0) \mapsto (x(0)e^{\lambda t},0)$. More generally, y evolves independently of x and is given by $y(t) = y(0)e^{\lambda t}$. We are left with an inhomogeneous equation for x:

$$\dot{x} = \lambda x + y(0)e^{\lambda t} \quad \text{with solution} \quad x(t) = x(0)e^{\lambda t} + y(0)te^{\lambda t}, \tag{6.25}$$

which is the subject of Prob. 6.10. To draw the corresponding phase portrait, we note that the slope of trajectories is given by $dy/dx = \dot{y}(t)/\dot{x}(t) = y(0)/(x(0) + y(0)(t + 1/\lambda))$. The slope approaches 0^- in the far past and 0^+ in the far future, so the flow is generally 'clockwise', see Fig. 6.6. The origin is an asymptotically stable degenerate node and the motion is like that of a critically damped oscillator. The same formulae apply also when $\lambda > 0$, in which case the origin is an *unstable degenerate node*. □

Let us now look at the **critically damped oscillator** of Sect. 6.4 with $\gamma = 2m\omega$ in more detail:

$$\left(\begin{smallmatrix} \dot{x} \\ \dot{p} \end{smallmatrix}\right) = \begin{pmatrix} 0 & 1/m \\ -k & -2\omega \end{pmatrix} \left(\begin{smallmatrix} x \\ p \end{smallmatrix}\right). \tag{6.26}$$

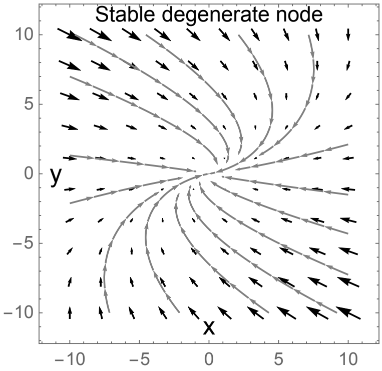

Figure 6.6: Phase portrait of stable degenerate node of the upper triangular system (6.24) for $\lambda = -1$. There is only one invariant subspace, the horizontal axis.

As noted, the coefficient matrix has the doubly degenerate eigenvalue $\lambda = -\omega$ with only one linearly independent eigenvector which we take as $\boldsymbol{w} = (1, -m\omega)^t$. To facilitate solving the equations, we will make a similarity transformation to a basis where A is upper/lower triangular (essentially in Jordan form). This basis consists of eigenvectors and generalized eigenvectors of A. Eigenvectors $\boldsymbol{w}$ are nontrivial solutions to $(A - \lambda I)\boldsymbol{w} = 0$, they lie in the kernel of $(A - \lambda I)$. Generalized eigenvectors are vectors that lie in the kernel of $(A - \lambda I)^p$ for some $p > 1$ but not in the kernel of $(A - \lambda I)^q$ for $q < p$. In our case $(A - \lambda I)^2$ is identically zero so we can take our generalized eigenvector to be any vector linearly independent of $\boldsymbol{w}$, say $\boldsymbol{w}' = (0, 1)^t$.

The resulting similarity matrix is

$$S = (\boldsymbol{w}, \boldsymbol{w}') = \left(\begin{smallmatrix} 1 & 0 \\ -m\omega & 1 \end{smallmatrix}\right) \quad \text{with inverse} \quad S^{-1} = \left(\begin{smallmatrix} 1 & 0 \\ m\omega & 1 \end{smallmatrix}\right). \tag{6.27}$$

Applying the similarity transformation we get $J = S^{-1}AS = (-\omega, 1/m | 0, -\omega)$ which is upper triangular. The ODE

$$\dot{\boldsymbol{r}} = A\boldsymbol{r} = SJS^{-1}\boldsymbol{r} \quad \text{becomes} \quad S^{-1}\dot{\boldsymbol{r}} = J(S^{-1}\boldsymbol{r}) \quad \text{where} \quad S^{-1}\boldsymbol{r} = \left(\begin{smallmatrix} x \\ m\omega x + p \end{smallmatrix}\right). \tag{6.28}$$

It is natural to define $y = m\omega x + p$, which evolves independently of x due to the triangular structure:

$$\left(\begin{smallmatrix} \dot{x} \\ \dot{y} \end{smallmatrix}\right) = \begin{pmatrix} -\omega & 1/m \\ 0 & -\omega \end{pmatrix} \left(\begin{smallmatrix} x \\ y \end{smallmatrix}\right) \quad \text{or} \quad \dot{y} = -\omega y \quad \text{and} \quad \dot{x} = -\omega x + y/m. \tag{6.29}$$

Thus

$$y(t) = y_0 e^{-\omega t} \quad \text{and} \quad x(t) = e^{-\omega t}\left(x_0 + y_0 t/m\right) \quad \text{where} \quad y_0 = m\omega x_0 + p_0. \tag{6.30}$$

The solution to the IVP may now be expressed as

$$x(t) = e^{-\omega t}\left[x_0(1 + \omega t) + \frac{p_0 t}{m}\right] \quad \text{and} \quad p(t) = m\dot{x} = e^{-\omega t}\left[-kx_0 t + p_0(1 - \omega t)\right]. \tag{6.31}$$

The origin ($x = 0, p = 0$) is an asymptotically stable degenerate node. $\boldsymbol{w}$ spans the only invariant subspace. Trajectories that do not start along $\boldsymbol{w}$ make roughly half a turn clockwise around the origin before reaching it. The phase portrait in the critically damped case may be viewed as resulting from the overdamped portrait when the eigenvectors $\boldsymbol{w}_\pm$ become collinear and the smaller wedges shrink letting the larger wedges become half-planes. Every trajectory that does not start along $\boldsymbol{w}$ crosses the equilibrium point $x = 0$ once (at $t = -mx_0/(m\omega x_0 + p_0)$, which may be negative) before eventually reaching the fixed point as $t \to \infty$. Similarly, every (possibly extended) trajectory comes to rest momentarily once at $t = p_0/(kx_0 + \omega p_0)$ before eventually coming to rest at the fixed point.

6.6* Trace-determinant classification of linear fixed points

Having worked out the example of the damped oscillator, we now return to the general linear vector field (6.5) on the phase plane and summarize the nature of its phase portrait. While the formulation in terms of eigenvalues allows us, for the most part, to classify fixed points of such vector fields, the (possibly complex) eigenvalues themselves depend only on two real numbers: the trace $\tau = a + d$ and determinant $\Delta = ad - bc$ of the coefficient matrix $A = (a, b|c, d)$. Thus, by and large, one obtains a more economical classification in terms of τ and Δ. In other words, although the space of linear systems defined by A is four-dimensional, the character of the system is largely determined[11] by just two real control parameters τ and Δ. In fact, the characteristic equation $\lambda^2 - \tau\lambda + \Delta = 0$ implies that the eigenvalues are

$$\lambda_\pm = \frac{1}{2}(\tau \pm \sqrt{\tau^2 - 4\Delta}) \quad \text{with} \quad \tau = \lambda_+ + \lambda_- \quad \text{and} \quad \Delta = \lambda_+\lambda_-. \tag{6.32}$$

In what follows, given a (τ, Δ) pair, we try to ascertain the nature of the phase portrait. To begin with, the sign of the discriminant $D = \tau^2 - 4\Delta$ tells us that $\lambda_\pm$ are (a) distinct and complex conjugates if $D < 0$, (b) real and distinct if $D > 0$ and (c) real and equal if $D = 0$. Evidently, the location of (τ, Δ) relative to the parabola $\Delta = \tau^2/4$ plays a crucial role (see Fig. 6.7).

At points above the parabola ($\Delta > \tau^2/4$), $D < 0$ and there are two main possibilities: (i) (stable) spiral sink if $\tau < 0$ and (ii) (unstable) spiral source if $\tau > 0$. At points below the parabola ($\Delta < \tau^2/4$) we have $D > 0$ and there are three main possibilities: (iii) saddle if $\Delta < 0$, as the eigenvalues have opposite signs, (iv) unstable node if $\Delta > 0$ and $\tau > 0$ since the eigenvalues are both positive and (v) stable node if $\Delta > 0$ and $\tau < 0$ since the eigenvalues are both negative. Special circumstances prevail on the boundaries between these five open regions (see Fig. 6.7).

1. **Boundary between spiral sources and sinks.** On the axis of the parabola (the ray $\tau = 0, \Delta > 0$), the eigenvalues are imaginary $\lambda_\pm = \pm i\sqrt{|D|}$ and the origin of the phase plane is a *center*. It is neutrally stable, as befits a system that is borderline between spiral sources and sinks.

---

[11] There are exceptional cases where the trace and determinant are not adequate to determine the character of the phase portrait. This happens if A has repeated eigenvalues, as we will see.

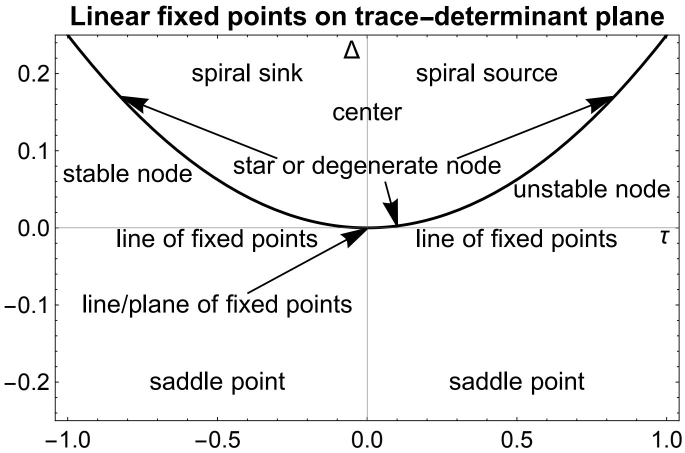

Figure 6.7: Nature of fixed points on the trace-determinant plane for a 2d linear system.

2. **Origin $\tau = \Delta = 0$.** The eigenvalues vanish and the origin $x = y = 0$ is no longer an isolated fixed point: we may either have a *plane of fixed points* (if A has two linearly independent eigenvectors so that $A = 0$) or a *line of fixed points* along the null space of A if A has only one linearly independent eigenvector (e.g., $A = (0, 1|0, 0)$). The fixed points are neutrally stable in the eigendirection and unstable in any other direction (recall (6.24) with $\lambda = 0$).

3. **Parabolic boundary between spirals and nodes**. On the parabola $\Delta = \tau^2/4$, the eigenvalues are real and equal $\lambda_\pm = \tau/2$. Let us suppose $\tau, \Delta \neq 0$. If A has two linearly independent eigenvectors, then A is a (nonzero) multiple of the identity and the origin is an unstable *symmetrical node (star)* if $\tau > 0$ and a stable symmetrical node if $\tau < 0$. On the other hand, if A is deficient and has only one independent eigenvector, then the origin is a stable/unstable *degenerate node* according as τ is negative or positive. This is illustrated by the example $A = (\lambda, 1|0, \lambda)$ where $\lambda = \tau/2 \neq 0$. The phase portrait of a degenerate node arises as the phase portrait of a node is morphed to lose one eigenvector. When both eigenvectors cease to be real, the node becomes a spiral.

4. The pair of rays $\Delta = 0, \tau \neq 0$ lie on the **boundary between saddles and nodes**. The eigenvalues are real and distinct $(\lambda_- = 0, \lambda_+ = \tau)$ and we have a *line of fixed points* along the null space of A. They are neutrally stable along the null space and unstable/stable in any other direction depending on whether $\tau \gtrless 0$.

These borderline cases are of two sorts. Centers lie on the dividing line between spiral sinks and spiral sources. A small change in (τ, Δ) can change the stability of a center. Nonisolated fixed points are similarly on the dividing line between stable/unstable nodes and saddles so that a small change in (τ, Δ) can alter the stability. By contrast, the stability of symmetrical and degenerate nodes is robust, although they lie on the borderline between nodes and spirals.

$*$ **Bifurcations.** A 1-parameter family of 2d linear vector fields would define a curve on the τ-Δ plane. When the curve crosses any of the above boundaries, the character of the phase portrait changes. Such changes are called bifurcations (Chap. 14) in the family of vector fields. For instance, a damped harmonic oscillator defines a family of vector fields (see Prob. 6.15). If we increase the damping γ holding the mass m and frequency ω fixed, the system goes from being underdamped to critically damped at $\gamma = 2m\omega$ and finally overdamped as the number of linearly independent *real* eigenvectors of A goes from zero to one to two. This corresponds to a qualitative change in the phase portrait, with the fixed point at the origin transitioning from a spiral sink to a stable node via a stable degenerate node at the bifurcation point $\gamma = 2m\omega$. □

6.7* Robustness of the linear theory

More generally, suppose we have a nonlinear vector field $\boldsymbol{v}(\boldsymbol{r})$ on the plane with a fixed point at $\boldsymbol{r}_*$. As described in (5.27), we may linearize $\boldsymbol{v}$ around the fixed point to arrive at the linear system

$$v^i(\boldsymbol{r}) = \frac{\partial v^i(\boldsymbol{r}_*)}{\partial x^j}(x^j - x^j_*) + \cdots \quad \text{where} \quad J^i_j = \frac{\partial v^i}{\partial x^j} \tag{6.33}$$

is the Jacobian matrix of first partials evaluated at the fixed point. J serves as the coefficient matrix A in (6.5). A natural question is whether we may trust the linearization of $\boldsymbol{v}$ to correctly capture the qualitative nature of the immediate vicinity of the fixed point. Below, we mention two general results which give sufficient conditions for the reliability of the linear approximation.

Centers in conservative systems. Here, we temporarily specialize to (2d) conservative systems. Suppose $\boldsymbol{r}_*$ is an isolated fixed point of $\boldsymbol{v}$ that lies at a minimum or maximum of the conserved quantity, which we denote $E(\boldsymbol{r})$. Then $\boldsymbol{r}_*$ is a (nonlinear) center. In other words, all trajectories that start sufficiently close to $\boldsymbol{r}_*$ are closed, and the local phase portrait is continuously deformable into (i.e., homeomorphic to) that of a linear center. The reason is that the graph of $E(\boldsymbol{r})$ over a sufficiently small neighborhood of $\boldsymbol{r}_*$ must look like a bowl with a unique minimum/maximum at $\boldsymbol{r}_*$, whence the level contours of E in the neighborhood must be closed curves. Each such closed level contour must be a trajectory (rather than a union of more than one trajectory) since there cannot be any fixed point at which the trajectory can stop, on account of $\boldsymbol{r}_*$ being isolated. We will meet examples of nonlinear centers in conservative systems such as the pendulum and anharmonic oscillator in Chap. 7 (see Fig 7.3 and Fig. 7.6).

Hyperbolic fixed points and Hartman-Grobman theorem. What can be said if our nonlinear system is not (or is not known to be) conservative? A useful result due to Hartman and Grobman [55] implies that the linearization may be trusted as long as it predicts a fixed point corresponding to a point away from the line $\Delta = 0$ or ray $\tau = 0, \Delta \geq 0$ on the τ-Δ plane. In other words, a linear spiral, node or saddle is a spiral, node or saddle of the corresponding nonlinear system (in the sense that the phase portrait of the nonlinear system in a neighborhood of the fixed point can be continuously deformed into that of its linearization). On the other hand, a linear center or nonisolated fixed point *may* or *may not* survive when the effects of nonlinearities are included[12]. However, unlike the neutrally stable center which can be a linear approximation to both a stable and an unstable spiral, the stability of a node (asymmetrical, symmetrical or degenerate) does not change due to nonlinear effects.

If we are only interested in the stability of a fixed point (and are willing to gloss over the difference between, say, a stable degenerate node and a stable node which, in any case, are continuously deformable into each other) then fixed points may be classified into those that have robust (linear) stability and those that are marginal. The robust ones are sinks (attractors), sources ('repellers' or attractors as $t \to -\infty$) and saddles, corresponding to eigenvalues of the linearization that have positive real parts, negative real parts or opposite signs respectively. The stability of such a fixed point is unchanged by nonlinear effects. The marginal ones are centers (with both eigenvalues imaginary) and nonisolated fixed points (where at least one eigenvalue vanishes): their stability can be altered by nonlinear effects. In other words, the marginal cases are those where at least one eigenvalue has zero real part. It is useful to introduce a common term for the robust cases: a *hyperbolic fixed point* is one at which all the eigenvalues of the linearization of the vector field have nonzero real parts (this applies to real autonomous systems of dimension one, two or higher). In the examples of Sect. 6.6*, the origin $\boldsymbol{r} = 0$ is a hyperbolic fixed point as long as it is an isolated fixed point and not a center. So saddles, nodes (symmetric or otherwise), spirals and degenerate nodes are all examples of hyperbolic fixed points[13].

The linear approximation faithfully captures the behavior in the neighborhood of a hyperbolic fixed point. The Hartman-Grobman theorem says that the phase portrait in the vicinity of a hyperbolic fixed point is topologically equivalent (or 'conjugate') to that of the linearized system. Topological equivalence means there is a homeomorphism (continuous map with continuous inverse, though not necessarily smooth) that maps the local phase portrait (an open neighborhood of the fixed point) to the whole phase plane of the linearized system, taking trajectories to trajectories while preserving the sense of time. Topologically equivalent phase portraits are continuously deformed versions of each other. For instance, a homeomorphism would take fixed points to fixed points, closed orbits to closed orbits and preserve the nature of homoclinic or heteroclinic trajectories.

6.8 Driven or forced oscillations

We now go from free to forced oscillations, which means the associated vector field becomes nonautonomous. Suppose in addition to a linear restoring force, the particle is subject to a prescribed time-dependent external force $F(t)$. Equation (6.2) for the small displacement x from equilibrium is then replaced by

$$m\ddot{x} + kx = F(t) \quad \text{or} \quad \ddot{x} + \omega^2 x = \frac{F(t)}{m} \quad \text{where} \quad \omega = \sqrt{\frac{k}{m}}. \tag{6.34}$$

---

[12] Degenerate nodes and star nodes are continuously deformable into ordinary nodes, so the distinction between node, degenerate node and symmetric node is not particularly useful beyond the linear theory.

[13] The name is a bit misleading: trajectories need not look like hyperbolae in the vicinity of a hyperbolic fixed point (except if it is a saddle)!

This equation of motion follows from the explicitly time-dependent Lagrangian $L = \frac{1}{2}m\dot{x}^2 - (\frac{1}{2}kx^2 - xF(t))$. The potential energy $-xF$ is the first nontrivial term in the Taylor expansion[14] of a time-dependent external potential energy in the small quantity x. Evidently, the driving force pumps energy into the particle's motion.

Equation (6.34) is an inhomogeneous linear 2nd order ODE. It can be written as a nonautonomous system of two 1st order equations and defines a time-dependent vector field. See Prob. 5.2 for how it can be re-expressed as a nonlinear autonomous system. Thus, we might expect forced oscillations to display novel phenomena not seen in linear free oscillations. Nevertheless, a form of the superposition principle still holds: if $F(t) = F_1(t) + F_2(t)$ is the sum of two forces, then $x(t) = x_1(t) + x_2(t)$ is the sum of the solutions for the individual forces[15].

Sinusoidal forcing. The general solution of (6.34) can be written as the sum of a particular solution x_p of the inhomogeneous equation and the general solution x_h of the homogeneous one[16]. To begin with, let us suppose that $F(t) = f\cos(\nu t + \beta)$ is sinusoidal in time, i.e., has a single frequency component so that (6.34) becomes

$$\ddot{x} + \omega^2 x = \frac{f}{m}\cos(\nu t + \beta). \tag{6.35}$$

More general driving forces can be Fourier synthesized by superposing sinusoids with different frequencies (see below). In our case, $x_h = a\cos(\omega t + \alpha)$ (6.3). A particular solution can be obtained by trying an ansatz (guess) $x_p = b\cos(\nu t + \beta)$ that is proportional to the driving force. One finds $b = f/m(\omega^2 - \nu^2)$ so that

$$x(t) = a\cos(\omega t + \alpha) + \frac{f}{m(\omega^2 - \nu^2)}\cos(\nu t + \beta) \quad \text{for} \quad \nu \neq \omega. \tag{6.36}$$

Thus, if $\nu \neq \omega$, the departure $x(t)$ from equilibrium is bounded in time and given by a superposition of two sinusoids. The resulting motion is periodic only if ω and ν are commensurate (i.e., ω/ν or ν/ω is rational). If the driving and natural frequencies are not commensurate, $x(t)$ is said to be quasiperiodic (see Footnote 24 of Chap. 2).

Equation (6.36) contains two constants of integration a and α, which are to be fixed by initial conditions. It is important to bear in mind that a and α could depend on the parameters ω, ν, f, m and β. Interestingly, the amplitude of the second term in (6.36) grows as the driving frequency ν approaches the natural frequency ω resulting in a *resonance*. On the face of it, (6.36) diverges as $\nu \to \omega$. However, this conclusion may not be correct: there could be cancellations with the first term if a and α are appropriately chosen. Empirically, one finds that at resonance, the amplitude of the oscillations are finite but grow with time until nonlinear effects can no longer be ignored. This suggests that we should choose a and α in such a way that (6.36) has a finite limit as $\nu \to \omega$. Another way to look at it is that the particular solution is not uniquely defined, we could add a homogeneous solution $\propto \cos(\omega t + \gamma)$ to a particular solution to get another particular solution. We may exploit this freedom to write (6.36) in the form

---

[14] $V(x,t) = V(0,t) + x(\partial_x V)(0,t) + \cdots$. $V(0,t)$ does not contribute to the equation of motion and we define $F(t) = (\partial_x V)(0,t)$.

[15] To solve the initial value problem, $x(0)$ and $\dot{x}(0)$ should also be expressed as the sum of the initial values for the individual forces.

[16] This is because the difference between 2 solutions of (6.34) is a solution of the corresponding homogeneous equation.

$$x(t) = \tilde{a}\cos(\omega t + \tilde{\alpha}) + \frac{f}{m(\omega^2 - \nu^2)}\left(\cos(\nu t + \beta) - \cos(\omega t + \beta)\right), \qquad (6.37)$$

with the understanding that $\tilde{a}$ and $\tilde{\alpha}$ are independent of ν. This choice (with $\gamma = \beta$) is motivated by the need to cancel the factor $\omega - \nu$ in the denominator of (6.36) in the limit $\nu \to \omega$. In fact, using the trigonometric identity

$$\cos(\nu t + \beta) - \cos(\omega t + \beta) = 2\sin\left(\frac{(\nu + \omega)}{2}t + \beta\right)\sin\left(\frac{(\omega - \nu)}{2}t\right), \qquad (6.38)$$

we find that in the resonant limit $\nu \to \omega$, the solution is given by (see Prob. 6.21)

$$x(t) = \tilde{a}\cos(\omega t + \tilde{\alpha}) + \frac{f}{2m\omega}t\sin(\omega t + \beta). \qquad (6.39)$$

Thus, at resonance, the amplitude of the oscillations grows linearly with time until the validity of the small oscillations approximation breaks down. This is an example of an *instability*. A sinusoidal driving force must have the *same* frequency as the unperturbed linear oscillator for an instability to develop. We will exploit this observation in (6.75) while discussing parametric oscillations and resonant amplification. Resonances will also make their presence felt in classical perturbation theory as we shall see in Sect. 7.5* on the Lindstedt-Poincaré method.

Beats. Slightly off resonance, we have the phenomenon of *beats*. Putting $\nu = \omega + \epsilon$ for small ϵ, (6.36) can be written as

$$\begin{aligned} x(t) &= a\cos(\omega t + \alpha) + b\cos(\nu t + \beta) = \Re\left[Ae^{i\omega t} + Be^{i(\omega+\epsilon)t}\right] = \Re C(t)e^{i\omega t} \\ \text{where} \quad & A = ae^{i\alpha}, \quad B = be^{i\beta} \quad \text{and} \quad C(t) = ae^{i\alpha} + be^{i(\beta + \epsilon t)}. \end{aligned} \qquad (6.40)$$

The modulus and argument of $C(t)$ vary over a time scale $2\pi/|\epsilon|$. Since $|\epsilon| \ll \omega$, $x(t) = \Re C(t)e^{i\omega t}$ may be regarded as an oscillation with time period $2\pi/\omega$ modulated by a slowly varying amplitude and phase. The amplitude

$$|C| = [a^2 + b^2 + 2ab\cos(\epsilon t + \beta - \alpha)]^{1/2} \qquad (6.41)$$

varies periodically between $|a - b|$ and $|a + b|$ with period $2\pi/|\epsilon|$. This is the phenomenon of beating: a high frequency oscillation modulated by a low frequency envelope. This is illustrated in Fig. 6.8.

General driving force

1. *Method of Fourier series:* If the driving force can be written as a sum of sinusoids,

$$F = f_0\cos(\omega t + \beta_0) + \sum\nolimits_{j,\nu_j \neq \omega} f_j\cos(\nu_j t + \beta_j), \qquad (6.42)$$

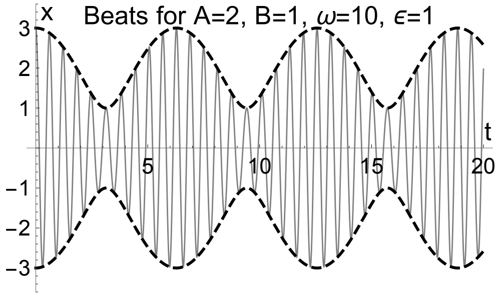

Figure 6.8: Time series of a signal $x(t)$ showing beating of a high frequency (ω) oscillation by a low frequency (ϵ) envelope whose amplitude varies periodically between $|A-B|$ and $|A+B|$.

then by the superposition principle mentioned at the beginning of Sect. 6.8, the solution of (6.34) is given by the Fourier series

$$x(t) = a\cos(\omega t+\alpha) + \frac{f_0}{2m\omega} t\sin(\omega t+\beta_0) + \sum_{j,\nu_j\neq\omega} \frac{f_j}{m(\omega^2-\nu_j^2)}\cos(\nu_j t+\beta_j). \tag{6.43}$$

Here, a and α are fixed by initial conditions.

2. *Reduction to quadrature.* Alternatively, following [83], (6.34) may be reduced to a first order equation by defining the complex function of time[17]

$$y = \dot{x} + i\omega x \quad \text{which satisfies} \quad \dot{y} - i\omega y = \frac{F(t)}{m}. \tag{6.44}$$

The latter is a linear inhomogeneous 1$^{\text{st}}$ order ODE. The general solution of the homogeneous equation is $y_h = Ae^{i\omega t}$ for integration constant A. To find a particular solution, we use the method of variation of constants (which goes back to Euler's and Lagrange's work in celestial mechanics) and try the ansatz $y_p = A(t)e^{i\omega t}$ leading to

$$\dot{A}e^{i\omega t} = \frac{F(t)}{m} \quad \text{or} \quad A(t) = \int \frac{F(t)}{m} e^{-i\omega t}. \tag{6.45}$$

Thus, we may write the solution of (6.34) as a Fourier-type integral

$$x(t) = \frac{1}{\omega}\Im y(t) \quad \text{where} \quad y(t) = e^{i\omega t}\left[y(0) + \int_0^t \frac{F(s)}{m} e^{-i\omega s}\right] \tag{6.46}$$

and $y(0) = \dot{x}(0) + i\omega x(0)$.

3. *Laplace transform:* The Laplace transform converts the linear differential equation (6.34) and initial conditions into a linear algebraic equation. In fact, suppose we

---

[17] Notice that the energy is given by $\frac{1}{2}my^*y$. Complex combinations of the position and momentum are also employed in the quantum mechanical treatment of the harmonic oscillator where (up to an additive constant) the Hamiltonian is factorized as a product of raising and lowering (creation and annihilation) operators which are Hermitian adjoints of each other.

define the Laplace transform

$$\tilde{F}(\nu) = \int_0^\infty F(t) e^{-\nu t}\, dt. \tag{6.47}$$

As long as $F(t)$ grows no faster than exponentially, this defines $\tilde{F}(\nu)$ for frequencies ν with sufficiently large real part. One finds that the Laplace transform of the second derivative in time $\ddot{x}$ is (see Prob. 6.24)

$$\tilde{\ddot{x}}(\nu) = \nu^2 \tilde{x}(\nu) - \nu x(0) - \dot{x}(0). \tag{6.48}$$

Thus, in the frequency domain, (6.34) becomes

$$(\nu^2 + \omega^2)\tilde{x}(\nu) - \nu x(0) - \dot{x}(0) = \frac{\tilde{F}(\nu)}{m} \tag{6.49}$$

resulting in

$$\tilde{x}(\nu) = \frac{1}{\nu^2 + \omega^2} \left[\frac{\tilde{F}(\nu)}{m} + \nu x(0) + \dot{x}(0) \right]. \tag{6.50}$$

Finally, $x(t)$ is obtained by inverting the Laplace transform via Mellin's Bromwich contour integral formula [8]

$$x(t) = \frac{1}{2\pi i} \int_{\mathcal{C}} \tilde{x}(\nu) e^{\nu t}\, d\nu \tag{6.51}$$

where the contour $\mathcal{C}$ goes from $\sigma - i\infty$ to $\sigma + i\infty$ with σ chosen so that $\mathcal{C}$ lies to the right of all singularities of $\tilde{x}(\nu)$.

4. *Method of impulsive force and Green's function.* In the method of Fourier series, we decomposed a general force as a linear combination of sinusoidal driving forces. Here, we think of a general time-dependent force as a linear combination of impulsive forces. An impulsive force $F_{t'}(t)$ at time t' is one that acts only at the instant $t = t'$ but nevertheless has a finite and nonzero impulse $\mathcal{I}$:

$$\int_{-\infty}^{\infty} F_{t'}(t)\, dt = \mathcal{I}. \tag{6.52}$$

An impulsive force can be expressed using the Dirac delta function:

$$F_{t'}(t) = \mathcal{I}\, \delta(t - t'). \tag{6.53}$$

Here, the Dirac delta function $\delta(t - t')$ vanishes for all $t \neq t'$ but diverges at $t = t'$ in such a way that the area under it is one:

$$\int_{-\infty}^{\infty} \delta(t - t')\, dt = 1. \tag{6.54}$$

As a consequence, integrating any function of t against the Dirac delta function $\delta(t - t')$ picks out the value of the function at $t = t'$:

$$\int_{-\infty}^{\infty} h(t)\, \delta(t - t')\, dt = h(t'). \tag{6.55}$$

Thus, we may express a given force as a linear combination of impulsive forces:

$$F(t) = \int_{-\infty}^{\infty} F(t')\delta(t-t')\,dt'. \tag{6.56}$$

Now, suppose we know the solution of the driven harmonic oscillator (6.34) for an impulsive force that acts at the instant t'. Such a solution is called a Green function and is denoted $G(t,t')$ to indicate that it depends both on the time t (at which we wish to know the particle's position) as well as on the time t' at which the impulsive force acted. We will soon see that the virtue of such a Green function is that it can be used to solve (6.34) for a general driving force that is synthesized from impulsive forces.

In more detail, suppose we know a Green function $G(t,t')$ satisfying[18]

$$\frac{d^2}{dt^2}G(t,t') + \omega^2 G(t,t') = \delta(t-t') \tag{6.57}$$

and the 'initial condition'

$$G(t,t') = 0 \quad \text{for} \quad t < t'. \tag{6.58}$$

The latter is reasonable since we have in mind that the particle was at rest before the impulsive force acted. Up to constant factors, $G(t,t')$ is the particle's position at time t if it was subject to an impulse at time t'.

Once we have $G(t,t')$, we may express the solution of (6.34) as

$$x(t) = \frac{1}{m}\int_{-\infty}^{\infty} G(t,t')\,F(t')\,dt'. \tag{6.59}$$

This is checked by applying the differential operator $\frac{d^2}{dt^2} + \omega^2$ to both sides and differentiating under the integral sign (see Prob. 6.25).

Finally, to find the Green function, we note that the solution of the inhomogeneous equation (6.57) may be expressed as the sum of a particular solution $G_p(t,t')$ and the general solution $G_h(t,t')$ of the homogeneous problem. The latter is given by

$$G_h(t,t') = c_1(t')\cos\omega t + c_2(t')\sin\omega t. \tag{6.60}$$

To find a particular solution, we use time-translation invariance to consider an ansatz of the form $G_p(t,t') = g(s)$ where g is a continuous function of the difference $s = t - t'$. Then using $\frac{d}{dt} = \frac{d}{ds}$ (see Prob. 6.26), (6.57) becomes

$$\left(\frac{d^2}{ds^2} + \omega^2\right) g(s) = \delta(s). \tag{6.61}$$

---

[18] One could introduce dimensional constants to make the RHS have dimensions of a force and G have dimensions of length. However, since the Green function is used as a technical tool, we avoid such constants.

The initial condition (6.58) becomes $g(s) = 0$ for $s < 0$. Since $\delta(s) = 0$ for $s > 0$, we must have $g(s) = a\cos\omega s + b\sin\omega s$ for $s > 0$. By continuity, we must have $g(0) = a = 0$. To fix b we examine what happens at $s = 0$. To this end, we integrate (6.61) from $s = -\epsilon$ to $s = \epsilon$ for a small $\epsilon > 0$. We get

$$\int_{-\epsilon}^{\epsilon} \ddot{g}(s)ds + \omega^2 \int_{-\epsilon}^{\epsilon} g(s)ds = 1. \tag{6.62}$$

The 2nd integral on the LHS vanishes as $\epsilon \to 0$ since g is continuous (and hence bounded). Thus, we get the condition

$$\dot{g}(0^+) - \dot{g}(0^-) = 1 \tag{6.63}$$

However, since $g(s) \equiv 0$ for $s < 0$, $\dot{g}(0^-) = 0$. Thus, we arrive at the second initial condition $\dot{g}(0^+) = 1$, which immediately implies $b\omega = 1$. It follows that a particular solution of (6.57) that also satisfies the IC (6.58) is

$$G_p(t,t') = \begin{cases} \frac{1}{\omega}\sin\omega(t-t') & \text{for} \quad t \geq t' \\ 0 & \text{for} \quad t \leq t'. \end{cases} \tag{6.64}$$

The Green function is therefore given by

$$G(t,t') = G_p(t,t') + c_1(t')\cos\omega t + c_2(t')\sin\omega t. \tag{6.65}$$

Since G_p already vanishes for $t < t'$, for G to satisfy (6.58) we must have $c_1(t') = c_2(t') = 0$ for $t' > t$. However, $c_{1,2}$ must be independent of t and the only way this can happen is for both of them to vanish. Thus we discover that the Green function for the harmonic oscillator is simply $G = G_p$. In conclusion, using (6.59) and (6.64), the solution to the forced oscillator may be expressed as a 'convolution'[19] of the force with the sine function:

$$x(t) = \frac{1}{m\omega}\int_{-\infty}^{t} \sin(\omega(t-t'))\, F(t')\, dt'. \tag{6.66}$$

Since cause must precede effect, only the force that acted prior to t can influence the particle's position at the instant t. We may think of (6.66) as the solution to the IVP[20] where the particle begins at rest at $x = 0$ in the distant past and is acted upon by a force till time t. It is interesting to think about the inverse problem: what force may be used to bring the particle to a desired state at time t if it began in the equilibrium state in the far past?

---

[19] The convolution of a function $f(t)$ with $s(t)$ is defined as $(f * s)(t) = \int f(t')s(t-t')dt'$.

[20] Instead of this IC in the far past, suppose we are interested in a particle which begins from rest at $t = t_1$ and is acted upon by a force $F(t)$ in addition to the linear restoring force. Then we may still use (6.66) provided we put $F(t) = 0$ for $t < t_1$, resulting in the lower limit of integration being advanced to t_1.

6.9* Driven damped oscillations

Combining the ideas from Sect. 6.4 and Sect. 6.8, we briefly consider the case of driven damped oscillations along the lines of [83]. For simplicity, consider sinusoidal forcing at a single frequency ν (i.e., a monochromatic driving force):

$$\ddot{x} + \frac{\gamma}{m}\dot{x} + \omega^2 x = (f/m)\cos\nu t. \tag{6.67}$$

Suppose the oscillator is underdamped, $\gamma < 2m\omega$. The general solution of the homogeneous equation is given by (6.14) while a particular solution (see Prob. 6.29) is $x_p = b\cos(\nu t + \delta)$ where

$$b = \frac{f/m}{\sqrt{(\omega^2-\nu^2)^2 + \nu^2\gamma^2/m^2}} \quad \text{and} \quad \delta = \arccos\frac{\omega^2-\nu^2}{[(\omega^2-\nu^2)^2+\nu^2\gamma^2/m^2]^{1/2}} \tag{6.68}$$

or $\delta = \arctan((\nu\gamma/m)/(\nu^2-\omega^2))$. Thus, we may write

$$x(t) = ae^{-\gamma t/2m}\cos\left(t\sqrt{\omega^2-\gamma^2/4m^2}+\alpha\right) + b\cos(\nu t+\delta). \tag{6.69}$$

The first term is a transient, it decreases exponentially and can be ignored for $t \gg 2m/\gamma$. However, unlike in the undamped case of (6.36), the amplitude b of the forced oscillations does not diverge as we approach resonance ($\nu \to \omega$). In fact, b is maximal at $\nu = \sqrt{\omega^2-\gamma^2/2m^2}$ (see Prob. 6.30). For weak damping $\gamma/m \ll \omega$, the maximum occurs close to the undamped resonance frequency ω and we will examine its vicinity by putting $\nu = \omega + \epsilon$ and keeping only the leading order terms in ϵ/ω. Thus,

$$b \approx \frac{f}{2m\omega\sqrt{\epsilon^2+\gamma^2/4m^2}} \quad \text{and} \quad \delta \approx \arccos\frac{-2\epsilon}{[4\epsilon^2+\gamma^2/m^2]^{1/2}} = \arctan\frac{\gamma}{2m\epsilon}. \tag{6.70}$$

Once the transient dies out, the oscillator reaches the 'steady state' $x \approx b\cos(\nu t + \delta)$ where all the energy injected by the driving force over one time period $2\pi/\nu$ is dissipated by friction in the same time interval.

How efficiently does the oscillator absorb energy as a function of the driving frequency? To find out, we evaluate the mean energy $\langle\dot{E}(\gamma)\rangle$ dissipated by the oscillator per unit time when averaged over one period. From Sect. 6.4 we know that $\dot{E} = 2F$ where $F = \frac{1}{2}\gamma\dot{x}^2$ is the dissipation function. Thus

$$\dot{E} = \gamma\dot{x}^2 = \gamma(-b\nu\sin(\nu t+\delta))^2 = \gamma b^2\nu^2\sin^2(\nu t+\delta). \tag{6.71}$$

Averaging over a period and using (6.70), we get

$$\langle\dot{E}\rangle(\nu) = \frac{\gamma f^2}{8m^2((\nu-\omega)^2+\gamma^2/4m^2)}. \tag{6.72}$$

This spectral distribution of average energy absorbed per unit time has a Lorentzian line shape as a function of ν. The oscillator is most efficient in absorbing energy at the resonant frequency $\nu = \omega$ with a maximal absorption rate $f^2/2\gamma$ that is inversely proportional to the damping coefficient. On the other hand, the width of the distribution, measured, say, via the full width at half maximum is γ/m (see Prob. 6.31). Thus, the Lorentzian becomes more sharply peaked as $\gamma \to 0$.

6.10 Parametric oscillations and resonant amplification

We consider here the situation arising from a periodic variation in the force constant parameter k appearing in the Lagrangian $\frac{1}{2}m\dot{x}^2 - \frac{1}{2}kx^2$ of an oscillator[21]. We have learned in Sect. 6.8 that even a small periodic driving force can lead to a resonant linear growth in the amplitude of free oscillations, provided the driving frequency matches the natural one. Small parametric oscillations (say of k) can also lead to amplification, though of a different character: exponential growth in time provided the frequency of parametric variation lies in certain bands of instability, the principal one being around twice the natural frequency. To see how this comes about, we consider an oscillator whose angular frequency differs from a constant ω_0 by a small amplitude sinusoidal variation at frequency $\nu \neq 0$:

$$\ddot{x} + \omega^2(t)x = 0 \quad \text{with} \quad \omega^2 = \omega_0^2(1 + h\cos\nu t) \quad \text{where} \quad 0 < h \ll 1. \tag{6.73}$$

A translation of time allows us to assume that the amplitude h is positive. The resulting linear equation is homogeneous[22]

$$\ddot{x} + \omega_0^2 x = -h\omega_0^2 \cos(\nu t)\, x. \tag{6.74}$$

In particular, this means that if the particle is initially at rest at equilibrium $(x, \dot{x} = 0)$, then parametric variation of the spring constant cannot excite it, unlike an external inhomogeneous driving force which *can* (see Sect. 6.8). Nevertheless, (6.74) may profitably be viewed as the equation for a driven oscillator where the driving force is proportional to the displacement x.

To heuristically identify the condition for a resonance, we suppose that $x \sim \cos\omega_0 t$ is oscillating with its natural frequency so that the effective driving force is proportional to

$$\cos\nu t \cos\omega_0 t = \frac{1}{2}\cos(\nu - \omega_0)t + \frac{1}{2}\cos(\nu + \omega_0)t. \tag{6.75}$$

Thus, the driving force in (6.74) can be viewed as a sum of two sinusoids with driving frequencies $\nu \pm \omega_0$. From our observation below (6.39), for a resonance to occur, we need either $\nu + \omega_0$ or $\nu - \omega_0$ to equal the natural frequency ω_0 on the LHS of (6.74). The nontrivial solution is $\nu = 2\omega_0$ so that the parametric oscillation must have *twice* the natural frequency to result in a resonance. Roughly, this may be achieved by giving a pendulum a small push inwards soon after it begins its return journey from both turning points. Evidently, this can lead to rapid amplification.

Following [83], we will determine the conditions for parametric resonance by focusing on the neighborhood of $\nu = 2\omega_0$ by putting $\nu = 2\omega_0 + \epsilon$ for $\epsilon \ll \omega_0$. We then look for an approximate solution of (6.74)

$$\ddot{x} + \omega_0^2\,(1 + h\cos(2\omega_0 + \epsilon)t)\, x = 0 \tag{6.76}$$

---

[21] The mass parameter m could also vary with time, but this can be absorbed into $k(t)$ via a reparametrization of time, see Prob. 6.33.

[22] This linear equation with periodically varying coefficients is essentially the Mathieu equation, see Sect. 13.4 for a general framework for analyzing such equations.

with frequency near resonance. To this end, we consider the ansatz

$$x(t) = a(t)\cos(\omega_0 + \epsilon/2)t + b(t)\sin(\omega_0 + \epsilon/2)t, \tag{6.77}$$

where $a(t)$ and $b(t)$ are slowly varying on a time scale of $2\pi/\omega_0$. Here, we ignore contributions from 'higher harmonics' with frequencies near $3\omega_0, 5\omega_0$, etc., that inevitably arise when an ansatz of the form (6.77) is inserted in (6.76); they turn out to be suppressed by powers of h [83].

Putting (6.77) in (6.76) and ignoring 2nd derivatives of the slowly varying functions as well as nonresonant terms that arise when products of trigonometric functions are written as sums, we obtain (see Prob. 6.34)

$$(2\dot{b} - \epsilon a + h\omega_0 a/2)\omega_0\cos(\nu t/2) - (2\dot{a} + \epsilon b + h\omega_0 b/2)\,\omega_0\sin(\nu t/2) \approx 0 \tag{6.78}$$

where $\nu = 2\omega_0 + \epsilon$. For this to be satisfied at all times, the coefficients must vanish, leading to two first order homogeneous linear equations

$$2\dot{b} = (\epsilon - h\omega_0/2)a = 0 \quad \text{and} \quad 2\dot{a} = -(\epsilon + h\omega_0/2)b. \tag{6.79}$$

Solutions may be sought in the form $a, b \propto e^{st}$. The proportionality constants cancel resulting in the condition

$$s^2 = (1/4)\left((h\omega_0/2)^2 - \epsilon^2\right). \tag{6.80}$$

Evidently, s^2 is either positive or negative, so that s is either real or purely imaginary. For exponential growth[23], s must be real, or $|\epsilon| < h\omega_0/2$. Thus, to leading order in h, amplification occurs provided the parametric oscillations have a frequency ν within $h\omega_0/2$ of twice the natural frequency of the oscillator:

$$2\omega_0 - \frac{h\omega_0}{2} < \nu < 2\omega_0 + \frac{h\omega_0}{2}. \tag{6.81}$$

As a consistency check, we notice that for such ν, the growth rate s is of order h so that the ignored 2nd derivatives $\ddot{a}$ and $\ddot{b}$ are of second order in the small amplitude h.

6.11 Problems

1. **Simple harmonic oscillator.** Consider the matrix $A = (0, 1/m| - k, 0)$ appearing in (6.4). The matrix exponential e^A is defined as $e^A = \sum_{n=0}^{\infty} A^n/n!$. Calculate e^{At}, express the answer in terms of trigonometric functions and thereby find the solution $(x(t)\ \ p(t))^t = e^{At}(x(0)\ \ p(0))^t$ to the IVP for the harmonic oscillator.
2. Suppose $\boldsymbol{w}_\pm$ are **eigenvectors** for the eigenvalues $\lambda_\pm$ of a real 2×2 matrix A. Assuming the eigenvalues are distinct, argue that the eigenvectors can be taken to have real components or to be complex conjugates of each other: $\boldsymbol{w}_- = \boldsymbol{w}_+^*$.

---

[23] Growing modes with $s > 0$ are of course paired with decaying modes $\propto e^{-st}$.

3. **Similarity transformation.** Suppose A is an $n \times n$ (real or complex) matrix with n linearly independent eigenvectors $Av_j = \lambda_j v_j$ for $j = 1, 2, \cdots, n$. Let $D = \operatorname{diag}(\lambda_1, \cdots, \lambda_n)$ be the diagonal matrix of eigenvalues and $S = (v_1, \cdots, v_n)$ be the matrix whose columns are the eigenvectors of A in the same order. Then show that S is invertible and that $AS = SD$ or $S^{-1}AS = D$. S is called a similarity transformation that diagonalizes A. If A is real symmetric ($A^t = A$) or complex Hermitian ($A^\dagger = A$), argue that S may be taken orthogonal ($S^t S = I$) or unitary ($S^\dagger S = I$), where † denotes the complex conjugate transpose.

4. **Simple harmonic oscillator.** Consider the harmonic oscillator $\dot{x} = p/m$ and $\dot{p} = -kx$ with $\omega = \sqrt{k/m}$. Take $\boldsymbol{r} = (x, p)$ so that $\dot{\boldsymbol{r}} = A\boldsymbol{r}$.

   a. Find A and its eigenvalues $\lambda_\pm$. Comment on the implications of the eigenvalues of A for the nature of the fixed point (and its stability) at $(x_* = 0, p_* = 0)$.
   b. Find the eigenvectors $\boldsymbol{w}_\pm$ of A corresponding to the eigenvalues $\lambda_\pm$ and show that they can be taken to be complex conjugates. For definiteness, try to ensure that the first component of both eigenvectors is 1 (choice of normalization).
   c. Use the eigenvalues and eigenvectors to write the general solution of the EOM of a harmonic oscillator as (for some complex number r_+, see Sect. 6.3):

$$\begin{aligned} x(t) &= 2(\Re r_+)\cos\omega t - 2(\Im r_+)\sin\omega t \quad \text{and} \\ p(t) &= 2m\omega\left[-\Re r_+ \sin\omega t - \Im r_+ \cos\omega t\right]. \end{aligned} \tag{6.82}$$

*5. For the **oscillator** $\ddot{x} = -\omega^2 x$, show that the **unique trajectory** connecting $x(t_i) = x_i$ and $x(t_f) = x_f$ assuming $\omega\,\Delta t \neq n\pi$ for any integer n is given by

$$x(t) = \frac{s_f x_i - s_i x_f}{\sin(\omega\Delta t)}\cos(\omega t) + \frac{c_i x_f - c_f x_i}{\sin(\omega\Delta t)}\sin(\omega t). \tag{6.83}$$

Here $\Delta t = t_f - t_i$. We use the abbreviations $c_i = \cos\omega t_i$, $s_f = \sin\omega t_f$, etc. What happens when $\omega\Delta t = n\pi$?

6. Argue why the phase point moves clockwise on the ellipses in the **phase portrait** of the **linear harmonic oscillator**. You may pick a suitable initial condition and use the nature of the restoring force. What are the semiaxes of the ellipses as a function of the energy? Also find the nullclines of the vector field, where do they intersect?

7. What are the **stable and unstable manifolds** W_s and W_u of a center? Why?

8. Can you construct a quantity with dimensions of length using the parameters m, k of the classical **harmonic oscillator**? What about in the quantum theory (i.e., including Planck's constant as a parameter)? Speculate on the qualitative implications.

9. Give an example of a 2×2 real matrix with only one linearly independent eigenvector. Find its eigenvalues and the **lone independent eigenvector**.

10. Solve the **inhomogeneous linear ODE** $\dot{x} = \lambda x + y_0 e^{\lambda t}$ with $x(0) = x_0$. Here, y_0 is a constant and $\lambda \neq 0$ is a real constant.

11. Where does a particle executing **simple harmonic oscillations** spend a majority of its time: near the equilibrium point or near the turning point?

$*$12. Suppose (x_*, y_*) is part of a 1-parameter family of fixed points. Give an example of a planar vector field (formula and phase portrait) for which the **stable and unstable manifolds** W_s, W_u of a suitable fixed point (x_*, y_*) are both nonempty. What can you say about W_s and W_u of (x_*, y_*) if the vector field is linear?

13. Consider the **damped linear oscillator** governed by Newton's equation $m\ddot{x} = -kx - \gamma\dot{x}$ for mass, spring constant and damping coefficient $m, k, \gamma > 0$ and $\omega = \sqrt{k/m}$.

    a. Express Newton's equation as a pair of coupled linear ODEs on the x-p phase plane where $p = m\dot{x}$. We denote the phase point $\boldsymbol{r} = (x, p)$.
    b. Find the fixed points of the corresponding vector field. Find the eigenvalues $\lambda_\pm$ of the coefficient matrix. Are the fixed points attractive? Why?
    c. For what parameter regime is the system said to be overdamped and why the name? Henceforth we work in the overdamped regime.
    d. What is the nature of the fixed point at the origin in the overdamped case and why? Is it Lyapunov stable?
    e. Find the eigenvectors $\boldsymbol{w}_\pm$ corresponding to $\lambda_\pm$. Take them to have positive second component. Try to express the components of $\boldsymbol{w}_\pm$ in terms of $\lambda_\pm$.
    f. Draw a picture indicating the eigenvectors (and their negatives) $\pm\boldsymbol{w}_\pm$ following the above convention. Hint: They should divide the phase plane into four *wedges* (sectors or regions) which you should number I,II, III and IV.
    g. Give a general formula for the trajectory $\boldsymbol{r}(t)$ in terms of $\lambda_\pm$ and $\boldsymbol{w}_\pm$.
    h. As $t \to \infty$, where do trajectories go, along which line and why?
    i. As $t \to -\infty$ along which line do trajectories lie and why?
    j. Sketch the phase portrait of the overdamped oscillator. Draw 1 trajectory (with direction) inside each of the 4 wedges and indicate the behavior of the trajectory as $t \to \pm\infty$. Also indicate the direction of the flow along $\pm\boldsymbol{w}_\pm$.
    k. Can a trajectory go through $x = 0$ before the mass comes to rest? If so, how many times? Draw such a phase plane orbit or argue why it is not possible.
    l. Can the particle come momentarily to rest before coming to rest permanently? If so, how many times can this happen?
    m. Sketch a graph of x vs t for one trajectory that lies in a small wedge (small opening angle) and one trajectory from a large wedge. Mention which wedge you choose in each case. Include all times from large negative to positive.
    n. Comment on what you expect to happen to $\pm\boldsymbol{w}_\pm$ in the critically damped limit. What happens to the wedges and phase portrait?

14. Draw the phase portrait corresponding to the strictly **upper triangular system** of (6.23): $\dot{x} = y$ and $\dot{y} = 0$. Give suitable physical interpretations for x and y. How does the phase portrait change if the coefficient matrix is replaced by its transpose?

$*15.$ Find the curve on the **trace-determinant plane** corresponding to the 1-parameter family of vector fields defined by $m\ddot{x} + kx + \gamma\dot{x} = 0$ for $m = k = 1$. Plot the curve on the τ-Δ plane to see where the **bifurcation** (see Chap. 14) occurs.

$*16.$ Consider a **damped oscillator** $\ddot{x} + \omega^2 x + (\gamma/m)\dot{x} = 0$. Let μ be the **exponential decay rate** $x(t) \sim e^{-\mu t}$.

a. Show that the exponential decay rate $\mu_{\rm c} = \omega$ for a critically damped oscillator ($\gamma_c = 2m\omega$) is larger than those (given in (6.18)) for underdamped and overdamped oscillators with the same values of m and ω.

b. Let us imagine tuning γ away from γ_c in both the under- and overdamped regimes. So let $\gamma_{\rm u} = 2m\omega - 2\epsilon$ for $0 < \epsilon < m\omega$ and $\gamma_{\rm o} = 2m\omega + 2\epsilon$ for $\epsilon > 0$. Show that (a) for $\epsilon < \epsilon_* = 2m\omega/3$ we have $2m\omega/3 < \gamma_{\rm u} < 2m\omega < \gamma_{\rm o} < 10m\omega/3$ and $\mu_{\rm u} > \mu_{\rm o}$ and (b) for $\epsilon > \epsilon_*$ we have $0 < \gamma_{\rm u} < 2m\omega/3$ and $\gamma_{\rm o} > 10m\omega/3$ and $\mu_u < \mu_{\rm o}$. At $\gamma_{\rm u} = 2m\omega/3$ and $\gamma_{\rm o} = 10m\omega/3$, what is the common decay rate $\mu_{\rm u} = \mu_{\rm o}$? In essence, this implies that there are underdamped oscillators that decay both faster and slower than a given overdamped oscillator and vice versa.

17. Show that Lagrange's equations augmented by the frictional force derived from the **dissipation function** $F = \frac{1}{2}\gamma_{ij}\dot{x}^i\dot{x}^j$ are equivalent to Eq. (6.22). Express the rate of change of mechanical energy $E = \dot{x}^i \frac{\partial L}{\partial \dot{x}^i} - L$ in terms of F.

$*18.$ Consider a particle of mass m moving on the real line subject to the **double-well potential** $V(x) = g(x^2 - a^2)^2$ for $g, a > 0$ and a frictional force $-\gamma\dot{x}$ for $\gamma > 0$. The equation of motion is $m\ddot{x} = -V'(x) - \gamma\dot{x}$. (a) Show that the attractors for the dynamics on the $(x, p = m\dot{x})$ phase plane lie at $(x = \pm a, p = 0)$ (b) By solving the EOM numerically for various ICs, find the basins of attraction of the two attractors. (c) What is the fate of points on the boundary between the two basins of attraction as $t \to \infty$?

19. A nontrivial example of a limit cycle arises in the **van der Pol equation**:

$$m\ddot{x} = -kx - \mu(x^2 - 1)\dot{x} \quad \text{for} \quad m, k, \mu > 0. \tag{6.84}$$

(a) Describe the qualitative physical character of the nonlinear term by comparing it with equations we have studied. (b) Write the equation as a $1^{\rm st}$ order pair and discuss the nature of its fixed points (by linearizing the vector field about them) as a function of the parameters m, k and μ. (c) For *large* x and p, approximate the equations by keeping only the leading terms and mention the qualitative behavior. Do x and/or p grow/decay/remain bounded?

20. Consider a Hamiltonian system with planar x-p phase space and real Hamiltonian $H(x, p)$. Suppose (x_*, p_*) is a **fixed point of the Hamiltonian vector field**.

a. Find the Jacobian matrix J of the linearization of the Hamiltonian vector field around the fixed point.

b. What is the trace of J? What are the possible forms of the eigenvalues of J?

   c. Assuming the eigenvalues are not both zero, to what sort of (linear) fixed points do the above possibilities correspond?
   d. For the free particle ($H = p^2/2m$), what are the fixed points of the Hamiltonian vector field? What is J at these fixed points and how many linearly independent eigenvectors does it have? Draw the phase portrait showing at least three qualitatively different trajectories.

21. **Resonance.** Verify that at resonance (when the driving frequency $\nu = \omega$), the solution to (6.35) is given by (6.39).
22. **Beats.** Use Eq. (6.37):

$$x(t) = \tilde{a}\cos(\omega t + \tilde{\alpha}) + \frac{f}{m(\omega^2 - \nu^2)}\left(\cos(\nu t + \beta) - \cos(\omega t + \beta)\right) \tag{6.85}$$

    as a starting point to discuss the phenomenon of beats for driving frequency $\nu = \omega + \epsilon$ with ϵ small. Here ω is the angular frequency of a sinusoidally driven harmonic oscillator.
23. **Forced oscillations.** Find an expression for the total energy transmitted to a particle (over all time $-\infty < t < \infty$) undergoing oscillations $[\ddot{x} + \omega^2 x = F/m]$ influenced by an external force $F(t)$. You may assume the particle begins at rest at the equilibrium point $x = 0$ in the far past when the force is turned on. Hint: Express the energy in terms of $y(t) = \dot{x} + i\omega x$.
24. Suppose $\tilde{x}(\nu) = \int_0^\infty x(t)e^{-\nu t}dt$ is the **Laplace transform** of $x(t)$. Use integration by parts to show that the Laplace transforms of $\dot{x}$ and $\ddot{x}$ are given by

$$\tilde{\dot{x}}(\nu) = \nu\tilde{x}(\nu) - x(0) \quad \text{and} \quad \tilde{\ddot{x}}(\nu) = \nu^2\tilde{x}(\nu) - \nu x(0) - \dot{x}(0). \tag{6.86}$$

25. Verify that if $G(t, t')$ is a **Green function** satisfying (6.57), then

$$x(t) = \frac{1}{m}\int_{-\infty}^{\infty} G(t, t')F(t')dt' \tag{6.87}$$

    solves the driven oscillator equation (6.34).
26. Suppose we make a change of variable from t to $s = t - t'$. Use the **chain rule** of differentiation to show that $d/dt = d/ds$.
27. **Fundamental theorem of calculus.** An antiderivative or primitive of a function $f(x, \alpha)$ with respect to x is a function $G(x, \alpha)$ with the property $\frac{\partial G}{\partial x} = f(x, \alpha)$. Here, α is a parameter. A primitive is usually written as an indefinite integral

$$\int^x f(x, \alpha)\, dx = G(x, \alpha) \tag{6.88}$$

    and is of course not unique (we may add to it any function of the parameter). According to the fundamental theorem of calculus (FTC),

$$\int_{x_1}^{x_2} f(x, \alpha)dx = G(x_2, \alpha) - G(x_1, \alpha). \tag{6.89}$$

Now we will suppose that the limits of integration also depend on the parameter α. Use the FTC to show that if

$$\begin{aligned} I(\alpha) &= \int_{a(\alpha)}^{b(\alpha)} f(x,\alpha)\,dx, \quad \text{then} \\ I'(\alpha) &= \int_{a(\alpha)}^{b(\alpha)} \frac{\partial f(x,\alpha)}{\partial \alpha}\,dx + f(b(\alpha),\alpha)b'(\alpha) - f(a(\alpha),\alpha)a'(\alpha). \end{aligned} \tag{6.90}$$

28. Verify by explicit differentiation and use of the FTC (Prob. 6.27) that (6.66):

$$x(t) = \frac{1}{m\omega}\int_{-\infty}^{t} \sin(\omega(t-t'))F(t')\,dt' \tag{6.91}$$

satisfies the **forced oscillator** equation (6.34).

29. Consider the **driven damped oscillator** equation $\ddot{x} + \frac{\gamma}{m}\dot{x} + \omega^2 x = (f/m)e^{i\nu t}$ where we use a complex force to avoid use of trigonometric identities and in anticipation of taking the real part. Find a particular solution by trying an ansatz with the same time-dependence as the driving force, i.e., $x_p = Be^{i\nu t}$. Take the real part and express it as $b\cos(\nu t + \delta)$ and find the amplitude b and initial phase δ.

30. Find the driving frequency ν at which the amplitude

$$b = (f/m)[(\omega^2-\nu^2)^2 + \nu^2\gamma^2/m^2]^{-1/2} \tag{6.92}$$

of the response of the **underdamped driven oscillator** is maximal.

31. Find the full width at half maximum of the **Lorentzian spectral distribution** of average rate of energy absorbed by a damped oscillator at late times:

$$\langle \dot{E} \rangle = (\gamma f^2/8m^2)[((\nu-\omega)^2 + \gamma^2/4m^2)]^{-1}. \tag{6.93}$$

32. Estimate the energy per unit time absorbed by a **damped driven oscillator** across all driving frequencies ν in the neighborhood of the resonant frequency ω. Show that it is $\approx \pi f^2/4m$, a value independent of ω and the damping coefficient γ.

33. Consider an oscillator with **time-dependent mass** and spring constant governed by the Lagrangian $L = \frac{1}{2}m(t)\dot{x}^2 - \frac{1}{2}k(t)x^2$. (a) Obtain the equation of motion. (b) Show that a reparametrization of time $t \to \tau$ given by $d\tau = dt/m(t)$ makes it possible to absorb the time-dependence of the mass into that of the spring constant. What is the resulting equation of motion for $x(\tau)$?

∗34. **Approximate condition for parametric resonance.** Derive Eq. (6.78)

$$\left(2\dot{b} - \epsilon a + h\omega_0 a/2\right)\omega_0\cos(\nu t/2) - (2\dot{a} + \epsilon b + h\omega_0 b/2)\,\omega_0\sin(\nu t/2) \approx 0 \tag{6.94}$$

where $\nu = 2\omega_0 + \epsilon$ is the parametric oscillation frequency. Hint: Put (6.77) in (6.76) and ignore appropriate slowly varying and nonresonant contributions.

Chapter 7

Nonlinear oscillations: pendulum and anharmonic oscillator

In Chapter 6, we discussed small amplitude oscillations of systems with one degree of freedom. In this chapter, we consider two important conservative systems with one degree of freedom that display oscillations that are not necessarily of small amplitude: the simple pendulum and the anharmonic oscillator. The first qualitative change is that the period of oscillations becomes amplitude-dependent. Unlike those of a harmonic oscillator, Hamilton's equations of motion here are nonlinear. This means the associated Hamiltonian vector field on phase space has components that are nonlinear functions of the coordinates on phase space. The phase portraits of these systems involve new features such as separatrices that separate qualitatively different types of behavior such as libration and rotation. Furthermore, in the case of the pendulum, the phase space is topologically nontrivial in the sense that it is a cylinder rather than the familiar position-momentum planar phase space ($\mathbb{R}^2$) of a point mass moving along a line. We also encounter new methods of solution, both exact (involving elliptic functions) and approximate (involving series expansions).

7.1 Simple pendulum: view from phase space

Recall from Sect. 1.5 that a simple pendulum consists of a point-like bob of mass m attached to the free end of a massless rigid rod of length ℓ clamped at a pivot. As shown in Fig. 7.1, the bob is free to move in a fixed vertical (x-y) plane subject to Earth's constant acceleration due to gravity of magnitude g. Newton's equation of motion (1.29) for the counterclockwise angle of deflection is the nonlinear ODE

$$\ddot{\theta} = -(g/\ell)\ \sin\theta = -\omega^2 \sin\theta \quad \text{where} \quad \omega = \sqrt{g/\ell}. \tag{7.1}$$

As shown in (1.31), this second order ODE admits a conserved energy

$$E = \frac{1}{2} m\ell^2 \dot{\theta}^2 + mg\ell(1-\cos\theta) = T + V. \tag{7.2}$$

Fig. 7.2a displays graphs of $\theta(t)$ for a few representative values of E.

Lagrangian and angular momentum. From Sect. 3.5, a Lagrangian for (7.1) is

$$L = T - V = \frac{1}{2} m\ell^2 \dot{\theta}^2 - mg\ell(1-\cos\theta). \tag{7.3}$$

The momentum canonically conjugate to θ is $p_\theta = \frac{\partial L}{\partial \dot{\theta}} = m\ell^2\dot{\theta}$ and Lagrange's equation $\dot{p}_\theta = -mg\ell\sin\theta$ reduces to (7.1). Note that p_θ is the z-component of angular

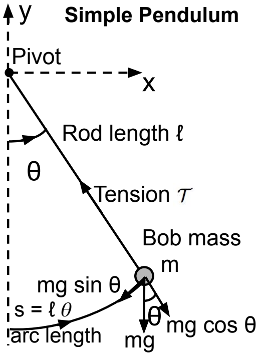

Figure 7.1: Simple pendulum free to oscillate in the vertical x-y plane.

momentum about the pivot. Indeed, suppose $\boldsymbol{r} = \ell\hat{r}$ is the radius vector of the bob with pivot as the origin and $\boldsymbol{p} = m\dot{s}\hat{\theta}$ its linear momentum, where $s = \ell\theta$ is the arc length. Then its angular momentum is

$$\boldsymbol{L} = \boldsymbol{r} \times \boldsymbol{p} = (\ell\hat{r}) \times (m\ell\dot{\theta}\hat{\theta}) = m\ell^2\dot{\theta}\,\hat{z} = p_\theta\hat{z}. \tag{7.4}$$

Angular momentum is *not* conserved[1] since there is a nonzero torque $\boldsymbol{\tau} = \boldsymbol{r} \times \boldsymbol{F}$ about the pivot. The force on the bob is the resultant of the radially inward tension and vertically downward force of gravity, but only gravity provides a nonzero torque that tends to restore the pendulum to its equilibrium position:

$$\boldsymbol{\tau} = \boldsymbol{r} \times \boldsymbol{F} = -\ell mg\sin\theta\,\hat{z}. \tag{7.5}$$

The evolution equation for angular momentum $\dot{\boldsymbol{L}} = \boldsymbol{\tau}$ (3.12) reduces to Lagrange's equation for p_θ. Though p_θ is *not* conserved, it becomes approximately conserved as the energy increases (see Fig. 7.2b). In the limit of high energies $E \gg mg\ell$, where most of the energy is kinetic $\frac{1}{2}m\ell^2\dot{\theta}^2 \gg mg\ell$, we may ignore the small gravitational force and the negligible torque it produces. In this limit, the pendulum executes nearly uniform circular motion at high angular speed $\dot{\theta} \gg \omega$.

Hamilton's equations. The Hamiltonian of the simple pendulum, as a function of phase space variables (θ and p_θ) is obtained via a Legendre transform (Sect. 3.15) from the Lagrangian

$$H(\theta, p_\theta) = \text{ext}_{\dot{\theta}}\left[p_\theta\dot{\theta} - L\right] = \frac{p_\theta^2}{2m\ell^2} + mg\ell(1-\cos\theta). \tag{7.6}$$

The Hamiltonian H is simply the energy $E = T + V$ (7.2) with $\dot{\theta}$ expressed in terms of p_θ. Hamilton's equations are the pair of first order differential equations

$$\dot{\theta} = \{\theta, H\} = \frac{\partial H}{\partial p_\theta} = \frac{p_\theta}{m\ell^2} \quad \text{and} \quad \dot{p}_\theta = \{p_\theta, H\} = -\frac{\partial H}{\partial \theta} = -mg\ell\sin\theta \tag{7.7}$$

---

[1] We note that the components of $\boldsymbol{L}$ in the swing plane of the simple pendulum (x and y components) *are* conserved. However, they are zero for all initial conditions.

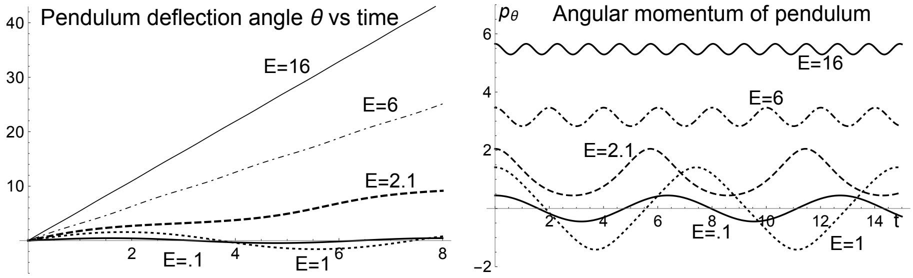

(a) (b)

Figure 7.2: (a) Pendulum deflection angle $\theta(t)$ (defined modulo 2π) at librational $(0 \le E < 2mg\ell)$ and rotational $(E > 2mg\ell)$ energies in units where $m = g = \ell = 1$. It is oscillatory at low energies and becomes linear for $E \gg 2mg\ell$. Small amplitude simple harmonic motion is approached as $E \to 0$. (b) Angular momentum $p_\theta = m\ell^2\dot{\theta}$ as a function of time. Notice that p_θ becomes approximately constant at high energies. ICs are chosen so that the bob starts moving counterclockwise $(p_\theta(0) > 0)$ at $t = 0$. It is instructive to compare this plot with Fig. 7.4b. As shown in (7.13), the time period grows without bound as $E \to 2mg\ell$.

where the Poisson brackets are the canonical ones:

$$\{\theta, \theta\} = \{p_\theta, p_\theta\} = 0 \quad \text{and} \quad \{\theta, p_\theta\} = 1, \tag{7.8}$$

since p_θ is the momentum canonically conjugate to θ in the Lagrangian (7.3).

Phase space and Hamiltonian vector field. The set of possible values of (θ, p_θ) comprise the phase space. The possible positions of the bob are given by points on a circle (denoted S^1) parametrized by the angle θ. For definiteness, we may suppose that $-\pi \le \theta \le \pi$ with both $\pm\pi$ corresponding to the upward orientation. On the other hand, angular momentum $p_\theta = m\ell^2\dot{\theta}$ can take any real value, $p_\theta \in \mathbb{R}$. If $p_\theta = 0$, the pendulum has zero angular velocity, as when it is at rest in equilibrium. A bob that rotates counterclockwise has $p_\theta > 0$, the faster it rotates, the higher p_θ is. If $p_\theta < 0$, the bob rotates clockwise.

Thus, the instantaneous state of the pendulum is determined by a point in the Cartesian product $S^1 \times \mathbb{R}$. This space (or manifold) may be viewed as an infinite circular cylinder (see Fig. 7.3). The motion of the pendulum defines a curve (phase trajectory) $(\theta(t), p_\theta(t))$ on this cylindrical phase space, the integral curve of the Hamiltonian vector field defined by Hamilton's equations (7.7). Its components are

$$v^\theta = \frac{p_\theta}{m\ell^2} \quad \text{and} \quad v^{p_\theta} = -mg\ell \sin\theta. \tag{7.9}$$

This vector field has precisely two fixed points: $(\theta^* = 0, p_\theta^* = 0)$ and $(\theta^* = \pi, p_\theta^* = 0)$ corresponding to static solutions with the pendulum hanging downwards or in an inverted position. Let us examine the neighborhood of these fixed points by linearizing the vector field around them. Putting $\theta = \theta^* + \delta\theta$ and $p = p^* + \delta p$ as in (5.27) we get

$$\frac{d}{dt}\begin{pmatrix}\delta\theta \\ \delta p_\theta\end{pmatrix} = \begin{pmatrix}0 & 1/m\ell^2 \\ \mp mg\ell & 0\end{pmatrix}\begin{pmatrix}\delta\theta \\ \delta p_\theta\end{pmatrix} \quad \text{for} \quad \theta^* = 0, \pi. \tag{7.10}$$

We see that the Jacobian matrix has trace $\tau = 0$ and determinant $\Delta = \pm g/\ell = \pm\omega^2$. From the classification of fixed points in Sect. 6.6*, we see that $(0,0)$ is a linear center (O-point) while $(\pi, 0)$ is a linear saddle (X-point). Can we trust these results of the linear theory? The answer is 'yes'. In fact, $(0,0)$ is a minimum of the Hamiltonian and must therefore be a center, as argued in Sect. 6.7*. On the other hand, by the Hartman-Grobman theorem of Sect. 6.7*, the linear saddle at $(\pi, 0)$ survives when nonlinearities are included.

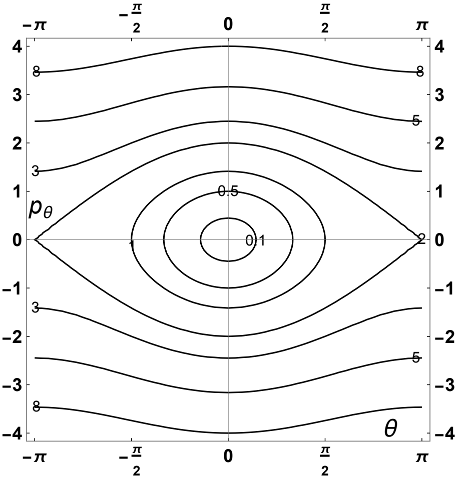

Figure 7.3: Energy level curves of the simple pendulum on its cylindrical phase space for $m = g = \ell = 1$. The value of energy on each curve is indicated. The right ($\theta = \pi$) and left ($\theta = -\pi$) edges of the diagram are to be identified, thus producing a cylinder with vertical axis parametrized by p_θ. Why are the energy level curves left-right and up-down symmetric? The direction of time along trajectories is 'clockwise'. The figure indicates that the origin is a center while ($\theta = \pi, p_\theta = 0$) is a saddle point. The energy $E = 2mg\ell$ level curve is a separatrix that demarcates the boundary between libration $E < 2mg\ell$ and rotation $E > 2mg\ell$.

Phase portrait. It is instructive to plot the trajectories on phase space. Since the Hamiltonian is a constant of motion, it is constant along trajectories. So each level curve[2] of the Hamiltonian is either a trajectory or a union of several trajectories with a common energy. The trajectory with least energy $(E = 0)$ is the one where the bob is permanently at rest at $\theta = 0$ with $p_\theta = 0$ (the O-point). As the bob is supplied with more energy, it oscillates about its stable equilibrium point in its *librational* phase. Conservation of energy allows us to find the maximum counterclockwise angle of deflection $\theta_{\max} = |\arccos(1 - E/mg\ell)|$ at which the bob comes instantaneously to rest (turning point). We see that energy $E = mg\ell(1 - \cos\theta_{\max})$ is an increasing function of $\theta_{\max}$: it goes from 0 to $2mg\ell$ as $\theta_{\max}$ increases from 0 to π. When $E = 2mg\ell$, we have an unstable equilibrium at the saddle point $\theta = \pm\pi, p_\theta = 0$. When $E > 2mg\ell$, the bob *rotates* around the pivot and there is no turning point or maximum angle of deflection. The phase portrait is shown in Fig. 7.3. Notice the separatrix that separates the librational trajectories from the rotational ones. The separatrices consist of the limiting trajectories with energy $E \to 2mg\ell^-$ where the bob just makes it to the top, either clockwise or counterclockwise. Librational trajectories are 'contractible' curves[3] on the cylindrical phase space while rotational trajectories are *not* contractible, they wind around the cylinder. In either case, as long as $E \neq 2mg\ell$ (see below), the trajectories are closed curves on phase space, indicating that the motion is periodic.

---

[2] The energy-E level set of H is the set of points on the phase space where $H = E$. Since this is one condition on the two variables θ and p_θ, level sets are typically 1d curves.

Time period. The time period is the minimum time taken for θ *and* p_θ to return to their initial values. As in Sect. 1.2, the time period of librational oscillations is twice the time taken for the bob to go between the turning points $\theta = \mp\theta_{\rm max}$. Since E (7.2) is an even function of θ, the period is

$$T(E) = 4\int_0^{\theta_{\rm max}} \frac{d\theta}{\sqrt{\frac{2}{m\ell^2}(E - mg\ell(1-\cos\theta))}} = \frac{2\sqrt{2}}{\omega}\int_0^{\theta_{\rm max}} \frac{d\theta}{\sqrt{\epsilon - (1-\cos\theta)}}. \tag{7.11}$$

Here, $\epsilon = E/mg\ell$ is the energy in units of the potential energy at the height of the pivot. For libration, $0 \leq E < 2mg\ell$ so $0 \leq \epsilon < 2$. When E approaches $2mg\ell$ from below, $\theta_{\rm max} \to \pi^-$ and

$$T(E = 2mg\ell) = \frac{2\sqrt{2}}{\omega}\int_0^{\pi} \frac{d\theta}{\sqrt{1+\cos\theta}}. \tag{7.12}$$

This integral diverges as the integrand has a simple pole at $\theta = \pi$. Indeed, if we put $\theta = \pi - x$, then $\cos(\pi - x) = -\cos x = -1 + \frac{1}{2}x^2 - \cdots$. At the threshold for rotational motion, the bob takes infinitely long to reach the vertically upward position. With some more effort (see Prob. 7.2), one may show that the time period diverges logarithmically as $E \to 2mg\ell^-$:

$$T(\epsilon) = -(2/\omega)\log[(2-\epsilon)/32] + \mathcal{O}(2-\epsilon) \quad \text{as} \quad \epsilon = E/mg\ell \to 2^-. \tag{7.13}$$

Though the time period diverges, it does so rather slowly (see Fig. 7.4b). Contrast this with the power-law divergence of the time period $T(E) \sim (-E)^{-3/2}$ in the Kepler problem (Prob. 2.17) and $T(E) \sim (-E)^{-1/2}$ for the sech^2 potential (Prob. 1.13). The time period as a function of $\theta_{\rm max}$ as well as energy is plotted in Fig. 7.4, showing the slow divergence as $\theta_{\rm max} \to \pi$. As $\theta_{\rm max} \to 0$, the period approaches the small oscillation value $2\pi\sqrt{\ell/g}$ of Sect. 1.5.

7.2* Introduction to Jacobi elliptic functions

The time-dependence of the deflection angle of a simple pendulum may be expressed in terms of the Jacobi[4] elliptic function sn [21,103]. In fact, elliptic functions

---

[3] A closed curve is contractible if it can be continuously deformed to a point while remaining on the phase space.

[4] The qualifier 'Jacobi' is used to distinguish them from the Weierstrass elliptic functions. See Prob. 7.4 for a relation between the Weierstrass $\wp$ function and the Jacobi elliptic functions.

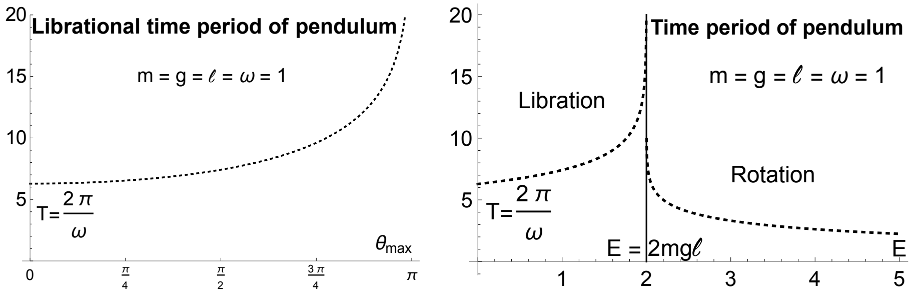

(a) (b)

Figure 7.4: Time period of simple pendulum versus (a) maximum angle of deflection $\theta_{\rm max}$ and (b) energy E in units of $mg\ell$ showing logarithmic divergence at libration to rotation transition at $E = 2mg\ell$. The asymmetry in the manner of divergence as $E \to \pm 2mg\ell$ can be understood intuitively. As $E \to 2mg\ell$ a librational period is roughly twice a rotational period since for libration, the bob must swing back and forth once while for rotation, it just needs to go round the circle once. Compare with Fig. 7.2b.

and the associated elliptic integrals[5] also arise in the solutions to several other mechanical systems. For instance, we will meet them in a quartic anharmonic oscillator in Sect. 7.5*, torque-free motion of an anisotropic rigid body in Sect. 8.13* and in the wobbling of a heavy symmetrical top in Sect. 8.15. Elliptic functions are examples of so-called *special functions*. Special functions usually refer to functions less familiar than rational, trigonometric or exponential functions but which arise in many problems of mathematics and physics and which often can be described in multiple equivalent/complementary ways (e.g., via differential equations, power series, integral representations, functional/recurrence relations and geometric constructions).

One way to motivate the Jacobi elliptic functions is via the differential equations they satisfy. Elliptic functions differ from some other special functions (such as the Legendre, Bessel or hypergeometric functions) in that they satisfy nonlinear rather than linear differential equations. Recall that the circular functions sine and cosine[6] may be defined by a pair of trigonometric evolution equations:

$$\sin' u = \cos u, \quad \cos' u = -\sin u \quad \text{with} \quad \sin 0 = 0, \quad \cos 0 = 1. \tag{7.14}$$

Primes denote differentiation in u, which is to be thought of as time. The Jacobi elliptic functions $\operatorname{sn}(u,k)$, $\operatorname{cn}(u,k)$ and $\operatorname{dn}(u,k)$ are defined via a system of 3 ODEs[7],

$$\operatorname{sn}'(u,k) \quad = \quad \operatorname{cn}(u,k)\operatorname{dn}(u,k), \quad \operatorname{cn}'(u,k) = -\operatorname{sn}(u,k)\operatorname{dn}(u,k) \quad \text{and}$$

---

[5] The name elliptic integrals is because they arise in finding the arc length of an ellipse, see Prob. 7.1. We will see that elliptic functions arise from inverting elliptic integrals. In a suitable limit, elliptic integrals can be expressed in terms of inverse trigonometric functions, so elliptic functions are a generalization of trigonometric functions.

[6] The name circular functions for $\cos\theta$ and $\sin\theta$ is because they are the Cartesian coordinates of a point on a unit circle at counterclockwise angle θ relative to the horizontal axis.

[7] They are closely related to Euler's equations for the components of angular momentum in the principal axis corotating frame of a rigid body subject to no external torque, see Sect. 8.13*.

$$\mathrm{dn}'(u,k) \quad = \quad -k^2\,\mathrm{sn}(u,k)\,\mathrm{cn}(u,k). \tag{7.15}$$

Here, u may be viewed as a rescaled time variable and $0 \le k \le 1$ is a parameter called the elliptic modulus[8]. Primes denote differentiation in u. These are supplemented by initial conditions

$$\mathrm{sn}(0,k) = 0, \quad \mathrm{cn}(0,k) = 1 \quad \text{and} \quad \mathrm{dn}(0,k) = 1. \tag{7.16}$$

Just as $\sin^2 u + \cos^2 u = 1$ is a constant of motion for the trigonometric evolution, we have two constants of motion for the evolution of elliptic functions

$$\mathrm{sn}^2 + \mathrm{cn}^2 = 1 \quad \text{and} \quad k^2\,\mathrm{sn}^2 + \mathrm{dn}^2 = 1 \quad \text{or} \quad \mathrm{dn}^2 - k^2\,\mathrm{cn}^2 = 1 - k^2. \tag{7.17}$$

These quadratic relations are established by explicit differentiation and use of initial conditions. We may use these quadratic relations to eliminate cn and dn from the system of ODEs and get a single ODE $\mathrm{sn}' = \mathrm{cn}\,\mathrm{dn}$. This implies

$$(\mathrm{sn}')^2 = (1 - \mathrm{sn}^2)(1 - k^2\,\mathrm{sn}^2) \quad \text{or} \quad du = \frac{ds}{\sqrt{(1-s^2)(1-k^2 s^2)}}. \tag{7.18}$$

Integrating from 0 to u and using $\mathrm{sn}(0) = 0$, we express the solution via quadrature

$$u(s) = \int_0^s \frac{dt}{\sqrt{(1-t^2)(1-k^2t^2)}} \equiv F(\arcsin s, k) \quad \text{for} \quad |s| \le 1. \tag{7.19}$$

This is called an *incomplete* (due to the variable upper limit) *elliptic integral*, of the first kind in Legendre normal form[9]. Inverting it gives another way [different from, but equivalent to the 3 ODEs (7.15)] of defining the Jacobi elliptic function $s = \mathrm{sn}(u,k)$. Elliptic functions may also be defined using power series expansions (they are complex analytic functions of both u and k though here we are only concerned with $0 \le k \le 1$ and real u) as well as via more geometric constructions [90].

To compare with how inverse trigonometric functions are defined, we let $k \to 0$ and see that the equation for dn becomes $\mathrm{dn}'(u,0) = 0$ so that $\mathrm{dn}(u,0) = 1$ and

$$\mathrm{sn}'(u,0) = \mathrm{cn}(u,0) \quad \text{and} \quad \mathrm{cn}'(u,0) = -\,\mathrm{sn}(u,0) \tag{7.20}$$

with initial conditions $\mathrm{sn}(0,0) = 0$ and $\mathrm{cn}(0,0) = 1$. So the elliptic functions reduce to trigonometric functions when the modulus k vanishes (see Fig. 7.5b):

$$\mathrm{sn}(u,0) = \sin(u), \quad \mathrm{cn}(u,0) = \cos(u) \quad \text{and} \quad \mathrm{dn}(u,0) = 1. \tag{7.21}$$

---

[8] The origin of the name modulus may be traced to the modulus (determinant) of certain 2×2 matrices that appear in the theory of elliptic curves.

[9] More generally, elliptic integrals arise when the integrand is a rational function of t and the square-root of a cubic or quartic polynomial in t with no repeated roots. Such general elliptic integrals can be reduced to integrals of rational functions and elliptic integrals of the first three kinds. The integrals are called hyperelliptic if the polynomial is of degree five or higher.

The differential equation becomes

$$\begin{aligned} \sin' u &= \sqrt{1-\sin^2 u} \quad \text{or} \quad \frac{ds}{\sqrt{1-s^2}} = du, \\ \text{so} \quad u &= \int_0^s \frac{dt}{\sqrt{1-t^2}} = \arcsin(s) \quad \Rightarrow \quad s = \sin u. \end{aligned} \tag{7.22}$$

We notice that $-\operatorname{sn}(-u,k)$, $\operatorname{cn}(-u,k)$ and $\operatorname{dn}(-u,k)$ satisfy the same ODEs (7.15) and initial conditions (7.16) as $\operatorname{sn}(u,k)$, $\operatorname{cn}(u,k)$ and $\operatorname{dn}(u,k)$. Assuming a unique solution to the initial value problem (see Sect. 5.3), sn must odd and cn, dn even:

$$\operatorname{sn}(-u,k) = -\operatorname{sn}(u,k), \quad \operatorname{cn}(-u,k) = \operatorname{cn}(u,k) \quad \text{and} \quad \operatorname{dn}(-u,k) = \operatorname{dn}(u,k). \tag{7.23}$$

For use in the pendulum problem, it is convenient to rewrite the incomplete elliptic integral (7.19) using the fairly natural change of variable $kt = \sin\frac{\theta}{2}$, which is valid provided $k \neq 0$. Then one finds that the elliptic function $s = \operatorname{sn}(u,k)$ results from inverting the incomplete elliptic integral

$$u(s,k) = \frac{1}{2}\int_0^{2\arcsin(ks)} \frac{d\theta}{\sqrt{k^2 - \sin^2\theta/2}} = \frac{1}{\sqrt{2}}\int_0^{2\arcsin(ks)} \frac{d\theta}{\sqrt{2k^2 - 1 + \cos\theta}}. \tag{7.24}$$

The complete elliptic integral is $u(1,k)$, obtained by letting the upper limit of integration be maximal[10]. We will see that the pendulum period is $4K(k)/\omega$, where K is the complete elliptic integral of the first kind, defined for $0 < k \leq 1$ by

$$\begin{aligned} K(k) &= \int_0^1 \frac{dt}{\sqrt{(1-t^2)(1-k^2t^2)}} = \frac{1}{2}\int_0^{2\arcsin k} \frac{d\theta}{\sqrt{k^2 - \sin^2\left(\frac{\theta}{2}\right)}} \\ &= \frac{1}{\sqrt{2}}\int_0^{2\arcsin k} \frac{d\theta}{\sqrt{2k^2 - 1 + \cos\theta}}. \end{aligned} \tag{7.25}$$

When $k \to 0$, we find from the first expression that $K(0) = \arcsin 1 = \pi/2$, which is one-fourth the period of circular functions. The other two expressions are not valid for $k = 0$ since the substitution $kt = \sin(\theta/2)$ is not meaningful when $k = 0$.

7.3* Time-dependence of pendulum in terms of elliptic functions

The solution of (7.1) is reduced to quadrature using the constancy of energy (7.2):

$$t - t_o = \int_{\theta(t_o)}^{\theta(t)} \frac{d\theta'}{\sqrt{\frac{2}{m\ell^2}[E - mg\ell(1-\cos\theta')]}}. \tag{7.26}$$

To find trajectories of energy E and $\theta(0) = 0$ we use dimensionless variables $\epsilon = E/mg\ell$ and $\tau = \omega t$ where $\omega = \sqrt{g/\ell}$ is the frequency of small oscillations. Then

$$\tau = \int_0^\theta \frac{d\theta'}{\sqrt{2(\epsilon - (1-\cos\theta'))}}. \tag{7.27}$$

---

[10] Notice that $s = \operatorname{sn} = 1$ is the largest value allowed by (7.17) for real sn and cn.

Comparing with the incomplete elliptic integral (7.24) for $s = \operatorname{sn}(u,k)$, we read off

$$u = \tau, \quad \theta = 2\arcsin ks \quad \text{and} \quad k = \sqrt{\epsilon/2}, \quad \text{provided} \quad 0 \le \epsilon \le 2. \tag{7.28}$$

Thus, the time-dependence of *librational trajectories* is given by

$$\theta_{\rm lib}(t) = 2\arcsin\left[k \operatorname{sn}(\omega t, k)\right]. \tag{7.29}$$

We check that this reduces to the known sinusoidal trajectory for low energies. If $E \gtrsim 0$ then $k \gtrsim 0$ and the argument of the arcsin is small ($|\operatorname{sn}| \le 1$ since $\operatorname{sn}^2 + \operatorname{cn}^2 = 1$), and we may replace $\arcsin(k \operatorname{sn})$ by $k \operatorname{sn}$. Moreover, for small k, $\operatorname{sn}(u,k) \approx \sin u$, so $\theta(t) \approx 2k\sin(\omega t)$, recovering the small amplitude sinusoidal oscillations of the deflection angle $\theta(t)$ studied in Sect. 1.5.

Notice that the elliptic modulus k monotonically increases with energy. As E goes from 0 to $2mg\ell$, ϵ increases from 0 to 2, k increases from 0 to 1 corresponding to an amplitude $\theta_{\max}$ increasing from 0 to π. We plot θ as a function of time in Fig. 7.5a for various E holding m, g, ℓ fixed. The increase in period and amplitude with E are evident. Also visible is the manner in which for small k, the angle approaches a sine function. As E increases, the bob spends more and more time around the vertically upward position ($|\theta| \lesssim \pi$), which is like a mountain pass or bottleneck.

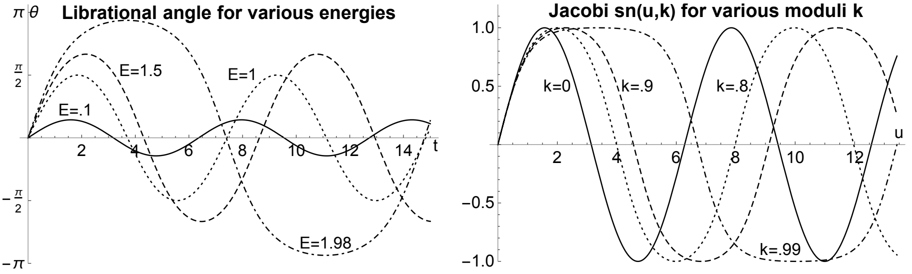

(a) (b)

Figure 7.5: (a) Deflection angle $\theta(t)$ for libration with $m = g = \ell = 1$. As $E \to 0$, $\theta(t) \to 2k\sin(\omega t)$ and the period approaches 2π. As $E \to 2mg\ell$, $\theta_{\max} \to \pi$ and the period diverges. (b) $\operatorname{sn}(u,k)$ approaches $\sin u$ for small k but has a diverging period as $k \to 1$

Time period for libration. The time period T for librational oscillations T may be expressed as a complete elliptic integral

$$\begin{aligned} T &= \frac{4}{\omega\sqrt{2}}\int_0^{\theta_{\max}} \frac{d\theta}{\sqrt{\epsilon - (1-\cos\theta)}} = \frac{4}{\omega\sqrt{2\epsilon}}\int_0^{\theta_{\max}} \frac{d\theta}{\sqrt{1-s^2}} \\ &= \frac{4}{\omega}\int_0^1 \frac{ds}{\sqrt{(1-s^2)(1-k^2s^2)}} = \frac{4}{\omega}K(k). \end{aligned} \tag{7.30}$$

As before, $k = \sqrt{\epsilon/2}$, $ks = \sin(\theta/2)$ and at the upper limit, $\cos\theta_{\max} = 1 - \epsilon$ implies $s_{\max} = 1$. T is a monotonically increasing function of E or $k = \sin(\theta_{\max}/2)$, as $(1 - k^2s^2)$ in the denominator decreases as k grows from 0 to 1. This is also evident in the following absolutely convergent series (see Prob. 7.3) with positive coefficients:

$$T = 2\pi\sqrt{\frac{l}{g}}\left[1 + \left(\frac{1}{2}\right)^2 k^2 + \left(\frac{1\cdot 3}{2\cdot 4}\right)^2 k^4 + \left(\frac{1\cdot 3\cdot 5}{2\cdot 4\cdot 6}\right)^2 k^6 + \cdots\right]. \tag{7.31}$$

We have already shown that the libration period $T(k)$ diverges as $k \to 1^-$. Finally, from (7.29) it follows that the elliptic function $\operatorname{sn}(u, k)$ is periodic with period $4K(k)$.

Rotational regime. For $\epsilon = E/mg\ell > 2$ we have rotational motion around the pivot, with the bob slowing down near the top. The motion is again periodic and the period is again given in terms of the complete elliptic integral of the 1^{st} kind (see Prob. 7.5)

$$T_{\text{rot}} = \frac{1}{\omega} \int_0^{2\pi} \frac{d\theta}{\sqrt{2\left(\epsilon - (1 - \cos\theta)\right)}} = \frac{2}{\omega}\kappa K(\kappa) \quad \text{where} \quad \kappa = \frac{1}{k} = \sqrt{\frac{2}{\epsilon}}. \quad (7.32)$$

With increasing energy, gravity becomes less relevant and the bob tends towards uniform circular motion. As $\epsilon \to \infty$, $\kappa \to 0$ and $T_{\text{rot}} \to 0$: the bob rotates very rapidly. The angle as a function of time for rotational motion may again be expressed in terms of Jacobi's sn function by inverting an incomplete elliptic integral of the first kind. Assuming $\theta(t = 0) = 0$,

$$t = \frac{1}{\omega} \int_0^{\theta} \frac{d\theta'}{\sqrt{2(\epsilon - (1 - \cos\theta'))}} \quad \Rightarrow \quad \theta_{\text{rot}}(t) = 2 \arcsin(\operatorname{sn}(\omega t/\kappa, \kappa)). \quad (7.33)$$

Separatrix solution. When $E = 2mg\ell$ ($\epsilon = 2, k = \kappa = 1$), nonconstant solutions are no longer periodic as $T \to \infty$ and the bob takes infinitely long to make it to the top from any initial location. There are two such trajectories (see Fig. 7.3) corresponding to clockwise and counterclockwise motion. Interestingly, the corresponding trajectories are expressible in terms of elementary functions (see Prob. 7.7)

$$\theta_{\text{sep}}(t) = \pm 2 \arcsin(\tanh(\omega t)). \quad (7.34)$$

7.4 Anharmonic oscillations: quartic double-well potential

A particle subject to a quadratic potential $\frac{1}{2}kx^2$ displays harmonic oscillations, with $x(t)$ given by a linear combination of sines and cosines, as discussed in Sect. 6.1. A potential that is *not* quadratic (usually a polynomial of degree > 2) is called anharmonic. The motion of a particle of mass m in the potential

$$V(x) = (g/4)(x^2 - a^2)^2 = \frac{g}{4}a^4 - \frac{g}{2}a^2x^2 + \frac{g}{4}x^4 \quad \text{with} \quad g, a > 0 \quad (7.35)$$

furnishes an example of anharmonic oscillations due to the confining quartic term in V. Fig. 7.6a shows why this potential is called a double-well potential. The additive constant in V does not affect the EOM. Newton's equation $m\ddot{x} = -V'(x) = ga^2x - gx^3$ is cubically nonlinear and leads to the autonomous Hamiltonian vector field

$$\dot{x} = p/m \quad \text{and} \quad \dot{p} = ga^2x - gx^3 \quad (7.36)$$

on the x-p phase plane shown in Fig. 7.6c. In the limit $g \to 0^-, a \to \infty$ holding $ga^2 = -k < 0$ fixed, we recover the equations (6.4) of a simple harmonic oscillator. For g and a^2 both positive, the linear force is destabilizing while the cubic force is restoring. Thus, we should expect the static solution at $x = 0$ to be unstable and

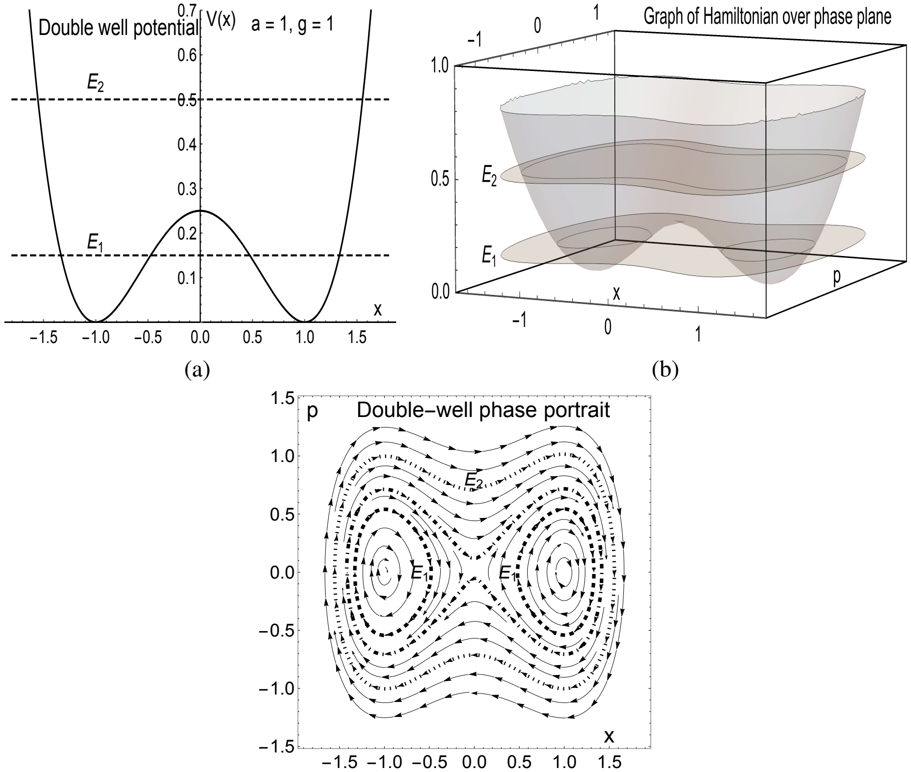

(a) (b)

(c)

Figure 7.6: (a) Double-well potential for $m = a = g = 1$ and $E_1 = 0.15, E_2 = 0.5$ (b) Graph of Hamiltonian $H(x,p)$ over the x-p phase plane. For $H = E_1$ the energy level set is a pair of closed curves while it is a single closed curve for $H = E_2$. (c) Phase portrait. The saddle point at the origin $(E = 1/4)$ is flanked by a pair of centers on either side. They are surrounded by a figure-8 shaped separatrix that partitions the phase plane into regions where the motion is confined to a well and the outer periphery where trajectories explore both wells.

nontrivial stable static solutions to exist on either side of it. In this section, we will draw some qualitative conclusions about this anharmonic oscillator. In Sect. 7.5* we will address the question of integrating the equations of the closely related anharmonic oscillator with cubic and linear *restoring* forces either exactly or approximately.

Like the pendulum, the double-well potential furnishes an example of a conservative system with saddles and centers. A graph of V (Fig. 7.6a) shows that there is a barrier of height $ga^4/4$ separating two potential wells[11]. There are three fixed points $(x_*, p_*) = (0,0), (a,0)$ and $(-a,0)$ corresponding to a particle at rest at the local extrema of V. Linearization around these fixed points leads to the Jacobians

$$J_{(0,0)} = \begin{pmatrix} 0 & 1/m \\ ga^2 & 0 \end{pmatrix} \quad \text{and} \quad J_{(\pm a,0)} = \begin{pmatrix} 0 & 1/m \\ -2ga^2 & 0 \end{pmatrix}. \tag{7.37}$$

---

[11] In Sect. 7.5* we will consider the anharmonic oscillator with $a^2 < 0$ so that there is a single well with no potential barrier.

While the trace $\tau = 0$ in all three cases, the determinant $\Delta_{(0,0)} = -ga^2/m < 0$ while $\Delta_{(\pm a,0)} = 2ga^2/m > 0$. Thus $(0,0)$ is a linear saddle while $(\pm a, 0)$ are linear centers. Though the Hartman-Grobman theorem of Sect. 6.7* guarantees that the phase portrait near the origin is homeomorphic to a saddle, it is noncommittal on whether the linear centers $(\pm a, 0)$ survive in the nonlinear theory. It turns out that $(\pm a, 0)$ are nonlinear centers: this is because they lie at local minima of the conserved energy $E = p^2/2m + (g/4)(x^2 - a^2)^2$. Fig. 7.6b displays a graph of the energy function over the x-p phase plane, showing that it has a bowl-like shape near $(\pm a, 0)$. The energy level contours are the curves along which horizontal planes intersect the graph. One finds that for $E < ga^4/4$, the level contours of energy are a pair of closed curves around $(\pm a, 0)$, so the latter are indeed centers. They correspond to oscillatory periodic motion around the minima $x = \pm a$ of V. As $E \to 0$, the level contours approach a pair of ellipses as is seen by Taylor expanding around $(x = \pm a, p = 0)$:

$$E = \frac{p^2}{2m} + ga^2(x \mp a)^2 + \mathcal{O}(x \mp a)^3. \tag{7.38}$$

The $E = ga^4/4$ level contour is a figure-8 shaped separatrix that is the union of two homoclinic orbits and the saddle point $(0,0)$. The homoclinic orbits correspond to trajectories where a particle approaches $x = 0$ as $t \to \pm\infty$ from either of the two wells. For $E > ga^4/4$, the level contours of E are 'large' closed curves corresponding to periodic motion that explores both wells (see Fig. 7.6c). As at the transition between libration and rotation in the simple pendulum, the period of oscillation diverges as $E \to ga^4/4$ either from above or below. The separatrix partitions the phase plane into regions where motion is confined/bound to one or other potential well and the region where the particle is deconfined/unbound and explores both wells.

7.5* Quartic oscillator: exact solution and Lindstedt-Poincaré method

We next consider a 1d anharmonic oscillator with linear and cubic restoring forces:

$$\ddot{x} + \omega_0^2 x = -gx^3 \quad \text{with} \quad g > 0. \tag{7.39}$$

This is sometimes referred to as the undamped and unforced Duffing equation. It differs from the double-well potential problem of Sect. 7.4 via the sign of the linear restoring force. The main challenge in solving this equation is its cubic nonlinearity, whose strength is proportional to g. The equation admits a conserved energy $E = \frac{1}{2}m\dot{x}^2 + V(x)$ where $V(x) = \frac{1}{2}m\omega_0^2 x^2 + \frac{1}{4}mgx^4$, which gives it the name quartic oscillator. From the standpoint of small oscillations discussed in Sect. 6.1, this V arises from expanding a more general potential around a minimum and keeping terms up the fourth degree in the displacement from equilibrium. The absence of a cubic term in V is a simplifying assumption, but is justified if the underlying potential possesses an $x \mapsto -x$ reflection symmetry. Physically, for any energy $E > 0$, a particle subject to (7.39) executes periodic oscillations between the turning points $\pm x_+$ where the amplitude

$$x_+ = \sqrt{y_+} \quad \text{and} \quad y_\pm = \frac{1}{g}\left[\pm\sqrt{\omega_0^4 + 4gE/m} - \omega_0^2\right] \equiv \frac{\pm\tilde{\omega}^2 - \omega_0^2}{g} \tag{7.40}$$

are the roots of the quadratic polynomial obtained by putting $y = x^2$:

$$E - V(x) = E - \frac{1}{2}m\omega_0^2 y - \frac{1}{4}mgy^2 = \frac{mg}{4}(y_+ - y)(y - y_-). \tag{7.41}$$

Exact solution via elliptic integrals. The solution of the equation of motion (7.39) may be reduced to quadrature. For instance, if the particle starts from the equilibrium point $x(0) = 0$ with rightward initial velocity, then t is given by

$$t = \int_0^x \frac{dx}{\sqrt{\frac{2}{m}\left(E - \frac{1}{2}m\omega_0^2 x^2 - \frac{1}{4}mgx^4\right)}} = \frac{1}{2}\sqrt{\frac{2}{g}}\int_0^{x^2} \frac{dy}{\sqrt{y(y_+ - y)(y - y_-)}}. \tag{7.42}$$

This is an incomplete elliptic integral of the first kind. Referring to Formula 5 of Sect. 3.131 on page 254 of [48] we may write

$$t = \sqrt{\frac{2}{g(y_+ - y_-)}}\, F\left(\arcsin\sqrt{\frac{(y_+ - y_-)x^2}{y_+(x^2 - y_-)}}, \sqrt{\frac{y_+}{y_+ - y_-}}\right). \tag{7.43}$$

This may be inverted using $\sin\varphi = \operatorname{sn}(u, k)$ if $F(\varphi, k) = u$ (see (7.19)) to express x as a function of t. In our case, the elliptic modulus is

$$k = \sqrt{\frac{y_+}{y_+ - y_-}} = \left(\frac{\tilde\omega^2 - \omega_0^2}{2\tilde\omega^2}\right)^{1/2} \quad \text{while} \quad u = t\sqrt{\frac{g(y_+ - y_-)}{2}} = \tilde\omega t. \tag{7.44}$$

It follows that

$$\frac{x^2(y_+ - y_-)}{y_+(x^2 - y_-)} = \operatorname{sn}^2(u, k) \quad \text{or} \quad x^2 = \frac{-y_+ y_- \operatorname{sn}^2(u, k)}{y_+ - y_- - y_+ \operatorname{sn}^2(u, k)}. \tag{7.45}$$

Thus, we arrive at a formula for the displacement in terms of the Jacobi sn function:

$$x(t)^2 = \frac{4(E/m)\operatorname{sn}^2(\tilde\omega t, k)}{2\tilde\omega^2 - (\tilde\omega^2 - \omega_0^2)\operatorname{sn}^2(\tilde\omega t, k)} \quad \text{where} \quad \tilde\omega = \omega_0\left(1 + 4gE/m\omega_0^4\right)^{1/4}. \tag{7.46}$$

To obtain $x(t)$, the positive square root is to be picked for $0 \le t \le T/2$ and the negative square root for $T/2 \le t \le T$, where T is the period of oscillations. From (7.43), the latter is given by a complete elliptic integral of the first kind

$$T = 4\int_0^{x_+} \frac{dx}{\sqrt{\frac{2}{m}(E - V(x))}} = \frac{4}{\tilde\omega}F(\arcsin 1, k) = \frac{4}{\tilde\omega}K(k). \tag{7.47}$$

To get a sense for the effect of the anharmonic force, let us consider our solution for small g. Since g is a dimensional quantity, what we really mean by weak nonlinearity is small values of the (unique independent) dimensionless combination $\alpha = gE/m\omega_0^4$. Thus, we focus on energies small compared to $m\omega_0^4/g$. We find for small α,

$$\tilde\omega = \omega_0\left[1 + \alpha - \frac{3\alpha^2}{2} + \cdots\right], \quad \tilde\omega^2 = \omega_0^2\left[1 + 2\alpha - 2\alpha^2 + \cdots\right] \text{ and } k^2 \approx \alpha. \tag{7.48}$$

Thus, when $\alpha \to 0$, the modulus k vanishes and $\tilde{\omega} \to \omega_0$. In this limit, $\mathrm{sn}(u,k) \to \sin\omega_0 t$ so that the solution (7.46) reduces to harmonic oscillations, as we expect:

$$x(t) \to \sqrt{\frac{2E}{m\omega_0^2}} \sin\omega_0 t \quad \text{as} \quad \alpha \to 0. \tag{7.49}$$

For future reference, it is instructive to find the leading departure from isochronous oscillations. The square of the amplitude is given by

$$x_+^2 = (2\omega_0^2\alpha/g)(1-\alpha+\cdots) = (2E/m\omega_0^2)(1-\alpha+\cdots). \tag{7.50}$$

Using the expansion $K(k) = (\pi/2)(1+k^2/4+\cdots)$ (see Prob. 7.3), we find that the time period acquires a dependence on energy or amplitude

$$T = \frac{2\pi}{\omega_0}\left(1-\frac{3\alpha}{4}+\cdots\right) = \frac{2\pi}{\omega_0}\left(1-\frac{3}{4}\frac{gE}{m\omega_0^4}+\cdots\right) = \frac{2\pi}{\omega_0}\left(1-\frac{3gx_+^2}{8\omega_0^2}+\cdots\right). \tag{7.51}$$

Lindstedt-Poincaré perturbation theory. We are lucky to have been able to solve the nonlinear EOM of the anharmonic oscillator using elliptic functions. However, elliptic integrals are not adequate if the potential is of degree 5 or higher, in which case we need hyperelliptic integrals, whose properties are even less familiar. For more general potentials, exact solutions are almost never possible. A complementary approach is to seek an approximate solution in terms of more elementary functions, that can be successively improved. The Lindstedt-Poincaré method is a perturbative approximation where one views the anharmonic force as a perturbation to the harmonic restoring force and attempts to express $x(t)$ in a series of successive approximations beginning with an appropriate solution of the harmonic oscillator. To this end, let us suppose that

$$x(t) = x_0(t) + gx_1(t) + g^2x_2(t) + \cdots. \tag{7.52}$$

Inserting this series in (7.39), and equating coefficients of like powers of g on either side, we get a sequence of equations:

$$\begin{aligned}
\text{at order } g^0 &: \quad \ddot{x}_0 + \omega_0^2 x_0 = 0,\\
g^1 &: \quad \ddot{x}_1 + \omega_0^2 x_1 = -x_0^3,\\
g^2 &: \quad \ddot{x}_2 + \omega_0^2 x_2 = -3x_0^2 x_1,\\
g^3 &: \quad \ddot{x}_3 + \omega_0^2 x_3 = -3(x_0^2 x_2 + x_0 x_1^2),\\
g^n &: \quad \ddot{x}_n + \omega_0^2 x_n = -\textstyle\sum_{p+q+r=n-1} x_p x_q x_r.
\end{aligned} \tag{7.53}$$

At the 0^{th} order, we recover the linear oscillator equation with solution $x_0 = a\cos\omega_0 t$ corresponding to the IC $x(0) = a$ and $\dot{x}(0) = 0$ where the particle starts from the turning point $a = x_+$. At the next order, we have an inhomogeneous equation, an oscillator with driving force determined by x_0. In fact, all the higher order equations are of the same sort: oscillators with driving terms determined by the lower order equations. So we hope to solve the equations successively and truncate the procedure after a few steps to obtain a desired accuracy. However, there is a hitch. At $\mathcal{O}(g)$,

$$\ddot{x}_1 + \omega_0^2 x_1 = -a^3\cos^3(\omega_0 t) = -(a^3/4)\left(3\cos\omega_0 t + \cos 3\omega_0 t\right). \tag{7.54}$$

The driving force $\propto \cos\omega_0 t$ has the same frequency ω_0 as the unperturbed oscillator and should lead to resonant amplification as explained below (6.39) in Sect. 6.8. In fact, imposing the IC $x(0) = x_0 + gx_1 = a$ and $\dot{x}(0) = 0$ we get

$$x_1(t) = a^3\left((1/32)(\cos 3\omega_0 t - \cos\omega_0 t) - (3/8)\omega_0 t \sin\omega_0 t\right). \tag{7.55}$$

This first order correction to the trajectory includes a *secular* term that grows linearly with time. Similar aperiodic and unbounded terms arise at higher orders in the perturbative expansion due to resonances. Unfortunately, this makes a truncation of the perturbation series a poor approximation since $|x(t)|$ is known to be periodic in time and also bounded above by x_+. These difficulties due to resonances are common to perturbative treatments of several classical systems. For instance, they arise in the three-body problem of celestial mechanics where one treats the effects of the Sun on the Earth-Moon system as a perturbation.

As noted in Sect. 1.3*, a key feature of anharmonic oscillations is that they are not isochronous: the period of oscillation (or frequency $\omega = 2\pi/T$) depends on the amplitude (or energy). The above series tries to express the periodic function $x(t)$ with a frequency $\omega(a)$ in terms of functions with frequencies ω_0 and multiples thereof ($3\omega_0$, etc.). The improved perturbative method proposed by Lindstedt and developed by Poincaré allows for an amplitude-dependent frequency ω that is expanded as a series[12]

$$\omega = \omega_0 + g\omega_1 + g^2\omega_2 + \cdots \quad \text{along with} \quad x = x_0 + gx_1 + \cdots \tag{7.56}$$

The unperturbed frequency ω_0 is the first approximation. To ensure that x inherits this new frequency, we define a rescaled time variable $\tau = \omega t$ and regard $x = x(\tau)$.

To determine the $x_n(\tau)$ we will as before insert (7.56) into (7.39) and compare coefficients of g^n. But this time, we will try to use the freedom to pick ω_n to ensure that the coefficients of resonant driving terms ($\propto \cos\omega t$) vanish so that secular terms are eliminated. To begin with, changing variables to τ, (7.39) becomes

$$\omega^2 \frac{d^2x}{d\tau^2} + \omega_0^2 x(\tau) = -gx^3(\tau) \quad \text{with} \quad x(0) = a \quad \text{and} \quad \dot{x}(0) = 0. \tag{7.57}$$

Dots denote τ derivatives. Inserting (7.56) in this, we get the sequence of equations:

$$\begin{aligned}
\omega_0^2(\ddot{x}_0 + x_0) &= 0, \\
\omega_0^2(\ddot{x}_1 + x_1) &= -x_0^3 + 2\omega_0\omega_1 x_0, \\
\omega_0^2(\ddot{x}_2 + x_2) &= -3x_0^2 x_1 - 2\omega_0\omega_1\ddot{x}_1 - (\omega_1^2 + 2\omega_0\omega_2)\ddot{x}_0 \\
&= -3x_0^2 x_1 + (2\omega_0\omega_2 - 3\omega_1^2)x_0 + \frac{2\omega_1}{\omega_0}x_0^3 + 2\omega_0\omega_1 x_1, \quad \text{etc.}
\end{aligned} \tag{7.58}$$

At order g^0 we have $x_0(\tau) = a\cos\tau$. The remaining equations are of driven oscillators with natural frequency 1 (in units of ω) subject to vanishing initial conditions

---

[12] For those familiar with quantum mechanical perturbation theory, the need to expand both ω and x should come as no surprise. For a system with Hamiltonian $H_0 + gH_1$, we expand both the wave function ψ (which plays the role of x) *and* the energy eigenvalues E in powers of the coupling g. Up to a factor of $\hbar$, E plays the role of the classical frequency ω.

$x_n(0) = \dot{x}_n(0) = 0$. For instance, at order g we have

$$\omega_0^2(\ddot{x}_1 + x_1) = -\frac{a^3}{4}(3\cos\tau + \cos 3\tau) + 2\omega_0\omega_1 a\cos\tau. \tag{7.59}$$

Requiring the coefficient of the resonant term $\cos\tau$ to vanish, we get $\omega_1 = 3a^2/8\omega_0$. The resulting resonance-free equation $\ddot{x}_1 + x_1 = -(a^3/4\omega_0^2)\cos 3\tau$, has the solution[13]

$$x_1 = -\frac{a^3}{32\omega_0^2}(\cos\tau - \cos 3\tau), \tag{7.60}$$

which has been cured of secular terms! Thus, to order g, the Lindstedt-Poincaré solution for oscillations with amplitude a starting at the turning point $x = a$ is

$$x(t) = a\cos\omega t - \frac{ga^3}{32\omega_0^2}(\cos\omega t - \cos 3\omega t) + \cdots \quad \text{where} \quad \omega = \omega_0 + \frac{3a^2 g}{8\omega_0} + \cdots \tag{7.61}$$

As anticipated, ω has acquired a dependence on a. The corresponding period is

$$T = \frac{2\pi}{\omega} \approx \frac{2\pi}{\omega_0}\left(1 - \frac{3ga^2}{8\omega_0^2}\right). \tag{7.62}$$

Remarkably, this agrees with the time period (7.51) obtained by expanding the exact expression (7.47) to leading order in g (the amplitude a was previously denoted x_+).

7.6 Problems

1. **Arc length of an ellipse.** Consider the ellipse $x^2/a^2 + y^2/b^2 = 1$ in parametric form $x = a\cos\theta$ and $y = b\sin\theta$ with $a \le b$ for definiteness. The line element along the circumference is $ds = \sqrt{dx^2 + dy^2}$. Show that the arc length of the portion of the ellipse between angles $0 \le \theta \le \phi$ is given by

$$\ell(0 \le \theta \le \phi) = b\int_0^\phi [1 - (1 - a^2/b^2)\sin^2\theta]^{1/2}\, d\theta. \tag{7.63}$$

   For $a \ne b$ this cannot be reduced to a trigonometric integral. It is an incomplete elliptic integral of the 2nd kind. It becomes a complete elliptic integral when $\phi = 2\pi$ and we get the perimeter of the ellipse. It is customary to denote $1 - a^2/b^2 = k^2$. Use an appropriate substitution to write the arc length in algebraic or Legendre normal form $\ell(0 \le \theta \le \phi) = b\int_0^{\sin\phi}\sqrt{(1 - k^2 s^2)/(1 - s^2)}\, ds$.

2. **Pendulum time period.** Show that the time period (7.11) of libration of the simple pendulum diverges logarithmically as $E \to 2mg\ell$ from below:

$$T(\epsilon) \to -\frac{2}{\omega}\log[2 - \epsilon] \quad \text{as} \quad \epsilon = \frac{E}{mg\ell} \to 2^-. \tag{7.64}$$

---

[13] The solution of the homogeneous equation is $\propto \cos\tau$ while a particular solution is obtained by considering the ansatz $b\cos 3\tau$ which has the same time-dependence as the driving force.

Hint: In (7.11), focus on the contribution from the vicinity of the upper limit of integration $\theta_{\max} = |\arccos(1-\epsilon)|$. Put $\delta = 2-\epsilon$, which is small and show that $\arccos(1-\delta) \approx \sqrt{2\delta}$. In the integrand, change variables to $x = \pi - \theta$ and show that $\cos\theta \approx -1 + x^2/2$ for small x. Keep only the dominant term in the integrand as $\epsilon \to 2^-$ and evaluate at the upper limit to get the advertised result. The rest of the integral gives finite contributions as $\epsilon \to 2^-$.

3. To illustrate the use of series expansions for **elliptic integrals**, let us find a 'low energy' expansion for the period of a simple pendulum with a bob of mass m suspended from a rigid rod of length ℓ from a fixed pivot and free to oscillate in a plane under Earth's gravitational acceleration g. Suppose the potential energy is chosen to vanish when the bob is at its lowest position. For low energies $E \gtrsim 0$, $\epsilon = E/mg\ell \gtrsim 0$ and $k = \sqrt{\epsilon/2} \gtrsim 0$. We wish to find a power series for the period of oscillation $T(k)$. Define the complete elliptic integral of the first kind by

$$K(k) = \int_0^1 [(1-s^2)(1-k^2s^2)]^{-1/2} ds \quad \text{for} \quad 0 \le k < 1. \tag{7.65}$$

(a) Show that the period of libration for $E < 2mg\ell$ is $T(k) = (4/\omega)K(k)$. (b) Obtain an expansion in powers of the elliptic modulus:

$$K(k) = \sum\nolimits_{n=0}^{\infty} \frac{1\cdot 3\cdot 5\cdots(2n-1)\, k^{2n}}{2^n\, n!} I_n \quad \text{where} \quad I_n = \int_0^1 \frac{s^{2n}\, ds}{\sqrt{1-s^2}}. \tag{7.66}$$

(c) Use the 'standard' definite integral

$$\int_0^{\pi/2} \sin^{2n}\theta\, d\theta = \sqrt{\pi}\Gamma(n+1/2)/2\Gamma(n+1) \tag{7.67}$$

and Gamma function properties $[\Gamma(\frac{1}{2}) = \sqrt{\pi}$ and $\Gamma(n+1) = n\Gamma(n)]$ to show that

$$I_n = \frac{\pi}{2}\, \frac{1\cdot 3\cdot 5\cdots(2n-1)}{2^n\, n!}. \tag{7.68}$$

(d) Obtain the following series expansion for the period of a pendulum

$$T(k) = 2\pi\sqrt{\ell/g}\left[1+\left(\frac{1}{2}\right)^2 k^2+\left(\frac{1\cdot 3}{2\cdot 4}\right)^2 k^4+\cdots+\left(\frac{(2n-1)!!}{(2n)!!}\right)^2 k^{2n}+\cdots\right]. \tag{7.69}$$

For small oscillations $(k \to 0)$ it reduces to $T = 2\pi\sqrt{\ell/g}$. Here, $n!! = n(n-2)\cdots$ is the product of all positive integers $\le n$ with the same parity as n. (e) Use the ratio test to argue that this series is absolutely convergent for $|k| < 1$.

∗4. The **Weierstrass elliptic function** $\wp(z)$ may be defined in terms of the Jacobi elliptic functions by $\wp(z) = e_2 + (e_1 - e_3)\,\mathrm{dn}^2(u,k)/\,\mathrm{sn}^2(u,k)$ where $u = z\sqrt{e_1 - e_3}$ and $k = \sqrt{(e_2 - e_3)/(e_1 - e_3)}$. Here e_1, e_2, e_3 are three constants that are assumed to add up to zero: $e_1 + e_2 + e_3 = 0$. (a) Show that $\wp(z)$ satisfies the Weierstrass differential equation $\wp'(z)^2 = 4(\wp(z) - e_1)(\wp(z) - e_2)(\wp(z) - e_3)$. Evidently, $e_{1,2,3}$ are the roots of the 'depressed' cubic polynomial on the RHS. (b) Show that $\wp'(z)^2 = 4\wp^3(z) - g_2\wp(z) - g_3$ where $g_1 = e_1 + e_2 + e_3 = 0$, $g_2 = -4(e_1e_2 + e_2e_3 + e_3e_1)$ and $g_3 = 4e_1e_2e_3$. (c) The modular discriminant of the cubic is defined as $\Delta = g_2^3 - 27g_3^2$. Show that $\Delta = 16[(e_1-e_2)(e_2-e_3)(e_3-e_1)]^2$ assuming $g_1 = 0$, so that Δ vanishes iff a pair of roots coincide.

5. Show that the time period (7.32) for **rotational motion** of a **simple pendulum** can be expressed in terms of the complete elliptic integral of the first kind:

$$T_{\text{rot}} = \frac{1}{\omega}\int_0^{2\pi} \frac{d\theta}{\sqrt{2\,(\epsilon - (1-\cos\theta))}} = \frac{2}{\omega}\kappa\, K(\kappa) \quad \text{where} \quad \kappa = \frac{1}{k} = \sqrt{\frac{2}{\epsilon}}. \qquad (7.70)$$

   Hint: Use the first formula in (7.25) for K and the substitution $t = \sin(\theta/2)$.

6. **Time period vs energy.** Consider the Kepler problem and the $-V_0\,\text{sech}^2(x/l)$ potential and the associated oscillation time periods $T(E)$. Which has a wider potential? By physical reasoning say for which potential $T(E)$ diverges faster as $E \to 0^-$. Omitting constants, recall the asymptotic functional form of $T(E)$ as a function of E for the three potentials Kepler, sech^2 and simple pendulum, as E approaches the borderline from bound/librational to scattering/rotational motion. Does the period of the pendulum diverge slower/faster than the other two?

7. Verify that at the transition from libration to rotation ($E = 2mg\ell$ or $\epsilon = 2$), the 'infinite period' **separatrix trajectories of the pendulum** may be obtained from the integrals $t = \pm(1/2\omega)\int_0^\theta \sec(\phi/2)d\phi$. Show that $\theta(t) = \pm 2\arcsin(\tanh(\omega t))$. Plot these solutions on the phase space, give the direction of motion and say where the bob spends a majority of its time. What is the other solution with this energy?

$*$8. **Isochrone problem.** We have observed that oscillations of a simple pendulum are not isochronous except in the small angle approximation. Huygens (1659) discovered that the time period of oscillations of a cycloidal pendulum [bob moving subject to gravity on a cycloid in a vertical plane (see Prob. 3.19) instead of a circle] is independent of amplitude. Show that this is indeed the case and establish that the time period is $4\pi\sqrt{R/g}$ where R is the radius of the circle that generates the cycloid and g is the acceleration due to gravity.

9. **Separatrices.** Consider a particle of mass m moving along the real line subject to the potential $V(x) = g(x^2 - a^2)^2$ with $g, a > 0$. (a) Give the algebraic equation (in terms of p and x) for the separatrices that divide the phase space between trajectories that are restricted to a single well from those that explore both wells. Specify the energy on the separatrices and draw a figure of the separatrices on the phase plane. (b) Find expressions (in x) for the possible slopes dp/dx of the separatrices. (c) Find the slopes dp/dx of the separatrices at the origin of phase space ($x = p = 0$) in terms of a, m, g. Check that the slope has the correct dimension. (d) Does the separatrix have a discontinuous slope at the origin or not?

10. Consider a particle of mass m moving on the x-y plane subject to the **quartic potential** $V = gx^2y^2$ for $g > 0$. The pair of straight lines $xy = 0$ are called **spikes**. Find Hamilton's and Lagrange's equations associated to $H = (1/2m)(p_x^2 + p_y^2) + gx^2y^2$. Find simple initial conditions for which the particle can escape to infinity along a spike. Plot the potential over the x-y plane. For a given energy $H = E$, sketch the part of the plane ('Hill' region) to which trajectories must be confined.

Chapter 8

Rigid body mechanics

A rigid[1] body is a system of particles such that the distances between any pair is fixed[2]. For instance, we could have four mass points m_a for $a = 1, 2, 3, 4$ arranged at the vertices of a regular tetrahedron and pairwise connected by rigid rods of negligible mass as shown in Fig. 8.1a. A continuous distribution of mass is also possible, as in a stone (see Fig. 8.1b). In this case, the discrete index a is replaced with the continuous location 'index' $\boldsymbol{r}$ and the masses of individual particles are replaced by the mass $dm(\boldsymbol{r}) = \rho(\boldsymbol{r})dV$ in any elemental volume dV around $\boldsymbol{r}$ where $\rho(\boldsymbol{r})$ is the local mass density. Many commonly encountered objects can be treated as rigid bodies. Examples include a point mass, a dumbbell, a plate, a cricket or golf ball, a boomerang, a top, a gyroscope, an asteroid and a spaceship. The concept is useful in quantum physics as well; e.g., the rotational energy levels (as opposed to the vibrational spectrum) of a molecule can be approximately understood by treating it as a rigid body.

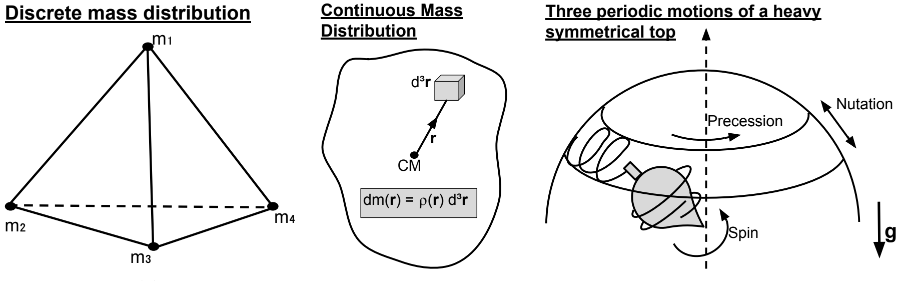
Discrete mass distribution
m1
m2
m3
m4
Continuous Mass Distribution
d³r
r
CM
dm(r) = ρ(r) d³r
Three periodic motions of a heavy symmetrical top
Nutation
Precession
Spin
g

(a) (b) (c)

Figure 8.1: (a) Tetrahedral rigid body (b) Continuous mass distribution in a rock (c) Spinning, precession and nutation (wobble or swaying) of a top in a gravitational field. The locus of the tip of the top is shown on a fictitious spherical surface.

Rigid body motion can range from simple to intricate. For instance, in the absence of external forces, the most general motion of a uniform solid sphere is a combination of steady spinning about an axis through its center while the center itself moves in a straight line. On the other hand, a (Lagrange) top with the lower end of its symmetry axis held fixed at a point on the ground in the uniform gravitational field of the Earth (as in Fig. 8.1c) executes a motion which involves spinning on its own axis, precession about a vertical axis parallel to the gravitational field and a wobble of the axis of spinning, called nutation (see Fig. Sect. 8.15). The three periodic motions have their own periods which, if incommensurate[3], prevent the top from returning to its initial orientation under time evolution. An anisotropic top (one that is not axisymmetric) with one point held fixed and subject to a uniform gravitational field typically displays chaotic motion although there are special cases where the dynamics is regular/integrable[4].

---

[1] The word *rigid* is used to distinguish a rigid body from a *deformable* body such as a stretched string, elastic solid or fluid (see Chap. 16). Indeed, the complexity of rigid body dynamics lies between that of a point particle and that of a deformable body.

[2] These are examples of holonomic constraints, see Footnote 30 of Sect. 3.5.

The motion of rigid bodies can also display interesting instabilities. For instance, consider a chalkboard duster, which is a cuboid having roughly uniform mass distribution with no two edges having equal lengths. It has 3 so-called principal axes passing through its center of mass and parallel to the edges. In the absence of significant external forces, it turns out that while the duster can be stably spun about the axes parallel to the longest and shortest edges, rotation about the 'middle' axis cannot be stably sustained, as we will learn in Sect. 8.12.

A rigid body is an elegant system to illustrate many of the principles and methods of mechanics that we have encountered. In fact, we will discuss the equations of rigid body motion from the Newtonian, Lagrangian, Hamiltonian and Poisson bracket formulations. Symmetries of the mass distribution of a rigid body will be exploited to simplify the equations of motion where possible. What is more, Euler suggested that it would help to use Galilean invariance of Newton's equations to transform from the lab frame to an inertial frame that moves (at the instant considered) with the center of mass of the rigid body. On the other hand, a rigid body also illustrates how the form of the equations change when going to a noninertial frame, here one that rotates with the body. This is again something that Euler understood and used to derive his celebrated equations for rigid body dynamics in a corotating frame (see Sect. 8.11).

We end this introduction with some (slightly advanced) remarks on practical and theoretical applications of rigid body dynamics. Gyroscopes furnish a practical application of the principles underlying rotational motion of a rigid body. A gyroscope is usually a disk-shaped rigid body (spheres are also used) which is free to spin in its plane about an axis through its center. The construction is such that when spinning, the orientation of this axis is unaltered even when the frame of the gyroscope is rotated. Furthermore, in the absence of external torques, the angular momentum of the gyroscope is conserved, whence the spin axis is fixed relative to an inertial frame even when the gyroscope is carried around. Thus, as long as external torques are negligible, the axis of a spinning gyroscope can be used to keep track of an initial reference direction during navigation on the Earth. Gyroscopes have also been used to look for subtle general relativistic effects. By measuring the change [relative to a distant guide star] in the spin axis (precession) of 4 gyroscopes, the Gravity Probe B experiment (2011) [housed in a polar Earth orbiting satellite] was used to check the geodetic and frame-dragging effects predicted by general relativity.

---

[3] Suppose T_p, T_s and T_n are the time periods of precession, spinning and nutation. They are said to be commensurate if the ratio of any pair of these is a rational number. This would imply that they have a least common integer multiple T_r after which time the top returns to its initial orientation. The periods are incommensurate if they are not commensurate.

[4] If the fixed point is the center of mass, then gravity imparts no torque and one gets the solvable quasiperiodic dynamics of an Euler-Poinsot top (1758) (see Sect. 8.13*). If the fixed point lies on the symmetry axis of a heavy symmetric top (the Lagrange top (1788) of Sect. 8.15), then again the dynamics is integrable. Sofya Kovalevskaya (1889) found a 3^{rd} case of integrable heavy top dynamics where two of the principal moments of inertia about the fixed point are equal to twice the third and the center of mass lies on the plane spanned by the first two principal axes of inertia.

Rotational dynamics of a rigid body gives us an example of a system whose configuration space is different from Euclidean space. In fact, it is the group $SO(3)$ of rotations of 3d Euclidean space. Euler's equations of rigid body dynamics can be fruitfully generalized to other groups, such as the one that appears in the incompressible flow of a dissipationless fluid (the group of diffeomorphisms of the fluid domain). Perhaps it is no coincidence that the equations of a rigid body and those of an inviscid and incompressible fluid are both due to Euler. Another generalization is to 'internal' groups of symmetries that arise in the physics of condensed matter, subatomic particles and strings; the corresponding dynamical systems are called nonlinear sigma models.

8.1 Lab and comoving frames

The motion of points in the rigid body may be described using the lab ('inertial', 'space' or 'fixed') frame. We will use a system of Cartesian coordinates X, Y, Z for the lab frame. The position vector of the point in the body labelled a, relative to the origin of the lab frame, is called $\mathscr{r}_a$ (see Fig. 8.2). The components of $\mathscr{r}_a$ relative to the lab axes are $\mathscr{r}_a = (X_a, Y_a, Z_a)$. The lab frame coordinates $X_a(t), Y_a(t), Z_a(t)$ of a point in the body, in general, change as the body moves. The center of mass (CM) of the body is the point $\boldsymbol{R} = (\bar{X}, \bar{Y}, \bar{Z})$ whose coordinates are

$$\bar{X} = \frac{1}{M}\sum\nolimits_a m_a X_a, \quad \bar{Y} = \frac{1}{M}\sum\nolimits_a m_a Y_a, \quad \bar{Z} = \frac{1}{M}\sum\nolimits_a m_a Z_a. \tag{8.1}$$

The sum on a is over all the mass points that make up the body of total mass $M = \sum_a m_a$. The CM is a distinguished point associated to a rigid body (however, it need not be inside the body, see Prob. 8.1). Thus, it is convenient to consider the location of a mass point labelled a, relative to the center of mass. The corresponding position vector relative to the CM is called $\boldsymbol{r}_a$. The components of $\boldsymbol{r}_a$ relative to the lab axes, in general, change with time. The position vector of the center of mass, relative to the center of mass is obviously the zero vector: $(1/M)\sum_a m_a \boldsymbol{r}_a = 0$.

We may also use a moving system of Cartesian coordinates $r_1 = x, r_2 = y, r_3 = z$ referred to the so-called comoving (or body-fixed or corotating) frame whose axes are rigidly fixed in the body and participate in its motion. The origin O of the comoving frame is most conveniently chosen to lie at the center of mass of the body, so $\sum_a m_a x_a = \sum_a m_a y_a = \sum_a m_a z_a = 0$. The comoving frame components (x_a, y_a, z_a) of a point $\boldsymbol{r}_a$ in the body are independent of time.

8.2 Configuration space and degrees of freedom

A point mass moving in 3d space has three degrees of freedom, its configuration space is 3d Euclidean space $\mathbb{R}^3$. If a rigid body is concentrated along a line (e.g., a pair of mass points connected by a slender rod of zero thickness or a straight wire or pen of negligible thickness) it is called a *rigid rotator*. A rigid rotator has three translational degrees of freedom, which may be regarded as specifying the location of the CM. Once the location of the CM has been fixed, the orientation of the pen is determined by the point on a unit sphere[5] (centered at the CM), at which the ray from the CM to the nib intersects it. Thus, a rigid rotator has five degrees of freedom and configuration space $\mathbb{R}^3 \times S^2$.

A noncollinear rigid body has six degrees of freedom[6]. We need three coordinates to locate the position of the CM. We are then free to rotate the rigid body about its center of mass in any manner. The orientation of the comoving frame relative to the lab frame is determined by such a rotation of 3d space. A rotation is determined by an axis (which can be taken as a unit vector) and an angle of rotation. We need two angles to define an axis and one to specify the angle of rotation. So rotations are a three-parameter family. Thus, a noncollinear rigid body has three translational and three rotational degrees of freedom. Moreover, rotations may be composed and inverted; they form the group of 3×3 special orthogonal matrices[7]. Thus, the configuration space of a noncollinear rigid body is $\mathbb{R}^3 \times SO(3)$.

$*$ **Remark.** Though we can specify a finite rotation by a vector (along the axis of rotation with length equal to the angle of rotation), the composition of rotations does not correspond to addition of these vectors, since rotations generally do not commute. The composition of rotations is modeled by multiplication of special orthogonal matrices. On the other hand, the composition of infinitesimal rotations is commutative to leading order and we will be able to represent the composition of infinitesimal rotations by vector addition. This is why we will soon be able to express angular velocity (which results from an infinitesimal rotation) as a vector. □

8.3 Infinitesimal displacement and angular velocity of rigid body

We begin our study of rigid body motion with the kinematical concepts of translational and angular velocities. An infinitesimal displacement of the body is expressible as a sum of an infinitesimal translation of the CM (O) to its final location (keeping the orientation of the body & comoving frame fixed) and an infinitesimal rotation (keeping the CM fixed) that orients the body (and comoving frame) appropriately. Moreover, any infinitesimal rotation about O is a rotation about some axis through O.

---

[5] The unit 2-sphere is defined as $S^2 = \{(x, y, z) \in \mathbb{R}^3 \text{ such that } x^2 + y^2 + z^2 = 1\}$.

[6] For example, a flat circular disk with a uniform mass distribution has 6 degrees of freedom: 3 translational, two to orient the symmetry axis and one corresponding to rotations about the axis. Though rotations about this axis are a symmetry of the mass distribution, the angular orientation about the axis *is* a degree of freedom. This is because the particles that make up the disk are classically distinguishable though they may be identical. More concretely, we could mark a point along the rim (without significantly altering the mass distribution) to keep track of the azimuthal orientation of the disk. Moreover, unlike rotations about the axis of a collinear rigid body, rotations of the disk about this axis have an associated rotational kinetic energy.

[7] The group $SO(3)$ of special orthogonal matrices consists of 3×3 real matrices R with $R^t R = RR^t = I$ and $\det R = 1$. Such matrices rotate vectors $\boldsymbol{x} \to R\boldsymbol{x}$. The first condition which involves the transpose, ensures preservation of length while the second excludes 'improper rotations' (which involve reflections in an essential way - for example the composition of a reflection in the xy plane followed by a reflection in the xz plane is in fact a rotation by π in the yz plane). Composition of rotations is given by matrix multiplication and in particular, the composition of two reflections (each with determinant -1) is a proper rotation. See also Prob. 3.24.

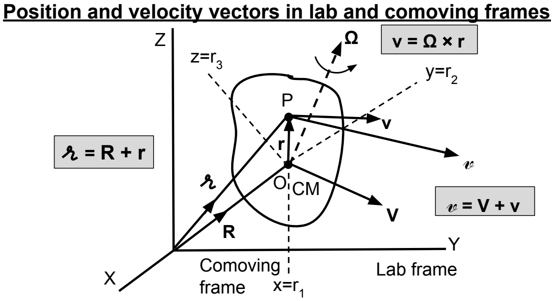

Figure 8.2: Position and velocity vectors of a marked point P in a rigid body with respect to the lab frame. The comoving frame is also indicated.

Let us denote by $\boldsymbol{\mathscr{r}}$ the position vector of a point P in the rigid body, relative to the origin of the lab frame (see Fig. 8.2). Suppose the same point has the position vector $\boldsymbol{r}$ relative to the CM. Then $\boldsymbol{\mathscr{r}} = \boldsymbol{R} + \boldsymbol{r}$ where $\boldsymbol{R}$ is the position vector of the CM relative to the origin of the lab frame. We will regard each of these three vectors as given by their components with respect to the lab axes.

Now, a small displacement $\delta\boldsymbol{\mathscr{r}}$ of P may be written as

$$\delta\boldsymbol{\mathscr{r}} = \delta\boldsymbol{R} + \delta\boldsymbol{\phi} \times \boldsymbol{r}. \tag{8.2}$$

Here, $\delta\boldsymbol{R}$ is the displacement of the CM. On the other hand, $\delta\boldsymbol{\phi} \times \boldsymbol{r}$ is the infinitesimal change in the position vector $\boldsymbol{r}$ (relative to the lab frame) due to a counterclockwise rotation about the axis $\widehat{\delta\boldsymbol{\phi}}$ along the Euler vector[8] $\delta\boldsymbol{\phi}$ (passing through the CM) by an angle $\delta\phi = |\delta\boldsymbol{\phi}|$. To see why, we note that the change in $\boldsymbol{r}$ under an infinitesimal counterclockwise rotation by angle $\delta\phi$ about $\delta\boldsymbol{\phi}$ is in magnitude

$$|\delta\boldsymbol{r}| = |\boldsymbol{r}|\, \sin\theta\, |\delta\boldsymbol{\phi}|, \tag{8.3}$$

where θ is the angle between $\delta\boldsymbol{\phi}$ and $\boldsymbol{r}$. For an infinitesimal rotation, $\delta\boldsymbol{r}$ is perpendicular to both $\boldsymbol{r}$ and $\delta\boldsymbol{\phi}$, as indicated in Fig. 3.7. Thus, $\delta\boldsymbol{r} = \delta\boldsymbol{\phi} \times \boldsymbol{r}$.

Example: Suppose we make a rotation by a small counterclockwise angle $\epsilon \ll 1$ about the $\hat{z}$ axis. This is encoded in the Euler vector $\delta\boldsymbol{\phi} = \epsilon\hat{z}$. The vector $\boldsymbol{r} = \hat{x}$ is transformed to $\boldsymbol{r}' \approx \boldsymbol{r} + \epsilon\hat{z} \times \hat{x} = \hat{x} + \epsilon\hat{y} = (1, \epsilon, 0)$. Notice that $|\boldsymbol{r}'| = \sqrt{1+\epsilon^2} = 1 + \mathcal{O}(\epsilon^2)$. We see that $\boldsymbol{r}'$ has the same length as $\boldsymbol{r}$ and lies in the first quadrant of the x-y plane, corresponding to a counterclockwise rotation by angle ϵ. In fact, $\delta\boldsymbol{r}$ is linearly related to $\boldsymbol{r}$ via an infinitesimal antisymmetric $\mathfrak{so}(3)$ matrix $u = \left(\begin{smallmatrix} 0 & -\epsilon & 0 \\ \epsilon & 0 & 0 \\ 0 & 0 & 0 \end{smallmatrix}\right)$: $\delta\boldsymbol{r} = \left(\begin{smallmatrix} 0 \\ \epsilon \\ 0 \end{smallmatrix}\right) = u \left(\begin{smallmatrix} 1 \\ 0 \\ 0 \end{smallmatrix}\right)$. Thus, we may also write $\boldsymbol{r}' = R\boldsymbol{r}$ where $R = I + u$ is the $SO(3)$ rotation matrix $\begin{pmatrix} \cos\epsilon & -\sin\epsilon & 0 \\ \sin\epsilon & \cos\epsilon & 0 \\ 0 & 0 & 1 \end{pmatrix}$ truncated to linear order in $\epsilon \ll 1$. See Prob. 8.14 for an explanation of the symbols $SO(3)$ and $\mathfrak{so}(3)$. □

---

[8] The Euler vector $\delta\boldsymbol{\phi}$ points along the axis of rotation (which is taken to be a unit vector) and has magnitude equal to the angle of rotation.

Dividing (8.2) by the time δt in which the infinitesimal motion took place,

$$\frac{\delta \mathpzc{r}}{\delta t} = \frac{\delta \boldsymbol{R}}{\delta t} + \frac{\delta \boldsymbol{\phi}}{\delta t} \times \boldsymbol{r}. \tag{8.4}$$

Now we let $\delta t \to 0$. If we denote the velocity vector of P relative to the origin of the lab frame by $\mathpzc{v} = d\mathpzc{r}/dt$, the translational velocity of the CM by $\boldsymbol{V} = d\boldsymbol{R}/dt$ and the angular velocity by $\boldsymbol{\Omega} = \lim_{\delta t \to 0} \delta\boldsymbol{\phi}/\delta t$, then

$$\mathpzc{v} = \boldsymbol{V} + \boldsymbol{\Omega} \times \boldsymbol{r} \quad \text{or} \quad \mathpzc{v} = \boldsymbol{V} + \mathbf{v} \quad \text{where} \quad \mathbf{v} = \boldsymbol{\Omega} \times \boldsymbol{r}. \tag{8.5}$$

The angular velocity vector $\boldsymbol{\Omega}$ points along the axis of right-handed rotation $(\widehat{\delta\boldsymbol{\phi}})$ passing through the CM. For example, an upright top that is just spinning uniformly counterclockwise at one radian per second about its symmetry axis has a constant $\boldsymbol{\Omega} = \hat{z}$. The angular velocity may of course change with time both in direction and magnitude. See Fig. 8.4 and Fig. 8.5 for examples of rotating rigid bodies and their angular velocity vectors.

$*$ **Change of origin.** How do the translational and angular velocities change if we shift the origin of the comoving frame to a point O$'$ different from the CM (O). Suppose O$'$ = O + $\boldsymbol{b}$. Then the position vector of P relative to O$'$ is $\boldsymbol{r}' = \boldsymbol{r} - \boldsymbol{b}$. Suppose further that $\boldsymbol{V}'$ and $\boldsymbol{\Omega}'$ are the translational and angular velocities of the rigid body relative to O$'$. Then the velocity $\mathpzc{v}$ of P is given by two equivalent expressions valid for any $\boldsymbol{r}$ in the body:

$$\mathpzc{v} = \boldsymbol{V} + \boldsymbol{\Omega} \times \boldsymbol{r} \quad \text{and} \quad \mathpzc{v} = \boldsymbol{V}' + \boldsymbol{\Omega}' \times \boldsymbol{r}' = \boldsymbol{V}' + \boldsymbol{\Omega}' \times (\boldsymbol{r} - \boldsymbol{b}), \tag{8.6}$$

We infer that $\boldsymbol{V}' = \boldsymbol{V} + \boldsymbol{\Omega} \times \boldsymbol{b}$ and $\boldsymbol{\Omega}' = \boldsymbol{\Omega}$. Although the translational velocity depends on the choice of origin, the angular velocity does not. We will find it useful to place the origin at the CM to simplify upcoming formulae for the kinetic energy and angular momentum of a rigid body by exploiting the identity $\sum m_a \boldsymbol{r}_a = 0$. □

More generally, for each mass point m_a in the rigid body, we denote by $\boldsymbol{r}_a$ its position vector relative to the CM,

$$\begin{aligned} \mathpzc{r}_a &= \boldsymbol{R} + \boldsymbol{r}_a, \quad \text{and differentiating in time,} \quad \mathpzc{v}_a = \boldsymbol{V} + \mathbf{v}_a \\ \text{where} \quad \boldsymbol{V} &= \dot{\boldsymbol{R}} \quad \text{and} \quad \mathbf{v}_a = \dot{\boldsymbol{r}}_a = \boldsymbol{\Omega} \times \boldsymbol{r}_a. \end{aligned} \tag{8.7}$$

Here, $\mathbf{v}_a = \dot{\boldsymbol{r}}_a$ is the velocity relative to the CM. Multiplying $\mathpzc{v}_a$ by the mass m_a, we get the momentum of the a^{th} particle relative to the lab frame:

$$\not{\mathpzc{p}}_a = m_a \boldsymbol{V} + \boldsymbol{p}_a \quad \text{where} \quad \boldsymbol{p}_a = m_a \mathbf{v}_a = m_a \boldsymbol{\Omega} \times \boldsymbol{r}_a. \tag{8.8}$$

The vector sum of all the momenta in the lab frame coincides with the center of mass momentum

$$\boldsymbol{P} = \sum\nolimits_a \not{\mathpzc{p}}_a = M\boldsymbol{V} + \boldsymbol{\Omega} \times \cancel{\sum\nolimits_a m_a \boldsymbol{r}_a} = M\boldsymbol{V}. \tag{8.9}$$

The sum vanishes as $\boldsymbol{r}_a$ are defined relative the the CM. The coordinates and momenta $(\mathpzc{r}_a, \not{\mathpzc{p}}_a)$ of all the particles in the body together specify the instantaneous state of the rigid body. To understand its dynamics, we examine its Lagrangian.

8.4 Kinetic energy and inertia tensor

Here, we wish to express the kinetic energy T of a rigid body in terms of its CM velocity $\boldsymbol{V}$ and angular velocity $\boldsymbol{\Omega}$. In doing so, we will discover a 3×3 matrix called the inertia tensor associated to the mass distribution of a rigid body. The inertia tensor plays a role in the rotational motion of a rigid body similar to that played by the total mass M in its translational motion. In fact, in the absence of external forces, the motion of a rigid body depends on its mass distribution only through the total mass and the inertia tensor (especially its eigenvalues, which are called the principal moments of inertia); the remaining details do not matter! In fact, in Sect. 8.5, we will classify rigid bodies based on the eigenvalues of their inertia tensors. Subsequently, we will deduce qualitative and quantitative features of rigid body motion based on the pattern of values of the principal moments of inertia (i.e., whether any vanish and possible degeneracies among the eigenvalues).

The kinetic energy T of a rigid body is a sum of free particle energies of each constituent mass point, whose velocity vector is $\boldsymbol{\mathscr{v}}_a$ relative to the lab frame. So

$$T = \sum\nolimits_a \frac{1}{2} m_a \boldsymbol{\mathscr{v}}_a^2 \equiv \sum \frac{1}{2} m \boldsymbol{\mathscr{v}}^2. \tag{8.10}$$

We will often suppress the index a labelling points. It appears on $\boldsymbol{r}$ and $\boldsymbol{\mathscr{v}}$ but not on $\boldsymbol{\Omega}$ or $\boldsymbol{V}$, which are properties of the body as a whole. Thus,

$$\begin{aligned} T &= \sum \frac{m}{2} (\boldsymbol{V} + \boldsymbol{\Omega} \times \boldsymbol{r})^2 = \sum \frac{m}{2} \boldsymbol{V}^2 + \sum m \boldsymbol{V} \cdot \boldsymbol{\Omega} \times \boldsymbol{r} + \sum \frac{m}{2} (\boldsymbol{\Omega} \times \boldsymbol{r})^2 \\ &= \frac{1}{2} M \boldsymbol{V}^2 + \boldsymbol{V} \cdot (\boldsymbol{\Omega} \times \cancel{\sum m \boldsymbol{r}}) + \frac{1}{2} \sum m \left[\Omega^2 r^2 - (\boldsymbol{\Omega} \cdot \boldsymbol{r})^2 \right]. \end{aligned} \tag{8.11}$$

Above, Ω, r are the magnitudes of $\boldsymbol{\Omega}, \boldsymbol{r}$. Thus, T may be written as a sum of the translational kinetic energy of a body of mass M located at the CM and the rotational kinetic energy $T_{\rm rot}$ about the CM:

$$T = \frac{1}{2} M \boldsymbol{V}^2 + \frac{1}{2} \Omega_i \Omega_j \sum m \left(r^2 \delta_{ij} - r_i r_j \right) = \frac{1}{2} M \boldsymbol{V}^2 + \frac{1}{2} \mathcal{I}_{ij} \Omega_i \Omega_j. \tag{8.12}$$

Inertia tensor. $T_{\rm rot}$ involves a 3×3 matrix called the inertia tensor, with components

$$\mathcal{I}_{ij} = \sum\nolimits_a m_a \left(r_a^2 \delta_{ij} - (r_a)_i (r_a)_j \right) \quad \text{or} \quad \mathcal{I}_{ij} = \iiint \rho(\boldsymbol{r}) \, \left(r^2 \delta_{ij} - r_i r_j \right) \, d^3\boldsymbol{r}. \tag{8.13}$$

The second formula applies to a rigid body with mass density ρ. It reduces to that for a system of point masses located at $\boldsymbol{r}_a$ if we take $\rho(\boldsymbol{r}) = \sum_a m_a \delta^3(\boldsymbol{r} - \boldsymbol{r}_a)$, where $\delta^3(\cdots)$ is the 3d Dirac delta function (see Appendix A.11*). The components of the inertia tensor are independent of time if $(r_a)_i$ are the components with respect to the comoving frame. The matrix $\mathcal{I}_{ij}$ is an intrinsic property of the mass distribution of the rigid body, the chosen origin and axes of the comoving frame. If instead, we use the components of $\boldsymbol{r}_a$ relative to the lab frame, then $\mathcal{I}_{ij}$ can be time-dependent.

The inertia matrix is a real and symmetric matrix $\mathcal{I}_{ij} = \mathcal{I}_{ji}$. It is a positive-semidefinite (or nonnegative) matrix in the sense that the associated quadratic form ('rotational kinetic energy') is manifestly nonnegative for any $\boldsymbol{\Omega}$:

$$T_{\rm rot} = \frac{1}{2}\mathcal{I}_{ij}\Omega_i\Omega_j = \frac{1}{2}\Omega^t\mathcal{I}\Omega = \sum\nolimits_a \frac{1}{2}m_a(\boldsymbol{\Omega}\times\boldsymbol{r}_a)^2 \geq 0. \tag{8.14}$$

The components of the inertia matrix with respect to the comoving frame are

$$\mathcal{I} = \sum_a \begin{pmatrix} m_a(y_a^2+z_a^2) & -m_a x_a y_a & -m_a x_a z_a \\ -m_a y_a x_a & m_a(z_a^2+x_a^2) & -m_a y_a z_a \\ -m_a z_a x_a & -m_a z_a y_a & m_a(x_a^2+y_a^2) \end{pmatrix}. \tag{8.15}$$

Evidently, it is the sum of inertia matrices of each mass point in the body. For a continuous mass distribution $\sum m(\cdots)$ is replaced with $\int \rho(\boldsymbol{r})(\cdots)\,dx\,dy\,dz$. The diagonal entries $\mathcal{I}_{11} = \sum m(y^2+z^2), \mathcal{I}_{22}$ and $\mathcal{I}_{33}$ are called the moments of inertia about the first, second and third axes of the comoving frame. In general, given any axis $\hat{\boldsymbol{n}}$, the moment of inertia about $\hat{\boldsymbol{n}}$ is defined as $\mathcal{I}_{\hat{\boldsymbol{n}}} = \sum_a m_a\rho_a^2$ where ρ_a is the perpendicular distance of point a from the axis. The parallel axis theorem [54] relates the moment of inertia about an axis through the CM to the moment of inertia about a parallel axis $\hat{\boldsymbol{p}}$: $\mathcal{I}_{\hat{\boldsymbol{p}}} = \mathcal{I}_{\rm cm} + Md^2$, where d is the distance between axes.

Being a real symmetric matrix, the inertia matrix may be diagonalized by an orthogonal transformation[9] S that rotates[10] the axes of the comoving frame: $S^{-1}\mathcal{I}S = D$. Here, D is the diagonal matrix of eigenvalues. As $\mathcal{I}$ is positive-semidefinite, the eigenvalues are nonnegative (see Prob. 8.2), they are called the principal moments of inertia, which we may order as $0 \leq \mathcal{I}_1 \leq \mathcal{I}_2 \leq \mathcal{I}_3$. The eigenvectors of the inertia matrix may be chosen orthonormal[11] and are called the principal axes of inertia. If the axes of the moving frame are chosen along the principal axes of inertia, then the inertia matrix is diagonal[12]

$$D = \sum_a \begin{pmatrix} m_a({y'}_a^2+{z'}_a^2) & 0 & 0 \\ 0 & m_a({z'}_a^2+{x'}_a^2) & 0 \\ 0 & 0 & m_a({x'}_a^2+{y'}_a^2) \end{pmatrix} = \begin{pmatrix} \mathcal{I}_1 & 0 & 0 \\ 0 & \mathcal{I}_2 & 0 \\ 0 & 0 & \mathcal{I}_3 \end{pmatrix}. \tag{8.16}$$

Here x'_a, y'_a, z'_a are the components of the position vector of a point in the body with respect to the principal axis frame. Note that the off-diagonal entries vanish due to cancellations $\sum_a m_a x'_a y'_a = 0$ although $m_a x'_a y'_a$ is, in general, nonzero for individual particles in the body. In the principal axis basis, the rotational kinetic energy is particularly simple:

---

[9] An orthogonal transformation is one that satisfies $SS^t = S^tS = \mathbf{1}$. The columns of S are the eigenvectors of $\mathcal{I}$ in the same order as that chosen for the eigenvalues that appear along the diagonal of D (see Appendix A). It is special orthogonal (i.e., a proper rotation) if $\det S = 1$.

[10] The comoving frame is orthonormal. Eigenvectors of $\mathcal{I}$ may also be chosen orthonormal. We simply rotate the comoving frame to make it point along the eigenvectors. If needed, we multiply some eigenvectors by -1 so that the eigenbasis has the same orientation as the rotated comoving frame. So no reflection is needed in the orthogonal transformation.

[11] Eigenvectors corresponding to distinct eigenvalues of a real symmetric matrix are orthogonal and can be normalized to have unit lengths [24]. If two eigenvalues coincide, the corresponding eigenvectors can be chosen as any two linearly independent vectors in the corresponding eigenplane; in particular, they can be chosen orthonormal.

[12] The principal moments of inertia satisfy a triangle inequality $\mathcal{I}_i + \mathcal{I}_j \geq \mathcal{I}_k$ where i, j, k are distinct indices taken from the set $\{1, 2, 3\}$. See Prob. 8.12.

$$T_{\text{rot}} = (1/2)\left(\mathcal{I}_1 \Omega_1^2 + \mathcal{I}_2 \Omega_2^2 + \mathcal{I}_3 \Omega_3^2\right). \tag{8.17}$$

8.5 Types of rigid bodies

As (8.17) shows, only the eigenvalues of the inertia tensor enter the formula for the rotational kinetic energy of a rigid body. Thus, in the absence of external forces, the pattern of eigenvalues of $\mathcal{I}$ determines the nature of the rotational motion. The remaining details of the mass distribution can play a role in the presence of external torques[13]. Thus, it is useful to classify rigid bodies based on their principal moments of inertia.

If the 3 principal moments of inertia are pairwise unequal, we call it an *anisotropic* rigid body. Most stones are anisotropic rigid bodies. If one pair coincide, it is called a *symmetrical top*[14], a uniform right circular cylinder is an example. For definiteness, if $\mathcal{I}_1 = \mathcal{I}_2$, then the corresponding two principal axes may be chosen to be any pair of linearly independent vectors in the corresponding x-y eigenplane. If all three eigenvalues coincide, it is called a *spherical top*. A solid spherical ball with uniform mass distribution is a simple example. The principal axes of inertia of a spherical top may be chosen as any three linearly independent vectors. Despite this freedom, we often pick the principal axes to form an orthonormal frame to simplify calculations.

Example: Uniform solid cube. Let us find the principal moments of inertia and principal axes of a uniform solid cube of side L and mass M. To make the determination of the inertia tensor simple, we choose coordinate axes that are parallel to the edges of the cube with origin at the center of the cube (see Fig. 8.3). Thus, the 6 corners of the cube are at $(L/2)(\pm 1, \pm 1, \pm 1)$. The density of the cube is a constant: $\rho = M/L^3$. The center of mass of the cube is then at $(0,0,0)$ since the three integrals $\bar{X} = \rho \int x\, dx\, dy\, dz$, $\bar{Y} = \rho \int y\, dx\, dy\, dz$ and $\bar{Z} = \rho \int z\, dx\, dy\, dz$ vanish on account of the integrands being odd. Next, we evaluate the components of the inertia tensor (8.15). For instance,

$$\mathcal{I}_{11} = \rho \int (y^2 + z^2) dx\, dy\, dz = 2\rho L^2 \int_{-L/2}^{L/2} y^2\, dy = 4\rho L^2 [y^3/3]_0^{L/2} = \frac{ML^2}{6}. \tag{8.18}$$

The other diagonal entries are seen to be equal $\mathcal{I}_{11} = \mathcal{I}_{22} = \mathcal{I}_{33}$. The off-diagonal entries vanish as the integrands are odd. E.g., $\mathcal{I}_{12} = -\rho \int xy\, dx\, dy\, dz = 0$. Thus, the inertia tensor of this cube is a multiple of the identity $\mathcal{I} = (ML^2/6)\mathbf{1}$. Consequently, every (nonzero)[15] vector is an eigenvector of $\mathcal{I}$ with eigenvalue $ML^2/6$. Hence, any three linearly independent vectors through the CM could be chosen to be the principal axes, though it is most convenient to take them parallel to the edges. Moreover, all three principal moments of inertia are equal to $ML^2/6$. It follows that a homogeneous cube is a spherical top! Additional examples of rigid bodies and their inertia tensors are discussed in Prob. 8.4, 8.5, 8.6 and 8.7. □

---

[13] For instance, for a symmetrical top held fixed at a point on its axis in a uniform gravitational field, the only other piece of information on the mass distribution that affects the rotational motion is the distance between the fixed point and the CM (see Sect. 8.15).

[14] Some authors use the word *top* to refer to a rigid body subject to gravity. For us, a top is simply a rigid body. A rigid body subject to gravity will be called a heavy top.

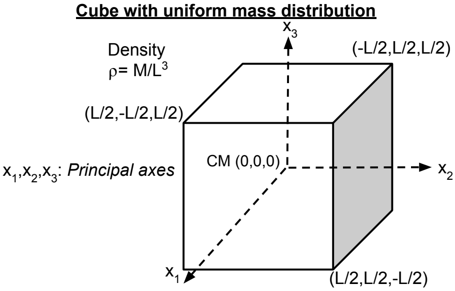

Figure 8.3: Homogeneous cube with a convenient choice of principal axes. The front, top and right faces are shown. It is a spherical top as the three principal moments of inertia are equal. In fact, the moment of inertia about any axis through the CM is $ML^2/6$.

$*$ **A spherical top need not have a spherically symmetric mass distribution.** In fact, any Platonic solid (tetrahedron, cube, octahedron, dodecahedron or icosahedron) or Archimedean solid with a uniform mass distribution is a spherical top. More generally, a rigid body with a pair of axes through the center of mass with three- or higher-fold symmetry is a spherical top. Furthermore, even an irregularly shaped body with nonuniform mass distribution can be turned into a spherical top by rescaling the mass distribution along two of its principal axes. □

Collinear rigid body or rigid rotator. If the body is concentrated along a straight line, say the z-axis, then it is called a rigid rotator and has no rotational inertia when spinning about the z-axis. Note that the mass distribution need not be uniform along the z-axis. Since $x = y = 0$ for all particles, the center of mass lies on the z-axis and the origin $z = 0$ may be chosen at the CM. We must have $\mathcal{I}_3 = 0$ and $\mathcal{I}_1 = \mathcal{I}_2 = \sum_a m_a z_a^2$. Note that two of the triangle inequalities introduced in Footnote 12 are saturated: $\mathcal{I}_1 + \mathcal{I}_3 = \mathcal{I}_2$ and $\mathcal{I}_2 + \mathcal{I}_3 = \mathcal{I}_1$. The principal axes of inertia can be taken to point along the z-axis and any pair of mutually orthogonal directions in the x-y plane.

Planar rigid body. Consider a rigid body that is concentrated on a plane (say the x-y plane), like a flat plate or sheet of cardboard. For all points on the body $z = 0$, so the center of mass lies on the x-y plane. It is clear from the explicit matrix representation (8.15) that $\mathcal{I}$ is block diagonal and that the z-axis is one of the principal axes. The other two lie in the x-y plane. Let us choose the x and y axes to point along these principal axes of inertia. The principal moments of inertia are $\mathcal{I}_1 = \sum my^2$, $\mathcal{I}_2 =$

---

[15] An eigenvector v is a nontrivial solution to the eigenvalue problem $Av = \lambda v$ for a matrix A and complex number λ. The zero vector v is always a solution for any A and for any λ, so it is not considered an eigenvector although it lies in the eigenspace spanned by any eigenvector.

$\sum mx^2$ and $\mathcal{I}_3 = \sum m(x^2 + y^2)$. Notice that one of the triangle inequalities of Footnote 12 is saturated: $\mathcal{I}_1 + \mathcal{I}_2 = \mathcal{I}_3$. This relation is called the **Perpendicular axis theorem**. For instance, the principal moments of inertia of a thin uniform square plate (see Prob. 8.4) are $ML^2/12, ML^2/12$ and $ML^2/6$. Despite appearances, it is a symmetrical top.

8.6 Angular momentum of a rigid body

The angular momentum of a rigid body is an important dynamical vector. We will soon formulate the equations of motion of a rigid body in terms of its linear and angular momenta (see Sect. 8.7). The angular momentum, like other dynamical vectors, depends on the choice of reference frame: its components depend on the choice of coordinate axes as well as an origin. For instance, we will find that in the absence of external torques, the components of the rotational angular momentum about the CM with respect to the lab frame are conserved and can therefore be used to restrict the possible types of motion. Furthermore, just as the linear momentum of a particle is linearly related to its velocity through multiplication by its mass, the angular momentum is linearly related to the angular velocity of a rigid body via the inertia tensor. However, since the inertia tensor is generally not a multiple of the identity, the angular momentum and angular velocity vectors need not point in the same direction, unlike the linear momentum and translational velocity. This relation between the two vectors has useful consequences. For instance, in the absence of external torques, the conservation of angular momentum and the form of the inertia tensor is used in Sect. 8.8 to infer the components of angular velocity and thereby deduce the nature of the rotational motion of a rigid body.

Angular momentum of CM motion and of rotation about CM. To begin with, we recall that the angular momentum of a system of particles is defined with respect to an origin. If we use the origin of the lab frame, then the position vector of a point labelled a in the rigid body is $\boldsymbol{\mathscr{r}}_a = \boldsymbol{R} + \boldsymbol{r}_a$ where $\boldsymbol{R}$ is the position vector of the center of mass. If $\boldsymbol{\mathscr{p}}_a$ is the lab-frame momentum of the same particle, we must have $\boldsymbol{\mathscr{p}}_a = m_a \boldsymbol{\mathscr{v}}_a = m_a \boldsymbol{V} + m_a \boldsymbol{\Omega} \times \boldsymbol{r}_a$ from (8.8). Thus, the 'total' angular momentum about the origin of the lab frame is

$$\boldsymbol{L}_{\text{tot}} = \sum_a \boldsymbol{\mathscr{r}}_a \times \boldsymbol{\mathscr{p}}_a = \sum_a \boldsymbol{R} \times \boldsymbol{\mathscr{p}}_a + \cancel{\sum_a m_a \boldsymbol{r}_a} \times \boldsymbol{V} + \sum_a m_a \boldsymbol{r}_a \times (\boldsymbol{\Omega} \times \boldsymbol{r}_a) . \quad (8.19)$$

Furthermore, the total momentum $\boldsymbol{P} = \sum_a \boldsymbol{\mathscr{p}}_a$ coincides with the CM momentum $M\boldsymbol{V}$ (8.9). Thus, the total angular momentum about the origin of the lab frame

$$\boldsymbol{L}_{\text{tot}} = \boldsymbol{R} \times \boldsymbol{P} + \sum\nolimits_a m_a \boldsymbol{r}_a \times (\boldsymbol{\Omega} \times \boldsymbol{r}_a) = \boldsymbol{L}_{\text{cm}} + \boldsymbol{L}_{\text{rot}} \qquad (8.20)$$

is a sum of a center of mass part $\boldsymbol{L}_{\text{cm}} = \boldsymbol{R} \times \boldsymbol{P}$ and a rotational part. $\boldsymbol{L}_{\text{cm}}$ is the angular momentum of the CM about the origin of the lab frame. $\boldsymbol{L}_{\text{rot}}$ also admits a nice interpretation. Consider an instant of time when the CM is moving at velocity $\boldsymbol{V}$. Imagine an inertial frame that moves with uniform velocity $\boldsymbol{V}$ relative to the lab frame and is centered at the CM at the instant considered. The CM is momentarily at rest in this frame. At this instant, the momentum of particle a with respect to this inertial frame is $\boldsymbol{p}_a = m_a \mathbf{v}_a = m_a \boldsymbol{\Omega} \times \boldsymbol{r}_a$ (8.8). Thus, we may interpret $\boldsymbol{L}_{\text{rot}}$ as the angular momentum relative to the CM in this inertial frame. Interestingly, $\boldsymbol{L}_{\text{rot}}$ also coincides with the angular momentum of the body relative to the CM in the lab frame! In fact,

$$\boldsymbol{L}_{\text{body}}^{\text{cm}-\text{lab}} = \sum\nolimits_a \boldsymbol{r}_a \times \not{p}_a = \cancel{\sum\nolimits_a m_a \boldsymbol{r}_a} \times \boldsymbol{V} + \sum\nolimits_a \boldsymbol{r}_a \times \boldsymbol{p}_a = \boldsymbol{L}_{\text{rot}}. \tag{8.21}$$

Henceforth, we will denote this rotational part of the angular momentum simply by the symbol $\boldsymbol{L}$:

$$\boldsymbol{L} = \boldsymbol{L}_{\text{rot}} = \boldsymbol{L}_{\text{body}}^{\text{cm}-\text{lab}} = \sum\nolimits_a \boldsymbol{r}_a \times \boldsymbol{p}_a = \sum\nolimits_a m_a (r_a^2 \boldsymbol{\Omega} - (\boldsymbol{\Omega} \cdot \boldsymbol{r}_a)\, \boldsymbol{r}_a). \tag{8.22}$$

In components,

$$L_i = \sum m \left(r^2 \delta_{ij} - r_i r_j \right) \Omega_j = \mathcal{I}_{ij} \Omega_j. \tag{8.23}$$

We see that the rotational angular momentum with respect to the CM is related to the angular velocity via the inertia matrix $\mathcal{I}$. This is analogous to how the translational momentum of a point particle is related to its velocity via the mass $\boldsymbol{p} = m\boldsymbol{v}$. Momentum always points in the same direction as velocity. But in general, angular momentum points in the same direction as angular velocity only for an isotropic rigid body, for which the inertia matrix is a multiple of the identity. For an anisotropic rigid body, $\boldsymbol{L}$ points in the same direction as $\boldsymbol{\Omega}$ only if a principal axis of inertia can be taken to point along $\boldsymbol{\Omega}$.

$*$ **Inertial vs comoving frames.** We note that $\boldsymbol{L}_{\text{rot}}$ is the angular momentum as defined by an inertial observer instantaneously stationed at the center of mass. It is different from the angular momentum about the CM defined by a noninertial observer who always moves and rotates with the body. According to such an observer, the momentum of each particle in the body is zero, so that the corresponding angular momentum is identically zero. However, there is something nontrivial in between: the components of $\boldsymbol{L}_{\text{rot}}$ referred to a comoving frame. We will examine the evolution of these components in Sect. 8.11. □

8.7 Equations of motion of a rigid body

The EOM of a rigid body made of N point masses can be written using Newton's second law in the lab (inertial) frame

$$m_a \ddot{\not{\boldsymbol{r}}}_a = \boldsymbol{f}_a \quad \text{for} \quad a = 1, \ldots, N. \tag{8.24}$$

Here, $\boldsymbol{f}_a$ is the force acting on the a^{th} particle, which in general is a sum of external forces and internal forces due to other particles in the rigid body. These are $3N$ second order equations. However, a generic[16] rigid body has only 6 degrees of freedom, irrespective of how large N may be. So the above equations are somewhat redundant: they do not make manifest the rigidity of the body. We should be able to formulate the EOM of a generic rigid body more economically in terms of just 6 second order ODEs without reference to individual mass points. We may regard the remaining $3N - 6$ equations (assuming $N \geq 3$) as simply encoding the rigidity of the body due to internal forces.

---

[16] If $N = 2$, then the rigid body has either 3 or 5 degrees of freedom depending on whether the two particles are always coincident or a nonzero distance apart.

The configuration of the rigid body may be specified by giving the location $\boldsymbol{R}$ of the center of mass and a rotation about the CM that brings the body to the desired orientation, relative to a reference orientation. We use $\boldsymbol{\phi} = (\phi_1, \phi_2, \phi_3)$ to denote three angles that specify the orientation of the rigid body. In Sect. 8.9, we will choose them to be the Euler angles, but we do not need them right now.

The EOM for the rigid body may be formulated as 1st order equations for the CM momentum $\boldsymbol{P}$ and for the angular momentum $\boldsymbol{L}$ about the CM. We will obtain these equations in the lab frame or any other inertial frame, the equations have the same form in all such frames by Galilean invariance (see Sect. 3.12). Note that the comoving frame is in general a noninertial frame, as the body may accelerate and rotate. We will transform the EOM to the comoving frame in Sect. 8.11.

Center of mass motion. Working in the lab frame, suppose $\boldsymbol{f}_a$ is the force on the a^{th} particle, then $\dot{\not{\boldsymbol{p}}}_a = \boldsymbol{f}_a$. Adding these for all the particles we get $\dot{\boldsymbol{P}} = \boldsymbol{F}$ where $\boldsymbol{P} = \sum_a \not{\boldsymbol{p}}_a = M\boldsymbol{V}$ is the total momentum and $\boldsymbol{F} = \sum \boldsymbol{f}_a$ is the total force acting on the body[17]. We need only include the external forces on the particles as the interparticle forces cancel by Newton's 3rd law. $\dot{\boldsymbol{P}} = \boldsymbol{F}$ is the equation of motion in the lab frame. By Galilean invariance, it takes the same form in any other inertial frame.

This equation may also be obtained from the Lagrangian[18]

$$L = T - U = \frac{1}{2} M \boldsymbol{V}^2 + \frac{1}{2} \mathcal{I}_{ij} \Omega_i \Omega_j - U(\boldsymbol{R}, \boldsymbol{\phi}) \quad \text{where} \quad \boldsymbol{V} = \dot{\boldsymbol{R}}. \tag{8.25}$$

The (external) potential U may also be regarded as a function of the positions of all the masses $U = \tilde{U}(\not{\boldsymbol{r}}_a)$. The corresponding EOM for $\boldsymbol{R}$ are seen to reproduce $\dot{\boldsymbol{P}} = \boldsymbol{F}$:

$$\frac{d}{dt}\frac{\partial L}{\partial \dot{R}_i} = \frac{d}{dt}\frac{\partial L}{\partial V_i} = \frac{\partial L}{\partial R_i} \quad \Rightarrow \quad M\dot{\boldsymbol{V}} \equiv \dot{\boldsymbol{P}} \;=\; -\frac{\partial U}{\partial \boldsymbol{R}} \;=\; \boldsymbol{F} = \text{ external force.} \tag{8.26}$$

Here we used the fact that the change in potential energy under a translation of the center of mass by $\delta\boldsymbol{R}$ is $\delta U = \sum_a \frac{\partial \tilde{U}}{\partial \not{\boldsymbol{r}}_a} \cdot \delta \not{\boldsymbol{r}}_a = -\sum_a \boldsymbol{f}_a \cdot \delta\boldsymbol{R}$ since all particles are translated by the same amount, $\delta \not{\boldsymbol{r}}_a = \delta\boldsymbol{R}$. So $\delta U = -\boldsymbol{F} \cdot \delta\boldsymbol{R}$ whence $\frac{\partial U}{\partial R_i} = -F_i$.

Rotational motion. Next, we compute the time derivative of the rotational angular momentum $\boldsymbol{L} = \sum_a \boldsymbol{r}_a \times \boldsymbol{p}_a$ (8.22) where $\boldsymbol{r}_a$ is the position vector of the a^{th} particle relative to the CM and $\boldsymbol{p}_a = \not{\boldsymbol{p}}_a - m_a\boldsymbol{V} = m_a\dot{\boldsymbol{r}}_a = m_a\mathbf{v}_a = m_a\boldsymbol{\Omega} \times \boldsymbol{r}_a$ (8.8) its momentum due to the rotation alone. As mentioned in Sect. 8.6, $\boldsymbol{L}$ is the angular momentum of the body relative to the CM in the lab frame. Moreover, $\dot{\boldsymbol{p}}_a = \boldsymbol{f}_a - m_a\dot{\boldsymbol{V}}$ where $\boldsymbol{f}_a$ is the force on this particle in the lab frame. Thus,

---

[17] In fact, the equation $\dot{\boldsymbol{P}} = \boldsymbol{F}$ relating the rate of change of total momentum to the vector sum of external forces is valid for any system of particles (e.g., two gravitating point masses in an external gravitational field) and is not restricted to rigid bodies. It is a consequence of Newton's second and third laws for the individual particles.

[18] The external potential energy U could depend both on the location $\boldsymbol{R}$ of the center of mass as well as on the orientation of the body, specified via the angular variables $\boldsymbol{\phi}$.

$$\dot{\boldsymbol{L}} = \sum_a (\cancel{\dot{\boldsymbol{r}}_a \times \boldsymbol{p}_a} + \boldsymbol{r}_a \times \dot{\boldsymbol{p}}_a) = \sum_a \boldsymbol{r}_a \times \boldsymbol{f}_a - \cancel{\sum_a m_a \boldsymbol{r}_a} \times \dot{\boldsymbol{V}} = \sum_a \boldsymbol{\tau}_a = \boldsymbol{\tau}. \tag{8.27}$$

Here, $\boldsymbol{\tau}$ is the total torque on the body about the CM (in fact, we may restrict to the external torque, see below). Since $\boldsymbol{L} = \mathcal{I}\boldsymbol{\Omega}$, we could also write $d(\mathcal{I}\boldsymbol{\Omega})/dt = \boldsymbol{\tau}$. This equation holds in the lab frame or any other inertial frame.

Equation (8.27) for $\dot{\boldsymbol{L}}$ also follows formally from the Lagrangian (8.25). At first, we are puzzled since we have (i) not specified the angles ϕ_i, (ii) not clarified the relation between Ω_i and $\dot{\phi}_i$ and (iii) not expressed the Lagrangian in terms of $\dot{\phi}_i$. All this will be done in Sect. 8.9 and Sect. 8.10 using the Euler angles. Here, we use the axis-angle representation of rotations and exploit the fact that to obtain the EL equations, it is enough to consider infinitesimal rotations. To begin with, we think of $\boldsymbol{\phi} = (\phi_1, \phi_2, \phi_3)$ as a vector specifying a rotation from a reference orientation. The unit vector along $\boldsymbol{\phi}$ is the axis of rotation while its magnitude is the counterclockwise angle of rotation. For an infinitesimal rotation, $\boldsymbol{\phi}$ reduces to the Euler vector $\delta\boldsymbol{\phi}$ of Footnote (8). What is more, $\boldsymbol{\Omega}$ was defined in Sect. 8.3 as the limit of $\delta\boldsymbol{\phi}/\delta t$ as $\delta t \to 0$. Thus, if $\boldsymbol{\phi} = \delta\boldsymbol{\phi}$ represents an infinitesimal rotation, then we are justified in taking $\Omega_i = \dot{\phi}_i$. Bearing this in mind, we evaluate the LHS of Lagrange's equations for the angular variables:

$$\frac{d}{dt}\frac{\partial L}{\partial \dot{\phi}_i} = \frac{d}{dt}\frac{\partial L}{\partial \Omega_i} = \frac{d}{dt}(\mathcal{I}_{ij}\Omega_j) = \dot{L}_i. \tag{8.28}$$

As for the RHS, we wish to show that $\frac{\partial L}{\partial \phi^i}$ or equivalently $-\frac{\partial U}{\partial \phi^i}$ are the components of the torque $\boldsymbol{\tau}$. To begin with, $\frac{\partial U}{\partial \phi^i}$ is defined as the limit of $\delta U/\delta\phi^i$ as the infinitesimal rotation specified by the Euler vector $\delta\boldsymbol{\phi} \to 0$. The change in potential energy δU due to an infinitesimal rotation specified by $\delta\boldsymbol{\phi}$ (about an axis passing through the CM) is minus the work done by the external forces[19]. Under a rotation about the CM, the center of mass $\boldsymbol{R}$ does not move, so $\delta \boldsymbol{\mathscr{r}}_a = \delta\boldsymbol{r}_a = \delta\boldsymbol{\phi} \times \boldsymbol{r}_a$. Consequently, the change in potential energy is (here $\boldsymbol{f}_a$ may be restricted to external forces)

$$\delta U = -\sum_a \boldsymbol{f}_a \cdot \delta \boldsymbol{\mathscr{r}}_a = -\sum_a \boldsymbol{f}_a \cdot (\delta\boldsymbol{\phi} \times \boldsymbol{r}_a) = -\delta\boldsymbol{\phi} \cdot \sum_a \boldsymbol{r}_a \times \boldsymbol{f}_a = -\delta\boldsymbol{\phi} \cdot \boldsymbol{\tau}. \tag{8.29}$$

From this we deduce that $\partial U/\partial\boldsymbol{\phi} = -\boldsymbol{\tau}$. So the Euler-Lagrange equations imply the law of evolution of angular momentum (relative to the CM) of the rigid body

$$\frac{d}{dt}\frac{\partial L}{\partial \dot{\boldsymbol{\phi}}} = \frac{\partial L}{\partial \boldsymbol{\phi}} \quad \Rightarrow \quad \dot{\boldsymbol{L}} = -\frac{\partial U}{\partial \boldsymbol{\phi}} = \boldsymbol{\tau} = \text{ external torque about the CM.} \tag{8.30}$$

In the absence of any external torque about the CM (e.g., if there are no external forces, so that U can be taken to vanish), the angular momentum of the rigid body about its CM is independent of time: $\dot{\boldsymbol{L}} = 0$.

---

[19] Internal forces between particles in the body can do work only if the body is deformed.

8.8 Force-free motion of rigid bodies

Now consider a rigid body in the absence of any external forces[20]. If the center of mass was initially at rest, it will remain so. More generally, the CM moves along a straight line since $\dot{\boldsymbol{P}} = M\ddot{\boldsymbol{R}} = \boldsymbol{F} = 0$ (8.26). Let us choose our inertial frame to move at velocity $\boldsymbol{V} = \dot{\boldsymbol{R}}$ relative to the lab, so that the CM is always at rest at its origin. Of course, the body could still rotate. Since there are no external forces, there are no external torques either, about any point. So the angular momentum about any point and in particular about the CM, $\boldsymbol{L} = \boldsymbol{L}_{\rm rot}$ must be constant in time[21] by (8.27). We may use the conservation of angular momentum and the formula $\boldsymbol{L} = \mathcal{I}\boldsymbol{\Omega}$ to understand many qualitative and quantitative aspects of the free rotational motion of spherical tops, rigid rotators and symmetrical tops, without attempting to solve the equations of motion explicitly. This is what we will do in the rest of this section. Some striking qualitative features emerge. For instance, all that a spherical top can do is to spin at a constant angular velocity about an axis that points along the conserved angular momentum vector and passes through the CM. The direction of this $\boldsymbol{L}$ vector is determined by initial conditions and the rate of spinning is determined in terms of its magnitude and the moment of inertia about the CM. A rigid rotator (collinear rigid body) on the other hand, must rotate uniformly in a plane perpendicular to the conserved $\boldsymbol{L}$ vector (see Fig. 8.4). In both these cases, the angular velocity vector $\boldsymbol{\Omega}$ is also conserved. A symmetrical top can do more *even* in the absence of an external torque. As illustrated in Fig. 8.5, it can spin steadily about its symmetry axis while the symmetry axis itself rotates (i.e., precesses) uniformly about the fixed direction of $\boldsymbol{L}$. This will be applied to the precession (‘Chandler wobble’) of the angular velocity vector of the Earth about its symmetry axis at the end of Sect. 8.11. An anisotropic rigid body can display more intricate motion, this will be examined in Sect. 8.12.

Free motion of a spherical top. For a spherical top, the principal moments of inertia $\mathcal{I}_1, \mathcal{I}_2, \mathcal{I}_3$ are equal and the inertia tensor $\mathcal{I} = \mathrm{diag}(\mathcal{I}_1, \mathcal{I}_2, \mathcal{I}_3)$ is a multiple of the 3×3 identity matrix. Thus $\boldsymbol{L} = \mathcal{I}_1\boldsymbol{\Omega}$, so the angular velocity and angular momentum both point in the same direction and are constant in time. In particular, force-free motion of a spherical top consists of uniform rotation about some axis (through the CM, see Prob. 8.15) that is fixed in the lab frame. The direction of this axis and the rate of rotation $\Omega = |\boldsymbol{\Omega}|$ are determined by initial conditions. The conserved energy $E = \frac{1}{2}\mathcal{I}_1(\Omega_1^2 + \Omega_2^2 + \Omega_3^2) = \frac{1}{2}\mathcal{I}_1|\boldsymbol{\Omega}|^2 = \frac{|\boldsymbol{L}|^2}{2\mathcal{I}_1}$ is also determined by initial conditions.

Free motion of a rigid rotator

Next, consider a rigid rotator (collinear rigid body of Sect. 8.5 or the rod in Fig. 8.4) subject to no forces, so that $\boldsymbol{L}$ is a constant vector. We will denote the axes of the lab frame by XYZ, principal axis frame by $x_1x_2x_3$ and body-fixed frame by xyz. Suppose we call the principal axis that points along the axis of the rotator x_3.

---

[20] While external forces like gravity are usually present, it may be possible to ignore the effect of the gravitational torque if the body has a large enough rotational kinetic energy.

[21] We note in passing that even in such a force-free situation, the components of $\boldsymbol{L}$, relative to a body-fixed frame, will in general depend on time.

Then the principal moments of inertia are $\mathcal{I}_1 = \mathcal{I}_2$ and $\mathcal{I}_3 = 0$. Since all the masses lie along the axis of the rotator, in the formula for angular momentum about the CM, $\boldsymbol{L} = \sum_a \boldsymbol{r}_a \times \boldsymbol{p}_a$, $\boldsymbol{r}_a$ is along the axis of the rotator. So the constant vector $\boldsymbol{L}$ must be orthogonal to the axis of the rotator at all times[22]. In other words, the rotator must rotate in a fixed plane in the lab frame. Let us call this the X-Y plane of the lab system, so that $\boldsymbol{L}$ points along $\hat{Z}$. Thus, for an infinitesimal rotation, $\delta\boldsymbol{\phi} \propto \hat{Z}$. It follows that the angular velocity $\Omega = \lim_{\delta t\to 0} \delta\boldsymbol{\phi}/\delta t$ also points along $\hat{Z}$ (see Fig. 8.4). Since $x_3 \perp Z$, it follows that $\Omega_3 = 0$.

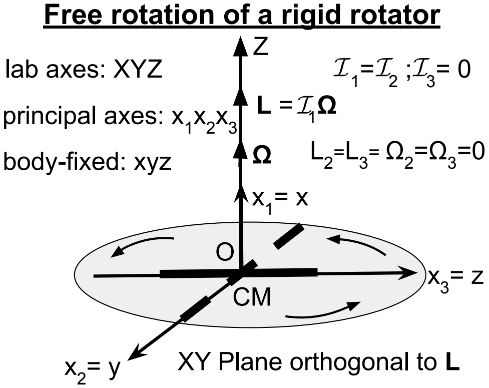
Free rotation of a rigid rotator
Z
lab axes: XYZ
$\mathcal{I}_1=\mathcal{I}_2$;$\mathcal{I}_3$= 0
principal axes: $x_1x_2x_3$
L = $\mathcal{I}_1$Ω
body-fixed: xyz
Ω
$L_2=L_3=\Omega_2=\Omega_3=0$
x_1= x
O
x_3= z
CM
x_2= y
XY Plane orthogonal to L

Figure 8.4: The most general free motion of a rigid rotator whose CM is fixed is a uniform rotation in a plane perpendicular to its angular momentum.

As the x_3 principal axis has been chosen along the axis of the rotator, $x_1 = x_2 = 0$ for all mass points and so the inertia tensor becomes the diagonal matrix $\mathcal{I} = \text{diag}(\mathcal{I}_1, \mathcal{I}_1, 0)$ irrespective of how we choose the x_1, x_2 axes in the plane orthogonal to x_3. It follows that $L_1 = \mathcal{I}_1\Omega_1$, $L_2 = \mathcal{I}_1\Omega_2$ while $L_3 = \Omega_3 = 0$. Thus $\boldsymbol{\Omega} = \boldsymbol{L}/\mathcal{I}_1$ must be a constant vector in space, just like $\boldsymbol{L}$ is. Moreover, the rate at which the rod rotates (axis 'precesses' about $\boldsymbol{L}$) is independent of time and equal to $|\boldsymbol{\Omega}| = L/\mathcal{I}_1$ where $L = |\boldsymbol{L}|$ is the magnitude of the constant angular momentum vector. So the most general free motion of a rigid rotator is uniform rotation in a plane fixed with respect to the lab frame and orthogonal to the direction of angular momentum.

We may also specify a convenient body-fixed frame xyz which is also a principal axis frame. We choose $z = x_3$ along the axis of the rotator ($\mathcal{I}_3 = 0$) and take $x = x_1$ along the fixed Z axis (direction of $\boldsymbol{L}$), which is a direction that is fixed both in the body and in space. Then $y = x_2$ must lie in the XY plane in such a way that xyz is a right-handed system. With these choices, we may write $\boldsymbol{L}$ and $\boldsymbol{\Omega}$ in terms of their components in both the lab and principal-axis-body-fixed frames:

---

[22] We could have reached this conclusion by a different argument as well. From $\boldsymbol{L} = \mathcal{I}\boldsymbol{\Omega}$ written in the principal axis basis, we see that the component of angular momentum in the direction of the axis of the rotator must vanish ($L_3 = \mathcal{I}_3\Omega_3 = 0$) irrespective of what Ω_3 is. So $\boldsymbol{L}$ must always point in a direction perpendicular to the axis of the rotator.

$$\boldsymbol{L} = L\hat{Z} = L\hat{x} \quad \text{and} \quad \boldsymbol{\Omega} = \frac{L}{\mathcal{I}_1}\hat{Z} = \frac{L}{\mathcal{I}_1}\hat{x}. \tag{8.31}$$

Free motion of symmetrical top

Force-free motion of a symmetric top is a combination of spinning on its axis and precession of the axis about a fixed direction in space, and at a fixed angle (there is no nutation in the absence of gravity). Let us understand why.

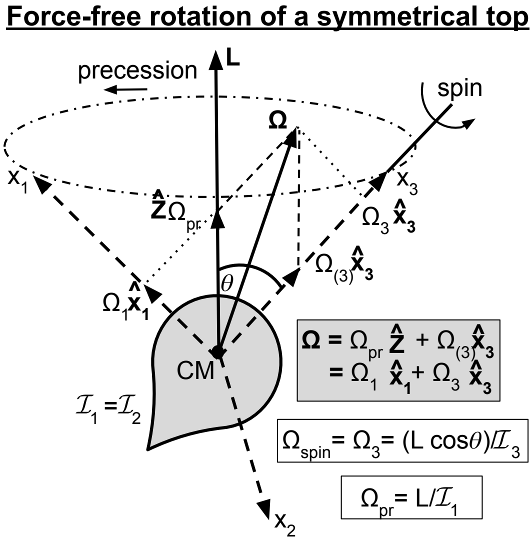
Force-free rotation of a symmetrical top
precession
L
spin
Ω
x_1
x_3
$\hat{Z}\Omega_{pr}$
$\Omega_3 \hat{x}_3$
$\Omega_{(3)} \hat{x}_3$
θ
$\Omega_1 \hat{x}_1$
CM
$\mathcal{I}_1 = \mathcal{I}_2$
$\boldsymbol{\Omega} = \Omega_{pr} \hat{Z} + \Omega_{(3)} \hat{x}_3 = \Omega_1 \hat{x}_1 + \Omega_3 \hat{x}_3$
$\Omega_{spin} = \Omega_3 = (L \cos\theta)/\mathcal{I}_3$
$\Omega_{pr} = L/\mathcal{I}_1$
x_2

Figure 8.5: Free motion of a symmetrical top. $\boldsymbol{L}$ is chosen along the Z-axis of the lab frame. The x_3 principal axis points along the top's axis while x_1 is chosen to lie in the x_3-Z plane. x_1 is not fixed in the body if it spins on its axis. $\boldsymbol{\Omega}$ lies in the plane of $\boldsymbol{L}$ and the axis and is decomposed in two different ways to find the spin and precession rates.

Choosing principal axes. Consider a symmetrical top with $0 < \mathcal{I}_1 = \mathcal{I}_2 \neq \mathcal{I}_3 \neq 0$. The angular momentum in space is of course a constant vector $\boldsymbol{L}$. Its conservation and the relation $\boldsymbol{L} = \mathcal{I}\Omega$ allow us to understand some aspects of the motion. Let us choose the Z axis of the lab frame along $\boldsymbol{L}$, as shown in Fig. 8.5. The third principal axis $x_3 = z$ is chosen along the axis of the top. The first two principal axes x_1, x_2 may be freely chosen orthogonal to x_3 since the corresponding eigenvalues are equal ($\mathcal{I}_1 = \mathcal{I}_2$). As a consequence of this degeneracy, not every such choice of principal axes is fixed in the body: a principal axis frame is not necessarily a body-fixed frame[23] (xyz) or vice versa. However, in this section, we do not need a comoving frame. In fact, it is not possible, in general, to specify a comoving frame relative to the lab frame, without prior knowledge of how the top moves! So we will simply choose a convenient set of principal axes x_1, x_2, x_3 in which $\mathcal{I}$ is diagonal. This frame will not qualify as a comoving frame.

---

[23] By contrast, for an anisotropic rigid body, the principal axes are uniquely determined (up to reflections and ordering) and the corresponding frame is automatically fixed in the body.

Let us choose the second principal axis x_2 to always be perpendicular to the plane spanned by $\boldsymbol{L}$ and the axis of the top[24]. Then x_1 must lie in the x_3-$\boldsymbol{L}$ plane in such a way that the x_1, x_2, x_3 axes form a right-handed orthonormal system. Since x_2 is orthogonal to $\boldsymbol{L}$, it follows that $L_2 = \boldsymbol{L} \cdot \hat{x}_2 = 0$. This implies $\Omega_2 = L_2/\mathcal{I}_2 = 0$ as $\mathcal{I}_2 \neq 0$. So $\boldsymbol{\Omega}$ always lies in the plane spanned by $\boldsymbol{L}$ and the axis of the top. It follows that the velocity of any point on the axis of the top, $\boldsymbol{v} = \boldsymbol{\Omega} \times \boldsymbol{r}$ always points perpendicular to that plane. So the axis of the top precesses about the direction of angular momentum in space, sweeping out a cone. Let us denote the angle between the axis of the top and $\boldsymbol{L}$ by θ. We now argue that θ is time-independent so that the cone has a fixed opening angle. For θ to change, the velocity $\boldsymbol{v}$ of a point on the axis of the top would need to have a component in the $\boldsymbol{L}$-x_3 plane. However, as noted above, $\boldsymbol{v}$ is always directed perpendicular to this plane. So θ must be fixed by initial conditions. We will see below, that the rate of precession and the length of $\boldsymbol{\Omega}$ are both constant in time. In addition to precessing about the Z axis, the top also spins about its own axis. We wish to find the angular speeds of precession $\Omega_{\rm pr}$ and spin $\Omega_{\rm spin}$ in terms of the opening angle θ, the constant magnitude of angular momentum $L = |\boldsymbol{L}|$ and the principal moments of inertia. It helps to expand $\boldsymbol{L}$ and $\boldsymbol{\Omega}$ in the principal axis basis. $\boldsymbol{\Omega} = \Omega_1 \hat{x}_1 + \Omega_3 \hat{x}_3$ and $\boldsymbol{L} = L_1 \hat{x}_1 + L_3 \hat{x}_3$ where $L_1 = L \sin\theta$ and $L_3 = L\cos\theta$ where θ is the angle between $\boldsymbol{L}$ and $\hat{x}_3$. By constancy of L and θ, the components L_1 and L_3 of $\boldsymbol{L}$ in the principal axis frame are independent of time. Similarly, $\Omega_1 = L\sin\theta/\mathcal{I}_1$ and $\Omega_3 = L\cos\theta/\mathcal{I}_3$ are also time-independent. So $\boldsymbol{\Omega}$ is a constant vector in the principal axis frame. But $\boldsymbol{\Omega}$ is *not* a constant vector in space, the $\boldsymbol{L}$-$\boldsymbol{\Omega}$ plane rotates about the Z axis. Physically, the direction of $\boldsymbol{\Omega}$ is the instantaneous axis of rotation. At any given instant, the top rotates infinitesimally about $\boldsymbol{\Omega}$ at a rate equal to $|\boldsymbol{\Omega}|$. However, since $\boldsymbol{\Omega}$ is not a constant vector, the axis of rotation keeps changing. The resulting rotational motion can be viewed as a combination of two periodic motions: spin and precession, whose rates we now determine.

Rate of spinning motion. The rate at which the top spins on its axis may be obtained by decomposing $\boldsymbol{\Omega}$ into two parts $\boldsymbol{\Omega} = \Omega_3 \hat{x}_3 + \Omega_1 \hat{x}_1$, the second term does not cause any spinning motion, it simply moves the axis of the top as a whole. On the other hand, an infinitesimal rotation about $\hat{x}_3$ causes the top to spin about its instantaneous axis of symmetry. Thus, $\Omega_3 \hat{x}_3$ may be identified as the angular velocity responsible for spinning motion. Consequently, $\Omega_{\rm spin} = \Omega_3 = \boldsymbol{\Omega} \cdot \hat{x}_3 = \frac{L_3}{\mathcal{I}_3} = \frac{L\cos\theta}{\mathcal{I}_3}$. Since θ is independent of time, the top spins at a constant rate on its axis. Moreover, a symmetric rigid body *must* spin on its axis, as long as ICs are such that $\theta \neq \pi/2$.

Precession rate. On the other hand, to find the precession rate of the axis of the top about the $\hat{Z}$ axis, we will decompose $\boldsymbol{\Omega}$ as a sum of two vectors, one of which does not cause any precession, while the other can be identified as the angular velocity of precession. Assuming $\theta \neq 0$, we use $\hat{x}_3$ and $\hat{Z}$ as a (generally nonorthogonal) basis to write $\boldsymbol{\Omega} = \Omega_{(3)} \hat{x}_3 + \Omega_{\rm pr} \hat{Z}$. The first term (which is *not* equal to $\Omega_3 \hat{x}_3$ in general) does not produce any displacement of the axis of the top. The magnitude of the second term $\Omega_{\rm pr}$ is the rate of precession[25]. An expression for $\Omega_{\rm pr}$ may be found by taking the dot product[26] of this nonorthogonal decomposition with $\hat{x}_1$ and using $\hat{x}_1 \cdot \hat{x}_3 = 0$:

---

[24] We exclude the case where the axis of the top points along $\boldsymbol{L}$. This case ($\theta = 0$) will be treated separately.

$$\Omega_1 = \boldsymbol{\Omega} \cdot \hat{x}_1 = \Omega_{\rm pr} \hat{Z} \cdot \hat{x}_1 = \Omega_{\rm pr} \sin\theta \quad \Rightarrow \quad \Omega_{\rm pr} = \frac{\Omega_1}{\sin\theta} = \frac{L_1}{\mathcal{I}_1 \sin\theta} = \frac{L}{\mathcal{I}_1}. \quad (8.32)$$

The rate of precession is constant. The axis of the top rotates uniformly about $\boldsymbol{L}$ in space. Since $\boldsymbol{\Omega}$ lies in the same plane as $\boldsymbol{L}$ and the axis of the top, it follows that $\boldsymbol{\Omega}$ also precesses about $\boldsymbol{L}$ at the same rate $\Omega_{\rm pr} = L/\mathcal{I}_1$. Interestingly, the rate of precession is independent of opening angle θ.

Space cone. Taking a dot product with $\hat{x}_3$, we get $\Omega_3 = \Omega_{\rm spin} = \Omega_{(3)} + \Omega_{\rm pr}\cos\theta$. Since $\Omega_{\rm spin}, \Omega_{\rm pr}$ and θ are all independent of time, so is $\Omega_{(3)}$. Thus, $\boldsymbol{\Omega}$ sweeps out a 'space cone' about $\boldsymbol{L}$ in the lab frame (see Prob. 8.21).

Axis along $\boldsymbol{L}$. So far, we excluded the case $\theta = 0$. Suppose the axis of the top ($\hat{x}_3$) always points along the fixed direction of angular momentum in space: $\boldsymbol{L} = L\hat{Z} = L\hat{x}_3$, so that $\theta = 0$. Then in any principal axis basis, $L_1 = L_2 = 0$ and $L_3 = L$. It follows that $\Omega_1 = L_1/\mathcal{I}_1 = 0$ and $\Omega_2 = L_2/\mathcal{I}_2 = 0$, so $\boldsymbol{\Omega} = \Omega_3\hat{x}_3 = (L/\mathcal{I}_3)\hat{Z}$. So like $\boldsymbol{L}$, $\boldsymbol{\Omega}$ too is a fixed vector in space. Its magnitude $\Omega = L/\mathcal{I}_3$ is the rate $\Omega_{\rm spin}$ at which the top spins on its axis. Since the axis always points in the same direction, it does not precess, $\Omega_{\rm pr} = 0$. We may obtain the case $\theta = 0$ as a limit of the previous analysis. For $\theta > 0$ we found $\Omega_{\rm spin} = L\cos\theta/\mathcal{I}_3$ which reduces to $L/\mathcal{I}_3$ in the limit $\theta \to 0$. To find the limiting value of the precession rate $\Omega_{\rm pr} = \frac{L_1}{\mathcal{I}_1 \sin\theta}$, we must bear in mind that as $\theta \to 0$, $L_1 \to 0$ as well. The physical process of taking the limit must be such that L_1 vanishes faster than $\sin\theta$, so that $\Omega_{\rm pr} \to 0$ as $\theta \to 0$.

8.9 Euler angles and rotations

The geometric approach of Sect. 8.8 used to study the free motion of a symmetric top has its limitations if we wish to study the motion of an anisotropic top or one that is subject to external forces. It helps to have a coordinate system on configuration space in which to write the equations of motion and look for solutions.

Euler angles are a way of parametrizing the rotational[27] degrees of freedom of a rigid body. They give us a way of specifying the orientation of a body-fixed or corotating frame xyz relative to an inertial frame XYZ. Since we are interested in the relative orientation (and not translational motion), we assume that the two frames have a common origin O (e.g., the center of mass). At any instant, the corotating frame is related to the fixed frame by a rotation, since both are right-handed orthonormal frames with a common origin. So Euler angles parametrize points on the rotation

---

[25] It is reasonable that $\Omega_{\rm pr}\hat{Z}$ is the precessional angular velocity. An infinitesimal rotation about $\hat{Z}$ makes the axis of the top sweep out a portion of the cone associated to precession.

[26] Note that the precession rate is *not* given by $\boldsymbol{\Omega} \cdot \hat{x}_1 = \Omega_1$. An infinitesimal rotation about $\hat{x}_1$ does not make the axis of the top sweep out a portion of the precessional cone.

[27] There are other ways of specifying a rotation in 3d. The axis-angle representation of rotations and the approach using Hamilton's quaternions are described in Appendix B.14*

group $SO(3)$. To set them up, we observe that the XY and xy planes intersect along a line called the line of nodes[28] (the dotted line in Fig. 8.6 that contains the segment ON). This line is of course orthogonal to both the $\hat{Z}$ and $\hat{z}$ axes, and the direction of ON is chosen along $\hat{Z} \times \hat{z}$. The orientation of the xyz axes relative to the fixed XYZ axes is specified as follows. θ is the angle between the Z and z axes. The line of nodes ON on the XY plane is fixed by saying that it makes an angle ϕ with the X axis. This fixes the xy plane as it must be perpendicular to z and contain the line of nodes. Finally, the x axis is fixed by saying it makes an angle ψ with the line of nodes. The Euler angles θ, ϕ and ψ are generalized coordinates that (locally) fix the angular orientation of a rigid body. The corresponding generalized velocities are their time derivatives $\dot{\theta}, \dot{\phi}$ and $\dot{\psi}$.

The Euler angles θ and ϕ are completely analogous to the polar (colatitude) and azimuthal (longitude) spherical polar coordinates. Together, they fix a point on the 2-sphere and thereby determine the orientation of the z axis relative to the lab frame (or equivalently, the orientation of the x-y plane). This implies $\theta \in [0, \pi]$ while ϕ is defined modulo 2π. Having fixed θ and ϕ, the last Euler angle ψ is used to orient the x and y axes on the plane perpendicular to $\hat{z}$ via a rotation about $\hat{z}$. Consequently, ψ is defined modulo 2π.

In fact, the analogy with spherical polar coordinates is apt. Recall from Appendix B.1 that a single chart of spherical polar coordinates does not cover the whole of the 2-sphere, which is the rotational configuration space of a collinear rigid body. Similarly, a single chart of Euler angles do not quite cover the rotation group, which is the rotational configuration space of a noncollinear rigid body. For instance, spherical coordinates breakdown (are 'singular' or not one-to-one) at the North pole, where $\theta = 0$ but ϕ is ill-defined. In a similar vein, when the XY and xy planes coincide (i.e., if $z = \pm Z$), $\theta = 0$ or $\theta = \pi$ but ϕ and ψ are not uniquely defined, as the line of nodes is not defined[29]. In these cases, the angle between the X and x axes can be used to specify the angular orientation of xyz relative to XYZ.

Obtaining the body-fixed frame by rotating the lab frame. The body-fixed frame xyz may be obtained from the lab frame XYZ by a sequence of three rotations by the Euler angles about suitably chosen axes. Suppose the body-fixed frame initially coincides with the lab frame. Then we first rotate the body frame by an angle $0 \leq \phi < 2\pi$ counterclockwise about the Z axis. As a result, the rotated $\hat{x}$ will now point along the desired line of nodes while $\hat{z}$ continues to coincide with $\hat{Z}$ (see Fig. 8.6). Under such a rotation, the coordinates of a point $P = (X, Y, Z)$ in the lab frame are

---

[28] The name *line of nodes* has its origin in celestial mechanics. Consider the Earth with its equatorial plane (the XY plane). The Moon's orbit around the Earth defines its orbital plane, say the xy plane. The ascending node is where the orbit of the Moon intersects the Earth's equatorial plane as it goes from the southern to the northern celestial hemisphere. The descending node is where it intersects the equatorial plane on its way down. The line of nodes passes through these two nodes and lies along the intersection of the Moon's orbital plane and the Earth's equatorial plane.

[29] Gimbal lock refers to situations where the Euler angles are not uniquely defined.

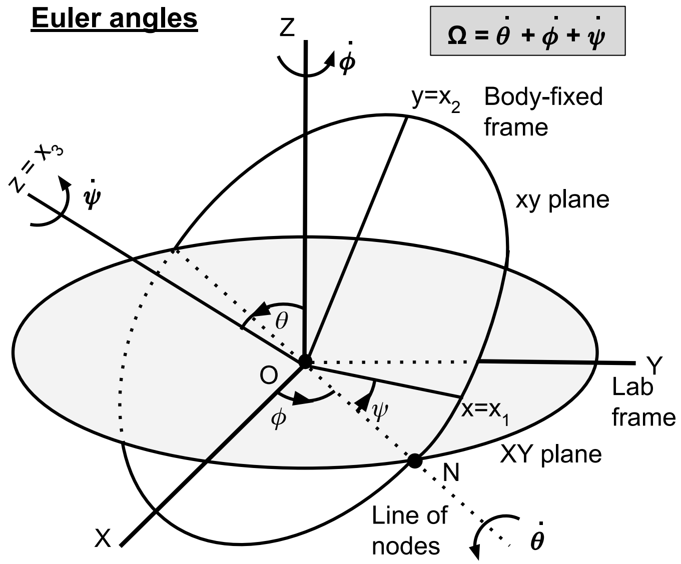

Figure 8.6: Euler angles and their time derivatives. The body-fixed frame xyz is obtained from the lab frame XYZ by a sequence of three rotations: (i) a counterclockwise rotation by angle ϕ about Z (ii) a counterclockwise rotation by angle θ about the new x axis (line of nodes), followed by (iii) a counterclockwise rotation by angle ψ about the new z axis.

now given in the new frame by (here, the superscript ^{t} denotes the transpose)

$$\begin{pmatrix} x' & y' & z' \end{pmatrix}^t = R^z_{-\phi} \begin{pmatrix} X & Y & Z \end{pmatrix}^t \tag{8.33}$$

where the rotation matrix[30] R^z_ϕ for a counterclockwise rotation is given in (8.36). Next, we rotate the body frame by an angle $0 \le \theta \le \pi$ counterclockwise about the new $\hat{x}$ axis (line of nodes). As a result of this, the new $\hat{z} = \hat{x}_3$ axis has reached its desired orientation. The coordinates of P with respect to the new axes are given by

$$\begin{pmatrix} x'' & y'' & z'' \end{pmatrix}^t = R^{x'}_{-\theta} \begin{pmatrix} x' & y' & z' \end{pmatrix}^t . \tag{8.34}$$

Finally, we rotate the body frame by an angle ψ counterclockwise about the new $\hat{z}$ axis. As a result, $\hat{x}$ moves off the XY plane and makes an angle ψ with the line of nodes, and reaches its desired orientation. The coordinates of the same point with respect to the moving frame become

$$\begin{pmatrix} x & y & z \end{pmatrix}^t = R^{z''}_{-\psi} R^{x'}_{-\theta} R^z_{-\phi} \begin{pmatrix} X & Y & Z \end{pmatrix}^t . \tag{8.35}$$

Now, the rotation matrices for counterclockwise rotations about the three axes are

$$R^z_\phi = \begin{pmatrix} \cos\phi & -\sin\phi & 0 \\ \sin\phi & \cos\phi & 0 \\ 0 & 0 & 1 \end{pmatrix}, \quad R^y_\theta = \begin{pmatrix} \cos\theta & 0 & \sin\theta \\ 0 & 1 & 0 \\ -\sin\theta & 0 & \cos\theta \end{pmatrix} \quad \text{and} \quad R^x_\theta = \begin{pmatrix} 1 & 0 & 0 \\ 0 & \cos\theta & -\sin\theta \\ 0 & \sin\theta & \cos\theta \end{pmatrix}. \tag{8.36}$$

---

[30] The appearance of $R^z_{-\phi}$ is because we are rotating the axes rather than the vector. Check by taking ϕ infinitesimal.

Thus, the lab and body-fixed coordinates are related by $(X\,Y\,Z)^t = R(x\,y\,z)^t$ where

$$R = R^z_\phi R^x_\theta R^z_\psi = \begin{pmatrix} \cos\phi\cos\psi - \cos\theta\sin\phi\sin\psi & -\cos\theta\cos\psi\sin\phi - \cos\phi\sin\psi & \sin\theta\sin\phi \\ \cos\psi\sin\phi + \cos\theta\cos\phi\sin\psi & \cos\theta\cos\phi\cos\psi - \sin\phi\sin\psi & -\cos\phi\sin\theta \\ \sin\theta\sin\psi & \cos\psi\sin\theta & \cos\theta \end{pmatrix} \tag{8.37}$$

for $0 \leq \theta \leq \pi$, $0 \leq \phi, \psi < 2\pi$. In effect, we have factorized any $R \in SO(3)$ as a product of three rotations about specially chosen axes, a result that goes back to Euler.

Example. What are the Euler angles corresponding to the identity element of $SO(3)$, $R = I$? From $R_{33} = 1$ we get $\theta = 0$, For $\theta = 0$ the above matrix reduces to $R = R^z_{\phi+\psi}$. Now $R^z_{\phi+\psi} = I$ iff $\phi + \psi$ is an integer multiple of 2π. Since $0 \leq \phi, \psi < 2\pi$, the only ways this can be satisfied are if $\theta = \phi = \psi = 0$ or $\theta = 0, \phi + \psi = 2\pi$. Thus, we have a 1-parameter family of Euler angles representing the identity rotation. In other words, Euler angles do not furnish a 1-1 coordinate system around the identity, they are 'singular' there. The situation is similar to that with polar coordinates (θ, ϕ) at the North pole of the 2-sphere, where $\theta = 0$ but ϕ can be any angle modulo 2π. □

8.10 Angular velocity and kinetic energy in terms of Euler angles

Angular velocity from generalized velocities. Now consider an infinitesimal rotation of the body (and comoving frame) that is made up of small increments $\delta\boldsymbol{\theta}, \delta\boldsymbol{\phi}, \delta\boldsymbol{\psi}$ in a small time δt. Here, $\delta\boldsymbol{\theta}$ denotes an infinitesimal rotation by angle $\delta\theta$ about a certain axis. From Fig. 8.6, we see that a small change in θ holding ϕ, ψ fixed is a rotation about the line of nodes. So we say that $\delta\boldsymbol{\theta}$ points along the line of nodes ON. Letting $\delta t \to 0$, $\dot{\boldsymbol{\theta}} = \dot\theta\,\hat{\text{ON}}$. Similarly, $\dot{\boldsymbol{\phi}}$ points along $\hat Z$ so $\dot{\boldsymbol{\phi}} = \dot\phi \hat Z$ and $\dot{\boldsymbol{\psi}} = \dot\psi\hat z$. We add up the effects of these three small rotations per unit time to get the angular velocity vector $\boldsymbol{\Omega} = \dot{\boldsymbol{\theta}} + \dot{\boldsymbol{\phi}} + \dot{\boldsymbol{\psi}}$ (recall from Sect. 8.2 that unlike finite rotations, infinitesimal rotations commute). Its components with respect to the corotating[31] frame xyz are denoted $\Omega_1, \Omega_2, \Omega_3$. We wish to express them in terms of the generalized velocities $\dot\theta, \dot\phi, \dot\psi$.

Let us denote by $\dot\theta_1, \dot\theta_2, \dot\theta_3$ the components of the vector $\dot{\boldsymbol{\theta}}$ in the three directions of the corotating xyz frame and similarly for $\dot\phi_i$ and $\dot\psi_i$; i.e., $\dot\theta_1 = \dot{\boldsymbol{\theta}} \cdot \hat x$, etc. Then by glancing (see below for an alternate approach) at Fig. 8.6 we determine the components:

$$\begin{aligned} \dot\theta_1 &= \dot\theta\cos\psi, \quad \dot\theta_2 = -\dot\theta\sin\psi \quad \text{and} \quad \dot\theta_3 = 0; \\ \dot\psi_1 &= \dot\psi_2 = 0 \quad \text{and} \quad \dot\psi_3 = \dot\psi \quad \text{while} \\ \dot\phi_1 &= \dot\phi\sin\theta\sin\psi, \quad \dot\phi_2 = \dot\phi\sin\theta\cos\psi \quad \text{and} \quad \dot\phi_3 = \dot\phi\cos\theta. \end{aligned} \tag{8.38}$$

In the last equation, we used the fact that $\hat Z$ is $\perp$ to the line of nodes. So the projection of $\dot{\boldsymbol{\phi}} \propto \hat Z$ onto the xy plane must also be perpendicular to the line of nodes. It follows that this projection makes an angle ψ with the y axis. Combining these, we get $\Omega_1 = \boldsymbol{\Omega}\cdot\hat x = (\dot{\boldsymbol{\theta}} + \dot{\boldsymbol{\phi}} + \dot{\boldsymbol{\psi}}) \cdot \hat x = \dot\theta_1 + \dot\phi_1 + \dot\psi_1$ etc:

$$\Omega_1 = \dot\theta\cos\psi + \dot\phi\sin\theta\sin\psi, \quad \Omega_2 = -\dot\theta\sin\psi + \dot\phi\sin\theta\cos\psi \quad \text{and} \quad \Omega_3 = \dot\psi + \dot\phi\cos\theta. \tag{8.39}$$

---

[31] The corotating frame need not be a principal axis frame. But we will soon choose it to be so, to keep the formulae simple.

See Prob. 8.13 for the converse.

Remark. It is possible to obtain (8.39) for the components of $\mathbf{\Omega}$ in the body frame using our formula (8.37) for the rotation R from lab to body frame. Indeed, let us define the angular velocity matrix[32] $\omega = R^{-1}\dot{R}$ in the body frame. Then $\mathbf{\Omega}$ is its 'dual' through contraction by the Levi-Civita symbol

$$\Omega_i = -(1/2)\epsilon_{ijk}\omega_{jk} \quad \text{or} \quad (\Omega_1, \Omega_2, \Omega_3) = -(\omega_{23}, \omega_{31}, \omega_{12}). \tag{8.40}$$

In fact, inverting (8.37) and using the Leibniz rule,

$$R^{-1} = R^z_{-\psi} R^x_{-\theta} R^z_{-\phi} \quad \text{and} \quad \dot{R} = R^z_{\dot{\phi}} R^x_{\theta} R^z_{\psi} + R^z_{\phi} R^x_{\dot{\theta}} R^z_{\psi} + R^z_{\phi} R^x_{\theta} R^z_{\dot{\psi}}. \tag{8.41}$$

Multiplying out the matrices, we find

$$\omega(t) = \begin{pmatrix} 0 & -\dot{\phi}\cos\theta - \dot{\psi} & \dot{\phi}\cos\psi\sin\theta - \dot{\theta}\sin\psi \\ \dot{\phi}\cos\theta + \dot{\psi} & 0 & -\dot{\theta}\cos\psi - \dot{\phi}\sin\theta\sin\psi \\ \dot{\theta}\sin\psi - \dot{\phi}\cos\psi\sin\theta & \dot{\theta}\cos\psi + \dot{\phi}\sin\theta\sin\psi & 0 \end{pmatrix}. \tag{8.42}$$

From this, we read off the components (8.39) of $\mathbf{\Omega}$. □

Rotational kinetic energy. Now, if x, y, z are taken to point along the principal axes of inertia, the formula for rotational kinetic energy (8.17) simplifies to $T = \frac{1}{2}\sum_j \mathcal{I}_j \Omega_j^2$, where $\mathcal{I}_j$ are the principal moments of inertia. We may substitute for $\Omega_{1,2,3}$ (8.39) to express the kinetic energy (of a generally *anisotropic rigid body*) in terms of the Euler angles and their time derivatives:

$$\begin{aligned} T_{\text{aniso}} &= \frac{\mathcal{I}_1}{2}\left(\dot{\theta}^2\cos^2\psi + \dot{\phi}^2\sin^2\theta\sin^2\psi + 2\dot{\theta}\dot{\phi}\sin\theta\sin\psi\cos\psi\right) \\ &\quad + \frac{\mathcal{I}_2}{2}\left(\dot{\phi}^2\sin^2\theta\cos^2\psi + \dot{\theta}^2\sin^2\psi - 2\dot{\theta}\dot{\phi}\sin\theta\cos\psi\sin\psi\right) \\ &\quad + \frac{\mathcal{I}_3}{2}\left(\dot{\psi}^2 + \dot{\phi}^2\cos^2\theta + 2\dot{\psi}\dot{\phi}\cos\theta\right). \end{aligned} \tag{8.43}$$

For a *symmetric top*, with $\mathcal{I}_1 = \mathcal{I}_2 \neq \mathcal{I}_3$ this simplifies

$$\begin{aligned} T_{\text{symm}} &= \frac{\mathcal{I}_1}{2}\left(\dot{\theta}^2 + \dot{\phi}^2\sin^2\theta\right) + \frac{\mathcal{I}_3}{2}\left(\dot{\psi} + \dot{\phi}\cos\theta\right)^2 \\ &= \frac{\mathcal{I}_1}{2}\left(\dot{\theta}^2 + \dot{\phi}^2\sin^2\theta\right) + \frac{\mathcal{I}_3}{2}\left(\dot{\psi}^2 + \dot{\phi}^2\cos^2\theta + 2\dot{\psi}\dot{\phi}\cos\theta\right). \end{aligned} \tag{8.44}$$

For a *spherical top* ($\mathcal{I}_1 = \mathcal{I}_2 = \mathcal{I}_3$), it further simplifies

$$T_{\text{sph top}} = \frac{1}{2}\mathcal{I}_1(\dot{\theta}^2 + \dot{\phi}^2 + \dot{\psi}^2 + 2\dot{\psi}\dot{\phi}\cos\theta). \tag{8.45}$$

---

[32] The formula $\omega = R^{-1}\dot{R}$ has a group theoretic meaning and is closely related to the Maurer-Cartan form of Appendix B.13*. A rotation matrix R defines a point on the rotational configuration space (the group $SO(3)$). The trajectory is a curve $R(t)$ while the entries of the tangent vector $\dot{R}$ are generalized velocities at $R(t)$. On the other hand, the angular velocity $\omega = R^{-1}\dot{R}$ is a tangent vector at the identity since it has been left-translated from R to the group identity via R^{-1}. Thus, ω lives in the Lie algebra $\mathfrak{so}(3)$ and must be an antisymmetric matrix (see Prob. 8.14). Finally, we use an isomorphism between the $\mathfrak{so}(3)$ and $\mathbb{R}^3$ Lie algebras (taking commutators of matrices to the (negative) cross product of vectors) (see Sect. 11.9.4*) to convert ω into the vector $\mathbf{\Omega}$ by contracting with the Levi-Civita symbol.

We could also obtain (8.44) for a *symmetric top* by a judicious choice of principal axes $x_1x_2x_3$. Let us choose the z axis along the third principal axis of inertia corresponding to $\mathcal{I}_3$. For a symmetric top with $\mathcal{I}_1 = \mathcal{I}_2$ we have the freedom of choosing the first two principal axes as any pair of orthogonal vectors perpendicular to $\hat{x}_3 = \hat{z}$. Let us choose (at the instant considered), the first principal axis $\hat{x}_1 = \hat{x}$ to point along the line of nodes ON. Then $\psi = 0$ at the instant considered (this does not mean $\dot{\psi}$ is zero!). $\hat{x}_2$ is then given by $\hat{x}_3 \times \hat{x}_1$. Equation (8.39) then gives, for a *symmetric top*:

$$\Omega_1 = \dot{\theta}, \quad \Omega_2 = \dot{\phi}\sin\theta \quad \text{and} \quad \Omega_3 = \dot{\psi} + \dot{\phi}\cos\theta. \tag{8.46}$$

Putting this in $\frac{1}{2}\sum_j \mathcal{I}_j\Omega_j^2$, we recover (8.44) for a symmetric top.

Rates of precession and spin for a symmetrical top $(\mathcal{I}_1 = \mathcal{I}_2)$**.** Let us now use these formulae in terms of Euler angles to find the rates of precession and spin of a freely rotating symmetrical top. As before, we assume $\boldsymbol{L} \propto \hat{Z}$ of the lab frame and choose the z axis of the corotating frame to point along the axis of the top. Then the rate at which the top spins on its axis is Ω_3. And the rate at which the axis of the top $(\hat{z})$ precesses about the angular momentum vector is equal to the rate at which the line of nodes goes round the $\hat{Z}$ axis, namely $\dot{\phi}$. We wish to express these rates in terms of L and θ. To introduce L, we first note that the components of angular momentum along the corotating axes are

$$L_1 = \mathcal{I}_1\Omega_1 = \mathcal{I}_1\dot{\theta}, \quad L_2 = \mathcal{I}_2\Omega_2 = \mathcal{I}_1\dot{\phi}\sin\theta, \quad L_3 = \mathcal{I}_3\Omega_3 = \mathcal{I}_3\left[\dot{\psi} + \dot{\phi}\cos\theta\right]. \tag{8.47}$$

On the other hand, since $\boldsymbol{L} \propto \hat{Z}$, its components along the corotating axes must be

$$L_1 = \boldsymbol{L}\cdot\hat{x} = 0, \quad L_2 = \boldsymbol{L}\cdot\hat{y} = L\sin\theta \quad \text{and} \quad L_3 = \boldsymbol{L}\cdot\hat{z} = L\cos\theta. \tag{8.48}$$

Comparing the two formulae, we get

$$\dot{\theta} = 0, \;\; \mathcal{I}_2\dot{\phi} = L \;\; \text{and} \;\; \mathcal{I}_3\left(\dot{\psi} + \dot{\phi}\cos\theta\right) = L\cos\theta \;\; \text{or} \;\; \dot{\psi} = L\cos\theta\left(\frac{1}{\mathcal{I}_3} - \frac{1}{\mathcal{I}_1}\right). \tag{8.49}$$

These relations are enough to give us an expression for the spinning rate Ω_3:

$$\text{rate of spin } = \boldsymbol{\Omega}\cdot\hat{z} = \Omega_3 = \frac{L_3}{\mathcal{I}_3} = \frac{L}{\mathcal{I}_3}\cos\theta. \tag{8.50}$$

The physical meaning of $\dot{\psi}$ will be revealed in Sect. 8.11. Meanwhile, we find the rate of precession, which turns out to be a constant:

$$\text{precession rate } = \Omega_{\text{pr}} = \dot{\phi} = \frac{L}{\mathcal{I}_2} = \frac{L}{\mathcal{I}_1}. \tag{8.51}$$

These formulae agree with what we obtained in Sect. 8.8. In particular, $0 = L_1 = \mathcal{I}_1\dot{\theta}$ so $\dot{\theta} = 0$: the axis of the symmetric top remains at a constant angle relative to $\boldsymbol{L}$.

8.11 Euler equations for a rigid body in body-fixed frame

As shown in Sect. 8.7, the EOM of a rigid body may be written as equations for the CM momentum $\boldsymbol{P} = M\boldsymbol{V}$ and the angular momentum $\boldsymbol{L} = \mathcal{I}\,\boldsymbol{\Omega}$ about the CM:

$$\frac{d\boldsymbol{P}}{dt} = \boldsymbol{F} = \sum\nolimits_a \boldsymbol{f}_a \quad \text{and} \quad \frac{d\boldsymbol{L}}{dt} = \boldsymbol{\tau} = \sum\nolimits_a \boldsymbol{r}_a \times \boldsymbol{f}_a \tag{8.52}$$

where $\boldsymbol{F}$ and $\boldsymbol{\tau}$ are the external force and external torque about the CM. Here, the rates of change of both $\boldsymbol{P}$ and $\boldsymbol{L}$ are measured with respect to an inertial observer (e.g., lab frame). Now, we wish to write these equations for the time evolution of the same vectors $\boldsymbol{P}$ and $\boldsymbol{L}$ but where their components are specified with respect to the (noninertial) comoving frame. The rotation of the frame imparts a time-dependence even to a vector that may be fixed in the lab frame, so we should expect the equations to look different.

Let $\boldsymbol{A}$ be a vector such as angular momentum or linear momentum of the rigid body or of a mass point. We wish to relate its time-dependence with respect to the lab frame to that in a frame rotating with instantaneous angular velocity $\boldsymbol{\Omega}$. If the vector is fixed in the rotating frame ($\dot{\boldsymbol{A}}_{\text{rot}} = 0$) then its time-dependence in the lab frame arises purely from the rotation and is given by $\dot{\boldsymbol{A}}_{\text{lab}} = \boldsymbol{\Omega} \times \boldsymbol{A}$. The reason is the same as the one we gave in deriving the equation $\boldsymbol{v} = \boldsymbol{\Omega} \times \boldsymbol{r}$ in (8.5). More generally, $\boldsymbol{A}$ may be changing with respect to the rotating frame as well. Combining these two[33],

$$\left(\frac{d\boldsymbol{A}}{dt}\right)_{\text{lab}} = \left(\frac{d\boldsymbol{A}}{dt}\right)_{\text{rot}} + \boldsymbol{\Omega} \times \boldsymbol{A}. \tag{8.53}$$

Thus, in the body-fixed frame, we have a system of six equations:

$$\dot{\boldsymbol{P}} + \boldsymbol{\Omega} \times \boldsymbol{P} = \boldsymbol{F} \quad \text{and} \quad \dot{\boldsymbol{L}} + \boldsymbol{\Omega} \times \boldsymbol{L} = \boldsymbol{\tau} \quad \text{where} \quad \boldsymbol{L} = \mathcal{I}\boldsymbol{\Omega}. \tag{8.54}$$

The dot denotes the time derivative of the components with respect to the comoving frame. Let us first focus on the evolution equation for $\boldsymbol{L}$, which was derived by Euler. In component form, the equations are related by cyclic permutation of indices:

$$\dot{L}_1 + (\Omega_2 L_3 - \Omega_3 L_2) = \tau_1, \quad \dot{L}_2 + (\Omega_3 L_1 - \Omega_1 L_3) = \tau_2, \quad \dot{L}_3 + (\Omega_1 L_2 - \Omega_2 L_1) = \tau_3. \tag{8.55}$$

The relation $L_i = \sum_j \mathcal{I}_{ij}\Omega_j$ is simplest in a principal axis frame, where $\mathcal{I}$ is diagonal. Therefore, we choose the axes of the corotating frame to point along the principal axes of inertia so that $L_i = \mathcal{I}_i \Omega_i$ for each $i = 1, 2, 3$. Assuming none of the principal moments of inertia vanish and defining $a_{ij} = \mathcal{I}_i^{-1} - \mathcal{I}_j^{-1}$, the Euler equations become the quadratically nonlinear ODEs

$$\dot{L}_1 + a_{23} L_2 L_3 = \tau_1, \quad \dot{L}_2 + a_{31} L_3 L_1 = \tau_2 \quad \text{and} \quad \dot{L}_3 + a_{12} L_1 L_2 = \tau_3. \tag{8.56}$$

In Prob. 8.24, we verify that the Euler equations can be written compactly as:

$$\dot{L}_i + \sum\nolimits_{j,k=1,2,3} \epsilon_{ijk} \frac{L_j L_k}{\mathcal{I}_j} = \tau_i \quad \text{for} \quad i = 1, 2, 3. \tag{8.57}$$

---

[33] One consequence is that $\left(\frac{d\boldsymbol{\Omega}}{dt}\right)_{\text{lab}} = \left(\frac{d\boldsymbol{\Omega}}{dt}\right)_{\text{rot}}$.

To find the evolution equations for the components of $\boldsymbol{\Omega}$ with respect to the body-fixed principal axes, we simply write $L_i = \mathcal{I}_i \Omega_i$ for each i in (8.56) to obtain

$$\begin{aligned} &\dot{\Omega}_1 + \left(\frac{\mathcal{I}_3 - \mathcal{I}_2}{\mathcal{I}_1}\right)\Omega_2\Omega_3 &=& \quad \tau_1, \quad \dot{\Omega}_2 + \left(\frac{\mathcal{I}_1 - \mathcal{I}_3}{\mathcal{I}_2}\right)\Omega_3\Omega_1 = \tau_2 \\ \text{and} \quad &\dot{\Omega}_3 + \left(\frac{\mathcal{I}_2 - \mathcal{I}_1}{\mathcal{I}_3}\right)\Omega_1\Omega_2 &=& \quad \tau_3. \end{aligned} \tag{8.58}$$

More generally, in a body-fixed frame,

$$\mathcal{I}_{ij}\frac{d\Omega_j}{dt} + (\boldsymbol{\Omega} \times \boldsymbol{L})_i = \tau_i. \tag{8.59}$$

Rate of change of kinetic energy. Recall that the kinetic energy of the rigid body is $T = (1/2)\mathcal{I}_{ij}\Omega_i\Omega_j$. Contracting (8.59) with Ω_i, we get

$$\mathcal{I}_{ij}\Omega_i\dot{\Omega}_j = \Omega_i\tau_i. \tag{8.60}$$

Using the symmetry of $\mathcal{I}$ and its constancy in a body-fixed frame, we recognize the left member as the rate of change of kinetic energy. Thus, we arrive at

$$\dot{T} = \boldsymbol{\Omega} \cdot \boldsymbol{\tau}. \tag{8.61}$$

This is the rotational analog of the formula $\dot{T} = \boldsymbol{v} \cdot \boldsymbol{F}$ for the rate of change of translational kinetic energy $T = (1/2)m\boldsymbol{v}^2$ of a point particle subject to a force $\boldsymbol{F}$.

Evolution of Euler angles. The Euler equations could be written as second order ODEs for the Euler angles by substituting for $\Omega_{1,2,3}$ in terms of $\dot{\theta}, \dot{\phi}$ and $\dot{\psi}$ using (8.39). But we could also regard them as first order equations specifying the evolution of the components of the angular momentum vector. Once the time evolution of L_i or Ω_i have been found, we would then find the time-dependence of the Euler angles by solving the 1st order equations (8.39). Knowledge of the Euler angles as functions of time would give us the orientation of the rigid body relative to the lab frame.

Coupling of rotational and translational motion. Let us now return to the full system of equations in (8.54). We begin by noting that the torque $\boldsymbol{\tau} = \sum_a \boldsymbol{r}_a \times \boldsymbol{f}_a$ on the RHS of the Euler equations in (8.54), depends on the instantaneous location and orientation of the body. The latter depends on the CM location $\boldsymbol{R}$, which must be determined from $\dot{\boldsymbol{R}} = \boldsymbol{P}$ by solving the momentum equations $\dot{\boldsymbol{P}} + \boldsymbol{\Omega} \times \boldsymbol{P} = \boldsymbol{F}$ in (8.54). Thus, the Euler equations in general are a complicated system that couple the rotational and translational motion. However, they simplify in the absence of external forces, in which case the equations for $\boldsymbol{L}$ *decouple* from those for $\boldsymbol{P}$. So for force-free motion, the three Euler equations for L_1, L_2, L_3 are a self-contained system of quadratically nonlinear ODEs for the rotational dynamics in the corotating principal axis frame. We will examine the physical and mathematical features of these equations in Sect. 8.12 and Sect. 8.14* and also solve them in Sect. 8.11 and Sect. 8.13*. There is another circumstance where the equations for a top simplify even in the presence of an external force (gravity), namely, when a point in the top is held fixed. This case for a heavy symmetrical top will be considered in Sect. 8.15.

Solving Euler's equations for force-free motion of a symmetric top

Let us consider the Euler equations (8.56) in the case of the free motion of a symmetric top with $0 < \mathcal{I}_1 = \mathcal{I}_2$. The axis of the top is the third principal axis, i.e., the z-axis of the comoving frame. Euler's equations become

$$\dot{L}_1 + aL_2L_3 = 0, \quad \dot{L}_2 - aL_3L_1 = 0 \quad \text{and} \quad \dot{L}_3 = 0 \quad \text{where} \quad a = \frac{1}{\mathcal{I}_1} - \frac{1}{\mathcal{I}_3}. \tag{8.62}$$

So L_3 is a constant while L_1 and L_2 obey the coupled equations

$$\dot{L}_1 + \omega L_2 = 0 \quad \text{and} \quad \dot{L}_2 - \omega L_1 = 0 \quad \text{where} \quad \omega = aL_3. \tag{8.63}$$

The general solutions depend on a multiplicative constant C and an additive phase δ

$$L_1 = C\cos(\omega t + \delta) \quad \text{and} \quad L_2 = C\sin(\omega t + \delta)\,. \tag{8.64}$$

Here, we may write $C^2 = L^2 - L_3^2$, where L^2 is the square of the magnitude of the angular momentum vector: $L_1^2 + L_2^2 + L_3^2 = L^2$, which has the same value in both lab and corotating frames. The motion of the angular momentum vector with respect to a frame fixed in the top is periodic in time. The component of $\boldsymbol{L}$ along the axis of the symmetric top is fixed while the component orthogonal to it rotates at an angular speed $|\omega|$.

Since $L_1 = \mathcal{I}_1\Omega_1, L_2 = \mathcal{I}_1\Omega_2$ and $L_3 = \mathcal{I}_3\Omega_3$, the same holds for the angular velocity vector, it rotates about the axis of the top at the constant rate $|\omega|$. In fact,

$$\Omega_3 = \frac{L_3}{\mathcal{I}_3} = \text{ constant}, \quad \Omega_1 = \frac{C}{\mathcal{I}_1}\cos(\omega t + \delta) \quad \text{and} \quad \Omega_2 = \frac{C}{\mathcal{I}_1}\sin(\omega t + \delta)\,. \tag{8.65}$$

In particular, Ω_3 is time-independent as is L_3. Seen from the body-fixed frame, the angular velocity vector $\boldsymbol{\Omega}$ precesses about the axis of the top at the angular rate $|\omega|$, sweeping out a so-called *body cone*[34] of opening angle $\arctan(C/\mathcal{I}_1\Omega_3)$. Similarly, the angular momentum vector $\boldsymbol{L}$ precesses about the axis of the top at the angular frequency $|\omega|$ and sweeps out a cone of constant opening angle $\theta = \arctan(C/L_3)$ where $C^2 = L^2 - L_3^2$. Combining (8.63) with (8.49) and (8.50), we deduce that $\omega = -\dot{\psi}$, which allows us to physically interpret $-\dot{\psi}$ as the rate at which $\boldsymbol{L}$ precesses around the z axis of the corotating frame. In hindsight, this is also evident in Fig. 8.6.

Earlier [in (8.50)], we found that $L_3 = L\cos\theta$ or $\Omega_3 = \frac{L}{\mathcal{I}_3}\cos\theta = \Omega_{\text{spin}}$, where θ is the Euler angle between the (constant) angular momentum vector in space and the instantaneous direction of the axis of the top. By both methods, we deduce that θ is independent of time. The axis of the top precesses at a constant angle around the fixed direction of angular momentum in the lab frame. If the angular velocity vector pointed along the axis of the top (i.e., if $C = 0$), then we would say that the top simply spun on its axis. For $C \neq 0$, the above solution describes the force-free motion of a top that is spinning on its own axis and precessing about an axis fixed in space. See Prob. 8.20 for the interesting limit in which a symmetrical top becomes a rigid rotator.

---

[34] The cone swept by $\boldsymbol{\Omega}$ relative to the inertial lab frame is called the space cone.

Finally, we observe that, the square of the length of the angular velocity vector is constant in time. To see this, we compute it in the comoving frame

$$\Omega^2 = \Omega_1^2 + \Omega_2^2 + \Omega_3^2 = \frac{C^2}{\mathcal{I}_1^2} + \frac{L_3^2}{\mathcal{I}_3^2} = \text{ constant.} \tag{8.66}$$

The *magnitude* of $\boldsymbol{\Omega}$ is of course the same in the corotating and lab frames, since rotations do not alter lengths of vectors.

Earth's torque-free precession. To first approximation, we may treat the Earth as a rigid body (ignoring the deformations due to tides and flows in its fluid interior). The Earth bulges out at the equator (see Sect. 1.5) and may be modeled as an oblate spheroid or ellipsoid of revolution: $\mathcal{I}_1 = \mathcal{I}_2 < \mathcal{I}_3$ where $\mathcal{I}_3$ is the moment of inertia about the axis of symmetry. Thus, we regard the Earth as a symmetric rigid body. The Earth's motion is of course subject to torques due to the Sun, Moon and other planets, but their effects on the rotational motion of the Earth are small and typically felt on long time scales [e.g., the axial precession (precession of the equinoxes) has a period of about 26,000 years]. So here we approximate the Earth's rotational dynamics as torque-free motion of a symmetric rigid body. The Earth spins on its axis about once per day. So from (8.50), $\Omega_3 = \Omega_{\text{spin}} \approx 2\pi/(1 \text{ day})$. Now, from (8.63), the angular speed ω at which the angular velocity vector of the Earth precesses about its axis (as viewed from the Earth) is given by $\omega = \Omega_3(\mathcal{I}_3 - \mathcal{I}_1)/\mathcal{I}_1$. For the Earth, $(\mathcal{I}_3 - \mathcal{I}_1)/\mathcal{I}_1 \approx 1/306$ [notice that this precession is absent if the Earth is a spherical top]. Thus, $\boldsymbol{\Omega}$ is expected to sweep out a cone about once every 306 days (this 'body cone' is about 10m wide on the Earth's surface). This precession was predicted by Euler (1749) but not detected for over a century since the period turned out to be somewhat larger as the Earth is not quite a rigid body. A 430 day precession was eventually detected by Chandler in 1891 ('Chandler wobble'). Much of the difference was explained by Simon Newcomb by estimating the effects due to the deformability of the Earth. Interestingly, Chandler discovered this wobble by looking for a periodicity in existing data. He succeeded where his predecessors failed as he did not restrict his attention solely to the period predicted by Euler. □

8.12 Ellipsoid of inertia and qualitative description of free motion of rigid body

Here, we describe a geometric approach to understanding the Euler equations (8.56) for the components of $\boldsymbol{L}$ in a corotating frame during torque-free motion of a generally anisotropic rigid body. We begin by noting that the rotational kinetic energy $T = \frac{1}{2}\mathcal{I}_{ij}\Omega_i\Omega_j$ is simplest in the principal axis basis:

$$T = \frac{L_1^2}{2\mathcal{I}_1} + \frac{L_2^2}{2\mathcal{I}_2} + \frac{L_3^2}{2\mathcal{I}_3}. \tag{8.67}$$

For torque-free motion, the rotational kinetic energy is constant in time:

$$\dot{T} = \frac{L_1\dot{L}_1}{\mathcal{I}_1} + \frac{L_2\dot{L}_2}{\mathcal{I}_2} + \frac{L_3\dot{L}_3}{\mathcal{I}_3} = -L_1L_2L_3\left(\frac{a_{23}}{\mathcal{I}_1} + \frac{a_{31}}{\mathcal{I}_2} + \frac{a_{12}}{\mathcal{I}_3}\right) = 0. \tag{8.68}$$

Similarly, the square of angular momentum $L^2 = L_1^2 + L_2^2 + L_3^2$ is conserved:

$$\begin{aligned} \frac{1}{2}\frac{dL^2}{dt} &= L_1\dot{L}_1 + L_2\dot{L}_2 + L_3\dot{L}_3 \\ &= -L_1(a_{23}L_2L_3) - L_2(a_{31}L_3L_1) - L_3(a_{12}L_1L_2) \\ &= -L_1L_2L_3(a_{23} + a_{31} + a_{12}) = 0. \end{aligned} \tag{8.69}$$

Unlike for the symmetric top of (8.66), Ω^2 is in general *not* conserved for force-free motion of an anisotropic top. Indeed, from (8.58) we find that

$$\frac{d\Omega^2}{dt} = 2\Omega_1\Omega_2\Omega_3\left(\frac{\mathcal{I}_2 - \mathcal{I}_3}{\mathcal{I}_1} + \frac{\mathcal{I}_3 - \mathcal{I}_1}{\mathcal{I}_2} + \frac{\mathcal{I}_1 - \mathcal{I}_2}{\mathcal{I}_3}\right). \tag{8.70}$$

The RHS clearly vanishes for a symmetric top, where two among $\mathcal{I}_1, \mathcal{I}_2$ and $\mathcal{I}_3$ are equal. However, for an anisotropic top, the RHS is generally nonzero, as the simple example $\mathcal{I}_1 = 1, \mathcal{I}_2 = 2, \mathcal{I}_3 = 3$ demonstrates.

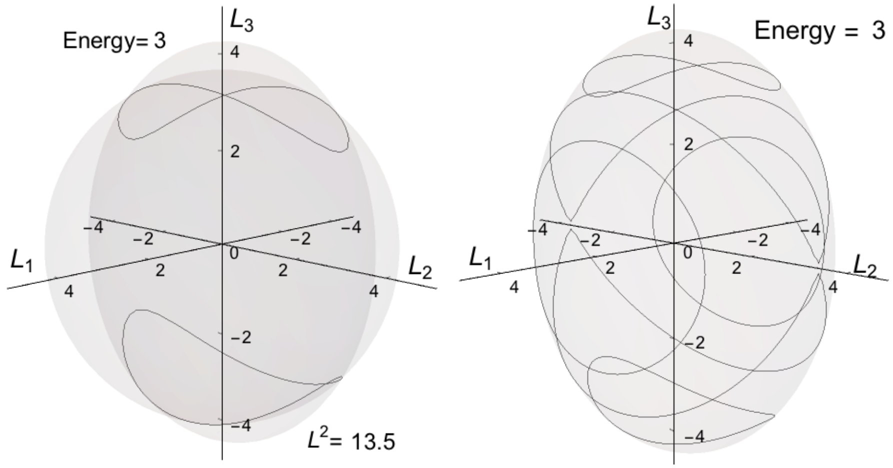

(a) Inertia ellipsoid, L^2 sphere (b) Trajectories on the inertial ellipsoid

Figure 8.7: (a) Intersection of energy ellipsoid and angular momentum sphere. (b) Trajectories of Euler equations on an energy level surface (inertia ellipsoid). Both figures are for $\mathcal{I}_1 = 1, \mathcal{I}_2 = 2, \mathcal{I}_3 = 3$ so that the first principal axis of the inertia ellipsoid is the shortest. The locus of the angular momentum vector with respect to the corotating principal axis frame $x_1 = L_1, x_2 = L_2, x_3 = L_3$ is shown. The simplest trajectories are the six points of intersection of the ellipsoid with the principal axes. These correspond to situations where $\boldsymbol{L}$ always points along one of the principal axes (this principal axis is then fixed in the lab frame as well) and describe a top spinning about that principal axis. [To get an idea of how the top behaves in the lab frame, one can imagine going to a frame where $\boldsymbol{L}$ is fixed and visualize how the principal axes (which are fixed in the body) rotate.] More generally, $\boldsymbol{L}$ traces out a closed curve that is centered around either the first or third axis. There are no such closed curves around the middle axis. This means rotation about the shortest and longest principal axes are stable while rotation about the second axis is unstable. In the latter case, the slightest perturbation will typically push $\boldsymbol{L}$ to a trajectory where it makes a large circuit around either the first or third axes. Notice the four limiting infinite period separatrix trajectories when $L^2 = 2E\mathcal{I}_2$ that begin and end at the points where the inertia ellipsoid intersects the second axis.

Thus, we have two conserved quantities among the three angular momentum components. We may use these to visualize the trajectories in the 3d phase space of angular momenta $\mathbb{R}^3$ with Cartesian coordinates L_1, L_2, L_3, as shown in Fig. 8.7. The conservation of total angular momentum implies that the trajectory must lie on the angular momentum sphere $L_1^2 + L_2^2 + L_3^2 = L^2$. The radius of the sphere is determined by the initial magnitude of the angular momentum vector. In addition, conservation of rotational kinetic energy implies that the trajectory must lie on an ellipsoid $H = \sum_i \frac{L_i^2}{2\mathcal{I}_i} = E$ with E determined by ICs. The semiaxes of this *ellipsoid of inertia* are $\sqrt{2E\mathcal{I}_i}$ for $i = 1, 2, 3$. Without loss of generality, let us assume that $\mathcal{I}_1 \leq \mathcal{I}_2 \leq \mathcal{I}_3$ so that $\mathcal{I}_1^{-1} \geq \mathcal{I}_2^{-1} \geq \mathcal{I}_3^{-1}$. Then we see that the energy satisfies the inequalities

$$\frac{L^2}{2\mathcal{I}_3} \leq E \leq \frac{L^2}{2\mathcal{I}_1} \quad \text{and consequently} \quad \sqrt{2E\mathcal{I}_1} \leq L \leq \sqrt{2E\mathcal{I}_3}. \tag{8.71}$$

These inequalities imply that the energy ellipsoid and angular momentum sphere always have nonempty intersection. In other words, the radius of the angular momentum sphere lies between the smallest and largest semiaxes of the ellipsoid of inertia.

Curves traced by tip of $\boldsymbol{L}$. As indicated in Fig. 8.7, the two quadric surfaces typically intersect along pairs of closed curves or points. Each such intersection set is a union of possible trajectories of the angular momentum vector, for given L^2 and E. This is similar to the double-well potential of Fig. 7.6, where energy level sets were often unions of two trajectories, each centered around one of the wells. Here, the two could correspond to clockwise and counterclockwise rotation. Let us find the types of curves traced out by the tip of the angular momentum vector.

There are six stationary points corresponding to: $L_{1,2,3} = \pm\sqrt{2E\mathcal{I}_{1,2,3}}$ with the other two components vanishing and with energy $E = L^2/2\mathcal{I}_{1,2,3}$. Verify that these are static solutions of (8.56). We will soon see that they correspond with steady rotation of the top about each principal axis.

More generally, suppose we keep E fixed and imagine varying L. When $L^2 = 2E\mathcal{I}_1$, there are two points of intersection, at $L_1 = \pm\sqrt{2E\mathcal{I}_1}, L_2 = L_3 = 0$. So the angular momentum vector is static in the comoving frame. It always points along (or opposite to) the principal axis (x_1-axis) corresponding to the smallest principal moment of inertia $\mathcal{I}_1$. It follows that $\Omega_1 = \sqrt{2E/\mathcal{I}_1}, \Omega_2 = \Omega_3 = 0$ so the angular velocity is constant and always along the x_1 principal axis of the body-fixed frame. We will see that this motion is stable in the sense that a small change in E or L results in a trajectory that always remains close to this one.

As L is increased slightly, the angular momentum sphere intersects the inertia ellipsoid in a pair of small closed curves encircling the L_1 axis (see the curves around the L_1 axis in Fig. 8.7b). So the static solutions of the previous paragraph (rotation of the body about the L_1 ($\pm x_1$) axis) are stable. The present solutions correspond to a time-dependent $\boldsymbol{L}$ in the body-fixed frame, whose terminus precesses around the $\pm x_1$-principal axis. Thus, the $\boldsymbol{L}$ vector relative to the body is periodic in time, it sweeps out a conical surface. The angular momentum vector relative to space is of course constant.

As $L^2 \to 2E\mathcal{I}_2$, the curves of intersection become larger and at $L^2 = 2E\mathcal{I}_2$, they are a pair of large ellipses that intersect at the points where the inertia ellipsoid meets the x_2 axis. $L_2 = \pm\sqrt{2E\mathcal{I}_2}, L_1 = L_3 = 0$ are static solutions corresponding to rotation about the $\pm x_2$-principal axis corresponding to the middle principal moment of inertia. However, rotation about the middle principal axis is unstable, since a small change in E or L^2 results in a trajectory that is not always close to $L_2 = \pm\sqrt{2E\mathcal{I}_2}$. The complement of these two static solutions in the pair of intersecting ellipses results in 4 separatrices. They separate the regions of phase space corresponding (broadly) to oscillations about rotation of the top about the largest and smallest principal axes.

As L^2 goes from $2E\mathcal{I}_2$ to $2E\mathcal{I}_3$, the curves of intersection shrink to a pair of closed curves around the x_3-axis and eventually end at the pair of static solutions $L_1 = L_2 = 0, L_3 = \pm\sqrt{2E\mathcal{I}_3}$ corresponding to stable rotation about the $\pm x_3$-axis.

All trajectories other than the separatrices are closed curves, so the motion on phase space of angular momenta is almost always periodic. While static solutions have a period zero (on the angular momentum phase space), we can interpret separatrices as trajectories with divergent period (as in the pendulum and double well problems of Eq. (7.34) and Sect. 7.4).

Instability in the rotation of a cuboid. A rapidly spun cuboid-shaped chalkboard duster (or tennis racquet) displays the above stability while rotating about its principal axes corresponding to its largest and smallest principal moments of inertia. One can stably get the duster to spin about either of these axes. On the other hand, it is not possible to get the duster to spin stably about its middle principal axis due to the above instability. [Hold the duster with two hands at the ends of the longest axis, which is oriented horizontally. Spin it about the longest axis while letting it go. The duster will of course drop to the floor, but if one watches carefully, one notices that the duster continues to spin about the long axis as it falls. Repeat the experiment while spinning it about the other two axes.] For instance, when spun about the middle axis, a small change in L^2 holding the energy fixed takes the angular momentum vector in the corotating frame to one of the large amplitude periodic orbits around one of the other axes (see Fig. 8.7b). This perturbed orbit is nearly a separatrix orbit that connects the unstable solutions $(L_1 = 0, L_2 = \pm\sqrt{2E\mathcal{I}_2}, L_3 = 0)$. In practice, this instability leads to interesting dynamical behavior: the body appears to repeatedly flip between roughly spinning clockwise and counterclockwise about the middle principal axis. This twisting phenomenon is called the **Dzhanibekov effect**, after a Russian cosmonaut who observed it in a spinning wing-nut aboard a space station in 1985. Of course, a spinning duster is not free but subject to the gravitational force of the Earth, which induces some coupling between the translational and rotational motion through the external torque (as discussed at the end of Sect. 8.11). It is also subject to damping. However, as long as the kinetic energy of rotation is large, we would expect to be able to ignore the effects of gravity and dissipation on the qualitative rotational behavior discussed above. This is confirmed by experiments on Earth and even more dramatically in 'microgravity' environments, such as a space station in free fall.

$*$ **Poinsot's characterization of torque-free motion.** Poinsot used the conservation of rotational kinetic energy $T = \frac{1}{2}\boldsymbol{\Omega}^t\mathcal{I}\boldsymbol{\Omega} = \frac{1}{2}\boldsymbol{L}\cdot\boldsymbol{\Omega}$ and the angular momentum vector $\boldsymbol{L} = \mathcal{I}\boldsymbol{\Omega}$ in space to describe the curve (called a polhode[35]) traced by the tip of the angular velocity vector $\boldsymbol{\Omega}$ on the inertia ellipsoid. In short, polhodes are curves traced by the point of contact as the inertia ellipsoid (with center fixed at the origin) rolls without slipping on the invariable plane. The latter is a fixed plane orthogonal to the conserved angular momentum vector $\boldsymbol{L}$. Let us see how this comes about. For the purposes of this discussion, we *define* the inertia ellipsoid as the set of points $\boldsymbol{\Omega}$ such that $(1/2)\boldsymbol{\Omega}^t\mathcal{I}\boldsymbol{\Omega} = T$ for fixed T. We imagine the inertia ellipsoid as being fixed in the body and participating in its motion. Now, at a time t when the angular velocity vector is $\boldsymbol{\Omega}$, the normal $\boldsymbol{n}$ to the inertia ellipsoid at the point $\boldsymbol{\Omega}$ points along the vector

---

[35] The term polhode meaning 'path of pole' (in Greek) was introduced by Louis Poinsot (1834) to describe the wobbling of the Earth about its rotation axis (see Sect. 8.11).

$$\boldsymbol{\nabla}((1/2)\boldsymbol{\Omega}^t\mathcal{I}\boldsymbol{\Omega}) = \mathcal{I}\boldsymbol{\Omega} = \boldsymbol{L}. \tag{8.72}$$

Since $\boldsymbol{n} \propto \boldsymbol{L}$, the tangent plane to the inertia ellipsoid at the point $\boldsymbol{\Omega}$ at the instant t is orthogonal to the fixed vector $\boldsymbol{L}$. In fact, we may show that the tangent plane is a fixed 'invariable' plane by establishing that its perpendicular distance d from the origin is independent of time. Indeed,

$$d = (\boldsymbol{L}/L) \cdot \boldsymbol{\Omega} = (2T/L). \tag{8.73}$$

Since L and T are conserved, so is d. Consequently, the tangent plane to the inertia ellipsoid (at the point $\boldsymbol{\Omega}$ where the instantaneous axis of rotation intersects it) is fixed in space. Thus, we have shown that as the rigid body rotates, the inertia ellipsoid (with center fixed at the origin) rolls without slipping on the invariable plane (see the figures in [54, 125]). The locus of the point of contact on the inertia ellipsoid is called the polhode while the locus of the point of contact on the invariable plane is called the herpolhode. Polhodes are generally connected closed curves (much like the loci of $\boldsymbol{L}$ in Fig. 8.7b) and consist of points on the inertia ellipsoid at which the tangent plane is at a constant distance d from the center. Herpolhodes are generally not closed curves, but fill annular regions (use your imagination of a rolling ellipsoid with fixed center to draw a figure). For torque-free motion of a symmetric top, Ω (8.66) becomes independent of time and polhodes are circles centered on the symmetry axis while herpolhodes reduce to circles on the invariable plane. In this case, by definition, they are the intersections of the body and space cones (swept by $\boldsymbol{\Omega}$) with the inertia ellipsoid and invariable plane respectively (see Sect. 8.11).

$*$ **Invariant tori from lab frame.** An anisotropic rigid body has three rotational degrees of freedom, its configuration space is the rotation group in three dimensions $SO(3)$ which may be parametrized by Euler angles. The corresponding phase space is six-dimensional, being parametrized by the Euler angles (generalized coordinates θ, ϕ, ψ) and their conjugate momenta p_θ, p_ϕ, p_ψ (see Prob. 8.22). For force-free rotational motion in this 6d phase space, we have four independent conserved quantities, the three components of angular momentum with respect to the lab frame and energy. Initial conditions fix their values $L_1 = \ell_1, L_2 = \ell_2, L_3 = \ell_3$ and $H = E$. Time evolution of the phase point (for given initial conditions) must therefore lie on the intersection of the level hypersurfaces of these four conserved quantities. This common level set is generically a 2d surface in the 6d phase space. It can be argued[36] that each connected component of this surface is a torus (surface of a vada/doughnut) since it must be compact[37] and admit a nonvanishing tangent vector field (the Hamiltonian vector field, which must be nonvanishing if $E > 0$). It is called an *invariant torus* since under time evolution, the phase point remains on the torus. For different constants ℓ_i, E, we get different tori, which together foliate the 6d phase space (see Sect. 11.7* for more on invariant tori). ☐

---

[36] The 2-sphere S^2 is compact and connected but does not admit a nonvanishing vector field: it is not possible to comb hair of nonzero length on a sphere (see Fig. B.5b). It can be shown

8.13* Solution of force-free Euler equations using Jacobi elliptic functions

Recall the Euler equations (8.56) for the components of $\boldsymbol{L}$ for force-free motion of an anisotropic rigid body in the corotating principal axis basis:

$$\dot{L}_1 = -a_{23} L_2 L_3, \quad \dot{L}_2 = -a_{31} L_3 L_1 \quad \text{and} \quad \dot{L}_3 = -a_{12} L_1 L_2. \tag{8.74}$$

Here, the constants $a_{ij} = \frac{1}{\mathcal{I}_i} - \frac{1}{\mathcal{I}_j}$. These equations bear a close resemblance to the three differential equations (7.15) for Jacobi elliptic functions:

$$\begin{aligned} \operatorname{sn}'(\tau,k) &= \operatorname{cn}(\tau,k)\operatorname{dn}(\tau,k), \quad \operatorname{cn}'(\tau,k) = -\operatorname{sn}(\tau,k)\operatorname{dn}(\tau,k) \\ \text{and} \quad \operatorname{dn}'(\tau,k) &= -k^2 \operatorname{sn}(\tau,k)\operatorname{cn}(\tau,k). \end{aligned} \tag{8.75}$$

However, while the former are manifestly symmetric under cyclic permutations $1 \to 2 \to 3 \to 1$, the latter do not quite display this symmetry. In fact, for any given anisotropic rigid body, the order of sizes of the principal moments of inertia breaks the cyclic symmetry. For definiteness, we may suppose that $\mathcal{I}_3 \geq \mathcal{I}_2 \geq \mathcal{I}_1$[38] (though the formulae given below also work for the opposite order). It is then possible to rescale time so that $L_{1,2,3}$ become proportional to cn, sn and dn if $L^2 \geq 2E\mathcal{I}_2$ (or dn, sn and cn if $L^2 \leq 2E\mathcal{I}_2$) for an appropriate elliptic modulus k. In fact, if $L^2 \geq 2E\mathcal{I}_2$, the reader is invited to verify that

$$\begin{aligned} L_1 &= \sqrt{\frac{\mathcal{I}_1(2E\mathcal{I}_3 - L^2)}{\mathcal{I}_3 - \mathcal{I}_1}} \operatorname{cn}(\tau,k), \quad L_2 = \sqrt{\frac{\mathcal{I}_2(2E\mathcal{I}_3 - L^2)}{\mathcal{I}_3 - \mathcal{I}_2}} \operatorname{sn}(\tau,k) \\ \text{and} \quad L_3 &= \sqrt{\frac{\mathcal{I}_3(L^2 - 2E\mathcal{I}_1)}{\mathcal{I}_3 - \mathcal{I}_1}} \operatorname{dn}(\tau,k) \end{aligned} \tag{8.76}$$

where

$$\tau = \gamma t \;\text{ with }\; \gamma = \sqrt{\frac{(\mathcal{I}_3 - \mathcal{I}_2)(L^2 - 2E\mathcal{I}_1)}{\mathcal{I}_1\mathcal{I}_2\mathcal{I}_3}} \quad \text{and} \quad k^2 = \frac{(\mathcal{I}_2 - \mathcal{I}_1)(2E\mathcal{I}_3 - L^2)}{(\mathcal{I}_3 - \mathcal{I}_2)(L^2 - 2E\mathcal{I}_1)}. \tag{8.77}$$

---

that a compact connected orientable surface with a nonvanishing vector field must be a torus. One can use the Liouville volume element (see Footnote 14 of Sect. 10.8) on the phase space to define an orientation for these 2d surfaces.

[37] Compact means closed and bounded. The surface is bounded since the Euler angles are bounded variables and the momenta cannot become unbounded as the kinetic energy is quadratic in velocities. It is closed since it is the intersection of inverse images of closed sets (single points) under continuous maps $L_1^{-1}(\ell_1) \cap L_2^{-1}(\ell_2) \cap L_3^{-1}(\ell_3) \cap H^{-1}(E)$.

[38] The radius of the L-sphere must lie between the smallest and largest semiaxes of the inertia ellipsoid, so $2E\mathcal{I}_1 \leq L^2 \leq 2E\mathcal{I}_3$ if $\mathcal{I}_1 \leq \mathcal{I}_2 \leq \mathcal{I}_3$.

The origin of time has been chosen[39] so that $L_2 = 0$ at $t = 0$. In Prob. 8.25, we show that $0 \le k^2 \le 1$. On the other hand, when $L^2 \le 2E\mathcal{I}_2$, we have

$$\begin{aligned} L_1 &= \sqrt{\frac{\mathcal{I}_1(2E\mathcal{I}_3 - L^2)}{\mathcal{I}_3 - \mathcal{I}_1}}\,\mathrm{dn}(\tau, k), \quad L_2 = \sqrt{\frac{\mathcal{I}_2(L^2 - 2E\mathcal{I}_1)}{\mathcal{I}_2 - \mathcal{I}_1}}\,\mathrm{sn}(\tau, k) \\ \text{and} \quad L_3 &= \sqrt{\frac{\mathcal{I}_3(L^2 - 2E\mathcal{I}_1)}{\mathcal{I}_3 - \mathcal{I}_1}}\,\mathrm{cn}(\tau, k) \end{aligned} \tag{8.78}$$

where

$$\tau = \gamma t \ \text{ with } \ \gamma = \sqrt{\frac{(\mathcal{I}_2 - \mathcal{I}_1)(2E\mathcal{I}_3 - L^2)}{\mathcal{I}_1\mathcal{I}_2\mathcal{I}_3}} \quad \text{and} \quad k^2 = \frac{(\mathcal{I}_3 - \mathcal{I}_2)(L^2 - 2E\mathcal{I}_1)}{(\mathcal{I}_2 - \mathcal{I}_1)(2E\mathcal{I}_3 - L^2)}. \tag{8.79}$$

The formulae for L_2, γ and k^2 in the two cases are related by $1 \leftrightarrow 3$ exchange while those for L_1 and L_3 are related by $\mathrm{cn} \leftrightarrow \mathrm{dn}$.

Example. Obtain (8.76) and (8.77) from the Euler equations. Comparing (8.74) with (8.75), we suppose that

$$L_1 = c_1\,\mathrm{cn}(\tau, k), \quad L_2 = c_2\,\mathrm{sn}(\tau, k) \quad \text{and} \quad L_3 = c_3\,\mathrm{dn}(\tau, k). \tag{8.80}$$

Other choices related by permutations are possible. We need to fix the five constants $c_{1,2,3}, \gamma$ and k in terms of $\mathcal{I}_{1,2,3}$, E and L^2. Putting (8.80) in the Euler equations and using (8.75) we get three algebraic conditions

$$\gamma c_1 = a_{23}c_2c_3, \quad \gamma c_2 = -a_{31}c_3c_1 \quad \text{and} \quad -\gamma k^2 c_3 = -a_{12}c_1c_2. \tag{8.81}$$

In addition, evaluating L^2 and E at $t = 0$ gives two quadratic relations:

$$c_1^2 + c_3^2 = L^2 \quad \text{and} \quad c_1^2/2\mathcal{I}_1 + c_3^2/2\mathcal{I}_3 = E. \tag{8.82}$$

They may be solved along with the quotient of the first two equations in (8.81) to get

$$c_1^2 = \frac{2E\mathcal{I}_3 - L^2}{\mathcal{I}_3 a_{13}}, \quad c_3^2 = \frac{L^2 - 2E\mathcal{I}_1}{\mathcal{I}_1 a_{13}} \quad \text{and} \quad c_2^2 = \frac{a_{13}}{a_{23}}c_1^2 = \frac{(2E\mathcal{I}_3 - L^2)}{\mathcal{I}_3 a_{23}} \tag{8.83}$$

as in (8.76). Putting these three back in (8.81) we get [in agreement with (8.77)],

$$\gamma^2 = \frac{a_{23}(L^2 - 2E\mathcal{I}_1)}{\mathcal{I}_1} \quad \text{and} \quad k^2 = \frac{\mathcal{I}_1 a_{12}}{\mathcal{I}_3 a_{23}}\frac{(2E\mathcal{I}_3 - L^2)}{(L^2 - 2E\mathcal{I}_1)}. \tag{8.84}$$

---

[39] In almost all solutions, there is a time where $L_2 = 0$. Exceptional solutions where L_2 is never zero cannot be represented this way. One could permute the elliptic functions to allow for some such solutions. An extreme case is a static solution of a spherical top with $L_1L_2L_3 \neq 0$ (i.e., with none of them zero), in which case there is no need to use elliptic functions. See Prob. 8.26 and Prob. 8.27.

Remarks: When the rigid body becomes a symmetric top [e.g., when $(\mathcal{I}_1 = \mathcal{I}_2)$ and $a_{12} \to 0$] the elliptic modulus $k \to 0$ and the elliptic functions reduce to trigonometric functions (see Sect. 7.2* and Prob. 8.26) and we recover the sinusoidal solutions of Sect. 8.11. Remarkably, the solutions of Euler's equations (8.74) are periodic even when the body is anisotropic. As we learned in Sect. 7.3*, the Jacobi elliptic functions are periodic with period given by four times the complete elliptic integral of the first kind (7.25). Thus, after a time $T = 4K(k)/\gamma$, the angular momentum and velocity vectors $\boldsymbol{L}$ and $\boldsymbol{\Omega}$ return to their initial directions relative to the corotating frame. However, in the anisotropic case, the motion of the top itself is not periodic. It can be shown (see Sect. 37 of [83] and Chap. VI of [133]) that while the Euler angles θ and ψ are periodic with the same period T, ϕ is only quasiperiodic [it evolves via a superposition of two periodic motions with periods T and T' which are incommensurate, see Footnote 24 of Chap. 2]. ☐

8.14* Poisson bracket formulation of Euler's equations

In Sect. 8.12, we addressed the qualitative nature and interpretation of solutions to the Euler equations (8.74) for torque-free motion of a generally anisotropic rigid body in the corotating principal axis frame. Analytic solutions in terms of Jacobian elliptic functions were obtained in Sect. 8.13*. Here, we turn to the Hamiltonian formulation of these equations, which reveals certain elegant structural features. The rigid body furnishes a simple physical example where noncanonical and degenerate Poisson structures, Casimir invariants and symplectic leaves play an essential role. These concepts (and their quantum counterparts) are useful in other physical systems like ideal fluids and the field theories of particle physics where pictorial or analytical solutions are typically not available.

The phase space we will deal with for the Euler equations is the angular momentum state space $\mathbb{R}^3$ of Sect. 3.26* with Cartesian coordinates L_1, L_2 and L_3, which are the components of $\boldsymbol{L}$ in the corotating frame. They satisfy the familiar angular momentum PBs[40] (3.129):

$$\{L_x, L_y\} = L_z \quad \text{and cyclic permutations,} \quad \text{or} \quad \{L_i, L_j\} = r_{ij}(L) = \epsilon_{ijk} L_k. \tag{8.85}$$

To obtain Euler's equations (8.74) (in the absence of external torques) we need to specify the Hamiltonian. It is natural to take the conserved kinetic energy (8.67) as Hamiltonian:

$$H = \frac{L_1^2}{2\mathcal{I}_1} + \frac{L_2^2}{2\mathcal{I}_2} + \frac{L_3^2}{2\mathcal{I}_3} = \sum\nolimits_j \frac{L_j L_j}{2\mathcal{I}_j}. \tag{8.86}$$

---

[40] Here, we are not particular about the up-down placement of indices, though repeated indices are summed. Strictly speaking, the components of angular momentum should be written L^i and the PB algebra should be written $\{L^i, L^j\} = r^{ij} = \epsilon^{ij}{}_k L^k$ while $H = \frac{1}{2}\mathcal{I}_{ij} L^i L^j$.

Hamilton's equations that follow[41] are then seen to agree with (8.57):

$$\dot{L}_i = -\{L_i, H\} = \left\{L_i, \sum\nolimits_j \frac{L_j L_j}{2\mathcal{I}_j}\right\} = \frac{L_j}{2\mathcal{I}_j}\{L_i, L_j\} = \sum_{jk} \epsilon_{ijk} \frac{L_j L_k}{\mathcal{I}_j}. \tag{8.87}$$

The Casimir invariant L^2. What is the nature of the other conserved quantity $L^2 = L_1^2 + L_2^2 + L_3^2$? Interestingly, we find that L^2 Poisson commutes with all the three coordinates on phase space:

$$\{L^2, L_j\} = 2L_i\{L_i, L_j\} = 2L_i\epsilon_{ijk}L_k = 0 \quad \text{for} \quad j = 1, 2, 3. \tag{8.88}$$

This vanishes since ϵ_{ijk} is antisymmetric under $i \leftrightarrow k$ while $L_i L_k$ is symmetric (see Prob. 8.29). By the Leibniz rule, this means L^2 commutes with any observable $f(L)$:

$$\{L^2, f(L)\} = \frac{\partial f}{\partial L_i}\{L^2, L_i\} = 0. \tag{8.89}$$

This makes L^2 (or any nonconstant function of L^2) very special: is it called a Casimir invariant or a Casimir for short[42]. If we think of $f(L)$ as a possible Hamiltonian, we conclude that L^2 is conserved (see (3.120)) irrespective of what the Hamiltonian is. From this viewpoint, the conservation of L^2 is kinematical, it does not depend on the dynamics. This has some interesting consequences that make the angular momentum Poisson algebra quite different from the canonical position-momentum PBs (3.126).

To begin with, the angular momentum phase space is 3-dimensional, unlike the canonical position-momentum PBs which are defined on an even-dimensional space ($\mathbb{R}^{2n}$ for a particle moving in n-dimensions). In particular, there is no splitting of the L_i into 'positions' and 'momenta'. What is more, the Poisson tensor $r_{ij}(\boldsymbol{L}) = \epsilon_{ijk}L_k$ is linear unlike the canonical one (3.134) which is a constant. Another key difference is that unlike L^2, there is no nonconstant function of positions and momenta that Poisson commutes with all the q^i and p_j (the center of the canonical Poisson bracket algebra is trivial, see Prob. 8.32).

Poisson tensor and symplectic leaves. When a Poisson algebra has Casimirs, we say that it is degenerate (see Sect. 3.26*). What this means, is that the Poisson tensor, regarded as a matrix field on phase space has zero determinant everywhere. In other words, it is not invertible: it has a nontrivial null space or kernel. The angular momentum Poisson tensor $r = r_{ij}\partial_{L_i} \otimes \partial_{L_j}$ in Cartesian coordinates leads to the antisymmetric matrix

$$r_{ij} = \epsilon_{ijk}L_k = \begin{pmatrix} 0 & L_3 & -L_2 \\ -L_3 & 0 & L_1 \\ L_2 & -L_1 & 0 \end{pmatrix}. \tag{8.90}$$

---

[41] The negative sign in Hamilton's equations compared to (3.117) is because the quadratic terms in Euler's equations are due to the transformation of the angular acceleration from the lab to the corotating frame, they do not arise from any external torque.

[42] See Sect. 3.26* for an introduction to Casimirs. An observable that commutes with all other observables is said to lie in the center of the Poisson algebra.

This matrix has determinant zero (in fact, any odd-dimensional antisymmetric matrix has zero determinant: see Prob. 8.30). It is easily verified that the 'radial' vector $\boldsymbol{L} = (L_1, L_2, L_3)$ is annihilated by r. In fact, this is equivalent to L^2 Poisson commuting with all components of $\boldsymbol{L}$:

$$r_{ij} L_j = \{L_i, L_j\} L_j = \frac{1}{2}\{L_i, L^2\} = 0. \tag{8.91}$$

The rank of r is two (the first two rows are linearly independent, for instance), so $\boldsymbol{L}$ is the only linearly independent vector in the null space of r.

The value of a Casimir cannot change with time, no matter what the Hamiltonian is. So the phase trajectories must lie on level sets of the Casimirs, which are called (symplectic) leaves of the Poisson manifold. The dynamics is confined to a leaf [which leaf depends on initial conditions]. Here, the level sets of $L_1^2 + L_2^2 + L_3^2$ consist of the point at the origin as well as the concentric spheres of radius L. These leaves foliate the phase space $\mathbb{R}^3$ in the sense that each point of phase space lies on precisely one leaf (see Fig. 3.13).

Though the Poisson tensor is not invertible on the full phase space, it becomes nondegenerate and invertible when restricted to a leaf, where it acquires a simple geometric meaning. This is most easily seen for the angular momentum Poisson tensor by expressing it in spherical polar coordinates

$$L_1 = L \sin\theta \cos\phi, \quad L_2 = L \sin\theta \sin\phi \quad \text{and} \quad L_3 = L\cos\theta. \tag{8.92}$$

In the (L, θ, ϕ) coordinates, the Poisson tensor is block diagonal[43] (see Prob. 8.31)

$$\tilde{r} = L^{-1} \csc\theta \begin{pmatrix} 0 & 0 & 0 \\ 0 & 0 & 1 \\ 0 & -1 & 0 \end{pmatrix} = L^{-1} \csc\theta (\partial_\theta \otimes \partial_\phi - \partial_\phi \otimes \partial_\theta). \tag{8.93}$$

The kernel of $\tilde{r}$ clearly consists of 'radial' vectors $\propto (1\ 0\ 0)$. On the other hand, when restricted to a spherical surface of constant L, $\tilde{r}$ is a 2×2 invertible matrix (the South-East block). Its inverse $\omega = \tilde{r}^{-1}$ is called the symplectic form on that sphere:

$$\omega_{ij} = L \sin\theta \begin{pmatrix} 0 & -1 \\ 1 & 0 \end{pmatrix} \quad \text{or} \quad \omega = \frac{1}{2} L \sin\theta (-d\theta \wedge d\phi + d\phi \wedge d\theta) = L \sin\theta \, d\phi \wedge d\theta. \tag{8.94}$$

Up to a factor of L, we see that this symplectic form ω is the usual area element[44] on the sphere of radius L. This is generally true, a symplectic form defines a notion of area for infinitesimal parallelograms in the phase space: if ∂_i, ∂_j are two coordinate tangent vectors, then the area of the parallelogram they define is $\omega(\partial_i, \partial_j)$.

---

[43] To obtain the components of $\tilde{r}$, we use the definition $\tilde{r}^{ij} = \{\xi^i, \xi^j\}$ where $\xi = (L, \theta = \arccos(L_3/L), \phi = \arctan(L_2/L_1))$. In particular, $\tilde{r}^{L\theta} = \{L, \theta\} = 0$ since L is a Casimir. The one nontrivial PB is $\tilde{r}^{\theta\phi} = \{\theta, \phi\}$ which turns out to equal $1/L \sin\theta$ (see Prob. 8.33).

[44] Poisson brackets $\{\cdot, \cdot\}$ (e.g., $\{x, p\} = 1$ or $\{L_x, L_y\} = L_z$) generally have dimensions of 1/action. Consequently, the Poisson tensor $r = r_{ij} \partial_i \otimes \partial_j$ also has dimensions of 1/action while its inverse, the symplectic form ω has dimensions of action. This is reasonable since action has the dimensions of area in phase space ($dx\, dp$). This is not the same as the geometric area, which for a surface in angular momentum space would have dimensions of (action)^2.

8.15 Motion of a heavy symmetrical (Lagrange) top

So far, we have mostly ignored the effect of gravity. Here, we consider the motion, subject to gravity[45], of a symmetrical top($\mathcal{I}_1 = \mathcal{I}_2$) whose bottom-most point O is held fixed (see Fig. 8.8a). Aside from this latter restriction and the disregard of friction, this models the motion of a toy top with principal moments of inertia $\mathcal{I}_1 = \mathcal{I}_2$ and $\mathcal{I}_3$ about the center of mass. The downward gravitational force exerts a torque on the top about the point O, which points along the line of nodes (perpendicular to both x_3 and Z). Thus, the angular momentum about O is generally not conserved.

Such a top is observed to display three types of oscillatory motions: spinning on its axis, precession of the axis about the vertical (direction of gravity) and a wobbling of the axis (nutation), as illustrated in Fig. 8.1c.

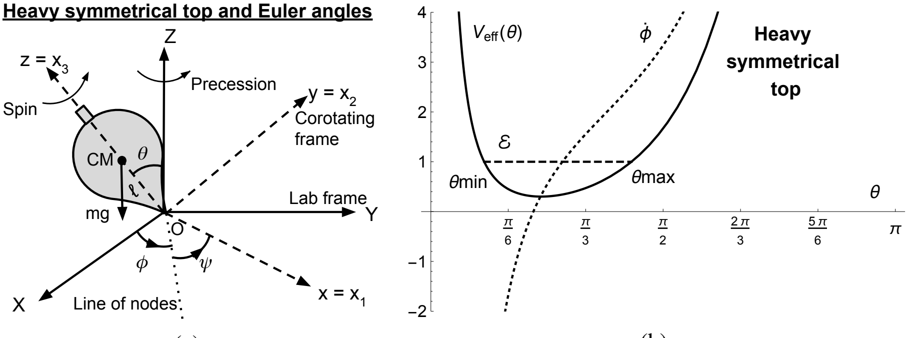

(a) (b)

Figure 8.8: (a) A heavy symmetrical top of mass m with lower vertex fixed at the origin of lab (XYZ) and corotating (xyz) frames. The X-Y and x-y planes intersect along the dotted line of nodes. (b) Effective potential $V_{\text{eff}}(\theta)$ (8.98) and precession rate $\dot{\phi}(\theta)$ (8.97) for a heavy symmetric top with $\mathcal{E}$ and turning points $\theta_{\min}$ and $\theta_{\max}$ indicated for $m = g = 1$, $l = 0.4$, $\mathcal{E} = 1, \mathcal{I}_1' = 0.3, p_\phi = 1$ and $p_\psi = 1.3$. The change in sign of $\dot{\phi}$ shows that for these values of constants, the top displays forward precession in the vicinity of $\theta_{\max}$ and backward precession in the vicinity of $\theta_{\min}$ as shown in Fig. 8.9c.

We will suppose that the top has a mass m and pick the origin of the lab and corotating frames to lie at O, which is assumed to be a distance l along the symmetry axis from the center of mass. By the parallel axis theorem of Sect. 8.5, the moment of inertia about an axis through O and perpendicular to the axis of the top is given by $\mathcal{I}_1' = \mathcal{I}_1 + ml^2$. It follows from (8.44) that the Lagrangian is given by

$$L = \frac{1}{2}(\mathcal{I}_1 + ml^2)(\dot{\theta}^2 + \dot{\phi}^2 \sin^2\theta) + \frac{1}{2}\mathcal{I}_3(\dot{\psi} + \dot{\phi}\cos\theta)^2 - mgl\cos\theta = T - V \quad (8.95)$$

and describes three degrees of freedom. Physically, the generalized velocities $\dot{\theta}$, $\dot{\phi}$ and $\dot{\psi}$ are related to the rates of nutation, precession and spinning motion. The energy $E = T + V$ is of course conserved, but it depends on all three velocities. Fortunately, two of them can be eliminated. There are two symmetries: rotations about the symmetry axis of the top and rotations about the vertical direction of gravity. Consequently, the Euler angles ψ and ϕ are cyclic coordinates leading to the conservation of the conjugate angular momentum components

---

[45] It is conventional to call a top subject to gravity a heavy top. A heavy symmetrical top is also called a Lagrange top. Such a top may also be analyzed in a corotating frame, see [106] for an elegant Hamiltonian approach to such an analysis.

$$p_\psi = \mathcal{I}_3 \left(\dot{\psi} + \dot{\phi} \cos\theta \right) \quad \text{and} \quad p_\phi = \left\{ \mathcal{I}_1' \sin^2\theta + \mathcal{I}_3 \cos^2\theta \right\} \dot{\phi} + \mathcal{I}_3 \dot{\psi} \cos\theta \tag{8.96}$$

along the x_3 and Z axes. They allow us to express $\dot{\phi}$ and $\dot{\psi}$ in terms of θ:

$$\dot{\phi} = \frac{p_\phi - p_\psi \cos\theta}{\mathcal{I}_1' \sin^2\theta} \quad \text{and} \quad \dot{\psi} = \frac{p_\psi}{\mathcal{I}_3} - \dot{\phi}\cos\theta. \tag{8.97}$$

Plugging these into $E = T + V$, the energy now looks like that of a particle with just one angular degree of freedom θ:

$$E = \frac{p_\psi^2}{2\mathcal{I}_3} + \frac{1}{2}\mathcal{I}_1' \dot{\theta}^2 + V_{\text{eff}}(\theta) \quad \text{where} \quad V_{\text{eff}} = \frac{(p_\phi - p_\psi \cos\theta)^2}{2\mathcal{I}_1' \sin^2\theta} + mgl\cos\theta. \tag{8.98}$$

Henceforth, we will use $\mathcal{E} = E - p_\psi^2/2\mathcal{I}_3$ for the conserved energy of precession, nutation and gravity, having removed the constant energy of spinning. Thus, the determination of $\theta(t)$ has been reduced to quadrature followed by a function inversion (in this case, inverting an elliptic integral)

$$t = \pm\sqrt{\frac{\mathcal{I}_1'}{2}} \int_{\theta_0}^{\theta} \frac{d\theta'}{\sqrt{\mathcal{E} - V_{\text{eff}}(\theta')}} = \mp \int_{\cos\theta_0}^{\cos\theta} \frac{du}{\sqrt{\chi(u)}} \tag{8.99}$$

Here $u = \cos\theta'$ with $0 \le \theta_0 \le \theta' \le \theta \le \pi$ and $\chi = (a + bu + cu^2 + du^3)/\mathcal{I}_1'^2$ with

$$a = 2\mathcal{I}_1'\mathcal{E} - p_\phi^2, \quad b = 2p_\phi p_\psi - d, \quad c = p_\psi^2 - 2\mathcal{I}_1'\mathcal{E} \quad \text{and} \quad d = 2mgl\mathcal{I}_1'. \tag{8.100}$$

The time-dependence of ϕ (precession) and ψ (spin) are found by integrating (8.97).

Even without evaluating any of these integrals, we may obtain a qualitative understanding of the dynamics by studying the effective potential[46] $V_{\text{eff}}(\theta)$ as in Chap. 1. For fixed values of the conserved quantities $\mathcal{E}, p_\psi$ and p_ϕ, the allowed range of values of θ is determined by the condition $\mathcal{E} \ge V_{\text{eff}}(\theta)$. As Fig. 8.8b shows, for $p_\phi \ne p_\psi$, $V_{\text{eff}}(\theta) \to \infty$ for $\theta \to 0^+, \pi^-$. For the chosen values, V_{eff} has one minimum in between and there are two roots $\theta_{\min} \le \theta_{\max}$ of the equation $\mathcal{E} = V_{\text{eff}}(\theta)$ that give the minimal and maximal inclination θ of the axis of the top as it precesses about the vertical. This up-down wobbling motion is called nutation and is not special to the values chosen. To demonstrate this, it is convenient to write the ODE for θ (8.98) in terms of $u = \cos\theta$, which must lie in the interval $|u| \le 1$:

$$\dot{u}^2 = \chi(u) = (1 - u^2)\left(\frac{2\mathcal{E}}{\mathcal{I}_1'} - \frac{2mgl}{\mathcal{I}_1'} u \right) - \frac{(p_\phi - p_\psi u)^2}{\mathcal{I}_1'^2}. \tag{8.101}$$

---

[46] V_{eff} can be negative, it is bounded below by $-mgl$ rather than zero.

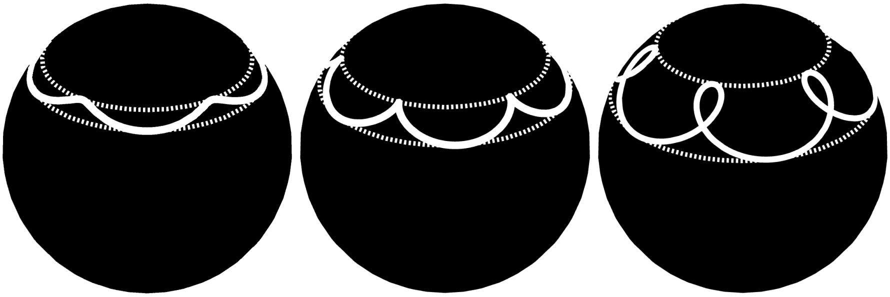

(a) (b) (c)

Figure 8.9: Locus of tip of a heavy symmetrical top (with $m = g = l = 1$, $\mathcal{I}_1' = 2.3$ and $p_\phi = 3$) on a sphere (with polar and azimuthal angles θ and ϕ) showing types of nutation and precession. (a) $\dot{\phi} > 0$: precession is monotonic, the curve is traversed rightward and has a continuously varying slope, though $\dot{\phi}$ is largest when $\theta = \theta_{\max}$ and smallest when $\theta = \theta_{\min}$, giving the curve its characteristic shape. Here, $p_\psi = 4$ and $\mathcal{E} = 0.72$. (b) $\dot{\phi}$ is positive but vanishes at $\theta = \theta_{\min}$, where precession momentarily stops. Here, $p_\psi = 4.17$ and $\mathcal{E} = 0.72$. (c) $\dot{\phi}$ takes both signs, allowing for back-and-forth precession. Here, $p_\psi = 4$ and $\mathcal{E} = 0.85$. Parameter values have been chosen to make the rate of precession slower than the rate of nutation and keep the tip of the top in the northern hemisphere.

For (8.101) to admit a solution, the real cubic polynomial $\chi(u)$ must be positive somewhere in the physical interval $|u| \leq 1$. Now, χ can have either one or three real roots. Where can they lie? We observe that $\chi(u) \to \infty$ as $u \to \infty$ and $\chi(1) < 0$. Thus, at least one real root must lie in the unphysical region $u > 1$. Moreover, $\chi(u) \to -\infty$ as $u \to -\infty$ and $\chi(-1) < 0$. Thus, for a nonempty set of nutation angles θ to exist, the other two roots $u_{\min}$ and $u_{\max}$ must also be real and lie in the physical region $-1 \leq u_{\min} \leq u_{\max} \leq 1$ as illustrated in Fig. 8.10.

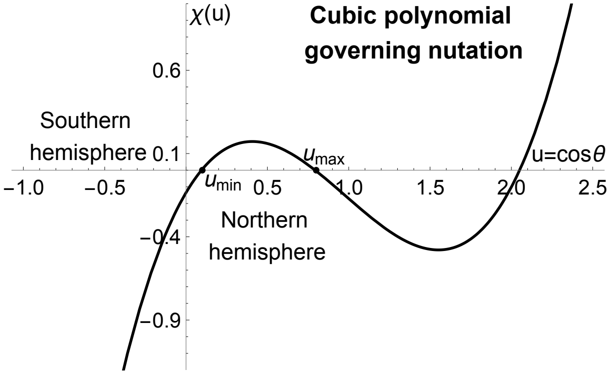

Figure 8.10: Graph of cubic polynomial $\chi(u)$ (8.101) showing two zeros $-1 \leq u_{\min} \leq u_{\max} \leq 1$ in the physical region and the third zero in the unphysical region $u > 1$. The range of nutation angles is given by $\arccos u_{\max} \leq \theta \leq \arccos u_{\min}$. We have taken $m = g = l = 1$, $\mathcal{I}_1' = 2.3$, $\mathcal{E} = 0.85$, $p_\phi = 2.15$ and $p_\psi = 3.1$.

The precession is simplest if $\dot{\phi}$ is either strictly positive or strictly negative, resulting in monotonic precession as in Fig. 8.9a. However, the precession need not be monotonic. This back-and-forth precession can happen if $\dot{\phi}$ switches sign, which happens if $p_\phi - p_\psi \cos\theta$ changes sign for $\theta_{\rm min} < \theta < \theta_{\rm max}$. The nature of precession and nutation are illustrated in Fig. 8.9 where the locus of the moving tip of the top

$$x(t) = \sin\theta(t)\cos\phi(t), \quad y(t) = \sin\theta(t)\sin\phi(t) \quad \text{and} \quad z(t) = \cos\theta(t) \quad (8.102)$$

is plotted on a unit sphere (in suitable units) centered at the fixed point O. The intermediate case of Fig. 8.9b occurs if $\dot{\phi}$ vanishes at a turning point of $V_{\rm eff}(\theta)$. In the case plotted, $\dot{\phi}$ vanishes at $\theta_{\rm min}$ (where $\dot{\theta} = 0$) so that precession momentarily stops when the nutation angle is minimal, producing a cusp. This happens if $\cos\theta_{\rm min} = p_\phi/p_\psi$.

Sleeping top. A heavy symmetrical top for which ICs are set up so that its axis is always vertical ($\theta = 0$ or $u = 1$) is called a sleeping top. We will show that if a top starts out vertically while spinning sufficiently fast, then it will sleep [i.e., neither precess ($\dot{\phi} = 0$) nor nutate ($\dot{\theta} = 0$)]. The essential idea is that to keep the top vertical, $\dot{u}^2 = \chi(u)$ must vanish at $u = 1$ and be negative elsewhere in the physical interval $-1 \le u \le 1$. To implement this idea, suppose the top starts out spinning vertically, so that $\theta(0) = 0$ or $u(0) = 1$ and $\dot{\phi}(0) = \dot{\theta}(0) = 0$. Then from (8.97), we must initially have $p_\phi = p_\psi$. In fact, this must hold at all times as p_ϕ and p_ψ are both conserved. Moreover, since it is conserved, the energy $\mathcal{E}$ (8.98) can be conveniently evaluated at $t = 0$, giving $\mathcal{E} = mgl$. Putting this and $p_\phi = p_\psi$ in (8.101), we get

$$\chi = \frac{2mgl}{\mathcal{I}_1'}(1-u^2)(1-u) - \frac{p_\psi^2}{\mathcal{I}_1'^2}(1-u)^2 = (1-u)^2\left[\frac{2mgl}{\mathcal{I}_1'}(1+u) - \frac{p_\psi^2}{\mathcal{I}_1'^2}\right]. \quad (8.103)$$

We infer that for a top that starts out spinning vertically, $\chi(u)$ must have a double zero at $u = 1$ while the third zero lies at $u_* = p_\psi^2/2mgl\mathcal{I}_1' - 1$. To keep the top from nutating, we need to prevent the cubic χ from being positive below $u = 1$. Since $\chi \to \pm\infty$ as $u \to \pm\infty$, this is ensured if $u_* \ge 1$ or $p_\psi^2 \ge 4mgl\mathcal{I}_1'$. From (8.97), this is the condition that to sleep, the top must spin sufficiently fast:

$$\dot{\psi}^2 \ge 4mgl(\mathcal{I}_1 + ml^2)/\mathcal{I}_3^2. \quad (8.104)$$

In practice, the spinning rate decreases with time due to friction, and a sleeping top eventually wakes up and starts nutating and precessing! ☐

8.16 Problems

1. **Center of mass.** Give an example of a rigid body whose center of mass is not a part of its mass distribution. What can be said about the CM of a convex body?
2. **Positive-semidefinite matrix.** Suppose a real symmetric matrix A is such that the associated quadratic form $\boldsymbol{v}^t A \boldsymbol{v} \ge 0$ for all vectors $\boldsymbol{v}$. Show that the eigenvalues of A are nonnegative.
3. **Mass density for point masses.** Suppose a rigid body of total mass M consists of point masses m_a located at $\boldsymbol{r}_a$ for $a = 1, \cdots, N$. (a) What mass density $\rho(\boldsymbol{r})$ does this correspond to? (b) Verify that the proposed ρ satisfies $\int \rho(\boldsymbol{r}) d\boldsymbol{r} = M$.

4. Consider a **uniform square plate** of side L, mass M and surface mass density σ. (a) Select a convenient right-handed orthonormal coordinate system and draw a diagram of the plate and the coordinate axes. (b) Where is the center of mass? Find its coordinates in the chosen coordinates. (c) Find all elements of the inertia matrix in a suitable basis with origin at the CM. Exploit the symmetries of the mass distribution to simplify the calculation. (d) Find the principal moments of inertia of the plate and check whether they satisfy/saturate the triangle inequalities. (e) Find the corresponding principal axes of inertia, are they uniquely determined? (f) Is the square plate a symmetric top? Why?

5. **Rigid rotator.** Consider a rigid rotator, a system of mass points m_a, $a = 1, \cdots, N$ that are concentrated along the z-axis at the locations z_a, defined so that the center of mass lies at $z = 0$ (and $x = y = 0$). Draw a figure indicating masses, origin and coordinate axes. What can you say about the off-diagonal elements of the inertia tensor? Find the principal moments of inertia of the rotator.

6. A **uniform circular disc** of radius R has mass M. The CM lies at the center of the disk. Let the z axis be perpendicular to the disk and the x, y axes be any pair of orthogonal axes in the plane of the disk, all passing through the center. Then show that the inertia matrix is diagonal in this basis and that the principal moments of inertia are $\mathcal{I}_x = \mathcal{I}_y = MR^2/4$ and $\mathcal{I}_z = MR^2/2$. Hint: $\int_0^\pi \sin^4\theta\, d\theta = 3\pi/8$.

7. **Coin.** Suppose the disk of Prob. 8.6 has a nonzero thickness h, so that it is a uniform right circular cylinder (coin) of mass M and radius R. Then show that the principal axes of inertia are the same as for the disk and that $\mathcal{I}_x = \mathcal{I}_y = (M/4)(R^2 + h^2/3)$ while $\mathcal{I}_z = MR^2/2$ is unaltered.

8. (a) Suppose a rigid body has a **plane of symmetry**: the mass distribution is symmetric about reflections in this plane. Assuming the origin lies at the CM, show that this plane must be orthogonal to a principal axis of inertia. (b) Show that an **axis of rotational symmetry** must be a principal axis and that the plane perpendicular to this axis and passing through the CM must be a principal plane spanned by principal axes corresponding to degenerate principal moments of inertial.

9. **Determinant of inertia tensor.** Recall from (8.15) that the inertia tensor is the sum of those for each point mass in the body: $\mathcal{I} = \sum_a \mathcal{I}_a$. (a) Show that $\det \mathcal{I}_a = 0$ for each a. (b) By a suitable choice of basis, show that one of the eigenvalues of $\mathcal{I}_a$ must vanish for each a. (c) Argue why this does not imply that $\det \mathcal{I}$ must vanish.

10. **Trace of inertia tensor.** Show that $\operatorname{tr}\mathcal{I} = 2\sum_a m_a r_a^2$.

11. Find out about a **boomerang, a gyroscope and a tippe-top**.

12. Show the **triangle inequality** among principal moments of inertia: $\mathcal{I}_i + \mathcal{I}_j \geq \mathcal{I}_k$ where i, j, k are distinct indices from $1, 2, 3$.

13. Express the **generalized velocities** associated to the **Euler angles** $(\dot\theta, \dot\phi, \dot\psi)$ in terms of the angular velocity components $\Omega_1, \Omega_2, \Omega_3$. Show that

$$\dot\theta = \Omega_1\cos\psi - \Omega_2\sin\psi, \quad \dot\phi = \frac{\Omega_1\sin\psi + \Omega_2\cos\psi}{\sin\theta}, \quad \dot\psi = \Omega_3 - \frac{\Omega_1\sin\psi + \Omega_2\cos\psi}{\tan\theta}. \tag{8.105}$$

14. (a) Suppose R is an element of the **special orthogonal group** $SO(3)$ consisting of 3×3 orthogonal matrices of unit determinant: $R^t R = I$, $\det R = 1$. Consider an element $R \approx I + u$ that is infinitesimally close to the identity element (u is treated to linear approximation). Show that the 3×3 matrix u must be antisymmetric for R to be an element of $SO(3)$. Such a u is said to lie in the **Lie algebra** $\mathfrak{so}(3)$ of the group $SO(3)$. (b) Suppose $\omega = R^{-1}\dot{R}$ where $R(t)$ is a curve on the rotation group $SO(3)$. Show that ω is antisymmetric. Hint: Differentiate the identity $R^t R = I$ in time and use it to compare ω and ω^t. It may help to work in components. (c) Show that the eigenvalues of R must be of the form $1, e^{i\theta}, e^{-i\theta}$ for some real angle θ. Geometrically interpret the eigenspace corresponding to the eigenvalue 1.

15. **Spin axis.** Consider motion of a rigid body in the absence of external forces discussed in Sect. 8.8. For definiteness, take it to be a spherical top. Can it spin about an axis that does not pass through the CM? Hint: Examine the motion of the CM.

16. **Free rotation of a rigid rotator.** Consider torque-free rotational motion of a rigid rotator with principal moments of inertia $\mathcal{I}_1 = \mathcal{I}_2, \mathcal{I}_3 = 0$ and use Euler angles to parametrize its orientation relative to a lab frame (see Fig. 8.6). Recall that the components of angular velocity relative to a comoving (xyz) frame are given in terms of Euler angles and their derivatives by (8.39). (a) Find an expression for the rotator Lagrangian in terms of coordinates and velocities by choosing comoving axes along principal axes $(x_1 x_2 x_3)$. The axis of the rotator is along $z = x_3$. (b) What is the configuration space of a rigid rotator that is free to rotate about its CM which is held fixed? Which Euler angles provide coordinates on the configuration space and what are their ranges? Identify any redundant coordinates. By redundant we mean neither the coordinate nor the corresponding generalized velocity appears in the Lagrangian. (c) Obtain conjugate momenta and identify (nonredundant) cyclic coordinates. (d) Find Lagrange's equations and express them as second order differential equations for the nonredundant Euler angles. (e) Show that $\theta(t) = \omega t$, $\phi(t) = \phi_o$, constant and $\psi(t) = 0$ for constant ω is a solution to the equations of motion. (f) Based on our study of the rigid rotator and the above example solution, say what the trajectories look like on the configuration space of a rigid rotator.

17. Consider **torque-free rotational motion of a symmetric top** with principal moments of inertia $0 < \mathcal{I}_1 = \mathcal{I}_2 < \mathcal{I}_3$. Denote the magnitude of angular momentum by $L = \sqrt{\boldsymbol{L} \cdot \boldsymbol{L}}$ and energy by E. (a) Write Euler's equations for the components of $\boldsymbol{L}$ with respect to a comoving frame by choosing the corotating axes along principal axes of inertial. Use the common notation $a_{ij} = \mathcal{I}_i^{-1} - \mathcal{I}_j^{-1}$, $a = a_{23}$, $\omega = aL_3$. (b) Write down the general solution of Euler's equations. (c) Find all static (time-independent) solutions (L_1, L_2, L_3) of Euler's equations. (d) Give the energy of each static solution. (e) Describe briefly in words the sort of motion each static solution represents. (f) Draw a picture of the ellipsoid of inertia and mark five qualitatively distinct curves/points of intersection with angular momentum spheres of various L^2. (g) Pick a static solution with minimal value of L for fixed E. Specify the solution (L_1, L_2, L_3) in terms of E and material constants. Comment on its stability with respect to a small increase in L holding E fixed.

18. Consider **torque-free motion of a symmetric top** $(\mathcal{I}_1 = \mathcal{I}_2)$, as discussed in

Sect. 8.8. Suppose the axis of the top makes an angle $\theta \neq 0$ with the fixed direction of $\boldsymbol{L}$. (a) Find the angle α between the angular velocity vector $\boldsymbol{\Omega}$ and angular momentum vector $\boldsymbol{L}$ (α is the opening angle of the space cone swept out by $\boldsymbol{\Omega}$). Express α in terms of θ, the principal moments of inertia and the magnitude of angular momentum L. How does α depend on time and L? (b) Suppose $\mathcal{I}_1 \to \mathcal{I}_3$ so that the symmetric top becomes a spherical top. Based on our study of the spherical top, what do you expect to happen to α? Is this expectation fulfilled by the above formula for α? (c) It can be shown that to take the limit of a rigid rotator (starting from a symmetric top), $\cos\theta$ must tend to zero faster than $\mathcal{I}_3$. Using this, find the limiting value of α for a rigid rotator. Does it agree with the value obtained in our study of a rigid rotator in Sect. 8.8?

19. Consider **torque-free rotational motion of a symmetric top** ($\mathcal{I}_1 = \mathcal{I}_2 \neq \mathcal{I}_3$) described via Euler angles. Let the corotating axes $x_1 = x, x_2 = y$, and $x_3 = z$ be chosen along principal axes of inertia. Write the Lagrangian and find the momenta conjugate to the Euler angles and identify which are conserved. From Fig. 8.6, guess which among p_θ, p_ϕ, p_ψ should correspond to the angular momentum component L_Z, and which should correspond to the $x_3 = z$ component L_z.

20. Consider **force-free motion of a symmetric top** with principal moments of inertia $\mathcal{I}_1 = \mathcal{I}_2 > \mathcal{I}_3 \geq 0$. Let the Euler angle θ be the angle between the fixed angular momentum vector in space $\boldsymbol{L} = L\hat{Z}$ and the axis of the top along $\hat{x}_3 = \hat{z}$. We use the same conventions as in Sect. 8.11. Recall the solution of Euler's equations:

$$L_3 = \text{const}, \quad L_1 = C\cos(\omega t + \delta), \quad L_2 = C\sin(\omega t + \delta) \tag{8.106}$$

where $\omega = L_3\left(\mathcal{I}_1^{-1} - \mathcal{I}_3^{-1}\right)$. (a) Relate ω to the generalized velocity $\dot{\psi}$ where ψ is one of the Euler angles. Refer to our discussion on the special choice of Euler angles for a symmetric top. (b) We now consider the limiting case of a rigid rotator by letting $\mathcal{I}_3 \to 0$ holding $\mathcal{I}_1 = \mathcal{I}_2$ and L fixed while ω remains finite. How must θ behave in the limit? (c) From your knowledge of the motion of a rigid rotator and above formulae, what are the limiting values of $\frac{\cos\theta}{\mathcal{I}_3}$, Ω_3 and ω? (d) Qualitatively describe what happens to the manner of rotation of the symmetric top when it becomes a rigid rotator.

21. **Space cone of symmetric top.** Show that the opening angle α of the space cone swept by the angular velocity vector $\boldsymbol{\Omega}$ in the torque-free motion of a symmetrical rigid body is given by $\cos\alpha = (\Omega_1 \sin\theta + \Omega_3\cos\theta)/\Omega$ in the notation of Sect. 8.8.

22. Find the **momenta** p_θ, p_ϕ and p_ψ **conjugate to** the **Euler angles** θ, ϕ and ψ that appear in the Lagrangian (8.43) for free motion of an anisotropic top. Solve for the velocities and thereby obtain the Hamiltonian as a function on phase space.

23. Recall the **Euler equations** (8.57) for force-free rotational motion of a rigid body in a principal axis corotating frame. (a) Suggest why $\dot{L}_i$ may be nonzero although there are no external torques. (b) What are the independent and dependent variables in the equations? Comment on their linearity/nonlinearity.

24. Show that the **Euler equations** $\dot{L}_1 + a_{23}L_2L_3 = \tau_1$ (and cyclic permutations

thereof) (8.57) can be written compactly using the Levi-Civita symbol:

$$\dot{L}_i + \sum_{j,k=1,2,3} \epsilon_{ijk} \frac{L_j L_k}{\mathcal{I}_j} = \tau_i \quad \text{for} \quad i = 1,2,3 \quad \text{where} \quad a_{ij} = \frac{1}{\mathcal{I}_i} - \frac{1}{\mathcal{I}_j}. \tag{8.107}$$

∗25. Recall from Sect. 8.13∗ that for an **anisotropic top** with principal moments of inertia $\mathcal{I}_1 \le \mathcal{I}_2 \le \mathcal{I}_3$, energy E and square of angular momentum $L^2 \ge 2E\mathcal{I}_2$,

$$k^2 = \frac{(\mathcal{I}_2 - \mathcal{I}_1)(2E\mathcal{I}_3 - L^2)}{(\mathcal{I}_3 - \mathcal{I}_2)(L^2 - 2E\mathcal{I}_1)}. \tag{8.108}$$

Show that k^2, which plays the role of the square of the **elliptic modulus**, lies between 0 and 1. Extend the argument to (8.79) for $L^2 \le 2E\mathcal{I}_2$.

∗26. Consider the solution to the **force-free Euler equations** for an anisotropic top in terms of **Jacobi elliptic functions** given in (8.76) and (8.78). Under what conditions can the elliptic modulus k vanish? Discuss the analytic & geometric nature of the limiting solutions when $k = 0$. Hint: There are 2 ways in which k can vanish.

∗27. Recall the elliptic function solution [(8.76) and (8.78)] of the **force-free Euler equations** for an anisotropic rigid body. (a) What are the two ways in which the **elliptic modulus** k can take the limiting value $k = 1$? (b) What is the geometric and physical nature of solutions for L_1, L_2 and L_3 in each case? (c) Comment on the time period and stability of trajectories when $k = 1$.

28. Consider the **Euler equations** (8.74) in the corotating frame for force-free motion of an **anisotropic rigid body** with principal moments of inertia $\mathcal{I}_3 > \mathcal{I}_2 > \mathcal{I}_1$. Suppose the magnitude of angular momentum has the critical 'intermediate' value $L = \sqrt{2E\mathcal{I}_2}$. (a) What is the physical nature of solutions of the Euler equations in this case? (b) Solve the Euler equations to find $L_{1,2,3}(t)$. Show that the nonconstant solutions are expressible in terms of hyperbolic functions, with

$$L_2(t) = \pm L \tanh(L\sqrt{a_{12}a_{23}}\,t) \quad \text{where} \quad a_{ij} = \mathcal{I}_i^{-1} - \mathcal{I}_j^{-1}. \tag{8.109}$$

Find the corresponding expressions for L_1 and L_3 and explain the significance of the ± signs. Hint: Use energy and angular momentum conservation to eliminate L_1 and L_3 and derive a nonlinear evolution equation for L_2.

29. **Contraction of symmetric and antisymmetric.** Show that the contraction of a symmetric tensor s_{ij} with an antisymmetric tensor a_{ij} is zero: $s_{ij}a_{ij} = 0$.

30. Show that any **odd-dimensional antisymmetric matrix** A has determinant zero.

∗31. Consider the **angular momentum Poisson algebra** $\{L^i, L^j\} = \epsilon_{ijk}L^k$. Identify the Poisson tensor $r^{ij}(L)$, a second rank antisymmetric contravariant tensor field. In the Cartesian coordinate basis $r = r^{ij}\partial_i \otimes \partial_j$ where $\partial_i = \frac{\partial}{\partial L^i}$.

a. Show that r^{ij} satisfies the Jacobi identity (quadratic first order PDEs).
b. Find the matrix r^{ij} in the Cartesian coordinate basis and find its kernel, which should consist of radial vectors $\propto \partial_r$.

c. Re-express r in the spherical polar coordinate basis ($\tilde{r}$) by finding the Jacobian matrix for the transformation. $\tilde{r}^{ab} = r^{ij} J_i^a J_j^b$. Here $J_i^a = \frac{\partial s^a}{\partial L^i}$ where $s = (\sqrt{L^2}, \theta, \phi)$ and $L^3 = L\cos\theta, L^1 = L\sin\theta\cos\phi, L^2 = L\sin\theta\sin\phi$. In other words, $\tilde{r} = J^t r J$. Note that J is not an orthogonal matrix with respect to the Euclidean inner product since the coordinate basis vectors $\partial_\theta, \partial_\phi$ are not unit vectors. Use this to show that r is nondegenerate when restricted to spheres of constant $(L^1)^2 + (L^2)^2 + (L^3)^2$, which is the only independent Casimir of the Poisson algebra (these are the symplectic leaves).

d. Restrict r to the 2d subspace spanned by $\partial_\theta, \partial_\phi$ to get a Poisson bivector field on the sphere of radius L, find its matrix elements.

e. Invert this restriction of r to get $\omega = r^{-1}$. Find the components of the symplectic form ω in the coordinate basis $\partial_\theta, \partial_\phi$, and show that it is a multiple of the area element on the sphere $\sin\theta\, d\theta \wedge d\phi$.

f. Check that ω_{ij} satisfies the Bianchi identity $\omega_{ij,k} + \omega_{ki,j} + \omega_{jk,i} = 0$, i.e., $d\omega = 0$ so it is a closed 2-form.

32. Show that there is no nonconstant function $C(q,p)$ that commutes with all the coordinates and momenta q^i, p_j of the canonical Poisson algebra of a particle moving in $\mathbb{R}^n$. Thus, the center of the canonical PB algebra is trivial, it has no **Casimirs**.

33. The antisymmetric **angular momentum Poisson tensor** in spherical polar coordinates is defined as $\tilde{r}^{ij} = \{\xi^i, \xi^j\}$, where $\xi^i = (L, \theta = \arccos(L_3/L), \phi = \arctan(L_2/L_1))$. (a) Argue that $\tilde{r}^{L\theta} = \tilde{r}^{L\phi} = 0$. So up to antisymmetry, $\tilde{r}^{\theta\phi}$ is the only independent entry. (b) Use the Leibniz rule to show that

$$\{\theta, \phi\} = -\csc\theta\cos^2\theta\, \partial_i(L_3/L)\partial_j(L_2/L_1)\{L_i, L_j\}. \tag{8.110}$$

(c) Show that $\partial_i(L_3/L) = \frac{1}{L^2}(L^2\delta_{3i} - L_3 L_i)$. (d) Show that $\partial_j(L_2/L_1) = \frac{1}{L_1^2}(L_1\delta_{2j} - L_2\delta_{1j})$. (e) Combine these to establish that $\{\theta, \phi\} = 1/(L\sin\theta)$.

34. Consider a rigid rotator ($I_3 = 0, I_1 = I_2$). Argue that its kinetic energy for rotational motion and its inertia tensor define a metric $g_{ij} = I_1(1, 0|0, \sin^2\theta)$ on its configuration space S^2 in polar coordinates θ, ϕ. Find the Riemann tensor, Ricci scalar and sectional curvature $K(\partial_\theta, \partial_\phi)$ in the 2-plane spanned by $\partial_\theta, \partial_\phi$ (see Appendix B.12.1). Show that $K = 1/I_1$ is a positive constant so that free rotational motion of a rigid rotator is geodesically stable. Generalize this to find inertia metrics on the rotational configuration spaces of a symmetric top, spherical top and anisotropic rigid body. In each case, find the sectional curvatures in the (Euler angle) coordinate 2-planes and comment on the occurrence of geodesic instabilities.

Chapter 9

Motion in noninertial frames of reference

Newton's 2^{nd} law generally holds only in inertial frames of reference[1]. However, there are physical situations where it is quite natural or necessary to study the equations of motion in a noninertial frame. For instance, a frame that is attached to a rotating rigid body is noninertial. In Sect. 8.11, we obtained Euler's equations for the linear and angular momenta in such a corotating frame and found that they involve new terms $\boldsymbol{\Omega} \times \boldsymbol{P}$ and $\boldsymbol{\Omega} \times \boldsymbol{L}$ depending on the instantaneous angular velocity $\boldsymbol{\Omega}$ of the frame. Moreover, we found that it was conceptually and technically beneficial to first solve Euler's equations in the corotating frame and then determine the orientation of the corotating frame relative to the lab frame. Another situation where the effects of a noninertial frame enter is in the motion of a simple pendulum where the Earth's rotation makes the lab frame noninertial and can cause the pendulum's oscillation plane to precess.

We begin this chapter by considering the motion of a particle in a frame that accelerates uniformly relative to an inertial frame. It turns out that Newton's 2^{nd} law is modified by a fictitious force proportional to the particle's mass and directed oppositely to the frame's acceleration. This pseudo force is similar to the force in a uniform gravitational field, an observation that led Einstein to the principle of equivalence.

We then address the question of determining the analog of Newton's equation of motion for a particle, when referred to a frame that is accelerating (nonuniformly) relative to an inertial frame. Although Newton's equation will not take the same form, Lagrange's equations written as $\frac{d}{dt}\frac{\partial L}{\partial \dot{q}} = \frac{\partial L}{\partial q}$ (3.21) *do* take the same form (as shown in Sect. 3.8 and Sect. 3.20*), though we need to transform the Lagrangian L to the new frame. Of course, one could transform Newton's equation of motion to the accelerating frame (see e.g., [68]). However, when it is available, it is more economical to transform one Lagrange function than three components of Newton's vector equation. We will exploit this feature to derive the equations of motion in an accelerating frame. The latter will be seen to involve new terms that are proportional to the particle's mass and are therefore called inertial fictitious forces. These include the so-called centrifugal and Coriolis forces. We will then specialize to the case of a uniformly rotating frame and explore a delightful analogy with the motion of a charged particle in a uniform magnetic field. The effect of the Coriolis force is vividly illustrated with the example of Foucault's pendulum. We end with a brief survey of the circular restricted three-body problem in a frame that rotates uniformly with the primaries. The centrifugal potential energy enters Roche's effective potential for the infinitesimal third mass. Although the Coriolis force does not contribute to Roche's potential, its effect is essential to understand the stability of Lagrange points.

---

[1] One needs to find out whether a frame is inertial by checking whether Newton's first law for isolated bodies holds to the desired accuracy. For many purposes, we may view a frame fixed in a lab on the Earth or the frame of the 'fixed stars' as inertial. As discussed in Sect. 3.12, a frame that is related to an inertial frame by a fixed translation of space or time, a fixed rotation (proper or improper) or a Galilean boost by a fixed velocity is inertial.

9.1 Uniformly accelerating frames and the equivalence principle

Suppose a particle of inertial mass $m_{\rm in}$ in an inertial frame K_0 is subject to a force $\boldsymbol{F}_0$. By Newton's $2^{\rm nd}$ law, it feels an acceleration $m_{\rm in}\boldsymbol{a}_0$. What is the nature of its dynamics as observed from a frame K' that is uniformly accelerating at the rate $\boldsymbol{A}$ relative to K_0? The acceleration of the particle in K' is related to that in K_0 by $\boldsymbol{a}' = \boldsymbol{a}_0 - \boldsymbol{A}$. Multiplying by $m_{\rm in}$,

$$m_{\rm in}\boldsymbol{a}' = m_{\rm in}\boldsymbol{a}_0 - m_{\rm in}\boldsymbol{A} = \boldsymbol{F}_0 - m_{\rm in}\boldsymbol{A}. \tag{9.1}$$

We will call $\boldsymbol{F}' = m_{\rm in}\boldsymbol{a}'$ the apparent force in K'. We assumed that the inertial mass of the particle is the same in both frames. Unlike in a frame that moves uniformly, the force seen in an accelerated frame is generally *not* the same as in an inertial frame. However, the apparent force in K' may be expressed as $\boldsymbol{F}' = \boldsymbol{F}_0 + \boldsymbol{F}_{\rm fict}$ where the so-called fictitious force is given by $\boldsymbol{F}_{\rm fict} = -m_{\rm in}\boldsymbol{A}$. Notice that $\boldsymbol{F}_{\rm fict}$ points oppositely to the direction of acceleration $\boldsymbol{A}$. Moreover, it is uniform, i.e., independent of location and proportional to the particle's inertial mass[2]. It is noteworthy that $\boldsymbol{F}_{\rm fict}$ arises from the acceleration of the frame rather than from interactions between particles, which explains the name fictitious. Thus, Newton's $2^{\rm nd}$ law in a frame that accelerates uniformly at the rate $\boldsymbol{A}$ is the same as that in an inertial frame, if we introduce a fictitious force $\boldsymbol{F}_{\rm fict} = -m_{\rm in}\boldsymbol{A}$ on each particle.

Principle of equivalence. Einstein noticed the similarity between the fictitious force $\boldsymbol{F}_{\rm fict} = -m_{\rm in}\boldsymbol{A}$ in a frame that accelerates at the rate $\boldsymbol{A}$ and the gravitational force $m_{\rm gr}\boldsymbol{g}$ on a particle of gravitational mass $m_{\rm gr}$ due to a uniform acceleration due to gravity $\boldsymbol{g} = -\boldsymbol{A}$ in an inertial frame. He wondered whether an observer in either frame can tell which force is responsible for the observed acceleration of particles.

To make the question more concrete, he proposed a thought (or 'gedanken') experiment (see also Prob. 9.2). Suppose an observer is in an elevator at rest in a uniform gravitational field of magnitude g pointing downwards. If the observer releases a ball from rest, it falls downwards with an acceleration $\boldsymbol{a} = (m_{\rm gr}/m_{\rm in})\boldsymbol{g}$. On the other hand, suppose the same elevator is isolated from gravitational forces and accelerates upwards at the constant rate $a = g$. If the ball is released in the same manner in this accelerating elevator, it accelerates downward at the rate g due to the fictitious force $\boldsymbol{F} = -m_{\rm in}\boldsymbol{g}$. As far as the observer is concerned, if $m_{\rm in} = m_{\rm gr}$, there is no way to distinguish between an accelerating elevator and a uniform gravitational field[3].

As mentioned in Sect. 3.3, there is experimental evidence that the gravitational and inertial masses of bodies can be taken equal. Thus, we have the principle of equivalence, which states that inertial and gravitational masses of any body are numerically equal $m_{\text{in}} = m_{\text{gr}}$ and that it is not possible to distinguish[4] between a uniform gravitational field with acceleration $\boldsymbol{g}$ (observed from an elevator that is at rest or moving uniformly) and a coordinate system (elevator) that accelerates at the rate $\boldsymbol{A} = -\boldsymbol{g}$.

---

[2] See Prob. 9.1 for an illustration of the effect of the fictitious force in an accelerating car.

[3] This is in a sense a constant acceleration version of Galileo's assertion that it is not possible to dynamically distinguish between two inertial frames in uniform relative motion.

9.2 Nonuniformly accelerated frames: Lagrangian approach

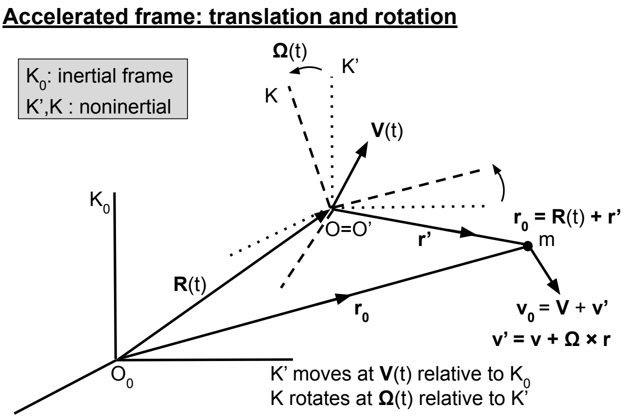
Accelerated frame: translation and rotation
K₀: inertial frame
K',K : noninertial
Ω(t)
K'
K
V(t)
K₀
O=O'
r₀ = R(t) + r'
r'
m
R(t)
r₀
v₀ = V + v'
v' = v + Ω × r
O₀
K' moves at V(t) relative to K₀
K rotates at Ω(t) relative to K'

Figure 9.1: Origin of the frame K' moves at (a possibly nonuniform) velocity $\boldsymbol{V}(t)$ relative to the inertial frame K_0. Frame K rotates at the rate $\boldsymbol{\Omega}(t)$ relative to K'.

As in our discussion of rigid body motion in Sect. 8.3, we may regard the general motion of a frame as a combination of translational and rotational motion. To this end, following the notation of [83], suppose K_0 is an inertial frame with respect to which the particle is located at $\boldsymbol{r}_0$, has velocity $\boldsymbol{v}_0 = \dot{\boldsymbol{r}}_0$ and Lagrangian $L_0 = \frac{1}{2}m\boldsymbol{v}_0^2 - U(\boldsymbol{r}_0)$. We wish to transform to a frame that is moving (at the instant considered) with translational velocity[5] $\boldsymbol{V}(t)$ and rotating with angular velocity $\boldsymbol{\Omega}(t)$ relative to K_0. We will do this in 2 steps: (a) first go to a frame K' that moves at translational velocity $\boldsymbol{V}(t)$ relative to K_0 and (b) next go to frame K whose origin always coincides with that of K' and which rotates with angular velocity $\boldsymbol{\Omega}$ relative to it, as pictured in Fig. 9.1. Here, it is supposed that $\boldsymbol{V}(t)$ and $\boldsymbol{\Omega}(t)$ are given vector functions of time. To begin with, the velocities in K_0 and K' are related via $\boldsymbol{v}_0 = \boldsymbol{v}' + \boldsymbol{V}(t)$ so that the Lagrangian in K' at first glance can be taken as

$$L'_{\text{temp}} = (m/2)\boldsymbol{v}'^2 + m\boldsymbol{v}' \cdot \boldsymbol{V} + (m/2)\boldsymbol{V}^2 - U(\boldsymbol{r}). \tag{9.2}$$

This form involving $\boldsymbol{V}$ and $\boldsymbol{V}^2$ (though correct and leading to the right EOM) is not very convenient. In particular, for a Galilean boost ($\boldsymbol{V}$ independent of time), this

---

[4] If one wishes to apply this idea to real gravitational fields and real elevators, then one needs to restrict to small 'local' regions, to avoid inhomogeneities in the gravitational field over large distances or, for instance, the possibility of the observer looking out of the elevator to determine whether it is falling or not relative to the Earth!

[5] By this we do not mean that $\boldsymbol{V}(t)$ has a constant direction. Rather, we mean that the origin of K moves at velocity $\boldsymbol{V}(t)$ with respect to K_0 and that the axes of K rotate at the instantaneous rate $\boldsymbol{\Omega}(t)$ relative to the axes of K_0.

Lagrangian does not resemble L_0 although a Galilean boost should be a symmetry of the equations of motion. We wish to use the freedom to subtract the time derivative of a function of coordinates and time from the Lagrangian to make the invariance under Galilean boosts manifest. To this end, we rewrite (9.2) as

$$L'_{\text{temp}} = \frac{1}{2}m\boldsymbol{v}'^2 - U(\boldsymbol{r}) - m\boldsymbol{r}' \cdot \dot{\boldsymbol{V}} + m\frac{d}{dt}\left(\boldsymbol{r}' \cdot \boldsymbol{V} + f(t)\right), \tag{9.3}$$

where $\dot{\boldsymbol{r}}' = \boldsymbol{v}'$ and $f(t) = \int^t \frac{1}{2}\boldsymbol{V}^2(t')\, dt'$ is any antiderivative of $\frac{1}{2}\boldsymbol{V}^2$. Since the time derivative term does not affect the EOM (as shown in Sect. 3.6), we may omit it and take our Lagrangian in K' to be

$$L' = \frac{1}{2}m\boldsymbol{v}'^2 - U - m\boldsymbol{r}' \cdot \dot{\boldsymbol{V}}. \tag{9.4}$$

This version is nice since it does not involve $\boldsymbol{V}$ or $\boldsymbol{V}^2$ and has the same form as L_0 for the special case of a Galilean boost (where $\dot{\boldsymbol{V}} = 0$). Here, U is now regarded as a function of $\boldsymbol{r}'$ where $\boldsymbol{r}_0 = \boldsymbol{R}(t) + \boldsymbol{r}'$ and $\boldsymbol{R}(t)$ is the position vector of the origin of K' with respect to the origin of K_0. This Lagrangian is explicitly time-dependent (if $\dot{\boldsymbol{V}}$ is not a constant) so that the corresponding Hamiltonian is *not* conserved (except for a uniformly accelerated frame). With $\boldsymbol{\nabla}'$ the gradient in $\boldsymbol{r}'$, the resulting EOM is

$$m\frac{d\boldsymbol{v}'}{dt} = -\boldsymbol{\nabla}'U - m\dot{\boldsymbol{V}}. \tag{9.5}$$

Compared to Newton's equation in K_0, we have a new inertial force (i.e., one that scales with the inertia m) proportional to the acceleration of K' relative to K_0 and directed oppositely. Such a force that arises from a change in frame is sometimes called a fictitious force[6]. We notice that it vanishes if K' moves at constant velocity relative to K_0, i.e., $\dot{\boldsymbol{V}} = 0$ and the two frames are related by a Galilean boost. This is as expected: Newton's equation should take the same form in all inertial frames.

Now, we transform from K' to the frame K with the same origin but which rotates at $\boldsymbol{\Omega}(t)$ relative to it. Since the origins coincide, the position vector $\boldsymbol{r}$ of the particle with respect to K is the same as $\boldsymbol{r}'$. However, as in (8.5), $\boldsymbol{v}' = \boldsymbol{v} + \boldsymbol{\Omega} \times \boldsymbol{r}$ where[7] $\boldsymbol{v} = \dot{\boldsymbol{r}}$. Putting this in (9.4), we get the Lagrangian in K:

$$L = \frac{1}{2}m\boldsymbol{v}^2 + m\boldsymbol{v} \cdot (\boldsymbol{\Omega} \times \boldsymbol{r}) + \frac{1}{2}m(\boldsymbol{\Omega} \times \boldsymbol{r})^2 - m\boldsymbol{r} \cdot \dot{\boldsymbol{V}} - U. \tag{9.6}$$

---

[6] As a simple illustration of this fictitious force consider the vertical motion of a particle of mass m viewed from an elevator that is accelerating upwards at the rate $\ddot{Y} = \dot{V} = a$ where $Y(t)$ is the height of the floor of the elevator above the ground (inertial frame). If y is the height of the particle with respect to the inertial frame and $\tilde{y}$ its height from the floor of the elevator, then $y = Y + \tilde{y}$. Moreover, $U = mgy$, so that $\frac{\partial U}{\partial \tilde{y}} = mg$. Thus the equation of motion in the inertial frame $m\ddot{y} = -mg$ becomes $m\ddot{\tilde{y}} = -mg - ma$ in the elevator frame. The fictitious inertial force is $-ma$. The Lagrangians in the inertial and noninertial frames are $L = \frac{1}{2}m\dot{y}^2 - mgy$ and $\tilde{L} = \frac{1}{2}m\dot{\tilde{y}}^2 - mg(Y + \tilde{y}) - ma\tilde{y}$. The $-mgY$ term can be dropped from the latter as it can be written as a time derivative.

[7] It arises from dividing $d\boldsymbol{r} + d\boldsymbol{\phi} \times \boldsymbol{r}$ by the small time interval dt in which the motion is a combination of a translation and an infinitesimal rotation (see Fig. 3.7) and taking $dt \to 0$.

Unlike (9.4), this Lagrangian has a term linear in the velocity $\boldsymbol{v} = \dot{\boldsymbol{r}}$, somewhat reminiscent of the Lagrangian (3.238) for a charged particle in a magnetic field. To identify the partial derivatives in Lagrange's equations, we write

$$\begin{aligned} dL &= \frac{\partial L}{\partial \boldsymbol{v}} \cdot d\boldsymbol{v} + \frac{\partial L}{\partial \boldsymbol{r}} \cdot d\boldsymbol{r} = m\boldsymbol{v} \cdot d\boldsymbol{v} + m d\boldsymbol{v} \cdot (\boldsymbol{\Omega} \times \boldsymbol{r}) + m\boldsymbol{v} \cdot (\boldsymbol{\Omega} \times d\boldsymbol{r}) \\ &\quad + m(\boldsymbol{\Omega} \times \boldsymbol{r}) \cdot (\boldsymbol{\Omega} \times d\boldsymbol{r}) - m\, d\boldsymbol{r} \cdot \dot{\boldsymbol{V}} - \boldsymbol{\nabla} U \cdot d\boldsymbol{r}. \end{aligned} \tag{9.7}$$

Using the identity $\boldsymbol{a} \cdot (\boldsymbol{b} \times \boldsymbol{c}) = (\boldsymbol{a} \times \boldsymbol{b}) \cdot \boldsymbol{c}$, we read off

$$\boldsymbol{p} = \frac{\partial L}{\partial \boldsymbol{v}} = m\boldsymbol{v} + m(\boldsymbol{\Omega} \times \boldsymbol{r}) \quad \text{and} \quad \frac{\partial L}{\partial \boldsymbol{r}} = m\boldsymbol{v} \times \boldsymbol{\Omega} + m(\boldsymbol{\Omega} \times \boldsymbol{r}) \times \boldsymbol{\Omega} - m\dot{\boldsymbol{V}} - \boldsymbol{\nabla} U. \tag{9.8}$$

We notice that the momentum $\boldsymbol{p}$ conjugate to $\boldsymbol{r}$ is not just the 'translational' momentum $m\boldsymbol{v}$ but includes a contribution from the rotation of the frame. This is reminiscent of the canonical momentum $\boldsymbol{p} = m\boldsymbol{v} + e\boldsymbol{A}/c$ of a charged particle in an electromagnetic field (3.153) with $\boldsymbol{\Omega} \times \boldsymbol{r}$ playing the role of the vector potential $\boldsymbol{A}/c$. Using $\dot{\boldsymbol{p}} = m\dot{\boldsymbol{v}} + m(\dot{\boldsymbol{\Omega}} \times \boldsymbol{r} + \boldsymbol{\Omega} \times \boldsymbol{v})$, Lagrange's equations

$$\dot{\boldsymbol{p}} = \frac{\partial L}{\partial \boldsymbol{r}} = \boldsymbol{p} \times \boldsymbol{\Omega} - m\dot{\boldsymbol{V}} - \boldsymbol{\nabla} U \quad \text{become} \tag{9.9}$$

$$m\dot{\boldsymbol{v}} = -\boldsymbol{\nabla} U - m\dot{\boldsymbol{V}} + m\boldsymbol{r} \times \dot{\boldsymbol{\Omega}} - 2m\boldsymbol{\Omega} \times \boldsymbol{v} - m\boldsymbol{\Omega} \times (\boldsymbol{\Omega} \times \boldsymbol{r}). \tag{9.10}$$

We have 3 new inertial fictitious forces associated with the rotation of K. The first $m\boldsymbol{r} \times \dot{\boldsymbol{\Omega}}$ is proportional to the moment of the angular acceleration of K and arises only if the rotation is nonuniform. The second $2m\boldsymbol{v} \times \boldsymbol{\Omega}$ is the Coriolis[8] force: it points in a direction orthogonal to the velocity of the particle as well as to the axis of rotation. It is reminiscent of the Lorentz force $(q/c)\boldsymbol{v} \times \boldsymbol{B}$ of Sect. 3.23*, with $2\boldsymbol{\Omega}$ playing the role of $\boldsymbol{B}/c$ and mass playing the role of charge. As with the magnetic force, it does no work on the particle (zero dot product with $\boldsymbol{v}$). Finally, we have the centrifugal force $-m\boldsymbol{\Omega} \times (\boldsymbol{\Omega} \times \boldsymbol{r})$ which points in a direction orthogonal to $\boldsymbol{\Omega}$ and away from the axis (centrifugal as opposed to centripetal) in the $\boldsymbol{r}$-$\boldsymbol{\Omega}$ plane. The centrifugal force has a magnitude $mr_\perp \Omega^2$ where $r_\perp$ is the particle's distance from the axis of rotation.

Example: planar motion viewed from a rotating frame. For instance, consider a particle of mass m moving on the x-y plane and viewed from a frame K (such as one attached to a merry-go-round) that rotates about the z-axis at the angular velocity $\boldsymbol{\Omega} = \Omega(t)\hat{z}$. Thus, $\boldsymbol{V} = 0$. This setup will be useful in our discussion of the Foucault pendulum in Sect. 9.4. Let us write (9.10) in cylindrical polar coordinates (r, θ, z) with $\hat{r} \times \hat{\theta} = \hat{z}$. For $z = 0$, from Appendix A.5 and Prob. 2.1 we have

$$\boldsymbol{r} = r\hat{r}, \quad \boldsymbol{v} = \dot{\boldsymbol{r}} = \dot{r}\hat{r} + r\dot{\theta}\hat{\theta} \quad \text{and} \quad \boldsymbol{a} = \dot{\boldsymbol{v}} = (\ddot{r} - r\dot{\theta}^2)\hat{r} + (r\ddot{\theta} + 2\dot{r}\dot{\theta})\hat{\theta}. \tag{9.11}$$

The fictitious forces are resolved into their radial and azimuthal components:

$$m\boldsymbol{r} \times \dot{\boldsymbol{\Omega}} = -mr\dot{\Omega}\hat{\theta}, \quad 2m\boldsymbol{v} \times \boldsymbol{\Omega} = -2m\dot{r}\Omega\hat{\theta} + 2mr\dot{\theta}\Omega\hat{r},$$

---

[8] Named after the French scientist Gaspard-Gustave de Coriolis who studied forces in rotating systems like waterwheels.

$$\text{while} \quad \boldsymbol{\Omega} \times \boldsymbol{r} = r\Omega\hat{\theta} \;\; \Rightarrow \;\; -m\boldsymbol{\Omega} \times (\boldsymbol{\Omega} \times \boldsymbol{r}) = mr\Omega^2 \hat{r}. \tag{9.12}$$

Thus, the radial component of the equation of motion (9.10) becomes

$$m(\ddot{r} - r\dot{\theta}^2) = -\hat{r} \cdot \boldsymbol{\nabla} U + 2mr\dot{\theta}\Omega + mr\Omega^2. \tag{9.13}$$

The LHS includes the radial and centripetal accelerations while the RHS includes contributions from the radial components of any real force, the Coriolis force and centrifugal force. The azimuthal component of the EOM is

$$m(r\ddot{\theta} + 2\dot{r}\dot{\theta}) = -\hat{\theta} \cdot \boldsymbol{\nabla} U - mr\dot{\Omega} - 2m\dot{r}\Omega. \tag{9.14}$$

The LHS includes the angular and Coriolis accelerations while the RHS receives contributions from the azimuthal components of any real force, the fictitious force due to any nonuniform rotation of K and the Coriolis force. □

9.3 Uniform rotation: Hamiltonian formulation and magnetic analog

We observe that the Lagrangian L (9.6) in frame K depends explicitly on time, through $\boldsymbol{V}(t)$ and $\boldsymbol{\Omega}(t)$. So, in general, there is no associated conserved energy. On the other hand, if there is no translational acceleration ($\dot{\boldsymbol{V}} = 0$) and the rotation is uniform ($\boldsymbol{\Omega}$ constant), then we get a time-independent Lagrangian

$$L = (m/2)\boldsymbol{v}^2 + m\boldsymbol{v} \cdot (\boldsymbol{\Omega} \times \boldsymbol{r}) + (m/2)(\boldsymbol{\Omega} \times \boldsymbol{r})^2 - U \tag{9.15}$$

and as in Sect. 3.9, an associated conserved energy. To find it, we recall that the momentum conjugate to $\boldsymbol{r}$ is $\boldsymbol{p} = m(\boldsymbol{v} + \boldsymbol{\Omega} \times \boldsymbol{r})$ so that the conserved energy in frame K is

$$E = \boldsymbol{p} \cdot \boldsymbol{v} - L = \frac{1}{2}m\boldsymbol{v}^2 + U - \frac{1}{2}m(\boldsymbol{\Omega} \times \boldsymbol{r})^2. \tag{9.16}$$

As we anticipated, there is no energy associated with the velocity-dependent Coriolis force. The new negative definite term in (9.16) is the centrifugal potential energy: $-\frac{1}{2}mr_\perp^2\Omega^2$. It is evidently more negative if the particle is farther away from the axis of rotation. Eliminating $\boldsymbol{v}$ in favor of $\boldsymbol{p}$, the Hamiltonian corresponding to (9.15) is

$$H = \frac{1}{2m}(\boldsymbol{p} - m\boldsymbol{\Omega} \times \boldsymbol{r})^2 - \frac{1}{2}m(\boldsymbol{\Omega} \times \boldsymbol{r})^2 + U = \frac{\boldsymbol{p}^2}{2m} - \boldsymbol{p} \cdot (\boldsymbol{\Omega} \times \boldsymbol{r}) + U. \tag{9.17}$$

The first term is similar to the Hamiltonian $(\boldsymbol{p} - q\boldsymbol{A}/c)^2/2m$ for a charged particle in a magnetic field (see (3.148) and Prob. 3.32) with $2\boldsymbol{\Omega}$ playing the role of the magnetic field $\boldsymbol{B}/c$ and $\boldsymbol{\Omega} \times \boldsymbol{r}$ the role of the vector potential $\boldsymbol{A}/c$ (see Prob. 3.31 and Prob. 9.3).

Pleasantly, upon use of the canonical PBs $\{r_i, p_j\} = \delta_{ij}$, the Hamiltonian (9.17) leads to the equation of motion (9.9) with $\dot{\boldsymbol{V}} = 0$. In fact, we find

$$\{p_i, H\} = \{p_i, -p_j(\boldsymbol{\Omega} \times \boldsymbol{r})_j + U\} = -p_j\epsilon_{jkl}\{p_i, \Omega_k r_l\} - \partial_i U = \epsilon_{jki}p_j\Omega_k - \partial_i U. \tag{9.18}$$

What does the other equation of motion $\dot{\boldsymbol{r}} = \{\boldsymbol{r}, H\}$ give? See Prob. 9.4.

Finally, let us relate the energy in the inertial and uniformly rotating frames in the absence of translational motion. If $\boldsymbol{V} = 0$, then $K_0 = K'$ so that $\boldsymbol{r}_0 = \boldsymbol{r}' = \boldsymbol{r}$ and

$\boldsymbol{v}_0 = \boldsymbol{v}' = \boldsymbol{v} + \boldsymbol{\Omega} \times \boldsymbol{r}$. An interesting implication is that the conjugate momenta in the frames K_0 and K are equal $\boldsymbol{p}_0 = m\boldsymbol{v}_0 = \boldsymbol{p}$, as are the corresponding angular momenta $\boldsymbol{L}_0 = \boldsymbol{r}_0 \times \boldsymbol{p}_0 = \boldsymbol{r} \times \boldsymbol{p} = \boldsymbol{L}$. The energy (9.16) may thus be expressed as

$$E = \frac{m}{2}(\boldsymbol{v}_0 - \boldsymbol{\Omega} \times \boldsymbol{r})^2 - \frac{m}{2}(\boldsymbol{\Omega} \times \boldsymbol{r})^2 + U = \frac{m}{2}\boldsymbol{v}_0^2 + U - m\boldsymbol{\Omega} \cdot (\boldsymbol{r} \times \boldsymbol{v}_0) = E_0 - \boldsymbol{L} \cdot \boldsymbol{\Omega}. \quad (9.19)$$

Thus, upon going to a uniformly rotating frame, the energy is reduced by $\boldsymbol{L} \cdot \boldsymbol{\Omega}$. This is the rotational analogue of what happens if we go from K_0 to a frame K moving at a constant velocity $\boldsymbol{V}$ so that $\boldsymbol{v}_0 = \boldsymbol{v} + \boldsymbol{V}$. In this case, show that $E = \frac{1}{2}m\boldsymbol{v}^2 = E_0 - \boldsymbol{p} \cdot \boldsymbol{V}$ up to a possible additive constant (see Prob. 9.5).

9.4 Precession of Foucault's pendulum

A Foucault pendulum is one with a heavy bob hung from a support by a long wire and free to swing in any direction. If the laboratory that houses the pendulum is an inertial frame then, ignoring friction, the tension in the wire and gravity are the only forces on the bob. As discussed in Sect. 1.5, the pendulum is expected to swing in a fixed plane (determined by initial conditions) with angular frequency $\omega = \sqrt{g/\ell}$ (for small oscillations). The Foucault pendulum was used to show that a lab on the Earth is not an inertial frame, by observing that the plane of oscillation of the pendulum precesses at a rate determined by the Earth's roughly constant angular velocity of rotation $\boldsymbol{\Omega}$ and the latitude λ of the lab ($\lambda = 0$ on the equator). The time period of this precession may be explained by invoking the Coriolis force due to the Earth's rotation on its axis.

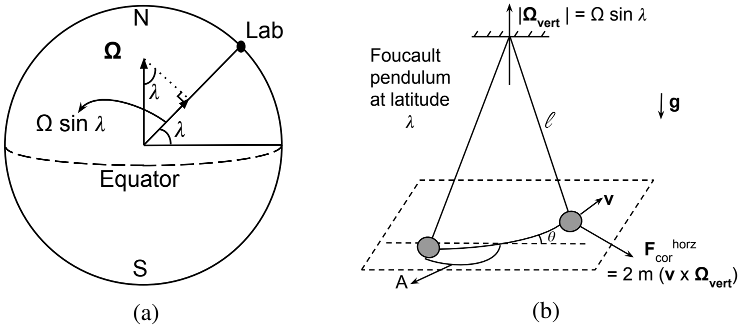

(a) (b)

Figure 9.2: (a) Vertical projection of the Earth's angular velocity at latitude λ is $\Omega \sin\lambda$. (b) Plane of oscillation of Foucault pendulum in a lab at latitude λ is specified by the angle θ of polar coordinates on the plane tangent to the Earth's surface.

To set up the problem, we use plane polar coordinates (r, θ) as in Fig. 9.2b to approximately locate the bob on the tangent plane to the Earth at the equilibrium location of the pendulum. If the lab were an inertial frame, then θ would be independent of time and for small oscillations, $r(t) = A \sin\omega t$ where A is the oscillation amplitude. Now recall from (9.10) that the Coriolis force is given by $-2m\boldsymbol{\Omega} \times \boldsymbol{v}$ where $\boldsymbol{\Omega}$ is the angular velocity of the Earth (it is ⊥ to the equatorial plane) and $\boldsymbol{v}$ the instantaneous velocity of the bob. For our purposes, $\boldsymbol{v}$ may be taken to lie approximately in the tangent plane to the Earth. We will resolve $\boldsymbol{\Omega}$ into a component $\boldsymbol{\Omega}_{\text{vert}}$ that points vertically upwards at the location of the lab and a component that is tangent to the Earth.

From Fig. 9.2a, $\boldsymbol{\Omega}_{\text{vert}}$ at latitude λ has a magnitude $\Omega \sin \lambda$ (this vertical component of $\boldsymbol{\Omega}$ vanishes along the equator). In addition to a vertical component (relative to the lab), the Coriolis force $-2m\boldsymbol{\Omega} \times \boldsymbol{v}$ generally has a component perpendicular to $\boldsymbol{v}$ in the horizontal r-θ plane. It arises from $\boldsymbol{\Omega}_{\text{vert}}$, which is orthogonal to $\boldsymbol{v}$ for small oscillations. This horizontal Coriolis force $\boldsymbol{F}_{\text{cor}}^{\text{horz}}$ can cause the pendulum's oscillation plane to change and is approximately $-2m\dot{r}(\Omega \sin \lambda)\,\hat{\theta}$ as $\boldsymbol{v} \approx \dot{r}\hat{r}$. Since gravity has no horizontal component and $\dot{\Omega} = 0$, the $\hat{\theta}$ component of the EOM (9.14) becomes

$$m(r\ddot{\theta} + 2\dot{r}\dot{\theta}) \approx -2m\dot{r}(\Omega \sin \lambda). \tag{9.20}$$

The simplest type of motion is where $\ddot{\theta} = 0$ and $\dot{\theta} = -\Omega \sin \lambda$ is constant. Thus, the simplest possibility is for the plane of oscillation of the pendulum to rotate at a constant angular speed $\Omega|\sin \lambda|$. The period of this precession is $T = 2\pi/\Omega|\sin \lambda|$. Foucault's pendulum was housed in the Pantheon in Paris, at a latitude $\lambda \approx 49°$N. Taking $2\pi/\Omega = 24$ hours and $\sin 49° \approx 3/4$, we find that Foucault's pendulum would precess once roughly every 32 hours. There is no such precession along the equator, where the horizontal Coriolis force vanishes. The precession period is 24 hours at the North (N) and South (S) poles. In fact, at N, the plane of oscillations of the pendulum is fixed in an inertial frame while the Earth rotates counterclockwise beneath it.

9.5* Circular restricted three-body problem

The restricted 3-body problem[9] is a simplified version of the 3-body problem (of Sect. 2.8*) where one of the masses m_3 is much lighter than the primaries $m_{1,2}$. Thus, m_1 and m_2 may be assumed to move in Keplerian orbits that are unaffected by m_3. The Sun-Earth-Moon system provides an example where we further have $m_2 \ll m_1$. In the planar circular restricted 3-body problem, the primaries move in fixed circular orbits around their common CM with angular speed $\Omega = (G(m_1 + m_2)/d^3)^{1/2}$ given by Kepler's 3rd law and m_3 moves in the same plane as $m_{1,2}$. Here, d is the separation between primaries. Thus, we may analyze the problem in a noninertial frame that rotates with the primaries at angular speed Ω, bringing the centrifugal and Coriolis forces into play. This system has one conserved quantity[10], the 'Jacobi integral' or energy of m_3 in the corotating frame of the primaries:

$$E = \left[\frac{1}{2}m_3\dot{r}^2 + \frac{1}{2}m_3 r^2\dot{\phi}^2\right] - \frac{1}{2}m_3\Omega^2 r^2 - Gm_3\left(\frac{m_1}{r_1} + \frac{m_2}{r_2}\right) \equiv T + V_{\text{eff}}. \tag{9.21}$$

As shown in Fig. 9.3a, r_1 and r_2 are the distances of m_3 from m_1 and m_2, while (r, ϕ) are the plane polar coordinates of m_3 in the corotating frame of the primaries with origin at their CM. The 'Roche' effective potential V_{eff}, named after the French astronomer Édouard Roche, includes a centrifugal contribution.

---

[9] This brief section is based on [72]. See [27, 106, 125] for more on this problem.

[10] This system has 2 degrees of freedom for the planar motion of m_3. Bruns (1887) and Poincaré (1889) [27, 133] essentially ruled out conserved quantities other than Jacobi's integral. So the restricted 3-body problem is not Liouville integrable in the sense of Sect. 11.7*. In fact, as mentioned in the discussion of homoclinic phenomena in Sect. 6.7*, it can display chaotic behavior.

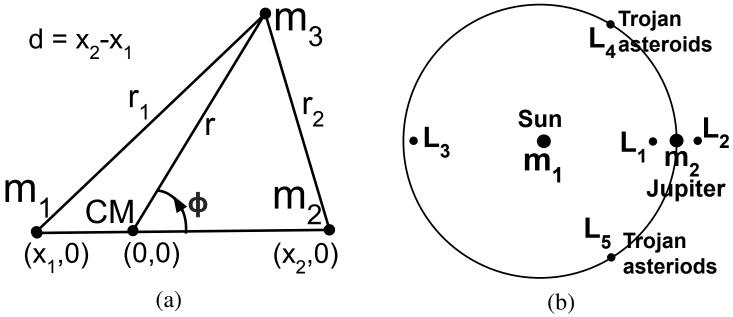

Figure 9.3: Circular restricted 3-body problem. (a) Coordinates of primaries ($m_{1,2}$) and secondary ($m_3 \ll m_{1,2}$) in the corotating frame of $m_{1,2}$. (b) Euler $(L_{1,2,3})$ and Lagrange $(L_{4,5})$ points for $m_1 \gg m_2 \gg m_{\text{asteroid}}$. Jupiter m_2 is in an approximately circular orbit around the Sun m_1. L_3 is closer to the Sun than Jupiter is. $L_{1,2}$ are symmetrically located on either side of Jupiter. L_4 & L_5 are equidistant from m_1 and m_2 and lie on the circular orbit of m_2.

In Sect. 2.8*, we described the Euler and Lagrange solutions to the 3-body problem, where each mass traverses a Keplerian orbit with one focus at the common CM. In the circular restricted 3-body problem, the primaries are in circular orbits around their CM. In a frame that rotates with the primaries, the possible locations of the infinitesimal third mass m_3 in the Euler and Lagrange solutions are called the Lagrange points (L_1, L_2, L_3) and (L_4, L_5) respectively (see Fig. 9.3b). The letter L stands both for Lagrange and for libration, which comes from the Latin word for 'balance'. As shown in Fig. 9.4, the Lagrange points lie at extrema of the Roche potential. If stable, an asteroid or satellite could occupy a Lagrange point. $L_{1,2,3}$ (also called Euler points) are saddle points of V_{eff} while $L_{4,5}$ are maxima. This suggests they are all unstable. However, V_{eff} does not include the effect of the Coriolis force since it does no work. A careful analysis [106, 125] shows that the Coriolis force stabilizes $L_{4,5}$. Euler points are always unstable while the Lagrange points $L_{4,5}$ are stable to small perturbations iff $(m_1 + m_2)^2 \geq 27 m_1 m_2$ [125]. More generally, in the unrestricted 3-body problem, the Lagrange equilateral solutions of Sect. 2.8* are stable iff Routh's (1877) inequality

$$(m_1 + m_2 + m_3)^2 \geq 27(m_1 m_2 + m_2 m_3 + m_3 m_1) \tag{9.22}$$

is satisfied. This happens, for instance, if one mass dominates the other two. Consequently, the Lagrange equilateral solutions are stable for the Sun-Jupiter-asteroid system. In fact, the Trojan asteroids are located at $L_{4,5}$ of the Sun-Jupiter system.

Although the Lagrange points $L_{1,2,3}$ are unstable, stable as well as unstable 'halo' and 'Lissajous' orbits around these points have been found numerically (the Mexican hat potential, Prob. 5.14 and Fig. 14.12b illustrate some ways this can happen in toy models). Stable orbits are useful. For instance, the LISA Pathfinder (a test mission for a space-based gravitational wave observatory) was placed around the L_1 point of the Sun-Earth system. The James Webb infrared space telescope (which images very old, distant or faint objects such as the earliest stars and galaxies to form) is positioned in a small orbit around L_2 while the Aditya solar mission satellite has been placed in a stable L_1 halo orbit 1.5 million km from the Earth[11]. By contrast with an observatory on the Earth or in a near-Earth orbit, a halo orbit around L_1 offers an uninterrupted view of the Sun (without eclipses) and is free of influences from the Earth's magnetic field and atmosphere, which should facilitate continuous observation and more accurate measurement of solar processes.

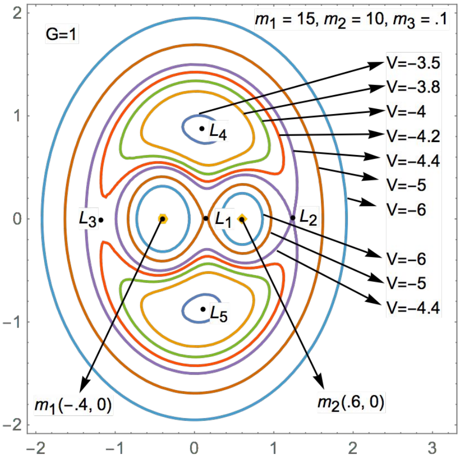

Roche effective potential for circular restricted three-body problem.

Lagrange points lie at extrema of Roche effective potential.

Hill region for E=-6 has 3 connected components.

Figure 9.4: Contours of Roche's effective potential in the corotating frame of the primaries for $G = 1, m_1 = 15, m_2 = 10$ and $m_3 = 0.1$. The trajectory of m_3 for given E is confined to the region $V_{\text{eff}}(x, y) \leq E$. Roche's lobes are the $V_{\text{eff}} = -5$ separatrices meeting at L_1.

9.6 Problems

1. A small bob of inertial and gravitational mass m_{in} and m_{gr} is suspended by a stretched string from the roof of a **car that accelerates** at the rate $\boldsymbol{A}$. The situation is viewed from the inertial frame of the road as well as from the accelerated frame of the car. Viewed from either frame, the string is seen to settle into a configuration where it hangs at a nonzero angle relative to the vertical, with the bob displaced towards the back of the car. If g is the magnitude of the acceleration due to gravity, show that the angle θ that the string makes with the vertical, as well as the tension T in the string are the same in both frames and given by

$$\theta = \arctan(m_{\text{in}} A / m_{\text{gr}} g) \quad \text{and} \quad T = (m_{\text{gr}}^2 g^2 + m_{in}^2 A^2)^{1/2}. \tag{9.23}$$

2. Consider an **elevator that is freely falling** in a uniform gravitational field. If a person in the elevator releases a ball from rest, what will it do and why?

---

[11] The Aditya space-based observatory will study the Sun's upper atmosphere, which includes the corona and chromosphere. One aim is to better understand the origin and dynamics of coronal mass ejections and solar flares by studying the coronal magnetic field and mechanisms for heat transfer in the plasma around the Sun. The dynamics of the solar atmosphere is also relevant to life on Earth: it affects near-Earth space weather which has implications for communications on the Earth and satellite operations.

3. Suppose the magnetic vector potential is given by $\boldsymbol{A}/c = \boldsymbol{\Omega} \times \boldsymbol{r}$. Calculate the **magnetic field** $\boldsymbol{B} = \boldsymbol{\nabla} \times \boldsymbol{A}$ and show that $\boldsymbol{B}/c = 2\boldsymbol{\Omega}$ by two methods: (a) use components and (b) use the identity [Whose is $\boldsymbol{\nabla} \cdot \boldsymbol{r}$ and what is $(\boldsymbol{\Omega} \cdot \boldsymbol{\nabla})\boldsymbol{r}$?]

$$\boldsymbol{\nabla} \times (\boldsymbol{f} \times \boldsymbol{g}) = \boldsymbol{f}(\boldsymbol{\nabla} \cdot \boldsymbol{g}) - \boldsymbol{g}(\boldsymbol{\nabla} \cdot \boldsymbol{f}) + (\boldsymbol{g} \cdot \boldsymbol{\nabla})\boldsymbol{f} - (\boldsymbol{f} \cdot \boldsymbol{\nabla})\boldsymbol{g}. \tag{9.24}$$

4. Work out the EOM for $\boldsymbol{r}$ implied by the Hamiltonian for a particle in a **uniformly rotating frame** (9.17) and canonical PBs. Show that $\dot{\boldsymbol{r}} = \frac{\boldsymbol{p}}{m} - \boldsymbol{\Omega} \times \boldsymbol{r}$.
5. **Energy transformation under a boost.** Suppose the Lagrangian is $L_0 = \frac{1}{2}mv_0^2$ in an inertial frame K_0. We boost to a new frame K moving at constant velocity $\boldsymbol{V}$ so that the velocity of the particle is $\boldsymbol{v}_0 = \boldsymbol{v} + \boldsymbol{V}$. Show that (a) the Lagrangian in K can be taken as $L = \frac{1}{2}m\boldsymbol{v}^2 + m\boldsymbol{v} \cdot \boldsymbol{V} + \frac{1}{2}m\boldsymbol{V}^2$, (b) the conjugate momenta $\boldsymbol{p}_0$ and $\boldsymbol{p}$ are equal and (c) that the conserved energies are related via $E = E_0 - \boldsymbol{p} \cdot \boldsymbol{V}$.

$*$6. Try to find the (approximate) coordinates of the **Lagrange points** of the circular restricted 3-body problem by determining the extrema of the **Roche potential**.

Chapter 10

Canonical transformations

In this chapter, we return to some structural features of classical mechanics, carrying on from where we left off in Chap. 3. Recall that canonical variables are a set of position-type and momentum-type coordinates q^i, p_i on phase space such that the equations of motion take the standard Hamiltonian form $\dot{q}^i = \frac{\partial H}{\partial p_i}$ and $\dot{p}_i = -\frac{\partial H}{\partial q^i}$ (3.78) for a suitable Hamiltonian $H(q,p)$ and $i = 1, \cdots, n$, where where n is the number of degrees of freedom. Roughly, we will define a canonical transformation as a change of phase space variables $(q^i, p_j) \mapsto (Q^i(q,p), P_j(q,p))$ such that the equations of motion, when transformed to the new variables, continue to take a Hamiltonian form. Canonical transformations bear a resemblance to some other transformations we encounter in mathematical physics. Recall from Appendix A.10 that an isomorphism L between vector spaces is one that preserves linear combinations: $L(au + bv) = aL(u) + bL(v)$ for any vectors u, v and scalars a, b. In other words, it preserves the linear structure of the space. An automorphism of a group (see Appendix B.13*) is a bijective map from a group to itself that preserves the group composition law. An isometry (see Footnote 28 of Appendix B.6*) is a map between spaces that preserves the distances between points. In a similar fashion, a canonical transformation is a change of coordinates on phase space that preserves the canonical Hamiltonian form of the equations of motion (Sect. 10.1). Interestingly, the same idea can also be expressed (see Sect. 10.2) in terms of Poisson brackets, without any reference to the Hamiltonian or Hamilton's equations: canonical transformations are those that preserve the canonical position-momentum PBs (3.126). This gives a way of constructing ('generating') transformations that will automatically ensure that the equations of motion (EOM) retain their Hamiltonian form. This feature can be exploited to change coordinates to ones where symmetries (when present) are more obvious and there are consequently more cyclic coordinates, making it easier to solve the EOM. In a similar vein, when there is a small parameter in the problem, one can sometimes make a succession of canonical transformations to bring the Hamiltonian to as simple a form as possible, order by order in a perturbation series in powers of the parameter.

Canonical transformations also have a geometric interpretation: they are transformations that preserve area elements in phase space (Sect. 10.4). This has far-reaching consequences for the nature of Hamiltonian mechanics and puts severe restrictions on the behavior of Hamiltonian vector fields (see Sect. 5.1) on phase space. For instance, as discussed in Sect. 10.8, their phase portraits cannot display nodes, spirals or limit cycles, though centers and saddle points are allowed. In particular, Hamiltonian systems cannot be dissipative or involve repellers or attractors. Another consequence is Liouville's theorem of Sect. 10.8: canonical transformations must preserve the volume of a region in phase space, although the region can be deformed beyond recognition. A prime example of a canonical transformation is time evolution and the preservation of phase volume has important consequences for trajectories. For instance, the Poincaré recurrence theorem (Sect. 10.9*) essentially states that for systems with a phase space of finite volume, almost all trajectories must eventually return arbitrarily close to where they began.

Canonical transformations can be composed and inverted: they form an infinite-dimensional group. Those that are close to the identity transformation are called infinitesimal, to distinguish them from other 'finite' canonical transformations. Remarkably, there is a beautiful correspondence between observables of a classical system and infinitesimal canonical transformations[1]. As we learn in Sect. 10.6, each dynamical variable in effect generates a canonical transformation. The most distinguished of these is the Hamiltonian, which generates time evolution. This observation also leads to a new viewpoint (Sect. 10.7) on symmetries, Noether's theorem and conserved quantities. In particular, we will discover that the conserved Noether charge of (3.49) may be interpreted as the infinitesimal generator of the canonical transformation that implements the symmetry.

Canonical transformations will also play an important role in Chapters 11 and 12. In Chap. 11, we will use them to distinguish between Hamiltonian systems that are solvable or integrable and those that are not. The former are distinguished by the existence of a canonical transformation to special canonical variables called angle-action variables. On the other hand, the Hamilton-Jacobi equation of Chap. 12 is an equation for the generating function of a canonical transformation. So it defines a sort of dynamics (or a path) on the group of canonical transformations. When the Hamilton-Jacobi equation admits a complete solution (e.g., via separation of variables), it gives an effective way of solving the initial value problem. Thus, canonical transformations can play a useful role in solving Hamiltonian systems.

Finally, a familiarity with of the structure of Hamiltonian mechanics in terms of canonical transformations allows us to understand much of the formalism of quantum mechanics, where unitary transformations play a similar role (see Sect. 10.3*). Moreover, the availability of canonical variables in a classical system makes it easier to pass to the corresponding quantum theory. Quantization involves representing classical observables as Hermitian linear operators on a vector space with inner product (Hilbert space) in such a way that the algebra of their commutators mimics their Poisson bracket algebra (at least to leading order in Planck's constant). For the canonical Poisson brackets, there is a standard representation (the Schrödinger representation) which allows us to set up the quantum theory without much ado. Thus, canonical variables and canonical transformations are of great conceptual and practical value in both the classical and quantum settings.

---

[1] As we will see in Sect. 10.10, something similar also applies to finite canonical transformations.

10.1 From point transformations to canonical transformations

Recall that the space of generalized coordinates and momenta (q, p) is called the phase space. Hamilton's equations $\dot{q}^i = \frac{\partial H}{\partial p_i}, \dot{p}_i = -\frac{\partial H}{\partial q^i}$ (3.78) may be easier to solve (or understand qualitatively) in some systems of coordinates and momenta compared to others. For instance, some symmetries may be more obvious in certain coordinate systems rather than others and be manifested via the presence of more cyclic coordinates.

Example: Cartesian to plane polar coordinates. For a particle in a central potential $V(r)$ on the plane, rotations about the origin are a symmetry and the angle θ is a cyclic coordinate. This makes the EOM simpler to handle in polar coordinates r and θ rather than in Cartesian coordinates x, y. In fact, from the Lagrangian

$$\begin{aligned} L(x,y,\dot{x},\dot{y}) &= \frac{1}{2}m\left(\dot{x}^2+\dot{y}^2\right) - V\left(\sqrt{x^2+y^2}\right) \\ &= \frac{1}{2}m\left(\dot{r}^2+r^2\dot{\theta}^2\right) - V(r) = \tilde{L}(r,\theta,\dot{r},\dot{\theta}), \end{aligned} \tag{10.1}$$

we see that θ is a cyclic coordinate and its conjugate momentum $p_\theta = \frac{\partial \tilde{L}}{\partial \dot{\theta}} = mr^2\dot{\theta}$ is conserved. As a consequence, the radial equation

$$\dot{p}_r = \frac{d}{dt}\frac{\partial \tilde{L}}{\partial \dot{r}} = \frac{\partial \tilde{L}}{\partial r} \quad \text{or} \quad m\ddot{r} = p_\theta^2/mr^3 - V'(r) \tag{10.2}$$

decouples from the angular one, making them easier to solve. On the other hand, neither $p_x = \partial L/\partial \dot{x} = m\dot{x}$ nor $p_y = \partial L/\partial \dot{y} = m\dot{y}$ is conserved and the Cartesian position coordinates satisfy coupled equations. Now, the Hamiltonian is given by

$$H = \frac{p_x^2}{2m} + \frac{p_y^2}{2m} + V(\sqrt{x^2+y^2}) = \frac{p_r^2}{2m} + \frac{p_\theta^2}{2mr^2} + V(r) = \tilde{H}(r,\theta,p_r,p_\theta). \tag{10.3}$$

One checks that the equations of motion take the same form in Cartesian and polar coordinates (as guaranteed by the argument in Sect. 3.20*):

$$\begin{aligned} & \dot{x} = \frac{\partial H}{\partial p_x}, \quad \dot{y} = \frac{\partial H}{\partial p_y}, \qquad \dot{p}_x = -\frac{\partial H}{\partial x}, \quad \dot{p}_y = -\frac{\partial H}{\partial y} \\ \Leftrightarrow \quad & \dot{r} = \frac{\partial \tilde{H}}{\partial p_r}, \quad \dot{\theta} = \frac{\partial \tilde{H}}{\partial p_\theta}, \qquad \dot{p}_r = -\frac{\partial \tilde{H}}{\partial r}, \quad \dot{p}_\theta = -\frac{\partial \tilde{H}}{\partial \theta}. \end{aligned} \tag{10.4}$$

Since the EOM take the same Hamiltonian form, we say that the transformation from Cartesian coordinates and conjugate momenta (x, y, p_x, p_y) to polar ones

$$r = \sqrt{x^2+y^2}, \quad \theta = \arccos\frac{x}{\sqrt{x^2+y^2}}, \quad p_r = \frac{xp_x + yp_y}{\sqrt{x^2+y^2}} \text{ and } p_\theta = xp_y - yp_x, \tag{10.5}$$

is a canonical transformation (CT). For future reference, we notice that in this transformation, the new positions (r, θ) do not depend on the old momenta (p_x, p_y). This is because the transformation arose from a change of variables on the $x-y$ configuration space with conjugate momenta changing in a manner specified by the Lagrangian. We also check (see Prob. 3.45) that the basic Poisson brackets among coordinates and momenta (3.126) are preserved:

$$\begin{aligned} &\{x,p_x\} = \{y,p_y\} = 1, \qquad \{x,p_y\} = \{y,p_x\} = \{x,y\} = \{p_x,p_y\} = 0 \quad \text{and} \\ &\{r,p_r\} = \{\theta,p_\theta\} = 1, \qquad \{r,p_\theta\} = \{\theta,p_r\} = \{r,\theta\} = \{p_r,p_\theta\} = 0. \end{aligned} \tag{10.6}$$

We will soon see that this connection between preserving the form of Hamilton's equations and that of the PBs is generally valid. □

Definition of a canonical transformation. Suppose we start with a system of coordinates q^i and conjugate momenta p_i, in which the EOM take the standard Hamiltonian form $\dot{q}^i = \frac{\partial H}{\partial p_i}, \dot{p}_i = -\frac{\partial H}{\partial q^i}$ for $i = 1,\ldots,n$. Such a system of coordinates and momenta is said to be canonical. Consider an invertible transformation from old variables (q^i, p_i) to new ones $(Q^i(q,p), P_i(q,p))$. Suppose the EOM in the new variables can be expressed in the Hamiltonian form $\dot{Q}^i = \frac{\partial \tilde{H}}{\partial P_i}, \dot{P}_i = -\frac{\partial \tilde{H}}{\partial Q^i}$ where $\tilde{H}(Q,P) = H(q(Q,P), p(Q,P))$ is the transformed Hamiltonian. If this can be done for any choice of old Hamiltonian H, then we will call the transformation canonical. In other words, a CT is a transformation between two sets of canonical variables, it preserves the form of Hamilton's equations. If we make a change of variables that is canonical, we do not need to transform the EOM. The latter are guaranteed to take the Hamiltonian form, so we may write them down once we obtain the transformed Hamiltonian. This is useful since there are ways to guarantee the canonicity of a transformation without any reference to the Hamiltonian or Hamilton's equations.

Transformations that are not canonical. To be sure, not every choice of coordinates and momenta is canonical. For example, notice that Hamilton's equations treat coordinates and momenta on a nearly equal footing. So suppose we simply swap them by defining $Q = p$ and $P = q$. Then the Hamiltonian may be written in terms of the new variables $H(q,p) = H(P,Q)$. The new Hamiltonian is then defined as $\tilde{H}(Q,P) = H(q(Q,P), p(Q,P)) = H(P,Q)$. We find that

$$\dot{Q} = \dot{p} = -\frac{\partial H}{\partial q} = -\frac{\partial \tilde{H}}{\partial P} \quad \text{and} \quad \dot{P} = \dot{q} = \frac{\partial H}{\partial p} = \frac{\partial \tilde{H}}{\partial Q}. \tag{10.7}$$

So the EOM in the new variables *do not* have the form of Hamilton's equations (3.78), they are off by a sign. So $(q,p) \mapsto (p,q)$ is *not* a canonical transformation. We may also check that the transformation *does not* preserve the basic PB

$$\{q,p\} = 1 \quad \text{while} \quad \{Q,P\} = \{p,q\} = -1. \tag{10.8}$$

Point transformation. In Sect. 3.20*, we saw that any change of coordinates alone ('*point transformation*' on configuration space) $q^i \to Q^i$, with the associated 'induced' change in momenta $P_i = \frac{\partial \tilde{L}}{\partial \dot{Q}^i}$ is automatically canonical. An example of such a canonical transformation is the one from Cartesian to polar coordinates for a particle on a plane. Interestingly, there are canonical transformations that are *more general* than those resulting from changes of coordinates on the configuration space $\mathcal{Q}$. Perhaps the simplest such examples are (1) $Q = p, P = -q$ and (2) $Q = -p, P = q$ which exchange coordinates and momenta up to a sign for one degree of freedom. Check that Hamilton's equations retain their form, as do the basic PBs (3.125). □

In the above examples of CTs, along with Hamilton's equations, the basic PBs among coordinates and momenta were preserved. This is generally true.

10.2 Form of Hamilton's equations is preserved iff PBs are preserved

It is worth noting that a transformation is canonical irrespective of what the Hamiltonian is. The form of Hamilton's equations must be unchanged for *any* smooth $H(q,p)$. This suggests it should be possible to state the condition of canonicity without reference to the Hamiltonian. This is indeed the case.

Proposition. A transformation preserves the form of Hamilton's equations (i.e., is canonical) if and only if it preserves the basic Poisson brackets.

Proof: For simplicity, we consider the case of one degree of freedom, though the argument can be extended, along similar lines, to more degrees of freedom. Suppose we make a smooth invertible change of coordinates and momenta $q \mapsto Q = Q(q,p)$ and $p \mapsto P = P(q,p)$. The inverse transformation expresses the old coordinates and momenta in terms of the new ones $q = q(Q,P)$ and $p = p(Q,P)$. The old coordinates satisfy canonical Poisson brackets $\{q,p\} = 1$, $\{q,q\} = \{p,p\} = 0$. Under this change, the old Hamiltonian $H(q,p)$ transforms into a new Hamiltonian $\tilde{H}(Q,P) = H(q(Q,P), p(Q,P))$. Suppose the above transformation preserves the form of Hamilton's equations. Denoting partial derivatives by subscripts,

$$\dot{q} = H_p \quad \text{and} \quad \dot{p} = -H_q \quad \text{while} \quad \dot{Q} = \tilde{H}_P \quad \text{and} \quad \dot{P} = -\tilde{H}_Q. \tag{10.9}$$

Then we will show that $\{Q,P\} = 1$. The other two Poisson brackets $\{Q,Q\}$ and $\{P,P\}$ vanish by antisymmetry.

By Hamilton's equations and the chain rule,

$$\dot{Q} = \tilde{H}_P = H_q\, q_P + H_p\, p_P = -\dot{p}\, q_P + \dot{q}\, p_P. \tag{10.10}$$

We also know that $\dot{Q} = Q_q \dot{q} + Q_p \dot{p}$. We want to equate these two expressions and extract information about the PB $\{Q,P\} = Q_q P_p - Q_p P_q$. As it is the partial derivatives of Q and P that appear in this PB, it is of interest to express q_P, p_P, etc., in terms of partial derivatives of Q and P using the following Lemma.

Lemma. The partial derivatives of the new coordinates and momenta are related to those of the old coordinates and momenta via

$$q_P = -\frac{Q_p}{\{Q,P\}}, \quad p_P = \frac{Q_q}{\{Q,P\}}, \quad p_Q = -\frac{P_q}{\{Q,P\}} \quad \text{and} \quad q_Q = \frac{P_p}{\{Q,P\}}. \tag{10.11}$$

Proof: Recall that for an invertible map of one variable, $x \to X(x) = f(x)$ with inverse $x = x(X) = f^{-1}(X)$ the derivatives are reciprocally related $\frac{dX}{dx} = \left(\frac{dx}{dX}\right)^{-1}$. This arises from differentiating the identity $(f \circ f^{-1})(X) = f(f^{-1}(X)) = X$ with respect to X. We get $f'(x)x'(X) = 1$ or $X'(x)x'(X) = 1$.

What is the analogous formula for the map $F : x^i = (q,p) \mapsto X^i = (Q,P)$? Here

$$F : \mathbb{R}^2 \to \mathbb{R}^2, \quad F(q,p) = (Q,P) \quad \text{and} \quad F^{-1} : \mathbb{R}^2 \to \mathbb{R}^2, \quad F^{-1}(Q,P) = (q,p). \tag{10.12}$$

In other words, $F^{-1}(\boldsymbol{X}) = \boldsymbol{x}$ or $F^i(\boldsymbol{x}) = X^i$. As before, $F \circ F^{-1}$ is the identity, so

$$F(F^{-1}(\boldsymbol{X})) = \boldsymbol{X} \quad \Rightarrow \quad F^i(\boldsymbol{x}(\boldsymbol{X})) = X^i, \;\; \text{and differentiating,} \quad \frac{\partial F^i}{\partial x^j}\frac{\partial x^j}{\partial X^k} = \delta^i_k. \tag{10.13}$$

Here, the Jacobian matrices of first partials are

$$\frac{\partial F^i}{\partial x^j} = \begin{pmatrix} \frac{\partial Q}{\partial q} & \frac{\partial Q}{\partial p} \\ \frac{\partial P}{\partial q} & \frac{\partial P}{\partial p} \end{pmatrix} \quad \text{and} \quad \frac{\partial x^j}{\partial X^k} = \begin{pmatrix} \frac{\partial q}{\partial Q} & \frac{\partial q}{\partial P} \\ \frac{\partial p}{\partial Q} & \frac{\partial p}{\partial P} \end{pmatrix}. \tag{10.14}$$

The above condition says that the matrix product must be the identity

$$\begin{pmatrix} \frac{\partial Q}{\partial q} & \frac{\partial Q}{\partial p} \\ \frac{\partial P}{\partial q} & \frac{\partial P}{\partial p} \end{pmatrix} \begin{pmatrix} \frac{\partial q}{\partial Q} & \frac{\partial q}{\partial P} \\ \frac{\partial p}{\partial Q} & \frac{\partial p}{\partial P} \end{pmatrix} = \begin{pmatrix} 1 & 0 \\ 0 & 1 \end{pmatrix}. \tag{10.15}$$

We get a system of 4 inhomogeneous linear equations for q_Q, q_P, p_Q and p_P:

$$Q_q q_P = -Q_p p_P, \;\; P_q q_P + P_p p_P = 1, \;\; P_q q_Q = -P_p p_Q, \;\; \text{and} \;\; Q_q q_Q + Q_p p_Q = 1. \tag{10.16}$$

These are, in fact, two pairs of linear equations in two unknowns each.

$$\begin{pmatrix} Q_q & Q_p \\ P_q & P_p \end{pmatrix}\begin{pmatrix} q_P \\ p_P \end{pmatrix} = \begin{pmatrix} 0 \\ 1 \end{pmatrix} \quad \text{and} \quad \begin{pmatrix} Q_q & Q_p \\ P_q & P_p \end{pmatrix}\begin{pmatrix} p_Q \\ q_Q \end{pmatrix} = \begin{pmatrix} 1 \\ 0 \end{pmatrix}. \tag{10.17}$$

Their solution involves the reciprocal of the determinant of the coefficient matrix, which is just the PB $\{Q,P\} = Q_q P_p - Q_p P_q$:

$$q_P = -\frac{Q_p}{\{Q,P\}}, \quad p_P = \frac{Q_q}{\{Q,P\}}, \quad p_Q = -\frac{P_q}{\{Q,P\}}, \quad q_Q = \frac{P_p}{\{Q,P\}}, \tag{10.18}$$

as desired. □

Armed with this Lemma, we return to (10.10) and the fact that the EOM retains its form in the new variables:

$$\dot Q = \tilde H_P = \frac{[\dot p Q_p + \dot q Q_q]}{\{Q,P\}} = \frac{\dot Q}{\{Q,P\}}. \tag{10.19}$$

For this equation to be satisfied we must have $\{Q,P\} = 1$. Similarly,

$$\dot P \;\; = \;\; -\tilde H_Q = -H_q q_Q - H_p p_Q = \dot p \frac{P_p}{\{Q,P\}} + \dot q \frac{P_q}{\{Q,P\}}$$

$$= \frac{1}{\{Q,P\}}\left[P_q\dot{q} + P_p\dot{p}\right] = \frac{\dot{P}}{\{Q,P\}}. \tag{10.20}$$

For this to hold, again we need $\{Q, P\} = 1$. Thus, we have shown that if Hamilton's equations retain their form in the new coordinates, then the transformation also preserves the form of the basic PBs.

Let us now prove the converse, namely, if the transformation $(q, p) \mapsto (Q, P)$ preserves the form of the PB, i.e., if $\{Q, P\} = 1$, then it must preserve the form of Hamilton's equations. So we must show that $\frac{\partial \tilde{H}}{\partial P} = \dot{Q}$ and $-\frac{\partial \tilde{H}}{\partial Q} = \dot{P}$. Let us compute

$$\frac{\partial \tilde{H}}{\partial P} = \frac{\partial H}{\partial q} q_{\scriptscriptstyle P} + \frac{\partial H}{\partial p} p_{\scriptscriptstyle P} = -\dot{p} q_{\scriptscriptstyle P} + \dot{q} p_{\scriptscriptstyle P} = \dot{p} Q_p + \dot{q} Q_q = \dot{Q}. \tag{10.21}$$

In the penultimate equality we used the Lemma and the assumption that $\{Q, P\} = 1$. So the 1^{st} of Hamilton's equations holds in the new variables! Similarly, we show that the 2^{nd} of Hamilton's equations also holds in the new variables

$$\frac{\partial \tilde{H}}{\partial Q} = \frac{\partial H}{\partial q}\frac{\partial q}{\partial Q} + \frac{\partial H}{\partial p}\frac{\partial p}{\partial Q} = -\dot{p} q_{\scriptscriptstyle Q} + \dot{q} p_{\scriptscriptstyle Q} = -\dot{p} P_p - \dot{q} P_q = -\dot{P}. \tag{10.22}$$

So we showed that if the transformation preserves the PB, then it is canonical (i.e., preserves the form of Hamilton's equations). □

A similar result holds for several degrees of freedom. Thus, the transformation as well as the new coordinates and momenta are said to be canonical provided Hamilton's equations retain their form

$$\dot{Q}^i = \frac{\partial \tilde{H}}{\partial P_i} \quad \text{and} \quad \dot{P}_i = -\frac{\partial \tilde{H}}{\partial Q^i} \tag{10.23}$$

or equivalently, if the Poisson brackets are preserved:

$$\{Q^i, P_j\} = \delta^i_j \quad \text{and} \quad \{Q^i, Q^j\} = 0 = \{P_i, P_j\} \quad \text{for all} \quad i, j. \tag{10.24}$$

Time evolution as a canonical transformation. Perhaps the most important examples of canonical transformations are furnished by time evolution by any fixed Hamiltonian H (which could depend explicitly on time). Let us indicate why this is true. Suppose $q(0), p(0)$ are canonical phase space variables describing the possible state of a particle at $t = 0$. Then $\{q(0), p(0)\} = 1$ while $\{q(0), q(0)\} = 0 = \{p(0), p(0)\}$. After a small time δt, the position and momentum are given by

$$q(\delta t) = q(0) + \delta t \frac{\partial H}{\partial p} + \mathcal{O}(\delta t^2) \quad \text{and} \quad p(\delta t) = p(0) - \delta t \frac{\partial H}{\partial q} + \mathcal{O}(\delta t^2), \tag{10.25}$$

where we made use of Hamilton's equations (3.78). To show that infinitesimal time evolution is a CT, we must show that $\{q(\delta t), p(\delta t)\} = 1$ and $\{q(0), q(0)\} = 0 = \{p(0), p(0)\}$. The latter follow by antisymmetry. We evaluate the former keeping terms up to order δt:

$$\{q(\delta t), p(\delta t)\} = \{q(0) + \delta t \frac{\partial H}{\partial p}, p(0) - \delta t \frac{\partial H}{\partial q}\} + \cdots$$

$$
\begin{aligned}
&= \{q(0),p(0)\} + \delta t\left(-\{q(0),\frac{\partial H}{\partial q}\} + \{\frac{\partial H}{\partial p},p(0)\}\right) + \cdots \\
&= 1 + \delta t(-H_{pq} + H_{qp}) + \mathcal{O}(\delta t)^2 = 1 + \mathcal{O}(\delta t)^2. \qquad (10.26)
\end{aligned}
$$

On the RHS, all quantities are evaluated at $t = 0$. More generally, the equal-time Poisson brackets of coordinates and momenta

$$\{q^i(t), p_j(t)\} = \delta^i_j \quad \text{and} \quad \{q^i(t), q^j(t)\} = \{p_i(t), p_j(t)\} = 0 \qquad (10.27)$$

are valid at all times t [see (10.48)]. Thus, the transformation

$$(q^i(t_1), p_i(t_1)) \mapsto (q^i(t_2), p_i(t_2)), \qquad (10.28)$$

which is a map from phase space to itself, is canonical for any two times t_1 and t_2. Keeping t_1 fixed and allowing t_2 to vary, Hamiltonian time evolution gives us a 1-parameter family of canonical transformations labelled by time t_2. □

Passive and active viewpoints. It is noteworthy that in this discussion, we have changed our perspective. In Sect. 10.1 and earlier in Sect. 10.2, we spoke of a change of phase space coordinates $(q,p) \mapsto (Q,P)$ as being canonical if the PBs are preserved. Here, we extend the concept to maps from phase space M to itself. Under a coordinate change, a physical point on phase space gets a new address. By contrast, under a map from M to M, a point (q,p) on phase space moves to a possibly different point (q',p') on M. We declare that the map is a CT if the primed quantities satisfy the same canonical PBs as the unprimed ones. Time evolution from t_1 to t_2 is evidently a map from M to M, since it takes any phase point to another phase point (along a trajectory). Thus (10.27), considered at two times t_1 and t_2, would imply that time evolution is a CT in this new sense. In what follows, we will use the term canonical transformation both for *passive* changes of coordinates on phase space and for *active* transformations that rearrange points on phase space while preserving the canonical PB relations. □

Unequal-time PBs. It may be noted that unequal-time Poisson brackets contain dynamical information and depend on the Hamiltonian (see Prob. 3.47). Equal-time PBs do not depend on the Hamiltonian and are in a sense kinematical. Unequal-time PBs $\{f(q(0),p(0)), g(q(t),p(t))\}$ may be reduced to equal-time PBs by solving the EOM and expressing $g(q(t),p(t))$ in terms of the initial values $q(0)$ and $p(0)$. □

10.3* Brief comparison of classical and quantum mechanical formalisms

We are now in a position to compare features of the Hamiltonian formalism of classical mechanics (CM) with the corresponding notions of quantum mechanics (QM). QM was developed in the first half of the 20th century to understand the properties of microscopic systems like atoms, molecules and photons. They displayed both wave-like and particle-like behavior depending on how they were observed. QM involves a new parameter, Planck's constant h, whose value is 6.6×10^{-34} Joule $\cdot$ sec. The smallness of h relative to quantities with the same dimensions encountered in macroscopic phenomena explains why quantum effects are often suppressed. Like CM, QM too has concepts of states and observables as well as time evolution. A key difference is that on account of the linear superposition principle (necessitated by observations of interference and diffraction of electron and atom 'matter waves') the quantum state space is a linear vector space unlike the classical phase space which is a manifold.

1. In CM, the space of (pure) states is the phase space, the space of positions and momenta. It is often the cotangent bundle[2] of the configuration space $\mathcal{Q}$. In QM, it is a vector space, the quantum mechanical Hilbert space[3] $\mathcal{H}$. Vectors in this space (up to scalar multiplication) are the possible states of the system, so linear combinations of states are also allowed states. $\mathcal{H}$ can typically be taken to be the space of square-integrable complex-valued functions on the classical configuration space: $L^2(\mathcal{Q},\mathbb{C})$. In the so-called position representation or basis, the states of a single particle moving in $\mathcal{Q}=\mathbb{R}^3$ are complex 'wave functions' $\psi(\boldsymbol{r})$ with $|\psi(\boldsymbol{r})|^2 d\boldsymbol{r}$ interpreted as the probability to find the particle in the infinitesimal volume $d\boldsymbol{r}$ around $\boldsymbol{r}$. The squared-norm $\int |\psi|^2 d\boldsymbol{r}$ must equal one, since this is the total probability to find the particle somewhere. This is why we insist on square-integrable functions on the classical configuration space, $L^2(\mathbb{R}^3,\mathbb{C})$ in this case. It turns out that we need to allow for complex vectors to accommodate the sort of wave phenomena observed in the quantum realm, which is somewhat different from that in classical sound or electromagnetic waves. Moreover, time evolution in QM is such that even if the initial state is real, it will in general become complex at the next instant. Probabilities, being proportional to the absolute square, remain real. Evidently, we use an infinite-dimensional vector space to model the translational states of motion of a particle (the need for an infinite-dimensional space will be clarified below). On the other hand, to model the spin states of a particle, a finite-dimensional complex vector space suffices: $\mathbb{C}^2$ for spin-$\frac{1}{2}$, $\mathbb{C}^3$ for spin 1 and so forth.
2. In CM, observables $f, g, \ldots$ are smooth real-valued functions on phase space. In QM, observables $(A, B, \ldots)$ are self-adjoint (Hermitian operators whose domain coincides with that of their Hermitian adjoints) linear operators on the quantum Hilbert space. Once a basis is chosen, we may represent quantum observables as (finite or infinite) matrices (see Appendix A.10). Self-adjointness is the analog of real-valuedness of classical observables, both of which ensure that results of measurements are real numbers. While each value of a classical dynamical variable f is a possible result of its measurement, the eigenvalues of A are the possible results when a quantum observable A is measured.

---

[2] Recall from Sect. 3.7, that velocity vectors at a point of $\mathcal{Q}$ span the tangent space to $\mathcal{Q}$ at that point. The vector space dual to the tangent space is the cotangent space and is spanned by momentum covectors. The union of all the cotangent spaces over each point of the configuration space is called the cotangent bundle.

[3] A Hilbert space is a complex vector space $\mathcal{H}$ (see Appendix A.10) with Hermitian positive-definite inner product $\langle\phi,\psi\rangle$. [See Sect. 18.3* for more on Dirac's bra-ket notation]. This means $\langle\phi,\psi\rangle = \langle\psi,\phi\rangle^*$, $\langle\psi,\psi\rangle \geq 0$ (with equality only if $\psi = 0$), linearity in ψ and consequently antilinearity in ϕ: $\langle a\phi, b\psi\rangle = a^* b\langle\phi,\psi\rangle$ and $\langle\phi_1+\phi_2,\psi_1+\psi_2\rangle = \langle\phi_1,\psi_1\rangle + \langle\phi_1,\psi_2\rangle + \langle\phi_2,\psi_1\rangle + \langle\phi_2,\psi_2\rangle$ for all vectors $\psi, \phi, \ldots$ and complex numbers a, b.

3. Classical observables form a commutative algebra under pointwise[4] multiplication. Thus $\alpha f + \beta g$ and $(fg)(\xi) = (gf)(\xi) = f(\xi)g(\xi)$ are observables for any $\alpha, \beta \in \mathbb{R}$ if f and g are. Linear operators on a quantum Hilbert space do not commute ($AB \neq BA$ for square matrices) in general: they form a noncommutative but associative $[(AB)C = A(BC)]$ algebra. What is more, the product of two Hermitian operators fails to be Hermitian if they do not commute. Nevertheless, it is possible to combine two observables to get a third in a different manner, as we discuss below.

4. The Poisson bracket of observables f and g in CM is another observable $\{f, g\}$. In QM, the role of the Poisson bracket is played by the commutator of operators (up to a factor of $i\hbar$). The commutator is defined as $[A, B] = AB - BA$ and one checks that $\frac{1}{i\hbar}[A, B]$ is Hermitian if A and B are. For e.g., the role of the canonical PB relation $\{x, p\} = 1$ for a particle in CM is played by the Heisenberg canonical commutation relation $\frac{1}{i\hbar}[\hat{x}, \hat{p}] = I$ where $\hat{x}$ and $\hat{p}$ are the position and momentum operators and I the identity operator. From this, we may deduce why we need an infinite-dimensional vector space to model the quantum states of a particle. For finite-dimensional ($n \times n$) matrices, the trace of the commutator $\operatorname{tr}[A, B]$ vanishes since $\operatorname{tr} AB = \operatorname{tr} BA = \sum_{1 \leq i,j \leq n} A_{ij} B_{ji}$. On the other hand, $\operatorname{tr} I = n$. So if $[\hat{x}, \hat{p}] = i\hbar I$ must hold, $\hat{x}$ and $\hat{p}$ cannot be finite-dimensional matrices. On the other hand, the trace of the commutator of a pair or infinite matrices can diverge, just like the trace of an infinite-dimensional identity matrix.

5. Classical time evolution of any observable f is governed by Hamilton's equation $\dot{f} = \{f, H\}$. In the quantum theory, an observable A evolves according to the Heisenberg equation of motion $i\hbar \partial_t \hat{A} = [\hat{A}, \hat{H}]$. Henceforth, we will often omit the hats on quantum observables.

6. A unitary transformation is a linear transformation U satisfying $U^\dagger U = U U^\dagger = I$. Unitary transformations, which act on states and observables via $|\psi\rangle \to |\psi'\rangle = U|\psi\rangle$ and $A \to A' = U A U^\dagger$, are quantum analogs of canonical transformations. Both preserve the structure of the formalism and the equations of motion. CTs preserve the basic PB relations while unitary transformations preserve the Heisenberg canonical commutation relations, since $[A', B'] = U[A, B]U^\dagger$ and in particular $[x', p'] = U[x, p]U^\dagger = U(i\hbar I)U^\dagger = i\hbar I$. For the same reason, unitary transformations leave the Heisenberg equations of motion invariant. Unitary transformations also preserve inner products (and consequently, the squared-norm $\langle\psi|\psi\rangle$) of a state:
$$\langle\phi'|\psi'\rangle = \langle U\phi|U\psi\rangle = \langle\phi|U^\dagger U\psi\rangle = \langle\phi|\psi\rangle. \tag{10.29}$$
Now, the norm of a state may be interpreted as the total probability of finding the system in some configuration. This makes unitary transformations appropriate for physical changes/processes in which probability is conserved.

7. In CM, time evolution is a 1-parameter family of canonical transformations (10.28) on phase space. In QM, time evolution (which conserves probabilities) is repre-

---

[4] *Pointwise* means f and g are multiplied at the same point ξ to get the value of fg at ξ.

sented by a 1-parameter family of unitary transformations on the quantum Hilbert space: $U(t,0) = e^{-iHt/\hbar}$ acts on the initial state $|\psi(0)\rangle$ to produce the state $|\psi(t)\rangle$.

$*$ **Schrödinger equation as Hamilton's equations.** Quite apart from the above analogies between classical and quantum mechanical formalisms, there is an amusing sense in which the Schrödinger equation $[i\hbar\partial_t|\psi(t)\rangle = \hat{H}|\psi(t)\rangle]$ for the time evolution of the state vector in QM can be thought of as Hamilton's equations for the coordinates on a suitable (linear) classical phase space equipped with a quadratic Hamiltonian. Let us illustrate this in the simplest case of a quantum system with Hilbert space $\mathcal{H} = \mathbb{C}$ with standard inner product. A state vector at each time t is just a complex number: $\psi(t) = a + ib$. If $\phi = c + id$ is another state vector, then their inner product is $\langle\psi|\phi\rangle = \psi^*\phi = (a-ib)(c+id) = ac + bd + i(ad - bc)$. The QM Hamiltonian $\hat{H}$ is a 1×1 Hermitian matrix, i.e., just a real number $\hat{H} = \varepsilon$. The Schrödinger equation $i\hbar\dot{\psi} = \hat{H}\psi$ is the pair of equations $\dot{a} = (\varepsilon/\hbar)b$ and $\dot{b} = -(\varepsilon/\hbar)a$. Now let us reinterpret these equations in terms of Hamiltonian mechanics. We first declare that the classical phase space M corresponding to $\mathcal{H} = \mathbb{C}$ is just the corresponding real vector space $\mathbb{R}^2$. The classical state corresponding to ψ is the 2-component real vector $\psi = \left(\begin{smallmatrix} a \\ b \end{smallmatrix}\right)$. We then use the imaginary part of the Hilbert space inner product to define a symplectic form (see Sect. 3.26*) on this classical state space. For two vectors ψ and ϕ, we define $\omega(\psi,\phi) = -\hbar\Im\langle\psi|\phi\rangle = -\hbar(ad - bc)$. It is easy to see that this is nondegenerate and skew-symmetric, since $\omega(\psi,\phi) = \psi^t\omega\phi$ for the invertible matrix $\omega = \hbar\left(\begin{smallmatrix} 0 & -1 \\ 1 & 0 \end{smallmatrix}\right)$. The corresponding Poisson tensor is $r = \omega^{-1}$ with nonzero entries $r^{12} = -r^{21} = 1/\hbar$. Now, we will regard $\psi^1 = a$ and $\psi^2 = b$ as coordinates on phase space. If $H(a,b)$ is the classical Hamiltonian, then Hamilton's equations are $\dot{\psi}^i = r^{ij}\partial_j H$. In components, these are the equations $\dot{a} = \hbar^{-1}\partial_b H$ and $\dot{b} = -\hbar^{-1}\partial_a H$. Requiring that these reproduce the components of Schrödinger's equation, we get the conditions $\partial_b H = \varepsilon b$ and $-\partial_a H = -\varepsilon a$. Integrating these, we obtain the classical Hamiltonian $H = (\varepsilon/2)(a^2 + b^2)$ up to an additive constant. Thus, we have realized Schrödinger's equation as Hamilton's equations for a suitable quadratic Hamiltonian! This construction may be generalized to other quantum systems with Hilbert spaces of larger dimension by using the imaginary part of the Hermitian inner product to regard the quantum state space as a symplectic vector space. The classical Hamiltonian must be quadratic on account of the linearity of Schrödinger's equation. E.g., for $\mathcal{H} = \mathbb{C}^2$ with $\psi = \left(\begin{smallmatrix} a_1+ib_1 \\ a_2+ib_2 \end{smallmatrix}\right)$ and $\hat{H} = \left(\begin{smallmatrix} \varepsilon_{11} & \alpha+i\beta \\ \alpha-i\beta & \varepsilon_{22} \end{smallmatrix}\right)$ one finds (see Prob. 10.3):

$$H = \frac{1}{2}\left[\varepsilon_{11}(a_1^2 + b_1^2) + \varepsilon_{22}(a_2^2 + b_2^2)\right] + \alpha(a_1a_2 + b_1b_2) - \beta(a_1b_2 - a_2b_1). \quad (10.30)$$

For a general method of realizing Schrödinger time evolution as Hamiltonian dynamics, see [67]. □

10.4 Canonical transformations: Area-preserving maps and integral invariants

Here, we give a geometric interpretation of canonical transformations on the phase plane and then briefly discuss the generalization to higher dimensional phase spaces.

For one degree of freedom, we have just one coordinate q and one canonically conjugate momentum p, which together parametrize the phase plane. There is only one nontrivial canonical PB $\{q, p\} = 1$ since $\{q, q\} = \{p, p\} = 0$ by antisymmetry. Thus, the map $(q, p) \mapsto (Q, P)$ is canonical iff $\{Q, P\} = 1$. This condition turns out to be equivalent to the condition that the Jacobian determinant for the change of variables be equal to one. On the other hand, we learn in calculus that the Jacobian determinant is precisely the factor that relates the old to the new area element on the phase plane. Thus, CTs for one degree of freedom coincide with transformations that preserve areas on the phase plane.

In more detail, suppose we map (q, p) to a new point with position $Q(q, p)$ and momentum $P(q, p)$. For the transformation to be canonical, the new variables must satisfy the same PB, i.e.,

$$1 = \{Q, P\} = \frac{\partial Q}{\partial q}\frac{\partial P}{\partial p} - \frac{\partial Q}{\partial p}\frac{\partial P}{\partial q}. \tag{10.31}$$

The quantity that appears above is in fact the determinant of the Jacobian matrix of 1st partials

$$\det J = \det \begin{pmatrix} \frac{\partial Q}{\partial q} & \frac{\partial Q}{\partial p} \\ \frac{\partial P}{\partial q} & \frac{\partial P}{\partial p} \end{pmatrix} = \frac{\partial Q}{\partial q}\frac{\partial P}{\partial p} - \frac{\partial Q}{\partial p}\frac{\partial P}{\partial q}. \tag{10.32}$$

We recall from calculus that the Jacobian determinant is the factor relating oriented area elements on phase space

$$dQ\, dP = (\det J)\, dq\, dp \quad \text{or} \quad dQ \wedge dP = (\det J)\, dq \wedge dp. \tag{10.33}$$

The wedge product (see Appendix B.6* and Appendix B.9*) of differentials is the analog of the cross product of coordinate tangent vectors. In vector calculus, the latter is used to define an 'area vector' (see Appendix A.1). So a CT for a system with one degree of freedom is simply a transformation that preserves the area element on phase space. Such a transformation is called area preserving. Conversely, any area preserving transformation (i.e., one with $\det J = 1$) is also a CT (i.e., with $\{Q, P\} = 1$). Note that if $dQ \wedge dP = -dq \wedge dp$, the transformation preserves magnitudes of areas but is orientation reversing.

Pictorially, what is an area-preserving map? The map $F : \mathbb{R}^2 \to \mathbb{R}^2$ specified by $q \to Q(q, p)$ and $p \to P(q, p)$ maps points on the plane to points on the plane. For example, it could be the translation map $q \to q + 1, p \to p + 2$ or a rotation. Under such a transformation, any domain $D \subset \mathbb{R}^2$ is mapped to a new one $D' = F(D)$. The map is area preserving if for any D with finite area, Ar(D) = Ar(D'), i.e., $\iint_D dqdp = \iint_{D'} dqdp$. The above condition guarantees this, since

$$\text{Ar}(D) = \iint_D dqdp = \int_{F(D)} \frac{dQdP}{\det J} = \iint_{D'} dQdP = \iint_{D'} dqdp = \text{Ar}(D'). \tag{10.34}$$

In the 2nd equality, we changed variables of integration, in the third we used $\det J = 1$ and finally relabelled the dummy variables of integration $Q \to q$ and $P \to p$.

What we have shown above is that CTs of the phase plane preserve areas. Reversing the steps, we also see that if a transformation preserves areas (and in particular, the infinitesimal area element), it must be canonical. Thus, area-preserving maps of the phase plane coincide with canonical transformations for one degree of freedom. Area-preserving maps include (but are not restricted to) rigid motions like translations and rotations of the *phase plane*. For example, time evolution by a generic Hamiltonian is a canonical transformation which in general will morph a disk on the phase plane into a complicated region having the same area.

$*$ **Generalization to more degrees of freedom.** For several degrees of freedom, CTs continue to have a geometric interpretation, though it is more intricate. We will see in Sect. 10.8 on the Liouville theorem, that a canonical transformation preserves volumes of regions in phase space (the determinant of the Jacobian continues to be unity). However, the condition of canonicity is stronger than the mere preservation of volumes. In fact, it can be shown that a transformation of coordinates and momenta is canonical provided it preserves the area elements in *every* two-dimensional tangent plane through each point in phase space [2]. The reason for this is not hard to understand. The information in the canonical PBs may be packaged in the symplectic 2-form ω (see (3.145) and (B.27)). Being a 2-form, ω may be evaluated on a pair of tangent vectors (B.24) to give a number: the area of the parallelogram spanned by the 2 vectors. If the transformation were canonical, ω would be preserved and consequently areas in each tangent plane would be preserved. $\square$

$*$ **Integral invariants.** Yet another equivalent condition for a map $f : M \to M$ of the phase space $M = \mathbb{R}^{2n}$ to be canonical is for it to leave unchanged the line integral $\oint_C p dq$ of the canonical Liouville 1-form $\alpha = p_i dq^i$ around any *closed* curve C on M. If C is mapped to fC, then this is the requirement that $\oint_C \alpha = \oint_{fC} \alpha$. On the other hand, if f is a canonical transformation and C any closed curve, then the conserved line integral $\oint_C p dq$ is called the Poincaré integral invariant[5]. We also say that $\alpha = p_i dq^i$ is a (relative) integral invariant [2] of the transformation. The symplectic form $\omega = d\alpha$ can be used to generate more integral invariants. For instance, as discussed above, a canonical transformation preserves the area of any surface S in phase space $\int_S \omega = \int_{fS} \omega$. We say that ω is an (absolute) integral invariant[6] of the canonical transformation. In fact, for a system with n degrees of freedom, each of the exterior powers $\omega, \omega^2 = \omega \wedge \omega, \cdots, \omega^n$ are absolute integral invariants (see Appendices B.9* and B.10* for the exterior algebra and integration of forms). What this means is that if Σ_{2k} for $k = 0, 1, \ldots, n$ is any $2k$-dimensional 'surface' in the phase space, then $\int_{\Sigma_{2k}} \omega^k = \int_{f\Sigma_{2k}} \omega^k$ where $f\Sigma_{2k}$ is the image of Σ_{2k} under the transformation. The special case $k = n$ is called Liouville's theorem, which will be discussed in Sect. 10.8.

---

[5] There is a generalization called the integral invariant of Poincaré-Cartan: $\oint_\gamma (p dq - H dt)$ where $H(q, p, t)$ is a (possibly time-dependent) Hamiltonian. Here, we consider the $2n+1$-dimensional extended phase space $\tilde{M} = \mathbb{R}^{2n} \times \mathbb{R}$ by including time as an extra variable and suppose γ is a closed curve in $\tilde{M}$ (points on γ need not have a common time). The graphs of trajectories that pass through points of γ form a tube in $\tilde{M}$. Suppose γ' is any other closed curve on this tube. Then $\oint_\gamma (p dq - H dt) = \oint_{\gamma'} (p dq - H dt)$. If γ, γ' are at distinct fixed times, then $dt = 0$ and this 'action' integral invariant reduces to the Poincaré integral invariant for the canonical transformation corresponding to time evolution. On the other hand, if H is not explicitly time-dependent and γ, γ' both lie on a common $2n$-dimensional constant H hypersurface, then we get $\int_\gamma p dq = \int_{\gamma'} p dq$. The latter differs from Poincaré's integral invariant since γ, γ' need not be curves with fixed times.

[6] The qualifiers *relative* and *absolute* for integral invariants convey that while in the former case the form is integrated over any *closed* curve/surface (more precisely 'chain'), in the latter

10.5 CTs preserve Poisson tensor and formula for PB of any pair of observables

We introduced canonical transformations in Sect. 10.1 as those changes of phase space coordinates that preserve the form of Hamilton's equations. Later, in Sect. 10.2 we showed that CTs preserve the basic PBs between coordinates and momenta. Here, we extend this to show that CTs also preserve the formula for the PB of any two dynamical variables. We then proceed to reformulate the condition for canonicity in terms of the Poisson tensor. Recall that the latter is the second rank antisymmetric contravariant tensor r^{ij} (see (3.134) and (3.186)) that has all the information on the Poisson brackets among the basic phase space variables. It has no new information, but is an economical way of packaging the information in the Poisson structure[7]. The condition for a transformation to be canonical becomes much shorter and easier to work with, when expressed in terms of the Poisson tensor. It also generalizes to any number of degrees freedom and allows us to interpret the condition in terms of the transformation properties of a tensor field. All this will also be illustrated in the simpler context of linear canonical transformations where things can be made very explicit.

In Sect. 10.2, we showed that CTs preserve the basic PB between coordinates and momenta. What about the PB between arbitrary observables f, g? In the old coordinates,

$$\{f, g\} \equiv \{f, g\}_{q,p} = \sum\nolimits_i \left(\frac{\partial f}{\partial q^i} \frac{\partial g}{\partial p_i} - \frac{\partial f}{\partial p_i} \frac{\partial g}{\partial q^i} \right). \tag{10.35}$$

It turns out that if $(q, p) \to (Q, P)$ is canonical (i.e., preserves the basic PB) then (and only then), the formula for $\{f, g\}$ may also be expressed as[8]

$$\{f, g\} = \sum\nolimits_i \left(\frac{\partial f}{\partial Q^i} \frac{\partial g}{\partial P_i} - \frac{\partial f}{\partial P_i} \frac{\partial g}{\partial Q^i} \right). \tag{10.36}$$

Let us show this for one degree of freedom (though the same calculation also works for n degrees of freedom by putting in the indices.) Now by definition, the chain rule and rearranging terms,

$$\{f, g\} \quad = \quad f_q g_p - f_p g_q$$

---

case the surface (or chain) need not be closed, it could have a boundary.

[7] For instance, suppose we begin with phase space variables that are not canonical and wish to transform to canonical variables. The condition for the transformation to have this property can be succinctly expressed in terms of the Poisson tensor.

[8] We are being economical with notation here. When we differentiate with respect to Q and P we regard $f = f(q(Q, P), p(Q, P))$.

$$\begin{aligned}
&= (f_Q Q_q + f_P P_q)(g_Q Q_p + g_P P_p) - (f_Q Q_p + f_P P_p)(g_Q Q_q + g_P P_q) \\
&= f_Q g_P (Q_q P_p - Q_p P_q) + f_P g_Q (P_q Q_p - P_p Q_q) \\
&\quad + f_Q g_Q (Q_q Q_p - Q_p Q_q) + f_P g_P (P_q P_p - P_p P_q) \\
&= (f_Q g_P - f_P g_Q)\{Q,P\} + f_Q g_Q \{Q,Q\} + f_P g_P \{P,P\}. \qquad (10.37)
\end{aligned}$$

The last two terms are identically zero by antisymmetry of the PB, but we displayed them as they help in writing the corresponding formula for n degrees of freedom:

$$\{f,g\} = \left(f_{Q^i} g_{P_j} - f_{P_j} g_{Q^i}\right)\{Q^i, P_j\} + f_{Q^i} g_{Q^j}\{Q^i, Q^j\} + f_{P_i} g_{P_j}\{P_i, P_j\}. \quad (10.38)$$

Thus, we see that

$$\{f,g\}_{q,p} = \sum\nolimits_{i=1}^{n} \left(\frac{\partial f}{\partial Q^i}\frac{\partial g}{\partial P_i} - \frac{\partial f}{\partial P_i}\frac{\partial g}{\partial Q^i}\right) = \{f,g\}_{Q,P} \quad (10.39)$$

iff the new coordinates and momenta satisfy canonical PB relations, i.e.,

$$\{Q^i, P_j\} = \delta^i_j \quad \text{and} \quad \{Q^i, Q^j\} = 0 = \{P_i, P_j\}. \quad (10.40)$$

Thus, a transformation is canonical iff the PB of any pair of observables is given by the same sort of formula, whether computed using the old or new variables:

$$(q,p) \mapsto (Q,P) \quad \text{is a CT iff} \quad \{f,g\}_{q,p} = \{f,g\}_{Q,P} \quad \text{for all} \quad f,g. \quad (10.41)$$

Yet another way of stating the canonicity of a transformation is that it preserves the Poisson tensor[9] introduced in (3.134). Suppose $\boldsymbol{\xi} = (\boldsymbol{q}, \boldsymbol{p})$ is the grand coordinate on phase space in the old variables and $\Xi = (\boldsymbol{Q}, \boldsymbol{P})$ is the new one[10]. Then the preservation of basic PBs means

$$\{\xi^i, \xi^j\} = r^{ij} = \{\Xi^i, \Xi^j\} \quad \text{or} \quad r^{ij} = \frac{\partial \Xi^i}{\partial \xi^k}\frac{\partial \Xi^j}{\partial \xi^l} r^{kl}. \quad (10.42)$$

In other words, a CT is one that leaves the Poisson tensor invariant, componentwise, just as an isometry leaves a metric tensor invariant. By the foregoing,

$$\{f,g\} = \{f,g\}_{q,p} = \sum\nolimits_{ij} \frac{\partial f}{\partial \xi^i}\frac{\partial g}{\partial \xi^j} r^{ij} = \sum\nolimits_{ij} \frac{\partial f}{\partial \Xi^i}\frac{\partial g}{\partial \Xi^j} r^{ij} = \{f,g\}_{Q,P} \quad (10.43)$$

where the *same* Poisson tensor r^{ij} appears in both expressions, though the differentiation is with respect to the old and new variables in the first and second respectively.

---

[9] Though it contains no new information beyond that in the individual PBs, the Poisson tensor gives us a compact way of expressing the condition for canonicity of a transformation. Everything is packaged in the single tensor r^{ij} and there is no need to write out all the basic PBs and require that they be preserved. Packaging this information in the Poisson tensor also allows us to formulate the condition in terms of the transformation property of a second rank contravariant tensor, a feature that is not revealed when all the PBs are written out.

[10] Ξ is the upper case version of the Greek letter ξ. It is pronounced xi.

Linear canonical transformations. An important special class of CTs are linear ones, where $\Xi^i = T^i_j \xi^j$ with T an invertible $2n \times 2n$ matrix. In this case, the Jacobian is $\frac{\partial \Xi^i}{\partial \xi^j} = T^i_j$ and the condition for canonicity becomes $r^{ij} = T^i_k T^j_l r^{kl}$. In matrix notation, this is the condition $TrT^t = r$. It is possible to express this condition in terms of the symplectic tensor or form $\omega = r^{-1}$ introduced in (3.144). Taking the inverse, one expresses the condition for canonicity as $\omega = (T^{-1})^t \omega T^{-1}$. Here T^{-1} gives the inverse transformation $\xi^i = (T^{-1})^i_j \Xi^j$ and it is canonical if $\xi \to \Xi = T\xi$ is. Now, denoting $M = T^{-1}$ we get $\omega = M^t \omega M$. Such a linear canonical transformation M is also called a linear symplectic transformation or simply a symplectic matrix. Linear canonical or symplectic transformations form a group, the symplectic group (see Prob. 10.14). For n degrees of freedom and phase space $\mathbb{R}^{2n}$, the symplectic group is denoted $Sp(2n, \mathbb{R})$ (see Prob. 10.15). ☐

10.6 Generating function for infinitesimal canonical transformations

The condition for a transformation from canonical variables (q^i, p_i) to new ones (Q^i, P_i) to be canonical is that the Poisson brackets must be preserved. It would be nice to find an explicit way of producing canonical transformations. Let us address this question for infinitesimal canonical transformations, those that depart infinitesimally from the identity $(Q^i = q^i, P_i = p_i)$. It turns out that any such canonical transformation can be expressed in terms of a single 'generating' function on phase space. In other words, we consider transformations of the form

$$Q^i = q^i + \delta q^i(q,p) \quad \text{and} \quad P_i = p_i + \delta p_i(q,p) \quad \text{where} \quad \delta q^i, \delta p_i \quad \text{are small.} \tag{10.44}$$

Note that we *do not* expand δq and δp in powers of q and p: we are not assuming that q and p are small. Now, we impose the conditions that the new coordinates and momenta satisfy canonical PBs up to terms quadratic in δq and δp for $1 \le i, j \le n$:

$$\begin{aligned} 0 &= \{Q^i, Q^j\} = \{q^i + \delta q^i, q^j + \delta q^j\} \approx \{q^i, \delta q^j\} + \{\delta q^i, q^j\} \\ 0 &= \{P_i, P_j\} \approx \{p_i, \delta p_j\} + \{\delta p_i, p_j\} \qquad \text{and} \\ \delta_{ij} &= \{Q^i, P_j\} \approx \{q^i, p_j\} + \{q^i, \delta p_j\} + \{\delta q^i, p_j\}. \end{aligned} \tag{10.45}$$

These lead to three sets of conditions

$$\frac{\partial \delta q^j}{\partial p_i} - \frac{\partial \delta q^i}{\partial p_j} = 0, \quad \frac{\partial \delta p_j}{\partial q^i} - \frac{\partial \delta p_i}{\partial q^j} = 0 \quad \text{and} \quad \frac{\partial \delta p_j}{\partial p_i} + \frac{\partial \delta q^i}{\partial q^j} = 0. \tag{10.46}$$

Thus, we have rewritten the conditions for an infinitesimal transformation to be canonical, as a system of homogeneous linear partial differential equations for the small changes in coordinates and momenta $\delta q^i(q,p)$ and $\delta p_i(q,p)$. They look formidable, though the solutions should obey the principle of linear superposition. In fact, on the face of it, there are more equations than unknowns for $n \ge 2$. Accounting for anti-symmetry, $\{Q^i, Q^j\} = 0$ gives one condition for each $n \ge i > j \ge 1$, which makes $(n^2 - n)/2$ equations, and the same number for $\{P_i, P_j\} = 0$. $\{Q^i, P_j\} = \delta^i_j$ gives n^2 more conditions. So we have $n^2 - n + n^2 = 2n^2 - n$ equations for $2n$ unknown functions δq^i and δp_i. However, the equations are not all independent and they admit an infinite-dimensional family of solutions! The key is to notice that the last set of equations, even for 1 degree of freedom $\frac{\partial \delta p}{\partial p} + \frac{\partial \delta q}{\partial q} = 0$ look like the condition for the divergence of a vector field on the plane $\boldsymbol{B} = (\delta q, \delta p)$ to vanish. Recall from Sect. 3.23* and Appendix A.8, that the divergence-free condition $\boldsymbol{\nabla} \cdot \boldsymbol{B} = 0$ on a magnetic field may be solved by introducing a vector potential: $\boldsymbol{B} = \boldsymbol{\nabla} \times \boldsymbol{A}$. This suggests we seek solutions in the form $\delta q = \frac{\partial f}{\partial p}$ and $\delta p = -\frac{\partial f}{\partial q}$. On the other hand, the first two systems of equations look like the conditions for the curl of a vector field on the plane to vanish. If $E = (E_x, E_y)$ is an electric field on a plane, then $\boldsymbol{\nabla} \times E = (\partial_x E_y - \partial_y E_x)\hat{z}$. Recall that if the curl of a vector field on the plane vanishes $\boldsymbol{\nabla} \times E = 0$, then we can express it as the gradient of a scalar function $E = -\boldsymbol{\nabla}\phi = (-\partial_x \phi, -\partial_y \phi)$. All this motivates us to express δq^i and δp_j as derivatives of a scalar function f. Check that equations (10.46) are identically satisfied if for $i = 1, \ldots, n$, we put

$$\delta q^i = \frac{\partial f}{\partial p_i} = \{q^i, f\} \quad \text{and} \quad \delta p_i = -\frac{\partial f}{\partial q^i} = \{p_i, f\} \tag{10.47}$$

for an arbitrary twice differentiable function $f(q, p)$ on phase space. We say that f is an infinitesimal generator for the above infinitesimal CT. The small quantity f generates the infinitesimal CT via the Poisson bracket, it is determined up to an additive constant. This freedom to add a constant is the analog of the invariance of the electric field upon adding a constant to the electrostatic potential ϕ. For the phase space $\mathbb{R}^{2n}$, all infinitesimal CTs may be obtained through appropriate choices of generators $f(q, p)$. It is also possible to build up finite CTs by composing a succession of infinitesimal ones (see Prob. 10.20). We will say more about finite CTs in Sect. 10.10.

We may of course compose CTs $(q, p) \to (Q, P) \to (\tilde{Q}, \tilde{P})$ to make new CTs and also invert a CT. Thus, canonical transformations form a group (see Appendix B.13*). We verify that $-f$ generates the inverse of the infinitesimal CT generated by f (each is defined up to an arbitrary constant). The identity CT is generated by $f = 0$ (or any constant f). Arbitrary smooth generating functions $f(q, p)$ parametrize the neighborhood of the identity element in the group of canonical transformations. In fact, infinitesimal canonical transformations form a linear space, since (10.46) is a system of homogeneous linear equations. Geometrically, this linear space can be viewed as the tangent space at the identity CT to the group of CTs. This tangent space at the identity is called the Lie algebra of the group of canonical transformations (see Appendix B.13*). Since we need infinitely many independent real parameters to specify a general smooth function $f(q, p)$ (such as all its Taylor coefficients along with additional data), the Lie algebra and group of CTs are both infinite-dimensional. To first approximation, check that $f + g$ generates the CT consisting of the composition of the infinitesimal CTs generated by f and g, in *either* order. But this approximation is a bit crude, the order *does* matter since the group of CTs is nonabelian. The nonabelian nature is encoded in the Lie bracket, which is just the PB of infinitesimal generators $\{f, g\}$ (see Prob. 10.11).

We already noted in (10.28) that Hamiltonian time evolution over any time interval is a CT since it preserves the PB among the q's and p's. The above result allows us to interpret infinitesimal time evolution as an infinitesimal CT and identify the corresponding generating function. Hamilton's equations (3.78) for evolution over a small time δt give, to leading order in δt,

$$Q^i \equiv q^i(t+\delta t) = q^i(t) + \delta t \frac{\partial H}{\partial p_i} \quad \text{and} \quad P_i \equiv p_i(t+\delta t) - \delta t \frac{\partial H}{\partial q^i}. \tag{10.48}$$

In this case the small change in coordinates and momenta are

$$\delta q^i = \frac{\partial (H\,\delta t)}{\partial p_i} = \{q^i, H\,\delta t\} \quad \text{and} \quad \delta p_i = -\frac{\partial (H\,\delta t)}{\partial q^i} = \{p_i, H\,\delta t\}. \tag{10.49}$$

From these equations we read off the infinitesimal generator of time evolution over a small time δt as $f = H(q,p)\ \delta t$. Notice that f is indeed a small quantity. We say that the Hamiltonian generates the infinitesimal CT corresponding to infinitesimal time evolution via the Poisson bracket. Note that these formulae are valid even if H depends explicitly on time. The generator would then change with time, but time evolution would nevertheless be a CT.

Infinitesimal CT generated by L_z. Like the Hamiltonian, every observable $f(q,p)$ generates an infinitesimal CT. For example, what infinitesimal CT does the angular momentum component ϵL_z generate? One finds, for instance,

$$\delta x = \{x, \epsilon L_z\} = \epsilon\{x, x p_y - y p_x\} = -\epsilon y \{x, p_x\} = -\epsilon y. \tag{10.50}$$

Proceeding in this way, we obtain

$$\delta x = -\epsilon y, \quad \delta y = \epsilon x, \quad \delta z = 0 \quad \text{and} \quad \delta p_x = -\epsilon p_y, \quad \delta p_y = \epsilon p_x, \quad \delta p_z = 0. \tag{10.51}$$

This CT is a counterclockwise rotation in the x-y plane and p_x-p_y plane by the small angle ϵ:

$$\begin{pmatrix} x' \\ y' \end{pmatrix} = \begin{pmatrix} \cos\epsilon & -\sin\epsilon \\ \sin\epsilon & \cos\epsilon \end{pmatrix} \begin{pmatrix} x \\ y \end{pmatrix} \approx \begin{pmatrix} 1 & -\epsilon \\ \epsilon & 1 \end{pmatrix} \begin{pmatrix} x \\ y \end{pmatrix}. \tag{10.52}$$

Similarly, we verify that L_x and L_y generate infinitesimal counterclockwise rotations in the y-z and z-x planes. More generally, as we shall explain below, $\boldsymbol{L} \cdot \hat{\boldsymbol{n}}$ generates infinitesimal counterclockwise rotations about the axis $\hat{\boldsymbol{n}}$. We say that angular momentum generates infinitesimal rotations. □

Infinitesimal CT generated by any observable. To proceed, it is useful to have an expression for the infinitesimal change in a general observable $g(q,p)$ due to a canonical transformation generated by $f(q,p)$. Since

$$\delta q^i = \{q^i, f\} = \frac{\partial f}{\partial p_i} \quad \text{and} \quad \delta p_i = \{p_i, f\} = -\frac{\partial f}{\partial q^i}, \tag{10.53}$$

we have

$$\delta g = \frac{\partial g}{\partial q^i}\delta q^i + \frac{\partial g}{\partial p_i}\delta p_i = \frac{\partial g}{\partial q^i}\frac{\partial f}{\partial p_i} - \frac{\partial g}{\partial p_i}\frac{\partial f}{\partial q^i} = \{g, f\}. \tag{10.54}$$

So the change in any observable is given by its PB with the infinitesimal generator.

Infinitesimal CT generated by angular momentum. In Fig. 3.7, we found the infinitesimal change in a vector $\boldsymbol{r}$ due to a rotation (by small angle θ) about axis $\hat{\boldsymbol{n}}$:

$$\delta \boldsymbol{r} = \theta \hat{\boldsymbol{n}} \times \boldsymbol{r}. \tag{10.55}$$

Let us compare this with the change in $\boldsymbol{r}$ generated by the angular momentum component $\theta \boldsymbol{L} \cdot \hat{\boldsymbol{n}}$. To begin with, the infinitesimal change in x_i generated by L_j is

$$\delta x_i = \{x_i, L_j\} = \epsilon_{jkl}\{x_i, x_k p_l\} = \epsilon_{jkl} x_k \delta_{il} = \epsilon_{ijk} x_k. \tag{10.56}$$

It follows that the change generated by $\theta \boldsymbol{L} \cdot \hat{\boldsymbol{n}}$ is

$$\delta x_i = \{x_i, \theta L_j n_j\} = \theta n_j \{x_i, L_j\} = \theta \epsilon_{ijk} n_j x_k = \theta\,(\hat{\boldsymbol{n}} \times \boldsymbol{r})_i. \tag{10.57}$$

Comparing with (10.55) we conclude that $\theta \boldsymbol{L} \cdot \hat{\boldsymbol{n}}$ generates an infinitesimal counterclockwise rotation by angle θ about the axis $\hat{\boldsymbol{n}}$.

This manner of transformation is not special to the position vector. Other vectors $\boldsymbol{v}$ (like momentum, angular momentum or the LRL vector in the Kepler problem of Sect. 3.24*) also transform in the same way under rotations:

$$\delta \boldsymbol{v} = \theta\, \hat{\boldsymbol{n}} \times \boldsymbol{v} \quad \text{and} \quad \{v_i, L_j\} = \epsilon_{ijk} v_k. \tag{10.58}$$

10.7 Symmetries & Noether's theorem in the Hamiltonian framework

In Sect. 3.10, we discussed point transformations of configuration space variables that are continuous symmetries of the Lagrangian of a mechanical system. Noether's theorem allowed us to associate a conserved quantity with each infinitesimal generator of such a symmetry. In Sect. 10.1, we showed that point transformations are a special class of a larger set of phase space transformations (canonical transformations) that preserve the form of Hamilton's equations and Poisson brackets. Thus, it is natural to ask if there is a version of Noether's theorem that applies to canonical transformations that are symmetries. But what do we mean by symmetries now? Earlier, a point transformation was a symmetry if it left the Lagrangian invariant. The corresponding concept in a phase space formulation would be to regard a CT as a symmetry if it left the Hamiltonian invariant. This would then guarantee that the differential equations of motion are also invariant under the CT. By doing this, we liberate ourselves from the confines of point transformations of coordinates. Thus, in the Hamiltonian formalism, we define a symmetry transformation as a canonical transformation $(q^i, p_i) \to (Q^i, P_i)$ that leaves the Hamiltonian invariant. The former condition ensures that a symmetry preserves the Poisson brackets. This feature allows us to obtain a conserved quantity from an infinitesimal symmetry, thereby generalizing Noether's theorem. Symmetries of the Hamiltonian[11] or equations of motion[12] that are not CTs, generally *do not* lead to conserved quantities.

---

[11] The discrete symmetry $q \to q, p \to -p$ of the Hamiltonian $H = p^2/2m + V(q)$ is not canonical. The continuous scaling symmetry $q \to \lambda q, p \to p$ of the free particle Hamiltonian $H = p^2/2m$ is not canonical. Neither of these lead to conserved quantities.

[12] For instance, the scaling symmetry (2.51) of the Kepler problem is not a CT (it does not preserve PBs, see Prob. 10.19) and it is not associated with any conserved quantity. It leaves the Hamiltonian unchanged up to an overall factor, which ensures that the EOM are invariant. There is a related dilation symmetry in the 3-body problem [72, 106] that is again not a CT and does not lead to a conserved quantity.

Let us begin with a few comments on what we mean by a symmetry of the Hamiltonian. For example, if the Hamiltonian is independent of a coordinate q, then it is invariant under translations of q, $H(q,p) = H(q+a,p)$. Translations $q \mapsto q+a$, $p \mapsto p$ are of course canonical transformations. The coordinate q is then cyclic and the conjugate momentum is conserved $\dot{p} = -\frac{\partial H}{\partial q} = 0$. More generally, a transformation is said to leave the Hamiltonian invariant if $H(q,p) = H(Q(q,p), P(q,p))$. It is important to distinguish between an invariant function and just a scalar function defined in Appendix B.3*. A scalar function on a manifold is one whose value at a physical location (point) does not depend on the coordinates we use to describe the location. A scalar function satisfies $\phi(q,p) = \phi(q(Q,P), p(Q,P))$ for all $q(Q,P), p(Q,P)$. In other words, its value at a point whose coordinates in the old system are (q,p) does not change if we express q, p in terms of some other arbitrarily chosen coordinates Q, P. The Hamiltonian of any system is a scalar function on phase space. On the other hand, an invariant function is a scalar function with the *additional property* that its value does not change if we *change the physical location* at which it is evaluated by a symmetry transformation, i.e., $H(q,p) = H(Q(q,p), P(q,p))$ where $(q,p) \to (Q,P)$ is not an arbitrary transformation, but a symmetry transformation.

Symmetries may be discrete or continuous. Continuous symmetries come in continuous families parametrized by real numbers. Let us focus on continuous symmetries that may be continuously deformed to the identity. Regarded as CTs, they can be built by composing a succession of infinitesimal CTs. Consider an infinitesimal symmetry. There must be a function on phase space $f(q,p)$ that generates it, called the generator of the symmetry. E.g., $f(q,p) = p_i a^i$ for a fixed vector $\boldsymbol{a}$ generates a translation of coordinates by $\boldsymbol{a}$, since

$$\delta q^i = \frac{\partial f}{\partial p^i} = a^i \quad \text{and} \quad \delta p_i = -\frac{\partial f}{\partial q^i} = 0. \tag{10.59}$$

Now from (10.54), the change in any observable g due to the symmetry transformation[13] generated by f is $\delta g = \{g, f\}$. In particular, since the Hamiltonian is invariant under a symmetry, we must have $0 = \delta H = \{H, f\} = 0$. By Hamilton's equation, this means $\dot{f} = \{f, H\} = 0$. It follows that the generator f of the symmetry is a constant of motion. Thus, we have a Hamiltonian version of Noether's theorem. In the above example, it means $p_i a^i$ is a conserved quantity if the Hamiltonian is invariant under translations of coordinates $q^i \mapsto q^i + a^i$.

Symmetries from conserved quantities. This viewpoint also allows us to associate an infinitesimal symmetry with any conserved quantity $f(q,p)$, namely the symmetry transformation it generates via the PB. This is a sort of converse to Noether's theorem.

---

[13] The discrete parity canonical transformation $(q,p) \to (-q,-p)$ is a symmetry of the Hamiltonian $H = p^2/2m + kq^2/2$. However, it does not lead to a Noether conserved quantity since it does not possess an infinitesimal generator.

10.8 Liouville's theorem

We will apply the idea of an infinitesimal generator for a CT to establish a theorem of Liouville on the geometric nature of canonical transformations. In Sect. 10.4, we showed that for one degree of freedom, CTs preserve areas in phase space. This is a special case of Liouville's theorem. For n degrees of freedom, it says that CTs preserve $2n$-dimensional 'volumes' in phase space. In other words, suppose a $2n$-dimensional region in phase space $D \subset \mathbb{R}^{2n}$ is mapped by a CT to a new region $D' \subset \mathbb{R}^{2n}$. Then $\mathrm{Vol}(D) = \mathrm{Vol}(D')$. Alternatively, it says that the canonical volume element[14] or measure Ω on phase space is invariant under a CT:

$$\Omega = dP_1 \wedge dQ^1 \wedge \cdots \wedge dP_n \wedge dQ^n = dp_1 \wedge dq^1 \wedge \cdots \wedge dp_n \wedge dq^n. \qquad (10.60)$$

See (B.19) for more on wedge products. For a general transformation, the determinant of the Jacobian matrix of first partials appears as a pre-factor on the RHS

$$J = \begin{pmatrix} \frac{\partial Q^i}{\partial q^j} & \frac{\partial Q^i}{\partial p_j} \\ \frac{\partial P_i}{\partial q^j} & \frac{\partial P_i}{\partial p_j} \end{pmatrix}_{2n\times 2n}, \qquad (10.61)$$

where each submatrix is an $n \times n$ block with $1 \le i, j \le n$. So Liouville's theorem says that $\det J = 1$ for a canonical transformation. Note that unlike for one degree of freedom, for $n > 1$, $\det J = 1$ is *not* a sufficient condition for a transformation to be canonical (see Sect. 10.4).

Let us establish Liouville's theorem for infinitesimal canonical transformations by using our expressions (10.47) for Q^i, P_j in terms of an infinitesimal generator[15] ϵf:

$$Q^i \approx q^i + \epsilon \frac{\partial f}{\partial p_i} \quad \text{and} \quad P_i \approx p_i - \epsilon \frac{\partial f}{\partial q^i}. \qquad (10.62)$$

Let us first look at the simple case of $n = 2$ degrees of freedom, where

$$Q^1 \approx q^1 + \epsilon f_{p_1}, \quad Q^2 \approx q^2 + \epsilon f_{p_2}, \quad P_1 \approx p_1 - \epsilon f_{q^1} \quad \text{and} \quad P_2 \approx p_2 - \epsilon f_{q^2}. \qquad (10.63)$$

Here, subscripts on f denote partial derivatives. In this case, the Jacobian matrix

$$J \approx I + \epsilon \begin{pmatrix} f_{q^1 p_1} & f_{q^2 p_1} & f_{p_1 p_1} & f_{p_1 p_2} \\ f_{q^1 p_2} & f_{q^2 p_2} & f_{p_1 p_2} & f_{p_2 p_2} \\ -f_{q^1 q^1} & -f_{q^2 q^1} & -f_{p_1 q^1} & -f_{p_2 q^1} \\ -f_{q^1 q^2} & -f_{q^2 q^2} & -f_{p_1 q^2} & -f_{p_2 q^2} \end{pmatrix} = I + \epsilon F \qquad (10.64)$$

---

[14] The canonical volume element Ω on phase space is proportional to the n^{th} exterior power of the canonical symplectic form $\omega = dp_i \wedge dq^i$, i.e., $\Omega = (1/n!)\omega^n$. Thus, Liouville's theorem says that Ω is an (absolute) integral invariant for any canonical transformation. See the remark on integral invariants in Sect. 10.4.

[15] ϵ is a small parameter which will help us keep track of infinitesimals, we will ignore quantities of order ϵ^2.

departs from the identity by an infinitesimal matrix whose entries are second partials of f. Now[16]

$$\det J = \det[I + \epsilon F] = 1 + \epsilon \operatorname{tr} F + \mathcal{O}(\epsilon^2) = 1 + \mathcal{O}(\epsilon^2) \tag{10.65}$$

since F is traceless[17]. So for two degrees of freedom we have shown that an infinitesimal CT preserves the (4-dimensional) volume element in phase space.

The case of n-degrees of freedom is analogous. The $2n \times 2n$ Jacobian matrix is made of $n \times n$ blocks

$$J = \begin{pmatrix} \delta_{ij} + \epsilon \frac{\partial^2 f}{\partial p_i \partial q^j} & \epsilon \frac{\partial^2 f}{\partial p_i \partial p_j} \\ -\epsilon \frac{\partial^2 f}{\partial q^i \partial q^j} & \delta_{ij} - \epsilon \frac{\partial^2 f}{\partial q^i \partial p_j} \end{pmatrix} \quad \Rightarrow \quad \det J \approx 1 + \epsilon \sum_{i=1}^{n} \frac{\partial^2 f}{\partial p_i \partial q^i} - \epsilon \sum_{i=1}^{n} \frac{\partial^2 f}{\partial q^i \partial p_i} = 1. \tag{10.66}$$

Thus, an infinitesimal CT preserves the volume element in phase space. Synthesizing a finite canonical transformation by composing a succession of N infinitesimal ones and letting $N \to \infty$ and $\epsilon \to 0$, we argue that finite canonical transformations also preserve the phase volume. To complete the proof, one needs to show that the terms of order ϵ^2 and higher do not contribute to the Jacobian of a finite CT.

In particular, Hamiltonian time evolution preserves phase volume. This is true even if the Hamiltonian depends explicitly on time. All we need is for the equations of motion to be expressible in Hamiltonian form $\dot{q}^i = \frac{\partial H}{\partial p_i}, \dot{p}_i = \frac{\partial H}{\partial q^i}$ and this is true even if the Lagrangian depends explicitly on time (see Sect. 3.14). At each instant of time, H generates an infinitesimal CT that preserves the phase volume. Of course, if H is explicitly time-dependent, the CT will change with time, but phase volume will still be preserved.

Hamiltonian vector field is divergence-free. Liouville's theorem on the preservation of phase volumes under time evolution (or more generally under any canonical transformation with an infinitesimal generator) can be interpreted geometrically in terms of the Hamiltonian vector field. In fact, our calculation to show that the determinant of the Jacobian is unity, also shows that the Hamiltonian vector field is divergence-free[18]. Indeed, Hamilton's equations define the vector field

$$\begin{pmatrix} \dot{x}^i \\ \dot{p}_i \end{pmatrix} = V_H = \begin{pmatrix} V_H^{x^i} \\ V_H^{p_i} \end{pmatrix} = \begin{pmatrix} \frac{\partial H}{\partial p_i} \\ -\frac{\partial H}{\partial x^i} \end{pmatrix} \quad \text{for} \quad i = 1, \cdots, n. \tag{10.67}$$

---

[16] Suppose the eigenvalues of $J = I + \epsilon F$ are $\lambda_1, \cdots, \lambda_{2n}$. Then from the characteristic equation $\det(J - \lambda I) = \det(\epsilon F - (\lambda - 1)I) = 0$ we see that the eigenvalues of ϵF are $\lambda_1 - 1, \cdots, \lambda_{2n} - 1$. Hence the eigenvalues of F are $f_1 = \frac{\lambda_1 - 1}{\epsilon}, \cdots, \frac{\lambda_{2n} - 1}{\epsilon}$. Thus $\det J = \lambda_1 \cdots \lambda_{2n} = (1 + \epsilon f_1) \cdots (1 + \epsilon f_{2n}) = 1 + \epsilon(f_1 + \cdots + f_{2n}) + \mathcal{O}(\epsilon^2) = 1 + \epsilon \operatorname{tr} F + \mathcal{O}(\epsilon^2)$. Alternatively, assuming the identity $\det J = \exp(\operatorname{tr} \log(I + \epsilon F))$, one may proceed by expanding in powers of ϵ.

[17] Equality of mixed partials is guaranteed by Clairaut's theorem if the 2nd partials exist and are continuous.

[18] The divergence of the time evolution vector field on phase space may, in some cases, be expressed as a sum of suitable 'Lyapunov exponents' (see Sect. 15.2* and (15.32)). For a Hamiltonian system, the sum of Lyapunov exponents vanishes as they come in pairs with opposite signs.

The divergence of the Hamiltonian vector field V_H is given by

$$\nabla \cdot V_H = \partial_{x^i} V_H^{x^i} + \partial_{p_i} V_H^{p_i} = \frac{\partial^2 H}{\partial x^i p_i} - \frac{\partial^2 H}{\partial p_i x^i} = 0. \tag{10.68}$$

As we will emphasize in our study of fluid mechanics, the divergence of a vector field measures the fractional rate at which the flow defined by the field alters infinitesimal volumes (see Sect. 19.5). A divergence-free vector field is volume preserving. Thus, Hamiltonian dynamics defines an incompressible flow on phase space.

Note that dissipative systems (e.g., ones with frictional forces) do not admit a standard Lagrangian or Hamiltonian description, there is no function $H(q, p, t)$ for which Hamilton's equations reproduce the equations of motion. In fact, a dissipative system is often taken as one for which volumes in phase space decrease with time. As illustrated in Sect. 6.4 for the damped harmonic oscillator $m\ddot{x} = -kx - \gamma\dot{x}$, irrespective of what initial conditions one considers, the mass comes to rest at the equilibrium point $(x = 0, m\dot{x} = 0)$, so the phase space area shrinks to zero.

Application to a gas. Consider the gas molecules in an isolated 3d container, modeled as a system of a very large number N of classical point particles (in practice, $N \sim 10^{24}$ is comparable to Avogadro's number). The phase space is $6N$ dimensional with coordinates $\boldsymbol{q}^1 \cdots \boldsymbol{q}^N, \boldsymbol{p}_1 \cdots \boldsymbol{p}_N$. Owing to the difficulty in determining the initial values of these variables, we may at best be able to say that the initial conditions lie within a certain region D of phase space. Each of the phase points in D will evolve in time and trace out a phase trajectory. In this manner, D itself will evolve in time to a new region D' which contains the possible phase points at a later time. Liouville's theorem says that D evolves in time as an 'incompressible fluid'. In general, the shape of the region will get distorted with time, while maintaining a constant $6N$-dimensional volume. In fact, under typical laboratory conditions, the gas reaches equilibrium at a common temperature with D developing dendritic structures allowing it to mix or spread out over the available phase space while maintaining its volume.

Lack of nodes, spirals and limit cycles in Hamiltonian systems. Liouville's theorem has other interesting consequences. For instance, it implies that Hamiltonian flows on the phase plane do not admit nodes and spirals (attractive or repulsive fixed points) or limit cycles[19]. Recall from Sect. 6.1 that an attractive fixed point is one with the property that all trajectories that begin in a sufficiently small (open) neighborhood tend to the fixed point as $t \to \infty$. The flow around an attractive or repulsive fixed point or limit cycle cannot preserve phase space area as the entire basin of attraction/repulsion (with nonzero area) is mapped by the flow (as $t \to \infty$ or $-\infty$) to a single point or a closed curve (having zero area). For the same reasons, attractive and repulsive fixed points are forbidden for Hamiltonian vector fields in any dimension. In fact, one does not need the Liouville property to conclude that Hamiltonian systems cannot have attractive or repulsive fixed points. This is true of any 'conservative' dynamical system. By a conservative system, here we mean one that has at least one conserved quantity C (a continuous function on phase space with $\dot{C} = 0$) that is not constant on any open subset of the phase space[20]. Now, if a conservative system had an attracting fixed point $\boldsymbol{r}_*$, then the conserved quantity would be constant throughout its basin of attraction. Since the basin of attraction includes an open set containing $\boldsymbol{r}_*$, the conserved quantity would be inadmissible. A similar argument applies to repelling fixed points. Though spirals and nodes are forbidden, planar Hamiltonian systems *can* have centers and saddles (as in the harmonic oscillator (Fig. 6.1a), pendulum (Fig. 7.3) and double-well potential (Fig. 7.6c)) or continuous families of fixed points (as for the free particle in Fig 3.2). In fact, if $\boldsymbol{r}_* = (x_*, p_*)$ is a fixed point of a planar Hamiltonian system, then the eigenvalues of the linearization around $\boldsymbol{r}_*$ must be of the form $\pm\lambda$ or $\pm i\omega$ with λ and ω real. This is a consequence of the form of Hamilton's equations. Indeed, the linearization (5.27) of the Hamiltonian vector field at the fixed point, $J = \begin{pmatrix} H_{px} & H_{pp} \\ -H_{xx} & -H_{xp} \end{pmatrix}$ is traceless, so that if the eigenvalues are real, they must be of the form $\pm\lambda$ while if they are complex conjugates, their real parts must vanish. For $\lambda, \omega \neq 0$, these correspond to linear saddles and centers (see Sect. 6.3). Both eigenvalues can vanish in various ways (depending on the order of the zero). This happens, for instance, in the case of a free particle $H = p^2/2m$:

---

[19] A limit cycle is an isolated periodic trajectory with the property that at least one other trajectory approaches it asymptotically (as $t \to \infty$ or as $t \to -\infty$). Isolated means there is no other periodic trajectory in its immediate neighborhood. On the phase plane, trajectories that begin nearby either spiral towards or away from a limit cycle.

$$\dot{x} = p/m \quad \text{and} \quad \dot{p} = 0 \quad \Rightarrow \quad J = \begin{pmatrix} 0 & 1/m \\ 0 & 0 \end{pmatrix}, \tag{10.69}$$

where the Jacobian has only one linearly independent eigenvector. There is a line of fixed points along the x-axis, with the flow being horizontal and to the right/left in the upper/lower half-planes.

10.9* Poincaré recurrence

Recurrence is a generalization of periodic behavior where one gives up exact return to the initial state for approximate return to the initial state to any prescribed accuracy. The Poincaré recurrence theorem concerns volume preserving flow (for instance, Hamiltonian dynamics) in a phase space of finite volume[21]. Subject to these hypotheses, it asserts that almost any trajectory that begins in any open subset of phase space will return to that subset infinitely many times. Though the result is quite natural if one keeps in mind the hypotheses, it led to much debate in the context of the kinetic theory of gases. Boltzmann offered a molecular explanation of the second law of thermodynamics (law of increase of entropy) for a dilute gas by proposing his transport equation [17, 59, 105] for the phase space distribution of molecules in a dilute gas and showing that it implied that his H-function was a decreasing function of time that asymptotically approached the value of entropy at equilibrium. This irreversibility was consistent with the observed behavior of a gas released from a small portion of a vacuum chamber: it expands into the whole chamber and thermalizes (the distribution of molecular speeds approaches the Maxwell-Boltzmann distribution corresponding to an equilibrium temperature). This seemed at odds with the Poincaré recurrence theorem which guaranteed a return arbitrarily close to the initial state. Indeed, we do not observe the gas released from a corner of a room to return to the corner. The apparent contradiction between thermal equilibration and recurrence could be resolved once it was realized that (a) initial states for which the gas returns to the corner are very rare and (b) that the typical time for the initial state of a gas to recur is very long compared to the equilibration time[22].

---

[20] Recall that in the harmonic oscillator and double-well potential problems, the energy level sets are curves or isolated points: these are not open subsets of the plane. A function that is constant on phase space is always trivially conserved, so we must exclude it to ensure that our definition does not classify every dynamical system as conservative!

[21] The analog of Poincaré recurrence does not directly apply to systems with infinite phase volume, infinitely many degrees of freedom or dissipation. However, it may be possible to relax the finite volume assumption if each trajectory is confined to a region of finite volume in phase space. On the other hand, Birkhoff recurrence [128] is an extension of the concept of Poincaré recurrence to continuum systems of fields.

The possibility of recurrence can also be related to the existence of conserved quantities. Conserved quantities place restrictions on the portion of phase space that a trajectory can explore. The more conserved quantities a system possesses, the more constrained the motion is and the easier it is for a trajectory to return to a neighborhood of the initial state. An extreme case is that of Liouville integrable systems (see Sect. 11.7*), which possess as many Poisson commuting conserved quantities as there are degrees of freedom. If the dynamics of such a system is such that trajectories are restricted to a bounded region of the phase space (so that trajectories cannot escape to 'infinity'), then almost all trajectories can be shown to be quasiperiodic (see Footnote 24 of Chap. 2) and consequently recurrent (in fact they must lie on invariant tori of various dimensions).

To begin with, we look at some examples to develop intuition about when a trajectory or a system as a whole may be recurrent. These examples will help us formulate conditions that will guarantee that a trajectory will eventually return to a prescribed neighborhood of an initial phase point[23].

1: Linear harmonic oscillator. Here $H = p^2/2m + m\omega^2 x^2/2$ and we have a center at the origin (see Fig. 6.1a). Every nonconstant trajectory is periodic with period $2\pi/\omega$. Thus, the system is recurrent. We notice that this happens even though the phase space has infinite volume (area). This suggests it is sufficient that trajectories be suitably confined to regions of finite volume in phase space.

2: The double-well potential. Here $H = p^2/2m + (g/4)(x^2 - a^2)^2$ with $g > 0$, so there is a saddle at the origin $(x = 0, p = 0)$ along with a pair of centers at $(\pm a, 0)$ (see Fig. 7.6c). All trajectories other than the two homoclinic ones are periodic. However, the period varies with energy and diverges as we approach the separatrix at $E =$

---

[22] Unfortunately, Boltzmann committed suicide partly as an outcome of the controversies surrounding the proof of his H-theorem on irreversible behavior in gases. Roughly, the critiques (Loschmidt's 'paradox' on time-reversal invariance and Zermelo's 'paradox' on Poincaré recurrence) were based on mechanics while the argument for irreversibility included both mechanical and probabilistic elements [31].

[23] We do not address the question of how long it may take for such recurrences to happen. This recurrence time depends on the system and neighborhood in phase space under consideration and could be very long for systems like a gas of molecules in a room.

$(g/4)a^4$ from above or below. Thus all trajectories other than those that begin on the homoclinic orbits return to the initial state, and the system is recurrent, though with a recurrence time that varies with location on phase space.

3: Irrational windings on a torus. Not all volume preserving flows need have fixed points or periodic trajectories. Consider flow on a 2-torus with 2π-periodic coordinates θ_1 and θ_2. We can view the phase space as the square $0 \le \theta_{1,2} \le 2\pi$ shown in Fig. 10.1b with the opposite edges identified. The evolution is defined by the equations

$$\dot\theta_1 = \omega_1 \quad \text{and} \quad \dot\theta_2 = \omega_2 \quad \text{where} \quad (\omega_1, \omega_2) \neq (0,0). \tag{10.70}$$

Since the frequencies are not both zero, the system does not possess any fixed points. If ω_1 or ω_2 vanishes, then all trajectories are periodic. Henceforth, where necessary, we assume that $\omega_1 \neq 0$ and $\omega_2 \neq 0$. The trajectories are straight lines on the square:

$$\theta_1 = \omega_1 t + \theta_1(0) \quad \text{and} \quad \theta_2 = \omega_2 t + \theta_2(0). \tag{10.71}$$

When a trajectory reaches an edge [say at $(\theta_1 = 2\pi, \theta_2)$], it continues from the opposite edge [say $(\theta_1 = 0, \theta_2)$] with the same slope and direction. So a trajectory on the phase square typically looks like a collection of oblique parallel lines with slope ω_2/ω_1. It is clear that the evolution preserves the area on the phase space measured with respect to the element $d\theta_1 \wedge d\theta_2$ [the wedge product was introduced in (B.19)]. In fact, if we postulate that θ_1 and θ_2 are canonically conjugate $\{\theta_1, \theta_2\} = 1$, we may derive the equations of motion (locally[24]) from the linear Hamiltonian $H = -\omega_2\theta_1 + \omega_1\theta_2$:

$$\dot\theta_1 = \{\theta_1, H\} = \omega_1 \quad \text{and} \quad \dot\theta_2 = \{\theta_2, H\} = \omega_2. \tag{10.72}$$

Both θ_1 and θ_2 evolve periodically in time, with periods $T_1 = 2\pi/\omega_1$ and $T_2 = 2\pi/\omega_2$. However, the superposition of these two periodic motions need not be periodic. If $T_1 = 2T_2$ then the phase trajectory is periodic with period T_1. More generally, if T_1 and T_2 are commensurate (i.e., if there exist integers m, n not both zero such that $mT_1 + nT_2 = 0$), then the periods have a 'least common integer multiple' (LCM) and the trajectory is periodic (it is a closed curve on the torus). On the other hand, if they are incommensurate (T_2/T_1 or T_1/T_2 is irrational), then the trajectory is not closed: it is as if the LCM has gone to infinity, the trajectory is aperiodic and keeps winding around the torus without ever returning to the initial state. In fact, one can show that for incommensurate frequencies, every trajectory is aperiodic and fills up the torus, in the sense that it comes arbitrarily close to any given point on the torus (see Fig. 10.1a). Thus, irrational windings on a torus provide an example of a volume preserving flow that displays recurrent motions without admitting any periodic trajectories.

4: Free particle and Kepler problem. Not all Hamiltonian systems display recurrence. In fact, free particle motion on a line is not recurrent in general. If it has nonzero initial momentum, the particle goes off to infinity without ever returning to a given neighborhood of the initial location: $x(t) = x(0) + p(0)t/m \to \pm\infty$ depending on the

---

[24] Note that this Hamiltonian is not globally well-defined on the torus: it is multivalued.

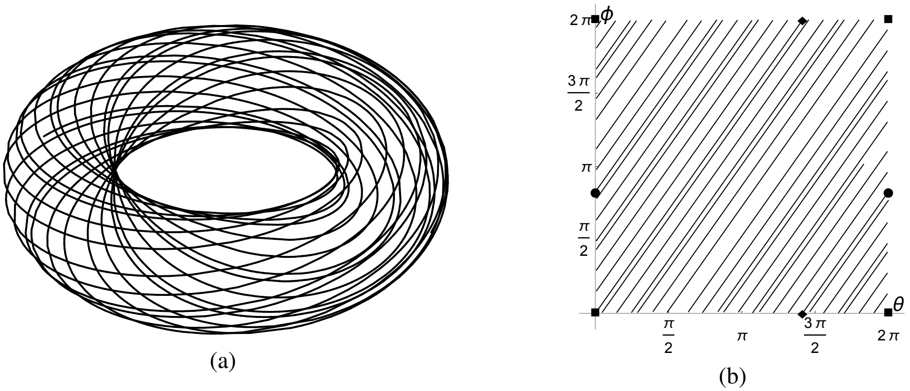
(a)

(b)

Figure 10.1: (a) Irrational windings on a torus: $\theta = \omega_1 t$ and $\phi = \omega_2 t$ for $0 \leq t \leq 100$ with $\omega_1 = 1, \omega_2 = \sqrt{2}$. The embedding used is $x = (R + r\cos\theta)\cos\phi$, $y = (R + r\cos\theta)\sin\phi$ and $z = r\sin\theta$ with $r = 1$ and $R = 3$. (b) $(\theta(t), \phi(t))$ plotted modulo 2π on a square with opposite edges identified (periodic boundary conditions). When the left and right edges are glued together we get a cylinder with vertical axis. Subsequently, when the cylinder is stretched and its bottom rim glued to its top rim, we get a torus. Viewed on the square, what this means, for instance, is that when the trajectory reaches the $\theta = 2\pi$ boundary, it continues at the same angle, starting from the point at the same height on the $\theta = 0$ boundary. A few examples of points on the rim of the square that are identified are indicated through common symbols.

sign of $p(0)$. Similarly, dynamics in the Kepler problem $H = (1/2m)\boldsymbol{p}^2 - GMm/|\boldsymbol{r}|$ is not recurrent. Trajectories with $H < 0$ are periodic, corresponding to elliptical orbits in configuration (position) space while trajectories with $H > 0$ fly off to infinity along hyperbolic orbits. These two examples indicate that having a phase space of infinite volume without any force to contain the motion (as in the harmonic oscillator) to a region of finite volume could come in the way of recurrence.

The Poincaré recurrence theorem. The theorem applies to volume preserving flow in a system with a phase space of any finite dimension with a finite phase volume. For Hamiltonian systems, the volume is naturally measured with respect to the canonical volume element of Footnote 14 of Sect. 10.8[25]. The theorem says that given any open set N_0 of initial conditions of positive volume in phase space, almost every trajectory that begins in it (with the possible exception of those beginning from a subset of zero volume) returns to N_0, and does so infinitely often.

Sketch of the proof. The proof exploits the preservation of phase volume (Liouville property for Hamiltonian systems) as well as the assumption of finite phase volume. Suppose we consider ICs lying in an open set N_0 (say an open ball) with necessarily nonzero volume. After a time t, N_0 evolves to a region N_t with the same volume. Now, the family of phase trajectories starting in N_0 trace out a tubular region (see

---

[25] These are simple sufficient conditions, they can sometimes be relaxed without losing recurrence, as the examples of the harmonic oscillator and double-well potential indicate. The recurrence theorem was conjectured by H. Poincaré in 1890 and proved by C. Carathéodory in 1919.

Fig. 10.2a) in phase space whose volume must be a nondecreasing function of time (invariably, its volume increases with time since the tubular region typically grows).

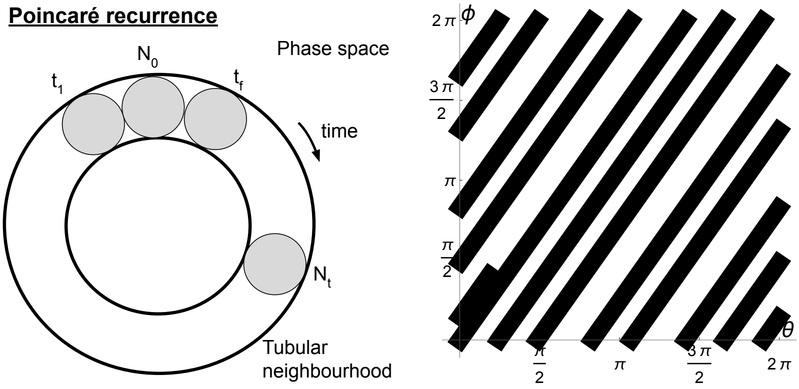

(a) (b)

Figure 10.2: (a) Time evolution of an open disk $N_0 \mapsto N_t$ forming a tubular neighborhood in a 2d phase space. This is a very simple example, not quite indicative the intricate dynamics that can occur, especially in phase spaces of higher dimensions. (b) Tubular neighborhood for irrational windings on a torus ($\theta = t, \phi = \sqrt{2}t$) for ICs in a neighborhood of (0,0) showing recurrence after a time $t_1 \approx 31.5$.

Step 1: One possibility is that N_t always[26] intersects N_0 in a set $\cap_{t\geq 0} N_t$ of nonzero volume. In this case, all trajectories in this intersection remain within it and the assertion of the theorem is true for this set, and we may proceed to *Step 2* (see below). On the other hand, suppose there is a first time $t = t_f$ at which the volume of $N_t \cap N_0$ drops to zero. In this case, we will argue that there must be a later time t_1 after which $N_{t_1+\epsilon}$ and N_0 intersect in a region of nonzero volume for any sufficiently small $\epsilon > 0$. This is because the volume of the phase tube is increasing but cannot exceed the total volume of the phase space. Thus, there must come a time when the phase tube 'intersects itself'. The 'first' such intersection must be of $N_{t_1+\epsilon}$ with N_0 rather than[27] with any $N_{t'>0}$. Thus, after a time t_1, $N_{t_1+\epsilon}$ and N_0 must intersect in a set of nonzero volume for any sufficiently small $\epsilon > 0$. Thus, trajectories starting from a nonzero fraction of the volume of N_0 return to N_0 after t_1.

---

[26] Although it has a phase space of infinite area, this would happen in the 1d harmonic oscillator $H = p^2/2m + kx^2/2$ if N_0 is, say, an open disk containing the origin $x = p = 0$. In particular, if $k = m = 1$, then phase points simply trace out circles centered at the origin so N_t would be a rotated version of N_0 and always intersect N_0 in a set of nonzero area.

[27] If we assume otherwise, we arrive at a contradiction. Suppose the first self intersection of the tube happens after a time t_1 where $N_{t_1+\epsilon}$ intersects $N_{t'}$ for some $t' > 0$ and any sufficiently small ϵ. But then, all points of $N_{t'}$ evolved back a time t' must lie in N_0. This would mean that the tube intersected itself at an earlier time than t_1, resulting in a contradiction. In fact, $N_{t_1+\epsilon-t'}$ would intersect N_0 in a set of positive volume, contradicting the assumption that the first self-intersection happened after a time t_1.

Step 2: We now apply the same argument to the remaining portion of N_0 (i.e., the interior of $N_0 \setminus N_{t_1}$[28]) to conclude that there is a time t_2 after which trajectories starting from a nonzero fraction of the volume of $N_0 \setminus N_{t_1}$ return to it. Proceeding in this manner, one argues that except possibly for a subset of zero volume, every trajectory starting in N_0 returns to N_0.

Step 3: Now we repeat the whole argument to show that almost every trajectory that begins in N_0 returns to N_0 twice and so on, thus establishing the theorem. □

Remarks. (a) We may choose N_0 as small as we like, to ensure a return to an arbitrarily small neighborhood of the initial state. However, this would typically come at the cost of a longer return time. The recurrence times tend to grow as the volume of N_0 is decreased (this is seen for irrational windings on a torus in Fig. 10.2b). (b) Note that the time at which the trajectory returns to N_0 for the second time need not be twice the time of first return. (c) There can be initial conditions in N_0 that never return to N_0: an example is provided by ICs that lie on homoclinic orbits in the double-well potential problem (see Fig. 7.6c). (d) There can be exceptional ICs and sets N_0 for which a trajectory returns to N_0 a finite number of times, and then stops doing so. □

10.10 Generating functions for finite canonical transformations

Transformations between different sets of canonical coordinates and momenta are called canonical transformations. Here we seek to express finite canonical transformations in terms of generating functions. We have already done this for infinitesimal canonical transformations in Sect. 10.6. To do so, we will use the variational principles of Sect. 3.19 for Hamilton's equations. We will find that, subject to some mild conditions, any differentiable functions of the form $F_1(q,Q,t), F_2(q,P,t), F_3(p,Q,t)$ and $F_4(p,P,t)$ can be used to generate finite canonical transformations for any fixed t. Before we explain how, let us make a few (somewhat advanced) general comments on the space of canonical transformations. As mentioned in Sect. 10.8, canonical transformations form a group since they can be composed and inverted to produce other canonical transformations. The group of CTs is very large, forming what one could call an infinite-dimensional manifold (see Prob. 10.10). For any fixed time t, the four types of generating functions may be regarded as furnishing four overlapping coordinate patches[29] on this infinite-dimensional group manifold. These generating functions will then be a very handy way of dealing with canonical transformations. For instance, in Chap. 12, we will discuss the Hamilton-Jacobi equation, which, in favorable cases, can be used to solve the equations of a Hamiltonian system. The HJ equation is an equation for the time evolution of a generating function (such as $F_2(q,P,t)$) and can itself be regarded as defining a sort of dynamical system on the group of CTs.

Consider the (possibly explicitly time-dependent) map from $(q^i, p_j) \mapsto (Q^i, P_j)$

---

[28] The set theoretic difference $A \setminus B$ is the set of all points in A that are not in B.

[29] These four types of functions are adequate for generating the CTs that we will encounter. We do not address the technical question of whether every CT can be obtained from a generator of one of these four sorts.

with the equations of transformation given by the functions

$$Q^i = Q^i(q,p,t) \quad \text{and} \quad P_i = P_i(q,p,t). \tag{10.73}$$

Such a change is canonical (for any fixed t) provided there is a new Hamiltonian $K(Q,P,t)$ (called $\tilde{H}$ in (10.3)) such that the EOM in the new variables take the same form as those in the old variables, i.e.,

$$\dot{Q}^i = \frac{\partial K}{\partial P_i} \quad \text{and} \quad \dot{P}_i = -\frac{\partial K}{\partial Q^i} \quad \text{while} \quad \dot{q}^i = \frac{\partial H}{\partial p_i} \quad \text{and} \quad \dot{p}_i = -\frac{\partial H}{\partial q^i}. \tag{10.74}$$

When the transformation is not explicitly dependent on time, $K(Q,P)$ is got by expressing q,p in terms of Q,P in the old Hamiltonian $H(q,p)$. We will see that essentially the same thing continues to be true, but with a slight modification. Now, our basic principle of consistency is that these two sets of Hamilton's equations should be equivalent in the sense that if we express Q and P in terms of q and p in the second set, they should reduce to the old Hamilton equations.

Each set of Hamilton's equations follows from the variational principle (3.107):

$$\delta \int_{t_i}^{t_f} \left[p_i \dot{q}^i - H(q,p)\right] dt = 0 \quad \text{and} \quad \delta \int_{t_i}^{t_f} \left[P_i \dot{Q}^i - K(Q,P,t)\right] dt = 0 \tag{10.75}$$

where t_i and t_f are initial and final times. The conditions for extrema of these two functionals $S_{\text{old}}[q,p]$ and $S_{\text{new}}[Q,P]$ are the same equations, just in different coordinates. We will now present a way in which this can happen. Let us define the functional

$$I[q,p,Q,P] = S_{\text{old}}[q,p] - S_{\text{new}}[Q,P] = \int_{t_i}^{t_f} \left(p\dot{q} - H - P\dot{Q} + K\right) dt. \tag{10.76}$$

Suppose I is stationary to first order with respect to small variations of $q^i(t)$, $p_i(t)$, $Q^i(t)$ and $P_i(t)$ holding the initial and final positions $q^j(t_{i,f})$ and $Q^j(t_{i,f})$ fixed. Now, if $\delta I = 0$, then $\delta S_{\text{old}} = \delta S_{\text{new}}$ and it follows that $\delta S_{\text{old}} = 0$ iff $\delta S_{\text{new}} = 0$. Thus, if $\delta I = 0$, then the two sets of Hamilton equations would be equivalent and consequently the transformation would be canonical. Next, we propose a way for $I[q,p,Q,P]$ to be stationary. Since the initial and final configurations are fixed, this can happen if I is independent of $p_j(t_{i,f})$, $P_j(t_{i,f})$ and other features of the paths with the exception of $q^j(t_{i,f})$ and $Q^j(t_{i,f})$. A sufficient condition for this is for the integrand in I to be the total time derivative of some function[30] $F_1(q,Q,t)$. For, then

$$I = \int_{t_i}^{t_f} \dot{F}_1 \, dt = F_1(q(t_f),Q(t_f),t_f) - F_1(q(t_i),Q(t_i),t_i) \tag{10.77}$$

and $\delta I = 0$ as q and Q are held fixed at the fixed times t_i and t_f. Note that F_1 cannot be taken as a function of p or P since $\delta p(t_i), \delta p(t_f), \delta P(t_i), \delta P(t_f)$ are unconstrained in Hamilton's variational principle and the total time derivative of such an F_1 would violate the constancy of I. In other words, a sufficient condition for the equations in both old and new variables to take the Hamiltonian form is for the relation

---

[30] We will need to impose some mild conditions of F_1 (including twice differentiability) to ensure that the transformation is invertible. More on this soon. The subscript on F_1 is in anticipation of other possibilities which will involve functions denoted F_2, F_3 and F_4.

$$p_i \dot{q}^i - H = P_i \dot{Q}^i - K + \frac{dF_1}{dt}, \tag{10.78}$$

to hold for some function $F_1(q,Q,t)$. Multiplying through by dt we get

$$p dq - H dt = P dQ - K dt + \frac{dF_1}{dt} dt. \tag{10.79}$$

This is the condition that the 1-form $pdq - PdQ - (H-K)dt$ be exact. That the independent variables in F_1 are q, Q and t is also consistent with the fact that the independent differentials appearing in the rest of the terms above are dt, dq and dQ. So, as an equation among the independent differentials dq, dQ and dt, we have

$$p dq - H dt = P dQ - K dt + \frac{\partial F_1}{\partial q} dq + \frac{\partial F_1}{\partial Q} dQ + \frac{\partial F_1}{\partial t} dt. \tag{10.80}$$

Comparing coefficients, we read off the relations

$$p = \frac{\partial F_1}{\partial q}, \quad P = -\frac{\partial F_1}{\partial Q} \quad \text{and} \quad K(Q,P,t) = H(q,p) + \frac{\partial F_1(q,Q,t)}{\partial t}. \tag{10.81}$$

$F_1(q,Q)$ is called the generator of the CT. The first two equations determine the equations of transformation. The first may be solved to find $Q = Q(q,p,t)$ and using it, the second expresses $P = P(q,p,t)$. The last relation fixes the new Hamiltonian in terms of the old one and the generator F_1. If F_1 does not depend explicitly on time, then it just says that $K(Q,P) = H(q(Q,P), p(Q,P)) = \tilde{H}(Q,P)$ as in (10.3). In general, the new and old Hamiltonians differ by the partial time derivative of the generator.

Condition on F_1 to be a generator. However, not every function $F_1(q,Q,t)$ is a legitimate generator. For example, $F_1(q,Q) = q + Q$ would imply $p = 1$ and $P = -1$ which in general cannot be solved to express Q, P in terms of q, p. Similarly, $F_1 = q^2 + Q^2$ also does not generate a CT since it implies $p = 2q, P = -2Q$ which cannot be solved to express Q, P as functions of q, p. On the other hand, a choice that *does* generate a CT is $F_1(q,Q) = qQ$. In this case, $Q = p$ and $P = -q$ and we have an exchange of coordinates and momenta up to a sign. What CT does $F_1 = -qQ$ generate?

Motivated by these examples, we observe that a necessary condition for $F_1(q,Q)$ to generate a CT is that the 'Hessian' of unlike second partials $\frac{\partial^2 F_1}{\partial q \partial Q}$ be nonvanishing[31]. This will allow us to use $p = \partial F_1(q,Q)/\partial q$ to solve for Q in terms of q, p, at least locally[32]. When the second partial is nonvanishing, $\partial F_1(q,Q)/\partial q$ depends nontrivially on Q which can then be solved for and then inserted in $P = -\frac{\partial F_1(q,Q)}{\partial Q}$ to express $P = P(q,p)$. □

---

[31] For more degrees of freedom, the Hessian $\frac{\partial^2 F_1}{\partial q^i \partial Q^j}$ of unlike 2^{nd} partials must be invertible.

[32] Recall from Sect. 3.6 that the acton functional on configuration space paths $S[q] = \int_{t_1}^{t_2} L(q,\dot{q},t)\, dt$ is unchanged upon augmenting the Lagrangian by the time derivative of a function $F(q,t)$. However, such an $F(q,t)$ does not generate a CT on phase space. On the other hand, point transformations on configuration space *can* be used to define CTs which, moreover, admit generating functions. This is explained later in this section.

Limitations of the generator $F_1(q,Q,t)$. The generator of a finite CT $F_1(q,Q,t)$ is distinct from the infinitesimal generator $f(q,p)$ encountered before. Unlike $f(q,p)$, which generates all infinitesimal CTs, $F_1(q,Q,t)$ does not generate all finite CTs. In particular, the identity transformation $Q = q, P = p$ is not expressible via a generating function $F_1(q,Q,t)$. The latter expresses

$$p = \frac{\partial F_1(q,Q)}{\partial q} = p(q,Q) \quad \text{and} \quad P = -\frac{\partial F_1(q,Q)}{\partial Q} = p(q,Q). \tag{10.82}$$

However, for the identity transformation, it is not possible to express P as a function of Q and q. On the other hand, F_1 is good at generating CTs that are in the vicinity of the one that exchanges coordinates and momenta up to a sign and a possible scaling, $Q = p/\lambda$, $P = -\lambda q$ that follows from the choice $F_1 = \lambda q Q$ for a nonzero real parameter λ.

Generator of second kind $F_2(q,P,t)$. To find a generator for other canonical transformations, we use the second variational principle $\tilde{S}[Q,P]$ (3.111) for Hamilton's equations. Here, the momenta are held fixed at the endpoints $\delta P(t_i) = \delta P(t_f) = 0$. For the old Hamilton equations, we use the first variational principle $S[q,p]$ where $\delta q(t_i) = \delta q(t_f) = 0$:

$$\delta \int_{t_i}^{t_f} [p\dot{q} - H(q,p)]\, dt = 0 \quad \text{and} \quad \delta \int_{t_i}^{t_f} [-Q\dot{P} - K(Q,P)]\, dt = 0. \tag{10.83}$$

These two variational principles give the same equations if the integrands differ by the total time derivative of a function $F_2(q,P,t)$ since δq and δP are held fixed at the endpoints. Proceeding as before,

$$p dq - H dt = -Q dP - K dt + \frac{\partial F_2}{\partial q} dq + \frac{\partial F_2}{\partial P} dP + \frac{\partial F_2}{\partial t}\, dt. \tag{10.84}$$

The resulting equations of transformation are

$$p = \frac{\partial F_2}{\partial q}, \quad Q = \frac{\partial F_2}{\partial P} \quad \text{and} \quad K = H + \frac{\partial F_2}{\partial t}. \tag{10.85}$$

F_2 is called a generator of the second kind. As before, we will need to assume that $\partial^2 F/\partial P \partial q \neq 0$. It is easily seen that if $F_2(q,P) = qP$, then the resulting transformation is the identity $Q = q, p = P$.

The most distinguished example of a generating function of type F_2 is Hamilton's principal function $S(q,P,t)$, which is a solution of the time-dependent Hamilton-Jacobi equation to be introduced in Sect. 12.1. In a similar vein, Hamilton's characteristic function $W(q,P)$ (see Sect. 11.2) which solves the time-independent Hamilton-Jacobi equation furnishes an example of a generator of type F_2, that does not depend explicitly on time.

Legendre transform from F_1 to F_2. The distinction between the generating functions $F_1(q,Q,t)$ and $F_2(q,P,t)$ lies in the independent variables they depend on. As we have seen, $F_1(q,Q,t)$ cannot be used to get the identity transformation and one checks that $F_2(q,P,t)$ cannot be used to get the exchange transformation $Q=p, P=-q$. But there are many CTs that may be generated by both[33] an $F_1(q,Q,t)$ and an $F_2(q,P,t)$. In these cases, one wonders whether F_1 and F_2 are related by a Legendre transform (see Sect. 3.15), as they depend on different variables but produce the same CT. Taking the difference between the differentials in (10.80) and (10.84),

$$pdq - Hdt = PdQ - Kdt + dF_1 \quad \text{and} \quad pdq - Hdt = -QdP - Kdt + dF_2 \tag{10.86}$$

we get

$$-QdP + dF_2 = PdQ + dF_1 \quad \Rightarrow \quad dF_2(q,P) = d\left[F_1(q,Q) + QP\right]. \tag{10.87}$$

where $P = -\frac{\partial F_1}{\partial Q}$. In other words, up to an additive constant, $F_2 = QP + F_1$ with P given as above, or in short,

$$F_2(q,P,t) = \text{ext}_Q\left[QP + F_1(q,Q,t)\right] \tag{10.88}$$

is the Legendre transform of F_1.

Generators of type $F_3(p,Q,t)$ and $F_4(p,P,t)$. We may obtain two more types of generators for finite canonical transformations by suitable choices of variational principles for the old and new Hamilton equations:

$$\tilde{S}[q,p] \quad \& \quad S[Q,P] \quad \rightsquigarrow \quad F_3(p,Q) \ \text{ while } \ \tilde{S}[q,p] \quad \& \quad \tilde{S}[Q,P] \quad \rightsquigarrow \quad F_4(p,P). \tag{10.89}$$

One finds

$$-qdp - Hdt = PdQ - Kdt + dF_3(p,Q,t) \tag{10.90}$$

which implies

$$q = -\frac{\partial F_3}{\partial p}, \quad P = -\frac{\partial F_3}{\partial Q} \quad \text{and} \quad K = H + \frac{\partial F_3}{\partial t}. \tag{10.91}$$

Similarly,

$$-qdp - Hdt = -QdP - Kdt + dF_4 \quad \Rightarrow \quad q = -\frac{\partial F_4}{\partial p}, \ Q = \frac{\partial F_4}{\partial P} \quad \text{and} \quad K = H + \frac{\partial F_4}{\partial t}. \tag{10.92}$$

As with $F_2(q,P)$, we may obtain $F_3(p,Q)$ and $F_4(p,P)$ via Legendre transforms:

$$\begin{aligned} F_3(p,Q) &= \text{ext}_q[F_1(q,Q) - qp] \quad \text{while} \\ F_4(p,P) &= \text{ext}_Q[QP + F_3(p,Q)] = \text{ext}_q[F_2(q,P) - pq]. \end{aligned} \tag{10.93}$$

No generating functions of type $F_5(q,p)$ or $F_6(Q,P)$. One wonders if there are generating functions $F_5(q,p)$ and $F_6(Q,P)$ for finite CTs. The above variational approach does not lead to such generators. In Hamilton's action principle, both q and p cannot be held fixed at the endpoints, so the total time derivative of F_5 (or F_6) would nontrivially modify Hamilton's equations and not lead to a CT in general.

---

[33] We will give examples in the context of the oscillator, see Sect. 11.3 and Prob. 11.3

Example 1: Point transformations. We began our study of canonical transformations in Sect. 10.1 with coordinate changes ('point' transformations) $Q^i(q)$ on configuration space $\mathcal{Q}$. The identity is included among such transformations. So let us look for a generator of type F_2 (named $W(q,P)$) that effects a change of coordinates on $\mathcal{Q}$, for simplicity for $n=1$ degree of freedom. We must have $Q=\frac{\partial W}{\partial P}$ and $p=\frac{\partial W}{\partial q}$. Integrating with respect to P, the first equation then implies

$$W(q,P) = PQ(q) + g(q), \tag{10.94}$$

for some function $g(q)$ of the old coordinates alone. Then $p = PQ'(q)+g'(q)$ or $P = (p-g'(q))/Q'(q)$. This determines the new momentum. A CT that effects a change of coordinates on $\mathcal{Q}$ is clearly not unique, $g(q)$ being an arbitrary function. Different functions $g(q)$ produce different possible new momenta. In our earlier discussion in Sect. 10.1 and Sect. 3.20*, the new momenta were determined using a Lagrangian. Specification of a Lagrangian $L(q,\dot{q})$, which 'induces' a change in momenta $P=\frac{\partial \tilde{L}}{\partial \dot{Q}}$ where $\tilde{L}(Q,\dot{Q}) = L(q(Q),\dot{q}(Q,\dot{Q}))$, is like selecting a specific function g. Of course, the simplest possibility is to take $g=0$, which we will see below corresponds to a Lagrangian with the standard kinetic terms.

Example 2: Cartesian to polar coordinates. Let us illustrate this with the example of the 'point' transformation from Cartesian to plane polar coordinates on configuration space. The old coordinates and momenta are x,y,p_x,p_y and the new coordinates and momenta are $r=\sqrt{x^2+y^2}, \theta = \arccos(x/r) = \arctan(y/x), p_r, p_\theta$ with p_r, p_θ yet to be determined. By the above arguments, the simplest generating function of the second type, that should take Cartesian to plane polar coordinates is one with $g=0$:

$$W(x,y,p_r,p_\theta) = Q^i(q)P_i = r(x,y)p_r + \theta(x,y)p_\theta = \sqrt{x^2+y^2}p_r + \arctan\left(\frac{y}{x}\right)p_\theta. \tag{10.95}$$

The new coordinates are given by partial derivatives of W and satisfy the defining relations as expected:

$$r = \frac{\partial W}{\partial p_r} = \sqrt{x^2+y^2} \quad \text{and} \quad \theta = \frac{\partial W}{\partial p_\theta} = \arctan\left(\frac{y}{x}\right). \tag{10.96}$$

The old momenta are given by the following partial derivatives of W:

$$p_x = \frac{\partial W}{\partial x} = \frac{x}{r}p_r - \frac{y}{r^2}p_\theta \quad \text{and} \quad p_y = \frac{\partial W}{\partial y} = \frac{y}{r}p_r + \frac{x}{r^2}p_\theta. \tag{10.97}$$

We may invert these relations and express p_r and p_θ in terms of the old coordinates and momenta

$$p_r = \frac{x}{r}p_x + \frac{y}{r}p_y = p_x\cos\theta + p_y\sin\theta = \boldsymbol{p}\cdot\hat{\boldsymbol{r}} \quad \text{and} \quad p_\theta = xp_y - yp_x = L_z. \tag{10.98}$$

We see that p_r and p_θ are the familiar radial and angular momenta. So our generating function reproduces the usual conjugate momenta that we derived in Sect. 10.1 using the standard Lagrangian $L=\frac{1}{2}m(\dot{r}^2+r^2\dot{\theta}^2) - V(r,\theta)$. On the other hand, if we took

$$W(x,y,p_r,p_\theta) = rp_r + \theta p_\theta + g(x,y) \quad \text{for} \quad g \neq 0, \tag{10.99}$$

then the resulting transformation would still be a CT, but the momenta $p_x = \frac{x}{r}p_r - \frac{y}{r^2}p_\theta + \frac{\partial g}{\partial x}$ and $p_y = \frac{\partial W}{\partial y} = \frac{y}{r}p_r + \frac{x}{r^2}p_\theta + \frac{\partial g}{\partial y}$, would not be the usual ones arising from the above Lagrangian. Can L be modified to accommodate the effect of g?

Example 3: Scaling. Another simple example of a CT is got by choosing $W(q,P) = \lambda q^i P_i$. The resulting CT is a scaling,

$$Q^j = \frac{\partial W}{\partial P_j} = \lambda q^j \quad \text{and} \quad p_i = \frac{\partial W}{\partial q^i} = \lambda P_i \quad \Rightarrow \quad P_i = \lambda^{-1} p^i. \tag{10.100}$$

The PB are preserved, $\{Q^i, P_j\} = \{\lambda q^i, \lambda^{-1} p_j\} = \delta^i_j$, etc. If $\lambda = 1 + \epsilon$ we get an infinitesimal scaling. We could also do a different rescaling in each of the q-p planes, by choosing $W(q,P) = \sum_i \lambda_i q^i P_i$. Choosing $\lambda = -1$, we see that reversing the signs of all coordinates and momenta $Q^i = -q^i, P_j = -p_j$ is a canonical transformation.

10.11 Problems

1. **Point transformation.** Consider a free particle moving on the real line with Lagrangian $L(q,\dot q) = \frac{1}{2}m\dot q^2$ and equation of motion $\ddot q = 0$. Suppose we make the change of coordinate to $Q = \tanh(q/a)$ where $a > 0$ is a constant length.

   a. Is this transformation invertible and/or smooth? What is the range of Q?
   b. Express the equation of motion $\ddot q = 0$ as a 2^{nd} order ODE for Q.
   c. Find the new Lagrangian $\tilde L(Q, \dot Q)$.
   d. Find the momentum P conjugate to Q from the transformed Lagrangian. Express P as a function of Q and $\dot Q$ and as a function of q and p.
   e. Find the new Hamiltonian $\tilde H(Q,P)$ from the old Hamiltonian.
   f. Find Hamilton's equations that follow from the new Hamiltonian $\tilde H(Q,P)$ [written as first order differential equations for Q and P].
   g. Check that Hamilton's equations for Q, P are equivalent to the 2^{nd} order ODE for Q obtained by transforming $\ddot q = 0$ above.
   h. Calculate the Legendre transform of the new Lagrangian $\tilde L(Q, \dot Q)$ and check that you get the new Hamiltonian $\tilde H(Q,P)$.
   i. Find the PB $\{Q,P\}$ (by differentiating in q and p) and compare with the canonical $\{q,p\}$ PB. Comment on the nature of this change of coordinates.

2. **Canonicity of center of mass and relative variables.** Let (r_1, p_1) and (r_2, p_2) be the canonically conjugate Cartesian coordinates and momenta of a pair of point particles of masses m_1, m_2 that move on a line (this is a 1d version of the two-body problem). Define the center of mass and relative positions and momenta by

   $$R = (m_1 r_1 + m_2 r_2)/M, \quad r = r_2 - r_1, \quad P = p_1 + p_2, \quad p = m(p_2/m_2 - p_1/m_1), \tag{10.101}$$

   where $M = m_1 + m_2$ and $m = m_1 m_2/M$. (a) Justify the formula for the relative momentum p. (b) Invert this transformation and express r_1, r_2, p_1, p_2 in terms of R, r, P, p. (c) Given that the old variables are canonical, what are the 6 (up to antisymmetry) basic PBs among them? (d) Determine whether this transformation is canonical by evaluating all the 6 relevant PBs among CM and relative variables.

$*3$. Consider a quantum system with Hilbert space $\mathcal{H} = \mathbb{C}^2$, state vector $\psi = \begin{pmatrix} a_1+ib_1 \\ a_2+ib_2 \end{pmatrix}$ and Hamiltonian operator $\hat{H} = \begin{pmatrix} \varepsilon_{11} & \alpha+i\beta \\ \alpha-i\beta & \varepsilon_{22} \end{pmatrix}$. Use the method of Sect. 10.3* to show that **Schrödinger's equation** can be expressed as **Hamilton's equations** for the classical Hamiltonian

$$H = \frac{1}{2}\left[\varepsilon_{11}(a_1^2+b_1^2) + \varepsilon_{22}(a_2^2+b_2^2)\right] + \alpha(a_1 a_2 + b_1 b_2) - \beta(a_1 b_2 - a_2 b_1) \tag{10.102}$$

on a classical state space $\mathbb{R}^4$ with coordinates given by the components of the column vector $\psi = (a_1, a_2, b_1, b_2)^t$.

$*4$. **Preservation of area elements.** Choose a simple example of a Hamiltonian system with 2 degrees of freedom. Attempt to verify that under time evolution, the area element in tangent 2-planes in phase space is preserved.

5. **Generator for infinitesimal canonical transformation.** Verify that equations (10.46) are identically satisfied if for $1 \le i \le n$, we put $\delta q^i = \frac{\partial f}{\partial p_i}$ and $\delta p_i = -\frac{\partial f}{\partial q^i}$ for an arbitrary twice differentiable function $f(q,p)$ on phase space.

6. Consider the **infinitesimal** ($|\epsilon| \ll 1$) **canonical transformation** (CT) $X = x + \delta x, P = p + \delta p$ generated by $f(x,p) = \epsilon p$ for a particle moving on a line. (a) Express the infinitesimal changes δx and δp in terms of partial derivatives as well as PBs. Find δx and δp. (b) Physically interpret this CT. (c) Find the Jacobian matrix $J = \frac{\partial(X,P)}{\partial(x,p)}$. (d) What property of J ensures that this is a CT?

7. Consider the **infinitesimal CT generated by the angular momentum** component ϵL_z for a particle moving in 3d. Write ϵL_z in terms of coordinates and momenta. Find the changes $\delta x, \delta y, \delta z$ and $\delta p_x, \delta p_y, \delta p_z$. Geometrically interpret this CT.

8. Find the **infinitesimal CT** (for 1 degree of freedom) generated by $f = \epsilon(x^2 + \alpha p^2)$ and give its geometric meaning in terms of the phase plane. Here ϵ is an infinitesimal parameter and α is a constant with appropriate dimensions to be found.

9. Consider a **free particle** of mass m moving on a line with coordinate q, canonically conjugate momentum p and Hamiltonian $H = \frac{p^2}{2m}$. Suppose we make the transformation to new variables $Q = q + kp, P = p$.

   a. What is the dimension of the constant k? Argue why the transformation is canonical. Under what circumstances is it an infinitesimal CT?
   b. Find a generating function $f(q,p)$ for the corresponding **infinitesimal canonical transformation** (up to an additive constant).
   c. Physically interpret the above infinitesimal CT and its generator by a suitable choice of k in terms of familiar physical quantities.

$*10$. Argue that the **group of CTs** of the q-p phase plane is infinite-dimensional. Hint: use the generating functions for either infinitesimal or finite CTs.

$*11$. Consider two infinitesimal CTs generated by functions f and g on phase space (say $\mathbb{R}^{2n}$). In general, the **composition of a pair of CTs** depends on the order of application: the group of CTs is nonabelian. Show that this nonabelian nature is captured to first approximation by the Poisson bracket of generators $\{f, g\}$. More precisely, suppose A is an observable on phase space and that $A \mapsto A_f$ via the generator f and $A_f \mapsto A_{g\circ f} = (A_f)_g$ when g follows f. Note that $g \circ f$ does not denote the composition of functions, but the composition of the CTs they generate. Concretely, we may regard $A = A(q,p)$, $A_f = A_f(q,p)$ and $A_{g\circ f} = A_{g\circ f}(q,p)$ as three different functions of the original coordinates and momenta on $\mathbb{R}^{2n}$. (a) Give expressions (using PBs) for $A_{g\circ f}$ and $A_{f\circ g}$ correct to *quadratic* order in the infinitesimal generators f and g. (b) Calculate the difference $A_{g\circ f} - A_{f\circ g}$ to leading nontrivial order in infinitesimals and show that it is given by a PB (of what?) with $\{f, g\}$. One may interpret this result as showing, in effect, that the PB of infinitesimal generators is the Lie bracket in the Lie algebra of the group of CTs.

$*$12. Verify the **associative law of composition of CTs** for infinitesimal CTs generated by three functions f, g and h. More precisely, suppose A is any observable and suppose $A_h = A + \{A, h\}$. Then $A_{g\circ h} \equiv (A_h)_g$, etc. Note that $g \circ h$ does not denote the composition of functions, but the composition of the CTs they generate. Verify that $A_{f\circ(g\circ h)} = A_{(f\circ g)\circ h}$ by showing that both are equal to

$$A + \{A, h\} + \{A_h, g\} + \{A_h + \{A_h, g\}, f\}. \tag{10.103}$$

13. **Generators for infinitesimal canonical transformations** on phase plane.

    a. Argue why the infinitesimal translation $Q = q + \epsilon_1$, $P = p + \epsilon_2$ is canonical.
    b. Find an infinitesimal generator $g(q,p)$ for the above infinitesimal translation.
    c. Consider the infinitesimal generator $f(q,p) = -\frac{1}{2}\theta(q^2 + p^2)$, where we suppress dimensional constants. Find the infinitesimal CT it generates.
    d. Plot on the q-p phase plane the effect of this infinitesimal CT on a typical phase point (q,p), i.e., indicate q, p and Q, P for small θ.
    e. State in words what infinitesimal canonical transformation f generates.

$*$14. **Symplectic group.** Suppose M is a linear symplectic transformation, i.e., a $2n \times 2n$ matrix that preserves the canonical symplectic tensor: $M^t \omega M = \omega$ where $\omega = (0, -I | I, 0)$. Show that the set of such symplectic matrices M forms a group. Show that the determinant of a 2×2 symplectic matrix must be one. Suppose $M = I + m$ is a symplectic matrix that departs infinitesimally from the identity matrix. What condition must m satisfy to linear order? What is the dimension of the space of such $2n \times 2n$ real matrices m? m is said to be an element of the Lie algebra of the symplectic group. What is the dimension of this group?

$*$15. Consider **finite linear canonical transformations** for one degree of freedom.

    a. Find all (finite) *linear* CTs $(q,p) \mapsto (Q,P)$ that fix the origin $(q = 0, p = 0)$. How many parameters are involved in their specification?
    b. Identify the matrix group of such CTs as a suitable special linear group. What is its dimension as a real manifold? Linear canonical transformations are also called linear symplectic transformations or symplectic matrices. For n degrees of freedom, the corresponding group is called the symplectic group Sp(2n, $\mathbb{R}$).

c. Find a generating function $W(q,P)$ for the above finite linear CTs by solving the relevant PDEs. Express the answer in terms of the parameters used to specify the above CTs. Mention in what cases there is no generator $W(q,P)$ of type 2 for the *above* CT. Give one such example with a suitable name.

16. Attempt to find a **generating function** for the finite CT to **center of mass and relative variables** in the 1d version of the Kepler problem discussed in Prob. 10.2.
17. For one degree of freedom, show that a transformation $(q,p) \mapsto (Q,P)$ generated by a function of old coordinates and new momenta $F_2(q,P) \equiv W(q,P)$ **preserves Poisson brackets**. Hint: It suffices to show that $\{Q,P\} = 1$.

$*$18. Argue that the set of all CTs of the q-p phase plane is not a linear space in the following sense. Via an explicit counter example, show that if $S(q,P)$ and $\tilde{S}(q,P)$ generate two **finite canonical transformations**, their sum need not generate a CT.

$*$19. **Keplerian mechanical similarity.** Recall the scaling transformation (Sect. 2.6*) for the Kepler problem $t \to t' = t/\lambda, \boldsymbol{r} \to \boldsymbol{r}' = \lambda^\gamma \boldsymbol{r}$ for $\gamma = -2/3$.

a. Under what circumstances can this transformation be considered infinitesimal?
b. Is this transformation a symmetry of Newton's equation of motion?
c. How does momentum $\boldsymbol{p}$ transform? Is the transformation canonical?
d. How do the Lagrangian and Hamiltonian transform? Is it a symmetry of the Lagrangian or Hamiltonian? Does one expect a Noether conserved quantity?

20. **Finite from infinitesimal CTs.** We illustrate how to get a finite canonical transformation by composing infinitesimal ones. Consider the infinitesimal generator $f(q,p) = -\frac{1}{2}\delta\theta(q^2+p^2)$ for a system with one degree of freedom and canonically conjugate phase space variables q,p. [In writing expressions such as q^2+p^2 we suppress constants which are necessary to make dimensions consistent.] (a) Find the infinitesimal CT $q \to Q = q + \delta q$, $p \to P = p + \delta p$ generated by $f(q,p)$. Express the answer in matrix form and identify the matrix T:

$$\binom{Q}{P} = [I + \delta\theta\, T]\binom{q}{p}. \tag{10.104}$$

(b) The effect of composing this infinitesimal CT twice is given by

$$\binom{Q}{P} = [I + \delta\theta\, T][I + \delta\theta\, T]\binom{q}{p}. \tag{10.105}$$

To get a finite CT, we compose n infinitesimal CTs generated by f, and let $n \to \infty$. Find how $\delta\theta$ must behave as $n \to \infty$ to ensure a finite limiting CT. Find the limiting CT and express it in matrix form $\binom{Q}{P} = A\binom{q}{p}$. Find a simple formula for the matrix A and show that the resulting finite CT is a rotation $Q = cq - sp$ and $P = sq + cp$ where $s = \sin\theta$ and $c = \cos\theta$. Relate the angle θ to $\delta\theta$ and n. (c) Verify that this CT preserves the basic Poisson bracket relations.

21. **Liouville's theorem for infinitesimal CTs for 1 degree of freedom.** Consider the infinitesimal CT $Q = q + \delta q, P = p + \delta p$ generated by $\epsilon f(q,p)$. (a) Express $\delta q, \delta p$ as derivatives of f. Write the 2×2 Jacobian matrix $J = \frac{\partial(Q,P)}{\partial(q,p)}$ explicitly with

entries expressed as partial derivatives of f. Write $J = I + \epsilon F$ for an appropriate matrix F. (b) Express $\det J$ as a quadratic polynomial in ϵ and show that the linear term is equal to the trace of F. Thus, find $\det J$ ignoring quadratic terms in ϵ.

$*$22. Suppose $J = I + \epsilon F$ where ϵ is a small parameter and J is a $2n \times 2n$ matrix as in the discussion of **Liouville's theorem**. Recall the identity $e^{\operatorname{tr} \log J} = \det J$ where $\log[I + \epsilon F]$ is defined by the logarithmic series. Find the *quadratic* Taylor polynomial for $\det J$ regarded as a series in ϵ.

$*$23. For one degree of freedom, find all **infinitesimal linear canonical transformations** $(q, p) \mapsto (Q, P)$ that fix the origin of the phase plane, i.e., $(0, 0) \mapsto (0, 0)$. What is the dimension of the space of such infinitesimal linear CTs? Find the generating function $f(q, p)$ for the most general such infinitesimal linear CT.

24. **Rotation of phase plane.** Consider the finite CT corresponding to a rotation of the phase plane (with dimensional constants suppressed) $Q = cq - sp$ and $P = sq + cp$ where $s = \sin\theta$ and $c = \cos\theta$.

    a. We seek a generating function of type-II, $W(q, P)$ for this CT. Write the equations of transformation for such a generator and find the 2 first order PDEs that $W(q, P)$ must satisfy to ensure it generates the above CT.
    b. Solve the PDE involving only one partial derivative $\frac{\partial W}{\partial q}$ and express the answer in terms of an arbitrary differentiable function g. What does g depend on?
    c. Determine g by imposing the other PDE. Find an ODE for g, solve it, and give a simple formula for the generating function $W(q, P)$.
    d. For $\theta = 0$, what does $W(q, P)$ reduce to, and what CT does it generate?
    e. Verify that the proposed $W(q, P)$ indeed generates the above finite rotation.
    f. Find a generating function of type $F_1(q, Q)$ that generates the same finite rotation via an appropriate Legendre transform from $W(q, P)$. This provides an example of a CT that admits a generator of both type I and II.
    g. Try to find a generator of type I for the identity CT, by letting the angle of rotation go to zero. What do you find?

25. Find a **generator** of 2^{nd} kind for the CT from plane polar to Cartesian coordinates.

26. State 5 **equivalent conditions** for a transformation $(q, p) \mapsto (Q(q, p), P(q, p))$ of the phase space $\mathbb{R}^2$ of a system with one real degree of freedom to be canonical. Mention three additional facts concerning **canonical transformations**.

27. **Generator for finite CT.** For n degrees of freedom, consider the transformation $Q^i = \lambda_i q^i$ and $P_i = \lambda_i^{-1} p_i$ (no sums on i). (a) Argue why it is canonical, describe its effect and give it a name. (b) Find a generator of type $W(q^i, P_j)$ for this CT and verify that it works. (c) Attempt to find a generating function of type $F_1(q, Q)$ by a suitable Legendre transform and indicate why it cannot be done. (d) Choosing all $\lambda_i = -1$, what CT do we get and what is a generator for it?

28. The **center of mass and relative positions and momenta** R, r, P, p in a 1d version of the Kepler 2 body problem are given by (10.101). We seek a **generating function** of the 2^{nd} kind $W(r_1, r_2, P, p)$ for the CT to CM and relative variables.

(a) Does this CT arise from a point transformation? Why? (b) Write the equations of transformation in terms of partial derivatives of W. (c) Find a generator W.

$*$29. The Jacobi identity is essential to showing that **time evolution** (or the flow generated by any observable via the PB) **preserves any PB relation**. Now suppose e, f and g are three observables with $\{e, f\} = g$. Under an infinitesimal transformation generated by an observable H, suppose $e \mapsto E = e + \delta e$, $f \mapsto F = f + \delta f$ and $g \mapsto G = g + \delta g$ where $\delta e = \{e, H\}$, $\delta f = \{f, H\}$ and $\delta g = \{g, H\}$. Then show that $\{E, F\} = G$. In particular, taking H to be the Hamiltonian, this shows that if $\{e, f\} = g$ at time t, then the same PB relation holds at $t + \delta t$. Conclude that the equal-time canonical PB relations $\{q^i, p_j\} = \delta^i_j$, $\{q^i, q^j\} = 0 = \{p_i, p_j\}$ are valid at any time if they were postulated to hold at $t = 0$ for $i = 1, \cdots, n$.

$*$30. Recall the **Kepler problem** (from Sect. 2.5*) for a particle in the central potential $V(r) = -\alpha/r$ in which the **LRL vector** $A_i = \epsilon_{ijk} p_j L_k - m\alpha \hat{r}_i$ is conserved.

a. Find the infinitesimal change in $1/r$ due to the CT generated by L_a. Give the answer without any calculation, but by pure reasoning about the nature of the CT generated by L_a and the nature of the observable $1/r$.
b. Find the change in r_i due to the infinitesimal CT generated by the angular momentum component L_a. Express δr_i via a PB and give a simple formula.
c. Find the infinitesimal change in $\hat{r}_i = \frac{r_i}{r}$ due to the CT generated by L_a.
d. Find the infinitesimal change in p_i due to the infinitesimal CT generated by L_a. We say that $\boldsymbol{r}$ and $\boldsymbol{p}$ transform as vectors under infinitesimal rotations.
e. Without calculation, make a conjecture for the infinitesimal change in the LRL vector components A_i under the infinitesimal CT generated by L_a.
f. Use the earlier results to calculate $\{A_i, L_a\}$ and check the conjecture. Hints: $\epsilon_{jik}\epsilon_{jab} = \delta_{ia}\delta_{kb} - \delta_{ib}\delta_{ka}$ and $\epsilon_{aij}(\boldsymbol{p} \times \boldsymbol{L})_j = p_a L_i - p_i L_a$.

$*$31. **Poincaré recurrence:** Let N_0 be a connected, simply connected (every closed curve can be shrunk to a point) open set in the phase space of a Hamiltonian dynamical system. There can be initial conditions lying in N_0 for which a trajectory that begins there returns to N_0 a finite number of times, and then stops doing so. Give an example where a trajectory intersects N_0 two times and never comes back after exiting for the second time. Hint: Try out the Hamiltonian systems we have studied. Use the freedom to pick N_0 as you wish.

$*$32. **Generating function for CT corresponding to finite time evolution.** Consider time evolution of a Hamiltonian system with 1 real degree of freedom. For any fixed time $T > 0$, both $(q(0), p(0))$ and $(q(T), p(T))$ are canonical variables on the phase plane. How might one go about finding a generating function for this finite canonical transformation. Begin first with the case where T is infinitesimal.

Chapter 11

Angle-action variables

In our discussion of canonical transformations (CTs) so far, the specific Hamiltonian of the system played no role. A transformation is canonical irrespective of what the Hamiltonian may be. Among canonical systems of coordinates and momenta on phase space, those which admit more cyclic coordinates *for a given Hamiltonian*, are more suited to solving Hamilton's equations for the given system. The momenta conjugate to cyclic coordinates are constants of motion, determined by the initial conditions. The best possibility is if all the coordinates (usually denoted θ^j) are cyclic. Then the Hamiltonian $H = H(I_1, \cdots I_n)$ is a function of the conjugate momenta alone, which are constants of motion: $\dot{I}_j = -\frac{\partial H}{\partial \theta^j} = 0$. Furthermore, the coordinates are then linear functions of time, since we may easily integrate Hamilton's equations:

$$\dot{\theta}^j = \partial_{I_j} H(I_1, \ldots, I_n) = \omega^j(I_1, \ldots, I_n) \quad \text{to get} \quad \theta^j(t) = \theta^j(0) + \omega^j t \tag{11.1}$$

and $I_j(t) = I_j(0)$. The 'frequencies' ω^j are *constant* in time. The coordinates θ^j are called angle variables and their conjugate constant momenta I_j are called action variables[1]. This terminology will be explained using the harmonic oscillator in Sect. 11.1.

Example. The position and momentum of a free particle $H = \frac{p^2}{2m}$ are angle and action variables since $\{q, p\} = 1$, momentum is conserved $p(t) = p(0)$ and position is linear in time $q(t) = q(0) + \frac{p(0)t}{m}$. In this case, the 'frequency' $\omega = p(0)/m$ is the constant velocity and H is clearly independent of the angle variable q. □

Based on examples such as the free particle and harmonic oscillator, there was a time when it was hoped that any Hamiltonian system could be 'solved analytically' by finding a canonical transformation to angle-action variables. For systems with one degree of freedom and conserved Hamiltonian, we will describe a procedure to transform to such variables in Sect. 11.4. For systems with more degrees of freedom, in a few favorable cases (e.g., the Kepler problem), it was possible to find such variables through educated guesswork. When this was not possible, an iterative procedure (e.g., the Birkhoff expansion and normal form) was proposed where one viewed the system Hamiltonian (e.g., $H = H_0 + gH_1$) as a perturbation to one (H_0) for which angle-action variables were already available. The idea was to construct angle-action variables for H in a series in powers of the coupling g, starting from those for H_0, by making a succession of canonical transformations[2]. This looked very promising, until it was discovered that for most systems, this series is not convergent and cannot directly be used to define angle-action variables. In current language, systems which admit a canonical transformation to angle-action variables are called completely integrable or Liouville integrable; they display relatively regular behavior. The remaining systems are not integrable, they display varying degrees of irregular or chaotic behavior, as we will encounter in Chap. 15.

---

[1] It is noteworthy that when they exist, angle-action variables for a given Hamiltonian are not uniquely determined. We may add a constant to the action or angle variables without affecting their Poisson brackets nor the conservation of the action variables. We may also rescale the action variables I_i by constants λ_i and the angle variables θ^i by $1/\lambda_i$ (for some nonzero constants $\lambda_1, \cdots, \lambda_n$) while retaining their status as angle-action variables. In fact, there is even more freedom in choosing angle-action variables, a feature we will comment on after Eq. (11.18).

In fact, generic n degree of freedom Hamiltonian systems do not admit angle-action variables. A prerequisite is that the system possesses n independent conserved quantities that are in involution (Poisson commute pairwise) so that they (or some functions of them) can serve as action variables. This brings into focus techniques to find conserved quantities. In Sect. 11.9*, we introduce one such technique, that of Lax pairs. When applicable, Lax pairs have far-reaching consequences for understanding integrability.

11.1 Angle-action variables for the harmonic oscillator

Recall from Sect. 6.1 that the harmonic oscillator Hamiltonian is $H = \frac{p^2}{2m} + \frac{1}{2}kq^2$ with $\omega = \sqrt{k/m}$. Hamilton's equations $\dot{q} = p/m$ and $\dot{p} = -kq$ imply Newton's equation $\ddot{q} = -\omega^2 q$, with solution

$$q(t) = A\sin(\omega(t-t_0)) \quad \text{and} \quad p(t) = Am\omega\cos(\omega(t-t_0)) \equiv B\cos(\omega(t-t_0)). \tag{11.2}$$

The phase point (q,p) for the solution with energy E moves clockwise on the q-p phase plane along an ellipse with semiaxes $A = \sqrt{2E/m\omega^2}$ and $B = \sqrt{2mE}$ (see Fig. 11.1a). The phase point begins at the northern-most point of the ellipse at $t = t_0$. Thus, we write

$$q(t) = \sqrt{\frac{2E}{m\omega^2}}\sin\theta(t) \quad \text{and} \quad p(t) = \sqrt{2mE}\cos\theta(t) \quad \text{where} \quad \theta(t) = \omega(t-t_0). \tag{11.3}$$

Our aim is to identify canonically conjugate angle and action variables for this system. $\theta(t)$ varies linearly with time, so it is a natural candidate for an angle variable. It is of course the angle subtended by the phase point with respect to the p axis measured clockwise. This explains the name angle. Taking a quotient, we express the angle variable in terms of q and p:

$$\theta = \arctan\left(m\omega q/p\right) = \arccos(p/\sqrt{2mE}) \quad \text{where} \quad E = p^2/2m + m\omega^2 q^2/2. \tag{11.4}$$

An action variable must be a constant of motion. Since there is only one degree of freedom, there can be at most one independent constant of motion, which can be

---

[2] One of the earliest significant uses of a succession of CTs to obtain an approximate series solution was by Charles Delaunay (1846) [52] in the Moon-Earth-Sun three-body problem. He made (via hand calculations) a succession of 505 CTs in a 7th order perturbative treatment of the 3d elliptical restricted 3-body problem and obtained the longitude and latitude of the Moon in trigonometric series of about 450 terms with secular terms (see Sect. 7.55) eliminated.

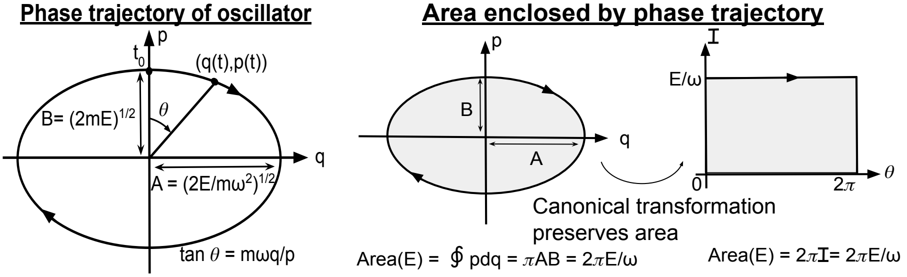
Phase trajectory of oscillator
p
t_0
(q(t),p(t))
B= $(2mE)^{1/2}$
θ
q
A = $(2E/m\omega^2)^{1/2}$
tan θ = mωq/p
Area enclosed by phase trajectory
p
B
A
q
I
E/ω
0
2π
θ
Canonical transformation
preserves area
Area(E) = $\oint$ pdq = πAB = 2πE/ω
Area(E) = 2πI= 2πE/ω

(a) (b)

Figure 11.1: (a) Elliptical phase trajectory of the harmonic oscillator on the q-p plane. (b) The canonical transformation from q-p to angle-action variables preserves area and can be used to deduce that $I = E/\omega$. Note that θ is 2π periodic, so the right and left edges of the rectangle on the θ-I plane are to be identified, making the trajectory periodic.

taken as energy E. All other constants of motion must be functions of energy. So we suppose that $I = I(E)$. We try to fix $I(E)$ by requiring that it be canonically conjugate to θ. Since I depends on q and p only via E, we have

$$\begin{aligned} 1 &= \{\theta, I\} = \frac{\partial \theta}{\partial q}\frac{\partial I}{\partial p} - \frac{\partial \theta}{\partial p}\frac{\partial I}{\partial q} = \frac{\partial \theta}{\partial q} I'(E) \frac{\partial E}{\partial p} - \frac{\partial \theta}{\partial p} I'(E) \frac{\partial E}{\partial q} \\ &= I'(E)\left[\frac{p}{m}\frac{\partial \theta}{\partial q} - kq\frac{\partial \theta}{\partial p}\right]. \end{aligned} \tag{11.5}$$

Taking the differential of $\tan\theta = \frac{m\omega q}{p}$ (11.4), we get (using $\cos^2\theta = p^2/2Em$)

$$d\theta = \sqrt{km}\left(\frac{dq}{p} - \frac{q\,dp}{p^2}\right)\cos^2\theta = \frac{\omega}{2E}\left(p\,dq - q\,dp\right), \tag{11.6}$$

from which we may read off $\frac{\partial \theta}{\partial q}$ and $\frac{\partial \theta}{\partial p}$. Thus, the condition that angle and action be canonically conjugate becomes an ODE for $I(E)$:

$$1 = I'(E)\frac{\omega}{E}\left(\frac{p^2}{2m} + \frac{1}{2}m\omega^2 q^2\right) \;\Rightarrow\; I'(E) = \frac{1}{\omega} \;\Rightarrow\; I(E) = \frac{E}{\omega} + c. \tag{11.7}$$

I is not uniquely determined, as mentioned earlier. For simplicity, we pick $c = 0$ and arrive at a pair of angle-action variables for the harmonic oscillator

$$\theta(q,p) = \arctan\left(\frac{m\omega q}{p}\right) \quad \text{and} \quad I(q,p) = \frac{E(q,p)}{\omega} = \frac{p^2}{2m\omega} + \frac{1}{2}m\omega q^2. \tag{11.8}$$

By construction, we know that $\theta(t) = \omega(t - t_0)$ is linear in time, I is constant in time and that they are canonically conjugate $\{\theta, I\} = 1$. Moreover, the Hamiltonian when expressed in angle-action variables $H(\theta, I) = \omega I$ is a function of I alone, the angle variable is a cyclic coordinate. The action variable I has dimensions of action, `energy × time`. As mentioned before, θ is the angle that the phase point makes with respect to the p axis clockwise. On the other hand, we notice that the action variable $I(E)$ is $1/2\pi$ times the area enclosed by the ellipse traced out by the phase point during one complete oscillation: the ellipse has semiaxes $A = \sqrt{2E/k}$ and $B = \sqrt{2mE}$ and area πAB:

$$I(E) = \frac{1}{2\pi}\text{Area}(E) = \frac{E}{\omega}. \tag{11.9}$$

We could have anticipated this relation between $I(E)$ and the area enclosed by the phase trajectory. It follows from the fact that a canonical transformation on the phase plane preserves areas. The area enclosed by a closed phase trajectory of energy E may be found in two sets of canonical coordinates and equated, as illustrated in Fig. 11.1b. On the one hand,

$$\text{Area}(E) = \oint p\, dq \tag{11.10}$$

where we choose a clockwise orientation since the phase trajectory went clockwise. On the other hand, by preservation of areas, we must have

$$\oint p\, dq = \oint I\, d\theta = \int_0^{2\pi} I(E) d\theta = 2\pi I(E) \tag{11.11}$$

by constancy of I along the trajectory. Again, we choose θ to increase clockwise. Thus $I(E) = \text{Area}(E)/2\pi$, as we found by explicit calculation.

Relation of action to time period. Suppose E is an energy for which the trajectory is periodic with period $T(E)$. This is of course always true for the harmonic oscillator with $E \geq 0$. As we might expect from (1.27), the action variable is related to the time period in a simple way: $I'(E) = T(E)/2\pi$. This is seen by differentiating in E:

$$I'(E) = \frac{1}{2\pi}\oint p'(E) dq = \frac{1}{2\pi}\sqrt{\frac{m}{2}}\oint \frac{dq}{\sqrt{E - V(q)}} = \frac{1}{2\pi}T(E). \tag{11.12}$$

We know the time period of harmonic oscillator trajectories, $T(E) = 2\pi/\omega$. This allows us to find the frequency of (11.1). Whatever θ may be, it must satisfy Hamilton's equation in the new variables,

$$\dot{\theta} = \frac{\partial H}{\partial I} = \frac{dE}{dI} = \frac{1}{I'(E)} = \frac{2\pi}{T(E)} = \frac{2\pi}{2\pi/\omega} = \omega. \tag{11.13}$$

We have found a CT to angle-action variables for the harmonic oscillator. What is the generator (in the sense of Sect. 10.10), of the finite canonical transformation from q, p to θ, I? The Hamilton-Jacobi equation gives us a method to find it.

11.2 Generator of CT to angle-action variables: Hamilton-Jacobi equation

Consider a dynamical system[3] with Hamiltonian $H(q,p)$ and canonical variables $\{q,p\} = 1$. An example to keep in mind is $H(q,p) = \frac{p^2}{2m} + V(q)$ and more specifically the harmonic oscillator. We are interested in trajectories with energy E. So

---

[3] Our notation will be for one degree of freedom, though some of this generalizes to $n > 1$ degrees of freedom. For a system with one degree of freedom with conserved Hamiltonian, one may usually pass to angle-action variables. But this is not always possible for systems with $n > 1$ degrees of freedom.

q, p must satisfy the condition $H(q,p) = E$. Now we seek a generator, of the sort introduced in Sect. 10.10, for a finite canonical transformation to new coordinates and momenta $Q = \theta, P = I$ where all coordinates are cyclic. In other words, the Hamiltonian $H(q,p) = K(P)$ depends only on the new momenta P. The new canonical variables would be angle-action variables: as $\dot{Q} = \frac{\partial K}{\partial P}$ are constant, the Q's evolve linearly in time. Moreover, $\dot{P} = -\frac{\partial K}{\partial Q} = 0$ so that the new momenta are constants of motion[4]. Hence we use the symbols I, θ in place of P, Q. Let us look for a generating function of the second type[5], depending on old coordinates and new momenta $F_2(q, I, t)$. In terms of F_2,

$$\theta = \frac{\partial F_2}{\partial I} \quad \text{and} \quad p = \frac{\partial F_2}{\partial q} \quad \text{and} \quad K = H + \frac{\partial F_2}{\partial t}. \tag{11.14}$$

Furthermore, let us consider only the case where F_2 is not explicitly dependent on time. This should be adequate for the harmonic oscillator since we found in Sect. 11.1 that $K = H$ simply by substitution while I and θ depended on time only via their dependence on q and p, and not explicitly. In this case, it is customary to denote $F_2(q, I) = W(q, I)$. The equations of transformation simplify to

$$\theta = \frac{\partial W(q,I)}{\partial I}, \qquad p = \frac{\partial W(q,I)}{\partial q} \quad \text{and} \quad K(I(q,p)) = H(q,p). \tag{11.15}$$

We hope that the trajectories of energy E are simpler to describe in terms of I and θ. Whatever this generating function W may be, it must satisfy the energy constraint $H(q,p) = E$, which is in general a nonlinear first order PDE for $W(\boldsymbol{q}, \boldsymbol{I})$. For the above example with one degree of freedom, it is

$$H\left(q, \frac{\partial W}{\partial q}\right) = E \quad \text{or} \quad \frac{1}{2m}\left(\frac{\partial W}{\partial q}\right)^2 + V(q) = E. \tag{11.16}$$

This equation is called the time-independent Hamilton-Jacobi (HJ) equation and W is called Hamilton's characteristic function. We will say more about the HJ equation in Chap. 12.

In general, W will generate a CT to new canonical variables. The HJ equation does not by itself pick out the CT to angle-action variables. To impose this additional requirement, we seek solutions $W(q, I)$ of the HJ equation subject to the condition that the action variable I be a constant of motion. This will ensure that θ is a cyclic coordinate, since $\partial_\theta K = -\dot{I} = 0$. Consequently, θ evolves linearly in time.

The time derivative of W is

$$\frac{dW(q,I)}{dt} = \frac{\partial W}{\partial q}\frac{dq}{dt} = p\dot{q} \quad \text{since} \quad \dot{I} = 0. \tag{11.17}$$

---

[4] Of course, there may not be n independent conserved quantities to serve as action variables. Then it is not possible to find angle-action variables and we say the system is not completely integrable. Note also that the action variables must Poisson commute with each other, so that they form a canonical family with their conjugate angle variables $\{\theta^i, I_j\} = \delta^i_j$, $\{I_i, I_j\} = \{\theta^i, \theta^j\} = 0$.

[5] At the end of this section, we will indicate how to proceed with a generator of type $F_1(q, \theta)$.

Thus, we must have

$$W(q(t), I) = W(q(t_0), I) + \int_{t_0}^{t} p\,\dot{q}\,dt = W(q(t_0), I) + \int_{q_0}^{q} p\,dx \qquad (11.18)$$

where $p(x, E) = \sqrt{2m(E - V(x))}$. Any such W is a solution of the HJ equation for some E as we check: differentiating the integral, $\frac{\partial W}{\partial q} = p = \sqrt{2m(E - V(q))}$ so that the time-independent HJ equation is satisfied. These solutions of HJ are parametrized by a 'constant of integration' $W(q(t_0), I)$ which can be an arbitrary function of the action variable, since it drops out of $\frac{\partial W}{\partial q}$. However, $W(q(t_0), I)$ *does* affect the dependence of W on I, and through this, it affects the angle variable $\theta = \frac{\partial W}{\partial I}$. In particular, we see that there are many sets of angle-action variables for the same system, obtained through different choices of the constant of integration.

The second term $\int_{q_0}^{q} p\,dx$ in (11.18) is the Euler-Maupertuis action. It depends on q via the upper limit of integration, while the dependence on I is through p:

$$p(x, I) = \sqrt{2m\,[E(I) - V(x)]}. \qquad (11.19)$$

For one degree of freedom, E must be a function of I as there is only one independent conserved quantity. More generally, E is a function of the action variables $E = K(I) = H(q, p)$ since the Hamiltonian in the new variables depends only on the action variables.

Remark. Alternatively, we could have used a generating function of type 1. If we use $F_1(q, \theta)$ instead of $W(q, I)$, then the HJ equation still reads $H(q, \frac{\partial F_1(q,\theta)}{\partial q}) = E$. Now, both q and θ depend on time and $\dot{F}_1 = (F_1)_q \dot{q} + (F_1)_\theta \dot{\theta} = p\dot{q} - I\dot{\theta}$. So unlike $\dot{W} = p\dot{q}$ (11.17), $\dot{F}_1$ involves two terms. Here, subscripts q and θ denote partial derivatives. The condition that I and θ be angle-action variables is imposed by requiring that both I and $\dot{\theta} \equiv \omega$ be constants. We could then integrate and find F_1 as we found W in (11.18), but with the extra term coming from $-I\dot{\theta}$. □

11.3 Generating function for CT to angle-action variables for linear oscillator

For the harmonic oscillator, we already found angle-action variables. We now seek a generating function from the original to angle-action variables:

$$(q, p) \quad \text{to} \quad I = \frac{E}{\omega} \quad \text{and} \quad \theta = \arctan\left[\frac{qm\omega}{p}\right]. \qquad (11.20)$$

A generating function for the CT to angle-action variables is provided by Hamilton's characteristic function $W(q, I)$ (11.18), which is a solution of the HJ equation:

$$W(q, I) = \int_0^q p\,dx = \int_0^q \sqrt{2m(I\omega - V(x))}\,dx \qquad (11.21)$$

where $\omega^2 = k/m$ and $V(x) = \frac{1}{2}kx^2$. We fixed the constant of integration by the convenient choice $W(0, I) = 0$. We evaluate the integral after rescaling variables[6]

$$\begin{aligned} W(q, I) &= 2I \int_0^{q\kappa} \sqrt{1-y^2}\, dy = I \left[q\kappa\sqrt{1-\kappa^2 q^2} + \arcsin{(q\kappa)} \right] \\ &= \frac{q}{2}\sqrt{2m\left(I\omega - \frac{1}{2}kq^2\right)} + I \arcsin\left(q\sqrt{\frac{k}{2I\omega}}\right). \end{aligned} \tag{11.22}$$

Pleasantly, this generating function takes a simpler form when expressed in terms of the old coordinate and the new coordinate (see Prob. 11.3):

$$F_1(q, \theta) = \frac{1}{2} m\omega q^2 \cot\theta. \tag{11.23}$$

The structure of this formula for F_1 could have been anticipated by dimensional analysis. The only dimensional quantities that F_1 (with dimensions of action) can depend on are m, ω and q and there is only one combination with dimensions of action: $m\omega q^2$. It follows that $F_1 = m\omega q^2 \times f_1(\theta)$ where $f_1(\theta)$ is a dimensionless function of θ. We show in Prob. 11.3 that $f_1 = \frac{1}{2}\cot\theta$. On the other hand, $W_1(q, I)$ (also with dimensions of action) can depend on m, ω, q *and* I, which allows for more possibilities in (11.22), see Prob. 11.2.

11.4 Angle-action variables for systems with one degree of freedom

Based on our experience with the harmonic oscillator, we briefly comment on a passage to angle-action variables for a system with one degree of freedom and conserved Hamiltonian of the form

$$H(q, p) = \frac{p^2}{2m} + V(q). \tag{11.24}$$

We will suppose that $V(q)$ is such that all the phase space trajectories are bounded and periodic in time as for $V(q) = \frac{1}{2}kq^2 + \alpha q^4$ with $k, \alpha > 0$. Further, assume that for a given energy, there is a unique periodic trajectory in phase space[7]. Then we *define* the action variable as the area enclosed by that phase trajectory:

$$I(E) = \frac{1}{2\pi}\oint p(E, q)\, dq = \frac{1}{2\pi}\oint \sqrt{2m\,(E - V(q))}\, dq. \tag{11.25}$$

Evaluating this integral and inverting the resulting expression, we get a formula for E as a function of I. As before, we look for a generating function of the 2^{nd} kind for the transformation to angle-action variables. We do this by solving the HJ equation via (11.18) with a convenient choice of constant of integration (set to zero below)

$$W(q, I) = \int_0^q p(E(I), x)\, dx = \int_0^q \sqrt{2m\,(E(I) - V(x))}\, dx. \tag{11.26}$$

---

[6] Use $\int \sqrt{1-y^2}\, dy = \frac{1}{2}\left(y\sqrt{1-y^2} + \arcsin y\right)$ and $y = \kappa x$ where $\kappa = \sqrt{k/2I\omega}$.

[7] There are potentials such as $V = -q^2 + q^4$ for which there may be more than one phase trajectory for a given energy. Then the action $I(E)$ is a multivalued function of energy.

The angle variable is *defined* as

$$\theta = \frac{\partial W}{\partial I} = E'(I) \int_0^q \frac{dx}{\sqrt{(2/m)(E(I)-V(x))}} = E'(I) T_I(0 \to q). \qquad (11.27)$$

Where $T_I(0 \to q)$ is the time taken for the trajectory with energy $E(I)$ to go from $x = 0$ to $x = q$. Moreover, $p = \frac{\partial W}{\partial q}$. By virtue of having a generating function, we are guaranteed that $\{\theta, I\} = 1$, i.e., they are canonically conjugate. Moreover, since $H = E(I) = K(I)$ is a function of I alone, θ is cyclic, I is conserved, and θ is linear in time. Thus, we have a way of identifying angle-action variables for such a system with one degree of freedom (see Sect. 11.5* and Sect. 15.4.3* for examples). There is a generalization of this method to certain systems with more degrees of freedom. It is the subject of the Liouville-Arnold theorem of Sect. 11.7* and Sect. 11.8*.

11.5* Angle-action variables for libration of the simple pendulum

Let us obtain angle-action variables (Θ, I) for the simple pendulum of Sect. 7.3* with Hamiltonian $H = \frac{p_\theta^2}{2ml^2} + mgl(1 - \cos\theta)$ and canonical variables with PB $\{\theta, p_\theta\} = 1$ and angular frequency $\omega = \sqrt{g/l}$. We will often abbreviate $p \equiv p_\theta$ and will restrict to the region of phase space inside the separatrix (see Fig. 7.3) where we have libration, i.e., $E < 2mgl$. The action variable (11.25) may be written as twice the integral between the turning points $\mp\theta_{\max} = \mp \arccos(1-\epsilon)$:

$$\begin{aligned} I(E) &= \frac{1}{2\pi} \oint p\, d\theta = \frac{\sqrt{2ml^2}}{2\pi} 2 \int_{-\theta_{\max}}^{\theta_{\max}} \sqrt{E - mgl(1-\cos\theta)}\, d\theta \\ &= \frac{\sqrt{2} m\omega l^2}{\pi} \int_{-\theta_{\max}}^{\theta_{\max}} \sqrt{\epsilon - (1-\cos\theta)}\, d\theta \end{aligned} \qquad (11.28)$$

where $\epsilon = E/mgl$. This implicitly expresses the energy E as a function of the action I. The integral can be expressed in terms of complete elliptic integrals of the first two kinds $K(k)$ (7.25) and $E(k) = \int_0^{\pi/2} \sqrt{1 - k^2 \sin^2\theta}\, d\theta$ [48]:

$$I(\epsilon) = (8m\omega l^2/\pi) \left[E(k) - (1-k^2)K(k)\right] \quad \text{where} \quad k = \sqrt{\epsilon/2}. \qquad (11.29)$$

As we expect from its interpretation as the area enclosed by the energy E orbit, the action variable is a monotonically increasing function of ϵ. In fact, plotting it shows that $I(\epsilon) \approx m\omega l^2 \epsilon$ for $0 \le \epsilon \le 1$. Hamilton's characteristic function $W(q, I)$ that generates the CT to angle-action variables is an incomplete elliptic integral:

$$\begin{aligned} W(q,I) &= \int_{\theta_0}^{\theta} p(\theta') d\theta' = \int_{\theta_0}^{\theta} \sqrt{(2ml^2)(E - mgl(1-\cos\theta))}\, d\theta \\ &= \sqrt{2} m\omega l^2 \int_{\theta_0}^{\theta} \sqrt{\epsilon - (1-\cos\theta)}\, d\theta. \end{aligned} \qquad (11.30)$$

If we evaluate this integral explicitly, then we could find the angle variable by differentiation $\Theta = \frac{\partial W}{\partial I}$ and $p = \frac{\partial W}{\partial \theta}$. However, there is another way of proceeding (see

Eq. (11.13)) that exploits our formula (7.30) for the librational time period $T(E)$ of a pendulum. Indeed, we have

$$\dot{\Theta} = \frac{dE}{dI} = \left(\frac{dI}{dE}\right)^{-1} = \frac{2\pi}{T(E)} = \frac{\pi\omega}{2K(k)} \quad \text{where} \quad k = \sqrt{\frac{E}{2mgl}} \tag{11.31}$$

and $K(k)$ is the complete elliptic integral of the first kind. Since the elliptic modulus k is a constant, the angle variable Θ varies linearly in time:

$$\Theta(t) = \frac{\pi\omega t}{2K(k)} + \Theta(0). \tag{11.32}$$

We will work with the initial condition $\Theta(0) = 0$ for simplicity. To specify the canonical transformation, let us now express the old variables θ, p_θ in terms of the new ones Θ, I. Recall from (7.29) that the librational trajectory with initial condition $\theta(0) = 0$ is given by $\theta(t) = 2\arcsin[k\,\mathrm{sn}(\omega t, k)]$. Substituting for t in terms of $\Theta(t)$ we get (note that the initial conditions for θ and Θ are consistent)

$$\theta(t) = 2\arcsin\left[k\,\mathrm{sn}\left(\frac{2K(k)\Theta(t)}{\pi}, k\right)\right]. \tag{11.33}$$

The old momentum is given by $p_\theta^2 = 2ml^2(E - mgl(1-\cos\theta))$. Show that it can be expressed as

$$p_\theta(t) = 2ml^2\omega k\,\mathrm{cn}\left(\frac{2K(k)\Theta(t)}{\pi}, k\right). \tag{11.34}$$

The last two equations give the old variables θ, p_θ in terms of the new angle Θ and action I, thus effectively specifying the canonical transformation (see Prob. 11.5).

11.6* Bohr-Sommerfeld quantization rule

Experimental measurements of emission and absorption frequencies of light from gases indicated the presence of discrete or line spectra. Understanding this 'quantization' of variables that were classically allowed to take a continuous range of values was one of the early challenges in the development of the quantum theory (well before the formulation of Heisenberg's matrix mechanics or Schrödinger's wave equation). The formula $E = I\omega$ (11.9) for the simple harmonic oscillator is a classical precursor of the quantum mechanical formula for its energy levels $E = \hbar(n + \frac{1}{2})\omega$ where $h = 2\pi\hbar$ is Planck's unit of action and $n = 0, 1, 2, \ldots$. Indeed, Ehrenfest proposed that it is the action variables of classical systems that may take discrete values (especially for bound states) in the quantum theory. A quantity that takes discrete values in the quantum theory (such as the number of nodes of a bound state wave function), cannot change under small slow perturbations[8] or continuous time evolution. He asserted that classical quantities that were 'ripe' for quantization should not only be conserved under Hamiltonian time evolution, but also be unchanged under some slow (i.e., adiabatic) perturbations of the system. It was found that the action variable $(1/2\pi)\oint p dq$ (11.25) is an *adiabatic invariant* of the classical system. If the spring constant is increased slowly, the energy of oscillations increases, but the action E/ω remains unchanged. These ideas are implemented in the semiclassical Bohr-Sommerfeld quantization rule $\oint p dq = nh$ for large integers $n \gg 1$.

---

[8] For instance, if we increase the length l of a 1d infinite potential well slowly, the energy of the n^{th} stationary state $E_n \propto n^2/l^2$ changes, but the number of nodes of the wave function does not.

To see where this quantization condition comes from, we restrict to a system with one degree of freedom for which angle-action variables θ, I are available. Suppose the original Hamiltonian $H(q,p)$ has been expressed in terms of the action variable $H = H(I)$ where $I = \frac{1}{2\pi}\oint p dq$. To pass to the quantum theory, we replace the time-independent HJ equation $H(I) = E$ by the time-independent Schrödinger equation $H(I)\psi = E\psi$ for the wave function $\psi(\theta)$. In the Schrödinger equation, I is 'represented' by the differential operator $-i\hbar\frac{\partial}{\partial\theta}$ leading to the eigenvalue problem

$$H\left(-i\hbar\frac{\partial}{\partial\theta}\right)\psi(\theta) = E\psi(\theta). \tag{11.35}$$

Here $H(I) = \omega I$ for the harmonic oscillator, but could be a nonlinear function of I for other systems which admit angle-action variables, such as the simple pendulum of Sect. 11.5*. Plane waves $\psi(\theta) = e^{iP\theta/\hbar}$ are solutions provided $H(P) = E$. Since classically, $H(I) = E$, we take $P = I$. What is more, if θ is an angle variable defined modulo 2π, then requiring the wave function to be singlevalued,

$$\psi(0) = \psi(2\pi) \quad \Rightarrow \quad e^{2\pi I/\hbar} = 1. \tag{11.36}$$

This leads to the Bohr-Sommerfeld quantization condition

$$I_n = \frac{1}{2\pi}\oint p dq = n\hbar, \quad \text{where } n \text{ is an integer.} \tag{11.37}$$

Thus, the quantum mechanical energy levels in the Bohr-Sommerfeld semiclassical treatment are given by $E_n = H(I_n) = H(n\hbar)$.

Harmonic oscillator. For the harmonic oscillator, $H(I) = \omega I$ (11.9) leading to the Bohr-Sommerfeld spectrum $E_n = n\hbar\omega$, which approaches the exact spectrum $\hbar\omega(n + \frac{1}{2})$ when n is a large integer.

Kepler problem. The Kepler problem for the reduced mass m (see Sect. 2.2) has three degrees of freedom. However, the square of angular momentum $\boldsymbol{L}^2 = l^2$ is conserved, so in spherical polar coordinates, the Hamiltonian [see (2.20) and (2.21)] $H = p_r^2/2m + V_{\text{eff}}$ where $V_{\text{eff}}(r) = l^2/2mr^2 - \alpha/r$, reduces to that of a system with one (radial) degree of freedom. The corresponding action variable following from (11.25) is

$$I = \frac{1}{\pi}\int_{r_-}^{r_+} \sqrt{2m\left(E - l^2/2mr^2 + \alpha/r\right)}\, dr, \tag{11.38}$$

where $0 < r_- < r_+$ are the radial turning points for bound ($E < 0$) trajectories, determined by $E = V_{\text{eff}}(r_\pm)$. Upon evaluating the integral (see Prob. 11.4), one gets $I = -l + \alpha/\sqrt{-2E/m}$, leading to the expression for the Hamiltonian $H(l, I) = -m\alpha^2/2(I + l)^2$. If we impose the Bohr-Sommerfeld semiclassical quantization condition (11.37), then both I and l (see Sect. 2.5*) must be integer multiples of $\hbar$. Denoting $(l + I)^2 = n^2\hbar^2$ for a 'principal quantum number' n, we recover the bound state spectrum (2.44) of the Hydrogen atom upon taking $\alpha = e^2/4\pi\epsilon_0$. Max Born used angle-action variables to find the spectrum of the Hydrogen atom.

11.7* Liouville integrability and KAM tori

The harmonic oscillator, simple pendulum and Kepler problem furnish examples of systems that are completely integrable or Liouville integrable. In general, a Hamiltonian system is said to be Liouville integrable if a transformation to angle-action variables can be found. As observed in (11.1), it is straightforward to write down the solution to the EOM in angle-action variables: $\theta^i(t) = \theta^i(0) + \omega^i t$ and $I_i(t) = I_i(0)$ where $\omega^i = \frac{\partial H}{\partial I_i}$. For a system with n degrees of freedom, a theorem[9] of Liouville and Arnold (see Sect. 11.8*) asserts that a transformation to angle-action variables can be found if the system admits n independent conserved quantities $F_1, \ldots, F_n$ in involution[10] (i.e., whose pairwise Poisson brackets vanish $\{F_i, F_j\} = 0$ for all $1 \le i, j \le n$).

The harmonic oscillator and simple pendulum, by virtue of being conservative (Hamiltonian) systems with just one degree of freedom, are automatically Liouville integrable with $F_1 = H$, the Hamiltonian. The Kepler problem with 3 degrees of freedom is also Liouville integrable: it has $n = 3$ conserved quantities in involution. As mentioned in Sect. 3.24*, these may be chosen as H, L_z, A_z or $H, L_z, \boldsymbol{L}^2$, etc.

When a system admits n conserved quantities in involution, the connected components of the common level sets of the conserved quantities F_i (when they are bounded) are a family of n-dimensional *invariant tori*. These tori typically foliate[11] the phase space. Recall that an n-dimensional torus is a Cartesian product of n circles $S^1 \times \cdots \times S^1$. For instance, the harmonic oscillator has one independent conserved quantity, the energy ($F_1 = H$), and its level sets are a family of concentric ellipses (deformable into circles) that foliate the phase plane as displayed in Fig. 6.1a. As with the harmonic oscillator, trajectories stay on the torus they begin on. The trajectory $I_i = I_i(0)$, $\theta^i = \theta^i(0) + \omega^i t$ is periodic or quasiperiodic according as the frequencies ω^i are commensurate or not (see Footnote 3 of Chap. 8). For instance, for $n = 2$, each torus has a fixed pair of associated frequencies ω^1, ω^2. If ω^1/ω^2 or ω^2/ω^1 is rational, then all trajectories on that torus are periodic (and quasiperiodic as in Fig. 10.1 if the period ratio is irrational). Interestingly, to solve the equations of motion for a system with n degrees of freedom via angle-action variables, we only need n conserved quantities. This is far fewer than the $2n-1$ conserved quantities that are required to determine the trajectory through the geometric constraints they impose on phase space (see Sect. 2.5*). Evidently, the requirement that the conserved quantities Poisson commute is a very strong condition, which allows us to solve Hamilton's equations.

---

[9] The converse is obvious. If there is a transformation to angle-action variables, then the action variables are automatically a set of n independent conserved quantities in involution.

[10] In quantum mechanics, conserved quantities in involution correspond to observables that are simultaneously measurable, they are represented by Hermitian operators that commute.

[11] Almost every point on phase space lies on precisely one such torus. A foliation of a manifold is like the layering of an onion. The tori are invariant in the sense that a trajectory that begins on a torus remains on that torus.

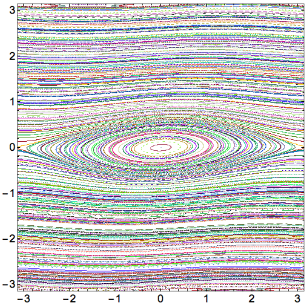

Figure 11.2: 1d KAM circles in the Chirikov-Taylor standard map of Sect. 15.1.2 on the θ-p phase torus [top-bottom and left-right edges identified] for perturbation parameter $\epsilon = \kappa = 0.1$. When $\kappa = 0$, all trajectories lie along horizontal circles. See Fig. 15.3 for further details.

KAM theorem: small departures from integrability. The most famous result on the behavior of Hamiltonian systems that are small departures from integrable systems is the KAM theorem [2, 65, 99, 106, 116] on the persistence of quasiperiodic motion. It was conjectured by A N Kolmogorov (1954) and eventually proved by V I Arnold (1963) and J Moser (1973). Here, one considers a system with Hamiltonian $H = H_0(I) + \epsilon H_1(\theta, I)$ that is a small perturbation of an integrable Hamiltonian H_0. For $j = 1, \cdots, n$, (θ^j, I_j) are angle-action variables for H_0. Aside from some technicalities (see Footnote 16), the phase space is foliated by invariant tori of H_0 that are labelled by values of the action variables. When $\epsilon = 0$, trajectories are confined to these invariant tori with time evolution being governed by $\dot{\theta}^j = \omega^j = \frac{\partial H_0}{\partial I_j}$. Now, a torus is called resonant if the associated frequencies are linearly dependent over the integers, i.e., $\boldsymbol{m} \cdot \boldsymbol{\omega} = \sum_j m_j \omega^j = 0$ for some integers m_j, not all zero. The resonant tori (which form a countable but dense set in the phase space) typically do not survive even for arbitrarily small ϵ. The main result of the KAM theorem is that subject to suitable hypotheses[12], most[13] tori survive (in a continuously deformed manner), for sufficiently small perturbations ϵ. In particular, the highly nonresonant tori[14] defined by frequencies for which $\boldsymbol{m} \cdot \boldsymbol{\omega}$ is sufficiently far from zero for all integer vectors $\boldsymbol{m}$, survive for small enough ϵ. An invariant torus T_0 of H_0 with frequency vector $\boldsymbol{\omega}_0$ is said to survive the perturbation if for each sufficiently small $\epsilon > 0$, there is a torus T_ϵ of $H_0 + \epsilon H_1$ with frequency vector $\boldsymbol{\omega}(\epsilon) = k(\epsilon)\boldsymbol{\omega}_0$ such that T_ϵ approaches T_0 and $k(\epsilon) \to 1$ continuously as $\epsilon \to 0$. Thus, although conserved quantities other than H typically cease to exist for $\epsilon > 0$, the dynamics continues to be relatively regular for small ϵ due to the survival of these invariant tori. The survival and gradual destruction of invariant tori as we move away from an integrable limit is illustrated in Fig. 11.2 and Figs. 15.3 and 15.16.

---

[12] For instance, the frequencies ω^j are assumed nondegenerate: $\det[\partial \omega^j / \partial I_k] \neq 0$. Thus, the frequencies depend on the torus being considered and can be used to label tori of H_0.

[13] By *most* we mean all except for a set of Lebesgue measure zero in the space of frequencies.

[14] A torus with frequencies ω^j is called highly nonresonant if it satisfies the diophantine condition $|\boldsymbol{m} \cdot \boldsymbol{\omega}| > K(\boldsymbol{\omega}) |\boldsymbol{m}|^{-(n+1)}$ for all n-tuples of integers $\boldsymbol{m}$ and some constant $K(\boldsymbol{\omega}) > 0$.

11.8* Liouville-Arnold theorem

This section is devoted to a statement and proof of the Liouville-Arnold theorem. Consider a system with Hamiltonian H and phase space $M = \mathbb{R}^{2n}$ with coordinates q^i and momenta p_j satisfying canonical PBs

$$\{q^i, p_j\} = \delta^i_j, \quad \{q^i, q^j\} = 0 \quad \text{and} \quad \{p_i, p_j\} = 0. \tag{11.39}$$

Now, suppose the system admits n independent conserved quantities $F_i(q,p)$ with the Hamiltonian being expressible as a function of them. Moreover, suppose the conserved quantities are in involution (i.e., they Poisson commute):

$$\dot{F}_i = 0 \quad \text{and} \quad \{F_i, F_j\} = 0 \quad \text{for} \quad i,j = 1,2,\ldots,n, \tag{11.40}$$

and that their common level sets $M_f = \{(q,p) | F_i = f_i \text{ for } 1 \leq i \leq n\} \subset \mathbb{R}^{2n}$ foliate the phase space. These common level sets are of course invariant under time evolution. Suppose further that M_f is compact[15] and connected. Then each M_f may be shown to be diffeomorphic to an n-dimensional ‘invariant’ torus T^n [2]. Under these hypotheses[16], the Liouville-Arnold theorem asserts that there is a canonical transformation from (q^i, p_j) to angle-action variables (θ^i, I_j) with the property that the Hamiltonian is a function of the action variables alone, i.e., $H = H(I_1, I_2, \cdots, I_n)$.

Outline of the proof. Although the F_i are conserved and in involution, they are not in general a natural choice for the action variables since it is not clear how to find canonically conjugate angle variables that evolve linearly in time. On the other hand, the harmonic oscillator of Sect. 11.1 with $n = 1$ suggests how one may proceed. In this case, energy $E = p^2/2m + m\omega^2 q^2/2$ is the only conserved quantity and $F_1 = E$.

---

[15] Level sets of conserved quantities can fail to be compact. For instance, consider a particle moving on the real line subject to the potential $V(q) = 1/(a^2 + q^2)$. Then the Hamiltonian $H = p^2/2m + V(q)$ is conserved, but for $H > 0$, its level sets are unbounded since the particle can escape to $q = \pm\infty$.

[16] Often, the integrals of motion F_i may not be independent on the whole phase space and angle-action variables may not exist everywhere. However, it is guaranteed that angle-action variables exist in some open neighborhood of any point (q,p) where the map $M \to \mathbb{R}^n$ taking $(q,p) \mapsto (F_1, F_2, \cdots, F_n)$ is regular. Here, regular means the Jacobian matrix of this map is of maximal rank n. The transformation to angle-action variables then defines a diffeomorphism from the open neighborhood to $T^n \times \mathbb{R}^n$ where T^n is the n-torus parametrized by the angles. Typically, at places where the F_i fail to be independent (i.e., where the rank of the above Jacobian drops), the invariant tori degenerate (drop in dimension or develop singularities). For instance, on a typical 4d symplectic leaf of the Rajeev-Ranken model [75], one has two generically independent conserved quantities in involution. A generic point on the leaf lies on an invariant 2-torus. However, at places where the conserved quantities develop relations, the 2-tori degenerate to horn tori, circles and points.

Also, $E = f_1$ is an ellipse (1d torus T^1) and the action variable is defined as (11.11)

$$I = \frac{1}{2\pi}\oint_{T_1} p dq, \quad \text{which turns out to equal} \quad \frac{E}{\omega}. \tag{11.41}$$

For n degrees of freedom, M_f is an n-dimensional torus $S^1 \times \cdots \times S^1$. So it has n independent noncontractible cycles Γ_k for $k = 1, 2, \cdots, n$. Fig. B.4 shows a 2-torus with two noncontractible cycles indicated. It is thus natural to define

$$I_k = \frac{1}{2\pi}\oint_{\Gamma_k} p_i dq^i. \tag{11.42}$$

On M_f, the momenta p_i are regarded as functions of the q's and f's. Indeed, assuming that the Jacobian matrix $\frac{\partial F_j}{\partial p_k}$ is nonsingular, we may express $p_i = p_i(q, f)$ by solving the equations $F_j(p, q) = f_j$. Now, we will show that I_k are unchanged under continuous deformations of the closed curves Γ_k on M_f, and therefore depend only on the values of the conserved quantities F defining the torus M_f. In particular, we will show that the line integral of the canonical Liouville 1-form $\alpha = p_i dq^i$ around a contractible closed contour on M_f vanishes. To show this, we differentiate the equation $F_i(q, p(q, f)) = f_i$ with respect to q^j and contract with $\frac{\partial F_m}{\partial p_j}$:

$$\frac{\partial F_i}{\partial q^j} + \frac{\partial F_i}{\partial p_k}\frac{\partial p_k}{\partial q^j} = 0 \quad \forall \; i, j \quad \Rightarrow \quad \frac{\partial F_m}{\partial p_j}\frac{\partial F_i}{\partial q^j} + \frac{\partial F_m}{\partial p_j}\frac{\partial F_i}{\partial p_k}\frac{\partial p_k}{\partial q^j} = 0 \quad \forall \; i, m. \tag{11.43}$$

Antisymmetrizing in the indices i and m gives

$$\{F_i, F_m\} + \sum_{j,k}\left(\frac{\partial F_m}{\partial p_j}\frac{\partial F_i}{\partial p_k}\frac{\partial p_k}{\partial q^j} - \frac{\partial F_i}{\partial p_j}\frac{\partial F_m}{\partial p_k}\frac{\partial p_k}{\partial q^j}\right) = 0. \tag{11.44}$$

The PB vanishes as the F's are in involution. Relabeling indices and using invertibility of $\frac{\partial F_i}{\partial p_k}$, we get

$$\sum_{j,k}\frac{\partial F_i}{\partial p_k}\frac{\partial F_m}{\partial p_j}\left(\frac{\partial p_k}{\partial q^j} - \frac{\partial p_j}{\partial q^k}\right) = 0 \quad \text{or} \quad \frac{\partial p_k}{\partial q^j} - \frac{\partial p_j}{\partial q^k} = 0. \tag{11.45}$$

The latter condition says that if we view p_k as the components of the canonical 1-form $\alpha = p_k dq^k$ on the torus M_f, then it is closed: $d\alpha = 0$. Stokes' theorem $\int_S d\alpha = \oint_{\partial S} \alpha$ (B.55) [where S is a surface whose boundary is ∂S] then implies that $\oint p_j dq^j$ vanishes around any contractible closed curve on the torus. More generally, if $\tilde\Gamma_k$ is a curve obtained by continuously deforming the cycle Γ_k and S is the strip whose boundary is the union of Γ_k and $\tilde\Gamma_k$ traversed backwards, then by Stokes' theorem,

$$\oint_{\Gamma_k} p_j dq^j - \oint_{\tilde\Gamma_k} p_j dq^j = \int_S \left(\frac{\partial p_i}{\partial q^j} - \frac{\partial p_j}{\partial q^i}\right) dq^j \wedge dq^i = 0. \tag{11.46}$$

Thus, I_k are well-defined functions of the F's: they are unchanged under continuous deformations of the n independent cycles Γ_k. As a consequence, they are conserved.

What is more, they are in involution:

$$\{I_i, I_j\} = \frac{\partial I_i}{\partial F_r}\frac{\partial F_r}{\partial q^k}\frac{\partial I_j}{\partial F_s}\frac{\partial F_s}{\partial p_k} - \frac{\partial I_i}{\partial F_r}\frac{\partial F_r}{\partial p_k}\frac{\partial I_j}{\partial F_s}\frac{\partial F_s}{\partial q^k} = \frac{\partial I_i}{\partial F_r}\frac{\partial I_j}{\partial F_s}\{F_r, F_s\} = 0. \tag{11.47}$$

Thus, I_k are candidate action variables. Can we find canonically conjugate variables that qualify as angle variables? We will define a set of variables θ^k conjugate to I_k by specifying a canonical transformation from $(q,p) \to (\theta, I)$. Inspired by what works for the harmonic oscillator, we pick an invariant torus defined by the values f_i of the constants F_i and consider a generating function of the 'second' kind

$$S(q, I) = \int_{q_0}^{q} p_j(q, f)dq^j. \tag{11.48}$$

By changing the invariant torus, the definition of S is extended to the whole phase space. The integral is along a curve on M_f from q_0 to q. Here, we regard p_j as functions of the q's and the f's (which may in turn be regarded as functions of the I's) obtained by solving $F_i(q,p) = f_i$. We have already shown that the canonical Liouville 1-form $\alpha = p_j dq^j$ is closed when restricted to M_f. This implies that $S = \int_{q_0}^{q} \alpha$ is invariant under continuous deformations of the path from q_0 to q. Thus, S may be regarded as a function of the endpoints. Changing the base point $q_0 \to q_0'$ will add to S a 'constant' $\int_{q_0}^{q_0'} p dq$ that depends on the I's. The equations of transformation for such a generating function of the second kind express the new coordinates and old momenta as

$$\theta^i = \frac{\partial S}{\partial I_i} \quad \text{and} \quad p_i = \frac{\partial S}{\partial q^i}. \tag{11.49}$$

The proposed angle variables θ^i depend on the base point, so they are far from unique. Having a generating function ensures that the transformation is canonical[17], i.e., the new variables are canonical:

$$\{\theta^j, \theta^k\} = 0, \quad \{I_j, I_k\} = 0 \quad \text{and} \quad \{\theta^j, I_k\} = \delta^j_k. \tag{11.50}$$

Moreover, since H was a function of the F's, it is a function of the action variables alone, $H = H(I_1, \cdots, I_n)$. In angle-action variables, Hamilton's equations become

$$\dot{I}_i = -\frac{\partial H}{\partial \theta^i} = 0 \quad \text{and} \quad \dot{\theta}^i = \frac{\partial H}{\partial I_i} \equiv \Omega^i(I). \tag{11.51}$$

Thus, the θ^i evolve linearly in time $\theta^k(t) = \Omega^k(I)t + \theta^k(0)$ while the action variables are conserved. The former generalize the variable $\theta = \arctan(m\omega q/p)$ of the harmonic oscillator, which is the angle around an invariant ellipse $(1/2)(p^2/m +$

---

[17] This was shown in Sect. 10.10. Another way to see this is to compute the exterior derivative $dS(q,I) = \frac{\partial S}{\partial q^i}dq^i + \frac{\partial S}{\partial I_i}dI_i = p_i dq^i + \theta^i dI_i$. Taking another exterior derivative, $d^2 S = 0$ or in other words, $\sum_i dp_i \wedge dq^i + \sum_j d\theta^j \wedge dI_j = 0$. Thus, the transformation preserves the form of the symplectic form: $\omega = dq^i \wedge dp_i = d\theta^j \wedge dI_j$, which means it is a symplectic diffeomorphism or canonical transformation.

$m\omega^2x^2) = E$. In fact, we will show that $\oint_{\Gamma_k} d\theta^i = 2\pi\delta^i_k$, so that θ^k may be viewed as the angle around the k^{th} cycle of an invariant torus. Indeed, using (11.42), (11.49) and observing that $dI_j = 0$ on M_f,

$$\oint_{\Gamma_k} d\theta^i = \frac{\partial}{\partial I_i}\oint_{\Gamma_k} dS(q,I) = \frac{\partial}{\partial I_i}\oint_{\Gamma_k}\left(p_i dq^i + \theta^j dI_j\right) = 2\pi\frac{\partial I_k}{\partial I_i} = 2\pi\delta^i_k. \tag{11.52}$$

Generating function and Poincaré's lemma. Since (q,p) and (θ, I) are both canonical coordinates on phase space, the symplectic form may be expressed in terms of either coordinate system: $dq^i \wedge dp_i = d\theta^i \wedge dI_i$. In other words, the difference between the two Liouville 1-forms must be closed: $d(p_i dq^i - I_i d\theta^i) = 0$. In his lectures on celestial mechanics, Poincaré developed the lemma that asserts that a closed form is locally exact. Thus, locally, there must be a function S such that $dS = pdq - Id\theta$. The generating function to angle-action variables is a Legendre transform of this S.

Remark on quasiperiodicity. The frequencies Ω^i vary from torus to torus, as they depend on the values of F_j or I_j. If the frequencies Ω^i on a given torus are commensurate (they have a least common finite integer multiple), then trajectories on that invariant torus are closed and the motion periodic. Generically, the frequencies are not commensurate and the trajectories on an invariant torus are not periodic, but rather quasiperiodic: a superposition of several incommensurate periodic motions. A quasiperiodic trajectory is not closed but dense on the torus: if we wait sufficiently long, it will come arbitrarily close to any given point on the torus without ever crossing itself (see Fig. 10.1). In this case, the dynamics is ergodic (time and ensemble averages agree) on the torus (though not on the full phase space). However, the time evolution is not sensitive to initial conditions and certainly not chaotic. □

Remark on commuting flows. Since the conserved quantities F_j are in involution, they generate n commuting flows. What does this mean? Each F_j generates a flow with a corresponding time t_j. The evolution of any observable, g under the flow generated by F_j is given by $\frac{dg}{dt_j} = \{g, F_j\}$. Since $\{F_i, F_j\} = 0$, all the F_is are conserved quantities for each of the flows. Thus, by sequentially choosing $F_1, F_2, \cdots$ as the Hamiltonian, we get a hierarchy of Liouville integrable systems. □

Remark on Frobenius theorem for vector fields. Suppose M is a smooth manifold and $V_{(1)}, \cdots V_{(m)}$ are a set of m vector fields on a region $U \subset M$ that form a subalgebra of the space of all vector fields on U, i.e., $[V_{(i)}, V_{(j)}] = \sum_k c^k_{ij} V_{(k)}$ for some functions c^k_{ij} on U. Then, the Frobenius theorem [113] says that the integral curves of these vector fields mesh together to form a family of submanifolds of M. The dimension of each submanifold is the dimension of the vector space spanned by the vector fields and is at most m. Each point of U lies on precisely one such submanifold, provided the dimension of span$(V_{(1)}, \cdots V_{(m)})$ is the same everywhere. The submanifolds fill up (foliate) U and each submanifold is called a leaf of the foliation. In the context of the Liouville-Arnold theorem, M is the $2n$ dimensional phase space, the vector fields V_{F_i} are the canonical vector fields (see Sect. 3.26*) associated to the n conserved quantities $F_1, \cdots, F_n$. Since F_i are independent and in involution, their canonical vector fields commute (3.194) and span an n-dimensional space. Their integral curves mesh together to form a family of n-dimensional submanifolds (the invariant tori M_f) which foliate M. □

11.9* Conserved quantities from a Lax pair

A Lax pair is a scheme for finding conserved quantities for some dynamical systems. The method relies on expressing the equations of motion in Lax form, by which we mean that the equations of motion are equivalent to the Lax equation

$$\dot{L} = [L, A] \equiv LA - AL, \tag{11.53}$$

where L and A are a pair of square matrices whose entries depend on the dynamical variables of the system. Once expressed in Lax form, it is possible to read off constants of motion: for instance, the eigenvalues of L are conserved. The idea goes back to Peter Lax [86] and, as we will learn, may also be viewed as expressing nonlinear equations of motion as compatibility conditions for a pair of auxiliary linear equations to have simultaneous solutions. Unfortunately, the scheme only works for special classes of mechanical systems and there is no general method to determine whether a given system admits a Lax pair or to find one when it does. However, if we are able to find a Lax pair then it usually leads to sufficiently many conserved quantities, which if in involution, would make the system Liouville integrable in the sense of Sect. 11.7*. Our treatment below will broadly follow that in [76] while much more on Lax pairs may be found in [6, 32].

11.9.1* Harmonic oscillator Lax pair

We will introduce the idea of a Lax pair through the example of the simple harmonic oscillator of Sect. 6.1. Since the Lax equation (11.53) is first order in time, we begin with the equations of motion written as a pair of first order ODEs for the displacement from equilibrium and linear momentum: $\dot{x} = p/m$ and $\dot{p} = -m\omega^2 x$. To make the upcoming equations dimensionally consistent, we will rewrite Hamilton's equations as equations for ωx and p/m, both of which have dimensions of velocity:

$$(\omega\dot{x}) = \omega(p/m) \quad \text{and} \quad (\dot{p}/m) = -\omega(\omega x). \tag{11.54}$$

We now seek a pair of matrices L, A such that these equations are equivalent to the Lax equation $\dot{L} = [L, A]$. Notice that the left members of (11.54) are linear in $\omega\dot{x}$ and $\dot{p}/m$. For $\dot{L} = [L, A]$ to share this feature, we shall pick the entries of L to be linear in ωx and p/m. The simplest possibility would be to suppose that L is a 2×2 matrix with real entries. To cut down from four to two independent equations, we will further suppose that L (and consequently $\dot{L}$) is symmetric and traceless. How shall we pick A? Notice from Prob. 11.7 that the commutator of a symmetric and an antisymmetric matrix is symmetric. Thus, it is natural to take A to be antisymmetric (see also Prob. 11.8). We will take A to be a constant matrix since that would ensure that $[L, A]$ is linear in ωx and p/m, just as the right sides of (11.54) are. A choice that does the job is

$$L = \begin{pmatrix} p/m & \omega x \\ \omega x & -p/m \end{pmatrix} \quad \text{and} \quad A = \begin{pmatrix} 0 & \omega/2 \\ -\omega/2 & 0 \end{pmatrix}. \tag{11.55}$$

In Prob. 11.9, we check that the four matrix elements of the Lax equation $\dot{L} = [L, A]$ are the same as Hamilton's equations (11.54) for the harmonic oscillator. Having found a Lax pair, we may use it to find conserved quantities. Before doing that, we observe that a Lax pair is not unique. Given a Lax pair that works, we may (i) add to L a time-independent matrix that commutes with A and (ii) add to A a matrix that commutes with L, without affecting the Lax equation.

11.9.2* Isospectral evolution and conserved quantities

The time evolution of the Lax matrix, governed by $\dot{L} = [L, A]$ is isospectral. For an $n \times n$ Lax matrix, this means that the eigenvalues of L (its spectrum) or equivalently, $\operatorname{tr} L^p$ for $p = 1, 2, \cdots, n$ (see Prob. 11.10) are independent of time.

Conservation of $\operatorname{tr} L^p$. We begin with the Lax equation, take its trace and use the fact that the trace of a commutator (for finite-dimensional matrices) vanishes:

$$L_t = \dot{L} = [L, A] \quad \Rightarrow \quad \operatorname{tr} \dot{L} = \operatorname{tr} [L, A] = 0. \tag{11.56}$$

Since the operations $\frac{d}{dt}$ and tr commute, $\operatorname{tr} L$ (i.e., the sum of its eigenvalues) is independent of time. Next, we compute the time derivative of L^2:

$$(L^2)_t = \dot{L}L + L\dot{L} = [L, A]L + L[L, A] = [L^2, A]. \tag{11.57}$$

Here, we used the Leibniz rule for commutators $[AB, C] = A[B, C] + [A, C]B$. Proceeding by induction, we show that (see Prob. 11.11)

$$(L^p)_t = [L^p, A] \quad \text{for} \quad p = 1, 2, 3 \cdots. \tag{11.58}$$

Taking a trace, we conclude that $\operatorname{tr} L^p$ is conserved for any positive integer p. Though it may seem that we have found an infinite number of conserved quantities, it is worth bearing in mind that there can be at most $2n - 1$ independent conserved quantities for a system with n degrees of freedom. This puts an upper bound on how many of the $\operatorname{tr} L^p$ can be independent.

Example. For the **harmonic oscillator**, the Lax matrix L in 11.55 is traceless. On the other hand, $(m/4) \operatorname{tr} L^2 = \frac{1}{2}(p^2/2m + m\omega^2 x^2)$ is the familiar conserved energy, which is also expressible as $E = -\frac{m}{2} \det L$. As expected, the traces of higher powers of L do not furnish any new conserved quantity, as we verify in Prob. 11.17. □

Conservation of eigenvalues of L. We may directly show that the eigenvalues of $L(t)$ are independent of time. One way to do this is to establish that $L(t)$ and $L(0)$ are similar matrices and to recall that matrices that differ by a similarity transformation have the same eigenvalues (Prob. 11.13). In fact, the solution of the Lax equation (11.53) can be expressed via a similarity transformation $L(t) = S(t)L(0)S^{-1}(t)$ where $S(t)$ is the (fundamental matrix) solution of the ODEs $\dot{S} = -AS$ with $S(0) = I$. In Prob. 11.14, we verify that this $L(t)$ satisfies the Lax equation.

Evolution of eigenvectors of L. The eigenvalues of L are conserved, but what about its eigenvectors? To find out, we differentiate the eigenvalue problem for L in time and use the Lax equation (11.53):

$$L\psi = \lambda\psi \quad \Rightarrow \quad L_t\psi + L\psi_t = \lambda_t\psi + \lambda\psi_t \quad \text{or} \quad (LA - AL)\psi + L\psi_t = \lambda_t\psi + \lambda\psi_t. \tag{11.59}$$

Rearranging and using $L\psi = \lambda\psi$, we get

$$(L-\lambda)A\psi + (L-\lambda)\psi_t = \lambda_t\psi \quad \Leftrightarrow \quad (L-\lambda)(\psi_t + A\psi) = \lambda_t\psi. \tag{11.60}$$

This equation says that if λ is conserved, $\psi_t + A\psi$ must lie in the λ-eigenspace of L. We have already assumed that ψ is an eigenvector of L with eigenvalue λ. So if the λ-eigenspace of L is 1-dimensional[18], then $\psi_t + A\psi$ must be a (possibly time-dependent and complex) multiple β of ψ:

$$\psi_t + A\psi = \beta\psi \quad \text{or} \quad \psi_t = (-A + \beta I)\psi. \tag{11.61}$$

In Prob. 11.15, we will indicate how β can be absorbed into A. Thus, assuming λ is a nondegenerate eigenvalue of L, the time evolution of the corresponding eigenvector is linear and governed by the Lax matrix A.

Lax equation as a compatibility condition. The Lax equation $L_t = [L, A]$ can be thought of as a compatibility condition between two linear equations. This is a useful viewpoint since it allows us to relate the usually nonlinear equations of motion of a system (that admits a Lax representation) to properties of linear equations[19]. To understand this, we reverse our viewpoint and begin with the pair of linear equations for the vector ψ, determined by the Lax pair (L, A):

$$L\psi = \lambda\psi \quad \text{and} \quad \psi_t = -A\psi \quad \text{for a constant } \lambda. \tag{11.62}$$

The first says that ψ is an eigenvector of L with time-independent eigenvalue λ while the second tells how the eigenvector evolves. To see how the Lax equation emerges, we differentiate the eigenvalue problem in time and use the second equation, to verify that for λ to be time-independent, L and A must satisfy the Lax equation $L_t = [L, A]$. Unlike above, here there is no need for λ to be a nondegenerate eigenvalue of L.

11.9.3* Toda chain: Flaschka's variables and a Lax pair

As a second example of a mechanical system with a Lax pair, we consider a chain of identical particles of mass m that interact with their nearest neighbors via nonlinear springs that exert exponential forces when stretched/compressed. This model for a 1d atomic crystal was introduced by Morikazu Toda in 1967. If x_i is the displacement of the i^{th} particle from equilibrium and p_i its momentum, then Newton's equations are

---

[18] Here, we will assume that the eigenvalues of L are nondegenerate. [This is the case for the harmonic oscillator Lax matrix L (11.55) which has, for any $E > 0$, two distinct eigenvalues ($\pm\sqrt{2E/m}$) and 1d eigenspaces (see Prob. 11.9).] However, this assumption is not needed to show that the eigenvalues are conserved, as the earlier similarity transformation approach demonstrates. See also Prob. 11.16 where we assume that L is Hermitian.

[19] When extended from mechanical systems to fields in one spatial dimension, the two 'auxiliary' linear equations allow us to reformulate the Lax pair scheme geometrically in terms of the flatness (zero curvature) of an appropriate space [77].

$$m\dot{x_i} = p_i \quad \text{and} \quad \dot{p_i} = \kappa \left(e^{-(x_i - x_{i-1})} - e^{-(x_{i+1}-x_i)} \right), \tag{11.63}$$

where κ is a force constant. Henceforth, we work in units where $\kappa = m = 1$ and consider an N-particle Toda chain with periodic boundary conditions: $x_{N+i} = x_i$ for $i = 1, 2, \ldots$. In this case, the particles may be viewed as lying on a circle, with $x_i = \theta_i$ being the angular displacement from equilibrium (Fig. 11.3). Flaschka [40] rendered quadratic the exponential nonlinearity in (11.63) by introducing the variables

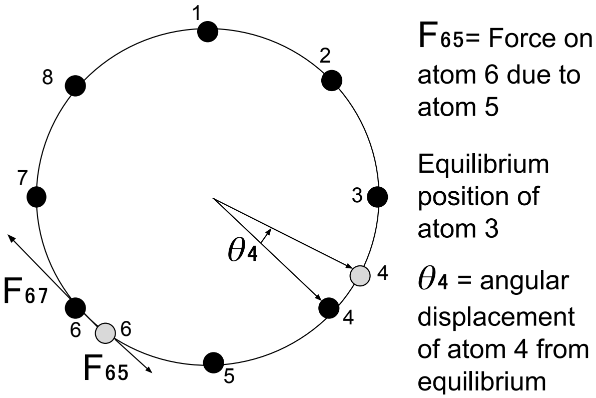
1
2
3
4
4
5
6
6
7
8
F67
F65
θ4
F65= Force on atom 6 due to atom 5
Equilibrium position of atom 3
θ4 = angular displacement of atom 4 from equilibrium

Figure 11.3: 8-particle Toda chain with periodic boundary conditions. Filled dots denote equilibrium positions while hollow dots are displaced positions of particles.

$$a_i = \frac{1}{2} e^{-(x_i - x_{i-1})/2} \quad \text{and} \quad b_i = -\frac{1}{2} p_{i-1}, \tag{11.64}$$

which evolve according to

$$\dot{a_i} = a_i(b_{i+1} - b_i) \quad \text{and} \quad \dot{b_i} = 2(a_i^2 - a_{i-1}^2). \tag{11.65}$$

These equations are equivalent to the Lax equation $\dot{L} = [L, A]$ if we define the essentially tridiagonal matrices

$$L = \begin{pmatrix} b_1 & a_1 & 0 & \cdots & a_N \\ a_1 & b_2 & a_2 & & \\ 0 & a_2 & b_3 & & \\ \vdots & & & \ddots & \\ a_N & & & & b_N \end{pmatrix} \quad \text{and} \quad A = \begin{pmatrix} 0 & -a_1 & 0 & \cdots & a_N \\ a_1 & 0 & -a_2 & \cdots & 0 \\ 0 & a_2 & 0 & \cdots & 0 \\ \vdots & & & & \vdots \\ -a_N & & & & 0 \end{pmatrix}. \tag{11.66}$$

Consequently, $\operatorname{tr} L^n$ for $n = 1, 2, \ldots, N$ or alternatively, the coefficients of the characteristic polynomial $\det(L - \lambda \mathbf{1})$ give us N conserved quantities [56]. The first two may be interpreted in terms of the total momentum and energy of the chain:

$$\operatorname{tr} L = \sum\nolimits_{i=1}^N b_i = -\frac{1}{2} \sum\nolimits_{i=1}^N p_{i-1} = -\frac{P}{2} \quad \text{and}$$

$$\operatorname{tr} L^2 \quad = \quad \sum\nolimits_{i=1}^{N} \left(2a_i^2 + b_i^2\right) = \frac{1}{2} \sum\nolimits_{i=1}^{N} \left(\frac{1}{2} p_i^2 + e^{-(x_i - x_{i-1})}\right) = \frac{E}{2}. \quad (11.67)$$

The reader is encouraged to check by explicit calculation that $\operatorname{tr} L^3$ is also conserved.

11.9.4* Euler-Poinsot top Lax pair: spectral parameter

As a third example, we discuss a Lax pair for the Euler equations for the torque-free rotational motion of a rigid body whose center of mass is held fixed. This will give us an opportunity to introduce the idea of a spectral parameter through an example. Recall from (8.55) that the components of angular momentum[20] $\boldsymbol{S} = (S_1, S_2, S_3)$ with respect to an orthonormal body-fixed frame centered at the CM evolve via the quadratically nonlinear equations $\dot{\boldsymbol{S}} = \boldsymbol{S} \times \boldsymbol{\Omega}$. Here, the angular momentum is related to the angular velocity ($\boldsymbol{S} = \mathcal{I}\boldsymbol{\Omega}$) via the inertia tensor $\mathcal{I}$. These equations are already in Lax form! To see this, we introduce the 3×3 traceless antisymmetric angular momentum and angular velocity matrices S and Ω by contracting with the Levi-Civita symbol of Prob. A.12 and Prob. 3.48:

$$S_{ij} = \epsilon_{ijk} S_k \quad \text{and} \quad \Omega_{ij} = \epsilon_{ijk} \Omega_k. \qquad (11.68)$$

Explicitly,

$$S = \begin{pmatrix} 0 & S_3 & -S_2 \\ -S_3 & 0 & S_1 \\ S_2 & -S_1 & 0 \end{pmatrix} \quad \text{and} \quad \Omega = \begin{pmatrix} 0 & \Omega_3 & -\Omega_2 \\ -\Omega_3 & 0 & \Omega_1 \\ \Omega_2 & -\Omega_1 & 0 \end{pmatrix}. \qquad (11.69)$$

One then verifies (see Prob. 11.20) that the cross product of vectors becomes the negative of the commutator of matrices, so that the Euler equations $\dot{\boldsymbol{S}} = \boldsymbol{S} \times \boldsymbol{\Omega}$ become $\dot{S} = [\Omega, S]$. Comparing with the Lax equation (11.53) we see that $(S, -\Omega)$ furnish a Lax pair for the Euler equations. Though S is traceless, $\operatorname{tr} S^2 = -2(S_1^2 + S_2^2 + S_3^2)$ is proportional to the square of angular momentum, which we recognize as a conserved quantity (in fact a Casimir invariant of the angular momentum Poisson algebra). Sadly, this Lax pair does not give us the other familiar quadratic conserved quantity, namely the rotational kinetic energy, which in a principal axis frame is $E = (1/2)(S_1^2/\mathcal{I}_1 + S_2^2/\mathcal{I}_2 + S_3^2/\mathcal{I}_3)$. This is because the Lax matrix S does not depend on the inertia tensor. Thus, we seek a new Lax pair which will give us both conserved quantities. This is achieved by making our Lax matrices depend on an arbitrary 'spectral parameter' λ that allows us to take a weighted sum of the original Lax matrices $(S, -\Omega)$ with matrices depending on the principal moments of inertia. For this purpose, it is convenient to package the principal moments of inertia in the diagonal matrix

$$\mathcal{J} = \operatorname{diag}(\mathcal{J}_1, \mathcal{J}_2, \mathcal{J}_3) \quad \text{with} \quad \mathcal{J}_1 = (1/2)(\mathcal{I}_2 + \mathcal{I}_3 - \mathcal{I}_1) \qquad (11.70)$$

and cyclic permutations thereof. Trial and error (see [77] for some motivation) and the requirement that the Lax equation $\dot{L} = [L, A]$ hold for any λ iff the Euler equations do, leads to a new Lax pair:

---

[20] We denote the angular momentum vector by $\boldsymbol{S}$ to distinguish it from the Lax matrix L.

$$\begin{aligned} L(\lambda) &= \mathcal{J}^2 + \frac{S}{\lambda} = \begin{pmatrix} \mathcal{J}_1^2 & S_3/\lambda & -S_2/\lambda \\ -S_3/\lambda & \mathcal{J}_2^2 & S_1/\lambda \\ S_2/\lambda & -S_1/\lambda & \mathcal{J}_3^2 \end{pmatrix} \quad \text{and} \\ A(\lambda) &= -(\lambda \mathcal{J} + \Omega) = -\begin{pmatrix} \lambda\mathcal{J}_1 & \Omega_3 & -\Omega_2 \\ -\Omega_3 & \lambda\mathcal{J}_2 & \Omega_1 \\ \Omega_2 & -\Omega_1 & \lambda\mathcal{J}_3 \end{pmatrix}. \end{aligned} \tag{11.71}$$

In Prob. (11.21), we verify that the condition that the Lax equation hold for any value of λ is equivalent to the Euler equations $\dot{S} = [\Omega, S]$. Thus, we have a Lax pair with spectral parameter for the torque-free Euler equations.

We may now use this to find conserved quantities. To begin with, $\operatorname{tr} L = \mathcal{J}_1^2 + \mathcal{J}_1^2 + \mathcal{J}_1^2$ is just a function of the constant principal moments of inertia, so it does not count as a dynamical variable. The traces of the next two powers of L are more interesting. We show in Prob. 11.22 that

$$\operatorname{tr} L^2 = \operatorname{tr} \mathcal{J}^4 - (2/\lambda^2)\boldsymbol{S}^2. \tag{11.72}$$

Since this is conserved for any λ and $\operatorname{tr} \mathcal{J}^4$ is a constant, it follows that the square of angular momentum $\boldsymbol{S}^2$ is conserved. Similarly, it is possible to express $\operatorname{tr} L^3$ as

$$\operatorname{tr} L^3 = \operatorname{tr} \left[\mathcal{J}^6 + \frac{3}{\lambda^2}\mathcal{J}^2 S^2\right] = \operatorname{tr} \mathcal{J}^6 - \frac{3}{\lambda^2}\left(\frac{(\operatorname{tr}\mathcal{I})^2 \boldsymbol{S}^2}{4} - \mathcal{I}_1\mathcal{I}_2\mathcal{I}_3 E\right). \tag{11.73}$$

Combining with the previous result, we deduce that the energy E is also conserved. Traces of higher powers of L cannot furnish more conserved quantities as the 3d angular momentum phase space can allow at most two independent conserved quantities. Thus, our new Lax pair with spectral parameter has allowed us to obtain all the conserved quantities of the Euler-Poinsot top.

More generally, a Lax pair for a continuum mechanical system in one spatial dimension usually (but not always, see Sect. 17.10*) means a Lax pair with spectral parameter [77]. The presence of the latter can often be exploited to find an infinite number of local[21] conserved quantities. Such a Lax pair is invariably also the basis for the Inverse Scattering Transform method for solving the initial value problem [6].

11.10 Problems

1. Verify that the function $W(q, I)$ given in (11.22) generates the desired canonical transformation to **angle-action variables** for the **harmonic oscillator**.
2. Use **dimensional analysis** to discuss the form of the generating function $W(q, I)$ (11.22) to angle-action variables for the **simple harmonic oscillator** with Hamiltonian $H = p^2/2m + m\omega^2 q^2/2$.
3. For the harmonic oscillator, find a simple **generating function of the first kind** $F_1(q, \theta)$ for a canonical transformation from the original variables q, p to angle-action variables θ, I. Hint: Use a Legendre transform.

---

[21] A local observable is one that depends on the fields and their derivatives (of finite order) at a spatial location.

4. Show that the (radial) **action variable** for the **Kepler problem** (11.38)

$$I = \frac{1}{\pi}\int_{r_-}^{r_+} \sqrt{2m\left(E - l^2/2mr^2 + \alpha/r\right)}\, dr = -l + \alpha/\sqrt{-2E/m}, \qquad (11.74)$$

where $r_+ > r_- > 0$ are the radial turning points for bound ($E < 0$) trajectories determined by $E = V_{\text{eff}}(r) = l^2/2mr^2 - \alpha/r$. Hint: Use the integral

$$\int_{r_-}^{r_+} \sqrt{(E - 1/r^2 + 1/r)}\, dr = -1 + 1/(2\sqrt{-E}) \qquad (11.75)$$

for $m = 1/2, \alpha = 1, l = 1$ and use dimensional analysis to reinstate m, α and l.

$*$5. Show that the deflection angle θ and angular momentum p_θ (old canonical variables) of a **pendulum** can be expressed in terms of angle Θ and action variables of Sect. 11.5* as given below. Where does the dependence on the action variable I enter?

$$\begin{aligned} \theta(t) &= 2\arcsin\left[k \;\operatorname{sn}\left(2K(k)\Theta(t)/\pi, k\right)\right] \quad \text{and} \\ p_\theta(t) &= 2ml^2\omega k \;\operatorname{cn}\left(2K(k)\Theta(t)/\pi, k\right). \end{aligned} \qquad (11.76)$$

$*$6. What happens to the **simple pendulum** formulae (11.76) in the limit of low energies (**small oscillations**)? Give the leading limiting behavior of $\Theta(t)$ as well as $\theta(t)$ and $p_\theta(t)$ and comment on whether they are as physically expected.

7. **Commutator.** Show that the commutator $[L, A]$ of symmetric (L) and antisymmetric (A) $n \times n$ matrices is symmetric.

8. Suppose L is a real symmetric square matrix. Show that for $[L, A]$ to be symmetric, A can differ from a real antisymmetric matrix at most by a multiple of the identity. How would augmenting A by a multiple of the identity affect the **Lax equation**?

9. (a) For the **harmonic oscillator Lax pair** (11.55), calculate $[L, A]$. Show that the matrix elements of the Lax equation are given by

$$\dot{L} = \begin{pmatrix} \dot{p}/m & \omega\dot{x} \\ \omega\dot{x} & -\dot{p}/m \end{pmatrix} = [L, A] = \begin{pmatrix} -\omega^2 x & \omega p/m \\ \omega p/m & \omega^2 x \end{pmatrix} \qquad (11.77)$$

and confirm that they are equivalent to Hamilton's equations. (b) Calculate the eigenvalues and eigenvectors of the harmonic oscillator Lax matrix L.

10. Suppose L is a diagonalizable $n \times n$ matrix. Show that $\operatorname{tr} L$ is the sum of its eigenvalues and more generally $\operatorname{tr} L^p$ is the sum of the p^{th} powers of its eigenvalues. Thus, the **eigenvalues** determine the **traces of powers** of L. Conversely, given $\operatorname{tr} L$, $\operatorname{tr} L^2, \cdots \operatorname{tr} L^n$, one may determine the eigenvalues. Demonstrate this for a 2×2 matrix. In particular, if $\operatorname{tr} L^p$ is conserved for all p, then the eigenvalues must also be conserved and vice versa.

11. Suppose $(L^p)_t = [L^p, A]$ for $p = 1, 2, \cdots, n$. Show that $(L^{n+1})_t = [L^{n+1}, A]$.

$*$12. Compare the **Heisenberg equation** of motion for the observable Q in the Heisenberg picture of quantum mechanics, $i\hbar\frac{dQ}{dt} = [Q, H]$ with the **Lax equation** $\dot{L} = [L, A]$. Could the former be used to find conserved quantities? If Q and H are operators on infinite-dimensional spaces, does $\operatorname{tr}[Q, H]$ have to vanish?

13. **Isospectrality.** Show that two matrices $L(t)$ and $L(0)$ that are related by a similarity transformation $L(t) = S(t)L(0)S^{-1}(t)$ have the same eigenvalues. Hint: Consider the eigenvalue problem $L(0)\psi = \lambda\psi$.

14. **Solution to the Lax equation.** Suppose $L(t) = S(t)L(0)S^{-1}(t)$ where $S(t)$ is the (fundamental) solution of the ODEs $\dot{S} = -AS$ with $S(0) = I$. Show that $L(t)$ satisfies the Lax equation $\dot{L} = [L, A]$. Hint: Differentiate $SS^{-1} = I$ in time to find an expression for the derivative of S^{-1}.

15. Suppose the **eigenvector** ψ of the **Lax matrix** L corresponding to eigenvalue λ evolves according to $\psi_t = (-A + \beta I)\psi$ for a scalar β. Argue that A may be redefined by absorbing β into it without affecting the Lax equation $L_t = [L, A]$.

$*$16. **Hermitian Lax matrix.** Suppose the Lax matrix L is Hermitian with respect to an inner product $(\cdot,\cdot)$ and suppose ψ is an eigenvector corresponding to the real eigenvalue λ. Show that $(L-\lambda)(\psi_t + A\psi) = \lambda_t\psi$. Use this to show that $\lambda_t = 0$.

17. Show that for $n = 1, 2, 3, \ldots$, the **harmonic oscillator Lax matrix** powers are

$$L^{2n} = \left(\frac{p^2}{m^2} + x^2\omega^2\right)^n I = \left(\frac{2E}{m}\right)^n I \quad \text{and} \quad L^{2n+1} = \left(\frac{2E}{m}\right)^n L. \tag{11.78}$$

Do the powers of L beyond the second furnish any new conserved quantities?

$*$18. **Toda chain conserved quantities.** (a) Show that the Flaschka variables satisfy the equations of motion (11.65). (b) Verify that the Lax equation for the L-A pair (11.66) is equivalent to these EOM. (c) Find an expression for $\operatorname{tr} L^3$ in terms of the positions and momenta of the particles in the Toda chain. (c) Verify using the Toda chain equations of motion that the total momentum P, energy E (11.67) and $\operatorname{tr} L^3$ are conserved.

19. **Vector to antisymmetric matrix.** If $S_{ij} = \epsilon_{ijk}S_k$ then show that $S_i = \frac{1}{2}\epsilon_{ijk}S_{jk}$.

20. Suppose we use the Levi-Civita symbol to map vectors in $\mathbb{R}^3$ to 3×3 antisymmetric matrices: $S_{ij} = \epsilon_{ijk}S_k$. Show that the **cross product** of two vectors $\boldsymbol{S} \times \boldsymbol{\Omega}$ is mapped to the **commutator of matrices** $[\Omega, S]$.

$*$21. **Euler equations.** Consider the **Lax pair with spectral parameter** $L(\lambda) = \mathcal{J}^2 + S/\lambda$ and $A(\lambda) = -(\lambda\mathcal{J} + \Omega)$ proposed in (11.71). (a) Show that

$$\dot{L} - [L, A] = \frac{1}{\lambda}\left(\dot{S} + [S, \Omega]\right) + [S, \mathcal{J}] + [\mathcal{J}^2, \Omega]. \tag{11.79}$$

(b) Show that the last two terms sum to zero. So the condition that the Lax equation hold for any λ is equivalent to the Euler equations in matrix form $\dot{S} = [\Omega, S]$.

$*$22. **Conserved quantities for Euler-Poinsot top.** Recall the Lax pair with spectral parameter (11.71) for the Euler-Poinsot top. Show that

$$\begin{aligned}\operatorname{tr} L^2 &= \operatorname{tr}\mathcal{J}^4 - \frac{2}{\lambda^2}\boldsymbol{S}^2 \\ \operatorname{tr} L^3 &= \operatorname{tr}\left[\mathcal{J}^6 + \frac{3}{\lambda^2}\mathcal{J}^2 S^2\right] = \operatorname{tr}\mathcal{J}^6 - \frac{3}{\lambda^2}\left(\frac{(\operatorname{tr}\mathcal{I})^2\boldsymbol{S}^2}{4} - \mathcal{I}_1\mathcal{I}_2\mathcal{I}_3 E\right).\end{aligned} \tag{11.80}$$

Chapter 12

Hamilton-Jacobi equation

So far, we have witnessed the evolution of the formulation of classical dynamics from Newton's equations, through Lagrange's equations and the principle of extremal action to Hamilton's equations, their formulation via Poisson brackets and their interpretation in terms of geodesics on configuration space or vector fields on phase space. In each of these viewpoints, trajectories as a function of time were to be obtained by solving certain ordinary differential equations (ODEs). In Chap. 10, we learned about canonical transformations (CTs), how they could be obtained via generating functions and that Hamiltonian time evolution defines a CT on phase space. In this chapter, we take up a new formulation of classical dynamics that is associated to the Hamilton-Jacobi (HJ) equation. Unlike the Newton/Euler-Lagrange and Hamilton equations, the Hamilton-Jacobi equation is a partial differential equation. It may be regarded as governing the evolution of a generating function [Hamilton's principal function $S(q, P; t)$] for a finite canonical transformation. This transformation, when it exists, re-expresses the EOM in variables where both the coordinates and momenta (and consequently the Hamiltonian as well) are constant in time! It is shown that when a *complete* solution to the HJ equation depending on sufficiently many free parameters can be found, such a CT exists and can be used to obtain trajectories starting from given initial conditions. We then describe the method of separation of variables, which in favorable cases, may be used to obtain complete solutions of the HJ equation by reducing it to a collection of independent 1^{st} order ODEs. This method turns out to be a classical counterpart of the method of separation of variables that is used to solve Schrödinger's equation in some quantum mechanics problems such as the hydrogen atom. In fact, we show that the nonlinear HJ equation may be obtained in a semiclassical limit[1] of Schrödinger's linear wave equation of quantum mechanics where the quantum wave function ψ is *approximated* by the exponential of Hamilton's principal function: $\psi \sim e^{iS/\hbar}$. We also show how the (time-independent) HJ equation can be regarded as the mechanical analog of the eikonal equation of geometrical optics, an observation that goes back to Hamilton's 'optico-mechanical analogy'. We then turn to another interpretation of Hamilton's principal function, as the action functional of Sect. 3.18* evaluated along a trajectory and regarded as a function of the endpoint of the trajectory. This allows us to derive the HJ equation without reference to canonical transformations. Finally, we provide an elegant geometric interpretation of Hamilton's principal function based on the idea of wavefronts from optics. It is shown that trajectories on configuration space are everywhere orthogonal to Hamilton-Jacobi wavefronts (level hypersurfaces of Hamilton's principal function), in a manner reminiscent of Huygens' construction in optics.

---

[1] This is a limit where Hamilton's principal function or other appropriate quantities with dimensions of action are large compared to Planck's constant $\hbar$. It may also be regarded as the limit $\hbar \to 0$, holding other appropriate quantities fixed.

The formulation of classical dynamics via the Hamilton-Jacobi PDE is both of practical and conceptual value. On the one hand, the method of separation of variables gives a systematic procedure for attempting to solve the evolution equations of Hamiltonian systems. The separation constants are then conserved quantities. As is the case with Newton's or Hamilton's equations, implementing the method requires some physical insight or ingenuity in the choice of coordinate systems. When all variables can be separated in the HJ equation [as in the free particle, harmonic oscillator, Kepler and Euler 3-body problems], we say that the system is (completely) solvable or Jacobi integrable[2] via separation of variables (SOV). When there is more that one coordinate system in which variables separate in the HJ equation, we say the system is super-integrable (the Kepler problem is an example). However, most systems cannot be solved by separation of variables. When this is the case (not for lack of trying), the system is designated nonintegrable via SOV. Nonintegrable systems often display varying degrees of irregular or chaotic behavior.

On the other hand, the HJ formulation of mechanics brings it closer to other branches of physics. For instance, it grew out of Hamilton's optico-mechanical analogy. The HJ equation is a first order PDE for a wave amplitude [Hamilton's principal function $S(q, P; t)$]. It turns out that to certain PDEs, one may associate a family of ODEs called the equations for its *characteristics*. The ODEs associated to the HJ equation are simply the equations of motion for trajectories. The characteristics (or characteristic curves) are the particle trajectories. In optics, the analog of the HJ equation is a wave equation (called the eikonal equation) for light propagation in a medium where the wavelength of light is small compared to the sizes of obstacles or the gradient length scale[3] of inhomogeneities in the refractive index. The corresponding characteristic curves in optics are light rays. Thus, light rays are the optical analogs of particle trajectories in mechanics. The prescient nature of Hamilton's optico-mechanical analogy can be gauged from what followed over the next century. First, a more accurate treatment of optics was discovered and found its expression in Maxwell's wave equations of electromagnetism (1861-62). The eikonal equation arises in a short-wavelength approximation to Maxwell's equations. Second, a more accurate version of mechanics was discovered and found its expression in Schrödinger's wave equation of quantum mechanics (1925-26). The HJ equation is the short-wavelength approximation to the Schrödinger equation, valid in the limit where the de Broglie wavelengths of matter waves are small compared to the gradient length scale of inhomogeneities in the potential $V(\boldsymbol{r})$. In fact, we often use the HJ equation to obtain an approximate solution to the Schrödinger equation via a scheme called the Jeffreys-Wentzel-Kramers-Brillouin (JWKB) approximation [114]. Thus, the Schrödinger equation of wave mechanics is the analog of the Maxwell equations of wave optics while the JWKB method is the mechanical analog of the eikonal approximation in optics.

---

[2] Solvability via separation of variables in the HJ equation (Jacobi integrability) is, on the face of it, different from Liouville integrability of Sect. 11.7*. However, the separation constants that result from a complete solution of the HJ equation via separation of variables must be in involution (since we will see that they can be taken as the new canonical momenta). So provided these constants of motion are independent, the system would satisfy the conditions for Liouville integrability. On the other hand, Liouville integrability, though it guarantees the existence of angle-action variables, does not suggest a coordinate system in which variables in the HJ equation can be separated. The HJ equation is generally not separable in angle-action variables since the Hamiltonian can depend on the action variables in a complicated way.

[3] By the gradient length scale we mean the length over which the refractive index changes significantly compared to its own value.

12.1 Time-dependent Hamilton-Jacobi evolution equation

Time evolution of a Hamiltonian system is particularly simple in angle-action variables, which were introduced in Chap. 11. When such canonically conjugate variables exist, the Hamiltonian is independent of all the angle variables (position coordinates). An even more extreme case of canonical variables is that in which the Hamiltonian is independent of all the coordinates as well as momenta, i.e., the Hamiltonian is a constant, which can be taken to vanish by a choice of additive constant in the energy of all states. Thus, for a system with n degrees of freedom, we imagine a set of *old* coordinates and momenta $(q^i, p_i)_{1\le i\le n}$ in which the problem is presented, as well as a set of *new* coordinates and momenta (Q^i, P_i) in which the transformed Hamiltonian of Sect. 10.10, $K = 0$. Hamilton's equations for K then imply that the new coordinates and momenta are *both* constant in time, and are therefore determined by their initial values: $Q^i(t) = Q^i(0) = \beta^i$ and $P_i(t) = P_i(0) = \alpha_i$. Time evolution[4] is very simple in such variables! However, it is not always possible to find canonical variables in which $K = 0$. When they exist, the generator of the canonical transformation to such variables must satisfy an interesting nonlinear first order partial differential equation (PDE) called the (time-dependent) Hamilton-Jacobi equation. For definiteness, let us look for a generating function of the second type $F_2(q, P, t)$ (10.85) for the transformation from $(q, p, H) \mapsto (Q, P, K)$ (see Prob. 12.1 for a formulation in terms of other generating functions). For reasons to be clarified later, it is customary in this context to denote F_2 by $S(q, P, t)$ and call it Hamilton's principal function. Recall from (10.85) that $p_i = \frac{\partial S}{\partial q^i}$ and that for the new Hamiltonian to vanish, S must satisfy[5]

$$K = H(q, p, t) + \frac{\partial S(q, P, t)}{\partial t} = 0 \qquad \text{or} \qquad H\left(q^i, \frac{\partial S}{\partial q^j}, t\right) + \frac{\partial S}{\partial t} = 0. \quad (12.1)$$

This is the Hamilton-Jacobi (HJ) equation. It is first order in time and a generally nonlinear PDE for the unknown generating function S in $n+1$ variables $q^1, \cdots, q^n, t$.

---

[4] The system looks static in the new variables. All the time evolution in the original variables has been encoded in the canonical transformation, which is time-dependent.

[5] If H is explicitly time-dependent, then one wonders whether we may end up with a new Hamiltonian $K(t)$ which is a constant on phase space, but a different constant at different times. Such a time-dependent K can be got rid of by adding to S a function $f(t)$ satisfying $K(t) = \frac{\partial f}{\partial t}$. So any residual time-dependence in the new Hamiltonian can be removed.

For a particle in a 1d potential $V(q)$, it is

$$\frac{\partial S}{\partial t} + \frac{1}{2m}\left(\frac{\partial S}{\partial q}\right)^2 + V(q) = 0. \tag{12.2}$$

Complete solution of HJ equation. To find a CT to constant coordinates and momenta, we will be interested in so-called 'complete integrals or complete solutions' of (12.1). A complete solution[6] is by definition one that depends on $n+1$ constants of integration which we shall denote by $\alpha_1, \cdots, \alpha_{n+1}$. They are indicated as arguments of Hamilton's principal function

$$S = S(q^1, \cdots q^n; \alpha_1, \cdots, \alpha_n; t). \tag{12.3}$$

We have not indicated the dependence on the last constant of integration α_{n+1}. The latter may be taken as an additive constant in S, since only derivatives of S appear in the HJ equation. We will choose $\alpha_{n+1} = 0$ since it will be seen not to enter the equations of transformation $p = \frac{\partial S}{\partial q}$, $Q = \frac{\partial S}{\partial P}$ and $K = H + \frac{\partial S}{\partial t}$. A possible origin of these constants of integration will be clarified when we discuss the method of separation of variables to solve the HJ equation in Sect. 12.3.

For now, let us illustrate the idea with the example of the free particle in 1d, where $V = 0$ in (12.2). It is straightforward to verify that a complete solution is given by

$$S(q, \alpha_1, \alpha_2, t) = -Et \pm q\sqrt{2mE} + \alpha_2 \tag{12.4}$$

for either sign. The first constant of integration $\alpha_1 = E$ is physically the conserved energy. The quantity $\pm\sqrt{2mE}$ has the meaning of linear momentum of the particle, which can have either sign depending on which way the particle is moving. In Sect. 12.3, we will discuss the procedure of separation of variables to solve the HJ equation where possible. In favorable cases (e.g., free particle, harmonic oscillator, Kepler & Euler 3-body problems, geodesics on a triaxial ellipsoid), the HJ PDE for a system with n degrees of freedom can be reduced to a set of n *decoupled first order* ODEs, whose solution by quadrature introduces the required constants of integration.

A virtue of a 'complete' solution of the HJ equation is that it provides a way of solving for the time evolution of the original mechanical system, i.e., of expressing $q^i(t)$ and $p_j(t)$ in terms of their initial values. First, we are free to take (i.e., *define*) the new constant momenta to equal[7] the constants of integration, i.e., $P_j = \alpha_j$. Then the equations of transformation (10.85) in terms of the generator S read

---

[6] A complete solution is not to be confused with a solution to the HJ PDE with specified initial and boundary values for $S(q,t)$. An 'incomplete' solution would be one that depends on less than $n+1$ free parameters. Such a partial solution cannot, by itself, be used to solve the initial value problem for Hamilton's equations.

[7] A complete solution of the HJ equation may not be unique. There may be more than one coordinate system in which variables may be separated in the HJ equation and a complete integral obtained. Given one complete integral, we still have a lot of freedom in choosing the new momenta P_j. For instance, we could take the P_j to be some n independent functions of the α_j. A convenient choice may depend on the physical interpretation of the resulting variables, as we observed for the free particle in (12.4). This freedom in approach does not take away from the typically unique solutions to Hamilton's equations for given initial conditions.

$$p_j = \frac{\partial S(q, \alpha, t)}{\partial q^j} \quad \text{and} \quad \beta^i = Q^i = \frac{\partial S(q, \alpha, t)}{\partial \alpha_i}. \tag{12.5}$$

The second equation may be used (assuming the Hessian $\partial^2 S/\partial q^j \partial \alpha_i$ is nonsingular) to solve for $q^i = q^i(\alpha, \beta, t)$. This may be put in the first equation to find $p_i = p_i(\alpha, \beta, t)$. Now, the solution of the mechanical problem in the sense mentioned above would be obtained if we express α_j, β^k in terms of the initial values of the old variables $q^i(0)$ and $p_i(0)$. To do this, let us consider these equations at $t = 0$. We get

$$p_j(0) = \frac{\partial S(q, \alpha, t)}{\partial q^j} \quad \text{and} \quad \beta^i = \frac{\partial S(q(t), \alpha, t)}{\partial \alpha_i} \quad \text{evaluated at } t = 0. \tag{12.6}$$

We may use the first equation to express α_i in terms of $q(0)$ and $p(0)$. Then the second gives us β^i in terms of $q(0)$ and $p(0)$. Using the above results, we get

$$q^i(t) = q^i(q(0), p(0), t) = q^i(\alpha, \beta, t) \quad \text{and} \quad p_i(t) = p_i(q(0), p(0), t) = p_i(\alpha, \beta, t). \tag{12.7}$$

These give the solution to the mechanical problem since they express the old coordinates and momenta in terms of their initial values.

For some purposes, we will consider a mechanical system as ‘solved’ if we can find a complete solution of the HJ PDE. As the forgoing indicates, this is still some way off from solving the IVP for the original coordinates and momenta, since one would still have to solve the algebraic/transcendental equations (12.5) to express the α_i in terms of the initial values $q^j(0)$ and $p_j(0)$. However, setting aside this inversion problem gives us a new and powerful notion of what it means to solve a mechanical system. However, as good as this sounds, it is rarely possible to find a complete solution of the HJ equation. Systems for which this is possible are ‘solvable’ or ‘integrable’, though in a manner different from Liouville integrability discussed in Sect. 11.7* (see also Footnote 2). Sometimes, one may only be able to find a solution S depending on less than $n + 1$ constants of integration. Fortunately, even this can be used to provide a partial understanding of the original mechanical problem (see Prob. 12.3). It is a bit like having less than a maximal set of conserved quantities.

Value of the Hamilton-Jacobi approach. At first sight, solving the HJ equation may appear to be a rather complicated and circuitous way of solving for the time evolution of a mechanical system. Indeed, it is a partial differential equation unlike the ODEs of Newton, Euler-Lagrange and Hamilton. However, a similar unfamiliarity presented itself when we first encountered the Euler-Lagrange variational principle or the Hamilton-Poisson bracket reformulation of Newton’s equations. Once one acquires some familiarity with it, the Hamilton-Jacobi equation will be seen to furnish not just an alternative way of solving a mechanical system when possible, but a truly new viewpoint on mechanics itself. Instead of finding $2n$ position and momentum functions of time, we now seek a single function S of n variables and time depending on n free parameters. Hamilton’s principal function S is a gadget from which all the coordinates and momenta can be obtained through differentiation and by solving the algebraic/transcendental equations (12.5). With a clever choice of coordinates, it may be feasible to solve the HJ equation through separation of variables (see Sect. 12.3). When one can separate variables in the HJ equation, the resulting decoupled ODEs are of 1^{st} order and their solution is reduced to quadrature. This is not a priori the case with Newton's 2^{nd} order ODEs. Furthermore, armed with examples and some physical insight, it may be possible to guess a form for Hamilton's principal function to find an approximate solution to the HJ equation. However, the HJ equation is not necessarily a 'better' way of solving/understanding a Hamiltonian system (compared to Newton's or Hamilton's equations or the principle of extremal action). The stark reality is that mechanical systems can be difficult to understand and we often need different approaches in distinct problems or multiple viewpoints for the same system. On the other hand, the Hamilton-Jacobi PDE *does* have distinct advantages in revealing deep connections of classical dynamics to geometrical optics (Hamilton's optico-mechanical analogy) and the Schrödinger formulation of quantum mechanics. We will briefly touch upon these connections in Sect. 12.2* and Sect. 12.5*. Remarkably, the solution of a mechanical system by separating variables in the HJ equation is what comes closest to how we solve for the stationary states of quantum mechanical systems like the hydrogen atom.

Remark. We introduced the HJ equation (12.1) as a means to find a CT to canonical variables that are constant in time. However, the equation itself is meaningful even when such variables do not exist. In particular, even when a *complete solution* of the HJ equation does not exist, the equation may still be solved as an *initial value problem* for Hamilton's principal function S. In fact, we will rederive the HJ equation in Sect. 12.4 and furnish an alternate physical interpretation for S in terms of the action. □

12.2* Connection of Hamilton-Jacobi to Schrödinger and eikonal equations

Let us pause and recall our development of the formalisms of mechanics. We began with Newton's formulation of mechanics in terms of a system of nonlinear ODEs (3.2) for Cartesian coordinates. We progressed to Lagrange's equations (3.21) which are still ODEs, but whose form is invariant under changes of coordinates on configuration space. Then came Hamilton's ODEs (3.78) which are form-invariant under canonical transformations on phase space. The Poisson bracket formulation of Hamilton's equations $\dot{f} = \{f, H\}$ (3.119) take the same form for *any* observable and any system of coordinates on phase space (canonical or not). The Hamilton-Jacobi equation (12.1) provides yet another formulation of Hamiltonian dynamics in terms of a single nonlinear first order PDE. This brings the equations of particle mechanics closer in spirit to the PDEs for waves: classical EM waves in the short-wavelength eikonal approximation and quantum matter waves in the semiclassical approximation. In fact, the Schrödinger equation for time evolution of the quantum wave function of a nonrelativistic particle of mass m in a potential V is

$$i\hbar\frac{\partial \Psi}{\partial t} = H\Psi = -\frac{\hbar^2}{2m}\boldsymbol{\nabla}^2\Psi + V\Psi. \tag{12.8}$$

For a free particle ($V = 0$), the stationary state wave function corresponding to energy E and momentum $\boldsymbol{p}$ is $\Psi(\boldsymbol{r}, t) \propto e^{i(\boldsymbol{p}\cdot\boldsymbol{r}-Et)/\hbar}$. For fixed E and $\boldsymbol{p}$, we see that Ψ has an essential singularity at $\hbar = 0$. Thus, the wave function itself does not have a good (classical) limit as $\hbar \to 0$. On the other hand, the quantity S defined by $\Psi = e^{iS/\hbar}$ is better placed to have a finite $\hbar \to 0$ limit. In fact, we have

$$\boldsymbol{\nabla}\Psi = \frac{i}{\hbar}\Psi\boldsymbol{\nabla}S \quad \text{and} \quad \boldsymbol{\nabla}^2\Psi = -\frac{1}{\hbar^2}\Psi\boldsymbol{\nabla}S\cdot\boldsymbol{\nabla}S + \frac{i}{\hbar}\Psi\boldsymbol{\nabla}^2 S, \tag{12.9}$$

so the Schrödinger equation becomes, upon cancelling $e^{iS/\hbar} \neq 0$,

$$-\frac{\partial S}{\partial t} = \frac{1}{2m}|\boldsymbol{\nabla}S|^2 + V - \frac{i\hbar}{2m}\boldsymbol{\nabla}^2 S. \tag{12.10}$$

No approximation has been made, although we assumed that Ψ is expressible as $e^{iS/\hbar}$ for some S[8]. Now, in the limit $\hbar \to 0$, we ignore the last term and notice that we get the Hamilton-Jacobi evolution equation:

$$\frac{\partial S}{\partial t} + \frac{|\boldsymbol{\nabla}S|^2}{2m} + V = 0 \quad \text{or} \quad \frac{\partial S}{\partial t} + H(q, \boldsymbol{\nabla}S) = 0. \tag{12.11}$$

It is in this sense that we may view the HJ equation as the semiclassical limit of the Schrödinger equation. It must be emphasized that we are not suggesting that the Schrödinger equation of quantum mechanics can be derived from the HJ equation; the latter is simply an approximation to the former in the limit $\hbar \to 0$.

Analogy with eikonal equation of optics. Suppose we are interested in the propagation of light of wave number k in an inhomogeneous optical medium with refractive index $n(\boldsymbol{r})$. This means the speed of light at the point $\boldsymbol{r}$ is $c/n(\boldsymbol{r})$ where c is the speed of light in vacuum. If we ignore effects of polarization, then light waves with harmonic time-dependence ($\sim e^{i\omega t}$) are governed by the scalar wave equation [106][9]

$$n(\boldsymbol{r})^2 k^2 \psi(\boldsymbol{r}) + \boldsymbol{\nabla}^2\psi(\boldsymbol{r}) = 0. \tag{12.12}$$

Now, if the wavelength $2\pi/k$ of light is small compared to the length scale over which the refractive index varies significantly, then we may make a short wavelength approximation called the eikonal approximation. By analogy with the semiclassical approximation to the Schrödinger equation, we change dependent variables from ψ to S via $\psi = e^{ikS}$. The 'eikonal' S has dimensions of length and we are interested in the limit of large k, just as we were interested in the limit of small $\hbar$ when we wrote the Schrödinger wave function as $\Psi = e^{iS/\hbar}$ in (12.8). As in (12.10), we find that $\boldsymbol{\nabla}^2\psi = k^2[-(\boldsymbol{\nabla}S)^2 + (i/k)\boldsymbol{\nabla}^2 S]\psi$. Thus, the wave equation (12.12) becomes

$$n(\boldsymbol{r})^2 - (\boldsymbol{\nabla}S)^2 + \frac{i}{k}\boldsymbol{\nabla}^2 S = 0. \tag{12.13}$$

---

[8] S would have to diverge at points where Ψ vanishes.

[9] This scalar wave equation may be viewed as an optical analog of the time-independent Schrödinger equation $[2m(E - V(\boldsymbol{r}))/\hbar^2]\psi + \boldsymbol{\nabla}^2\psi = 0$ for a particle in the potential $V(\boldsymbol{r})$.

In the short wavelength limit, $k \to \infty$ and we get the so-called eikonal equation of geometrical optics:

$$n(\boldsymbol{r})^2 = (\boldsymbol{\nabla} S)^2. \tag{12.14}$$

This is the optical analog of the time-independent HJ equation $(\boldsymbol{\nabla} S)^2 = 2m(E - V(\boldsymbol{r}))$ (11.16) for a particle in the potential $V(\boldsymbol{r})$. Evidently, in this optico-mechanical analogy, which goes back to Hamilton [93], the square of the refractive index $n(\boldsymbol{r})^2$ plays the role of $2m(E - V(\boldsymbol{r}))$.

12.3 Separation of variables in the Hamilton-Jacobi equation

Ironically, after the advent of quantum mechanics [114], some of us are more familiar with solving the Schrödinger equation (12.8) than its classical predecessor, the HJ equation. We may use this experience to motivate the method of separation of variables (SOV) to solve the HJ equation. Recall that if the Hamiltonian is not explicitly dependent on time, then we may multiplicatively separate the time-dependence by writing $\Psi(t, q) = T(t)\psi(q)$. The wave function $\psi(q)$ must solve the time-independent Schrödinger's eigenvalue problem $H\psi = E\psi$ where the energy eigenvalue E is also the separation constant. Moreover, $T(t) = e^{-iEt/\hbar}$. Since $\Psi \sim e^{iS/\hbar}$, multiplicative separation of variables in the quantum wave function is replaced by additive SOV in Hamilton's principal function. In more detail, if the Hamiltonian $H(q, p)$ is not explicitly dependent on time (so that H is a constant of motion), then we may seek a solution of the HJ equation $H(q, \frac{\partial S}{\partial q}) + \frac{\partial S}{\partial t} = 0$ (12.1) in the form

$$S(q, P, t) = W(q, P) - Et. \tag{12.15}$$

We find that (12.1) is satisfied provided W solves the time-independent HJ equation for Hamilton's characteristic function (which we met earlier in Sect. 11.2):

$$E = H\left(q, \partial_q W\right). \tag{12.16}$$

Free particle in 1d. The simplest case is $H = p^2/2m$. The HJ equation is

$$\partial_t S + (1/2m)\left(\partial_q S\right)^2 = 0. \tag{12.17}$$

Since H is time-independent, we put $S = -Et + W(q, P)$ to get the time-independent Hamilton-Jacobi equation $(1/2m)(\partial_q W)^2 = E$. Up to an additive constant, $W(q) = \pm q\sqrt{2mE}$. Thus, we have found a complete solution $S = -Et \pm q\sqrt{2mE}$ of the HJ equation depending on one constant of integration. For convenience, we take this constant of integration as $\alpha = P = \pm\sqrt{2mE}$. So

$$S = -\frac{P^2}{2m}t + qP + \text{constant}. \tag{12.18}$$

We notice that $W(q, P) = qP$ generates the identity CT, while S deviates from the identity by an amount that grows linearly with time, as we might expect. The additive constant in S may be set to zero. The first equation of transformation says $p = \frac{\partial S}{\partial q} = P$. So the old momentum equals the conserved new momentum. Thus,

$P = p(0)$ (the sign of $p(0)$ determines the choice of sign in P). The second equation of transformation gives us the new coordinate

$$Q = \frac{\partial S}{\partial P} = q - \frac{Pt}{m} = q(t) - \frac{p(0)t}{m}. \tag{12.19}$$

Since the new coordinate is guaranteed to be a constant of motion, we evaluate it at $t = 0$ and find $Q = q(0)$. Thus the new coordinate is equal to the initial location. This allows us to solve the initial value problem: $q(t) = q(0) + p(0)t/m$. Finally, the new Hamiltonian vanishes by construction: $K = H + \frac{\partial S}{\partial t} = E - E = 0$.

The free particle in 3d. This may be treated similarly. The HJ equation

$$\partial_t S + (1/2m)\left(\left(\partial_{q^1} S\right)^2 + \left(\partial_{q^2} S\right)^2 + \left(\partial_{q^3} S\right)^2\right) = 0, \tag{12.20}$$

reduces to the time-independent HJ equation $2mE = \left[\frac{\partial W}{\partial q^1}\right]^2 + \left[\frac{\partial W}{\partial q^2}\right]^2 + \left[\frac{\partial W}{\partial q^3}\right]^2$ upon putting $S = -Et + W(q)$. We further separate variables by taking $W = W_1(q^1) + W_2(q^2) + W_3(q^3)$ to get

$$W_1'(q^1)^2 + W_2'(q^2)^2 + W_3'(q^3)^2 = 2mE. \tag{12.21}$$

Since the RHS is a constant and the LHS is a sum of terms depending on different variables, each must be a constant that we denote α_j^2. The new momenta P_j are taken to equal the α_j,

$$W_1'(q^1)^2 = P_1^2, \quad W_2'(q^2)^2 = P_2^2 \quad \text{and} \quad W_3'(q^3)^2 = P_3^2 \tag{12.22}$$

where $(1/2m)(P_1^2 + P_2^2 + P_3^2) = E$. We have a complete solution of the HJ equation depending on 3 constants of integration (P_1, P_2 and P_3):

$$S = -(1/2m)(P_1^2 + P_2^2 + P_3^2)t + q^1 P_1 + q^2 P_2 + q^3 P_3. \tag{12.23}$$

A 4^{th} constant of integration is an additive constant that we omit. Partial derivatives of Hamilton's principal function with respect to the old coordinates give

$$p_j = \partial_{q^j} S \quad \Rightarrow \quad p_j = P_j. \tag{12.24}$$

So the constant new momenta are just the old momenta, which must therefore be constants of motion $P_i = p_i = p_i(0)$. Partial derivatives of S with respect to the new momenta give the new coordinates

$$Q^i = \frac{\partial S}{\partial P_i} \quad \Rightarrow \quad Q^i = -\frac{tP_i}{m} + q^i. \tag{12.25}$$

Since Q^i must be constant, we evaluate them at $t = 0$ and find $Q^i = q^i(0)$ are just the initial values of the old coordinates. Thus the solution of the initial value problem is

$$q^i(t) = q^i(0) + p_i(0)t/m. \tag{12.26}$$

For the free particle we were able to separate all the variables (t, q^1, q^2, q^3) in the HJ equation and write Hamilton's principal function as a sum of terms involving just one variable each. The HJ equation for a free particle is said to be separable. If the time-dependent HJ equation is separable, we may reduce it to a collection of first order ODEs, each of which is solved separately (typically by quadrature).

Circularly symmetric 2d potential. Here, in polar coordinates, the Hamiltonian is

$$H = \frac{p_r^2}{2m} + \frac{p_\phi^2}{2mr^2} + V(r) \quad \text{where } p_r = m\dot{r} \text{ and } p_\phi = mr^2\dot{\phi} \tag{12.27}$$

and $V(r) = \frac{1}{2}kr^2 + gr^4$ could be a quartic potential. Separating time via $S = W - Et$, we get the time-independent HJ equation

$$(1/2m)\left(\partial_r W\right)^2 + (1/2mr^2)\left(\partial_\phi W\right)^2 + V(r) = E. \tag{12.28}$$

Writing $W(r,\phi) = W_1(r) + W_2(\phi)$ we get

$$2mr^2\left[E - (1/2m)W_1'(r)^2 - V(r)\right] = W_2'(\phi)^2 = l^2 \tag{12.29}$$

where l^2 must be a constant since LHS and RHS depend on r and ϕ exclusively. Thus, $W_2 = l\phi$ where $l = p_\phi$ can have either sign. The determination of W_1 is reduced to quadrature: it may be expressed as an elliptic integral for the above quartic potential V (see Prob. 12.8). This leads to a complete solution of the HJ equation depending on two constants of integration E and l. The corresponding dynamical variables H and p_ϕ Poisson commute with each other. This is generally true.

Spherically symmetric potential in 3d. A 3d generalization is a particle subject to a central potential. The time-independent HJ equation separates in spherical polar coordinates (r, θ, ϕ). It also admits 3 pairwise commuting constants of motion, usually taken to be the Hamiltonian, the square of angular momentum L^2 and the component of angular momentum in any particular direction (say, L_z). The system is solvable by separation of variables and also Liouville integrable in the sense of Sect. 11.7*. However, note that the $\mathbb{R}^6$ phase space is not necessarily foliated by 3-tori: trajectories could escape to infinity, as for the Newtonian gravitational potential $-\alpha/r$.

Planar Euler three-body problem. The Euler 3-body problem [72] concerns the dynamics of a point mass m subject to the gravitational potential[10] of two fixed primary masses m_1 and m_2. If initial conditions are chosen so that m is confined to a plane containing m_1 and m_2, we get the planar problem with Hamiltonian

$$H = \frac{1}{2m}\left(p_x^2 + p_y^2\right) - \frac{\mu_1}{r_1} - \frac{\mu_2}{r_2}. \tag{12.30}$$

Here, $r_{1,2}$ are the distances of m from $m_{1,2}$, $\mu_{1,2} = Gm_{1,2}m$ and (x,y) are the Cartesian coordinates of m. The HJ equation can be separated in elliptical coordinates[11] (ξ, η), whose level curves are mutually orthogonal confocal ellipses and hyperbolae with m_1 and m_2 at the foci $2f$ apart (see Fig. 12.1):

$$x = f\,\cosh\xi\,\cos\eta \quad \text{and} \quad y = f\,\sinh\xi\,\sin\eta. \tag{12.31}$$

Roughly, ξ and η are like r and θ of plane polar coordinates.

---

[10] The quantum version of the Euler 3-body problem can be used to model the dynamics of the electron in the hydrogen molecular ion H_2^+, with the two protons assumed to be at rest.

[11] A three-dimensional generalization, ellipsoidal coordinates, were used by Jacobi to separate variables in the problem of free particle (geodesic) motion on a triaxial ellipsoid.

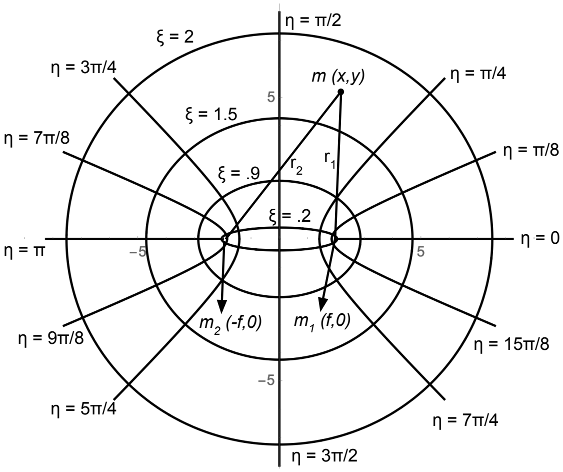

Figure 12.1: The primaries are at the foci $(\pm f, 0)$ of an elliptical coordinate system on the x-y plane. The distances of m from $m_{1,2}$ are $r_{1,2} = f(\cosh\xi \mp \cos\eta)$. The level curves of ξ and η are confocal ellipses and hyperbolae. Units are chosen so that $f = 2$.

Writing (12.30) in elliptical coordinates, putting $W(\xi,\eta) = W_1(\xi) + W_2(\eta)$ and using $p_\xi = W_1'(\xi)$ and $p_\eta = W_2'(\eta)$, the time-independent HJ equation becomes

$$E = \frac{W_1'(\xi)^2 + W_2'(\eta)^2 - 2mf(\mu_1+\mu_2)\cosh\xi - 2mf(\mu_1-\mu_2)\cos\eta}{2mf^2(\cosh^2\xi - \cos^2\eta)}. \tag{12.32}$$

Rearranging,

$$\begin{aligned} &W_1'^2 - 2Emf^2\cosh^2\xi - 2mf(\mu_1+\mu_2)\cosh\xi \\ &= -W_2'^2 - 2Emf^2\cos^2\eta + 2mf(\mu_1-\mu_2)\cos\eta = \alpha, \end{aligned} \tag{12.33}$$

where α is a separation constant. The decoupled ODEs for $W_1(\xi)$ and $W_2(\eta)$ may be solved using elliptic functions. Since α is conserved, it must Poisson commute with the Hamiltonian, making the system Liouville integrable in the sense of Sect. 11.7*. ‘Whittaker’s constant’ $w = -2mf^2E - \alpha$ is expressible as[12] [51, 133]

$$\begin{aligned} w &= \boldsymbol{L}_1 \cdot \boldsymbol{L}_2 + 2mf\,(-\mu_1\cos\theta_1 + \mu_2\cos\theta_2) \\ &= m^2 r_1^2 r_2^2\,\dot\theta_1\dot\theta_2 + 2fm\,(-\mu_1\cos\theta_1 + \mu_2\cos\theta_2)\,. \end{aligned} \tag{12.34}$$

Here, $\theta_{1,2}$ are the angles between the position vectors $\boldsymbol{r}_{1,2}$ and the positive x-axis and $\boldsymbol{L}_{1,2} = mr_{1,2}^2\dot\theta_{1,2}\hat z$ are the angular momenta about the two primaries (Fig. 12.1). Although m is no longer confined to a plane, the 3d Euler 3-body problem is also Liouville integrable as it admits 3 independent conserved quantities in involution: the Hamiltonian, the x-component of angular momentum and Whittaker’s constant [51].

---

[12] When the primaries coalesce at the origin ($f \to 0$), w reduces to the conserved quantity $\boldsymbol{L}^2$ of the planar Kepler problem.

Separation of variables in quantum mechanics. As mentioned, this additive separation of variables $S = -Et + W(q)$ in the classical HJ equation is replaced in quantum mechanics (QM) by the multiplicative factorization $\Psi(q,t) = e^{-iEt/\hbar}\psi(q)$ in the Schrödinger equation for a system with conserved energy. Moreover, the energy eigenfunction ψ is related to Hamilton's characteristic function via $\psi(q) \propto e^{iW(q)/\hbar}$ in the semiclassical limit $\hbar \to 0$. The further additive SOV for Hamilton's characteristic function $W(q) = W_1(q^1) + W_2(q^2)$ is replaced in QM by the multiplicative separation of variables $\psi(q^1,q^2) = \psi_1(q^1)\psi_2(q^2)$ which is used to separate the radial and angular variables in problems such as the hydrogen atom. □

12.4 Hamilton's principal function is action as a function of endpoint of a trajectory

In Sect. 12.1, we introduced Hamilton's principal function $F_2(q,P,t) = S(q,P,t)$ as a possible generating function of a CT to coordinates and momenta which are time-independent. A necessary condition[13] for this was that S must satisfy the time-dependent HJ equation (12.1). Interestingly, the HJ equation arises in another way, which allows us to interpret Hamilton's principal function in terms of the action (which is the reason we use the same letter S for both). To see this, we compute the time derivative of an F_2 that satisfies the HJ equation

$$\begin{aligned} \dot{F}_2 = \frac{\partial F_2}{\partial q^i}\dot{q}^i + \frac{\partial F_2}{\partial t} &= p_i\dot{q}^i - H = L \quad \text{which implies} \\ F_2(q(t),t) - F_2(q(t_0),t_0) &= \int_{t_0}^{t} [p\dot{q} - H]dt'. \end{aligned} \tag{12.35}$$

Thus, up to an additive constant (more on this shortly), $S = F_2$ is the Hamilton-Lagrange action that appears in Hamilton's variational principle of Sect. 3.5. But now, it is regarded as a *function* of the (variable) final location and final time of a *trajectory* (as in Sect. 3.18*) rather than as a *functional* of a whole *path* holding the endpoints fixed[14]. Furthermore, the variables conjugate to the (final) coordinates and time, namely the (final) momenta and Hamiltonian, are expressed as partial derivatives

$$p_i(t) = \frac{\partial F_2}{\partial q^i} \quad \text{and} \quad H(q(t),p(t),t) = -\frac{\partial F_2}{\partial t}. \tag{12.36}$$

In fact, we already showed in (3.102) that the action regarded as a function of the endpoint of a trajectory satisfies what we now call the HJ equation!

Note that to specify a trajectory that begins at fixed $q(t_0) = q_0$, we need to say what the initial momenta are. So $F_2(q(t),t)$ also depends on the initial momenta $p(t_0)$, though we did not indicate this explicitly above. It is through these initial momenta and initial coordinates that Hamilton's principal function $F_2 = S(q,P,t)$ acquires a dependence on P_i. Indeed, for the free particle, we showed in Sect. 12.3

---

[13] This is not sufficient, one needs a complete solution to the HJ equation to find such a CT.

[14] Recall that a trajectory is a path (in this context, a path on phase space) that satisfies the equations of motion.

that we could take $P_i = p_i(t_0)$. In general, the relation is obtained by evaluating $p_i = \partial S(q,P,t)/\partial q^i$ at $t = t_0$.

Just as Hamilton's principal function is related to the Hamilton-Lagrange action, Hamilton's characteristic function $W(q,P)$ (12.15) is related to the Euler-Maupertuis action (1.26). To see this, we compute

$$\frac{dW}{dt} = \frac{\partial W}{\partial q^i}\dot{q}^i + \frac{\partial W}{\partial P_i}\dot{P}_i = p_i \dot{q}^i. \qquad (12.37)$$

Thus $W(q(t),P) = W(q(t_0),P) + \int_{t_0}^{t} p_i \dot{q}^i \, dt'$ where the integration is along the trajectory which starts at $q(t_0)$ at t_0 with initial momentum $p(t_0)$. Here, the constant P is determined in terms of $q(t_0), p(t_0)$ using $p(t_0) = \partial_q W(q,P)|_{t=t_0}$. So Hamilton's characteristic function is the Euler-Maupertuis action evaluated on a trajectory with fixed initial point and viewed as a function the endpoint.

12.5* Geometric interpretation of HJ: trajectories and HJ wavefronts

Hamilton's principal function $S(q,P,t)$ may be given a geometric interpretation that allows us to relate it to the wavefronts encountered in optics[15]. For fixed constant new momenta P, we think of $S(q,P,t)$ as a time-dependent scalar function of q on the n-dimensional configuration manifold $\mathcal{Q}$. Then at each instant of time, $S(q,P,t)$ defines a family of hypersurfaces[16] in $\mathcal{Q}$, namely, the constant S hypersurfaces of dimension $n-1$. We will call these constant S hypersurfaces *wavefronts*. These are to be regarded as the instantaneous wavefronts of a propagating wave/disturbance that is governed by the HJ wave equation $\frac{\partial S}{\partial t} + H(q, \frac{\partial S}{\partial q}) = 0$. At a given time, each wavefront is labeled by the value of S on it. As time progresses, the wavefront with a given value of $S = S_0$ moves. In addition, we also have a family of curves in $\mathcal{Q}$, namely the trajectories for various possible initial locations $q^i(0)$ and fixed initial momenta $p_i(0) = \frac{\partial S}{\partial q^i}$, which are determined by the constants P_j and $q^i(0)$. Now, let us display a geometric relation between the wavefronts and trajectories by first examining the solution of the free particle HJ equation.

Free particle moving in 2d: From Sect. 12.3, Hamilton's principal function is $S = -Et + xP_1 + yP_2$ where $\boldsymbol{q} = (x,y)$, P_1 and P_2 are constants and $2mE = P_1^2 + P_2^2$. At any fixed time t_0, the constant $S = S_0$ hypersurfaces are a family of lines $xP_1 + yP_2 = S_0 + Et_0$. These are the wavefronts at $t = t_0$, they are the lines perpendicular to the vector (P_1, P_2). Though individual wavefronts move, the set of wavefronts at any other time is the same set of lines as at t_0. This is because the Hamiltonian is time-independent. On the other hand, trajectories are $(x(t), y(t)) = (x_0 + \frac{P_1 t}{m}, y_0 + \frac{P_2 t}{m})$. Subtracting, trajectories are the family of lines $P_2 x - P_1 y = P_2 x_0 - P_1 y_0$, which is the same as $(P_2, -P_1) \cdot (x,y) = P_2 x_0 - P_1 y_0$. In other words, trajectories are the lines (not necessarily through the origin), orthogonal to the vector $(P_2, -P_1)$. Since the normal (P_1, P_2) to the wavefronts is perpendicular to the normal $(P_2, -P_1)$ to the trajectories, it follows that the *trajectories are everywhere orthogonal to the wavefronts*, as shown in Fig. 12.2.

---

[15] Such analogies between optics and mechanics played an important role in Hamilton's development of both subjects in the early 1800s. In the 1920s, Schrödinger and de Broglie were partly motivated by Hamilton's optico-mechanical analogy in their development of wave mechanics for quantum mechanical phenomena in atomic physics.

[16] A hypersurface is a manifold of dimension one less than that of the ambient space.

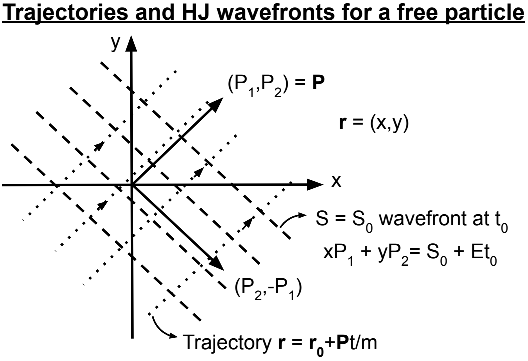

Figure 12.2: Wavefronts of Hamilton's principal function (level hypersurfaces of S) are orthogonal to trajectories $\boldsymbol{r}(t)$ of a free particle moving on the plane with given momentum $\boldsymbol{P} = \boldsymbol{p}(0)$. While wavefronts (dashed) evolve via the HJ equation, trajectories (dotted) are governed by Lagrange's equations.

A free particle in 3d. Here, the complete solution of the HJ equation is

$$S = -Et + xP_1 + yP_2 + zP_3 \quad \text{where} \quad 2mE = P_1^2 + P_2^2 + P_3^2. \tag{12.38}$$

In this case, the constant S hypersurfaces are planes orthogonal to the vector $\boldsymbol{P} = (P_1, P_2, P_3)$, i.e., $(x, y, z) \cdot (P_1, P_2, P_3) = S + Et = \text{const}$. The wavefronts evolve but the set of all wavefronts is independent of time. Trajectories are still straight lines $\boldsymbol{r} = \boldsymbol{r}_0 + \boldsymbol{P}t/m$. So trajectories are parallel to the vector $\boldsymbol{P}$ which is everywhere normal to the wavefronts. It follows that free particle trajectories are everywhere orthogonal to the wavefronts.

Particle subject to a potential moving on a Riemannian manifold: The orthogonality between HJ wave fronts and trajectories is not restricted to 'solvable' systems that admit a complete solution to the HJ equation. In fact, as in Sect. 3.27*, let us consider a Lagrangian system whose configuration space is a Riemannian manifold $\mathcal{Q}$ with metric m_{ij} and whose kinetic energy is quadratic in velocities $L = \frac{1}{2} m_{ij} \dot{q}^i \dot{q}^j - V(q)$. In this case, the conjugate momenta are $p_i = m_{ij} \dot{q}^j$ and the Hamiltonian is $H = \frac{1}{2} m^{ij} p_i p_j + V(q)$ (see Prob. 3.33). For $V = 0$, Lagrange's equations are the geodesic equations $\ddot{q}^l + \Gamma^l_{ij} \dot{q}^i \dot{q}^j = 0$. The HJ equation for Hamilton's principal function $S(q, P, t)$ is

$$\frac{\partial S}{\partial t} + \frac{1}{2} m^{ij} \frac{\partial S}{\partial q^i} \frac{\partial S}{\partial q^j} + V(q) = 0 \quad \text{where} \quad p_j = \frac{\partial S}{\partial q^j}. \tag{12.39}$$

For a free particle moving in 2d or 3d Euclidean space, we found that the trajectories are orthogonal to the wavefronts (level hypersurfaces of S) at each point. We will now show that the same holds for the above Lagrangian system even with a potential.

A normal vector n to a hypersurface of constant S is given by the gradient of S (see Footnote 96 of Sect. 3.25*). It has components $n^i = (\text{grad } S)^i = m^{ij}\partial_j S$. Since S is a generating function of second type, $n^i = m^{ij} p_j = \dot{q}^j$. But this just says that the velocity vector at a point along a trajectory is normal to the wavefront through that point. Thus, the trajectories are everywhere normal to the HJ wavefronts!

Classical version of 'wave-particle' duality. We have come to the remarkable conclusion that the same classical system can be described either via point particle trajectories that solve a system of ODEs (Lagrange's or Hamilton's equations), or via evolving wavefronts obtained from solving the HJ PDE. This may be viewed as a classical wave-particle duality, a forerunner of the quantum one. Sometimes, the trajectories are called characteristic curves and Hamilton's ODEs are called the equations for the characteristics associated to the Hamilton-Jacobi PDE.

Geodesic equation from HJ equation. One may use this connection between trajectories and wavefronts to give an alternate derivation of the geodesic equation (3.199) (for the kinetic metric m_{ij}) on $\mathcal{Q}$ from the HJ equation, by considering the special case $V = 0$. If $x^i(t)$ is a curve whose tangent vector $\dot{x}$ equals the normal to the HJ wavefront at every point, then

$$\dot{x}^i = m^{ij}\partial_j S. \tag{12.40}$$

Now, we will eliminate S and obtain a differential equation for $x^i(t)$. We differentiate once in time and use $\dot{S} = \partial_t S + \partial_k S \dot{x}^k$, the HJ equation $\partial_t S = -H = -\frac{1}{2} m_{ij}\dot{x}^i \dot{x}^j$ and the fact that $\partial_j S = p_j = m_{jk}\dot{x}^k$:

$$\begin{aligned}
\ddot{x}^i &= m^{ij}{}_{,k}\dot{x}^k \partial_j S + m^{ij}\partial_j\partial_t S + m^{ij}\partial_j\partial_k S\,\dot{x}^k \\
&= m^{ij}{}_{,k}\dot{x}^k p_j - m^{ij}\partial_j H + m^{ij}\partial_j p_k \dot{x}^k \\
&= m^{ij}{}_{,k}\dot{x}^k m_{jl}\dot{x}^l - m^{ij}\frac{1}{2} m_{kl,j}\dot{x}^k\dot{x}^l + m^{ij} m_{kl,j}\dot{x}^k\dot{x}^l \\
&= \left[m^{ij}{}_{,k} m_{jl} + (1/2) m^{ij} m_{kl,j} \right] \dot{x}^k \dot{x}^l.
\end{aligned} \tag{12.41}$$

The subscript $,k$ denotes partial differentiation with respect to x^k. We also used $\partial_j \dot{x}^k = \frac{d}{dt}\delta^k_j = 0$. Differentiating the identity $m^{ij} m_{jl} = \delta^i_l$ in x^k one has $m^{ij}{}_{,k} m_{jl} + m^{ij} m_{jl,k} = 0$. Exploiting the symmetry of $\dot{x}^l \dot{x}^k$ under $k \leftrightarrow l$, we find that the curve $x(t)$ satisfies the geodesic equation familiar from Sect. 3.27*

$$\ddot{x}^i + (1/2) m^{ij}\left(m_{jl,k} + m_{jk,l} - m_{kl,j}\right)\dot{x}^k \dot{x}^l = 0. \tag{12.42}$$

Remark. If $V \neq 0$, then trajectories are not geodesics with respect to the metric m_{ij}, but they remain orthogonal to the wavefronts, as shown above. This suggests that there may be some other metric that is conformal[17] to m_{ij} with respect to which trajectories are geodesics. This is indeed the case: the relevant metric is the Jacobi-Maupertuis metric of Sect. 3.28*. □

---

[17] Conformal metrics assign the same angle between a pair of tangent vectors at a point but possibly different lengths to tangent vectors.

12.6 Problems

1. In Sect. 12.1 we introduced the Hamilton-Jacobi equation for a generating function (of type 2) of a canonical transformation to variables in which the Hamiltonian vanishes. Find the corresponding Hamilton-Jacobi equations for generating functions of type 1, 3 and 4 and compare and contrast them. Loosely, we may speak of the **HJ equation in position and in momentum space**.

2. Consider the **oscillator** $H = \frac{p^2}{2m} + \frac{1}{2}m\omega^2 q^2$ with spring constant $k = m\omega^2$.

   a. Use an Euler-Maupertuis action integral to solve the time-independent HJ equation and find a **generating function** $W(q, I)$ for the **canonical transformation to angle-action variables** $I = E/\omega$ and $\theta = \arctan(m\omega q/p)$.

   b. Verify that this function W generates a canonical transformation to the above angle-action variables. In other words, show explicitly that

   $$\partial_q W = p = \sqrt{2m(E-V)} \quad \text{and} \quad \partial_I W = \theta = \arcsin\left(q\sqrt{m\omega/2I}\right). \tag{12.43}$$

   Why is this different-looking formula for θ also valid?

   c. Use the above $W(q, I)$ to find a generating function of the first kind $F_1(q, \theta)$ for the same canonical transformation. Give the explicit formula for I as a function of θ, q as well as a simple formula for $F_1(q, \theta)$.

∗3. Suppose we have an **incomplete solution** $S(q^1 \cdots q^n; \alpha_1, \cdots, \alpha_p; t)$ of the time-dependent **Hamilton-Jacobi equation** for a mechanical system, depending on less than n constants of integration ($p < n$, setting aside the overall additive constant in S). Try to examine to what extent this can be used to understand the time evolution of the coordinates and momenta of the system. Try to construct an explicit example of a system where this happens. Hint: To get started, one could take a complete integral and simply assign a numerical value to one of the constants of integration and see how this comes in the way of implementing the procedure of Sect. 12.1.

∗4. **Complex exponential.** Consider the function of a complex variable $z \mapsto w = e^z$. Given a fixed $w \neq 0$, identify a countably infinite collection of complex numbers z such that $e^z = w$. Display a typical such w in the interior of the first quadrant of the complex plane and the corresponding values of z in a figure.

5. **Free particle HJ equation.** Consider a particle free to move on a line with Hamiltonian $H = p^2/2m$. Work out the 'complete' solutions of the time-dependent HJ equation and find Hamilton's principal function. But unlike in Sect. 12.3, make a different choice for the new momentum $P = \alpha$ (such as E or $2mE$). For such a choice, the new 'momentum' may not have the physical dimensions of momentum, but that is all right. Express the new constant coordinate and momentum Q and P in terms of the initial values of the old ones $q(0), p(0)$. Show that Q, P are canonically conjugate even with this altered choice. Use the HJ approach to find the trajectory $q(t), p(t)$ in terms of $q(0)$ and $p(0)$ and show that you get the expected answer even with this altered choice of new coordinates and momenta.

6. Consider a **projectile moving under Earth's downward gravity**: $H = (p_x^2 + p_y^2 + p_z^2)/2m + mgz$.

   a. Write the time-dependent HJ equation for Hamilton's principal function S and the time-independent HJ equation for Hamilton's characteristic function W after separating the time variable.

   b. Solve for W by further SOV and find a complete solution of the HJ equation, identifying integration constants and choosing suitable constant new momenta.

   c. Find the constant new coordinates from S and express $x(t), y(t), z(t)$ as functions of time and the new coordinates and momenta. Show that x, y are linear in time, that z is a quadratic function of time, and that the projection of the trajectory on the x-y plane is a straight line, thus recovering the parabolic trajectory. [You need not express the new coordinates and momenta in terms of the initial values of the old ones.]

$*$7. **Particle on a sphere.** Consider a particle of mass m moving on a sphere of radius a, governed by the Hamiltonian $H = \boldsymbol{L}^2/2ma^2 + mga\cos\theta$ where $\boldsymbol{L}$ is its angular momentum, g the magnitude of the acceleration due to gravity and θ the polar angle of spherical coordinates. (a) Argue that apart from gravity, this describes a free particle (constrained to move on a sphere). (b) Show that

$$H = (1/2ma^2)(p_\theta^2 + p_\phi^2/\sin^2\theta) + mga\cos\theta, \tag{12.44}$$

where $p_\theta = ma^2\dot{\theta}$ and $p_\phi = ma^2\sin^2\theta\dot{\phi}^2$ are the momenta conjugate to the polar and azimuthal angles. (c) Separate variables in the HJ equation by writing Hamilton's characteristic function as $W(\theta, \phi) = W_1(\theta) + W_2(\phi)$. (d) Reduce the ODEs for W_1 and W_2 to quadrature. (e) Evaluate the integrals when $g = 0$ and compare with Prob. 3.17. (f) For $g \neq 0$, mention the type of integrals obtained and try to evaluate them.

8. Recall the **separation of variables** in the HJ equation for a particle in a **circularly symmetric quadratic + quartic potential** $V = \frac{1}{2}kr^2 + gr^4$. Express the radial part of Hamilton's characteristic function $W_1(r)$ (12.29) as an elliptic integral.

9. **Brachistochrone problem.** Recall from Prob. 3.19 that a 'Lagrangian' for the extremization of time in this problem may be taken as $L(y, y') = \sqrt{(1 + y'^2)/2gy}$. Here $y' = dy/dx$ and x plays the role of time in conventional systems. (a) Show that the 'momentum' p conjugate to y is $p = y'\sqrt{2gy(1 + y'^2)}$. (b) Show that y' can be expressed in terms of y and p via $y' = p/\sqrt{(2gy)^{-1} - p^2}$. (c) Define the Hamiltonian $H = py' - L$ via a Legendre transform. Show that $H(y, p) = -\sqrt{(2gy)^{-1} - p^2}$. (d) Show that the corresponding Hamilton-Jacobi equation for $S(x, y)$ is given by $S_x^2 + S_y^2 = (2gy)^{-1}$ with subscripts denoting partial derivatives. (e) What are the dimensions of L, gy, y', p and H?

10. **Planar Kepler problem.** Consider the planar Kepler problem (Sect. 2.3) in polar coordinates (r, ϕ) with Hamiltonian $H = p_r^2/2m + p_\phi^2/2mr^2 - \alpha/r$. Reduce the time-independent HJ equation for energy E to quadratures by separation of

variables: $W(r, \phi) = W_1(r) + W_2(\phi)$. Interpret the separation constants. Explain how to obtain the orbit equation $r(\phi)$ and the time-dependence of r along an orbit.

11. **Planar Euler 3-body problem.** (a) Obtain the time-independent HJ equation (12.32) for the planar Euler 3-body problem. (b) Show that variables may be separated in elliptical coordinates (ξ, η) and reduce the HJ equation to the pair of ODEs (12.33). (c) Try to express $W_1(\xi)$ and $W_2(\eta)$ in terms of standard elliptic integrals (in Legendre normal form). (d) Show that the separation constant α in (12.33) is related to Whittaker's constant (12.34) via $w = -2mf^2E - \alpha$.

Chapter 13

Normal modes of oscillation and linear stability

In Chap. 6, we studied small oscillations around a stable equilibrium state of a system with one degree of freedom. This led us to the harmonic oscillator. What if two or more simple harmonic oscillators or pendula executing small oscillations (without damping and driving forces) interact with each other weakly? To uncover some of the new phenomena that can arise, we begin this chapter in Sect. 13.1 by examining elementary examples of small oscillations in a system with two degrees of freedom: pendula coupled by a spring and a diatomic molecule[1]. The resulting coupled small oscillations are widely encountered in physical systems, typically at low energies or more generally around a stable equilibrium state. In Sect. 13.2 we use the two degree of freedom undamped double pendulum[2] (a simple pendulum with a second pendulum suspended from its bob) as a concrete context to introduce some general techniques used to study small oscillations in a system with more than one degree of freedom. As in Chap. 6, the first step is to linearize the equations of motion to obtain a system of linear ODEs with *constant coefficients*. The main complication is that the various degrees of freedom generally satisfy coupled equations. A key idea is to make a linear change of variables to *normal modes*. The latter satisfy *uncoupled* equations that are easier to solve, as explained in Sect. 13.2.2. Degrees of freedom that satisfy uncoupled equations evolve independently of each other. If the initial state is an excitation along only one normal mode, then other normal modes cannot get activated during subsequent time evolution via the linearized equations of motion. Based on this example, we present in Sect. 13.3* a general framework for studying normal modes of oscillation of a mechanical system with several degrees of freedom around a static equilibrium state. Perhaps not surprisingly, tools from linear algebra [eigenvalue problems and diagonalization of matrices, introduced in Appendix A.10] play a prominent role.

In Sect. 13.4, we progress from small oscillations around a static solution to those around a periodic solution. These could arise, for instance, due to Solar perturbations to the Moon's Keplerian orbit around the Earth. We focus on the question of whether a periodic trajectory (with period T in phase space) is stable or not to small perturbations. Upon linearizing the equations of motion around the periodic solution, we obtain (a system of) linear ODEs with *periodic coefficients* having period T. The simplest example of such an equation is the second order Mathieu equation[3]. Important progress in the study of such systems was made by the mathematician Gaston

---

[1] One could also have a particle moving on a plane while attached to walls via springs.

[2] The double pendulum will continue to give us company in Chap. 15, where we will examine large amplitude and chaotic oscillations in the double pendulum.

[3] Émile Mathieu encountered this equation in the somewhat different context of vibrations of the elliptical disk-shaped membrane of a drum.

Floquet who studied linear differential equations with periodic coefficients in his PhD dissertation and thereafter (1879-1884), and whose name is associated with this theory. Interestingly, the same kinds of equations also arise in the quantum mechanical study of particle motion in a periodic potential, as in Felix Bloch's 1928 analysis of electron motion in a crystal lattice, in the context of electrical conduction in solids. To understand the (linear) stability of a periodic orbit, we examine the evolution of a trajectory that begins nearby, i.e., whether it oscillates around the orbit, approaches it or wanders away from it. In the small deviation approximation, this is encoded in a time evolution matrix. Of particular interest is the question of where a trajectory that begins nearby ends up after one time period T of the unperturbed orbit. This information is packaged in a matrix M called the monodromy[4] matrix, which is a linear map on the tangent space at the start of the periodic orbit. Composing the monodromy matrix with itself (M^2) allows us to determine the fate of the perturbed solution after time $2T$ and so on. The analogs of normal modes are played by the eigenvectors of the monodromy matrix. The stability of the periodic solution is then determined by studying the spectrum of M: roughly, eigendirections corresponding to eigenvalues of magnitude less than unity are stable and those corresponding to eigenvalues of magnitude greater than unity are unstable.

These general constructions are then illustrated in Sect. 13.4.5* by examining the Kapitza pendulum, which is a simple pendulum with its rod attached to a support that oscillates either vertically or horizontally. The oscillation of the support is regarded as the unperturbed periodic motion, while the swinging of the pendulum is the small perturbation. For sinusoidal vertical oscillations, it turns out that the linearized equations reduce to the second order Mathieu equation. By studying its monodromy matrix, we find that this vertical oscillation of the pivot can render a Kapitza pendulum unstable via a mechanism that should remind us of parametric resonance from Sect. 6.10. Even more surprisingly, we show that an inverted pendulum (with bob pointing up) can be stabilized through a vertical vibration of the support[5].

13.1 Elementary examples of coupled small oscillations

13.1.1 Normal modes of two weakly coupled pendula undergoing small oscillations

Consider a pair of identical plane pendula of length ℓ and bob mass m. From Sect. 1.5, *small* oscillations of the deflection angles θ_1 and θ_2 are governed by the EOM

$$m\ell\ddot{\theta}_1 = -mg\theta_1 \quad \text{and} \quad m\ell\ddot{\theta}_2 = -mg\theta_2 \tag{13.1}$$

in the angular (tangential) directions. Now, we let the pendula interact weakly[6] by connecting their bobs by a spring with force constant k whose natural length is equal to the distance between the two supports (see Fig. 13.1).

---

[4] Monodromy comes from the Greek words $\mu o\nu \acute{o}\varsigma$ (single) and $\delta\rho\acute{o}\mu\iota o$ (road or racecourse).

[5] In a somewhat similar spirit, it is possible to balance a stick vertically on one's palm through rapid horizontal movements of the palm. On the other hand, the downward-hanging pendulum is unstable if the pivot oscillates rapidly in a horizontal direction (it cannot oscillate stably about the downward vertical). However, in the latter case, there is a nonzero acute angle (relative to the vertical) about which such a pendulum can stably oscillate [106].

[6] Replacing the spring by a rigid rod would result in a 'strong' interaction between pendula.

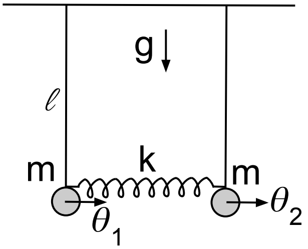

Figure 13.1: First (left) and second (right) pendula coupled by a spring.

Suppose the 2^{nd} pendulum swings to the right slightly ($\theta_2 > 0$) while $\theta_1 = 0$. Then, the spring expands by a length $\approx \ell\theta_2$ and exerts a force $\approx k\ell\theta_2$ to the right on the 1^{st} pendulum and an equal and opposite force $\approx k\ell\theta_2$ to the left on the 2^{nd} pendulum. Similarly, if $\theta_2 = 0$ and $\theta_1 > 0$, then there is a leftward force $\approx k\ell\theta_1$ on the 1^{st} pendulum and an equal and opposite rightward force of approximate magnitude $k\ell\theta_1$ on the 2^{nd}. By the superposition principle, the EOM of the coupled pendula are:

$$\begin{aligned} m\ell\ddot{\theta}_1 &= -mg\theta_1 - k\ell(\theta_1 - \theta_2) \quad \text{and} \\ m\ell\ddot{\theta}_2 &= -mg\theta_2 + k\ell(\theta_1 - \theta_2). \end{aligned} \tag{13.2}$$

Introducing $\omega = \sqrt{g/\ell}$ and $\tilde{\omega} = \sqrt{k/m}$, we get the linear equations of motion

$$\ddot{\theta}_1 + (\omega^2 + \tilde{\omega}^2)\theta_1 = \tilde{\omega}^2\theta_2 \quad \text{and} \quad \ddot{\theta}_2 + (\omega^2 + \tilde{\omega}^2)\theta_2 = \tilde{\omega}^2\theta_1. \tag{13.3}$$

The terms on the RHS couple the equations. The evolution of θ_1 depends on θ_2 and vice-versa. The degrees of freedom or ‘modes’ θ_1 and θ_2 are coupled.

Normal modes are variables built from θ_1 and θ_2 that evolve independently of each other. It is easy to find normal modes in this example: we simply add and subtract the two equations. If we denote $\theta_+ = \theta_1 + \theta_2$ and $\theta_- = \theta_1 - \theta_2$, then

$$\ddot{\theta}_+ + \omega^2\theta_+ = 0 \quad \text{and} \quad \ddot{\theta}_- + (\omega^2 + 2\tilde{\omega}^2)\theta_- = 0. \tag{13.4}$$

We see that $\theta_\pm$ evolve independently: they are normal modes of our coupled pendula. Each satisfies the equation for a harmonic oscillator (6.2) with the solutions

$$\theta_+(t) = A_+\cos(\omega t + \phi_+) \quad \text{and} \quad \theta_-(t) = A_-\cos\left(\sqrt{\omega^2 + 2\tilde{\omega}^2}t + \phi_-\right). \tag{13.5}$$

Here, $\phi_\pm$ are a pair of initial phases. Each of the normal modes is periodic in time, but the time periods $T_+ = 2\pi/\omega$ for θ_+ and $T_- = 2\pi/\sqrt{\omega^2 + 2\tilde{\omega}^2}$ for θ_- are distinct as long as $\tilde{\omega} \neq 0$. What is the pattern of oscillation in each of the normal modes?

1. In the θ_+ normal mode, ICs are such that $A_- = 0$ so that $\theta_1 - \theta_2 = 0$ at all times. Thus, both deflection angles are always equal, the pendula swing ‘in phase’ and the spring is never compressed nor elongated. The frequency and time period are the same as for the uncoupled pendula.

2. In the θ_- normal mode, ICs are such that $A_+ = 0$ so that $\theta_1 = -\theta_2$ at all times. The pendula are 'out of phase': they swing in opposite directions with the same amplitude. The angular frequency $\sqrt{\omega^2 + 2\tilde{\omega}^2}$ exceeds that of the individual pendula since the spring is either compressed or elongated leading to a larger restoring force compared to when gravity alone acts. The factor of 2 arises because both bobs simultaneously compress or expand the spring in the θ_- normal mode.

For other initial conditions, both normal modes are excited. In fact, due to the linearity of the EOM, the general solution is a linear combination of normal modes:

$$\begin{aligned}\theta_1 &= \frac{1}{2}(\theta_+ + \theta_-) = (A_+/2)\cos(\omega t + \phi_+) + (A_-/2)\cos\left(\sqrt{\omega^2 + 2\tilde{\omega}^2}t + \phi_-\right), \\ \theta_2 &= \frac{1}{2}(\theta_+ - \theta_-) = (A_+/2)\cos(\omega t + \phi_+) - (A_-/2)\cos\left(\sqrt{\omega^2 + 2\tilde{\omega}^2}t + \phi_-\right)\end{aligned} \quad (13.6)$$

It is natural to ask if the general solution is periodic. If the ratio of T_+/T_- is rational, say p/q where p, q are coprime positive integers, then both θ_1 and θ_2 are periodic with period given by the least common integer multiple $T = qT_+ = pT_-$. On the other hand, if T_+ and T_- are incommensurate (i.e., T_+/T_- is irrational or $T_\pm$ linearly independent over the integers) then the resulting motion is not periodic[7] and it is as though the least common integer multiple has gone to infinity. Such motion is called quasiperiodic (or conditionally periodic): a linear superposition of incommensurate periodic motions. In the incommensurate case, although the motion is not periodic, $\theta_{1,2}$ will return to values arbitrarily close to their initial values if we wait long enough. This is because the irrational ratio T_+/T_- can be approximated to any desired precision by the ratio p/q of sufficiently large coprime positive integers p and q.

13.1.2 Normal modes of a diatomic molecule

Next, we consider small longitudinal oscillations (without collisions) of a diatomic molecule modeled as a pair of point particles (each of mass m) connected by a spring with force constant k. As shown in Fig. 13.2, we will choose the x-axis along the 'longitudinal' direction defined by the line from the first mass to the second mass in the undisturbed equilibrium state. The undisturbed equilibrium positions of the masses are denoted $\bar{x}_1$ and $\bar{x}_2$ (which are independent of time) with $\bar{x}_2 - \bar{x}_1$ being the natural length of the spring.

For simplicity, we restrict to small oscillations along the x axis. If the first mass moves to the right, the spring is compressed resulting in a restoring force on it pointing to the left. If the second mass moves to the right, the spring is expanded and the restoring force on the first mass acts to the right. Thus, by Hooke's law we get the equation of motion for x_1:

$$m\ddot{x}_1 = -k(x_1 - \bar{x}_1) + k(x_2 - \bar{x}_2). \quad (13.7)$$

Similarly, the EOM for x_2 is given by

$$m\ddot{x}_2 = k(x_1 - \bar{x}_1) - k(x_2 - \bar{x}_2). \quad (13.8)$$

---

[7] See Footnote 24 of Chap. 2.

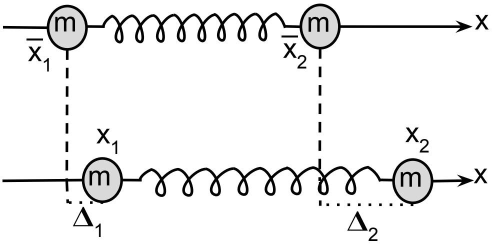

Figure 13.2: *Undisturbed* (upper) and *disturbed* (lower) configurations of a diatomic molecule executing small oscillations. The first mass is the one to the left.

This formula is consistent with Newton's 3rd law, which implies that the force on the first mass due to a small displacement of the second must be equal and opposite to the force on the second. These are a pair of coupled inhomogeneous linear ODEs for x_1 and x_2. It would be nice to decouple them by passing to suitable normal modes.

Since $\ddot{\bar{x}}_{1,2} = 0$, the equations only involve the departures from equilibrium locations. So we introduce the variables $\Delta_1 = x_1 - \bar{x}_1$ and $\Delta_2 = x_2 - \bar{x}_2$, in terms of which the EOM become

$$m\ddot{\Delta}_1 = -k(\Delta_1 - \Delta_2) \quad \text{and} \quad m\ddot{\Delta}_2 = k(\Delta_1 - \Delta_2). \tag{13.9}$$

These are a pair of coupled homogeneous linear equations for $\Delta_1(t)$ and $\Delta_2(t)$. We may obtain uncoupled equations by introducing analogs of center of mass and relative variables $\Delta_+ = \Delta_1 + \Delta_2$ and $\Delta_- = \Delta_1 - \Delta_2$. These satisfy the equations

$$\ddot{\Delta}_+ = 0 \quad \text{and} \quad \ddot{\Delta}_- = -2(k/m)\Delta_-. \tag{13.10}$$

$\Delta_\pm$ are normal modes of our diatomic molecule. Each evolves independently of the other, so ICs may be chosen so that only one of the normal modes is excited.

The normal mode Δ_+ is called a *zero mode* since it has zero angular frequency ω_+ when written as $\ddot{\Delta}_+ + \omega_+^2\Delta_+ = 0$. It displays the dynamics of a free particle. Moreover, in this mode, $\Delta_- = 0$, so $\Delta_1 = \Delta_2$ and therefore, $x_1 - \bar{x}_1$ and $x_2 - \bar{x}_2$ are equal at all times. Thus, the two masses move together uniformly either to the right or left. Hence, in the Δ_+ 'translational' mode, the molecule as a whole moves uniformly without any internal vibration.

The normal mode Δ_- is oscillatory with angular frequency $\omega_- = \sqrt{2k/m}$. In this mode, $\Delta_+ = \Delta_1 + \Delta_2 = 0$, so the two masses move in opposite directions, either both compressing or expanding the spring. This results in double the restoring force that would arise if just one mass was compressing/expanding the spring. In this mode, the molecule as a whole is at rest and displays purely vibrational motion.

13.2 Double pendulum: formulation and small oscillations

The double pendulum (see Fig. 13.3) is a delightfully simple system with rich dynamics, that serves as a model for conservative coupled oscillations. It can be assembled in the lab or at home and is fun to play with. We shall use it to illustrate methods we have encountered, as well as new ones. The double pendulum is an autonomous Hamiltonian system with a minimal number of degrees of freedom displaying both regular and chaotic dynamics (see Sect. 15.4) in various energy regimes. As a general rule of thumb, if a system admits more conserved quantities, then the dynamics is more restricted[8] and may display more regularity (an extreme case is integrability as described in Sect. 11.7*). A system with 2 degrees of freedom has a 4d phase space. If the Hamiltonian (energy) H is conserved, the trajectory must lie on a 3d constant energysubmanifold (hypersurface) of phase space, determined by initial conditions[9]. If there is another conserved quantity C functionally independent of energy, then each trajectory must lie on the intersection of a constant H and constant C submanifold, which is in general a 2d surface in phase space. We see that the presence of more conserved quantities restricts the dynamics.

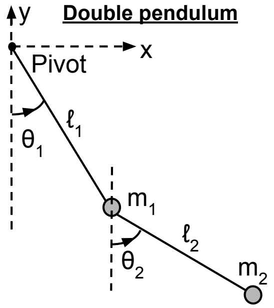

Figure 13.3: Double pendulum with two bobs of masses m_1, m_2 suspended from a fixed support with massless rods of lengths l_1, l_2 free to move in a vertical (x-y) plane.

13.2.1 Energy, Lagrangian and equations of motion

We consider a double pendulum with ‘lower’ bob of mass m_2 suspended by a massless rod of length l_2 from an ‘upper’ bob of mass m_1 which is in turn suspended from a fixed pivot by a massless rod of length l_1 (see Fig. 13.3). The system has 2 degrees of freedom, it is free to move in a vertical plane subject to gravity. The rods make angles θ_1 and θ_2 counterclockwise relative to the downward vertical. The Cartesian coordinates of the two bobs are $\boldsymbol{r}_1 = (x_1, y_1)$ and $\boldsymbol{r}_2 = (x_2, y_2)$ where

---

[8] A conserved quantity reduces the dimension of the available phase space that a trajectory can explore. A weaker but more general possibility is the existence of an invariant hypersurface in phase space that separates the latter into an ‘inside’ and an ‘outside’. Such an invariant surface can place restrictions on trajectories [E.g., an invariant circle on a plane prevents trajectories beginning inside from going outside and forces trajectories that begin on the circle to remain on it.]. The KAM theorem of Sect. 11.7* guarantees the existence of invariant toroidal submanifolds in the phase space of a system whose Hamiltonian differs from that of an integrable system by a (usually nonintegrable) small perturbation. However, these invariant tori need not always separate the phase space into disconnected regions [E.g., a circle in $\mathbb{R}^3$ does not divide it into an inside and an outside.]. Note that the equations of linear systems are typically solvable through a passage to normal modes, as we shall demonstrate for small oscillations of a double pendulum.

[9] Even if the system does not possess any conserved quantity, a given trajectory may not explore (almost) the whole of the phase space due to dynamical barriers. See Fig. 15.15 for examples of a few possibilities on a ‘Poincaré surface’ within an energy hypersurface.

$$\begin{aligned} x_1 &= l_1 \sin\theta_1 \quad \text{and} \quad y_1 = -l_1\cos\theta_1 \quad \text{while} \\ x_2 &= l_1\sin\theta_1 + l_2\sin\theta_2 \quad \text{and} \quad y_2 = -l_1\cos\theta_1 - l_2\cos\theta_2. \end{aligned} \tag{13.11}$$

Assuming that the potential energy vanishes when both bobs hang downwards ($\theta_1 = \theta_2 = 0$), the potential and kinetic energies are (see Prob. 13.5)

$$\begin{aligned} V &= -m_1 g l_1(\cos\theta_1 - 1) - m_2 g[l_1(\cos\theta_1 - 1) + l_2(\cos\theta_2 - 1)] \quad \text{and} \\ T &= \frac{m_1}{2}\left(\dot{x}_1^2 + \dot{y}_1^2\right) + \frac{m_2}{2}\left(\dot{x}_2^2 + \dot{y}_2^2\right) \\ &= \frac{m_1}{2} l_1^2\dot{\theta}_1^2 + \frac{m_2}{2}\left[l_1^2\dot{\theta}_1^2 + l_2^2\dot{\theta}_2^2 + 2l_1 l_2 c_{12}\dot{\theta}_1\dot{\theta}_2\right]. \end{aligned} \tag{13.12}$$

We abbreviated $\sin(\theta_1 - \theta_2) = s_{12}$ and $\cos(\theta_1 - \theta_2) = c_{12}$. For simplicity, we take bobs of equal masses m and rods of equal length l. In this case, $0 \le V \le 6mgl$ while $0 \le T < \infty$. The configuration space of the double pendulum is a 2-torus, the Cartesian product of circles: $\mathbb{T}^2 = S^1 \times S^1$ with θ_1 and θ_2 each specifying a point on a circle S^1. The Lagrangian is $T - V$:

$$L = \frac{ml^2}{2}\left[2\dot{\theta}_1^2 + \dot{\theta}_2^2 + 2c_{12}\dot{\theta}_1\dot{\theta}_2\right] + mgl\left[2\cos\theta_1 + \cos\theta_2\right] - 3mgl. \tag{13.13}$$

The momenta conjugate to θ_1 and θ_2 are

$$p_1 = \frac{\partial L}{\partial\dot{\theta}_1} = ml^2\left[2\dot{\theta}_1 + c_{12}\dot{\theta}_2\right] \quad \text{and} \quad p_2 = \frac{\partial L}{\partial\dot{\theta}_2} = ml^2\left[\dot{\theta}_2 + c_{12}\dot{\theta}_1\right]. \tag{13.14}$$

The phase space of the double pendulum is four-dimensional, with coordinates $\theta_1 \in S^1, \theta_2 \in S^1$ and $p_1, p_2 \in \mathbb{R}$. It is the Cartesian product of a 2-torus $\mathbb{T}^2 = S^1 \times S^1$ and a plane $\mathbb{R}^2$ and may be regarded as the cotangent bundle (see Footnote 2 of Sect. 10.3*) of the 2-torus. The conjugate momenta do not coincide with the angular momenta [$\boldsymbol{L}_a = m\boldsymbol{r}_a \times \dot{\boldsymbol{r}}_a$ for $a = 1, 2$] of the individual bobs:

$$\boldsymbol{L}_1 = ml^2\dot{\theta}_1\,\hat{z} \quad \text{and} \quad \boldsymbol{L}_2 = ml^2[(1 + c_{12})(\dot{\theta}_1 + \dot{\theta}_2)]\hat{z}. \tag{13.15}$$

However, they are related. For instance, their sum is the z-component of the total angular momentum: $\boldsymbol{L} = \boldsymbol{L}_1 + \boldsymbol{L}_2 = (p_1 + p_2)\hat{z}$. The 'generalized forces' are

$$\frac{\partial L}{\partial\theta_1} = -ml\left[2g\sin\theta_1 + ls_{12}\,\dot{\theta}_1\dot{\theta}_2\right] \quad \& \quad \frac{\partial L}{\partial\theta_2} = ml\left[ls_{12}\,\dot{\theta}_1\dot{\theta}_2 - g\sin\theta_2\right]. \tag{13.16}$$

Lagrange's equations of motion are the pair of 2nd order nonlinear ODEs

$$2\ddot{\theta}_1 + c_{12}\ddot{\theta}_2 + s_{12}\dot{\theta}_2^2 + 2\omega^2\sin\theta_1 = 0 \qquad \text{and} \qquad \ddot{\theta}_2 + c_{12}\ddot{\theta}_1 - s_{12}\dot{\theta}_1^2 + \omega^2\sin\theta_2 = 0. \tag{13.17}$$

They involve only one[10] material parameter, the frequency $\omega = \sqrt{g/l}$. Upon expressing the generalized velocities in terms of momenta,

$$\dot\theta_1 = \frac{p_1 - c_{12}p_2}{ml^2(1+s_{12}^2)} \quad \text{and} \quad \dot\theta_2 = \frac{2p_2 - c_{12}p_1}{ml^2(1+s_{12}^2)}, \tag{13.18}$$

we find the conserved Hamiltonian $H = p_1\dot\theta_1 + p_2\dot\theta_2 - L = T + V$:

$$H = \frac{p_1^2 + 2p_2^2 - 2c_{12}p_1p_2}{2ml^2(1+s_{12}^2)} - mgl[2\cos\theta_1 + \cos\theta_2] + 3mgl. \tag{13.19}$$

The remaining pair of Hamilton's equations are

$$\begin{aligned} \dot p_1 &= f - 2mgl\sin\theta_1 \quad \text{and} \quad \dot p_2 = -f - mgl\sin\theta_2 \quad \text{where} \\ f &= \frac{s_{12}}{ml^2(1+s_{12}^2)^2}\left[c_{12}(p_1^2 + 2p_2^2) - \left(2 + c_{12}^2\right)p_1p_2\right]. \end{aligned} \tag{13.20}$$

The conserved energy may also be expressed in terms of coordinates and velocities:

$$E = \frac{1}{2}ml^2\left[2\dot\theta_1^2 + \dot\theta_2^2 + 2c_{12}\dot\theta_1\dot\theta_2\right] - mgl[2\cos\theta_1 + \cos\theta_2] + 3mgl. \tag{13.21}$$

The energy is minimal ($E = 0$) when the bobs are at rest at the stable equilibrium configuration $\theta_1 = \theta_2 = 0$.

13.2.2 Normal modes of a double pendulum

Aside from the energy, the double pendulum does not possess any other obvious conserved quantity. In fact, we will argue in Sect. 15.4 that it *cannot* have any other conserved quantity. In the absence of additional conserved quantities, the double pendulum is not Liouville integrable in the sense of Sect. 11.7* and it has not been possible to reduce its equations of motion (EOM) to quadratures. Unsurprisingly, it has not been possible to solve the EOM of a double pendulum in closed form (not even with elliptic or other such special functions!). However, if the deflection angles are always small, we may linearize the EOM around the stable equilibrium state and solve them. An extra conserved quantity emerges in this limit and the motion reduces to the integrable dynamics of a pair of coupled harmonic oscillators. Let us see why.

If both $|\theta_1|, |\theta_2| \ll 1$, we may approximate the trigonometric functions $\cos$ and $\sin$ by their quadratic Taylor polynomials in the kinetic and potential energies, so that the resulting equations of motion become linear. The Lagrangian becomes

$$L = \frac{1}{2}ml^2\left[2\dot\theta_1^2 + \dot\theta_2^2 + 2\dot\theta_1\dot\theta_2\right] - mgl\left[\theta_1^2 + \frac{1}{2}\theta_2^2\right] = T - V. \tag{13.22}$$

---

[10] This means solutions to the equations of motion are independent of the mass m of the bobs and can depend on g and l only through the combination g/l. In other words, we may double the lengths of the rods and double the strength of gravity without affecting the nature of the motion. The appearance of m in H is because we have rescaled it to have dimensions of energy.

The conjugate momenta are

$$p_1 = ml^2\left(2\dot{\theta}_1 + \dot{\theta}_2\right) \quad \text{and} \quad p_2 = ml^2\left(\dot{\theta}_1 + \dot{\theta}_2\right) \tag{13.23}$$

and the angular velocities of the bobs are

$$\dot{\theta}_1 = (1/ml^2)(p_1 - p_2) \quad \text{and} \quad \dot{\theta}_2 = (1/ml^2)(2p_2 - p_1). \tag{13.24}$$

As in (13.17), the EOM depend only on one physical parameter $\omega^2 = g/l$:

$$2\ddot{\theta}_1 + \ddot{\theta}_2 + 2\omega^2\theta_1 = 0 \quad \text{and} \quad \ddot{\theta}_1 + \ddot{\theta}_2 + \omega^2\theta_2 = 0. \tag{13.25}$$

The corresponding conserved energy is $H = T + V$ with V from (13.22):

$$H = \frac{ml^2}{2}\left[2\dot{\theta}_1^2 + \dot{\theta}_2^2 + 2\dot{\theta}_1\dot{\theta}_2\right] + V = \frac{1}{2ml^2}\left[p_1^2 + 2p_2^2 - 2p_1p_2\right] + V. \tag{13.26}$$

The EOM are now a pair of *coupled* second order *linear* ODEs with constant coefficients. Since the equations are linear, it is reasonable to expect that we can make a linear change of variables from θ_1, θ_2 to a new pair of 'normal mode' variables $\xi_\pm(\theta_1, \theta_2)$ which satisfy a pair of *uncoupled* linear ODEs. The mathematical tools to effect this transformation come from linear algebra.

Linear algebraic method to find normal modes. Let us first write the equations of motion in matrix form:

$$\frac{d^2}{dt^2}\begin{pmatrix} 2 & 1 \\ 2 & 2 \end{pmatrix}\begin{pmatrix} \theta_1 \\ \theta_2 \end{pmatrix} = -2\omega^2\begin{pmatrix} \theta_1 \\ \theta_2 \end{pmatrix}. \tag{13.27}$$

If we let B be the constant coefficient matrix,

$$B = \begin{pmatrix} 2 & 1 \\ 2 & 2 \end{pmatrix} \quad \text{and} \quad \theta = \begin{pmatrix} \theta_1 \\ \theta_2 \end{pmatrix}, \quad \text{then} \quad \frac{d^2}{dt^2}(B\theta) = -2\omega^2\theta. \tag{13.28}$$

The matrix B has distinct eigenvalues $\lambda_\pm = 2 \pm \sqrt{2}$, and therefore can be diagonalized by a similarity transformation[11] (see Appendix A.10). The eigenvectors corresponding to these eigenvalues may be taken as

$$a_+ = \frac{1}{2}\begin{pmatrix} 1 \\ \sqrt{2} \end{pmatrix} \quad \text{and} \quad a_- = \frac{1}{2}\begin{pmatrix} 1 \\ -\sqrt{2} \end{pmatrix}. \tag{13.29}$$

---

[11] Readers acquainted with elementary quantum mechanics would be familiar with symmetric or Hermitian matrices which model observables of quantum systems. They have real eigenvalues and can be diagonalized by orthogonal or unitary transformations. In classical mechanics, the coefficient matrix B of a linear system need not be real symmetric or even normal (B does not commute with its transpose) with respect to the Euclidean inner product. As a consequence, the eigenvectors of B are generally not pairwise orthogonal and the similarity transformation S that diagonalizes it is typically not orthogonal. Unlike in quantum mechanics, orthogonality or the lack thereof does not have a direct physical significance here. Interestingly, as we will see in Sect. 13.3*, B is invariably the 'quotient' of two symmetric matrices.

The eigenvectors $a_\pm$ are technical tools to help us diagonalize B. They will help us find the physically significant normal modes, which evolve independently of each other. A similarity transformation that diagonalizes B may be represented by a matrix S whose columns are the eigenvectors of B:

$$S^{-1}BS = D \quad \text{where} \quad S = \frac{1}{2}\begin{pmatrix} 1 & 1 \\ \sqrt{2} & -\sqrt{2} \end{pmatrix}, \quad S^{-1} = \begin{pmatrix} 1 & \frac{1}{\sqrt{2}} \\ 1 & -\frac{1}{\sqrt{2}} \end{pmatrix} \tag{13.30}$$

and $D = \text{diag}(\lambda_+, \lambda_-)$. The equations of motion may then be written

$$\frac{d^2}{dt^2} SDS^{-1}\theta = -2\omega^2\theta \quad \Rightarrow \quad D\frac{d^2}{dt^2}(S^{-1}\theta) = -2\omega^2(S^{-1}\theta). \tag{13.31}$$

Since D is a diagonal matrix, these are uncoupled equations for the components of $S^{-1}\theta$. Thus, if we denote

$$S^{-1}\theta = \xi = \begin{pmatrix} \xi_+ \\ \xi_- \end{pmatrix} = \begin{pmatrix} \theta_1 + \frac{\theta_2}{\sqrt{2}} \\ \theta_1 - \frac{\theta_2}{\sqrt{2}} \end{pmatrix} \quad \text{and} \quad 2\omega^2 D^{-1} = \begin{pmatrix} \frac{2\omega^2}{\lambda_+} & 0 \\ 0 & \frac{2\omega^2}{\lambda_-} \end{pmatrix} = \begin{pmatrix} \omega_+^2 & 0 \\ 0 & \omega_-^2 \end{pmatrix}, \tag{13.32}$$

then the components $\xi_\pm$ evolve via *decoupled* 2^{nd} order linear ODEs:

$$\ddot{\xi}_+(t) = -\omega_+^2\xi_+(t) \quad \text{and} \quad \ddot{\xi}_-(t) = -\omega_-^2\xi_-(t) \quad \text{where} \quad \omega_\pm^2 = \frac{2\omega^2}{\lambda_\pm}. \tag{13.33}$$

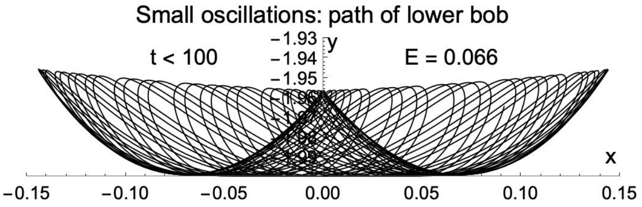
Small oscillations: path of lower bob

Figure 13.4: Small oscillations of a double pendulum governed by (13.25) for $m = l = g = 1$ [starting from rest at $\theta_1(0) = -\theta_2(0) = \pi/15$]. (a) Trajectory (locus) of the lower bob on the vertical x, y plane of Fig. 13.3 for $0 \leq t \leq 100$. The trajectory of the 'upper' bob is not shown, it simply lies on the arc of a circle. Note that the trajectory of the bob can intersect itself on the plane of the pendulum's oscillations but not on phase space. It shows aperiodic but quasiperiodic and visually 'regular' motion.

Basic features of normal modes. The decoupled angles $\xi_\pm(t)$ are called normal modes of the system. The significance of normal modes is that they evolve independently of each other and since the evolution equations are linear, they furnish a basis in which to express the general solution. For instance, if the pendulum is set into motion with an excitation along the ξ_+ mode, subsequent evolution (in the small angle approximation) will be such that $\xi_- = \theta_1 - \theta_2/\sqrt{2}$ always remains zero. In this pattern of oscillation, the deflection angle of the lower bob θ_2 is always $\sqrt{2}$ times that of the upper bob, with both being either clockwise or counterclockwise at any instant of time. From (13.33), the normal mode solutions $\xi_\pm(t)$ are periodic functions of time with time periods

$$T_\pm = \frac{2\pi}{\omega_\pm} = \frac{2\pi}{\omega}\sqrt{1 \pm \frac{1}{\sqrt{2}}}. \tag{13.34}$$

Furthermore, they may be expressed in terms of trigonometric functions

$$\xi_+(t) = c_1\cos(\omega_+ t) + c_2 \sin(\omega_+ t) \quad \text{and} \quad \xi_-(t) = c_3\cos(\omega_- t) + c_4\sin(\omega_- t). \tag{13.35}$$

The four coefficients c_i are to be fixed using the initial conditions. The original deflection angles are determined via $\theta = S\xi$:

$$\theta_1 = \frac{1}{2}\left(\xi_+ + \xi_-\right) \quad \text{and} \quad \theta_2 = \frac{1}{\sqrt{2}}\left(\xi_+ - \xi_-\right). \tag{13.36}$$

Thus, we have arrived at the general solution to the IVP for small oscillations of a double pendulum. Note that the general motion of the double pendulum in the small angle approximation is not periodic (see Fig. 13.4). In (13.36), $\theta_{1,2}$ are linear combinations of periodic functions whose periods are not in rational ratio:

$$\frac{T_+}{T_-} = \frac{\omega_-}{\omega_+} = \sqrt{\frac{\lambda_+}{\lambda_-}} = 1 + \sqrt{2} \notin \mathbb{Q}. \tag{13.37}$$

The resulting motion of each bob is called *quasiperiodic* (see Footnote 24 of Chap. 2). If the ratio of periods were rational, then any linear combination would be periodic with a period given by the least common multiple of T_+ and T_-. One consequence of quasiperiodicity is that the double pendulum, in general, does not return to its initial state, but approaches it arbitrarily closely if we are willing to wait long enough (see Fig. 13.5). However, if initial conditions are chosen so that only one of the two normal modes ξ_+ or ξ_- is present (e.g., if $c_3 = c_4 = 0$), then the motion is periodic.

Conserved energies of normal modes. We may use the normal modes to find a new conserved quantity for small oscillations of a double pendulum. As for the harmonic oscillator, from (13.33)

$$\ddot{\xi}_+ = -\omega_+^2 \xi_+ \quad \text{and} \quad \ddot{\xi}_- = -\omega_-^2 \xi_-, \tag{13.38}$$

we infer that the 'energy' of each normal mode is a constant of motion[12]:

$$H_+ = \frac{1}{4} m l^2 \lambda_+ \left[\dot{\xi}_+^2 + \omega_+^2 \xi_+^2\right] \quad \text{and} \quad H_- = \frac{1}{4} m l^2 \lambda_- \left[\dot{\xi}_-^2 + \omega_-^2 \xi_-^2\right]. \tag{13.39}$$

The total energy

$$H = \frac{1}{2} m l^2 [2\dot{\theta}_1^2 + \dot{\theta}_2^2 + 2\dot{\theta}_1\dot{\theta}_2] + mgl[\theta_1^2 + \frac{1}{2}\theta_2^2] \tag{13.40}$$

---

[12] The constant pre-factors $ml^2\lambda_\pm$ have been chosen to ensure that $H_\pm$ have dimensions of energy and so that we may interpret $H_+ + H_-$ as the total energy. The need for the weights $\lambda_\pm$ may be anticipated from the appearance of $D = \text{diag}(\lambda_1, \lambda_2)$ on the LHS of (13.31). Upon writing ω in terms of $\omega_\pm$, $\lambda_\pm$ emerge as pre-factors in the energy expressions.

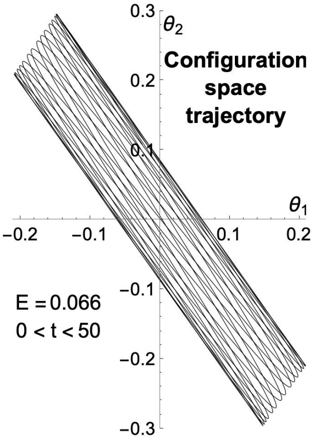

Figure 13.5: Trajectory on the θ_1-θ_2 configuration space showing quasiperiodic small oscillations of a double pendulum (13.25) for $m = l = g = 1$ [starting from rest at $\theta_1(0) = -\theta_2(0) = \pi/15$]. Poincaré sections give another insightful way of visualizing trajectories in phase space. See Fig. 15.12 of Chap. 15 and the accompanying discussion for the Poincaré section of a quasiperiodic trajectory of small oscillations of a double pendulum.

is of course also conserved. Are H, H_+ and H_- functionally independent? This is unlikely since we would expect the total energy to be a sum of energies contributed by the various normal modes, which do not interact with each other. In fact, we will show that $H = H_+ + H_-$. To see this, we write H as a quadratic form and then express θ_i in terms of normal modes $\xi_\pm$. To begin with,

$$\begin{aligned} H &= \frac{ml^2}{2} \begin{pmatrix} \dot\theta_1 \\ \dot\theta_2 \end{pmatrix}^t \begin{pmatrix} 2 & 1 \\ 1 & 1 \end{pmatrix} \begin{pmatrix} \dot\theta_1 \\ \dot\theta_2 \end{pmatrix} + mgl \begin{pmatrix} \theta_1 \\ \theta_2 \end{pmatrix}^t \begin{pmatrix} 1 & 0 \\ 0 & \frac{1}{2} \end{pmatrix} \begin{pmatrix} \theta_1 \\ \theta_2 \end{pmatrix} \\ &= \frac{ml^2}{2} \dot\theta^t \tau \dot\theta + mgl\, \theta^t v \theta \quad \text{where } \tau = \begin{pmatrix} 2 & 1 \\ 1 & 1 \end{pmatrix} \text{ and } v = \begin{pmatrix} 1 & 0 \\ 0 & \frac{1}{2} \end{pmatrix}. \end{aligned} \tag{13.41}$$

The kinetic and potential matrices τ and v are not uniquely defined. We may add any antisymmetric matrices to τ and v without affecting the formula for energy. However, we will take them to be symmetric, which is necessary to ensure that (a) τ and v are uniquely defined, (b) Lagrange's equations[13] may be written as in (13.42) and (c) the diagonalization formulae (13.43) hold.

Diagonalization of τ and v. Now recall that S was the similarity transformation (13.30) that diagonalized the coefficient matrix $S^{-1}BS = D$ in the EOM (13.28)

---

[13] The associated Lagrangian and equations of motion for small oscillations are

$$L(\theta, \dot\theta) = \frac{ml^2}{2} \dot\theta^t \tau \dot\theta - mgl\, \theta^t v \theta \quad \text{and} \quad ml^2 \tau \ddot\theta = -2mglv\theta. \tag{13.42}$$

Only the symmetric parts of τ and v contribute to L. In writing the EOM, we have assumed that τ and v are symmetric. If they are not, then they must be replaced by $(\tau + \tau^t)/2$ and $(v + v^t)/2$ in the EOM. Comparing with the EOM $B\ddot\theta = -2\omega^2\theta$ (13.28) where $\omega = \sqrt{g/l}$, we infer that $B = v^{-1}\tau = \left(\begin{smallmatrix} 2 & 1 \\ 2 & 2 \end{smallmatrix}\right)$, in agreement with (13.28).

and that the normal modes were found to be $\xi = S^{-1}\theta$. Interestingly, the kinetic and potential matrices τ and v are also diagonalized upon pre- and post-multiplication by S^t and S, i.e.,

$$S^t \tau S = D/2 = (1/2)\,\mathrm{diag}(\lambda_+, \lambda_-) \quad \text{and} \quad S^t v S = I/2. \tag{13.43}$$

This is verified in Prob. 13.10 by explicit calculation[14]. Formulae (13.43) are in fact true for any symmetric kinetic and potential matrices τ and v and any number of degrees of freedom. To see this, let us write the conserved energy in two different ways. First, from (13.31), the EOM in terms of normal modes is $D\ddot{\xi} = -2\omega^2\xi$. Taking the dot product with $\dot{\xi}$ we find that the quantity $\frac{1}{2}\dot{\xi}^t D\dot{\xi} + \omega^2\xi^t\xi$ is conserved. On the other hand, the conserved energy (13.41) is given by

$$H = (ml^2/2)\dot{\theta}^t\tau\dot{\theta} + mgl\theta^t v\theta = (ml^2/2)\dot{\xi}^t S^t\tau S\dot{\xi} + mgl\xi^t S^t v S\xi. \tag{13.44}$$

Both these conserved quantities are obtained by contracting the EOM with the velocity as an integrating factor. They are quadratic in the normal modes and their generalized velocities and contain no additive constants. Thus, they must be equal up to a multiplicative constant. This must be true for any ξ and $\dot{\xi}$ and so we deduce that

$$(ml^2/2)S^t\tau S = \mu D/2 \quad \text{and} \quad mglS^t v S = \mu(g/l)I \tag{13.45}$$

for some constant μ. In writing these formulae, we have assumed that $S^t\tau S$ and $S^t v S$ are real symmetric, which is true iff τ and v are symmetric (their antisymmetric parts do not contribute to (13.44) and therefore cannot be constrained). Inserting the numerical values and comparing any one pair of matrix elements, we find that $\mu = ml^2/2$. Physically, it is reasonable that $S^t\tau S$ and $S^t v S$ are diagonal, since the normal modes evolve independently of each other and there is no kinetic or potential energy of interaction between the normal modes.

Thus, we may write the total energy as

$$\begin{aligned} H &= \frac{ml^2}{2}\,\dot{\xi}^t\,(S^t\tau S)\,\dot{\xi} + mgl\;\xi^t\,(S^t v S)\,\xi \\ &= \lambda_+\frac{ml^2\dot{\xi}_+^2}{4} + \lambda_-\frac{ml^2\dot{\xi}_-^2}{4} + \lambda_+\frac{mgl}{2\lambda_+}\xi_+^2 + \lambda_-\frac{mgl}{2\lambda_-}\xi_-^2 = H_+ + H_-. \end{aligned} \tag{13.46}$$

In the last step, we used $\omega_\pm^2 = 2\omega^2/\lambda_\pm$ to write

$$\frac{mgl}{\lambda_\pm} = \frac{ml^2\omega^2}{\lambda_\pm} = \frac{1}{2}ml^2\,\omega_\pm^2. \tag{13.47}$$

As a consequence of (13.46), only two among H, H_1 and H_2 are independent conserved quantities. Thus, we have identified a second conserved quantity for small oscillations of a double pendulum. In the limit of low energies, the motion of a double pendulum is integrable[15] (in fact, we have found the general solution (13.35) explicitly). Before we attempt to study the dynamics of a double pendulum at higher energies in Sect. 15.4, we will discuss some general features of small oscillations around static and periodic solutions.

---

[14] The different transformation laws for B on the one hand and τ and v on the other, is attributable to the fact that while the former is a $(1,1)$ tensor, the latter are $(0,2)$ tensors (E.g., $\theta^t v\theta = v_{ij}\theta^i\theta^j$, see Appendix B.6* for the definition). This is consistent with the quotient formula $B = v^{-1}\tau$ of Footnote 13 where v^{-1} is viewed as a $(2,0)$ tensor and $B^i_k = v^{ij}\tau_{jk}$.

Remark: The EOM (13.27) may also be written as a system of four 1st order linear ODEs for the phase space variables θ_i, p_i:

$$\frac{d}{dt}\begin{pmatrix}\theta_1\\ \theta_2\\ p_1\\ p_2\end{pmatrix} = \begin{pmatrix} 0 & 0 & \frac{1}{ml^2} & -\frac{1}{ml^2}\\ 0 & 0 & -\frac{1}{ml^2} & \frac{2}{ml^2}\\ -2mgl & 0 & 0 & 0\\ 0 & -mgl & 0 & 0\end{pmatrix}\begin{pmatrix}\theta_1\\ \theta_2\\ p_1\\ p_2\end{pmatrix} \quad \text{or} \quad \frac{d\psi}{dt} = A\psi. \tag{13.48}$$

This implies that $\psi(t) = e^{At}\psi(0)$. By solving the equations of motion, we have in effect calculated the matrix exponential. □

13.3* Normal modes around a static equilibrium: general framework

In Sect. 13.2.2, we studied small oscillations of a double pendulum and discovered that the coupled motion of the two bobs could be separated by a passage to normal modes. Much of what we did can be generalized to small oscillations of systems with any (finite) number of degrees of freedom.

Linear system defined by mass and spring constant matrices. To describe the method, we consider a Lagrangian of the form $L = \frac{1}{2}g_{ij}(q)\dot{q}^i\dot{q}^j - U(q)$ where $g_{ij}(q)$ is a positive-semidefinite[16] $n \times n$ matrix on an n-dimensional configuration space and $U(q)$ is a potential energy[17]. Lagrange's equations take the form

$$\frac{d}{dt}\left(g_{ij}(q)\dot{q}^j\right) + \frac{\partial U}{\partial q^i} = 0. \tag{13.49}$$

If q_0 is an extremum of U, then $\frac{\partial U}{\partial q^i}(q_0) = 0$ and a static solution of the EOM is

$$q^i(t) \equiv q_0^i \quad (\text{so that } \dot{q}^i(t) \equiv 0). \tag{13.50}$$

For the double pendulum, $\theta_1 = \theta_2 \equiv 0$ is a static solution. If a static solution occurs at an isolated local minimum of the potential, we expect it to be stable under small perturbations, and may look for small[18]oscillations around the static solution. In this case, we expect the departure from equilibrium $x^i = q^i - q_0^i$ to remain small at all times. Consequently, the Lagrangian may be expanded to quadratic order (so that the EOM become linear) in x by Taylor expanding $g_{ij}(q)$ and $U(q)$ around $q = q_0$:

---

[15] One could attempt to include some nonlinear (anharmonic) effects in a perturbative approximation by retaining up to cubic terms in a Taylor expansion of the Hamiltonian. However, the integrability of the dynamics does not, in general, survive beyond the harmonic approximation.

[16] A positive-semidefinite real matrix is a symmetric matrix whose eigenvalues are nonnegative. It is positive-definite if the eigenvalues are strictly positive. If we do not require the matrix to be symmetric, its eigenvalues may not be real. The product of two positive-definite matrices that commute is again positive-definite while the sum of two such matrices is positive-definite irrespective of whether they commute (see Prob. 13.7).

[17] For the double pendulum of Sect. 13.2.1, $g_{ij} = ml^2 \left(\begin{smallmatrix} 2 & c_{12}\\ c_{12} & 1\end{smallmatrix}\right)$ where $c_{12} = \cos(\theta_1 - \theta_2)$ and $U(\theta) = -mgl(2\cos\theta_1 + \cos\theta_2) + 3mgl$.

$$L = \frac{1}{2} g_{ij}(q_0)\dot{x}^i\dot{x}^j - U(q_0) - \frac{1}{2}\frac{\partial^2 U(q_0)}{\partial q^i \partial q^j} x^i x^j + \mathcal{O}(x^3). \tag{13.51}$$

We may take $U(q_0) = 0$, as a constant addition to the potential U does not affect the EOM. Let us introduce the symbol $m_{ij} = g_{ij}(q_0)$ for the mass matrix and

$$k_{ij} = \frac{\partial^2 U(q_0)}{\partial q^i \partial q^j} \tag{13.52}$$

for the Hessian spring constant matrix. Like m_{ij}, the spring constant matrix k_{ij} too is symmetric. It too must be a positive-definite matrix since q_0 is a minimum of U. The Lagrangian to quadratic approximation around equilibrium is then

$$L = \frac{1}{2} m_{ij}\dot{x}^i\dot{x}^j - \frac{1}{2} k_{ij} x^i x^j. \tag{13.53}$$

For instance, small oscillations of a double pendulum[19] about the minimum energy static solution are governed by the Lagrangian (13.22) with $x = (\theta_1, \theta_2)$ and the positive-definite matrices[20]

$$M = ml^2 \begin{pmatrix} 2 & 1 \\ 1 & 1 \end{pmatrix} \quad \text{and} \quad K = mgl \begin{pmatrix} 2 & 0 \\ 0 & 1 \end{pmatrix}. \tag{13.54}$$

The corresponding equations of motion are a system of n homogeneous linear 2nd order ODEs with constant coefficients

$$m_{ij}\ddot{x}^j + k_{ij} x^j = 0 \quad \text{or} \quad M\ddot{x} = -Kx, \tag{13.55}$$

defined by a pair of real symmetric positive-definite matrices $M = m_{ij}$ and $K = k_{ij}$, which act on the vector space $V \cong \mathbb{R}^n$ in which x lives. Linearity of the equations means the space of solutions $x(t)$ is a linear space: we may add and rescale solutions by real numbers to get other solutions. This system of ODEs admits a conserved energy $E = \frac{1}{2}\dot{x}^t M \dot{x} + \frac{1}{2} x^t K x$. The momentum conjugate to x^i is $p_i = m_{ij}\dot{x}^j$. If the matrix elements of M^{-1} are denoted m^{ij} ($m^{ij} m_{jk} = \delta^i_k$), then the Hamiltonian is

$$H = (1/2) m^{ij} p_i p_j + (1/2) k_{ij} x^i x^j. \tag{13.56}$$

---

[18] Given a fault tolerance, a simple way of checking that oscillations are small is to examine whether the contribution of the ignored cubic or higher order terms to the energy of the approximate oscillatory solution lies within the desired margin of error.

[19] Comparing the equations of motion $M\ddot{x} = -Kx$ (13.55) and $B\ddot{\theta} = -2\omega^2\theta$ from (13.28) we may write the coefficient matrix B of Sect. 13.2.2 in terms of the mass and spring constant matrices of this section: $B = v^{-1}\tau = 2\omega^2 K^{-1} M$.

[20] Since k and m are already in use for the spring constant and mass of a spring with one degree of freedom, here we use capital letters M, K for the mass and spring constant matrices and the small letters m_{ij} and k_{ij} for their matrix elements.

Finding the solution $x^i(t)$ via 'separation of variables'. To find $x^i(t)$, we try to separate the time and vectorial dependences by making the ansatz $x^i(t) = v^i f(t)$ where $v^i \in \mathbb{R}^n$ is a constant vector and f a real function of time. One hopes that there are sufficiently many separable solutions to span the space of all solutions[21]. Then

$$(Mv)\ddot{f} = -(Kv)f \quad \text{or} \quad (Mv)(\ddot{f}/f) = -Kv. \tag{13.57}$$

The RHS is time-independent while the LHS depends on time via the scalar $\ddot{f}/f$. The only way for this equation to hold at all times is for $\ddot{f}/f$ to be a negative[22] constant, say $-\omega^2$. Thus, $\ddot{f} = -\omega^2 f$, leading to the solution $f = A\cos\omega t + B\sin\omega t$. Sometimes, one simply says $f \sim e^{i\omega t}$ with the understanding that the real and imaginary parts are the linearly independent real solutions. However, not all values of ω may be physically allowed. To find the legitimate ones, we notice that the vector v must satisfy a linear equation which is reminiscent of an eigenvalue problem (see Appendix A.10):

$$(-\omega^2 M + K)v = 0. \tag{13.58}$$

For nontrivial solutions v to exist, the matrix of coefficients must have zero determinant, leading to the characteristic equation for ω^2:

$$\det(-\omega^2 M + K) = 0. \tag{13.59}$$

This equation in general has n roots ω_α^2 for $\alpha = 1, 2, \cdots, n$ (including possibly repeated roots), which must all be real and positive if K and M are positive-definite matrices, as noted above. Even if we do not appeal to the positivity of M and K, physically the roots ω^2 may be argued to be positive since otherwise $\omega = \pm i\gamma$ would be purely imaginary and the independent solutions $\propto e^{\pm\gamma t}$ would either grow or decay exponentially in time and this would violate conservation of energy H (13.56). Growing solutions would also violate the stability of the static solution q_0. Alternatively, we could multiply the linear equation by M^{-1}, to get a standard eigenvalue equation[23]

$$\left(M^{-1}K\right)\, v = \omega^2 v. \tag{13.60}$$

Note that the product of two positive-definite matrices need not be positive-definite, nor even symmetric (see Prob. 13.7). Despite this, our earlier argument surrounding

---

[21] The point is that 'separable' solutions are easier to find than solutions to the initial value problem, but can be used to synthesize the latter. For systems with finitely many degrees of freedom n, any solution may be written as a linear combination of separable solutions. This will follow from the linear independence of the n normal mode eigenvectors. The corresponding question for systems with infinitely many degrees of freedom is more delicate.

[22] That the constant must be negative is seen by multiplying by v^t from the left and using the fact that both M and K are positive-definite matrices so that their diagonal matrix elements $\langle v|K|v\rangle$, $\langle v|M|v\rangle$ in the 'state' v must be positive (see Sect. 18.3* for more on Dirac's bra-ket notation.). Here, we use the result that if the eigenvalues λ_i of a symmetric matrix A are positive, then $\langle\psi|A|\psi\rangle > 0$ for any $\psi \neq 0$. This may be shown by expanding $\psi = c_i v_i$ in the orthonormal eigenbasis of A ($Av_i = \lambda_i v_i$) and noting that $\langle\psi|A|\psi\rangle = \sum_i c_i^2 \lambda_i > 0$.

[23] Assuming M is positive-definite, M^{-1} too is positive-definite, as is seen by going to the basis in which M is diagonal. M^{-1} is also diagonal in this basis, with positive eigenvalues equal to the reciprocals of those of M.

(13.57) tells us that if M and K are positive-definite, then the n eigenvalues ω_α^2 for $\alpha = 1, \dots n$ are real and positive.

Example of $M^{-1}K$: For small oscillations of a double pendulum, from (13.54),

$$M^{-1}K = \frac{1}{ml^2}\begin{pmatrix} 1 & -1 \\ -1 & 2 \end{pmatrix} mgl \begin{pmatrix} 2 & 0 \\ 0 & 1 \end{pmatrix} = \frac{g}{l}\begin{pmatrix} 2 & -1 \\ -2 & 2 \end{pmatrix}. \tag{13.61}$$

Notice that $M^{-1}K$ is not a symmetric matrix, and that M and K do not commute in this example. Yet, $M^{-1}K$ has positive eigenvalues $(g/l)(2 \pm \sqrt{2})$. □

Expanding arbitrary oscillations in normal modes. Recall that the EOM (13.55) are linear. Thus, the principle of linear superposition of solutions applies. In particular, we would like to expand a small oscillatory mode as a linear combination of the normal modes [as in (13.65)]. For this, we need to know whether $M^{-1}K$ has n linearly independent eigenvectors. Since $M^{-1}K$ may not be symmetric and its eigenvalues ω^2 (13.60) [which we have argued are real] may not be distinct[24], we wonder if it has n linearly independent eigenvectors v in the eigenvalue problem (13.60). Fortunately, it can be shown that $M^{-1}K$ is not deficient[25]. In the Remark at the end of this section, we show that there is a basis (in general not related to the original one by an orthogonal transformation) in which M is the identity and K is symmetric, so that the eigenvalue problem (13.60) reduces to that for a symmetric matrix[26]. Thus, we are guaranteed that n linearly independent eigenvectors ['normal modes' $v_{(\alpha)}$] exist, corresponding to the n real and positive eigenvalues

$$\omega_\alpha^2 = \langle v_{(\alpha)}|K|v_{(\alpha)}\rangle / \langle v_{(\alpha)}|M|v_{(\alpha)}\rangle. \tag{13.62}$$

Since $M^{-1}K$ may not be symmetric, the $v_{(\alpha)}$ may not be orthogonal[27], as we found for the double pendulum. Thus, we have n normal modes of small oscillations with eigenfrequencies ω_α for $\alpha = 1, 2, \dots, n$:

$$\xi_{(\alpha)}(t) = v_{(\alpha)}\left[c_1^{(\alpha)}\cos(\omega_\alpha t) + c_2^{(\alpha)}\sin(\omega_\alpha t)\right] \qquad \text{(no sum on } \alpha\text{)}. \tag{13.63}$$

Physically, the vector $v_{(\alpha)}$ for each α is a direction in the tangent space[28] to the configuration space at the equilibrium point q_0. The corresponding normal mode is an oscillation in that direction. Here, $c_{1,2}^{(\alpha)}$ are constants of integration. In terms of the normal modes, the equations of motion decouple for each eigenfrequency,

---

[24] An $n \times n$ matrix with distinct eigenvalues is guaranteed to have n linearly independent eigenvectors. To see this, recall from Footnote 9 of Chap. 6 that corresponding to each eigenvalue, there is at least one eigenvector and that eigenvectors corresponding to distinct eigenvalues are linearly independent.

[25] An $n \times n$ matrix is deficient if it does not have n linearly independent eigenvectors. A necessary (but not sufficient) condition for a matrix to be deficient, is for it to have at least one repeated eigenvalue.

[26] Symmetry/lack of symmetry of a matrix is not always preserved by a change of basis. For instance, nonorthogonal transformations can convert some nonsymmetric matrices into symmetric ones. See Prob. 13.13 for explicit examples.

[27] The $v_{(\alpha)}$ can be chosen orthogonal if M and K commute, so that $M^{-1}K$ is symmetric.

[28] The eigenvectors can be taken to be real. This is because $M^{-1}K$ is a real matrix and the eigenvalue ω^2 is also real. So if v is an eigenvector, so is its complex conjugate v^*. So either v is real or $(v + v^*)/2$ and $(v - v^*)/2i$ are real eigenvectors corresponding to the same eigenvalue.

$$\ddot{\xi}_{(\alpha)}(t) = -\omega_\alpha^2 \, \xi_{(\alpha)}(t) \qquad \text{(no sum on } \alpha\text{)}. \tag{13.64}$$

The general solution of the equations $M\ddot{x} + Kx = 0$ for small vibrations is a linear combination of normal modes:

$$x(t) = \sum\nolimits_\alpha \xi_{(\alpha)}(t) = \sum\nolimits_{\alpha=1}^{n} \left[c_1^{(\alpha)} \cos(\omega_\alpha t) + c_2^{(\alpha)} \sin(\omega_\alpha t) \right] v_{(\alpha)}. \tag{13.65}$$

A negative eigenvalue ω^2 (i.e., imaginary ω) would imply that the static solution is, in general, exponentially unstable in the linear approximation. Small perturbations would grow exponentially (or decay if $c_1 = 0$) with time $\xi = (c_1 e^{|\omega| t} + c_2 e^{-|\omega| t})v$, and the quadratic energy (13.56) would generally not be conserved. This happens if we were perturbing around a static solution q_0 that is not a local minimum, but a local maximum or saddle point of the potential. Of course, this cannot happen if both M and K are positive-definite matrices.

A 'zero mode' corresponding to a zero eigenvalue $\omega^2 = 0$ could grow linearly with time $\xi = (c_1 + c_2 t)v$ since $\ddot{f} = 0$. In this case, the static solution is said to be marginally unstable within the linear approximation. This happens, for instance, if the static solution q_0 is one among a continuously infinite family of degenerate minima of the potential, such as at one of the minima of the 'Mexican hat' potential $U(x,y) = (x^2 + y^2 - 1)^2$. The corresponding zero mode points in the direction in which the potential is flat, i.e., along the valley of the Mexican hat potential.

Remark: Basis in which mass and spring constant matrices are symmetric. Another way to reduce the equation $(-M\omega^2 + K)v = 0$ (13.60) to a standard eigenvalue problem is given here, emphasizing concepts from tensor algebra introduced in Appendix B.6*. We are given a vector space V along with a pair of covariant symmetric positive-definite tensors $M = m_{ij}$ and $K = k_{ij}$. We may regard M as defining a positive-definite inner product on V. Let e_i denote the standard basis vectors for V with components $(e_i)^j = \delta_i^j$. Explicitly, $e_1 = (1000\cdots)^t, e_2 = (0100\cdots)^t$, etc., with ^{t} denoting the transpose. The inner products of basis vectors are defined as $(e_i, e_j) = m_{ij}$. For a general pair of vectors $u = u^i e_i$ and $v = v^j e_j$, their inner product is $(u,v) = m_{ij} u^i v^j$ with $(u,u) > 0$ for all $u \neq 0$, since the kinetic energy $(\frac{1}{2} m_{ij} \dot{x}^i \dot{x}^j)$ is positive for *any* velocity vector $u = \dot{x}$. Then, there is a basis for V consisting of vectors f_α, which are orthonormal with respect to this inner product $(f_\alpha, f_\beta) = \delta_{\alpha\beta}$. The f_α basis vectors are some linear combinations of the e_i, $f_\alpha = T_\alpha^i e_i$, so

$$\delta_{\alpha\beta} = (f_\alpha, f_\beta) = (T_\alpha^i e_i, T_\beta^j e_j) = T_\alpha^i T_\beta^j (e_i, e_j) = T_\alpha^i T_\beta^j m_{ij}. \tag{13.66}$$

In other words, in the standard basis e_i, M is the matrix with entries m_{ij}, while in the f_α basis, M is the identity matrix. Note that being a covariant tensor (see Appendix B.6*) of rank two, M transforms via '$T \cdots T^t$' (rather than '$T^{-1} \cdots T$'), which is *not* a similarity transformation[29], and in particular *does not* preserve the eigenvalues of

---

[29] A mixed tensor with one upper and one lower index h_j^i transforms via $T^{-1} h T$.

m_{ij}. In the new basis, M is the identity, all of whose eigenvalues are equal to one. Analogously, K transforms as a covariant symmetric tensor to

$$\tilde{k}_{\alpha\beta} = T^i_\alpha T^j_\beta k_{ij}. \tag{13.67}$$

Finally, the vector $v = v^i e_i$ also has new components in the f basis. Indeed,

$$f_\alpha = T^i_\alpha e_i \quad \Rightarrow \quad e_i = (T^{-1})^\alpha_i f_\alpha \quad \Rightarrow \quad v = \tilde{v}^\alpha f_\alpha \quad \text{where} \quad \tilde{v}^\alpha = (T^{-1})^\alpha_i v^i. \tag{13.68}$$

So the linear equation for v is transformed from

$$(-m_{ij}\omega^2 + k_{ij})v^j = 0 \quad \text{to} \quad (-\delta_{\alpha\beta}\omega^2 + \tilde{k}_{\alpha\beta})\tilde{v}^\beta = 0 \quad \text{or} \quad \tilde{k}_{\alpha\beta}\tilde{v}^\beta = \omega^2 \tilde{v}_\alpha \tag{13.69}$$

which is now a standard eigenvalue problem for a real symmetric matrix $\tilde{k}_{\alpha\beta}$. □

13.4 Small perturbations around a periodic solution

In Sect. 13.1, Sect. 13.2.2 and Sect. 13.3*, we studied small oscillations around a static solution. This is what results when the static solution is stable to small perturbations. More generally, we could consider a time-dependent solution (perhaps even an approximate one) and ask about its stability to perturbations around it. The simplest of time-dependent solutions are periodic ones with period T, so we will focus on these. A physically interesting and nontrivial example concerns the stability of the Moon's approximately Keplerian orbit around the Earth when subject to solar perturbations. This problem was investigated by Hill [52].

We will find that the EOM for small perturbations around a periodic solution take the same form (13.55) as for oscillations around a static solution, but with the spring constant matrix k_{ij} being replaced by one with time-dependent but T-periodic entries determined by the unperturbed solution. As outlined in the introduction to Chap. 13, we will then develop a method (based on the 'monodromy matrix') to study the stability of the periodic solution by examining the fate of the perturbation after a time[30] T, $2T$ and so on. Loosely, the role of normal modes will be played by the eigenvectors of the monodromy matrix, while its eigenvalues govern stability.

Consider a system with Lagrangian $L = \frac{1}{2}m_{ij}\dot{q}^i\dot{q}^j - V(q)$, where for simplicity we take m_{ij} constant. We now suppose that $q_0(t)$ is a periodic solution with period T:

$$m_{ij}\ddot{q}_0^j + \frac{\partial V(q_0)}{\partial q^i} = 0 \ \text{ for } \ 1 \le i \le n, \ \text{ with } \ q_0(t+T) = q_0(t) \ \ \forall\, t. \tag{13.70}$$

This is common in potential wells or planetary orbits. We seek a nearby solution of the form $q^i(t) = q_0^i(t) + x^i(t)$, where x^i is a perturbation treated to linear order:

$$m_{ij}(\ddot{q}_0^j + \ddot{x}^j) + \frac{\partial V(q_0(t))}{\partial q^i} + \frac{\partial^2 V(q_0(t))}{\partial q^i \partial q^j} x^j + \mathcal{O}(x^2) = 0. \tag{13.71}$$

---

[30] We will learn that perturbations to a periodic solution are generally not periodic and that this can be regarded as an example of spontaneous symmetry breaking.

Ignoring higher order terms, we get a system of 2^{nd} order homogeneous linear ODEs with periodic coefficients for the perturbation $x(t)$:

$$m_{ij}\ddot{x}^j + k_{ij}(t)x^j = 0, \quad \text{where} \quad k_{ij}(t) = \frac{\partial^2 V(q_0(t))}{\partial q^i \partial q^j} \quad \text{and} \quad k_{ij}(t+T) = k_{ij}(t). \tag{13.72}$$

The time-dependent spring 'constants' $k_{ij}(t)$ inherit the periodicity of the unperturbed solution $q_0(t)$, since the Hessian of the potential is evaluated at $q_0(t)$. The simplest case is that of one degree of freedom

$$m\,\ddot{x}(t) + k(t)\,x(t) = 0. \tag{13.73}$$

An interesting example is $k(t)/m = a - 2q\cos 2t$, which leads to Mathieu's equation (see Sect. 6.10 and Sect. 13.4.5*).

Hill's equation. Such ODEs were studied by the American mathematical astronomer George Hill in the context of solar perturbations to the Moon's periodic motion around the Earth [52] and also by the French mathematician Gaston Floquet [61]. For the Earth-Moon-Sun system, $q_0(t)$ is an approximate periodic solution (when the Sun's effect is ignored), namely the Earth and Moon going round their common center of mass in nearly circular orbits with a common period of about $T = 1$ month. Here, $q_0(t) + x(t)$ is the perturbed lunar orbit when effects of the Sun's gravity are included to first order.

Bloch wave function. A mathematically similar equation to (13.73) (for $n = 1$) arises in quantum mechanics when considering the time-independent Schrödinger eigenvalue problem for a particle moving in one dimension subject to a periodic potential $V(x)$, such as the electrostatic potential felt by an electron in an ionic crystal:

$$-\frac{\hbar^2}{2m}\psi''(x) + (V(x) - E)\psi(x) = 0. \tag{13.74}$$

Here, one considers a 1 dimensional crystal with spacing between adjacent ions equal to a. The crystal as a whole is of length L, but we assume that $L \gg a$ so that the effects of the edges of the crystal can be ignored. This is often implemented via periodic boundary conditions on the wave function (as would be the case if the ions are arranged on a circle). To relate the linearized Newton equation (13.73) to the Schrödinger eigenvalue equation (13.74) in a periodic potential, $x(t)$ is replaced by the 'Bloch' wave function $\psi(x)$ and time t is replaced by the spatial coordinate x. Moreover, the periodic spring coefficient $k(t)$ is replaced by the periodic potential difference $E - V(x)$, while the inertia m is replaced by the constant $\hbar^2/2m$. Although the time-independent Schrödinger eigenvalue equation (13.74) and linearized Newton equation (13.73) are mathematically similar, their physical interpretations are quite different. While Schrödinger's equation is linear even in the absence of any approximation, Newton's equation is linear only for small perturbations $x(t)$. While classically $x(t)$ is a real perturbation to a periodic classical solution $q_0(t)$, the generally complex electron wave function $\psi(x)$ is not really a perturbation, but rather is considered in the presence of a 'background' periodic ionic potential $V(x)$.

Spontaneous symmetry breaking. A qualitative feature of an ODE with periodic coefficients is that the solutions need not have the same periodicity, nor even be periodic at all. In fact, we are familiar with this phenomenon from the simplest such equation. The harmonic oscillator equation $m\ddot{x} + kx = 0$ describes oscillations around a static equilibrium ($x = 0$). Here, the coefficients m and k are independent of time, and therefore periodic with period 0. Nevertheless, solutions are not constant functions, they are periodic with period $T = 2\pi\sqrt{m/k}$. Loosely, this may be regarded as an example of '*spontaneous symmetry breaking*'. A symmetry of the equation of motion, (i.e., time-translation invariance) is not realized in some or all solutions.

Bloch's theorem. For an electron in a periodic potential (crystal lattice), Bloch's theorem [4] (in 1d) states that the energy eigenfunctions can be expressed as $\psi(x) = e^{ikx}u(x)$ where $u(x)$ is periodic with the same period L as the crystal lattice. The 'crystal momentum wavevector' k can take a continuous range of values lying within the so-called first Brillouin zone (fundamental domain of the reciprocal lattice). As a consequence, $\psi(x)$ does not share the periodicity of the crystal, though it is periodic up to a phase:

$$\psi(x+L) = e^{ikL}\psi(x). \tag{13.75}$$

We will encounter similar phenomena elsewhere as well [see Eq. (13.99)].

13.4.1 Formulation as a system of first order equations

In the simplest case of one degree of freedom, the equation for small oscillations around a periodic solution takes the form $m\ddot{x} + k(t)x(t) = 0$ with $k(t+T) = k(t)$ for all t. It is convenient to rewrite this as a pair of first order equations on phase space

$$\frac{d}{dt}\begin{pmatrix} x(t) \\ p(t) \end{pmatrix} = \begin{pmatrix} 0 & m^{-1} \\ -k(t) & 0 \end{pmatrix}\begin{pmatrix} x(t) \\ p(t) \end{pmatrix} \quad \text{and denote} \quad A(t) = \begin{pmatrix} 0 & m^{-1} \\ -k(t) & 0 \end{pmatrix}. \tag{13.76}$$

$A(t)$ is periodic with period T. These equations follow from the (explicitly time-dependent) Hamiltonian $H = \frac{p^2}{2m} + \frac{1}{2}k(t)x^2$. Let $\psi(t) = (x(t), p(t))^t$ denote the instantaneous 'state vector' of the system. Then the equation takes the form $\dot{\psi}(t) = A(t)\psi(t)$. Notice the formal similarity of $\dot{\psi} = A\psi$ with the time-dependent Schrödinger equation of quantum mechanics $i\hbar\dot{\psi} = H(t)\psi$. However, unlike the typically Hermitian Hamiltonian $H(t)$ in quantum mechanics, here $A(t)$ is not Hermitian, but traceless. As we shall see in Sect. 13.4.2*, this ensures that time evolution preserves phase space volume, since $\operatorname{tr} A$ is proportional to the infinitesimal change in volume. Analogously, in quantum mechanics, hermiticity of the Hamiltonian ensures that time evolution preserves probabilities.

For n degrees of freedom, the equation $m_{ij}\ddot{x}^j + k_{ij}x^j = 0$ may similarly be formulated as a first order system. We first define the momenta $p_i = m_{ij}\dot{x}^j$. Then

$$\dot{x}^i = m^{il}p_l \quad \text{and} \quad \dot{p}_j = -k_{jk}x^k \quad \Rightarrow \quad \frac{d}{dt}\begin{pmatrix} x^i \\ p_j \end{pmatrix} = \begin{pmatrix} 0 & m^{il} \\ -k_{jk}(t) & 0 \end{pmatrix}\begin{pmatrix} x^k \\ p_l \end{pmatrix} \tag{13.77}$$

where m^{il} are the entries of the inverse matrix m^{-1}. We see that the $2n \times 2n$ matrix $A(t) = \left(\begin{smallmatrix} 0 & m^{-1} \\ -k & 0 \end{smallmatrix}\right)$ is again traceless. These equations for small oscillations again follow from an explicitly time-dependent Hamiltonian

$$H(x,p,t) = \frac{1}{2} m^{il} p_i p_l + \frac{1}{2} k_{jk}(t)\, x^j x^k. \tag{13.78}$$

As before, we define the 'state vector' $\psi(t) = (x^i, p_j)^t$, in terms of which $\dot{\psi}(t) = A(t)\psi(t)$. Here too, $A(t+T) = A(t)$ inherits the periodicity of the solution $q_0(t)$.

13.4.2* Time evolution matrix

Our aim here is to understand and obtain an expression for the solution of the evolution equation for small perturbations (13.76):

$$\dot{\psi}(t) = A(t)\psi(t) \quad \text{given the initial state} \quad \psi(0). \tag{13.79}$$

Here $\psi(t) = (x^1(t), \cdots, x^n(t), p_1(t), \cdots, p_n(t))^t$ is a $2n$-component column vector representing the instantaneous state of the perturbed system. The solution of this equation up to time t, for an arbitrary initial state $\psi(0)$, is usefully encoded in a gadget called the time evolution matrix $U(t,0)$. Being a system of $2n$ first order linear equations, there are $2n$ possible linearly independent initial conditions which may conveniently be taken as the standard basis vectors for $\mathbb{R}^{2n}$: $(1,0,\cdots)^t$, $(0,1,\cdots)^t, \cdots$ and $(0,0,\cdots 0,1)^t$. The solution of the IVP (13.79) for each of these ICs may be regarded as a column vector. The time evolution matrix $U(t,0)$ is the result of assembling all these column vectors in a $2n \times 2n$ matrix. By construction, $U(0,0)$ is the identity matrix. The matrix $U(t,0)$ has complete information on the evolution of small perturbations. For instance, given an initial perturbation $\psi(0)$, it will evolve into $\psi(t) = U(t,0)\psi(0)$ after a time t. Thus, it is useful to have a formula for U in terms of the coefficient matrix $A(t)$. From (13.79) we should expect U to be the matrix exponential of A, provided A is independent of time. However, here A is T-periodic in time. Remarkably, the concept of the exponential may be generalized to that of the time-ordered exponential, in terms of which we will express $U(t,0)$. Along the way, we will uncover some nice properties of U. For instance, on account of the tracelessness of A, it has unit determinant (it is unimodular), which ensures that time evolution preserves phase space volume. Our labors will also have payoffs elsewhere in physics:

1. The time evolution matrix arises in quantum mechanics (QM), where it is unitary rather than unimodular. It is used to develop the path integral formulation [114].
2. In Sect. 15.2*, the singular values of $U(t,0)$ will be used to define Lyapunov exponents, which have information on the stability of trajectories of a dynamical system.
3. The idea of an 'ordered' exponential is useful in classical and quantum field theory. For instance, it arises in gauge theories in the guise of the path-ordered exponential or Wilson loop variable[31], whose behavior for large closed curves γ gives a way of understanding whether quarks are confined inside protons [58].

---

[31] The Wilson loop observable is $W(\gamma) = \operatorname{tr} P \exp \oint_\gamma A_\mu dx^\mu$ where $A_\mu(x)$ for $\mu = 0,1,2,3$ are the space-time components of the gauge field (scalar and vector potentials in electromagnetism).

4. In integrable field theories such as the nonlinear Schrödinger equation in one spatial dimension (see Prob. 19.49), the transition matrix [76, 77] is a path-ordered exponential and its trace is a generating series for (an infinite sequence of) conserved quantities.

Often, the time evolution matrix $U(t,0)$ has more information than we are interested in. If we are particularly interested in the stability of the unperturbed T-periodic orbit $q_0(t)$, then we will see that it suffices to consider what happens to a perturbation after a time $T, 2T, 3T$ and so on. This behavior is encoded in the monodromy matrix $M = U(T,0)$ and its powers M^2, M^3, etc. We will find that the spectrum of M has information on the stability of the 'background' periodic orbit and that its eigenvectors loosely play the role of normal modes.

Let us now derive a formula for $U(t,0)$. Given $\psi(0)$, the linear equation for small perturbations $\dot{\psi}(t) = A(t)\psi(t)$ determines the state ψ at subsequent times. For instance if t is small, then

$$\psi(t) = (1 + A(0)\,t)\psi(0) + \mathcal{O}(t^2). \tag{13.80}$$

To get ψ after a longer time, we compose time evolution over several short times:

$$\psi(t) = \lim_{n\to\infty} (1+A((n-1)t/n))(1+A((n-2)t/n))\dots(1+A(t/n))(1+A(0))\psi(0). \tag{13.81}$$

We will give an alternate formula shortly, but for now we notice that, since the equation is linear, $\psi(t)$ must depend linearly on the initial state. Thus, we may write

$$\psi(t) = \begin{pmatrix} x(t) \\ p(t) \end{pmatrix} = U(t,0)\begin{pmatrix} x(0) \\ p(0) \end{pmatrix} = U(t,0)\psi(0), \tag{13.82}$$

where $U(t,0)$ is a 2×2 time evolution matrix.

For n degrees of freedom we again have $\dot{\psi} = A(t)\psi(t)$ where the $2n \times 2n$ matrix $A(t) = \begin{pmatrix} 0 & m^{-1} \\ -k & 0 \end{pmatrix}$ in (13.77) is block off diagonal and traceless and we may write $\psi(t) = U(t,0)\psi(0)$. $U(t,0)$ satisfies the same 1st order ODE as $\psi(t)$:

$$AU(t,0)\psi(0) = \dot{\psi} = \dot{U}(t,0)\psi(0) \quad \forall \quad \psi(0) \quad \Rightarrow \quad \dot{U}(t,0) = A(t)U(t,0) \tag{13.83}$$

with the IC $U(0,0) = I$. More generally, one defines $U(t,t')$ via

$$\psi(t) = U(t,t')\psi(t') \quad \text{for any} \quad t \geq t'. \tag{13.84}$$

It is convenient to combine the ODE and initial condition into an integral equation

$$U(t,0) = I + \int_0^t A(t')U(t',0)\,dt'. \tag{13.85}$$

Notice that (13.83) is similar to the equation for the time evolution operator in QM $i\hbar\dot{U}(t,0) = H(t)U(t,0)$ where $H(t)$ is the Hamiltonian. As in QM, from its definition ($\psi(t) = U(t,t')\psi(t')$), U satisfies a composition law or reproducing property[32]

$$U(t,t'') = U(t,t')U(t',t'') \quad \text{for any} \quad t \geq t' \geq t''. \tag{13.86}$$

---

[32] To show (13.86) one may also check that both the LHS and RHS satisfy the same differential equation $\dot{U} = A(t)U$ and IC and then appeal to the uniqueness of solutions.

However, there are some differences as well.

Time evolution matrix is unimodular. Unlike the Hermitian Hamiltonian $H(t)$ in QM, the matrix $A(t)$ is not Hermitian in general. However, it is traceless. Using this, one may show (see below) that unlike in QM where $U(t,0)$ is *unitary*, here $U(t,0)$ is *unimodular*. Alternatively, from (10.48), we know that Hamiltonian evolution, even by a time-dependent Hamiltonian, defines a canonical transformation. Since we have linearized the EOM, the time evolution matrix defines *linear* canonical transformations between tangent spaces to the phase space along the unperturbed trajectory. By Liouville's theorem, these CTs must preserve the volume element on phase space (area element for one degree of freedom). Now the linear transformation $U(t+\delta t, t)$ taking $(x(t), p(t))$ to $(x(t+\delta t), p(t+\delta t))$ is also the Jacobian of this transformation. Since it preserves volumes, the Jacobian U must have unit determinant[33].

Proving $\det U = 1$ is easy when A is time-independent. Then $U(t,0) = e^{tA}$ and $\log\det U = \operatorname{tr}\log e^{tA} = \operatorname{tr}(tA) = 0$. More generally, for short times,

$$U(t,0) = I + \int_0^t A(t')dt' + \mathcal{O}(t^2). \tag{13.87}$$

Using $\det(I+\epsilon A) \approx 1 + \epsilon \operatorname{tr} A$ for small ϵ, we get

$$\det U(t,0) \approx 1 + \int_0^t \operatorname{tr} A(t')\, dt' = 1 + \mathcal{O}(t^2). \tag{13.88}$$

Infinitesimal time evolution preserves the unimodularity of U. For longer times, we write $U(t,t_0)$ as a product of several short-time evolutions and let the time step $\to 0$:

$$U(t,t_0) = U(t,t_{n-1})U(t_{n-1},t_{n-2})\cdots U(t_2,t_1)U(t_1,t_0). \tag{13.89}$$

Here, for simplicity, we take $t_{i+1} - t_i = \Delta t = (t-t_0)/n$ to be constant, though one could have variable time steps as well. Then defining $t_n \equiv t$, which is held fixed,

$$\det U(t,t_0) = \prod_{i=0}^{n-1} \det U(t_{i+1},t_i) = \prod_{i=0}^{n-1}(1+\mathcal{O}(\Delta t)^2) \to 1 \quad \text{as} \quad n\to\infty. \tag{13.90}$$

Unimodularity of U can also be established using the identity $\log\det U = \operatorname{tr}\log U$. One first shows that

$$\frac{d}{dt}\log\det U(t,0) = \operatorname{tr}\dot{U}U^{-1} = \operatorname{tr} A = 0 \tag{13.91}$$

and then uses $\det U(0,0) = 1$ to deduce that $\det U(t,0) = 1$ at all $t > 0$.

Time-ordered exponential series. By iterating the integral equation (13.85), we get a series for the time evolution operator:

$$U(t,0) \quad = \quad I + \int_0^t dt'\, A(t') + \int_0^t dt' A(t') \int_0^{t'} dt''\, A(t'') + \cdots$$

---

[33] For 1 degree of freedom, we show in Prob. 10.15 that a linear CT is an element of $SL_2(\mathbb{R})$.

$$= \quad I + \sum_{n=1}^{\infty} \iiint_{t \geq t_1 \geq t_2 \geq \cdots t_n \geq 0} dt_1 \cdots dt_n \; A(t_1)A(t_2)\cdots A(t_n). \quad (13.92)$$

To make this series look like the exponential series (to which it must reduce if A is time-independent), we begin by noticing that the $n = 1$ term is an integral over an interval $t \geq t_1 \geq 0$. The next is an integral over a triangle $t \geq t_1 \geq t_2 \geq 0$. The $n = 3$ term is an integral over a pyramid/tetrahedron and so on. These can be re-expressed as integrals over an interval, a square, a cube and so on. To see this, we first observe that the $n = 2$ term can be written as an integral over either of two triangles in the square $0 \leq t_1, t_2 \leq t$:

$$\int_{t \geq t_1 \geq t_2 \geq 0} dt_1 dt_2 A(t_1)A(t_2) = \int_{t \geq t_2 \geq t_1 \geq 0} dt_1 dt_2 A(t_2)A(t_1). \qquad (13.93)$$

The integrands in both cases are such that the A at the earlier time appears to the right. Thus, if we introduce the time ordering operation that places matrices in a product with ‘younger ones to the right’:

$$\mathcal{T}(A(t_1)A(t_2)) = \begin{cases} A(t_1)A(t_2) & \text{if} \quad t_1 \geq t_2 \\ A(t_2)A(t_1) & \text{if} \quad t_2 \geq t_1, \end{cases} \qquad (13.94)$$

we may write the $n = 2$ term as:

$$\int_0^t dt_1 \int_0^{t_1} dt_2 \; A(t_1)A(t_2) = \frac{1}{2} \int_0^t dt_1 \int_0^t dt_2 \; \mathcal{T}(A(t_1)A(t_2)). \qquad (13.95)$$

In effect, we have expressed an integral over the triangle $t \geq t_1 \geq t_2 \geq 0$ in the t_1-t_2 plane as half the integral over a square. Similarly, for $n = 3$ we may express the integral over the pyramid $t \geq t_1 \geq t_2 \geq t_3 \geq 0$ as one-sixth of that over a cube in the 3d t_1-t_2-t_3 space. Continuing in this manner, we get

$$\begin{aligned} &\textstyle\int_0^t dt_1 \int_0^{t_1} dt_2 \cdots \int_0^{t_{n-1}} dt_n \; A(t_1)A(t_2)\cdots A(t_n) \\ &= \tfrac{1}{n!} \textstyle\int_0^t \cdots \int_0^t dt_1 dt_2 \cdots dt_n \mathcal{T}[A(t_1)A(t_2)\cdots A(t_n)]. \end{aligned} \qquad (13.96)$$

Thus, $U(t,0)$ may be expressed as a time-ordered exponential series:

$$U(t,0) = \sum\nolimits_{n=0}^{\infty} \frac{1}{n!} \int_0^t dt_1 \cdots \int_0^t dt_n \mathcal{T}[A(t_1)\cdots A(t_n)] \equiv \mathcal{T} \exp \int_0^t A(s) ds. \quad (13.97)$$

In short, we extended the integrals over each of the simplices[34] $t \geq t_1 \geq \cdots \geq t_n \geq 0$ to the full hypercube $[0,t]^n$ by dividing by $n!$, but needed to make sure the matrices

---

[34] A point, a line segment, a triangular surface and a solid tetrahedron are examples of 0,1,2 and 3-dimensional simplices. In general, given $n+1$ points $x_0, x_1, \cdots, x_n \in \mathbb{R}^n$, the n-simplex they determine is the set of points given by the weighted sums $\sum_{i=0}^n w_i x_i$ for arbitrary nonnegative weights satisfying $\sum_{i=0}^n w_i = 1$. Here, we assume that $x_j - x_0$ for $j = 1, \ldots, n$ are n linearly independent vectors in $\mathbb{R}^n$.

$A(t_i)$ in the product are ordered with 'younger ones to the right'. This series[35] is called the time-ordered exponential, denoted symbolically by $\mathcal{T}\exp$. Note that in general, it is *not* the exponential of $\int_0^t A(s)\,ds$, though it reduces to this if A is time-independent or if the matrices $A(s)$ commute at distinct times.

A virtue of $U(t, t_0)$ is that its columns are solutions of the original equation $\dot{\psi} = A(t)\psi(t)$, as is easily seen from $\dot{U}(t, t_0) = A(t)U(t, t_0)$. Since $\det U \neq 0$, the columns of U are a complete set of $2n$ linearly independent solutions to the equation for small oscillations. The IC for the p^{th} column is a vector with a 1 in the p^{th} row and zeros elsewhere. Thus, U is called the fundamental matrix solution. Every solution of $\dot{\psi} = A(t)\psi$ with prescribed ICs is a linear combination of the columns of U.

13.4.3* Monodromy matrix

So far, we have not used the T-periodicity of $A(t)$. Here, we are interested in the behavior of U after one period, i.e., $U(t+T, t)$. The reproducing formula implies that

$$U(t+T, 0) = U(t+T, t)U(t, 0). \tag{13.98}$$

The matrix $U(t+T, t)$ advances a solution $\psi(t)$ of (13.79) by one period of the unperturbed trajectory $q_0(t)$:

$$\psi(t+T) = U(t+T, t)\psi(t). \tag{13.99}$$

What is more, by periodicity of A, it follows that $U(t+T, t)$ is independent of t, since the time-ordered exponential series (13.97) for $U(t+T, t)$ only involves integrals of A over a complete period. So we may unambiguously denote $U(t+T, t)$ by $M(T)$, which is called the monodromy matrix

$$M(T) = U(t+T, t) = \mathcal{T}\exp\int_t^{t+T} A(s)\,ds = \mathcal{T}\exp\int_0^T A(s)\,ds. \tag{13.100}$$

Being a special case of the time evolution operator, $\det M = 1$. Thus, from (13.99), $\psi(t+T) = M\psi(t)$. In other words, *the solution $\psi(t)$ is periodic up to multiplication by a unimodular matrix* [see (13.75) for a wave mechanical analog]. In our language, this is one of the main results of Floquet's theory. It finds application in Bloch's analysis of the energy eigenfunctions of an electron in a 1d periodic potential, which underpins the band theory of electrons in a crystal.

13.4.4* Stability of a periodic solution

We will now explain that long-term (linear) stability of the original periodic solution $q_0(t)$ is largely governed by the spectrum of M. After one period T of the unperturbed motion, the initial perturbation $\psi(0)$ becomes $\psi(T) = M\psi(0)$. After

---

[35] If $A(t)$ is uniformly bounded, i.e., if the largest eigenvalue of A is bounded above by some constant Λ for all times in the interval $[0, t]$, then the norm of this sum of operators is dominated by a constant multiple of the exponential series $\sum(\Lambda t)^n/n! = e^{\Lambda t}$. In this case, the series (13.97) is absolutely convergent.

n time periods, $\psi(nT) = M^n\psi(0)$. For long-term stability, we would want $\psi(nT)$ to remain bounded as $n \to \infty$ for any choice of $\psi(0)$. This puts restrictions on the monodromy matrix M, which is a real matrix with unit determinant. It defines a finite linear canonical transformation (see Sect. 10.5 and Prob. 10.14). To determine M explicitly for given $A(t)$ is usually quite hard, requiring numerical calculations, but a lot can be said about the qualitative nature of the motion, if the spectrum (eigenvalues[36] $m_1, m_2, \cdots$) of M is known. Let us consider the simplest example of one degree of freedom, where M is a 2×2 matrix with product of eigenvalues $\mu_1\mu_2 = 1$. There are three cases to consider, and the analysis is simplest in a basis in which M is either diagonal or takes a canonical form.

1. If the eigenvalues are **real and unequal**, then M is diagonalizable via a similarity transformation $S^{-1}MS = D$ where $D = \mathrm{diag}(\mu, 1/\mu)$. The eigenvalues must both have the same sign. One of the eigenvalues is necessarily larger than 1 in magnitude, say $1/\mu$. An initial state $\psi(0)$ that has a component in the direction of the corresponding eigenvector will grow exponentially with time since $D^n = \mathrm{diag}(\mu^n, \mu^{-n}) \to \mathrm{diag}(0, \pm\infty)$ as $n \to \infty$. So if the monodromy matrix has real and distinct eigenvalues, the periodic solution $q_0(t)$ is in general linearly unstable. Now using calculus, one may show that for $0 < |\mu| < 1$, $|\mu + 1/\mu| > 2$ (see Prob. 13.23). Thus, in this regime of instability, $|\operatorname{tr} M| > 2$.
2. If the eigenvalues are **real and equal** $\mu_1 = \mu_2 = 1$, or $\mu_1 = \mu_2 = -1$ then M in general cannot be diagonalized, though it is similar to a Jordan matrix $S^{-1}MS = J = \left(\begin{smallmatrix} \pm 1 & c \\ 0 & \pm 1 \end{smallmatrix}\right)$ and
$$J^n = \begin{pmatrix} 1 & nc \\ 0 & 1 \end{pmatrix} \quad \text{or} \quad J^n = (-1)^n \begin{pmatrix} 1 & -nc \\ 0 & 1 \end{pmatrix}. \tag{13.101}$$
   Working in the Jordan basis, we see that a perturbation that initially has a component in the second direction, grows linearly with time ($t = nT$) if $c \neq 0$. So if $M \neq \pm I$ has coincident real eigenvalues, then the periodic solution is linearly unstable in general. It is stable if $M = \pm I$. What is more, the eigenvalues are real and equal[37] iff $\operatorname{tr} M = \pm 2$. Thus we see that when $|\operatorname{tr} M| = 2$, additional information is needed to determine stability of the periodic solution $q_0(t)$.
3. Finally, if M has a **nonreal** eigenvalue, then both eigenvalues must be nonreal and complex conjugates of each other ($\mu \neq \mu^*$), since the characteristic equation has real coefficients. Moreover, $|\mu|^2 = \mu\mu^* = \det M = 1$, so the eigenvalues have unit absolute values. Let $\mu = e^{i\theta} = a + ib$ with a, b real and $a^2 + b^2 = 1$. Since it has distinct eigenvalues, M may be diagonalized by a nonreal similarity transformation $S^{-1}MS = D = \mathrm{diag}(e^{i\theta}, e^{-i\theta})$ and $D^n = \mathrm{diag}(e^{in\theta}, e^{-in\theta})$. It is clear that the matrix elements do not grow in magnitude, so we expect stability. However, x and p are real, and M cannot be diagonalized by a real similarity transformation. Nevertheless, it may be brought by a similarity transformation to

---

[36] Note that $(1/T)\log m_i$ are called the Floquet exponents and their real parts are called Lyapunov exponents. For more on Lyapunov exponents, see Sect. 15.2*.

[37] Verify this by finding the roots of $\mu + 1/\mu = \pm 2$.

the real Jordan form $J = \begin{pmatrix} \cos\theta & \sin\theta \\ -\sin\theta & \cos\theta \end{pmatrix}$ corresponding to a rotation in the phase plane and $J^n = \begin{pmatrix} \cos n\theta & \sin n\theta \\ -\sin n\theta & \cos n\theta \end{pmatrix}$ is also a rotation. It is clear that perturbations do not grow in size in this case. If $\theta = 2\pi(p/q)$ is a rational multiple of 2π (with p, q coprime), then the perturbation $\psi(t)$ is periodic with period qT. Notably, in this third case of stability, $|\operatorname{tr} M| = 2|\cos\theta| < 2$.

In summary, the eigenvalues of the monodromy matrix determine the stability of the unperturbed periodic trajectory $q_0(t)$. For one degree of freedom, the *stability index* $\sigma = \operatorname{tr} M$ controls stability. If $|\sigma| > 2$ we have instability, stability for $|\sigma| < 2$ while $\sigma = 2$ is marginal.

13.4.5* Kapitza pendulum with oscillating support: Mathieu equation

A pendulum with vertically oscillating support is called a Kapitza pendulum after the Russian physicist Pyotr Kapitza who explained some of its remarkable features. A sufficiently rapid vertical vibration can stabilize a pendulum that is balanced on its head. On the other hand, parametric oscillations due to the vibrating support can render librational motion unstable for certain ranges of parameters.

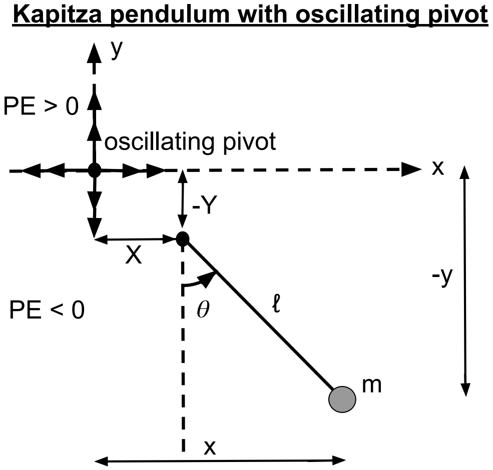

Figure 13.6: Kapitza pendulum with oscillating support.

Suppose the instantaneous coordinates of the support are $(X(t), Y(t))$, where X and Y are measured to the right and upwards as in Fig. 13.6. The coordinates of the bob are then

$$x = X + l\sin\theta \quad \text{and} \quad y = Y - l\cos\theta. \tag{13.102}$$

The kinetic and potential energies are

$$\begin{aligned} T &= \frac{m}{2}\left(\dot{x}^2 + \dot{y}^2\right) = \frac{m}{2}\left[\dot{X}^2 + \dot{Y}^2 + l^2\dot{\theta}^2 + 2l(\dot{X}\cos\theta + \dot{Y}\sin\theta)\dot{\theta}\right] \quad \text{and} \\ V &= mg(Y - l\cos\theta). \end{aligned} \tag{13.103}$$

The zero of V has been chosen at the height of the undisturbed support. Since $X(t)$ and $Y(t)$ are prescribed functions of time, the terms proportional to $\dot{X}^2$, $\dot{Y}^2$ and Y

are time derivatives and do not contribute to Lagrange's equations. Thus, we take

$$L = T - V = \frac{m}{2}\left[l^2\dot{\theta}^2 + 2l(\dot{X}\cos\theta + \dot{Y}\sin\theta)\dot{\theta}\right] + mgl\cos\theta. \tag{13.104}$$

For small oscillations around $\theta = 0$, we expand in $\xi = \theta$ and keep up to quadratic terms while dropping constants:

$$L_{\theta=0} \approx \frac{1}{2}ml^2\dot{\xi}^2 + ml\dot{X}\dot{\xi} + ml\dot{Y}\xi\dot{\xi} - \frac{1}{2}mgl\xi^2. \tag{13.105}$$

Similarly, to investigate the possibility of small oscillations around $\theta = \pi$, we expand to quadratic order in $\xi = \theta - \pi$:

$$L_{\theta=\pi} \approx \frac{1}{2}ml^2\dot{\xi}^2 - ml\dot{X}\dot{\xi} - ml\dot{Y}\xi\dot{\xi} + \frac{1}{2}mgl\xi^2. \tag{13.106}$$

The resulting equations of motion are

$$l\ddot{\xi} + (g + \ddot{Y})\xi + \ddot{X} = 0 \quad \text{and} \quad l\ddot{\xi} - (g + \ddot{Y})\xi - \ddot{X} = 0. \tag{13.107}$$

In this approximation, the horizontal motion of the support introduces an external driving while the vertical motion, if oscillatory, produces parametric oscillations as in Sect. 6.10. To focus on the latter, we will put $X(t) \equiv 0$ and suppose that $Y(t) = -b\cos\nu t$ with $b > 0$ (the sign of b can be reversed by a change in phase) to obtain

$$\ddot{\xi} \pm \left(\omega_0^2 + \frac{b\nu^2}{l}\cos\nu t\right)\xi = 0 \quad \text{where} \quad \omega_0 = \sqrt{\frac{g}{l}}. \tag{13.108}$$

For oscillations around $\theta = 0$ (the upper sign), this equation has the same form as (6.74) with $h = (b/l)(\nu^2/\omega_0^2)$. If the amplitude of oscillation of the support is much less than the length of the rod ($b \ll l$), then $h \ll 1$. Consequently, from (6.81) we can expect parametric resonance (instability) for $|\nu - 2\omega_0| < \frac{1}{2}h\omega_0 = b\nu^2/2l\omega_0$. Here, we will go a step further by looking for regions of stability/instability in the space of physical parameters by treating (13.108) by the monodromy matrix method of Sect. 13.4.4*. To place (13.108) in the context of small perturbations around a periodic solution, we view the vertical oscillation of the pivot as the background 'periodic solution' while the swinging of the pendulum is the small perturbation.

To identify the relevant (dimensionless) parameters we pass to a nondimensional time $\tau = \nu t/2$. Then $\xi = \xi(\tau)$ evolves according to the Mathieu equation:

$$\ddot{\xi} \pm 4\left(\frac{\omega_0^2}{\nu^2} + \frac{b}{l}\cos 2\tau\right)\xi = 0 \quad \text{or} \quad \ddot{\xi} + (a - 2q\cos 2\tau)\xi = 0, \tag{13.109}$$

Evidently, there are two relevant dimensionless parameters: the squared ratio of natural swinging to pivot frequencies $a = \pm 4\omega_0^2/\nu^2$ and the ratio of lengths $q = \mp 2b/l$. Let us get a sense for interesting values of these parameters. We expect parametric resonance when $\nu \approx 2\omega_0$, which corresponds to $a \approx 1$ (for oscillations around $\theta = 0$). Interestingly, the inverted pendulum corresponds to $a < 0$. On the other

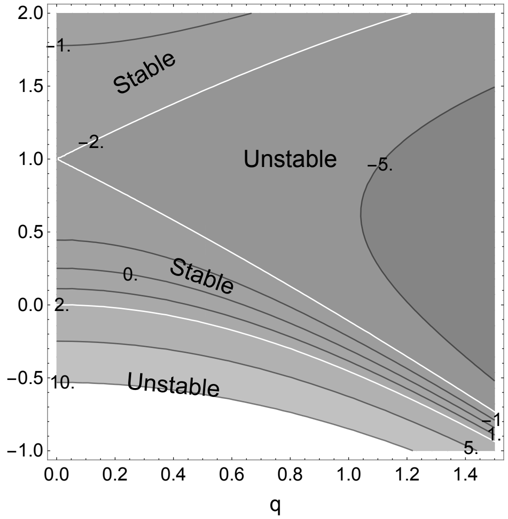

Figure 13.7: Level contours of the stability index σ on the q-a plane for the Kapitza pendulum with oscillating support. $|\sigma| < 2$ implies stability. $q = 2b/l$ is the ratio of the amplitude of the oscillating support to the length of the pendulum rod. $a = 4\omega_0^2/\nu^2$ is proportional to the squared ratio of natural to pivot frequencies. The downward hanging pendulum ($a > 0$) displays an instability around parametric resonance $a = 1$ or $\nu = 2\omega_0$. The inverted pendulum ($a < 0$) can be stabilized by the vibrating pivot.

hand, q is small if the pendulum rod is long compared to the amplitude of pivot oscillations. Since the sign of q can be changed by changing the origin of time, we may take $q = 2b/l$ in both cases and treat it as positive.

Equation (13.109) may be written in first order form as in (13.76):

$$\frac{d}{d\tau}\psi = A\psi \quad \text{where} \quad \psi = \begin{pmatrix} \xi \\ \dot{\xi} \end{pmatrix} \quad \text{and} \quad A(\tau) = \begin{pmatrix} 0 & 1 \\ a - 2q\cos 2\tau & 0 \end{pmatrix}. \tag{13.110}$$

The coefficient matrix is π periodic: $A(\tau + \pi) = A(\tau)$. In terms of the time evolution matrix (13.82), the monodromy matrix is $M = U(\pi, 0)$. The magnitude of the stability index $\sigma(a, q) = \operatorname{tr} M$ determines linear stability. It turns out that σ can be expressed in terms of the values and derivatives of Mathieu functions. Indeed, the fundamental matrix solution $U(\tau, 0)$ is determined by solutions of (13.109) satisfying the ICs $\xi_1(0) = 1, \dot{\xi}_1(0) = 0$ and $\xi_2(0) = 0, \dot{\xi}_2(0) = 1$. These solutions can be expressed in terms of the odd and even Mathieu functions $S_{a,q}(\tau)$ and $C_{a,q}(\tau)$, which are special solutions of (13.109) with $S(0) = 0$ and $\dot{C}(0) = 0$ that are odd and even in τ. Their properties are tabulated in Chap. 20 of [1], in Sect. 6.9 and Sect. 8.6 of [48] and built into software packages such as Mathematica [134]. Indeed, one easily verifies that

$$\xi_1(\tau) = \frac{S(\tau)\dot{C}(0) - \dot{S}(0)C(\tau)}{W(S,C)} \quad \text{and} \quad \xi_2(\tau) = \frac{S(0)C(\tau) - S(\tau)C(0)}{W(S,C)}. \tag{13.111}$$

Here $W(S, C)$ is the Wronskian of the odd and even solutions

$$W(S,C)(\tau) = S(\tau)\dot{C}(\tau) - \dot{S}(\tau)C(\tau). \tag{13.112}$$

The significance of the Wronskian is explored in Prob. 13.24, where it is shown that W is independent of time τ. From the discussion below (13.97), the time evolution matrix is then given by $U = \begin{pmatrix} \xi_1 & \xi_2 \\ \dot{\xi}_1 & \dot{\xi}_2 \end{pmatrix}$. Evaluating at $\tau = \pi$ and taking the trace, we get an expression for the stability index

$$\sigma(a, q) = \operatorname{tr} M = \frac{S(0)\dot{C}(\pi) - \dot{S}(0)C(\pi) + (\pi \leftrightarrow 0)}{W(S, C)}. \tag{13.113}$$

Using the tabulated values of Mathieu functions, the level contours of σ are plotted on the q-a plane in Fig. 13.7, showing regions of stability and instability. As anticipated, the downward hanging pendulum ($a > 0$) is unstable in a wedge around parametric resonance ($a = 1$ or $\nu = 2\omega_0$). Interestingly, we also see that the inverted pendulum ($a < 0$) can be stabilized by the vibrating pivot for certain parameter values.

For rapid oscillations of the support ($\nu \gg \omega$), one may average over the motion of the pivot to obtain an 'effective' Lagrangian for the slower angular motion of the bob. See Sect. 30 of [83] and Sect. 8.10 of [107] where it is shown that for sufficiently rapid *horizontal* motion of the support, the vertically downward-hanging pendulum is unstable, though there are two stable extrema of the effective potential on either side.

13.5 Problems

1. Consider the two **weakly coupled pendula** studied in Sect. 13.1.1. Find conserved energies for each of the normal modes and combine them to get a conserved energy for the coupled pendula and express it in the original θ_1, θ_2 variables.
2. (a) Say what it means for 2 time periods $T_1 > 0, T_2 > 0$ to be **commensurate or incommensurate**. What does being commensurate imply for the combined dynamics given by a linear combination of the two normal modes? (b) Suppose there are 3 normal modes with (positive, nonzero) periods T_1, T_2, T_3. Give 2 examples of such time periods which one would consider (E1) commensurate and (E2) incommensurate, with a line of justification for each. (c) Suggest a definition for what is meant by 3 time periods being commensurate. Give an easily checked necessary and sufficient condition for 3 time periods to be commensurate.
3. **Lagrangian for coupled pendula.** Propose a Lagrangian for the linear equations describing small oscillations of a pair of pendula that interact via a spring, as discussed in Sect. 13.1.1. Verify that Lagrange's equations reproduce (13.2). Interpret the terms in the Lagrangian.
4. Use normal modes to obtain the general solution ($x_1(t)$ and $x_2(t)$) of the EOM of the **diatomic molecule** studied in Sect. 13.1.2.
5. Consider a **double pendulum** with 'lower' bob of mass m suspended by a massless rod of length l from an 'upper' bob of mass m which is in turn suspended from a fixed pivot by a massless rod of length l (see Fig. 13.3). The system is free to move in a vertical plane subject to gravity. The rods make angles θ_1, θ_2 counterclockwise relative to the downward vertical. The Cartesian coordinates of the two bobs are $\boldsymbol{r}_1 = (x_1, y_1)$ and $\boldsymbol{r}_2 = (x_2, y_2)$ where

$$x_1 = l \sin\theta_1 \quad \text{and} \quad y_1 = -l\cos\theta_1 \quad \text{while}$$

$$x_2 = l\sin\theta_1 + l\sin\theta_2 \quad \text{and} \quad y_2 = -l\cos\theta_1 - l\cos\theta_2. \tag{13.114}$$

Choose the potential energy to vanish when $\theta_1 = \theta_2 = 0$.

a. Find the potential & kinetic energies and Lagrangian. Use the abbreviations $c_1 = \cos\theta_1, s_2 = \sin\theta_2, c_{12} = \cos(\theta_1 - \theta_2), s_{12} = \sin(\theta_1 - \theta_2)$, etc.
b. Identify the configuration manifold and convenient coordinates on it.
c. Identify an interesting continuous symmetry $\theta_i \to \theta_i + \delta\theta_i$ of the Lagrangian in the absence of the gravitational force.
d. Find the momenta p_1, p_2 conjugate to θ_1, θ_2.
e. Find the angular momenta $\boldsymbol{L}_1, \boldsymbol{L}_2$ of the two bobs.
f. Try to find a relation among $p_1, p_2, \boldsymbol{L}_1$ and $\boldsymbol{L}_2$ and identify its physical meaning and significance in the context of the above symmetry.
g. Express the generalized velocities $\dot\theta_i$ in terms of the generalized coordinates and momenta. Show that you get

$$\dot\theta_1 = \frac{p_1 - c_{12}p_2}{ml^2(1+s_{12}^2)} \quad \text{and} \quad \dot\theta_2 = \frac{2p_2 - c_{12}p_1}{ml^2(1+s_{12}^2)}. \tag{13.115}$$

h. Find the conserved total energy and Hamiltonian, show that you get

$$\begin{aligned} E &= (ml^2/2)\left[2\dot\theta_1^2 + \dot\theta_2^2 + 2c_{12}\dot\theta_1\dot\theta_2\right] + mgl[3 - 2\cos\theta_1 - \cos\theta_2], \\ H &= 1/(2ml^2(1+s_{12}^2))\left[p_1^2 + 2p_2^2 - 2c_{12}p_1p_2\right] + V. \end{aligned} \tag{13.116}$$

6. Consider a **triple pendulum**, i.e., a double pendulum with a third mass suspended from the ‘lower’ bob by a massless rigid rod, all free to move in a vertical plane. How many degrees of freedom does it have? What is the configuration space as a manifold? What are a convenient set of coordinates on this configuration space?

7. A **positive-semidefinite matrix** A is a real symmetric matrix whose eigenvalues are nonnegative. (a) Show that a matrix is positive-semidefinite iff all its diagonal matrix elements are nonnegative, i.e., $v^tAv \geq 0$ for any vector v. (b) Show that the sum of 2 positive-semidefinite matrices is positive-semidefinite. (c) Show that the product of 2 such matrices that commute is positive-semidefinite.

$*$8. Consider the **double pendulum** in the **small oscillation** approximation. (a) Identify the Riemannian metric g_{ij} on the torus $S^1 \times S^1$ defined by the kinetic energy $T = \frac{1}{2}g_{ij}\dot\theta^i\dot\theta^j$ in the small oscillation approximation. (b) Is it a flat/curved metric? Find out by calculating the Riemann tensor (see Appendix B.12.1*). (c) Is the picture of this torus as the surface of a vada/tyre-tube embedded in 3d Euclidean space $\mathbb{R}^3$, a geometrically faithful (i.e., isometric) depiction?

9. Find the **eigenvalues and eigenvectors** of the matrix $B = (2,1|2,2)$ that arises as a coefficient matrix in the small oscillation approximation to the double pendulum.

10. **Diagonalizing** τ, v**.** Show by explicit matrix multiplication that the kinetic and potential matrices (13.41) for small oscillations of a double pendulum are diagonalized by the transformation S that diagonalizes the coefficient matrix B of (13.30):

$$S^t\tau S = D/2 = (1/2)\,\mathrm{diag}(\lambda_+, \lambda_-) \quad \text{and} \quad S^tvS = I/2. \tag{13.117}$$

11. **Quasiperiodic motion.** Show that a superposition of two periodic motions is not periodic if the ratio of individual periods is irrational. In other words, suppose $f_1(t)$ and $f_2(t)$ are periodic functions with periods T_1 and T_2. Then argue that $f_1 + f_2$ is not periodic if T_1/T_2 is irrational. Hint: Try to prove this by contradiction.
12. **Small oscillations of a double pendulum.** Consider the double pendulum in the small oscillations approximation $|\theta_i| \ll 1$, with Hamiltonian
$$H(\theta_i, p_i) = (1/2ml^2)\left[p_1^2 + 2p_2^2 - 2p_1p_2\right] + mgl\left[\theta_1^2 + (\theta_2^2/2)\right]. \qquad (13.118)$$
Show that a constant energy $H = E$ hypersurface is contained in a bounded region of phase space. Why is this intuitively/physically expected?
13. **Similarity transformation.** Find a basis change (similarity transformation S) that converts the nonsymmetric matrix $M^{-1}K = (g/l)\begin{pmatrix} 2 & -1 \\ -2 & 2 \end{pmatrix}$ into a real symmetric matrix. Hint: You could transform to the eigenbasis, what S does this correspond to and is it an orthogonal matrix? Which other bases is $M^{-1}K$ diagonal in?
14. Use methods of Sect. 13.3* to write H (13.56) as a sum of **normal mode energies**.
15. **Normal modes.** In Sect. 13.3*, we considered small oscillations around a local minimum q_0 of the potential $U(q)$. Think about how the discussion that follows would change if q_0 were an extremum but not a local minimum. Comment on the eigenvalues of the Hessian spring constant matrix k_{ij} of U at q_0 and the eigenvalues ω^2 of the coefficient matrix $M^{-1}K$ (13.60) and their physical interpretation. What does this imply for the time-dependence of normal modes?
16. What can you say in general about the **level hypersurfaces** (in phase space) of two **conserved quantities** that are functionally dependent on each other.
17. Recall that in the **small angle approximation**, the dynamics of a **double pendulum** decouples for normal modes. The Hamiltonian of the double pendulum may be expressed as a sum of normal mode energies $H = H_+ + H_-$ where
$$\frac{H_\pm}{\lambda_\pm} = \frac{p_\pm^2}{4ml^2} + \frac{ml^2}{4}\omega_\pm^2\xi_\pm^2 \quad \text{with } \lambda_\pm = 2 \pm \sqrt{2}, \;\; \omega_\pm = \frac{2\omega^2}{\lambda_\pm} \;\text{ and }\; p_\pm = ml^2\dot{\xi}_\pm. \qquad (13.119)$$
What are the PBs among p_+, p_-, ξ_+, ξ_-? Use the harmonic oscillator to find **angle-action variables** for small oscillations of a double pendulum and express them in terms of the old canonical variables ξ_+, p_+, ξ_-, p_-. You may first take $l = 1$.
18. Argue that for fixed $t > 0$, the **cube** $t \geq t_1, t_2, t_3 \geq 0$ is the union of six equally voluminous **tetrahedra**, which are disjoint except that they may share boundaries. Hint: The first tetrahedron may be taken to be $t \geq t_1 \geq t_2 \geq t_3 \geq 0$.

$*$19. **Jordan normal form.** Consider the matrix $M = \begin{pmatrix} -5 & 4 \\ -9 & 7 \end{pmatrix}$ representing a linear transformation acting on $\mathbb{R}^2$ in the standard basis.

   a. Find $\det M, \ \operatorname{tr} M$.
   b. Deduce its eigenvalues and also find the characteristic polynomial of M.
   c. Find linearly independent eigenvectors u corresponding to each eigenvalue. To avoid fractions, normalize all eigenvectors so that their upper component is 2.

d. Can M be diagonalized by a change of basis? Why?

e. There is a basis for $\mathbb{R}^2$ consisting of eigenvectors and generalized eigenvectors of M in which M takes a simple form. A generalized eigenvector $v \neq 0$ is one which is annihilated by $(M - \mu I)^2$ in this case. Find all such v and pick one really simple $\tilde{v}$ that is linearly independent of the genuine eigenvectors u.

f. Check that $(M - \mu I)\tilde{v} = cu$ is proportional to an eigenvector u with eigenvalue μ. Why did this have to be the case?

g. Now find the matrix $\tilde{J}$ representing M in the new basis consisting of $u, \tilde{v}$. Mention any plausible features of $\tilde{J}$ that are manifest. Hint: The matrix $\tilde{J} = S^{-1}MS$ where the columns of S are $u, \tilde{v}$ *in that order*. S is the similarity transformation from the old to the new basis.

h. To get the Jordan normal form J of M we want the north-east corner entry in J to be equal to 1 (first superdiagonal). This is achieved by picking a generalized eigenvector v so that the above proportionality constant is $c = 1$. Can you see why this is the case? Find a generalized eigenvector v so that $(M - \mu I)v = u$. Show that such a v is not unique. So for definiteness, choose the upper component of v to be 1.

i. Find the Jordan normal form of M, $J = S^{-1}MS$ using the above choice of v.

j. The Jordan form helps us understand what M does when it acts repeatedly, which will be useful in analyzing systems subject to forces that oscillate periodically in time. Find M^{100} using the similarity transformation to Jordan form. Notice that this is substantially easier than direct calculation of M^{100}.

20. Suppose the **monodromy matrix** for small perturbations around a periodic orbit is

$$M = \begin{pmatrix} -5 & 4 & 0 & 0 \\ -9 & 7 & 0 & 0 \\ 0 & 0 & 1/\sqrt{2} & 1/\sqrt{2} \\ 0 & 0 & -1/\sqrt{2} & 1/\sqrt{2} \end{pmatrix}. \tag{13.120}$$

How many degrees of freedom does the system have? What can you say about the stability of the orbit to perturbations in various directions?

∗21. **Transformation of covariant tensor.** Explain if the following statement is true or false. A covariant tensor of rank two $K = k_{ij}$ under a change of vector space basis $e_i \mapsto f_\alpha = S^i_\alpha e_i$ transforms via a similarity transformation $\tilde{k}_{\alpha\beta} = (S^{-1})^i_\alpha k_{ij} S^j_\beta$.

∗22. Formulate the **Schrödinger eigenvalue problem** for a particle moving along a line in a potential $V(x)$, $[-\frac{\hbar^2}{2m}\psi''(x) + V(x)\psi(x) = E\psi(x)]$ as a pair of first order ODEs and write it in matrix form $\phi' = A\phi$. Find the coefficient matrix A and show that it is traceless but not symmetric in general.

23. Suppose the real eigenvalue μ of the **monodromy matrix** satisfies $0 < |\mu| < 1$. Show that $|\mu + 1/\mu| > 2$. This establishes that the trace of a 2×2 monodromy matrix exceeds 2 in magnitude if the eigenvalues are real and unequal.

24. Define the **Wronskian** $W(f, g)(t) = \det \begin{pmatrix} f & g \\ \dot{f} & \dot{g} \end{pmatrix} = f\dot{g} - \dot{f}g$ of two solutions of the second order ODE $\ddot{\xi} + \omega(t)\xi = 0$. Show that W is time-independent.

Chapter 14

Bifurcations: qualitative changes in dynamics

We have seen in Chap. 5 that a (continuous-time) dynamical system can be viewed as a system of 1^{st} order ODEs. The latter define a vector field on the phase space. It is often the case that the vector field depends continuously on one or more 'control' parameters such as coupling constants or interaction strengths, masses of particles, material constants or growth rates. Furthermore, the nature of the dynamics may change significantly as these parameters are varied. These changes are reflected in the structure of the phase portrait of the vector field. For instance, the nature of fixed points and limit cycles can undergo qualitative changes known as *bifurcations*, as a control parameter a is varied across a critical value a_c, at the bifurcation point. Although we focus on vector fields in this chapter, bifurcations also occur in discrete-time dynamical systems such as iterations of maps. Bifurcations are widely encountered in practice (e.g., in the buckling of a column, in airplane wing flutter and in chemical oscillations [99, 122]) and are like thermal phase transitions such as the melting of ice or the paramagnetic to ferromagnetic transition in a magnet at its Curie temperature. Near a bifurcation, one may sometimes identify scaling laws and exponents much like those in critical phenomena associated to phase transitions. The buckling of a card or column due to compressional stresses can be modeled via a bifurcation in a vector field. At a bifurcation, fixed points (which may model equilibria of a mechanical system) or limit cycles (which may model self-sustained oscillations) may be created or destroyed or their stability may change. These changes are sometimes also associated to the transition from regular to irregular or chaotic motion. For instance, the development of instabilities in fluid flows and the transition from regular or laminar to turbulent flow of a fluid can involve (a succession of) bifurcations. The transition from regularity to widespread chaos in the logistic map (see Sect. 15.1.3), the Hénon-Heiles system (see Sect. 15.4 and [87, 126]) and the three-rotor problem [73, 78] are associated with a cascade or accumulation of an infinite sequence of bifurcations. In this chapter, we introduce some examples of bifurcations of vector fields on the real line and on the Euclidean plane. Some of these will be relevant to the logistic map and Lorenz model to be taken up in Chap. 15. Although most realistic systems involve more degrees of freedom, the essential dynamics in the vicinity of a bifurcation can, in many cases, be distilled to that involving just a few degrees of freedom.

14.1 Bifurcations of vector fields on the real line

The buckling or bending of a horizontal rectangular card compressed between two opposite edges using two fingers provides an example of a bifurcation in one dimension. The compressional stress F is the control parameter while a measure of departure of the card from flatness (e.g., height of center relative to compressed edges) is the dynamical variable. For a range of small F, the card has only one stable equilibrium: it is flat. At a critical compression $F_{\rm cr}$, it bends either upwards or downwards. Thus, for compression above the threshold value, we have two stable equilibria (card bent upwards or downwards) and one unstable equilibrium (flat card) as shown in Fig. 14.1. This is an example of a pitchfork bifurcation. It is associated with spontaneous breaking of the up-down reflection symmetry. We will soon see how to model the essence of this situation using a vector field on a line. In what follows, we will examine three types of bifurcations in one dimension: saddle-node, transcritical and pitchfork.

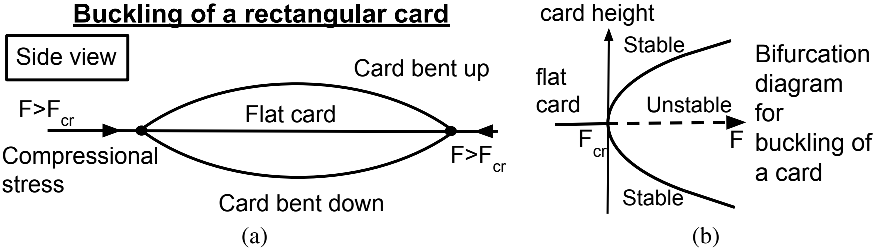

Figure 14.1: (a) Buckling of a card subjected to a compressional stress above a critical value. (b) *Bifurcation diagram* showing possible (stable and unstable) equilibrium heights of middle of card as a function of compressional stress F (both below and above $F_{\rm cr}$).

14.1.1* Saddle-node bifurcation

Imagine a dynamical system defined by a vector field $v(x)$ that depends on a real control parameter a. We shall focus on the fixed points x_* of v and examine how they move as a is varied. In a saddle-node bifurcation, as a is (say) increased across a critical value a_c, two fixed points merge and annihilate leaving no fixed point. Decreasing a across a_c would describe the 'pair production' of two fixed points. The name 'saddle-node' comes from a generalization of this bifurcation to flows on the plane (see Sect. 14.2.1*).

The prototypical family of vector fields displaying such a bifurcation is $v(x;a) = a + x^2$. The bifurcation point is $a_c = 0$. Fig. 14.2 shows that for $a < 0$, v has 2 fixed points: $x_* = \sqrt{-a}$ is unstable while $x_* = -\sqrt{-a}$ is stable. They coalesce at the half-stable fixed point $x_* = 0$ as $a \to 0^-$. For $a > 0$, there are no fixed points. The *bifurcation diagram* in Fig. 14.2 showing the locations of the fixed points on the a-x plane indicates why a saddle-node bifurcation is also called a fold or turning point bifurcation. Similarly, $v(x;a) = a - x^2$ displays a saddle-node bifurcation where a pair of fixed points emerge as a increases beyond $a_c = 0$. These quadratic vector fields are not just simple examples, they are canonical/normal forms of vector fields displaying a saddle-node bifurcation (in the neighborhood of the bifurcation point and in the vicinity of the merging fixed points)[1]. Indeed, without loss of generality, we may take the bifurcation point to be $a_c = 0$ and the point of coalescence of fixed points to be $x = 0$. Then $v(x;a)$ must be parabolic in x for x and a near zero in order for there to be two merging fixed points. This may also be seen by Taylor expanding a vector field $v(x;a)$ that displays a saddle-node bifurcation at (x_*, a_c). Indeed,

---

[1] Somewhat more precisely, a vector field displaying a saddle-node bifurcation can (in a neighborhood of a_c and the point of coalescence) be continuously mapped to the normal form.

$$\begin{aligned} v(x;a) &= v(x_*;a_c) + (x - x_*)\partial_x v(x_*;a_c) + (a - a_c)\partial_a v(x_*;a_c) \\ &\quad + (1/2)(x - x_*)^2 \partial_x^2 v(x_*;a_c) + \cdots . \end{aligned} \tag{14.1}$$

Now $v(x_*, a_c) = 0$ as x_* is a fixed point when $a = a_c$. Moreover, $\partial_x v(x_*;a_c) = 0$ as the graph of v must be tangent to the x-axis when $a = a_c$ so that v can have a double zero corresponding to the coalescence of fixed points. Neglecting higher order terms, we get the canonical form $v(x;a) = \alpha(a - a_c) + \beta(x - x_*)^2$.

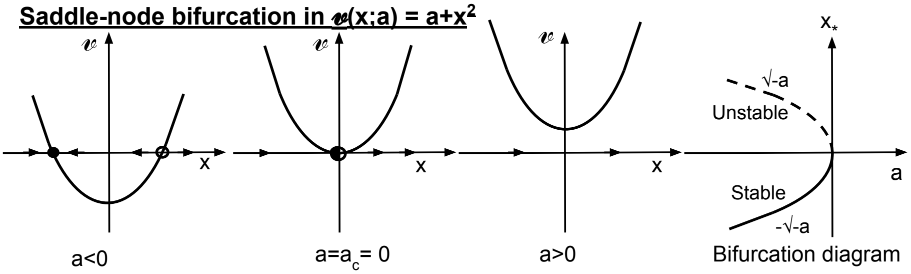

Figure 14.2: Saddle-node bifurcation showing annihilation of stable and unstable fixed points.

14.1.2* Transcritical bifurcation

This describes a situation where a fixed point x_* exists for all parameter values, but whose stability changes as a is varied. For instance, x_* may go from being stable to unstable as a crosses a_c. This is achieved by making another fixed point ‘pass through’ x_* and ‘exchange’ stabilities with it. The following normal form demonstrates the phenomenon. Consider

$$v(x) = ax - x^2 = x(a - x) = -(x - a/2)^2 + a^2/4. \tag{14.2}$$

$x_* = 0$ is clearly always a fixed point. A second fixed point located at $x_{**} = a$ moves to the right as a increases past $a_c = 0$ (see Fig. 14.3). For $a < 0$, the fixed point at the origin is stable while the one at a is unstable. At $a = 0$, $v = -x^2$ and the fixed points merge at the origin, which is half-stable. Finally, for $a > 0$ the origin becomes unstable while $x_{**} = a$ is stable. The bifurcation diagram in Fig. 14.3 shows that the fixed points have exchanged stabilities via the bifurcation at $a = 0$.

The logistic equation[2], considered for real N, K and r,

$$\dot{N} = v(N) = rN(1 - N/K) = (r/K)N(K - N), \tag{14.3}$$

---

[2] The logistic equation is a model for the dynamics of the population $(N(t) \geq 0)$ of a species. It postulates that the per-capita growth rate $\dot{N}/N$ is a constant $r > 0$ for small N so that small populations grow exponentially. However, as the population grows, pressure on resources leads to a decrease in the per-capita growth rate, which eventually drops to zero when the population reaches the carrying capacity $K > 0$. The vector field $v(N)$ has two fixed points. The zero population fixed point $N_* = 0$ is unstable while the carrying capacity $N_* = K$ is stable: any nonzero population always tends monotonically to the carrying capacity as $t \to \infty$.

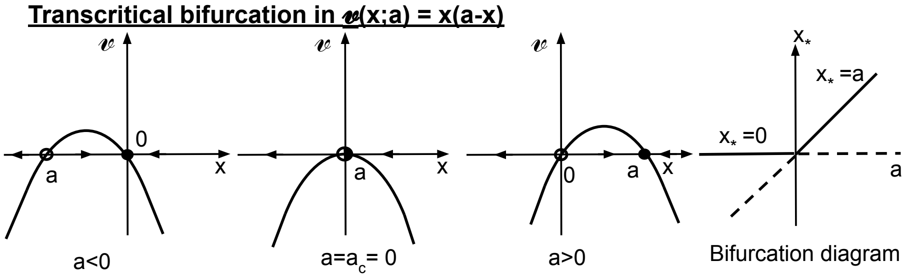

Figure 14.3: Transcritical bifurcation in 1d.

displays a transcritical bifurcation of the $N_* = 0$ (zero population) fixed point as the carrying capacity K slides past $K_c = 0$ provided $\tilde{r} = r/K > 0$ is held *fixed*. For $K < 0$, $N_* = 0$ is stable as $v'(0) = K\tilde{r} < 0$ while $N_* = K$ is unstable. The two fixed points exchange stabilities at $K_c = 0$ with the zero population fixed point becoming unstable and $N_* = K$ becoming stable for $K > 0$.

We will encounter another example of a transcritical bifurcation in the logistic map of Sect. 15.1.3 where the trivial and nontrivial fixed points exchange stabilities when the control parameter crosses unity.

There are variants of this transcritical bifurcation where the stability of a fixed point changes as a parameter is varied. (i) For the linear vector field $v(x) = ax$, $x_* = 0$ changes from being stable for $a < 0$ to unstable for $a > 0$. At $a = 0$, we have a line of fixed points: the vector field vanishes. (ii) Returning to the logistic equation, $\dot{N} = v(N) = rN(1 - N/K)$, suppose we now hold K fixed and let r vary. Then the zero population fixed point $N_* = 0$ goes from being stable for $r < 0$ to unstable for $r > 0$. On the other hand, the fixed point $N_* = K$ at the carrying capacity goes from being unstable to stable as r increases past the bifurcation point $r_c = 0$. Interestingly, at $r = 0$, v vanishes identically and we have a line of fixed points. Though the fixed points at 0 and K exchange stabilities at $r_c = 0$, they do not merge at r_c. Neither fixed point moves, and it is as if they exchange stabilities through an action at a distance via the line of fixed points. We might use the name *transcritical bifurcation with action at a distance* for exchange of stabilities of this sort.

14.1.3* Pitchfork bifurcations

Pitchfork bifurcations are named after an agricultural tool that looks like a *Trishul* or trident. It has a long handle and three tines or prongs. Pitchfork bifurcations are typically seen in systems with a discrete parity or left-right ($\mathbb{Z}/2\mathbb{Z} = \mathbb{Z}_2$) symmetry. In the bending of a card (see Fig. 14.1), one stable flat (parity invariant) equilibrium configuration becomes unstable at the bifurcation point (critical compressional stress) where two stable equilibria with opposite parities are born. Though the word bifurcation is standard, pitchfork trifurcation describes the situation more accurately.

There are two types of pitchfork bifurcations: supercritical and subcritical. The former is associated with the bending of a card or buckling of a column under a weight as well as to second order or continuous phase transitions while the latter is associated with first order or discontinuous phase transitions in thermal physics.

14.1.3.1* Supercritical pitchfork bifurcation

The normal form in this case is

$$\dot{x} = ax - x^3 = x(a - x^2). \tag{14.4}$$

This ODE has an $x \to -x$ parity symmetry. This means that every trajectory is either parity neutral or comes paired with another trajectory related to it by a parity transformation. This applies to fixed points as well (which are static trajectories). For $a < 0$, the origin $x_* = 0$ is the only fixed point, and it is stable: $v'(0) = a$ so that trajectories approach the origin exponentially fast with time constant $1/|a|$. When $a = 0$, the vector field has a triple zero at $x_* = 0$, which is still a stable fixed point, though the linear decay time constant diverges. So trajectories that start at x_0 at $t = 0$, i.e., $x(t) = \operatorname{sgn}(x_0)\,(2t + 1/x_0^2)^{-1/2}$ approach the origin as a power-law rather than exponentially. This is similar to critical slowing down (p.643 of [100]) in the vicinity of a 2$^{\text{nd}}$ order phase transition in classical statistical mechanics. Finally, when $a > 0$, we have three fixed points, an unstable one at $x_* = 0$ and two stable 'nontrivial' fixed points at $x_* = \pm\sqrt{a}$. The bifurcation diagram in Fig. 14.4 looks like a horizontal pitchfork with prongs pointing to the right. The connection to the bending of the card in Fig. 14.1 is evident. This pitchfork bifurcation is called *supercritical* to signify that the nontrivial fixed points that are born at the bifurcation are stable. A supercritical bifurcation is safe in the sense that although ICs close to the fixed point $x_* = 0$ are no longer attracted to it when $a > 0$, they are nevertheless attracted to a fixed point that gets arbitrarily close to $x_* = 0$ as $a \to 0^+$.

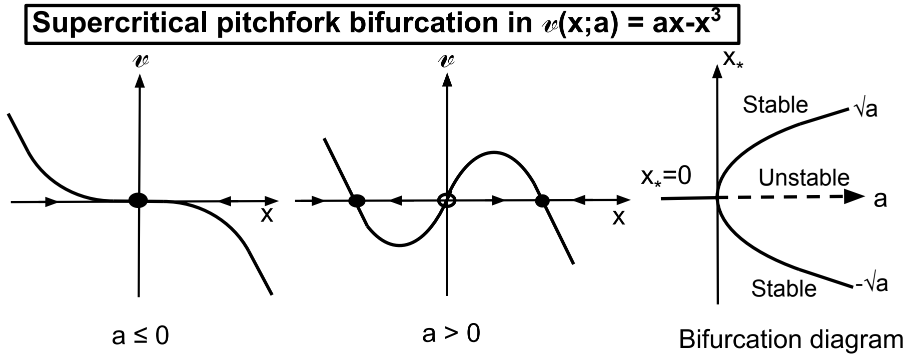

Figure 14.4: Supercritical pitchfork bifurcation in 1d.

It is instructive to look at the potential (5.15) for the vector field $v(x) = ax - x^3$. It is a quartic potential

$$\phi(x) = -\frac{1}{2}ax^2 + \frac{1}{4}x^4 \quad \text{with} \quad v = -\phi'. \tag{14.5}$$

Viewed as a potential for a particle moving on the line, we see that the quartic term is attractive/stabilizing. For $a < 0$, ϕ has only one extremum, a global minimum at $x_* = 0$, the minimum becomes very flat at the critical point $a = 0$ while it turns into a double-well potential for $a > 0$.

The *basin of attraction* (see Sect. 5.1) of a fixed point x_* is the set of ICs x_0 for which $x(t) \to x_*$ as $t \to \infty$. In the above case, $x_* = 0$ is a global attractor for $a \leq 0$. For $a > 0$, the two fixed points $x_* = \pm\sqrt{a}$ have basins of attraction consisting of the positive and negative half lines $x_0 > 0$ and $x_0 < 0$, while $x_0 = 0$ is the only point in the basin of attraction of the unstable fixed point at $x_* = 0$.

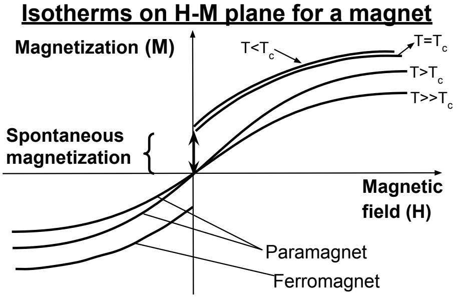

Figure 14.5: Plot of magnetization M (in a magnetic domain) versus applied magnetic field H for various temperatures. For $T > T_c$ (temperature above the Curie temperature, paramagnetic phase) $M = \chi H$ for small H (linear response regime) while M saturates for large H. For $T \leq T_c$ (ferromagnetic phase) there is a residual (spontaneous) magnetization even when $H \to 0^{\pm}$. There is a 2^{nd} order phase transition at T_c.

Analogy with 2^{nd} order phase transitions. A system with a $\mathbb{Z}_2$ symmetry displaying a 2^{nd} order phase transition is a 2d Ising spin system where 'spins' which can either point up or down are located on a square lattice. Neighboring spins tend to align due to the exchange interaction between spins, but thermal fluctuations can prevent all spins from being aligned. The system as a whole is invariant under reversal of the sign of all spins. It displays a 2^{nd} order paramagnetic to ferromagnetic transition as the temperature is lowered below the Curie temperature T_c (see Fig. 14.5). In the paramagnetic phase, the net magnetization ($\propto$ total spin) is zero in the absence of an external magnetic field (due to thermal fluctuations) corresponding to the single fixed point $x_* = 0$. In the ferromagnetic phase, there is a nonzero net 'spontaneous' magnetization with all spins in a magnetic domain pointing either up or down (corresponding to the stable fixed points $x_* = \pm\sqrt{a}$). In the vicinity of the 2^{nd} order phase transition at T_c, there are long-range fluctuations, one of whose effects is that one needs to average over a very large number of configurations to reliably calculate mean values in a Gibbs ensemble. This is one manifestation of critical slowing down. Moreover, correlation functions display power-law decay at T_c, while away from the critical temperature, they decay exponentially. This is somewhat similar to what we found for the rate of approach/emergence to/from the fixed point $x_* = 0$.

14.1.3.2* Subcritical pitchfork bifurcation

Reversing the sign of the quartic term in the potential ϕ (14.5) or the cubic term in v (14.4) leads to a subcritical pitchfork bifurcation. Thus we consider

$$\dot{x} = v(x) = ax + x^3 = x(a + x^2) \tag{14.6}$$

which corresponds to the quartic potential $\phi(x) = -\frac{1}{2}ax^2 - \frac{1}{4}x^4$.

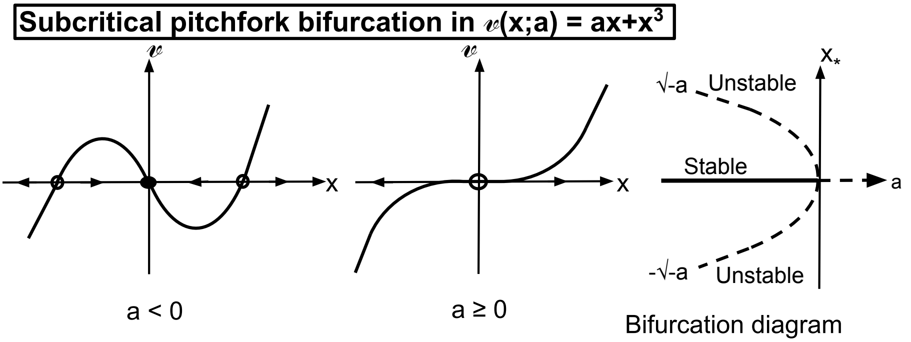

Figure 14.6: Subcritical or backward pitchfork bifurcation in 1d.

As shown in Fig. 14.6, for $a < 0$, there are three fixed points $x_* = 0$ (stable) and $x_* = \pm\sqrt{-a}$ (unstable). When $a \to 0^-$, the three fixed points merge into a single unstable fixed point at $x_* = 0$ which then survives as an unstable fixed point for $a > 0$. The bifurcation diagram for a subcritical pitchfork bifurcation looks like a laterally inverted version of the supercritical one, except that the nontrivial fixed points are unstable in the subcritical case, while they were stable in the supercritical case. It is called subcritical to convey that the nontrivial fixed points $x_* = \pm\sqrt{-a}$ are unstable. What is more, for $a \geq 0$, the origin is very unstable and all nonconstant trajectories blowup in finite time. This is easily seen for $a = 0$, where the solution to the IVP is $x(t) = \text{sgn}(x_0)(1/x_0^2 - 2t)^{-1/2}$. We see that $x(t) \to \pm\infty$ according as $\text{sgn}(x_0) = \pm 1$ at the blowup time $t_b = 1/2x_0^2$ for any nonzero x_0.

In practice, additional nonlinear effects would become important once the solutions grow sufficiently. The simplest parity symmetric model incorporating these is

$$\dot{x} = v(x) = ax + x^3 - x^5. \tag{14.7}$$

It is clear that $x_* = 0$ is always a fixed point, linearly stable for $a < 0$ and unstable for $a > 0$. The other fixed points are roots of the quartic equation $a + x^2 - x^4 = 0$:

$$x_*^{\pm\pm} = \pm\left[(1/2)(1 \pm \sqrt{1 + 4a})\right]^{1/2}. \tag{14.8}$$

For $a < a_s = -1/4$, $x_* = 0$ is the only fixed point. For $-1/4 < a < 0$ there are four nontrivial fixed points $x_*^{\pm\pm}$. While $x_*^{\pm,-}$ are unstable, $x_*^{\pm,+}$ are stable. For $a > 0$ we have only two nontrivial fixed points $x_*^{\pm,+}$, both of which are stable. This vector field displays both a subcritical pitchfork bifurcation at $a = 0$ as well as a pair of saddle-node bifurcations at $a_s = -1/4$ where the stable ($x_*^{\pm,+}$) and unstable ($x_*^{\pm,-}$) large-amplitude fixed points are born.

Fig. 14.7 shows the potential $\phi(x) = -ax^2/2 - x^4/4 + x^6/6$ in the three qualitatively different regions: (a) $a < -1/4$, (b) $-1/4 < a < 0$ and (c) $a > 0$. For $a < -1/4$, the quartic term does not have a chance to play a qualitative role (for small x it is dominated by the quadratic term with large coefficient, while for large x it is dominated by the x^6 term!) and ϕ has only one extremum, a global minimum

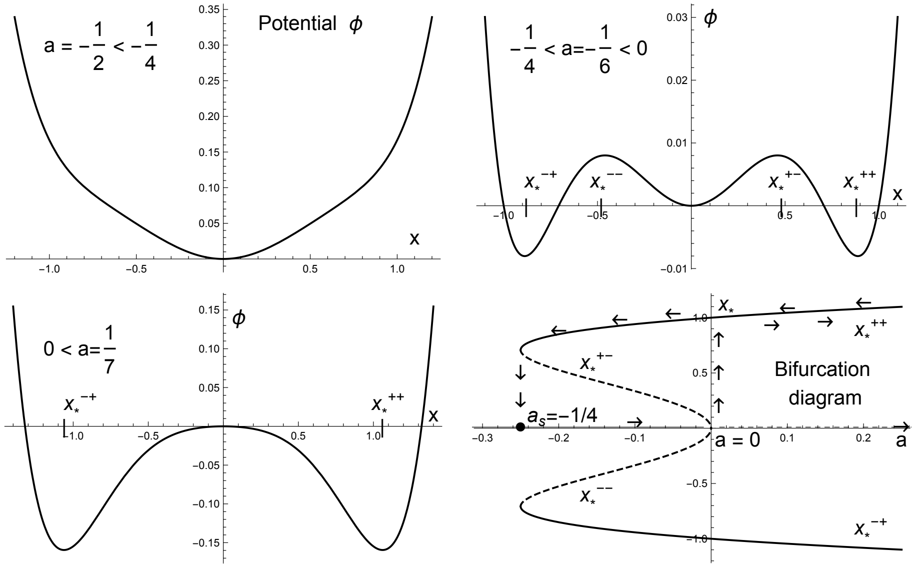

Figure 14.7: Potential $\phi = -ax^2/2 - x^4/4 + x^6/6$ and bifurcation diagram for $\dot{x} = v(x) = ax + x^3 - x^5$ which displays a subcritical pitchfork bifurcation stabilized by large amplitude fixed points $x_*^{\pm +}$. Extrema of the potential are fixed points. The dashed and solid lines represent unstable and stable fixed points. There are two saddle-node bifurcations at $a_s = -1/4$ and a subcritical pitchfork bifurcation at $a = 0$. The arrows show hysteresis.

at $x_* = 0$. For $-1/4 < a < 0$, there is a local minimum at $x_* = 0$, a pair of local maxima at $x_*^{\pm,-}$ and a pair of local minima at $x_*^{\pm,+}$. Finally, for $a > 0$, ϕ has a local maximum at $x_* = 0$ and a pair of global minima at $x_*^{\pm,+}$.

Interestingly, this system can display jumps. Thus, unlike the supercritical bifurcation that is associated to second order (continuous) phase transitions, the subcritical one is associated to first order (discontinuous) phase transitions. Indeed, as illustrated in Fig. 14.7, suppose we begin with the system in its unique stable equilibrium $x_* = 0$ for $a < -1/4$ and imagine slowly increasing a. As the trivial fixed point is linearly stable up to $a = 0^-$, the system remains at $x_* = 0$. At $a = 0$, the slightest perturbation causes the system to make a discontinuous transition or 'jump' from $x_* = 0$ to one of the two 'far-away' stable fixed points $x_* = x_*^{\pm,+}$ (this makes a subcritical bifurcation 'unsafe'). Suppose it jumps to the 'upper' branch $x_*^{+,+}$. With further increase in a, the system remains in the stable equilibrium $x_*^{+,+}$. Now, suppose a is decreased. Interestingly, the system remains in the state $x_*^{+,+}$ even when a is decreased below $a = 0$, as it is a stable state. In other words, the system does not retrace its path even when the control parameter retraces its path! Hysteresis is the name for this lack in reversibility, it is seen in ferromagnets and is exploited in computer hard disk memories. A second jump occurs when a is decreased down to $a_s = -1/4$ at which point the nontrivial fixed points cease to exist and the system jumps back to the stable equilibrium $x_* = 0$.

14.2 Bifurcations in two dimensions

We now move to bifurcations of 2d vector fields. In addition to the change in character of fixed points (as in 1d), here we also have the possibility of limit cycles changing stability or being created or destroyed. The linear stability of a fixed point in 2d is largely governed by the eigenvalues $\lambda_{1,2}$ of the linearization of the vector field around the fixed point. A change in stability occurs when one or both eigenvalues cross the imaginary axis in the complex eigenvalue plane, with the left half-plane corresponding to stability and the right to instability (as time-dependence involves $e^{\lambda_1 t}$ and $e^{\lambda_2 t}$, see Sect. 6.3). Since we consider real vector fields, the eigenvalues must either both be real ($\lambda_1, \lambda_2 \in \mathbb{R}$) or complex conjugates $\lambda_\pm = \nu \pm i\omega$. In the former case, bifurcations can occur when either λ_1 or λ_2 vanishes while in the latter case, bifurcations occur when the real parts vanish and $\lambda_\pm = \pm i\omega$. We begin with examples of the *zero eigenvalue* bifurcations, which include saddle-node, transcritical and pitchfork bifurcations on the plane. All these involve 'collisions' between fixed points. We then turn to the imaginary eigenvalue case where limit cycles can be created or destroyed.

14.2.1* Saddle-node, transcritical and pitchfork bifurcations

The saddle-node, transcritical and pitchfork bifurcations generalize in a straightforward manner from one to two and higher dimensions. The flow in all but one direction is passive (attractive or repulsive) and the change in character of the vector field is essentially confined to one direction (say x). In 2d, normal forms can be chosen to involve decoupled pairs of differential equations for x and y.

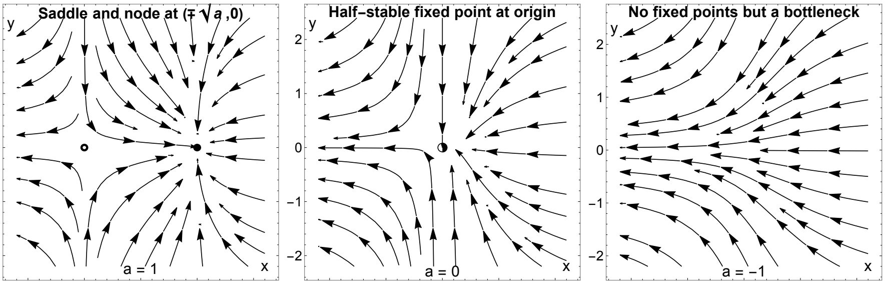

Figure 14.8: Saddle-node bifurcation in 2d for $\dot{x} = a - x^2$ and $\dot{y} = -y$ as a is decreased.

Saddle-node bifurcation. This bifurcation is exemplified by the normal form

$$\dot{x} = a - x^2 \quad \text{and} \quad \dot{y} = -y. \tag{14.9}$$

As a is varied, this vector field displays the basic mechanism by which fixed points can be produced or annihilated in pairs. While $y(t) = y(0)e^{-t}$ approaches zero exponentially fast, the dynamics in the x direction is as in Sect. 14.1.1*. Fig. 14.8 shows that for $a > 0$, we have a saddle at $(-\sqrt{a}, 0)$ and a stable node at $(\sqrt{a}, 0)$. As a decreases to zero, the saddle and node coalesce at a partly stable-partly unstable fixed point at the origin, whose basin of attraction is the closed right half-plane. This explains the name saddle-node bifurcation. There are no fixed points when $a < 0$. However, for $a \lesssim 0$, there is a remnant of the fixed point around $(0, 0)$. Though the flow is generally up/downwards and leftwards (towards an unstable direction of the erstwhile saddle), trajectories are slowed down as they pass through a bottleneck around the origin.

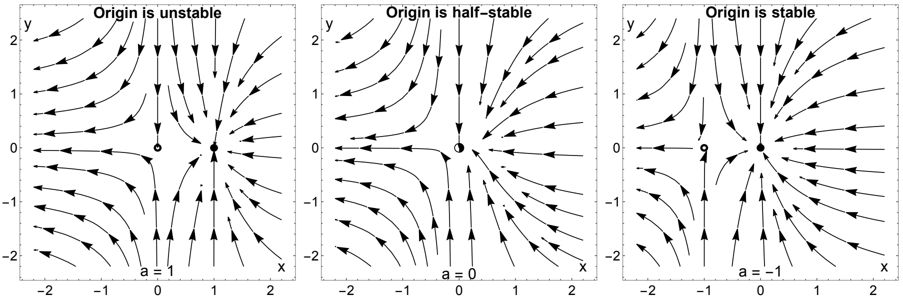

Figure 14.9: Exchange of stabilities via a transcritical bifurcation in 2d for the vector field $\dot{x} = x(a - x)$ and $\dot{y} = -y$. The origin goes from unstable (a saddle) to stable (a node) as a is decreased below zero.

Transcritical bifurcation. Analogously, the transcritical bifurcation of Sect. 14.1.2* generalizes to 2d. The canonical form is

$$\dot{x} = x(a - x) \quad \text{and} \quad \dot{y} = -y. \tag{14.10}$$

As shown in Fig. 14.9, this vector field has fixed points at $(0, 0)$ and $(a, 0)$. For $a < 0$, the origin is a stable node and $(a, 0)$ is a saddle. As a increases past 0, the fixed point at $(a, 0)$ passes through the origin and exchanges stabilities with it. As a result, for $a > 0$, the origin becomes a saddle while $(a, 0)$ becomes a stable node.

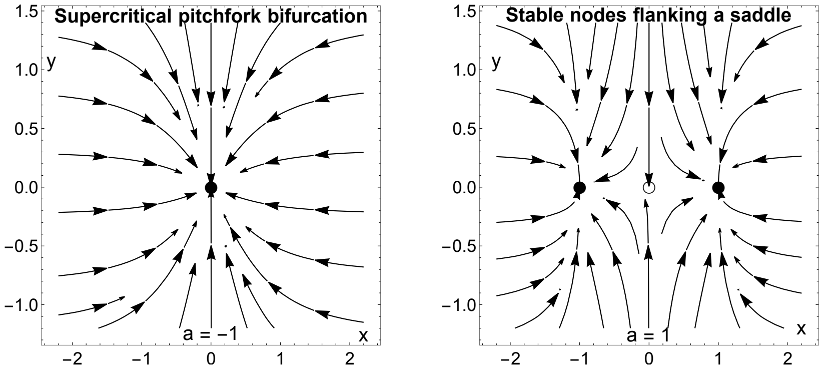

Figure 14.10: Supercritical pitchfork bifurcation in $\dot{x} = ax - x^3, \dot{y} = -y$. The nontrivial fixed points born at the bifurcation are stable nodes making it safe.

Pitchfork bifurcation. The supercritical and subcritical bifurcations in 2d (illustrated in Fig. 14.10 and Fig. 14.11) are typified by the vector fields

$$\dot{x} = x(a - x^2), \quad \dot{y} = -y \quad \text{and} \quad \dot{x} = x(a + x^2), \quad \dot{y} = -y. \tag{14.11}$$

In the supercritical case, we go from a single fixed point, a stable node at the origin for $a < 0$ to a saddle at the origin flanked by two stable nodes at $(\pm\sqrt{a}, 0)$ when a exceeds zero. In the subcritical case (see Fig. 14.11), a stable node at the origin is flanked by a pair of saddles at $(\pm\sqrt{-a}, 0)$ for $a < 0$. When $a > 0$, the origin is the only fixed point, a saddle. The main distinction is that while the nontrivial fixed points that germinate at the bifurcation are stable in the supercritical case, they are unstable for subcritical bifurcations.

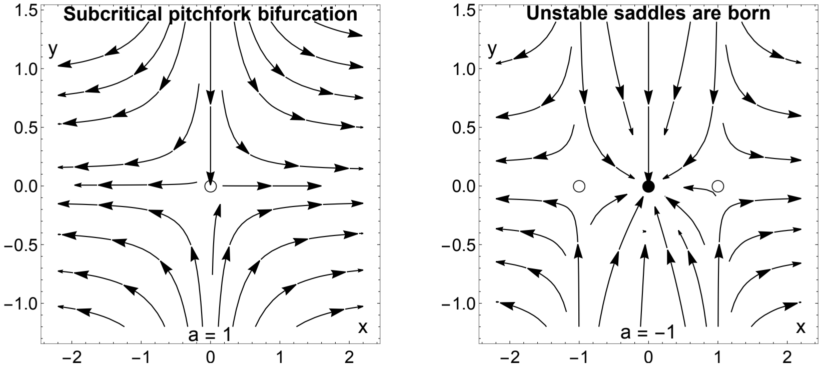

Figure 14.11: Subcritical pitchfork bifurcation in $\dot{x} = ax + x^3, \dot{y} = -y$. The nontrivial fixed points born at the bifurcation are unstable saddles making it dangerous.

Remarks. In these three examples of bifurcations, a stable fixed point underwent a change in stability as the control parameter was varied. The Jacobian of the vector field around a stable fixed point generically has a pair of eigenvalues that lie in the left half of the complex eigenvalue plane. These eigenvalues could both be negative (as for a stable node) or be complex conjugates (as in the case of a spiral sink). The bifurcation is associated with a change in stability. This typically happens when one or both eigenvalues reach the imaginary axis or cross over to the right half-plane. In the above examples, we were dealing with real eigenvalues (since nodes and saddles were involved) and one of the eigenvalues reached $\lambda = 0$ at the bifurcation point. Thus, they are called zero-eigenvalue bifurcations. The other possibility where a pair of complex conjugate eigenvalues in the left half-plane together cross the imaginary axis is qualitatively different and leads to Hopf bifurcations, which we turn to next. □

14.2.2* Hopf bifurcations

Unlike the saddle-node, transcritical and pitchfork bifurcations of Sect. 14.2.1* which involve collisions between fixed points, Hopf bifurcations do not. A Hopf bifurcation is one way in which a limit cycle can be created or destroyed. Though Hopf bifurcations are not direct generalizations of 1d bifurcations, they bear some resemblance to pitchfork bifurcations. They can occur in a state space of dimension two or more. We will illustrate Hopf bifurcations on the phase plane using a pair of simple examples[3].

---

[3] Hopf's theorem [80] gives conditions for the existence and stability of limit cycles that may germinate at a Hopf bifurcation around a fixed point of a planar vector field.

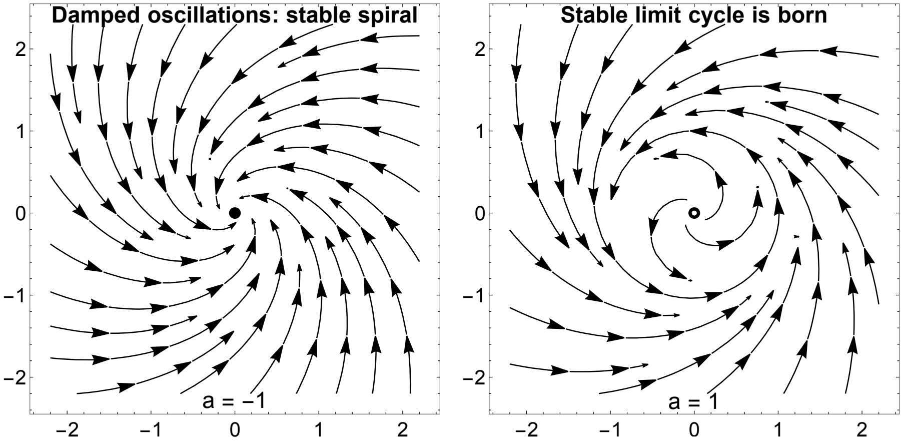

(a) (b)

Figure 14.12: Supercritical Hopf bifurcation of (14.12). (a) Stable spiral for $a = -1$ transitions to (b) a stable limit cycle for $a = 1$. Here $b = \omega = 1$.

Supercritical Hopf bifurcation. A supercritical Hopf bifurcation is somewhat analogous to a supercritical pitchfork bifurcation. Thus, we have a stable fixed point $\boldsymbol{r}_*$ when the control parameter is on one side of a critical value, say $a < a_c$. However, rather than being a stable node, it is a spiral sink. Hence, for $a < a_c$, the system displays damped oscillations before settling down to the fixed point. On the other hand, for $a > a_c$, the fixed point becomes a spiral source. However, stability is not entirely lost, since the spiral approaches a stable limit cycle of roughly elliptical shape that goes round $\boldsymbol{r}_*$. What this means in practice is that the exponential decay to an equilibrium state becomes slower as $a \to a_c^-$. Beyond a_c, the equilibrium state becomes unstable and the system flutters/oscillates about it with relatively small amplitude. One says that the supercritical Hopf bifurcation is safe or soft. A prototypical vector field displaying a supercritical Hopf bifurcation is given in plane polar coordinates by

$$\dot{r} = ar - r^3 \quad \text{and} \quad \dot{\theta} = \omega + br^2. \tag{14.12}$$

For $a \leq 0$, $\boldsymbol{r}_* = 0$ is a stable spiral (see Fig. 14.12a). The approach to the origin goes from exponentially fast to a power-law as $a \to 0^-$. When $a > 0$, the origin is a spiral source. However, the unstable spiral growth saturates (due to the stabilizing effect of the $-r^3$ term, see Fig. 14.12b) at a stable limit cycle given by the circle $r = \sqrt{a}$ on which $\dot{r} = 0$ and $\dot{\theta} = \omega + ab$. The behavior of eigenvalues of the Jacobian is most easily examined in Cartesian coordinates $x = r\cos\theta$ and $y = r\sin\theta$, where

$$\begin{aligned} \dot{x} &= \cos\theta\,\dot{r} - r\sin\theta\,\dot{\theta} = x(a-r^2) - y(\omega + br^2) \\ &= ax - \omega y + \mathcal{O}(x^3, y^3, \cdots) \\ \text{and} \qquad \dot{y} &= \sin\theta\,\dot{r} + r\cos\theta\,\dot{\theta} = y(a-r^2) + x(\omega + br^2) \\ &= \omega x + ay + \mathcal{O}(x^3, y^3, \cdots). \end{aligned} \tag{14.13}$$

Thus, the linearization around the fixed point at the origin is given by $J = \left(\begin{smallmatrix} a & -\omega \\ \omega & a \end{smallmatrix}\right)$ with the eigenvalues $\lambda = a \pm i\omega$. Evidently, the eigenvalues cross the imaginary axis from the left to right half-plane as a increases past zero.

Subcritical Hopf bifurcations are dangerous since after the bifurcation, stable oscillations are rendered unstable and trajectories jump to some ‘far-away’ attractor (a fixed point, a limit cycle, infinity or even a chaotic attractor, as in the case of the Lorenz model of Sect. 15.5*). This is illustrated by the vector field in polar coordinates

$$\dot{r} = ar + r^3 - r^5 \quad \text{and} \quad \dot{\theta} = \omega + br^2. \tag{14.14}$$

The linearization around the fixed point at the origin,

$$\begin{aligned} \dot{x} &= \frac{x}{r}\dot{r} - y\dot{\theta} = x(a + r^2 - r^4) - y(\omega + br^2) \approx ax - \omega y \quad \text{and} \\ \dot{y} &= \frac{y}{r}\dot{r} + x\dot{\theta} = y(a + r^2 - r^4) + x(\omega + br^2) \approx \omega x + ay, \end{aligned} \tag{14.15}$$

leads to the same Jacobian $J = \left(\begin{smallmatrix} a & -\omega \\ \omega & a \end{smallmatrix}\right)$ as in the supercritical case. As before, when a increases past 0, the eigenvalues $a \pm i\omega$ cross over to the right half-plane making the origin an unstable fixed point. What makes this example different is that the r^3 term in (14.14) is now destabilizing. As in the subcritical pitchfork example of Sect. 14.1.3.2*, this is balanced by a stabilizing r^5 term. The latter will be seen to lead to a large-amplitude limit cycle to which trajectories can flow after the bifurcation.

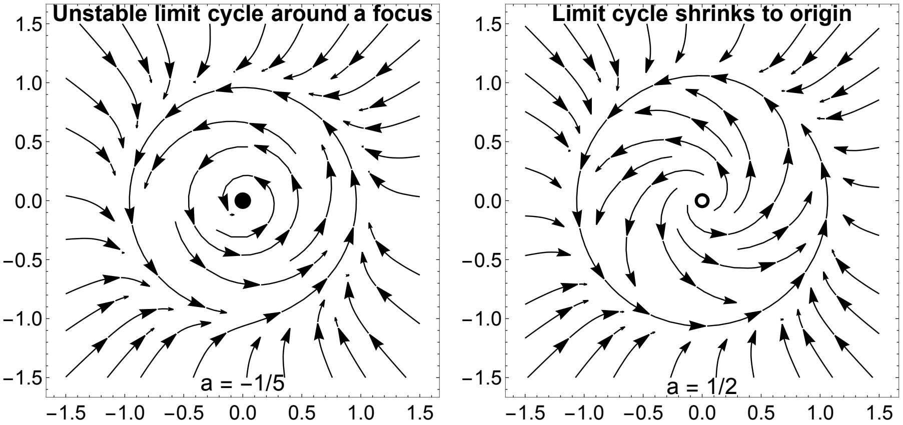

(a) (b)

Figure 14.13: Subcritical Hopf bifurcation of (14.14). (a) Stable spiral (focus) surrounded by an unstable circular limit cycle and a larger stable limit cycle for $a = -1/5$. (b) Unstable spiral with trajectories attracted to a large amplitude limit cycle for $a = 1/2$. Here $b = \omega = 1$.

Indeed, for $-1/4 < a < 0$, there is a spiral sink at the origin surrounded by an unstable limit cycle at $r^2 = (1 - \sqrt{1+4a})/2$ which is in turn surrounded by a larger stable limit cycle at $r^2 = (1 + \sqrt{1+4a})/2$ (see Fig. 14.13a). So for $-1/4 < a < 0$ the system displays decaying oscillations for small amplitude initial conditions. As $a \to 0^-$, the unstable limit cycle shrinks to the origin turning it into an unstable spiral shown in Fig. 14.13b. The decaying oscillations morph into growing oscillations at the subcritical Hopf bifurcation at $a = 0$. In this example, these growing trajectories are then attracted to the limit cycle at $r^2 = (1 + \sqrt{1 + 4a})/2$. This limit cycle is 'far-away' in the sense that it does not shrink to the origin as $a \to 0$.

As in the 1d example of Sect. 14.1.3.2*, this system displays hysteresis. When a is decreased from positive values, the large amplitude oscillations persist all the way down to $a = -1/4$. At this point, the stable and unstable limit cycles collide and annihilate in a saddle-node bifurcation of cycles and we are left with a spiral sink at the origin for $a < -1/4$.

In addition to Hopf bifurcations, there are other ways in which limit cycles can be created or destroyed in 2d. These are classified as global bifurcations as they involve large portions of the phase plane. (a) We already encountered the **saddle-node or fold bifurcation of cycles** at $a = -1/4$ in the example of (14.14). Here, a stable and unstable limit cycle that exist for $a > -1/4$ annihilate and cease to exist for $a < -1/4$. At $a = -1/4$ they coalesce to form a half-stable cycle. (b) **Saddle-node infinite period bifurcation:** Here, a limit cycle develops a bottleneck and a half-stable fixed point is born on the cycle at the bifurcation point, leading to a divergence of the period. Subsequently, the fixed point splits into a pair of fixed points on the erstwhile cycle in a saddle-node bifurcation. A simple example demonstrating this phenomenon is $\dot{r} = r(1 - r^2)$ and $\dot{\theta} = a - \sin\theta$ at $a = 1$ (see Prob. 14.4). (c) **Homoclinic or saddle-loop bifurcation:** In this case, a limit cycle moves close to a saddle point and touches it when the control parameter reaches its critical value. As should be plausible from our examples in Sect. 5.2* and Prob. 5.6, this results in a divergence of the period of the limit cycle and the cycle turns into a homoclinic orbit.

14.3 Problems

1. Consider the **linear vector field** $v(x) = ax$ and discuss the stability of its fixed points as a function of the control parameter a. Clarify the nature of bifurcations and draw the bifurcation diagram.
2. Consider the family of **1d vector fields** $\dot{x} = v(x) = \beta \tanh x - x$ with real β a control parameter. Sketch the phase portraits and plot $v(x)$ for three qualitatively different β. Show that it displays a bifurcation (what type of bifurcation is it?) and find the bifurcation point β_c and the fixed point x_* at β_c. Draw a bifurcation diagram and explain how the character of the phase portrait changes.
3. Consider the real vector field $\dot{x} = v(x) = ax + x^3$, which we have argued displays a **subcritical pitchfork bifurcation** at $a_c = 0$. Draw phase portraits and the corresponding potential $\phi(x)$ for typical values of a. Draw a bifurcation diagram.

$*$4. **Limit cycle & SNIP bifurcation.** Consider the vector field $\dot{r} = r(1 - r^2)$ and $\dot{\theta} = a - \sin\theta$ introduced in Sect. 14.2.2*. Find the limit cycle and fixed points and their stability as a function of a. Find the bottleneck. Draw phase portraits to show that this vector field displays a saddle-node infinite period bifurcation at $a = 1$.

5. Examine the bifurcation in a **damped harmonic oscillator** (Sect. 6.11) as the control parameter $a = \gamma/2m\omega$ is changed, taking it from an underdamped $(a < 1)$ to an overdamped oscillator $(a > 1)$ via a critically damped oscillator at $a_c = 1$.

Chapter 15

From regular to chaotic motion

Several of the classical mechanical systems many of us encounter in our early education, such as the free particle, harmonic oscillator, Kepler problem and Euler-Poinsot top display motion that is relatively regular and predictable[1]. In fact, all these systems are solvable or integrable. Thus, it may come as a surprise that most mechanical systems have parameter regimes where they display rather irregular (also known as stochastic[2] or more accurately chaotic[3]) behavior that seems unpredictable. This is despite the fact that these systems are deterministic: their dynamics is defined by differential or difference equations that completely determine the state at later times given the current state. One reason for this chaotic behavior is extreme (e.g., exponential) sensitivity to initial conditions. By this, we mean that two initial states that differ a wee bit but are qualitatively similar, can display markedly different behavior upon being evolved for moderate lengths of time. Stated differently, the knowledge of the initial state to a given accuracy permits determination of the final state to a far lesser accuracy.

It is not just students of physics who may be surprised by the possibility of chaotic behavior. Most scientists till the late 19th century were unaware of it. In fact, chaos itself was discovered serendipitously by Poincaré while working on the stability of the solar system and the three-body problem of celestial mechanics [27, 72]. Even after Poincaré's work, the physical significance and ubiquity of chaos remained largely unrecognized (though some mathematical progress was made by G Birkhoff, J E Littlewood, M L Cartwright, A N Kolmogorov and others) till the 1960s and 1970s, when a combination of puzzling experimental results, availability of electronic computers and theoretical insight made it possible to explore chaotic behavior in certain model systems which initiated the development of a systematic theory. Notable among these are Boris Chirikov's study of Hamiltonian chaos [his resonance criterion for the transition to stochasticity [87] in a model for plasma confinement and discovery of chaos in the standard map], Michel Hénon and Carl Heiles' identification of a simple 2 degree of freedom Hamiltonian model for the motion of a star around a galactic center, which turned out to display remarkable chaotic phenomena [87, 126], Edward Lorenz's discovery [88] of sensitive dependence on initial conditions and chaos in his truncated system of differential equations for atmospheric convection [39], Stephen Smale's pioneering elucidation of the dynamics of the horseshoe map [57] and Mitchell Feigenbaum's discovery of universality [37] in the logistic difference equation (logistic map) [99]. In fact, chaotic behavior has been observed in a variety of natural phenomena and mathematical models arising in the physical, biological, economic and social sciences [44]. For instance, Robert May [89] emphasized chaotic behavior in the logistic difference equation regarded as a model for population dynamics while Benoit Mandelbrot discovered fractals in a plethora of settings in his study of 'roughness': financial markets, coastlines, mountains, ferns, tree bark, lightning, etc. Fractals also arise in various guises (such as attractors) in chaotic dynamical systems (see e.g., Sect. 15.1.3). Aside from the Chirikov, Hénon-Heiles and Lorenz differential equations, the other models just mentioned are discrete-time dynamical systems defined by difference equations. These discrete-time systems[4] were sometimes inspired by continuous-time systems (pendulum or kicked rotor for the standard map, van der Pol oscillator for the horseshoe and fluid turbulence in Feigenbaum's work) but can be of interest in their own right and sometimes provide simpler contexts in which to study complicated dynamical behavior. In fact, we have already encountered a discrete-time dynamical system: iterations of the monodromy matrix as a tool to study the stability of periodic trajectories in Sect. 13.4.4*. What is more, it is much easier to numerically simulate a difference equation on a computer (or calculator) and readily observe the types of behavior it displays as parameters are varied. Another difference is that while vector fields need to be at least 3 dimensional to display chaotic behavior (as a consequence of the Poincaré-Bendixon theorem of Sect. 5.4*), iterations of maps of 1d state spaces can already be chaotic[5].

---

[1] We have in mind periodic or quasiperiodic trajectories or escape to infinity in a simple way.

[2] 'Stochastic' is meant to convey seemingly random behavior. The word stochastic is often used in a technically different sense to describe random phenomena such as Brownian motion, which are usually modeled as nondeterministic dynamical systems.

[3] *Kháos* is the Greek word for an abyss and portrays an incomprehensibly difficult situation.

For this reason, we begin this chapter with a brief glimpse of the transition to chaotic behavior in two discrete-time systems: the standard and logistic maps. We will then consider two continuous-time systems: (a) the double pendulum, which is a Hamiltonian system and (b) the Lorenz oscillator, which models the driven dissipative process of atmospheric convection and whose investigation heralded the modern theory of chaos. Along the way, we will introduce some general phenomena associated with chaotic systems and tools to study them. These include Lyapunov exponents, Poincaré return maps and homoclinic tangles.

15.1 Chaos in iterations of a map

A (self) *map* is a function f from a set M to itself, $f : M \to M$. The set M is regarded as the state space of the dynamical system and is usually a (differentiable) manifold. For instance, it could be the unit interval $[0, 1]$, real line, unit square $[0, 1] \times [0, 1]$ or Euclidean plane. Simple examples of functions include $f(x) = (1/4)x(1-x)$ on the unit interval or $f(x, y) = (x^2 - y^2, 2xy)$ on the plane. Time is discrete and taken to be the nonnegative integers $0, 1, 2, \ldots$. The dynamics is specified by repeated application or *iteration* of f. Many of the concepts familiar from continuous-time dynamical systems carry over to iterations of a map. Thus, starting with an initial state x_0, we get its orbit[6] (or trajectory) $x_0, x_1 = f(x_0), x_2 = f(f(x_0)) \equiv f_2(x_0), x_3 = f(f(f(x_0))) = f_3(x_0)$, etc., or $x_{n+1} = f(x_n)$. The iterate f_n encodes the result of time evolution after time n. The orbit of x_0 may be displayed as a sequence of points (iterates of x_0) on the state space M (see Fig. 15.1a). An orbit is periodic with period p if p is the smallest positive integer such that $f_p(x_0) = x_0$. An orbit with period one is the analog of a static solution: x_0 is a fixed point if $f(x_0) = x_0$. For instance, $x = 0$ is a fixed point of $f = 4x(1-x)$ while $x = (5 \pm \sqrt{5})/8$ lie on an orbit of period two. Moreover, if x lies on an orbit of period p, then it must be a fixed point of f_p (the converse is not quite true, see Prob. 15.3). A periodic orbit is an example of a regular trajectory. Still regular, but not periodic are what we will call quasiperiodic orbits. Examples are displayed in Fig. 15.1a. On the other hand, in a chaotic orbit, the iterates x_n wander around a bounded portion of M in an irregular fashion and can seem to fill up open subsets of M (see Fig. 15.3). Chaos is associated with instabilities[7] and sensitivity to initial conditions, whereby orbits starting from two infinitesimally separated initial conditions exponentially deviate from each other and become uncorrelated. A quantitative measure of this exponential sensitivity to ICs is the Lyapunov exponent, which we define in Sect. 15.1.1. Next, we illustrate some of the dynamical features that can arise in iterations of a map by discussing two examples: the Chirikov-Taylor standard map (Sect. 15.1.2) and the logistic map (Sect. 15.1.3). Both display regular as well as chaotic behavior as a control parameter is varied.

---

[4] Many interesting discrete-time systems arise through iterations of a self-map of a state space (see Sect. 15.1). They could also arise through 'symbolic dynamics' applied, say, to a continuous-time system where one keeps track only of a denumerable set of mutually exclusive 'events' denoted by symbols; then each trajectory is replaced by a symbol sequence.

[5] If a map of an n-dimensional state space is invertible, then it cannot be chaotic if $n < 2$. On the other hand, the (necessarily invertible) Poincaré return map on a 2d surface of section in the 3d phase space of a chaotic vector field can display chaos. Noninvertible maps such as the logistic map can be chaotic even when $n = 1$.

15.1.1 Lyapunov exponent and sensitivity to initial conditions

A quantitative measure of the sensitivity to initial conditions is the Lyapunov exponent. Here, we introduce it for maps of one real variable. It measures the (exponential) rate of separation of orbits that begin nearby. For $|\delta_0| \ll 1$, let x_0 and $x_0 + \delta_0$ be two nearby ICs. After n iterations of a map of one variable, let δ_n denote the separation between the orbits. If δ_n grows exponentially with n, i.e., $|\delta_n| \to |\delta_0| e^{\lambda n}$ as $n \to \infty$ and $\delta_0 \to 0$, then we say that λ is the Lyapunov exponent for the orbit through x_0. More precisely,

$$\lambda(x_0) = \lim_{n \to \infty} \lim_{\delta_0 \to 0} \frac{1}{n} \log \left| \frac{\delta_n}{\delta_0} \right| . \tag{15.1}$$

From the definition, we should expect $\lambda < 0$ in the absence of any instability (e.g., if neighboring orbits converge to a fixed point or periodic orbit) while $\lambda > 0$ in the presence of exponential instabilities and sensitive dependence on ICs characteristic of chaos. When $\lambda > 0$, its reciprocal, sometimes called the Lyapunov time, tells us roughly how long we can make reliable predictions. It is noteworthy that (a) λ is not a short-time property and (b) a positive Lyapunov exponent does not imply that the separation between orbits that begin nearby grows without bound. One can have a positive Lyapunov exponent even in a state space that has a finite extent, such as the interval $[0,1]$. The limit $\delta_0 \to 0$ ensures that one can have ‘exponential growth in separation’ as $n \to \infty$ even in a bounded region (see also Footnote 19).

---

[6] If f is an invertible map, with inverse denoted f^{-1}, then we may extend time to the negative integers $-1, -2, \ldots$ and define backward time evolution by $x_{-1} = f^{-1}(x_0)$ and more generally $x_{-n-1} = f^{-1}(x_{-n})$ for $n = 0, 1, 2, \cdots$.

[7] The simplest example of an instability is that of a fixed point. As with vector fields on phase space in Sect. 5.2*, there is a simple criterion (see Prob. 15.4) for the linear stability of a fixed point: x_* is stable if the *magnitude* of the 'stability coefficient' $f'(x_*)$ is < 1, unstable if $|f'(x_*)| > 1$. The test is inconclusive if $|f'(x_*)| = 1$. If $f'(x_*) = 0$ then x_* is called *superstable*. See Prob. 15.5 for a generalization to the stability of periodic orbits.

For a differentiable map f, we may derive a formula for $\lambda(x_0)$ in terms of f. To begin with,

$$\frac{\delta_n}{\delta_0} = \frac{f_n(x_0+\delta_0) - f_n(x_0)}{\delta_0} \to f_n'(x_0) \quad \text{as} \quad \delta_0 \to 0. \tag{15.2}$$

Now, by the chain rule, denoting $x_n = f(x_{n-1})$ we have

$$f_n'(x_0) = f'(x_{n-1}) f'(x_{n-2}) \cdots f'(x_1) f'(x_0). \tag{15.3}$$

Thus,

$$\lambda(x_0) = \lim_{n\to\infty} \frac{1}{n} \sum_{j=0}^{n-1} \log |f'(x_j)|. \tag{15.4}$$

In other words, the Lyapunov exponent is the average of the logarithms of the magnitudes of the derivatives of f along the orbit of x_0. We will illustrate the idea of a Lyapunov exponent by evaluating it for various orbits in the logistic map in Sect. 15.1.3.

15.1.2 Chirikov-Taylor standard map: a kicked rotor

The ‘standard map’ [99] is a discrete-time dynamical system defined by the pair of coupled nonlinear difference equations

$$\theta_{n+1} = \theta_n + p_{n+1} \quad \text{and} \quad p_{n+1} = p_n - \kappa \sin\theta_n \tag{15.5}$$

for the instantaneous state (θ_n, p_n) of the system. Here, $n = 0, 1, 2, \ldots$ labels discrete time and the coupling constant κ controls the size of the nonlinearity. The map was introduced by Bryan Taylor in modeling the motion of charged particles in strong magnetic fields and independently by Boris Chirikov (1969) to model resonance phenomena in Hamiltonian systems. In Prob. 15.8, these equations are expressed in the conventional form $\xi_{n+1} = f(\xi_n)$ where f is a self-map of the θ-p plane. Thus, given initial conditions (θ_0, p_0), we study the iterates (θ_n, p_n) of a map of the θ-p plane.

Interpretation as discretized pendulum equations. Equations (15.5) are perhaps most simply interpreted (for small positive[8] κ and with a rescaled momentum, see Prob. 15.6) as a finite difference approximation to Hamilton’s equations for a simple

---

[8] Some authors use $K = -\kappa$ with $K > 0$. Our convention (with $\kappa > 0$) places the trivial fixed point at the origin (stable equilibrium point of a pendulum) and facilitates comparison with libration and rotation of a pendulum for small positive κ. Note that reversing the sign of κ can be compensated for by the shift $\theta \to \theta + \pi$. So it is sufficient to consider $\kappa \geq 0$.

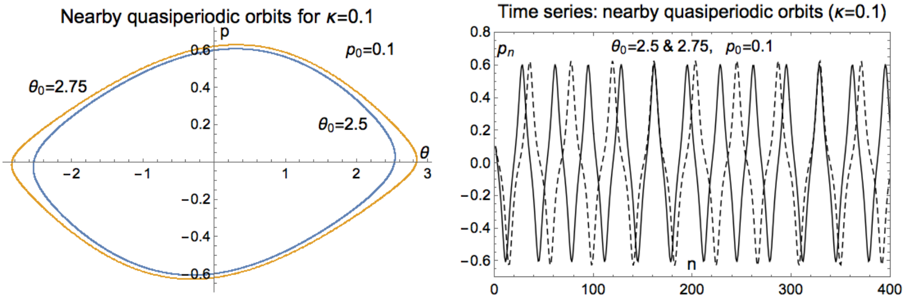

(a) (b)

Figure 15.1: (a) Iterates of the standard map for small $\kappa = 0.1$ showing 'quasiperiodic' orbits concentrated on closed curves on phase space. Changing ICs by 10% produces a nearby orbit with slightly different shape. (b) Linearly interpolated time series of p_n for the two orbits, showing regular dynamics.

pendulum $\dot{\theta} = p_\theta / m\ell^2$ and $\dot{p}_\theta = -mg\ell \sin\theta$ (7.7), where θ and p_θ are the deflection angle from the downward vertical and angular momentum. Given that the standard map is a discretization of a Hamiltonian system, it is perhaps not surprising that (15.5) is a canonical transformation of the θ-p phase space. What is more, since the pendulum has 1 degree of freedom, (15.5) is an area-preserving map as shown in Prob. 15.8 (see also Sect. 10.4). The standard map inherits the parity symmetry of the pendulum: $(\theta_n \to -\theta_n, p_n \to -p_n)$ which is evident in the orbits shown in Figs. 15.1a and 15.3. However, unlike the pendulum, (15.5) (for $\kappa \neq 0$) does not possess a conserved quantity (i.e., a dynamical variable independent of n). Evidence for this will be provided in Fig. 15.3 where orbits will be seen to explore 2d regions of phase space and are not confined to 1d level curves of a possible conserved quantity[9]. In fact, we will find that the standard map displays more complicated dynamics than the pendulum which is integrable and (aside from separatrices) admits only periodic solutions.

Interpretation as a kicked rotor. We may also view (15.5) as a Poincaré map (see Fig. 15.10 and Sect. 15.4.1*) or stroboscopic[10] description of the evolution of a kicked rotor (or rotator): a pendulum which is free to rotate about a pivot in a plane and whose bob is subject to no force besides an impulsive 'gravitational' force ($\propto -\kappa \sin\theta_n$) at unit time intervals. These kicks prevent the pendulum from conserving energy (see Prob. 15.13) but may be modeled by the explicitly time-dependent Hamiltonian: $H = p^2/2 - \kappa \cos\theta \sum_{j\in\mathbb{Z}} \delta(t-j)$. This allows the Chirikov-Taylor map to display much richer dynamics than the simple pendulum.

Considering θ_n and p_n modulo 2π. Given its interpretation as a deflection angle, it is natural to consider θ_n modulo 2π. In the standard map, one also takes p_n to be defined mod 2π, though this is not meaningful in the pendulum. This is because (15.5) has

---

[9] In fact, we will say that iterations of a map $f(x, y)$ of a 2d state space is integrable if there is a real function $C(x, y)$ such that $C \circ f = C$. Since $C(f(x, y)) = C(x, y)$, C remains constant under iterations and plays the role of a conserved quantity.

[10] A stroboscopic lamp is one that produces flashes of light at regular intervals of time and can be used to capture snapshots of an event such as a dance performance.

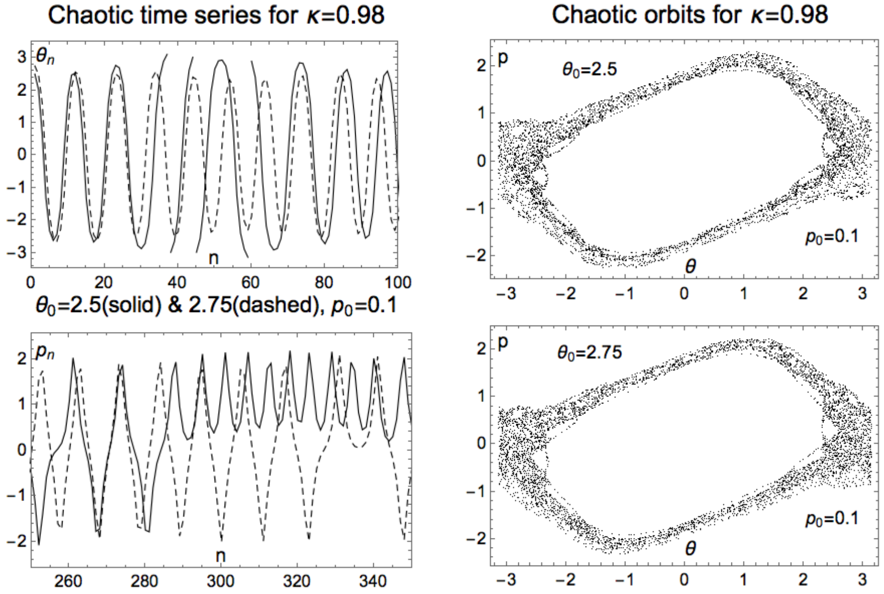

(a) (b)

Figure 15.2: Iterates of the standard map for $\kappa = 0.98$ showing aperiodic chaotic orbits. (a) Changing ICs by 10% [$\theta(0) = 2.5$ to $\theta(0) = 2.75$ holding $p(0) = 0.1$ fixed] produces qualitatively different orbits as seen from the (linearly interpolated modulo 2π) θ_n and p_n time series. (b) Although over moderate times, the two chaotic orbits explore different parts of the phase space, over long times ($\sim$ 5000 iterates), both chaotic orbits explore similar parts of the phase space, suggesting that reliable statistical predictions of time-averages *can* be made in spite of the chaos.

a 2π 'periodicity' in momentum as well. More precisely, if the momenta of two ICs (θ_0, p_0) and $(\theta_0, p_0 + 2\pi q)$ differ by an integer multiple of 2π, then their iterates retain the same difference in momentum: (θ_n, p_n) and $(\theta_n, p_n + 2\pi q)$. Thus, it suffices to consider p_n modulo 2π. Consequently, we will take the phase space of the standard map to be a 2-torus, i.e., a $2\pi \times 2\pi$ square with periodic boundary conditions (BCs)[11].

---

[11] This is just as well since we wish to use the standard map as a model for chaos. An unbounded phase space can be detrimental to the development of chaos, since even if there is sensitivity to ICs, trajectories could fly off to infinity in a regular manner preventing certain other features of chaotic dynamics from being manifested. Some phenomena associated with chaotic systems include sensitivity to ICs (instabilities), denseness of periodic orbits and mixing, see Sect. 1.8 of [26]. In Footnote 13, we point out the need for both stretching and folding to generate chaos in iterations of maps. While stretching generates sensitivity to ICs, the presence of periodic orbits is symptomatic of a tendency to fold. Heuristically, stretching and folding together generate mixing as in the mixing of salt when kneading dough. So it is perhaps not unreasonable to suppose that the presence of any two of these phenomena would guarantee the third. In a different direction, it is worth noting that even if trajectories escape to infinity over long times, they could display *transient* chaos at intermediate times as happens in the three-body problem.

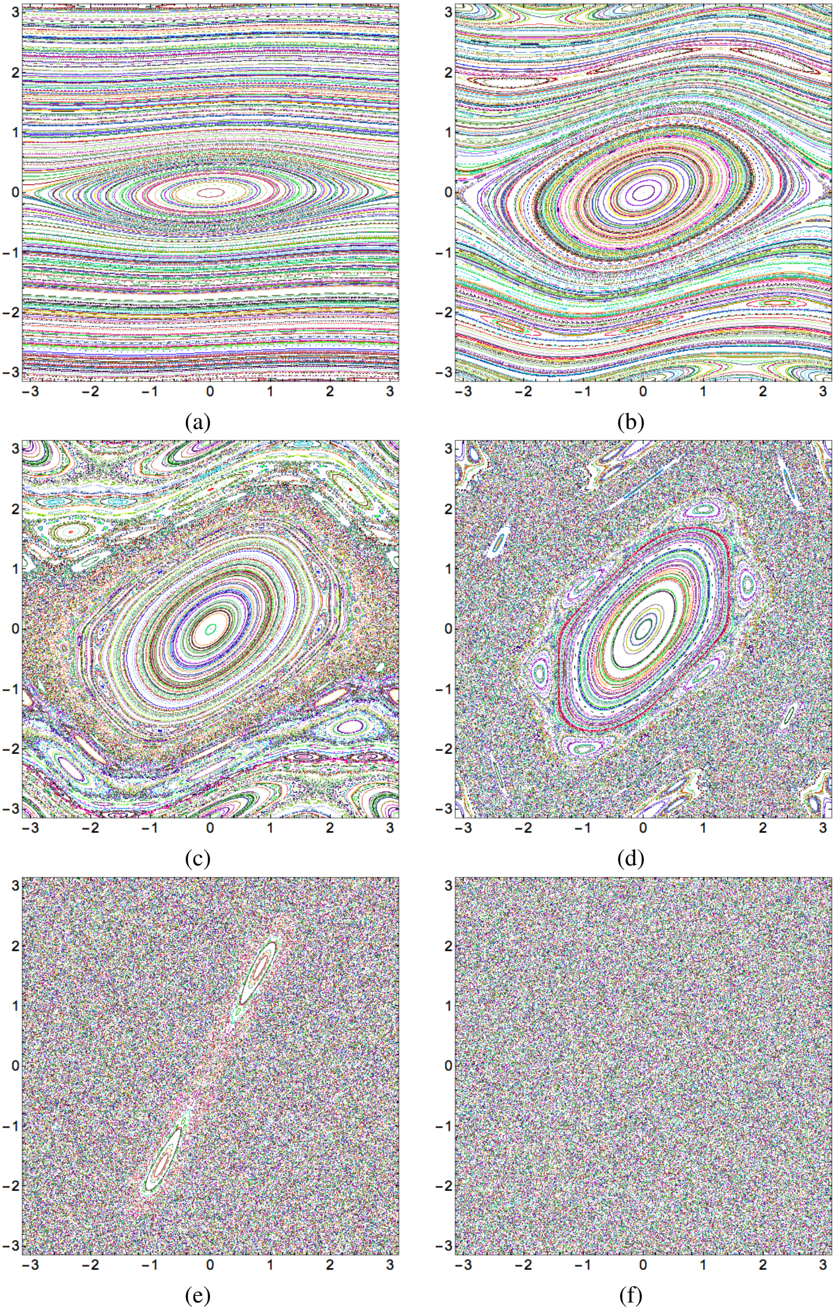

(a) (b) (c) (d) (e) (f)

Figure 15.3: Standard map on the θ-p plane: 500 iterates each for 400 orbits with random ICs. (a) $\kappa = 0.1$ (quasiperiodic orbits concentrated on KAM curves), (b) $\kappa = 0.5$ (quasiperiodic, some chaos near unstable fixed point), (c) $\kappa = 0.98$ (transition to widespread chaos), (d) $\kappa = 1.5$, (e) $\kappa = 4.5$ and (f) $\kappa = 100$ (nearly global chaos).

Dynamics of the standard map as κ is increased from zero. For $\kappa = 0$, $p_0 = p_1 = p_2 = \cdots$ is conserved while $\theta_n = \theta_0 + np_0$ is linear modulo 2π, resulting in horizontal periodic or quasiperiodic orbits on the θ-p square according as the angular velocity or 'rotation number' $p_0/2\pi$ is rational or irrational. The standard map is called a twist map since orbits with larger p_0 rotate faster, thereby 'twisting' the phase square. As shown in Figs. 15.1 and 15.3a, for $\kappa \ll 1$, the dynamics is not highly sensitive to ICs and orbits for various initial conditions are either periodic or more frequently 'quasiperiodic', i.e., not returning to the initial state but densely filling up 1d curves (see Sect. 11.7*) lying either roughly horizontally in phase space (KAM curves) or encircling the elliptic fixed point at the origin. The surviving KAM curves arise from nonresonant circles of the $\kappa = 0$ system with sufficiently irrational rotation numbers. The presence of invariant curves keeps the dynamics relatively regular as points are confined to them or between them. As κ is increased, we first see elliptic island chains forming, as in Fig. 15.3b. Subsequently, orbits tend to become increasingly complicated and beyond $\kappa_c \approx 0.97$, there ceases to be any KAM curve running from $\theta = -\pi$ to $\theta = \pi$ and we have a transition to widespread chaos[12]. While there continue to be periodic and quasiperiodic orbits for some special ICs, they are interwoven with 'chaotic' orbits that explore (and seem to densely fill up) 2d regions in an irregular fashion, as illustrated in Fig. 15.3. These chaotic orbits are quite sensitive to initial conditions, as shown in Fig. 15.2. However, we find that over long times, two chaotic orbits that begin from slightly different initial conditions can explore similar regions of phase space. When this happens, robust averages over long times can plausibly be computed despite the sensitivity to ICs. As κ is further increased, most ICs lead to chaotic orbits, which also begin to occupy nearly the entire phase space, as we see in Fig. 15.3. However, even for large κ, chaos may not be truly global. In fact, it is known [33] that arbitrarily close to any given κ, the standard map admits plenty of elliptic islands of stability.

15.1.3 Logistic map: period doubling, chaos, Cantor dust and Lyapunov exponent

Our next example of a discrete-time dynamical system is the logistic difference equation or logistic map [89],

$$x_{n+1} = rx_n(1 - x_n) = rx_n - rx_n^2 \tag{15.6}$$

for a dynamical variable x_n that takes values in the unit interval $[0, 1]$. Here, the fixed real parameter $r \geq 0$. The logistic map is not invertible[13], it is generally 2 to 1. It is called unimodal[14], since the graph of $f(x) = rx(1 - x)$ has a single maximum for

---

[12] The work of John Greene [87], shows that the last invariant KAM circles to be destroyed have rotation numbers ($p_0/2\pi$) that differ at most by an integer from the golden mean $[(1 + \sqrt{5})/2]$, which is in a sense the most irrational among irrational numbers.

[13] For a map of $[0, 1]$ to be chaotic, it must involve both stretching (to generate sensitivity to ICs) and folding (to keep orbits bounded). Folding makes it noninvertible. This is vividly illustrated in the manner in which some bakers knead dough and is captured in the baker's map [99] as well as in doubling modulo unity and the tent map (see Prob. 15.14 and Prob. 15.17).

[14] A bimodal function is one whose graph resembles the profile of the back of a camel with two humps. The terminology is related to the shape of a signal in Fourier space. A largely

$x \in [0,1]$ with $f(0) = f(1) = 0$. Many of its qualitative properties carry over to other unimodal maps. We may interpret $x_n \in [0,1]$ as the population of a species of insects in a region (in units of the carrying capacity of the region) at the n^{th} instant of time. Given an initial population x_0, (15.6) is a crude model to determine the populations at subsequent times by iterating the function $f(x)$. The logistic map is a discrete version of the logistic differential equation $\dot{N} = rN(1 - N/K)$ (14.3) of Sect. 14.1.2*. As observed there, r may be interpreted as a linear growth rate, while units have been chosen so that the analog of the carrying capacity K is 1. The $-rx_n^2$ term in (15.6) models the effect of finite resources and tends to prevent the population from growing without bound. The logistic map is, in a sense, simpler than the standard map since it involves only one difference equation. However, unlike the standard map that arose from a Hamiltonian system, the logistic differential equation is not Hamiltonian as it admits attractive fixed points.

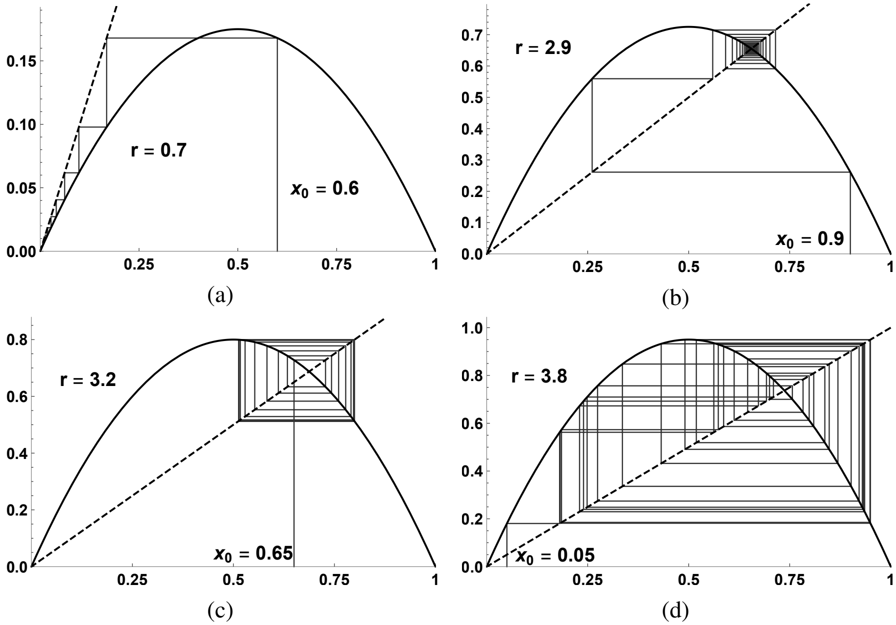

Figure 15.4: Cobweb diagrams for the logistic map showing (a) convergence to the trivial fixed point, (b) convergence to the nontrivial fixed point $1 - 1/r$, (c) convergence to a period two orbit and (d) a chaotic orbit.

Fixed points and their stability. To begin with, we will restrict r to the range $0 \leq r \leq 4$. This ensures that $f(x) = rx(1-x)$ takes values within the unit interval $[0,1]$ so that it may be iterated[15]. Fixed points [x_* such that $f(x_*) = x_*$] lie at the abscissae

---

monochromatic signal would have a peak around a single frequency (Fourier mode). A bimodal one would have peaks around two Fourier modes.

[15] A cobweb diagram (see Fig. 15.4) is a way to find and display the iterates of f. Begin by drawing the graphs of the functions $y = f(x)$ and $y = x$ on the unit interval $0 \leq x \leq 1$. Start at the point $(x_0, f(x_0))$ on the graph of $y = f(x)$ with abscissa x_0. Then draw a horizontal

of the intersections of the graph of $f(x)$ with the graph of the identity function x. One (trivial) fixed point always exists, at $x = 0$. Since $f'(0) = r$, it is stable for $0 \leq r < 1$ and unstable for $1 < r < 4$. For $r > 1$ we have a second fixed point at $x_* = 1 - 1/r$. Since $f'(x_*) = 2 - r$, this nontrivial fixed point is stable for $1 < r < 3$ and unstable for $r > 3$. For $r < 1$, all orbits are attracted to $x = 0$: the population dwindles to zero as the growth rate is insufficient (see Prob. 15.19). For instance, for $x_0 = r = 1/2$, the first few iterates are

$$\frac{1}{2}, \frac{1}{8}, \frac{7}{128}, 0.0258484, 0.0125901, 0.00621581, 0.00308859, 0.00153952, \ldots \tag{15.7}$$

For $r_0 = 1 < r < r_1 = 3$, all orbits (other than the one at $x = 0$) are attracted to the fixed point at $x_* = 1 - 1/r$. In other words, the number of individuals eventually approaches a nonzero self-sustaining population. For instance, taking $r = 2$ and $x_0 = 1/4$ we find that the iterates rapidly approach $x_* = 1/2$ (see also Prob. 15.19):

$$x_0 = 0.25, \quad x_1 = 0.375, \quad x_2 = 0.46875, \quad x_3 = 0.498047, \quad x_4 = 0.499992, \cdots. \tag{15.8}$$

Notice that at $r = 1$, the trivial $(x = 0)$ and nontrivial $(x_* = 1 - 1/r)$ fixed points 'collide'. In fact, the two fixed points exchange stabilities as r crosses 1 with the trivial one going from being stable to unstable while x_* goes from unstable to stable. Thus, we have a *transcritical bifurcation* (see Sect. 14.1.2*) at $r = 1$.

As r approaches $r_1 = 3$, the convergence to x_* slows down in a manner reminiscent of critical slowing down (see Sect. 14.1.3.1*) in the vicinity of a second order phase transition. This is illustrated in Fig. 15.5a.

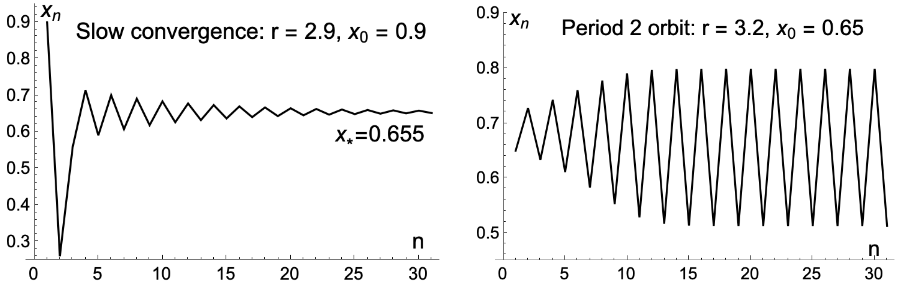

(a) (b)

Figure 15.5: (a) Iterates converging slowly to the nontrivial fixed point $x_* = 1 - 1/r$ for $r = 2.9 < r_1 = 3$. (b) Convergence to period 2 orbit for $r_1 < r < r_2$.

Periodic orbits and period doubling cascade. One consequence of the above discussion is that for $r < r_1 = 3$, there are no periodic orbits aside from fixed points. When the growth rate exceeds $r_1 = 3$, there is no stable fixed point to which trajectories can be attracted. However, there can be nontrivial periodic orbits. Let us first look for an orbit of period two. The quartic equation $f(f(x)) = x$ has four roots, two

---

line to the graph of $y = x$ meeting it at the point $(f(x_0), f(x_0))$. The abscissa of this point is the first iterate $x_1 = f(x_0)$. This process is then repeated to get $x_2 = f(x_1)$, etc.

of which [0 and $1 - 1/r$] correspond to fixed points. Factoring these out, we get the quadratic equation

$$r^2x^2 - r(1+r)x + (1+r) = 0 \quad \text{with roots} \quad x_\pm = \frac{1}{2r}\left[1 + r \pm \sqrt{r^2 - 2r - 3}\right]. \tag{15.9}$$

We verify that $f(x_\pm) = x_\mp$ so x_+ and x_- lie on an orbit of period two[16]. This period two orbit exists as long as the discriminant $r^2 - 2r - 3 > 0$, which is the same as $r > r_1 = 3$. Is this period two orbit stable and does it serve as an attractor for other orbits? Since it is a fixed point of the second iterate f_2, it is stable provided $|f_2'(x_\pm)| < 1$. In fact, $f_2'(x_+) = f_2'(x_-)$, for by the chain rule,

$$f_2'(x_+) = f'(f(x_+))f'(x_+) = f'(x_-)f'(x_+) \tag{15.10}$$

is symmetric in $x_\pm$. From (15.9) we get $f_2'(x_\pm) = 4 + 2r - r^2$. The period 2 orbit is stable if $|f_2'(x_\pm)| < 1$, which happens provided $r_1 = 3 < r < r_2 = 1 + \sqrt{6} \approx 3.449$. Numerical experiments show that most initial states are attracted to this period 2 orbit for $r_1 < r < r_2$. For this range of values of r, the population at late times switches back and forth between the two characteristic values $x_\pm$ (see Fig. 15.5b). For instance, taking $r = 3.2$ and $x_0 = 0.65$, we find the orbit approaches $x_\pm = 0.799455, 0.513045$:

$$\begin{array}{cccccc} 0.65, & 0.728, & 0.633651, & 0.74284, & 0.611293, & 0.760365, \\ 0.583073, & 0.777916, & 0.55284, & 0.791065, & 0.528899, & 0.797328, \\ 0.517108, & 0.799063, & 0.513795, & 0.799391, & 0.513168, & 0.799445. \end{array} \tag{15.11}$$

The story so far can be summarized as follows: (a) for $0 < r < 1$, the zero population fixed point is a global attractor, (b) for $r_0 = 1 < r < r_1 = 3$ almost all trajectories are attracted to the fixed point at $x_* = 1 - 1/r$ and (c) for $r_1 = 3 < r < r_2 \approx 3.449$ we have a period two attractor. As r is further increased, we will continue to look for periodic orbits that can serve as attractors for the dynamics.

The condition $f_3(x) = x$ leads to two period three orbits provided the discriminant of a sixth degree polynomial is positive. We find (see Prob. 15.23) that period three orbits exist only for $r > 1 + 2\sqrt{2} \approx 3.828$. What then is the attractor when the period two orbit becomes unstable at $r \approx 3.449$?

Proceeding as before, and aided by numerical experiments, one finds that for $r_2 \approx 3.449 \lesssim r \lesssim r_3 \approx 3.544$ there is a stable period 4 orbit obtained by solving $f_4(x) = x$. Most trajectories for these r are attracted to this period 4 orbit (see Fig. 15.6a and Prob. 15.21). E.g., taking $r = 3.5$ and $x_0 = 0.7$, the first 36 iterates are:

$$\begin{array}{cccc} 0.7, & 0.735, & 0.681712, & 0.759432, \\ 0.639433, & 0.806955, & 0.545225, & 0.867841, \\ 0.401425, & 0.84099, & 0.46804, & 0.871425, \\ 0.392152, & 0.834291, & 0.483873, & 0.87409, \\ 0.385199, & 0.828873, & 0.49645, & 0.874956, \\ 0.382928, & 0.82703, & 0.50068, & 0.874998, \\ 0.382817, & 0.826938, & 0.50089, & 0.874997. \end{array} \tag{15.12}$$

---

[16] This period 2 orbit could also have been discovered by finding the points at which the graph of $y = x$ intersects that of the second iterate $f_2(x)$.

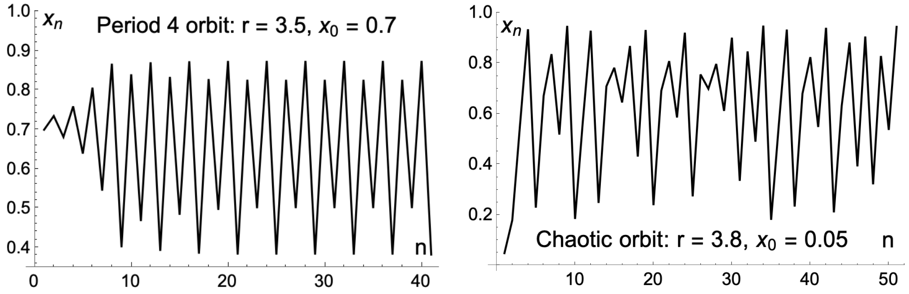

(a) (b)

Figure 15.6: (a) Convergence of iterates to a period 4 orbit of the logistic map for $r_2 < r < r_3$. (b) An aperiodic orbit of the logistic map for $r > r_\infty$.

Putting things together, the period of the attractor doubled from 1 to 2 at r_1 and from 2 to 4 at r_2. We say that there have been period-doubling bifurcations at $r_1 = 3$ and $r_2 = 1 + \sqrt{6} \approx 3.449$. This pattern repeats itself. As r is increased beyond $r_3 \approx 3.544$, a period 8 attractor is born followed by a period 16 attractor (at $r_4 \approx 3.564$) and so on. What is more, if r_n denotes the value of r at which a period 2^n orbit first becomes an attractor, then the sequence

$$r_1 = 3, \quad r_2 \approx 3.44949, \quad r_3 \approx 3.54409, \quad r_4 \approx 3.5644, \quad r_5 \approx 3.568759, \ldots \tag{15.13}$$

converges to $r_\infty \approx 3.569946$. Remarkably, the ratio of lengths of successive bifurcation intervals approaches a geometric sequence with common ratio

$$\delta \equiv \lim_{n \to \infty} \frac{r_n - r_{n-1}}{r_{n+1} - r_n} \approx 4.66920. \tag{15.14}$$

Other unimodal maps also display a similar 'cascade' of period doubling bifurcations. Though the numerical values of r_n depend on the details of the map, Feigenbaum [37] discovered that the ratio δ is independent of those details; it is universal. He developed a method to compute δ inspired by the renormalization group methods used to find critical exponents of second order phase transitions in statistical physics.

Chaos. As soon as r exceeds r_∞, there is no periodic orbit to serve as an attractor with a finite number of points. The dynamics is found to be chaotic: successive iterates x_n wander aperiodically around the unit interval while displaying great sensitivity to initial conditions, which we shall soon quantify using Lyapunov exponents. Fig. 15.6b displays the iterates in one such 'chaotic' orbit.

However, in the middle of this chaos (for $r_\infty < r < 4$), there are islands of stability. Parameter intervals open up where we have stable periodic orbits with heretofore unseen periods [e.g., 3, 5, 6, 7 and so forth], with each one undergoing a cascade of period doubling bifurcations! In fact, every integer makes its appearance as the period of an attractor in some (small) parameter window.

Attractor diagram. The dynamics of the logistic map may be summarized in an attractor or orbit diagram (or bifurcation diagram, see Fig. 15.7), where we display the

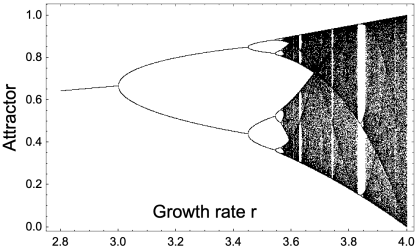

Figure 15.7: Attractor for the logistic map plotted for a range of values of r. The diagram has a self-similar (or fractal) structure, with the whole orbit diagram reappearing in compressed form from certain critical values of r after the onset of chaos at $r_\infty = 3.569946$. As r decreases from 4, the chaotic attractor [0,1] splits into 2, 4, 8 ... bands. The band doublings accumulate [99] geometrically at r_∞ with the same asymptotic common ratio δ of (15.14).

attractors for each value of r. The nontrivial fixed point x_* is seen to bifurcate into the period two attractor at $r_1 = 3$, both branches of which bifurcate into the period 4 attractor and so on. These bifurcations are supercritical pitchfork bifurcations (see Sect. 14.1.3.1*) since the fixed points of the iterate f_{n+1} that are born at the bifurcation are stable, while the fixed point of f_n becomes unstable. Chaos is seen to set in beyond $r_\infty \approx 3.569946$, where the dynamics is very sensitive to initial conditions (see the discussion on Lyapunov exponents below).

Logistic map for $r = 4$. The limiting case $r = 4$ deserves special mention. In this case, one may show (see Prob. 15.17) that (15.6) admits period k orbits for each $k = 1, 2, 3, \ldots$ and that they are all unstable. Moreover, these periodic orbits form a dense but countable subset of the unit interval $[0, 1]$. As a consequence, arbitrarily close to any initial condition x_0, there is one that lies on a periodic orbit. Setting aside this dense set of periodic orbits (that has measure zero in the unit interval), the remaining ICs form an uncountable set and lead to aperiodic 'chaotic' orbits. Thus, a randomly chosen IC would lie on a chaotic orbit. Understanding these features is facilitated by an equivalence between the $r = 4$ logistic map and the tent map

$$y_{n+1} = g(y_n) = 1 - 2|y_n - 1/2|. \tag{15.15}$$

In fact, putting $x_n = \sin^2(\pi y_n/2)$ in (15.6), we get $\sin^2(\pi y_{n+1}/2) = \sin^2(\pi y_n)$. This can hold only if $\pi y_{n+1}/2 = \pm\pi y_n + m\pi$ for some integer m. Further, requiring that both y_n and y_{n+1} lie in the unit interval, we find two possibilities: (a) if $y_n \in [0, 1/2]$ then we need to pick the positive sign and $m = 0$, leading to $y_{n+1} = 2y_n$ and (b) if $y_n \in [1/2, 1]$, then we need to pick the negative sign and $m = 1$, leading to $y_{n+1} = -2y_n + 2$. Combining these, we get $y_{n+1} = g(y_n)$ (15.15) where the graph of g is shaped like a tent with base 1 and height 1. The tent map involves both stretching (by a factor of two) and folding (to ensure it is a self-map of the interval). The stretching leads to an exponential sensitivity to ICs that we will soon quantify via a Lyapunov exponent.

Logistic map for $r > 4$. The logistic map is interesting even for $r > 4$, although in this case, $f(x) = rx(1 - x)$ does not map the unit interval back into itself. Nevertheless, some interesting things happen. For most initial conditions $x_0 \in [0, 1]$, successive iterates x_n approach $-\infty$ as $n \to \infty$, so that the long-time behavior is predictable. This is also true of any point outside the unit interval, its iterates remain outside the unit interval and eventually approach $-\infty$. However, there is an infinite set of isolated points in $[0, 1]$ that stay within the unit interval upon successive application of f. This subset is a 'Cantor' set. Let us sketch why. To begin with, we note that there are only two fixed points 0 and $x_* = 1 - 1/r$ (with $3/4 < x_* < 1$), both of which are linearly unstable for $r > 4$ since $f'(0) = r > 4$ and $f'(x_*) = 2 - r < -2$. Nevertheless, certain ICs are attracted to these fixed points: for instance $f(1) = 0$ and $f(1 - x_*) = x_*$. We now wish to characterize the points in $[0, 1]$ that always remain in the unit interval. From the foregoing discussion, this is the complement of the set of points that after a finite number of iterates land outside the unit interval. We will find the points that remain in the unit interval by successively deleting from $[0, 1]$ the points that leave the unit interval after $1, 2, 3, \ldots$ iterates. The points that remain form an analog of the middle-thirds Cantor set[17].

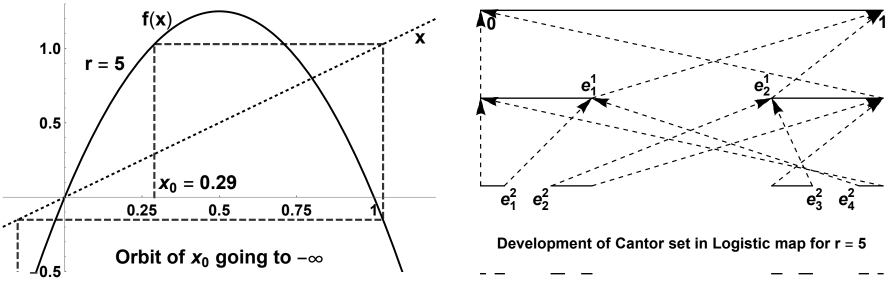

(a) (b)

Figure 15.8: (a) Cobweb diagram for $r = 5$ and $x_0 = 0.29$ showing that $f(x_0)$ lies outside the unit interval and that successive iterates fly off to $-\infty$. (b) 'Surviving' intervals (solid horizontal lines) in $[0, 1]$ for $r = 5$ after the first 3 iterates of f. The dashed arrows indicate the images of the endpoints under f.

We first observe (see the cobweb diagram in Fig. 15.8a) that if $x_0 \in [0, 1]$ is such that $f(x_0) > 1$, then its iterates $(x_1 > 1 > 0 > x_2 > x_3 \cdots)$ eventually tend to $-\infty$. Let $0 < e_1^1 < e_2^1 < 1$ be the two points with $f(e_1^1) = f(e_2^1) = 1$. They are

$$e_{1,2}^1 = (1/2)[1 \mp \sqrt{1 - 4/r}], \tag{15.16}$$

with e standing for 'endpoint'. Thus, points in the open interval (e_1^1, e_2^1) that is symmetrically located about $x = 1/2$ leave the unit interval after one iterate, never to return. On the other hand, the points in the 'surviving intervals' $[0, e_1^1] \cup [e_2^1, 1]$ remain in the unit interval after 1 iteration. Next, let $e_1^2 < e_4^2$ and $e_2^2 < e_3^2$ be the roots of

---

[17] To construct the middle-thirds Cantor 'ternary' set, we begin with the unit interval $[0, 1]$ and remove the open interval $(1/3, 2/3)$ leaving two closed intervals: $[0, 1/3] \cup [2/3, 1]$. Next, we remove the open middle third of each of these intervals and repeat this process ad infinitum. The points that remain form the Cantor ternary set, which has the structure of a fractal with noninteger dimension [122].

$f(x) = e_1^1$ and $f(x) = e_2^1$ respectively. Then $f_2(e_j^2) = 1$ for $1 \leq j \leq 4$ and the points in the intervals (e_1^2, e_2^2) and (e_3^2, e_4^2) leave the unit interval after 2 iterations. The surviving set after 2 iterations is the union $[0, e_1^2] \cup [e_2^2, e_1^1] \cup [e_2^1, e_3^2] \cup [e_4^2, 1]$. This is illustrated in Fig. 15.8b. At each successive iteration, the surviving intervals are split into two with the points roughly in the middle of each being expelled from unit interval. At the n^{th} iterate, 2^n new endpoints e_j^n for $1 \leq j \leq 2^n$ are generated through the roots of the quadratic equations

$$f(e_j^n) = \begin{cases} e_j^{n-1} & \text{for} \quad 1 \leq j \leq 2^{n-1} \quad \text{and} \\ e_{2^n-j+1}^{n-1} & \text{for} \quad 2^{n-1} < j \leq 2^n. \end{cases} \tag{15.17}$$

Thus, there are 2^n surviving disjoint intervals after n iterations. As $n \to \infty$, the surviving intervals approach a Cantor set or dust of isolated points. Moreover, we note that $f_n(e_j^n) = 1$ so that $f_{n+1}(e_j^n) = 0$ for $1 \leq j \leq 2^n$. So the endpoints e_j^n are mapped to 0 after $n + 1$ iterations. Interestingly, the nontrivial fixed point $x_* = 1 - 1/r$ and its preimages (points such that $f_p(x) = x_*$ for $p = 1, 2, 3, \ldots$) do not arise as endpoints e_j^n for any finite n. Nevertheless, these points remain in the unit interval (they are all attracted to x_*). Thus, they must lie in the Cantor set but arise as limit points rather than as end points.

Lyapunov exponent for Logistic map. For the logistic map, $f'(x) = r(1 - 2x)$ and (15.4) may be used to estimate Lyapunov exponents for orbits through selected x_0 at various growth rates r. Though λ can depend[18] on the initial state x_0, one finds that all orbits with a common attractor have essentially the same Lyapunov exponent (see Fig. 15.9). Heuristically, the initial transients hardly contribute to (15.4) in the limit $n \to \infty$; it is the tail of the orbit that largely determines λ. Thus, for the logistic map, λ is essentially a function only of r. For orbits that tend to a fixed point or to a periodic attractor, λ turns out to be negative as anticipated. For instance, when $0 < r < 1$, all orbits approach the trivial fixed point $x = 0$ at which $f'(0) = r$. Ignoring the transients, we estimate $\lambda \approx \log r$ for $0 < r < 1$. Similarly, for $1 < r < 3$, orbits are attracted to the fixed point $x_* = 1 - 1/r$ and we then estimate that $\lambda \approx \log |2 - r|$ for $1 < r < 3$. In both cases, $\lambda < 0$. Moreover, λ vanishes at the bifurcation points $r_0 = 1$ and $r_1 = 3$. In Prob. 15.26, we find a similar formula for $r_1 < r < r_2$. The presence of periodic attractors (as well as numerical calculations displayed in Fig. 15.9) show that the Lyapunov exponent λ remains nonpositive for $r < r_\infty \approx 3.569946$. Thereafter, λ becomes positive (indicating chaotic instabilities) and generally increases with r except for sharp dips to negative values within islands of stability where periodic attractors exist. For $r = 4$ we may estimate λ through the equivalence with the tent map (15.15). Noting that for the tent map, $|g'(y)| = 2$ for all y, we deduce from (15.4) that $\lambda = \log 2$ in agreement with our numerical estimate shown in Fig. 15.9b.

---

[18] To eliminate the dependence on x_0, one could average the Lyapunov exponent $\lambda(x_0)$ over all x_0 lying in a common basin of attraction. The average would most naturally be computed with respect to a measure (satisfying the Frobenius-Perron equation [99]) that is invariant under the dynamics.

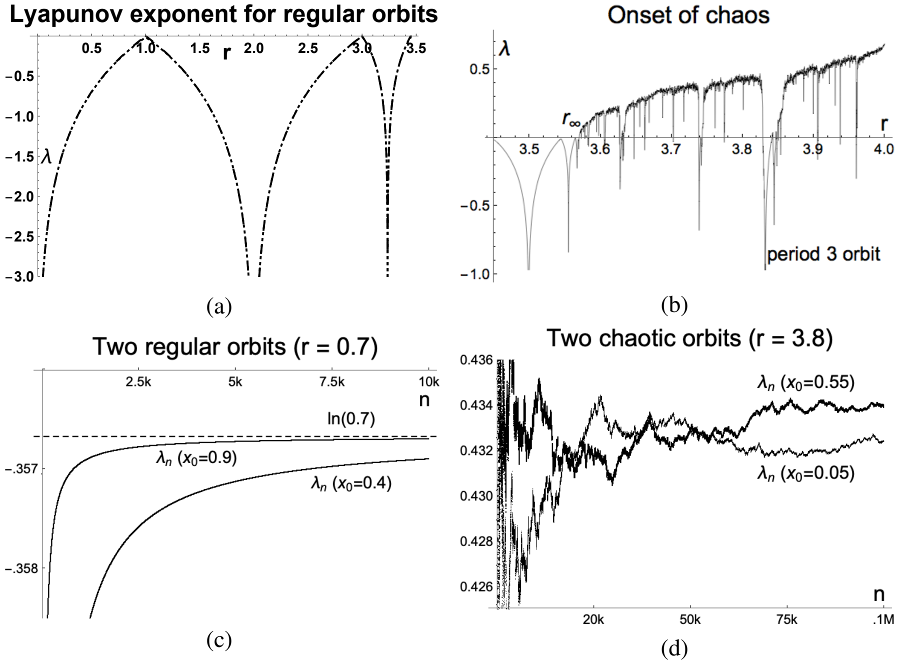

(a) (b)

(c) (d)

Figure 15.9: Lyapunov exponent for the logistic map. (a) For $0 < r < r_2 \approx 3.45$, numerically computed λ (dotted) are nearly indistinguishable from analytical estimate (dashed) for period one and period two attractors. (b) Numerically computed λ for $r_2 < r < 4$ shows a transition to positive values accompanying the onset of chaos at $r_\infty \approx 3.57$. The sharp dips for $r > r_\infty$ occur in windows where periodic attractors arise. As $r \to 4$, $\lambda \to \log 2 \approx .693$ as expected from the tent map. In (a) and (b) the sums are truncated after $n = 500$ terms. Convergence of partial sums of (15.4) to a nearly common Lyapunov exponent for (c) two regular orbits tending to the nontrivial fixed point for $r = 0.7$ and (d) two chaotic orbits at $r = 3.8$, showing insensitivity to ICs.

15.2* Lyapunov exponents for continuous-time dynamical systems

Having discussed Lyapunov exponents for the discrete-time logistic map, we will now extend the concept to continuous-time dynamical systems. The idea will be illustrated in the context of the double pendulum and Lorenz oscillator in Sect. 15.4 and Sect. 15.5*. Consider a dynamical system defined by the first order ODEs

$$\dot{x}^i = v^i(x) \tag{15.18}$$

for the vector field v on the n-dimensional phase space M. As in Sect. 15.1.3 (see (15.1)), Lyapunov exponents measure the exponential rate of divergence[19] of trajectories that begin near a prescribed trajectory. To make precise the idea of 'near', we linearize the ODEs (15.18) for small perturbations $\delta x(t)$ to the solution $x(t)$:

---

[19] This idea does not require trajectories to keep growing apart exponentially: the available phase space volume and nonlinear effects may not permit this. It is also not a concept tied to short-time behavior. Linearization of the flow around a given trajectory allows one to consistently speak of long-term exponential growth even in a bounded region of phase space by

$$\frac{d\delta x^i(t)}{dt} = \frac{\partial v^i(x(t))}{\partial x^j}\delta x^j(t), \quad \text{for} \quad i = 1, \cdots, n, \tag{15.19}$$

where we omitted all nonlinear terms. Evaluated at $x(t)$, the $n \times n$ matrix $\partial v^i/\partial x^j$ is called the linearization or Jacobian matrix[20] of the vector field around the trajectory. Now, suppose $x(t)$ for $0 \le t < \infty$ is a trajectory that starts from $x(0)$. Then these linear ODEs may be used to evolve a small perturbation or tangent vector $u(0) \in T_{x(0)}M$ forward in time to arrive at a tangent vector $u(t) \in T_{x(t)}M$. We then define the Lyapunov exponent associated to the state-perturbation[21] pair $(x(0), u(0))$ as

$$\lambda(x(0), u(0)) = \lim_{t\to\infty} \frac{1}{t} \log \frac{||u(t)||}{||u(0)||} \tag{15.20}$$

where $||u||$ is a suitable notion of length for tangent vectors to M. Evidently, λ measures the exponential rate at which a tangent vector is stretched as it evolves along the trajectory $x(t)$. However, there is an n-dimensional space of possible initial perturbations $u(0)$. How do we account for them? To do so, we draw inspiration from the time evolution matrix that we used in Sect. 13.4.2* to study the stability of a periodic solution.

Lyapunov spectrum. The linearized equations (15.19) define a linear time evolution map $L(t, 0)$ from the tangent space $T_{x(0)}M \cong \mathbb{R}^n$ to $T_{x(t)}M \cong \mathbb{R}^n$. It is the solution of the linear system

$$\frac{d}{dt}L(t, 0) = A(t)L(t, 0) \quad \text{where} \quad A^i_j(t) = \frac{\partial v^i(x(t))}{\partial x^j(t)} \quad \text{and} \quad L(0, 0) = I. \tag{15.21}$$

It may be expressed as a time-ordered exponential (13.97):

$$L(t, 0) = \mathcal{T} \exp \int_0^t A(x(\tau))\, d\tau. \tag{15.22}$$

This linear transformation[22] has n (generally complex) eigenvalues $\mu_1(t), \ldots, \mu_n(t)$. If $x(t)$ were periodic with period τ, then it is natural to take $t = \tau$ and call $\mu_i(\tau)$ the Floquet exponents. We would define the Lyapunov exponents λ_i as the real[23] parts of $(1/\tau) \log \mu_i(\tau)$. These λ_i measure the rate of exponential growth or decay

---

focusing on the tangent space at each point along a trajectory (roughly, by sending the initial perturbation to zero, we can have long-term exponential growth in a bounded region).

[20] For a Hamiltonian system, Liouville's theorem on the preservation of phase volume implies that this Jacobian must be traceless.

[21] The Lyapunov exponent $\lambda(x(0), \alpha u(0)) = \lambda(x(0), u(0))$ is independent of the length of $u(0)$, since the evolution (15.19) is linear and (15.20) involves a ratio of lengths.

[22] In practice, we may choose any basis (not necessarily orthonormal) $u_1(0), \cdots, u_n(0)$ for $T_{x(0)}M$. Each of the $u_j(0)$ evolves under (15.19) to a vector $u_j(t) \in T_{x(t)}M$. In the basis where $u_j(0)$ is the j^{th} column of the identity, $L(t, 0)$ is the fundamental solution of (15.19).

[23] The imaginary part has information on how a perturbation winds or rotates during a period.

of perturbations. To capture the exponential rate of growth or decay of perturbations to an aperiodic orbit, we first eliminate the rotational part by considering the singular values[24] $s_1, \cdots, s_n$ of $L(t, 0)$. When the limits exist, we will define the spectrum of Lyapunov exponents $\lambda_1, \cdots, \lambda_n$ associated to the point $x(0) \in M$ by the formulae

$$\lambda_j(x(0)) = \lim_{t\to\infty} \frac{1}{t} \log s_j(t) \quad \text{for} \quad j = 1, \cdots, n. \tag{15.23}$$

Numerical estimation of Lyapunov spectrum. We often wish to estimate Lyapunov exponents numerically by cutting off the limiting procedures in (15.20) and (15.23) at a large but finite time $t_{\max}$ to arrive at 'finite-time' Lyapunov exponents. In practice, it can be challenging to use (15.23) to calculate the finite-time Lyapunov spectrum numerically if the largest of the Lyapunov exponents $\lambda_{\max}$ is positive. This is because, generically, all the tangent vectors $u_j(t)$ grow in length with their components in the direction corresponding to $\lambda_{\max}$ growing exponentially fast $\propto e^{\lambda_{\max} t}$. Due to truncation errors, after moderate times, all the u_j begin to point in essentially the same direction and cease to furnish a basis for the tangent space. In a similar way, if we try to use (15.20) to calculate $\lambda(x(0), u(0))$ we invariably arrive at the largest Lyapunov exponent (LLE), irrespective of the choice of initial perturbation $u(0)$.

We may attempt to reduce truncation errors and circumvent this numerical difficulty by breaking up the long time $[0, t_{\max}]$ into a large number N of shorter intervals, say of equal duration $\tau = t_{\max}/N$. The time evolution matrix $L(t_{\max}, 0)$ is then the composition of the individual time evolution matrices

$$L(t_{\max}, 0) = L(t_{\max}, (N-1)\tau) \cdots L(2\tau, \tau) L(\tau, 0). \tag{15.24}$$

The individual time evolution matrices are constructed as in Sect. 13.4.2*. For k a nonnegative integer $< N$, we begin with the standard basis $\frac{\partial}{\partial x^i}$ for coordinate vector fields at $x(k\tau)$, which may be expressed in this basis as the vectors $(1, 0, 0 \ldots, 0)$, $(0, 1, 0, \ldots, 0)$, etc. Then the columns of $L((k+1)\tau, k\tau)$ are the images of these standard basis vectors under the linearized time evolution (15.19) along the trajectory from $x(k\tau)$ to $x((k+1)\tau)$. After composing the individual time evolution matrices, we proceed to calculate the singular values of $L(N\tau, 0)$ and the Lyapunov exponents by truncating the limit in (15.23) at $t_{\max} = N\tau$. As N increases (holding τ fixed), we look for convergence of the finite-time exponents to asymptotic values that are not sensitive to small changes in τ. The method can be used to find the Lyapunov spectrum for the Lorenz oscillator and the LLE of the double pendulum. However, if the LLE is positive and slow convergence necessitates a large number of steps N, then numerical difficulties can arise in reliably composing the individual time evolution matrices and extracting the singular values of $L(t_{\max}, 0)$. Due to the multiple scales in the problem, the entries of $L(t_{\max}, 0)$ can differ enormously (by factors such as $e^{(\lambda_1 - \lambda_2)t_{\max}}$) and round-off errors become significant.

Gram-Schmidt orthogonalization. An alternative algorithm to numerically obtain the Lyapunov spectrum attempts to decouple the dynamics corresponding to distinct

---

[24] The singular values of L are the square-roots of the eigenvalues of the real symmetric positive-semidefinite matrix $L^t L$ or equivalently $L L^t$

Lyapunov exponents. We begin with an arbitrary orthonormal[25] basis $u_1(0)$, ..., $u_n(0)$ for $T_{x(0)}M$. We then choose a time step τ and evolve each of the $u_j(0)$ according to (15.19) for $0 \leq t \leq \tau$ to obtain tangent vectors $u_j(\tau) \in T_{x(\tau)}M$. In general, $u_j(\tau)$ are not orthogonal nor of unit length since linearized time evolution can stretch/contract and rotate the tangent vectors. What is more, all the u_j would have acquired significant components in the direction corresponding to the LLE and progressively smaller components in directions corresponding to the lesser Lyapunov exponents. To start extracting this information, we use Gram-Schmidt orthogonalization to define an orthogonal basis $v_1^{(1)}, \cdots, v_n^{(1)}$ (and corresponding orthonormal basis $w_1, w_2, \cdots, w_n$) at $T_{x(\tau)}M$:

$$\begin{aligned} v_1^{(1)} &= u_1(\tau), \quad w_1 = v_1^{(1)}/||v_1^{(1)}|| \\ v_2^{(1)} &= u_2(\tau) - \langle u_2(\tau), w_1\rangle w_1, \quad w_2 = v_2^{(1)}/||v_2^{(1)}|| \cdots \\ v_n^{(1)} &= u_n(\tau) - \sum_{i=1}^{n-1} \langle u_n(\tau), w_i\rangle w_i, \quad w_n = v_n^{(1)}/||v_n^{(1)}||. \end{aligned} \tag{15.25}$$

Here, $\langle \cdot, \cdot \rangle$ is the inner product on tangent vectors to M at $x(\tau)$ and $\langle v, v\rangle = ||v||^2$. Note that the order does not matter: any of the $u_j(\tau)$ could be taken to be v_1 and so on. The idea is that $v_1^{(1)}$ points predominantly in the direction corresponding to the LLE, $v_2^{(1)}$ primarily in the direction corresponding to the next largest Lyapunov exponent and so on. Moreover, the lengths of the $v_j^{(1)}$ contain information on how much the original unit vectors $u_j(0)$ have been stretched. Thus, our first crude approximation to the Lyapunov spectrum is

$$\lambda_j^{(1)} = \frac{1}{\tau} \log ||v_j^{(1)}|| \quad \text{for} \quad j = 1, 2, \cdots, n. \tag{15.26}$$

The w_j, being orthonormal lack this stretching information, but point approximately in the Lyapunov eigendirections and we take them as the initial orthonormal tangent vectors for the linearized time evolution from $t = \tau$ to $t = 2\tau$. We repeat this procedure N times and thereby perform the linearized time evolution from $t = 0$ to $t = N\tau$ resulting in the sequence of orthogonal frames $v_j^{(k)} \in T_{x(k\tau)}M$ for $k = 1, \ldots, N$ and $j = 1, \ldots, n$. The corresponding approximation to the Lyapunov spectrum after N time steps is

$$\lambda_j^{(N)} = \frac{1}{N\tau} \sum_{k=1}^{N} \log ||v_j^{(k)}|| \quad \text{for} \quad j = 1, \ldots, n. \tag{15.27}$$

We will use this algorithm to calculate the Lyapunov spectrum for the double pendulum and for the Lorenz oscillator in Sect. 15.4.1* and Sect. 15.5* where the dimension of M is $n = 4$ and $n = 3$ respectively. One finds that the results do not depend significantly on the choice of time step τ.

---

[25] The phase space M is viewed as a submanifold of Euclidean space $\mathbb{R}^p$ of sufficiently large dimension $p \geq n$. We use the inner product on coordinate basis vectors in any tangent space to M induced (see (B.42) for the induced metric) by the Euclidean inner product in $\mathbb{R}^p$. Any choice of coordinates and positive-definite inner product $\langle \cdot, \cdot \rangle$, in the limit of a large number of time steps, should lead to the same Lyapunov spectrum.

Qualitative discussion of properties of Lyapunov exponents. As we found for the logistic map in Sect. 15.1.3, points on phase space that lie in the basin of attraction of a common attractor (e.g., fixed point, periodic/quasiperiodic orbit, fractal set or the whole phase space) tend to have nearly the same numerically calculated Lyapunov exponents, making the concept robust. Heuristically, the Lyapunov exponents measure the rate at which the sides of the parallelepiped $u_1(0), \cdots, u_n(0)$ stretch or contract as they evolve linearly via (15.19) along the unperturbed trajectory $x(t)$. If these tangent vectors simply rotated and did not stretch, then the eigenvalues μ_j of the time evolution matrix would be complex numbers of unit magnitude and all the Lyapunov exponents would vanish. More commonly, some exponents are positive, some negative and some may vanish.

Lyapunov exponent along a trajectory. Interestingly, at any point $x(0)$, the Lyapunov exponent (15.20) in the direction along the trajectory through $x(0)$ must vanish if the trajectory does not approach a fixed point. To see why this is the case, we first note that (15.18) implies

$$\frac{d\dot{x}^i}{dt} = \frac{\partial v^i}{\partial x^j}\dot{x}^j. \tag{15.28}$$

Thus, the velocity vector to a trajectory satisfies the linearized evolution equation (15.19). It follows that under linearized evolution, $\dot{x}(0) \mapsto \dot{x}(t)$:

$$L(t,0)\dot{x}(0) = \dot{x}(t) = v(x(t)). \tag{15.29}$$

Putting this in definition (15.20),

$$\lambda(x(0), \dot{x}(0)) = \lim_{t\to\infty} \frac{1}{t} \log \frac{||L(t,0)\dot{x}(0)||}{||\dot{x}(0)||} = \lim_{t\to\infty} \frac{1}{t}[\log ||v(x(t))|| - \log ||v(x(0))||] = 0, \tag{15.30}$$

since $v(x(t))$ does not approach a zero and we are dividing by t. A Hamiltonian system does not have attractive fixed points, so this suggests that Hamiltonian systems may always possess a vanishing Lyapunov exponent. This is indeed true (see below).

Sum rule for Lyapunov exponents. Furthermore, Lyapunov exponents (at a point $x(0)$ along a trajectory $x(t)$) are constrained by the divergence of the vector field as encoded in the sum rule[26]

$$\lambda_1(x(0)) + \cdots + \lambda_n(x(0)) = \lim_{t\to\infty} \frac{1}{t} \int_0^t (\boldsymbol{\nabla} \cdot \boldsymbol{v})(x(\tau))\, d\tau. \tag{15.32}$$

To establish this, we notice that from (15.23),

$$\sum\nolimits_j \lambda_j(x(0)) \quad = \quad \lim_{t\to\infty} \frac{1}{t} \sum\nolimits_j \log s_j(t) = \lim_{t\to\infty} \frac{1}{2t} \log\det L^t(t,0)L(t,0)$$

---

[26] Heuristically, this is to be expected since the divergence of a vector field measures the fractional rate at which infinitesimal volumes $\delta\Omega(x(0))$ change (see Sect. 19.5):

$$(\boldsymbol{\nabla} \cdot \boldsymbol{v})(x(0)) = \lim_{\delta\Omega\to 0} \lim_{t\to 0} \frac{1}{t\, \delta\Omega(x(0))} \left[\delta\Omega(x(t)) - \delta\Omega(x(0))\right]. \tag{15.31}$$

Crudely, viewing the Lyapunov exponents as the exponential rates of stretching over short times, $\delta\Omega(x(t)) \sim e^{\lambda_1 t} e^{\lambda_2 t} \cdots e^{\lambda_n t} \delta\Omega(x(0))$ so that (13.91) becomes a sum of Lyapunov exponents.

$$= \lim_{t\to\infty} \frac{1}{t} \log\det L(t,0) = \lim_{t\to\infty} \frac{1}{t} \int_0^t \boldsymbol{\nabla} \cdot \boldsymbol{v}(x(\tau))\, d\tau. \quad (15.33)$$

In the last step we used (15.21) to deduce that [see (13.91)]

$$\frac{d}{dt} \log\det L(t,0) = \frac{d}{dt} \operatorname{tr} \log L = \operatorname{tr} \dot{L} L^{-1} = \operatorname{tr} A = \boldsymbol{\nabla} \cdot \boldsymbol{v}, \quad (15.34)$$

whence $\log\det L(t,0) = \int_0^t \boldsymbol{\nabla} \cdot \boldsymbol{v}(x(\tau))\, d\tau$. In particular, the sum of Lyapunov exponents mush vanish in a volume preserving flow.

Largest Lyapunov exponent and chaos. Of particular significance, is the largest Lyapunov exponent (LLE, also called the maximal Lyapunov exponent), which controls the rate of most rapid growth of perturbations around the trajectory that starts at $x(0)$. Evidently, a positive maximal Lyapunov exponent is a harbinger of exponential instability and can contribute to the development of chaos. However, a positive LLE is not sufficient for chaos. For instance, an unstable fixed point such as at the origin of the linear system $\dot{x} = ax$ for $a > 0$ (or $\dot{x}_i = a_{ij} x_j$ where a_{ij} has at least one positive eigenvalue) leads to a positive Lyapunov exponent $\lambda = a$, but the system is not chaotic, trajectories simply fly off to infinity in a regular fashion. Exponential instability of trajectories that are moreover confined[27] to a bounded region usually leads to chaotic behavior.

Pairing of Lyapunov exponents in Hamiltonian systems. If all the Lyapunov exponents are negative, then the evolution is dissipative and perturbations die out. For a conservative Hamiltonian system, Liouville's theorem tells us that time evolution preserves volumes in phase space. This implies that the linearized time evolution matrix $L(t,0)$ must have unit determinant, which in turn implies that the sum of Lyapunov exponents must vanish (as does the divergence of a Hamiltonian vector field (see (15.32) and Sect. 10.8)). In fact, Hamiltonian time evolution, being a family of canonical transformations, also preserves the symplectic form. This can be used to show that the Lyapunov exponents come in $(\lambda, -\lambda)$ pairs[28]. To see this, we note that $L(t,0)$ must be a linear canonical transformation, one that satisfies $L^t \omega L = \omega$ where $\omega = (0, -I|I, 0)$ is the canonical symplectic form (3.145). In other words, $L = \omega^{-1}(L^t)^{-1}\omega$. Now, the eigenvalues of L are the zeros of its characteristic polynomial. However, L and L^{-1} share the same characteristic polynomial:

$$\det(L - \mu I) = \det(\omega^{-1}(L^t)^{-1}\omega - \mu I) = \det((L^{-1})^t - \mu\omega\omega^{-1}) = \det(L^{-1} - \mu I), \quad (15.35)$$

and therefore must have the same eigenvalues. The eigenvalues of L^{-1} are the reciprocals of those of L. Hence, if μ is an eigenvalue of L, so must $1/\mu$ (recall that $\det L = 1 \neq 0$). Since Lyapunov exponents are $t \to \infty$ limits of $(1/t)\log|\mu(t)|$, they must come in $(\lambda, -\lambda)$ pairs. Furthermore, there are as many vanishing pairs of Lyapunov exponents as there are independent conserved quantities[29] in involution [43]. In the extreme case of a Liouville integrable system (see Sect. 11.7*), all the Lyapunov exponents vanish.

---

[27] In the language of homoclinic phenomena (see Fig. 15.10b), the unstable manifold needs to fold and intersect the stable manifold for chaos to occur.

[28] The $\lambda \to -\lambda$ symmetry of the Lyapunov spectrum of a Hamiltonian system is symptomatic of its time-reversal invariance. Heuristically, a growing direction must come paired with a decaying direction.

15.3* Poincaré return map and Homoclinic tangle

Lyapunov exponents quantify the (exponential) sensitivity to initial conditions, which is a characteristic feature of chaotic systems. Another feature of chaotic systems is a homoclinic tangle. In fact, chaos was first 'sighted' by Poincaré in the late 1800s when he discovered a homoclinic tangle while studying the stability of the solar system in the context of the gravitational three-body problem. Here, we give a brief introduction to the phenomenon of a homoclinic tangle. For this, we will consider a vector field $\dot{\boldsymbol{r}} = \boldsymbol{v}(\boldsymbol{r})$ with a fixed point $\boldsymbol{r}_*$ (see Chap. 5), define the notions of stable and unstable manifolds and then examine the dynamics in the vicinity of the fixed point via a Poincaré return map on a surface of section.

Stable and unstable manifolds. The stable and unstable manifolds W_s and W_u of a fixed point $\boldsymbol{r}_*$ are the sets of points (other than $\boldsymbol{r}_*$) that approach it as $t \to \pm\infty$. For a sink or attractor (e.g., spiral or node on the phase plane), W_u is empty while W_s is the basin of attraction (it includes all points in a sufficiently small open neighborhood of $\boldsymbol{r}_*$). For a source/repeller, W_s is empty while W_u is the 'basin of repulsion' and includes an open neighborhood of $\boldsymbol{r}_*$. Saddles have nonempty stable as well as unstable manifolds. For the dipole field of (5.28) W_s and W_u coincide except along the axis of the dipole (see Fig. 5.9c).

Poincaré section and return map. For dynamical systems with a phase space of dimension 3 or more, Poincaré developed a discrete-time dynamics on surfaces that bear his name. For definiteness, suppose we have a dynamical system with a 3d phase space (it could be a constant energy hypersurface of a Hamiltonian system with two degrees of freedom). A Poincaré surface S is a 2d hypersurface[30] in this 3d phase space. The Poincaré return map is a discrete-time dynamics on S defined as follows (see Fig. 15.10a). Given a point $p_0 \in S$, generically the trajectory starting at p_0 does not lie on S and intersects S next at some point p_1. The map $p_0 \mapsto p_1$ is the Poincaré return map. It may be iterated $p_0 \mapsto p_1 \mapsto p_2 \mapsto \cdots$ to obtain a discrete-time dynamics on S. We will call this sequence of points on S the Poincaré section associated to the trajectory through p_0. A fixed point p_* of the return map is a point that is mapped to itself $p_* \mapsto p_*$. For example, p_* could be a fixed point of the original continuous-time dynamics which happens to lie on S. The concepts of stable and unstable manifolds can be extended to fixed points of the return map. The stable manifold W_s of p_* consists of points $p_0 \neq p_*$ on S whose forward iterates

---

[29] If H is the only conserved quantity, then two Lyapunov exponents vanish. One corresponds to a direction along the Hamiltonian flow (trajectory) and the other to one transversal to the level hypersurface of H. The same applies to any other conserved quantity.

[30] A hypersurface is the name given to a manifold of dimension one less than that of the ambient space. If the state space were n dimensional, then a Poincaré surface is an $n-1$ dimensional hypersurface.

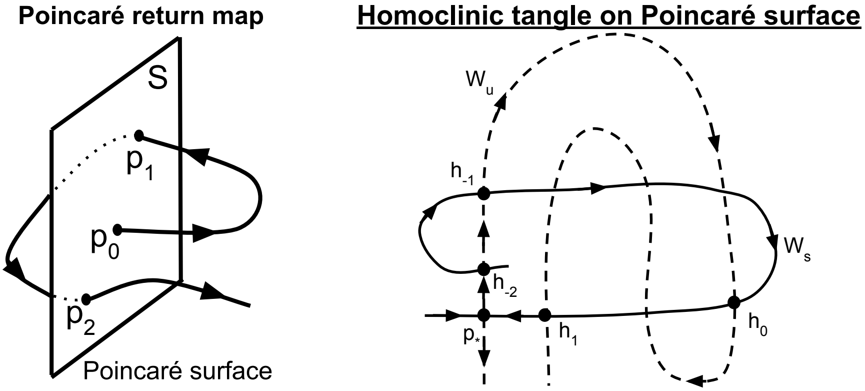

(a) (b)

Figure 15.10: (a) First return map $p_0 \mapsto p_1$ on a Poincaré surface S in phase space. (b) Homoclinic tangle around a saddle point p_* on a Poincaré surface S showing homoclinic points h_n that lie at intersections of the stable and unstable manifolds W_s and W_u of p_*. h_1 is the image of h_0 while h_{-1} is its pre-image under the return map. W_s is the union of points whose iterates approach p_* while W_u is the union of points whose backward iterates approach p_*.

$p_0 \mapsto p_1 \mapsto p_2 \mapsto \cdots \mapsto p_n \mapsto \cdots$ approach p_* as $n \to \infty$. Thus, W_s is a union of many such sequences and can look like a curve on S ending at p_*. Similarly, the unstable manifold W_u of p_* consists of points on S which when iterated backwards in discrete time approach p_*.

Homoclinic points and tangle. Now, if p_* is a saddle point of the original continuous-time dynamics, Poincaré discovered that remarkable things happen when the stable and unstable manifolds of p_* intersect. Such a point of intersection of W_s and W_u is called a homoclinic point[31]; it is not another fixed point. Thus, a homoclinic point $h \in S$ is one that approaches p_* when iterated both forward and backward in discrete time under the Poincaré return map! He realized that if there is one homoclinic point h_0, then there is automatically a doubly infinite sequence of homoclinic points obtained by forward and backward iterates of h_0 under the return map. This sequence of homoclinic points $\cdots h_{-m}, \cdots, h_{-2}, h_{-1}, h_0, h_1, h_2, \cdots, h_n \cdots$ accumulates at the fixed point p_* as either m or $n \to \infty$. Consequently, the stable and unstable manifolds W_u and W_s fold and intersect in an intricate manner called a homoclinic tangle (see Fig. 15.10b). This leads to a very complicated flow pattern around p_* for the original vector field, which we now associate with chaotic systems[32]. In fact, a homoclinic tangle implies sensitive dependence on initial conditions, as we will see by considering three types of ICs. If an IC lies on W_s, then successive iterates asymptotically approach p_*. An IC on W_u (that is not a homoclinic point) leads to an orbit that does not tend to p_*, but approaches p_* when evolved backwards in time. Finally, an IC that does not lie on either W_u or W_s wanders around without approaching p_* either in forward or backward time. Since W_u and W_s fold and intersect infinitely often forming a tangle around p_*, there are ICs of all three types arbitrarily close to one another. Positive Lyapunov exponents help to quantify this sensitive dependence on ICs. More on homoclinic phenomena may be found in [57, 65, 99].

---

[31] When they intersect, W_s and W_u usually intersect transversally (i.e., at a nonzero angle). A point at which they intersect with vanishing angle is called a *homoclinic tangency*. A homoclinic tangency signals the onset of a homoclinic tangle. Indeed, suppose we have a vector field depending continuously on a real 'control parameter' a. As a crosses a critical value a_c, we may imagine that W_s and W_u go from being nonintersecting to crossing each other. Typically, at $a = a_c$, the stable and unstable manifolds display a homoclinic tangency.

[32] However, this does not happen for autonomous vector fields in 2d. As explained in the context of the Poincaré-Bendixon theorem in Sect. 5.4*, one needs a 3 or higher dimensional phase space (in which the Poincaré slice sits) for homoclinic phenomena and chaos to be possible.

15.4 Hamiltonian chaos: order-chaos-order transition in a double pendulum

In Sect. 15.1, we studied chaos in discrete-time systems (iterations of a map). We now move to continuous-time systems which may broadly be classified into conservative and dissipative. This section is devoted to the transition from regularity to chaos in a conservative system while Sect. 15.5* deals with the dissipative Lorenz model.

In conservative Hamiltonian systems, the Hamiltonian structure leads to distinctive phenomena and theoretical control over the dynamics [99, 126]. The preservation of the symplectic structure in phase space places restrictions: phase space volume (Sect. 10.8) and areas in all tangent 2-planes (Sect. 10.4) must be conserved, thus precluding nodes and limit cycles. The KAM (Sect. 11.7*) and Poincaré-Birkhoff (Sect. 15.4.1*) theorems control the manner in which integrability can give way to chaos as parameters are varied, with surviving invariant tori, centers and saddles playing a prominent role. By the Poincaré-Bendixon theorem of Sect. 5.4*, we need at least two degrees of freedom (or a 4d phase space) for chaos to be possible. If there is not any coordinate system in which one may separate variables in the Hamilton-Jacobi equation (as in Sect. 12.3), then the system fails to be solvable by separation of variables and could display chaotic behavior. There are several simple examples of nonseparable potentials on 2 and 3 dimensional configuration spaces that display chaotic behavior in appropriate parameter regimes. These include (i) the Hénon-Heiles system of planar stellar motion around a galactic center [87, 126] modeled by $H = (1/2)(p_x^2 + p_y^2 + x^2 + y^2) + \lambda(x^2 y - y^3/3)$, (ii) certain anharmonic oscillators such as $H = (1/2)(p_x^2 + p_y^2) + ((1-\lambda)/12)(x^4 + y^4) + \frac{1}{2}x^2 y^2$ [66, 136], (iii) pendula such as the (planar) elastic pendulum and the double pendulum studied here and (iv) three-body problems such as the planar circular restricted three-body problem of celestial mechanics (see Sect. 9.5*) and the three-rotor problem [73].

We now return to the double pendulum of Sect. 13.2 and use it as a place to study some aspects of the transition from regular to chaotic motion in a Hamiltonian system. It gives us a context in which to introduce and illustrate general ideas such as Poincaré sections, Lyapunov exponents and spontaneous symmetry breaking, which are useful in the study of many nonlinear and chaotic systems. Recall that the double pendulum consists of an 'upper' bob of mass m [attached to the end of a rod of length l which is suspended from a fixed pivot] and a 'lower' bob, also of mass m, attached to the end of a rod of length l which is suspended from the upper bob. Both rods are assumed rigid and of insignificant mass, while the bobs are point-like. As shown in Fig. 15.11, the pendulum is free to move in a vertical plane (the x-y plane with origin at the fixed pivot) subject to a constant downward acceleration due to gravity of magnitude g.

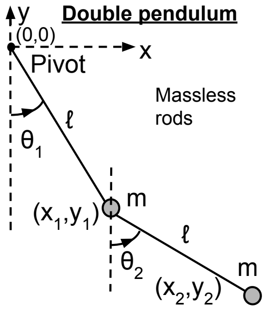

Figure 15.11: Double pendulum with two equally massive bobs suspended from a fixed support with massless rods of length l free to move in a vertical plane subject to gravity.

The double pendulum has two degrees of freedom: the angles θ_1 and θ_2 made by the two rods relative to the vertical. It has only one conserved quantity that we are aware of, the total energy or Hamiltonian, which restricts the motion to a constant energy 3d hypersurface in its 4d phase space. The energy E (say, in units of mgl) may be regarded as a control parameter[33] that can take any value from 0 to ∞.

Resumé of the order-chaos-order dynamics of the double pendulum. We will now outline the changes in the dynamics of the double pendulum as its energy E is increased from 0 to ∞. We will see that it is integrable in both limits and displays an order-chaos-order transition with increasing energy.

Infinitesimal and moderately low energies. As we learned in Sect. 13.2.2, at very low energies $0 \leq E \ll mgl$, the double pendulum executes oscillations of small amplitude ($|\theta_{1,2}| \ll 1$) that can be decomposed into a pair of normal modes. Thus, at low energies, to leading approximation, we have two independent conserved quantities, the energies of the two normal modes (13.39) with the total energy being their sum (13.40). These normal mode Hamiltonians Poisson commute with each other. Therefore the limiting low energy system is Liouville integrable in the sense of Sect. 11.7*. As a consequence, the dynamics at low energies (even in the absence of any approximation) is relatively regular. In fact, the trajectory on the configuration space (the 2-torus $S^1_{\theta_1} \times S^1_{\theta_2}$) is quasiperiodic (to leading approximation), being the superposition of the periodic motions of the two normal modes, whose periods are incommensurate.

As the energy is increased, the motion ceases to be quasiperiodic but continues to be relatively regular. We demonstrate this via numerical solutions to the EOM. To visualize the trajectories, we plot the locus of the bobs in the vertical plane. However, such a figure rapidly becomes unwieldy since the configuration space trajectory can keep crossing itself and over time resembles a ball of wool. To visualize trajectories in a more controlled manner, one needs to give up some of the details. Poincaré sections introduced in Sect. 15.4.1* strike a balance. Poincaré surfaces are 2d surfaces in a 3d constant energy hypersurface of the 4d phase space, on which the points of intersection with a trajectory are recorded to produce the Poincaré sections corresponding to an orbit[34]. We will learn how one can distinguish periodic, quasiperiodic and irregular trajectories through examination of their Poincaré sections. We note here that at low energies, Poincaré sections (see Fig. 15.12) are concentrated along 1d 'KAM' curves.

---

[33] By this we mean that as the energy is varied, the nature of the dynamics changes. The ratio of masses of the bobs may also be regarded as a control parameter. Unlike the latter, the energy is a dynamical variable. However, E may be regarded as a control parameter since it is conserved in time. By contrast, we may not regard the angles (θ_1, θ_2) as control parameters.

Intermediate energies. As the energy is increased, points on Poincaré sections go from being concentrated on 1d KAM curves to densely exploring 2d regions, due to the absence of an additional conserved quantity or sufficiently many invariant surfaces in phase space to restrict the motion (see Fig. 15.15). This signals the onset of chaos[35]. We observe an extreme sensitivity to initial conditions in this chaotic phase: trajectories with nearly the same initial conditions rapidly deviate from each other and become uncorrelated. This is manifested in the positivity of the largest Lyapunov exponent. The exponential sensitivity[36] to initial conditions coupled with the confinement of trajectories to a bounded energy hypersurface is typical of chaotic systems. Additionally, the bobs begin to wind around their pivots, signaling a change in topology from purely librational to a combination of rotational and librational motion. The degree of chaos gradually increases till a single trajectory explores practically the entire Poincaré surface in a phase of 'global' chaos. As the energy is further increased, the dynamics progressively becomes more regular, with Poincaré sections becoming concentrated on what begin to look like 1d curves.

High energy or zero gravity limit. At high energies $E \gg mgl$, the kinetic energies of the bobs far exceeds the gravitational potential energy, which is bounded above by $6mgl$. In fact, the limit $E \to \infty$ may also be regarded as the one where gravity is very weak ($g \to 0$). When the gravitational torque is ignored, an additional conserved quantity emerges: the total angular momentum L_z of the bobs about the support. Moreover, L_z Poisson commutes with the Hamiltonian. Thus, the zero gravity double pendulum is also integrable. In Sect. 15.4.3*, we study this limiting case. Conservation of E and L_z are used to reduce the EOM to quadrature (involving a hyperelliptic integral) and also to classify the possible types of motion. These results are used to validate our numerical solutions at relatively high energies as well as to predict some of the patterns on the high energy Poincaré sections. In summary, the double pendulum displays order-chaos-order behavior with increasing energy[37].

---

[34] Though they are discrete-time snapshots of a trajectory, 2d Poincaré surfaces [for a Hamiltonian system with 3d energy hypersurfaces] capture the dynamics in a relatively faithful manner. For instance, a generic trajectory will (repeatedly) intersect such a Poincaré surface, unlike a 2d surface in a 4d energy hypersurface. In general, a Poincaré surface is chosen to have codimension one in the ambient space.

[35] Chirikov's overlap of 'resonances' is a criterion for the onset of chaos. We refer the reader to [87] for a discussion of this phenomenon.

[36] Typically, trajectories move away from each other exponentially fast for short/moderate times. The boundedness of energy hypersurfaces puts an upper bound on how long this exponential growth can go on although it can go on indefinitely in the tangent spaces along a trajectory, see Footnote 19.

15.4.1* Poincaré sections and onset of chaos

The phase space M of the double pendulum is four-dimensional. It is the Cartesian product of a 2-torus $\mathbb{T}^2 = S^1 \times S^1$ and a plane $\mathbb{R}^2$ parametrized by angular coordinates $\theta_{1,2} \in S^1$ and conjugate momenta[38] $p_{1,2} \in \mathbb{R}$:

$$p_1 = ml^2(2\dot{\theta}_1 + c_{12}\dot{\theta}_2) \quad \text{and} \quad p_2 = ml^2(\dot{\theta}_2 + c_{12}\dot{\theta}_1). \tag{15.36}$$

It is challenging to visualize trajectories on M. However, since the energy (13.19):

$$H = \frac{1}{2ml^2(1+s_{12}^2)}\left[p_1^2 + 2p_2^2 - 2c_{12}p_1p_2\right] - mgl[2\cos\theta_1 + \cos\theta_2] + 3mgl \tag{15.37}$$

is conserved, each trajectory is confined to a 3d hypersurface in phase space.

Boundedness of constant energy hypersurfaces. We will now argue that the constant energy ($H = E$) subsets M_E of phase space are bounded and closed. This will mean, in particular, that a trajectory cannot escape to infinity or acquire an infinite velocity. This is unlike the Kepler problem, where a comet with positive energy can escape to infinity while a zero impact parameter trajectory can approach the force center with speed increasing without bound[39].

The constant energy hypersurface M_E is a compact (bounded and closed[40]) 3d manifold since $\theta_{1,2} \in S^1$ are always bounded while $|p_1|$ and $|p_2|$ are also bounded due to the conservation of energy. To see this boundedness, we first notice that the potential energy $V = 3mgl - mgl[2\cos\theta_1 + \cos\theta_2]$ is bounded both above and below: $0 \le V \le 6mgl$. Thus, for fixed E, the kinetic energy $T = E - V$ (which is manifestly positive from its expression in Cartesian coordinates, $(m/2)(\dot{x}_1^2 + \dot{y}_1^2 + \dot{x}_2^2 + \dot{y}_2^2)$) is also bounded above: $0 \le T \le E$. Hence from (15.37),

$$|T| = T = \frac{1}{2ml^2(1+s_{12}^2)}\left[p_1^2 + 2p_2^2 - 2c_{12}p_1p_2\right] \ge \frac{1}{4ml^2}\left[p_1^2 + 2p_2^2 - 2|p_1||p_2|\right]. \tag{15.38}$$

Here, we replaced $(1 + s_{12}^2)$ by the larger quantity 2 and subtracted the larger quantity $2|p_1||p_2|$ instead of $2p_1p_2c_{12}$. The RHS may be expressed as a sum of two squares:

$$E \ge T \ge \frac{1}{4ml^2}\left[(|p_1| - |p_2|)^2 + p_2^2\right]. \tag{15.39}$$

Consequently, both $|p_2|$ and $|p_1| - |p_2|$ are bounded above. It follows that $|p_1|$ is also bounded. Thus, any constant E submanifold of phase space is bounded.

---

[37] The 3-rotor problem [73, 74] furnishes another example of order-chaos-order behavior.

[38] Here, we use the short forms $c_{12} = \cos(\theta_1 - \theta_2)$ and $s_{12} = \sin(\theta_1 - \theta_2)$.

[39] The boundedness of M_E will also contribute to the chaotic behavior of trajectories: nearby trajectories of moderate energy have a tendency to move apart exponentially fast but are forced to turn around due to the boundedness of M_E, producing an intricate tangle of trajectories!

[40] It is a closed set since it is the inverse image of a closed set (the single point set $\{E\}$ with $E \in \mathbb{R}$) under a continuous map given by the Hamiltonian $H : M \to \mathbb{R}$.

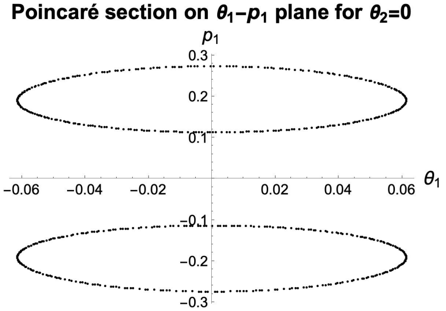

Figure 15.12: Numerically obtained Poincaré sections for the double pendulum in the small angle approximation (13.25) with $m = 1$, $l = 1$, $g = 1$, and starting from rest at $\theta_1(0) = -\theta_2(0) = \pi/15$ and $E = 0.0658$. 588 points are shown for $0 \le t \le t_{\max} = 1000$. The points lie on a pair of closed curves, indicating that the trajectory is quasiperiodic. It also suggests the presence of two conserved quantities and an absence of chaos. Here, the lower curve corresponds to $\dot{\theta}_2 > 0$ and the upper one to $\dot{\theta}_2 < 0$ at the points of intersection. In principle, a Poincaré plot must include all points of intersection when the evolution is extended indefinitely in time. In practice, numerically obtained trajectories are available only for a limited duration. However, as the figure indicates, a reasonably clear Poincaré section emerges for $0 \le t \le 1000$ and our eyes are able to plausibly fill in the gaps! As further evidence for the reliability of the plot, we verified that the qualitative nature of the section does not change upon doubling $t_{\max}$ or changing initial conditions while keeping E small.

Poincaré sections. It is difficult to plot or visualize trajectories in a 3d constant energy hypersurface[41]. This is where the Poincaré plots introduced in Sect. 15.3* come to our aid. In the present context, a Poincaré surface is a 2d slice through a constant energy hypersurface M_E (see Fig. 15.10a). For example, we could choose a Poincaré surface corresponding to $\theta_1 = 0$, i.e., focus on those instants when the first bob hangs vertically downward. This 2d surface may be parametrized by θ_2 and p_2 (very roughly, the 'phase space' of the second bob). The fourth coordinate p_1 at any point on this surface is fixed[42] by the condition $H(\theta_1 = 0, \theta_2, p_1, p_2) = E$. Now, we begin with an initial condition $(\theta_2^{(0)}, p_2^{(0)})$ on this slice and evolve the trajectory forward in time till it intersects this slice again, say at $(\theta_2^{(1)}, p_2^{(1)})$ with $\dot{\theta}_1 \ge 0$. The map

$$(\theta_2^{(0)}, p_2^{(0)}) \mapsto (\theta_2^{(1)}, p_2^{(1)}) \quad \text{is called the Poincaré return map.} \tag{15.40}$$

The Poincaré map gives us a natural example of a discrete-time dynamical system like the ones of Sect. 15.1. Iterating this map, we mark the sequence of points $[(\theta_2^{(n)}, p_2^{(n)})$

---

[41] Though it is a 3d manifold, it may not be possible to visualize M_E as a subset of $\mathbb{R}^3$. A lower dimensional example will indicate why. Suppose the phase space was $\mathbb{R}^3$ and the Hamiltonian was $x^2 + y^2 + z^2$. Energy hypersurfaces are then 2-spheres $x^2 + y^2 + z^2 = E$. Though a spherical surface is 2-dimensional, it cannot be embedded in the plane $\mathbb{R}^2$; we need at least two planar patches to cover the 2-sphere. M_E is a 3d analog of the 2-sphere; it is compact (closed and bounded) and lacks a boundary.

[42] There are usually two values of p_1 that satisfy this condition, corresponding to clockwise and counterclockwise motion of the first bob as it passes through $\theta_1 = 0$. We are free to focus on one of them to uniquely specify the state. For definiteness, we restrict attention to $\dot{\theta}_1 \ge 0$.

for $n = 0, 1, 2, \ldots]$ where the trajectory intersects the Poincaré surface. We will call this set of points the Poincaré section of the trajectory corresponding to the chosen surface. It is possible to obtain Poincaré sections (see Fig. 15.12) for various trajectories by numerically integrating the equations of motion up to a time $t_{\max}$ of our choosing.

Poincaré sections can convey a great deal of qualitative information on the nature of the dynamics. To begin with, a periodic trajectory would typically intersect a Poincaré surface at a finite number of (e.g., two) points[43]. On the other hand, a quasiperiodic trajectory such as one that is an incommensurate superposition of two periodic motions, would lie on a torus in the phase space (see Fig. 10.1a) and would typically intersect a Poincaré surface at points lying along a 1d curve (or several disconnected curves). So a Poincaré section consisting of a finite number of points or with points lying along curves indicates a periodic or quasiperiodic trajectory.

More generally, if there is a second conserved quantity Q independent of H, then each trajectory is confined to a 2d surface (in the 4d phase space) on which level hypersurfaces of H and Q intersect. This 2d surface (determined by ICs) generically intersects a given Poincaré slice along a 1d curve. So if there is a 2^{nd} conserved quantity, we expect the points in any Poincaré section to lie along a 1d curve (or union of curves). If Q is 'nearly conserved' (as happens with the angular momentum of a double pendulum at high energies), then we would expect the points in any Poincaré section to be concentrated in a neighborhood of 1d curves. If there is no conserved quantity other than H, then points on a Poincaré slice can fill out 2d regions unless the trajectory lies on an invariant surface, such as a surviving (nonresonant) torus that appears in the KAM theorem of Sect. 11.7*. In all cases, since the constant energy hypersurface is bounded, the points in a Poincaré section must lie in a bounded region.

Small oscillations at low energies. We begin here with the double pendulum treated in the low energy (small angle) approximation (13.25). Numerically obtained trajectories show that points on a Poincaré surface lie along 1d curves as shown in Fig. 15.12. This indicates there is a second conserved quantity. In fact, we already found two conserved quantities for small oscillations: the energies of the two normal modes $H_\pm$ (13.39) with the total energy $H = H_+ + H_-$ being their sum. Small oscillations of a double pendulum define a Liouville integrable system and one can use the normal modes to find angle-action variables (see Prob. 13.17). As explained in Sect. 11.7*, this means that the 4d phase space is foliated by a two-parameter family of invariant 2-tori, which are the common level sets of H_+ and H_- [the two parameters being the numerical values of H_+ and H_-]. The points on Poincaré sections are concentrated on 1d curves given by the intersection of these invariant tori with the Poincaré surface.

Though the motion is not periodic (only quasiperiodic), small oscillations of the double pendulum are regular, as displayed in Fig. 15.14a. What is more, trajectories starting from nearby initial conditions remain nearby for long times (see Fig. 15.13a).

---

[43] In exceptional cases, if the trajectory is not transversal [transversal means intersects it at a nonzero angle] to the Poincaré surface, it could be tangent to the slice at one or more points or even lie on the slice for some duration of time.

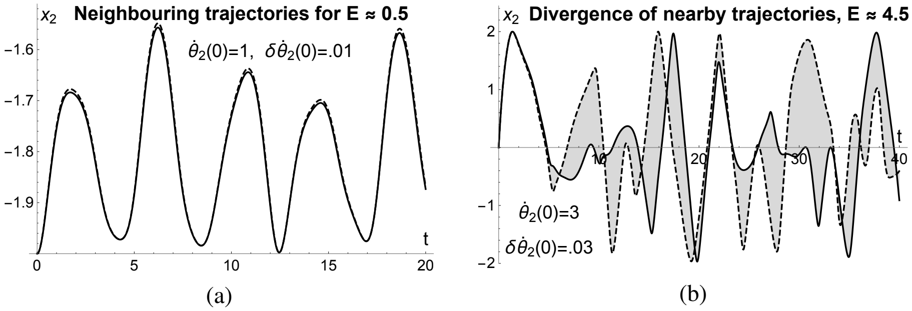

Figure 15.13: (a) Abscissa of 2^{nd} bob for two neighboring trajectories with $E = 0.5, 0.51$. The nonzero ICs $\dot\theta_2(0) = 1$ (solid curve) and 1.01 (dashed curve) differ by 1%. The trajectories remain nearby and the dynamics is close to linear. (b) Sensitive dependence of $x_2(t)$ on ICs for neighboring chaotic trajectories with $E = 4.5, 4.59$ (ICs $\dot\theta_2(0) = 3, 3.03$ are 1% apart). The shaded region encloses the deviation. Here, $m = l = g = 1$ corresponding to the linear time scale $T = 2\pi\sqrt{l/g} \approx 6.28$. Thus, while in (a) approximate knowledge of the initial state guarantees knowledge of the final state to a similar accuracy, in (b) this is certainly not the case.

Onset of chaos. As the energy is increased and oscillations become larger, $H_\pm$ are no longer (approximately) conserved, though the total energy is. For relatively low E (say $E \lesssim 1$ in units where $m = g = l = 1$), Poincaré sections for several initial conditions are still concentrated near deformed 1d curves, as shown in Fig. 15.16, indicating that $H_\pm$ are 'approximately' conserved. More accurately, though $H_\pm$ are not conserved, many of the invariant tori survive (though their shapes may deform) so that trajectories that start on them remain confined to these 2d KAM surfaces in phase space. These surviving tori intersect Poincaré surfaces along 1d KAM curves as in the $E = 0.5$ Poincaré plots in Figs. 15.15 and 15.16. Thus, invariant tori serve as a replacement for conserved quantities when the latter cease to exist. This survival of invariant tori beyond the small oscillations integrable limit can be established using perturbation theory and forms the subject of KAM theory (see Sect. 11.7* and [2, 99, 106]).

Prior to the onset of widespread chaos, Poincaré sections display interesting features. For instance, the Poincaré plot at $E = 1$ in Fig. 15.16 shows several orbits that are concentrated on 1d curves that look like deformed circles. These are called 'resonance' islands. Some of these resonance islands are seen to form chains enclosing centers and separated by saddle points. This pattern of alternating centers and saddles is the subject of the Poincaré-Birkhoff theorem [99]. Chaotic orbits tend to make their first appearance in the vicinity of saddle points. As E is increased, the size of some of these resonance islands grows, allowing them to 'overlap'. Chirikov argued that this overlap of resonances is associated to the onset of widespread chaos [87].

As the energy is increased to intermediate values (e.g., Fig. 15.14b or $E = 1.5$ in Fig. 15.16), the motion becomes increasingly irregular. Points on Poincaré sections 'diffuse' out of the 1d curves to which they used to be confined and progressively fill up 2d regions as in the $E = 4$ plot of Fig. 15.15, indicating that the dynamics is chaotic. This spreading-out of orbits provides numerical evidence that energy

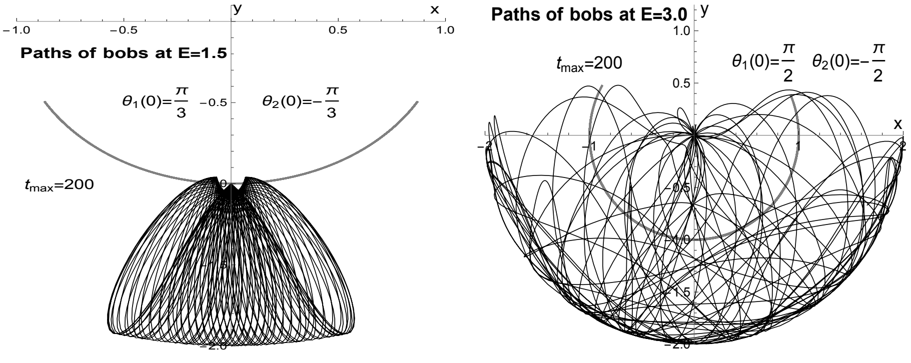

(a) (b)

Figure 15.14: Curves traced by bobs of a double pendulum on the vertical x-y plane for $m = g = l = 1$. (a) Moderately low energy ($E = 1.5$ for $0 \leq t \leq 200$, bobs starting from rest at $\theta_1(0) = -\theta_2(0) = \pi/3$) oscillation showing some regularity. (b) Intermediate energy oscillation ($E = 3$ for $0 \leq t \leq 200$, starting from rest at $\theta_1(0) = -\theta_2(0) = \pi/2$) showing irregular motion. The 'upper' bob always lies on the 'upper' circle of radius $l = 1$, though its trajectory can be quite irregular. The curve traced by the 'lower' bob is more complicated.

is the lone conserved quantity. The surviving invariant tori[44] are islands of regular (quasiperiodic) motion between regions of chaos. As we move farther away from integrability by increasing E, most invariant tori cease to exist and most of the phase space is filled by any one chaotic trajectory: we reach a globally chaotic phase (e.g., $E = 4$ in Fig. 15.16).

Sensitivity to initial conditions. A hallmark of chaos is sensitivity to initial conditions. This means two trajectories with slightly differing ICs could get quite far apart and display qualitatively different behavior. This feature makes chaotic systems behave unpredictably despite being deterministic. For the double pendulum, this is illustrated in Fig. 15.13 where we plot the horizontal coordinate of the second bob for trajectories with ICs that differ by 1%. In units where $m = g = l = 1$, the coordinates are seen to remain nearby at $E = 0.5$. At $E \approx 4.5$ they only agree for short times $\lesssim 2\pi\sqrt{l/g}$ and subsequently move apart and appear uncorrelated. In a chaotic regime, nearby trajectories typically diverge exponentially fast. Lyapunov exponents defined via the linearized evolution around a given trajectory and introduced in Sect. 15.2*, provide a way of quantifying this. Of these, the largest Lyapunov exponent λ_1 or $\lambda_{\max}$ gives the leading exponential rate of divergence, heuristically $|\delta \boldsymbol{r}(t)| \propto e^{\lambda_1 t}|\delta \boldsymbol{r}(0)|$. A positive λ_1 is characteristic of chaotic instabilities. In Fig. 15.17a, we plot the largest finite-time Lyapunov exponent (LLE) $\lambda_1(t)$ for a chaotic trajectory with energy $E = 4$ (in units where $m = g = l = 1$) that lies in the band of global chaos.

---

[44] The linearized equations of motion (13.25) define an integrable system which is a good approximation at low energies. This integrable system has the same phase space as the full double pendulum, and this phase space is foliated by invariant tori whose (quadratic) energies (13.26) are the sum of the two normal mode energies. Now, as nonlinearities are included [so that the equations become applicable at higher energies], some of these tori cease to exist while others survive with deformed shapes.

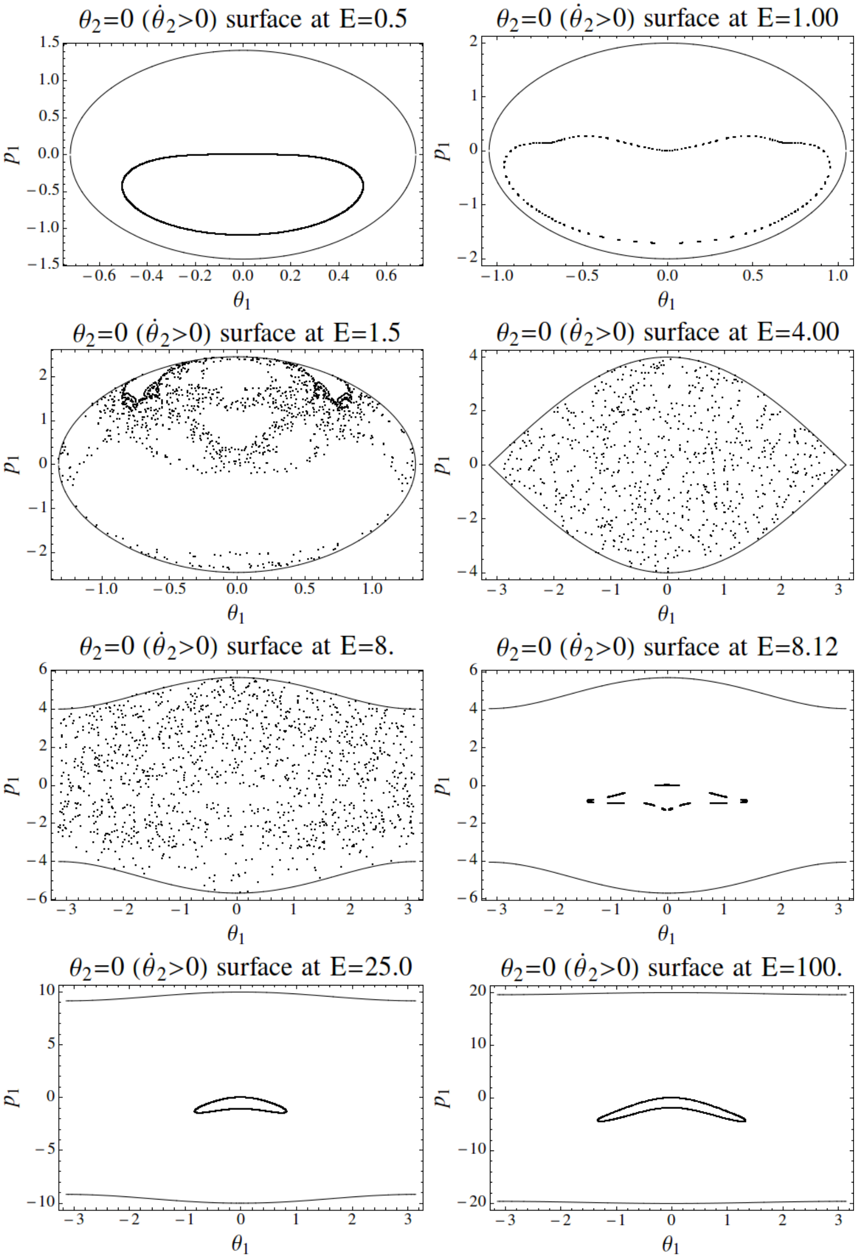

Figure 15.15: Poincaré sections on $\theta_2 = 0$ surface (parametrized by θ_1 and p_1) for trajectories ($t_{\max} \approx 10^3$-10^4) of increasing energy E in units where $m = l = g = 1$. In the initial state, the bobs hang downwards ($\theta_1(0) = \theta_2(0) = 0$) with the lower bob pushed to the right with twice the angular velocity of the upper bob, which is pushed to the left ($p_1(0) = 0$, $p_2(0) = \sqrt{E}$, $\dot\theta_1 = -p_2$, $\dot\theta_2 = 2p_2$). The Hill region goes from being contractible to wrapping around the θ_1-p_1 cylinder at $E = 4$. An order-chaos-order transition occurs with increasing energy.

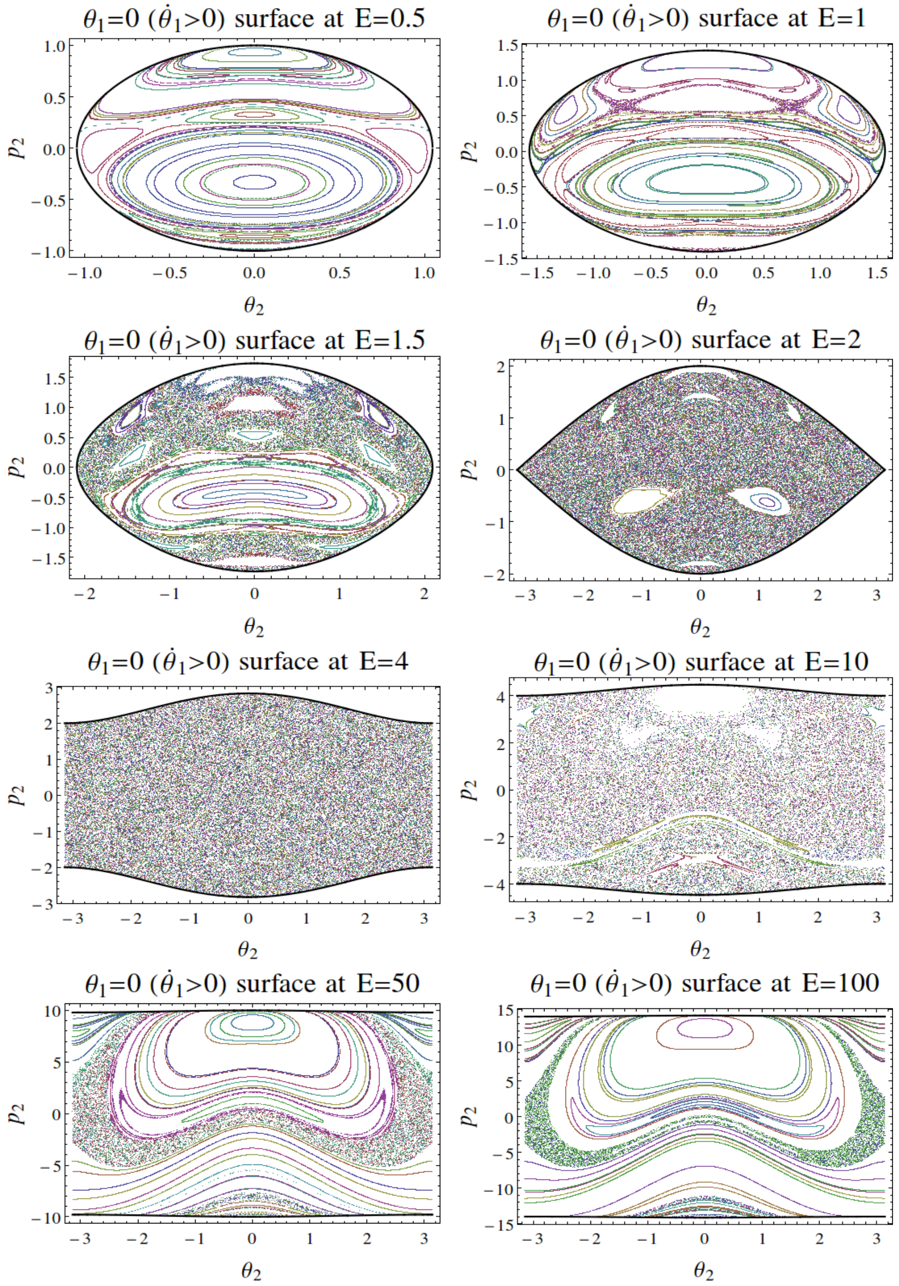

Figure 15.16: Order-chaos-order transition: For each of several energies, 40-60 randomly chosen ICs with $\theta_1(0) = 0$ are evolved forward in time till $t_{\max} = 10^3 - 10^4$. Points where the trajectories intersect the $\theta_1 = 0$ surface with $\dot\theta_1 \geq 0$ are shown on the Hill region parametrized by θ_2 and p_2. These correspond to instants where the upper bob points vertically downwards and is moving counterclockwise.

We see that $\lambda_1(t)$ appears to approach a positive limiting value ≈ 0.4 as t grows. The finite-time LLEs for several chaotic trajectories are plotted as a function of energy in Fig. 15.17b. We see that $\lambda_1 \to 0$ even for chaotic trajectories at low energies where the dynamics is predominantly regular. As the dynamics becomes more chaotic and we enter the globally chaotic phase around $E = 4$, λ_1 increases. Interestingly, the LLE for chaotic trajectories at higher energies ($E = 50, 100$), can exceed those for their counterparts in the globally chaotic phase. Evidently, the larger energies available and other dynamical features can enhance the sensitivity to ICs although chaotic trajectories occupy a smaller fraction of the phase space.

Due to the boundedness of energy hypersurfaces in the double pendulum, trajectories cannot keep growing apart exponentially, as a positive LLE might suggest based on the linearized evolution around a trajectory. Nonlinear effects ensure that the separation between trajectories saturates. Nevertheless, the sensitivity to ICs can magnify small errors in numerical solutions and make it difficult to make long-term predictions[45]. However, we find that this does not affect our ability to numerically obtain[46] Poincaré sections in the chaotic phase. In fact, a wide variety of numerically generated irregular orbits that begin nearby all produce essentially the same Poincaré section. Thus, the chaotic sections of Fig. 15.16 are robust despite the discretization and roundoff errors present in numerical solutions.

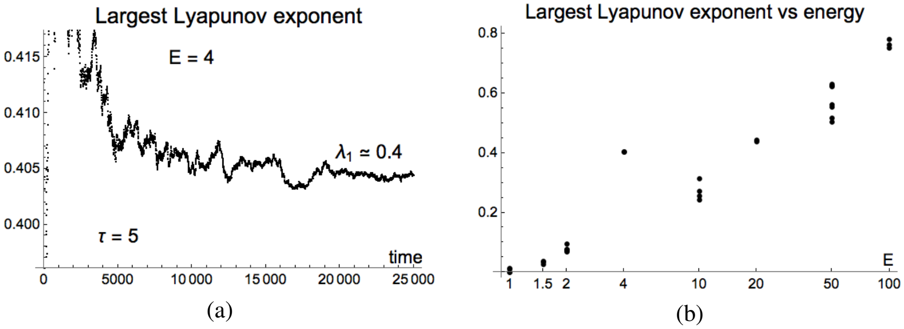

Figure 15.17: (a) Numerically computed largest finite-time Lyapunov exponent $\lambda_1(t)$ from formula (15.20) for a chaotic trajectory of the double pendulum with energy $E = 4$ when $m = l = g = 1$ showing approach to a positive asymptotic value for large t. The solution of the linearized equations was rescaled to unit length after every interval of time $\tau = 5$. (b) Largest finite-time Lyapunov exponent for chaotic trajectories at a few energies (on a log scale). The spread in values of λ_1 at a given energy is due to the dependence on ICs and due to statistical errors. The time $t_{\max}$ used in estimating finite-time Lyapunov exponents is $\sim 10^4$.

Hill region on Poincaré surfaces. We observe that the points on the Poincaré plots on the $\theta_2 = 0$ surfaces of Fig. 15.15 or $\theta_1 = 0$ surfaces of Fig. 15.16, are confined to well-defined regions. The boundaries of these 'Hill' regions[47] (indicated in black) are determined by energy conservation. For instance, putting $\theta_2 = 0$ in the Hamiltonian (15.37) and imposing $H = E$, we get

---

[45] Setting aside the boundedness of M_E, to ensure that 2 trajectories at time t are within ϵ of one another, we'd typically need to ensure that at $t = 0$, they were within $e^{-\lambda t}\epsilon$ of each other.

[46] This is related to the shadowing property of certain chaotic systems: there is an exact trajectory starting from a nearby IC that remains close to a numerically obtained trajectory.

$$2ml^2(E+2mgl(\cos\theta_1-1)) = (1+\sin^2\theta_1)^{-1}\left(p_1^2+2p_2^2-2p_1p_2\cos\theta_1\right). \quad (15.41)$$

To find the bounding curves $p_1^{\max,\min}(\theta_1)$, we extremize over possible values of p_2 by differentiating in p_2 holding E, θ_1 and p_1 fixed, resulting in $p_2 = (p_1/2)\cos\theta_1$. Inserting this in (15.41) we obtain

$$p_1^{\max,\min} = \pm\sqrt{4ml^2}\,(E+2mgl(\cos\theta_1-1))^{1/2}. \quad (15.42)$$

A similar procedure (see Prob. 15.29) leads to the boundary of the Hill region on the $\theta_1 = 0$ surface:

$$p_2^{\max,\min} = \pm\sqrt{2ml^2}\,(E+mgl(\cos\theta_2-1))^{1/2}. \quad (15.43)$$

These Hill regions may be viewed as subsets of the θ_1-p_1 and θ_2-p_2 cylinders. As Fig. 15.15 shows, they display a libration to rotation 'topological' transition as the energy is increased. More precisely, in the former case, from (15.42), for $E < 4mgl$, the range of allowed values of θ_1 is restricted to $|\theta_1| < \arccos(1-E/2mgl)$ so that the first bob cannot rotate about the pivot. For $E > 4mgl$ there is no such restriction, so θ_1 can reach $\pm\pi$ allowing the first bob to rotate about the pivot. Consequently, the Hill region goes from being simply connected (see Appendix B.2*) to wrapping around the θ_1-p_1 cylinder and becoming multiply connected.

Spontaneous symmetry breaking. This is a phenomenon where a symmetry of the equations of motion (or Hamiltonian/Lagrangian) is not a symmetry of a particular trajectory. We have encountered spontaneous symmetry breaking while studying perturbations of a static or periodic solution in Sect. 13.4 or in the bending of a card in Sect. 14.1 and will see it in the supercritical pitchfork bifurcation in the Lorenz oscillator of Sect. 15.5* as well as in the transition to turbulence in Sect. 19.16. In the double pendulum, the discrete transformation $\theta_2 \to -\theta_2$ is a symmetry of (i) the Hamiltonian (15.37) for $\theta_1 = 0$ and of (ii) the boundary of the corresponding Hill region. For low energies, all the orbits whose Poincaré sections are shown in Fig. 15.16 display this symmetry. However, around $E = 2$, when the dynamics is predominantly chaotic, some regular orbits do not display this $\theta_2 \to -\theta_2$ symmetry. We say that the symmetry is spontaneously broken[48]. However, in many chaotic orbits at the same energy, the symmetry remains unbroken. On average, the Poincaré section of a chaotic orbit is left-right symmetric so that the symmetry is respected in a statistical sense, although the scatterplot is not left-right symmetric pointwise.

---

[47] Hill regions are named after the 19th century American mathematical astronomer George W Hill who worked on the Sun-Moon-Earth and other problems of celestial mechanics. Here, we will use the phrase 'Hill region at energy E' for the portion of a (Poincaré) surface that lies within the constant energy hypersurface M_E.

[48] The symmetry is still present in the sense that the mirror image of any orbit is also an orbit, though perhaps a different one.

15.4.2* Return to regularity at high energies

At high energies $E \gg 6mgl$, the Poincaré sections of Fig. 15.15 and Fig. 15.16 display more regularity[49]. The return map no longer explores as much of the Hill region as at intermediate energies and Poincaré sections gradually get concentrated along 1d curves. Let us understand why.

When the energy is very large, most of it is kinetic since the gravitational potential energy (15.37) is bounded above by $6mgl$. Numerical solutions (e.g., for $E = 100mgl$ or more) show that on average, the bobs rotate rapidly either clockwise or counter-clockwise depending on ICs. However, superposed on this mean rotational motion, depending on the initial conditions, there can be oscillations. For example, if we start from the stable equilibrium state and give the lower bob a large angular velocity, then one finds that the angular velocities $\dot{\theta}_1$ and $\dot{\theta}_2$ oscillate roughly periodically about nonzero mean values, so that the two pendula rotate about their supports. However, the rotation is not uniform, the relative angle $\theta = \theta_1 - \theta_2$ oscillates roughly periodically around 0 with a nonzero amplitude, as the bobs continually exchange kinetic energy. In particular, unlike the simple pendulum at high energies, the bobs *need not* approach uniform circular motion, although that too is possible if ICs are chosen appropriately. Nevertheless, when $E \gg 6mgl$, we should, as a first approximation, be able to ignore the torque due to the gravitational force. As a consequence, total angular momentum $\boldsymbol{L}$ should be conserved at asymptotically high energies. The expression (13.15) for $\boldsymbol{L} = \boldsymbol{L}_1 + \boldsymbol{L}_2 = L_z\hat{z}$ may also be obtained using Noether's theorem of Sect. 3.10. The Lagrangian (13.13) upon ignoring gravity

$$L_{g=0} = T = (1/2)ml^2[2\dot{\theta}_1^2 + \dot{\theta}_2^2 + 2\cos(\theta_1 - \theta_2)\dot{\theta}_1\dot{\theta}_2] \qquad (15.44)$$

is invariant under (infinitesimal) rotations of the pendulum as a whole: $\theta_{1,2} \to \theta_{1,2} + \delta\phi$. Noether's theorem then guarantees the conservation of

$$p_1\,\delta\theta_1 + p_2\,\delta\theta_2 = \delta\phi\, ml^2[2\dot{\theta}_1 + c_{12}\dot{\theta}_2] + \delta\phi\, ml^2[\dot{\theta}_2 + c_{12}\dot{\theta}_1]. \qquad (15.45)$$

Since $\delta\phi$ is arbitrary, we omit it to get an expression for the conserved angular momentum

$$L_z = ml^2\left[(2 + c_{12})\dot{\theta}_1 + (1 + c_{12})\dot{\theta}_2\right] = p_1 + p_2. \qquad (15.46)$$

Numerical solutions show that L_z fluctuates around a mean value. As the energy increases, the fluctuations in L_z get smaller. In the limit of infinite energy, L_z is exactly conserved, just as for the simple pendulum (see Fig. 7.2b). Thus, at asymptotically high energies, we have two independent Poisson commuting conserved quantities (L_z and H) on a 4d phase space and should expect the dynamics to become regular (in fact, Liouville integrable, see Sect. 11.7*). In other words, the double pendulum should display order-chaos-order behavior as the energy is increased from 0 to ∞.

---

[49] Though chaotic trajectories occupy a smaller fraction of the phase space at high energies, they can still be very sensitive to ICs. In fact, as Fig. 15.17b shows, the largest finite-time Lyapunov exponent for chaotic trajectories at $E = 50$ or 100 are more than in the phase of global chaos (typified by $E = 4$) in units where $m = g = l = 1$.

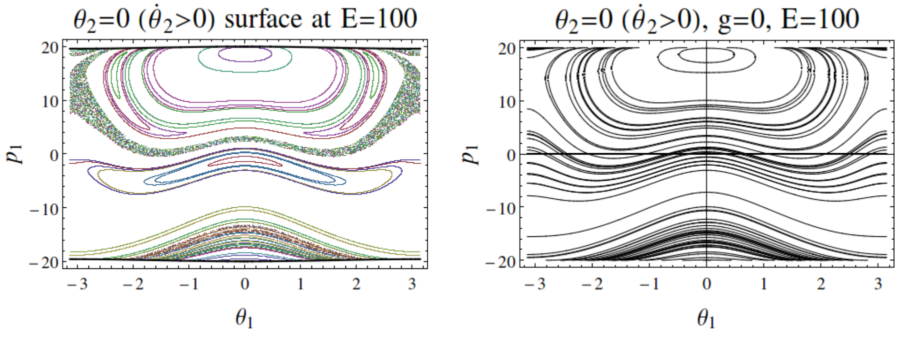

(a) (b)

Figure 15.18: Comparison of (a) Poincaré sections on $\theta_2 = 0$ plane (with $\dot\theta_2 > 0$ and parametrized by θ_1 and p_1) at high energy ($E = 100$ for $m = l = g = 1$) with (b) level curves of energy on the same surface in the zero gravity ($g = 0$) double pendulum. If the condition[50] $\dot\theta_2 > 0$ were not imposed, the curves would intersect each other and the figure would not be clear. The Poincaré surface is restricted to the energetically allowed Hill region. The various Poincaré sections in (a) correspond to 60 initial values of (approximately conserved) angular momentum $|L_z| < 31$ while the curves in (b) correspond to the same (conserved) L_z values. We see that the $g = 0$ model captures the gross features and shapes of Poincaré sections at this high energy, though it does not include the chaotic trajectories that survive at this energy. Note that the Hill boundary is not a limiting trajectory for $g = 0$.

In fact, we may use the conservation of H and $L_z = p_1 + p_2$ at high energies to infer the shapes of Poincaré plots. For instance, on the $\theta_2 = 0$ surface at a fixed energy E, $p_2 = L_z - p_1$ can be eliminated and p_1 and θ_1 must satisfy the relation

$$\begin{aligned} 2ml^2E(1+s_1^2) &= p_1^2 + 2(L_z - p_1)^2 - 2c_1p_1(L_z-p_1) \quad \text{or} \\ (3+2c_1)p_1^2 - 2L_z(2+c_1)p_1 &+ 2\left(L_z^2 - ml^2E(1+s_1^2)\right) = 0, \end{aligned} \tag{15.47}$$

where $c_1 = \cos\theta_1$ and $s_1 = \sin\theta_1$. The corresponding curve on the $\theta_1 = 0$ surface (cylinder parametrized by θ_2 and p_2) is determined by the relation

$$2ml^2E(1+s_2^2) = (L_z - p_2)^2 + 2p_2^2 - 2c_2p_2(L_z - p_2). \tag{15.48}$$

These relations (for large E and L_z) define closed curves on the $\theta_2 = 0$ and $\theta_1 = 0$ surfaces along which points of the Poincaré return map may be expected to be concentrated. Numerically obtained Poincaré sections at relatively high energies shown in Fig. 15.18 are seen to follow many of these curves.

---

[50] In Fig. 15.18a, $\dot\theta_2 > 0$ means we record only those instants where the lower bob passes counterclockwise through the downward vertical. In Fig. 15.18b, with $g = 0$, this condition is imposed using Hamilton's equation $\dot\theta_2 = \frac{\partial H}{\partial p_2}$. Along a level curve of L_z with $E = 100$ and $\theta_2 = 0$ on the θ_1-p_1 plane, $\frac{\partial H}{\partial p_2} = (2p_2 - c_1p_1)/[ml^2(1+s_1^2)]$ (13.18) varies. We retain the portion where $\frac{\partial H}{\partial p_2} > 0$. This corresponds to $2p_2 > c_1p_1$, or eliminating $p_2 = L_z - p_1$, the condition $p_1(1 + c_1/2) < L_z$. For given L_z, we restrict the curve to points (θ_1, p_1) that satisfy this condition.

15.4.3* Understanding the zero gravity double pendulum

At high energies, the dynamics of the double pendulum approaches that of the zero gravity ($g = 0$) double pendulum. The latter is an interesting system in its own right. Crucially, unlike the simple pendulum where turning off gravity reduces it to a free particle moving on a circle with Hamiltonian $H = p_\theta^2/2ml^2$, the zero gravity double pendulum is nontrivial since the two bobs are nonlinearly coupled even when $g = 0$:

$$H = [2ml^2(1+s_{12}^2)]^{-1}\left[p_1^2 + 2p_2^2 - 2c_{12}p_1p_2\right]. \tag{15.49}$$

Nevertheless, as we remarked in Sect. 15.4.2*, the zero gravity limit of the double pendulum should be somewhat simpler due to the presence of two Poisson commuting conserved quantities. In fact, we may use the conservation of $L_z = p_1 + p_2$ and H to 'decouple' the relative motion from the mean motion and reduce the EOM to quadratures. Though the resulting integrals are not elementary (they are hyperelliptic), we will express the relative motion in terms of a vector field on the circle. The techniques of Chapters 5 and 6 will then help us classify all possible qualitative motions of the zero gravity double pendulum.

From (13.18) and (13.20), the equations of motion for $g = 0$ are

$$\begin{aligned}\dot\theta_1 &= \frac{p_1 - c_{12}p_2}{ml^2(1+s_{12}^2)}, \quad \dot\theta_2 = \frac{2p_2 - c_{12}p_1}{ml^2(1+s_{12}^2)} \quad \text{and} \\ \dot p_1 &= -\dot p_2 = f = \frac{s_{12}}{ml^2(1+s_{12}^2)^2}\left[c_{12}(p_1^2+2p_2^2) - \left(2+c_{12}^2\right)p_1p_2\right]. \end{aligned} \tag{15.50}$$

Due to rotation invariance, only the relative angle $\theta = \theta_1 - \theta_2$ appears in H (15.49) and on the RHS of the EOM (15.50). It is then natural to introduce the center of mass (or mean) and relative coordinates and momenta

$$\Theta = \frac{1}{2}(\theta_1+\theta_2), \quad L_z = p_1 + p_2 \quad \text{and} \quad \theta = \theta_1 - \theta_2, \quad p = (p_1 - p_2)/2. \tag{15.51}$$

Conversely, $p_{1,2} = (1/2)L_z \pm p$ and $\theta_{1,2} = \Theta \pm \theta/2$. The factors of 2 have been chosen to make this a canonical transformation:

$$\{\theta, p\} = \{\Theta, L_z\} = 1 \quad \text{and} \quad \{\theta, L_z\} = \{\Theta, p\} = \{\Theta, \theta\} = \{L_z, p\} = 0. \tag{15.52}$$

For brevity, we will use the symbols $s = \sin\theta$ and $c = \cos\theta$. The Hamiltonian is independent of the CM angle Θ:

$$H(\cancel{\Theta}, L_z, \theta, p) = \frac{(2c+3)p^2 - L_z p - (2c-3)L_z^2/4}{2ml^2(1+s^2)}. \tag{15.53}$$

This ensures that the conjugate momentum L_z is conserved. The relative motion decouples from the CM motion:

$$\dot\theta = \frac{(2c+3)p - L_z/2}{ml^2(1+s^2)} \quad \text{and} \quad \dot p = \frac{(c+1)(c+2)p^2 - L_z cp - L_z^2(c-1)(c-2)/4}{ml^2(1+s^2)^2/s}. \tag{15.54}$$

Once these equations for θ and p have been solved for any given L_z, the mean motion may be determined by integrating Hamilton's equation for the CM angle:

$$\dot{\Theta} = -\frac{2p + (2c-3)L_z}{4ml^2(1+s^2)}. \tag{15.55}$$

By transforming to CM and relative variables[51], we have reduced the coupled system (15.50) to what may be called a triangular system by analogy with Gaussian elimination [121] for systems of linear equations.

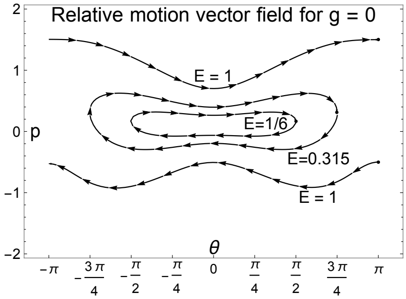

Figure 15.19: Phase portrait for $L_z = 1$ on the θ-p phase cylinder of the vector field (15.54) governing relative motion of the zero gravity double pendulum. Librational and rotational trajectories corresponding to a few values of E (in units of $L_z^2/2ml^2$ for $m = l = 1$) are displayed. They correspond to the lower bob oscillating about or going round the upper bob. For more on the possible types of qualitative motion, see Fig. 15.20.

We now focus on the relative motion governed by (15.54) and (15.53), which is described by a conservative system with just one degree of freedom on a cylindrical θ-p phase space. The equations (15.54) are still highly nonlinear. We plot a numerically obtained phase portrait of the associated vector field $(\dot{\theta}, \dot{p}) = (v^\theta(\theta, p), v^p(\theta, p))$ in Fig. 15.19, which indicates the possibility of both librational and rotational motion. To understand these and other possibilities and when they can occur, we notice that despite the nonlinearities, we may use the conservation of H to eliminate

$$p_\pm = \frac{L_z/2 \pm \sqrt{(1+s^2)(2ml^2E(2c+3) - L_z^2)}}{(2c+3)} \tag{15.56}$$

and obtain a self-contained first order ODE for θ:

$$\dot{\theta} = v(\theta) = \pm\frac{1}{ml^2}\sqrt{\frac{2ml^2E(2c+3) - L_z^2}{1+s^2}}. \tag{15.57}$$

The two signs correspond to increasing and decreasing relative angle θ. For instance, when θ reaches a turning point (a zero of $v(\theta)$) in finite time, the sign of $\dot{\theta}$ must be reversed, just as with a particle oscillating in a harmonic trapping potential. Using

---

[51] These are not angle-action variables of Chap. 11, as H depends on θ so that p is not conserved. Moreover, $\dot{\Theta}$ is in general not constant in time.

$\dot{c} = -s\dot{\theta}$ we write this in algebraic form,

$$ml^2\dot{c} = \mp\frac{\sqrt{(1-c^2)(2-c^2)(2ml^2E(2c+3)-L_z^2)}}{2-c^2}. \tag{15.58}$$

This leads to a hyperelliptic abelian integral since the integrand is a rational expression in c and the square root of an irreducible quintic polynomial in c. Thus, we have reduced the zero gravity limit to three quadratures (for θ followed by p and then Θ).

Action variable for relative motion. As noted in Footnote 51, Θ, θ, L_z, p are not angle-action variables. However, for fixed L_z, $H(L_z, \theta, p)$ (15.53) describes a system with 1 degree of freedom. From the Hamilton-Jacobi theory of Sect. 11.4, an action variable for the relative motion is $I = \frac{1}{2\pi}\oint p\, d\theta$, with p given by (15.56). For example, if $\pm\theta_*$ are the turning points for libration[52], then since $p_+ - p_-$ is an even function,

$$2\pi I = \int_{-\theta_*}^{\theta_*} p_+(\theta)\, d\theta + \int_{\theta_*}^{-\theta_*} p_-(\theta)\, d\theta = 2\int_0^{\theta_*} [p_+ - p_-]\, d\theta. \tag{15.59}$$

Changing variables to $c = \cos\theta$, one obtains a complete hyperelliptic integral:

$$\frac{1}{2}\pi I = \int_{\cos\theta_*}^{1} \frac{\sqrt{(1-c^2)(2-c^2)(2ml^2E(2c+3)-L_z^2)}}{(2c+3)(1-c^2)}\, dc. \tag{15.60}$$

The corresponding generating function W and angle variable may be obtained by the procedure outlined in Sect. 11.4. ☐

Qualitative description of motion. Even without evaluating these integrals, we may gain qualitative insight into the dynamics of θ by examining the vector field[53] $\dot{\theta} = v(\theta)$ defined by (15.57). In fact, this is a family of vector fields on a circle (or an arc of a circle parametrized by θ) depending on the two control parameters $L_z \in \mathbb{R}$ and $E \geq 0$. Depending on their values, the upper half of the L_z-E parameter plane[54] may be divided into the following regions and their boundaries (see Fig. 15.20), where qualitatively distinct physical behavior is manifested. Each of these types of motion is a possible manner of oscillation of a double pendulum at asymptotically high energies.

1. *Forbidden region:* When $10ml^2E < L_z^2$ the quantity under the square-root in (15.57) is negative for all θ and no dynamics is possible (see Prob. 15.33). In other words, the bobs must have a minimal energy for them to possess a given L_z.
2. *Libration:* If $L_z^2/10ml^2 < E < L_z^2/2ml^2$, corresponding to the region between the parabolas in Fig. 15.20, $v(\theta)$ has two zeros at $\pm\theta_*$ where

$$\cos\theta_* = L_z^2/4ml^2E - 3/2 \quad \text{and} \quad \pi > \theta_* > 0. \tag{15.61}$$

---

[52] In the rotational phase, we get $2\pi I_\pm = \int_{-\pi}^{\pi} p_\pm d\theta$ with signs chosen according to the direction of rotational motion.

[53] See Sect. 5.2* for background on vector fields on the line and circle. New features arise here since $v(\theta)$ is double-valued (due to the ± signs) and since $v'(\theta)$ can become unbounded.

[54] Compare with the trace-determinant classification of linear vector fields on the plane discussed in Sect. 6.6*.

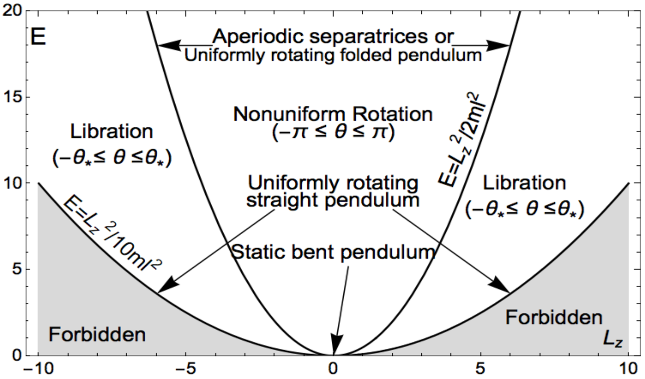

Figure 15.20: Upper half L_z-E parameter plane for the zero gravity double pendulum showing distinct types of motion governed by the vector field $v(\theta)$ of (15.57) for $m = l = 1$.

The relative angle θ is restricted to the interval $|\theta| \le \theta_* < \pi$. Depending on the sign of v in (15.57), the flow is either towards θ_* or towards $-\theta_*$. What is more, one checks that $|v'(\theta_*)|$ diverges as a power law. In fact for $v > 0$, the difference quotient is given by

$$\frac{\pm v(\pm\theta_*) \mp v(\pm\theta_* \mp \epsilon)}{\epsilon} \sim \mp\sqrt{\frac{4E\sin\theta_*}{ml^2(1+\sin^2\theta_*)\epsilon}} \quad \text{as} \quad \epsilon = |\theta_* - \theta| \to 0^+, \tag{15.62}$$

where one choses either the upper or lower signs. The signs on the RHS are reversed for $v < 0$. So for $v > 0$, the fixed point θ_* is reached within a finite time. In fact, the limiting time taken for θ to go from $-\theta_*$ to θ_* is given by a complete hyperelliptic integral:

$$\text{Time}(-\theta_* \to \theta_*) = \int_{-\theta_*}^{\theta_*} \frac{d\theta}{|v(\theta)|} \equiv \frac{T(\theta_*)}{2}. \tag{15.63}$$

Though θ_* is reached in finite time, θ prefers not to stay there. Indeed, for $v < 0$, the fixed point θ_* is infinitely unstable, so we expect[55] that once θ reaches θ_*, $\dot\theta$ and v will switch sign and reverse the motion. Thus, this is a 'librational' regime, with relative angle θ oscillating periodically between $\pm\theta_*$ with period $T(\theta_*)$. In other words, *the* 2^{nd} *bob oscillates about the first one without going round it.* Between the parabolas, we also have the constant fixed point solutions $\theta = \pm\theta_*$, which however are unstable for the reasons mentioned.

3. *Bobs move steadily in unison as a long straight pendulum:* This possibility occurs on the boundary between the forbidden and libration regions. On the two arcs of

---

[55] The phase portrait (Fig. 15.19) of the 2d vector field $v(\theta, p)$ (15.54) governing relative motion on the cylindrical θ-p phase space illustrates that trajectories in this regime are contractible closed curves corresponding to periodic librational motion. Observe that though $\dot\theta = 0$ at $\theta = \pm\theta_*$, $\dot p$ calculated using (15.56) is nonzero when this happens, forcing the trajectory to continue, unlike at the fixed points of the sliding friction vector field of Prob. 5.5.

the parabola $10ml^2E = L_z^2$ with $L_z \neq 0$, the range of librational angles shrinks, and the two zeros of $v(\theta)$ coalesce: $\pm\theta_* \to 0$. Thus, the only possibility is for the relative angle $\theta = \theta_1 - \theta_2$ to vanish at all times. This means the two bobs move in unison with the two rods stretched out straight. Here $p = L_z/10$ and $\dot{\Theta} = L_z/5ml^2$ are both constants. Thus $\Theta = \theta_1 = \theta_2$ are all linear in time and the long pendulum rotates uniformly.

4. *Rotation:* If $2ml^2E > L_z^2$ [corresponding to the region above the upper parabola in Fig. 15.20], the quantity under the square-root in (15.57) is strictly positive and $v(\theta)$ is defined on the whole circle and has no zeros. Depending on ICs, the relative angle $\theta = \theta_1 - \theta_2$ is either monotonically increasing or monotonically decreasing. If we regard θ_1 and θ_2 as the angular positions of two runners on a circular racetrack, then one of them keeps 'lapping' the other.

5. *Aperiodic separatrices or folded pendulum:* On the two arcs of the upper parabola $E = L_z^2/2ml^2$ with $L_z \neq 0$, the zeros of v merge at $\theta_* = \pm\pi$. When approached from the librational regime, the time period of $\theta(t)$ diverges since $|v'(\pm\pi)| = \sqrt{2E/ml^2}$ is finite and the relative angle $\theta = \theta_1 - \theta_2$ takes infinitely long to go between $-\pi$ and π, resulting in an aperiodic separatrix. For these values of L_z and E we also have the possibility of $\theta \equiv \theta_* = \pm\pi$, i.e., a permanently folded double pendulum. In this case, $p = L_z/2 = \pm\sqrt{ml^2E/2}$ and $\dot{\Theta} = L_z/ml^2 = \pm\sqrt{2E/ml^2}$ are both constant. Thus, the folded pendulum rotates uniformly (either clockwise or counterclockwise) and there is no energy exchanged between the bobs.

6. *Static bent pendulum:* Finally, when $E = L_z = 0$, $v(\theta)$ is identically zero and every point on the circle is a fixed point. In this case, any initial angle θ is maintained unchanged for all time. What is more, $p \equiv 0$ and $\dot{\Theta} \equiv 0$ so that θ_1 and θ_2 take arbitrary fixed values. Physically, these are static solutions of (15.50) where the double pendulum looks like a bent rod that does not rotate ($p_1 = p_2 = 0$). A bent pendulum is a static solution: there is no gravity to straighten it or make it fall!

This completes our enumeration of the possible qualitative motions of a double pendulum in the absence of gravity (or at asymptotically high energies). Some of these possibilities for relative motion are illustrated in Fig. 15.19.

15.5* Chaos in Lorenz's model for convection

The Lorenz equations $\dot{\boldsymbol{r}} = \boldsymbol{v}(\boldsymbol{r})$ are three 1st order ODEs for $\boldsymbol{r} = (x, y, z)$:

$$\dot{x} = \sigma(y - x), \quad \dot{y} = \rho x - y - xz \quad \text{and} \quad \dot{z} = xy - \beta z. \tag{15.64}$$

The Lorenz model has a 3d phase space unlike the 4d phase space of the double pendulum. However, unlike the latter, it is not Hamiltonian nor even conservative. In fact, it may be regarded as a simplified description of a driven dissipative system.

The Lorenz equations were introduced in 1963 by Edward Norton Lorenz [88] as a truncated model for atmospheric Rayleigh-Bénard convection cells in a shallow two-dimensional fluid layer warmed from below and cooled from above [39]. He viewed it as a 'toy' system to study the weather and obtained it by reducing a larger system of 12 ODEs used in studying convection. The modes x and y are measures of the velocity and temperature convection rates in the convective roll patterns while z is proportional to the vertical convective heat transfer. The three *positive* parameters ρ, σ and β are constants proportional to the Rayleigh number, Prandtl number[56] and a geometric aspect ratio. Of the three, ρ is the main control parameter while σ and β may be taken fixed under typical conditions. The Rayleigh number Ra is a dimensionless parameter associated to convection in buoyancy driven flows as in a layer of fluid that is heated from below. While gravity tries to keep the heavy fluid down, the heating from below drives it upwards. Ra is the ratio of the time scale for diffusive/conductive heat transfer to that for convective heat transfer. It may be increased by increasing the temperature of the lower plate. If Ra is small, heat transfer is through conduction while it is convective for larger Ra. The flow goes from regular (laminar) to irregular (turbulent) with increasing Ra. Thus, we should expect the Lorenz system to display a transition from regular to chaotic behavior as $\rho \propto$ Ra is increased. In Lorenz's original work, he took $\rho = 28, \sigma = 10$ and $\beta = 8/3$ and found the system to behave chaotically. In addition to convection, the Lorenz equations can also be used to model (geo)dynamos, lasers and water wheels [122].

We will view (15.64) as defining a vector field for a dynamical system whose phase space is $\mathbb{R}^3$. We will soon see that the Lorenz system is not conservative and is not translation or rotation invariant. So concepts like energy, momentum and Poisson brackets are not directly helpful in analyzing it. However, (15.64) possesses a discrete symmetry. In the x, y, z variables, the Lorenz equations are quadratically nonlinear and invariant under the reflection symmetry $(x, y, z) \to (-x, -y, z)$ which we may think of as relating clockwise to counterclockwise motion in convection cells.

If we ignore all interaction terms, then the resulting linear system

$$\dot{x} = -\sigma x, \quad \dot{y} = -y \quad \text{and} \quad \dot{z} = -\beta z \tag{15.65}$$

is dissipative and would imply that x, y and z each decays monotonically and exponentially to zero. The full system is of course much richer. We will study some basic properties of (15.64) using the tools from Chapters 5, 6, 14 and elsewhere.

Fixed points. For $\rho \leq 1$ the trivial fixed point $x_* = y_* = z_* = 0$ is the only one, while for $\rho > 1$ two additional nontrivial fixed points emerge. In fact, the conditions for the Lorenz vector field to vanish are

$$\dot{x} = 0 \;\Rightarrow\; x = y, \quad \dot{y} = 0 \;\Rightarrow\; x(\rho - 1 - z) = 0 \quad \text{and} \quad \dot{z} = 0 \;\Rightarrow\; x^2 = \beta z. \tag{15.66}$$

The second equation implies either $x = 0$ or $z = \rho - 1$. If $x = 0$, then $x_* = y_* = z_* = 0$ is the only possibility. If $z = \rho - 1$ then $x^2 = \beta(\rho - 1)$, which has nontrivial real solutions only if $\rho > 1$. Thus, for $\rho \leq 1$, $\boldsymbol{r}_* = 0$ is the only fixed point. What is more, for $\rho < 1$, we will soon use a Lyapunov function (see Sect. 5.4*) to show that $\boldsymbol{r}_* = 0$ is a *global attractor*, so that all trajectories eventually reach $\boldsymbol{r}_* = 0$ (see Fig. 15.21a). Thus, the dynamics is relatively benign for $\rho < 1$.

---

[56] The Prandtl number Pr is a ratio of kinematic viscosity (19.115) to thermal diffusivity (18.4). It measures the ratio of the rates of momentum and heat diffusion. For Pr $\ll 1$, heat diffuses faster than momentum, so heat transfer is via conduction rather than convection.

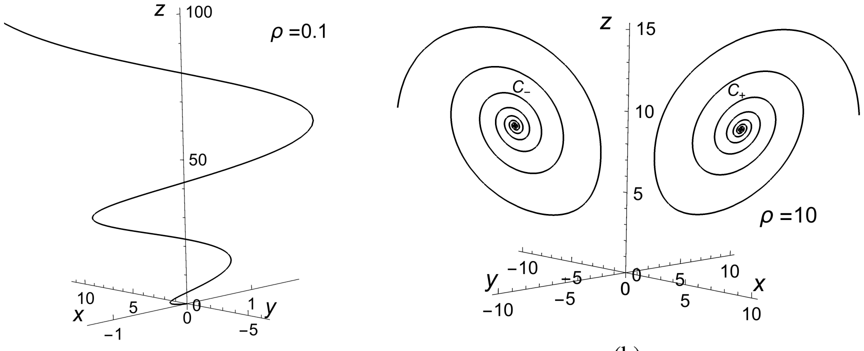

(a)

(b)

Figure 15.21: (a) Trajectory from (-1,10,100) approaches the global attractor at the origin for $\rho = 1/10$ (note axis scales). (b) Trajectories starting from $(\pm 10, \pm 10, 10)$ approaching the stable fixed points $C_\pm = (\pm 2\sqrt{6}, 2\sqrt{6}, 9)$ for $\rho = 10$. In all cases, $\sigma = 10$ and $\beta = 8/3$.

On the other hand, for $\rho > 1$ we have, in addition to the trivial fixed point, two nontrivial fixed points (see Fig. 15.21b)

$$C_\pm = (x_* = \pm\sqrt{\beta(\rho - 1)},\ y_* = x_*,\ z_* = \rho - 1). \tag{15.67}$$

Notice that $C_\pm$ merge with the trivial fixed point as $\rho \to 1^+$. The trivial fixed point at the origin corresponds to the absence of convection and no horizontal or vertical temperature variation. The nontrivial fixed points $C_\pm$ correspond to steady clockwise or counterclockwise convection, which explains the symbol C. As we might expect, the system displays a supercritical pitchfork bifurcation (see Sect. 14.1.3.1*) at $\rho = 1$, which is associated with the spontaneous breaking of the above discrete symmetry. It is supercritical since $C_\pm$ are stable for $\rho \gtrsim 1$.

Stability of trivial fixed point. To examine linear stability of fixed points, we consider the Jacobian matrix:

$$J = \left(\frac{\partial v^i}{\partial x^j}\right)_{\boldsymbol{r}_*} = \begin{pmatrix} -\sigma & \sigma & 0 \\ \rho - z_* & -1 & -x_* \\ y_* & x_* & -\beta \end{pmatrix}. \tag{15.68}$$

At the trivial fixed point, $J(\boldsymbol{r}_* = 0) = \begin{pmatrix} -\sigma & \sigma & 0 \\ \rho & -1 & 0 \\ 0 & 0 & -\beta \end{pmatrix}$, and the linearized flow in the z direction decouples and is stable. The restriction of J to the x-y plane is a 2×2 matrix with trace $\tau = -(1 + \sigma) < 0$ and determinant $\Delta = \sigma(1 - \rho)$ (see Sect. 6.6*). Moreover, the discriminant is positive:

$$D = \tau^2 - 4\Delta = \sigma^2 + 2\sigma + 1 - 4\sigma + 4\rho\sigma = (\sigma - 1)^2 + 4\rho\sigma. \tag{15.69}$$

Thus, if $0 < \rho < 1$, $\Delta > 0$ and the origin is a stable node while if $\rho > 1$, it becomes a saddle point since $\Delta < 0$. This may also be seen from the characteristic equation $(\lambda + \beta)(\lambda^2 + (\sigma + 1)\lambda + \sigma(1 - \rho)) = 0$ whose roots are

$$\lambda_\pm = (1/2)(\tau \pm \sqrt{D}) \quad \text{and} \quad \lambda_3 = -\beta. \tag{15.70}$$

Contraction of volumes. The divergence of the vector field $\boldsymbol{v}$ controls how infinitesimal volumes in the x-y-z phase space change with time (see Sect. 19.5). If $(\delta V)(\boldsymbol{r})$ is the volume of an infinitesimal region located at $\boldsymbol{r}$,

$$\frac{1}{\delta V}\frac{d}{dt}(\delta V)(\boldsymbol{r}) = (\boldsymbol{\nabla}\cdot\boldsymbol{v})(\boldsymbol{r}) = \operatorname{tr} J = -(\sigma+1+\beta). \tag{15.71}$$

Since $\boldsymbol{\nabla}\cdot\boldsymbol{v}$ is strictly negative and independent of location, little volumes located anywhere in phase space will shrink exponentially in time for any positive σ and β. The system is dissipative in this sense. Thus, any 3d space of initial conditions will eventually shrink (be attracted) to a set of zero volume. This attractor could be one or more fixed points or a limit cycle or invariant surface or some less familiar invariant set of points with zero volume. We will see that the Lorenz system does not admit any invariant surfaces that enclose a finite volume, but that the other possibilities do occur for various values of ρ.

Origin is a global attractor when $\rho < 1$. Consider the nonnegative function

$$\phi = (1/2)\left(x^2/\sigma + y^2 + z^2\right). \tag{15.72}$$

We will show that for $\rho < 1$, ϕ is a Lyapunov function (see Sect. 5.4*) for (15.64). It is clear that ϕ vanishes only at the trivial fixed point $\boldsymbol{r}_* = 0$ and has concentric ellipsoids as its level surfaces. It remains to show that ϕ is monotonically decreasing along the flow, so that every trajectory must approach $\boldsymbol{r} = 0$ as $t \to \infty$. In fact,

$$\begin{aligned}\dot{\phi} &= x\dot{x}/\sigma + y\dot{y} + z\dot{z} = (xy - x^2) + (\rho xy - y^2 - \cancel{xyz}) + (\cancel{xyz} - \beta z^2)\\ &= -(x^2 - (\rho+1)xy + y^2 + \beta z^2)\\ &= -\left[(x - ((\rho+1)/2)\,y)^2 + [1 - ((\rho+1)/2)^2]y^2 + \beta z^2\right], \end{aligned}\tag{15.73}$$

where we have completed a square. Now for $\rho < 1$, $\rho+1 < 2$ so that $((\rho+1)/2)^2 < 1$, Thus, for $\beta > 0$ and $\rho < 1$, $\dot{\phi} < 0$. What is more, when $\rho < 1$ we observe that for $\dot{\phi}$ to vanish, each of the three terms in (15.73) must vanish. This happens only if $x = y = z = 0$, so that ϕ is strictly decreasing along the flow away from the origin. Thus, for $\rho < 1$, any trajectory that begins away from $\boldsymbol{r} = 0$ must approach the trivial fixed point as $t \to \infty$. This implies that for $\rho < 1$, there cannot be any limit cycles, nontrivial invariant manifolds or chaos. What is the nature of the dynamics for $\rho > 1$?

Stability of nontrivial fixed points $C_\pm$. The nontrivial fixed points $C_\pm$ (which exist only for $\rho > 1$) can be stable or unstable depending on the values of ρ, σ and β. For the values chosen by Lorenz ($\rho = 28, \sigma = 10$ and $\beta = 8/3$), they are unstable: two of the eigenvalues of J have positive real parts: $\lambda_3 \approx -13.9, \lambda_\pm \approx 0.09 \pm 10.2i$. On the other hand, holding σ, β fixed, for a smaller ρ (e.g., $\rho = 18$) they are stable $\lambda_3 \approx -13.21, \lambda_\pm = -.23 \pm 8.3i$. So we might suspect a change in stability of $C_\pm$ at a critical value ρ_H (named since it turns out to be a Hopf bifurcation) at which $\lambda_\pm$ cross the imaginary axis. To find where this occurs, we note that the Jacobians at $C_\pm$,

$$J(C_\pm) = \begin{pmatrix} -\sigma & \sigma & 0 \\ 1 & -1 & \mp\sqrt{\beta(\rho-1)} \\ \pm\sqrt{\beta(\rho-1)} & \pm\sqrt{\beta(\rho-1)} & -\beta \end{pmatrix} \tag{15.74}$$

have the characteristic polynomial

$$\lambda^3 + (1+\beta+\sigma)\lambda^2 + \beta(\rho+\sigma)\lambda + 2\beta\sigma(\rho-1). \tag{15.75}$$

On the other hand, at the transition, the eigenvalues must be of the form $\lambda = \pm i\omega$ and λ_3 for $\omega, \lambda_3 \in \mathbb{R}$ leading to the characteristic polynomial

$$(\lambda - i\omega)(\lambda + i\omega)(\lambda - \lambda_3) = \lambda^3 - \lambda_3\lambda^2 + \omega^2\lambda - \omega^2\lambda_3. \tag{15.76}$$

Comparing, $\lambda_3 = -(1+\beta+\sigma)$ [corresponding to a stable direction], $\omega^2 = \beta(\rho_H + \sigma)$ and $\omega^2\lambda_3 = -2\beta\sigma(\rho_H - 1)$. The latter 2 equations admit only one solution

$$\rho_H = \sigma(\sigma+\beta+3)/(\sigma-\beta-1). \tag{15.77}$$

Here we assume $\sigma > \beta + 1$ so that $\rho_H > 0$ [when $\rho > 1$ and $\sigma < \beta + 1$, the nontrivial fixed points $C_\pm$ are unstable]. For Lorenz's values, the inequality is satisfied and $\rho_H = 470/19 \approx 24.7368$, which lies between $\rho = 18$ and $\rho = 28$ we considered above. Thus, $C_\pm$ are linearly stable provided $1 < \rho < \rho_H$.

Subcritical Hopf bifurcation. As $\rho \to \rho_H$ from below, one can show (see [99, 122]), that the stable fixed points $C_\pm$ undergo a subcritical Hopf bifurcation (see Sect. 14.2.2*). This means unstable limit cycles shrink to $C_\pm$ as $\rho \to \rho_H^-$ and render the nontrivial fixed points unstable for $\rho > \rho_H$. So for $\rho > \rho_H$, generic trajectories cannot approach $C_\pm$ nor the trivial fixed point and do not have the above limit cycles to tend to either. What can trajectories do? Can they approach limit cycles? Lorenz argued (using a discrete-time 'Lorenz map') that any limit cycles would have to be unstable. Can they approach some invariant surface, such as a torus (and become quasiperiodic)?

No invariant surfaces enclosing finite (nonzero) volume in Lorenz system. We may argue that the Lorenz system cannot have any invariant surfaces that enclose a finite volume (e.g., a closed and bounded surface such as a sphere or a torus or a Riemann surface of higher genus). Indeed, suppose there is such an invariant surface Σ, then the 3d region Ω inside Σ must also be invariant under the flow. In particular, the volume of Ω must be conserved in time. However, this contradicts the previously established (15.71) exponential decrease in volume of any region of the phase space.

Trajectories cannot escape to infinity. Can trajectories fly off to infinity? This too is not possible, as can be shown by finding a trapping surface. For example, consider the ellipsoids E_K defined by the level surfaces $F = K$ of the function

$$F(x,y,z) = \rho x^2 + \sigma y^2 + \sigma(z-2\rho)^2. \tag{15.78}$$

We will show that if K is chosen sufficiently large, then every trajectory that begins on E_K remains inside it. Given any initial condition, there will then be such a trapping surface containing it, establishing that trajectories cannot escape to infinity. To see this, we will show that the vector field points inwards on E_K for K big enough. Now, an outward normal on E_K and the Lorentz vector field are given by

$$\boldsymbol{\nabla} F = (2\rho x, 2\sigma y, 2\sigma(z-2\rho)) \quad \text{and} \quad \boldsymbol{v} = (\sigma(y-x), \rho x - y - xz, xy - \beta z). \tag{15.79}$$

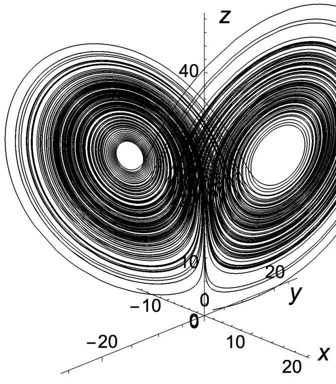

Aperiodic bounded trajectory (ρ=28)

Figure 15.22: A 'chaotic' trajectory starting from (1,1,1) in the Lorenz model for $\rho = 28, \sigma = 10$ and $\beta = 8/3$. The trajectory 'goes round' the 'left lobe' a few times before switching to the right lobe. The lobes are located around the unstable fixed points $C_\pm$. This winding and switching continues indefinitely with no apparent regularity.

For $\boldsymbol{v}$ to point inwards on E_K we need $\boldsymbol{v} \cdot \boldsymbol{\nabla} F < 0$. Now,

$$\begin{aligned} \boldsymbol{v} \cdot \boldsymbol{\nabla} F &= 2\sigma \left[\cancel{\rho x y} - \rho x^2 + \cancel{\rho x y} - y^2 - \cancel{xyz} + \cancel{xyz} - \cancel{2\rho x y} - \beta z^2 + 2\rho\beta z\right] \\ &= -2\sigma \left[\rho x^2 + y^2 + \beta(z-\rho)^2 - \beta\rho^2\right]. \end{aligned} \tag{15.80}$$

For this to be negative we need

$$\rho x^2 + y^2 + \beta(z-\rho)^2 > \beta\rho^2. \tag{15.81}$$

Here, β and ρ are fixed. This condition says that (x, y, z) must lie outside a certain ellipsoid. Though they have different centers and semiaxes, by choosing K sufficiently big, we may ensure E_K lies outside this ellipsoid, thereby ensuring the condition is satisfied. Thus, we have our trapping ellipsoids guaranteeing that trajectories cannot escape to infinity.

As a consequence, for $\rho > \rho_H$, trajectories are confined to a large ellipsoid in phase space but are generically not attracted to any fixed point, limit cycle or invariant surface enclosing a nonzero volume. This nonperiodic and non-quasiperiodic bounded motion may be shown via Lyapunov exponents, introduced in Sect. 15.2*, to display extreme sensitivity to initial conditions, with the associated difficulty in making reliable long-term predictions. Fig. 15.23 shows that the largest Lyapunov exponent is positive for $\rho > \rho_H$ and roughly increases with ρ. The dynamics is said to be chaotic. Due to the shrinking of phase space volume, trajectories must approach an attractor of zero volume, it is called a strange attractor and is a fractal set. A typical trajectory for Lorenz's values of parameters is displayed in Fig. 15.22. For more on the Lorenz attractor and chaos in the Lorenz system, see [99, 122].

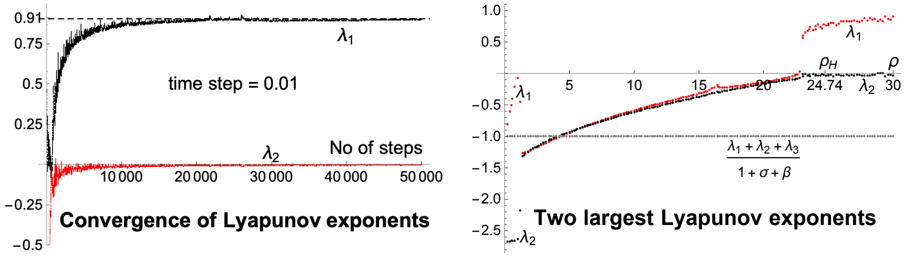

(a) (b)

Figure 15.23: (a) For $\rho = 28$, convergence of largest Lyapunov exponent λ_1 ($\to 0.9$ roughly as the reciprocal of N) and λ_2 ($\to 0.0$) as the number N of time steps [of size $\tau = 0.01$] is increased up to 50,000 starting from $(x = 1, y = 2, z = 3)$. The asymptotic value $\lambda_1 \approx 0.9$ was verified to be independent of ICs [IC (1,2,3) and (1,1,1) give $\lambda_1 = 0.908, 0.903$] and small changes in τ. (b) Two largest finite-time Lyapunov exponents λ_1 (dots), λ_2 (diamonds) [for a trajectory starting from $(x = 1, y = 2, z = 3)$] versus ρ for $\sigma = 10$ and $\beta = 8/3$. The sum rule $\lambda_1+\lambda_2+\lambda_3 = \boldsymbol{\nabla}\cdot\boldsymbol{v} = -(\sigma+1+\beta) = -13\frac{2}{3}$, which is satisfied to high accuracy, determines λ_3. A transition from negative to positive λ_1 occurs a little before $\rho = \rho_H \approx 24.7$, where $C_\pm$ cease to be stable and significant instabilities set in, leading to chaos. There is a fluctuation around $\rho = 1$, where there is a supercritical pitchfork bifurcation. Moreover, $\lambda_1 \approx \lambda_2$ in between. We use $\tau = 0.1$ and $N = 1000$ in these calculations.

15.6 Problems

1. Consider the maps defined by **iterations** of the **monotonic** (and hence invertible) **functions** $f(x) = x^2$ and $g(x) = \sqrt{x}$ on the interval $[0, 1]$. Find the asymptotic behavior of all orbits and argue that their dynamics is not chaotic.

*2. **Stroboscopic sampling.** Explain how one may construct an invertible discrete-time dynamical system (map) on an n dimensional state space by sampling solutions to a system of n autonomous first order ODEs at equally spaced times.

3. Suppose x is a **fixed point of the** n^{th} **iterate** of the map f. Show that the orbit of x is periodic with a period p that divides n (i.e., n/p is an integer). Provide an example to show that the period p can be less than n.

4. **Stability of a fixed point.** Suppose x_* is a fixed point of the differentiable map $f(x)$, say from $\mathbb{R} \to \mathbb{R}$. Show that x_* is stable (asymptotically as $n \to \infty$) if $|f'(x_*)| < 1$ and unstable if $|f'(x_*)| > 1$. Proceed by estimating the magnitude of the difference between x_* and the iterates of a nearby point $x = x_*+\delta$: $|f(x)-x_*|$, $|f(f(x))-x_*|, \cdots, |f_n(x)-x_*|$ for $n = 1, 2, 3, \ldots$. Hint: Show that the derivative of f_n at a fixed point is the n^{th} power of $f'(x_*)$.

5. **Stability of a periodic orbit.** Suppose $\mathcal{O}_p = \{x_0, x_1 = f(x_0), \ldots, x_{p-1} = f(x_{p-2})\}$, with $f(x_{p-1}) = x_0$ is a period-p orbit for iterations of the map f of the real line. Define the 'stability coefficient' $\mu(\mathcal{O}_p) = f'(x_0)f'(x_1)\cdots f'(x_{p-1})$. Argue that $\mathcal{O}_p$ is stable to small perturbations if $|\mu| < 1$ and unstable if $|\mu| > 1$.

*6. **Pendulum to standard map.** Here we set up a finite difference approximation to Hamilton's equations for a simple pendulum [$\dot{\theta} = p_\theta/m\ell^2$ and $\dot{p}_\theta = -mg\ell\sin\theta$ (7.7)] that take the form of the standard map difference equations (15.5). Proceed by defining a sequence of times $t_n = n\delta$ for $n = 0, 1, 2, \ldots$ with a time step δ and let $\theta(t_n) \equiv \theta_n$, etc. Use a backward difference (see Sect. 17.2) discretization for the time derivative $[\dot{\theta}(t) \approx (\theta(t) - \theta(t-\delta))/\delta]$ to show that Hamilton's equations upon rescaling $p_n = (\delta/m\ell^2)p_\theta(t_n)$ may be approximated by the Chirikov-Taylor difference equations with $\kappa = \omega^2\delta^2$ where $\omega^2 = g/\ell$. What are the dimensions of κ, p_n and θ_n? What sort of discretization scheme do you need for $\dot{p}$?

7. Find the **orbits of the standard map** (15.5) for $\kappa = 0$ and determine when they are periodic and when they are quasiperiodic, based on ICs.
8. Write the **standard map** $\theta_{n+1} = \theta_n + p_{n+1}$ and $p_{n+1} = p_n - \kappa \sin\theta_n$ (15.5) in the form $\xi_{n+1} = f(\xi_n)$ where $\xi_n = (\theta_n, p_n)^t$ is a column vector and f a self-map of the plane. Compute the Jacobian and show that f is **area-preserving**.
9. We view the **standard map** (15.5) as taking old angle and momentum to new ones:

$$\Theta = \theta + p - \kappa \sin\theta \quad \text{and} \quad P = p - \kappa \sin\theta. \tag{15.82}$$

Since it is area-preserving, it is reasonable to view it as a finite canonical transformation. Find a **generating function** of the first kind $F_1(\theta, \Theta)$ (10.81) that generates this transformation, i.e., with $p = \frac{\partial F_1}{\partial \theta}$ and $P = -\frac{\partial F_1}{\partial \Theta}$.

10. For $\kappa \neq 0$, show that there are only 2 **fixed points** for the **standard map** on the $[0, 2\pi] \times [0, 2\pi]$ square: $(\theta, p) = (0, 0)$ and $(\pm\pi, 0)$. What happens for $\kappa = 0$?
11. **Stability of fixed points of the standard map.** Calculate the eigenvalues of the Jacobian matrix of the standard map at the fixed points $(\theta = 0, p = 0)$ and $(\pm\pi, 0)$. Use these to comment on the stability of these fixed points as a function of κ. Find the corresponding eigenvectors and plot their directions (when they are real). Hint: If the magnitude of an eigenvalue exceeds one, it corresponds to an unstable direction. Recall our discussion of the stability of a periodic solution of a continuous-time system via repeated application of the monodromy matrix in Sect. 13.4.4*.

$*$12. Write a computer program to compute (and plot on phase space) the first 500 **iterates of the standard map** (15.5) for a random initial state (θ_0, p_0) with (a) $\kappa = 0.1$, (b) $\kappa = 0.5$, (c) $\kappa = 0.98$, (d) $\kappa = 1.5$, (e) $\kappa = 4.5$ and (f) $\kappa = 100$. Describe the resulting orbits. Keeping other quantities fixed, increase θ_0 by 1% and check whether the resulting orbit is significantly different.

$*$13. Use the **simple pendulum** to propose an 'energy' E_n for the **Chirikov-Taylor system**. It must reduce to the pendulum energy in the appropriate limit. Examine the behavior of E_n under iterations of the standard map for various values of κ. Is this energy constant, periodic, quasiperiodic or seemingly random?

$*$14. **Doubling modulo one.** A simple example of a discrete-time chaotic dynamical system, albeit without any control parameter, is the doubling map modulo 1 [25, 99, 106] on the unit interval [0,1]. Here, $f(x) = 2x$ modulo 1. This map is conveniently analyzed using the binary representation of x. If $x = b_1/2 + b_2/2^2 + \cdots + b_n/2^n$ with $b_i = 0$ or 1 is a number in the unit interval, then we write $x = 0.b_1 b_2 b_3 \cdots$. (a) Show that $f(x) = 0.b_2 b_3 b_4 \cdots$. This map is an example of a Bernoulli shift. (b) Show that $x = 0$ is the only fixed point. (c) Show that there is precisely one orbit of period two and find the points on it; express them in both binary and decimal fractional notation. Observe that they are fixed points of the second iterate $f(f(x)) = 2^2 x$ (mod 1). (d) Find all other periodic orbits. Hint. They are fixed points of the iterates $f_n(x) = 2^n x$ (mod 1). (e) Argue that any rational number $x \in [0,1]$ is attracted to one of these periodic orbits under iterations of this map. Hint: a rational number has an eventually repeating binary expansion. (f) Irrational numbers in the unit interval lie on chaotic orbits. Try to display the orbit of $\sqrt{2} - 1$. Since most numbers are irrational, the typical orbit is chaotic. Nevertheless, observe that this chaotic system has a (countably) infinite and dense collection of periodic orbits. This too is typical of globally chaotic systems. (g) Show that all these periodic orbits are unstable. The Bernoulli shift is sensitive to ICs. A change in b_{20} has a negligible effect of $\mathcal{O}(2^{-20})$ on the initial state, but after 19 time steps, it results in a change of $O(1)$.

$*$15. **Complex dynamics.** Examine the dynamics of the map of one complex variable $z \mapsto f_0(z) = z^2$ with particular attention to how it behaves on the unit circle $|z| = 1$. Experiment with iterations of $f_c(z) = z^2 + c$ where c is a fixed complex number. For fixed c, the Julia subset of the complex plane is the set of points z whose orbits are chaotic. The Fatou set is its complement, consisting of regular orbits. The Mandelbrot set is the set of points $c \in \mathbb{C}$ such that the orbit of $z = 0$ is bounded.

16. Construct two examples of **unimodal maps** on the unit interval $[0, 1]$ (other than the logistic map) using trigonometric and piecewise linear functions.

$*$17. **Logistic map to tent map.** Show that the logistic map of the unit interval for $r = 4$, $x_{n+1} = rx_n(1-x_n)$ can be transformed into the 'tent' map $y_{n+1} = 1-2|y_n-1/2|$ via $x = \sin^2(\pi y/2)$. Show that points on periodic orbits of the tent map are dense in the unit interval and that all periodic orbits are unstable.

18. **Logistic map period 2.** Find a value of r for which $x = 1/2$ lies on a period two orbit of the logistic map $x_{n+1} = rx_n(1 - x_n)$ on the unit interval.

19. **Cobweb diagrams.** Draw cobweb diagrams for the logistic map for (a) $r = 1/2$ and (b) $r = 2$ showing that orbits are attracted to the trivial and nontrivial fixed points at (a) $x = 0$ and (b) $x_* = 1 - 1/r$ respectively.

$*$20. For the logistic map, explore the **nonlinear stability** of the fixed point $x_* = 1-1/r$ when $r = 3$. Take a nearby x_0 and compute its iterates to formulate a conjecture.

$*$21. With the help of symbolic computation, find the 12^{th} degree polynomial equation for **period 4 orbits** of the logistic map after factoring out the known fixed point and period two orbits from $f_4(x) = x$. For values of r in the range $[r_2, r_3]$, verify that this equation has 4 real zeros lying in the unit interval. For instance, for $r = 3.5$, they are given by $0.38282, 0.500884, 0.826941$ and 0.874997. By choosing random initial states x_0, verify that iterates of x_0 approach this period 4 orbit.

22. Use the value of the **Feigenbaum constant** $\delta = 4.66920$ to approximately predict the numerical values of r_6 and r_7 at which the period 2^6 and period 2^7 orbits of the logistic map first become attractors. You may assume that the asymptotic $n \to \infty$ behavior of the sequence r_n is a good approximation for $n = 5, 6, 7, \ldots$.

$*23.$ Use symbolic computation to find the 8^{th} degree polynomial equation $f_3(x) - x = 0$ where f_3 is the 3^{rd} iterate of the logistic map. Divide by the known factors coming from fixed points $x(x - (1 - 1/r))$ to arrive at a 6^{th} degree polynomial for nontrivial **period 3 orbits**. Find its discriminant $\Delta_3(r)$. Observe that up to manifestly positive factors, $\Delta_3(r) \propto r^2 - 2r - 7$. Show that $\Delta_3(r) > 0$ provided $r > 1 + 2\sqrt{2}$. Conclude that period 3 orbits can exist only for $r \gtrsim 3.828$.

$*24.$ **Quasiperiodic orbits.** For iterations of a map of a 2d phase space, we made a distinction between periodic, quasiperiodic and chaotic orbits in the context of the standard map. For a map of a 1d state space (such as the logistic map), discuss whether it is meaningful to speak of quasiperiodic orbits.

$*25.$ Try to formulate what it means for iterations of a map to be **time-reversal** (T) invariant. One would like the definition to be such that the standard map is T-invariant while the logistic map is not. Why?

26. By ignoring initial transients, find an analytical estimate for the **Lyapunov exponent** of the **logistic map** for initial conditions that lie in the basin of attraction of a period two orbit. Apply this to the period two attractor for $r_1 = 3 < r < r_2 = \sqrt{6} + 1$ and thereby obtain an approximate expression for $\lambda(r)$ in this interval.

27. As in Prob. 15.26, ignore initial transients to estimate the **Lyapunov exponent** for an orbit that lies in the basin of attraction of a **period** n **orbit**. Show that $\lambda \approx \frac{1}{n} \log |f_n'(x_*)|$ where x_* is any point on the period n orbit.

$*28.$ Numerically solve the EOM of a **double pendulum**. Use it to estimate the **largest Lyapunov exponent** at a point on a chaotic trajectory.

$*29.$ **Hill regions.** For the **double pendulum**, show that the boundary of the Hill region on the $\theta_1 = 0$ Poincaré surface at energy E is given by the curves

$$p_2^{\max,\min} = \pm\sqrt{2ml^2}\left(E + mgl(\cos\theta_2 - 1)\right)^{1/2}. \qquad (15.83)$$

Use this to find the range of allowed values of θ_2 on the $\theta_1 = 0$ surface (θ_2-p_2 cylinder) for any given energy. Find the energy at which the libration-to-rotation transition in θ_2 takes place. This is the energy at which the second bob goes from purely librational to a combination of librational and rotational motion.

$*30.$ Write a computer program to solve the differential equations of the **double pendulum** numerically. Make a movie showing the motion of the bobs. Plot **Poincaré sections** of the sort shown in this chapter. Try to reproduce and improve upon all the figures shown in the text.

$*31.$ Build/buy a **double pendulum**, play with it and observe the transition to chaos.

32. For the relative motion of the **zero gravity double pendulum**, find $\dot{p}$ (15.56) at the fixed points $\pm\theta_*$ of the vector field $v(\theta)$ on the arc of a circle.

33. Show that there is no dynamics in the **zero gravity double pendulum** if $10ml^2E < L_z^2$ where E and L_z are the conserved energy and angular momentum of the bobs.

34. Explain in what sense the EOM (15.54) and (15.55) for the **zero gravity double pendulum** are triangular in center of mass and relative variables.

$*$35. Consider a **driven damped simple pendulum** with EOM $ml\ddot{\theta} = -mg\sin\theta - \gamma\dot{\theta} + f\sin(2\pi\nu t)$ for the counterclockwise angle of deflection θ from the downward vertical. The constants $\gamma > 0$ and f control the friction and external torque at the pivot while m, l and g are the mass of bob, length of rod and acceleration due to gravity. (a) Write the EOM as an autonomous system with a 3d phase space. (b) Use numerical solutions to show that the system displays both regular and chaotic motion depending on values of parameters and initial conditions.

Chapter 16

Dynamics of continuous deformable media

Continuum mechanics begins by dealing with the nonrelativistic classical dynamics of continuous deformable media. Examples are oscillations of stretched strings, heat conduction in rods, elastic motion of solids (rods/beams), motion of fluids[1] (air, water) and plasmas (ionized gases), in roughly increasing order of complexity. All of these systems involve a very large number of molecules (or degrees of freedom) and we will treat them as continuous mass/charge distributions with an infinite number of degrees of freedom. Thus, unlike particle mechanics, continuum mechanics deals with fields (see Appendix B). Examples of fields include the height of a stretched string, temperature, elastic displacement, mass density, velocity, pressure, internal energy, specific entropy, charge density, current density, electric and magnetic fields. While a classical point particle is *somewhere* at any given time, a classical field is *everywhere* at any given instant! Thus, continuum mechanics is a collection of (primarily nonrelativistic, classical) field theories. Electromagnetism and gravitation are other examples of field theories, though they often involve relativistic and/or quantum effects.

Due to the larger number of degrees of freedom, the dynamics of deformable bodies is generally more complicated than that of point particles or rigid bodies. In fact, we can imagine a rigid body becoming deformable by relaxing the constraints that fix the distances between its constituents.

There are two principal formalisms for treating mechanics of continuous media, the so-called Lagrangian and Eulerian descriptions. The former is closer to our treatment of systems of particles: we follow the motion of each molecule or fluid element (to be defined in Sect. 19.1) or bit of string. For example, if a fluid element occupied the location $\boldsymbol{a}$ at $t = 0$, then we seek the trajectory $\boldsymbol{r}(\boldsymbol{a}, t)$ of this fluid element, which should be determined by Lagrange's equations (ironically, this treatment was originally attempted by Euler). The Lagrangian description is particularly useful if we have some way of keeping track of which material element is where. This is usually not possible in a flowing liquid or gas, but is possible in a vibrating string since the bits of string are ordered and may be labeled by their location along the string or by their horizontal coordinate x for small vertical vibrations of a string that does not 'bend over'. For an elastic solid, the corresponding variable is the local displacement field $\boldsymbol{s}(\boldsymbol{r}, t)$ or $\boldsymbol{\xi}(\boldsymbol{r}, t)$ which represents the departure from the equilibrium location of the element that was originally at $\boldsymbol{r}$. In a fluid like air or water, it is difficult to follow the motion of individual fluid elements due to the tendency to mix. So Euler developed the so-called Eulerian description, which attempts to understand the dynamics of quantities (Eulerian variables) such as density $\rho(\boldsymbol{r}, t)$, pressure $p(\boldsymbol{r}, t)$, velocity $\boldsymbol{v}(\boldsymbol{r}, t)$ and temperature $T(\boldsymbol{r}, t)$ in a fluid at a specified *observation point* $\boldsymbol{r}$ at time t. However, it must be emphasized that the laws of mechanics (Newton's laws) apply to material particles or fluid elements, not to points of observation, so one must reformulate the equations of motion so that they apply to the Eulerian variables. The equations of motion in continuum mechanics are invariably expressed as partial differential equations for fields (such as the density of a fluid or height of a string at a given location and time). Thus, we are dealing with the classical dynamics of fields. We will begin with the Lagrangian description of the vibration of a stretched string in Chap. 17. For small vibrations, this is governed by d'Alembert's wave equation. Chap. 18 deals with Fourier's equation for the diffusion or conduction of heat and its role in Brownian motion. Conduction produces heat transport largely through random local molecular vibrations that are transmitted to neighboring molecules. On the other hand, large-scale coherent motion of molecules results in fluid flows, a topic that we take up in Chap. 19, especially from an Eulerian perspective. Fluid dynamics displays both wave-like and diffusive behavior, so it will draw on some of the ideas from the two preceding chapters.

---

[1] Collectively, sand grains sometimes flow like a fluid, though individual grains display properties normally associated with a solid.

Chapter 17

Vibrations of a stretched string and the wave equation

Our first example of a continuum mechanical system is a stretched string free to execute small vibrations in a direction transverse to that in which it is stretched. A vina (veena), sitar or guitar string or a rubber band are possible realizations. The equation of motion for small fluctuations in the height of a stretched string, known as the d'Alembert wave equation, turns out to be universal. It can be used to model small amplitude waves in a wide variety of physical systems such as (a) sound waves in air describing oscillations in pressure or density, (b) electromagnetic or light waves where the components of the electric and magnetic field oscillate, (c) gravitational waves describing oscillations in the metric tensor of space-time, (d) elastodynamic seismic waves describing oscillations of material in the Earth and (e) scalar waves describing oscillations of a classical massless Klein-Gordon field. These examples usually involve additional features such as oscillations in more than one dimension, polarization (vectorial character of electric and magnetic fields or tensorial character of the gravitational metric tensor field) or a combination of transverse and longitudinal oscillations (as in shear and compressional seismic waves) or quantum effects and those of a nonzero mass (as in the application of the Klein-Gordon field to π mesons in particle physics). Despite this, the stretched string gives us a simple context in which to learn about some essential features of all these waves when their amplitude is small.

For concreteness, we suppose the string is stretched horizontally (say, between a pair of clamps) and is free to vibrate in a vertical plane. Stretching the string subjects it to a tension along its length, which is assumed constant for simplicity. We begin in Sect. 17.1 by deriving the equation for small oscillations by considering the forces acting on small bits of the string, whose inertia is determined by the mass density of the string. Newton's second law for the string segment relates its vertical acceleration ($\times$ mass) to the tensional forces exerted on it due to the neighboring segments. The resulting equation for small amplitude oscillations is the celebrated one-dimensional d'Alembert wave equation for the instantaneous height $u(x,t)$ of the string at horizontal location x. The equation is named after the French mathematical physicist Jean le Rond d'Alembert, who found a formula for certain solutions of the wave equation.

The wave equation is a linear partial differential equation that generalizes to fields, the linear ODEs of particle mechanics for small oscillations around a static equilibrium that we encountered in Sect. 6.1 and in Chap. 13. In fact, the wave equation can be written as an infinite collection of linear ODEs in more than one way. For instance, in Sect. 17.2 we write it as a system of ODEs by discretizing the spatial coordinate so that it takes values on an equally spaced grid of points. The resulting equations are *coupled*, since neighboring string segments interact with each other. In Sect. 17.3, we use separation of space and time variables to discover normal modes of vibration (standing wave harmonics), in terms of which the wave equation splits into an infinite tower of *uncoupled* ODEs. These normal modes are then synthesized via a Fourier series to obtain a solution to the initial value problem (IVP) for a stretched string. Another kind of wave on a stretched string is a traveling wave: a disturbance that propagates along the string at constant velocity while maintaining its shape. Remarkably, as discovered by d'Alembert, the solution to the IVP for the wave equation (for an infinite string) can be written as a sum of a left-moving and a right-moving traveling wave (see Sect. 17.4). The speeds of these traveling waves are fixed by the mass density and tension in the string. The structure of d'Alembert's solution also allows us to explain how causality is implemented in solutions to the wave equation.

In Sect. 17.5, we view the wave equation as a continuum version of Newton's second law and derive a (globally) conserved energy for transverse vibrations. Being a continuum system, the energy density is spatially distributed over the length of the string and satisfies a local conservation law, which governs how the energy density can move around the string. We also derive local conservation laws for transverse and longitudinal momenta in Sect. 17.6. There are analogous conservation laws for the energy and momentum of electromagnetic waves. To relate these conservation laws to symmetries via Noether's theorem, we first use the conserved energy to propose Lagrangian and Hamiltonian-Poisson bracket formulations for the wave equation in Sect. 17.7. This then allows us, in Sect. 17.8, to relate the time-translation, vertical and horizontal space-translation symmetries of the string (for suitable boundary conditions) to the conserved energy, transverse and longitudinal momenta. What is more, using a Fourier representation for the string profile, we show that the Lagrangian for the stretched string admits an infinite number of cyclic coordinates which lead to an infinite number of conserved quantities!

In Sect. 17.9, we return to traveling waves and explain the concept of phase velocity of a Fourier mode, as well as the group velocity of a wave packet that is obtained by superposing a collection of Fourier modes. These ideas are used to explain the sense in which the wave equation is nondispersive and contrast it with the dispersive nature of the quantum mechanical Schrödinger wave equation.

The presence of an infinite number of conserved quantities and its solvability by separation of variables and Fourier series reflect the integrability of the wave equation as a mechanical system. In Sect. 17.10* we explore another aspect of this integrability: a Lax pair for the (1^{st} order) wave equation. This extends to continuum systems of fields, the concept of a Lax pair for a mechanical system with finitely many degrees of freedom introduced in Sect. 11.9*. What is more, it turns out that the Lax pair for the linear nondispersive wave equation can be generalized to the KdV equation, which is in many ways a universal equation for nonlinear dispersive waves in 1 spatial dimension.

17.1 Wave equation for transverse vibrations of a stretched string

One of the simplest mechanical systems with a continuously infinite number of degrees of freedom is a vibrating stretched string. We will consider the special case where, in equilibrium, the string is stretched between two clamps at $x = 0$ and $x =$

ℓ as shown in Fig. 17.1a. We ignore gravity for now since the tensional forces in the string often dominate especially when the string is stretched (in a limp string, tension can be weaker). We shall call the direction in which the string is stretched, the ‘horizontal’ direction. The string is free to move only in one direction (vertical) transverse to the direction in which it is stretched. We assume the string has a mass per unit length of ρ. The instantaneous configuration of the string is specified by giving the height $u(x,t)$ of the string above the horizontal position x at time t.

Tensional forces on a string segment. Since the string is stretched, there are tension forces that act on any segment of the string, tangentially at either end of the segment, tending to elongate the segment, as shown in Fig. 17.1b. Unless otherwise mentioned, we will assume that the tension in the string is a constant τ. When the string is horizontal, the tensions at either end of any segment are horizontal, equal and opposite in direction so that the string is in equilibrium. At the endpoints, the tension is balanced by the outward forces applied by the clamps.

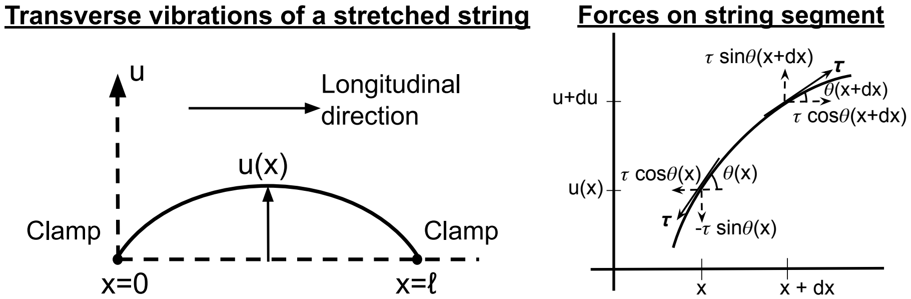

(a) (b)

Figure 17.1: (a) Transverse motion of a stretched string clamped at its endpoints. (b) Tensional forces on a portion of a stretched string. Observe that the net vertical force on this string segment is downward directed, tending to restore the segment to its equilibrium location.

Note that the length of the string is not fixed, it can stretch to a length more than ℓ, for instance when it is plucked as in a vina. When the string is displaced from equilibrium by small vertical displacements, tensional forces on the ends of a small segment are not necessarily horizontal. But to a good approximation, the horizontal components of tension are equal and opposite, ensuring that there is no longitudinal/horizontal movement of the string. On the other hand, the vertical components of tension are in general unequal and result in a vertical acceleration of the segment. We will soon estimate these vertical components. As shown in Fig. 17.1b, consider a small segment of string between horizontal locations x and $x+dx$ with corresponding heights $u(x)$ and $u(x+dx) \approx u+du$. We suppose that the tangent to the string at any point x makes a counterclockwise angle $\theta(x)$ with respect to the horizontal. Then since we assume the inclination angles are small,

$$\cos\theta(x) \approx 1 - \frac{\theta(x)^2}{2} \approx 1 \quad \text{and} \quad \sin\theta(x) \approx \tan\theta(x) \approx \frac{\partial u}{\partial x} = u_x \equiv u'(x). \tag{17.1}$$

Now, the horizontal components of tension at the right and left ends of the segment are

$\tau(x+dx)\cos\theta(x+dx)$ and $-\tau(x)\cos\theta(x)$. Since we are assuming that the string does not move horizontally, these must be equal and opposite (this is possible if τ is independent of x). More generally, we must account for horizontal motion as well. We will temporarily allow for nonconstant τ just to see how it affects the equation for transverse motion. The vertical components of tension at the right and left ends of the segment are

$$\tau(x+dx)\sin\theta(x+dx)\hat{z} \approx (\tau u')(x+dx)\hat{z} \quad \text{and} \quad -\tau(x)\sin\theta(x)\hat{z} \approx -(\tau u')(x)\hat{z}. \tag{17.2}$$

Thus, the net upward force on the segment is

$$F_{\text{up}} = (\tau u')(x+dx) - (\tau u')(x) \approx \partial_x(\tau(x)u'(x))\, dx. \tag{17.3}$$

Newton's 2^{nd} law for the string. We begin by observing that the length of the string segment in Fig. 17.1b is $|dx|$ up to terms quadratic in small quantities:

$$\sqrt{dx^2+du^2} \approx |dx|\left[1+(1/2)(\partial u/\partial x)^2\right] \approx |dx|. \tag{17.4}$$

Thus Newton's second law '$F = ma$' for the segment, whose mass is $\rho(x)\,dx$ is

$$F_{\text{up}} = (\tau u_x)_x\, dx = \rho\, dx\, u_{tt}. \tag{17.5}$$

Thus, the equation of motion for small transverse (1d) vibrations of the stretched string is $(\tau u_x)_x = \rho u_{tt}$. If the tension τ is a constant, then we get the standard form of d'Alembert's wave equation:

$$\frac{\partial^2 u}{\partial x^2} = \frac{1}{c^2}\frac{\partial^2 u}{\partial t^2} \quad \text{where} \quad c = \sqrt{\frac{\tau}{\rho}} \tag{17.6}$$

has dimensions of a speed and will be seen to be the speed at which waves propagate on the string.

The wave equation $u_{tt} = c^2 u_{xx}$ is a linear, homogeneous partial differential equation (PDE) second order in both space and time derivatives. PDEs involve derivatives with respect to more than one independent variable (x, t here) while ordinary differential equations (ODEs) involve derivatives only in one independent variable (t in Newton's equation for a point particle). The wave equation is linear since it involves only the first power of the unknown function (dependent variable) u. It is time-reversal invariant [see (1.3)] in the sense that $u(-t)$ is a solution if $u(t)$ is one. So a movie of a solution played backwards is also a solution.

Hyperbolic character. The wave equation is hyperbolic, which means it describes wave-like disturbances, as we shall see. Roughly, the name hyperbolic comes from the shape of the dispersion relation curve $\omega^2 = c^2k^2$ in the k-ω plane that the wave number k and frequency ω must obey for the real and imaginary parts of the plane wave ansatz $u = e^{i(kx-\omega t)}$ to satisfy the wave equation (see Prob. 17.2). The analogy with a hyperbola is more obvious if the wave equation is augmented with a term $\propto u$. Plane waves are special solutions of the wave equation which are labelled by a wave number k and associated frequency $\omega(k)$; they can be superposed to obtain more general solutions of the wave equation. The meanings of ω and k will be clarified in Sect. 17.3, while the term ‘plane wave’ and the idea of a dispersion relation will be explained in Sect. 17.9. The hyperbolic wave equation is to be contrasted with Helmholtz’s equation $u_{xx} + u_{yy} = \kappa^2 u$ (or Laplace’s equation when $\kappa = 0$) which is elliptic and Fourier’s heat equation $u_t = \alpha u_{xx}$ (see Chap. 18) which is parabolic in the sense that their dispersion curves are shaped like an ellipse and (up to a factor of i) a parabola respectively (see Prob. 17.3 and Prob. 17.4). Unlike the wave-like character of hyperbolic equations, parabolic equations display damped evolution. Elliptic equations like the Laplace, Helmholtz or Poisson equations do not describe propagation in time but can model static configurations such as an electrostatic or gravitational potential.

Initial and boundary conditions. We are interested in solving the initial-boundary value problem for the string. The wave equation is second order in time and requires two initial conditions (say at $t = 0$), just like Newton’s equation. These can be the initial height $u(x, t = 0)$ and the initial velocity of the string $u_t(x, t = 0)$. In addition, we need to specify what happens at the boundaries. The boundary conditions corresponding to a string clamped at the endpoints $[u(x = 0, t) = u(x = \ell, t) = 0]$ are called Dirichlet boundary conditions (BCs)[1]. Other BCs are also of interest. For example, we might have an end (say at $x = 0$) of the string free to move up and down (though not horizontally), so that the slope of the string vanishes at the endpoint. This could be implemented by attaching the left end of the string to a massless ring free to move vertically without friction on a pole. This means u has zero slope at the left endpoint, one cannot apply a vertical force on the ring since it yields, it has no inertia. This leads to the free or open or Neumann boundary condition[2] $\frac{\partial u}{\partial x} = 0$ at $x = 0$. We could also consider an infinite string with decaying BCs: $u(x, t) \to 0$ as $|x| \to \infty$. All of the above are homogeneous boundary conditions. On the other hand, a BC such as $u(0, t) = 1$ is inhomogeneous. In particular, the sum of two solutions with inhomogeneous BCs would not satisfy the BCs and the superposition principle for the linear wave equation would not apply. Sometimes, we consider mixed (different types of BCs on different parts of the boundary) or Robin BCs (named after the French mathematical physicist Victor Robin) where a linear combination of u and u_x is specified on the boundaries. The nature of solutions and the physics they model depend crucially on boundary conditions. It is important to recognize that without suitable BCs, the wave equation is in general underdetermined and may have multiple solutions for given initial conditions. □

If we were to include the weight of string segments (gravitational force due to constant acceleration due to gravity g), show that the equation for small vibrations of a horizontally stretched string becomes the linear inhomogeneous PDE

$$(1/c^2)u_{tt} = u_{xx} - (g/c^2). \tag{17.7}$$

---

[1] The same boundary conditions were used by the German mathematician Lejeune Dirichlet in his pioneering work on the boundary value problem for Laplace’s equation.

[2] Free boundary conditions are named after the German mathematical physicist Carl Neumann who studied the Dirichlet problem and its extensions.

We note in passing that the wave equation for small oscillations of a stretched string is Lorentz invariant (see Eq. (4.42) of Sect. 4.10*) (with c interpreted as the speed of light) even though the underlying system is nonrelativistic. This is associated with the linear 'dispersion relation' $\omega = \pm ck$ (see Sect. 17.9) for small oscillations. This is an artifact of ignoring nonlinearities.

Comparing (17.6) with Newton's or Lagrange's equations of mechanics, $u(x)$ is the analog of the generalized coordinate and x labels the 'particles' in the string. The configuration space is the set of possible instantaneous locations of the string segments, i.e., the space of twice differentiable functions $u(x)$ on the interval $[0, \ell]$ that vanish at the end-points. This is an infinite-dimensional space, reflecting the fact that a string has infinitely many degrees of freedom[3]. The equations of continuum mechanics (e.g., fluid mechanics, electrodynamics, general relativity, elasticity) are typically systems of partial differential equations and the wave equation is a prototype. What is more, as we will learn in Sect. 17.7, the wave equation admits both Hamiltonian-Poisson bracket and Lagrangian formulations.

17.2 Finite differences: wave equation as a system of ODEs

We may regard a partial differential equation such as the wave equation as a large (infinite) system of coupled ODEs, one ODE for each value of x. This viewpoint can be useful in seeking numerical solutions through discretization and truncation. To see this, we consider the wave equation, for definiteness, on the real line $-\infty < x < \infty$ and imagine discretizing the spatial coordinate $\ldots x_{-2}, x_{-1}, x_0 = 0, x_1, x_2, x_3, \ldots$ with uniform spacing δx. The first derivative may be approximated as a forward or backward difference:

$$u'_{\rm fd}(x_i) = \frac{1}{\delta x}(u(x_{i+1}) - u(x_i)) \quad \text{or} \quad u'_{\rm bd}(x_i) = \frac{1}{\delta x}(u(x_i) - u(x_{i-1})). \tag{17.8}$$

If we assemble the values of u in a vector $(u(x_i))_{i\in\mathbb{Z}}$, then we may write the forward and backward difference approximants to the first derivative as upper and lower triangular matrices with entries along the diagonal and the first super- or subdiagonal

$$\left[\frac{d}{dx}\right]_{\rm fd} \approx \frac{1}{\delta x}\begin{pmatrix} \vdots & \vdots & \vdots & \vdots & \vdots & \vdots & \vdots \\ \cdots & -1 & 1 & 0 & 0 & 0 & \cdots \\ \cdots & 0 & -1 & 1 & 0 & 0 & \cdots \\ \cdots & 0 & 0 & -1 & 1 & 0 & \cdots \\ \cdots & 0 & 0 & 0 & -1 & 1 & \cdots \\ \cdots & 0 & 0 & 0 & 0 & -1 & \cdots \\ \vdots & \vdots & \vdots & \vdots & \vdots & \vdots & \vdots \end{pmatrix} \quad \text{and} \quad \left[\frac{d}{dx}\right]_{\rm bd} \approx \frac{1}{\delta x}\begin{pmatrix} \vdots & \vdots & \vdots & \vdots & \vdots & \vdots & \vdots \\ \cdots & 1 & 0 & 0 & 0 & 0 & \cdots \\ \cdots & -1 & 1 & 0 & 0 & 0 & \cdots \\ \cdots & 0 & -1 & 1 & 0 & 0 & \cdots \\ \cdots & 0 & 0 & -1 & 1 & 0 & \cdots \\ \cdots & 0 & 0 & 0 & -1 & 1 & \cdots \\ \vdots & \vdots & \vdots & \vdots & \vdots & \vdots & \vdots \end{pmatrix} \tag{17.9}$$

With decaying BCs, d/dx is a real antisymmetric operator $(u, v') = -(u', v)$ where $(u, v) = \int u(x)v(x)dx$ is the L^2 inner product on functions that vanish at the boundaries. This is reflected in the relation $(d/dx)_{\rm bd} = -(d/dx)^t_{\rm fd}$ where t denotes the transpose. Now, the finite difference approximation to the second derivative can be obtained in several ways[4]. For instance, we could apply the forward difference twice or the backward difference twice or compose the forward and backward difference operators (in either order). We prefer the third option as the resulting matrix is symmetric, as is the operator d^2/dx^2 with vanishing/decaying BCs. Thus, we take

---

[3] These degrees of freedom can be taken as the continuously infinite collection of heights $u(x)$ for all $x \in [0, \ell]$. However, to describe most configurations of a stretched string, it suffices to use the countably infinite sequence of Fourier coefficients $A_0, A_1, \ldots, B_0, B_1, \ldots$ introduced in Sect. 17.3. Note also that the continuous function $u(x)$ is determined by its values at the (countably infinite set of) rational numbers in the interval $[0, \ell]$.

$$\frac{d^2}{dx^2} \approx \frac{1}{(\delta x)^2} \begin{pmatrix} \vdots & \vdots & \vdots & \vdots & \vdots & \vdots & \vdots \\ \ldots & -2 & 1 & 0 & 0 & 0 & \ldots \\ \ldots & 1 & -2 & 1 & 0 & 0 & \ldots \\ \ldots & 0 & 1 & -2 & 1 & 0 & \ldots \\ \ldots & 0 & 0 & 1 & -2 & 1 & \ldots \\ \ldots & 0 & 0 & 0 & 1 & -2 & \ldots \\ \vdots & \vdots & \vdots & \vdots & \vdots & \vdots & \vdots \end{pmatrix}. \tag{17.10}$$

Now, we may write the wave equation as an infinite collection of ODEs:

$$\frac{1}{c^2}\frac{\partial^2 u(x_i,t)}{\partial t^2} = \frac{1}{(\delta x)^2}\left(u(x_{i+1},t) - 2u(x_i,t) + u(x_{i-1},t)\right) \tag{17.11}$$

for $i = \ldots, -2, -1, 0, 1, 2, \ldots$. The equations are *coupled* since the evolution of $u(x_i,t)$ depends on $u(x_{i+1},t)$ and $u(x_{i-i},t)$. This system of ODEs can be solved (say, on a computer after restricting i to a finite range $|i| \leq i_{\max}$) with suitable initial and BCs. Remarkably, there is *another* way of converting the wave equation into an infinite array of ODEs, this time uncoupled! This is by the method of separation of variables and Fourier series, which we turn to next.

17.3 Separation of variables, normal modes and solution by Fourier series

On account of the linearity of the wave equation (17.6) subject to homogeneous BCs (say Dirichlet or Neumann), the superposition principle applies. Linear combinations of solutions are again solutions. The solution space forms a linear space. This suggests that if we can find a sufficiently large set of linearly independent solutions, we may be able to express a solution of interest as a linear combination of them (see Sect. 13.2.2 for a mechanical example).

The wave equation $u_{tt} = c^2 u_{xx}$ is a partial differential equation for an unknown height function u dependent on two independent variables t, x. Let us look for solutions which are a product of a function of t and a function of x: $u(x,t) = X(x)T(t)$. We hope that solutions of this separable type form a basis for the space of all solutions of interest. We also hope that X and T will be determined by simpler ODEs compared to the PDE for u. Indeed, we find, wherever the quotients in (17.12) make sense[5],

---

[4] Depending on context, an appropriate choice of finite difference approximant may be made to help us reduce computational complexity or reduce numerical errors or ensure that certain properties (such as symmetries) are implemented to machine precision. Since computational time and memory are limited, truncation and roundoff errors can affect the reliability and accuracy of numerical solutions. The effects of roundoff errors can be quite dramatic in chaotic systems (as observed by Edward Lorenz [88]) where sensitivity to initial conditions could magnify the effects of small errors and lead to a loss in predictive power.

$$X(x)\ddot{T}(t) = c^2 T(t) X''(x) \quad \Rightarrow \quad \frac{\ddot{T}(t)}{T(t)} = c^2 \frac{X''(x)}{X(x)} = -\omega^2. \tag{17.12}$$

Now, the LHS is a function of t alone, while the RHS is a function of x alone. Thus, both must equal the same 'separation' constant, which we called $-\omega^2$ for some real number ω. We anticipate that the constant must be negative for vibrational motion. This is because $-\omega^2 = \frac{\ddot{u}}{u}$ is the ratio of the acceleration of the string element to its displacement from the mean position. As in Hooke's law, this quotient must be negative for the tension in the string to be a restoring force (see Fig. 17.1). Alternatively, $c = \sqrt{\tau/\rho} > 0$ and the second derivative ∂_x^2 is a negative-definite operator[6] on functions $X(x)$ that vanish at the endpoints of the interval. Thus, our PDE has reduced to a pair of ODEs for each allowed (though yet to be determined) value of ω^2:

$$\ddot{T}(t) = -\omega^2 T(t) \quad \text{and} \quad X''(x) = -k^2 X(x). \tag{17.13}$$

Here, $k = \omega/c$ is called the angular wave number. Remarkably, the ODEs for one value of ω^2 are not coupled to those for any other value of ω^2. Contrast this with the ODEs we got by finite differences in Sect. 17.2.

These ODEs are in fact eigenvalue problems. For example, the first is the eigenvalue problem for the (infinite-dimensional) operator d^2/dt^2 with $T(t)$ the eigenvector and $-\omega^2$ the eigenvalue. To make the connection to finite-dimensional matrix eigenvalue problems more explicit, we could discretize time and represent T by the column vector whose entries are $T(t_i)$ where t_i are a suitable set of times, say $\delta t(\ldots, -3, -2, -0, 1, 2, 3, \ldots)$ where δt is a small time step. Then, we may represent the operator d^2/dt^2 in this basis by a tridiagonal real symmetric matrix, a few of whose 'middle' rows and columns are

$$\frac{d^2}{dt^2} \approx \frac{1}{(\delta t)^2} \begin{pmatrix} \vdots & \vdots & \vdots & \vdots & \vdots & \vdots & \vdots \\ \ldots & -2 & 1 & 0 & 0 & 0 & \ldots \\ \ldots & 1 & -2 & 1 & 0 & 0 & \ldots \\ \ldots & 0 & 1 & -2 & 1 & 0 & \ldots \\ \ldots & 0 & 0 & 1 & -2 & 1 & \ldots \\ \ldots & 0 & 0 & 0 & 1 & -2 & \ldots \\ \vdots & \vdots & \vdots & \vdots & \vdots & \vdots & \vdots \end{pmatrix} \quad \text{where} \quad T \approx \begin{pmatrix} \vdots \\ T(-2\delta t) \\ T(-\delta t) \\ T(0) \\ T(\delta t) \\ T(-2\delta t) \\ \vdots \end{pmatrix} \tag{17.14}$$

corresponding to the finite difference approximation of the second derivative:

$$\ddot{T}(t) \approx \frac{1}{\delta t}\left(\frac{T(t+\delta t) - T(t)}{\delta t} - \frac{T(t) - T(t-\delta t)}{\delta t}\right) = \frac{T(t+\delta t) - 2T(t) + T(t-\delta t)}{(\delta t)^2}. \tag{17.15}$$

---

[5] Remarkably, we will see that the quotients $\ddot{T}(t)/T(t)$ and $X''(x)/X(x)$ are well-defined in a limiting sense even when the denominators vanish. The prototypical example illustrating this is $X(x) = \sin(\pi x/\ell)$.

[6] A symmetric or Hermitian operator M is negative-definite if its eigenvalues are < 0, or equivalently, if all its diagonal matrix elements $v^\dagger M v$ are < 0 for any nonzero state/vector v and its Hermitian adjoint $v^\dagger$. Show or recall from quantum mechanics that the first derivative is antisymmetric: $\partial_x^\dagger = -\partial_x$ so that $\partial_x^2 = -\partial_x^\dagger \partial_x$. Finally, show that $A^\dagger A$ and $AA^\dagger$ are positive-definite operators for any operator A with adjoint $A^\dagger$.

A similar matrix representation[7] applies, mutatis mutandis, to d^2/dx^2.

Normal modes. The first ODE in (17.13) $\ddot{T} = -\omega^2 T$ is *formally* the same as Newton's equation for a harmonic oscillator[8], as is the second. So we can write their general solutions as

$$T(t) = A\cos\omega t + B\sin\omega t \quad \text{and} \quad X(x) = C\cos kx + D\sin kx. \tag{17.16}$$

Here, ω and k can both be taken nonnegative, as we will soon discover. The clamping of endpoints of the string (Dirichlet BCs) implies $X(0) = X(\ell) = 0$, so we must have $C = 0$ and $\sin k\ell = 0$. So $k\ell = n\pi$ where n is an integer. Thus the eigenvalues are $-\omega_n^2 = -(n\pi c/\ell)^2$ and $-k_n^2 = -(n\pi/\ell)^2$. It suffices to take $n \geq 1$ since the negative values give (linearly dependent) solutions that only differ by a sign and $n = 0$ gives the zero solution. So we may write any separable solution of the wave equation as

$$u_n(x,t) = (A_n\cos\omega_n t + B_n\sin\omega_n t)\sin\frac{n\pi x}{\ell} \quad \text{where} \quad \omega_n = \frac{n\pi c}{\ell}. \tag{17.17}$$

Each of these solutions for $n = 1, 2, 3, \ldots$ is called a *normal mode* of oscillation.

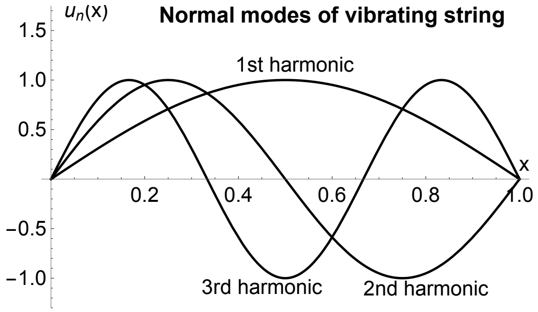

Figure 17.2: Normal modes $u_n(x,0) = \sin(n\pi x/\ell)$ of a vibrating string clamped at $x = 0$ and $x = 1$: fundamental, 2nd harmonic and 2nd overtone.

The mode $n = 1$ is called the fundamental or 1st harmonic, $n = 2$ the 2nd harmonic or first overtone and so on (see Fig. 17.2). Normal modes are periodic functions of x and t. At any t, a normal mode has a definite angular wave number k_n and spatial wavelength $\lambda_n = 2\pi/k_n = 2\ell/n$. At any fixed x, it has a definite angular frequency $\omega_n = ck_n$ and time period of oscillation $T_n = 2\pi/\omega_n$. $\nu_n = \omega_n/2\pi$ is the frequency at which every point along the string vibrates about its mean position. As opposed to a normal mode, a more general motion of a stretched string does not have such a definite wavelength and time period, indeed it need not even be periodic in time! Moreover, these normal modes do not necessarily satisfy the prescribed initial conditions. But since the wave equation is linear, we can take linear combinations of normal modes to produce new solutions. The most general such linear combination is a Fourier series

---

[7] Boundary conditions may be encoded as conditions on the components of the column vector representing the discretized and truncated version of $X(x)$. Think of ways to impose periodic, Dirichlet, Neumann and decaying boundary conditions.

[8] It is notable that Newton's 2nd law for the harmonic oscillator $\ddot{\delta}(t) = -\omega^2\delta(t)$ where $\delta(t)$ is the displacement of a particle from equilibrium is *not* an eigenvalue problem since $\omega = \sqrt{k/m}$ here is a fixed constant determined by the spring constant k and particle mass m.

$$u(x,t) = \sum\nolimits_{n=1}^{\infty} \left(A_n \cos\omega_n t + B_n \sin\omega_n t\right) \sin\frac{n\pi x}{\ell}. \tag{17.18}$$

The Fourier coefficients A_n, B_n must decay sufficiently fast as $n \to \infty$ to ensure that the sum converges ($|A_n|, |B_n| \sim 1/n^2$ will do). The theorems of Fourier series [24] tell us that we can represent any continuous function of x that vanishes at the endpoints $(0,\ell)$ as a Fourier sine series (at any t). So we may try to fit the ICs by a suitable choice of A_n, B_n for $n \geq 1$. They are fixed by the initial height and velocity of the string

$$u(x,0) = \sum\nolimits_{n=1}^{\infty} A_n \sin\frac{n\pi x}{\ell} \quad \text{and} \quad \dot{u}(x,0) = \sum\nolimits_{n=1}^{\infty} B_n \omega_n \sin\frac{n\pi x}{\ell} \tag{17.19}$$

where $\omega_n = n\pi c/\ell$. The initial height and velocity must vanish at $x = 0, \ell$ so that the BCs are satisfied. Using the orthogonality of $\sin(n\pi x/\ell)$ on the interval $[0,\ell]$ for $n = 1, 2, 3, \ldots$ and the fact that the average value (over a period) of the square of the sine function is a half, we find[9] the Euler-Fourier formulae

$$A_n = \frac{2}{\ell}\int_0^{\ell} u(x,0) \sin\left(\frac{n\pi x}{\ell}\right) dx \quad \text{and} \quad B_n = \frac{2}{n\pi c}\int_0^{\ell} \dot{u}(x,0) \sin\left(\frac{n\pi x}{\ell}\right) dx. \tag{17.20}$$

Thus, we have solved the initial-boundary value problem for the motion of a stretched string clamped at the endpoints. It is instructive (see Prob. 17.11) to plot a movie of one such solution by choosing a simple initial condition such as an isosceles triangular initial height, zero initial velocity and truncating the Fourier series (see Fig. 17.3).

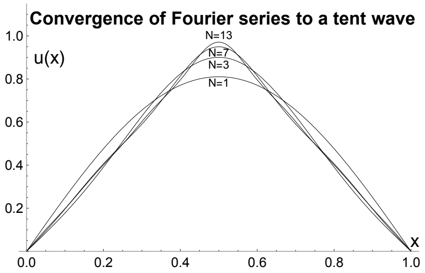

Figure 17.3: Truncations of a Fourier sine series after 1, 3, 7 and 13 terms are seen to be converging to a triangular wave of width $\ell = 1$ and height $a = 1$. Here, the even Fourier coefficients vanish while the odd ones are $A_n = (-1)^{(n-1)/2} 8a/n^2\pi^2$.

Hence, a general vibration of a stretched string involves a superposition of several normal modes and does not possess a definite wave number or time period. However, we will see that in general, higher harmonics cost more energy to excite. We might anticipate this since the restoring force was found to be proportional to $u''(x)$. Higher harmonics $\sin(n\pi x/\ell)$, for $n \gg 1$ are rapidly oscillating functions with large second derivatives ($\propto n^2$), so they involve significant forces on the string segments. We would expect much energy to be stored in the oscillatory motion of a higher harmonic.

---

[9] We multiply both sides by $\sin(m\pi x/\ell)$ and integrate over $x \in [0,\ell]$ for integer m and consider the cases $m = n$ and $m \neq n$. Use $2\sin\alpha\sin\beta = \cos[\alpha-\beta] - \cos[\alpha+\beta]$.

17.4 Right- and left-moving waves and d'Alembert's solution

By playing with a stretched string, we may discover the phenomenon of a transverse wave that moves along a string[10]. A vertical disturbance somewhere along a string can propagate elsewhere. This is because the vertical component of tension causes the neighboring string element to move vertically, and the process goes on. The simplest such wave is a traveling wave: a wave that maintains its profile as it moves at constant speed (say $c > 0$) along the string (either to the right or left, see Fig. 17.4). For example, if $u(x,0) = f(x)$ is the initial height profile, then $u(x,t) = f(x-ct)$ is a right-moving wave and $u(x,t) = f(x+ct)$ is a left-moving wave.

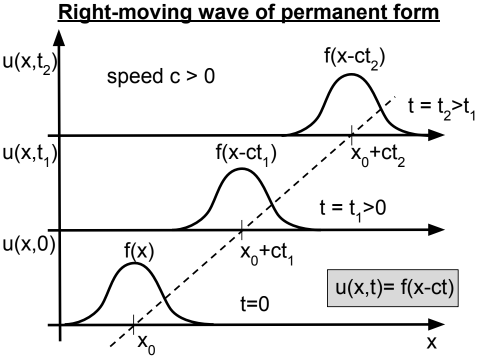

Figure 17.4: Snapshots of right-moving traveling wave $u(x,t) = f(x-ct)$ of permanent form at $t_2 > t_1 > t_0 = 0$ (here $c > 0$). In particular, the center of the pulse moves rightwards at constant speed $x_{\text{center}} = x_0 + ct$.

Now, we investigate whether it is possible to describe the solution of the wave equation (17.6) in terms of traveling waves. Recall that the height $u(x,t)$ of a stretched string executing small transverse vibrations must be annihilated by the wave operator or d'Alembertian $\Box = \frac{1}{c^2}\partial_t^2 - \partial_x^2$ (4.42). D'Alembert's approach to solving the wave equation arises from factorizing $\Box$ into a pair of first order operators. Let us consider the wave equation on the real line $-\infty < x < \infty$ subject to the ICs

$$u(x,t=0) = h(x) \quad \text{and} \quad \dot{u}(x,0) = v(x). \tag{17.21}$$

The wave equation may be factorized in two ways:

$$\left(c^{-2}\partial_t^2 - \partial_x^2\right)u = \left(c^{-1}\partial_t - \partial_x\right)\left(c^{-1}\partial_t + \partial_x\right)u = \left(c^{-1}\partial_t + \partial_x\right)\left(c^{-1}\partial_t - \partial_x\right)u = 0. \tag{17.22}$$

We assume that we are considering functions for which mixed partials are equal $\partial_t\partial_x u = \partial_x\partial_t u$; this is true provided the mixed partials exist and are continuous (Clairaut's theorem). It follows that if u is annihilated by either $\partial_- = c^{-1}\partial_t - \partial_x$ or

---

[10] For instance, tie one end of a long string to a hook on a wall and stretch it horizontally by pulling at the other end. Now shake the free end once up and down and watch the wave-like disturbance propagate towards the hook, get reflected and come back. Moreover, two such waves moving in opposite directions can collide and superpose.

$\partial_+ = c^{-1}\partial_t + \partial_x$, then it will satisfy the wave equation[11]. Let us consider these first order equations. We notice that for any differentiable functions f and g of one variable, $u(x,t) = f(x-ct)$ satisfies $\partial_+ u = 0$ while $u(x,t) = g(x+ct)$ is annihilated by ∂_-. Thus, for any, say, twice differentiable functions f and g,

$$u(x,t) = f(x-ct) + g(x+ct) \tag{17.23}$$

is a solution of the wave equation. As noted, for $c > 0$, $f(x-ct)$ is a right-moving wave with speed c and initial profile (at $t = 0$) given by the function $f(x)$. The shape of the wave $f(x-ct)$ is unaltered as it travels to the right. Similarly, for $c > 0$, $g(x+ct)$ is a left-moving wave. Thus, we have found that any linear superposition of such right- and left-moving waves is a solution of (17.6).

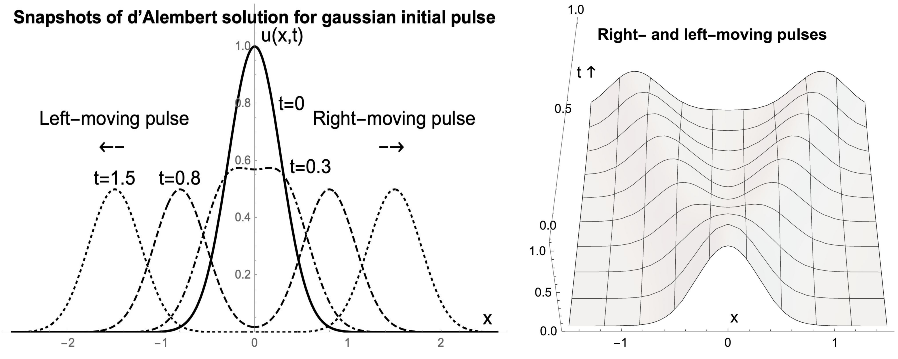

(a) (b)

Figure 17.5: (a) Snapshots of d'Alembert solution (17.27) for Gaussian initial height profile $h(x) = e^{-x^2/a^2}$ with $a = 0.4$ and zero initial velocity $v(x)$. (b) Space-time diagram of evolution of same pulse showing emergence of right- and left-moving waves which essentially retain their shapes while moving outward.

Solution of IVP. One wonders whether such superpositions of right- and left-moving waves are adequate to solve the initial value problem for a stretched string[12]. We will see that this is indeed the case on an infinite domain. To solve the IVP, we wish to fix f and g in terms of the initial data. We have

$$u(x,0) = f(x) + g(x) = h(x) \quad \text{and} \quad \dot{u}(x,0) = -cf'(x) + cg'(x) = v(x). \tag{17.24}$$

Integrating the latter equation with integration constant K, we get

$$f(x) + g(x) = h(x) \quad \text{and} \quad -f(x) + g(x) = \frac{1}{c}\int_{x_0}^{x} v(\xi)\, d\xi + K. \tag{17.25}$$

---

[11] These are sufficient but not necessary conditions for solving (17.6). But as we will soon see, functions of these special sorts can be used to obtain the solution to the IVP on a line.

[12] It can be shown (see Prob. 17.14) that the initial value problem for the wave equation has a unique solution. So the solution we find here in terms of left- and right-moving waves and expressed in terms of initial height and initial velocity is the only one.

Adding and subtracting, we solve for f, g in terms of the initial data:

$$\begin{aligned} f(x) &= \frac{1}{2}\left(h(x) - \frac{1}{c}\int_{x_0}^{x} v(\xi)\, d\xi - K\right) \quad \text{and} \\ g(x) &= \frac{1}{2}\left(h(x) + \frac{1}{c}\int_{x_0}^{x} v(\xi)\, d\xi + K\right). \end{aligned} \tag{17.26}$$

K and x_0 are not part of the initial data, so we hope to get rid of them. Fortunately, we are not interested in f and g, but in $u(x,t) = f(x-ct) + g(x+ct)$. Adding, we express the solution entirely in terms of initial height and velocity

$$u(x,t) = \frac{1}{2}\left[h(x-ct) + h(x+ct) + \frac{1}{c}\int_{x-ct}^{x+ct} v(\xi)\, d\xi\right]. \tag{17.27}$$

It is instructive to plot a movie of this solution, e.g., for zero initial velocity and a Gaussian initial height profile $h(x) = e^{-x^2/a^2}$. One finds two little waves (of roughly half the initial height) moving away from $x = 0$, as shown in Fig. 17.5.

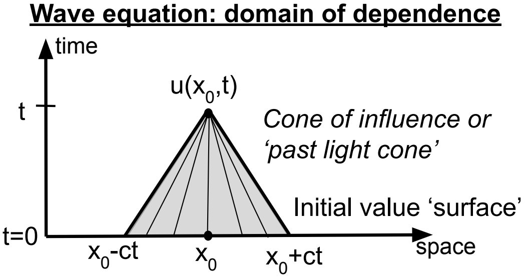
Wave equation: domain of dependence
time
t
u(x0,t)
Cone of influence or 'past light cone'
Initial value 'surface'
t=0
x0-ct
x0
x0+ct
space

Figure 17.6: Space-time diagram showing domain of dependence of solution of wave equation.

Remark. The height at x_o at time t depends on the initial ($t = 0$) height h at points $x_o - ct$ and $x_o + ct$. So the initial height only at points a distance ct from the observation point x_o can affect the height at the point of observation. This indicates that these 'signals' that communicate the information in the initial height distribution $h(x)$ travel at the speed[13] c. On the other hand, the initial transverse velocity $v(x)$ only at points within a distance ct from the observation point can affect the height at the observation point. These latter influences can travel at any speed from zero up to c. Combining these two observations, we may display the locations at the initial instant of time that can influence the current configuration of the string at x_o. The resulting space-time diagram (Fig. 17.6) showing the *domain of dependence* takes the shape of a *past 'light cone'* (compare with Fig. 4.6). Note that the transverse velocity of the string at time t can be obtained by differentiating (17.27) in time, as in Prob. 17.6:

$$\partial_t u(x,t) = \frac{1}{2}\left[ch'(x+ct) - ch'(x-ct) + v(x+ct) + v(x-ct)\right]. \tag{17.28}$$

---

[13] Note that the speed at which these (longitudinal) signals travel is quite distinct from the instantaneous vertical velocity $\dot{u}$ of a point on the string.

On the other hand, the second time derivative $\ddot{u}(x,t)$ can be obtained in two different ways: either differentiate (17.28) in t or differentiate (17.27) twice in x and use the wave equation. We verify in Prob. 17.6 that both give the same result. □

17.5 Conserved energy of small oscillations of a stretched string

Since we have not incorporated dissipative effects and are not supplying energy or applying external forces to the string at any $t > 0$, we expect the vibrating string to have a conserved energy. Let us derive an expression for it following what we did for Newton's equation. Recall from (1.2) and Prob. 1.3 that we multiplied $m\ddot{q}_i + \frac{\partial V}{\partial q_i} = 0$ by the integrating factor $\dot{q}_i$ and summed over the degrees of freedom i. The resulting expression was the statement that the time derivative of energy is zero. So let us begin with Newton's equation for a string in its pristine form (17.5) and multiply by u_t

$$\begin{aligned} \rho u_{tt}\, dx = (\tau u_x)_x\, dx \quad &\Rightarrow \quad \rho u_t u_{tt}\, dx - u_t(\tau u_x)_x\, dx = 0 \\ &\Rightarrow \quad \frac{1}{2}\rho(u_t^2)_t\, dx - u_t(\tau u_x)_x\, dx = 0. \end{aligned} \tag{17.29}$$

For a string between $x = a, b$, we sum over degrees of freedom by integrating over x:

$$\partial_t \int_a^b \frac{1}{2}\rho u_t^2\, dx - \int_a^b u_t(\tau u_x)_x\, dx = 0. \tag{17.30}$$

We assumed $\rho(x)$ is independent of time. The first term is the time derivative of what looks like a kinetic energy by analogy with a point particle:

$$\frac{m}{2}\sum\nolimits_i \dot{q}_i^2 \to \int_a^b \frac{1}{2}\,\rho\, u_t^2\, dx. \tag{17.31}$$

So we would like to express the second term as the time derivative of a potential energy. To do so, we first integrate by parts to obtain

$$\partial_t \int_a^b \frac{1}{2}\rho u_t^2\, dx - [\tau u_t u_x]_a^b + \int_a^b \tau u_x u_{tx}\, dx = 0. \tag{17.32}$$

The boundary term vanishes if we use Dirichlet or free boundary conditions ($u = 0$ or $u_x = 0$ at $x = a, b$) or even periodic boundary conditions ($\tau(a) = \tau(b)$, $u(a,t) = u(b,t)$, $u_x(a,t) = u_x(b,t)$). Assuming $\tau(x)$ is independent of time, we get

$$\partial_t \int_a^b \rho \frac{u_t^2}{2}\, dx + \partial_t \int_a^b \frac{1}{2}\tau\, u_x^2\, dx = 0. \tag{17.33}$$

Thus the conserved energy is a sum of kinetic and potential energies

$$E = T + V = \int_a^b \left[\frac{1}{2}\rho u_t^2 + \frac{1}{2}\tau u_x^2\right] dx = \int_a^b \mathcal{E}\, dx \quad \text{with} \quad \frac{dE}{dt} = 0. \tag{17.34}$$

This calculation is valid even if ρ and τ depend on x. T is a sum of kinetic energies for vertical motion of the bits of string. T and V are separately nonnegative. Thus $E \geq 0$, with equality iff the string is in equilibrium (say $u(x,t) = 0$). The energy density $\mathcal{E}(x,t)$ 'moves around the string' in such a way that the total energy is conserved.

Interpretation of potential energy. The potential energy V is a gradient energy, it is proportional to the square of the gradient (slope) of the string profile. However, the string cannot have a nonzero constant slope if it is clamped at the same height at either end, it must bend. In fact, the potential energy can be regarded as an energy stored in the curvature/bending of the string. Assuming τ is independent of x, we integrate by parts to write $V = -\int \frac{1}{2}\tau u u_{xx}\, dx$. Here u_{xx} measures the curvature of the string profile. We also see that for fixed A_n and B_n, higher ($n \gg 1$) normal modes of oscillation $\sin(n\pi x/\ell)$ in (17.18) store more potential energy, since higher Fourier modes are more undulatory and have higher second spatial derivatives. □

We verify that the energy is conserved using (17.5) and integration by parts

$$\begin{aligned}\dot{E} &= \int [\rho u_t u_{tt} + \tau u_x u_{xt}]\, dx \\ &= \int \left[\rho u_t \frac{1}{\rho}(\tau u_x)_x - (\tau u_x)_x u_t + \partial_x(\tau u_x u_t)\right] dx = [\tau u_x u_t]_a^b = 0. \quad (17.35)\end{aligned}$$

We assumed that the boundary term $[\tau u_x u_t]_a^b$ vanishes. This is automatic if u or u_x vanish at the endpoints, which is the case for a clamped string (Dirichlet BCs) or a string with free boundary conditions ($u_x = 0$). Thus, the energy of the string is conserved. It was initially supplied to the string when set in motion through the initial gradients in the string profile $u_x(t = 0)$ and initial velocity of the string $u_t(t = 0)$.

17.6 Three local conservation laws for the wave equation

Energy. Energy is locally conserved in the sense that the energy density $\mathcal{E} = \frac{1}{2}\rho u_t^2 + \frac{1}{2}\tau u_x^2$ satisfies a *continuity equation* $\partial_t \mathcal{E} + \partial_x j = 0$ for an energy current density $j = -\tau u_x u_t$. Indeed,

$$\partial_t \mathcal{E} = \rho u_t u_{tt} + \tau u_x u_{xt} = u_t(\tau u_x)_x + (\tau u_x u_t)_x - (\tau u_x)_x u_t = (\tau u_x u_t)_x. \quad (17.36)$$

The presence of a local conservation law implies that the energy density flows like a fluid, it can move from place to place on the string due to the flux[14] of the energy current, but cannot jump discontinuously from one place to another. This is analogous to how the movement of electric charges is associated to an electric current. It also ensures that the total energy is 'globally' conserved if the current vanishes at the boundaries (taken to be at $x = 0$ and $x = \ell$ here) or is equal at the boundaries:

$$\dot{E} = \partial_t \int_0^\ell \mathcal{E}\, dx = -\int_0^\ell \partial_x j\, dx = j(0) - j(\ell) = 0. \quad (17.37)$$

This is the case for clamped ends, periodic BCs (u and u_x ℓ-periodic) as well as for decaying BCs on an infinite domain. In general, the rate of increase of energy in a fixed interval $[a,b]$ is equal to the energy flux across its boundary. If $j(a)$ and $j(b)$ are the inward and outward fluxes across the left and right boundaries, then

---

[14] The flux of a current $\boldsymbol{j}$ across a surface element $\hat{n}dS$ is $\boldsymbol{j} \cdot \hat{n}dS$. It measures the amount of charge crossing the surface per unit time. In 1d, the boundary surface of an interval $[a, b]$ is just the pair of points $x = a, b$ with oppositely directed outward unit normals ($\hat{x}$ at b and $-\hat{x}$ at a), so the flux of the current $\boldsymbol{j} = j\hat{x}$ is $j(b) - j(a)$.

$$\frac{d}{dt}\int_a^b \mathcal{E}\,dx = j(a) - j(b). \tag{17.38}$$

With suitable BCs, local conservation laws generally imply global conservation laws.

Transverse momentum. For free ($u_x(a) = u_x(b) = 0$) or periodic BCs, the quantity $Q = \int_a^b \rho u_t\,dx$ is a constant of motion. This is checked by integrating by parts:

$$\dot{Q} = \int_a^b \rho u_{tt}\,dx = \int_a^b (\tau u_x)_x\,dx = [\tau u_x]_a^b = 0. \tag{17.39}$$

Here, a, b could either or both be infinite. Physically, $\rho u_t dx$ is the vertical component of momentum of a string element. So Q is the total transverse momentum of the string. We expect it to be conserved provided there is no external vertical force, like gravity. Notice that Q is generally *not* conserved for Dirichlet BCs. This is to be expected in that case, since there would be a vertical force on the string at the clamps.

Like energy, transverse momentum too is locally conserved. What we mean is that we can find a current density j such that $\partial_t(\rho u_t) + \partial_x j = 0$. In fact, using the wave equation $\rho u_{tt} = (\tau u_x)_x$ we find that the required current density is $j = -\tau u_x$:

$$\partial_t(\rho u_t) - \partial_x(\tau u_x) = 0. \tag{17.40}$$

We say that the wave equation can be expressed in local conservation form.

Longitudinal momentum. There is another conserved momentum if the total horizontal (longitudinal) force vanishes and ρ and τ are independent of x. This longitudinal momentum[15] is $P = \int_a^b \rho u_t u_x\,dx$. It is conserved with periodic BCs on (a,b), a limiting case of which is decaying BCs on $(-\infty,\infty)$. In fact, using (17.5),

$$\begin{aligned}\dot{P} &= \int_a^b \rho\,(u_{tt}u_x + u_t u_{xt})\,dx = \int_a^b \left[\tau u_{xx}u_x + \frac{1}{2}\rho(u_t^2)_x\right] dx \\ &= \int_a^b \left[\frac{1}{2}\tau u_x^2 + \frac{1}{2}\rho u_t^2\right]_x dx = 0.\end{aligned} \tag{17.41}$$

---

[15] Despite the name ‘longitudinal momentum’, the string does not move longitudinally. As we will see in Sect. 17.8, P arises from a symmetry of the wave equation (for suitable BCs) and associated Lagrangian under longitudinal translations. Momentum is the name given to the Noether conserved quantity following from space translation-invariance.

It is generally *not* conserved for Dirichlet BCs. P too arises from a local conservation law, with the current given by the negative of the energy density[16]:

$$\partial_t(\rho u_t u_x) = \left[\frac{\tau}{2}u_x^2 + \frac{\rho}{2}u_t^2\right]_x \quad \Rightarrow \quad (\rho u_t u_x)_t - \mathcal{E}_x = 0. \tag{17.42}$$

It turns out that Q and P may be obtained from symmetries of the wave equation via Noether's theorem (see Sect. 17.8). To understand this, we will use a Lagrangian formulation of the wave equation.

17.7 Lagrangian and Hamiltonian for stretched string

The possible instantaneous configurations of a vibrating stretched string are the heights $u(x)$ for $0 \leq x \leq \ell$. So the configuration space is a space of functions, it is not finite-dimensional. The generalized coordinates are the values of the function $u(x,t)$ for $0 \leq x \leq \ell$ at a given time t. The generalized velocities at time t are $u_t(x,t)$. We will show that a Lagrangian for small transverse oscillations of the stretched string is

$$L = \int_0^\ell \frac{1}{2}\left[\rho(u_t)^2 - \tau(u_x)^2\right] dx \equiv \int_0^\ell \mathcal{L}\, dx, \tag{17.43}$$

where $\mathcal{L}$ is called the Lagrangian density. This formula is simply $L = T - V$, obtained from our earlier formula for the conserved energy $E = T + V$ (17.34). Similar formulae hold for the electromagnetic field; $\mathcal{L} = \frac{1}{2}(\boldsymbol{E}^2 - \boldsymbol{B}^2)$ and $\mathcal{H} = \frac{1}{2}(\boldsymbol{E}^2 + \boldsymbol{B}^2)$ where $\boldsymbol{E}$ and $\boldsymbol{B}$ are the electric and magnetic fields in Heaviside-Lorentz units (see Footnote 40 of Sect. 2.7*). The analogy is even closer if $\boldsymbol{E}$ and $\boldsymbol{B}$ are expressed as derivatives of the scalar and vector potentials as in Prob. B.12.

The principle of extremal action states that the equations of motion are the conditions for the action $S = \int_{t_1}^{t_2} L dt$ to be stationary for arbitrary small variations $u(x,t) \to u(x,t) + \delta u(x,t)$ holding the initial and final string profile $u(x,t_1)$ and $u(x,t_2)$ fixed. In other words, we ask for the 'trajectory' $u(x,t)$ of the string for times $t_1 \leq t \leq t_2$ for prescribed initial and final profiles. The trajectory is the $u(x,t)$ for which δS vanishes to first order in small variations $\delta u(x,t)$. If we view $u(x,t)$ as defining a surface over a rectangle ($0 \leq x \leq \ell$, $t_1 \leq t \leq t_2$) in the x-t plane, then $u + \delta u$ represents a nearby surface which coincides with the original surface along the edges $t = t_1, t_2$ ($\delta u(x,t_1) = \delta u(x,t_2) = 0$). This is illustrated in Fig. 17.7.

Euler-Lagrange equations. In general, for a Lagrangian density $\mathcal{L}$ that depends on u and its time and space derivatives u_t, u_x, u_{xx}, the Euler-Lagrange conditions for S to be stationary (subject to suitable BCs such as clamped, decaying, etc.) are

$$\frac{\partial}{\partial t}\frac{\partial \mathcal{L}}{\partial u_t} = \frac{\partial \mathcal{L}}{\partial u} - \frac{\partial}{\partial x}\left(\frac{\partial \mathcal{L}}{\partial u_x}\right) + \partial_x^2\left(\frac{\partial \mathcal{L}}{\partial u_{xx}}\right). \tag{17.44}$$

---

[16] There are similar globally and locally conserved quantities in electromagnetism. The Maxwell equations in the absence of sources conserve energy, the three components of linear momentum (the Poynting vector) and three components of angular momentum of the electromagnetic field. Here too, the energy current vector and momentum density vector are essentially the same. In fact, energy, linear and angular momentum are conserved for any system of fields that is time-translation, space-translation and rotation invariant. One use of conserved quantities is to check the accuracy of numerical schemes used to solve the equations.

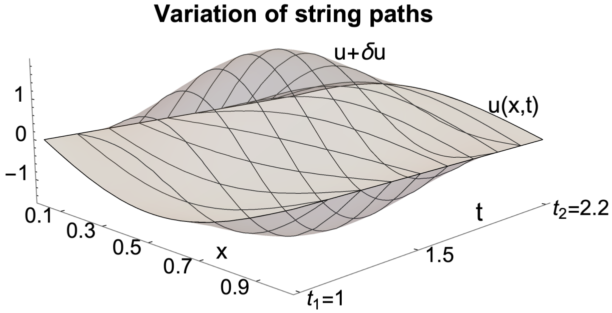

Figure 17.7: Infinitesimal variation $u(x,t)+\delta u(x,t)$ of a 'path' $u(x,t)$ of a stretched string clamped at $x=0, \ell=1$. The variation is such that the initial and final configurations are held fixed $\delta u(x,t_1)=\delta u(x,t_2)=0$ for all x with $t_1=1$ and $t_2=2.2$. The mesh curves give the instantaneous string height profiles for u and $u+\delta u$ at some intermediate times. Due to Dirichlet boundary conditions, $u(0,t)=u(\ell,t)=\delta u(0,t)=\delta u(\ell,t)=0$ at all times. The surfaces $u(x,t)$ and $(u+\delta u)(x,t)$ over the rectangle $[0,\ell]\times[t_1,t_2]$ in the x-t plane are seen to intersect in this example. Compare with Fig. 3.3.

To see this, we simply set the first variation of the action $S=\int \mathcal{L} dx\, dt$ to zero after integrating by parts in t in the 2^{nd} term, x in the 3^{rd} term and twice in x in the 4^{th} term. Up to boundary terms, we get:

$$\begin{aligned}\delta S &= \int_{t_1}^{t_2}\int_0^\ell \left[\frac{\partial \mathcal{L}}{\partial u}\delta u+\frac{\partial \mathcal{L}}{\partial u_t}\delta u_t+\frac{\partial \mathcal{L}}{\partial u_x}\delta u_x+\frac{\partial \mathcal{L}}{\partial u_{xx}}\delta u_{xx}\right] dx\, dt \\ &= \iint \left[\frac{\partial \mathcal{L}}{\partial u}-\partial_t\left(\frac{\partial \mathcal{L}}{\partial u_t}\right)-\partial_x\left(\frac{\partial \mathcal{L}}{\partial u_x}\right)+\partial_x^2\left(\frac{\partial \mathcal{L}}{\partial u_{xx}}\right)\right]\delta u\, dx\, dt. \quad (17.45)\end{aligned}$$

Since $\delta u(x,t)$ is arbitrary for $0<x<\ell$ and $t_1<t<t_2$, the integrand must vanish, giving us (17.44). The boundary terms from the first two integrations by parts are

$$\int_0^\ell dx\left[\frac{\partial \mathcal{L}}{\partial u_t}\delta u\right]_{t_1}^{t_2} \quad \text{and} \quad \int_{t_1}^{t_2} dt\left[\frac{\partial \mathcal{L}}{\partial u_x}\delta u\right]_0^\ell. \quad (17.46)$$

The integrand in the first case vanishes since $\delta u(x,t_1)=\delta u(x,t_2)=0$. The second integrand vanishes if, say, the variations respect clamped ($\delta u(0,t)=\delta u(\ell,t)=0$) or decaying BCs or even Neumann BCs as $\frac{\partial \mathcal{L}}{\partial u_x}\propto u_x$ for the Lagrangian proposed. Try to show that the boundary terms coming from two integrations by parts in the 4^{th} term also vanish subject to suitable BCs.

For the Lagrangian density in (17.43), the EL equation is $\partial_t(\rho u_t)=\partial_x(\tau u_x)$ or $\rho u_{tt}=\partial_x(\tau u_x)$ since $\rho(x)$ is not dependent on time. When ρ,τ are constants, this reduces to the familiar form of the wave equation $u_{tt}=c^2u_{xx}$ with $c^2=\tau/\rho$.

Conjugate momentum. The momentum conjugate to the coordinate $u(x,t)$ is defined as the variational or functional derivative:

$$\pi(x,t)=\frac{\delta L}{\delta u_t(x)}=\rho u_t(x,t). \quad (17.47)$$

Variational derivatives are evaluated using the same rules as for partial derivatives: linearity and the Leibniz rule, treating u and u_t as independent. Just as the basic partial derivative $\frac{\partial x^i}{\partial x^j} = \delta^i_j$ is expressed in terms of the Kronecker delta, the basic variational derivative is written in terms of the Dirac delta:

$$\frac{\delta u(x)}{\delta u(y)} = \delta(x-y), \quad \frac{\delta u_x(x)}{\delta u(y)} = \partial_x \delta(x-y), \ldots \quad \text{and} \quad \frac{\delta u_t(x)}{\delta u_t(y)} = \delta(x-y). \tag{17.48}$$

Thus, the second term in (17.43) does not contribute and we get

$$\frac{\delta L}{\delta u_t(x)} = \int \rho u_t(y) \frac{\delta u_t(y)}{\delta u_t(x)} dy = \int \rho u_t(y) \delta(x-y) dy = \rho u_t(x). \tag{17.49}$$

Hamiltonian. The Hamiltonian is the Legendre transform of the Lagrangian

$$H[u,\pi] = \text{ext}_{u_t} \int_0^\ell \left[\pi u_t - \mathcal{L}\right] dx = \int_0^\ell \left[\frac{\pi^2}{\rho} - \frac{\rho}{2}\frac{\pi^2}{\rho^2} + \frac{\tau}{2} u_x^2\right] dx = \int_0^\ell \left[\frac{\pi^2}{2\rho} + \frac{\tau u_x^2}{2}\right] dx. \tag{17.50}$$

The extremization is with respect to the ‘velocities’ $u_t(x,t)$ at *all* x. The conditions for extrema recover the definition of the conjugate momentum $\pi = \delta L/\delta u_t$:

$$\frac{\delta}{\delta u_t(y)} \int_0^\ell \left[\pi(x) u_t(x) - \mathcal{L}\right] dx = 0. \tag{17.51}$$

Evidently, H is the energy expressed in terms of u and π instead of u and u_t. Integrating by parts assuming clamped or free boundaries, we may also express it as

$$H[u,\pi] = \int_0^\ell \left[\frac{1}{2\rho}\pi^2 - \frac{1}{2} u (\tau u_x)_x\right] dx \quad \text{assuming} \quad [\tau u u_x]_0^\ell = 0. \tag{17.52}$$

Hamilton’s equations. Hamilton’s equations are the first order equations

$$u_t(x) = \frac{\delta H}{\delta \pi(x)} = \frac{\pi(x)}{\rho} \quad \text{and} \quad \pi_t(x) = -\frac{\delta H}{\delta u(x)} = (\tau u_x)_x. \tag{17.53}$$

Here, the variational derivatives are calculated treating u and π as independent. For instance, from (17.50), we get for $0 < y < \ell$,

$$\begin{aligned} \frac{\delta H}{\delta u(y)} &= \int \frac{\tau}{2} 2 u_x \frac{\delta u_x(x)}{\delta u(y)} dx = \int \tau u_x \partial_x \delta(x-y) dx \\ &= -\int (\tau u_x)_x \delta(x-y) dx = -(\tau u_y)_y. \end{aligned} \tag{17.54}$$

We have integrated by parts in the penultimate step. The boundary term $[\tau u_x \delta(x-y)]_0^\ell$ does not contribute[17] since $\delta(x-y)$ vanishes for $x = 0, \ell$. Combining Hamilton’s equations, we get the 2nd order wave equation $\rho u_{tt} = (\tau u_x)_x$ or $u_{tt} = c^2 u_{xx}$ for constant tension, as desired.

---

[17] It would also not contribute for Neumann BCs where $u_x(0) = u_x(\ell) = 0$.

The equal-time **Poisson brackets** between canonically conjugate variables are

$$\{u(x), \pi(x')\} = \delta(x - x') \quad \text{and} \quad \{u(x), u(x')\} = \{\pi(x), \pi(x')\} = 0. \qquad (17.55)$$

The equations of motion written using PBs take the form $\partial_t f = \{f, H\}$ for any dynamical variable f. Taking $f = u(x,t)$ we get

$$\begin{aligned} u_t &= \int_0^\ell \left\{ u(x), \frac{\pi(y)^2}{2\rho} + \frac{\tau u_y^2}{2} \right\} dy \\ &= \int_0^\ell \left[\frac{\pi(y)}{\rho} \{u(x), \pi(y)\} + \tau u_y \partial_y \{u(x), u(y)\} \right] dy \\ &= \int_0^\ell \frac{\pi(y)}{\rho} \delta(x-y) dy = \frac{\pi(x)}{\rho}. \end{aligned} \qquad (17.56)$$

Similarly, we verify in Prob. 17.9 that $\partial_t \pi(x,t) = \{\pi(x), H\}$ gives the second of Hamilton's equations in (17.53).

17.8 Conserved quantities from Noether's theorem

The simplest version of Noether's theorem in classical mechanics (Sect. 3.10) states that if the Lagrangian is invariant under the infinitesimal coordinate transformation $q^i \to q^i + \delta q^i$, then the quantity $Q = \sum_i p_i \delta q^i$ is conserved, $\dot{Q} = 0$. The generalization to our system of fields is that if $u(x) \to u(x) + \delta u(x)$ is an infinitesimal symmetry of the Lagrangian, then $Q = \int \pi(x,t) \delta u(x,t) dx$ is conserved.

The Lagrangian $L = \frac{1}{2} \int \left(\rho u_t^2 - \tau u_x^2 \right) dx$ (17.43) is invariant under translations in u and x. So we may use Noether's theorem to find the corresponding conserved quantities. They turn out to be the conserved momenta Q and P found in Sect. 17.6.

Under an infinitesimal translation $x \to x + \epsilon$, $u(x) \to u(x+\epsilon) \approx u(x) + \epsilon u_x$. The Lagrangian is translation-invariant in x provided the string is homogeneous (τ, ρ independent of x) and we have either periodic or decaying BCs. Dirichlet BCs would violate translation invariance due to the fixed positions of the clamps. Since $\pi = \rho u_t$, Noether's theorem implies the conservation of $\epsilon \int \rho u_t u_x \, dx$, which we recognize as being proportional to the longitudinal momentum P of Sect. 17.6.

Under a translation (constant shift) $u \to u + \epsilon$, the Lagrangian (17.43) does not change since it only involves derivatives of u. If, in addition, the BCs are also invariant (this is the case for free boundary conditions or periodic BCs, but not for Dirichlet BCs), then we may apply Noether's theorem to deduce that $Q = \int \pi(x) \delta u(x) \, dx = \epsilon \int \rho u_t \, dx$ is conserved. Omitting the constant ϵ we recover the conserved transverse momentum of Sect. 17.6.

The transverse momentum Q may be interpreted as the conserved momentum conjugate to a cyclic coordinate in the Lagrangian (17.43). Indeed, suppose we have periodic BCs (by this we mean that u and u_x each takes the same value at $x = 0$ and at $x = \ell$), then we may expand the height $u(x,t)$ in a Fourier series[18]

$$u(x,t) = a_0(t) + \sum\nolimits_{n \geq 1} a_n(t) \cos\left(\frac{2n\pi x}{\ell} \right) + \sum\nolimits_{n \geq 1} b_n(t) \sin\left(\frac{2n\pi x}{\ell} \right). \qquad (17.57)$$

---

[18] Note that $\cos(\pi x/\ell)$ and the derivative of $\sin(\pi x/\ell)$ do not satisfy periodic boundary conditions. This is the reason for the factor of 2 in the arguments.

The zeroth Fourier mode $a_0 = \frac{1}{\ell}\int_0^\ell u(x,t)\,dx$ is the average height. Using orthogonality of sines and cosines and the fact that the average value of their squares over a period is a half, we get, for $n \geq 1$,

$$a_n = \frac{2}{\ell}\int_0^\ell u(x)\cos\left(\frac{2n\pi x}{\ell}\right) \quad \text{and} \quad b_n = \frac{2}{\ell}\int_0^\ell u(x)\sin\left(\frac{2n\pi x}{\ell}\right). \tag{17.58}$$

The infinite collection of Fourier coefficients a_0, a_n and b_n furnish coordinates on the configuration space of the vibrating string. Thus, we are changing variables from the values of u at various x to the Fourier coefficients. We find

$$\begin{aligned} u_t &= \dot{a}_0 + \sum\nolimits_{n\geq 1}\left[\dot{a}_n\cos(2n\pi x/\ell) + \dot{b}_n\sin(2n\pi x/\ell)\right] \quad \text{and} \\ u_x &= (2\pi/\ell)\sum\nolimits_{n\geq 1} n\left[-a_n\sin(2n\pi x/\ell) + b_n\cos(2n\pi x/\ell)\right]. \end{aligned} \tag{17.59}$$

The new velocities are $\dot{a}_0, \dot{a}_n, \dot{b}_n$. The Lagrangian is expressed in terms of the Fourier coefficients and their velocities using orthogonality of the sines and cosines:

$$L = \int_0^\ell \left[\frac{1}{2}\rho u_t^2 - \frac{1}{2}\tau u_x^2\right] dx = \frac{\rho\ell}{2}\left[\dot{a}_0^2 + \frac{1}{2}\sum_{n\geq 1}\left(\dot{a}_n^2 + \dot{b}_n^2\right)\right] - \frac{\tau\pi^2}{\ell}\sum_{n=1}^{\infty} n^2(a_n^2 + b_n^2). \tag{17.60}$$

All Fourier coefficients would be cyclic if $\tau = 0$. For nonzero tension, we see that a_0 is the only cyclic coordinate, it does not appear in L, though its velocity $\dot{a}_0$ does. The momentum conjugate to the 'zero mode' a_0 is

$$\pi_0 = \frac{\partial L}{\partial \dot{a}_0} = \frac{\partial T}{\partial \dot{a}_0} = \rho\ell\dot{a}_0 = \rho\ell\frac{1}{\ell}\int_0^\ell u_t\,dx = \int_0^\ell \rho u_t\,dx = Q. \tag{17.61}$$

So the conserved charge Q corresponding to symmetry under translations in the height $u \to u + \epsilon$ is the same as the momentum conjugate to the cyclic coordinate a_0.

In fact, the wave equation admits an *infinite number* of conserved quantities. See Prob. 17.16 for a way to identify them using the above Lagrangian.

17.9 Dispersion relation, phase and group velocities

As discussed in Sect. 17.1 and Prob. 17.2, the 1d wave equation $u_{tt} = c^2 u_{xx}$ admits 'traveling wave' solutions of the form $u \propto \sin(kx - \omega t)$ or $\cos(kx - \omega t)$ [which are conveniently regarded as the real and imaginary parts of $e^{i(kx-\omega t)}$], provided the angular frequency ω and wave number k satisfy the *dispersion relation* $\omega^2 = c^2k^2$. For $k > 0$ and $c > 0$, the two solutions $\omega = \pm ck$ correspond to right- and left-moving waves (such as $\cos(kx - ckt)$ and $\cos(kx + ckt)$) that move at the *phase velocities* $c_p = \omega/k = \pm c$. Similar waves played a role in d'Alembert's solution of the wave equation in Sect. 17.4, where the idea of a traveling wave and its speed of propagation were introduced. The name phase velocity is used for ω/k, since it determines the propagation velocity of a point $x(t)$ at which the phase of the exponential $e^{i(kx-\omega t)}$ takes a specified value. Indeed, putting $kx(t) - \omega t = kx_0$ implies $x(t) = x_0 + (\omega/k)t$.

Analogously, the 1^{st} order wave equation $u_t = cu_x$ has the dispersion relation $\omega = -ck$ and admits only unidirectional propagation for given k: left-moving waves for $k, c > 0$. Similarly, $u_t = -cu_x$ admits only right-moving waves with dispersion relation $\omega = ck$. More generally, the 3d wave equation $u_{tt} = c^2\boldsymbol{\nabla}^2 u$ admits plane wave solutions $u_{\boldsymbol{k}}(\boldsymbol{r}, t) = e^{i(\boldsymbol{k}\cdot\boldsymbol{r}-\omega t)}$ for any wave vector $\boldsymbol{k}$ provided the angular frequency satisfies the dispersion relation $\omega^2 = c^2|\boldsymbol{k}|^2$. We call this a plane wave as $u_{\boldsymbol{k}}(\boldsymbol{r}, t)$ is constant on any plane orthogonal to the wave vector $\boldsymbol{k}$. These planes are the 'wavefronts'. If we take $\omega = c|\boldsymbol{k}|$, this wave travels in the direction of $\boldsymbol{k}$ at a phase velocity $c_p = \omega/k = c$.

In all these cases, the phase speeds of all Fourier modes k are the same. Such an equation is called nondispersive. More general solutions of these linear equations may be obtained by superposing plane waves with different wave numbers k:

$$u(x,t) = \int \tilde{u}(k) e^{i(kx-\omega(k)t)}\, dk. \tag{17.62}$$

If $\tilde{u}(k)$ is a function peaked around some $k = k_0$, the resulting $u(x, t)$ typically looks like a wave packet peaked around some $x_0(t)$. Since the individual modes travel at the same speed, they tend to stay together and the wave packet retains its shape as it moves with the same speed c_p.

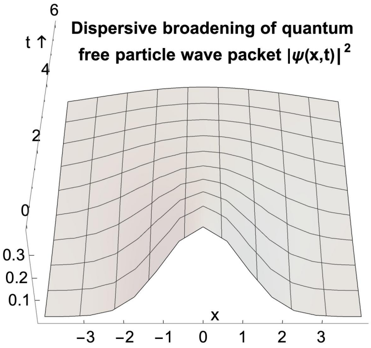

Figure 17.8: Dispersive broadening of a free particle Gaussian wave packet in 1d quantum mechanics. The probability density $|\psi(x,t)|^2 = e^{-x^2/2a(t)^2}/\sqrt{2\pi}a(t)$ where $a(t) = (a^2 + \hbar^2 t^2/4a^2m^2)^{\frac{1}{2}}$ is plotted over the x-t plane in units where the initial width $a = 1$ and the particle mass and Planck's constant $m = \hbar = 1$.

Dispersive evolution. On the other hand, for a dispersive equation such as the free particle Schrödinger wave equation $i\hbar\dot{\psi}(x,t) = -(\hbar^2/2m)\psi''(x)$, modes with different wave numbers k move at different phase speeds $c_p = \hbar k/2m$ and a wave packet tends to spread out (see Fig. 17.8 and Prob. 17.10). It can be shown that the packet as a whole moves at the group velocity $c_g = \frac{d\omega}{dk}$ evaluated at $k = k_0$. This is obtained using a stationary phase approximation to evaluate the Fourier integral (17.62) for $u(x,t)$ to find that $x_0(t) \approx c_g t$. The argument is as follows. Let us suppose that $\tilde{u}(k)$ is peaked around k_0, then the primary contribution to the integral can be expected to come from a neighborhood of k_0. Now, at any fixed time, the phase $e^{i(kx-\omega(k)t)}$ is a unimodular complex number pointing in different directions in the complex plane for different values of k. For most values of x, the phase is a rapidly changing function of k, resulting in efficient cancellations among contributions from different values of k in the vicinity of k_0. This is called destructive interference and produces a small value of $u(x,t)$. On the other hand, constructive interference can happen around certain special values of x where the phase is roughly constant, i.e., stationary with respect to small changes in k around k_0. The condition for the phase to be stationary is

$$x - \frac{d\omega}{dk}t = 0 \quad \text{implying that} \quad x_0(t) = c_g(k_0)t. \tag{17.63}$$

Thus, we see that the location $x_0(t)$ of the peak in $u(x,t)$ moves with the group velocity $c_g(k_0) = d\omega/dk$ evaluated at $k = k_0$. ☐

17.10* Lax pair for the first order wave equation

Recall from Sect. 11.9* that a Lax formulation involves finding a pair of matrices (or operators) L and A whose matrix elements depend on the dynamical variables in such a way that the Lax equation $L_t = [L, A]$ is equivalent to the equations of motion. Since the Lax equation is first order in time, it is particularly suited to equations of motion that are first order in time.

The wave equation $u_{tt} = c^2 u_{xx}$ is second order in time. We could write it as the pair of first order Hamilton equations (17.53). However, there is a somewhat simpler option that will allow us to illustrate the idea of a Lax pair for a continuum system. Recall from d'Alembert's approach of Sect. 17.4, that solutions of the wave equation can be expressed as sums of solutions of the pair of first order wave equations $u_t \pm c u_x = 0$. Thus, we will look for a Lax pair for the first order wave equation

$$u_t = -c u_x, \tag{17.64}$$

which describes right-moving waves for $c > 0$. Left-moving waves may be got by reversing the sign of c. Since this is a PDE for a system with infinitely many degrees of freedom, we expect to need Lax matrices that are infinite-dimensional. So it makes sense to look for differential operators L and A. In fact, one can find a Lax pair almost by inspection. The obvious choice for L is the multiplication operator $L_0 = u$, from which we get $\partial_t L_0 = u_t$, as desired. Next, A must be a differential operator such that $[u, A] = -c u_x$. Now notice[19] that for any function f,

$$[u, \partial_x] f = u f_x - \partial_x(uf) = -u_x f \quad \text{so that} \quad [u, \partial_x] = -u_x. \tag{17.65}$$

Thus, we immediately arrive at the choice $A = c\partial_x$ to supplement the Lax operator $L_0 = u$. While this is a legitimate Lax pair for the unidirectional wave equation $u_t + c u_x = 0$, it has its limitations. For instance, the eigenvalue problem for L_0, namely $u\psi = \lambda\psi$ for a nonconstant wave height $u(x)$ (that must decay to 0 as $|x| \to \infty$) has no nontrivial/nonsingular[20] solutions for the wave function $\psi(x)$.

---

[19] In quantum mechanics, this is the commutator of a potential u with the momentum operator divided by $-i\hbar$.

[20] For $(u - \lambda)\psi$ to vanish, either u must be constant and equal to the eigenvalue λ or ψ must

Schrödinger Lax operator. To find a more convenient Lax operator, we recall that one may add to L_0 an operator that is independent of time and commutes with $A = c\partial_x$. Derivatives commute, so we are free to add to L_0 constant multiples of ∂_x or ∂_x^2, etc. Since $L_0 = u$ is Hermitian for real u, it would be simplest to retain this feature, which would also guarantee that its conserved eigenvalues are real. The simplest possibilities are

$$L_1 = -i\partial_x + u \quad \text{and} \quad L_2 = -\partial_x^2 + u. \tag{17.66}$$

The signs and factors are chosen to remind us of the momentum $(p = -i\hbar\partial_x)$ and kinetic energy $(p^2/2m = -(\hbar^2/2m)\partial_x^2)$ operators in quantum mechanics. The operator L_2 appears in Sturm-Liouville theory [24] and is also the quantum Hamiltonian operator in the Schrödinger equation for a particle in the 1d potential u, whence it is called the Schrödinger operator. The eigenvalue problem for the 1d Schrödinger operator is very well studied and is easily interpreted in terms of the bound and scattering stationary states (discrete and continuous energy levels) of a particle in the potential u. The other option L_1 is perhaps less familiar, although it can be interpreted as a covariant derivative or as the mechanical momentum of a charged particle minimally coupled to a one-dimensional magnetic 'vector potential' u (see Sect. 3.23*). The corresponding eigenvalue problem $L_1\psi = \lambda\psi$ has a continuous spectrum consisting of all real λ with eigenfunctions $\psi(x) = \psi(x_0)\exp\int_{x_0}^{x}(\lambda - u(x'))dx'$.

On balance, one opts to work with the Schrödinger operator L_2, due to its familiarity, rich spectral features and physical interpretation. This turns out to pay handsome dividends: the same Schrödinger Lax operator will turn out to work for the KdV equation as well as for an infinite 'KdV hierarchy' of integrable nonlinear wave equations with suitable choices for the second Lax matrix A. For instance, in Prob. 17.20 we verify that the Lax pair

$$L = -\partial_x^2 + u \quad \text{and} \quad A = 4\partial_x^3 - 6u\partial_x - 3u_x \tag{17.67}$$

leads to the KdV equation $u_t - 6uu_x + u_{xxx} = 0$.

Infinitely many conserved quantities. Having found a Lax pair for $u_t + cu_x = 0$, the obvious next step is to use it to find conserved quantities. It turns out that this is more involved than for the mechanical systems of Sect. 11.9.2*. The main complication is that $L = -\partial_x^2 + u$ for a u that vanishes as $x \to \infty$ is an unbounded operator on an infinite-dimensional vector space. Its spectrum is not bounded above and so $\operatorname{tr} L^n$ is formally infinite. The eigenvalues are still conserved, but it is not clear whether or how these can be expressed as integrals of functions of u and its spatial derivatives. Fortunately, the physical interpretation of the eigenvalue problem $L\psi = \lambda\psi$ as the study of bound and scattering states in the potential u comes to our rescue. One can show that in addition to the spectrum, the transmission amplitude for scattering in the potential $u(x,t)$ is conserved if u satisfies the first order wave equation. Exploiting such ideas, one can find an infinite sequence of local conserved quantities for (17.64).

---

vanish. If $u = x$ then ψ can be taken to be the Dirac delta distribution. For more general u, ψ would have to vanish outside the support of u and be infinite on the support of u. These types of singular eigenfunctions are not convenient for our purposes.

The first few of these are:

$$Q_0 = \int \frac{u}{2}\, dx, \qquad Q_1 = \int \frac{u^2}{2}\, dx, \quad Q_2 = \int \left(\frac{u_x^2}{2} + u^3 \right)\, dx$$
$$\text{and} \qquad Q_3 = \frac{1}{2} \int \left[5u^4 + 10uu_x^2 + u_{2x}^2 \right]\, dx. \tag{17.68}$$

The procedure to obtain these is sketched in [77], while additional details may be found in [32, 34]. The virtue of these methods based on scattering theory is their generality. It turns out that Q_n are conserved not just for the first order wave equation but also for the KdV equation and the rest of the equations in the KdV hierarchy! Similar methods also apply to other field equations (such as the nonlinear Schrödinger equation and the sine-Gordon equation) in 1d that admit a Lax representation.

Here, we will settle for less and use elementary methods to derive another infinite sequence of conserved quantities for the wave equation (17.64). In fact, the wave equation is in local conservation form $u_t + cu_x = 0$. So $C_1 = \int_{-\infty}^{\infty} u\, dx$ is conserved subject to decaying boundary conditions ($u \to 0$ as $x \to \pm\infty$). Multiplying (17.64) by u leads to another local conservation law: $(u^2)_t + c(u^2)_x = 0$. Thus, $C_2 = \int_{-\infty}^{\infty} u^2\, dx$ is a second conserved quantity. Proceeding this way, we obtain an infinite sequence of local conservation laws

$$(u^n)_t + c(u^n)_x = 0, \quad \text{so that} \quad C_n = \int_{-\infty}^{\infty} u(x,t)^n\, dx \tag{17.69}$$

is conserved for any $n = 1, 2, 3, \ldots$.

17.11 Problems

1. **Variable tension and density.** Consider small transverse vibrations of height $u(x,t)$ of a stretched string of variable tension $\tau(x)$ and density $\rho(x)$. Find the vertical force on a string segment and show that Newton's second law implies the generalized wave equation

$$\rho(x) u_{tt} = \partial_x \left(\tau(x) u_x \right). \tag{17.70}$$

2. Find the **dispersion relation** expressing the angular frequency ω as a function of k which ensures that the plane wave $\sin(kx - \omega(k)t)$ is a solution of the 1d **wave equation** $u_{tt} = c^2 u_{xx}$. Deduce why the equation is called hyperbolic.
3. **Dispersion relation for heat equation.** Find the dispersion relation expressing the angular frequency ω as a function of wave number k, which ensures that the plane wave $e^{i(kx-\omega(k)t)}$ is a solution of the 1d heat equation $u_t = \alpha u_{xx}$. Deduce that the resulting solution is damped in time and observe why the heat equation is called parabolic.
4. **Helmholtz equation.** Find the relation among the components of the wave vector k_x, k_y, which ensures that the ansatz $u = e^{i(k_x x + k_y y)}$ is a solution of the Helmholtz equation $u_{xx} + u_{yy} = -\kappa^2 u$. Plot the curve defined by the relation in the k_x-k_y plane. Deduce why the Helmholtz equation is called elliptic.

5. Derive (17.28) for $\partial_t u$ from the **d'Alembert solution** of the wave equation (17.27).
6. Find $\partial_t^2 u$ from (17.28) and also from **d'Alembert's solution** (17.27) using the wave equation. Verify that the two agree.
7. Express the **potential energy** of a stretched string $V = \int_0^\ell \frac{1}{2}\tau u_x^2 \, dx$ in terms of the second spatial derivative of the height u, assuming the tension τ is independent of location. Does the expression you obtain hold for clamped and/or free boundaries?
8. **Conservation of energy.** Use the wave equation to directly verify that the energy $E = \int (\frac{1}{2}\rho u_t^2 + \frac{1}{2}\tau u_x^2)\, dx$ of a string is conserved subject to both clamped and free boundary conditions. You may assume that u is such that time derivatives can be taken inside the integral and that ρ and τ are both constants.

$*$9. Use the canonical PBs (17.55) and Hamiltonian (17.50) to show that **Hamilton's equation** $\partial_t \pi(x,t) = \{\pi(x), H\}$ for the stretched string reduces to $\pi_t = (\tau u_x)_x$. Hint: derivatives can be pulled out of PBs $\{u(y), u_x(x)\} = \partial_x \{u(y), u(x)\}$.

10. **Dispersive and nondispersive waves.** For linear PDEs with constant coefficients such as the wave equation, we may associate a dispersion relation between angular frequency ω and wave number k (more generally wave vector $\boldsymbol{k}$). By this we mean the relation between ω and k that must hold for the traveling wave $e^{i(kx-\omega t)}$ to be a solution. Find the dispersion relation $\omega(k)$ for the following equations. In each case compute the phase speed $c_p = |\omega/k|$ and the group speed $c_g = |\frac{d\omega}{dk}|$. If the phase speed is independent of wave number, we say the equation is nondispersive. Classify the equations as dispersive/nondispersive.

    a. The d'Alembert wave equation $u_{tt} = c^2 u_{xx}$.
    b. The first order wave equation $u_t = c u_x$.
    c. The Fourier heat conduction equation $u_t = \alpha u_{xx}$.
    d. The linearized KdV equation $u_t = \beta u_{xxx}$.
    e. The Schrödinger wave equation $i\hbar\psi_t = -(\hbar^2/2m)\psi_{xx}$.

11. **Fourier series solution.** Consider the wave equation on the interval $[0,\ell]$, $u_{tt} = c^2 u_{xx}$ with Dirichlet BCs $u(0,t) = u(\ell,t) = 0$. The string is released from rest after being plucked upwards to form an isosceles triangle of height a.

    a. What is $u(x,0)$? Find the Fourier series representation of the initial height profile $u(x,0)$. How fast do the Fourier coefficients decay?
    b. Write down the Fourier series for $u(x,t)$ obeying the above initial and boundary conditions.
    c. Suppose $c = a = \ell = 1$. Give the formula for the Fourier coefficients and for $u(x,t)$. Plot the approximate wave height $u(x,0)$ at $t = 0$ by retaining 1,2,3 and 4 terms in the Fourier series.
    d. Plot a movie of an approximate solution to this initial value problem by truncating the Fourier series after 4 terms.

12. **Noether's theorem.** A version of Noether's theorem states that if $u \to u + \delta u$ is an infinitesimal symmetry of the Lagrangian, then the Noether charge $Q = \int \pi(x,t)\delta u(x,t)dx$ is conserved. Here π is the momentum conjugate to u and $L = \int(\frac{1}{2}\rho u_t^2 - \frac{1}{2}\tau u_x^2)dx$ is the Lagrangian for small transverse oscillations of a stretched string, say on $-\infty < x < \infty$ with decaying BCs.

    a. Consider small constant shifts $u \to u + \epsilon$. Show that L is invariant under such a shift and obtain the corresponding conserved quantity and interpret it.
    b. Consider small constant shifts $x \to x + \epsilon$. Find δu. Show that L is invariant under this infinitesimal transformation and obtain the corresponding Noether charge and verify that it is conserved.

13. **Factorizing the 2d Laplacian.** Suppose $z = x + iy$ and $\bar{z} = x - iy$ where x and y are real. Suppose f is a function of x and y or equivalently of z and $\bar{z}$.

    a. Express $\partial_z = \frac{\partial}{\partial z}$ and $\partial_{\bar{z}} = \frac{\partial}{\partial \bar{z}}$ as linear combinations of ∂_x and ∂_y when acting on f.
    b. Factorize the Laplace operator in two dimensions $\partial_x^2 + \partial_y^2$ just as we did for d'Alembert's wave operator.

14. **Uniqueness.** Suppose $u(x,t)$ and $\tilde{u}(x,t)$ are 2 solutions of the wave equation subject to the same ICs $u(x,0) = \tilde{u}(x,0) = h(x), \dot{u}(x,0) = \dot{\tilde{u}}(x,0) = v(x)$ and the same BCs, say clamped at $x = 0, l$. Use the conservation of energy to show that $u(x,t) = \tilde{u}(x,t)$, i.e., the solution of the initial-boundary value problem is unique. Hint: Consider $w(x,t) = u(x,t) - \tilde{u}(x,t)$. What can you say about w?

*15. **Euler-Lagrange equations.** Show that the boundary terms coming from two integrations by parts in the 4th term of (17.45) vanish subject to suitable BCs.

*16. **Conserved quantities for the wave equation.** We expressed the Lagrangian for the wave equation on an interval of length ℓ with periodic boundary conditions in terms of Fourier coefficients of the wave height u and their velocities (17.60):

$$L = \int_0^\ell \left[\frac{\rho}{2}u_t^2 - \frac{\tau}{2}u_x^2\right]dx = \frac{\rho\ell}{2}\left[\dot{a}_0^2 + \frac{1}{2}\sum_{n\geq 1}\left(\dot{a}_n^2 + \dot{b}_n^2\right)\right] - \frac{\tau\pi^2}{\ell}\sum_{n=1}^{\infty} n^2(a_n^2 + b_n^2). \tag{17.71}$$

a_0 is the only cyclic coordinate and its conjugate momentum $\pi_0 = \rho\ell\dot{a}_0$ is conserved. We can find additional cyclic coordinates by going to 'polar-coordinates' in the a_n, b_n planes. Let $a_n = r_n\cos\theta_n$ and $b_n = r_n\sin\theta_n$. (a) Write the Lagrangian in terms of a_0, r_n, θ_n and their velocities. (b) Identify infinitely many cyclic coordinates. What are the conserved conjugate momenta? Express them in terms r_n and θ_n as well as a_n and b_n (and their velocities). Give a descriptive name for these conserved quantities. Examine whether they could be associated to conservation laws.

*17. **KdV equation.** Consider the nonlinear KdV equation $u_t + 6uu_x + u_{xxx} = 0$ where $u(x,t)$ is a real wave amplitude for $-\infty < x < \infty$.

a. Express the KdV equation in local conservation form. Identify the locally conserved density and corresponding current density j. Hint: To do this does not require a Lagrangian.
b. What is the globally conserved quantity M that follows from this conservation law? Give suitable boundary conditions for which $dM/dt = 0$.
c. Multiply the KdV equation by u. Express the resulting equation in local conservation form, identify the density, current and globally conserved quantity.
d. A constant $u(x,t) = h$ is clearly a solution of the KdV equation. Consider a small perturbation $u = h + v$ and obtain a linear PDE for v, treating it as small compared to h. This is the linearized KdV equation.
e. Find the dispersion relation for the linearized KdV equation.
f. Find the phase and group velocities c_p and c_g for the linearized KdV equation.
g. Write the general solution of the linearized KdV equation.

$*$18. **Finite difference approximation to the second derivative.**

a. Write down an $\infty \times \infty$ real-symmetric matrix A that approximates the second derivative operator by considering finite differences of a function f of a real variable x with spatial increments δx.
b. Truncate the matrix A to three rows and three columns and find its eigenvalues and eigenvectors, assuming $\delta x = 1$ for simplicity.
c. Find a 5×5 truncation of the second derivative operator. Find its eigenvalues and eigenvectors. Plot the eigenvectors as discrete sequences. Write a computer program to do this for a 100×100 and 175×175 truncations. Look for any patterns.
d. What are the eigenvalues and eigenvectors of d^2/dx^2 on the real line?
e. Examine whether the eigenvalues and eigenvectors of the 3×3 and 5×5 and larger truncations approximate those of d^2/dx^2 in a suitable sense.

$*$19. For the **first order wave equation** $u_t + cu_x = 0$, find **local conservation laws** for which the globally conserved charges are Q_0, Q_1 and Q_2 given in (17.68).

$*$20. Show that the **Lax equation** $L_t = [L, A]$ for the pair $L = -\partial_x^2 + u$ and $A = 4\partial_x^3 - 6u\partial_x - 3u_x$ is equivalent to the **KdV equation** $u_t - 6uu_x + u_{xxx} = 0$.

Chapter 18

Heat diffusion equation and Brownian motion

In this chapter, we continue our exploration of continuum mechanics by studying the simplest model for diffusion: Fourier's heat equation. This is another of the basic linear partial differential equations of mathematical physics, like the elliptic Poisson and Laplace equations and the hyperbolic wave equation encountered earlier in Footnote 48 of Sect. 2.7* and in Chap. 17. However, as we will learn, Fourier's heat equation describes a dissipative process, that of heat conduction and is classified as a parabolic equation (see Prob. 17.3). Consequently, its solutions are not wave-like[1] as typified by those of d'Alembert's wave equation, but describe temperature distributions that usually approach a static equilibrium state which depends on the behavior at boundaries. The heat equation is often not encountered in a treatment of mechanics. This is because it usually arises from a treatment of a gas or solid, based not on microscopic laws of mechanics, but on Fourier's empirical macroscopic law of heat conduction[2]. However, the heat equation is central to continuum mechanics and we have a vested interest in discussing heat diffusion since it will provide a stepping stone to our treatment of velocity diffusion[3] in a viscous fluid in Sect. 19.16. Moreover, the heat conduction equation provides an important example of a dissipative system to complement the many conservative systems we have encountered in this book. Dissipation and diffusion are ubiquitous in nature and the heat equation is a simple equation for treating a large class of stochastic processes such as the diffusion of particles, temperature and velocity, Brownian motion and random walks. For example, the price of a stock-option as a function of time may be treated as a stochastic process. This is modeled by the Black-Scholes equation, which in appropriate variables is the heat equation. Generalizations of the heat equation include the renormalization group equation in quantum field theory and statistical physics and the equation for Ricci flow used to study the geometry of manifolds.

In Sect. 18.1, we begin by deriving the heat equation from Fourier's law of heat diffusion. Basic features and properties such as boundary conditions, its lack of invariance under time-reversal, its tendency to smooth the temperature profile, the maximum principle and the uniqueness of solutions to its initial value problem (IVP) are briefly discussed. Next, in Sect. 18.2, we discuss the separation of space and time variables in the heat equation. We synthesize separable solutions via Fourier series to find the solution of the IVP for the heat equation on a one-dimensional rod that is insulated at its ends. Section 18.3* concerns the heat kernel[4] for the heat equation on the infinite real line. The heat kernel consists of the matrix elements of a linear operator that can be used to evolve a temperature distribution forward in time. In this sense, it is similar to the time evolution matrix encountered in our treatment of small perturbations around a periodic solution in Sect. 13.4.2* or in defining Lyapunov exponents in Sect. 15.2* and the time evolution operator for the Schrödinger equation in quantum mechanics from Sect. 10.3*. Section 18.4 is devoted to Brownian motion. After an overview (Sect. 18.4.1) of the phenomenon and the role it played in the establishment of the molecular structure of matter, in Sect. 18.4.2* we present a random walk model for Brownian motion and explain the emergence of the diffusion equation in a probabilistic treatment of Brownian movement.

---

[1] Hyperbolic equations display what we intuitively mean by wave-like behavior, i.e., roughly oscillatory conservative propagation of disturbances. See [132] for more on this.

[2] Deriving the heat equation from molecular dynamics is more involved as it requires a coarse-graining or averaging over microscopic degrees of freedom to arrive at an effective equation for the macroscopic temperature.

[3] By this, we mean the diffusion of velocity from a fast-moving layer of fluid to a neighboring slow-moving layer resulting in a reduction of the velocity gradient.

18.1 Obtaining the heat equation and its basic properties

Suppose we have a body with some initial (absolute) temperature[5] distribution $T(\boldsymbol{r}, t = 0)$. We wish to know how this temperature distribution evolves with time. Empirically, it is found that the heat flux between bodies or parts of a body grows with the temperature difference. Fourier's law of heat diffusion states that the heat flux density vector (with units of energy per unit time crossing unit area normal to the heat flux vector) is proportional to the negative gradient in temperature

$$\boldsymbol{q} = -k\boldsymbol{\nabla} T \quad \text{where } k \text{ is the thermal conductivity.} \tag{18.1}$$

For a perfect thermal insulator, k would be zero. If $d\boldsymbol{S} = \hat{\boldsymbol{n}} dS$ is a small area (vector), then the heat flux across it (energy crossing it per unit time) is given by $\boldsymbol{q} \cdot d\boldsymbol{S}$.

Consider gas in a fixed volume V. The increase in internal energy

$$U = \int_V \rho c_v T(\boldsymbol{r}, t)\, d\boldsymbol{r}, \tag{18.2}$$

where T is the absolute temperature, must be due to the influx of heat across its surface ∂V. This is a consequence of the first law of thermodynamics, if we assume no work is done on the gas[6] and that there are no sources/sinks of energy inside the gas. Thus

$$\int_V \partial_t(\rho c_v T) d\boldsymbol{r} = -\int_{\partial V} \boldsymbol{q} \cdot \hat{\boldsymbol{n}}\, dS = \int_{\partial V} k\boldsymbol{\nabla} T \cdot \hat{\boldsymbol{n}}\, dS = k \int_V \boldsymbol{\nabla} \cdot \boldsymbol{\nabla} T\, d\boldsymbol{r}. \tag{18.3}$$

We used Gauss' divergence theorem to convert the surface integral to a volume integral taking $\hat{\boldsymbol{n}}$ to be the outward pointing normal to the surface. Here, c_v is the specific heat per unit mass at constant volume (since no work is done) and ρ is the density of the gas. Since the volume V is arbitrary, the integrands must be equal and Fourier's heat diffusion equation follows:

---

[4] The concept of an integral kernel was introduced in Footnote 24 of Chap. 1.

[5] Absolute temperature is defined through the 2$^{\text{nd}}$ law of thermodynamics. The Kelvin scale is a scale of absolute temperature.

[6] The first law of thermodynamics for a gas states that $\Delta U = \Delta Q + \Delta W$. Here, ΔU is the increase in internal energy of the gas, and it is a sum of the heat added ΔQ and the work ΔW done on the gas. If no work is done and there are no sources of heat in the interior, then ΔU must be due to the heat transferred across the boundary.

$$\frac{\partial T}{\partial t} = \alpha \boldsymbol{\nabla}^2 T \quad \text{where} \quad \alpha = \frac{k}{\rho c_v} \quad \text{is called the thermal diffusivity.} \tag{18.4}$$

The diffusivity $\alpha \geq 0$ has dimensions of area per unit time[7]. Since the heat equation is linear and only involves derivatives of temperature, we are free to rescale the absolute temperature or add a constant to it. Consequently, the heat equation applies even if we use the Centigrade or Fahrenheit scales in place of an absolute temperature scale such as the Kelvin scale.

Boundary and initial conditions (BCs and ICs). Interesting boundary conditions for the heat equation arise when the temperature on the boundary of the body is held fixed or the body is insulated ($\hat{\boldsymbol{n}} \cdot \boldsymbol{\nabla} T = 0$). For definiteness, consider heat conduction on a slender 1d rod that extends from $x = 0$ to $x = \ell$. If the endpoints are held at fixed temperatures T_0 and T_1, then we have Dirichlet BCs: $T(0,t) = T_0$ and $T(\ell,t) = T_1$ at all times t. If the ends are insulated, it means the heat flux vanishes at the ends. This leads to Neumann boundary conditions $T'(0,t) = T'(\ell,t) = 0$ from (18.1).

Unlike the wave equation (17.6), the heat equation (18.4) is first order in time and requires only one piece of initial data, which may be taken as the initial temperature distribution $T(x,0)$. We are then interested in solving the initial-boundary value problem for the heat equation.

Time reversal. The heat equation (18.4) is *not* time-reversal invariant: i.e., it is not invariant under $t \to -t$: the LHS reverses sign but the RHS does not. In other words, the movie of a solution of the heat equation played backwards is generally *not* a possible solution of the heat equation. The heat equation does not describe a conservative system, heat diffusion is an example of a *dissipative* process. Useful energy stored in the initial temperature distribution is lost with an attendant rise in entropy. Unlike the time-reversal invariant wave equation, the heat equation *does not* admit a Hamiltonian or Lagrangian formulation of the usual sort. However, dissipative does not mean nothing is conserved. For instance, the average temperature of an insulated rod of length ℓ, $\bar{T}(t) = (1/\ell)\int_0^\ell T(x,t)dx$ is independent of time (see Prob. 18.2)! In fact, this is valid in any dimension and is a consequence of the fact that the heat equation is in local conservation form $T_t - \alpha \boldsymbol{\nabla} \cdot (\boldsymbol{\nabla} T) = 0$.

Smoothing property and equilibrium. Heat diffusion tends to *smooth* the temperature distribution. By Fourier's law, temperature differences tend to even out (unless they are maintained by external agents). Even a discontinuous initial temperature distribution such as the Heaviside step function[8] $\theta(x)$ becomes a smooth temperature distribution after an arbitrarily short time. [By contrast, the wave equation does not smooth the initial wave height distribution.] From empirical observations (and solutions of the heat equation), as $t \to \infty$, T approaches an equilibrium (steady) temperature distribution where net heat flow stops. The approach to equilibrium is typically exponentially fast, as we shall see. The equilibrium distribution is usually determined by boundary conditions (but could depend on the initial condition due to conservation laws such as that of the mean temperature in an insulated rod) and serves as an *attractor* for the dynamics. For instance, the equilibrium temperature distribution in an insulated rod is simply uniform.

---

[7] The diffusion equation can be used to describe the diffusion of heat, material/molecules, momentum, velocity, vorticity, etc. In each case, where an analog of Fourier's law holds, there is an analog of the thermal conductivity k, but it has a dimension depending on context. By contrast, diffusivities such as α always have dimensions of an areal speed and can be compared to know the relative rates of diffusion.

[8] $\theta(x) = 0$ for $x < 0$ and equals 1 for $x > 0$. It is often convenient to define $\theta(0) = 1/2$.

Backward time evolution. The backward time evolution of the heat equation is often ill-posed. This means that while we can specify practically any initial temperature distribution and evolve it forwards in time, it cannot always be evolved backwards, such a solution may not exist. For instance, we can take a Heaviside step function in temperature $T(x,0) = \theta(x)$ and evolve it forward from $t = 0$ to $t = \infty$, the sharp jump in temperature will get smoothed out. On the other hand, there is no temperature distribution that upon evolution from $t = -\infty$ (or $t = -t_0 < 0$) reaches the above step function. Physically, heat evolution describes a process with increasing entropy[9] and tendency to smooth sharp temperature differences (due to Fourier's law). $T(x,0)$ is discontinuous and it is plausible that $T(x,0)$ is a rather specially arranged state with low entropy. It is not possible that a rod whose temperature distribution has been evolving for some time while increasing its entropy and smoothing $T(x)$ can arrive at the special discontinuous state $T(x,0)$.

Note that there are initial states that *can* be evolved backwards in time for some duration. For instance, suppose we perform the forward evolution of the heat equation from $t = -10$ to $t = 0$ starting from some $T(x,-10)$ and ending at some $T(x,0)$. In this case, we *can* evolve the state $T(x,0)$ backwards in time, at least till $t = -10$.

Maximum and Minimum Principles. Roughly, these state that the temperature determined by the heat equation must remain bounded between the minimum and maximum values that the ICs and BCs involve[10]. See [64] and the remark in Sect. 18.3*.

Uniqueness of solutions. When it exists, let us sketch why the solution to the IVP for the heat equation on the spatial interval $0 \le x \le \ell$ is unique subject to suitable boundary conditions (here, we consider Dirichlet and Neumann BCs). Suppose $T_1(x,t)$ and $T_2(x,t)$ are both solutions of the heat equation with the same initial condition

---

[9] The entropy of a macroscopic state of a thermodynamic system is (in units of Boltzmann's constant), the logarithm of the volume of the set of all microstates that correspond to the given macrostate. A macrostate might be specified by macroscopic variables such as temperature and density, while a microstate would be specified by the positions and momenta of all the molecules in the system. A specially arranged macrostate with discontinuous temperature would have relatively fewer microstates corresponding to it.

[10] This is similar to the maximum principle for Laplace's equation ($\nabla^2 u = 0$) for an electrostatic potential in a region without charges. It essentially says that a nonconstant harmonic function on an open bounded domain $\Omega \in \mathbb{R}^n$ cannot have a local maximum in Ω. So its maximum on the closure of Ω must occur on the boundary $\partial\Omega$.

$T_1(x,0) = T_2(x,0) = f(x)$ and the same boundary conditions (which must necessarily be compatible with the initial condition). We wish to show that $T_1(x,t) = T_2(x,t)$ at all $t > 0$ or equivalently that $T = T_1 - T_2 \equiv 0$ at all x and $t > 0$. By linearity, $T = T_1 - T_2$ is also a solution to the heat equation satisfying the initial condition $T(x,0) \equiv 0$. The boundary condition on $T = T_1 - T_2$ is $T = 0$ or $dT/dx = 0$ (at $x = 0, \ell$) in the Dirichlet and Neumann cases. Since there is no temperature gradient for T initially (both in the interior and at the boundaries or as they are approached), the corresponding heat flux density vector (18.1) vanishes everywhere at $t = 0$. Consequently, physically we would not expect any redistribution of the temperature. This would imply that $T(x,t)$ must remain zero at all subsequent times. This is also a consequence of the maximum and minimum principles[11].

18.2 Solution of initial value problem on an interval by Fourier's series

Fourier developed his series to solve the heat equation. Let us consider the heat equation[12] $u_t = \alpha u_{xx}$ on the interval $0 \le x \le \ell$ with the ends insulated so that $u_x(0,t) = u_x(\ell,t) = 0$ (Neumann BC). We wish to solve the IVP to determine how the temperature distribution evolves with time from a given initial distribution $u(x,0) = f(x)$ satisfying $f'(0) = f'(\ell) = 0$. Intuitively, we expect inhomogeneities in the initial temperature distribution to be ironed out and for the temperature all along the rod to settle down at a single temperature $\bar{u} = (1/\ell)\int f(x)dx$ determined by the conservation of the mean temperature mentioned earlier. How does this equilibration occur?

Separation of variables. As with the wave equation, we make the separation of variables ansatz $u(x,t) = X(x)T(t)$ and obtain

$$\frac{\dot{T}}{T} = \alpha\frac{X''}{X} = \text{constant} = -\kappa < 0. \qquad (18.5)$$

Here, κ is a separation constant chosen positive so that the boundary conditions may be nontrivially imposed and so that the time-dependence is a decaying rather than growing exponential: we expect equilibration[13] to a steady state rather than a blowing up of the temperature distribution as time evolves.

The ODEs for X and T have the general solutions

$$X(x) = A\cos\sqrt{\kappa/\alpha}x + B\sin\sqrt{\kappa/\alpha}x \quad \text{and} \quad T(t) = Ce^{-\kappa t}. \qquad (18.6)$$

The Neumann BCs $X'(0)T(t) = 0$ and $X'(\ell)T(t) = 0$ for all times imply $X'(0) = X'(\ell) = 0$. The left BC implies $B = 0$ while

$$X'(\ell) = -A\sqrt{\kappa/\alpha}\,\sin(\sqrt{\kappa/\alpha}\ell) = 0 \quad \Rightarrow \quad \kappa = \frac{n^2\pi^2}{\ell^2}\alpha. \qquad (18.7)$$

---

[11] To be applicable, one needs to place some (continuity) restrictions on T, T_t and T_{xx} [64].

[12] Here onwards, we use u rather than T for the temperature.

[13] By equilibration we mean the approach to a steady equilibrium state. For instance, the temperature in a finite rod whose ends are thermally insulated is observed to approach (exponentially fast as $t \to \infty$) a uniform distribution with temperature equal to the average of the initial temperature distribution.

where n is an integer. We will denote κ by κ_n. Thus, the linearly independent separable solutions to the heat equation with insulated endpoints are the 'normal modes'

$$u_n(x,t) = A_n e^{-\kappa_n t} \cos(n\pi x/\ell) \quad \text{for} \quad n = 0, 1, 2, 3 \ldots . \tag{18.8}$$

Unlike in the wave equation, these modes are not oscillatory. Since $\kappa_n = (n^2\pi^2/\ell^2)\alpha$ grow quadratically with n, the higher modes decay faster with time. The $n = 0$ mode dominates at large times t, while the $n = 1$ mode controls the rate of approach to equilibrium. We may now form a linear combination of these modes to arrive at a Fourier series solution of the heat equation with Neumann boundary conditions:

$$u(x,t) = \sum\nolimits_{n=0}^{\infty} A_n e^{-\kappa_n t} \cos(n\pi x/\ell). \tag{18.9}$$

The Fourier coefficients A_n are determined by imposing the initial condition

$$u(x,0) = f(x) = \sum\nolimits_n A_n \cos(n\pi x/\ell). \tag{18.10}$$

As before, we get the Euler-Fourier formulae

$$A_0 = \frac{1}{\ell}\int_0^\ell f(x)\,dx \quad \text{and} \quad A_n = \frac{2}{\ell}\int_0^\ell f(x)\cos(n\pi x/\ell)\,dx \;\; \text{for} \;\; n = 1, 2, 3 \ldots . \tag{18.11}$$

What if the ends are maintained at a fixed temperature u_0, namely the temperature of the heat bath or surroundings in which the rod is immersed? Can we use the Fourier series method to solve the corresponding IVP? See Prob. 18.4.

18.3* Heat kernel: time evolution operator for heat equation

In this section, we find the 'time evolution operator' for the heat equation on an infinite rod. As in Sect. 13.4.2*, it is a linear transformation that takes as input, the initial temperature distribution and produces as output, the temperature distribution after a desired time. Since the state space of the heat equation is infinite-dimensional (all possible temperature distributions), the corresponding transformation is infinite-dimensional. In fact, it is convenient to regard the heat evolution operator as an integral operator that is specified in terms of its integral kernel. As we shall learn, the integral kernel[14] of a linear operator encodes the matrix elements of the operator, say, in the position basis. In fact, we have already met the idea of the integral kernel of a linear operator in Sect. 1.3* (see Footnote 24). The integral kernel of the heat evolution operator is called the heat kernel. We begin by defining it and then obtain a formula for it.

The heat equation for the temperature distribution $u(x,t)$ on an infinite rod with thermal diffusivity $\alpha > 0$ is

$$\partial_t u(x,t) = \alpha \nabla^2 u(x,t) \quad \text{with initial temperature distribution} \quad u(x,0). \tag{18.12}$$

---

[14] A Green function (6.59) is another example of the integral kernel of a linear operator.

Here $\nabla^2 = \partial_x^2$ in 1d. We will comment on the generalization to higher dimensions at the end of this section. A solution[15] may be expressed in terms of the integral kernel of the heat evolution operator $h_t = e^{\alpha t \nabla^2}$. The latter is defined via the convergent exponential series, which produces a differential operator of infinite order

$$h_t = e^{\alpha t \nabla^2} = I + \alpha t \nabla^2 + \frac{\alpha^2 t^2 \nabla^4}{2!} + \cdots . \tag{18.13}$$

Differentiating term by term, h_t is seen to satisfy the heat equation (h_t and the Laplacian commute)

$$\partial_t h_t = \alpha \nabla^2 h_t \quad \text{with initial condition} \quad h_{t\to 0^+} = I. \tag{18.14}$$

Dirac's notation for vectors and operators: If $|e_i\rangle$ for $i \in I$ is a basis for a (finite-dimensional) vector space, we may (in a unique manner) write a vector as a linear combination $|v\rangle = \sum_i |e_i\rangle v_i$ and thereby define the components v_i of v. If the space is an inner product space and the basis is orthonormal $\langle e_i|e_j\rangle = \delta_{ij}$, then taking an inner product with e_j we may express $v_j = \langle e_j|v\rangle$. Since the basis is orthonormal, we also have the completeness relation $\sum_i |e_i\rangle\langle e_i| = I$, which expresses the identity as a sum of outer products: this is easily checked for any basis vector and by linearity holds in general: $\sum_i |e_i\rangle\langle e_i|e_k\rangle = |e_k\rangle = I|e_k\rangle$. Similarly, we define the components of a linear transformation by the way it acts on the basis vectors $A|e_j\rangle = \sum_i |e_i\rangle A_{ij}$. Again, taking an inner product with e_k and using orthonormality, we express the components of A as the inner products ('matrix elements') $\langle e_k|A|e_j\rangle = A_{kj}$. This allows us to write A as a linear combination of outer products of basis vectors $A = \sum_{ij} A_{ij}|e_i\rangle\langle e_j|$. Combining this expression with $|v\rangle = \sum_k |e_k\rangle v_k$ we may write $A|v\rangle = \sum_{ij} |e_i\rangle A_{ij} v_j$ or $(Av)_i = \sum_j A_{ij} v_j$.

These formulae can be formally extended to infinite-dimensional inner product spaces [Hilbert spaces of functions such as square-integrable ones, denoted $L^2(\mathbb{R})$]. A convenient basis is that of position eigenstates $|x'\rangle$ which are orthogonal, Delta normalized $\langle x'|x''\rangle = \delta(x' - x'')$ and satisfy the completeness relation $\int dx |x\rangle\langle x| = I$. They are eigenstates of the position multiplication operator $(Mf)(x) = xf(x)$, i.e., $x|x'\rangle = x'|x'\rangle$ or $x\delta(x - x') = x'\delta(x - x')$. Another basic operator is differentiation $(Df)(x) = f'(x)$ or more generally the partial derivative on $L^2(\mathbb{R}^n)$. The second derivative D^2 is similarly defined, as is the Laplacian ∇^2.

Integral kernel of an operator. Given an operator A on a function space, we have the notion of its integral kernel $A(x, y)$ defined via $(Af)(x) = \int A(x, y) f(y) dy$. In Dirac notation, $A(x, y) = \langle x|A|y\rangle$. Check that the integral kernel of the position operator is $M(x, y) = x\delta(x - y) = y\delta(x - y)$. Show that the integral kernel of the differentiation operator is $D(x, y) = \partial_x \delta(x - y) = -\partial_y \delta(x - y)$. Similarly, show that $D^2(x, y) = \partial_x^2 \delta(x - y) = \partial_y^2 \delta(x - y)$ and that the integral kernel of the Laplacian in 3d is $\langle \boldsymbol{x}|\nabla^2|\boldsymbol{y}\rangle = \nabla_{\boldsymbol{x}}^2 \delta^3(\boldsymbol{x} - \boldsymbol{y})$.

---

[15] We have in mind decaying BCs $u(x, t) \to 0$ as $|x| \to \infty$, although the same heat kernel also works for other BCs such as Neumann. Essentially, the integral in (18.18) must converge.

The heat kernel. Let us define the heat kernel $h_t(x,y)$ as the integral kernel of the heat evolution operator $h_t = e^{\alpha t \nabla^2}$ (18.13), which acts on functions via

$$(h_t f)(x) = \int h_t(x,y) f(y)\, dy. \tag{18.15}$$

In more detail, $h_t(x,y)$ is the matrix element of h_t between position eigenstates. In Dirac notation, $h_t(x,y) = \langle x|h_t|y\rangle$. The heat equation and IC for h_t (18.14) may be expressed in terms of the heat kernel[16]:

$$\partial_t h_t(x,y) = \alpha \nabla_x^2 h_t(x,y) \quad \text{with} \quad \lim_{t\to 0^+} h_t(x,y) = \delta(x-y). \tag{18.16}$$

The 1^{st} statement is verified using the matrix elements of the Laplacian $\langle x|\nabla^2|z\rangle = \nabla_x^2 \delta(x-z)$. Taking matrix elements of (18.14) we get $\langle x|\partial_t h_t|y\rangle = \partial_t h_t(x,y)$, while

$$\begin{aligned} \langle x|\alpha \nabla^2 h_t|y\rangle &= \alpha \int \langle x|\nabla^2|z\rangle \langle z|h_t|y\rangle dz \\ &= \alpha \int \nabla_z^2 \delta(x-z) h_t(z,y) dz = \alpha \nabla_x^2 h_t(x,y), \end{aligned} \tag{18.17}$$

where we integrated by parts twice. The second statement uses the fact that the matrix elements of the identity between position eigenstates is the Dirac delta function. Note that $h_t(x,y)$ has dimensions of $1/L^d$ where d is the spatial dimension.

A solution of the heat equation with decaying BCs and any[17] initial temperature distribution $u(x,0)$ may be expressed in terms of the heat kernel:

$$u(x,t) = \int_{-\infty}^{\infty} h_t(x,y) u(y,0)\, dy. \tag{18.18}$$

To see this, we check using (18.16) that the RHS satisfies the heat equation with initial condition $u(x,0)$. Tikhonov's theorem mentioned in Footnote 16 implies that the solution (18.18) is the unique solution of the IVP. In other words, integration against the heat kernel transforms the initial temperature distribution into the one at time t.

Taking $u(y,0) = \delta(y)$, we see that $h_t(x) \equiv h_t(x,0)$ may be interpreted as the temperature at x at time t if the initial temperature distribution is a Dirac delta function supported at $x = 0$. [Of course, this $u(y,0)$ and $h_t(x)$ do not have dimensions of temperature. One could use the linearity of the heat equation to multiply by a dimensional constant to ensure that u has dimensions of temperature, but this constant plays no role in what follows.]

---

[16] The solution of the IVP (18.16) [called a fundamental solution of the heat equation on the real line] is unique if we impose decaying BCs. We could add to $h_t(x,y)$ any solution of the heat equation that vanishes as $t \to 0^+$ to get another fundamental solution. However, Tikhonov's theorem [16] implies that such 'homogeneous' solutions must grow faster than exponentially as $|x| \to \infty$. They are inadmissible if there is no heat entering from $x = \pm\infty$.

[17] The initial distribution $u(x,0)$ must of course be such that the integral in (18.18) exists.

Guessing the heat kernel. Before trying to determine $h_t(x)$ by solving the heat equation let us try to guess its behavior. Physically we heat the center of an (infinitely) long rod to a high temperature while keeping the rest of it at zero temperature, then withdraw the heat source and watch the temperature redistribute. We expect the heat to flow out symmetrically in either direction from $x = 0$. The temperature at $x = 0$ should gradually decrease and the temperature distribution should gradually widen. Suppose we guess that the distribution is a Gaussian, $h_t(x) = N(t)e^{-x^2/a(t)^2}$. The width $a(t)$ of the Gaussian must have dimensions of length and can depend only on time and α. Putting $a^2 \propto t^{2\nu}\alpha^\gamma$ we get $\nu = 1/2$ and $\gamma = 1$ by dimensional analysis, so $h_t(x) \sim N(t)e^{-x^2/b\alpha t}$ for some dimensionless numerical constant b.

Since we expect the temperature at $x = 0$ to decrease with time, $N(t)$ must be a monotonically decreasing function of time. So we might suppose $N(t) \propto 1/t^\mu$ for some $\mu > 0$. To determine the exponent μ, we note that the 'total temperature' $\int h_t(x)dx$ is conserved (assuming $h_t(x) \to 0$ as $|x| \to \infty$) and by the initial condition its value is unity. So h_t must have dimensions of an inverse length. Consequently, $N(t) = N_0/\sqrt{\alpha t}$ for some positive numerical constant N_0. In fact, one may determine N_0 in terms of b by requiring $\int h_t(x)\, dx = 1$ at all $t \geq 0$. Thus, on physical grounds, we guess that as $t \to \infty$, the heat escapes to infinity and the temperature at all points drops to zero: this is the expected equilibrium state.

Finding the heat kernel by Fourier analysis. Going beyond guesswork, to derive a formula for the heat kernel on the real line, we note that the heat equation and initial condition for $h_t(x, y)$ is invariant under the translations $x \to x + a, y \to y + a$. In other words, if $h_t(x, y)$ is a solution with IC $\delta(x - y)$ then so is $h_t(x - a, y - a)$. Taking $a = y$ we see that $h_t(x - y, 0) \equiv h_t(x - y)$ is a solution[18] of the heat equation with IC $\delta(x - y)$. By uniqueness, it follows that the heat kernel is a function only of the difference in positions $h_t(x, y) = h_t(x - y)$. Thus, we have reduced the job of finding the heat kernel to finding a time-dependent function $h_t(x)$ of one rather than two arguments. To solve the equation

$$\partial_t h_t(x) = \alpha \nabla_x^2 h_t(x) \quad \text{with initial condition} \quad h_0(x) = \delta(x), \tag{18.19}$$

we go to momentum space via a Fourier transform (see Appendix A.11*), since ∂_x^2 is diagonal in momentum space. Differentiation in x becomes multiplication by ip (see Prob. A.36) and this will allow us to convert the PDE into a system of ODEs. We begin with formulae (A.63) and (A.67) for the Fourier transform and its inverse:

$$\tilde{h}_t(p) = \int_{-\infty}^{\infty} h_t(x)e^{-ipx}\, dx \quad \text{and} \quad h_t(x) = \int_{-\infty}^{\infty} \tilde{h}_t(p)e^{ipx}\, \frac{dp}{2\pi}. \tag{18.20}$$

Then, the heat equation for $h_t(x)$ implies

$$\int_{-\infty}^{\infty} \left[(\partial_t + \alpha p^2)\tilde{h}_t(p)\right] e^{ipx} \frac{dp}{2\pi} = 0 \quad \forall\ x \ \text{ and for any } \ t > 0. \tag{18.21}$$

---

[18] There is a slight abuse of notation here. We use the same symbol h_t to denote a function of two variables and the function of one variable obtained using translation invariance.

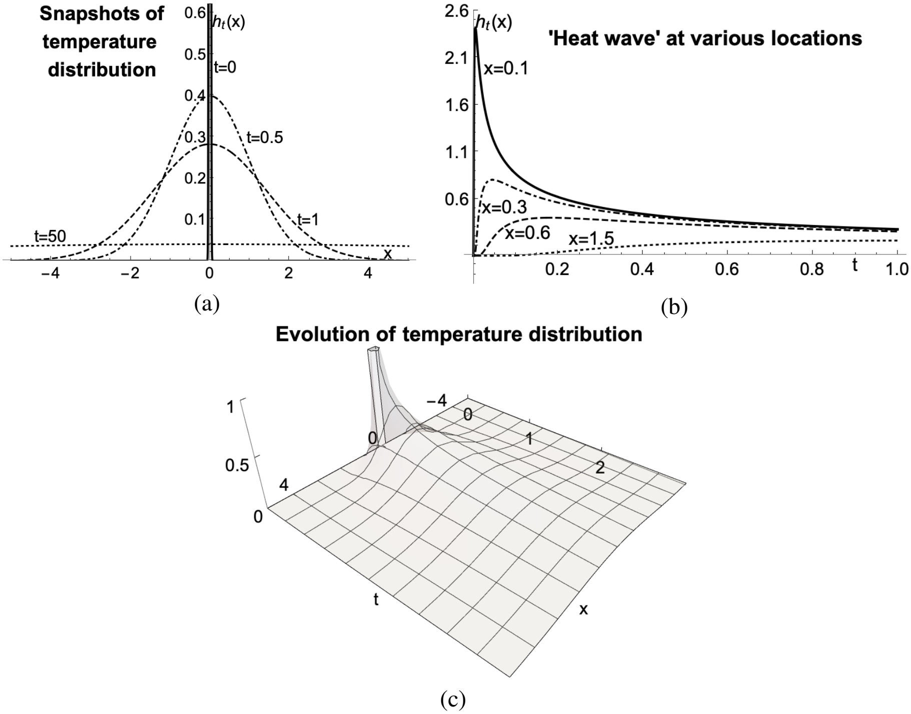

Figure 18.1: (a) Snapshots of temperature distribution $h_t(x)$ vs x at $t = .5, 1, 50$ starting from a Dirac delta distribution at $t = 0$ showing broadening. (b) Temperature $h_t(x)$ vs t at specific locations showing initial growth and subsequent power-law $1/\sqrt{t}$ decay. (c) Heat kernel on x-t plane. The term 'heat wave' is meant to convey that at a given location, the temperature increases from zero, reaches a peak and then decreases monotonically.

This can be true for all x only if the quantity in parentheses vanishes. So the heat equation in momentum space becomes

$$\partial_t \tilde{h}_t(p) = -\alpha p^2 \tilde{h}_t(p) \quad \text{and has the solution} \quad \tilde{h}_t(p) = A e^{-\alpha p^2 t}. \tag{18.22}$$

The constant of integration $A = \tilde{h}_0(p) = 1$ by the initial condition $h_0(x) = \delta(x)$. Now, we go back to position space and integrate by 'completing the square' (see also Prob. A.37):

$$\begin{aligned} h_t(x) &= \frac{1}{2\pi}\int_{-\infty}^{\infty} dp\, e^{-\alpha t\left(p^2 - \frac{ipx}{\alpha t}\right)} \\ &= \frac{1}{2\pi} e^{-\frac{x^2}{4\alpha t}} \int_{-\infty}^{\infty} dp\, e^{-\alpha t (p - \frac{ix}{2\alpha t})^2} = \frac{1}{\sqrt{4\pi\alpha t}} e^{-\frac{x^2}{4\alpha t}}. \end{aligned} \tag{18.23}$$

Thus, confirming our guess, the heat kernel is the Gaussian (see Fig. 18.1)

$$h_t(x, y) = \frac{1}{\sqrt{4\pi\alpha t}} e^{-\frac{(x-y)^2}{4\alpha t}}. \tag{18.24}$$

This formula says that if the initial temperature is Delta distributed at $x = 0$, then as time elapses, the temperature $h_t(x,0)$ at any fixed location $x \neq 0$ first grows with time, reaches a maximum and then decays to zero as the power $t^{-1/2}$. On the other hand, at any fixed time $t > 0$, the temperature rapidly decays to zero as x moves away from the origin.

Remarks:

1. Since the heat kernel $h_t(x,y)$ is positive, it follows from (18.18) that if $u(x,0)$ is nonnegative, $u(x,t)$ will also be nonnegative. It can also be shown that the temperature at any spot on the rod cannot (for $t > 0$) exceed the maximal value of the initial temperature distribution. This is physically expected due to the heat flux from hot to cold regions. Similar results hold for the heat equation on a bounded domain and go under the name Maximum and Minimum Principles. Essentially, the temperature must remain bounded between the maximum and minimum temperatures that the initial and boundary conditions involve.
2. Notice also that even an infinitely discontinuous initial temperature distribution $\delta(x)$ evolves into a smooth distribution $h_t(x)$ at any $t > 0$.
3. In d dimensions, the heat kernel is the product of d 1-dimensional heat kernels:

$$h_t(\boldsymbol{x},\boldsymbol{y}) = \frac{1}{(4\pi\alpha t)^{d/2}} e^{-\frac{(\boldsymbol{x}-\boldsymbol{y})^2}{4\alpha t}}. \tag{18.25}$$

18.4 From Brownian motion to the diffusion equation

In this section, we discuss Brownian motion and its connection to the diffusion equation[19]. Despite being a classical phenomenon, Brownian motion is rather different from the motion of pendula or billiard balls. In fact, it provides an example of a physical process to which the 'zeroth law' of mechanics (see Sect. 3.3) does not apply: the trajectory of a Brownian particle is very irregular and cannot be modeled as a differentiable function of time (see Fig. 18.2). What is more, due to its stochastic nature, it is not fruitful to try to predict the position of a Brownian particle as a function of time in a manner that worked for planets. Instead, one follows a statistical approach. This gives us an opportunity to introduce probabilistic reasoning and techniques to complement the more analytic or geometric methods employed elsewhere. Last but not least, the physics of Brownian motion is very interesting. Among other things, it allowed scientists (at the turn of the 20th century) to quantitatively infer the atomic structure of matter without being able to 'see' atoms and molecules.

18.4.1 Brownian motion and the atomic hypothesis

A small particle such as a pollen grain suspended in a stationary homogeneous liquid at a fixed temperature is found to move around in a seemingly unpredictable manner: jagged trajectories that abruptly change direction as seen in Fig. 18.2. This phenomenon is called Brownian motion, named after Robert Brown, a Scottish botanist who described it in 1828 when observing pollen grains suspended in water. He was not the first to observe the phenomenon. Among others, the Dutch microscopist and microbiologist Antonie van Leeuwenhoek (1632-1723) also mentions it. For a long time it was widely believed that the jiggling motion was because the particles were alive and self-propelled. An electrical origin was also suspected. In the second half of the $19^{\rm th}$ century, explanations based on heat and kinetic theory were proposed (e.g., by Christian Wiener in 1863 and subsequently by Father Carbonnelle [102]). According to kinetic theory, a gas or fluid is made of molecules which are in random thermal motion with a mean kinetic energy that is proportional to the absolute temperature. It was proposed that the irregular motion of a Brownian particle was due to frequent collisions with the (invisible) fluid molecules. Louis Georges Gouy (1888) performed careful experiments and provided arguments supporting the kinetic theory explanation. The main qualitative conclusions based on his and other experiments were as follows [97, 102]. *(a) A Brownian particle's motion is very irregular. The trajectory appears to have no tangent. (b) Grains appear to move independently even when they come within a distance comparable to their linear dimensions; forces between grains do not seem to play a role. (c) Smaller grains display greater jiggling motion. (d) The density and composition of the particles has no effect on their motion. (e) A less viscous fluid supports more vigorous Brownian motion. (f) Brownian motion is more active the higher the temperature of the fluid. (g) If the temperature is maintained, Brownian motion does not cease.* These observations supported the idea that Brownian motion is due to bombardment of pollen grains by the much more numerous and small fluid molecules. Experiments were performed to quantitatively test the kinetic origin of Brownian motion. According to equipartition of kinetic energy in thermal equilibrium, it was expected that the translational kinetic energy of the Brownian particles must be of the same order as that of the gas molecules. Attempts were made to measure the speed of Brownian particles and thereby deduce their kinetic energies. However, the values obtained differed greatly and the inescapable conclusion was that the speed of a granule was 'not accessible to measurement' [102]. In other words, the trajectory of a Brownian particle on the length scales of interest (above a micrometer or so) cannot be modeled as a differentiable curve[20].

---

[19] We will also reinterpret the heat kernel as the probability density of a Brownian particle

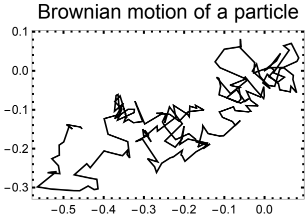

Figure 18.2: Sample trajectory of a Brownian particle that starts from the origin of the plane. The trajectory is plotted for $0 \leq t \leq 0.1$ with straight lines connecting the positions recorded at time instants 0.0005 apart.

---

[20] By contrast, the fluid molecules are much tinier (smaller than a nanometer) and their trajectories *can* be modeled as smooth curves (essentially straight lines except when molecules come close) on scales above a nanometer or so.

In 1905, Albert Einstein proposed a quantitative theory of Brownian motion [36]. Interestingly, he was not aware of the phenomenon when he developed his theory. He was looking for ways of testing the hypothesis that gases are made of atoms and molecules of finite sizes. He realized that if the atomic hypothesis and the kinetic theory of gases were correct, then although the gas molecules were too small to be seen, there would be a random movement of suspended particles which *could* be observed. Thus, he proposed that Brownian movement was due to repeated collisions of the micron-sized pollen grain with molecules of water. An important part of Einstein's treatment was to circumvent the question of the velocity of a Brownian particle.

The trajectory of a planet may be found by using Newton's law of gravity and his equations of motion, as in Chap. 2. Since Brownian motion (as envisaged by Einstein) involves random kicks, it is not feasible to predict the trajectory of a particular pollen grain. Einstein pioneered a statistical approach by considering the probability density $p(\boldsymbol{r}, t)$ of finding a Brownian particle at position $\boldsymbol{r}$ at time t. He argued that $p(\boldsymbol{r}, t)$ must satisfy the diffusion equation $p_t = D\boldsymbol{\nabla}^2 p$ (18.4) where D is the diffusion constant, which could be measured by observing Brownian motion. He then used heuristic arguments to relate D to other physical quantities: $D = \mu k_b T$. Here, k_b is Boltzmann's constant, T the absolute temperature and μ the mobility[21] of the particle [with dimensions of time per unit mass]. For a spherical particle of radius a moving (not too fast) through a viscous medium of mass density ρ and kinematic viscosity ν, Stokes showed [see (19.126)] that the damping force is $\boldsymbol{F}_{\rm damp} = -\lambda \boldsymbol{v}$ where $\lambda = 6\pi a \rho \nu$. In this case, Einstein's arguments using osmotic pressure allow one to deduce that the mobility is $\mu \approx 1/\lambda$ leading to the relation $D \approx k_b T/(6\pi a \rho \nu)$. A larger diffusion constant D leads to a more vigorous Brownian motion. Notice that the dependence on temperature, coefficient of viscosity and particle size are in line with what Gouy and others deduced from experiments. Einstein's relation[22] would allow one to measure Boltzmann's constant and estimate Avogadro's number $N_A = R/k_b$ where $R \approx 8.31 JK^{-1} mol^{-1}$ is the universal gas constant whose value had already been measured. Experimentally checking whether the statistical properties of Brownian motion match those expected from the diffusion equation, measuring D and using it to estimate Avogadro's number would provide strong evidence for the reality of atoms and molecules.

Predictions of Einstein's theory of Brownian motion were tested by the French physicist Jean Perrin (1909) and his student Chaudesaigues (1908) in a series of difficult experiments that allowed them to measure Avogadro's number ($N_A \approx 6 \times 10^{23}$) and provide evidence for the atomic hypothesis [102]. Perrin received the 1926 Nobel prize for his *work on the discontinuous structure of matter*.

---

[21] The idea is to consider a particle subject to an external force (like gravity) in a viscous medium with damping force proportional to the particle's velocity. In such a situation, the particle acquires a terminal speed due to a balance between the external and damping forces. The mobility is the ratio of the terminal speed to the applied force.

[22] Independently of Einstein, the Polish physicist Marian Smoluchowski (1906) developed a more detailed dynamical probabilistic theory of Brownian motion. He recovered Einstein's formula for the diffusion constant with some additional numerical factors. So it is called the Einstein-Smoluchowski relation.

18.4.2* Random walk model and the diffusion equation

To develop a quantitative probabilistic picture of Brownian motion, we will model it as a scaled[23] continuum limit of a random walk of a particle that can move on the sites of a lattice. For simplicity, we will consider the case of one spatial dimension.

Random walk on a 1d lattice. Suppose a particle can be located at the sites of a uniformly spaced one-dimensional lattice $x_j = j\Delta x$ where $j = 0, \pm 1, \pm 2, \ldots$. Here, Δx is a fixed lattice spacing. The particle's position is recorded at the discrete times $t_i = i\Delta t$ for $i = 0, 1, 2, \ldots$, where Δt is a fixed time interval (see Fig. 18.3). Moreover, if at time t_i, the particle is at position x_j then we assume that at time $t_i + \Delta t$, it is at either of its neighboring sites $x_j \pm \Delta x$ with equal probability. In particular, the shift in the particle's position is assumed independent of its previous motion.

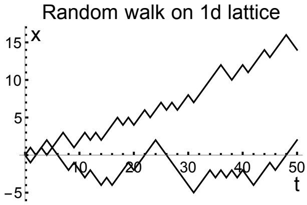

Figure 18.3: Two sample space-time trajectories or time series of a random walk on a 1d lattice. Here $\Delta x = \Delta t = 1$. The particle's positions at successive instants of time are joined by straight lines to guide the eyes.

Let the real random variable $\xi(t)$ denote the position of the particle at time t (it being understood that t must be one of the discrete times t_i). We call it a random variable since in each realization of the random walk, $\xi(t)$ (for a fixed t) would potentially have a different value. The random walk we have described has the properties of space- and time-translation invariance. This is because the rules governing displacements are independent of time and the same irrespective of the current location. This means the statistical properties of $\xi(t)$ (relative to $\xi(0)$) [such as its mean, variance and higher moments, see Footnote 18 of Chap. 3] can depend on the distance from the starting location and time elapsed but not on the starting point $\xi(0)$ or initial time. In other words, the probability distribution[24] of $\xi(t) - \xi(0)$ is the same as that of $\xi(t + t_*) - \xi(t_*)$ for any t_*. Henceforth, we will assume, for definiteness, that the particle begins at the point $x = 0$ at time $t = 0$, so that $\xi(0) = 0$.

Mean and variance of the displacement. After n time steps ($t = n\Delta t$) the particle would have undergone n displacements, S_n to the right and $n - S_n$ to the left. Thus,

$$\xi(t) = S_n \Delta x - (n - S_n)\Delta x = (2S_n - n)\Delta x. \tag{18.26}$$

---

[23] The scaling limit introduced in Eq. (18.34) allows us to go from a discrete space-time to a continuous one while replacing a binomial random variable with a Gaussian one.

[24] The probability distribution of a random variable ξ is the set of probabilities $\mathbf{P}\{x' \le \xi \le x''\}$ for all $x' \le x''$. For a continuous random variable, it may be expressed as an integral over a probability density function $\mathbf{P}\{x' \le \xi \le x''\} = \int_{x'}^{x''} p_\xi(x)dx$.

Since the probability to hop to the right and left are equal, the average position[25] $\langle \xi(t) \rangle = 0$, provided n is even. Now, we are going to exploit the independence of displacements on the history of the particle's motion to find its variance[26]. Suppose s is an intermediate time in the sequence ($0 \leq s \leq t$). Then we may write

$$\xi(t) = [\xi(s) - \xi(0)] + [\xi(t) - \xi(s)]. \tag{18.27}$$

Due to space-time translation invariance, the probability distribution of $\xi(t) - \xi(s)$ is the same as that of $\xi(t-s) = \xi(t-s) - \xi(0)$. Moreover, due to the lack of memory, the increments $\xi(s) - \xi(0) = \xi(s)$ and $\xi(t) - \xi(s)$ are independent random variables[27]. In Prob. 18.14, we show that the variance of a sum of independent random variables is the sum of their variances. Thus, the variance of $\xi(t)$ (denoted $\text{ var } (t)$) is the sum

$$\text{var } (t) = \text{ var } (s) + \text{ var } (t-s) \quad \text{for} \quad 0 \leq s \leq t. \tag{18.28}$$

Putting $s = s_1$ and $t - s = s_2$ we have $\text{ var } (s_1 + s_2) = \text{ var } (s_1) + \text{ var } (s_2)$ for all discrete times $s_1, s_2 \geq 0$. It follows that the variance must be proportional to time: $\text{var}\, \xi(t) = 2Dt$. Aside from the conventional factor of two, the proportionality constant D with dimensions of area per unit time is called the diffusion constant or diffusivity. This linear growth of the variance is also observed experimentally.

Bernoulli trials and the diffusion constant. We wish to find the probability distribution of $\xi(t)$. Since the particle's motion is memoryless, successive displacements are independent and may be viewed as Bernoulli trials[28] with probabilities of success and failure ($p = q = \frac{1}{2}$) being the probabilities to move a step to the right and left. Thus, S_n is the number of successes in n Bernoulli trials[29]. It can be shown[30] that

---

[25] By average or expectation value of position $\langle \xi(t) \rangle$, we mean the arithmetic mean of the positions (after $n = t/\Delta t$ steps) in N realizations of the random walk as $N \to \infty$. In a similar manner, we may define the expectation value of other random variables. For example, the average $\langle \xi(t)^2 \rangle$ is called the mean square value of $\xi(t)$.

[26] The variance of a random variable ξ is defined as the mean square value of $\xi - \langle \xi \rangle$. In other words, $\text{ var } (\xi) = \langle (\xi - \langle \xi \rangle)^2 \rangle = \langle \xi^2 \rangle - \langle \xi \rangle^2$. For future use, we note that the variance of a constant vanishes while $\text{ var } (c\xi) = c^2 \text{ var } (\xi)$ for any real constant c.

[27] Events A_1 and A_2 are statistically independent if the probability that both occur factorizes as a product: $\mathbf{P}(A_1 A_2) = \mathbf{P}(A_1)\mathbf{P}(A_2)$. Real random variables ξ_1 and ξ_2 are independent if the events $x_1' \leq \xi_1 \leq x_1''$ and $x_2' \leq \xi_2 \leq x_2''$ are independent for all $x_1' \leq x_1''$ and $x_2' \leq x_2''$. It follows that ξ_1 and ξ_2 are independent if their joint probability density $p_{\xi_1,\xi_2}(x_1, x_2)$ factorizes as the product of individual probability densities $p_{\xi_1}(x_1) p_{\xi_2}(x_2)$. In particular, the expectation value of a product of independent random variables factorizes $\langle \xi_1 \xi_2 \rangle = \langle \xi_1 \rangle \langle \xi_2 \rangle$.

[28] Bernoulli trials are identical independent experiments in each of which an event A may occur with probability $0 \leq p \leq 1$ and fail to occur with probability $q = 1 - p$.

[29] For each $k = 1, 2, \ldots, n$, we introduce the 'Bernoulli' random variable β_k associated to the k^{th} Bernoulli trial, taking the values 1 or 0 depending on whether the trial is a success or a failure. Then $S_n = \beta_1 + \cdots + \beta_n$. Since the trials are independent, the probability of k successes is given by the binomial distribution $\mathbf{P}\{S_n = k\} = \binom{n}{k} p^k q^{n-k}$.

[30] Since the Bernoulli random variables β_k for $k = 1, \cdots, n$ are independent and identically distributed, the mean and variance of the binomial distribution are given by $\langle S_n \rangle = n \langle \beta_1 \rangle = n(0 \cdot q + 1 \cdot p) = np$ and $\text{ var } (S_n) = n \text{ var } (\beta_1) = n(\langle \beta_1^2 \rangle - \langle \beta_1 \rangle^2) = n(\langle \beta_1 \rangle - p^2) = n(p - p^2) = npq$ since $\beta_1^2 = \beta_1$ as it can only take the values 0 and 1.

$\langle S_n \rangle = np = n/2$ and $\text{var } S_n = npq = n/4$. We combine this with $\text{var } \xi = 2Dn\Delta t$ to write D in terms of Δx and Δt. In fact, from (18.26) and Footnote 26,

$$\text{var } \xi = \text{var } [(2S_n - n)\Delta x] = 4(\Delta x)^2 \text{ var } S_n = n(\Delta x)^2 \quad \Rightarrow \quad D = (\Delta x)^2/2\Delta t. \tag{18.29}$$

Diffusion equation for the Brownian probability density. Equation (18.29) is a key result. It will help us derive an equation for the probability $p(x_j, t_i)$ that the Brownian particle is at site x_j at time t_i. Given the distribution at t_i, what is the probability of the particle being at x_j at time t_{i+1}? A moment's thought leads us to the equation

$$p(x_j, t_{i+1}) = p(x_j, t_i) + \left[\frac{1}{2}p(x_{j+1}, t_i) + \frac{1}{2}p(x_{j-1}, t_i) - p(x_j, t_i)\right]. \tag{18.30}$$

The first term on the RHS is the existing probability to be at x_j. It can increase if the particle is present at either of the neighboring sites $x_{j\pm1}$ and hops to x_j. In either case, the probability of hopping to x_j is $1/2$. Finally, the probability can decrease if the particle was at x_j, in which case it must hop (with probability one) to one of the neighboring sites. To take a continuum limit, we let the space and time spacings $\Delta x, \Delta t \to 0$ and $n \to \infty$ in such a way that the diffusion constant D remains fixed, as does the time elapsed $t = n\Delta t$. To take this limit in (18.30), we insert the factor $1 = 2D\Delta t/(\Delta x)^2$ from (18.29) and write

$$p(x_j, t_{i+1}) = p(x_j, t_i) + \frac{2D\Delta t}{2(\Delta x)^2}\left[p(x_{j+1}, t_i) + p(x_{j-1}, t_i) - 2p(x_j, t_i)\right]. \tag{18.31}$$

Rearranging, we get

$$\frac{p(x_j, t_{i+1}) - p(x_j, t_i)}{\Delta t} = D\frac{p(x_{j+1}, t_i) - 2p(x_j, t_i) + p(x_{j-1}, t_i)}{(\Delta x)^2}. \tag{18.32}$$

Comparing with (17.8) and (17.11), we recognize that the quotients on the LHS and RHS are finite difference approximants to the first and second derivatives in t and x. Thus, in the limit, we get a PDE that is identical to the heat equation (18.4) in one dimension, with the diffusion constant D playing the role of thermal diffusivity α:

$$\frac{\partial p(x,t)}{\partial t} = D\frac{\partial^2 p(x,t)}{\partial x^2}. \tag{18.33}$$

Thus, we have shown that the heat equation also governs the time evolution of the probability density of the position ξ of a Brownian particle modeled via the continuum limit of the above random walk. To find an explicit expression for $p(x,t)$ we may solve (18.33) subject to the initial condition that the particle was at $x = 0$ at $t = 0$, as done in Sect. 18.3*, resulting in the Gaussian formula $p(x,t) = h_t(x, 0)$ (18.24). As an alternative, we give below a method based on probability theory.

Brownian probability distribution from limit theorem. To find the probability distribution of ξ, it is helpful to relate it to a normalized binomial random variable S_n^* with zero mean and unit variance:

$$S_n^* = \frac{S_n - n/2}{\sqrt{n/4}} = \frac{2S_n - n}{\sqrt{n}} = \frac{\xi}{\Delta x\sqrt{n}} = \frac{\xi}{\sqrt{2Dt}}. \tag{18.34}$$

Now we let $n \to \infty$ and $\Delta t \to 0$ holding $t = n\Delta t$ fixed and also let $\Delta x \to 0$ in such a way that D remains fixed. In this limit, the De Moivre-Laplace limit theorem [110] applies and the distribution of the normalized binomial random variable S_n^* approaches a standard Gaussian with probability density $p_{S^*}(y) = e^{-y^2/2}/\sqrt{2\pi}$:

$$\lim_{n\to\infty} \mathbf{P}\{y' \le S_n^* \le y''\} = \frac{1}{\sqrt{2\pi}} \int_{y'}^{y''} e^{-y^2/2}\, dy \tag{18.35}$$

Changing variables to $\xi = \sqrt{2Dt}S^*$ so that $x = \sqrt{2Dt}y$ and $dx = \sqrt{2Dt}dy$, we get the probability density of the Brownian particle at time t:

$$p_{S^*}(y)dy = p_\xi(x)dx \quad \Rightarrow \quad p_\xi(x) = (4\pi Dt)^{-1/2} e^{-x^2/4Dt}. \tag{18.36}$$

$p_\xi(x)dx$ is the probability to find the particle in an interval of size dx around x at time t. Notice that $p_\xi(x)$ is the same as the heat kernel $h_t(x,0)$ (18.24) with $\alpha \mapsto D$. Thus, it is not a surprise (see Prob. 18.15) that $p_\xi(x)$ satisfies the diffusion equation (18.33).

18.5 Problems

1. What are the **dimensions** of thermal conductivity k and specific heat c_v? Verify that diffusivity $\alpha = k/\rho c_v$ has dimensions of area per unit time.
2. **Local conservation law.** Show that the heat equation in 1d can be written in local conservation form. Derive a conserved quantity for suitable boundary conditions.

∗3. Give an example of an initial temperature distribution $u(x,0)$ on a rod $(0 \le x \le \ell)$ that evolves under the heat equation in distinct ways for two different BCs. Hint: ensure that the IC satisfies both **Dirichlet and Neumann** BCs at $t = 0$ and argue what the distribution of temperature at late times would be in each case.

∗4. Adapt the **Fourier series method** of Sect. 18.2 for the solution of the heat equation for an insulated rod to a rod whose ends are held at a common temperature u_0. What if the ends are maintained at different temperatures u_L and u_R?

∗5. Show that the **integral kernels** of the following operators are as given. (a) The position multiplication operator: $M(x,y) = x\delta(x-y) = y\delta(x-y)$. (b) The differentiation operator: $D(x,y) = \partial_x\delta(x-y) = -\partial_y\delta(x-y)$. (c) $D^2(x,y) = \partial_x^2\delta(x-y) = \partial_y^2\delta(x-y)$. (d) The Laplacian in 3d: $\langle \boldsymbol{x}|\boldsymbol{\nabla}^2|\boldsymbol{y}\rangle = \boldsymbol{\nabla}_{\boldsymbol{x}}^2\delta^3(\boldsymbol{x}-\boldsymbol{y})$.

∗6. **Heat kernel.** Recall that by translation-invariance, the heat kernel in 1d $h_t(x,y) = h_t(x-y)$ is a function of one spatial variable. The Fourier transform $\tilde{h}_t(p) = \int h_t(x)e^{-ipx}dp/2\pi$ satisfies the heat equation in momentum space $\partial_t\tilde{h}_t(p) = -\alpha p^2\tilde{h}_t(p)$ with the initial condition $\tilde{h}_0(p) = 1$. Invert the Fourier transform to find an explicit expression for $h_t(x)$. Give the final expression for the heat kernel $h_t(x,y)$ including all numerical factors. Hint: show that $\int_{-\infty}^{\infty} e^{-\beta q^2}\, dq = \sqrt{\pi/\beta}$.

7. **Peak temperature.** Suppose $h_t(x)$ is the temperature (in appropriate units) at time t on an infinite slender rod evolving via the heat equation $\partial_t h_t = \alpha\partial_x^2 h_t(x)$ with the initial condition $h_0(x) = \delta(x)$. Find the time $t_{\max}$ at which the temperature at a point x_0 is maximal. Before determining $t_{\max}$ exactly, use dimensional analysis to propose a formula for $t_{\max}$. Comment on $t_{\max}$ for the location $x_0 = 0$.

8. Guess a formula for the **heat kernel** $h_t(\boldsymbol{x}, \boldsymbol{y})$ in d-dimensional Euclidean space where $\boldsymbol{x}, \boldsymbol{y} \in \mathbb{R}^d$. It is the solution to the heat equation $\partial_t h_t(\boldsymbol{x}, \boldsymbol{y}) = \alpha \boldsymbol{\nabla}^2 h_t(\boldsymbol{x}, \boldsymbol{y})$ subject to the initial condition $h_0(\boldsymbol{x}, \boldsymbol{y}) = \delta^d(\boldsymbol{x} - \boldsymbol{y})$. Make sure you get the dimensions right and indicate any dimensionless numerical factors that could appear.
9. Use formula (18.24) for the heat kernel in 1 dimension to arrive at formula (18.25) for the **heat kernel in d dimensions**. Hint: Use the separability of the Laplace operator in Cartesian coordinates to write $h_t(\boldsymbol{x}, \boldsymbol{y})$ as a product.
10. **Smoothing property of heat equation.** Give an explicit example to show that a discontinuous temperature profile at $t = 0$ can become smooth (C^∞ as a function of position) at any time $t > 0$ while evolving according to the 1d heat equation.

$*$11. **Polynomial solutions to the heat equation.** (a) Verify that the following polynomials in x and t are solutions to the heat equation $u_t = u_{xx}$ (in units where the diffusivity $\alpha = 1$). (1) $p_1 = x$, (2) $p_2 = x^2/2! + t$, (3) $p_3 = x^3/3! + tx$, (4) $p_4 = x^4/4! + tx^2/2 + t^2/2$. (b) Show that these may be generalized to polynomials

$$p_n(x,t) = \sum\nolimits_{k=0}^{[n/2]} \frac{t^k}{k!} \frac{x^{n-2k}}{(n-2k)!} \tag{18.37}$$

of degree n in x and $[n/2]$ in t, where $[\cdot]$ denotes the greatest integer part. Note that these solutions are unbounded in space and also in time (with the exception of p_1). Comment on the ICs and BCs that these *temperature polynomials* satisfy.

$*$12. **Similarity solutions of the heat equation.** Consider the scaling form $u(x,t) = f(\xi)/\sqrt{t}$ where the scaling variable $\xi = x/\sqrt{t}$. (a) Show that u solves the 1d heat equation $u_t = \alpha u_{xx}$ provided the scaling function f satisfies the linear ODE with variable coefficients $2\alpha f'' + \xi f' + f = 0$. (b) Verify the dimensional consistency of this equation. (c) Look for solutions of this linear ODE. (d) Arrive at the proposed scaling form by supposing that $t^\beta u(x,t)$ depends on x and t only via the combination $\xi = x t^\gamma$ for some real numbers β and γ. (e) Try to identify a scaling symmetry of the heat equation that underlies similarity solutions. Hint: Recall the scaling symmetry (2.51) of the Kepler problem.

$*$13. **Maximum Principle.** Look up the Maximum Principles for the Laplace and heat equations and understand their physical meanings.

14. **Variance and covariance.** Given random variables ξ, η, a measure of their correlation is the covariance $\text{cov}(\xi, \eta) = \langle (\xi - \langle \xi \rangle)(\eta - \langle \eta \rangle) \rangle$. The variance of a random variable is $\text{var}(\xi) = \text{cov}(\xi, \xi)$. (a) Show that $\text{var}(\xi + \eta) = \text{var}(\xi) + \text{var}(\eta) + 2\,\text{cov}(\xi, \eta)$. (b) If ξ and η are independent, show that $\text{cov}(\xi, \eta) = 0$. Deduce that the variance of the sum of independent random variables is the sum of variances.
15. **Diffusion equation from Brownian probability.** Show by differentiation that the probability density of a one-dimensional Brownian random walk, $p_\xi(x;t) = (4\pi D t)^{-1/2} \exp(-x^2/4Dt)$ satisfies the diffusion equation $u_t = D u_{xx}$.
16. Numerically generate a **random walk** on a 1d lattice and plot sample trajectories.

Chapter 19

Introduction to fluid mechanics

Fluid flows are all around us: the air through our nostrils, tea stirred in a cup, water down a river and charged particles in the ionosphere. The flow of fluids can be fascinating to watch [10,96,129]. It is also an interesting branch of physics to which many of the best scientists from the early days of Leonardo da Vinci, Isaac Newton, Daniel Bernoulli and Leonhard Euler have contributed. Fluid dynamics finds application in numerous areas: flight of airplanes and birds, weather prediction, blood flow in the heart and blood vessels, waves on the beach, ocean currents and tsunamis, flows in the molten metallic core of the Earth, controlled nuclear fusion in a tokamak, jet engines in rockets, motion of charged particles in the solar corona and astrophysical jets, accretion disks around active galactic nuclei, formation of clouds, melting of glaciers, climate change, sea level rise, traffic flow, building pumps and dams, etc. Fluid flows can range from regular and predictable (laminar) to seemingly disorganized and unpredictable (turbulent) while displaying remarkable patterns.

We believe[1] we know the macroscopic physical laws governing fluid motion. In the absence of dissipation, they are the local conservation laws of mass, momentum and energy along with a thermodynamic equation of state. The resulting equation for the flow velocity in ‘ideal’ (dissipationless) flow goes back to the work of Euler (1757). In the presence of dissipation (viscosity, thermal conductivity, etc.), local conservation of mass continues to hold although the ideal momentum and energy equations are modified (in the simplest possible way) using empirical macroscopic laws of Newton and Fourier governing diffusion of momentum and heat to arrive at the equations for viscous flow. The corresponding equation for the flow velocity was introduced by Claude-Louis Navier (1822) and George Gabriel Stokes (1845). It is important to bear in mind that these equations of macroscopic fluid mechanics were postulated based on empirical observations, macroscopic conservation laws and the principles of minimality and simplicity rather than by a direct application of Newton’s second law to individual molecules. In fact, these equations were proposed well before the molecular structure of matter was established. What is more, although we now know the laws of molecular dynamics accurately, it has not been possible to rigorously deduce the equations of fluid mechanics from them[2]. In this framework, the equations of fluid mechanics have to be validated by comparing their predictions[3] with macroscopic experimental measurements and observations. Fortunately, in many cases where such comparisons have been possible, there is evidence in favor of the fluid equations. However, there are situations where one needs to modify them (e.g., to account for a nonlinear stress-strain relation or the polymeric structure of constituent molecules) or abandon them (e.g., when one is interested in phenomena on molecular length scales).

---

[1] Unlike in the application of Newton’s laws to a pair of point particles or a rigid body, there are significant approximations, imprecise notions of averaging and plausible assumptions involved in arriving at the equations governing macroscopic fluid motion.

[2] Well after their formulation, some of these macroscopic fluid equations (especially for dilute gases, but not for liquids) have been shown (by L Boltzmann, S Chapman, D Enskog and others [18, 19, 43, 47]) to follow from the molecular kinetic theory of gases through a coarse-graining procedure based on some plausible assumptions and approximations. In this chapter,

19.1 Fluid element, local thermal equilibrium and dynamical fields

In a fluid description, we do not follow the microscopic positions and velocities of individual molecules. We focus instead on macroscopic fluid variables such as velocity, pressure, density, energy and temperature that we assign to a *fluid element* by averaging over it. By a fluid element (sometimes called a material element), we mean a sufficiently large collection of molecules so that concepts such as 'volume occupied' make sense and yet small in extent compared to the macroscopic length scales of phenomena we wish to describe. Thus, quantities such as the density and velocity will be assumed not to vary appreciably over a fluid element. For example, we could divide a bucket with about 10^{23} molecules into 10^3 fluid elements, each containing 10^{20} molecules. Thus, we model a fluid as a continuum system with an essentially infinite number of degrees of freedom[4]. The fluid description applies to phenomena on length scales large compared to the typical mean free path between collisions of molecules. On shorter length scales, the fluid description breaks down[5], though Boltzmann's kinetic theory of molecules applies.

A flowing fluid is generally *not* in global thermal equilibrium. What this means is that it may not be possible to assign a common temperature to all parts of a fluid, and heat could be transported between parts of a fluid. Nevertheless, collisions between molecules typically establish local thermodynamic equilibrium so that we may assign a local absolute temperature T, pressure p and density ρ to fluid elements, satisfying an equation of state (such as that of an ideal gas[6] $p = \rho RT/\mu$). Sometimes, it is convenient to replace some of these thermodynamic state variables with specific entropy

---

we will introduce the equations of fluid mechanics from a macroscopic viewpoint and make no attempt to derive them from kinetic theory.

[3] As in the rest of continuum mechanics, the evolution equations of fluid dynamics are partial differential equations. However, these equations are nonlinear and despite much progress since the time of Euler, Navier and Stokes, it is still a challenge to calculate (even with the best of computers) many features of commonly occurring flows [23, 41].

[4] To specify the pattern of a flow we must, among other things, specify the fluid velocity at each of the infinitely many points in the container.

[5] In going from a molecular description to a fluid description, we replace sums over individual molecules by integrals over the region occupied by the fluid, with fluid elements roughly playing the role of infinitesimal integration elements. A system with a very large but finite number of molecular degrees of freedom is approximated by a continuum system with infinitely many degrees of freedom.

[6] Here $R = 8.314$ Joules per Kelvin per mole is the universal gas constant and μ the molar mass, 12 grams per mole for Carbon-12

s (entropy S per unit mass) or specific internal energy ϵ (energy per unit mass) or specific volume $v = 1/\rho$. Each of these quantities could vary from one fluid element to another and also with time. From an Eulerian standpoint, at each location $\boldsymbol{r}$ in a fluid at time t, we have the dynamical fields of density $\rho(\boldsymbol{r}, t)$, pressure $p(\boldsymbol{r}, t)$, specific entropy $s(\boldsymbol{r}, t)$, temperature $T(\boldsymbol{r}, t)$, etc. In addition to these scalar fields (see Appendix A.8), we have the velocity vector field $\boldsymbol{v}(\boldsymbol{r}, t)$ that is instantaneously tangent to the flow at each point $\boldsymbol{r}$.

19.2 Fluid statics: aero- or hydrostatics

Before considering fluid flows in more detail, we briefly remark upon the special situation that prevails when the fluid is not in motion in the inertial frame considered. This is usually called hydrostatics or sometimes aerostatics (if one wishes to emphasize that the density is inhomogeneous). In fluid static equilibrium, each fluid element is at rest due to a balance between surface and body forces. Surface forces are those that act on the element across its boundary due to material just outside the surface. The most common body force is gravity, which acts over the whole volume of the fluid element. To obtain the equations of hydrostatic equilibrium, we consider a small fluid element of mass $\delta m = \rho\, \delta V$ occupying a volume δV. The external body force such as gravity acting on the fluid element is $\boldsymbol{f} \delta V$ where $\boldsymbol{f}$ is the body force per unit volume ($\boldsymbol{f} = \rho \boldsymbol{g}$ for gravity, where $\boldsymbol{g}$ is the acceleration vector due to gravity). In addition, we have the surface force due to the pressure exerted on the fluid element by the fluid surrounding the element. To calculate this, assume the fluid element is an infinitesimal cuboid with sides of length dx, dy and dz.

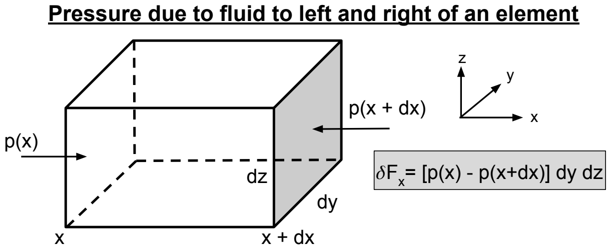
Pressure due to fluid to left and right of an element
p(x)
p(x + dx)
dz
dy
x
x + dx
z
y
x
δF_x = [p(x) - p(x+dx)] dy dz

Figure 19.1: Horizontal force on a fluid element due to material to the left and right.

As shown in Fig. 19.1, the net pressure force in the $\hat{x}$ direction is the product of the area $dydz$ and pressure difference between the left and right faces: $\delta F_x \approx -\frac{\partial p}{\partial x} dx \times dydz$. The negative sign is because pressure tends to compress the element and the net force is leftward if p on the right face is larger than on the left face. Thus, the total pressure force on the fluid element is

$$\delta \boldsymbol{F}_{\text{pressure}} = \delta F_x \hat{x} + \delta F_y \hat{y} + \delta F_z \hat{z} = -(\boldsymbol{\nabla} p)\, \delta V. \tag{19.1}$$

For the element to be in static equilibrium, we must have

$$\boldsymbol{f} - \boldsymbol{\nabla} p = 0 \quad \text{or} \quad \boldsymbol{\nabla} p = \rho \boldsymbol{g}. \tag{19.2}$$

where $\boldsymbol{f}$ and $\boldsymbol{g}$ are the body forces per unit volume and mass respectively. This is one equation for two unknown functions, the pressure and density. It is usually supplemented by an 'equation of state' relating pressure to density. For an incompressible liquid, ρ can often be assumed to be a constant. For an ideal gas at a fixed temperature T, the equation of state is $p = \rho RT/\mu$ where μ is the molar mass and R the universal gas constant. This is usually written as Boyle's law $(p/p_o) = (\rho/\rho_o)$ where p_o is the pressure at a reference density ρ_o. If the pressure and density variations are at constant entropy (reversible adiabatic process) rather than constant temperature, the corresponding formula is $(p/p_o) = (\rho/\rho_o)^\gamma$ (see Prob. 19.2 and Sect. 19.8) where the adiabatic index $\gamma = C_p/C_v$ is the ratio of heats capacities at constant pressure and volume (see Prob. 19.1). □

Example: Atmospheric pressure. For example, let us find the density and pressure as a function of height z in the atmosphere, assuming it is in aerostatic equilibrium and treating the temperature and acceleration due to gravity as independent of height. The force balance equation reduces to

$$\frac{\partial p}{\partial z} = -g\rho(z) \quad \text{or} \quad \frac{dp}{p} = -\frac{g\rho_o}{p_o} \quad \Rightarrow p(z) = p(0)e^{-\rho_o g z/p_o}. \tag{19.3}$$

Thus, the pressure and density decrease exponentially with height if we ignore the temperature and gravity variations. Prob. 19.3 treats this aerostatic situation with the isentropic equation of state $p \propto \rho^\gamma$, which is more realistic. □

A frequently encountered circumstance is one where the body force field per unit mass is the (negative) gradient of a potential $\boldsymbol{g} = -\boldsymbol{\nabla}\varphi$. Such a force is called *conservative*. Then $\boldsymbol{\nabla} p = -\rho\boldsymbol{\nabla}\varphi$. If, moreover, the density is a constant, we have $\boldsymbol{\nabla}(\frac{p}{\rho} + \varphi) = 0$. So $p/\rho + \varphi$ must be a constant. In particular, an equipotential surface must also be a surface of constant pressure (an isobar). For example, the free surface of a liquid is an isobar (pressure equal to atmospheric pressure), and hence must also be an equipotential surface within these approximations.

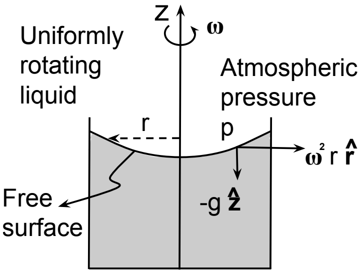

Figure 19.2: Parabolic free surface of a uniformly rotating liquid.

Example: Free surface of rotating liquid. Let us apply (19.2) to determine the shape of the free surface of a liquid that is rotated at a constant angular velocity $\omega\hat{z}$ in a bucket (cf. Fig. 19.2). After some time, the surface of the liquid is found to reach an equilibrium shape. The body forces per unit mass are gravity $-g\hat{z}$ and the centrifugal force $r\omega^2\hat{r}$ where we use cylindrical coordinates r, θ, z. Thus, the body force per unit mass is the negative gradient of the effective potential $\varphi = gz - \frac{1}{2}r^2\omega^2$. Once the liquid settles into equilibrium, $p/\rho + gz - \frac{1}{2}\omega^2 r^2$ is a constant. On the free surface, the pressure is constant, equal to atmospheric pressure. So the equation for the free surface

$gz - \frac{1}{2}\omega^2 r^2 =$ constant, describes a paraboloid obtained by rotating the parabola $gz - \frac{1}{2}\omega^2 x^2 =$ constant, about the z axis. □

19.3 Flow visualization: streamlines, streaklines and pathlines

In fluid mechanics, when we speak of the velocity of a flow, we are referring not to the random thermal motions of individual molecules (which can be rather jagged, as observed in Brownian motion) but to the velocity of the overall flow. The latter is smoother since an average over molecules in each fluid element has been performed to arrive at the flow velocity field.

If the velocity vector field at every point of observation is independent of time, we say the velocity field is steady, $\boldsymbol{v}(\boldsymbol{r},t) = \boldsymbol{v}(\boldsymbol{r})$. More generally, we will say that a fluid flow is steady if the velocity, density, pressure, temperature, specific entropy, etc., are independent of time at every point of observation. To aid in the visualization of a flow we define the concepts of streamlines, streaklines and pathlines. All three coincide for a steady flow, though not in general. For steady flow, they are the 'field lines' or integral curves (see Sect. 5.1) of the velocity vector field, i.e., curves that are everywhere tangent to $\boldsymbol{v}(\boldsymbol{r})$ (see Fig. 19.3a). They are the trajectories of test particles moving in the steady flow, i.e., solutions of the ODEs and initial conditions

$$\frac{d\boldsymbol{r}}{ds} = \boldsymbol{v}(\boldsymbol{r}(s)) \quad \text{and} \quad \boldsymbol{r}(s_o) = \boldsymbol{r}_o. \tag{19.4}$$

Here, s is the parameter along the integral curve, it is the time that parametrizes the trajectory of the test particle moving in the steady flow. If we write these in Cartesian components $\boldsymbol{r}(s) = (x(s), y(s), z(s))$ and $\boldsymbol{v}(\boldsymbol{r}) = (v_x(\boldsymbol{r}), v_y(\boldsymbol{r}), v_z(\boldsymbol{r}))$, then the ODEs for field lines become

$$\frac{dx}{ds} = v_x, \quad \frac{dy}{ds} = v_y \quad \text{and} \quad \frac{dz}{ds} = v_z \quad \text{or} \quad \frac{dx}{v_x} = \frac{dy}{v_y} = \frac{dz}{v_z} = ds. \tag{19.5}$$

Streamlines. More generally, consider a possibly nonsteady flow. Streamlines at the observation time t_o are defined as the integral curves of the velocity field $\boldsymbol{v}(\boldsymbol{r}, t_o)$. The streamline through any point of observation P with position vector $\boldsymbol{r}(P)$ at a given time t_o is tangent to the velocity vector $\boldsymbol{v}(\boldsymbol{r}(P), t_o)$. At a given instant of time, streamlines cannot intersect. Since the flow may not be steady, the streamlines will in general change with time. Streamlines of the velocity field are analogous to the field lines of a (generally time-dependent) electric or magnetic field. In particular, for a divergence-free ($\boldsymbol{\nabla} \cdot \boldsymbol{v} = 0$) flow (see Sect. 19.5), streamlines cannot emerge or spread out from a point or region, just as magnetic field lines cannot. A flow that is spatio-temporally regular is called laminar. An example is the slow, steady flow of water through a pipe, where streamlines are parallel as in Fig. 19.3a.

Streamlines have information on the current flow. For example, we could draw the streamlines of the monsoon winds over the Indian peninsula at the onset of the South-West monsoon on June 5, 2012. These streamlines changed with time and partly reversed direction during the 'receding' North-East monsoon in November 2012.

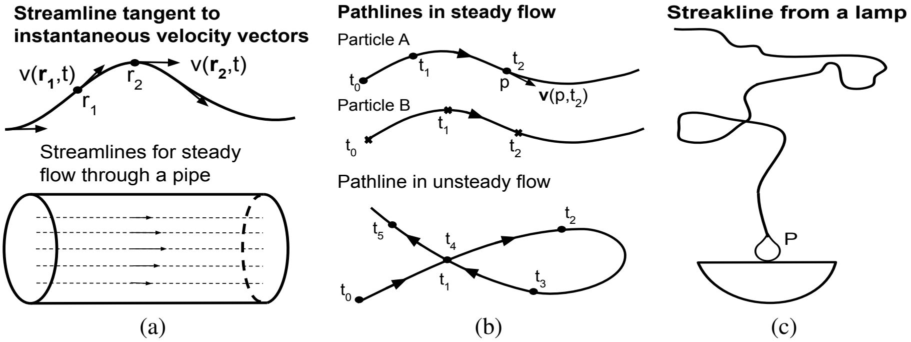

Figure 19.3: (a) Streamlines encode the instantaneous flow pattern. (b) Pathline of a speck of sawdust as it is carried by a flow. (c) Caricature of a streakline in the air above a lamp's burning wick at the point P. The burning wick introduces particles of soot into the air, which are carried by the air flow. The curve along which the soot lies at a given time is the instantaneous streakline. A burning incense stick also produces a streakline if we ignore the slow movement of the point of injection (reduction in length of the stick as it burns).

Pathlines are the trajectories of individual fluid particles. For example, if we introduced a small speck of saw dust[7] (which reflects light) into the fluid and took a movie of its trajectory, we would get its pathline (see Fig. 19.3b). At any point P along a pathline, it is tangent to the velocity vector at P at the time the particle passed through P. Pathlines can intersect themselves or even retrace themselves, for instance if a fluid particle goes round and round in a container. Two pathlines can intersect if the point of intersection corresponds to a different time on each of the two trajectories. For example, two different dust particles may pass through the same point in a room on two different days.

Streaklines. Suppose a small quantity of dye is continuously injected into a fluid flow at a fixed point of injection P. The dye is so chosen that the dye particles do not diffuse in the fluid. Rather, a dye particle tends to stick to the first fluid particle it encounters and flows along with it. So the dye released at time t sticks to the fluid particle that passes through P at time t and is then carried by that particle. The resulting highlighted curve is the *streakline* through P as illustrated in Fig. 19.3c. So at a given time of observation $t_{\rm obs}$, a streakline is the locus of all current locations of particles that passed through P at some time $t \leq t_{\rm obs}$ in the past. Unlike streamlines, streaklines provide information on the history of the flow. Streaklines for a given flow are governed by three quantities: the point of injection P, the time of observation $t_{\rm obs}$ and the time when the injection of dye began t_i. Such a streakline always begins at P and extends to a point determined by t_i when injection began. In practice, streaklines get blurred by diffusion of the dye in the fluid, however they are reasonably sharp for a time short compared to the diffusion time scale.

---

[7] Leonardo da Vinci (1452-1519) suspended fine sawdust in water and observed the motion of the saw dust as it was carried by the flow. By contrast, pollen grains were used by Robert Brown (1827) to reveal the random thermal motion of molecules under a microscope (see Sect. 18.4).

19.4 Material derivative

In the Eulerian description of fluid motion, we are interested in the time development of various fluid dynamical variables such as velocity, pressure, density and temperature at a given point of observation $\boldsymbol{r} = (x, y, z)$ in the container. This is reasonable if we are interested in predicting the weather changes at the point of observation over the course of time. For instance, the change in density at a fixed location is $\frac{\partial \rho(\boldsymbol{r})}{\partial t}$. However, different fluid particles will arrive at the point $\boldsymbol{r}$ as time passes. It is also of interest to know how the corresponding dynamical variables evolve, not at a fixed location but for a fixed small fluid element, as in a Lagrangian description. This is especially important since the dynamical laws of mechanics apply directly to the fluid particles, not to the point of observation. So, we may ask how a variable changes along the flow, so that the observer is always attached to a fixed fluid element (or 'material element') and travels along its pathline. For instance, the change in density of a fluid element in a small time dt as it moves from location $\boldsymbol{r}$ to $\boldsymbol{r} + d\boldsymbol{r}$ is

$$d\rho = \rho(\boldsymbol{r} + d\boldsymbol{r}, t + dt) - \rho(\boldsymbol{r}, t) \approx d\boldsymbol{r} \cdot \boldsymbol{\nabla}\rho + \frac{\partial \rho}{\partial t}\, dt. \tag{19.6}$$

We divide by dt, take the limit $dt \to 0$ and observe that $\boldsymbol{v} = \frac{d\boldsymbol{r}}{dt}$ is the velocity of the fluid at the point $\boldsymbol{r}$ at time t. Thus, the instantaneous rate of change of density of a fluid element that is located at $\boldsymbol{r}$ at time t is

$$\frac{D\rho}{Dt} \equiv \frac{d\rho}{dt} = \frac{\partial \rho}{\partial t} + \boldsymbol{v} \cdot \boldsymbol{\nabla}\rho = (\partial_t + v_x \partial_x + v_y \partial_y + v_z \partial_z)\, \rho. \tag{19.7}$$

$\frac{D}{Dt} = \frac{d}{dt} \equiv \frac{\partial}{\partial t} + \boldsymbol{v} \cdot \boldsymbol{\nabla}$ is called the material[8] (also total, substantial, convective) derivative. It can be used to express the rate of change of a physical quantity (velocity, pressure, temperature, etc.) associated to a fixed fluid element, i.e., along the flow specified by the velocity field $\boldsymbol{v}$. This formula for the material derivative bears a resemblance to the rigid body formula (8.53) relating the time derivatives of a vector relative to the lab and corotating frames: $\left(\frac{d\boldsymbol{A}}{dt}\right)_{\text{lab}} = \left(\frac{d\boldsymbol{A}}{dt}\right)_{\text{rot}} + \boldsymbol{\Omega} \times \boldsymbol{A}$. A quantity f (could be a scalar or a vector) is said to be conserved along the flow or dragged by the flow if its material derivative vanishes $\frac{Df}{Dt} = 0$.

Since $\frac{D}{Dt}$ is a first order partial differential operator, Leibniz's product rule of differentiation holds for scalar functions f, g: $\frac{D(fg)}{Dt} = f\frac{Dg}{Dt} + \frac{Df}{Dt}g$. Similarly, for a scalar f and vector field $\boldsymbol{w}$, we check in Prob. 19.4 that the Leibniz rule holds

$$\frac{D(f\boldsymbol{w})}{Dt} = \frac{Df}{Dt}\,\boldsymbol{w} + f\frac{D\boldsymbol{w}}{Dt}. \tag{19.8}$$

19.5 Compressibility, incompressibility and divergence of velocity field

We define a flow to be incompressible if the volume occupied by any fixed fluid element[9] (not necessarily small) remains constant in time although its shape may change. This is approximately true for water flowing in a hose pipe. Generally, liquids tend to be incompressible, they offer a large opposing force to attempts to change volume. Gases are more compressible, and high speed flows in gases tend to be compressible. However, the same material (like air) under different conditions may behave differently, depending on the speed of the flow in comparison to the speed of sound, as we will explain later in this section.

---

[8] The adjectives *material* or *substantial* are meant to convey that D/Dt is a rate of change computed while moving with the material or substance.

[9] By a fixed fluid element we mean a fixed collection of molecules. One can think of them as being surrounded by an imaginary impermeable membrane that instantaneously assumes the

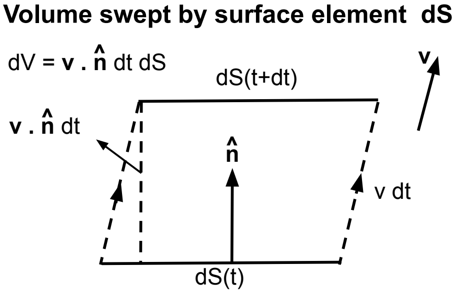

Figure 19.4: Surface element $d\boldsymbol{S} = \hat{\boldsymbol{n}}\, dS$ is carried by a flow $\boldsymbol{v}$ over a time dt sweeping out a volume $dV = \boldsymbol{v} \cdot \hat{\boldsymbol{n}}\, dt\, dS$. The figure shows a side view of the volume.

To clarify the idea of incompressibility, we ask how the volume V of a region Ω occupied by a fluid changes with time[10], i.e., we seek an expression for $\frac{dV}{dt}$. Suppose Ω is bounded by a surface $S = \partial\Omega$ with outward area element $d\boldsymbol{S}$ and outward unit normal $\hat{\boldsymbol{n}}$ such that $d\boldsymbol{S} = \hat{\boldsymbol{n}}\ dS$. In a small time dt, the region Ω changes by a movement of its bounding surface[11] in the direction of $\boldsymbol{v}$. At a point $\boldsymbol{r}$ on $\partial\Omega$, the surface element dS moves out a perpendicular distance $\boldsymbol{v} \cdot \hat{\boldsymbol{n}}\ dt$ where $\boldsymbol{v}$ is the fluid velocity at the point $\boldsymbol{r}$ (see Fig. 19.4). Thus, the change in volume $dV(dS)$ due to the area element dS moving out a bit is $\boldsymbol{v} \cdot \hat{\boldsymbol{n}}\ dt\ dS$. To include the contributions of all area elements, we integrate over the entire bounding surface to arrive at

$$\frac{dV}{dt} = \int_S \boldsymbol{v} \cdot \hat{\boldsymbol{n}}\, dS = \int_\Omega \boldsymbol{\nabla} \cdot \boldsymbol{v}\ d\boldsymbol{r}. \tag{19.9}$$

The last equality uses Gauss' divergence theorem to transform the surface integral into a volume integral. Since this is true for a fluid parcel of any volume (above molecular sizes), let us specialize to a small fluid element Ω (so that $\boldsymbol{\nabla} \cdot \boldsymbol{v}$ is roughly constant over its extent) at location $\boldsymbol{r}$ having volume δV. Then,

$$\frac{d\delta V}{dt} = \frac{D\,\delta V}{Dt} \approx (\boldsymbol{\nabla} \cdot \boldsymbol{v})\,(\delta V) \quad \text{or} \quad \boldsymbol{\nabla} \cdot \boldsymbol{v} = \lim_{V \to 0} \frac{1}{V}\frac{dV}{dt} = \lim_{V \to 0} \frac{d \log V}{dt}. \tag{19.10}$$

So the divergence of the velocity field is the fractional rate of change of volume of a small fluid element.

---

shape of the region they occupy.

[10] Here, $\frac{dV}{dt}$ is not the material derivative in the strict sense of Sect. 19.4, since V is not a local field. However, it is similar in spirit as it is the rate of change of volume following the flow.

[11] We neglect the infinitesimal change in the area dS of the surface element due to the flow. The change in volume due to such a change is of second order in infinitesimals. The surface area of a material element can change even in incompressible flow.

A flow is incompressible if each fluid element maintains its volume during the flow, i.e., $\frac{dV}{dt} = 0$ for all V (above molecular scales). It follows that a flow is incompressible iff the velocity field is divergence-free: $\boldsymbol{\nabla} \cdot \boldsymbol{v} = 0$.

Examples. A simple example of an incompressible flow is one where the density of the fluid is the same everywhere and at all times. In fact, if the density ρ is a constant, then the volume of an element is a fixed multiple $(1/\rho)$ of its mass. However, the mass of a *material* element is conserved, so its volume must remain constant. A more general example of an incompressible flow is one where the density of a given fluid element is constant in time, though different fluid elements may have different densities. This happens for horizontal flows in the atmosphere, where the density is stratified by height though the flow is horizontal. Note that the same fluid (e.g., air) under different conditions may exhibit incompressible and compressible flows. The study of compressible flows is usually termed gas dynamics or aerodynamics, while the study of incompressible flows is often termed hydrodynamics.

Compressibility and bulk modulus. Incompressibility means the volume of a fluid element does not change irrespective of the pressure applied across its surface. A measure of the compressibility[12] of a flow is the *compressibility* $\kappa = -\frac{1}{V}\frac{\partial V}{\partial p}$. The negative sign ensures that $\kappa \geq 0$, since pressure tends to decrease volume in most materials. Thus, $\kappa \to 0$ in an incompressible flow. The reciprocal of compressibility is called the bulk modulus K. Since the mass of a fluid element is conserved, incompressibility may be taken to mean that the density does not change with applied pressure. Indeed, since $\rho \propto 1/V$, we may write the compressibility[13] also as $\kappa = \frac{1}{\rho}\frac{\partial \rho}{\partial p}$. □

Relation to speed of sound. Intuitively, a sound wave is a wave of compression and expansion. As we will learn in Sect. 19.10, a sound wave propagates changes in density and travels at the speed c_s where $c_s^2 = \left(\frac{\partial p}{\partial \rho}\right)_s$ (for flow with constant specific entropy s). Evidently, c_s grows as the compressibility κ decreases. Solids tend to be less compressible than gases. As a consequence, sound propagates faster in steel than in air and we can hear an approaching train on a railway track earlier than it is heard through the air. If the flow velocity $|\boldsymbol{v}|$ is small compared to the speed of sound c_s, then the flow can usually be approximated as incompressible[14]. In fact, we may regard a strictly incompressible flow as one where the speed of sound is infinite. Crudely, any attempt by the flow to alter the density of a fluid element is immediately wiped out since sound travels much faster than the flow and irons out the change. □

---

[12] Intuitively, compressibility measures how much the volume of a fluid element decreases in response to a unit increase in applied pressure. To make compressibility independent of the size of the fluid element, we divide by its volume to arrive at an intensive variable κ.

[13] In evaluating this partial derivative using the thermodynamic equation of state (see Sect. 19.8), a third variable such as temperature or entropy is held fixed. So one has slightly different notions of compressibility depending on what is held fixed.

[14] The Mach number $M = |\boldsymbol{v}|/c_s$ (which could depend on location and time) is a way of quantifying this. The Mach number is zero in incompressible flow. Flow in regions where $M < 1$ is called subsonic while it is supersonic where $M > 1$.

Incompressibility in 2d: stream function. The condition for a vector field on the x-y plane to be incompressible can be solved in terms of a scalar *stream function* $\psi(x,y)$. Indeed, suppose $\boldsymbol{v} = (u(x,y), v(x,y), 0)$, then $\boldsymbol{\nabla} \cdot \boldsymbol{v} = 0$ becomes the condition $u_x + v_y = 0$, where subscripts denote partial derivatives. Now, if

$$u = \psi_y \quad \text{and} \quad v = -\psi_x, \tag{19.11}$$

then the incompressibility condition is identically satisfied. In 3d vector notation, we can regard $\psi(x,y)\hat{z}$ as a vector potential for the incompressible velocity field: $\boldsymbol{v} = \boldsymbol{\nabla} \times (\psi\hat{z})$, which is then automatically divergence-free. This is similar to how the solenoidal magnetic field is expressed in terms of a vector potential $\boldsymbol{B} = \boldsymbol{\nabla} \times \boldsymbol{A}$ in electrodynamics. □

To sum up, we introduced the idea of incompressibility via the divergence of $\boldsymbol{v}$ and then discussed the physical meaning of compressibility in terms of the density ρ. Pleasantly, the divergence-free condition $\boldsymbol{\nabla} \cdot \boldsymbol{v} = 0$ may be expressed in terms of the material derivative of ρ via the continuity equation, as we will see in Sect. 19.6.

19.6 Local conservation of mass: continuity equation

The total mass of fluid in a given fluid element remains constant in time, since material does not enter or leave the element. Consider a small fluid element of volume δV in the vicinity of the point $\boldsymbol{r}$ where the fluid density is $\rho(\boldsymbol{r})$ at time t. Then the mass of the fluid element is $\delta m = \rho\,\delta V$. The material derivative of δm must vanish. Using the Leibniz rule (19.8) and (19.10) we get for any small δV,

$$0 = \frac{D\,\delta m}{Dt} = \frac{D(\rho\,\delta V)}{Dt} = \frac{D\rho}{Dt}\,\delta V + \rho\,\frac{D\,\delta V}{Dt} = \left(\frac{D\rho}{Dt} + \rho\boldsymbol{\nabla}\cdot\boldsymbol{v}\right)\delta V. \tag{19.12}$$

Thus, we arrive at the *continuity equation* expressing conservation of mass

$$\frac{D\rho}{Dt} + \rho\,\boldsymbol{\nabla}\cdot\boldsymbol{v} = 0. \tag{19.13}$$

We immediately see that if the density is constant along the flow ($\frac{D\rho}{Dt} = 0$), then the flow is divergence-free ($\boldsymbol{\nabla}\cdot\boldsymbol{v} = 0$) and incompressible. Expanding the material derivative, we get

$$\frac{\partial\rho}{\partial t} + \boldsymbol{v}\cdot\boldsymbol{\nabla}\rho + \rho\,\boldsymbol{\nabla}\cdot\boldsymbol{v} = 0. \tag{19.14}$$

In particular, if $\rho = \rho_0$ is constant in both time and space, then the flow must be incompressible. On the other hand, if the flow is incompressible, i.e., $\boldsymbol{\nabla}\cdot\boldsymbol{v} = 0$, then the density must be constant along the flow, $\frac{D\rho}{Dt} = \frac{\partial\rho}{\partial t} + (\boldsymbol{v}\cdot\boldsymbol{\nabla})\rho = 0$. We say the density is advected or transported by an incompressible flow.

Combining the last two terms in (19.14), the continuity equation can be written in local conservation form (see Sect. 17.6):

$$\frac{\partial\rho}{\partial t} + \boldsymbol{\nabla}\cdot(\rho\boldsymbol{v}) = 0. \tag{19.15}$$

We say that ρ is the locally conserved mass density and $\rho\boldsymbol{v}$ is the corresponding mass current density. The continuity equation says that the rate of change of density at a point is balanced by the divergence of the mass current density. We may also write (19.15) in integral form, by integrating over a region Ω that is *fixed* in space (does not move with the flow) and applying Gauss' divergence theorem:

$$\int_\Omega \frac{\partial \rho}{\partial t}\, d\boldsymbol{r} + \int_\Omega \boldsymbol{\nabla}\cdot(\rho\boldsymbol{v})\, d\boldsymbol{r} = 0 \quad \text{or} \quad \frac{d}{dt}\int_\Omega \rho\, d\boldsymbol{r} + \int_{S=\partial\Omega} \rho\boldsymbol{v}\cdot d\boldsymbol{S} = 0. \quad (19.16)$$

The 1^{st} term is the rate of increase of mass inside a fixed volume Ω. The 2^{nd} gives the outward flux of mass across the boundary S. So mass is neither created nor destroyed: it can only move around *continuously*, hence the name 'continuity' equation. If Ω is the entire flow domain, then the first term is the rate of increase of mass of the fluid as a whole, which must vanish provided the mass flux across the boundary is zero.

19.7 Euler equation for inviscid flow

An inviscid (sometimes called ideal) fluid flow is one where no resistance is offered to changes in shape that are not accompanied by a change in volume. We will elaborate on this shortly. In particular, ideal fluids assume the shape of the container; they lack a rigidity of form. This means that in an ideal flow, the force acting on a material element (anywhere in the fluid) across its surface, due to the material outside, is everywhere normal to the surface. Tangential surface forces tend to *shear* the element and change its shape without affecting its volume. On the other hand, normal surface forces tend to compress or expand[15] the element and thereby change its volume. The inward directed normal surface force per unit area is called pressure p. So in an inviscid flow, tangential or shearing stresses vanish irrespective of the location and orientation of the surface. In viscous flows, tangential forces typically arise between layers of fluid in relative motion. Thus, tangential forces are absent in hydrostatics.

Stress tensor[16]**.** In general, forces need not be either normal or tangential to surfaces[17] in the fluid, and they could vary in magnitude and direction with location. The stress tensor is a quantity that encodes the force per unit area acting across an element of surface. Let $\hat{\boldsymbol{n}}\,\delta S$ be a small surface element of area δS, with unit normal $\hat{\boldsymbol{n}}$, centered at $\boldsymbol{r}$. Let $\boldsymbol{F}(\hat{\boldsymbol{n}}\,\delta S, \boldsymbol{r})$ be the force that acts across the surface, its magnitude must be proportional to the area δS. Precisely, it is the force on the material on the side to which $\hat{\boldsymbol{n}}$ points, due to the material on the other side, as shown in Fig. 19.5. In general, $\boldsymbol{F}$ and $\hat{\boldsymbol{n}}$ point in different directions and are related by a linear transformation, the transformation of stress. If we choose to write all vectors in some basis, e.g., resolve them according to Cartesian components, then this linear relation may be written as

$$\boldsymbol{F}_i(\hat{\boldsymbol{n}}\,\delta S, \boldsymbol{r}) = \sum\nolimits_j T_{ij}(\boldsymbol{r}) n_j\, \delta S. \quad (19.17)$$

---

[15] Normal surface forces that tend to expand an element are called tensile stresses, as is the case in an elastic rod that is being stretched. Tensile stresses correspond to a *negative* pressure.

[16] Here, we introduce the stress tensor in general, not necessarily for inviscid flow.

[17] These may be external or, more frequently, hypothetical internal surfaces in the fluid.

The 3×3 matrix $T_{ij}(\boldsymbol{r})$ is called the stress tensor field. It depends only on the location $\boldsymbol{r}$ and not on the surface or $\hat{\boldsymbol{n}}$. By choosing a surface whose normal $\hat{\boldsymbol{n}}$ points in the j^{th} direction, we see that T_{ij} is then the i^{th} component of the force acting on the material towards the j^{th} direction of a surface of unit area whose normal points in the j^{th} direction. Alternatively, suppose δS is a small surface with normal $\hat{\boldsymbol{n}}$, then $\sum_j T_{ij} n_j (\delta S)$ is the i^{th} component of the force acting on the material on the side to which the normal $\hat{\boldsymbol{n}}$ points.

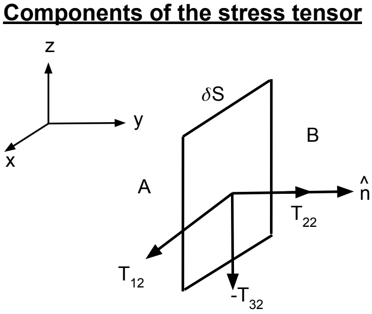

Figure 19.5: Components of the force due to fluid A on fluid B across a small surface with unit normal $\hat{\boldsymbol{n}}$ which here points along $\hat{y}$. T_{32} is the third component of the force on the material located on the second direction of the surface.

Example: stress tensor in hydrostatics and inviscid flow. By definition, hydrostatic pressure acts normal to any surface. So consider a small cuboid with axes along Cartesian axes. It follows that $T_{ij} = 0$ for $i \neq j$, as there are no tangential stresses. Moreover, $T_{33} = p$ since the force across the top surface (whose normal points along $\hat{z}$) due to the fluid below, is $p\hat{z}$. We get the same answer by considering the bottom surface. Proceeding in this way, $T_{ij} = p\delta_{ij}$. This formula for the stress tensor due to hydrostatic pressure is independent of basis: multiples of the identity matrix have the same components in any basis. More generally, the absence of tangential stresses in an inviscid flow irrespective of orientation of surfaces implies that the stress tensor is diagonal in every basis, and must be proportional to the identity: $T_{ij} = p\delta_{ij}$. □

Euler equation. To derive the equation of motion for an inviscid flow, consider a small fluid element of mass $\delta m = \rho\, \delta V$ occupying a volume δV and having instantaneous velocity $\boldsymbol{v}$. Let us write Newton's 2^{nd} law for this fluid element. The change in its velocity in a time dt as it is displaced from $\boldsymbol{r}$ to $\boldsymbol{r} + d\boldsymbol{r}$ is

$$d\boldsymbol{v} = \boldsymbol{v}(\boldsymbol{r} + d\boldsymbol{r}, t + dt) - \boldsymbol{v}(\boldsymbol{r}, t) \approx \frac{\partial \boldsymbol{v}}{\partial t} dt + (d\boldsymbol{r} \cdot \boldsymbol{\nabla})\boldsymbol{v}. \tag{19.18}$$

Dividing by dt, letting $dt \to 0$ and noting that $d\boldsymbol{r}/dt = \boldsymbol{v}$, we obtain its acceleration: $D\boldsymbol{v}/Dt \equiv \partial \boldsymbol{v}/\partial t + (\boldsymbol{v} \cdot \boldsymbol{\nabla})\boldsymbol{v}$. The material derivative $D\boldsymbol{v}/Dt$ differs from the partial derivative by the quadratically nonlinear 'advection' term $(\boldsymbol{v} \cdot \boldsymbol{\nabla})\boldsymbol{v}$. By Newton's 2^{nd} law, the force acting on the element must equal $\rho\, \delta V\, \frac{D\boldsymbol{v}}{Dt}$.

We consider two sorts of forces acting on the fluid element. There can be an external force field such as gravity (called a body force) acting on the fluid. It may be expressed as $\boldsymbol{f}\delta V$ where $\boldsymbol{f}(\boldsymbol{r})$ is the body force per unit volume (e.g., $\boldsymbol{f} = \rho \boldsymbol{g}$ where

$\boldsymbol{g}$ is the acceleration due to gravity). In addition, we have the surface force due to the pressure exerted on the element by the fluid surrounding the element. To calculate this, assume the fluid element is a cuboid with sides dx, dy, dz. The net pressure force in the $\hat{x}$ direction is the product of the area $dy\,dz$ and pressure differential between the two faces: $\delta F_x = -\frac{\partial p}{\partial x} dx \times dy\,dz$. The $-$ sign arises because if p is greater on the right face of the element compared to the left face, then the net force would be leftward. Thus, the total surface force[18] on the fluid element is $\delta \boldsymbol{F} = -(\boldsymbol{\nabla} p)\delta V$. Thus, Newton's 2^{nd} law for the fluid element reads

$$\rho\,\delta V\,\frac{D\boldsymbol{v}}{Dt} = -(\boldsymbol{\nabla} p)\,\delta V + \boldsymbol{f}\,\delta V. \tag{19.20}$$

Dividing by δV, we get Euler's celebrated equation of motion[19] for an inviscid fluid. It must be considered in conjunction with the continuity equation (19.13)

$$\frac{\partial \boldsymbol{v}}{\partial t} + \boldsymbol{v}\cdot\boldsymbol{\nabla}\boldsymbol{v} = -\frac{1}{\rho}\boldsymbol{\nabla} p + \frac{\boldsymbol{f}}{\rho} \quad \text{and} \quad \frac{D\rho}{Dt} + \rho\boldsymbol{\nabla}\cdot\boldsymbol{v} = 0. \tag{19.22}$$

Notice that the Euler equation is quadratically nonlinear in $\boldsymbol{v}$ due to the $\boldsymbol{v}\cdot\boldsymbol{\nabla}\boldsymbol{v}$ advection term. This makes it difficult to solve but also allows it to describe a wide variety of ideal flows. A vector identity (see Prob. 19.8) allows us to write the advection term in terms of the *vorticity* $\boldsymbol{w} = \boldsymbol{\nabla}\times\boldsymbol{v}$ and a gradient term:

$$\frac{\partial \boldsymbol{v}}{\partial t} + \boldsymbol{w}\times\boldsymbol{v} = -\frac{1}{\rho}\boldsymbol{\nabla} p - \frac{1}{2}\boldsymbol{\nabla} v^2 + \frac{\boldsymbol{f}}{\rho} \tag{19.23}$$

Here $\boldsymbol{w}\times\boldsymbol{v}$ is called the vortex force per unit mass or Lamb vector. We will have more to say about vorticity in Sect. 19.11.

The Euler and continuity equations are first order in time derivatives of $\boldsymbol{v}$ and ρ. So we need to specify the initial values $\rho(\boldsymbol{r},0)$ and $\boldsymbol{v}(\boldsymbol{r},0)$, to be able to evolve them forward in time[20]. However, these are still only four evolution equations for five

---

[18] More generally, the force due to pressure across the surface $\partial(\delta V)$ of the element is

$$\delta\boldsymbol{F}_{\text{surface}} = -\int_{\partial(\delta V)} p\hat{\boldsymbol{n}}\,dS = -\int_{\delta V} \boldsymbol{\nabla} p\,dV \approx -\boldsymbol{\nabla} p\,\delta V. \tag{19.19}$$

We have used a corollary of Gauss' divergence theorem (see Prob. 19.5) to convert the surface integral to a volume integral and taken $\boldsymbol{\nabla} p$ to be constant over the small volume δV. The minus sign is because $\hat{\boldsymbol{n}}$ is the outward-pointing normal.

[19] The Euler equation can be written in terms of the stress tensor $T_{ij} = p\delta_{ij}$

$$\partial_t v_i + v_j\partial_j v_i = -\frac{1}{\rho}\partial_j T_{ij} + \frac{1}{\rho} f_i \quad \text{in Cartesian components.} \tag{19.21}$$

The equation may be generalized to viscous flows by including tangential stresses in T_{ij} (see Sect. 19.16). Here, repeated indices are summed and no distinction is made between upper and lower indices.

[20] In addition, we need to impose suitable *boundary conditions*. The Euler and continuity equations are first order in space derivatives, and we may impose conditions on the boundary

unknown functions (density, pressure and three components of the velocity field). In particular, we have not specified how the pressure evolves in time. We will address this question for adiabatic flow in Sect. 19.8. Here, we deal with the slightly simpler case of incompressible constant density flow.

Pressure for constant density flow. If $\rho(\boldsymbol{r},t) = \bar{\rho}$ is a constant in space and time, then the continuity equation (19.14) implies $\boldsymbol{\nabla} \cdot \boldsymbol{v} = 0$. Taking the divergence of the Euler equation (19.22) (in the absence of external body forces), the time derivative term is eliminated leaving us with a nondynamical 'constraint' equation

$$\boldsymbol{\nabla}^2 p = -\bar{\rho}\, \boldsymbol{\nabla} \cdot (\boldsymbol{v} \cdot \boldsymbol{\nabla} \boldsymbol{v}). \tag{19.24}$$

If we view the RHS as a source, this is Poisson's equation[21] for p. It can be solved with suitable boundary conditions, say using Green's function for the Laplace operator. For decaying BCs, we have

$$p(\boldsymbol{r},t) = \frac{\bar{\rho}}{4\pi} \int \frac{\boldsymbol{\nabla} \cdot (\boldsymbol{v} \cdot \boldsymbol{\nabla} \boldsymbol{v})(\boldsymbol{r}')}{|\boldsymbol{r} - \boldsymbol{r}'|} d\boldsymbol{r}'. \tag{19.25}$$

Thus, for constant density, we have been able to eliminate the pressure from the Euler equation, which becomes an evolution equation for $\boldsymbol{v}$ alone. We say that in constant density flow, the pressure is not dynamical. It does not obey an independent evolution equation but is determined by the instantaneous velocity distribution. See Prob. 19.7 for the case of incompressible flow with variable density. □

19.8 Ideal adiabatic flow: entropy advection and equation of state

As pointed out below Eq. (19.22), the Euler and continuity equations (19.22) are generally an underdetermined system: they do not tell us how the pressure evolves. To understand how the pressure evolves, we need to broaden our physical perspective. Recall from Sect. 19.1 that a fluid can usually be considered to be in local thermal equilibrium. This means there is a local temperature field $T(\boldsymbol{r},t)$ that, along with the pressure and density, satisfies an equation of state ($p = \rho k_b T/m$ for an ideal gas with molecular mass μ.). To find the remaining dynamical equation, it is fruitful to ask how the conjugate variable to T, i.e., the entropy evolves. For a dissipationless flow, it is physically reasonable to suppose that the entropy of a fluid element remains constant in time, just as its mass does. In other words, there is no entropy production or heat exchanged between fluid elements. Such a flow is called adiabatic.

---

values of $\boldsymbol{v}$ and ρ. On fixed impenetrable boundaries, the normal component $\boldsymbol{v} \cdot \hat{\boldsymbol{n}}$ must vanish. In the absence of viscosity, the tangential component of $\boldsymbol{v}$ is unconstrained on boundaries. In unbounded regions, we typically have decaying BCs: $\boldsymbol{v} \to 0$ and $\rho \to \rho_0$ as $|\boldsymbol{r}| \to \infty$.

[21] In electrostatics, when the electric field is expressed in terms of an electrostatic potential ($\boldsymbol{E} = -\boldsymbol{\nabla}\phi$), Gauss' law $\boldsymbol{\nabla} \cdot \boldsymbol{E} = \rho/\epsilon_0$ leads to Poisson's equation $\boldsymbol{\nabla}^2\phi = -\rho/\epsilon_0$, where $\rho(\boldsymbol{r})$ is the electric charge density. The solution involves the Coulomb potential, which is essentially the Green function of the Laplace operator: $\phi = \frac{1}{4\pi\epsilon_0} \int \frac{\rho(\boldsymbol{r}')}{|\boldsymbol{r}-\boldsymbol{r}'|} d\boldsymbol{r}'$. See Footnote 48 of Sect. 2.7* and Sect. 6.8.

Dynamics of specific entropy. Now consider a small fluid element of volume δV and let s denote the specific entropy field (entropy per unit mass). Then the entropy of the fluid element is $\rho\, s\, \delta V$. If this is conserved as the element moves around, then its material derivative must vanish. Using the Leibniz rule and (19.10), we get

$$\frac{D(\rho s \delta V)}{Dt} = \rho s(\boldsymbol{\nabla}\cdot\boldsymbol{v})\delta V + \delta V \frac{D(\rho s)}{Dt} = 0 \quad \text{or} \quad \partial_t(\rho s) + \boldsymbol{\nabla}\cdot(\rho s \boldsymbol{v}) = 0. \quad (19.26)$$

In other words, the entropy per unit volume ρs is locally conserved[22] with the corresponding entropy current given by $\rho s \boldsymbol{v}$. Using the continuity equation (19.14), the adiabaticity of the flow implies that s is advected by $\boldsymbol{v}$:

$$\partial_t s + \boldsymbol{v}\cdot\boldsymbol{\nabla} s = 0. \quad (19.27)$$

This is our third evolution equation. The pressure is then determined by the equation of state, which may be regarded as a relation among s, p and ρ. For instance, for an ideal gas with constant specific heat ratio $\gamma = c_p/c_v$, the equation of state is

$$s = c_v \log\left(\frac{p/\bar{p}}{(\rho/\bar{\rho})^\gamma}\right) \quad (19.28)$$

for some reference values $\bar{p}$ and $\bar{\rho}$ (see Prob. 19.9).

Internal energy or pressure equation. We may also combine this equation of state (19.28), the entropy advection equation (19.27) and the continuity equation (19.14) to derive an evolution equation for pressure (see Prob. 19.11):

$$\left(\frac{p}{\gamma-1}\right)_t + p\boldsymbol{\nabla}\cdot\boldsymbol{v} + \boldsymbol{\nabla}\cdot\left(\frac{p\boldsymbol{v}}{\gamma-1}\right) = 0. \quad (19.29)$$

This is called the internal energy equation since $p/(\gamma-1)$ will be interpreted as the internal energy density of an ideal gas (see Sect. 19.13).

Homentropic and barotropic flow. Homentropic flow is a situation where the entropy advection equation (19.27) can be eliminated. Here, the specific entropy $s = s_0$ is independent of both space and time and (19.27) is identically satisfied. Moreover, the equation of state then becomes a relation between ρ and p. In general, a relation between ρ and p is called a barotropic relation. For example[23], for homentropic flow of an ideal gas with adiabatic index γ, the barotropic relation can be written as $(p/p_0) = (\rho/\rho_0)^\gamma$ for some reference values p_0 and ρ_0. For barotropic flow, pressure $p(\boldsymbol{r}, t)$ is determined by the instantaneous density $\rho(\boldsymbol{r}, t)$ and we do not need to supplement the continuity and Euler equations by a third evolution equation.

---

[22] Integrating over the flow domain and assuming the entropy flux across the boundary vanishes, we arrive at the global conservation of entropy $\frac{d}{dt}\int \rho\, s\, d\boldsymbol{r} = 0$.

[23] Another example of barotropic flow is the isothermal inviscid compressible flow of an ideal gas. The barotropic relation is $p = \rho k_b T/m$ where T is the constant temperature and m the mass of a molecule. In this case, the role of specific enthalpy is played by the specific Gibbs free energy $g(\rho) = (k_b T/m)\log(\rho/\rho_0)$ which is determined up to a constant by $\boldsymbol{\nabla} g = (\boldsymbol{\nabla} p)/\rho$.

Remark. Note that for $\gamma = 1$, the barotropic relation for homentropic flow of an ideal gas becomes $p = (p_0/\rho_0)\rho$ where p_0/ρ_0 is a constant. Comparing with the ideal gas law $p = (k_b T/m)\rho$, we infer that the temperature in such a flow, $T = mp_0/k_b\rho_0$, is spatially constant and independent of time. Thus, such a flow must be isothermal. However, not all isothermal flows arise this way. A gas with $\gamma = c_p/c_v \neq 1$ can display an isothermal flow. □

An important consequence of a barotropic relation expressing $\rho = \rho(p)$ is that the pressure term on the RHS of the Euler equation (19.23) can be expressed as a gradient:

$$\frac{\nabla p}{\rho} = \nabla h \quad \text{where} \quad h(p) = \int_{p_0}^{p} \frac{dp'}{\rho(p')} \quad \text{so} \quad \nabla h = h'(p)\nabla p = \frac{1}{\rho}\nabla p. \tag{19.30}$$

For barotropic (homentropic) flow of an ideal gas,

$$\frac{\nabla p}{\rho} = \gamma\frac{p_0}{\rho_0}\left(\frac{\rho}{\rho_0}\right)^{\gamma-1}\frac{\nabla\rho}{\rho} = \frac{\gamma}{\gamma-1}\nabla\left(\frac{p}{\rho}\right) \quad \Rightarrow \quad h = \frac{\gamma}{\gamma-1}\left(\frac{p}{\rho}\right). \tag{19.31}$$

Here, $h(\rho)$ is called the specific enthalpy or enthalpy per unit mass[24]. If, in addition, the body force per unit mass can be expressed as a gradient, $\boldsymbol{f}/\rho = -\nabla\varphi$ [i.e., body force is conservative], then the RHS of Euler's equation (19.22) becomes a gradient:

$$\frac{D\boldsymbol{v}}{Dt} = \partial_t\boldsymbol{v} + \boldsymbol{v}\cdot\nabla\boldsymbol{v} = -\nabla(h+\varphi). \tag{19.32}$$

What is more, using the identity (19.129) to write the advection term in terms of the vortex force, the Euler equation becomes

$$\partial_t\boldsymbol{v} + \boldsymbol{w}\times\boldsymbol{v} = -\nabla(\sigma+\varphi) \quad \text{where} \quad \sigma = h + \frac{1}{2}v^2. \tag{19.33}$$

Here, σ is called the *stagnation enthalpy*, it reduces to the enthalpy at a stagnation point (i.e., one where $\boldsymbol{v} = 0$).

19.9 Bernoulli's equation

Bernoulli's principle for steady flow. Recall from Sect. 19.3, that a fluid flow is steady if $\boldsymbol{v}, \rho, p$, etc., are not explicitly dependent on time. In its simplest form, Bernoulli's principle concerns a drop in pressure along a streamline in places where a steady constant density flow speeds up. Euler's equation (19.33) for a steady homentropic flow with specific enthalpy $h(\rho)$ and body force potential φ is

$$\boldsymbol{v}\times\boldsymbol{w} = \nabla\left(\frac{1}{2}\boldsymbol{v}^2 + h + \varphi\right) \quad \text{where} \quad \boldsymbol{w} = \nabla\times\boldsymbol{v}. \tag{19.34}$$

---

[24] The first law of thermodynamics $dU = TdS - pdV$, when written in terms of enthalpy $H = U + pV$ instead of internal energy U, becomes $dH = TdS + Vdp$. For an isentropic process $dS = 0$, so $dh = dp/\rho$. Here $V = M/\rho$ is the volume, M the mass of fluid, $h = H/M$ the enthalpy per unit mass, T absolute temperature and S the entropy.

For example, $\varphi = gz$ for the gravitational body force, where z is the vertical height and g the magnitude of the acceleration due to gravity. The left member is orthogonal to $\boldsymbol{v}$, so upon taking the dot product with the velocity field, we get Bernoulli's equation:

$$\boldsymbol{v} \cdot \boldsymbol{\nabla} \mathcal{B} = 0 \quad \text{where} \quad \mathcal{B} = \frac{1}{2}\boldsymbol{v}^2 + h + \varphi. \tag{19.35}$$

Thus, the component of the gradient of the Bernoulli specific energy $\mathcal{B}$ along the velocity vector field is zero. If $\boldsymbol{r}(s)$ is a streamline[25], then Bernoulli's equation becomes

$$\frac{d\boldsymbol{r}}{ds} \cdot \boldsymbol{\nabla} \mathcal{B} = 0 \quad \text{or} \quad \frac{d\mathcal{B}(\boldsymbol{r}(s))}{ds} = 0. \tag{19.36}$$

So in steady flow, $\mathcal{B} = \frac{1}{2}\boldsymbol{v}^2 + h + \varphi$ is constant along streamlines. Note that $\mathcal{B}$ will, in general, take different values for different streamlines. Now recall that the enthalpy per unit mass is $h = \varepsilon + \frac{p}{\rho}$ where ε is the internal energy per unit mass, p the pressure and ρ the density. Thus, for steady homentropic inviscid flow subject to a conservative body force, Bernoulli's equation says that along streamlines,

$$\mathcal{B} = \frac{1}{2}v^2 + \varepsilon + \frac{p}{\rho} + \varphi \quad \text{is conserved.} \tag{19.37}$$

If the flow is incompressible, then ρ is constant along the flow and, in particular, along streamlines of the steady flow. Suppose the internal energy density of the fluid is also constant along the flow. Then we find that $\frac{1}{2}\rho v^2 + p + \rho\varphi$ is constant along streamlines. If in addition, the body force potential φ does not vary along the streamline (as for horizontal streamlines in a vertical gravitational field), then $\frac{1}{2}\rho v^2 + p$ is constant along streamlines. In other words, in regions of high pressure along a streamline, the fluid speed must be low and vice-versa. Such a situation is approximately encountered in laminar flow through a cylindrical pipe of varying cross section. On account of mass conservation, the water speeds up in regions where there is a constriction in the pipe. At such constrictions, the pressure drops, as can be demonstrated by comparing the pressure with atmospheric pressure (a lower pressure supports a shorter vertical column of water against atmospheric pressure).

Bernoulli equation for unsteady flow. There is a version of the Bernoulli equation (19.35) that applies to unsteady flows, though in the restricted context of barotropic potential flow ($\boldsymbol{v} = \boldsymbol{\nabla}\phi$). Potential flow is irrotational $\boldsymbol{w} = \boldsymbol{\nabla} \times \boldsymbol{v} = 0$, so the vortex force vanishes and the Euler equation (19.33) for barotropic flow subject to a body force derived from a potential ($\boldsymbol{f}/\rho = -\boldsymbol{\nabla}\varphi$) becomes

$$\frac{\partial \boldsymbol{v}}{\partial t} = -\boldsymbol{\nabla} h - \boldsymbol{\nabla}\left(\frac{1}{2}v^2\right) - \boldsymbol{\nabla}\varphi \quad \text{or} \quad \boldsymbol{\nabla}\left(h + \frac{\partial \phi}{\partial t} + \frac{1}{2}v^2 + \varphi\right) = 0. \tag{19.38}$$

The quantity in parentheses must be independent of location but could depend on time. Thus, we arrive at the unsteady Bernoulli equation for barotropic potential flow:

$$\frac{\partial \phi}{\partial t} + h + \frac{1}{2}(\boldsymbol{\nabla}\phi)^2 + \varphi = B(t). \tag{19.39}$$

---

[25] A streamline $\boldsymbol{r}(s)$ is an integral curve of the velocity vector field: $\frac{d\boldsymbol{r}}{ds} = \boldsymbol{v}(\boldsymbol{r}(s))$. Here, s is a parameter along the streamline.

The simplest case is that of constant density, were $h = p/\rho$. Unlike Bernoulli's equation (19.35) for steady flow, (19.39) holds throughout the fluid and is not associated with streamlines. The unsteady Bernoulli equation may also be interpreted as an evolution equation for the velocity potential ϕ. It can also be used to eliminate the pressure p in favor of the velocity potential when computing the force due to pressure[26] on a body immersed in a fluid [70].

19.10 Sound waves in homentropic flow

By sound waves, we usually mean small oscillations of the density, pressure and velocity fields around a 'background' flow. They arise in compressible flows, where regions of compression and rarefaction can form and propagate. It is these pressure variations that our ears receive and help us perceive as sound. For simplicity, we shall consider sound waves in the background of a motionless homogeneous fluid.

Notice first that in the absence of body forces, a fluid at rest ($\boldsymbol{v} = 0$) with *constant* pressure and density ($p = p_0$, $\rho = \rho_0$) is a static solution to the continuity and Euler equations (19.22):

$$\partial_t \rho + \boldsymbol{\nabla} \cdot (\rho \boldsymbol{v}) = 0 \quad \text{and} \quad \rho(\partial_t \boldsymbol{v} + \boldsymbol{v} \cdot \boldsymbol{\nabla} \boldsymbol{v}) = -\boldsymbol{\nabla} p. \tag{19.40}$$

Now suppose the still fluid suffers a disturbance resulting in small variations

$$\boldsymbol{v} = 0 + \boldsymbol{v}_1(\boldsymbol{r}, t), \quad \rho = \rho_0 + \rho_1(\boldsymbol{r}, t) \quad \text{and} \quad p = p_0 + p_1(\boldsymbol{r}, t). \tag{19.41}$$

The perturbations $\boldsymbol{v}_1(\boldsymbol{r}, t), p_1(\boldsymbol{r}, t)$ and $\rho_1(\boldsymbol{r}, t)$ must be such that $\boldsymbol{v}, p$ and ρ satisfy the continuity and Euler equations with $\boldsymbol{v}_1, p_1, \rho_1$ treated to linear order. However, we need to supplement (19.40) with another equation, as we currently have only four equations for five unknowns: ρ, p and the 3 components of $\boldsymbol{v}$. Following Laplace, we will consider the physically realistic case of sound waves in adiabatic flow of an ideal gas[27]. As discussed in (19.27), specific entropy is advected by adiabatic flow: $\partial_t s + \boldsymbol{v} \cdot \boldsymbol{\nabla} s = 0$. A steady uniform specific entropy $s = s_0$ is clearly a valid background solution. Putting $s = s_0 + s_1(\boldsymbol{r}, t)$ and linearizing around the static homogeneous background, we get

$$\partial_t s_1 + \boldsymbol{v}_1 \cdot \boldsymbol{\nabla} s_1 \approx \partial_t s_1 = 0. \tag{19.42}$$

The simplest solution is the one with vanishing entropy perturbation $s_1(\boldsymbol{r}, t) \equiv 0$, corresponding to homentropic flow $s(\boldsymbol{r}, t) \equiv s_0$. In particular, the specific entropy of every fluid element is the same and remains that way at all times. Now, for homentropic flow, the thermodynamic equation of state relating p, ρ and s reduces to a barotropic relation between pressure and density $p = p(\rho, s_0)$ [such as $p/p_0 = (\rho/\rho_0)^\gamma$ for adiabatic flow of an ideal gas]. Inserting (19.41) in the barotropic relation and using the leading Taylor approximation, we get

---

[26] If S is a surface with fluid to one side of it, then the force on the surface due to fluid pressure is given by $\int_S p\, \hat{\boldsymbol{n}}\, dA$ where dA is the area element and $\hat{\boldsymbol{n}}$ is the unit normal pointing away from the fluid.

[27] In his Principia, Newton computed the speed of sound in air assuming the flow to be isothermal. This was found not to be a particularly good approximation, since there are temperature fluctuations in a sound wave. Laplace's assumption of adiabatic flow led to a value closer to experimental measurements ($c_s^2 = \gamma p/\rho$ for an ideal gas).

$$p = p_0 + \left(\frac{\partial p}{\partial \rho}\right)_{\rho_0, s_0} \rho_1 + \cdots \quad \Rightarrow \quad p_1 \approx \left(\frac{\partial p}{\partial \rho}\right)_{\rho_0, s_0} \rho_1. \tag{19.43}$$

Thus, the small pressure and density variations are proportional. The constant of proportionality[28] is denoted (celeritas means velocity in Latin)

$$c_s^2 = \left(\frac{\partial p}{\partial \rho}\right)_{\rho_0, s_0} = \frac{K_s}{\rho_0} \tag{19.44}$$

and has dimensions of the square of a speed. We will show that c_s (called the adiabatic sound speed) is the speed at which sound waves propagate. To do so, we derive an equation for sound waves by linearizing the continuity and Euler equations around a motionless fluid. Ignoring products of small quantities $\boldsymbol{v}_1, p_1$ and ρ_1, the continuity and Euler equations

$$\begin{aligned} \partial_t(\rho_0 + \rho_1) + \boldsymbol{\nabla} \cdot ((\rho_0 + \rho_1)\boldsymbol{v}_1) &= 0 \quad \text{and} \\ (\rho_0 + \rho_1)(\partial_t \boldsymbol{v}_1 + \boldsymbol{v}_1 \cdot \boldsymbol{\nabla} \boldsymbol{v}_1) &= -\boldsymbol{\nabla}(p_0 + p_1) \end{aligned} \tag{19.45}$$

become

$$\partial_t \rho_1 + \rho_0 \boldsymbol{\nabla} \cdot \boldsymbol{v}_1 = 0 \quad \text{and} \quad \rho_0 \partial_t \boldsymbol{v}_1 = -\boldsymbol{\nabla} p_1. \tag{19.46}$$

Putting $p_1 = c_s^2 \rho_1$ and taking a divergence, the linearized Euler equation becomes

$$\rho_0 \partial_t (\boldsymbol{\nabla} \cdot \boldsymbol{v}_1) = -c^2 \boldsymbol{\nabla}^2 \rho_1. \tag{19.47}$$

Eliminating $\boldsymbol{\nabla} \cdot \boldsymbol{v}_1 = -\rho_0^{-1} \partial_t \rho_1$ using the continuity equation, we get

$$\partial_t^2 \rho_1 = c_s^2 \boldsymbol{\nabla}^2 \rho_1, \tag{19.48}$$

which we recognize as the 3d d'Alembert wave equation for density variations. From our discussion of the wave equation in Sect. 17.4, we deduce that c_s may be interpreted as the speed at which sound waves propagate. The corresponding equations for pressure and velocity perturbations are the subject of Prob. 19.13.

As we might physically expect from Sect. 19.5, for incompressible flow ($\rho = \rho_0, \rho_1 = 0$), the sound speed $c_s^2 = \frac{p_1}{\rho_1} = \frac{\delta p}{\delta \rho} \to \infty$ as the density variations are vanishingly small even for large pressure variations. Thus, sound waves travel much faster than the fluid in the incompressible limit and the Mach number $M = |\boldsymbol{v}|/c_s$ tends to zero. Sound waves are expelled from the spectrum of wave-like disturbances in this limit.

---

[28] Here, K_s is the isentropic bulk modulus (see Sect. 19.5), a measure of stiffness of the medium.

19.11 Vorticity and its evolution

Vorticity $\boldsymbol{w} = \boldsymbol{\nabla} \times \boldsymbol{v}$ is the curl of the velocity field[29]. Unlike $\boldsymbol{v}$, which is a polar vector (reverses sign under the reflection $\boldsymbol{r} \to -\boldsymbol{r}$), $\boldsymbol{w}$ is a pseudovector or axial vector (no change in sign under reflections, see Sect. 3.13*). Since the divergence of a curl vanishes, vorticity is solenoidal: $\boldsymbol{\nabla} \cdot \boldsymbol{w} = 0$. Vorticity has dimensions of (1/time) and is a measure of local rotation in a flow. A flow without vorticity is called irrotational[30]. For example, a bucket of fluid rigidly rotating at small angular velocity $\boldsymbol{\Omega} = \Omega \hat{z}$ has the azimuthal velocity field $\boldsymbol{v}(r, \theta, z) = \boldsymbol{\Omega} \times \boldsymbol{r} = \Omega r \hat{\theta}$ in cylindrical coordinates (see Fig. 19.6a). The corresponding vorticity $\boldsymbol{w} = \boldsymbol{\nabla} \times \boldsymbol{v} = \frac{1}{r} \partial_r (r v_\theta) \hat{z}$ is vertically upwards and constant over the bucket. In fact, as pointed out by Stokes, $\boldsymbol{w} = 2\Omega \hat{z}$ has a magnitude of twice the angular speed Ω. Eddies or vortices are manifestations of vorticity in a flow. They are ubiquitous[31] in flows and can come in various sizes: in a wash basin, in the sea and in the atmosphere.

Given a closed contour C in a fluid, the *circulation* $\Gamma(C) = \oint_C \boldsymbol{v} \cdot d\boldsymbol{l}$ measures how much $\boldsymbol{v}$ 'goes round' C. For a simple closed contour C, Stokes' theorem implies that the circulation is the flux of vorticity across any surface S in the fluid that spans C (i.e., whose boundary ∂S is C):

$$\Gamma(C) = \oint_C \boldsymbol{v} \cdot d\boldsymbol{l} = \int_S (\boldsymbol{\nabla} \times \boldsymbol{v}) \cdot d\boldsymbol{S} = \int_S \boldsymbol{w} \cdot d\boldsymbol{S} \quad \text{where} \quad \partial S = C. \tag{19.49}$$

Enstrophy. The square of the L^2 norm of vorticity $\int \boldsymbol{w}^2 \, d\boldsymbol{r}$ is called enstrophy. It is a global measure of vorticity. We will see that it is conserved in incompressible barotropic 2d flows, but not in 3d, where it can grow due to 'vortex stretching'.

Example: shear flow. Shears are large scissors used, for instance, to trim the wool of sheep. The blades of the scissors are said to slide over each other in a 'shearing' motion. By analogy, a flow is a shear flow if layers if fluid slide over each other at different speeds. The shear flow $\boldsymbol{v}(x, y, z) = (u(y), 0, 0)$ with horizontal streamlines illustrated in Fig. 19.6b is an example of a flow with vorticity. Here, horizontal layers of fluid move at different speeds depending on their height y, leading to the vorticity $\boldsymbol{w} = \boldsymbol{\nabla} \times \boldsymbol{v} = -u'(y) \hat{z}$. When there is a velocity differential between two layers of fluid, one can imagine that a little windmill placed there would start spinning. In fact, eddies can be produced as the interface 'curls up'. □

Example: point-like vortex. For $\alpha > 0$, the planar azimuthal velocity field $\boldsymbol{v}(r, \theta) = \frac{\alpha}{r} \hat{\theta}$ shown in Fig. 19.6c has counterclockwise circular streamlines. It has no vorticity

---

[29] In general, the vorticity field need not be orthogonal to velocity. The flow helicity density $\mathscr{K} = \boldsymbol{v} \cdot \boldsymbol{w}$ is a local measure of the extent to which $\boldsymbol{v}$ and $\boldsymbol{w}$ fail to be orthogonal (see Prob. 19.22). Flow helicity density is a pseudoscalar, it changes sign under reflections.

[30] Potential flow, i.e., where $\boldsymbol{v} = \boldsymbol{\nabla} \phi$ is the gradient of a scalar velocity potential is irrotational. Locally, an irrotational velocity field must be a gradient.

[31] There are many names for vortex-like structures: swirls, whirlpools, whorls, cyclones, hurricanes, typhoons, tornadoes, maelstroms, etc. Leonardo da Vinci was fascinated by vortices. Many of his sketches contain detailed illustrations of eddies in fluids. He even noticed similarities between the train of vortices in the wake behind a flat plate and braided hair!

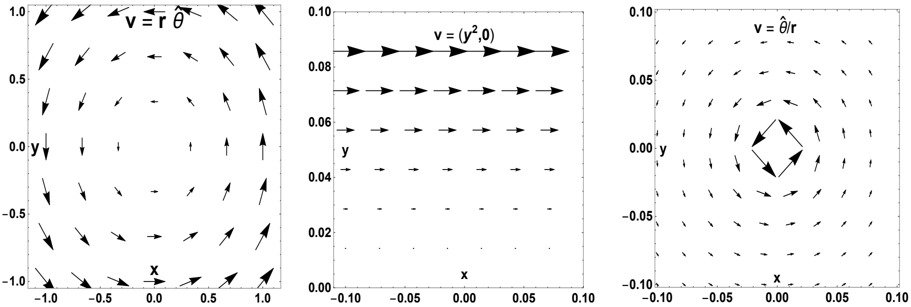

(a) (b) (c)

Figure 19.6: Velocity vector field for (a) rigidly rotating bucket of fluid $\boldsymbol{v} = \Omega r\hat{\theta}$ for $\Omega = 1$, (b) shear flow $\boldsymbol{v}(x, y) = (u(y), 0)$ for $u(y) = y^2$ and (c) point-like vortex $\boldsymbol{v} = (\alpha/r)\hat{\theta}$ for $\alpha = 1$.

$\boldsymbol{w} = \frac{1}{r}\partial_r(r\frac{\alpha}{r})\hat{z} = 0$ except at $r = 0$: $\boldsymbol{w} = 2\pi\alpha\delta^2(\boldsymbol{r})\hat{z}$. Thus, the vorticity is concentrated at the origin. The constant $2\pi\alpha$ comes from requiring the flux of $\boldsymbol{w}$ to equal the circulation of $\boldsymbol{v}$ around any contour enclosing the origin

$$\oint \boldsymbol{v} \cdot d\boldsymbol{l} = \oint (\alpha/r) r \, d\theta = 2\pi\alpha. \tag{19.50}$$

If we include the vertical z direction, this point vortex becomes a 'line' vortex, with vorticity concentrated along the z axis. More generally, vortices can take the shape of tubes and rings (see Sect. 19.12). Smoke rings are examples of vortex tubes. Dolphins blow vortex rings in water and chase them. Kelvin and Helmholtz discovered many interesting properties of vortex tubes. Inviscid fluid flow tends to stretch and bend vortex tubes while carrying them along. They survive in the absence of viscosity but dissipate due to friction (see Sect. 19.16). □

Vorticity evolution. Let us obtain the equation for vorticity by taking the curl of the Euler equation. It is simplest to do this for barotropic (e.g., homentropic) flow of a fluid subject to a conservative body force. Thus, we suppose that $\boldsymbol{\nabla} p/\rho = \boldsymbol{\nabla} h$ and that the body force per unit mass is $\boldsymbol{f}/\rho = -\boldsymbol{\nabla}\varphi$, so that (19.33) becomes

$$\partial_t \boldsymbol{v} + \boldsymbol{w} \times \boldsymbol{v} = -\boldsymbol{\nabla}\left(h + \varphi + (1/2)\boldsymbol{v}^2\right). \tag{19.51}$$

Taking a curl, the RHS vanishes and we get the vorticity evolution equation

$$\frac{\partial \boldsymbol{w}}{\partial t} + \boldsymbol{\nabla} \times (\boldsymbol{w} \times \boldsymbol{v}) = 0. \tag{19.52}$$

In this form, both the pressure and density have been eliminated from the Euler equation! This comes at the cost of making it second order in spatial derivatives of $\boldsymbol{v}$. Using $\boldsymbol{\nabla} \cdot \boldsymbol{w} = 0$ and the vector identity

$$\boldsymbol{\nabla} \times (\boldsymbol{w} \times \boldsymbol{v}) = ((\boldsymbol{\nabla} \cdot \boldsymbol{v}) + \boldsymbol{v} \cdot \boldsymbol{\nabla})\, \boldsymbol{w} - ((\boldsymbol{\nabla} \cdot \boldsymbol{w}) + \boldsymbol{w} \cdot \boldsymbol{\nabla})\, \boldsymbol{v}, \tag{19.53}$$

the evolution equation for vorticity becomes

$$\frac{D\boldsymbol{w}}{Dt} - (\boldsymbol{w} \cdot \boldsymbol{\nabla})\boldsymbol{v} + (\boldsymbol{\nabla} \cdot \boldsymbol{v})\boldsymbol{w} = 0. \tag{19.54}$$

Notice that if the flow is incompressible ($\boldsymbol{\nabla}\cdot\boldsymbol{v} = 0$), the last term vanishes and we get $\frac{D\boldsymbol{w}}{Dt} = (\boldsymbol{w}\cdot\boldsymbol{\nabla})\boldsymbol{v}$. One consequence of this equation is that vorticity is *frozen* into an inviscid barotropic flow, as we will see in Sect. 19.12. Heuristically, what this means is that vortices (more precisely vortex tubes or rings) are dragged along by the flow field $\boldsymbol{v}$. This can be expressed in terms of the Lie dragging of vorticity by the flow, as we will show in Prob. 19.16.

Advection of vorticity in 2d incompressible barotropic flow. Vorticity behaves in a particularly simple manner in 2d incompressible barotropic flows. Consider flow on a portion of the x-y plane, so that $\boldsymbol{v} = (u, v, 0)$ while the vorticity points vertically $\boldsymbol{w} = \boldsymbol{\nabla}\times\boldsymbol{v} = w\,\hat{z}$ where[32] $w = v_x - u_y$. It follows that $(\boldsymbol{w}\cdot\boldsymbol{\nabla})\boldsymbol{v} = 0$ and (19.54) becomes $\frac{D\boldsymbol{w}}{Dt} = 0$. Thus, vorticity is advected by a planar incompressible barotropic flow. In particular, the vorticity of a fluid element is constant as the element moves around. Using incompressibility ($\boldsymbol{\nabla}\cdot\boldsymbol{v} = 0$), this can be expressed as a local conservation law for w:

$$\frac{D\boldsymbol{w}}{Dt} = 0 \quad\Rightarrow\quad \frac{\partial w}{\partial t} + \boldsymbol{v}\cdot\boldsymbol{\nabla}w = 0 \quad\Rightarrow\quad \frac{\partial w}{\partial t} + \boldsymbol{\nabla}\cdot(w\boldsymbol{v}) = 0. \tag{19.55}$$

Multiplying by w, we get a local conservation law for w^2 as well:

$$\frac{1}{2}\frac{\partial w^2}{\partial t} + \boldsymbol{\nabla}\cdot\left(\frac{1}{2}w^2\boldsymbol{v}\right) = 0. \tag{19.56}$$

In fact, proceeding this way, one may show (see Prob. 19.17) that w^n is locally conserved with the current $w^n\boldsymbol{v}$ for $n = 1, 2, 3, \ldots$. Integrating over the plane and assuming $\boldsymbol{v}$ vanishes on boundaries and sufficiently fast at infinity, we get conservation laws for the moments of vorticity

$$\frac{d}{dt}\int w^n\,dx\,dy = 0 \quad \text{for} \quad n = 1, 2, 3, \ldots. \tag{19.57}$$

Enstrophy is defined as the integral of the square of vorticity. Thus, enstrophy and its higher cousins[33] are invariants for 2d incompressible barotropic flows.

19.12 Vortex tubes: Kelvin and Helmholtz theorems

In three dimensions, vorticity is frozen (19.54) into inviscid isentropic (barotropic) flow. One manifestation of this is Kelvin's theorem on conservation of circulation.

Vorticity is the curl of the velocity field just as the magnetic field is the curl of a vector potential $\boldsymbol{A}$ (3.147). Like the magnetic flux across an oriented surface S, we may consider the flux Γ of vorticity across a surface S in a fluid. By Stokes' theorem,

$$\Gamma = \int_S \boldsymbol{w}\cdot d\boldsymbol{S} = \int_S (\boldsymbol{\nabla}\times\boldsymbol{v})\cdot d\boldsymbol{s} = \oint_C \boldsymbol{v}\cdot d\boldsymbol{r} \tag{19.58}$$

is the circulation (19.49) or line integral of $\boldsymbol{v}$ around the directed closed curve $C = \partial S$ that bounds S (see Fig. 19.7a).

---

[32] The (negative) Laplacian of the stream function ψ (19.11) is the vorticity component w in 2d incompressible flow. In fact, $w = v_x - u_y = -(\psi_{xx} + \psi_{yy}) = -\boldsymbol{\nabla}^2\psi$.

[33] In fact, subject to suitable behavior at the boundary, the integral of any function of vorticity (that can be approximated by polynomials) is conserved.

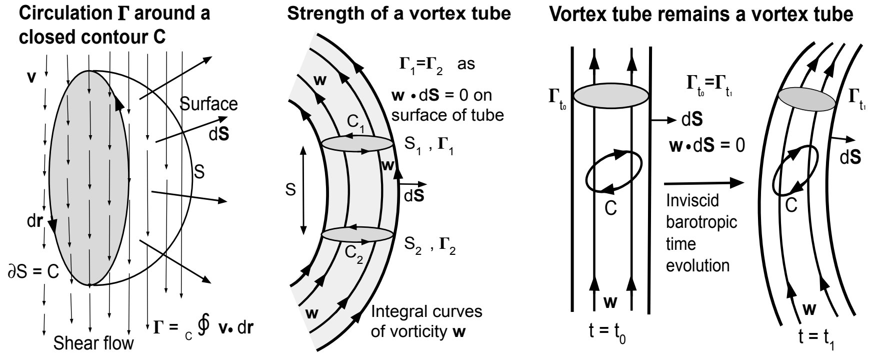
Circulation Γ around a closed contour C
v
Surface
dS
S
dr
∂S = C
Γ = ∮C v• dr
Shear flow
Strength of a vortex tube
Γ1=Γ2 as
w •dS = 0 on surface of tube
w
C1
S1 , Γ1
w
S
dS
S2 , Γ2
C2
w
Integral curves of vorticity w
Vortex tube remains a vortex tube
Γt0
Γt0=Γt1
dS
w•dS = 0
C
Inviscid barotropic time evolution
w
t = t0
Γt1
dS
C
w
t = t1

(a) (b) (c)

Figure 19.7: (a) Circulation around a closed contour. (b) Integral curves of vorticity. Strength of a vortex tube is independent of choice of encircling closed contour. C_1 and C_2 wind once around the tube, they are noncontractible. (c) A vortex tube remains a vortex tube under inviscid barotropic flow. The curve C is a contractible closed curve lying on the surface of the tube, it does not wind around the tube. $d\boldsymbol{S}$ is an area element on the surface of the vortex tube.

Kelvin's law: conservation of circulation around a material loop. Suppose C_t at time t is a closed material contour. Then $\Gamma(C_t)$ is conserved as C_t is transported by an inviscid (possibly compressible) barotropic flow subject to conservative body forces. Let us show that the time derivative[34] of Γ vanishes:

$$\frac{d\Gamma}{dt} = \oint_{C_t} \frac{D\boldsymbol{v}}{Dt} \cdot d\boldsymbol{r} + \oint_{C_t} \boldsymbol{v} \cdot \frac{Dd\boldsymbol{r}}{Dt}. \tag{19.59}$$

Since C_t moves with the flow, we used material derivatives and the product rule that it satisfies. The velocity $\boldsymbol{v}(\boldsymbol{r},t)$ is that of a moving material element and we must also account for the motion of the material element $d\boldsymbol{r}$ itself. For barotropic flow with conservative body forces, Euler's equation (19.33) says that $\frac{D\boldsymbol{v}}{Dt} = -\boldsymbol{\nabla}(h+\varphi)$. On the other hand, the material derivative of a material line element is its fluid velocity element: $\frac{Dd\boldsymbol{r}}{Dt} = d\boldsymbol{v}$ and $\boldsymbol{v}\cdot d\boldsymbol{v} = \frac{1}{2}d(\boldsymbol{v}^2) = \frac{1}{2}\boldsymbol{\nabla}\boldsymbol{v}^2 \cdot d\boldsymbol{r}$. Thus, by Stokes' theorem,

$$\frac{d\Gamma}{dt} = \oint_{C_t} \boldsymbol{\nabla} \cdot \left(-h - \varphi + \frac{1}{2}\boldsymbol{v}^2\right) \cdot d\boldsymbol{r} = 0 \tag{19.60}$$

as it is the line integral of a gradient around a closed curve. It follows that the circulation around a closed fluid contour is constant in time.

Alternatively, the flux of vorticity across any surface that moves with the fluid is constant in the absence of viscosity, provided the sum of pressure and body forces per unit mass may be expressed as a gradient. Loosely, in the absence of viscosity, eddies and vortices cannot develop in a barotropic flow that was initially irrotational.

---

[34] $d\Gamma/dt$ refers to the rate of change in the circulation around a material contour, as it is carried around by the flow. $\Gamma(C_t)$ depends on a whole contour and is not a function of one position like the field $\boldsymbol{v}(\boldsymbol{r},t)$. Bearing this in mind, one could equally well use the notation $D\Gamma/Dt$ for $d\Gamma/dt$.

Vortex tube. Like any other field line defined in Sect. 5.1, a vortex line is an integral curve of the vorticity field $\boldsymbol{w}$ at a given instant of time. Given any closed curve C in the fluid, consider the vortex lines through C. They form a surface, called a vortex tube, as shown in Fig. 19.7. The vorticity is everywhere tangent to a vortex tube. A vortex tube of infinitesimal cross section is called a vortex filament. We now describe **Helmholtz's theorem** on vortex tubes, which states that inviscid barotropic flow carries vortex tubes to vortex tubes of the same strength.

Strength of a vortex tube. At an initial time t_0, a vortex tube can be assigned a strength, the circulation $\Gamma(C)$ around a closed curve C that winds around the tube once. To be meaningful, this strength should be independent of the choice of closed loop C. This is indeed true. Suppose C_1 and C_2 are two curves winding around the vortex tube once each. For simplicity, we assume that they do not intersect[35]. Let S_1 and S_2 be any two surfaces with $\partial S_1 = C_1, \partial S_2 = C_2$ (see Fig. 19.7b). We assume that $S_{1,2}$ are chosen not to intersect. Consider the portion of the vortex tube between S_1 and S_2. Its interior is a solid cylindrical region R with closed surface $\partial R = \Sigma = S \cup S_1 \cup S_2$ where S is the tubular surface of the vortex tube. The flux of vorticity across Σ must vanish by the divergence theorem: $\int_\Sigma \boldsymbol{w} \cdot d\boldsymbol{S} = \int_R \boldsymbol{\nabla} \cdot (\boldsymbol{\nabla} \times \boldsymbol{v}) d\boldsymbol{r}$. Thus, assigning suitable orientations,

$$0 = \cancel{\int_S \boldsymbol{w} \cdot d\boldsymbol{S}} + \int_{S_1} \boldsymbol{w} \cdot d\boldsymbol{S} + \int_{S_2} \boldsymbol{w} \cdot d\boldsymbol{S} = \oint_{C_1} \boldsymbol{v} \cdot d\boldsymbol{l} - \oint_{C_2} \boldsymbol{v} \cdot d\boldsymbol{l}. \qquad (19.61)$$

The integral over S vanishes since vorticity is tangential to a vortex tube. Thus, $\Gamma(C_1) = \Gamma(C_2)$: the circulation around a vortex tube is independent of the choice of encircling contour. As a consequence, *a vortex tube cannot abruptly end in the fluid*, it must close on itself to form a vortex ring or end on a boundary.

Vortex tubes evolve into vortex tubes. Inviscid isentropic flow takes a vortex tube to another vortex tube. This is a manifestation of the freezing-in of vorticity into the velocity field. To show this, we consider a vortex tube at t_0 and follow its surface as it moves with the flow up to a final time $t_1 > t_0$. We wish to show that the new tube is a vortex tube, i.e., that the vorticity is everywhere tangent to it. To this end, consider a contractible[36] closed curve $C(t_0)$ lying on the initial vortex tube, the flow maps it to a new contractible closed curve $C(t_1)$ lying on the final tube, as shown in Fig. 19.7c. By Kelvin's theorem, $\Gamma(C(t_0)) = 0 = \Gamma(C(t_1))$. Now, suppose S is the portion of the new tubular surface enclosed by $C(t_1)$, i.e., $\partial S = C(t_1)$. Then

$$0 = \Gamma(C(t_1)) = \int_S \boldsymbol{w} \cdot d\boldsymbol{S}. \qquad (19.62)$$

By suitably repositioning and shrinking $C(t_0)$, this is true for an infinitesimal closed curve $C(t_1)$ around any point on the new tube. Thus, we conclude that $\boldsymbol{w} \cdot d\boldsymbol{S} = 0$ at every point of the new tube. In other words, the vorticity is everywhere tangent to the new tube, which must therefore be a vortex tube.

---

[35] If C_2 is a closed curve that winds once around the vortex tube and intersects C_1, then we may still conclude that $\Gamma(C_1) = \Gamma(C_2)$ by choosing a third contour C_3 which does not intersect either C_1 or C_2 and use the argument that follows to show $\Gamma(C_1) = \Gamma(C_2) = \Gamma(C_3)$

[36] 'Contractible' means the closed curve can be continuously shrunk to a point while remaining on the surface of the tube.

Strength of a vortex tube is time-independent. Suppose $C(t)$ is a closed material contour winding once round a vortex tube as it evolves in time. By Kelvin's theorem, strength of the vortex tube $\Gamma(C(t))$ is independent of time.

19.13 Conservation of energy, (angular) momentum and helicity

We have already encountered two local conservation laws: that for mass, the continuity equation $\partial_t \rho + \boldsymbol{\nabla} \cdot (\rho \boldsymbol{v}) = 0$ (19.15) and that for entropy in ideal adiabatic flow, $\partial_t(\rho s) + \boldsymbol{\nabla} \cdot (\rho s \boldsymbol{v}) = 0$ (19.26). Integrating over the flow domain and assuming the corresponding fluxes across the boundary vanish, we get the conservation of the total mass and entropy of the fluid. There are four more such local (and corresponding global) conservation laws: for energy, linear momentum, angular momentum and helicity which, we discuss below.

Conservation of energy. By analogy with the kinetic energy $\frac{1}{2}mv^2$ of a particle we expect a fluid flow to have a kinetic energy $\int \frac{1}{2}\rho v^2 \, d\boldsymbol{r}$. In addition, we might expect a potential energy which could variously be thought of as an internal energy or compressional energy or thermal energy. From the equipartition principle in the kinetic theory of a gas at temperature T, each (translational, rotational, vibrational) degree of freedom of a molecule has an associated energy $\frac{1}{2}k_b T$, where k_b is Boltzmann's constant. So if there are N molecules of the gas with f degrees of freedom each, the internal energy is $(f/2)Nk_bT$. For example, a monatomic gas has $f = 3$ translational degrees of freedom, so that its internal energy takes the familiar form $(3/2)Nk_bT$. More generally, a gas with specific heat ratio γ has in effect $f = 2/(\gamma - 1)$ degrees of freedom[37]. Furthermore, if we trade the temperature for pressure using the ideal gas equation of state $pV = Nk_bT$ we find that the internal energy of a homogeneous ideal gas at equilibrium in a volume V is $pV/(\gamma - 1)$. A flowing fluid may be regarded as a collection of small volumes $d\boldsymbol{r}$ each in local thermal equilibrium with pressure $p(\boldsymbol{r})$. Thus, the internal or potential energy density of an ideal gas is $\mathcal{U} = p/(\gamma - 1)$. Adding the kinetic and potential energies, we guess that the total energy of a fluid composed of an ideal gas with specific heat ratio γ is

$$E = \int \left[\frac{1}{2}\rho v^2 + \frac{p}{\gamma - 1}\right] d\boldsymbol{r} = \int \mathcal{E} \, d\boldsymbol{r} \qquad (19.63)$$

---

[37] Consider N molecules of an ideal gas satisfying the equation of state $pV = Nk_bT$. The caloric condition from the Joule-Thomson porous plug experiment [38] says that the internal energy of such a gas is independent of volume occupied and depends only on the temperature, $U = U(T, \cancel{V})$. Thus $dU = C_v dT$ where $C_v(T)$ is called the heat capacity at constant volume. Putting these in the first law of thermodynamics ($\delta Q = dU + pdV$), we get $\delta Q = (C_v + Nk_b)dT - Vdp$. Now, the heat capacity at constant pressure is $C_p = (\delta Q/\delta T)_p$. Thus, $C_p - C_v = Nk_b$. What is more, from the kinetic theory of gases [118], one estimates that $C_v = (f/2)Nk_b$ where f is the number of degrees of freedom (translational, rotational and possibly vibrational) of the molecule: $C_v = (3/2)Nk_b$ for monatomic, $(7/2)Nk_b$ for diatomic and $3Nk_b$ for noncollinear polyatomic. Thus, we find that $\gamma = C_p/C_v = 1 + Nk_b/C_v = 1 + 2/f$.

where $\mathcal{E}$ is the energy density. To confirm our guess, we now show that $\mathcal{E}$ satisfies a local conservation law. To do so, we combine the inviscid adiabatic evolution equations for ρ, $\boldsymbol{v}$ (19.22) and p (19.29) in the absence of external forces (see also, Prob. 19.19).

$$\rho_t = -\boldsymbol{\nabla}\cdot(\rho\boldsymbol{v}), \quad \boldsymbol{v}_t = -\boldsymbol{v}\cdot\boldsymbol{\nabla}\boldsymbol{v} - \frac{\boldsymbol{\nabla}p}{\rho}, \quad \frac{p_t}{\gamma-1} = -p\boldsymbol{\nabla}\cdot\boldsymbol{v} - \frac{\boldsymbol{\nabla}\cdot(p\boldsymbol{v})}{\gamma-1}, \tag{19.64}$$

to evaluate the time derivative of the internal energy density

$$\mathcal{E}_t = -\frac{v^2}{2}\boldsymbol{\nabla}\cdot(\rho\boldsymbol{v}) - \rho\boldsymbol{v}\cdot(\boldsymbol{v}\cdot\boldsymbol{\nabla})\boldsymbol{v} - \boldsymbol{v}\cdot\boldsymbol{\nabla}p - p\boldsymbol{\nabla}\cdot\boldsymbol{v} - \frac{\boldsymbol{\nabla}\cdot(p\boldsymbol{v})}{\gamma-1}. \tag{19.65}$$

Using the Leibniz rule $\boldsymbol{\nabla}\cdot(g\boldsymbol{u}) = \boldsymbol{\nabla}g\cdot\boldsymbol{u}+g\boldsymbol{\nabla}\cdot\boldsymbol{u}$ for any function g and vector field $\boldsymbol{u}$, the first 2 terms may be combined as a divergence, as can the last 3 (see Prob. 19.18). Thus, in the absence of external forces, we get the local conservation law

$$\frac{\partial\mathcal{E}}{\partial t} + \boldsymbol{\nabla}\cdot\left(\frac{v^2}{2}\rho\boldsymbol{v} + \frac{\gamma}{\gamma-1}p\boldsymbol{v}\right) = 0. \tag{19.66}$$

The quantity in parentheses is the energy current vector. This formula holds for adiabatic flow as well as the special case of homentropic or barotropic flow where p is a function of ρ. Integrating (19.66) over the flow domain, it follows that the total energy (19.63) is conserved if the flux of the energy current across the boundary vanishes. This happens, for instance, with decaying boundary conditions ($\boldsymbol{v} \to 0, \rho \to \rho_0$ sufficiently fast as $|\boldsymbol{r}| \to \infty$) or periodic boundary conditions in a cuboid.

Barotropic energy density. In homentropic flow, we have the barotropic relation $p = p_0(\rho/\rho_0)^\gamma$ corresponding to the specific enthalpy $h(\rho) = (\gamma/(\gamma-1))p/\rho$ (19.31). In this case, the potential energy density $\mathcal{U} = p/(\gamma-1)$ becomes $\mathcal{U}(\rho) = p_0(\rho/\rho_0)^\gamma/(\gamma-1)$. We notice that $\mathcal{U}(\rho)$ is an antiderivative of the specific enthalpy: $\mathcal{U}'(\rho) = h(\rho)$. This relation holds more generally for any barotropic relation between p and ρ, as one may check (see also Sect. 19.14*).

Energy in incompressible limit. In the incompressible case ($\boldsymbol{\nabla}\cdot\boldsymbol{v} = 0$), we continue to have local and global conservation laws for energy, though there is no compressional potential energy. In this case, the time derivative of the kinetic energy density may be expressed as a divergence using the Euler equation $\boldsymbol{v}_t + \boldsymbol{v}\cdot\boldsymbol{\nabla}\boldsymbol{v} = -\boldsymbol{\nabla}p/\rho$ and continuity equation $\rho_t + \boldsymbol{v}\cdot\boldsymbol{\nabla}\rho = 0$:

$$\left(\frac{1}{2}\rho v^2\right)_t = -\frac{1}{2}v^2\boldsymbol{v}\cdot\boldsymbol{\nabla}\rho - \rho\boldsymbol{v}(\boldsymbol{v}\cdot\boldsymbol{\nabla})\boldsymbol{v} - \boldsymbol{v}\cdot\boldsymbol{\nabla}p. \tag{19.67}$$

As before, the first two terms combine to give the divergence of $-\frac{1}{2}\rho v^2\boldsymbol{v}$ while the last one is the divergence of $-p\boldsymbol{v}$ since $\boldsymbol{\nabla}\cdot\boldsymbol{v} = 0$. Thus, we obtain the local conservation law for energy in incompressible hydrodynamics:

$$\partial_t\left(\frac{1}{2}\rho v^2\right) + \boldsymbol{\nabla}\cdot\left\{\left(p + \frac{1}{2}\rho v^2\right)\boldsymbol{v}\right\}. \tag{19.68}$$

We may obtain this equation by letting $\gamma \to \infty$ in (19.66). This is reasonable, since $\gamma = \infty$ corresponds to zero internal degrees of freedom $f = 2/(\gamma - 1) = 0$, which means the gas molecules have no internal/random thermal/compressional energy; all the energy comes from the large-scale motion of the gas via the velocity field.

Conservation of linear momentum. By analogy with particle mechanics, we would expect the linear momentum of a fluid to be given by the vector $\boldsymbol{P} = \int \rho \boldsymbol{v} \, d\boldsymbol{r}$. We will show that with suitable BCs, $\boldsymbol{P}$ is constant in time and that the momentum density $\rho \boldsymbol{v}$ is locally conserved. In fact, it satisfies the momentum equation:

$$\partial_t(\rho v_i) + \partial_j \Pi_{ij} = 0 \quad \text{where} \quad \Pi_{ij} = p\delta_{ij} + \rho v_i v_j. \tag{19.69}$$

This equation is obtained by combining the continuity (19.15) and Euler (19.22) equations in the absence of external forces. Indeed, one finds that

$$\partial_t(\rho v_i) = -v_i \partial_j(\rho v_j) - \rho v_j \partial_j v_i - \partial_i p = -\partial_i p - \partial_j(\rho v_i v_j) = -\partial_j \Pi_{ij}. \tag{19.70}$$

It holds independent of how pressure evolves and is thus valid both for adiabatic as well as incompressible flow. The symmetric 2^{nd} rank momentum current tensor $\Pi_{ij} = T_{ij} + \rho v_i v_j$ is related to the stress tensor of Sect. 19.7. Its divergence appears in (19.69). Integrating over the flow domain Ω, we get the conservation of momentum:

$$\frac{dP_i}{dt} = -\int_\Omega \partial_j \Pi_{ij} d\boldsymbol{r} = -\int_{\partial\Omega} \Pi_{ij} n_j dS = 0. \tag{19.71}$$

Here, n_j are the components of the unit normal on the boundary surface $\partial\Omega$. We used the divergence theorem to convert the volume integral into a surface integral and assumed that the flux of momentum across the boundary vanishes (this is the case, for instance, with decaying BCs in $\Omega = \mathbb{R}^3$ or with periodic BCs in a cuboid).

Conservation of angular momentum. It is natural to define the angular momentum density (relative to $\boldsymbol{r} = 0$) as $\mathcal{L} = \boldsymbol{r} \times \rho \boldsymbol{v}$, where $\rho \boldsymbol{v}$ is the momentum density. In components, $\mathcal{L}_i = \rho \epsilon_{ijk} x_j p_k$. It satisfies the local conservation law

$$\partial_t \mathcal{L}_i + \partial_l \Lambda_{il} = 0 \quad \text{where} \quad \Lambda_{il} = \epsilon_{ijk} x_j \Pi_{kl} \tag{19.72}$$

is the angular momentum current tensor, which is built from the momentum tensor Π. This is checked by evaluating $\partial_t \mathcal{L}_i$ using (19.69), see Prob. 19.20. It is valid irrespective of how pressure evolves (incompressible, barotropic, adiabatic, etc.) but assumes there are no external or viscous forces. The total angular momentum $\boldsymbol{L} = \int \mathcal{L} d\boldsymbol{r}$ is conserved with suitable BCs, such as decaying BCs in an infinite domain. Moreover, in an infinite domain, $\boldsymbol{L}$ is independent of the choice of origin since $\boldsymbol{r}$ is a dummy variable of integration. On the other hand, in axisymmetric domains such as a circular cylinder or torus, the component of angular momentum along the symmetry axis is conserved provided there is no flux of angular momentum across the boundary.

Flow helicity and its conservation. Flow helicity is defined as $\mathcal{K} = \int \boldsymbol{v} \cdot \boldsymbol{w} \, d\boldsymbol{r}$. Helicity density $\mathscr{K} = \boldsymbol{v} \cdot \boldsymbol{w}$ is proportional to the component of vorticity in the direction of velocity[38]. Though $\boldsymbol{w} = \boldsymbol{\nabla} \times \boldsymbol{v}$, it is not necessarily orthogonal to $\boldsymbol{v}$. A fluid flow has helicity, for instance, if streamlines are shaped like helices. Helicity may also be regarded as measuring the extent to which vortex lines wind around streamlines (see Prob. 19.22 and Sect. 3.12 of [111]). The examples of rotational planar flows in Sect. 19.11 have zero helicity as we argue in Prob. 19.21. However, it is not difficult to come up with helical flows. The toy example $\boldsymbol{v} = (z, x, y)$ of Prob. 19.22 is one with nonvanishing $\mathscr{K} = \boldsymbol{v} \cdot \boldsymbol{w}$. We will show that helicity is an integral invariant for inviscid homentropic (barotropic) flow subject to conservative body forces (see Prob. 19.24 for what goes wrong without the barotropic assumption). In fact, $\boldsymbol{v} \cdot \boldsymbol{w}$ satisfies a local conservation law:

$$\frac{\partial(\boldsymbol{v} \cdot \boldsymbol{w})}{\partial t} + \boldsymbol{\nabla} \cdot ((\sigma + \varphi)\boldsymbol{w} + (\boldsymbol{w} \times \boldsymbol{v}) \times \boldsymbol{v}) = 0. \tag{19.73}$$

To show this, we note that the Euler equation (19.33) $\boldsymbol{v}_t + \boldsymbol{w} \times \boldsymbol{v} = -\boldsymbol{\nabla}(\sigma + \varphi)$ and the vorticity evolution equation (19.52) give

$$\boldsymbol{w} \cdot \boldsymbol{v}_t = -\boldsymbol{w} \cdot \boldsymbol{\nabla}(\sigma + \varphi) \quad \text{and} \quad \boldsymbol{v} \cdot \boldsymbol{w}_t = -\boldsymbol{v} \cdot \boldsymbol{\nabla} \times (\boldsymbol{w} \times \boldsymbol{v}). \tag{19.74}$$

This implies

$$\partial_t(\boldsymbol{v} \cdot \boldsymbol{w}) = -\boldsymbol{w} \cdot \boldsymbol{\nabla}(\sigma + \varphi) - \boldsymbol{v} \cdot \boldsymbol{\nabla} \times (\boldsymbol{w} \times \boldsymbol{v}). \tag{19.75}$$

We want to write the RHS as a divergence. The first term is a divergence since $\boldsymbol{w}$ is solenoidal: $\boldsymbol{w} \cdot \boldsymbol{\nabla}(\sigma + \varphi) = \boldsymbol{\nabla} \cdot ((\sigma + \varphi)\boldsymbol{w})$. For the second term we use the vector identity of Prob. 19.23 to write:

$$\boldsymbol{\nabla} \cdot ((\boldsymbol{w} \times \boldsymbol{v}) \times \boldsymbol{v}) = \boldsymbol{v} \cdot \boldsymbol{\nabla} \times (\boldsymbol{w} \times \boldsymbol{v}) - \cancel{(\boldsymbol{w} \times \boldsymbol{v}) \cdot (\boldsymbol{\nabla} \times \boldsymbol{v})}. \tag{19.76}$$

Combining these, we obtain the local conservation law (19.73). Integrating over the flow domain, flow helicity is conserved ($d\mathcal{K}/dt = 0$) provided the flux of the helicity current across the boundary vanishes.

$*$ **Helicity as a Casimir.** In fact, flow helicity is more than just a conserved quantity, it is a Casimir invariant of the Poisson algebra (19.77) for barotropic flow. This means $\mathcal{K}$ Poisson commutes with any observable (functional $G[\rho, \boldsymbol{v}]$ of ρ and $\boldsymbol{v}$.). Thus, it is conserved no matter what the formula for the Hamiltonian $H[\rho, \boldsymbol{v}]$ is! This is shown in Prob. 19.32. In this sense, flow helicity is like the square of angular momentum L^2 in the Euler-Poinsot top of Sect. 8.14*. In fact, it is often useful to think of the Euler equations for barotropic flow as an infinite-dimensional generalization of the Euler equations for a rigid body. See [3] and [107] for more on this viewpoint.

19.14* Hamiltonian and Poisson brackets for inviscid flow

Having established the conservation of energy in adiabatic, barotropic and incompressible flow in Sect. 19.13, it is natural to seek a Hamiltonian formulation of fluid mechanics where the energy plays the role of the Hamiltonian. To do this, we need appropriate Poisson brackets that will lead to the equations of motion. It turns out that the relevant PBs among fluid variables $(\rho, \boldsymbol{v}, s, p)$ is noncanonical: there is no separation of physical variables into position-type and momentum-type variables[39]. Such brackets were first proposed by Lev Landau (1941) while attempting a quantum theory of superfluid Helium II [82]. Ironically, Landau's quantum mechanical commutation relations preceded the corresponding classical PBs, which were made precise and generalized to charged fluids (magnetohydrodynamics) by Morrison and Greene in 1980 [91]. Landau arrived at his brackets by treating a fluid as a collection of particles whose positions and momenta satisfied canonical commutation relations. We shall not reproduce Landau's derivation [82] but go straight to the resulting PBs, which have an elegance of their own[40].

---

[38] The significance of helicity was pointed out relatively recently, by H K Moffat in 1969 [111]. A similar concept arises in particle physics, where helicity is the component of spin along the momentum of a particle.

Barotropic flow Poisson brackets. For compressible barotropic flow, the nonzero equal-time PBs (up to antisymmetry) among the velocity and density variables are:

$$\{\boldsymbol{v}(\boldsymbol{x}), \rho(\boldsymbol{y})\} = \boldsymbol{\nabla}_{\boldsymbol{y}} \delta(\boldsymbol{x}-\boldsymbol{y}) \quad \text{and} \quad \{v_i(\boldsymbol{x}), v_j(\boldsymbol{y})\} = \frac{\epsilon_{ijk} w_k}{\rho} \delta(\boldsymbol{x}-\boldsymbol{y}). \tag{19.77}$$

Evidently, these are noncanonical PBs. Notice that variables at distinct spatial locations commute. At the same location, the PB can be divergent, being given by multiples of the Dirac δ function (see Appendix A.11*) and its derivatives. While the PB between velocity components is proportional to the vorticity divided by density, that between velocity and density is a 'constant': the gradient of $\delta(\boldsymbol{x}-\boldsymbol{y})$ is not dependent on dynamical variables. The appearance of the Dirac δ function may look foreboding, but is the natural generalization of the Kronecker delta ($\{x_i, p_j\} = \delta_{ij}$) to the fields of continuum mechanics. What is more, in practice, one or other of the spatial variables $\boldsymbol{x}, \boldsymbol{y}$ is integrated after multiplying by some fields, so one may use the defining property $\int \delta(\boldsymbol{x}-\boldsymbol{y}) f(\boldsymbol{y}) d\boldsymbol{y} = f(\boldsymbol{x})$ to work with them. For instance, let us see how these PBs along with the Hamiltonian for barotropic flow

$$H = \int \left[\frac{1}{2}\rho v^2 + \mathcal{U}(\rho)\right] d\boldsymbol{r} \quad \text{where} \quad \mathcal{U}'(\rho) = h(\rho) \tag{19.78}$$

lead to the continuity equation (19.15). Here $h(\rho)$ is the specific enthalpy. Since density commutes with itself, we have (see also Prob. 19.25)

$$\begin{aligned} \partial_t \rho(\boldsymbol{x}) &= \{\rho(\boldsymbol{x}), H\} = \int \frac{\rho(\boldsymbol{y})}{2} \{\rho(\boldsymbol{x}), v(\boldsymbol{y})^2\} d\boldsymbol{y} = \int \rho(\boldsymbol{y}) \boldsymbol{v}_i(\boldsymbol{y}) \{\rho(\boldsymbol{x}), \boldsymbol{v}_i(\boldsymbol{y})\} d\boldsymbol{y} \\ &= \int \rho(\boldsymbol{y}) \boldsymbol{v}_i(\boldsymbol{y}) \partial_{y^i} \delta(\boldsymbol{x}-\boldsymbol{y}) d\boldsymbol{y} = -\int \boldsymbol{\nabla}_{\boldsymbol{y}} \cdot (\rho(\boldsymbol{y}) \boldsymbol{v}(\boldsymbol{y})) \delta(\boldsymbol{x}-\boldsymbol{y}) d\boldsymbol{y} \\ &= -\boldsymbol{\nabla}_{\boldsymbol{x}} \cdot (\rho(\boldsymbol{x}) \boldsymbol{v}(\boldsymbol{x})). \end{aligned} \tag{19.79}$$

We integrated by parts in the penultimate step to obtain (19.15). We begin to see how these novel PBs conspire to do their job. A similar calculation (see Prob. 19.26) leads to the Euler equation (19.32) in the absence of external body forces.

---

[39] Clebsch potentials furnish canonical variables for a fluid, see Sect. 19.15*.

[40] For instance, in the incompressible case, these PBs are the natural ones on the dual of the Lie algebra of incompressible velocity vector fields [3, 107].

Recall from (3.118) that the position-momentum PBs $\{x^i, p_j\} = \delta^i_j$ may be expressed as PBs between general observables $\{f(x,p), g(x,p)\} = \sum_i (\frac{\partial f}{\partial x^i}\frac{\partial g}{\partial p_i} - \frac{\partial f}{\partial p^i}\frac{\partial g}{\partial x_i})$. In a similar vein, (19.77) may be written as a PB between functionals of ρ and $\boldsymbol{v}$:

$$\{F, G\} = \int \left[\frac{\boldsymbol{w}}{\rho} \cdot \left(\frac{\delta F}{\delta \boldsymbol{v}} \times \frac{\delta G}{\delta \boldsymbol{v}}\right) - \frac{\delta F}{\delta \boldsymbol{v}} \cdot \boldsymbol{\nabla} G_\rho + \frac{\delta G}{\delta \boldsymbol{v}} \cdot \boldsymbol{\nabla} F_\rho\right] d\boldsymbol{r}. \tag{19.80}$$

Here, subscripts $F_\rho = \frac{\delta F}{\delta \rho}$ denote functional derivatives. In Prob. 19.27, we verify that taking $F = \boldsymbol{v}(\boldsymbol{x})$ and $G = \rho(y)$ or $G = \boldsymbol{v}(\boldsymbol{y})$, we recover (19.77).

Ideal adiabatic flow Poisson brackets. The Hamiltonian formulation for barotropic flow may be generalized to the inviscid adiabatic compressible flow of Sect. 19.8. In this case, we have an additional field, the specific entropy. The relevant PBs[41] were introduced in the work of Morrison and Greene [91]:

$$\begin{aligned} \{\boldsymbol{v}(\boldsymbol{x}), \rho(\boldsymbol{y})\} &= \boldsymbol{\nabla}_y \delta(\boldsymbol{x}-\boldsymbol{y}), \;\; \{\boldsymbol{v}(\boldsymbol{x}), s(\boldsymbol{y})\} = \frac{\boldsymbol{\nabla} s}{\rho}\delta(\boldsymbol{x}-\boldsymbol{y}) \\ \text{and} \quad \{v_i(\boldsymbol{x}), v_j(\boldsymbol{y})\} &= \frac{\epsilon_{ijk} w_k}{\rho}\delta(\boldsymbol{x}-\boldsymbol{y}). \end{aligned} \tag{19.81}$$

Aside from antisymmetry, the other PBs such as $\{\rho(\boldsymbol{x}), s(\boldsymbol{y})\}$ are postulated to vanish. We may use these PBs to obtain the equations of inviscid adiabatic compressible flow of an ideal gas, by taking the conserved energy (19.63) as the Hamiltonian:

$$H = \int \left[\frac{1}{2}\rho \boldsymbol{v}^2 + \frac{p}{\gamma - 1}\right] d\boldsymbol{r}. \tag{19.82}$$

For instance, the entropy advection equation (19.27) is obtained from this Hamiltonian by noting that pressure (being a function of ρ and s) commutes with s:

$$\begin{aligned} \partial_t s(\boldsymbol{x}) &= \{s(\boldsymbol{x}), H\} = \int \rho(\boldsymbol{y}) v_i(\boldsymbol{y}) \{s(\boldsymbol{x}), v_i(\boldsymbol{y})\} d\boldsymbol{y} \\ &= -\int v_i(\boldsymbol{y}) \partial_{y^i} s(\boldsymbol{y}) \delta(\boldsymbol{x}-\boldsymbol{y}) d\boldsymbol{y} = -\boldsymbol{v} \cdot \boldsymbol{\nabla} s(\boldsymbol{x}). \end{aligned} \tag{19.83}$$

The same calculation as in the barotropic case (19.79) leads to the continuity equation. Obtaining the Euler equation for ideal adiabatic flow (19.22) is left as an exercise (see Prob. 19.33). For this purpose, it is useful to work out (see Prob. 19.28) the PB of velocity with pressure for an ideal gas with polytropic exponent γ:

$$\{\boldsymbol{v}(\boldsymbol{x}), p(\boldsymbol{y})\} = \gamma p(\boldsymbol{y}) \boldsymbol{\nabla}_{\boldsymbol{y}} \left(\frac{\delta(\boldsymbol{x}-\boldsymbol{y})}{\rho(\boldsymbol{y})}\right) + \frac{\boldsymbol{\nabla} p}{\rho}\delta(\boldsymbol{x}-\boldsymbol{y}). \tag{19.84}$$

---

[41] The arguments of s and ρ in the $\{\boldsymbol{v}(\boldsymbol{x}), s(\boldsymbol{y})\}$ PB can be taken as either $\boldsymbol{x}$ or $\boldsymbol{y}$ as $\delta(\boldsymbol{x}-\boldsymbol{y})$ vanishes when they are unequal.

Incompressible flow Poisson brackets. Finally, we come to the case of incompressible constant density flow, where $\rho(\boldsymbol{r},t) = \rho_0$. Thus, there is just one dynamical field, the velocity $\boldsymbol{v}(\boldsymbol{r})$, which is a divergence-free vector field ($\boldsymbol{\nabla} \cdot \boldsymbol{v} = 0$). Incompressible vector fields form a subalgebra of the Lie algebra of all differentiable vector fields on the flow domain. Indeed, one checks that the Lie bracket (or commutator) of incompressible vector fields

$$[\boldsymbol{u}, \boldsymbol{v}] = \boldsymbol{u} \cdot \boldsymbol{\nabla} \boldsymbol{v} - \boldsymbol{v} \cdot \boldsymbol{\nabla} \boldsymbol{u}, \tag{19.85}$$

is again divergence-free (see Prob. 19.34). Observables of incompressible fluid dynamics are functionals of the velocity field. There is a natural PB between two functionals $F[\boldsymbol{v}]$ and $G[\boldsymbol{v}]$ of incompressible vector fields:

$$\{F(\boldsymbol{v}), G(\boldsymbol{v})\} = -\int \frac{1}{\rho_0} \boldsymbol{v} \cdot \left[F_{\boldsymbol{v}}^{\perp}, G_{\boldsymbol{v}}^{\perp}\right] \, d\boldsymbol{r}. \tag{19.86}$$

This is what one obtains from (19.80) upon assuming that $\rho = \rho_0$ is a nondynamical constant (see Prob. 19.29) and that $(\delta F/\delta \boldsymbol{v})^{\perp}$ and $(\delta G/\delta \boldsymbol{v})^{\perp}$ are the divergence-free projections introduced below. The latter condition ensures that their commutator is solenoidal, which guarantees that (19.86) satisfies the Jacobi identity.

Divergence-free projection. Helmholtz's theorem allows us to uniquely decompose a vector field (that decays sufficiently fast at ∞) as a sum of a curl-free and a divergence-free part. These two parts may be expressed in terms of scalar and vector potentials: $\boldsymbol{v} = \boldsymbol{\nabla}\phi + \boldsymbol{\nabla} \times \boldsymbol{A}$. In particular, given any vector field $\boldsymbol{v}$, we may define its projection to the divergence-free subspace as[42]

$$\boldsymbol{v}^{\perp} = \mathbb{P}\boldsymbol{v} = \boldsymbol{v} - \boldsymbol{\nabla}\phi. \tag{19.87}$$

It follows that $\boldsymbol{\nabla} \cdot \boldsymbol{v}^{\perp} = 0$. Having a formula for ϕ (determined only up to an additive constant) will help us fix the divergence free part of $\boldsymbol{v}$. In fact, taking a divergence, we find that ϕ must satisfy Poisson's equation: $\boldsymbol{\nabla}^2\phi = \boldsymbol{\nabla} \cdot \boldsymbol{v}$. Requiring ϕ to vanish as $|\boldsymbol{r}| \to \infty$, we get [see Footnote 21]

$$\phi(\boldsymbol{r}) = -\frac{1}{4\pi} \int \frac{\boldsymbol{\nabla} \cdot \boldsymbol{v}(\boldsymbol{s})}{|\boldsymbol{r} - \boldsymbol{s}|} d\boldsymbol{s}. \tag{19.88}$$

By contrast, $\boldsymbol{A}$ is determined up to the gradient of a scalar (see Prob. 19.35). □

Incompressible Euler equation. To define time evolution, we take the Hamiltonian to be the kinetic energy, as there is no compressional potential energy:

$$H = \int \frac{1}{2} \rho_0 \boldsymbol{v}(\boldsymbol{r})^2 \, d\boldsymbol{r}. \tag{19.89}$$

We now show that the incompressible Euler equation $[\boldsymbol{v}_t + \boldsymbol{v} \cdot \boldsymbol{\nabla} \boldsymbol{v} = -(1/\rho_0)\boldsymbol{\nabla} p]$ follows from (19.89) and (19.86). To evaluate the PBs (19.86) in $\boldsymbol{v}_t = \{\boldsymbol{v}, H\}$, we need the functional derivatives

$$\frac{\delta H}{\delta \boldsymbol{v}} = \rho_0 \boldsymbol{v} \quad \text{and} \quad \frac{\delta v_i(\boldsymbol{x})}{\delta v_j(\boldsymbol{y})} = \delta_{ij}\delta(\boldsymbol{x} - \boldsymbol{y}) \equiv W_{j;i}(\boldsymbol{y}; \boldsymbol{x}). \tag{19.90}$$

---

[42] In particular, the projection of a gradient is zero.

Here, $W_{j;i}(\boldsymbol{y};\boldsymbol{x})$ is the j^{th} component at location $\boldsymbol{y}$ of a vector field that depends parametrically on $\boldsymbol{x}$ and i. While $\delta H/\delta \boldsymbol{v}$ is divergence-free (since $\boldsymbol{v}$ is), W is not:

$$(\boldsymbol{\nabla}\cdot W)_i(\boldsymbol{y};\boldsymbol{x}) = \partial_{y^j} W_{j;i}(\boldsymbol{y};\boldsymbol{x}) = \partial_{y^j}\delta_{ij}\delta(\boldsymbol{x}-\boldsymbol{y}) = \partial_{y^i}\delta(\boldsymbol{x}-\boldsymbol{y}) \not\equiv 0. \quad (19.91)$$

Its divergence-free projection is given by (19.87):

$$\mathbb{P}W_{j;i}(\boldsymbol{y};\boldsymbol{x}) = \delta_{ij}\delta(\boldsymbol{x}-\boldsymbol{y}) - \partial_{y^j}\phi_i(\boldsymbol{y};\boldsymbol{x}). \quad (19.92)$$

Here, the scalar potential (19.88) is

$$\phi_i(\boldsymbol{y};\boldsymbol{x}) = -\int \frac{(\boldsymbol{\nabla}\cdot W)_i(\boldsymbol{s};\boldsymbol{x})}{4\pi|\boldsymbol{y}-\boldsymbol{s}|}d\boldsymbol{s} = -\int \frac{\partial_{s^i}\delta(\boldsymbol{x}-\boldsymbol{s})}{4\pi|\boldsymbol{y}-\boldsymbol{s}|}\,d\boldsymbol{s} = \frac{1}{4\pi}\partial_{x^i}\frac{1}{|\boldsymbol{y}-\boldsymbol{x}|}. \quad (19.93)$$

Thus,

$$\mathbb{P}W_{j;i}(\boldsymbol{y};\boldsymbol{x}) = \delta_{ij}\delta(\boldsymbol{x}-\boldsymbol{y}) - \frac{1}{4\pi}\partial_{x^i}\partial_{y^j}|\boldsymbol{x}-\boldsymbol{y}|^{-1}. \quad (19.94)$$

Now,

$$\begin{aligned}\{v_i(\boldsymbol{x}),H\} &= -\int v_j(\boldsymbol{y})\left[\mathbb{P}W_{k;i}(\boldsymbol{y};\boldsymbol{x})\partial_{y^k}v_j(\boldsymbol{y}) - v_k(\boldsymbol{y})\partial_{y^k}\mathbb{P}W_{j;i}(\boldsymbol{y};\boldsymbol{x})\right]d\boldsymbol{y}\\ &= A+B+C+D. \end{aligned} \quad (19.95)$$

The first 3 integrals are evaluated using integration by parts, $\boldsymbol{\nabla}\cdot\boldsymbol{v}=0$ and the fact that $|\boldsymbol{x}-\boldsymbol{y}|^{-1}$ is Green's function for the Laplacian: $\boldsymbol{\nabla}_y^2|\boldsymbol{x}-\boldsymbol{y}|^{-1} = -4\pi\delta(\boldsymbol{x}-\boldsymbol{y})$ (see Footnote 21):

$$\begin{aligned} A &= -\int v_j(\boldsymbol{y})\delta_{ik}\delta(\boldsymbol{x}-\boldsymbol{y})\partial_{y^k}v_j(\boldsymbol{y})d\boldsymbol{y} = -\frac{1}{2}\partial_i\boldsymbol{v}^2,\\ B &= \int v_j(\boldsymbol{y})v_k(\boldsymbol{y})\partial_{y^k}\delta_{ij}\delta(\boldsymbol{x}-\boldsymbol{y})d\boldsymbol{y} = -\boldsymbol{v}\cdot\boldsymbol{\nabla}v_i \quad \text{and}\\ C &= \frac{1}{4\pi}\int v_j(\boldsymbol{y})\partial_{x^i}\partial_{y^k}|\boldsymbol{x}-\boldsymbol{y}|^{-1}\partial_{y^k}v_j(\boldsymbol{y})d\boldsymbol{y} = \frac{1}{2}\partial_i\boldsymbol{v}^2. \end{aligned} \quad (19.96)$$

The fourth integral involves two integrations by parts:

$$\begin{aligned} D &= -\frac{1}{4\pi}\int v_j(\boldsymbol{y})v_k(\boldsymbol{y})\partial_{y^k}\partial_{x^i}\partial_{y^j}|\boldsymbol{x}-\boldsymbol{y}|^{-1}d\boldsymbol{y}\\ &= -\frac{1}{4\pi}\partial_{x^i}\int\frac{\boldsymbol{\nabla}\cdot((\boldsymbol{v}\cdot\boldsymbol{\nabla})\boldsymbol{v})(\boldsymbol{y})}{|\boldsymbol{x}-\boldsymbol{y}|}d\boldsymbol{y} \equiv -\frac{1}{\rho_0}\partial_i p(x). \end{aligned} \quad (19.97)$$

Up to an additive constant, we have defined a function p with dimensions of pressure by dividing by the constant density ρ_0. Thus, we get the evolution equation

$$\boldsymbol{v}_t + \boldsymbol{v}\cdot\boldsymbol{\nabla}\boldsymbol{v} = -\frac{1}{\rho_0}\boldsymbol{\nabla}p \;\text{ with }\; \boldsymbol{\nabla}\cdot\boldsymbol{v}=0 \;\text{ and }\; \boldsymbol{\nabla}^2 p = -\rho_0\boldsymbol{\nabla}\cdot(\boldsymbol{v}\cdot\boldsymbol{\nabla}\boldsymbol{v}). \quad (19.98)$$

Now, comparing this with the Euler equation (19.22) we see that p may be interpreted as the mechanical pressure. Thus, we have arrived at a Hamiltonian-Poisson bracket formulation of the constant density incompressible Euler equation.

19.15* Clebsch variables and Lagrangian for ideal flow

As we learned in Sect. 19.14*, the Poisson brackets among velocity, density, pressure and specific entropy are not canonical. Thus, we are led to ask whether one can find canonically conjugate fluid variables[43]. It turns out that these are furnished by variables that go back to the work of Alfred Clebsch (1859).

Velocity potential as conjugate to density. To begin with, we notice that the ρ-$\boldsymbol{v}$ equal-time PB $\{\rho(\boldsymbol{x}), \boldsymbol{v}(\boldsymbol{y})\} = \boldsymbol{\nabla}_{\boldsymbol{y}}\delta(\boldsymbol{x}-\boldsymbol{y})$ (19.77) can be made to look canonical if $\boldsymbol{v}$ happens to be the gradient of a velocity potential ($\boldsymbol{v}(\boldsymbol{y}) = \boldsymbol{\nabla}_{\boldsymbol{y}}\phi(\boldsymbol{y})$) and we postulate that

$$\{\rho(\boldsymbol{x}), \phi(\boldsymbol{y})\} = \delta(\boldsymbol{x}-\boldsymbol{y}), \quad \{\rho(\boldsymbol{x}), \rho(\boldsymbol{y})\} = 0 = \{\phi(\boldsymbol{x}), \phi(\boldsymbol{y})\}. \tag{19.99}$$

These canonical PBs would then imply that velocity components commute:

$$\{v_i(\boldsymbol{x}), v_j(\boldsymbol{y})\} = \{\partial_{x^i}\phi(\boldsymbol{x}), \partial_{y^j}\phi(\boldsymbol{y})\} = \partial_{x^i}\partial_{y^j}\{\phi(\boldsymbol{x}), \phi(\boldsymbol{y})\} = 0. \tag{19.100}$$

Pleasantly, this agrees with (19.77), since vorticity vanishes for potential flow.

Clebsch variables for barotropic flow. Evidently, to deal with flows with vorticity, we need to generalize the formula $\boldsymbol{v} = \boldsymbol{\nabla}\phi$. Such a generalization was found by Clebsch in 1859. Let us first consider the case of homentropic or barotropic flow so that we need not concern ourselves with a dynamical entropy. Clebsch found a way of parametrizing such a velocity field in terms of three 'potentials' ϕ, λ and μ:

$$\boldsymbol{v} = \boldsymbol{\nabla}\phi + (\lambda/\rho)\boldsymbol{\nabla}\mu. \tag{19.101}$$

Unlike the Helmholtz decomposition of a vector field as the sum of curl-free and divergence-free parts (see Prob. 19.35), the Clebsch representation expresses $\boldsymbol{v}$ as a sum of curl-free and helicity-free summands (see Prob. 19.36). In a sense, we have traded the three components of $\boldsymbol{v}$ for the three Clebsch potentials[44]. It is also reasonable to have a total of four fields ρ, ϕ, λ and μ, so that they can be split evenly into 'position-type' and 'momentum-type' variables. Later in this section, we will interpret the Clebsch potentials as Lagrange multipliers. The vorticity is given by

$$\boldsymbol{w} = \boldsymbol{\nabla}\times\boldsymbol{v} = \boldsymbol{\nabla}(\lambda/\rho)\times\boldsymbol{\nabla}\mu. \tag{19.102}$$

Now, we postulate the canonical[45] equal-time PBs among Clebsch variables:

$$\{\rho(\boldsymbol{r}), \phi(\boldsymbol{r}')\} = \{\lambda(\boldsymbol{r}), \mu(\boldsymbol{r}')\} = \delta(\boldsymbol{r}-\boldsymbol{r}'). \tag{19.103}$$

---

[43] By this we mean a collection of fields $q^i(\boldsymbol{r}), p_j(\boldsymbol{r})$, half of which are like position variables and the other half like momentum variables satisfying the PBs $\{q^i(\boldsymbol{r}), p_j(\boldsymbol{r}')\} = \delta^i_j\delta(\boldsymbol{r}-\boldsymbol{r}')$.

[44] However, the Clebsch potentials are not uniquely determined by $\boldsymbol{v}$ and ρ. To begin with, we may add constants to ϕ and μ without altering $\boldsymbol{v}$. In fact, there are more 'gauge transformations' one can make without affecting $\boldsymbol{v}$ (see Prob. 19.39).

[45] The division of λ by ρ in (19.101) is to ensure that λ and μ may be taken to be canonically conjugate.

Up to antisymmetry, the remaining PBs vanish (e.g., $\{\lambda(\boldsymbol{x}), \lambda(\boldsymbol{y})\} = \{\mu(\boldsymbol{x}), \phi(\boldsymbol{y})\} = 0$). Using these, we evaluate

$$\{\rho(\boldsymbol{x}), \boldsymbol{v}(\boldsymbol{y})\} = \{\rho(\boldsymbol{x}), \boldsymbol{\nabla_y}\phi(\boldsymbol{y}) + \frac{\lambda}{\rho}\boldsymbol{\nabla_y}\mu(\boldsymbol{y})\} = \boldsymbol{\nabla_y}\{\rho(\boldsymbol{x}), \phi(\boldsymbol{y})\} = \boldsymbol{\nabla_y}\delta(\boldsymbol{x}-\boldsymbol{y}), \tag{19.104}$$

which is as desired. The velocity-velocity PB (see Prob. 19.41 and Prob. 19.42) also agrees with (19.77):

$$\{v_i(x), v_j(y)\} = \frac{1}{\rho}\left(\partial_i\left(\frac{\lambda}{\rho}\right)\partial_j\mu - \partial_j\left(\frac{\lambda}{\rho}\right)\partial_i\mu\right)\delta(x-y) = \frac{1}{\rho}\epsilon_{ijk}w_k\delta(x-y). \tag{19.105}$$

The arguments of the functions multiplying $\delta(x-y)$ can be taken as x or y. Thus, the Clebsch variables furnish canonical (or Darboux) coordinates for barotropic flow.

Clebsch variables for adiabatic flow. More generally, for adiabatic flow, the Clebsch representation [137] of the velocity field is given by

$$\boldsymbol{v} = \boldsymbol{\nabla}\phi + (\lambda/\rho)\boldsymbol{\nabla}\mu + (\alpha/\rho)\boldsymbol{\nabla}s \tag{19.106}$$

where s is specific entropy and α another Clebsch potential. Thus, we have six[46] fields, which are postulated to satisfy canonical PBs:

$$\{\rho(\boldsymbol{r}), \phi(\boldsymbol{r}')\} = \{\alpha(\boldsymbol{r}), s(\boldsymbol{r}')\} = \{\lambda(\boldsymbol{r}), \mu(\boldsymbol{r}')\} = \delta(\boldsymbol{r}-\boldsymbol{r}'), \tag{19.107}$$

with other PBs vanishing (up to antisymmetry). These PBs may be seen to reproduce those for adiabatic compressible flow (19.81). The equations of motion for the Clebsch potentials ϕ, λ, μ and α will be obtained shortly. As one might anticipate, the one for ϕ is a generalization of the unsteady Bernoulli equation (19.39).

Hamiltonian. The Hamiltonian in terms of Clebsch variables is

$$H = \int \mathcal{H}\, d\boldsymbol{r} = \int \left[\frac{\rho}{2}\left(\boldsymbol{\nabla}\phi + \frac{(\lambda\boldsymbol{\nabla}\mu + \alpha\boldsymbol{\nabla}s)}{\rho}\right)^2 + \rho\,\varepsilon(\rho, s)\right] d\boldsymbol{r}. \tag{19.108}$$

Here, $\mathcal{U} = \rho\varepsilon$ is the potential energy density and $\varepsilon(\rho, s)$ the specific internal energy. For an ideal gas, $\mathcal{U} = p/(\gamma-1)$ where pressure[47] is to be expressed in terms of ρ and s using the equation of state (19.28). Hamilton's equations $\partial_t f = \{f, H\}$ for $f = \rho, \boldsymbol{v}$ and s then reproduce the continuity, Euler and entropy advection equations as in Sect. 19.14*.

---

[46] The six Clebsch variables cannot be uniquely determined by the five physical fields v_x, v_y, v_z, ρ, s. See Prob. 19.39 for a 'gauge freedom' in choosing Clebsch potentials that already exists in the barotropic case.

[47] Pressure is also related to the specific internal energy via the thermodynamic relation $p = \rho^2\frac{\partial\varepsilon}{\partial\rho}$, which comes from $p = -\frac{\partial U}{\partial V}$ at constant entropy.

Lagrangian and equations of motion. The advantage of having Clebsch variables is that they can be used to give a Lagrangian formulation for the equations of inviscid flow. Since the equations of motion are first order in time derivatives, the relevant Bateman-Thellung Lagrangian density $\mathcal{L}_1 = \rho_t\phi + \lambda_t\mu + \alpha_t s - \mathcal{H}$ [12,127] is linear (rather than quadratic) in generalized velocities[48]

$$\mathcal{L}_1 \quad = \quad \rho_t\phi + \lambda_t\mu + \alpha_t s - \frac{\rho}{2}\left(\boldsymbol{\nabla}\phi + \frac{(\lambda\boldsymbol{\nabla}\mu + \alpha\boldsymbol{\nabla}s)}{\rho}\right)^2 - \rho\,\varepsilon(\rho,s). \quad (19.109)$$

$\mathcal{L}_1$ depends on the 6 fields $f = \rho, \phi, \lambda, \mu, \alpha$ and s and their space or time derivatives. As in (17.44), the Euler-Lagrange (EL) equation for a field f is given by

$$\frac{\partial}{\partial t}\frac{\partial \mathcal{L}_1}{\partial f_t} = \frac{\partial \mathcal{L}_1}{\partial f} - \boldsymbol{\nabla}\cdot\frac{\partial \mathcal{L}_1}{\partial \boldsymbol{\nabla} f}. \quad (19.110)$$

For example, $\partial\mathcal{L}_1/\partial\alpha = -\boldsymbol{v}\cdot\boldsymbol{\nabla}s$ and $\partial\mathcal{L}_1/\partial\alpha_t = s$, so the EL equation for α gives the advection of specific entropy: $\frac{Ds}{Dt} = \partial_t s + \boldsymbol{v}\cdot\boldsymbol{\nabla}s = 0$ (19.27). Similarly, the one for λ implies that μ is advected[49]: $\frac{D\mu}{Dt} = 0$. On the other hand, $\mathcal{L}_1$ is independent of ϕ_t while $\partial\mathcal{L}_1/\partial\phi = \rho_t$ and $\partial\mathcal{L}_1/\partial\boldsymbol{\nabla}\phi = -\rho\boldsymbol{v}$. Thus, the EL equation for ϕ is the continuity equation $\partial_t\rho + \boldsymbol{\nabla}\cdot(\rho\boldsymbol{v}) = 0$. Now, $\partial\mathcal{L}_1/\partial\boldsymbol{\nabla}s = -\alpha\boldsymbol{v}$ while $\partial\mathcal{L}_1/\partial s = \alpha_t - \rho\partial\varepsilon/\partial s = \alpha_t - \rho T$, where we used the relation following from the first and second laws of thermodynamics for reversible processes $TdS = dU + pdV$. So the EL equation for s gives the evolution equation $\alpha_t + \boldsymbol{\nabla}\cdot(\alpha\boldsymbol{v}) = \rho T$. Proceeding as above, the EL equation for μ says that λ is locally conserved: $\lambda_t + \boldsymbol{\nabla}\cdot(\lambda\boldsymbol{v}) = 0$. The EL equation for ρ is quite interesting. We have $\partial\mathcal{L}_1/\partial\rho_t = \phi$ and

$$\begin{aligned}\frac{\partial\mathcal{L}_1}{\partial\rho} &= -\frac{1}{2}v^2 - \frac{\rho}{2}2\boldsymbol{v}\cdot\left(-\frac{1}{\rho^2}(\lambda\boldsymbol{\nabla}\mu + \alpha\boldsymbol{\nabla}s)\right) - \varepsilon - \rho\frac{\partial\varepsilon}{\partial\rho}\\ &= -\frac{1}{2}v^2 + \boldsymbol{v}\cdot(\boldsymbol{v} - \boldsymbol{\nabla}\phi) - \varepsilon - \frac{p}{\rho},\end{aligned} \quad (19.111)$$

upon using $p = \rho^2\partial\varepsilon/\partial\rho$. Thus, we get a sort of time-dependent Bernoulli equation:

$$\phi_t - \frac{\boldsymbol{v}^2}{2} + \boldsymbol{v}\cdot\boldsymbol{\nabla}\phi + \varepsilon(\rho,s) + \frac{p}{\rho} = 0. \quad (19.112)$$

Taking its divergence and combining with the other equations, one obtains the Euler equation for $\boldsymbol{v}$ (19.22), see Prob. 19.40. [Note that for incompressible flow with constant entropy and constant density $\bar\rho$, both λ and μ are advected by $\boldsymbol{v} = \boldsymbol{\nabla}\phi + (\lambda/\bar\rho)\boldsymbol{\nabla}\mu$ and could be expected to furnish canonical variables, while ϕ is determined in terms of them by the divergence-free condition $\boldsymbol{\nabla}\cdot\boldsymbol{v} = 0$.]

Interpretation of Lagrangian. Integrating by parts in t in the action $S = \int \mathcal{L}_1\,dt\,d\boldsymbol{r}$, we get other possible Lagrangian densities with the same equations of motion. For instance, we have

$$\mathcal{L}_2 \quad = \quad -\rho\phi_t - \lambda\mu_t - \alpha s_t - \mathcal{H} \quad \text{and}$$

---

[48] See Prob. 3.39, Prob. 3.40 and [124] for more on Lagrangians linear in velocities.

[49] This means that μ and s of a fluid element are the same as their values at $t = 0$

$$\mathcal{L}_3 \quad = \quad \rho\left(\frac{\boldsymbol{v}^2}{2}-\varepsilon\right)+\phi\left(\rho_t+\boldsymbol{\nabla}\cdot(\rho\boldsymbol{v})\right)-\lambda\frac{D\mu}{Dt}-\alpha\frac{Ds}{Dt}. \tag{19.113}$$

$\mathcal{L}_3$ has a nice interpretation. Its first term is the difference between kinetic and potential energy densities, as one might expect. However, the action principle for inviscid adiabatic flow is not merely the extremization of this difference. The remaining three terms can be regarded as imposing constraints via the method of Lagrange multipliers (see Sect. 3.16*). The first imposes the condition that mass must be locally conserved, with ϕ being the corresponding Lagrange multiplier. The second requires that μ be advected by $\boldsymbol{v}$ with λ being the multiplier. Finally, in the last term, the Lagrange multiplier α imposes the adiabatic flow condition, namely the advection of specific entropy (19.27). There are of course other choices of Lagrangian densities obtained via integration by parts. Taken together, we may interpret the Clebsch potentials as Lagrange multipliers imposing constraints[50].

19.16 Navier-Stokes equation for incompressible viscous flow

If viscous dissipative effects are included, the Euler equation (19.22) for inviscid flow is modified. The simplest case is that of incompressible flow, where (19.22) is augmented by a viscous term $\propto \boldsymbol{\nabla}^2\boldsymbol{v}$ to obtain the Navier-Stokes (NS) equation[51]:

$$\rho\frac{\partial\boldsymbol{v}}{\partial t}+\rho\boldsymbol{v}\cdot\boldsymbol{\nabla}\boldsymbol{v}=-\boldsymbol{\nabla}p+\boldsymbol{f}+\mu\boldsymbol{\nabla}^2\boldsymbol{v} \quad \text{with} \quad \boldsymbol{\nabla}\cdot\boldsymbol{v}=0. \tag{19.115}$$

Here, $\boldsymbol{f}$ is the body force per unit volume and μ is called the dynamic viscosity, which has been assumed constant[52]. One also introduces the kinematic viscosity $\nu = \mu/\rho$ with dimensions of a diffusivity [areal speed (L^2/T)]. If density variations are insignificant, then ν may also be taken to be a constant, as we shall do wherever convenient. The word shear[53] viscosity is often used for ν since, as we shall soon see, it is the coefficient of friction between layers of fluid that slide over each other.

The viscous term can be motivated through an analogy with the heat equation $\partial_t T = \alpha\boldsymbol{\nabla}^2 T$ (18.4) which describes diffusion of heat from hot to cold regions. Similarly, shear viscosity causes diffusion of velocity from a fast layer to a neighboring slow layer of fluid. By analogy with heat diffusion, velocity diffusion is described by

---

[50] Note however, that these 'constraints' are not simply conditions on the initial data but evolution equations.

[51] Using (19.129), the advection term in NS may be written in terms of the Lamb vector:

$$\partial_t\boldsymbol{v}+\boldsymbol{w}\times\boldsymbol{v}=-\frac{1}{\rho}\boldsymbol{\nabla}p-\frac{1}{2}\boldsymbol{\nabla}\boldsymbol{v}^2+\frac{\boldsymbol{f}}{\rho}+\nu\boldsymbol{\nabla}^2\boldsymbol{v}. \tag{19.114}$$

[52] The dynamic viscosity μ can vary with location, especially if there are significant inhomogeneities in temperature. If μ is nonuniform, then the i^{th} component of the viscous term in (19.115) becomes $\partial_j(\mu\partial_j v_i)$, see (19.116).

[53] The other type of viscosity is bulk or volume viscosity, which has to do with friction from compression of the fluid. It is absent in incompressible flows. See equation (19.121).

$\nu \boldsymbol{\nabla}^2 \boldsymbol{v}$, with shear viscosity ν playing a role analogous to thermal diffusivity α. If water in a cup is stirred and left to itself, viscosity brings it to rest, just as heat diffusion uniformizes the temperature distribution to zero in a rod with ends held at $T = 0$.

The NS equation has not been derived from molecular dynamics except for dilute gases. It is the simplest equation consistent with physical requirements and symmetries, that can be used to describe macroscopic viscous fluid motion. As with other physical models, its validity is to be checked by comparing its predictions with experimental measurements, which have largely confirmed its reliability.

No-slip boundary condition. The Navier-Stokes equation (19.115) is 2^{nd} order in space derivatives unlike the inviscid Euler equation (19.22), which is 1^{st} order. The viscous term is called a singular perturbation (see Footnote 7 of Sect. 5.2*), it increases the spatial order by one and necessitates an additional boundary condition (BC). In addition to the impenetrable BC on solid boundaries[54], one typically imposes the 'no-slip' BC which requires that the tangential component of $\boldsymbol{v}$ on solid boundaries must vanish. There is empirical support for the no-slip boundary condition: (a) running a fan does not remove the dust accumulated on its blades and (b) material accumulates on the sides of drain pipes even if the flow is quite fast.

Stress and rate of strain tensors. As we did with the Euler equation in (19.21), we may write the incompressible NS equation (19.114) in the absence of external body forces in terms of a stress tensor:

$$\partial_t v_i + v_j \partial_j v_i = -\frac{1}{\rho}\partial_j T_{ij} \quad \text{where} \quad T_{ij} = p\delta_{ij} - \mu(\partial_i v_j + \partial_j v_i). \tag{19.116}$$

The term $\partial_i v_j$ in T_{ij} does not contribute to the EOM through the divergence of the stress tensor $\partial_j T_{ij}$ because the flow is incompressible ($\partial_j v_j = 0$). However, we include it to make T_{ij} a symmetric tensor[55]. Evidently, pressure[56] enters through the isotropic part[57] (part that is a multiple of the identity) while the viscous forces enter through its nonisotropic part (traceless part: $-2\mu\partial_i v_i = 0$)[58]. This reinforces our introduction of pressure as a normal surface force, while shear viscosity is a tangential surface force. The (negative of the) nonisotropic part of T_{ij} is denoted d_{ij} and is called the deviatoric stress tensor. It must be symmetric and traceless: $d_{ij} = d_{ji}$ and $d_{ii} = 0$. For an incompressible viscous fluid, we have postulated that $d_{ij} = \mu(\partial_i v_j + \partial_j v_i)$. We notice that the deviatoric stress can be nonzero only if the fluid is in motion ($\boldsymbol{v} \neq 0$). In fact, one needs more than just a flow, one needs appropriate velocity gradients to be nonvanishing. It is convenient at this stage to introduce the rate of strain tensor[59] $e_{ij} = \frac{1}{2}(\partial_i v_j + \partial_j v_i)$, in terms of which, our postulate becomes $d_{ij} = 2\mu e_{ij}$. This is an instance of Newton's law for a fluid, stating that the deviatoric stress is linearly related to (here proportional to) the rate of strain[60]. In fact, one could start more generally by postulating that the deviatoric stress is linear[61] in velocity gradients $d_{ij} = A_{ijkl}\partial_k v_l$ for some constant 4^{th} rank tensor A_{ijkl}, and use the assumption of isotropy of the fluid[62] and the symmetry of d_{ij} to show that one must have $d_{ij} = 2\mu e_{ij}$ for an incompressible flow (see Prob. 19.44). This completes our analogy between heat and velocity diffusion. Just as the heat flux vector (18.1) is proportional to the temperature gradient, the viscous stress is proportional to the velocity gradient.

---

[54] The impenetrable BC is $\boldsymbol{v} \cdot \hat{\boldsymbol{n}} = 0$, where $\hat{\boldsymbol{n}}$ is the outward normal on boundaries.

[55] Taking T_{ij} symmetric could be regarded as an attempt at being elegant without affecting the equation of motion. However, it is helpful elsewhere. E.g., Batchelor (p.11 of [11]) argues that the stress tensor must be symmetric for the rate of change of angular momentum of a fluid element to equal the torque on the element due to surface forces. It also needs to be symmetric if the fluid (say, in a gaseous star) is to be consistently coupled to (i.e., act as a source for) the gravitational field in Einstein's general theory of relativity.

[56] As in the incompressible Euler equation, the pressure may be eliminated via the constraint equation obtained by taking the divergence of the NS equation and using $\boldsymbol{\nabla} \cdot \boldsymbol{v} = 0$ (see (19.24) and Prob. 19.7).

[57] An isotropic second rank tensor t_{ij} is one that does not define any preferred direction. Eigenvectors of the matrix t_{ij} define preferred directions. So for a matrix to be isotropic, every vector must be an eigenvector. This is the case if it is a multiple of the identity. Since multiples of the identity are invariant under changes of basis, this concept is basis-independent.

[58] Sometimes, it is imprecisely said that pressure is the diagonal part and the viscous forces are the off-diagonal part of the stress tensor: this is a basis-dependent statement.

Deviatoric stress for shear flow. To get a feeling for the deviatoric stress, let us consider a horizontal shear flow with $\boldsymbol{v} = (u(y), 0, 0)$. In this case, the only independent deviatoric stress tensor component is

$$T_{12} = T_{21} = -d_{12} = -2\mu e_{12} = -\mu(\partial_1 v_2 + \partial_2 v_1) = -\mu u'(y). \qquad (19.117)$$

Evidently, this viscous stress arises from the relative motion of horizontal layers.

Poiseuille flow in a pipe. This is steady laminar flow of a viscous fluid with constant density ρ through a long horizontal cylindrical pipe of length ℓ and uniform circular cross section of radius $a \ll \ell$, with axis along the z-axis. It is induced by a pressure drop Δp between the inlet and outlet of the pipe, with effects of gravity being insignificant. For sufficiently small[63] pressure gradients and away from the inlet and outlet, the flow is found to settle into a steady axisymmetric pattern. It is an example of a shear flow: faster at the center of the pipe and tapering off to zero on the walls, where it satisfies the no-slip BC. We will work in cylindrical coordinates and suppose that the flow velocity is independent of z and is purely axial $\boldsymbol{v} = u(r)\hat{z}$, while the pressure could depend on r and z. The time derivative and advection terms vanish in the incompressible NS equation $\rho(\boldsymbol{v}_t + \boldsymbol{v}\cdot\boldsymbol{\nabla}\boldsymbol{v}) = -\boldsymbol{\nabla}p + \mu\boldsymbol{\nabla}^2\boldsymbol{v}$ as the flow is steady and lacks a radial velocity component. Moreover, the radial component of NS implies $\partial p/\partial r = 0$, so $p = p(z)$. Separating variables in the z-component of NS,

---

[59] The velocity gradient $\partial_i v_j$ can be written as a sum of its symmetric and antisymmetric parts $\partial_i v_j = e_{ij} + w_{ij}$ where $e_{ij} = \frac{1}{2}(\partial_i v_j + \partial_j v_i)$ is the rate of strain tensor and $w_{ij} = \frac{1}{2}(\partial_i v_j - \partial_j v_i)$ is the vorticity tensor: $w_i = \epsilon_{ijk} w_{jk}$. The name *rate of strain* is because $e_{ij} \sim \frac{\partial}{\partial x_i}\frac{Dx_j}{Dt}$ involves a time derivative (rate) as well as a fractional displacement (strain).

[60] This is the fluid analog of Hooke's law for an elastic solid: stress being proportional to strain or more precisely, the stress tensor being linearly related to the strain tensor.

[61] A linear relation between two vectors (e.g., $L_i = \mathcal{I}_{ij}\Omega_j$) involves a 2^{nd} rank tensor. Similarly, a linear relation between two second rank tensors involves a fourth rank tensor.

[62] A fluid is isotropic if its intrinsic properties are independent of the direction in which they are measured. A liquid crystal with elongated molecules that are aligned using electromagnetic fields is an anisotropic fluid, as are some states of polymers. By intrinsic properties, we mean things like the refractive index or shear viscosity and not the shape of the container or features of a particular flow of the fluid, which may have a specific direction. Isotropy of a fluid implies that if it admits a flow in one direction, it would admit the same type of flow in any other direction (with suitably oriented boundaries). The isotropy of a fluid and that of a tensor are distinct concepts. The stress tensor of a viscous isotropic fluid is anisotropic.

[63] As Δp is increased, the flow becomes unsteady and makes a transition to turbulence.

$$\mu\boldsymbol{\nabla}^2\boldsymbol{v} = \frac{\mu}{r}\partial_r(r\partial_r u(r))\hat{z} = \frac{\partial p}{\partial z}\hat{z}, \tag{19.118}$$

we infer that the pressure gradient must be a constant, $dp/dz = -\Delta p/\ell < 0$. Upon imposing the BC $u(a) = 0$, we find a parabolic radial profile for the longitudinal velocity and an azimuthal vorticity that is counterclockwise viewed from the outlet:

$$u(r) = \frac{\Delta p}{4\mu\ell}(a^2 - r^2) \quad \text{and} \quad \boldsymbol{w} = -u'(r)\hat{\phi} = \frac{r\Delta p}{2\mu\ell}\hat{\phi}. \tag{19.119}$$

Evidently, the flow is helicity-free. The mass of fluid passing through a cross section of the pipe per unit time, is called the mass flow rate:

$$\dot{M} = \int \rho\boldsymbol{v}\cdot d\boldsymbol{S} = \int_0^{2\pi} d\phi \int_0^a \rho u(r)\, r\, dr = \frac{\pi a^4\Delta p}{8\nu\ell}. \tag{19.120}$$

Here, $\mu = \rho\nu$. The corresponding volume flow rate $\dot{V} = \dot{M}/\rho$ is given by the Hagen-Poiseuille equation $\dot{V} = \pi a^4\Delta p/8\mu\ell$.

Navier-Stokes for compressible flow. For compressible flow, there are two types of viscous terms, essentially because there are two vectors that can be constructed from second derivatives of velocity: the Laplacian $\boldsymbol{\nabla}^2\boldsymbol{v}$ and the gradient of the divergence $\boldsymbol{\nabla}(\boldsymbol{\nabla}\cdot\boldsymbol{v})$. For uniform dynamic shear viscosity μ and bulk viscosity ζ, the compressible Navier-Stokes equation takes the form [11]

$$\rho\frac{D\boldsymbol{v}}{Dt} = \boldsymbol{f} - \boldsymbol{\nabla}p + \mu\left(\boldsymbol{\nabla}^2\boldsymbol{v} + \frac{1}{3}\boldsymbol{\nabla}(\boldsymbol{\nabla}\cdot\boldsymbol{v})\right) + \zeta\boldsymbol{\nabla}(\boldsymbol{\nabla}\cdot\boldsymbol{v}). \tag{19.121}$$

Here p is the mechanical pressure, the isotropic part of the stress tensor. In a flowing viscous fluid, the mechanical pressure can differ from the thermodynamic pressure that appears in the thermodynamic equation state. □

Vorticity evolution and diffusion. The equation for evolution of vorticity may be obtained by taking the curl of (19.114). For a *conservative* body force and *constant density*, it takes a particularly simple form (see Prob. 19.45):

$$\partial_t\boldsymbol{w} + \boldsymbol{\nabla}\times(\boldsymbol{w}\times\boldsymbol{v}) = \nu\boldsymbol{\nabla}^2\boldsymbol{w} \quad \text{where} \quad \boldsymbol{\nabla}\cdot\boldsymbol{v} = 0. \tag{19.122}$$

We see that each component of vorticity must satisfy the linear diffusion equation ($\partial_t\boldsymbol{w} = \nu\boldsymbol{\nabla}^2\boldsymbol{w}$) modified by the curl of the nonlinear vortex force. Thus, unlike in inviscid flow studied in Sect. 19.11 and Sect. 19.12, vorticity can diffuse between regions and is not simply frozen into the velocity field. In particular, vortex tubes can lose their strength with time and dissipate. In viscous flows, vorticity is often generated near boundaries (even if not initially present) and then diffuses to the bulk of the fluid.

Reynolds number and similarity principle. Suppose we consider water with uniform velocity $U\hat{x}$ flowing along a broad and deep channel. It meets a cylindrical obstacle of diameter L and flows round it creating a pattern as in Fig. 19.8a. It turns out that if we double the speed U and halve the diameter L, then the same flow pattern results. This is the 'similarity' principle named after Osborne Reynolds, who did careful experiments with fluids flowing through a pipe in the late 1800s. More precisely, incompressible flows[64] with the same Reynolds number $\mathcal{R}$ are identical when compared at a reference scale. Reynolds' similarity principle is quite useful in practice: it is exploited to study the flow around an aircraft by using a flow with the same $\mathcal{R}$ around a scaled-down version of the aircraft placed in a wind tunnel, leading to significant cost savings.

To see how this arises, let us use the scales L and U (which are an appropriate geometric length and typical flow speed) to define dimensionless (primed) variables

$$\boldsymbol{r}' = \boldsymbol{r}/L, \quad \boldsymbol{v}' = \boldsymbol{v}/U \quad \text{and} \quad t' = Ut/L. \tag{19.123}$$

We denote by $\boldsymbol{\nabla}'$, the gradient with respect to $\boldsymbol{r}'$. Then, the Navier-Stokes equation (19.122) for incompressible constant density flow (in vorticity form) becomes

$$\frac{\partial \boldsymbol{w}'}{\partial t'} + \boldsymbol{\nabla}' \times (\boldsymbol{w}' \times \boldsymbol{v}') = \left(\frac{\nu}{LU}\right) \boldsymbol{\nabla}'^2 \boldsymbol{w}' \quad \text{with} \quad \boldsymbol{\nabla}' \cdot \boldsymbol{v}' = 0, \tag{19.124}$$

where $\boldsymbol{w}' = \boldsymbol{\nabla}' \times \boldsymbol{v}'$. Thus, two flows with the same Reynolds number $\mathcal{R} = LU/\nu$ lead to the same equation, and are therefore simply rescaled versions of each other. The Reynolds number $\mathcal{R}$ is a dimensionless parameter that may be interpreted as a measure of the ratio of inertial to viscous terms in the NS equation (19.115):

$$\frac{\text{inertial force}}{\text{viscous force}} = \frac{|\boldsymbol{v} \cdot \boldsymbol{\nabla} \boldsymbol{v}|}{|\nu \boldsymbol{\nabla}^2 \boldsymbol{v}|} \approx \frac{U^2/L}{\nu U/L^2} = \frac{LU}{\nu} = \mathcal{R}. \tag{19.125}$$

When $\mathcal{R}$ is small (e.g., in slow creeping flow), viscous forces dominate over the nonlinear inertial forces and the flow is regular or laminar, or even steady [$\boldsymbol{v}(\boldsymbol{r}, \not{t})$ and $p(\boldsymbol{r}, \not{t})$ independent of time when there is a suitable driving force to balance dissipation]. At low $\mathcal{R}$, one could ignore the nonlinear inertial advection term $\boldsymbol{v} \cdot \boldsymbol{\nabla} \boldsymbol{v}$ in NS, resulting in the Stokes flow approximation. On the other hand, when $\mathcal{R}$ increases (say, as the flow speeds up), the streamlines become convoluted, the flow becomes increasingly irregular, seemingly unpredictable and is called turbulent.

Stokes flow past a sphere. Stokes studied steady creeping viscous constant ρ flow with asymptotic[65] velocity $\boldsymbol{U}$ around a sphere of radius a. For steady ($\partial_t \boldsymbol{v} = 0$) creeping flow ($\mathcal{R} = aU/\nu \ll 1$), (19.115) reduces to the linear equation

$$0 = -\boldsymbol{\nabla} p + \mu \boldsymbol{\nabla}^2 \boldsymbol{v} \quad \text{with} \quad \boldsymbol{\nabla} \cdot \boldsymbol{v} = 0. \tag{19.126}$$

---

[64] The flows could be steady or unsteady, laminar or turbulent.

[65] By going to a frame that moves with the asymptotic velocity of the fluid, the problem may be mapped to that of a sphere moving at $-\boldsymbol{U}$ through a fluid asymptotically at rest.

The dimensional parameters in the problem are U, a and $\mu = \rho\nu$. Thus, on dimensional grounds, the magnitude of the force that the fluid exerts on the sphere must be $F \propto \mu a U$. A detailed calculation (see Sect. 20 of [85]) shows that the proportionality constant is 6π. In other words, the drag force on a sphere moving at velocity $\boldsymbol{U}$ through a fluid asymptotically at rest is $-6\pi a\mu\boldsymbol{U}$ in the Stokes flow approximation. More generally, even if we drop the assumptions of steady creeping flow, dimensional analysis (see Prob. 19.48) implies that the magnitude of the drag force may be written as $F = \frac{1}{2}C_D(\mathcal{R})\pi a^2\rho U^2$ for a dimensionless function $C_D(\mathcal{R})$, called the drag coefficient. What the Stokes approximation shows is that $C_D \to 12/\mathcal{R}$ as $\mathcal{R} \to 0$. This has been experimentally validated. In other words, the drag coefficient is proportional to speed at low speeds. As $\mathcal{R}$ is increased, there are deviations from Stokes' formula as the flow ceases to be steady. It becomes roughly periodic in time (but still laminar) and then becomes increasingly turbulent: vortices are generated in a boundary layer around the sphere and are carried downstream in a turbulent wake. This change in flow pattern with increasing $\mathcal{R}$ is described below in the context of flow past a cylinder.

Flow past a cylinder: transition to turbulence[66]**.** Let us consider flow of water, entering uniformly from the far left and flowing to the right with asymptotic velocity $U\hat{x}$ as in Fig. 19.8a. The water meets a fixed vertical right circular cylinder of diameter L with axis along $\hat{z}$. We shall denote the Cartesian components of the flow velocity by $\boldsymbol{v} = (u, v, w)$. At very low $\mathcal{R} = LU/\nu \approx .16$, the flow around the cylinder is laminar (steady, i.e., time-translation invariant) and displays several symmetries, as shown in Fig. 19.8a: (a) $y \to -y$ (reflections in $z - x$ plane), (b) z translation-invariance and (c) left-right symmetry with respect to the center of the cylinder ($x \to -x$ and $(u, v, w) \to (u, -v, -w)$). All these are symmetries of Stokes flow, which results from ignoring the body force term and nonlinear advection term in NS (19.115). At $\mathcal{R} \approx 1.5$, a marked left-right asymmetry develops between the upstream and downstream regions. At $\mathcal{R} \approx 5$, there is a change in the topology of the flow: the flow downstream of the obstacle no longer hugs the cylindrical surface, it detaches from the surface. This is called flow separation and is associated with the formation of recirculating standing eddies downstream of the cylinder (see Fig. 19.8b). These eddies were not present at smaller $\mathcal{R}$ or far upstream of the cylinder; they are generated and diffuse from a *boundary layer* around the obstacle, where the effect of viscosity is very significant. Far from the obstacle, the flow is nearly irrotational.

At $\mathcal{R} \approx 40$, the flow ceases to be approximately steady, but is periodic in time at each point. At $\mathcal{R} \gtrsim 40$, recirculating eddies are periodically shed (alternatively from either side of the cylinder) to form the celebrated von Kármán vortex street[67] sketched in Fig. 19.9a. The z-translation invariance along the axis of the cylinder is spontaneously broken when $\mathcal{R} \sim 40 - 75$. At higher $\mathcal{R} \sim 200$, the flow becomes chaotic with a turbulent 'boundary layer' around the cylinder. At $\mathcal{R} \sim 1800$, only about two vortices in the von Kármán vortex street are distinct, before merging into

---

[66] Excellent photographs illustrating the transition to turbulence in flow past a cylinder may be found in [129].

[67] Vortex streets also appear behind an obstacle in a river, in clouds passing around a high pressure region, past the wings of insects and birds, etc.

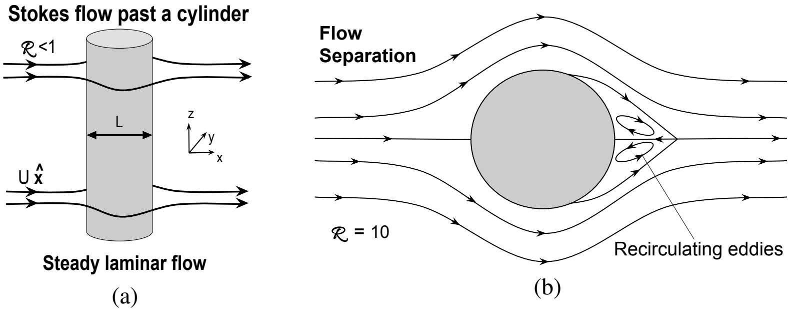

Figure 19.8: Flow past a cylinder. (a) Side view of Stokes flow at $\mathcal{R} \lesssim 1$. (b) Top view at $\mathcal{R} \approx 10$ showing detachment of the flow and recirculating eddies downstream of the cylinder.

a quasiuniform turbulent wake (see Fig. 19.9b). At much higher $\mathcal{R}$, many of the symmetries of NS are restored in a statistical sense and turbulence is called fully-developed. This spontaneous breaking and statistical restoration of symmetries of the equations and boundary conditions is typical of the transition from laminar flow to fully developed turbulence.

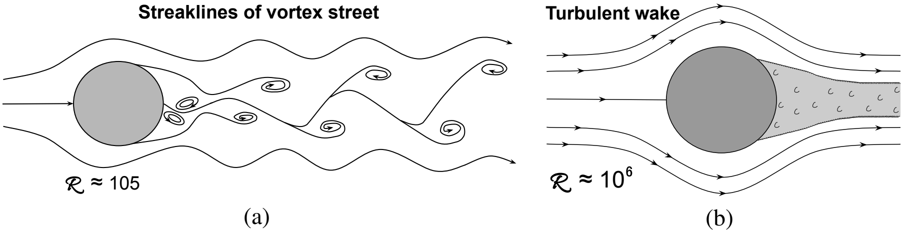

Figure 19.9: Flow past a cylinder. (a) Top view of streaklines at $\mathcal{R} \approx 105$ showing alternate shedding of eddies and development of vortex street consisting of two parallel rows of staggered vortices. (b) Sketch of turbulent wake downstream of cylinder at $\mathcal{R} \approx 10^6$.

By turbulence, we usually mean irregular[68] behavior (chaos) in a driven dissipative system with a large number of degrees of freedom. Without a driving force (say stirring or pumping in the water), the turbulence decays. In the absence of dissipation, we would have Hamiltonian chaos modeled, for instance, by the Euler equation. In a turbulent flow, the velocity field $\boldsymbol{v}(\boldsymbol{r}, t)$ appears random in time and highly disordered in space. Turbulent flows exhibit a wide range of length scales[69]: from the system size, size of obstacles, through large vortices down to the smallest ones at the so-called Taylor microscale where dissipation occurs. What is more, even at a fixed location $\boldsymbol{r}_0$, the time series of velocity $\boldsymbol{v}(\boldsymbol{r}_0, t)$ tends to be very different in distinct experiments with approximately the same initial and boundary conditions. Nevertheless, the time average $\bar{\boldsymbol{v}}(\boldsymbol{r}_0)$ tends to be the same in all realizations. Unlike individual flow realizations, statistical properties of turbulent flow are empirically reproducible.

---

[68] This includes intermittency, one of whose manifestations is irregular alteration between chaos and apparently periodic behavior.

[69] The range of length scales where inertial forces ($\propto \boldsymbol{v} \cdot \boldsymbol{\nabla} \boldsymbol{v}$) dominate over viscous forces ($\propto \nu \boldsymbol{\nabla}^2 \boldsymbol{v}$) is called the inertial range. Dissipation typically occurs at smaller length scales.

They typically depend on $\mathcal{R}$ and BCs.

The study of fluid flow including the Navier-Stokes and Euler equations is a major branch of engineering, physics and mathematics. Though simple to write down, these equations are notoriously hard to solve in most physically interesting situations, primarily due to the nonlinearities arising from the advection term and the resulting coupling of a large number of degrees of freedom and length scales. For instance, we do not yet have an effective analytical method of predicting the features of the flow past a cylinder as $\mathcal{R}$ is varied or the values of $\mathcal{R}$ at which qualitative changes[70] in the flow pattern occur. However, some things have been done: von Kármán showed that the vortex street is stable for certain ranges of parameters. Numerical simulations can reproduce some of the observed features. As happened near the cylinder, the conditions at boundaries and interfaces encode important physical effects, but can add to the complications. Some of these effects can be understood using boundary layer theory, an asymptotic approximation method pioneered by Ludwig Prandtl. In fact, there is a million dollar Clay Millennium Prize attached to understanding whether the solution to NS for smooth initial data exists and is smooth or whether the solution could hit a singularly in finite time (as in the example of a finite-time blowup in Sect. 5.3). The wider challenge lies in deducing the observed, often complex patterns of flow[71] from the known laws governing fluid motion. This often requires a mix of physical insight, experimental data, mathematical techniques and computational methods.

19.17 Problems

1. **Heat capacities** at constant volume and pressure are $C_v = \left(\frac{\delta Q}{\delta T}\right)_V = T\left(\frac{\partial S}{\partial T}\right)_V$ and $C_p = \left(\frac{\delta Q}{\delta T}\right)_p = T\left(\frac{\partial S}{\partial T}\right)_p$, where δQ is the heat added reversibly to a gas, T its absolute temperature and S its entropy. Use the 1st and 2nd laws of thermodynamics $dU = TdS - pdV$ and the definition of enthalpy in terms of internal energy $H = U + pV$ to express C_v and C_p as partial derivatives of U and H. For N molecules of an ideal gas ($pV = Nk_bT$) show that $C_p = C_v + Nk_b$ and that $\gamma = C_p/C_v > 1$.
2. **Adiabatic process for an ideal gas.** Show that for an ideal gas undergoing a reversible adiabatic process, pV^γ is constant. Hint: By the first law of thermodynamics, the infinitesimal heat added to the gas is $dU + pdV = 0$ where $dU = C_v dT$ is the increase in internal energy. Use the results of Prob. 19.1.
3. **Atmospheric pressure.** It is observed that temperature $T(z)$, density $\rho(z)$ and pressure $p(z)$ all decrease with height z in the atmosphere. We wish to find the

---

[70] Qualitative changes typically occur when the existing flow is unstable to perturbations which grow, leading to a new flow pattern. For instance, steady shear flow can be susceptible to the Kelvin-Helmholtz instability: the interface between two layers of fluid moving at different velocities is unstable to short wavelength perturbations that grow, leading, for instance, to the ‘roll-up’ of a vortex sheet. Another common instability is the Rayleigh-Taylor instability of the interface between a dense fluid and a rare fluid that lies beneath it.

[71] In particular, one would like to develop a statistical understanding of turbulent flows.

temperature and pressure gradients in a simple model for the atmosphere where we ignore the variation of the acceleration due to gravity (g) with height. We assume that the air is an ideal gas satisfying the ideal gas law $p = \rho RT/\mu$ where μ is the molar mass. Since air is a poor conductor we will assume that parcels of air move without much heat exchange with surroundings (i.e., adiabatically and reversibly), so we may assume that any two among p, ρ, T satisfy the adiabatic relation. We will assume a steady state where layers of air in the atmosphere are in mechanical equilibrium due to a balance of their weight by the upward pressure gradient.

a. Find the differential condition for mechanical equilibrium of a thin layer of air of surface area A at height z and thickness dz.
b. Show that the variation of pressure satisfies $dp/p = -(\mu g/RT)dz$. Here, μ is the average molar mass for air and g the acceleration due to gravity.
c. Show that the temperature gradient dT/dz is a constant κ (assuming g is constant). Find an expression for κ in terms of the adiabatic index γ.
d. Find the numerical value of the temperature gradient by taking reasonable values for the constants.
e. Find a differential equation for the variation of pressure with height in the form $dp/dz = f(p, z)$, assuming temperature on the Earth's surface $(z = 0)$ is T_0.
f. Find a formula for $p(z)$, assuming the pressure at $z = 0$ is p_0.
g. Find the variation of acceleration due to gravity with height z above the Earth's surface. Show that $g(z) = g/(1 + z/R)^2$ where $R \approx 6371$ km is the radius of the Earth and g the acceleration due to gravity at the surface. Long range commercial aircraft fly at a height of $h_{\text{plane}} \approx 10$ km. Find g at h_{plane} given that it is about 9.81 m/s^2 at the surface.

4. Check the **Leibniz rule** $\frac{D(f\boldsymbol{w})}{Dt} = \frac{Df}{Dt}\boldsymbol{w} + f\frac{D\boldsymbol{w}}{Dt}$ (19.8) for the material derivative.
5. **Gauss' divergence theorem** relates the integral over a volume V of the divergence of a vector field $\boldsymbol{q}$ to the flux of the vector field across its bounding surface ∂V:

$$\int_V \boldsymbol{\nabla} \cdot \boldsymbol{q}\, dV = \int_{\partial V} \boldsymbol{q} \cdot \hat{\boldsymbol{n}}\, dA. \tag{19.127}$$

The outward pointing normal on ∂V is $\hat{\boldsymbol{n}}$. By choosing $\boldsymbol{q}$ appropriately, obtain the following Corollary of the divergence theorem for any scalar function p:

$$\int_V \boldsymbol{\nabla} p\, dV = \int_{\partial V} p\, \hat{\boldsymbol{n}}\, dA. \tag{19.128}$$

6. Consider inviscid **constant density flow** of an ideal gas. How are the pressure and temperature determined? Are they independent propagating degrees of freedom?
7. **Incompressible flow with variable density.** Consider Euler's equation for incompressible flow with density that is not necessarily constant. Give the evolution equation for ρ and find a nonevolutionary constraint equation for the pressure.

8. Establish the **vector identity**

$$(\boldsymbol{v}\cdot\boldsymbol{\nabla})\boldsymbol{v} = \boldsymbol{\nabla}\left(\frac{1}{2}v^2\right) + (\boldsymbol{\nabla}\times\boldsymbol{v})\times\boldsymbol{v}. \tag{19.129}$$

   Hint: Find the i^{th} component of the left and right sides by using (3.249).

9. **Specific entropy.** Derive the formula $s = c_v \log\left(\frac{p/\bar{p}}{(\rho/\bar{\rho})^\gamma}\right)$ for the specific entropy of an ideal gas with specific heat ratio $\gamma = c_p/c_v$. The specific heat (per unit mass) at constant volume is c_v, while $\bar{\rho}$ and $\bar{p}$ are reference density and pressure. The corresponding equation expressing the entropy of a monatomic ideal gas in terms of mass density and internal energy density is called the Sackur-Tetrode equation. Hint: For n moles of an ideal gas, $p = nRT/V$ and the change in internal energy is $dU = C_v dT$ with heat capacity C_v independent of V (this is called the caloric condition, $U(T,V) = U(T)$ is independent of volume). Use the 1st law of thermodynamics $\delta Q = dU + pdV$ along with the 2nd law expressing the exactness of $\frac{\delta Q}{T} = dS$ for an infinitesimal reversible process to derive the formula for specific entropy assuming that the gas is calorically perfect (C_v independent of T, usually a reasonable first approximation).

10. **Specific entropy for isothermal flows.** Consider an ideal gas with molecular mass m that satisfies the caloric condition and undergoes isothermal motions. (a) Use the 1st and 2nd laws of thermodynamics to show that its specific entropy is $s = \bar{s} + (k_b/m)\log(\bar{\rho}/\rho)$ where $\bar{\rho} = m\bar{p}/k_b T$ is a reference density. (b) Verify that the specific entropy expression from Prob. 19.9 reduces to this for isothermal flows. Hint: $c_p - c_v = k_b/m$. (c) Deduce that in an isothermal flow, the specific entropy obeys the evolution equation $\partial_t s + \boldsymbol{v}\cdot\boldsymbol{\nabla}s = (k_b/m)\boldsymbol{\nabla}\cdot\boldsymbol{v}$. Comment on what happens if the flow is incompressible.

*11. **Ideal gas internal energy equation.** (a) Derive the internal energy equation for the adiabatic dynamics of an ideal gas with constant specific heat ratio $\gamma = c_p/c_v$:

$$\left(\frac{p}{\gamma-1}\right)_t + p\boldsymbol{\nabla}\cdot\boldsymbol{v} + \boldsymbol{\nabla}\cdot\left(\frac{p\boldsymbol{v}}{\gamma-1}\right) = 0. \tag{19.130}$$

   Here, $p/(\gamma-1)$ is the internal energy density. Express it in terms of the temperature T of an ideal monatomic gas. This equation is not in local conservation form. In principle, how must one modify it to get an equation in local conservation form? Hint: Begin with the equation of state for an ideal gas relating entropy to p and ρ and use the entropy advection and continuity equations. (b) Express the temperature of such a gas in terms of p and ρ, given that its molecular mass is m.

12. Consider **isothermal compressible inviscid flow** of an ideal gas with molecular mass m at temperature T. What is the barotropic relation (and analog of specific enthalpy) that supplements the continuity and Euler equations of such a flow. What is the speed of sound waves in isothermal disturbances around such a fluid at rest?

13. **Sound waves.** In (19.48) we obtained the wave equation for small amplitude density perturbations in a sound wave. What are the corresponding equations for pressure, velocity and temperature perturbations p_1, $\boldsymbol{v}_1$ and T_1? To obtain the equation

for T_1, you may assume the fluid to be an ideal gas. Assuming that $\boldsymbol{v}_1 = \boldsymbol{\nabla}\phi_1$ is a potential vector field, show that there is a suitable ϕ_1 that satisfies the wave equation.

14. **Adiabatic and isothermal sound speeds.** Find an expression for the adiabatic (constant specific entropy) sound speed c_s for sound waves in an ideal gas (with specific heat ratio γ) around the state with constant density and pressure ρ_0, p_0. What is the corresponding isothermal sound speed c_T? Which is larger?

15. **Vorticity in rotating bucket.** Find the vorticity for the azimuthal velocity field $\boldsymbol{v} = \Omega r\hat{\theta}$ in cylindrical polar coordinates. Here, Ω is a constant angular speed.

$*$16. **Freezing-in of vorticity.** Combine the continuity and vorticity (19.54) equations for a barotropic flow to obtain the following form of the freezing-in of $\boldsymbol{w}/\rho$ into the flow:

$$(\boldsymbol{w}/\rho)_t + \mathcal{L}_{\boldsymbol{v}}(\boldsymbol{w}/\rho) = 0. \tag{19.131}$$

Show that when the flow is incompressible, vorticity itself is frozen into the flow: $\boldsymbol{w}_t + \mathcal{L}_{\boldsymbol{v}}\boldsymbol{w} = 0$. Here, the Lie derivative of the vector field $\boldsymbol{u}$ along $\boldsymbol{v}$ is $\mathcal{L}_{\boldsymbol{v}}\boldsymbol{u} = \boldsymbol{v}\cdot\boldsymbol{\nabla}\boldsymbol{u} - \boldsymbol{u}\cdot\boldsymbol{\nabla}\boldsymbol{v}$. Verify that $\mathcal{L}_{\boldsymbol{v}}\boldsymbol{u} = [\boldsymbol{v}, \boldsymbol{u}]$ is also the commutator of vector fields. We may regard the derivative $\partial_t + \mathcal{L}_{\boldsymbol{v}}$ as the derivative along the flow.

17. Consider **incompressible barotropic flow** on the x-y plane with the z-component of **vorticity** given by w. Use the local conservation law: $(w^2)_t + \boldsymbol{\nabla}\cdot(w^2\boldsymbol{v})$ (19.56) to derive a local conservation law for w^3. Try to extend it to w^n for $n = 4, 5, \cdots$.

18. **Leibniz rule.** (a) Establish the Leibniz rule $\boldsymbol{\nabla}\cdot(f\boldsymbol{u}) = \boldsymbol{\nabla}f\cdot\boldsymbol{u} + f\boldsymbol{\nabla}\cdot\boldsymbol{u}$ for a scalar function f and vector field $\boldsymbol{u}$. (b) Use it to show that

$$\boldsymbol{\nabla}\cdot\left(\frac{v^2}{2}\rho\boldsymbol{v}\right) = \frac{v^2}{2}\boldsymbol{\nabla}\cdot(\rho\boldsymbol{v}) + \rho\boldsymbol{v}\cdot(\boldsymbol{v}\cdot\boldsymbol{\nabla})\boldsymbol{v}. \tag{19.132}$$

It may help to write the second term in components. (c) Similarly, show that

$$\boldsymbol{\nabla}\cdot\left(\frac{\gamma}{\gamma-1}p\boldsymbol{v}\right) = v\cdot\boldsymbol{\nabla}p + p\boldsymbol{\nabla}\cdot\boldsymbol{v} + \boldsymbol{\nabla}\cdot\left(\frac{p\boldsymbol{v}}{\gamma-1}\right). \tag{19.133}$$

19. Consider **inviscid adiabatic compressible flow** in the presence of a **conservative body force** per unit volume $\boldsymbol{f} = -\rho\boldsymbol{\nabla}\varphi$, so that the Euler equation becomes $\boldsymbol{v}_t + \boldsymbol{v}\cdot\boldsymbol{\nabla}\boldsymbol{v} = -(1/\rho)\boldsymbol{\nabla}p - \boldsymbol{\nabla}\varphi$. What are the dimensions of φ? Can you modify $\mathcal{E} = \frac{1}{2}\rho\boldsymbol{v}^2 + p/(\gamma-1)$ to obtain a **locally conserved energy** for such a flow?

20. **Local conservation of angular momentum.** Show that the angular momentum density $\mathcal{L}_i = \rho\epsilon_{ijk}x_jp_k$ satisfies the local conservation law $\partial_t\mathcal{L}_i + \partial_l\Lambda_{il} = 0$ where $\Lambda_{il} = \epsilon_{ijk}x_j\Pi_{kl}$ and Π_{kl} is the momentum current tensor (19.69). Hint: Use $\partial_lx_j = \delta_{lj}$.

21. **Helicity density for planar flow.** Show that the helicity density $\boldsymbol{v}\cdot\boldsymbol{w}$ of a planar velocity field of the form $\boldsymbol{v} = (u(x,y), v(x,y), 0)$ always vanishes.

22. Consider the velocity fields (a) $\boldsymbol{v} = (z, x, y)$ and (b) $\boldsymbol{v} = (z, x, 0)$ in Cartesian coordinates. In each case, evaluate $\boldsymbol{w} = \boldsymbol{\nabla}\times\boldsymbol{v}$ and **helicity density** $\boldsymbol{v}\cdot\boldsymbol{w}$. Plot $\boldsymbol{v}$ and describe its integral curves. Describe the shapes of vortex lines and specify

the level surfaces of helicity density. Qualitatively describe the relative orientation of vorticity and velocity integral curves.

23. **Divergence of a cross product.** Establish the vector identity $\boldsymbol{\nabla} \cdot (\boldsymbol{A} \times \boldsymbol{B}) = \boldsymbol{B} \cdot \boldsymbol{\nabla} \times \boldsymbol{A} - \boldsymbol{A} \cdot \boldsymbol{\nabla} \times \boldsymbol{B}$ which is useful in deriving local conservation laws. Hint: Write out both sides in components. See [60] for a compilation of vector identities.

∗24. Consider flow that is not necessarily barotropic, governed by the Euler equation

$$\boldsymbol{v}_t = -\boldsymbol{w} \times \boldsymbol{v} - \frac{\boldsymbol{\nabla} p}{\rho} - \frac{1}{2}\boldsymbol{\nabla} v^2. \tag{19.134}$$

Show that the **time derivative of helicity density** can 'almost' be expressed as a local conservation law:

$$(\boldsymbol{w} \cdot \boldsymbol{v})_t + \boldsymbol{\nabla} \cdot \left(\frac{v^2}{2}\boldsymbol{w} + (\boldsymbol{w} \times \boldsymbol{v}) \times \boldsymbol{v} + \frac{\boldsymbol{\nabla} p}{\rho} \times \boldsymbol{v} \right) = -2\boldsymbol{w} \cdot \frac{\boldsymbol{\nabla} p}{\rho}. \tag{19.135}$$

The term on the RHS is generally not a divergence. Since $\boldsymbol{\nabla} \cdot \boldsymbol{w} = 0$, it *is* a divergence iff $(\boldsymbol{\nabla} p)/\rho$ is the gradient of a scalar $(\boldsymbol{\nabla} h)$, this is the case if ρ is a constant or if the flow is barotropic. This explains our assumption in deriving (19.73). How is the above equation modified in the presence of a body force?

25. Show that the **density-velocity Poisson bracket** $[\{\boldsymbol{v}(\boldsymbol{x}), \rho(\boldsymbol{y})\} = \boldsymbol{\nabla}_{\boldsymbol{y}} \delta(\boldsymbol{x} - \boldsymbol{y})]$ (19.77) may also be expressed as

$$\{\rho(\boldsymbol{x}), \boldsymbol{v}(\boldsymbol{y})\} = \boldsymbol{\nabla}_{\boldsymbol{y}} \delta(\boldsymbol{x} - \boldsymbol{y}) = -\boldsymbol{\nabla}_{\boldsymbol{x}} \delta(\boldsymbol{x} - \boldsymbol{y}). \tag{19.136}$$

∗26. Show that the **Euler equation** $\boldsymbol{v}_t + \boldsymbol{v} \cdot \boldsymbol{\nabla} \boldsymbol{v} = -\boldsymbol{\nabla} h$ is **Hamilton's equation** $\boldsymbol{v}_t = \{\boldsymbol{v}, H\}$ for the Hamiltonian (19.78) and PBs (19.77) for barotropic flow.

∗27. Show that the **barotropic flow Poisson brackets** (19.80) between functionals F and G of ρ and $\boldsymbol{v}$ imply the Landau PBs among ρ and $\boldsymbol{v}$ (19.77). Hint: Take $F = v_i(\boldsymbol{x})$ and $G = \rho(y)$ or $G = v_j(\boldsymbol{y})$ and evaluate the functional derivatives.

28. **Velocity-pressure PB.** Show using the PBs (19.81) that the velocity-pressure PB for adiabatic flow of an ideal gas with polytropic exponent γ is given by (19.84)

∗29. **Incompressible flow PB.** Suppose $F[\boldsymbol{v}]$ and $G[\boldsymbol{v}]$ are independent of density and that $\rho = \rho_0$ is a constant in the PBs for barotropic flow (19.80). Show that these PBs then reduce to those for incompressible flow (19.86), assuming the functional derivatives of F and G are divergence-free. Hint: Use the vector identity $(\boldsymbol{\nabla} \times \boldsymbol{A}) \cdot \boldsymbol{B} - \boldsymbol{A} \cdot \boldsymbol{\nabla} \times \boldsymbol{B} = \boldsymbol{\nabla} \cdot (\boldsymbol{A} \times \boldsymbol{B})$ and assume surface terms can be ignored. You will also need the vector identity (which you must establish)

$$\boldsymbol{\nabla} \times (\boldsymbol{A} \times \boldsymbol{B}) = \boldsymbol{A}(\boldsymbol{\nabla} \cdot \boldsymbol{B}) - \boldsymbol{B}(\boldsymbol{\nabla} \cdot \boldsymbol{A}) + (\boldsymbol{B} \cdot \boldsymbol{\nabla})\boldsymbol{A} - (\boldsymbol{A} \cdot \boldsymbol{\nabla})\boldsymbol{B}. \tag{19.137}$$

30. Show that the **functional derivative of helicity** $\mathcal{K} = \int \boldsymbol{v} \cdot \boldsymbol{w} \, d\boldsymbol{r}$ with respect to the velocity field is twice the vorticity field: $\frac{\delta \mathcal{K}}{\delta v_i(z)} = 2 w_i(z)$. You may assume that the velocity field $\to 0$ at infinity or on boundaries.

31. Suppose the velocity vector field $v(\boldsymbol{r})$ is an **eigenvector of the curl operator**, i.e., $\boldsymbol{\nabla} \times \boldsymbol{v} = \lambda \boldsymbol{v}$ where λ is a constant (in (a) and (b) λ can be a scalar function). (a) Show that this flow has no vortex force. (b) Show that the corresponding vorticity $\boldsymbol{w} = \boldsymbol{\nabla} \times \boldsymbol{v}$ field is a steady solution of the Euler equations for constant density flow. (c) Assuming $\boldsymbol{v}$ is not irrotational, show that the helicity of this flow is nonzero. (d) Find an example of a **vortex force-free flow**.

∗32. **Helicity as a Casimir.** Show that the helicity $\mathcal{K} = \int \boldsymbol{v} \cdot \boldsymbol{w}\, d\boldsymbol{r}$ is a Casimir invariant of the Poisson algebra (19.80) of observables for barotropic flow in $\mathbb{R}^3$ with decaying BCs. In other words, show that $\{\mathcal{K}, G[\rho, \boldsymbol{v}]\} = 0$ for any functional G of ρ and $\boldsymbol{v}$. Hint: Start with a functional of ρ or $\boldsymbol{v}$ alone.

∗33. **Hamiltonian formulation for adiabatic flow.** Show that the Hamiltonian (19.82) for ideal adiabatic flow of a gas with polytropic exponent γ along with the PBs (19.81) and (19.84) leads to the Euler equation $\boldsymbol{v}_t + \boldsymbol{v} \cdot \boldsymbol{\nabla} \boldsymbol{v} = -(1/\rho)\boldsymbol{\nabla} p$.

34. **Commutator of divergence-free vector fields.** Suppose $\boldsymbol{u}$ and $\boldsymbol{v}$ are divergence-free: $\boldsymbol{\nabla} \cdot \boldsymbol{u} = \boldsymbol{\nabla} \cdot \boldsymbol{v} = 0$. Then show that their Lie bracket or commutator $[\boldsymbol{u}, \boldsymbol{v}] = \boldsymbol{u} \cdot \boldsymbol{\nabla} \boldsymbol{v} - \boldsymbol{v} \cdot \boldsymbol{\nabla} \boldsymbol{u}$ is also divergence-free.

35. **Helmholtz decomposition.** Consider the Helmholtz decomposition (Sect. 19.14*) of a vector field $\boldsymbol{v} = \boldsymbol{\nabla} \phi + \boldsymbol{\nabla} \times \boldsymbol{A}$. Find a formula for $\boldsymbol{A}$ in a suitable *gauge*, i.e., by exploiting the freedom to add to $\boldsymbol{A}$ the gradient of a scalar. Hint: Find $\boldsymbol{\nabla} \times \boldsymbol{v}$.

36. **Clebsch decomposition and helicity.** Consider the velocity vector field $\boldsymbol{v} = \tilde{\lambda} \boldsymbol{\nabla} \mu$. Show that the corresponding vorticity is $\boldsymbol{w} = \boldsymbol{\nabla} \tilde{\lambda} \times \boldsymbol{\nabla} \mu$. Conclude that $\boldsymbol{v}$ is helicity-free: $\boldsymbol{v} \cdot \boldsymbol{w} = 0$.

37. **Incompressible flow Clebsch decomposition.** Show that ϕ is not an independent degree of freedom in the Clebsch decomposition of an incompressible velocity field $\boldsymbol{v} = \boldsymbol{\nabla} \phi + \tilde{\lambda} \boldsymbol{\nabla} \mu$. How can ϕ be eliminated?

38. **Incompressible flow Clebsch variables.** Suppose an incompressible velocity field is expressed as $\boldsymbol{v} = \boldsymbol{\nabla} \times \boldsymbol{A} = \boldsymbol{\nabla} \phi + \alpha \boldsymbol{\nabla} \beta$ and consequently $\boldsymbol{w} = \boldsymbol{\nabla} \times \boldsymbol{v} = \boldsymbol{\nabla} \alpha \times \boldsymbol{\nabla} \beta$. Show that (a) $\boldsymbol{v}^2 = \boldsymbol{A} \cdot \boldsymbol{w} - \boldsymbol{\nabla} \cdot (\boldsymbol{v} \times \boldsymbol{A})$. (b) $\boldsymbol{A} \cdot \boldsymbol{w} = \boldsymbol{\nabla} \cdot (\beta \boldsymbol{A} \times \boldsymbol{\nabla} \alpha) - \beta \boldsymbol{v} \cdot \boldsymbol{\nabla} \alpha$ and (c) $\boldsymbol{A} \cdot \boldsymbol{w} = -\boldsymbol{\nabla} \cdot (\alpha \boldsymbol{A} \times \boldsymbol{\nabla} \beta) + \alpha \boldsymbol{v} \cdot \boldsymbol{\nabla} \beta$.

∗39. **Gauge invariance of Clebsch representation.** Show that the transformation [112]

$$\phi \mapsto \phi' = \phi + f(\tilde{\lambda}, \mu, t), \quad \tilde{\lambda} \mapsto \tilde{\lambda}' = g(\tilde{\lambda}, \mu, t), \quad \mu \mapsto \mu' = h(\tilde{\lambda}, \mu, t) \tag{19.138}$$

leaves $\boldsymbol{v} = \boldsymbol{\nabla} \phi + \tilde{\lambda} \boldsymbol{\nabla} \mu$ unchanged if the functions f, g, h satisfy the conditions

$$\frac{\partial f}{\partial \mu} + g \frac{\partial h}{\partial \mu} = \tilde{\lambda} \quad \text{and} \quad \frac{\partial f}{\partial \tilde{\lambda}} + g \frac{\partial h}{\partial \tilde{\lambda}} = 0. \tag{19.139}$$

40. **Euler equation from Lagrangian.** Derive the Euler equation (19.22) by taking the divergence of the evolution equation (19.112) for the Clebsch velocity potential ϕ obtained from the Bateman-Thellung Lagrangian in Sect. 19.15*.

∗41. **Velocity PBs from Clebsch variables.** For the velocity field $\boldsymbol{v} = \boldsymbol{\nabla} \phi + (\lambda/\rho) \boldsymbol{\nabla} \mu$, use the canonical PBs (19.103) between Clebsch variables to show that

$$\{v_i(x), v_j(y)\} \quad = \quad \left[\frac{\lambda(y) \partial_j \mu}{\rho^2(y)} \partial_i - \frac{\lambda(x) \partial_i \mu}{\rho^2(x)} \partial_j \right] \delta(x - y)$$

$$+\frac{1}{\rho(x)\rho(y)}[-\lambda(x)\partial_j\mu(y)\partial_i + \partial_i\mu(x)\lambda(y)\partial_j]\delta(x-y). \quad (19.140)$$

Here $\partial_i = \partial_{x^i}$, $\partial_j = \partial_{y^j}$. Use $f\partial_i\delta(x-y) = \partial_i(f\delta(x-y)) - (\partial_i f)\delta(x-y)$ to rewrite terms and argue that the total derivative terms cancel, leading to (19.105).

42. (a) Show that the **vorticity field** $\boldsymbol{w} = \boldsymbol{\nabla}(\lambda/\rho)\times\boldsymbol{\nabla}\mu$ **is solenoidal** for any Clebsch potentials λ,μ and density ρ. (b) Show that $\epsilon_{ijk}w_k = \partial_i(\lambda/\rho)\partial_j\mu - \partial_j(\lambda/\rho)\partial_i\mu$.
43. Express the **specific internal energy** ε of an ideal gas with specific heat ratio γ in terms of the density and specific entropy.
44. **Newton's law for a fluid** states that the deviatoric stress is linear in the rate of strain: $d_{ij} = A_{ijkl}\partial_k v_l$, where A_{ijkl} are the constant Cartesian components of a rank-4 tensor. If the fluid is isotropic, A_{ijkl} must be an isotropic tensor and expressible as a linear combination of products of Kronecker delta symbols. Use isotropy for an incompressible flow to show that $d_{ij} = 2\mu e_{ij}$ for some constant μ, where $e_{ij} = (1/2)(\partial_i v_j + \partial_j v_i)$ is the rate of strain tensor.
45. **Vorticity evolution in viscous flow.** Show that the evolution equation for vorticity in viscous incompressible flow may be written as

$$\partial_t\boldsymbol{w} + \boldsymbol{\nabla}\times(\boldsymbol{w}\times\boldsymbol{v}) = -\frac{1}{\rho^2}\boldsymbol{\nabla}p\times\boldsymbol{\nabla}\rho + \boldsymbol{\nabla}\times\frac{\boldsymbol{f}}{\rho} + \nu\boldsymbol{\nabla}^2\boldsymbol{w}. \quad (19.141)$$

Hint: Show that $\boldsymbol{\nabla}\times(f\boldsymbol{v}) = f\boldsymbol{\nabla}\times\boldsymbol{v} + \boldsymbol{\nabla}f\times\boldsymbol{v}$, for any $f, \boldsymbol{v}$.

46. Find a **stress tensor** $T_{ij} = p\delta_{ij} + \cdots$ for the **Navier-Stokes equation** (19.121) for compressible flow in the absence of an external force. Can it be taken symmetric?
47. Change to dimensionless 'primed' variables (19.123) in the Navier-Stokes equation (19.122) for incompressible constant density flow in vorticity form. Show that it can be written in terms of the dimensionless **Reynolds number** as in (19.124).
48. **Drag force on a sphere.** The drag force F for constant density flow at asymptotic speed U past a sphere of radius a can depend on ρ, U, a and ν. (a) Argue that $F \propto \rho U^b \nu^c a^d$ where $b = d$ and $c = 2 - d$ and thereby deduce that $F \propto \rho\mathcal{R}^d\nu^2$. (b) Show that $F_D = \frac{1}{2}C_D(\mathcal{R})\,\pi a^2\,\rho U^2$ for some function C_D of $\mathcal{R} = aU/\nu$.

*49. **Nonlinear Schrödinger equation.** The classical nonlinear Schrödinger equation (NLSE) is used to model the dynamics of Bose-Einstein condensates (BECs, e.g., ultracold dilute atomic Bose gases such as Rubidium-87) in a 'mean field' approximation. The one-dimensional version is relevant to BECs in cigar-shaped traps. The nonlinear Schrödinger field is a complex scalar field $\psi(x,t)$ that evolves according to the cubically nonlinear PDE called the nonlinear Schrödinger equation:

$$i\partial_t\psi = -\beta\partial_x^2\psi + \kappa|\psi|^2\psi. \quad (19.142)$$

β and κ are constant real parameters. We work with decaying boundary conditions on the real line: $|\psi(x,t)| \to 0$ sufficiently fast as $x \to \pm\infty$ at all times t. (a) Use the NLSE and its complex conjugate to show that $N = \int \psi^*\psi\,dx$ is conserved[72].

---

[72] Up to a dimensionful multiplicative constant, the eigenvalues of a quantum operator associated to N are interpreted as the possible numbers of particles in the condensate.

(b) Verify that the energy

$$H = \int \left(\beta |\partial_x \psi|^2 + \frac{1}{2}\kappa |\psi(x)|^4 \right) dx = \int \left(-\beta \psi^* \partial_x^2 \psi + \frac{1}{2}\kappa |\psi(x)|^4 \right) dx \tag{19.143}$$

is also independent of time. (c) Infer the dimensions $[\beta] = L^2/T$, $[\psi] = [\psi^*] = (ML/T)^{1/2}$ and $[\kappa] = 1/ML$. (d) Argue that one may always take $\beta > 0$. (Hint. Take the complex conjugate of the NLSE). Assuming this has been done, the equation is called repulsive or defocusing if $\kappa > 0$ and attractive or focusing if $\kappa < 0$. When $\kappa = 0$, (19.142) reduces to the free particle linear Schrödinger equation of quantum mechanics $[i\hbar \partial_t \psi = -(\hbar^2/2m)\psi'']$, which explains the name. However, the name can be misleading, as ψ here is a classical field, not a quantum wave function. (e) Show that the 'field momentum' $P = i \int \psi^* \psi' \, dx$ is a third conserved quantity. (f) Show that N, H and P are real. (g) Taking H as the Hamiltonian, show that the NLSE admits a Hamiltonian-Poisson bracket formulation if we postulate the PBs

$$\{\psi(x), \psi^*(x')\} = -i\delta(x - x'), \quad \{\psi(x), \psi(x')\} = \{\psi^*(x), \psi^*(x')\} = 0. \tag{19.144}$$

We may interpret the PBs as saying that $\pi = i\psi^*$ is the field conjugate to ψ. (h) Show that Hamilton's equation for ψ^* is the complex conjugate NLSE. (i) Verify that $\{N, H\} = 0$, $\{P, H\} = 0$. (j) Find $\{N, P\}$. (k) Show that the Lagrangian resulting from an (inverse) Legendre transform $\int \pi \dot{\psi} \, dx - H$ where $\pi = i\psi^*$ is

$$L = \int \left[i\psi^* \dot{\psi} + \beta \psi^* \partial_x^2 \psi - \frac{1}{2}\kappa \psi^* \psi^* \psi \psi \right] dx. \tag{19.145}$$

(l) Verify that the Euler-Lagrange equation for ψ^* and ψ are the NLSE and its complex conjugate. (m) Apply Noether's theorem to the global $U(1)$ symmetry $\psi \to e^{i\theta}\psi$ to deduce the conservation of N. (n) Deduce the conservation of P from invariance of L under space translations. (o) In fact, the 1d NLSE admits an infinite number of independent conserved quantities and is an integrable system with infinitely many degrees of freedom. Find out more about this.

Appendix A

Mathematical and kinematical background

Here we provide a brief and informal introduction to some mathematical and kinematical concepts that are useful in our study of classical mechanics. Vectors in Euclidean space (Appendix A.1) furnish a basic example of a vector space. The associated notion of linear combinations of vectors with real scalar coefficients leads us to the concept of linear (in)dependence. The dot or scalar product encodes geometric notions such as lengths, projections and angles while the cross product encodes areas of parallelograms. Together, they allow us to define right-handed orthonormal bases or frames. Physically, they are used to define concepts such as the work done by a force and the angular momentum of a particle. In Appendix A.2, we use these ideas to introduce the position coordinates and position, infinitesimal displacement, velocity and acceleration vectors of a particle moving in Euclidean space. Circular motion (Appendix A.3) and motion with constant acceleration (Appendix A.4) provide examples where explicit formulae for these quantities can be written down. While Cartesian coordinates are the simplest way of specifying the location of a particle in Euclidean space, curvilinear coordinates such as plane and spherical polar coordinates (Appendices A.5 and A.6) provide alternatives that are convenient when there is rotational symmetry around a central object. By contrast with Cartesian coordinates, new terms arise when we express the velocity and acceleration vectors in polar coordinates since the radial and angular directions change with location, as we will see in Appendix A.5.

Taylor series allow us to approximate functions in the vicinity of a point by polynomials. They are useful, for instance, in modeling the force felt by a particle around a point of stable equilibrium. In Appendix A.7, we discuss Taylor series for functions of one and two variables and also introduce the differential and partial derivatives of a function, which feature in the Taylor 'expansion'.

In Appendix A.8, we progress from scalars and vectors at *one* point to a smoothly varying assignment of scalars or vectors to *every* point of a region in Euclidean space. This leads to the concept of scalar and vector fields, which allow us to model quantities like the pressure and velocity of a flowing fluid or the gravitational potential energy and force felt by massive particles in the vicinity of a star. Combining these fields with (multivariable) differential calculus allows us to introduce three notions of first order derivatives: the gradient of a scalar field and the divergence and curl of a vector field. The gradient tells us in which direction a scalar function increases most rapidly and enables us to write a conservative force field in terms of a scalar potential. The divergence quantifies the compressibility of a flow while the curl measures its vorticity (tendency to circulate). Gauss' and Stokes' theorems (Appendix A.9) relate the integrals of a gradient, curl or divergence over a curve, surface or volume to the values of the scalar and vector fields on the boundaries. They help us formulate physical laws governing the conservation of mass, electromagnetic phenomena and heat diffusion and allow us to relate the circulation of a fluid flow around a closed curve to the flux of its vorticity across a spanning surface.

Appendix A.10 is a primer on linear algebra: vector spaces with bases, linear transformations between vector spaces, their representation by matrices and eigenvalue problems. Physical systems typically display small oscillations when perturbed around a stable static equilibrium state. These oscillations are treated by linearizing the equations of motion around the equilibrium state as done in Chap. 13. Although oscillations are generally not periodic, they may often be decomposed into a combination of periodic 'normal modes'. This phenomenon is elegantly captured by the framework of an eigenvalue problem for a linear transformation on a vector space. Linearization of the equations of motion corresponds to approximating the arena for the dynamics by a vector space with the information in the equations encoded in a matrix that represents a linear transformation in a suitable basis. The eigenvectors of this matrix correspond to the normal modes while its eigenvalues are related to the oscillation frequencies. The decomposition is achieved via the diagonalization of the matrix by a change of basis for the vector space.

We end in Appendix A.11* with a brief introduction to the Fourier transform. It is an integral transform that takes a function of a position coordinate x and produces one of a wave number k. The Legendre transform of Sect. 3.15 may be regarded as an approximation to the Fourier transform (see Footnote 61 of Sect. 3.15). A utility of the Fourier transform derives from that fact that it converts differentiation with respect to x into multiplication by ik. Thus, linear partial differential equations such as the heat equation can be converted into systems of ordinary differential equations (18.22) by 'going' to Fourier or wave number space. We will also meet the Fourier transform while studying scattering in Sect. 2.71. By trying to evaluate the Fourier transform of a constant, we discover the Dirac delta function, a distribution that is infinite at one point and zero everywhere else. The delta function is useful in modeling an impulsive force (6.53) or the density distribution of a point mass (see Prob. A.38) or in defining Green's function of a differential operator (6.57).

A.1 Vectors in Euclidean space

Vectors provide a convenient way of writing the equations of physics in compact form. This compact form can often reveal symmetries and structural features of equations (such as behavior under transformation to a rotated or boosted frame) that may otherwise be obscured. They also allow us to exploit tools from linear algebra and geometry. Vector notation offers an economy of symbols: in his formulation of the equations of electromagnetism, Maxwell needed 6 letters of the alphabet (E, F, G, H, I and J) for the components of the electric and magnetic fields[1]. Vector notation (introduced in the work of Oliver Heaviside and Josiah Willard Gibbs who developed vector calculus for treating problems of electromagnetism) allows us to manage with two ($\boldsymbol{E}, \boldsymbol{H}$) or just one letter F for the electromagnetic field. Moreover, written in vector form, it is easier to recognize the symmetries of Maxwell's equations[2].

---

[1] This explains our current use of $\boldsymbol{H}$ for the magnetic field.

Three dimensional (3d) Euclidean space is the space around us in which we observe the motion of objects from cricket balls, birds and airplanes to planets and stars. We imagine it to extend indefinitely in all directions. We pick a point in this space and designate it as the origin. A nonzero vector $\boldsymbol{v}$ in 3d Euclidean space is a directed line segment (represented by an arrow as in Fig. A.1) emanating from the origin. It has a magnitude (or length, norm or modulus) denoted $|\boldsymbol{v}| = v$ (which is a positive real number determined using a measuring scale) and a direction (which is specified with respect to the origin and relative to other objects[3]). Additionally, there is the zero vector $\mathbf{0}$, which is the only vector with zero length, it may be regarded as pointing in all directions. It is distinct from the real number 0. While the tip of the arrow representing the $\mathbf{0}$ vector lies at the origin of 3d space, 0 is a point on the real line. Examples: (i) The vector that points from the origin to the instantaneous location of a particle is called its position vector. (ii) The velocity of a particle and the force acting on it are vectors that emanate from the location of the particle.

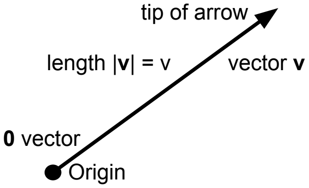

Figure A.1: A vector as an arrow from an origin. Without reference objects, it is not possible to specify the direction of $\boldsymbol{v}$. This is called isotropy of Euclidean space, where all directions from a point look the same. Inclusion of reference objects in Euclidean space help to fix directions.

The multiplication of a vector $\boldsymbol{v}$ by the real number α (also called a real scalar) denoted $\alpha\boldsymbol{v}$ is a vector in the same or opposite direction as $\boldsymbol{v}$ (according as $\alpha \geq 0$ or $\alpha \leq 0$) that has the length $|\alpha||\boldsymbol{v}|$. In particular, $1\boldsymbol{v} = \boldsymbol{v}$ and $0\boldsymbol{v} = \mathbf{0}$ is the zero vector. A *unit vector* is one with unit length (length one). Given a nonzero vector $\boldsymbol{a}$, the associated unit vector $\hat{\boldsymbol{a}}$ is obtained by 'normalization', i.e., dividing it by its norm: $\hat{\boldsymbol{a}} = \boldsymbol{a}/|\boldsymbol{a}| = (1/a)\boldsymbol{a}$.

The sum of the vectors $\boldsymbol{a}$ and $\boldsymbol{b}$ is the vector that points (from the common origin) along the diagonal of the parallelogram with adjacent sides $\boldsymbol{a}$ and $\boldsymbol{b}$, as in Fig. A.2a. Evidently, the order does not matter: $\boldsymbol{a} + \boldsymbol{b} = \boldsymbol{b} + \boldsymbol{a}$. We say that the addition of vectors is commutative or abelian. In particular, $\mathbf{0} + \boldsymbol{v} = \boldsymbol{v}$ for any vector $\boldsymbol{v}$.

The set of all vectors in 3d Euclidean space (with a fixed origin) equipped with the operations of addition of vectors and multiplication of vectors by real numbers

---

[2] In fact, although Maxwell's equations are invariant under rotations and translations, they are not invariant under Galilean transformations to a boosted frame of reference. The latter highlights an inconsistency between Newtonian mechanics and electromagnetic theory. This inconsistency was resolved in the special theory of relativity by replacing Galilean transformations with Lorentz transformations which were all along a symmetry of Maxwell's equations.

[3] Given an origin we need at least two other reference points that are not collinear with the origin to be able to specify directions of all nonzero vectors.

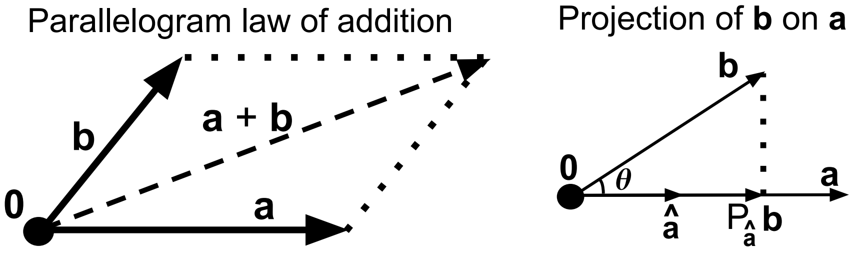

(a) (b)

Figure A.2: (a) $\boldsymbol{a}+\boldsymbol{b}$ is the vector that points along the diagonal of the parallelogram defined by $\boldsymbol{a}$ and $\boldsymbol{b}$. Clearly $\boldsymbol{a}+\boldsymbol{b}=\boldsymbol{b}+\boldsymbol{a}$. (b) The orthogonal projection $P_{\hat{\boldsymbol{a}}}\boldsymbol{b}$ of $\boldsymbol{b}$ on $\boldsymbol{a}$ depends on $\boldsymbol{a}$ only through $\hat{\boldsymbol{a}}$.

is called a 3d real vector space and is denoted $\mathbb{R}^3$. The space of vectors on the 2d Euclidean plane with a chosen origin forms the 2d real vector space denoted $\mathbb{R}^2$.

Dot or scalar product. For two vectors in $\mathbb{R}^3$, we define their dot product as the real number $\boldsymbol{a}\cdot\boldsymbol{b}=ab\cos\theta$ where θ is the angle between the vectors in either direction. It is also called the scalar product (or inner product) since the result is a real number. The dot product is commutative: $\boldsymbol{a}\cdot\boldsymbol{b}=\boldsymbol{b}\cdot\boldsymbol{a}$. We can turn things around. Suppose we did not know the angles between vectors but were given the dot product[4] of any pair of vectors. Then we may define the angle between $\boldsymbol{a}$ and $\boldsymbol{b}$ as $\theta=\arccos(\frac{\boldsymbol{a}\cdot\boldsymbol{b}}{ab})$. In particular, two vectors are orthogonal or perpendicular if $\boldsymbol{a}\cdot\boldsymbol{b}=0$. What is more, we may recover the length of a vector from its dot product with itself: $a=\sqrt{\boldsymbol{a}\cdot\boldsymbol{a}}$. Geometry has to do with angles, lengths, notions of parallel and perpendicular, etc. Thus, we may say that the geometry of Euclidean space is encoded in the dot product of vectors. The dot product arises naturally in mechanics. For instance, the work done by a force is an example of a scalar product. Suppose a force $\boldsymbol{F}$ acts on a particle and displaces it infinitesimally by the vector $d\boldsymbol{s}$. Then the infinitesimal work done by the force is the scalar product $\boldsymbol{F}\cdot d\boldsymbol{s}$.

Projection of a vector on another vector. Given $\boldsymbol{b}$ and a nonzero vector $\boldsymbol{a}$ we define the component of $\boldsymbol{b}$ in the direction of $\boldsymbol{a}$ by $\boldsymbol{b}\cdot\hat{\boldsymbol{a}}=b\cos\theta$ where θ is the angle between the vectors in either direction. The component is a real number, it can be positive, negative or zero. It does not depend on the length of $\boldsymbol{a}$. The orthogonal projection of $\boldsymbol{b}$ on $\boldsymbol{a}$ denoted $P_{\hat{\boldsymbol{a}}}\boldsymbol{b}$ is the vector $P_{\hat{\boldsymbol{a}}}\boldsymbol{b}=(\boldsymbol{b}\cdot\hat{\boldsymbol{a}})\hat{\boldsymbol{a}}$ indicated in Fig. A.2b. It is a vector that points in the direction of $\hat{\boldsymbol{a}}$ or $-\hat{\boldsymbol{a}}$ and has a magnitude equal to the absolute value of the component of $\boldsymbol{b}$ along $\hat{\boldsymbol{a}}$.

Cross or vector product. The vector or cross product $\boldsymbol{a}\times\boldsymbol{b}$ is a vector with magnitude $ab\sin\theta\geq 0$ where θ is the angle between the vectors chosen to satisfy $0\leq\theta\leq\pi$. Its direction is determined by the right hand thumb rule: if the fingers of the right hand curl from $\boldsymbol{a}$ to $\boldsymbol{b}$ then the cross product points in the direction of the thumb. In particular, $\boldsymbol{a} \times \boldsymbol{b}$ points in a direction perpendicular to both $\boldsymbol{a}$ and $\boldsymbol{b}$. Moreover, the cross product is antisymmetric: $\boldsymbol{a} \times \boldsymbol{b} = -\boldsymbol{b} \times \boldsymbol{a}$. In particular, $\boldsymbol{a} \times \boldsymbol{a} = \mathbf{0}$. Examples: (i) The 'torque' due to a force $\boldsymbol{F}$ acting on a particle with position vector $\boldsymbol{r}$ relative to a given origin is defined as the cross product $\boldsymbol{\tau} = \boldsymbol{r} \times \boldsymbol{F}$. How might a force point so that it imparts no torque on the particle? (ii) The area of a parallelogram spanned by the vectors $\boldsymbol{a}$ and $\boldsymbol{b}$ (in that order) is fruitfully regarded as the vector $\boldsymbol{a} \times \boldsymbol{b}$. Its magnitude is the numerical value of the more familiar 'area' $ab \sin\theta$.

---

[4] To qualify as a dot product, a rule assigning a real number to any pair of vectors must satisfy some conditions inspired by the Euclidean dot product: it must be symmetric [$\boldsymbol{a}\cdot\boldsymbol{b}=\boldsymbol{b}\cdot\boldsymbol{a}$], linear [$(\boldsymbol{a}+\boldsymbol{b})\cdot\boldsymbol{c}=\boldsymbol{a}\cdot\boldsymbol{c}+\boldsymbol{b}\cdot\boldsymbol{c}$ and $(\alpha\boldsymbol{a})\cdot\boldsymbol{b}=\alpha\boldsymbol{a}\cdot\boldsymbol{b}$ for any real scalar α] and positive [$\boldsymbol{a}\cdot\boldsymbol{a}\geq 0$ with equality only if $\boldsymbol{a}=0$].

Linear combinations and (in)dependence of vectors. Given vectors $\boldsymbol{u}$ and $\boldsymbol{v}$ and real numbers α and β, the vector $\alpha\boldsymbol{u} + \beta\boldsymbol{v}$ is called a linear combination[5]. Two vectors $\boldsymbol{u}$ and $\boldsymbol{v}$ are linearly dependent if one is a multiple of the other, i.e., if they point in the same or opposite directions. In other words, $\boldsymbol{u} = \alpha\boldsymbol{v}$ or $\boldsymbol{v} = \beta\boldsymbol{u}$ for some real numbers α and β. So when they are dependent, there is a linear combination $\boldsymbol{u} - \alpha\boldsymbol{v}$ or $\boldsymbol{v} - \beta\boldsymbol{u}$ that vanishes. We need to allow for both possibilities. For instance, if $\boldsymbol{u} = 0\boldsymbol{v}$ and $\boldsymbol{v} \neq \mathbf{0}$, then β is formally infinite and we do not have a relation of the sort $\boldsymbol{v} = \beta\boldsymbol{u}$. In summary, $\boldsymbol{u}$ and $\boldsymbol{v}$ are linearly dependent if there are real numbers a, b (not both zero) such that $a\boldsymbol{u} + b\boldsymbol{v} = \mathbf{0}$. The zero vector $\mathbf{0}$ and any vector $\boldsymbol{u}$ are always linearly dependent since $\mathbf{0} = 0\boldsymbol{u}$. On the other hand, $\boldsymbol{u}$ and $\boldsymbol{v}$ are said to be linearly independent if they point in different directions (i.e., are neither parallel nor antiparallel). Equivalently, two vectors are linearly independent iff[6] the parallelogram they span has nonzero area (see Prob. A.6). Prob. A.8 contains yet another equivalent condition: $\boldsymbol{u}$ and $\boldsymbol{v}$ are linearly independent if $a\boldsymbol{u} + b\boldsymbol{v} = \mathbf{0}$ implies that both a and b are zero. These ideas generalize to more than two vectors. For instance, three vectors are linearly independent iff the volume of the parallelepiped they define is nonzero. In particular, three vectors cannot be linearly independent in $\mathbb{R}^2$ (see Prob. A.9). More generally, vectors $\boldsymbol{v}_1, \boldsymbol{v}_2, \boldsymbol{v}_3, \cdots$ are said to be linearly independent if the only linear combination $c_1\boldsymbol{v}_1 + c_2\boldsymbol{v}_2 + c_3\boldsymbol{v}_3 + \cdots$ that vanishes is the one where $c_1 = c_2 = c_3 = \cdots = 0$. In other words, the only linear combination that vanishes is the trivial one.

Cartesian axes and orthonormal frame. Cartesian axes are any choice of mutually perpendicular axes x, y, z emanating from the origin in $\mathbb{R}^3$. Any point P in $\mathbb{R}^3$ can then be assigned three Cartesian coordinates (x, y, z) which are the perpendicular distances of P from the yz, zx and xy planes. It is conventional to use x, y, z both for the axes and for the coordinates of a point relative to these axes. At any point (x, y, z) we denote by $\hat{x}$ (more precisely $\hat{x}(P)$) the unit vector in the direction of increasing x holding y and z fixed[7]. The unit vectors $\hat{y}$ and $\hat{z}$ are similarly defined, see Fig. A.3a. At the origin, $\hat{x}, \hat{y}$ and $\hat{z}$ (more precisely $\hat{x}(0)$, etc.) are unit vectors along the Cartesian axes. They are orthonormal in the sense that they each have unit norm and are mutually perpendicular:

$$\hat{x} \cdot \hat{x} = \hat{y} \cdot \hat{y} = \hat{z} \cdot \hat{z} = 1 \quad \text{and} \quad \hat{x} \cdot \hat{y} = \hat{y} \cdot \hat{z} = \hat{z} \cdot \hat{x} = 0. \tag{A.1}$$

---

[5] The set of vectors $\alpha\boldsymbol{u} + \beta\boldsymbol{v}$ for all real α and β is called the *linear span* of $\boldsymbol{u}$ and $\boldsymbol{v}$. The set is a vector space and is called the vector space spanned by $\boldsymbol{u}$ and $\boldsymbol{v}$. It is a subspace of the vector space in which $\boldsymbol{u}$ and $\boldsymbol{v}$ live.

[6] The word iff is short-hand for 'if and only if'.

[7] The unit vectors $\hat{x}$ at two different points are related by parallel translation.

The $(\hat{x}, \hat{y}, \hat{z})$ frame is called right-handed if $\hat{x} \times \hat{y} = \hat{z}$ (rather than $-\hat{z}$, in which case it is left-handed, see Fig. A.3b). What are $\hat{y} \times \hat{z}$ and $\hat{z} \times \hat{x}$? Conventionally one works with right-handed frames unless otherwise specified.

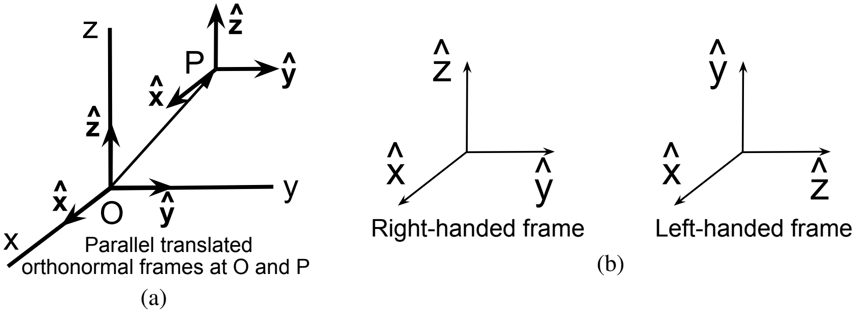

Figure A.3: (a) Orthonormal frames at O and P are related by parallel translation. (b) Right-handed ($\hat{x} \times \hat{y} = \hat{z}$) and left-handed ($\hat{x} \times \hat{y} = -\hat{z}$) orthonormal frames.

Orthonormal basis. At any point P, the vectors $\hat{x}, \hat{y}$ and $\hat{z}$ form a basis for the 3d vector space $\mathbb{R}^3$ of vectors emanating from that point (see Fig. A.3a). By this, we mean that they are linearly independent and any vector can be written (uniquely) as a linear combination of them: $\boldsymbol{a} = a_x\hat{x} + a_y\hat{y} + a_z\hat{z}$. Focusing on vectors emanating from the origin, the three real numbers a_x, a_y and a_z are the Cartesian coordinates of the tip of the vector $\boldsymbol{a}$. They are also the components of $\boldsymbol{a}$ along the three coordinate frame vectors since $a_x = \boldsymbol{a} \cdot \hat{x}$, etc. Notice that $a_x\hat{x} = P_{\hat{x}}\boldsymbol{a}$ is the projection of $\boldsymbol{a}$ along $\hat{x}$. We say that the vector $\boldsymbol{a}$ has been resolved into its components and written as a sum of its orthogonal projections along the orthonormal basis vectors. When the basis vectors are clear from the context, we may also write $\boldsymbol{a}$ as the ordered triple $\boldsymbol{a} = (a_x, a_y, a_z)$. Verify that the dot product of $\boldsymbol{a} = a_x\hat{x} + a_y\hat{y} + a_z\hat{z}$ and $\boldsymbol{b} = b_x\hat{x} + b_y\hat{y} + b_z\hat{z}$ is $\boldsymbol{a} \cdot \boldsymbol{b} = a_xb_x + a_yb_y + a_zb_z$. See Prob. A.10 for the components of the vector product.

A.2 Position coordinates and velocity and acceleration vectors

The instantaneous location of a particle moving in 3d Euclidean space may be specified by its Cartesian coordinates $(x(t), y(t), z(t))$. As the particle moves, it traces out a directed curve parametrized by increasing time, called its trajectory. The instantaneous location of a particle is the same no matter which coordinate system we use to describe it. The latter is simply a convenient way of specifying the ‘address’ of a point. For instance, the Cartesian coordinates x, y, z depend on the choice of origin and orientation of axes. If we change these, we will get a different set of coordinates to describe the same physical location of the particle at a given time. Operationally, two people following different coordinate systems to track the trajectory of a particle will meet each other at the common instantaneous location of the particle (see Prob. A.16).

The vector that points from the origin of Cartesian coordinates to the instantaneous position of the particle has components $(x(t), y(t), z(t))$. It is called the position vector $\boldsymbol{r}(t) = x(t)\hat{x} + y(t)\hat{y} + z(t)\hat{z}$. While such a designation is convenient for some purposes, it is important to bear in mind that the location of a particle is a point in space rather than a vector: it is not physically associated to a direction and the location of the particle does not come with any intrinsic notion of an origin or a length.

The infinitesimal displacement of a particle over a time $[t, t + \delta t]$ *does* define a vector, albeit a vector with infinitesimal length $\delta \boldsymbol{r}(t) = \boldsymbol{r}(t + \delta t) - \boldsymbol{r}(t)$. The concept of infinitesimal displacement defines an origin, namely the initial location of the particle (at time t). The infinitesimal displacement vector then points from this origin to the final location of the particle (at time $t + \delta t$). The concept of infinitesimal displacement does not define a coordinate frame, it only defines an origin and a vector $\delta \boldsymbol{r}$. It is convenient to resolve $\delta \boldsymbol{r}$ along the axes of the previously introduced Cartesian orthonormal frame (see Fig. A.3a) with origin at $\boldsymbol{r}(t)$ and write

$$\delta \boldsymbol{r}(t) = (x(t + \delta t) - x(t))\hat{x} + (y(t + \delta t) - y(t))\hat{y} + (z(t + \delta t) - z(t))\hat{z}. \quad \text{(A.2)}$$

The velocity of the particle is defined as the limiting value of the difference quotient

$$\boldsymbol{v}(t) = \frac{d\boldsymbol{r}(t)}{dt} \equiv \lim_{\delta t \to 0} \frac{\delta \boldsymbol{r}(t)}{\delta t}. \quad \text{(A.3)}$$

The velocity defines a vector that points from the instantaneous location in the direction of motion. It is a tangent vector to the trajectory. Its magnitude is called the instantaneous speed of the particle. Note that the origin from which the velocity vector points moves with the particle. It is convenient to resolve $\boldsymbol{v}$ along the axes of the Cartesian orthonormal frame with origin at the current location of the particle. Denoting time derivatives with over-dots,

$$\boldsymbol{v}(t) = \dot{x}\hat{x} + \dot{y}\hat{y} + \dot{z}\hat{z} \quad \text{(A.4)}$$

The time-derivative of the velocity is the acceleration, which is the vector

$$\boldsymbol{a}(t) = \ddot{x}(t)\hat{x} + \ddot{y}(t)\hat{y} + \ddot{z}(t)\hat{z}. \quad \text{(A.5)}$$

It is the limit of the difference quotient $(\boldsymbol{v}(t + \Delta t) - \boldsymbol{v}(t))/\Delta t$ as $\Delta t \to 0$. It may be regarded as a vector emanating from the instantaneous location of the particle. See Prob. A.17 for an example.

A.3 Circular motion: uniform and nonuniform

Uniform circular motion. Suppose a particle moves counterclockwise on the circle $x^2 + y^2 = \ell^2$ of radius ℓ in the x-y plane at a constant angular speed $\omega > 0$ radians per second. Assuming it starts from the point $(\ell, 0)$ at $t = 0$, at time t, the particle would have traced an arc of the circle subtending an angle ωt at the center of the circle, as displayed in Fig. A.4. Thus, its location at time t may be given by the Cartesian coordinates $x(t) = \ell \cos \omega t$ and $y(t) = \ell \sin \omega t$. As shown in Fig. A.4, the position vector of the particle relative to the origin lying at the center of the circle is $\boldsymbol{r}(t) = \ell \cos \omega t\, \hat{x} + \ell \sin \omega t\, \hat{y}$. The velocity vector is given by

$$\boldsymbol{v}(t) = \dot{\boldsymbol{r}}(t) = -\ell\omega \sin \omega t\, \hat{x} + \ell\omega \cos \omega t\, \hat{y}, \quad \text{(A.6)}$$

since $\hat{x}$ and $\hat{y}$ are constant in magnitude and direction. The speed of the particle $v = |\boldsymbol{v}(t)| = \sqrt{\boldsymbol{v} \cdot \boldsymbol{v}} = \ell\omega$ is constant as must be the case for uniform circular motion. The particle goes round the circle once in a time $T = 2\pi\ell/v = 2\pi/\omega$. The particle covers 2π radians in a time $2\pi/\omega$ resulting in an angular speed of ω radians per second (angular speed is sometimes called angular frequency). Notice that $\boldsymbol{v} \cdot \boldsymbol{r} = 0$ so that the velocity is perpendicular to the radius vector and thus tangent to the circular trajectory.

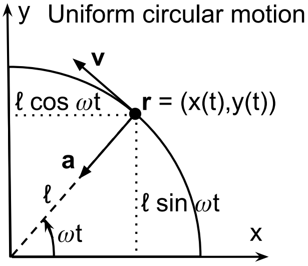

Figure A.4: Uniform circular motion of a particle at angular speed ω showing position or radius vector $\boldsymbol{r}$, tangential or azimuthal velocity $\boldsymbol{v} = \dot{\boldsymbol{r}}$ and centripetal acceleration $\boldsymbol{a} = \dot{\boldsymbol{v}}$.

The acceleration

$$\boldsymbol{a}(t) = \dot{\boldsymbol{v}}(t) = -\ell\omega^2 \cos\omega t \hat{x} - \ell\omega^2 \sin\omega t \hat{y} = -\omega^2 \boldsymbol{r}(t) \qquad \text{(A.7)}$$

has the constant magnitude $|\boldsymbol{a}(t)| = \ell\omega^2$ and points radially inwards. The latter feature leads to the name 'centripetal acceleration' as centripetal means 'seeking the center' in Latin (see Prob. A.18).

Suppose there is a radially inward force $\boldsymbol{F}$ (like a person tugging at a string with a stone tied at the other end and rotated) that is responsible for this circular motion. Noting that the infinitesimal displacement $d\boldsymbol{r}$ of the particle is tangent to the circle we see that $\boldsymbol{F} \cdot d\boldsymbol{r} = 0$ as $\boldsymbol{F}$ is perpendicular to $d\boldsymbol{r}$. Thus, a radially inward force does no work in moving a particle along a circular trajectory.

Nonuniform circular motion. In nonuniform motion of a particle around a circle of radius ℓ, the angular speed is not necessarily constant. Thus, the angular position of the particle $\theta(t)$ need not be a linear function of time. Hence, we may model this motion via the position vector

$$\boldsymbol{r}(t) = \ell(\cos\theta(t), \sin\theta(t)) = \ell(\cos\theta(t)\hat{x} + \sin\theta(t)\hat{y}). \qquad \text{(A.8)}$$

If we denote $\omega(t) = \dot{\theta}$, then the angular speed of such a particle is $|\omega(t)| = |\dot{\theta}|$, which could vary with time. The velocity of such a particle is

$$\boldsymbol{v}(t) = \ell\dot{\theta}(-\sin\theta(t), \cos\theta(t)). \qquad \text{(A.9)}$$

Notice that $\boldsymbol{v} \cdot \boldsymbol{r} = 0$. So $\boldsymbol{v}$ always points tangent to the circle as it must for a particle confined to the circle. However, the linear speed $\ell|\dot{\theta}|$ may vary with time. Using the product rule of differentiation, the acceleration is given by

$$\boldsymbol{a} = \dot{\boldsymbol{v}} = \ell\ddot{\theta}(-\sin\theta, \cos\theta) - \ell\dot{\theta}^2(\cos\theta, \sin\theta). \qquad \text{(A.10)}$$

The first term points tangentially (counterclockwise or clockwise depending on the sign of $\ddot{\theta}$), and is called the angular acceleration while the second term points radially inwards and is called the centripetal acceleration. Thus $\boldsymbol{a} \cdot \boldsymbol{v} \neq 0$ in general for nonuniform circular motion.

Remark on rotating vectors. We found that the velocity of a particle moving on a circle is orthogonal to its radius vector: $\boldsymbol{v} \cdot \boldsymbol{r} = \dot{\boldsymbol{r}} \cdot \boldsymbol{r} = 0$. In fact, for uniform circular motion, we also found that $\dot{\boldsymbol{v}} \cdot \boldsymbol{v} = 0$. Let us comment on the significance such formulae. Suppose a vector $\boldsymbol{b}$ is such that it is orthogonal to its time derivative: $\boldsymbol{b} \cdot \dot{\boldsymbol{b}} = 0$. This means $\boldsymbol{b}^2 = \boldsymbol{b} \cdot \boldsymbol{b}$ has zero time derivative so $\boldsymbol{b}$ has a constant length. Geometrically, $\boldsymbol{b} \cdot d\boldsymbol{b} = 0$ implies that the infinitesimal change in $\boldsymbol{b}$ has no component along $\boldsymbol{b}$; so $\boldsymbol{b}$ cannot elongate or shrink and therefore must maintain its length. Consequently, $\boldsymbol{b}$ can only rotate, though not necessarily at a constant rate. What we mean is that if the vectors $\boldsymbol{b}(t)$ are all parallel translated (if necessary) to emanate from a common origin, then the tip of $\boldsymbol{b}(t)$ must lie on a circle (or sphere, if the motion was in 3d). This is obviously the case for the position vector $\boldsymbol{r}$ of a particle executing circular motion. It also applies to the velocity $\dot{\boldsymbol{r}}$ as well as the acceleration $\dot{\boldsymbol{v}}$ of a particle undergoing uniform circular motion.

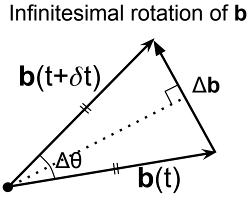

Figure A.5: Exaggerated view of infinitesimal rotation of a vector $\boldsymbol{b}$ through an angle $\Delta\theta$. $\Delta\boldsymbol{b} = \boldsymbol{b}(t+\delta t) - \boldsymbol{b}(t)$ is the base of an isosceles triangle.

Let us obtain a formula for $|d\boldsymbol{b}/dt|$. Suppose $\Delta\boldsymbol{b} = \boldsymbol{b}(t+\Delta t) - \boldsymbol{b}(t)$ is the infinitesimal change in $\boldsymbol{b}$. Since the length of $\boldsymbol{b}$ does not change, the three vectors $\boldsymbol{b}(t)$, $\boldsymbol{b}(t+\Delta t)$ and $\Delta\boldsymbol{b}$ form an isosceles triangle with $\Delta\boldsymbol{b}$ as base (see Fig. A.5). Let us denote the angle at the apex of this isosceles triangle by $\Delta\theta$, which is the angle of rotation. Then

$$|\Delta\boldsymbol{b}| = |2b\sin(\Delta\theta/2)| \approx b|\Delta\theta| \quad \text{for} \quad \text{small } \Delta\theta. \tag{A.11}$$

We have used the linear Taylor approximation for the sine function (see Appendix A.7). Taking the limit $\Delta t \to 0$,

$$\left|\frac{d\boldsymbol{b}}{dt}\right| = b\left|\frac{d\theta}{dt}\right|. \tag{A.12}$$

Here, $|d\theta/dt|$ is the angular speed of $\boldsymbol{b}$. We may apply this to circular motion where $\boldsymbol{b} = \boldsymbol{r}$ is the radius vector of the particle and $\dot{\boldsymbol{b}} = \boldsymbol{v}$ is its velocity. Then the linear speed of the particle is $v = r|\omega|$ where $\omega = d\theta/dt$ is the angular velocity (positive for counterclockwise motion). Note that v and ω need not be constant. Uniform circular motion is a special case where ω is a constant.

Remark. See Sect. 3.10 for how the position vector $\boldsymbol{r}$ behaves under a rotation of 3d Euclidean space. In some contexts, it is helpful to view a vector as an ordered triple that transforms in the same way as the position vector under a rotation. See Sect. 3.13* for more on this. □

A.4 Integration of kinematical equations: uniform acceleration

If the forces on a particle are known, then one may use Newton's 2^{nd} law to find its acceleration. This is called the dynamical part of the problem of motion, since it depends on the forces and interactions. The kinematical part of the problem of motion is to determine the velocity of the particle and its trajectory from its acceleration. Suppose we are given the acceleration of a particle as a function of time. Then the velocity must satisfy $\frac{d\boldsymbol{v}}{dt} = \boldsymbol{a}(t)$. This is a 1^{st} order ordinary differential equation (ODE) since it only involves the first derivative. The independent variable is t and the vector $\boldsymbol{v}(t)$ is called the unknown or dependent variable. Integrating $d\boldsymbol{v}(t') = \boldsymbol{a}(t')dt'$ from t_0 to t, we get

$$\boldsymbol{v}(t) = \boldsymbol{v}(t_0) + \int_{t_0}^{t} \boldsymbol{a}(t')dt'. \tag{A.13}$$

In addition to knowledge of the acceleration at all times from t_0 to t, we need three initial conditions (ICs), namely the three Cartesian components of $\boldsymbol{v}(t_0)$ to determine the velocity at subsequent times. The problem of determining velocity has been reduced to quadratures, i.e., to evaluating integrals (see Footnote 18 of Chap. 1). The step from velocity to position involves one more integration and another set of 3 ICs:

$$\dot{\boldsymbol{r}}(t) = \boldsymbol{v}(t) \quad \Rightarrow \quad \boldsymbol{r}(t) = \boldsymbol{r}(t_0) + \int_{t_0}^{t} \boldsymbol{v}(t')dt'. \tag{A.14}$$

In effect, we have solved the 2^{nd} order ODE $\ddot{\boldsymbol{r}}(t) = \boldsymbol{a}(t)$ in two steps. Evaluating these integrals for a specific acceleration may or may not be analytically feasible. A simple example where the integrals can be evaluated in closed form is that of uniform acceleration: $\boldsymbol{a}(t) = \boldsymbol{a}$. In this case, $\boldsymbol{v}(t) = \boldsymbol{v}(t_0) + (t - t_0)\boldsymbol{a}$. Integrating once more,

$$\boldsymbol{r}(t) = \boldsymbol{r}(t_0) + (t - t_0)\boldsymbol{v}(t_0) + \frac{1}{2}(t^2 - t_0^2)\boldsymbol{a} - (t - t_0)t_0\boldsymbol{a}. \tag{A.15}$$

This formula simplifies if $t_0 = 0$:

$$\boldsymbol{r}(t) = \boldsymbol{r}(0) + t\boldsymbol{v}(0) + \frac{1}{2}t^2\boldsymbol{a}. \tag{A.16}$$

A.5 Plane polar coordinates

Plane polar coordinates (r, θ) are often more convenient than Cartesian coordinates (x, y) in treating systems where there is circular symmetry about a point. For example, this happens in treating planar motion of planets or electrons around the Sun or a nucleus. Suppose we are given horizontal and vertical x and y axes with origin O at the center of rotational symmetry. A point P with abscissa x and ordinate y is assigned the radial coordinate $r = \sqrt{x^2+y^2}$ which is the distance of P from O. The azimuthal angle θ is the counterclockwise angle the radius vector $\boldsymbol{r} = x\hat{x} + y\hat{y}$ makes with the horizontal axis. Thus,

$$r = \sqrt{x^2+y^2} \quad \text{and} \quad \theta = \arccos(x/r), \tag{A.17}$$

where the value of arccos is fixed using the quadrant in which (x, y) lies. Conversely $x = r\cos\theta$ and $y = r\sin\theta$. Notice that θ is defined modulo 2π with $\theta = -\pi$ and π both corresponding to the negative x-axis. There is a more serious problem at the origin, where θ can be assigned any value depending on how we approach the origin. One says that polar coordinates 'break down' at the origin.

Recall that the constant x and constant y curves (the level curves of x and y) are mutually orthogonal straight lines parallel to the y and x axes respectively. By contrast, the constant θ curves are rays emanating radially outwards from the origin while the constant r curves are concentric circles centered at O. This is why polar coordinates are called curvilinear. Despite being curvilinear, the level curves of r and θ are mutually orthogonal.

Unit vectors $\hat{r}$ and $\hat{\theta}$. At the point (r, θ) on the plane, we define $\hat{r}$ and $\hat{\theta}$ to be the unit vectors pointing in the direction of increasing r holding θ fixed and vice versa. As shown in Fig. A.6a, while $\hat{r}$ points radially outwards, $\hat{\theta}$ points in the azimuthal direction (counterclockwise tangentially to the circle of radius r).

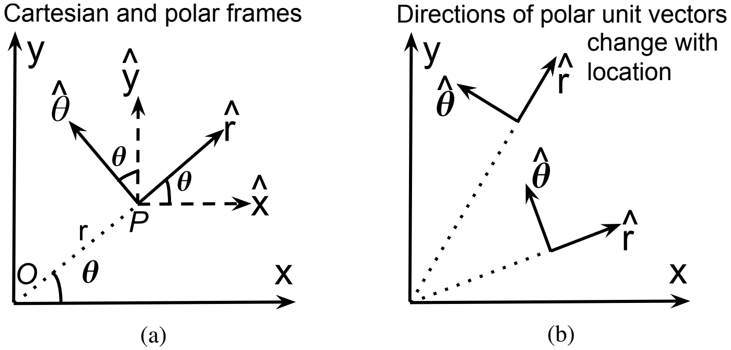

(a) (b)

Figure A.6: (a) Cartesian and plane polar orthonormal frames at a point P on the plane with coordinates (r, θ). (b) Unlike $\hat{x}$ and $\hat{y}$, directions of polar unit vectors $\hat{r}$ and $\hat{\theta}$ change with location.

The Cartesian frame $(\hat{x}, \hat{y})$ furnishes one basis for vectors at any point on the plane. We may therefore expand $\hat{r}$ and $\hat{\theta}$ in the $(\hat{x}, \hat{y})$ basis. Some trigonometry gives

$$\hat{r} = \cos\theta\,\hat{x} + \sin\theta\,\hat{y} \quad \text{and} \quad \hat{\theta} = -\sin\theta\,\hat{x} + \cos\theta\,\hat{y}. \tag{A.18}$$

In fact, Fig. A.6a shows that the $\hat{r}$-$\hat{\theta}$ frame is obtained from the $\hat{x}$-$\hat{y}$ frame through a rotation by angle θ counterclockwise. Thus, we should not be surprised to find that $\hat{r}$ and $\hat{\theta}$ are orthonormal,

$$\hat{r}\cdot\hat{\theta} = 0 \quad \text{and} \quad \hat{r}\cdot\hat{r} = \hat{\theta}\cdot\hat{\theta} = 1 \tag{A.19}$$

and thus furnish another basis (away from the origin). We may thus write $\hat{x}$ and $\hat{y}$ as linear combinations of $\hat{r}$ and $\hat{\theta}$:

$$\hat{x} = \cos\theta\,\hat{r} - \sin\theta\,\hat{\theta} \quad \text{and} \quad \hat{y} = \sin\theta\,\hat{r} + \cos\theta\,\hat{\theta}. \tag{A.20}$$

Unlike $\hat{x}$ and $\hat{y}$ which point in the same direction everywhere and may be obtained by parallel translation from the origin, the directions of $\hat{r}$ and $\hat{\theta}$ change with location, as shown in Fig. A.6b. This leads to new features when a particle's velocity and acceleration are written in polar coordinates.

Position coordinate and velocity vector. The position vector $\boldsymbol{r}$ of a particle located at point P with coordinates (x, y) can now be expressed in polar coordinates. We parallel transport the position vector $\boldsymbol{r}$ from the origin to P and then write it as a linear combination of $\hat{x}$ and $\hat{y}$ or $\hat{r}$ and $\hat{\theta}$ at P:

$$\boldsymbol{r} = x\hat{x} + y\hat{y} = r\cos\theta\hat{x} + r\sin\theta\hat{y} = r\hat{r}. \tag{A.21}$$

Although the particle moves, the directions and magnitudes of $\hat{x}$ and $\hat{y}$ do not change with location. Thus, in the Cartesian frame, the particle's velocity and acceleration are $\boldsymbol{v} = \dot{x}\hat{x} + \dot{y}\hat{y}$ and $\boldsymbol{a} = \ddot{x}\hat{x} + \ddot{y}\hat{y}$. To find the analogous expressions in the polar coordinate frame, we suppose that $\boldsymbol{r}(t) = r(t)\hat{r}(t)$ is the position vector of the particle at time t. As it moves along a trajectory, the radial coordinate r can change, but so can the direction of the unit vector $\hat{r}(t)$. Thus, its velocity is given by

$$\boldsymbol{v}(t) = \dot{\boldsymbol{r}}(t) = \dot{r}\,\hat{r} + r\frac{d\hat{r}}{dt}. \tag{A.22}$$

While $\dot{r}\hat{r}$ is what we might naively guess as the radial velocity, the other term comes from the change in direction of the basis vector $\hat{r}$.

Let us take a moment to find the rates of change of $\hat{r}(t)$ and $\hat{\theta}(t)$. Being unit vectors, their change can only come from a change in their direction. For instance,

$$\hat{r} = \cos\theta\hat{x} + \sin\theta\hat{y} \quad \Rightarrow \quad \dot{\hat{r}} = -\sin\theta\,\dot{\theta}\,\hat{x} + \cos\theta\,\dot{\theta}\,\hat{y} = \dot{\theta}\hat{\theta}. \tag{A.23}$$

Thus, the change in $\hat{r}$ is always in the azimuthal $\hat{\theta}$ direction, as illustrated in Fig. A.7. Similarly, the rate of change of $\hat{\theta}$ always points radially:

$$\hat{\theta} = -\sin\theta\hat{x} + \cos\theta\hat{y} \quad \Rightarrow \quad \dot{\hat{\theta}} = -\cos\theta\,\dot{\theta}\,\hat{x} - \sin\theta\,\dot{\theta}\,\hat{y} = -\dot{\theta}\,\hat{r}. \tag{A.24}$$

Putting these together, we get the decomposition of the velocity of the particle in the polar coordinate basis: $\boldsymbol{v} = \dot{r}\,\hat{r} + r\,\dot{\theta}\,\hat{\theta}$. We say that $\boldsymbol{v}\cdot\hat{r} = \dot{r}$ is the radial velocity while $\boldsymbol{v}\cdot\hat{\theta} = r\dot{\theta}$ is the angular or azimuthal component of velocity. For *circular motion* at a constant radius ℓ, $\dot{r} = 0$ and $\boldsymbol{v} = \ell\dot{\theta}\hat{\theta}$ is purely azimuthal. The linear speed of such a particle is $v = \ell|\dot{\theta}|$ while its angular speed is $|\dot{\theta}| = v/\ell$.

Acceleration in polar coordinates. We may differentiate $\boldsymbol{v}$ to find the acceleration:

$$\boldsymbol{a} = \dot{\boldsymbol{v}} = \frac{d}{dt}(\dot{r}\,\hat{r} + r\,\dot{\theta}\,\hat{\theta}) = \ddot{r}\,\hat{r} + \dot{r}\frac{d\hat{r}}{dt} + \dot{r}\dot{\theta}\hat{\theta} + r\ddot{\theta}\hat{\theta} + r\dot{\theta}\frac{d\hat{\theta}}{dt}. \tag{A.25}$$

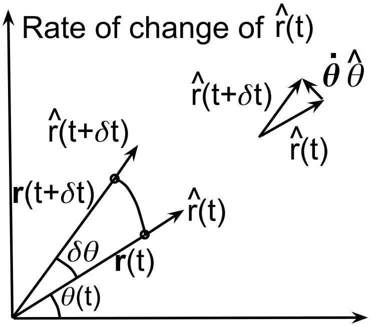

Figure A.7: A particle moves from $\boldsymbol{r}(t)$ to $\boldsymbol{r}(t+\delta t)$ in a time δt. The change in $\hat{r}$ points in the azimuthal direction, as shown in the inset with parallel translated vectors.

Using $\dot{\hat{r}} = \dot{\theta}\hat{\theta}$ and $\dot{\hat{\theta}} = -\dot{\theta}\hat{r}$, we get

$$\boldsymbol{a} = (\ddot{r} - r\dot{\theta}^2)\hat{r} + (r\ddot{\theta} + 2\dot{r}\dot{\theta})\hat{\theta}. \tag{A.26}$$

The terms in $\boldsymbol{a}$ have distinct origins. (i) $\ddot{r}\hat{r}$ is the part of the radial acceleration coming from a change in the radial component of velocity. (ii) $-r\dot{\theta}^2\hat{r}$ is the centripetal acceleration familiar from uniform circular motion. It always points radially inwards. (iii) $r\ddot{\theta}\hat{\theta}$ is the angular acceleration that comes from the varying angular speed of the particle. (iv) $2\dot{r}\dot{\theta}\hat{\theta}$ is called the Coriolis acceleration, it is present whenever both r and θ change with time.

A.6 Spherical polar coordinates

Spherical polar coordinates (r, θ, ϕ) displayed in Fig. A.8 are convenient when we have rotational symmetry about a central object (e.g., the Sun in the solar system or nucleus in an atom) in 3d Euclidean space. Given a point P with Cartesian coordinates (x, y, z) and position vector $\boldsymbol{r}$ relative to the origin, the radial coordinate r is the distance of P from the origin $r = \sqrt{x^2 + y^2 + z^2}$. Evidently, $0 \le r < \infty$. The *polar angle* θ is the angle that the vector $\boldsymbol{r}$ makes with the upward vertical z axis. Thus, $\theta = \arccos(z/r)$. Notice that $0 \le \theta \le \pi$ with $\theta = 0$ and $\theta = \pi$ corresponding to the positive and negative z axis. If we regard P as a point on the Earth [with the origin of spherical polar coordinates at the center of the Earth and $\hat{z}$ pointing from the origin to the North pole] then $\theta = \pi/2 - \psi$ where ψ is the angle of the latitude through P. Next, suppose we orthogonally project the position vector onto the x-y plane. This projected vector has length $r \sin\theta = \sqrt{x^2 + y^2}$. The *azimuthal angle* ϕ is defined as the angle that this projection makes with the x axis, measured counterclockwise[8]. Thus, $\phi = \arccos(x/\sqrt{x^2 + y^2})$ and $\tan\phi = y/x$. Notice that $0 \le \phi < 2\pi$. Again, viewing P as a point on the Earth with the x axis passing through the prime meridian, ϕ is the angle of the longitude through P.

Alternatively, we may write

$$z = r\cos\theta, \quad x = r\sin\theta\cos\phi \quad \text{and} \quad y = r\sin\theta\sin\phi. \tag{A.27}$$

---

[8] Spherical polar coordinates break down along the z axis, where ϕ is not uniquely defined: it can be assigned any value $0 \le \phi < 2\pi$.

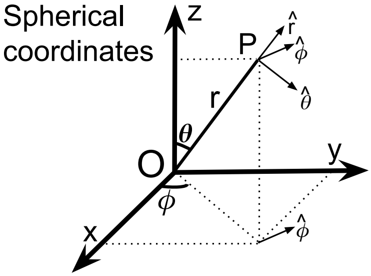

Figure A.8: Spherical polar coordinates (r, θ, ϕ) of a point P along with the unit vectors $(\hat{r}, \hat{\theta}, \hat{\phi})$ at P, which form a right-handed orthonormal frame. The projection of the position vector $\boldsymbol{r}$ to the x-y plane makes an angle ϕ with the x axis. $\hat{\phi}$ is the unit vector in the direction of increasing ϕ holding r and θ fixed. $\hat{\phi}$ is parallel to the x-y plane. The parallel translate of $\hat{\phi}$ to the tip of the projection of $\boldsymbol{r}$ is also shown and leads to the formula for $\hat{\phi}$ in (A.28).

Next, at a point with coordinates (r, θ, ϕ), we introduce the unit vectors $\hat{r}, \hat{\theta}$ and $\hat{\phi}$ in the directions of increasing r, θ and ϕ holding the other two fixed. The position vector of a particle located at (x, y, z) is then given by $\boldsymbol{r} = x\hat{x} + y\hat{y} + z\hat{z} = r\hat{r}$. Moreover, Fig. A.8 helps us express the spherical polar unit vectors as linear combinations of the Cartesian basis vectors:

$$\begin{aligned} \hat{r} &= \cos\theta\,\hat{z} + \sin\theta(\cos\phi\,\hat{x} + \sin\phi\,\hat{y}), \\ \hat{\theta} &= -\sin\theta\,\hat{z} + \cos\theta(\cos\phi\,\hat{x} + \sin\phi\,\hat{y}) \quad \text{and} \\ \hat{\phi} &= -\sin\phi\,\hat{x} + \cos\phi\,\hat{y}. \end{aligned} \tag{A.28}$$

Verify that $(\hat{r}, \hat{\theta}, \hat{\phi})$ is a right-handed orthonormal system. The velocity and acceleration vectors of a particle moving in 3d may be expressed in the spherical polar basis just as we did in Appendix A.5 for a particle on the plane with plane polar coordinates.

A.7 Taylor series

Taylor series for one variable. Suppose $f(x)$ is the force felt by a particle at the position x along a line. We are often interested in describing small oscillations of the particle in the neighborhood of an equilibrium point x_0. Although f may be a complicated function of position, for this purpose, it is usually sufficient to approximate f by a polynomial in the vicinity of x_0. A Taylor polynomial provides such an approximation, assuming f is continuous and sufficiently differentiable. By continuity, $f(x) \approx f(x_0)$ is our zeroth order approximation to the value of f for x near x_0. The next possibility is to approximate f by a linear function near x_0. It is natural to take the slope of this linear function to be the derivative of f at x_0, so that we approximate the graph of f by the tangent through the point $(x_0, f(x_0))$. This leads to the first order or linear Taylor approximation

$$f(x) \approx f(x_0) + f'(x_0)(x - x_0). \tag{A.29}$$

Note that if x_0 is an equilibrium point, then $f'(x_0)$ would vanish. To indicate that $x - x_0$ is small, we will denote it by $\Delta x = x - x_0$, and denote $f(x) - f(x_0) = \Delta f$.

Then we have $\Delta f \approx f'(x_0)\Delta x$. This is of course only an approximation, but one which improves as $\Delta x \to 0$. It is also convenient to introduce the *differential* of f, which at x is written $df(x) = f'(x)dx$ where dx is called the differential of x. The derivative denoted $f'(x)$ or df/dx is the limit of $\Delta f/\Delta x$ as $\Delta x \to 0$. For example, $d\sin x = \cos x\, dx$. The differential of a function is also called a 1-form. The next step is to approximate f in the vicinity of x_0 by a quadratic function whose $2^{\rm nd}$ derivative is the same as that of f. In other words, we approximate the graph of f near x_0 by a parabola whose curvature matches that of f at x_0 (see Fig. A.9).

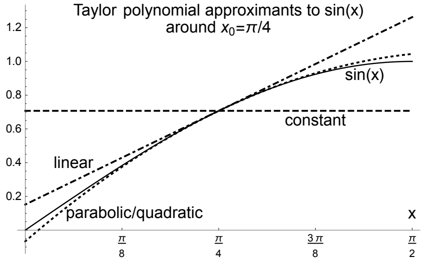

Figure A.9: Graph of $f(x) = \sin x$ (solid) compared with those of its constant (dashed), linear (dot-dashed) and quadratic (dotted) Taylor polynomials at $x_0 = \pi/4$ showing increasingly accurate approximations. For instance, at $x = \pi/8$, the first three Taylor polynomials have the numerical values $\approx 0.707, 0.429$ and 0.375, while $\sin(\pi/8) \approx 0.383$.

More generally, if f is n times differentiable at x_0, we have the $n^{\rm th}$ order Taylor polynomial approximation for small $x - x_0$:

$$\begin{aligned} f(x) \quad &\approx \quad f(x_0) + f'(x_0)(x-x_0) + \frac{1}{2}f''(x_0)(x-x_0)^2 + \frac{1}{3!}f'''(x_0)(x-x_0)^3 \\ &\quad + \cdots + \frac{1}{n!}f^{(n)}(x_0)(x-x_0)^n, \end{aligned} \tag{A.30}$$

where $f^{(n)}(x_0)$ is the $n^{\rm th}$ derivative of f at x_0. The factors of $1/2, 1/3!$, etc., are chosen so that the first n derivatives of the Taylor polynomial at $x = x_0$ match those of f. For many of the functions we encounter, the Taylor series, obtained by letting $n \to \infty$, converges to the function $f(x)$ for x in a neighborhood of x_0. Such functions are called real analytic[9] at x_0.

For example, show that the Taylor series for $1/(1-x)$ around $x = 0$ is given by a geometric series $(1-x)^{-1} = 1 + x + x^2 + \cdots$. This series converges to $1/(1-x)$ for $|x| < 1$. Show that the Taylor series for e^x around $x = 0$ is given by

$$e^x = 1 + x + \frac{x^2}{2!} + \cdots + \frac{x^n}{n!} + \cdots . \tag{A.31}$$

---

[9] A real-valued function that is continuous in some domain is said to be of type C^0 in that domain (see Prob. A.20). A function that is differentiable with continuous first derivative is said to be of class C^1 in that domain. Similarly, we have the notion of C^k functions for $k = 1, 2, 3, \ldots$: k times continuously differentiable functions. A function that is C^k for all $k = 0, 1, 2, 3, 4, \ldots$ is said to be smooth or C^∞. A function whose Taylor series converges to the function in some domain is called real analytic or of type C^ω. See Prob. A.21.

This series converges for any x and is said to have an infinite radius of convergence. The binomial series is a very useful Taylor series around $x = 0$:

$$(1+x)^\nu = 1 + \nu x + \frac{\nu(\nu-1)}{1\cdot 2}x^2 + \frac{\nu(\nu-1)(\nu-2)}{1\cdot 2\cdot 3}x^3 + \dots. \tag{A.32}$$

It converges for $|x| < 1$ and any real number ν. For a positive integer $\nu = n$, this series terminates and we recover the binomial expansion with coefficients given by combinatorial factors: $(1+x)^n = \sum_{r=0}^{n}\binom{n}{r}x^r$.

Taylor series for two variables. For a real function $f(x, y)$ of two variables, we have the Taylor expansion of f around a point (x_0, y_0):

$$\begin{aligned} f(x,y) \quad &= \quad f(x_0,y_0) + \frac{\partial f}{\partial x}(x-x_0) + \frac{\partial f}{\partial y}(y-y_0) + \frac{1}{2}\left[\frac{\partial^2 f}{\partial x^2}(x-x_0)^2 + \frac{\partial^2 f}{\partial y^2}(y-y_0)^2\right. \\ &\quad \left. + \frac{\partial^2 f}{\partial x \partial y}(x-x_0)(y-y_0) + \frac{\partial^2 f}{\partial y \partial x}(y-y_0)(x-x_0)\right] + \cdots \end{aligned} \tag{A.33}$$

where all the partial derivatives[10] are evaluated at (x_0, y_0). The mixed second partials $\frac{\partial^2 f}{\partial x \partial y}$ and $\frac{\partial^2 f}{\partial y \partial x}$ are equal assuming they are continuous (this is called Clairaut's or Schwarz's Theorem, see Prob. A.23). One way to obtain this series is to treat y as fixed and first write down a Taylor series in x around x_0 with coefficients being functions of y. Then we expand these coefficients in a Taylor series in y around $y = y_0$. Just as for functions of one variable, the first partials may be combined in the differential $df = \frac{\partial f}{\partial x}dx + \frac{\partial f}{\partial y}dy$. It is often convenient to regard the second partials as the entries of a symmetric 2×2 matrix called the Hessian $\begin{pmatrix} \frac{\partial^2 f}{\partial x^2} & \frac{\partial^2 f}{\partial x \partial y} \\ \frac{\partial^2 f}{\partial y \partial x} & \frac{\partial^2 f}{\partial y^2} \end{pmatrix}$.

A.8 Some vector calculus: grad, div and curl

Scalar fields. At a given instant of time, the pressure $p(\boldsymbol{r})$ in the atmosphere is a real number (scalar) that depends on location $\boldsymbol{r}$. The pressure function is an example of a scalar field[11] defined on a region in 3d Euclidean space. A scalar field assigns a real number to each point $\boldsymbol{r}$. We will suppose that the real number varies sufficiently smoothly as the location changes. This is usually physically justified and allows us to use tools from calculus. Simple examples include (i) $p(\boldsymbol{r}) = \boldsymbol{a}\cdot\boldsymbol{r}$ where $\boldsymbol{a}$ is a fixed vector and (ii) $p(\boldsymbol{r}) = \sigma\boldsymbol{r}\cdot\boldsymbol{r} = \sigma(x^2+y^2+z^2)$ where σ is a real constant. A scalar field on the plane may be visualized via a contour plot: a plot of the level curves (curves along which the field is constant) of the scalar function in the region of interest. For example, the level curves of x^2+y^2 are concentric circles centered at the origin. Fig. 3.12 displays level curves of a pair of quadratic functions on the plane. For a function of three variables, level curves are replaced by level surfaces in $\mathbb{R}^3$.

---

[10] To calculate a partial derivative with respect to y we simply differentiate the function with respect to y treating x as fixed.

[11] The notion of a field introduced here is different from the algebraic notion of a field (e.g., field of real or complex numbers).

Vector fields. Similarly, we have the concept of a vector field: a smoothly varying vector $\boldsymbol{v}(\boldsymbol{r})$ at each location $\boldsymbol{r}$. The gravitational force felt by a point mass m at various points above the Earth's surface defines a vector field. A vector field may be visualized by drawing arrows pointing along $\boldsymbol{v}(r)$ at each point $\boldsymbol{r}$. See Figs. 5.1, 5.3 and 5.9 for examples. The density of arrows around $\boldsymbol{r}$ encodes the magnitude of the vector field at $\boldsymbol{r}$. The magnitude may also be encoded in the lengths of the arrows. The flow velocity at each point of a steadily flowing fluid is an example of a vector field. A vector field on the plane is of the form $\boldsymbol{v} = f(x,y)\hat{x} + g(x,y)\hat{y}$. For instance, $\boldsymbol{v} = \hat{x}$ is a constant vector field of unit length that points in the $\hat{x}$ direction everywhere. A radially outward pointing vector field is $\boldsymbol{v}(\boldsymbol{r}) = \boldsymbol{r} = x\hat{x} + y\hat{y}$, its magnitude at $\boldsymbol{r}$ is equal to the distance from the origin.

Gradient of a scalar field. Given a scalar field $\phi(\boldsymbol{r})$, its gradient is a vector field denoted grad $\phi(\boldsymbol{r})$ or $\boldsymbol{\nabla}\phi(\boldsymbol{r})$ where $\boldsymbol{\nabla}$ is the Greek letter nabla. In Cartesian coordinates,

$$\text{grad } \phi(\boldsymbol{r}) = \boldsymbol{\nabla}\phi(\boldsymbol{r}) = \frac{\partial \phi}{\partial x}\hat{x} + \frac{\partial \phi}{\partial y}\hat{y} + \frac{\partial \phi}{\partial z}\hat{z}. \tag{A.34}$$

For many purposes, we may regard $\boldsymbol{\nabla}$ as the vector first order differential operator $\boldsymbol{\nabla} = \hat{x}\frac{\partial}{\partial x} + \hat{y}\frac{\partial}{\partial y} + \hat{z}\frac{\partial}{\partial z}$. Examples: (i) If $\phi(x,y) = x$ then $\boldsymbol{\nabla}\phi = \hat{x}$ is a constant vector field pointing in the x direction at all points of $\mathbb{R}^2$. (ii) If $\phi = \frac{1}{2}(x^2 + y^2 + z^2)$, then $\boldsymbol{\nabla}\phi = x\hat{x} + y\hat{y} + z\hat{z} = r\hat{r}$ is a radially outward pointing vector field on $\mathbb{R}^3$, with magnitude equal to the distance from the origin. The gradient allows us to write the first order Taylor polynomial in a nice way. Recall that for a differentiable function $\phi(x,y,z)$, we have

$$\phi(\boldsymbol{r} + \delta\boldsymbol{r}) \approx \phi(\boldsymbol{r}) + \frac{\partial \phi}{\partial x}\delta x + \frac{\partial \phi}{\partial y}\delta y + \frac{\partial \phi}{\partial z}\delta z \tag{A.35}$$

where $\delta\boldsymbol{r} = \delta x\,\hat{x} + \delta y\,\hat{y} + \delta z\,\hat{z}$. We recognize the last three terms as the dot product of $\boldsymbol{\nabla}\phi$ and $\delta\boldsymbol{r}$. Thus $\phi(\boldsymbol{r} + \delta\boldsymbol{r}) \approx \phi(\boldsymbol{r}) + \delta\boldsymbol{r} \cdot \boldsymbol{\nabla}\phi$. This formula holds in any dimension.

Interpretation of gradient. At any location $\boldsymbol{r}$, $\boldsymbol{\nabla}\phi$ is a vector that points in the direction of most rapid increase of ϕ. To see why, it is helpful to introduce the level surfaces of ϕ, which are surfaces in $\mathbb{R}^3$ on which ϕ is a constant. For ϕ to change most rapidly, we must move from $\boldsymbol{r}$ along a vector that has no component along the level surface through $\boldsymbol{r}$, i.e., orthogonal to the level surface (see Fig. 3.12). We will now argue that at any point $\boldsymbol{r}$, $\boldsymbol{\nabla}\phi(\boldsymbol{r})$ is also orthogonal to the level surface through $\boldsymbol{r}$. Suppose $\boldsymbol{v}$ is a vector at $\boldsymbol{r}$ of small magnitude, then the linear Taylor approximation gives $\phi(\boldsymbol{r} + \boldsymbol{v}) \approx \phi(\boldsymbol{r}) + \boldsymbol{v} \cdot \boldsymbol{\nabla}\phi$. Now, $\boldsymbol{v}$ is tangent to the level surface through $\boldsymbol{r}$ if $\phi(\boldsymbol{r}+\boldsymbol{v}) - \phi(\boldsymbol{r})$ vanishes to first order in $\boldsymbol{v}$. This happens precisely when $\boldsymbol{v} \cdot \boldsymbol{\nabla}\phi = 0$. Thus, $\boldsymbol{\nabla}\phi$ must be perpendicular to the level surface of ϕ and must point either in the direction of most rapid increase or decrease of ϕ. Taking $\boldsymbol{v} = \epsilon\boldsymbol{\nabla}\phi$ for $0 < \epsilon \ll 1$, we find that $\phi(\boldsymbol{r} + \epsilon\boldsymbol{\nabla}\phi) \approx \phi(\boldsymbol{r}) + \epsilon|\boldsymbol{\nabla}\phi|^2 > \phi(\boldsymbol{r})$. Thus we conclude that $\boldsymbol{\nabla}\phi$ must point in the direction of most rapid increase of ϕ.

If ϕ is regarded as a potential function, then its level surfaces are referred to as equipotential surfaces. E.g., (i) For $\phi(x,y) = x$, the level curves are lines parallel to the y axis, and $\boldsymbol{\nabla}\phi = \hat{x}$ points perpendicular to these lines in the direction of most rapid increase in ϕ. (ii) For $\phi = \frac{1}{2}(x^2 + y^2 + z^2)$, the level surfaces are concentric spheres centered at the origin and $\boldsymbol{\nabla}\phi = \boldsymbol{r}$ is perpendicular to these surfaces.

Line integral. Given a vector field $\boldsymbol{v}(\boldsymbol{r}) = (v_x, v_y, v_z)(\boldsymbol{r})$ in three-dimensional space and a parametrized curve $\boldsymbol{\gamma}(t) = (x(t), y(t), z(t))$ for $0 \leq t \leq 1$, we may define the 'line integral' or 'contour integral' of $\boldsymbol{v}$ along $\boldsymbol{\gamma}$ as the real number

$$\int_{\gamma} \boldsymbol{v} \cdot d\boldsymbol{\gamma} = \int_0^1 \boldsymbol{v} \cdot \frac{d\boldsymbol{\gamma}}{dt} dt = \int_0^1 \left[v_x \frac{dx}{dt} + v_y \frac{dy}{dt} + v_z \frac{dz}{dt} \right] dt. \tag{A.36}$$

Here, $\dot{\boldsymbol{\gamma}} = \frac{d\boldsymbol{\gamma}}{dt} = \dot{x}\hat{x} + \dot{y}\hat{y} + \dot{z}\hat{z}$ is a vector field along the curve $\boldsymbol{\gamma}$ (it is not defined elsewhere in $\mathbb{R}^3$). At each fixed t, it is the tangent vector to the curve at the point $\boldsymbol{\gamma}(t)$ as shown in Fig. A.10.

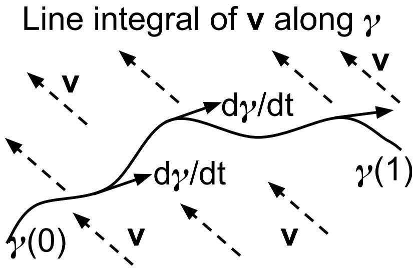

Figure A.10: Contour γ along which the line integral of the vector field $\boldsymbol{v}$ is evaluated.

For example, if $\boldsymbol{\gamma}$ is the helix $(\cos t, \sin t, t)$, then $d\boldsymbol{\gamma} = (-\sin t, \cos t, 1)dt$. We may consider $d\boldsymbol{\gamma}$ as the differential of the map $\boldsymbol{\gamma} : [0, 1] \to \mathbb{R}^3$. The work done by a force field $\boldsymbol{F}(\boldsymbol{r})$ in moving a particle along a curve $\boldsymbol{\gamma}$ is an important example of a line integral: $W_{\boldsymbol{F}}(\boldsymbol{\gamma}) = \int_\gamma \boldsymbol{F} \cdot d\boldsymbol{\gamma}$.

In general, the line integral depends on the values of $\boldsymbol{v}$ all along the curve $\boldsymbol{\gamma}$. However, if $\boldsymbol{v}$ is the gradient of a scalar, $\boldsymbol{v} = \boldsymbol{\nabla}\phi$, then the line integral can be evaluated in terms of the values of ϕ at the endpoints:

$$\begin{aligned} \int_\gamma \boldsymbol{\nabla}\phi \cdot d\boldsymbol{\gamma} &= \int_0^1 \left(\frac{\partial\phi}{\partial x}\frac{dx}{dt} + \frac{\partial\phi}{\partial y}\frac{dy}{dt} + \frac{\partial\phi}{\partial z}\frac{dz}{dt} \right) dt \\ &= \int_0^1 \frac{d\phi(\boldsymbol{r}(t))}{dt} dt = \phi(\boldsymbol{r}(1)) - \phi(\boldsymbol{r}(0)). \end{aligned} \tag{A.37}$$

Here, we viewed $\phi(x(t), y(t), z(t))$ as a function of t and used the chain rule to differentiate it with respect to t. In particular, if $\boldsymbol{\gamma}$ is a closed curve, then $\boldsymbol{r}(0) = \boldsymbol{r}(1)$ and the line integral of a gradient vanishes $\oint_\gamma \boldsymbol{\nabla}\phi \cdot d\boldsymbol{\gamma} = 0$. Here $\oint$ denotes a line integral around a closed contour.

A vector field that is the gradient of a scalar field is called a gradient vector field. In mechanics, if a force field $\boldsymbol{F}(\boldsymbol{r})$ is the (negative) gradient of a scalar field (or 'potential' $\phi(\boldsymbol{r})$), then it is called a conservative force field. The work done by a conservative force field $-\boldsymbol{\nabla}\phi$ depends only on the initial and final locations of the particle, and not on other details of the path taken. A conservative force field does no work in moving a particle around a closed curve.

Divergence of a vector field. The divergence of a vector field $\boldsymbol{v}$, denoted $\boldsymbol{\nabla} \cdot \boldsymbol{v}$ or div $\boldsymbol{v}$ is a scalar field. In Cartesian coordinates, it is defined as $\boldsymbol{\nabla} \cdot \boldsymbol{v} = \frac{\partial v_x}{\partial x} + \frac{\partial v_y}{\partial y} + \frac{\partial v_z}{\partial z}$. Intuitively, the divergence measures how much a vector field is expanding or contracting at a point. For instance, if $\boldsymbol{v}$ is the velocity field of a flowing fluid, then as shown in Sect. 19.5, $\boldsymbol{\nabla} \cdot \boldsymbol{v}(\boldsymbol{r})$ is the fractional rate of change of volume of a small parcel of fluid at r. A vector field with constant Cartesian components has zero divergence: the arrows representing the vector field are parallel and have the same magnitude everywhere. The vector field $\boldsymbol{v} = x\hat{x} + y\hat{y} + z\hat{z}$ should be expected to have a positive divergence everywhere as it represents a radially expanding flow: in fact, we check that it has divergence 3 everywhere.

If $\boldsymbol{v} = \boldsymbol{\nabla}\phi$ is a gradient, then its divergence

$$\boldsymbol{\nabla} \cdot \boldsymbol{v} = \boldsymbol{\nabla} \cdot \boldsymbol{\nabla}\phi = \frac{\partial^2 \phi}{\partial x^2} + \frac{\partial^2 \phi}{\partial y^2} + \frac{\partial^2 \phi}{\partial z^2} \tag{A.38}$$

is a scalar field called the Laplacian of ϕ and denoted $\boldsymbol{\nabla}^2\phi$. The 'Laplace operator' $\boldsymbol{\nabla}^2 = \partial_x^2 + \partial_y^2 + \partial_z^2$ is a rotationally invariant second order differential operator that we will meet in the heat (18.4) and wave equations (19.48).

Curl of a vector field. The curl of a vector field $\boldsymbol{v}$ is the vector field whose Cartesian components are given by

$$\boldsymbol{\nabla} \times \boldsymbol{v} = (\partial_y v_z - \partial_z v_y)\hat{x} + (\partial_z v_x - \partial_x v_z)\hat{y} + (\partial_x v_y - \partial_y v_x)\hat{z}. \tag{A.39}$$

Here, ∂_x is short-hand for $\frac{\partial}{\partial x}$, etc. The 2nd and 3^{3rd} terms are obtained from the 1st by cyclically permuting $x \to y \to z \to x$. Being formally a cross product of $\boldsymbol{\nabla}$ and $\boldsymbol{v}$, the formula for the curl should remind us of the angular momentum $\boldsymbol{L} = \boldsymbol{r} \times \boldsymbol{p} = (yp_z - zp_y)\hat{x} + (zp_x - xp_z)\hat{y} + (xp_y - yp_x)\hat{z}$ of a particle. In fact, the curl is a measure of local rotation in a vector field. If $\boldsymbol{v}$ is the velocity field of a fluid, then $\boldsymbol{\nabla} \times \boldsymbol{v}$ is the vorticity field of the flow and is a local measure of angular velocity or circulation. Examples of rotational flows with vorticity may be found in Sect. 19.11.

Curl-free and divergence-free vector fields and the Helmholtz decomposition. (i) There is a simple way of constructing a curl-free vector field: take the gradient of a scalar. A gradient vector field has vanishing curl due to the equality of mixed partials:

$$\boldsymbol{\nabla}\times\boldsymbol{\nabla}\phi = (\partial_y\partial_z\phi - \partial_z\partial_y\phi)\hat{x} + (\partial_z\partial_x\phi - \partial_x\partial_z\phi)\hat{y} + (\partial_x\partial_y\phi - \partial_y\partial_x\phi)\hat{z} = 0. \tag{A.40}$$

Intuitively, a gradient vector field points in the direction of most rapid increase of ϕ and cannot 'circulate'. (ii) Similarly, there is a nice way of constructing a divergence-free vector field: take the curl of any vector field $\boldsymbol{A}$. In other words, the divergence of a curl is identically zero:

$$\boldsymbol{\nabla} \cdot (\boldsymbol{\nabla} \times \boldsymbol{A}) = \partial_x(\partial_y A_z - \partial_z A_y) + \partial_y(\partial_z A_x - \partial_x A_z) + \partial_z(\partial_x A_y - \partial_y A_x) = 0, \tag{A.41}$$

again by the equality of mixed partials. (iii) The Helmholtz decomposition expresses a vector field, quite generally, as a sum of curl-free and divergence-free vector fields: $\boldsymbol{v} = \boldsymbol{\nabla}\phi + \boldsymbol{\nabla} \times \boldsymbol{A}$. This decomposition is useful in fluid mechanics, see Sect. 19.14* and Prob. 19.35.

A.9 Stokes', Green's and Gauss' integral theorems

In Appendix A.8 we showed that the integral of a gradient $\boldsymbol{\nabla}\phi$ along a contour $\gamma : [0,1] \to \mathbb{R}$ was equal to the difference between the values of ϕ at the end and beginning of the contour. The latter difference may itself be viewed as an integral over the boundary of γ, denoted $\partial\gamma$, which is the set consisting of two points: the final and initial points on the contour. Thus, we rewrite (A.37) as

$$\int_\gamma \boldsymbol{\nabla}\phi \cdot d\boldsymbol{\gamma} = \int_{\partial\gamma} \phi = \phi(\boldsymbol{\gamma}(1)) - \phi(\boldsymbol{\gamma}(0)). \tag{A.42}$$

The minus sign for the initial point is to take into account that γ is oriented from initial to final point. There are higher dimensional analogs of this integral formula, concerning the surface integral of a curl (Stokes' theorem) and the volume integral of a divergence (Gauss' theorem). Suppose $\boldsymbol{v}$ is a vector field and S a 2d surface (with area element $d\boldsymbol{S}$) with boundary given by the curve ∂S. Stokes' theorem says that

$$\int_S (\boldsymbol{\nabla} \times \boldsymbol{v}) \cdot d\boldsymbol{S} = \oint_{\partial S} \boldsymbol{v} \cdot d\boldsymbol{l}. \tag{A.43}$$

In particular, if $\boldsymbol{v} = \boldsymbol{\nabla}\phi$ is the gradient of a scalar, then $\boldsymbol{\nabla} \times \boldsymbol{v} = 0$ from (A.40) and Stokes' theorem says that $\oint \boldsymbol{v} \cdot d\boldsymbol{l} = 0$. On the other hand, suppose Ω is a 3d region bounded by the surface $\partial\Omega$, then Gauss' divergence theorem states that

$$\int_\Omega (\boldsymbol{\nabla} \cdot \boldsymbol{v}) d\boldsymbol{r} = \int_{\partial\Omega} \boldsymbol{v} \cdot d\boldsymbol{S}. \tag{A.44}$$

Green's theorem is a planar version of Stokes' theorem. Suppose $\boldsymbol{v} = v_x \hat{x} + v_y \hat{y}$ is a vector field on the x-y plane and let S be a region in the plane bounded by the curve ∂S. Then $\boldsymbol{\nabla} \times \boldsymbol{v}$ has only a z component while $d\boldsymbol{S} = dx\, dy\, \hat{z}$ and $d\boldsymbol{l} = dx\, \hat{x} + dy\, \hat{y}$, so that (A.43) becomes

$$\int_S (\partial_x v_y - \partial_y v_x) dx\, dy = \oint_{\partial S} (v_x dx + v_y dy). \tag{A.45}$$

Green's theorem leads to a line integral representation of the area of a region S on the plane. We pick a planar vector field $\boldsymbol{v}$ such that the z-component of its curl is a constant, say $v_x = -y, v_y = x$. Then

$$\text{Area}(S) = \int_S dx dy = \frac{1}{2} \oint_{\partial S} (x\, dy - y\, dx). \tag{A.46}$$

Generalizations of Gauss' and Stokes' theorems may be found in (B.55).

Conservative force from path-independence of work: Let $\boldsymbol{F}$ be a force field in $\mathbb{R}^3$ (or a simply connected domain D in $\mathbb{R}^3$, i.e., one where any closed curve may be continuously shrunk to a point). Suppose the work done by $\boldsymbol{F}$ when a particle is moved between any 2 points $\boldsymbol{a}, \boldsymbol{b}$ in D is the same for any two paths traversed by the particle, i.e., $\int_{\gamma_1} \boldsymbol{F} \cdot d\boldsymbol{r} = \int_{\gamma_2} \boldsymbol{F} \cdot d\boldsymbol{r}$ (these paths need not be trajectories). Then by considering the closed curve $C = \gamma_1 \cup \bar{\gamma}_2$ obtained by traversing γ_2 in the reverse direction after γ_1, we deduce that $\oint_C \boldsymbol{F} \cdot d\boldsymbol{r} = 0$ for any closed curve C in D. By Stokes' theorem, $\int_S (\boldsymbol{\nabla} \times \boldsymbol{F}) \cdot d\boldsymbol{S} = 0$ where S is any surface in D whose boundary is C. However, since C is arbitrary, we conclude that $\int_S (\boldsymbol{\nabla} \times \boldsymbol{F}) \cdot d\boldsymbol{S} = 0$ for every surface S in D. Taking S arbitrarily small, we find that $\boldsymbol{F}$ must be curl-free. Now, a curl-free vector field in a simply-connected domain can always be expressed as the gradient of a scalar (this is called the Poincaré lemma). Thus, if the work done by a force is path-independent for any two initial and final positions in a simply-connected domain, then the force field must be conservative.

A.10 Vector spaces, matrices and eigenvalue problems

We now return to vector spaces introduced through the examples of two- and three-dimensional Euclidean space in Appendix A.1. The notion of a vector subspace spanned by a set of vectors helps us introduce the concept of a basis for a vector space and its dimension. This brings us to the key idea of a linear transformation between vector spaces and its representation by a matrix once bases are chosen for the spaces. The matrix that represents a linear map is not unique, and we learn how it transforms when bases are changed. The same applies to the representation of vectors by components arranged in columns or rows. The rest of this section is devoted eigenvalue problems. In favorable cases, eigenvalues and eigenvectors of a linear transformation allow us to find a basis in which the matrix representing it is diagonal. This *diagonalization* of a square matrix by a 'similarity' transformation is helpful in disentangling coupled modes of a linear system into 'normal modes' that evolve independently according to their characteristic frequencies or growth/decay rates.

Subspace, span, basis and dimension. We define a *real vector space* V to be a set of elements ('vectors') $u, v, w, \ldots$ that is closed under linear combinations: $\alpha u + \beta v \in V$ for any $\alpha, \beta \in \mathbb{R}$ and $u, v \in V$. In a complex vector space, the 'scalar' coefficients α, β can be complex. In particular, any vector space includes the zero vector. The set of vectors emanating from a fixed origin in 3d Euclidean space, denoted $\mathbb{R}^3$, is an example. A subset $W \subseteq V$ that is a vector space with respect to the operations inherited from V is called a *subspace*. For example, the set of all real multiples of a nonzero vector v is the (one-dimensional) vector subspace spanned by v. Similarly, the space of 'horizontal' vectors in $\mathbb{R}^3$ is a subspace which we may identify as $\mathbb{R}^2$. The set of real linear combinations of a collection of vectors is called the vector subspace *spanned* by them. If u and v are linearly independent, then they span a 2d vector space consisting of all linear combinations $\alpha u + \beta v$. A *basis* for V is an (ordered) collection of linearly independent vectors $e_1, e_2, \ldots, e_n \in V$ which span V. Every vector in V is expressible in a unique manner as a linear combination of the basis vectors: $v = v_1 e_1 + v_2 e_2 + \cdots + v_n e_n$. The real numbers $v_1, \cdots, v_n$ are called the *components* of v in this basis and v is conventionally represented by the column vector $v = \begin{pmatrix} v_1 \\ v_2 \\ \cdot \\ \cdot \\ v_n \end{pmatrix}$. The *dimension* of a vector space is the cardinality (number of elements) of any basis. The standard basis for $\mathbb{R}^3$ is $e_1 = \hat{x}, e_2 = \hat{y}$ and $e_3 = \hat{z}$; it is a 3-dimensional real vector space. In this basis, the basis vectors themselves are represented by the column vectors

$$\hat{x} = \begin{pmatrix} 1 \\ 0 \\ 0 \end{pmatrix}, \quad \hat{y} = \begin{pmatrix} 0 \\ 1 \\ 0 \end{pmatrix} \quad \text{and} \quad \hat{z} = \begin{pmatrix} 0 \\ 0 \\ 1 \end{pmatrix} \quad \text{while} \quad \boldsymbol{r} = \begin{pmatrix} x \\ y \\ z \end{pmatrix} \tag{A.47}$$

represents the vector $\boldsymbol{r} = x\hat{x} + y\hat{y} + z\hat{z}$. Euclidean space $\mathbb{R}^n$ is the standard example of an n-dimensional vector space. The vector space with only one element (the zero vector) is called the trivial vector space and has dimension zero.

Linear maps, kernel, isomorphism. Suppose we have two real vector spaces D (the domain) and T (the target). A linear transformation $L : D \to T$ is a linear map that assigns a vector in T to each vector in D. In other words, L must preserve linear combinations: $L(\alpha u + \beta v) = \alpha L(u) + \beta L(v)$ for all $u, v \in D$ and $\alpha, \beta \in \mathbb{R}$. In particular, L must preserve the origin: $L(0) = 0$. An example of a linear map is the scaling $L(u) = 5u$ for all $u \in D$; in this case, the target T is the same as the domain. A translation is not a linear map: $A(u) = u + 1$ does not preserve the origin, it is an example of a so-called affine transformation. The orthogonal projection from $\mathbb{R}^2$ to the horizontal axis is an example of a linear map (see Fig. A.2b and Prob. A.32). A linear map L is one-one or injective if $L(u) = L(v)$ implies $u = v$. Scaling by a nonzero scalar ($L(u) = \lambda u$) is a 1-1 map, it fails to be injective precisely when $\lambda = 0$. In general, using linearity, we may check that L is injective iff 0 is the only vector that it maps to zero (see Prob. A.27). Vectors that L maps to zero form a subspace of D called the kernel or null space of L. Thus, L is injective if it has trivial kernel. For example, the orthogonal projection from $\mathbb{R}^2$ to the horizontal axis has kernel given by the subspace of vertical vectors. On the other hand, the kernel of the zero map ($L(u) = 0$ for all u) consists of all of D. Two vector spaces D and T are isomorphic if there is an injective linear map L that maps D onto T. In this case, L is invertible and L^{-1} maps T injectively onto D. Isomorphic vector spaces are linear algebraically identical but may be geometrically or physically distinct. For example, the $x - y$ and $x - z$ planes in $\mathbb{R}^3$ are isomorphic: a rotation by 90° about the x-axis furnishes an isomorphism. When an isomorphism exists, it is generally far from unique. More generally, every real vector space of dimension n is isomorphic to $\mathbb{R}^n$.

Matrix of a linear transformation. Suppose $L : \mathbb{R}^q \to \mathbb{R}^p$ is a linear transformation. To know a linear transformation, it suffices to know what it does to a set of basis vectors. For, given any vector $v = \sum_{j=1}^q v_j e_j \in \mathbb{R}^q$, linearity determines that $L(v) = \sum_j v_j L(e_j)$. Now, suppose $f_1, \cdots, f_p$ is a basis for the target $\mathbb{R}^p$. Then we may expand each $L(e_j)$ as a linear combination of the f's. Concretely, we may write

$$L(e_j) = \sum_{i=1}^{p} f_i L_{ij} \quad \text{for each} \quad j = 1, \cdots, q. \tag{A.48}$$

The set of real numbers L_{ij} for $1 \leq i \leq p$ and $1 \leq j \leq q$ may be arranged as a rectangular array with p rows and q columns, with L_{ij} appearing in the i^{th} row and j^{th} column. This array is called the matrix of the linear transformation L with respect to the bases $\{e_j\}$ and $\{f_i\}$. For example, the entries in the first column L_{i1} (for $1 \leq i \leq q$) are the coefficients that appear in the expansion of the image of the first basis vector: $L(e_1)$. Suppose $\{e_j\}$ and $\{f_i\}$ basis vectors for $\mathbb{R}^q$ and $\mathbb{R}^p$. In the selfsame bases, they are represented by column vectors with a 1 in the j^{th} row and i^{th} row and zeros elsewhere:

$$e_1 = \begin{pmatrix} 1 \\ 0 \\ \cdot \\ \cdot \\ 0 \end{pmatrix}, \quad e_2 = \begin{pmatrix} 0 \\ 1 \\ \cdot \\ \cdot \\ 0 \end{pmatrix}, \quad \cdots, e_q = \begin{pmatrix} 0 \\ 0 \\ \cdot \\ \cdot \\ 1 \end{pmatrix}, \quad \text{etc.} \tag{A.49}$$

Then $L(e_1)$ is the column vector $(L_{11}, L_{21}, \cdots, L_{p1})^t$ where t denotes the transpose. With this choice of bases, the j^{th} column of the matrix L consists of the image of the j^{th} basis vector e_j.

Examples. The identity map I from $\mathbb{R}^2 \to \mathbb{R}^2$ takes $e_1 \to e_1$ and $e_2 \to e_2$. Thus, it is represented by the matrix $\left(\begin{smallmatrix} 1 & 0 \\ 0 & 1 \end{smallmatrix}\right)$. The zero map takes $e_{1,2} \to 0$ and is represented by $\left(\begin{smallmatrix} 0 & 0 \\ 0 & 0 \end{smallmatrix}\right)$. Under the orthogonal projection from $\mathbb{R}^2$ to the x-axis, $e_1 = \hat{x} \mapsto e_1$ and $e_2 = \hat{y} \mapsto 0$ so that it is represented by $\left(\begin{smallmatrix} 1 & 0 \\ 0 & 0 \end{smallmatrix}\right)$. A scaling of all vectors by λ is represented by the matrix $\left(\begin{smallmatrix} \lambda & 0 \\ 0 & \lambda \end{smallmatrix}\right)$. A reflection through the origin takes $\hat{x} \to -\hat{x}$ and $\hat{y} \to -\hat{y}$ and is represented by $\left(\begin{smallmatrix} -1 & 0 \\ 0 & -1 \end{smallmatrix}\right)$. A counterclockwise rotation by 90° takes $e_1 \to e_2$ and $e_2 \to -e_1$, its matrix in this basis is $\left(\begin{smallmatrix} 0 & -1 \\ 1 & 0 \end{smallmatrix}\right)$. In general, if $L(e_1) = ae_1 + be_2$ and $L(e_2) = ce_1 + de_2$, then L is represented by the matrix $\left(\begin{smallmatrix} a & c \\ b & d \end{smallmatrix}\right)$.

If $L : U \to V$ and $M : V \to W$ are a pair of linear maps, then we may compose them to get a linear map $M \circ L : U \to W$ defined as $(M \circ L)(u) = M(L(u))$. The matrix representing the composition may be shown to be the product of matrices $(M \circ L)_{ik} = \sum_j M_{ij} L_{jk}$. Since composition of maps is associative, it follows that matrix multiplication is associative as well: $N(ML) = (NM)L$. If L is the identity map $L : V \to V$ ($L(v) = v$ for all $v \in V$), then in any basis, it is represented by the identity matrix I, whose entries are given by the Kronecker symbol $I_{ij} = \delta_{ij}$ (1 if $i = j$ and zero otherwise). On the other hand, if $Lv = 0$ for all v, then L is represented by the zero matrix. A vector v that is mapped to 0 by L is said to be annihilated by L. The rank of a matrix is the number of linearly independent rows or equivalently, the number of linearly independent columns. An $n \times n$ matrix L is invertible iff its rank is maximal (equal to n); this happens precisely when $\det L \neq 0$. For example, the rank of the $n \times n$ identity matrix is n, that of the zero matrix is 0 and that of a projection is the dimension of the subspace to which it projects. In general, the dimension of a square matrix is the sum of its rank and the dimension of its kernel.

Effect of change of basis. Suppose we change the basis used for the target space. In place of $\{f_j\}$ we use a new basis $\{f'_j\}$. We will suppose the old basis vectors are given by the following linear combinations[12] of the new ones:

$$f_j = \sum\nolimits_{k=1}^{p} f'_k S_{kj} \quad \text{for} \quad j = 1, \cdots, p. \tag{A.50}$$

What are the entries of the matrix L representing the linear transformation in this new basis for T? Writing (henceforth, repeated indices are summed over their range)

$$L(e_j) = f_i L_{ij} = f'_k S_{ki} L_{ij} = f'_k L'_{kj}, \tag{A.51}$$

---

[12] For $\{f'\}$ To qualify as a basis, the change needs to be invertible. In other words, the coefficients S_{kj} must be the entries of an invertible matrix.

we infer that $L'_{kj} = S_{ki}L_{ij}$. Thus, the new matrix L' differs from the old one via multiplication on the left by the matrix of coefficients S.

Similarly, suppose we change the basis used for the domain $e_j = e'_k T_{kj}$. Then

$$L(e_j) = L(e'_k T_{kj}) = T_{kj} L(e'_k) = f_i L_{ij}. \tag{A.52}$$

Multiplying by $(T^{-1})_{jm}$ and summing over j on either side, we get

$$L(e'_m) = f_i L_{ij} (T^{-1})_{jm}. \tag{A.53}$$

Comparing with $L(e'_m) = f_i L'_{im}$, we infer that $L'_{im} = L_{ij}(T^{-1})_{jm}$.

Combining, we conclude that under changes of basis of T and D by S and T, the matrix representing a linear map $L : D \to T$ transforms to $L' = SLT^{-1}$. In the special case where $D = T = V$ and $L : V \to V$, under a change of basis $e_i = e'_j S_{ji}$, the matrix representing L is transformed to $L' = SLS^{-1}$. This is called a similarity transformation or conjugation of L by S.

Now recall that $\det(AB) = \det A \det B$ for square matrices A and B. Consequently, the determinant of L is independent of the choice of basis: $\det SLS^{-1} = \det L$. The trace of a square matrix L is defined as the sum of its diagonal entries: $\operatorname{tr} L = \sum_i L_{ii}$. Now, for a pair of square matrices, $\operatorname{tr} AB = \operatorname{tr} BA = \sum_{i,j} A_{ij}B_{ji}$. Thus, $\operatorname{tr} L' = \operatorname{tr} SLS^{-1} = \operatorname{tr} L$ is independent of the choice of basis.

Eigenvalue problem for a square matrix. Suppose the domain and target spaces of a linear transformation L are the same vector space $V = \mathbb{R}^n$ with basis $e_1, \cdots, e_n$. In this basis, L is represented by an $n \times n$ square matrix[13] with entries L_{ij}. Thus, L transforms a vector $v \in V$ represented by the column vector with components v_j to the column vector Lv with components $L_{ij}v_j$. The vectors that behave in the simplest way are those that are sent to a multiple of themselves. The equation $Lv = \lambda v$ is called the eigenvalue problem for L. A nonzero solution v is called an eigenvector of L corresponding to the eigenvalue or characteristic value λ. The complex numbers λ for which the eigenvalue problem can be solved nontrivially are called the eigenvalues[14] of L and together comprise its spectrum. The zero vector $v = 0$ is not considered an eigenvector of L since it automatically solves $Lv = \lambda v$ for any λ. The set of solutions[15] v (including 0) to the eigenvalue problem for a fixed λ forms a vector subspace of V called the λ eigenspace V_λ. The dimension of the λ eigenspace is called the geometric multiplicity of λ: it is the number of linearly independent eigenvectors corresponding to the eigenvalue λ. The λ eigenspace is an invariant subspace for L in the sense that if $v \in V_\lambda$ then Lv also lies in V_λ since $L(Lv) = L(\lambda v) = \lambda(Lv)$.

---

[13] The transpose of a square matrix is the matrix L^t with ij entry L_{ji}. A matrix that is its own transpose is called real symmetric. Verify that $(LM)^t = M^t L^t$. The determinant of a square matrix is the same as that of its transpose: $\det L = \det L^t$. A complex matrix H is Hermitian if $H_{ij} = H^*_{ji}$, i.e., $H = H^\dagger \equiv (H^*)^t$. A complex matrix U is unitary if $UU^\dagger = I$.

[14] *Eigen* is a German word meaning ‘ones own’. Like its eigenvalues, the eigenvectors of L are special vectors associated to L and are like its private property!

[15] Note that if v is an eigenvector corresponding to eigenvalue λ, then so is cv for any nonzero scalar c. So eigenvectors are defined up to scalar multiples.

This is a useful feature if we wish to apply L repeatedly (as in discrete- or continuous-time evolution problems): $Lv = \lambda v$ implies $L^2 v = \lambda^2 v$, $L^3 v = \lambda^3 v$, etc. Thus, an eigenvector does not 'mix' with other vectors under repeated application of L.

Characteristic equation. The eigenvalue problem $Lv = \lambda v$ can be considered a homogeneous linear system of equations $(L - \lambda I)v = 0$ where I is the $n \times n$ identity matrix. A nontrivial solution (eigenvector) exists iff $L - \lambda I$ has nontrivial kernel, which happens iff $\det(L - \lambda I) = 0$. This is an n^{th} degree polynomial equation in λ called the *characteristic equation*:

$$\det(L - \lambda I) = \det \begin{pmatrix} L_{11}-\lambda & L_{12} & \cdots & L_{1n} \\ L_{21} & L_{22}-\lambda & L_{23} & \cdots \\ \vdots & \vdots & \vdots & \vdots \\ L_{n1} & L_{n2} & \cdots & L_{nn-\lambda} \end{pmatrix} = 0. \qquad (A.54)$$

For example, the characteristic equation of the matrix $L = \left(\begin{smallmatrix} 1 & 2 \\ 2 & 4 \end{smallmatrix}\right)$ is

$$\det \left(\begin{smallmatrix} 1-\lambda & 2 \\ 2 & 4-\lambda \end{smallmatrix}\right) = (1-\lambda)(4-\lambda) - 4 = \lambda(\lambda - 5) = 0. \qquad (A.55)$$

The eigenvalues are $\lambda = 0, 5$ and the corresponding eigenvectors (up to scalar multiples) can be taken as $\left(\begin{smallmatrix} 2 \\ -1 \end{smallmatrix}\right)$ and $\left(\begin{smallmatrix} 1 \\ 2 \end{smallmatrix}\right)$. The determinant of L is 0, which is the same as the product of eigenvalues. Notice that the trace of L is 5, which coincides with the sum of its eigenvalues. These relations hold for any matrix.

The characteristic polynomial $\det(L - \lambda I)$ has n roots $\lambda_1, \lambda_2, \cdots, \lambda_n$, which are the n (generally complex) eigenvalues of L. Generically, they are distinct, but it may happen that some of the eigenvalues coincide. We may assign an algebraic multiplicity to each eigenvalue: it is the order of the corresponding zero of the characteristic polynomial. An eigenvalue with algebraic multiplicity one is called nondegenerate. The sum of algebraic multiplicities of the eigenvalues must equal n. A matrix is deficient if the geometric multiplicity of some eigenvalue is strictly less than its algebraic multiplicity. Such a matrix is 'lacking' in linearly independent eigenvectors. For example, the matrix $N = (0, 1|0, 0)$ has one eigenvalue $\lambda = 0$, its algebraic multiplicity is two, but the 0 eigenspace is one-dimensional: there is only one linearly independent eigenvector $(0 \;\; 1)^t$. The $n \times n$ identity matrix is not deficient: its only eigenvalue 1 has both algebraic and geometric multiplicities equal to n. So degenerate eigenvalues do not always lead to a deficiency.

Accounting for multiplicity, the characteristic polynomial may be factorized as

$$\det(L - \lambda I) = (\lambda_1 - \lambda)(\lambda_2 - \lambda) \cdots (\lambda_n - \lambda). \qquad (A.56)$$

It is convenient to multiply by $(-1)^n$ so that the polynomial is monic, i.e., λ^n has coefficient 1. Expanding out the product, the characteristic equation becomes

$$(-1)^n \det(L - \lambda I) = \lambda^n + c_{n-1}\lambda^{n-1} + c_{n-2}\lambda^{n-2} + \cdots + c_1\lambda + c_0 = 0. \quad (A.57)$$

Setting $\lambda = 0$, we see that the constant term is the determinant up to a possible sign and this may also be identified with the product of eigenvalues

$$(-1)^n \det L = c_0; \quad \det L = \lambda_1 \lambda_2 \cdots \lambda_n. \qquad (A.58)$$

Moreover, $-c_{n-1}$, the coefficient of $-\lambda^{n-1}$ is the sum of the eigenvalues $\lambda_1 + \lambda_2 + \cdots + \lambda_n$. It turns out that this is the trace of L. The eigenvalues of L^t are the same as the eigenvalues of L. This is because $\det(L^t - \lambda I) = \det(L - \lambda I)$, so L and L^t have the same characteristic polynomial.

One of the main uses of eigenvectors is to try to employ them to furnish a basis for the vector space on which L acts. The following fundamental result facilitates this. The eigenvectors corresponding to a pair of distinct eigenvalues are always linearly independent. To see this, suppose $Lv = \lambda v$ and $Lw = \mu w$ are two (nonzero) eigenvectors corresponding to distinct eigenvalues $\lambda \neq \mu$. Suppose $v = \alpha w$ are linearly dependent. Then $Lv = \lambda v$ and also $Lv = L\alpha w = \alpha\mu w = \mu v$ so that $(\lambda - \mu)v = 0$ or $\lambda = \mu$, contradicting the hypothesis. This extends to any number of distinct eigenvalues. One can show inductively that eigenvectors corresponding to a set of distinct eigenvalues are linearly independent. It follows that if an $n \times n$ matrix has n distinct eigenvalues, then the corresponding n eigenvectors are linearly independent and span the whole vector space. So matrices with n distinct eigenvalues are not deficient. When eigenvalues coincide as a parameter is varied, the corresponding eigenvectors may remain independent (as in $(1+\delta, 0|0, 1-\delta)$) or become collinear (e.g., $(1+\delta, 1|0, 1+2\delta)$). Deficiencies arise in the latter case (see Sect. 6.5).

Cayley-Hamilton Theorem. The matrix $L = (1, 2|2, 4)$ has the characteristic equation $\lambda^2 - 5\lambda = 0$ and it is easily checked that $L^2 = (5, 10|10, 20) = 5L$. The Cayley-Hamilton theorem states that any matrix satisfies its own characteristic equation. Suppose the eigenvalues of $n \times n$ matrix L are $\lambda_1, \cdots, \lambda_n$, then the characteristic equation is

$$P(\lambda) = (\lambda - \lambda_1)(\lambda - \lambda_2)\cdots(\lambda - \lambda_n) = 0. \tag{A.59}$$

We will show that $P(L) = 0$ assuming L is not deficient. In other words, we assume that the eigenvectors $v_1, v_2, \cdots, v_n$ of L span the vector space V so that any vector u may be expressed as $u = u_1 v_1 + u_2 v_2 + \cdots + u_n v_n$. Now consider the matrix $P(L) = (L - \lambda_1)(L - \lambda_2)\cdots(L - \lambda_n)$. The order of the factors does not matter since L commutes with its powers. We will show that $P(L)$ annihilates any vector u. It will then follow that $P(L)$ must be the zero matrix. To begin with, notice that $(L - \lambda_1)u_1 v_1 = 0$. Next, consider $(L - \lambda_2)(L - \lambda_1)$. This matrix annihilates any linear combination of the eigenvectors v_1 and v_2 since the right factor annihilates v_1 while the left factor annihilates v_2. Continuing this way

$$P(L)(u_1 v_1 + u_2 v_2 + \cdots + u_n v_n) = 0, \tag{A.60}$$

implying that $P(L)$ must be the zero matrix. Since the characteristic equation is a polynomial of degree n, the Cayley-Hamilton theorem allows us to express L^q for $q \geq n$ as a linear combination of $I, L, L^2, \cdots, L^{n-1}$. For the 2×2 matrix we started with, $L^n = 5^{n-1} L$ for $n = 2, 3, \ldots$.

Diagonalization of a nondeficient square matrix. Suppose $L : V \to V$ is a linear map represented by the $n \times n$ real matrix L_{ij} in a basis $\{e_i\}$ for V. We will suppose that L is not deficient[16], i.e., that it possesses n linearly independent eigenvectors

---

[16] Deficient matrices are not diagonalizable, but can be brought to Jordan normal form. See Sect. 6.5 for an example.

$v_1, \cdots, v_n$: $Lv_j = \lambda_j v_j$. These eigenvectors consequently furnish a basis for V, called the eigenbasis of L. Some conditions that ensure that L is nondeficient include: (i) L has n distinct eigenvalues, (ii) L is a real symmetric or antisymmetric matrix ($L^t = L$ or $L^t = -L$), (iii) L is an orthogonal matrix $L^t L = I$ and (iv) L is normal, i.e., it commutes with its transpose ($[L, L^t] = LL^t - L^t L = 0$). We may then show that L is diagonal in its eigenbasis, with diagonal entries given by its eigenvalues $\lambda_1, \lambda_2, \cdots, \lambda_n$ in the same order as the eigenvectors in the eigenbasis. In other words, L is conjugate to the diagonal matrix $\Lambda = \mathrm{diag}(\lambda_1, \cdots, \lambda_n)$ via the similarity transformation S whose columns are the eigenvectors of L: $S^{-1} L S = \Lambda$. Thus, the change from the original basis (A.49) to the eigenbasis[17] diagonalizes L. These statements are easily verified once we note that the eigenvalue equations $Lv_i = \lambda_i v_i$ can be summarized as

$$\begin{aligned} LS &= S\Lambda \quad \text{where} \quad S = \left(v_1 \; v_2 \; \cdots \; v_n \right), \\ LS &= \left(Lv_1 \; Lv_2 \; \cdots \; Lv_n \right) \quad \text{and} \quad S\Lambda = \left(\lambda_1 v_1 \; \lambda_2 v_2 \; \cdots \; \lambda_n v_n \right). \end{aligned} \tag{A.61}$$

Taking the trace of $S^{-1} L S = \Lambda$ we find that $\mathrm{tr}\, L = \mathrm{tr}\, \Lambda$. Thus, the trace of a diagonalizable matrix is the sum of its eigenvalues. This is in fact true of all matrices, as mentioned while discussing the characteristic polynomial.

Returning to our example $L = (1, 2|2, 4)$, recall that the eigenvalues are $\lambda_1 = 0$ and $\lambda_2 = 5$. We take the corresponding eigenvectors to have unit norm $v_1 = \frac{1}{\sqrt{5}}(2, -1)^t$ and $v_2 = \frac{1}{\sqrt{5}}(1, 2)^t$. In this case, $\Lambda = \mathrm{diag}(0, 5)$ and $S^{-1} L S = \Lambda$ where

$$S = (1/\sqrt{5}) \begin{pmatrix} 2 & 1 \\ -1 & 2 \end{pmatrix} \quad \text{and} \quad S^{-1} = (1/\sqrt{5}) \begin{pmatrix} 2 & -1 \\ 1 & 2 \end{pmatrix}. \tag{A.62}$$

Notice that L is a symmetric matrix and that by normalizing the eigenvectors, S could be taken to be orthogonal: $S^t S = I$. This is generally true: a symmetric matrix may be diagonalized by an orthogonal matrix.

A.11* Fourier transform

Given a function of one real variable $f(x)$, its Fourier transform is defined as the (generally complex-valued) function[18] of another real variable k:

$$\tilde{f}(k) = \int_{-\infty}^{\infty} f(x) e^{-ikx} \, dx. \tag{A.63}$$

The coordinate x is said to lie in position space while the wave number k lies in Fourier-space or loosely, momentum space. $\tilde{f}(k)$ is called the k^{th} Fourier mode of the function $f(x)$. If f is real-valued, then we verify that its Fourier transform has the symmetry $\tilde{f}^*(k) = \tilde{f}(-k)$. Fourier transforms are a continuum version of Fourier series discussed in Eq. 17.18 of Sect. 17.3 with the discrete mode number n playing the role of k.

---

[17] It is noteworthy that nonreal eigenvalues of a real matrix must come in complex conjugate pairs as must the corresponding eigenvectors. A real matrix with a nonreal eigenvalue is not diagonalizable over the real numbers but may be diagonalizable over the complex numbers.

[18] For this integral to exist, it is sufficient that f be absolutely integrable (i.e., of class L^1, $\int |f(x)| \, dx < \infty$) or square integrable (i.e., of class L^2, $\int |f(x)|^2 dx < \infty$).

A key property of the Fourier transform is that differentiation in position space becomes multiplication by ik in Fourier space (see Prob. A.36) so that linear differential equations in position space become algebraic equations in Fourier space. We will exploit this feature in treating partial differential equations such as the heat equation in Sect. 18.3*.

Fourier transform of a constant and the Dirac delta function. If $f(x) \equiv 1$, then $\tilde{f}(k)$ vanishes whenever $k \neq 0$ due to cancellation among phases e^{ikx}. If $k = 0$, then the Fourier transform diverges like the length of the spatial region parametrized by x. A careful treatment allows us to take the Fourier transform of $f = 1$ to be the Dirac delta function supported[19] at the origin $k = 0$:

$$\int_{-\infty}^{\infty} e^{-ikx}\, dx = 2\pi\delta(k). \tag{A.64}$$

The latter is defined by the condition that[20]

$$\int_{-\infty}^{\infty} \tilde{g}(k)\, 2\pi\delta(k)\, \frac{dk}{2\pi} = \tilde{g}(0) \tag{A.65}$$

for any continuous function $\tilde{g}(k)$. In other words, integration against the Dirac delta function[21] supported at the origin picks out the value of the function at $k = 0$.

Inverse Fourier transform. The original function $f(x)$ may be synthesized as a linear combination of its Fourier modes. This is done via an inverse Fourier transform[22]:

$$f(x) = \int_{-\infty}^{\infty} \tilde{f}(k)\, e^{ikx} \frac{dk}{2\pi}. \tag{A.67}$$

This formula is checked by inserting (A.63) on the RHS and using the integral representation and defining property of the Dirac delta function:

$$\begin{aligned}\int_{-\infty}^{\infty} \tilde{f}(k)\, e^{ikx} \frac{dk}{2\pi} &= \iint_{-\infty}^{\infty} f(y) e^{-iky}\, dy\, e^{ikx} \frac{dk}{2\pi} = \int dy f(y) \int e^{ik(x-y)} \frac{dk}{2\pi} \\ &= \int_{-\infty}^{\infty} dy f(y) \delta(x-y) = f(x).\end{aligned} \tag{A.68}$$

---

[19] The support of a function is the closure of the set on which it is nonzero.

[20] Conventionally, all integrals over Fourier space are performed with respect to the measure $dk/2\pi$. For consistency, delta functions in momentum space come with a prefactor of 2π.

[21] We may think of the Dirac delta 'function' $\delta(x)$ as a limit of gaussians centered at the origin as their widths and heights go to zero and infinity while holding the area under the graphs fixed at one: $\delta(x) = \lim_{a\to 0} (\pi a^2)^{-1/2} \exp(-x^2/a^2)$.

[22] The Fourier transform and its inverse may be extended to functions on $\mathbb{R}^n$:

$$\tilde{f}(\boldsymbol{k}) = \int f(\boldsymbol{x}) e^{-i\boldsymbol{k}\cdot\boldsymbol{x}} d^n x \quad \text{and} \quad f(\boldsymbol{x}) = \int \tilde{f}(\boldsymbol{k}) e^{i\boldsymbol{k}\cdot\boldsymbol{x}} \frac{d^n k}{(2\pi)^n}. \tag{A.66}$$

We have suppressed the limits of integration ($\pm\infty$) in some places. For instance, if all Fourier modes are equal to unity, $\tilde{f}(k) = 1$ then $f(x) = \delta(x)$. Thus, while a constant function of x has only one nonvanishing Fourier mode, the delta function has all Fourier modes equal to each other. Interestingly, the Fourier transform of a Gaussian is again a Gaussian. Verify that for any length $a > 0$,

$$\int_{-\infty}^{\infty} e^{-x^2/2a^2} e^{-ikx}\, dx = a\sqrt{2\pi}\, e^{-a^2k^2/2}. \tag{A.69}$$

Convolution. The Fourier transform of a product of functions $(fg)(x) = f(x)g(x)$ is the 'convolution' $(\tilde{f} * \tilde{g})(k)$ of Fourier transforms. To find a formula, we write

$$\begin{aligned} \widetilde{(fg)}(k) &= \int f(x)g(x)e^{-ikx}\, dx = \int\int \tilde{f}(l)e^{ilx}\frac{dl}{2\pi}\int \tilde{g}(m)e^{imx}\frac{dm}{2\pi}e^{-ikx}dx \\ &= \int \tilde{f}(l)\tilde{g}(m)\frac{dl}{2\pi}\frac{dm}{2\pi}\int e^{i(l+m-k)x}dx = \int \tilde{f}(l)\tilde{g}(m)\frac{dl\, dm}{4\pi^2}2\pi\delta(l+m-k) \\ &= \int \tilde{f}(l)\tilde{g}(k-l)\frac{dl}{2\pi} = (\tilde{f} * \tilde{g})(k). \end{aligned} \tag{A.70}$$

A.12 Problems

1. **Law of cosines.** Suppose θ is the angle between vectors $\boldsymbol{a}$ and $\boldsymbol{b}$. Show the law of cosines $c^2 = a^2 + b^2 + 2ab\cos\theta$ for $\boldsymbol{c} = \boldsymbol{a} + \boldsymbol{b}$.
2. **Dependence of torque on origin.** How does the torque $\boldsymbol{\tau}$ due to a force $\boldsymbol{F}$ on a particle change if the origin $\boldsymbol{O}$ for position vectors is shifted to $\boldsymbol{O}' = \boldsymbol{O} + \boldsymbol{a}$? Relate the torques with respect to the two origins. Draw a figure to illustrate.
3. **Origin and angular momentum.** A particle moves uniformly counterclockwise along a circle on a horizontal plane. Comment on the direction of its angular momentum $\boldsymbol{L}$ if (a) the origin is at the center of the circle and (b) the origin is at a point on the horizontal plane lying outside the disk defined by the circle.
4. **Square of cross product.** Suppose $\boldsymbol{\Omega}$ and $\boldsymbol{r}$ are a pair of vectors. Find an expression for $|\boldsymbol{\Omega} \times \boldsymbol{r}|^2$ purely in terms of dot products of the vectors $\boldsymbol{\Omega}$ and $\boldsymbol{r}$.
5. **Direction of cross product.** Consider a particle that moves on a sphere, its position vector $\boldsymbol{r}$ is defined relative to the center of the sphere. The sphere rotates (counterclockwise when viewed from above) about a vertical axis through its center at the angular speed Ω. The angular velocity vector $\boldsymbol{\Omega}$ has magnitude Ω and points upwards. Comment on the direction of the vector $-\boldsymbol{\Omega} \times (\boldsymbol{\Omega} \times \boldsymbol{r})$. Draw a figure to clarify.
6. Show that $\boldsymbol{u}$ and $\boldsymbol{v}$ are **linearly independent** if and only if $\boldsymbol{u} \times \boldsymbol{v} \neq \boldsymbol{0}$.
7. **Nonassociativity of cross product.** Give an example of vectors $\boldsymbol{a}, \boldsymbol{b}, \boldsymbol{c}$ in 3d Euclidean space to show that the cross product is not associative in general.
8. **Linear independence.** Show that vectors $\boldsymbol{u}$ and $\boldsymbol{v}$ point in different directions (not parallel/antiparallel) if and only if $a\boldsymbol{u} + b\boldsymbol{v} = \boldsymbol{0}$ implies that both $a, b = 0$.
9. **Maximal number of independent vectors.** (a) Show that three vectors in $\mathbb{R}^2$ cannot be linearly independent. (b) In $\mathbb{R}^n$ what is the maximum number of vectors that can be linearly independent?

10. **Components of cross product.** Express the Cartesian components of the cross product $\boldsymbol{a} \times \boldsymbol{b}$ in terms of those of $\boldsymbol{a}$ and $\boldsymbol{b}$ by using $\hat{x} \times \hat{y} = \hat{z}$, etc.

11. **Scalar triple product.** Show that $\boldsymbol{a} \cdot (\boldsymbol{b} \times \boldsymbol{c}) = \boldsymbol{c} \cdot (\boldsymbol{a} \times \boldsymbol{b}) = \boldsymbol{b} \cdot (\boldsymbol{c} \times \boldsymbol{a})$ by working with the Cartesian components of the three vectors.

12. Define the **Levi-Civita symbol** (a real number) ϵ_{ijk} for integers $1 \leq i, j, k \leq 3$ (not necessarily distinct) by the conditions (i) $\epsilon_{123} = 1$ and (ii) ϵ_{ijk} reverses sign under exchange of any pair of indices [e.g., $\epsilon_{ijk} = -\epsilon_{jik}$]. Find ϵ_{213}, ϵ_{312}, ϵ_{321}, ϵ_{112}, ϵ_{313} and ϵ_{222}.

13. **Scalar triple product and Levi-Civita symbol.** If a_i, b_j, c_k are the Cartesian components of three vectors in $\mathbb{R}^3$, then verify that $\boldsymbol{a} \cdot (\boldsymbol{b} \times \boldsymbol{c}) = \sum_1^3 \epsilon_{ijk} a_i b_j c_k$.

$*$14. **Product of Levi-Civita symbols.** Suppose i, j, k, l, m, n can each take values among $1, 2, 3$. (a) Show that

$$\epsilon_{ijk}\epsilon_{lmn} = \det \begin{pmatrix} \delta_{il} & \delta_{im} & \delta_{in} \\ \delta_{jl} & \delta_{jm} & \delta_{jn} \\ \delta_{kl} & \delta_{km} & \delta_{kn} \end{pmatrix}. \tag{A.71}$$

Hint: How does the LHS behave under suitable exchanges of indices? (b) What does this formula reduce to for $\sum_i \epsilon_{ijk}\epsilon_{imn}$?

15. **Orthogonal transformation.** Suppose we make a linear change from Cartesian coordinates (x, y) to new coordinates (u, v) on the plane, given by $u = ax + by$ and $v = cx + dy$ for some real constants a, b, c, d. It is possible to show (you are not asked to do this) that vectors pointing in the direction of increasing u and v holding the other fixed are given by $\boldsymbol{u} = a\hat{x} + b\hat{y}$ and $\boldsymbol{v} = c\hat{x} + d\hat{y}$ where $\hat{x}$ and $\hat{y}$ are the usual unit vectors in the directions of increasing x and y respectively. Find conditions on (a, b, c, d) to guarantee that $\boldsymbol{u}$ and $\boldsymbol{v}$ are orthonormal. Interpret the answer in terms of the matrix $(a, b|c, d)$.

16. **Transformation of coordinates.** According to Galileo, the coordinates of a particle are (x, y) with respect to a given origin O and choice of x and y axes. (a) Suppose Newton picks an origin located at $\boldsymbol{a}$ relative to O and axes parallel to those of Galileo. What are the coordinates of the particle according to Newton? (b) What are the coordinates according to Newton if his coordinate axes were rotated counterclockwise by $\pi/4$ relative to those of Galileo?

17. **Velocity and acceleration along a helical trajectory.** Suppose a particle has a helical trajectory in 3d space given by the position vector $\boldsymbol{r}(t) = \cos t\ \hat{x} + \sin t\ \hat{y} + t\ \hat{z}$. Find the velocity and acceleration vectors. Plot the trajectory. Indicate the directions of the velocity and acceleration vectors at a point on the trajectory.

18. **Uniform circular motion.** Suppose $\boldsymbol{a}(t)$ is the acceleration vector of a particle undergoing uniform circular motion at angular speed ω counterclockwise around a circle of radius ℓ with position vector $\boldsymbol{r}$ relative to the center of the circle. Find $\boldsymbol{v} = \dot{\boldsymbol{r}}$, $\boldsymbol{a}$ and $\dot{\boldsymbol{a}}$. Find $\boldsymbol{r} \cdot \boldsymbol{v}$ and $\boldsymbol{v} \cdot \boldsymbol{a}$ and show that $\boldsymbol{a} \cdot \dot{\boldsymbol{a}} = 0$. What does $\boldsymbol{a} \cdot \dot{\boldsymbol{a}} = 0$ imply for the length of $\boldsymbol{a}$? How does the $\boldsymbol{a}$ vector evolve in time? Which way does the jolt or jerk vector $\dot{\boldsymbol{a}}$ point?

19. **Spherical polar coordinates.** Consider spherical polar coordinates (r, θ, ϕ). The radial, polar and azimuthal coordinates are defined in terms of Cartesian coordinates in $\mathbb{R}^3$ via $z = r\cos\theta$, $x = r\sin\theta\cos\phi$ and $y = r\sin\theta\sin\phi$. (a) Express r, θ, ϕ in terms of x, y, z. (b) Find the ranges of r, θ and ϕ and mention where the spherical polar coordinates are not uniquely defined. (c) If $\hat{r}, \hat{\theta}, \hat{\phi}$ are the unit vectors in the directions of increasing r, θ, ϕ, then use a figure to show that

$$\begin{aligned} \hat{r} &= \cos\theta\,\hat{z} + \sin\theta(\cos\phi\,\hat{x} + \sin\phi\,\hat{y}), \\ \hat{\theta} &= -\sin\theta\,\hat{z} + \cos\theta(\cos\phi\,\hat{x} + \sin\phi\,\hat{y}) \quad \text{and} \\ \hat{\phi} &= -\sin\phi\,\hat{x} + \cos\phi\,\hat{y}. \end{aligned} \tag{A.72}$$

(d) Verify that $(\hat{r}, \hat{\theta}, \hat{\phi})$ is a right handed orthonormal frame. (e) If $\boldsymbol{r}(t) = r(t)\hat{r}(t)$ is the position vector of the trajectory of a particle, show that $\dot{\hat{r}} = \dot{\theta}\hat{\theta} + \dot{\phi}\sin\theta\hat{\phi}$. (f) Qualitatively explain the vanishing coefficient of $\hat{r}$ in $\dot{\hat{r}}$. (g) Find the radial, polar and azimuthal components of the particle's velocity and (h) its acceleration.

20. **Differentiable but derivative discontinuous.** Consider the function defined as $f(x) = x^2\sin(1/x)$ for $x \neq 0$ and $f(0) = 0$. Show that f is differentiable but that its derivative is not continuous at $x = 0$.

21. **Smooth but not analytic function.** Consider the function on the real line $f(x) = \exp(-1/x^2)$. We define its value and that of its derivatives at $x = 0$ by taking limits as $x \to 0$. Show that f and all its derivatives vanish at $x = 0$. Recalling Footnote 9, argue that f is smooth but not real analytic at $x = 0$. To what function does the Taylor series converge?

22. **Taylor series.** (a) Recall the Taylor series $1/(1-x) = 1 + x + x^2 + \ldots$. Evaluate the function at $x = 0.1$ and $x = 1.1$. Compare these values with those obtained from Taylor polynomials of degrees $1, 2, 3$ and 4. (b) Show that the Taylor series for $1/\sqrt{1+x}$ around $x = 0$ is given by $1/\sqrt{1+x} = 1 - x/2 + 3x^2/8 + \cdots$. (c) Find the Taylor series for $\cos x$, $\sin x$ and $\log(1+x)$ around $x = 0$. (d) Consider $f(x) = 1/x(1-x)$. What goes wrong if we try to develop a Taylor series for f around $x = 0$? Look up the idea of a Laurent series.

23. **Equality of mixed partials (Clairaut's theorem).** Evaluate the second partials $\frac{\partial^2 f}{\partial x \partial y}$ and $\frac{\partial^2 f}{\partial y \partial x}$ of $f(x, y) = \cos(xy)$ and show that they are equal.

24. **Gradient of a scalar field.** Consider the scalar field $\psi = 1/\sqrt{x^2 + y^2 + z^2}$ defined using Cartesian coordinates in $\mathbb{R}^3$ with the origin left out. (a) Find the gradient of ψ for x, y, z not all zero. After obtaining the answer in Cartesian coordinates, re-express ψ and the final answer for the gradient in spherical polar coordinates. (b) Say in words which way $\boldsymbol{\nabla}\psi$ points and why and how its magnitude varies. Plot this vector field on a suitably chosen plane through the origin. Does the choice of plane matter? Why or why not?

25. **Force from a potential.** Suppose a potential in 3d Euclidean space is given by $V = \alpha/r^n$ where r is the radial distance from the origin, $\alpha > 0$ a real constant and n a real number. (a) Find the associated force $\boldsymbol{F} = -\boldsymbol{\nabla}V$ and express it in

spherical polar coordinates. (b) For $n = -2$ write V and $\boldsymbol{F}$ in Cartesian coordinates. (c) Describe the resulting $\boldsymbol{F}$ for $n = -2$ by saying whether the force is attractive/repulsive (relative to the origin), how it behaves with distance and give it a suitable name using standard terminology. Plot the graph of $V(r)$.

26. **Uniqueness of linear combinations.** Suppose $\{e_1, \cdots, e_n\}$ are linearly independent vectors in an n-dimensional vector space V. We have argued that any vector in V can be expressed as a linear combination of the e's. Show that the coefficients in the linear combination are uniquely determined.
27. **Kernel of a linear map.** Suppose $L : D \to T$ is a linear map between vector spaces. The kernel $\ker L$ is defined as the set of vectors $v \in D$ with $L(v) = 0$. (a) Show that $\ker L$ is a subspace of D. (b) Show that L is 1-1 iff $\ker L$ is trivial.
28. The **Pauli matrices** are $\sigma_1 = (0,1|1,0)$, $\sigma_2 = (0,-i|i,0)$ and $\sigma_3 = (1,0|0,-1)$. (a) Verify that the entries are $(\sigma_1)_{ab} = 1 - \delta_{ab}$, $(\sigma_2)_{ab} = i(-1)^a(1-\delta_{ab})$ and $(\sigma_3)_{ab} = (-1)^{a-1}\delta_{ab}$. Show that (b) $\sigma_a\sigma_b = \delta_{ab}I + i\epsilon_{abc}\sigma_c$ and (c) $[\sigma_a, \sigma_b] = 2i\epsilon_{abc}\sigma_c$. (d) What is the determinant, trace and square of each Pauli matrix?
29. Find the **characteristic equation**, eigenvalues and corresponding linearly independent eigenvectors of the **Pauli matrix** $\sigma_1 = (0,1|1,0)$.
30. Show that the eigenvalues of a **real symmetric matrix** are real, that the corresponding eigenvectors can be chosen real and that eigenvectors corresponding to distinct eigenvalues are orthogonal.
31. Give an example of a 2 × 2 matrix that is **invertible but not diagonalizable**.
32. A **projection matrix** is a real symmetric matrix satisfying $P^2 = P$. Comment on its eigenvalues, their algebraic and geometric multiplicities, $\operatorname{tr} P$ and the rank of P. Is a projection diagonalizable and if so what are its entries in its eigenbasis?
33. Consider the **rotation matrix** $R = (\cos\theta, \sin\theta| - \sin\theta, \cos\theta)$. Show that $R^t R = I$, i.e., it is orthogonal. Show that its characteristic polynomial is $\lambda^2 - 2\lambda\cos\theta + 1 = 0$ and that its eigenvalues are $e^{\pm i\theta}$. Find the corresponding eigenvectors and a similarity transformation S that diagonalizes it: $S^{-1}RS = \Lambda = \text{diag}(e^{i\theta}, e^{-i\theta})$. Can S be chosen to be an orthogonal (or unitary) matrix?
34. **Exponential.** Suppose A is diagonalizable via a similarity transformation. Use this to find an expression for $e^A = I + A + A^2/2! + \cdots$ and apply it to $A = i\theta\sigma_1$.
35. **Symmetry of the Fourier transform of a real function.** If $f(x)$ is real, show that its Fourier transform $\tilde{f}(k)$ satisfies $\tilde{f}^*(k) = \tilde{f}(-k)$.
36. **Fourier transform of the derivative.** Show that $\widetilde{f'}(k) = ik\tilde{f}(k)$.
37. **Fourier transform of a Gaussian.** Complete the square to show that

$$\int_{-\infty}^{\infty} e^{-x^2/2a^2} e^{-ikx}\, dx = a\sqrt{2\pi}\, e^{-a^2k^2/2} \quad \text{for any } a > 0. \tag{A.73}$$

38. **Mass density of point masses.** Find the mass density $\rho(\boldsymbol{r})$ of a pair of point masses m_1 and m_2 located at the points $\boldsymbol{r}_1$ and $\boldsymbol{r}_2$. If there are no other masses present, verify from your formula that the total mass in space is equal to $m_1 + m_2$.

Appendix B

Primer on manifolds, tensors and groups

In Chap. 3 we have used the terms manifold (for the configuration or phase space of a mechanical system), group (for symmetries such as the set of Galilean transformations) and Lie algebra (for the Poisson brackets among conserved quantities L_i, K_j, H of the Kepler problem or the components of angular momentum L_x, L_y, L_z). In Chap. 3 and elsewhere, we also encounter the notions of vector fields, covector fields, differential forms, wedge products, tensor fields and exterior, Lie and covariant differentiation on a manifold. These are part of the mathematical language of classical mechanics. Among other things, they help us study systems whose configuration or phase space is not Euclidean space ($\mathbb{R}^n$ for some $n = 1, 2, 3, \cdots$) but a space such as a circle, sphere (see the example in Sect. 3.26*), torus, hyperboloid and so forth. In this appendix, we introduce these notions along with examples. Books such as [94, 95, 113, 120, 135] may be consulted for much more on these topics.

B.1 The concept of a manifold

By a manifold, we have in mind a space like a circle (denoted S^1), the plane, the surface of a sphere (S^2) or the 3d Euclidean space $\mathbb{R}^3$ in which a particle can move. A manifold is a space where every point[1] has an open neighborhood[2] that looks like[3] Euclidean space $\mathbb{R}^n$ for some fixed positive integer n, which is called the dimension of the manifold. By considering sufficiently many such overlapping open neighborhoods of points, we obtain an open covering of the space. Thus, roughly, a manifold is a space that can be covered by charts or 'coordinate' patches, as in Fig. B.1a and

---

[1] In Appendix B.10* we will extend the concept of a manifold to one with a boundary. The points on the boundary will not have open neighborhoods and need to be treated differently.

[2] The open neighborhoods we have in mind are simple ones: they must come in one piece and be contractible (shrunk continuously to a point). In 1d they are open intervals on the real line (a, b) or bent (continuously deformed) versions thereof. In 2d they are open disks $x^2 + y^2 < 1$ or stretched/bent (continuously deformed) versions of disks. In 3d they are continuous deformations of open balls $x^2 + y^2 + z^2 < 1$. The open interval, disk and ball is each continuously deformable into $\mathbb{R}, \mathbb{R}^2$ and $\mathbb{R}^3$. Similarly, we have open balls in higher dimensions. They are our neighborhoods. By contrast, a pair of disjoint intervals on the real line does not come in one piece and may be shrunk to a pair of points but not to a single point. Similarly, an annulus $1 < x^2 + y^2 < 2$ can be shrunk to a circle but not to a point.

[3] By 'looks like', we mean *continuously deformable into*. A rubber balloon undergoes continuous deformation as it is inflated. More precisely, by 'looks like', we mean *homeomorphic to*. A homeomorphism is a continuous map with a continuous inverse. An untied balloon is homeomorphic to a disc-shaped rubber sheet since the latter can be stretched into a balloon without tearing the rubber sheet.

Fig. B.2a. The charts together are said to furnish an atlas for the manifold. The terminology is borrowed from cartography, where an atlas consists of several overlapping charts which can, for instance, together describe a continent.

The idea is to use existing notions on smooth functions, vector fields, differentials and Cartesian tensors on $\mathbb{R}^n$ to develop corresponding notions for the manifold via a combination of patchwork and consistency conditions between overlapping charts. It took a long time for a satisfactory definition of a manifold to be arrived at (in the work of Hermann Weyl (1912) and Hassler Whitney (1930s)), with examples playing a key role. In this appendix, we will introduce a number of concepts and technical terms from the theory of manifolds. The reader who is meeting these for the first time should not despair, as they are invariably accompanied by illustrative examples.

Analogy with cell phone networks and cartography. The idea of covering a space with overlapping patches of a simple sort is practically realized in cell phone networks, which we caricature now. For instance, a city is covered by cells (say disks), each serviced by a cell phone tower. Each point in the city lies in at least one such cell and communication to/from the cell phone is transmitted via some protocols associated to the corresponding tower (manner of storage, encryption, etc.). If a phone lies in the intersection of two cells, then two towers can simultaneously communicate with it. The data received by the two towers can be related to each other via a suitable transformation between the protocols followed by each tower. This is crucial when a person is traveling in the back seat of a car and speaking on a cell phone. When moving from one cell to another, the two towers must agree on what the person is saying when the phone is in the intersection, before the 'future' tower takes over from the 'past' tower. Evidently, the city is our manifold and the cells are our coordinate patches. The transformations between data received by two towers from the overlap of two cells play the role of transition functions that we will soon encounter. A similar analogy, which explains much of the terminology, may be made with cartography, where the charts or maps prepared by two explorers have to be related (e.g., the scales of magnification may be different) in regions they both explore. ☐

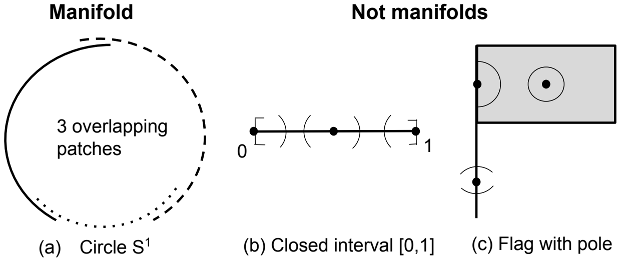

Figure B.1: (a) The circle manifold S^1 covered here by three overlapping open neighborhoods. (b) The closed interval $[0, 1]$ is *not* a manifold as 0 and 1 do not have open neighborhoods: it is a manifold with boundary. (c) A flag with pole is not a manifold: open neighborhoods do not all have the same dimension (1 on the pole and 2 on the flag) and the neighborhoods of all points do not look alike.

Coordinate charts and transition functions. Returning to our definition of a manifold, why do we insist on open neighborhoods of the same dimension to cover a manifold? Examples of spaces we do not want to regard as manifolds will reveal why. For instance, the closed interval $C = [0, 1] \subset \mathbb{R}^1$ is *not* a manifold[4]. The points 0 and 1 do not have any open neighborhoods[5] lying in C while all other points $0 < x < 1$ have open neighborhoods (see Fig. B.1) of the form $(x - \epsilon, x + \epsilon) \subset C$ for some sufficiently small ϵ [we could take ϵ to be the smaller of $x/2$ and $(1 - x)/2$]. Intuitively, C looks different in the vicinity of 0 and 1 from how it looks elsewhere. We do not want to allow such 'inhomogeneities' in a manifold. This is why we insist on open neighborhoods. Similarly, the space that is shaped like the multiplication sign × is not a manifold: it looks different at the center and the extremes compared to how it looks elsewhere. A cloth flag attached to a pole is also not a manifold: points on the lower part of the pole look different from points on the cloth: the former typically have 1d open neighborhoods while the latter typically have 2d open neighborhoods (see Fig. B.1). This is why we insist that all neighborhoods have the same dimension.

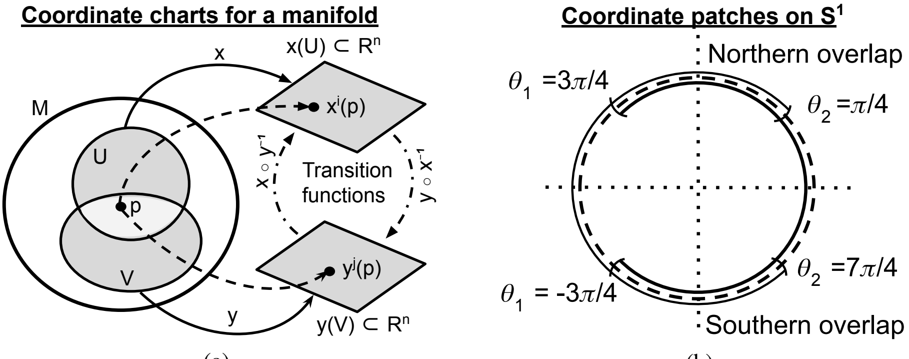

(a) (b)

Figure B.2: (a) Coordinate charts and transition functions for a manifold M (which can be thought of as the surface of a sphere S^2). (b) Overlapping coordinate patches for the circle S^1 (dashed curve) as a manifold. A minimum of two (open) coordinate patches is needed to cover the circle: here they are the Eastern and Western patches indicated by thick and thin solid curves. The angle θ is measured counterclockwise from the the horizontal axis.

On the other hand, the unit circle S^1 defined as the set of points (x, y) on the plane with $x^2 + y^2 = 1$ is a one-dimensional manifold. As shown in Fig. B.2b, the circle can be covered by two patches: the Eastern and Western neighborhoods $-3\pi/4 < \theta_1 < 3\pi/4$ and $\pi/4 < \theta_2 < 7\pi/4$ defined in terms of a polar angle measured counterclockwise with respect to the positive x-axis. θ_1 and θ_2 are called local[6] coordinates in their respective patches. Thus, the circle is one-dimensional. Each of these angular patches is continuously deformable (by stretching) into the real line $\mathbb{R}$ since every open interval can be continuously mapped to the whole real line (e.g., $\tan : (-\pi/2, \pi/2) \to \mathbb{R}$). These patches intersect in a pair of 'upper' and 'lower' intervals: running from North-East to North-West and from South-West to South-East.

---

[4] However, $[0, 1]$ may be viewed as the manifold $(0, 1)$ with boundary included, see Appendix B.10*.

[5] Neighborhoods of 0 such as $[0, 1/2)$ are 'closed-open'.

[6] *Local* means coordinates are defined on a patch rather than *globally* on the whole manifold.

When a point lies in such an intersection, either of the coordinates can be expressed in terms of the other via a 'transition function' or coordinate transformation. For the circle, we have in the upper intersection $\theta_1 = \theta_2$ and in the lower intersection $\theta_1 = \theta_2 - 2\pi$. The manifold is differentiable if these transition functions between coordinate systems in each such intersection is a differentiable map from $\mathbb{R}^n \to \mathbb{R}^n$ (or between open subsets of $\mathbb{R}^n$ which are homeomorphic to $\mathbb{R}^n$). In the circle example, the transition functions are linear maps of one real variable, so the circle is a differentiable manifold of dimension one. If the transition functions are infinitely differentiable (as is the case here), we say the manifold is smooth[7] or C^∞. Note that the circle cannot be covered by a single open chart: the largest ones such as $-\pi < \theta_1 < \pi$ unfortunately exclude one point while $-\pi < \theta_1 \leq \pi$ or $0 \leq \theta_1 \leq 2\pi$ fail to be open subsets of $\mathbb{R}$.

Sometimes we are lucky, and a single coordinate patch is sufficient to cover the whole manifold or the portion we are interested in. This is the case with the plane or a disk ($x^2 + y^2 < 1$) or 3d Euclidean space $\mathbb{R}^3$, which can be covered by a single patch with, say, Cartesian coordinates. In particular, $\mathbb{R}^n$ for each[8] $n = 1, 2, 3, \ldots$ is automatically a smooth manifold, as are all the open subsets of $\mathbb{R}^n$ that may be continuously shrunk to a single point. Unfortunately, the circle, which is a 1d manifold, is not an open subset of $\mathbb{R}^1$ and S^2 is not an open subset of $\mathbb{R}^2$, so we cannot cover them with a single chart[9] and need to work harder to find an atlas for these manifolds. The circle or the 2-sphere S^2 require a minimum of two coordinate patches. For S^2, the patches (each continuously deformable into a disk) consisting of all latitudes strictly above the Tropic of Capricorn and all latitudes strictly below the Tropic of Cancer furnish one possible atlas. These patches intersect over the tropics.

Given a manifold M, suppose a point $p \in M$ lies in the intersection of two coordinate patches so that p may be assigned the coordinates $x = (x^1, \cdots, x^n)$ or $y = (y^1, \cdots y^n)$. Then the 'transition function' from x to y is given by the equations for the coordinate transformation $y^i = y^i(x)$ and conversely $x^j = x^j(y)$ for $1 \leq i, j \leq n$. For the manifold to be smooth, both the transformation $x \mapsto y$ and its inverse $y \mapsto x$ must be smooth[10] maps between open subsets of $\mathbb{R}^n$ (see Fig. B.2a).

Refining an atlas. Given a smooth manifold (which must necessarily come with an atlas of smoothly interrelated coordinate charts), we are free to add a chart to the atlas, provided we are consistent. For instance, if the new chart with coordinate y overlaps an existing chart with coordinate x, the transformation $y = y(x)$ and its inverse must be smooth. For the Euclidean plane, the Cartesian coordinates $(x^1 \in \mathbb{R}, x^2 \in \mathbb{R})$ furnish a one-chart atlas. Suppose we wish to add a chart consisting of plane polar coordinates $(y^1 = r, y^2 = \phi)$. We can do this provided we choose the polar coordinate chart to be an open set on which the transformation to/from Cartesian coordinates is smooth. This is the case, for instance, if we choose the polar coordinate chart to be defined on $\mathbb{R}^2$ with the origin and negative horizontal axis excluded so that $y^1 = r \in (0, \infty)$ and $y^2 = \phi \in (-\pi, \pi)$. The Cartesian product $(0, \infty) \times (-\pi, \pi)$ is clearly an open subset of $\mathbb{R}^2$ continuously deformable into $\mathbb{R}^2$. Note that if we retained the negative real axis, the patch consisting of the punctured plane (plane with the origin removed) would not be continuously deformable into $\mathbb{R}^2$. In this region of overlap we have the familiar coordinate transformation $y^1 = \sqrt{(x^1)^2 + (x^2)^2}$ and $y^2 = \arctan(x^2/x^1)$ and the inverse transformation $x^1 = y^1 \cos y^2$ and $x^2 = y^1 \sin y^2$ which are both seen to be smooth. The smoothness of the transition function would fail at the origin.

---

[7] If the transition functions are continuous, we call it a C^0 manifold or a topological manifold. If they are once differentiable with a continuous derivative, we call it a C^1 manifold. More generally, we have the notion of a C^k manifold if the transition functions are continuously differentiable k times for some $k = 0, 1, 2, \ldots$.

[8] For some purposes, it is convenient to regard $\mathbb{R}^0$ as a zero-dimensional manifold with only one point. A zero-dimensional manifold is either a point or a discrete set of points. For example, the zero-dimensional sphere S^0 is the pair of points $\{-1, 1\}$ satisfying $x^2 = 1$ in $\mathbb{R}^1$.

[9] If we could cover S^1 with a single chart, the chart (and hence S^1) would be an open subset of $\mathbb{R}^1$. Note, however, that merely being an open subset of $\mathbb{R}^n$ does not mean we can cover a manifold with a single chart, since our charts are assumed to be homeomorphic to open balls. For instance, the annulus $1 < x^2 + y^2 < 2$ is an open subset of $\mathbb{R}^2$, but we need a minimum of two charts to cover it.

[10] $y^i(x)$ is smooth if partial derivatives of all orders ($\partial y^i/\partial x^j, \partial^2 y^i/\partial x^j \partial x^k, \cdots$) exist.

Maps between manifolds: homeomorphisms, diffeomorphisms. Having defined manifolds, we can now consider maps between manifolds. We will use such maps to say when two manifolds are to be considered the same. Two manifolds are topologically equivalent (or homeomorphic) if they are related by an invertible continuous map. The surface of a cube can be continuously deformed into that of a sphere, so they are homeomorphic. If two differentiable manifolds can be related via an invertible differentiable map, then they are called diffeomorphic.

To make precise the notion of a continuous, differentiable or smooth map between manifolds, we make use of the corresponding concept for maps between Euclidean spaces or open subsets thereof. So to begin with, a map $f : \mathbb{R}^p \to \mathbb{R}^q$ given by $y^i = f^i(x)$ is continuous if y^i are continuous functions of x^j. It is differentiable if all the first partials $\frac{\partial y^i}{\partial x^j}$ exist (it is continuously differentiable if these partial derivatives exist and are continuous). Finally, it is smooth if partial derivatives of all orders exist. Moving on from Euclidean spaces to manifolds, a map $\phi : M^p \to N^q$ is continuous/differentiable/smooth if in each coordinate patch, the corresponding maps between $\mathbb{R}^p$ and $\mathbb{R}^q$ are continuous/differentiable/smooth. For consistency, if coordinate patches overlap, then the individual maps should agree on the overlap.

Two manifolds M, N are said to be homeomorphic if there is a continuous bijective (one-to-one and onto) map $f : M \to N$ with continuous inverse. They are diffeomorphic if continuity is replaced with smoothness. Homeomorphic or diffeomorphic manifolds must have the same dimension and cannot be distinguished insofar as their topological/smooth structure is concerned. The circles $x^2 + y^2 = 1, x^2 + y^2 = 2$ and the ellipse $x^2 + 2y^2 = 1$ are all diffeomorphic (see Prob. B.3) as are the sphere $x^2 + y^2 + z^2 = 1$ and the ellipsoid $x^2 + y^2 + 2z^2 = 1$ or the open interval $(0, 1)$ and the real line $\mathbb{R}$ (see Prob. B.4). On the other hand, the surface of a cube is not smooth (due to the sharp edges and corners), so it is not diffeomorphic to the sphere, though the two are homeomorphic. Similarly, the surface of a sphere and that of a torus (inflated tyre tube or vadai) are not homeomorphic: one can show that there is no continuous bijection between them since the latter has a 'hole/handle' which the former lacks.

The concept of a manifold that we have defined does not possess any notion of distances between points or lengths of tangent vectors or angles between tangent vectors. To define these 'geometric' concepts we need additional structure on the manifold, such as a metric (see Appendix B.6*). At present, our manifolds are either topological manifolds (if the transition functions are continuous) or differentiable/smooth manifolds (if the transition functions are differentiable/smooth). Thus, our manifolds currently lack any geometric rigidity of shape or size. In particular, the surface of a triaxial ellipsoid ($x^2/a^2 + y^2/b^2 + z^2/c^2 = 1$ with no two among a^2, b^2, c^2 equal) and that of a round sphere ($x^2 + y^2 + z^2 = 1$) are identical as topological or smooth manifolds since they can be continuously or smoothly deformed into each other.

B.2* Submanifolds, connected and simply connected manifolds

It is tempting to think of a submanifold as a subset of a manifold M that acquires a manifold structure when charts of M are suitably restricted. However, this is a little too restrictive for some purposes. While the unit circle $x^2+y^2 = 1$ is a submanifold of the Euclidean x-y plane $\mathbb{R}^2$ in this sense, we would also like to admit the cubic curve and 3-petaled rose shown in Fig. B.3 (c) and (d) (but not the cardioid (a) and cycloid (b)) as suitable submanifolds of $\mathbb{R}^2$. On the face of it, these curves are not manifolds due to the self-intersections. However, there is a simple way to view them as images of bona fide manifolds sitting inside ('included in') the plane. Without attempting to be very precise, we outline a framework for the idea of a submanifold. Given an n-dimensional manifold M, an s-dimensional manifold S ($s \leq n$) and an 'inclusion' map $i : S \hookrightarrow M$, we can specify what we mean by immersed and embedded submanifolds. For example, S could be $\mathbb{R}$, thought of as an infinitely long (or open stretch of) rope and M could be the plane $\mathbb{R}^2$. The inclusion map is some way of laying the rope on the plane. The question is one of whether S sits inside M in a sufficiently nice way. For example, we readily admit the x-axis contained in $\mathbb{R}^2$ and the interval $(0,1) \subset \mathbb{R}$ as submanifolds. Questions arise, for instance, when the image of S in M involves sharp corners (as in the curve that looks like the character V or the cardioid and cycloid of Fig. B.3 (a) and (b)) or self-intersections (as in the curve that looks like α or the 3-petaled rose of Fig. B.3(d)). Very roughly, if the tangent to S behaves nicely (sharp corners are absent), we will say that S is an immersed submanifold while we will call it an embedding if it has neither sharp corners nor self-intersections. The manner in which S sits inside M can be encoded in properties of the inclusion map $i : S \hookrightarrow M$ which takes any point $x \in S$ to the corresponding point $i(x) \in M$. If the derivative of the inclusion map, which is the $n \times s$ Jacobian matrix of first partials, has the maximum possible rank[11] s everywhere, then S is said to be an immersed submanifold (this eliminates sharp corners but allows for self-intersections, as in the symbol α or the planar cubic curve $y^2 = x^3 + x^2$ of Fig. B.3(c)). Thus, in an immersion, the inclusion map need not be 1-1, though its derivative must be 1-1. An immersion where the inclusion map is also 1-1 (this eliminates self-intersections) is called an embedding. The n-sphere $S^n = \{\boldsymbol{x} \in \mathbb{R}^{n+1} \text{ such that } (x^1)^2 + (x^2)^2 + \cdots + (x^{n+1})^2 = 1\}$ is an embedded submanifold of $\mathbb{R}^{n+1}$ for $n = 0, 1, 2, \ldots$. An important theorem of Whitney states that essentially any smooth n-dimensional manifold M (defined as above using an atlas) can be realized as a smoothly embedded submanifold[12] of $\mathbb{R}^{2n}$.

---

[11] The row (column) rank of a matrix is the number of linearly independent rows (columns). The rank of a matrix is the larger of its row and column ranks.

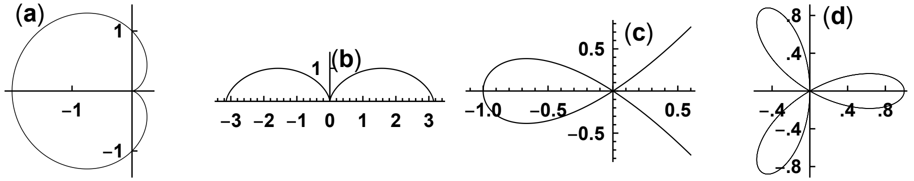

Figure B.3: Plane curves (a) cardioid $x = \cos t(1 - \cos t), y = \sin t(1 - \cos t)$ (b) cycloid $x = (t - \sin t)/2, y = (1 - \cos t)/2$ (c) cubic $y^2 = x^3 + x^2$ and (d) 3-petaled rose $r = \cos 3\theta$ given in parametric, implicit and polar forms. The cardioid and cycloid fail to be immersed submanifolds of the plane since the rank of their Jacobians drop from 1 to 0 at the sharp corners. E.g., for the cycloid, the transpose of the Jacobian is $J^t = (\dot{x}, \dot{y}) = ((1 - \cos t)/2, (\sin t)/2) = (0, 0)$ at $t = 2n\pi$ where n is an integer. The cubic curve and the rose are immersions but not embeddings: they have no sharp corners but display self-intersections. If we think of the image curve as the path traced by an ant walking on the plane, the Jacobian is the velocity vector. If the ant does not momentarily come to rest, its path may be modeled as an immersion (self-intersections occur when an ant returns to an earlier location while at a sharp corner, the ant must momentarily come to rest and abruptly change direction). If the curve is the world line of a massive particle in space-time parametrized by proper time, then it must be an embedding since the 4-velocity (4.33) cannot vanish and the world line cannot have self-intersections.

Connected and simply connected manifolds. A manifold is connected if it comes in one piece. For example, the disjoint union of two open real intervals $(0, 1) \cup (2, 3)$ is not connected. To define the concept of connectedness, we imagine a point-like ant walking on the manifold M. If it can reach any point from any other point via a continuous path $\gamma(t)$ that lies in M, then M is connected. More precisely, M is path connected if any two points $p, q \in M$ can be joined by a continuous path $\gamma : [0, 1] \to M$ with $\gamma(0) = p$ and $\gamma(1) = q$. For example, $\mathbb{R}^n$ and S^n for $n = 1, 2, 3, \ldots$ are connected. If a manifold is not path connected, then it is called disconnected. The real line punctured[13] at the origin is a disconnected manifold. For a disconnected manifold, the connected component of $p \in M$ is the submanifold consisting of points $q \in M$ that can be reached from p via continuous paths lying in M. The line punctured at the origin has two connected components $(-\infty, 0)$ and $(0, \infty)$. The connected component of the point 2 is the right half-line. Similarly, $S^0 = \{-1, 1\}$ is disconnected, it has two connected components: $\{-1\}$ and $\{1\}$. A connected manifold M is called simply connected if any nontrivial closed curve in M can be continuously deformed (shrunk) to a point while remaining in M. The two-sphere S^2 is simply connected, a rubber band on a globe can always be shrunk to a point while remaining on the globe. On the other hand, S^1, the torus, the surface of an infinite circular cylinder and the punctured plane are all connected but not simply connected (see Fig B.4).

---

[12] In favorable cases, one may be able to embed the n-dimensional manifold M in a Euclidean space of dimension less than $2n$, as is the case with $S^n \hookrightarrow \mathbb{R}^{n+1}$.

[13] To puncture the line $\mathbb{R}$ is to remove (or excise) one point from it.

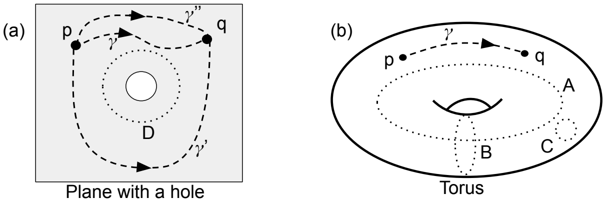

Plane with a hole

Torus

Figure B.4: (a) The plane with a hole (disk excised) is homeomorphic to the once punctured plane. Any two points p, q can be joined by a continuous path γ: it is path connected. However, it is not simply connected: the closed curve D cannot be continuously shrunk to a point. It is *multiply connected*: there are many paths from p to q that are not continuously deformable into each other: direct (γ), around the hole (γ'), winding twice around the hole, etc. Though γ is *not* homotopic to γ' (they cannot be continuously deformed into each other), γ and γ'' are homotopic to each other (a rubber band stretched from p to q along γ can be deformed to γ''). A homotopy between $\gamma, \gamma'' : [a,b] \to M$ is a continuous map $\Gamma : [a,b] \times [0,1] \to M$ with $\Gamma(t;0) = \gamma(t)$ and $\Gamma(t;1) = \gamma''(t)$. (b) The torus too is path connected but not simply connected: the closed curves A, B winding around the torus cannot be shrunk to a point, though C can. C is a *contractible* closed curve or one that is *homotopic* to a point.

B.3* Smooth functions or scalar fields

In essence, a smooth real function (or a 'scalar field') f on a smooth manifold M is a way of assigning a smoothly varying real number to each point on the manifold. They are important since the observables or dynamical variables of a mechanical system are smooth functions on the phase space manifold. More precisely, scalar fields are smooth real-valued functions of the coordinates in any given patch with the consistency condition that, when $p \in M$ lies in the intersection of coordinate patches, the value of the function at p must be the same irrespective of which coordinate system is used to describe p. In other words, if the function is described by the formulae $f(x)$ and $g(y)$ in two coordinate patches, then we must have $g(y(x)) = f(x)$ at each point p of the overlap. Sometimes, we turn this around and say that given a scalar field $f(x)$ in one coordinate system, under a change from $x \mapsto y$ given by the transformation $y = y(x)$ (and its inverse $x = x(y)$), the formula for the function becomes $F(y) = f(x(y))$. Henceforth, we will mostly take this second viewpoint and speak in terms of how objects transform under a change of coordinates in a region of overlap between two coordinate patches. The space of smooth functions on M is denoted $C^\infty(M)$ or $\mathcal{F}(M)$. If M is the phase space of a classical system, then the set of observables is given by $\mathcal{F}(M)$. It is a commutative algebra: it is closed under real linear combinations $af + bg \in \mathcal{F}$ and pointwise products $(fg)(x) = f(x)g(x) = g(x)f(x) = (gf)(x)$ for all $f, g \in \mathcal{F}(M)$, with products distributing over sums. The property $fg = gf$ encodes the fact that classical observables commute under multiplication, a feature that is not always true in the quantum theory, where observables are Hermitian operators.

B.4* Vector fields

Given local coordinates x^i in a chart on an n-dimensional manifold M, we have the notion of coordinate vector fields. These are defined as the first order partial differential operators $\frac{\partial}{\partial x^1}, \frac{\partial}{\partial x^2}, \cdots, \frac{\partial}{\partial x^n}$, which are often abbreviated ∂_{x^i} or ∂_i for $i = 1, \cdots, n$. Geometrically, we may think of the coordinate vector fields at a point p as tangent vectors to M at p. For instance, ∂_1 is the tangent vector to the coordinate curve parametrized by x^1 passing through p holding $x^2, \cdots, x^n$ fixed. As a consequence, ∂_x is a tangent vector field on the $x-y$ plane $\mathbb{R}^2$ that points rightward at every point, as shown in Fig. B.5a. These coordinate vector fields furnish a basis for more general vector fields on M. A general vector field is given by a linear combination

$$v = \sum\nolimits_{i=1}^{n} v^i(x)\frac{\partial}{\partial x^i} \equiv v^i(x)\partial_i. \tag{B.1}$$

A vector field restricted to a point $p \in M$ is called a tangent vector at p. The set of tangent vectors at p is the tangent space $T_p(M)$, a real vector space of dimension n. The coordinate tangent vectors $\partial_1, \cdots, \partial_n$ at p furnish a basis[14] for $T_p(M)$. E.g., the tangent space to the 2-sphere at a point on the equator may be visualized as a vertical tangent plane spanned by the coordinate tangent vectors $\frac{\partial}{\partial\phi}$ and $\frac{\partial}{\partial\theta}$ (see Fig. B.5b).

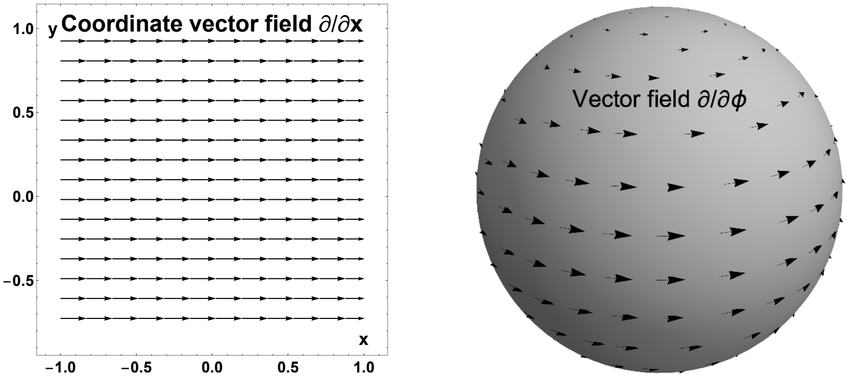

(a) (b)

Figure B.5: (a) Coordinate vector field ∂_x on the x-y plane. (b) Azimuthal coordinate vector field $\partial_\phi = -y\partial_x + x\partial_y$ on the unit sphere with the z-axis pointing vertically upwards. At the North and South poles $x = y = 0$ and $z = \pm 1$. At the poles, ∂_ϕ vanishes, they are zeros of ∂_ϕ. In fact, there is no nonvanishing smooth vector field on a sphere: loosely speaking, it is not possible to comb hair on the sphere. Here, a smooth distribution of hair combed tangent to a sphere may be regarded as a vector field on the sphere. The vector field has a zero at a bald spot where there is no hair.

The set of n functions $v^i(x)$ are called the components of v in the coordinate basis. Though each is a function within a coordinate patch, they do not transform as scalar functions under a change of coordinates. The components of a vector field have a special transformation law that follows from the chain rule in multivariable calculus. Suppose the same vector field is expressed in another coordinate system y^i:

$$v = \tilde{v}^j(y)\frac{\partial}{\partial y^j}. \tag{B.2}$$

---

[14] A *noncoordinate basis* for vector fields is a collection of n vector fields $e_1, \cdots, e_n$ that are linearly independent at each point but whose pairwise commutators $[e_i, e_j]$ are not all zero. The latter condition ensures that they are not expressible as ∂_{x^i} in any local coordinate system x^i.

Since $y = y(x)$, we may relate the two sets of coordinate vector fields via a Jacobian:

$$\frac{\partial}{\partial x^i} = \frac{\partial y^j}{\partial x^i}\frac{\partial}{\partial y^j} = J^j_i \frac{\partial}{\partial y^j} \quad \text{so that} \quad v = v^i \frac{\partial}{\partial x^i} = v^i \frac{\partial y^j}{\partial x^i}\frac{\partial}{\partial y^j}. \tag{B.3}$$

Comparing with (B.2) we find how the components of a vector field transform:

$$\tilde{v}^j(y) = v^i(x(y))\frac{\partial y^j}{\partial x^i} \quad \text{or} \quad \tilde{v}^j = J^j_i v^i. \tag{B.4}$$

Thus, the components of a vector field transform via the Jacobian matrix[15]: the new j^{th} component is a linear combination of all the old components (quite unlike how n scalar fields would transform). Such a transformation is called *contravariant*. The prefix *contra*[16] arises from the manner in which the coordinate vector fields transform, i.e., via the inverse of the Jacobian matrix[17]:

$$\frac{\partial}{\partial y^j} = \frac{\partial x^i}{\partial y^j}\frac{\partial}{\partial x^i} = (J^{-1})^i_j \frac{\partial}{\partial x^i}. \tag{B.5}$$

Thus, tangent vector fields are also called contravariant vector fields. A vector field on a smooth manifold is called smooth if the components $v^i(x)$ are smooth functions of the coordinates in each patch. The matrix elements J^j_i entering the transformation formula for v^i between overlapping coordinate patches are automatically smooth since the manifold is smooth.

A vector field v can act on a function on M and give its derivative 'along' v:

$$v(f) = v^i \frac{\partial f}{\partial x^i}. \tag{B.6}$$

$v(f)$ is a function on M and generalizes the concept of the directional derivative[18] $\boldsymbol{v} \cdot \boldsymbol{\nabla} f$ from vector calculus in $\mathbb{R}^3$. Evidently, a vector field acts linearly on the space of functions: $v(af + bg) = av(f) + bv(g)$ for any pair of scalar fields f, g and real numbers a, b. Since a vector field is a first order differential operator, v acts as a derivation on the space of functions: verify that the Leibniz rule $v(fg) = fv(g) + v(f)g$ is satisfied. Thus, we may view a vector field simply as a linear map from $\mathcal{F}(M) \to \mathcal{F}(M)$ that satisfies the Leibniz rule. The set of vector fields on M is denoted Vect(M), it is an infinite-dimensional real vector space since the coefficients

---

[15] We may view this as the product of a matrix with a column vector by regarding J^j_i as the entry in the j^{th} row and i^{th} column of a square matrix J and v^i as the element in the i^{th} row of a column vector.

[16] In Appendix B.5* we will meet covector fields. Coordinate covector fields (B.9) transform via J rather than J^{-1}, so covector fields are called *covariant*.

[17] The Jacobians for $x \mapsto y$ and $y \mapsto x$ are inverse matrices. This is seen by using the chain rule to differentiate $x^i(y(x)) = x^i$ with respect to x^k to get $\frac{\partial x^i}{\partial y^j}\frac{\partial y^j}{\partial x^k} = \delta^i_k$.

[18] $v(f)$ is also called the Lie derivative of f along v and denoted $\mathcal{L}_v f$. To find $\mathcal{L}_v f$ at a point $x_0 \in M$, we consider the integral curve $x(t)$ (B.7) of v through x_0 with $x(0) = x_0$. Then $\mathcal{L}_v f = \lim_{s\to 0}[\{f(x(s)) - f(x(0))\}/s]$.

v^i can be arbitrary smooth functions in any given patch. For instance, a large class of vector fields on the real line can be written as $\sum_{l=0}^{\infty} c_l x^l \partial_x$ where $c_0, c_1, \ldots$ are suitable real coefficients. $\text{Vect}(M)$ may also be viewed as a module[19] over the ring of functions on M: $fv + gw \in \text{Vect}(M)$ if $v, w \in \text{Vect}(M)$ and $f, g \in \mathcal{F}(M)$. In particular, we may multiply a vector field by a scalar field to get another vector field.

$*$ **Gradient of a function.** The gradient of a scalar function f is an example of a vector field. However, to define it, we need additional structure on the manifold. For instance, we may combine the notion of the differential of a function and the inverse of a metric tensor to define the gradient $(\text{grad}\, f)^i = (\boldsymbol{\nabla} f)^i = g^{ij}\partial_j f$. These concepts will be introduced in Appendix B.5* and Appendix B.6*. □

Integral curves of a vector field. Given a vector field v on a manifold, it defines a flow on the manifold. By this, we mean that there is a family of curves on M that are everywhere tangent to v. Precisely, the integral curve through the point $x_0 \in M$ is the solution $x^i(t)$ to the system of first order ODEs

$$\frac{dx^i}{dt} = v^i(x) \quad \text{with} \quad x^i(0) = x_0. \tag{B.7}$$

For examples, figures and much more on integral curves of vector fields, see Chap. 5.

Commutator of vector fields. Given a pair of differentiable vector fields on a manifold M, we may define their commutator, which is another vector field. In local coordinates, suppose $u = u^i\partial_i$ and $v = v^i\partial_i$. Then their commutator $[u, v]$ is

$$[u, v] = (u^j\partial_j v^i - v^j\partial_j u^i)\partial_i. \tag{B.8}$$

By making a change of coordinates, one may check that this first order differential operator transforms as a contravariant vector field. Given a function $f : M \to \mathbb{R}$, both $u(v(f))$ and $v(u(f))$ are functions on M. The commutator $[u, v]f$ measures the extent to which the two differ (see Prob. B.6). Notably, $u(v(f))$ and $v(u(f))$ involve both first and second order derivatives, so the composition of vector fields is not a vector field. Pleasantly, we verify that these second order derivatives cancel out in the commutator. The latter is also called the Lie bracket of vector fields since it is linear[20]

---

[19] A module over a ring is a generalization of the concept of a vector space over a field like the real or complex numbers. Here, a field is an algebraic concept distinct from the differential geometric concepts of scalar, vector and tensor fields. Multiplication, addition and division by nonzero elements are defined in a field. Elements of the ring, like those of a field can be added and multiplied in a manner satisfying the distributive law. A key difference is that not all nonzero elements of the ring may have reciprocals (multiplicative inverses) and division is therefore not defined. The integers $\mathbb{Z}$ form a ring but not a field. For the ring of functions, only those functions that are nowhere zero have reciprocals. As with vectors in a vector space, elements of a module can be multiplied (say from the left) by scalars that come from the ring, with multiplication distributing over addition. Our main example is the module of vector fields over the commutative ring of functions on a manifold. We cannot always divide a vector field by a function since the latter may have zeros. Sometimes, we may circumvent this by adding the 'point at infinity', define $1/0 = \infty$ and turn the ring of rational functions into a field.

[20] Note that $[fu, v] \neq f[u, v]$ in general for a nonconstant smooth function f, see Prob. B.8.

$[au + bv, w] = a[u, w] + b[v, w]$, antisymmetric $[u, v] + [v, u] = 0$ and satisfies the Jacobi identity $[u, [v, w]] + [w, [u, v]] + [v, [w, u]] = 0$ (Prob. B.7) for any three vector fields u, v and w and real numbers a, b. Consequently, the linear space of vector fields $\mathrm{Vect}(M)$ equipped with the commutator Lie bracket is called a real Lie algebra (see Appendix B.13* for a definition and more examples of Lie algebras). The commutator $[u, v]$ is also called the Lie derivative of v along u and is written $\mathcal{L}_u v = [u, v]$. From (B.8), we see that the Lie derivative[21] of v along u includes two contributions: the first is the 'obvious' change in v in the direction of u while the second accounts for the fact that the components of u themselves change with location. Finally, we note that given a smooth function f, the Lie derivative of a vector field satisfies the Leibniz rule: $\mathcal{L}_u(fv) = (\mathcal{L}_u f)v + f\mathcal{L}_u v$, as we verify in Prob. B.8.

B.5* Covector fields or 1-forms

Motivating examples. On the Euclidean plane, the differentials dx and dy are examples of covector fields or 1-forms. They are to be thought of as dual to the coordinate vector fields $\frac{\partial}{\partial x}$ and $\frac{\partial}{\partial y}$ via the 'pairing' $dx(\partial_x) = 1, dx(\partial_y) = 0, dy(\partial_x) = 0$ and $dy(\partial_y) = 1$ which is defined to be linear: for instance, $dx(f\partial_x + g\partial_y) = f dx(\partial_x) + g dx(\partial_y) = f(x, y)$ for any two smooth functions f and g. A general covector field is a linear combination $\phi = a(x, y)dx + b(x, y)dy$ where a and b are smooth functions. A 1-form is also called a Pfaffian differential expression after the German mathematician J F Pfaff who studied equations[22] of the form $a(x, y, z)dx + b(x, y, z)dy + c(x, y, z)dz = 0$. Physically, for a particle moving on a plane, while the velocity $\dot q(t) = \dot q^1(t)\partial_x + \dot q^2(t)\partial_y$ is a tangent vector at each point $(x(t), y(t))$ on a trajectory, the momentum $p(t) = p_1 dx + p_2 dy$ is a covector at each such point (see Sect. 3.7) on the configuration plane. Another example of a 1-form is the Liouville 1-form $pdq = p_i dq^i$. This is to be regarded as a 1-form on the phase space of a mechanical system that is furnished with canonical (Darboux) coordinates (q^i, p_j). Covector fields are also encountered on the thermodynamic state space. According to the 1st law of thermodynamics, the infinitesimal heat added to a gas is given by the action of the heat 1-form $\phi = dU + pdV$ (U, p and V are the internal energy, pressure and volume of the gas) on the tangent vector representing the infinitesimal process[23].

---

[21] It is tempting to mimic the geometric approach to the Lie derivative of a function given in Footnote 18 to define $\mathcal{L}_u v$ as the $s \to 0$ limit of a difference quotient $\{v(x(s)) - v(x(0))\}/s$, where $x(t)$ is the integral curve (B.7) of u through x_0 with $x(0) = x_0$. However, there is a difficulty since $v(x(s))$ and $v(x(0))$ live in different tangent spaces and cannot be subtracted. One needs a way to 'push' one of the vectors to the tangent space where the other lives before subtracting. This can be done using the pushforward defined in Appendix B.8*.

[22] The Pfaffian differential equation $\phi = a\,dx + b\,dy + c\,dz = 0$ is said to be integrable if it admits an integrating denominator $T(x, y, z)$ (or integrating factor $1/T$) such that $\phi/T = dS$ is an exact differential. Then $dS = 0$ and the solutions of the Pfaffian differential equation are given by $S(x, y, z) = \sigma$ for any constant σ.

[23] The thermodynamic state space is a 3d manifold with coordinates U, V, S. An infinitesimal process is represented by a tangent vector $v = a\partial_U + b\partial_V + c\partial_S$. The work done in this infinitesimal process is $pdV(v) = pb$ and the heat added is $a + pb$. Equilibrium states form a 2d hypersurface determined by an equation of state (EOS). Tangent vectors to this EOS surface

If the process is reversible, the second law postulates that $\phi = TdS$, where T and S are the absolute temperature and entropy.

Dual to tangent space. More generally, a covector field or covariant vector field or 1-form is simply a (smoothly varying) assignment of a covector at each point of a manifold. In more detail, given local coordinates x^i in a patch, we have the coordinate basis 1-forms given by the differentials of the coordinates $dx^1, \cdots, dx^n$. At a point $p \in M$, the basis 1-forms $dx^i(p)$ are said to span the cotangent space to M at p. The cotangent space is denoted $T_p^*(M)$ and is the vector space dual to the tangent space $T_p(M)$. Indeed, $\{dx^i\}$ is the dual basis to $\{\partial_i\}$ defined via the pairing $dx^i(\partial_j) = \delta^i_j$. In general, a covector field on M is a linear combination of the basis 1-forms $\phi = \phi_i(x)dx^i$. The n real-valued quantities $\phi_i(x)$ in a coordinate patch are called the components of the covector field. As with the components of a vector field, they are not scalar functions on M but satisfy a special transformation law. Indeed, suppose y^j is another local coordinate system defined on a chart that has an overlap with that of the x^i. On the overlap, the coordinate 1-forms are related by the chain rule

$$dy^j = \frac{\partial y^j}{\partial x^i} dx^i = J^j_i \, dx^i. \tag{B.9}$$

We see that coordinate 1-forms transform via the Jacobian matrix (as opposed to its inverse, as was the case for coordinate vector fields in (B.5)). For this reason, covector fields are called covariant vector fields. Now suppose the same covector field ϕ is expressed in the y basis: $\phi = \tilde{\phi}_j(y)dy^j = \tilde{\phi}_j J^j_i dx^i$. Comparing, we see that the components of a covector field transform via the inverse of the Jacobian[24]:

$$\phi_i = \tilde{\phi}_j \frac{\partial y^j}{\partial x^i} \quad \text{or} \quad \tilde{\phi}_j = (J^{-1})^i_j \phi_i. \tag{B.10}$$

Compare this with the corresponding formula (B.4) for components of a vector field. If the components of ϕ in all charts are smooth functions of the local coordinates on a smooth manifold, then ϕ is called a smooth covector field. Since covectors are dual to vectors at each point of M, covector fields are linear functions on the space of vector fields. The value of $\phi = \phi_i dx^i$ on the vector field $v = v^j \partial_j$ is the smooth function or scalar field

$$\phi(v) = \phi_i dx^i(v^j \partial_j) = \phi_i v^j dx^i(\partial_j) = \phi_i v^j \delta^i_j = \phi_i(x) v^i(x). \tag{B.11}$$

We used linearity of the action of a covector on a vector to pull the components $v^j(x)$ out. $\phi(v)$ is called the contraction of ϕ with v. More generally, for vector fields v, w,

$$\phi(fv + gw) = f\,\phi(v) + g\,\phi(w) \quad \text{for any} \quad f, g \in \mathcal{F}(M). \tag{B.12}$$

The space of covector fields on M is denoted $\Omega^1(M)$ and is dual to Vect(M) over $\mathcal{F}(M)$. In particular, if ϕ and ψ are 1-forms and f, g scalar fields, then $f\phi + g\psi$ is also a 1-form. Note that $f\phi = \phi f$, the order does not matter.

---

represent infinitesimal reversible processes.

[24] If we view $(J^{-1})^i_j$ as the entry in the i^{th} row and j^{th} column of a matrix and ϕ_i as the entry in the i^{th} column of a row vector, then this is the product (from the left) of a row vector with the square matrix J^{-1} producing the row vector with j^{th} column entry $\tilde{\phi}_j$.

On the other hand, we can also evaluate a vector field v on a 1-form ϕ to get a scalar field. In fact, since they are dual bases, we also have $\partial_i(dx^j) = \delta_i^j$ so that $v(\phi) = v^j\partial_j(\phi_i dx^i) = v^i\phi_i = \phi(v)$. This allows us to reinterpret vector fields as linear functions on the space of 1-forms. This viewpoint will soon be useful in generalizing vector fields to contravariant tensor fields.

An important class of 1-forms are **differentials of functions** on M: $\phi = df = \frac{\partial f}{\partial x^i}dx^i$. So the partial derivatives of a function should be thought of as components of a covector rather than a vector[25]. Sometimes, it is convenient to regard functions as covector fields of degree zero and call $\mathcal{F}(M)$ $\Omega^0(M)$. Thus, the differential d is a linear map (over $\mathbb{R}$) from $\Omega^0(M)$ to $\Omega^1(M)$ satisfying the Leibniz rule.

Lack of a canonical isomorphism. The tangent space $T_p(M)$ and the cotangent space $T_p^*(M)$ are both n-dimensional real vector spaces and are therefore isomorphic. However, there is no preferred or canonical isomorphism between them. If a basis, such as a coordinate basis is chosen for vector fields then one gets an isomorphism that maps ∂_i to dx^i and vice versa. However, this depends on the choice of coordinates[26]. Thus, given a smooth manifold, there is no distinguished or natural way to relate vectors to covectors, there are many ways to do this, but none of them is special. The situation changes if the manifold is equipped with a metric tensor. In this case, there is a standard way (called *lowering an index*) of mapping vectors to covectors, which does not depend on the coordinates chosen, as we will see in Appendix B.6*.

B.6* Tensors of rank two and 2-forms

Vector fields $v = v^i\partial_i$ that we encountered in Appendix B.4* are called contravariant tensor fields of rank one (or of type (1,0) as their components (v^i) have one upper index), while 1-forms introduced in Appendix B.5* are called covariant tensor fields of rank one (or of type (0,1)). More generally, one may define tensors of higher rank that find varied uses in physics and mathematics. For instance, as we will see later in this section, the metric is a symmetric tensor of rank two that is used to define lengths and angles on a manifold while the symplectic form is an antisymmetric second rank tensor on phase space that arises in Hamilton's equations.

At a point $p \in M$ lying in a patch with local coordinates x^i, we may consider the tensor product of the tangent space with itself $T_p(M) \otimes T_p(M)$. This is the space of dimension n^2 with basis consisting of $\partial_i \otimes \partial_j$ for $1 \le i, j \le n$. A type (2,0) tensor field or second rank contravariant tensor field is then a linear combination

$$t = t^{ij}(x)\partial_i \otimes \partial_j. \tag{B.13}$$

---

[25] There is a related vector field, the gradient of f, introduced in Appendix B.4*. However, it requires an inverse metric tensor for its definition $(\text{grad}\, f)^i = g^{ij}\partial_j f$. The components of *df* and grad f are numerically equal if $g^{ij} = \delta^{ij}$, see Appendix B.6*.

[26] For example, on $\mathbb{R}$ with coordinate x, we have an isomorphism mapping $dx \leftrightarrow \partial_x$. If we change to a new coordinate $y = 2x$, then $dy = 2dx$ and $\partial_y = \frac{1}{2}\partial_x$. The new isomorphism between cotangent and tangent spaces $dy \leftrightarrow \partial_y$ is *different* since it takes dx to $\frac{1}{4}\partial_x$. Thus, there are many isomorphisms between the spaces of covectors and vectors, none of which can be considered coordinate-independent or standard.

Without further ado, we note that upon changing coordinates $x \mapsto y$, the components t^{ij} transform via the Jacobian matrix, just as for contravariant vector fields, except that there are now two Jacobian factors

$$t = \tilde{t}^{kl} \frac{\partial}{\partial y^k} \otimes \frac{\partial}{\partial y^l} \quad \text{where} \quad \tilde{t}^{kl} = J_i^k J_j^l t^{ij} \quad \text{and} \quad J_i^k = \frac{\partial y^k}{\partial x^i}. \tag{B.14}$$

Just as vector fields act linearly on 1-forms to produce functions, second rank contravariant tensors act bilinearly[27] on a pair of 1-forms to produce functions:

$$t(\phi, \psi) = t^{ij} \partial_i \otimes \partial_j (\phi_k dx^k, \psi_l dx^l) = t^{ij} \phi_k \psi_l \partial_i (dx^k) \partial_j (dx^l) = t^{ij} \phi_i \psi_j. \tag{B.15}$$

Poisson tensor. A physically important example of a (2,0) tensor is the Poisson tensor on the phase space of a mechanical system: $r = r^{ij} \partial_i \otimes \partial_j$ of (3.134) and Sect. 3.26*, which has the further property of antisymmetry: $r^{ij} = -r^{ji}$. The Poisson bracket of a pair of smooth functions (observables) is the function $\{f, g\} = r(df, dg) = r^{ij} \partial_i f \partial_j g$. For a particle moving on a line, $M = \mathbb{R}^2$ with canonical coordinates $\xi = (q, p)$ and $r^{ij} = (0, 1| -1, 0)$. Given a Hamiltonian function H on phase space, the Poisson tensor allows us to define the Hamiltonian vector field V_H. It is the vector field which acts on any 1-form ϕ via $V_H(\phi) = r(\phi, dH)$. The Hamiltonian vector field defines time evolution of any observable through $\dot{f} = V_H(df)$. Trajectories on phase space are the integral curves of V_H. They are governed by the ODEs $\dot{\xi}^i = V_H^i = r^{ij} \partial_j H$. For the canonical Poisson tensor on $\mathbb{R}^2$, they reduce to Hamilton's canonical equations $\dot{\xi}^1 = \dot{q} = r^{12} \partial_2 H = \frac{\partial H}{\partial p}$ and $\dot{\xi}^2 = \dot{p} = r^{21} \partial_1 H = -\frac{\partial H}{\partial q}$. $\square$

Similarly, we have covariant tensor fields of rank two or tensors of type (0,2):

$$t = t_{ij} dx^i \otimes dx^j, \tag{B.16}$$

which are linear combinations of the tensor products of the coordinate basis covector fields. Such a tensor transforms via two factors of the inverse Jacobian:

$$\tilde{t}_{kl} = (J^{-1})_k^i (J^{-1})_l^j \, t_{ij}. \tag{B.17}$$

In summary, each upper index on a tensor transforms via J and each lower one via J^{-1}. Covariant tensors of rank two can act on a pair or vector fields and produce a scalar function, they are bilinear maps from Vect(M)× Vect(M) to $\mathcal{F}(M)$.

Metric tensor. An important example of a 2nd rank covariant tensor field is the metric tensor $g = g_{ij} dx^i \otimes dx^j$, which has the further property of being symmetric $g_{ij} = g_{ji}$ and nondegenerate [g_{ij} an invertible matrix]. A metric allows us to generalize the concept of the dot product of vectors in Euclidean space to tangent vectors at a point p on a manifold M. We have encountered it as the mass metric in a Lagrangian quadratic in velocities (3.42). A metric is called Riemannian if g_{ij} is a positive-definite matrix at every point on the manifold. If the positive-definiteness condition is dropped, it is called pseudo-Riemannian (this case includes the Lorentzian metric tensor of space-time; e.g., Minkowski space of Sect. 4.10* in Cartesian coordinates $x^\mu = (ct, x, y, z)$ has the metric given by the constant diagonal matrix $g_{\mu\nu} = \mathrm{diag}(1, -1, -1, -1)$ where $\mu, \nu = 0, 1, 2, 3$). A virtue of an invertible metric tensor is that it defines an isomorphism from vectors to covectors: $v \mapsto v'$ where $v'_i = g_{ij} v^j$. The inverse metric with components g^{ij} maps covectors to vectors $g^{ij} v'_j = v^i$. Thus, on a Riemannian manifold, the tangent and cotangent spaces are canonically isomorphic. We say that the metric and its inverse can be used to lower and raise indices. In particular, we may use the inverse metric g^{ij} to define the *gradient of a function* (see Appendix B.4*) by raising the index of the components of the 1-form df: $(\mathrm{grad}\, f)^i = (\boldsymbol{\nabla} f)^i = g^{ij} \partial_j f$.

---

[27] $t(\phi, \psi)$ is bilinear if it is linear in *both* the entries. For instance, $t(f\phi_1 + g\phi_2, \psi) = ft(\phi_1, \psi) + gt(\phi_2, \psi)$ for any functions f, g and 1-forms ϕ_1, ϕ_2, ψ. Bilinearity is a consequence of the definition of a dual space: vector fields are dual to 1-forms and act linearly on 1-forms (as discussed in Appendix B.5*). So pairs of vectors fields (written as a tensor product $\partial_i \otimes \partial_j$) act linearly on pairs of 1-forms (ϕ, ψ).

A metric tensor gives a manifold a rigid geometric shape[28]. The square of the length of the vector $v = v^i \partial_i \in T_p M$ is defined as

$$g(v, v) = g_{ij} dx^i \otimes dx^j (v^k \partial_k, v^l \partial_l) = g_{ij} v^i v^j. \tag{B.18}$$

Given a pair of tangent vectors $u, v \in T_p M$, their inner product (see Footnote 43 in Sect. 3.9) is defined as $g(u, v) = g_{ij} u^i v^j$. The cosine of the angle between them is $g(u, v)/\sqrt{g(u, u) g(v, v)}$. See Sect. 3.27* for how a metric is used to define lengths of curves and the notion of geodesics. □

Two-forms. An antisymmetric second rank covariant tensor is called a 2-form. To make the antisymmetry manifest, one defines the wedge product[29]

$$dx^i \wedge dx^j = dx^i \otimes dx^j - dx^j \otimes dx^i \tag{B.19}$$

and writes a 2-form with antisymmetric components ω_{ij} as (show the 2^{nd} equality!)

$$\omega = \omega_{ij} dx^i \otimes dx^j = \frac{1}{2} \omega_{ij} dx^i \wedge dx^j. \tag{B.20}$$

Note that $dx^1 \wedge dx^1 = 0$, etc. Geometrically, two-forms are related to area elements in a manifold. The familiar area 'element' $dx\, dy$ on a plane is more precisely the 2-form

---

[28] The surface of a round sphere and an ellipsoid are diffeomorphic, they have the same topology. However, they differ geometrically: notions of lengths of tangent vectors and angles between them differ. When the distances between corresponding points on two diffeomorphic manifolds are the same, the notions of lengths and angles are preserved and the two manifolds are said be isometric (have the same geometry). This happens when the diffeomorphism preserves the metric tensor. A page of a book and a cylinder are isometric since the page can be bent into a cylinder without stretching or tearing.

[29] The wedge product can be written as a sum over permutations of two objects: $dx^1 \wedge dx^2 = \sum_{\sigma \in S_2} \mathrm{sgn}(\sigma) dx^{\sigma(1)} \otimes dx^{\sigma(2)}$. Here S_2 is the permutation or symmetric group consisting of two elements, the identity ($\sigma(1) = 1, \sigma(2) = 2$) and the exchange transposition ($\sigma(1) = 2, \sigma(2) = 1$). $\mathrm{sgn}(\sigma)$ is the sign of the permutation: -1 to the power of the number of pairwise transpositions needed to write σ as a product of exchanges. The identity has sign $+1$ and the exchange has sign -1.

$dx \wedge dy$. The antisymmetry of the wedge product allows us to encode the orientation of the area element, which in vector calculus is conveyed by the inward/outward normal in an 'infinitesimal area vector' $dx\, dy\, \hat{\boldsymbol{n}}$ on a surface parametrized by x and y. Moreover, as explained in Footnote 98 of Sect. 3.25*, in Euclidean space $\mathbb{R}^3$ with Cartesian coordinates, the components of the wedge product of 1-forms df and dg are related to those of the cross product $\boldsymbol{\nabla} f \times \boldsymbol{\nabla} g$ whose magnitude measures the area of a parallelogram.

The space of 2-forms is denoted $\Omega^2(M)$. Recall that functions can also be regarded as 0-forms and that we could go from functions to 1-forms by taking the differential: $df = (\partial_i f) dx^i$. The differential of a function is also called its exterior derivative. Interestingly, there is a similar way of going from 1-forms to 2-forms by (exterior) differentiation. Given a 1-form $\phi = \phi_j dx^j$, we *define* its exterior derivative

$$\omega = d\phi = d\phi_j \wedge dx^j, \tag{B.21}$$

which is a 2-form. To find its components we write

$$d\phi = \frac{\partial \phi_j}{\partial x^i} dx^i \wedge dx^j = \frac{1}{2}(\partial_i \phi_j - \partial_j \phi_i) dx^i \wedge dx^j \quad \text{whence} \quad \omega_{ij} = \partial_i \phi_j - \partial_j \phi_i. \tag{B.22}$$

We used the antisymmetry of the wedge product in the second step, relabelled indices and used the definition (B.20) to identify the antisymmetric tensor ω_{ij}.

However, unlike ordinary differentiation that can be done repeatedly to produce higher order derivatives of a function, the square of the exterior derivative vanishes[30]. Indeed, using the definition in (B.21), the exterior derivative of the 1-form df is

$$d(df) = d(\partial_j f) dx^j = (\partial_i \partial_j f) dx^i \wedge dx^j = 0. \tag{B.23}$$

Here $\partial_i \partial_j f$ is symmetric under $i \leftrightarrow j$ exchange due to the equality of mixed partials, while the wedge product $dx^i \wedge dx^j$ is antisymmetric, so the sum vanishes. Thus, $d^2 f = 0$. This identity is a generalization of the vector identity $\boldsymbol{\nabla} \times (\boldsymbol{\nabla} f) = 0$ valid for real-valued functions on Euclidean space $\mathbb{R}^3$.

Just as a 1-form acts linearly on vector fields to produce functions $\phi(v) = \phi_i v^i$, a 2-form acts as a skew-symmetric bilinear map from pairs of vector fields to $\mathcal{F}(M)$:

$$\omega(u, v) = \omega_{ij} dx^i \otimes dx^j (u^k \partial_k, v^l \partial_l) = \omega_{ij} dx^i (u^k \partial_k) dx^j (v^l \partial_l) = \omega_{ij} u^i v^j. \tag{B.24}$$

Here, the 1st (2nd) factor in a tensor product acts on the 1st (2nd) entry of the ordered pair (u, v). We used linearity of the action of forms on vector fields (B.11) and the pairing $dx^i(\partial_k) = \delta^i_k$.

A 2-form can be used to define an area for infinitesimal parallelograms in each tangent space to a manifold. For example, if ∂_i, ∂_j are two coordinate tangent vectors at x, then the area of the parallelogram they span is defined as $\omega(\partial_i, \partial_j) = \omega_{ij}(x)$.

---

[30] We say that the exterior derivative is nilpotent of degree two: $d^2 = 0$

Physical examples of 2-forms. (i) An interesting example of a 2-form is the electromagnetic field strength tensor F, which is a 2-form on the 4-dimensional Minkowski space-time of Sect. 4.10*. It is the exterior derivative of the 1-form 'gauge potential':

$$A = A_\mu dx^\mu \quad \text{and} \quad F = dA = \frac{1}{2} F_{\mu\nu} dx^\mu \wedge dx^\nu \quad \text{where} \quad F_{\mu\nu} = \partial_\mu A_\nu - \partial_\nu A_\mu \tag{B.25}$$

as in (B.22). Here $\mu, \nu = 0,1,2,3$ and $A_\mu = (\phi, -\boldsymbol{A})$ is a combination of the scalar and vector potentials of electrodynamics introduced in Sect. 3.23*. In Prob. B.12 we show that the electric and magnetic fields appear as the components of F. (ii) An example of a 1-form in mechanics is the so-called canonical or Liouville 1-form on the $2n$-dimensional phase space $M = \mathbb{R}^{2n}$ of a system with n-degrees of freedom:

$$\alpha = p_i dq^i = p_1 dq^1 + p_2 dq^2 + \cdots + p_n dq^n. \tag{B.26}$$

As in (3.133), $\xi = (q^1, \cdots, q^n, p_1, \cdots p_n)$ together furnish coordinates on M. Notice that α has no components along the dp_i. Its exterior derivative is a 2-form

$$\begin{aligned} \omega &= d\alpha = dp_i \wedge dq^i = -dq^i \wedge dp_i = -(dq^1 \wedge dp_1 + \cdots + dq^n \wedge dp_n) \\ &= \frac{1}{2}(-dq^1 \wedge dp_1 - \cdots - dq^n \wedge dp_n + dp_1 \wedge dq^1 + \cdots + dp_n \wedge dq^n). \end{aligned} \tag{B.27}$$

From this we may read off the antisymmetric components of $\omega = \frac{1}{2}\sum_{a,b=1}^{2n} \omega_{ab} d\xi^a \wedge d\xi^b$. The only nonzero ones are:

$$\omega_{i,n+i} = -1 \quad \text{and} \quad \omega_{n+i,i} = 1 \quad \text{for} \quad i = 1, 2, \ldots, n. \tag{B.28}$$

Comparing with (3.145), we see that ω is the canonical symplectic 2-form (the inverse of the canonical Poisson tensor $\omega_{ab} r^{bc} = \delta_a^c$). For 1 degree of freedom, $\alpha = p dq$ and

$$\omega = \frac{1}{2}(-dq \wedge dp + dp \wedge dq) = \frac{1}{2}(\omega_{11} dq \wedge dq + \omega_{12} dq \wedge dp + \omega_{21} dp \wedge dq + \omega_{22} dp \wedge dp) \tag{B.29}$$

so that $\omega_{12} = -\omega_{21} = -1$ and $\omega_{11} = \omega_{22} = 0$ and $\omega = \left(\begin{smallmatrix} 0 & -1 \\ 1 & 0 \end{smallmatrix}\right)$. Referring back to our discussion of the Poisson tensor earlier in this section, we observe that given a Hamiltonian function H on phase space, the Hamiltonian vector field is defined via $\omega(\cdot, V_H) = dH(\cdot)$. In components, $\omega_{ab} V_H^b = \partial_a H$ or inverting, $V_H^c = r^{ca} \partial_a H$.

Mixed second rank tensors. Aside from contravariant and covariant tensors, we also have mixed second rank tensors[31] of type (1,1): $t = t^i_j \partial_i \otimes dx^j$. They transform via one Jacobian and one inverse Jacobian factor: $\tilde{t}^k_l = J^k_i (J^{-1})^j_l t^i_j$. A (1,1) tensor restricted to a point $p \in M$ can be viewed as a linear transformation on the tangent space $T_p(M)$. Indeed, contracting it with a tangent vector gives another tangent vector:

$$t(\cdot, v) = t^i_j \partial_i(\cdot) dx^j (v^k \partial_k) = t^i_j v^j \partial_i(\cdot) \quad \text{or} \quad v^i \mapsto v'^i = t^i_j v^j. \tag{B.30}$$

---

[31] We have arbitrarily chosen to place the ∂_i ahead of the dx^j in the tensor product. The opposite order can also be followed throughout.

The $\cdot$ is a placeholder for an unspecified 1-form that t could act on via the first slot. Similarly, $t^i_j v^j \partial_i(\cdot)$ is the action of a vector field on an unspecified 1-form. The components t^i_j of a (1,1) tensor define a matrix in the coordinate basis, and the above transformation rule written in matrix notation, $\tilde{t} = JtJ^{-1}$ is just a similarity transformation!

B.7* Higher rank tensor fields and forms

More generally, we have tensor fields of type (p, q) for $p, q \geq 0$ which, in local coordinates, are given by the linear combinations

$$t = t^{i_1 \cdots i_p}_{j_1 \cdots j_q} \partial_{i_1} \otimes \cdots \otimes \partial_{i_p} \otimes dx^{j_1} \otimes \cdots \otimes dx^{j_q}. \tag{B.31}$$

Their components transform via p factors of J for upper indices and q factors of J^{-1} for lower indices. Such a tensor field can act linearly on p one-forms and q vector fields to produce a function: $t(\phi, \psi, \cdots, u, v, \cdots) = t^{i_1 \cdots i_p}_{j_1 \cdots j_q} \phi_{i_1} \psi_{i_2} \cdots u^{j_1} v^{j_2} \cdots$. Thus, algebraically, (p, q) tensor fields are simply multilinear maps from p copies of $\Omega^1(M)$ and q copies of Vect(M) to the space of scalar functions on M. For instance, $t(f\phi_1 + g\phi_2, \ldots) = ft(\phi_1, \ldots) + gt(\phi_2, \ldots)$ for any scalar functions f and g.

Of particular importance are the p-forms, which are covariant antisymmetric tensor fields[32] of rank p (or of type $(0, p)$),

$$\omega = \omega_{i_1 \cdots i_p} dx^{i_1} \otimes \cdots \otimes dx^{i_p}. \tag{B.32}$$

Antisymmetry means the components are antisymmetric under interchange of *any* pair of indices. As a consequence, a p-form on an n dimensional manifold must be identically zero if $p > n$ (at least one basis 1-form must appear twice in the tensor product, which when contracted with an antisymmetric coefficient, must vanish). Forms can be written as linear combinations of p-fold wedge products of coordinate 1-forms, which are obtained by antisymmetrizing the p-fold tensor product:

$$\omega = \frac{1}{p!} \omega_{i_1 \cdots i_p} \, dx^{i_1} \wedge \cdots \wedge dx^{i_p}. \tag{B.33}$$

For instance, a three-fold wedge product is a sum over all permutations of three objects (which comprise the symmetric group[33] S_3) weighted by the signs of the permutations

---

[32] We may take linear combinations of p-forms ω, ψ: $f\omega + g\psi$ for any smooth functions f, g to produce other p-forms. The space of p-forms is denoted $\Omega^p(M)$.

[33] The symmetric group on 3 letters (Appendix B.13*) has $3! = 6$ elements. The identity $\sigma(i) = i$ denoted $(1)(2)(3)$ has sign 1. There are three pairwise transpositions $(12)(3)$, $(1)(23)$ and $(2)(31)$ which have sign -1. For example (23) means 2 and 3 are mapped to each other. Thus, $(1)(23)$ means $\sigma(1) = 1, \sigma(2) = 3, \sigma(3) = 2$. There are also two cyclic permutations $(123) = (12)(23)$ and $(132) = (12)(13)$ which have been written as products of pairwise exchanges composed from right to left. Here (132) means $\sigma(1) = 3, \sigma(3) = 2$ and $\sigma(2) = 1$. In the composition $(12)(13)$, 3 is mapped to 1 which is then mapped to 2, so that 3 is on the whole mapped to 2. On the other hand, 2 is directly mapped to 1. The cyclic permutations have sign $+1$ as they are products of an even number of transpositions. See also Footnote 29.

(see Footnote 29):

$$\begin{aligned} dx^1 \wedge dx^2 \wedge dx^3 &= \sum\nolimits_{\sigma \in S_3} \operatorname{sgn}(\sigma)\, dx^{\sigma(1)} \otimes dx^{\sigma(2)} \otimes dx^{\sigma(3)} \\ &= dx^1 \otimes dx^2 \otimes dx^3 - dx^2 \otimes dx^1 \otimes dx^3 - dx^1 \otimes dx^3 \otimes dx^2 \\ &- dx^3 \otimes dx^2 \otimes dx^1 + dx^2 \otimes dx^3 \otimes dx^1 + dx^3 \otimes dx^1 \otimes dx^2. \end{aligned} \tag{B.34}$$

An example of a 3-form on $\mathbb{R}^3$ is the **Euclidean volume form** whose components in Cartesian coordinates are given in terms of the Levi-Civita symbol:

$$\Omega = \frac{1}{3!}\epsilon_{ijk} dx^i \wedge dx^j \wedge dx^k. \tag{B.35}$$

Combining the six nonzero terms using the antisymmetry of the wedge product, we verify in Prob. B.15 that Ω is simply the familiar volume element $\Omega = dx^1 \wedge dx^2 \wedge dx^3$. The Levi-Civita symbol generalizes to $\mathbb{R}^n$: $\epsilon_{i_1 \cdots i_n}$ is antisymmetric under every exchange of indices and satisfies $\epsilon_{12\cdots n} = 1$. For example, on $\mathbb{R}^2$ with Cartesian coordinates $x^i = (x, y)$, we have the volume form $\Omega = \frac{1}{2}\Omega_{ij} dx^i \wedge dx^j$ where $\Omega_{ij} = \epsilon_{ij}$. Thus $\Omega = dx \wedge dy$. Now suppose we change to polar coordinates $\tilde{x}^i = (r, \theta)$ via $x = r\cos\theta, y = r\sin\theta$. Then the inverse Jacobian is $(J^{-1})^k_i = \frac{\partial x^k}{\partial \tilde{x}^i} = (x/r, -y|y/r, x)$. The components of Ω in the new coordinates are $\tilde{\Omega}_{ij} = (J^{-1})^k_i (J^{-1})^l_j \Omega_{kl}$. One finds $\tilde{\Omega}_{ij} = (0, r| - r, 0)$ so that the volume form in polar coordinates is $\Omega = \frac{1}{2}(r dr \wedge d\theta - r d\theta \wedge dr) = r dr \wedge d\theta$. We notice that the prefactor r is $\det J^{-1}$. This is generally true: volume elements transform via a Jacobian determinant.

$*$ **Levi-Civita tensor density.** In Prob. 3.48 (see also Sect. 3.13*), we defined the Levi-Civita symbol to have the same components in any coordinate system. Suppose $x^i \to \tilde{x}^i$, is a change of coordinates, then $\tilde{\epsilon}_{ijk} = \epsilon_{ijk}$. What is more, for any invertible matrix A, we have the identity (see Prob. B.16)

$$\epsilon_{ijk} = \det A^{-1}\, A^l_i A^m_j A^n_k\, \epsilon_{lmn}. \tag{B.36}$$

Applying this to the inverse Jacobian matrix $A = J^{-1}$ where $(J^{-1})^l_i = \frac{\partial x^l}{\partial \tilde{x}^i}$, we get

$$\tilde{\epsilon}_{ijk} = \epsilon_{ijk} = \det\left(\frac{\partial \tilde{x}^a}{\partial x^b}\right) \frac{\partial x^l}{\partial \tilde{x}^i} \frac{\partial x^m}{\partial \tilde{x}^j} \frac{\partial x^n}{\partial \tilde{x}^k} \epsilon_{lmn}. \tag{B.37}$$

If the determinant did not appear on the right, ϵ_{ijk} would transform as the components of a $(0, 3)$ tensor. To account for the first power of the Jacobian determinant, we say that ϵ_{ijk} transform as the components of a tensor density of weight 1. □

B.8* Pushforward and pullback of tensors

Given a pair of smooth manifolds X and Y with dimensions n and n' and a smooth map $\phi : X \to Y$, we may, in favorable cases, use ϕ to move tensor fields between the manifolds. This finds application, for instance, in deducing the induced metric on a submanifold embedded in Euclidean space. However, moving tensors only works in certain directions. Forms and more generally covariant tensor fields on Y may be 'pulled back' to X, the pullback being denoted ϕ^*. On the other hand, vector fields (and more generally contravariant tensor fields) on X may, in some cases, be 'pushed forward' to Y via ϕ_*. Combining these, if ϕ is a diffeomorphism (*invertible* smooth map with smooth inverse) then the pullback and pushforward via ϕ and ϕ^{-1} may be used to move arbitrary tensor fields in either direction.

Pullback. The simplest tensor field is a scalar function. Given a smooth function $f : Y \to \mathbb{R}$, its pullback is the function $\phi^* f : X \to \mathbb{R}$ defined as $(\phi^* f)(x) = f(\phi(x))$ for any $x \in X$. In other words, we simply compose f with ϕ to go from X to $\mathbb{R}$ in two steps, $\phi^* f : X \xrightarrow{\phi} Y \xrightarrow{f} \mathbb{R}$. For example, suppose $\phi : S^2 \to \mathbb{R}^3$ is the map $\phi(\theta, \varphi) = (x = \sin\theta\cos\varphi, y = \sin\theta\sin\varphi, z = \cos\theta)$ and let $f(x, y, z) = z$ be the height function. Then the pullback $(\phi^* f)(\theta, \varphi) = \cos\theta$ is the function that assigns the cosine of the polar angle to any point on the sphere. On the other hand, it is generally not possible to define the pushforward of a function. For this reason, we will view scalar functions as covariant (rather than contravariant) tensors of rank zero.

More generally, the gadget that helps us do this pushing and pulling is the linearization or differential $d\phi$ of the map ϕ. Suppose x^i and y^j are local coordinates on X and Y and $y = \phi(x)$ or $y^j = \phi^j(x)$. Then the linearization at the point x is represented by the $n' \times n$ Jacobian matrix with entries $\frac{\partial \phi^j}{\partial x^i}$. Next, given a 1-form $\omega_j dy^j$ on Y we define its pullback at a point $x \in X$, denoted $(\phi^*\omega)(x)$ via

$$(\phi^*\omega)_i(x) = \frac{\partial \phi^j}{\partial x^i}\omega_j(\phi(x)). \tag{B.38}$$

Notice that no assumption on the invertibility of ϕ has been made. This suggests why it is not possible, in general, to pushforward a differential form. If ϕ is invertible (say when $X = Y$ and ϕ is a diffeomorphism), we may multiply by the inverse Jacobian and formally recover the coordinate transformation formula of (B.10). However, there is a conceptual difference: while a map $\phi : X \to X$ actively moves points around, a coordinate transformation only relabels them. The generalization to the pullback of covariant rank-p tensor fields (including p-forms) is:

$$(\phi^*\omega)_{i_1\cdots i_p}(x) = \frac{\partial \phi^{j_1}}{\partial x^{i_1}} \cdots \frac{\partial \phi^{j_p}}{\partial x^{i_p}}\omega_{j_1\cdots j_p}(\phi(x)). \tag{B.39}$$

Evidently, the pullback of a smooth function is the special case when $p = 0$.

Pushforward. Pushing forward vector fields or contravariant tensors is not so straightforward. To begin with, we note that the linearization of ϕ defines a linear transformation $d\phi$ between tangent spaces. If $y = \phi(x)$, then $d\phi(x) : T_x X \to T_y Y$. Once coordinates are chosen, this map is represented by the $n' \times n$ Jacobian matrix. Now if $v = v^i \partial_{x^i} \in T_x X$, then it is natural to define its pushforward to be the image of the vector v under the linear transformation $d\phi$. Thus, we are tempted to define the pushforward $\phi_* v$ as the vector field whose components at $y = \phi(x)$ are given by

$$(\phi_* v)^j(y) = \frac{\partial \phi^j}{\partial x^i} v^i(x) \quad \text{for} \quad j = 1, 2, \ldots, n'. \tag{B.40}$$

Note that if ϕ is not surjective (say, if $n' > n$) then this does not define a vector field on all of Y. Nevertheless, we can try to define a pushforward vector field on the image

$\phi(X) \subset Y$. However, there is a further difficulty with (B.40): suppose ϕ is many to one with $y = \phi(x_1) = \phi(x_2)$. Then it may happen that the Jacobians $\frac{\partial \phi^j}{\partial x^i}$ at x_1 and x_2 are not the same giving rise to an ambiguity in the definition of the vector field. This difficulty does not arise when ϕ is one-to-one and we can write $x = \phi^{-1}(y)$ on the RHS of (B.40) to arrive at a pushforward vector field $\phi_* v$ on $\phi(X)$. See Prob. B.17 for a simple example. The definition has a straightforward generalization to rank p contravariant tensor fields for any $p = 1, 2, \ldots$:

$$(\phi_* t)^{j_1 \cdots j_p}(y) = \frac{\partial \phi^{j_1}}{\partial x^{i_1}} \frac{\partial \phi^{j_2}}{\partial x^{i_2}} \cdots \frac{\partial \phi^{j_p}}{\partial x^{i_p}} t^{i_1 \cdots i_p}(x). \tag{B.41}$$

As before, we notice the formal similarity with the coordinate transformation laws [e.g., (B.14)] for contravariant tensor fields when X and Y are the same manifold. What is more, if ϕ is a diffeomorphism then it is both injective and surjective so that (B.41) unambiguously defines a pushforward tensor field on all of Y.

Pullback of a metric: induced metric via an example. Consider the unit sphere S^2 ($x^2 + y^2 + z^2 = 1$) embedded as a submanifold of $\mathbb{R}^3$. If we use polar coordinates ($\xi^1 = \theta, \xi^2 = \varphi$) on S^2, the embedding is defined by a smooth map $\phi : S^2 \to \mathbb{R}^3$ given by $\phi(\theta, \varphi) = (x = \sin\theta\cos\varphi, y = \sin\theta\sin\varphi, z = \cos\theta)$. Now, $\mathbb{R}^3$ has the standard flat Euclidean metric whose components in Cartesian coordinates are $g_{ij} = \delta_{ij}$. We may pullback this rank-2 covariant symmetric tensor field to get an 'induced' metric h_{ab} on S^2 with components

$$h_{ab} = (\phi^* g)_{ab} = \frac{\partial \phi^i}{\partial \xi^a} \frac{\partial \phi^j}{\partial \xi^b} g_{ij}. \tag{B.42}$$

This formula defines the induced metric and is of course not special to the above example. In the case of the embedding $\phi : S^2 \hookrightarrow \mathbb{R}^3$, the induced metric $h_{ab}(\theta, \varphi)$ is the familiar 'round sphere' metric. Its components are obtained in Prob. B.19.

B.9* Exterior algebra, exterior derivative and Bianchi's identity

Exterior algebra. In Appendix B.5* and Appendix B.6*, we introduced 1- and 2-forms. One-forms can be used to describe the momentum of a particle on the configuration space of a mechanical system, the Liouville form '$p\, dq$' on phase space, the infinitesimal heat added to a gas in a thermodynamic process or the electromagnetic 'scalar' and 'vector' potentials. Two-forms are used to model infinitesimal area elements, the electromagnetic field strength tensor $F_{\mu\nu}$ and the symplectic form ω_{ij} in mechanics. Furthermore, the wedge product of two 1-forms was seen to produce a 2-form. On the other hand, the differential or exterior derivative of a function df was shown to give a 1-form, while the exterior derivative of a 1-form led to a 2-form. In this section, we extend the wedge product and exterior derivative to forms of any rank (introduced in Appendix B.7*) and also discuss an analog of the Leibniz rule for the exterior derivative of a wedge product. The space of differential forms with these algebraic properties is called the exterior algebra. These developments are then applied to understand some properties of the symplectic form ω of Hamiltonian mechanics introduced in (3.144) and (B.27) and further discussed in Sect. 3.26*.

Recall from Appendix B.7*, that a differential form of order $p = 0, 1, 2, \ldots$ or p-form ω in a patch with coordinates x^i is a linear combination of p-fold wedge products of coordinate 1-forms:

$$\omega = \frac{1}{p!}\omega_{i_1\cdots i_p} dx^{i_1} \wedge \cdots \wedge dx^{i_p}. \tag{B.43}$$

Given any smooth p-forms ω, ψ and smooth functions f, g, $f\omega + g\psi$ is also a smooth p-form. Thus, the space of p-forms denoted $\Omega^p(M)$ is said to be a module (see Footnote 19) over the ring of smooth real-valued functions on M ($\mathcal{F}(M)$ of Appendix B.3*).

Owing to the antisymmetry of $dx^{i_1} \wedge \cdots \wedge dx^{i_p}$ there are no nonzero p forms for $p > n$ on a manifold of dimension n. For instance on $\mathbb{R}$, there is only one coordinate 1-form dx and the only possible coordinate basis 2-form $dx \wedge dx$ vanishes by antisymmetry (there is no concept of area on a line). On $\mathbb{R}^2$, we have two coordinate basis 1-forms dx and dy, one independent basis 2 form $dx \wedge dy = -dy \wedge dx$ and no nonzero 3-forms as $dx \wedge dy \wedge dx$, etc., all vanish. In fact, the number of linearly independent p-forms at a point is the binomial coefficient $\binom{n}{p}$ since each choice of p distinct coordinate 1-forms $dx^{i_1}, \ldots, dx^{i_p}$ furnishes one coordinate basis p-form $dx^{i_1} \wedge \ldots \wedge dx^{i_p}$. In particular, there is only one ($= \binom{n}{0}$) independent 0-form and one ($= \binom{n}{n}$) independent n-form. What we mean is that any 0-form is some smooth function times the constant function 1 and any n-form is some smooth function times the volume form $dx^1 \wedge \cdots \wedge dx^n$.

We may take the direct sum of the spaces of p-forms to obtain the $\sum_{p=0}^{n} \binom{n}{p} = 2^n$ dimensional space of all differential forms on M:

$$\Omega(M) = \oplus_{p=0}^{n} \Omega^p(M). \tag{B.44}$$

In addition to taking linear combinations of forms, we may take their wedge product. For the coordinate basis forms

$$(dx^{i_1} \wedge \cdots \wedge dx^{i_p}) \wedge (dx^{i_{p+1}} \wedge \cdots \wedge dx^{i_{p+q}}) = dx^{i_1} \wedge \cdots \wedge dx^{i_{p+q}}. \tag{B.45}$$

For example, $(dx \wedge dy) \wedge (dz \wedge dw) = dx \wedge dy \wedge dz \wedge dw$. By repeated use of the antisymmetry property $dx^i \wedge dx^j = -dx^j \wedge dx^i$, we may show that the wedge product of a p-form ω and a q-form ψ is (anti)commutative:

$$\omega \wedge \psi = (-1)^{pq} \psi \wedge \omega. \tag{B.46}$$

Let us explain the origin of the sign. Suppose $\omega = dx$ and $\psi = dy \wedge dz$ so that $p = 1$ and $q = 2$. Then dx has to 'pass through' dy and dz producing two minus signs resulting in $dx \wedge (dy \wedge dz) = (-1)^{1\cdot 2}(dy \wedge dz) \wedge dx$. Similarly, suppose we consider $(dx \wedge dy) \wedge (du \wedge dv \wedge dw)$. Here we move dy first through the 3-form picking up a $(-1)^3$ and then move dx and get another $(-1)^3$. Thus we see the emergence of p factors of $(-1)^q$ leading to the sign $(-1)^{pq}$.

Equipped with this wedge product, $\Omega(M)$ is called the exterior algebra. A special case is the wedge product of a p-form ω and a 0-form f: $\omega \wedge f = (-1)^0 f \wedge \omega = f\omega$.

Exterior derivative. The exterior derivative may be extended to a map from p-forms to $(p+1)$-forms: $d : \Omega^p(M) \to \Omega^{p+1}(M)$ for any $p = 0, 1, 2, \ldots$ satisfying the three axioms:

1. Linearity: $d(a\omega + b\psi) = ad\omega + bd\psi$ for any $a, b \in \mathbb{R}$ and p-forms ω, ψ.
2. Leibniz (antiderivation) rule: $d(\omega \wedge \phi) = d\omega \wedge \phi + (-1)^p \omega \wedge d\phi$ where $\omega \in \Omega^p(M)$ and ϕ is any form.
3. Nilpotent[34] of degree two: $d^2\omega = 0$ for any p-form ω.

The need for the minus sign in this Leibniz rule is already evident if we consider the wedge product of a 1-form $\phi = \phi_j dx^j$ and a zero form f. Now $\phi \wedge f = f \wedge \phi = f\phi$. We will calculate $d(\phi \wedge f)$ from first principles and see the emergence of the minus sign. In fact, using $d\phi = \partial_i \phi_j dx^i \wedge dx^j$, we get

$$\begin{aligned} d(\phi \wedge f) &= d(f\phi) = \partial_i(f\phi_j) dx^i \wedge dx^j = ((\partial_i f)\phi_j + f\partial_i \phi_j)\, dx^i \wedge dx^j \\ &= df \wedge \phi + f d\phi = -\phi \wedge df + d\phi \wedge f = d\phi \wedge f - \phi \wedge df. \end{aligned} \quad \text{(B.47)}$$

Closed and exact forms on a manifold M. A p-form ω such that $d\omega = 0$ is said to be closed. On the other hand, if $\omega = d\phi$ for some $(p-1)$-form ϕ, then ω is said to be exact (generalizing the idea of an exact differential). Since $d^2 = 0$, an exact form is automatically closed. The quotient linear space of closed p-forms modulo exact p-forms is called the p^{th} cohomology (group) of the manifold M. The homogeneous Maxwell equations $\boldsymbol{\nabla} \cdot \boldsymbol{B} = 0$ and $\frac{1}{c}\frac{\partial \boldsymbol{B}}{\partial t} + \boldsymbol{\nabla} \times \boldsymbol{E} = 0$ are together the statement that the Faraday 2-form $F = (1/2)F_{\mu\nu} dx^\mu \wedge dx^\nu$ on Minkowski space-time $\mathbb{R}^4$ (with $x^\mu = (ct, x, y, z)$ for $\mu = 0, 1, 2, 3$) is a closed 2-form. Here, $F_{0i} = E_i$ and $F_{ij} = -\epsilon_{ijk} B_k$ for $1 \leq i, j, k \leq 3$. Since $\mathbb{R}^4$ has trivial cohomology groups, F must be exact and expressible as $F = dA$ for some 'gauge potential' 1-form $A = A_\mu dx^\mu$. This is why we may express $\boldsymbol{B} = \boldsymbol{\nabla} \times \boldsymbol{A}$ and $\boldsymbol{E} = -\boldsymbol{\nabla}\phi - c^{-1}\frac{\partial \boldsymbol{A}}{\partial t}$ in terms of the scalar and vector potentials which are the components of $A_\mu = (\phi, -\boldsymbol{A})$ (see Sect. 3.23* and Prob. B.12). □

Symplectic form and Bianchi's identity. Suppose $\alpha = p_i dq^i$ is the canonical Liouville 1-form on the phase space $\mathbb{R}^{2n}$ of a mechanical system with n degrees of freedom. Then we have seen that the canonical symplectic form is given by $\omega = d\alpha = dp_i \wedge dq^i$. It follows that $d\omega = d^2\alpha = 0$. In other words, the canonical symplectic form is closed. More generally (see Prob. 3.60) the Jacobi identity implies that the inverse ω of any invertible (but not necessarily canonical) Poisson tensor r satisfies the Bianchi identity. We now verify that the Bianchi condition (3.257) is simply the statement that $d\omega = 0$. Indeed, using linearity and the Leibniz rule,

$$d\omega = \frac{1}{2} d(\omega_{jk} dx^j \wedge dx^k) = \frac{1}{2}(\partial_i \omega_{jk}) dx^i \wedge dx^j \wedge dx^k. \quad \text{(B.48)}$$

Since $dx^i \wedge dx^j \wedge dx^k$ is antisymmetric under exchange of any pair of indices, only the similarly antisymmetric part of $\partial_i \omega_{jk}$ can contribute. Antisymmetrizing as in (B.34), we write

---

[34] $d^2 = 0$ is a generalization of the vector calculus identities $\boldsymbol{\nabla} \times \boldsymbol{\nabla} f = 0$ and $\boldsymbol{\nabla} \cdot (\boldsymbol{\nabla} \times \boldsymbol{v}) = 0$ for any smooth function f and vector field $\boldsymbol{v}$ in $\mathbb{R}^3$.

$$\begin{aligned} d\omega &= \frac{1}{12}\left(\partial_i\omega_{jk} - \partial_j\omega_{ik} - \partial_k\omega_{ji} - \partial_i\omega_{kj} + \partial_k\omega_{ij} + \partial_j\omega_{ki}\right) dx^i \wedge dx^j \wedge dx^k \\ &= (1/3!)\left(\partial_i\omega_{jk} + \partial_k\omega_{ij} + \partial_j\omega_{ki}\right) dx^i \wedge dx^j \wedge dx^k, \end{aligned} \tag{B.49}$$

where we used the antisymmetry of ω in the last step. Thus $(d\omega)_{ijk} = \partial_i\omega_{jk} + \partial_k\omega_{ij} + \partial_j\omega_{ki}$, so that $d\omega = 0$ iff the Bianchi condition (3.257) is satisfied. We begin to see the economy and clarity that the use of differential forms can bring to tensor calculus. What is more, given a smooth 'Hamiltonian' function H on M, we may use ω to define a vector field v_H called the Hamiltonian vector field via the formula

$$v_H(\cdot) = \omega^{-1}(\cdot, dH). \tag{B.50}$$

Here ω^{-1} is a contravariant (antisymmetric) second rank tensor that can act on a pair of 1-forms, one of which is chosen to be dH. The resulting object is a vector field as it can act linearly on an (unspecified) 1-form. We will see concrete examples of Hamiltonian vector fields in Sect. 5.1.

More generally, even if we do not have canonical (q-p-type) coordinates on phase space and do not have available the canonical Liouville 1-form $\alpha = p_i dq^i$, we may still wish to define a symplectic form using physical or geometric considerations. From the foregoing, the essential conditions it must satisfy are invertibility and the Bianchi identity. Thus, one defines a symplectic manifold as a sufficiently smooth manifold that is equipped with a closed nondegenerate (i.e., invertible) two-form ω called the symplectic form. Though it is required to be closed, ω need not be exact[35].

B.10* Integration on manifolds and Stokes' theorem

We now move from the exterior differential calculus to the integral calculus on a manifold. This will allow us to generalize the concepts of line, surface and volume integrals to manifolds. To do this, we first need the idea of an oriented manifold.

Orientability of a manifold. We may orient a curve γ in 3d space by placing arrows on it so that the curve is traversed in only one direction. A parametrized curve $\gamma(s) : [0,1] \to \mathbb{R}^3$ with $\dot\gamma \neq 0$ everywhere has a natural orientation, namely the direction in which $\dot\gamma$ points (which is the same as that of increasing s). If $\dot\gamma$ vanishes somewhere, we would not know which way the arrow points there. Moreover, we can also have the situation where the parametrized curve γ retraces the image so that there would be points on the curve where the arrow points in both directions. This may be avoided by assuming that $\dot\gamma \neq 0$. Given a vector field $\boldsymbol{v}$ and such a curve

---

[35] The symplectic form (3.192) on the 2-sphere S^2, given by $\omega = -l \sin\theta \, d\theta \wedge d\phi$ (for $l \neq 0$) is closed (being a top degree form) but not exact. To show this, we note that $\int_{S^2} \omega = -4\pi l$ is proportional to the surface area of the unit sphere. If $\omega = d\alpha$, then by Stokes' theorem (B.55), this integral must vanish, since S^2 has no boundary: $\int_{S^2} d\alpha = \int_{\partial S^2} \alpha = 0$. Thus, ω cannot be exact. However, locally in a coordinate patch, it can be written as $\omega = d\alpha$ for $\alpha = l\cos\theta \, d\phi$ (local exactness is called the Poincaré lemma). The problem is that α cannot be smoothly extended to a 1-form on all of S^2.

$\boldsymbol{\gamma}$, we may define the line element $d\boldsymbol{\gamma} = \dot{\boldsymbol{\gamma}}(t)dt$ and the line integral of $\boldsymbol{v}$ along $\boldsymbol{\gamma}$: $\int_\gamma \boldsymbol{v}\cdot d\boldsymbol{\gamma}$. Note that $\boldsymbol{\gamma}$ need not be an integral curve of $\boldsymbol{v}$. One verifies that this line integral is reparametrization invariant[36]. Indeed, suppose $s = s(t) : [0,1] \to [0,1]$ is a reparametrization (invertible map) and let $\tilde{\gamma}(t) = \gamma(s(t))$. Then

$$\int \boldsymbol{v}\cdot d\tilde{\boldsymbol{\gamma}} = \int_0^1 v_j \frac{d\tilde{\gamma}^j}{dt} dt = \int_0^1 v_j \frac{d\gamma^j}{ds}\frac{ds}{dt} dt = \int_0^1 v_j \frac{d\gamma^j}{ds} ds = \int \boldsymbol{v}\cdot d\boldsymbol{\gamma}. \quad \text{(B.51)}$$

For a 2d surface Σ embedded in $\mathbb{R}^3$, we usually speak of an outward or inward pointing unit normal at each point of Σ. When Σ is defined by the condition $C(x,y,z) = 0$, the normal in the direction of increasing C is given by the unit vector along the gradient $\boldsymbol{\nabla} C$. To be well-defined (unambiguous), when the normal is followed around any closed loop on Σ, it must return to its original direction. When this happens, we say that the surface is oriented. In vector calculus, this normal to the surface is used to define a vectorial area element $(\hat{n} dS)$ that goes into the definition of surface integrals. These concepts can be generalized to manifolds of any dimension and are used to define integration on manifolds. An n-dimensional manifold is orientable if it admits a nonvanishing[37] form of top degree n (called a volume form). The choice of such a form is called an orientation. On $\mathbb{R}^2$ we usually choose the orientation as given by $dx \wedge dy$, the choice $dy \wedge dx$ is equally valid, but would correspond to reversing the orientation. On $\mathbb{R}^n$, the standard volume form is $dx^1 \wedge \cdots \wedge dx^n$. Admitting a volume form is equivalent to the Jacobian determinants of all the transition functions between coordinate charts being positive, so that all the coordinate charts have a common orientation[38] and the atlas may be called an oriented atlas. The two-sphere is orientable since the symplectic form (3.192) on S^2 is a nonvanishing 2-form (proportional to the standard area form). For a surface in $\mathbb{R}^3$, orientability allows us to unambiguously distinguish two sides of the surface. The Möbius strip is not orientable[39]: one can go from the 'upper' side of the surface to the 'lower' side at the same point by taking a walk on the strip; this is not possible on a cylindrical surface or on a sphere, which are orientable.

---

[36] When we use a line integral (3.6) to model the work $W = \int \boldsymbol{F}\cdot d\boldsymbol{\gamma}$ done by a force field as a particle moves along a path, we are asserting that the work done is independent of how fast the particle moves at various places along the path.

[37] A p-form ω is nonvanishing if at each point on the manifold, $\omega(u, v, \ldots) \neq 0$ for any p linearly independent tangent vector fields $u, v, \cdots$.

[38] It is possible to concoct a nonoriented atlas. Consider the Euclidean plane $\mathbb{R}^2$ and define a new manifold via two overlapping patches. The left patch $x < 1$ and the right patch $x > -1$. On the left patch we define local coordinates $\xi^1 = x, \xi^2 = y$ while on the right patch we define local coordinates $\eta^1 = y, \eta^2 = x$. They overlap along the strip $-1 < x < 1$ where the point (x, y) has two addresses or sets of coordinates: (ξ^1, ξ^2) and (η^1, η^2). The transition functions are $\eta^1 = \xi^2$ and $\eta^2 = \xi^1$ resulting in an off-diagonal Jacobian matrix $\frac{\partial \eta^i}{\partial \xi^j} = (0, 1|1, 0)$ with determinant -1. Through this atlas, we have defined a manifold that is not orientable, the two charts have opposite orientations.

[39] A cylinder is constructed by taking a rectangular page from a tall book and pasting the two short edges together: the left of the bottom edge to the left of the top edge. The Möbius strip is obtained by twisting the bottom edge once before pasting it onto the top edge, so that the left of the bottom edge is joined to the right of the top edge.

Riemannian volume form. On an oriented n-dimensional Riemannian or pseudo-Riemannian manifold M with nondegenerate metric g, one has a natural volume form ω_g. In local coordinates x^i, it is $\omega_g = \sqrt{|\det g|}\, dx^1 \wedge \cdots \wedge dx^n$. Since g_{ij} is invertible, $\det g \neq 0$ so that this is a nonvanishing form. Let us check that this formula holds in any coordinate system. As noted in Appendix B.7*, under a coordinate change $x^i \to y^i$ a volume form $f(x) dx^1 \wedge \cdots \wedge dx^n$ (where f is a scalar function) transforms to $\det J^{-1} f(x(y)) dy^1 \wedge \cdots \wedge dy^n$ where $(J^{-1})^i_j = \frac{\partial y^i}{\partial x^j}$ is the inverse Jacobian matrix. If the transformation is orientation-preserving, then $\det J^{-1} > 0$. However, $\sqrt{|\det g|}$ is not a scalar function since the metric components transform to $\tilde{g}_{ij} = g_{kl}(J^{-1})^k_i (J^{-1})^l_j$. Hence, $\det \tilde{g} = \det g \det((J^{-1})^t) \det J^{-1}$. Consequently,

$$\begin{aligned} \sqrt{|\det g|} dx^1 \wedge \cdots \wedge dx^n &= \frac{\sqrt{|\det \tilde{g}|}}{\det J^{-1}} \det J^{-1} dy^1 \wedge \cdots \wedge dy^n \\ &= \sqrt{|\det \tilde{g}|} dy^1 \wedge \cdots \wedge dy^n. \end{aligned} \tag{B.52}$$

We see that in any coordinate system, the Riemannian volume form has the same expression. What is more, if one takes any orthonormal basis $\phi^1, \phi^2, \cdots, \phi^n$ for 1-forms on M, then $\omega = \pm \phi^1 \wedge \phi^2 \wedge \cdots \wedge \phi^n$. For example, consider 3d Euclidean space $\mathbb{R}^3$. In Cartesian coordinates, the Euclidean metric has components $g_{ij} = \delta_{ij}$ with unit determinant and the Euclidean volume form is $\omega = dx^1 \wedge dx^2 \wedge dx^3$. In spherical polar coordinates, the nonzero metric components are $g_{rr} = 1, g_{\theta\theta} = r^2, g_{\phi\phi} = r^2 \sin^2\theta$ so that $\det g = r^4 \sin^2\theta$ and the volume form becomes $\omega = r^2 \sin\theta dr \wedge d\theta \wedge d\phi$. On the other hand, the inverse metric is $g^{ij} = \text{diag}(1, 1/r^2, 1/(r^2 \sin^2\theta))$ so that the coordinate 1-forms have squared-lengths $g^{-1}(dr, dr) = 1, g^{-1}(d\theta, d\theta) = 1/r^2, g^{-1}(d\phi, d\phi) = 1/r^2 \sin^2\theta$. It follows that $\{dr, r d\theta, r \sin\theta d\phi\}$ is an orthonormal basis for 1-forms. We see that their wedge product is the volume form ω.

Integration of forms. In vector calculus, we define line integrals, surface integrals and volume integrals. These are examples of the integration of a 1-form along a curve, a 2-form over a surface and a 3-form over a 3d manifold. More generally, a p-form ψ may be integrated over an oriented p-dimensional manifold M to obtain a real number denoted $\int_M \psi$. To evaluate the integral, the manifold is covered by nonoverlapping cells and their boundaries (each lying within a coordinate chart) and the integral is a sum of contributions from each cell[40]. In each cell, the integral is evaluated as in multivariable calculus. In more detail, the p-form ψ can be written as $\psi = f\omega$ where f is a scalar and ω the volume form. Moreover, within a patch with coordinates $x^1, \cdots, x^p$, the volume form may be written as $\omega = \mu(x) dx^1 \wedge \cdots \wedge dx^p$ for some nonvanishing function μ. Then the contribution of the cell C is $\int_C \psi = \int_{x(C)} f(x)\mu(x) dx^1 \cdots dx^p$ where $x(C)$ is the image of the cell in $\mathbb{R}^p$. Examples: (i) We may integrate the 1-form

---

[40] If ψ has bounded components, the boundaries between cells do not contribute to $\int_M \psi$ so it does not matter if these boundaries are omitted or counted a finite number of times.

$\psi = f(x)dx$ over the submanifold $I = (1,2) \cup (3,6)$ of $\mathbb{R}$:

$$\int_I \psi \equiv \int_1^2 f(x)dx + \int_3^4 f(x)dx + \int_4^6 f(x)dx. \tag{B.53}$$

Here we have chosen the 'increasing' orientation $\omega = dx$ (as opposed to $-dx$) and broken I into three cells. (ii) The polar coordinate patch $x^i = (\theta, \phi)$ along with its boundary covers the unit sphere S^2. So the integral of the 2-form $\psi = f\omega$ on S^2 may be expressed as

$$\int_{S^2} \psi = \int_{x(S^2)} f(\theta,\phi)\, \sin\theta\, d\theta \wedge d\phi \equiv \int_0^{2\pi} d\phi \int_0^{\pi} d\theta\, f(\theta,\phi) \sin\theta. \tag{B.54}$$

The orientation has been chosen so that for $f = 1$, the integral of $\omega = \sin\theta d\theta \wedge d\phi$ over S^2 gives the area 4π of the unit sphere.

Manifold with boundary. To discuss Stokes' theorem, we need to generalize the notion of a manifold to include manifolds with boundary. By the definition of Appendix B.1, the closed unit disk D ($x^2 + y^2 \leq 1$) contained in the plane is not a manifold, since points of D on the rim (with $x^2 + y^2 = 1$) do not have open neighborhoods lying within D. For points on the rim, we will allow neighborhoods of a different sort: roughly those shaped like a half Moon that include nearby points on the rim. There is an obvious sense in which the unit circle S^1 is the boundary of D, which we indicate via $\partial D = S^1$. The set theoretic difference $D \setminus \partial D$ is the open unit disk, it is called the interior of D. More generally, a manifold with boundary is a (topological) space M with two types of points: (a) *interior points* which together comprise an n-dimensional manifold (i.e., which have open neighborhoods homeomorphic to $\mathbb{R}^n$ or the n-ball $B_n : x_1^2 + \cdots + x_n^2 < 1$) and (b) *boundary points* which together comprise an $n-1$ dimensional manifold called the boundary (∂M) consisting of points of M which have a neighborhood homeomorphic to a half space ($\boldsymbol{x} \in \mathbb{R}^n$ with $x_1 \geq 0$) or half ball ($\boldsymbol{x} \in B_n$ with $x_1 \geq 0$) with the homeomorphism taking the boundary points to points with $x_1 = 0$.

Stokes' theorem. Suppose $\omega = d\phi$ is an exact p-form on a p-dimensional manifold M with boundary denoted ∂M. Then Stokes' theorem

$$\int_M d\phi = \int_{\partial M} \phi \tag{B.55}$$

expresses the integral of ω over M as that of the $(p-1)$-form ϕ over the $(p-1)$-dimensional boundary ∂M. In particular, the integral of an exact form over a manifold without boundary vanishes. This is a generalization of Gauss' divergence theorem and Stokes' theorem from vector calculus (see Prob. B.23):

$$\int_\Omega \boldsymbol{\nabla} \cdot \boldsymbol{v}\, d^3r = \int_{\partial\Omega} \boldsymbol{v} \cdot d\boldsymbol{S} \quad \text{and} \quad \int_S (\boldsymbol{\nabla} \times \boldsymbol{v}) \cdot d\boldsymbol{S} = \oint_{\partial S} \boldsymbol{v} \cdot d\boldsymbol{l}. \tag{B.56}$$

Here, Ω is a 3d region in $\mathbb{R}^3$ while S is a surface in $\mathbb{R}^3$. In fact, (B.55) is also a generalization of the fundamental theorem of calculus for the integral of a 1-form over an interval $M = [a, b] \subset \mathbb{R}$: $\int_M f'(x)dx = \int_{\partial M} f = f(b) - f(a)$. Here f is a zero form and the boundary ∂M is the 0-dimensional disconnected manifold consisting of two points a, b. The orientation of the interval gives ∂M an orientation ($+1$ at b and -1 at a) leading to the relative sign on the RHS.

B.11* Covariant derivative

The laws governing the dynamics of physical systems (especially continuum mechanical systems with infinitely many degrees of freedom, see Chap. 16) are often formulated in terms of (partial) differential equations involving scalar, vector and tensor fields. Given a p-form, we have learned (in Appendix B.9*) how to take its exterior derivative using partial derivatives and the Leibniz rule to arrive at a p+1-form. What about the derivative of a vector field v? If one is given another vector field u, then as in Appendix B.4*, one may differentiate v along the integral curves of u to arrive at the Lie derivative $\mathcal{L}_u v = [u, v]$ (an example of this is the Lie derivative of the vorticity along the velocity field of a fluid). In the absence of such a u, one could consider the partial derivatives $\partial_i v^j$. Unfortunately, the partial derivatives of a vector field do not form the components of a tensor. As we will soon show, although $\partial_i v^j$ has one upper and one lower index, it does not transform as a (1,1) tensor field. In the absence of additional structure (like another vector field), it is not possible to differentiate a vector field (or other contravariant tensors or covariant tensors that are not antisymmetric) in a manner that produces a tensor. An advantage of working with tensors is that they have a coordinate-independent meaning (as multilinear maps) although one may choose to write their components in a particular coordinate system with simple transformation properties under a change of coordinates. However, if the manifold is equipped with a metric tensor g_{ij} (as may arise from a kinetic energy quadratic in velocities or from the geometry of space or space-time), then it is possible to 'covariantly' differentiate a vector field to arrive at a $(1, 1)$ tensor field $\boldsymbol{\nabla}_i v^j dx^i \otimes \partial_j$. This notion of covariant differentiation (discovered by Christoffel and further developed by Ricci and Levi-Civita) is also called the Levi-Civita connection) can be extended to other tensor fields in such a way that it satisfies the Leibniz rule and reduces to the partial derivative for functions. It turns out that in Euclidean space ($\mathbb{R}^n$ with the metric δ_{ij} in Cartesian coordinates), the covariant derivative reduces to the partial derivative. However, the covariant derivative is essential if we wish to use curvilinear coordinates in Euclidean space or work on a curved manifold such as a sphere or hyperboloid. In fact, we have already met the covariant derivative in our discussion of the geodesic equation in (3.214) of Sect. 3.27*, where we noted that the tangent vector to a geodesic is covariantly constant along the geodesic.

There are several ways of introducing the covariant derivative such as by (a) postulating axioms (such as linearity and the Leibniz rule) it must satisfy, (b) using the geometric notion of parallel transport and (c) combining the partial derivative with the Christoffel symbols from the geodesic equation and requiring tensorial behavior under coordinate transformations. Since we already have a provisional formula (3.214) for the covariant derivative[41]:

$$\nabla_j v^i = \partial_j v^i + \Gamma^i_{jk} v^k, \tag{B.57}$$

we will follow approach (c). In other words, we will examine how $\partial_j v^i$ transforms under a coordinate change and observe that it fails to behave like a (1,1) tensor. Then, we will use our definition (3.200) of the Christoffel symbols to similarly observe that they do not transform as a tensor. The offending terms in the transformation laws for the partial derivative and Christoffel symbols will be seen to cancel, allowing $\nabla_j v^i$ to transform as the components of a (1,1) tensor.

Thus, suppose we make a change of coordinates $x^i \mapsto \tilde{x}^i(x)$ under which the components of the vector field v^i become $\tilde{v}^i = \frac{\partial \tilde{x}^i}{\partial x^j} v^j$. Then the components of the partial derivatives of $\tilde{v}^i$ are

$$\frac{\partial \tilde{v}^i}{\partial \tilde{x}^j} = \frac{\partial}{\partial \tilde{x}^j}\left(\frac{\partial \tilde{x}^i}{\partial x^k} v^k\right) = \frac{\partial \tilde{x}^i}{\partial x^k}\frac{\partial x^l}{\partial \tilde{x}^j}\frac{\partial v^k}{\partial x^l} + \frac{\partial^2 \tilde{x}^i}{\partial x^l \partial x^k}\frac{\partial x^l}{\partial \tilde{x}^j} v^k. \tag{B.58}$$

The first term on the RHS is all there would have been if $\frac{\partial v^i}{\partial x^j}$ transformed as a (1,1) tensor. The second term with the second derivative is an inhomogeneous nontensorial term. In particular, unlike a tensor, which vanishes in all coordinate systems, if it vanishes in one, $\partial_j v^i$ fails to have this property. Next, we use the transformation law for the metric to find how the term involving Christoffel symbols

$$\Gamma^i_{jk} = \frac{1}{2} g^{il}\left(\partial_j g_{lk} + \partial_k g_{lj} - \partial_l g_{jk}\right) \tag{B.59}$$

transforms. To make a long story short (see Prob. B.25) one finds that

$$\tilde{\Gamma}^i_{jk}\tilde{v}^k = \frac{\partial \tilde{x}^i}{\partial x^k}\frac{\partial x^l}{\partial \tilde{x}^j}\Gamma^k_{lm} v^m - \frac{\partial^2 \tilde{x}^i}{\partial x^l \partial x^k}\frac{\partial x^l}{\partial \tilde{x}^j} v^k. \tag{B.60}$$

Again, the first term is all there would have been if $\Gamma^i_{jk} v^k$ transformed as a (1,1) tensor. Interestingly, the second (inhomogeneous) term cancels the corresponding one in (B.58) so that the covariant derivative transforms as a (1,1) tensor.

Remarks. (a) As mentioned, we define the covariant derivative of a scalar function as its partial derivative: $\nabla_i f = \partial_i f$. Thus $\nabla_i f$ are the components of a 1-form. (b) Equipped with formula (B.57), it is now easy to check that the covariant derivative of a vector field fv satisfies the Leibniz rule (see Prob. B.24)

$$\nabla_i (f v^j) = (\partial_i f) v^j + f \nabla_i v^j \quad \text{for any scalar function } f. \tag{B.61}$$

(c) In Riemannian geometry, the analog of the divergence of a vector field is the covariant divergence: $\nabla \cdot v = \partial_i v^i + \Gamma^i_{ij} v^j$. (d) The covariant derivative of v along a vector field u is defined as having the components $(\nabla_u v)^i = u^j \nabla_j v^i$. We check that it is linear in u in the sense that $\nabla_{fu+hw} v = f \nabla_u v + h \nabla_w v$ for any scalar functions

---

[41] It is noteworthy that the proposed formula (B.57) for the covariant derivative is linear in the components of v, this will allow it to satisfy appropriate Leibniz-type rules of differentiation.

f, h and vector fields u, v, w. (e) If $\boldsymbol{\nabla}_{\dot{x}} v = 0$, we say that v is parallel transported along curve $x(t)$. (f) A vector field v whose covariant derivative along itself vanishes ($\boldsymbol{\nabla}_v v = 0$) is called a *geodesic vector field*. The integral curves of a geodesic vector field are geodesics. This is not a surprise. We have already verified in (3.215) that the tangent to a geodesic is covariantly constant along the geodesic: $\boldsymbol{\nabla}_{\dot{x}} \dot{x} = 0$. ☐

Covariant derivative of other tensors. The covariant derivative can be generalized to other tensor fields. To begin with, one postulates that it reduces to the partial derivative on smooth functions $\boldsymbol{\nabla}_i f = \partial_i f$. Next, proceeding as for vector fields, we propose a formula for the covariant derivative of a 1-form $\phi_i dx^i$:

$$\boldsymbol{\nabla}_i \phi_j = \partial_i \phi_j - \Gamma_{ij}^k \phi_k, \tag{B.62}$$

and check that the RHS transforms as a (0,2) tensor field.

Since a 1-form and a vector field can be contracted to obtain a function (on which the covariant derivative reduces to the partial derivative), we should expect a Leibniz-like identity among covariant derivatives of 1-forms, vector fields and their contraction. In fact, we verify in Prob. B.27 that

$$\boldsymbol{\nabla}_i(\phi_j v^j) = \partial_i(\phi_j v^j) = (\boldsymbol{\nabla}_i \phi_j) v^j + \phi_j \boldsymbol{\nabla}_i v^j. \tag{B.63}$$

The extension to higher rank tensor fields is obtained by requiring $\boldsymbol{\nabla}$ to be a linear map (over $\mathbb{R}$) from the space of (p, q) tensors to $(p, q+1)$ tensors that satisfies the Leibniz rule: $\boldsymbol{\nabla}(s \otimes t) = \boldsymbol{\nabla} s \otimes t + s \otimes \boldsymbol{\nabla} t$ where s, t are a pair of tensor fields. This leads, for instance, to a formula for the covariant derivative of a (0,2) tensor (which can be regarded as a linear combination of tensor products of pairs of (0,1) tensors)[42]:

$$\boldsymbol{\nabla}_i t_{jk} = \partial_i t_{jk} - \Gamma_{ij}^l t_{lk} - \Gamma_{ik}^l t_{jl}. \tag{B.64}$$

We show in Prob. B.28 that the metric is 'compatible with the connection': it is covariantly constant: $\boldsymbol{\nabla}_i g_{jk} = 0$. This ensures that parallel transport, that one can define using the Christoffel connection, preserves the inner products of vectors.

B.12* Curvature on a Riemannian manifold

Recall (from Sect. 3.27*) that geodesics are curves that extremize the distance between a pair of points on a Riemannian manifold (manifold M with a metric tensor g). They play the same role that straight lines play in Euclidean space. The separation between straight lines on the Euclidean plane typically grows linearly with time. Based on this, we say that the Euclidean plane is flat. On the other hand, the separation between geodesics on the round sphere (which are great circles like longitudes on the Earth) oscillates in time. We say that the round sphere is positively curved. Interestingly, on a hyperboloid or saddle, geodesics typically separate exponentially fast: these surfaces are said to be negatively curved. Somewhat more precisely, curvature measures the behavior of the separation between geodesics that begin nearby. Gauss gave a way of quantifying the curvature of surfaces embedded in $\mathbb{R}^3$ without any reference to geodesics, that nevertheless captures this behavior of geodesics. This notion of curvature is called Gaussian curvature[43]. It is a generalization of the curvature of a plane curve $y = f(x)$, which is measured by f'' if the curve is rotated to make f' vanish at the point of interest.

---

[42] In general, aside from the partial derivative, the covariant derivative of a tensor involves one term with Christoffel symbols for each index of the tensor (with a negative sign for lower/covariant indices).

Geodesics and their separation are relevant to the behavior of mechanical systems. For instance, the rotational motion of an Euler top (see [3, 106, 107] and Prob. 8.34) is along geodesics of the inertia metric on its configuration space (the rotation group $SO(3)$). More generally, the trajectories of a system with kinetic energy bilinear in velocities may be interpreted as reparametrized geodesics of the Jacobi-Maupertuis metric on configuration space (see Sect. 3.28*). Consequently, the manner in which geodesics separate can encode information on the stability of a mechanical system (see Prob. 3.65 and [72, 73]). Since the configuration space of a mechanical system can have dimension more than two, it would be nice to have a notion of curvature for general Riemannian manifolds. Remarkably, Riemann developed such a generalization of Gaussian curvature to manifolds of any dimension. As with Gaussian curvature, Riemannian curvature is defined without reference to geodesics. Following Christoffel, in Appendix B.12.1*, we will formulate it in terms of the covariant derivative of Appendix B.11*. Then in Appendix B.12.2* we will relate it to the separation between geodesics by deriving the geodesic deviation equation and finding Riemann's curvature hidden inside it.

B.12.1* Riemann-Christoffel curvature tensor

Here, we define the Riemann-Christoffel notion of curvature on an n-dimensional manifold M with metric tensor g. Suppose u and v are a pair of vector fields: we may think of these as the velocity vector of a geodesic and the separating vector to a nearby geodesic. The Riemannian curvature $R(u,v)$ takes vector fields to vector fields via

$$R(u,v)w = [\boldsymbol{\nabla}_u, \boldsymbol{\nabla}_v]w - \boldsymbol{\nabla}_{[u,v]}w. \tag{B.65}$$

Here, $\boldsymbol{\nabla}_u$ is the covariant derivative along the vector field u introduced in Appendix B.11*, $[\boldsymbol{\nabla}_u, \boldsymbol{\nabla}_v]w = \boldsymbol{\nabla}_u(\boldsymbol{\nabla}_v w) - \boldsymbol{\nabla}_v(\boldsymbol{\nabla}_u w)$ and $[u,v]$ is the commutator of vector fields. It is clear that $R(u,v) = -R(v,u)$ is antisymmetric and that it is a measure of the lack of commutativity of covariant derivatives. Remarkably, despite the appearance of all these derivatives, $R(u,v)w$ does not depend on the derivatives of u, v or w.

---

[43] Let Σ be a surface embedded in $\mathbb{R}^3$. At each point $p \in \Sigma$, we have the tangent plane $T_p\Sigma$. A normal plane N_p through p is one that is orthogonal to $T_p\Sigma$. The osculating circle associated to a normal plane N_p is the best quadratic approximation (near p) to the curve of intersection between N_p and Σ. The maximum and minimum radii $R_{1,2}$ of osculating circles through p are called the principle radii of curvature at p. The Gaussian curvature $K(p)$ is defined to have a magnitude equal to $1/R_1R_2$. Its sign is positive/negative according as the centers of the corresponding osculating circles lie on the same/opposite sides of Σ. Gauss showed that his curvature is an intrinsic property of Σ, it does not depend on the embedding in $\mathbb{R}^3$. It is invariant under isometries [deformations of the surface that preserve lengths and angles].

In fact, R behaves linearly (over the ring of functions on M) in all three arguments[44]. This establishes that $R(u,v)$ is a $(1,1)$ tensor and that R is a tensor of type $(1,3)$: it acts multilinearly on triples of vector fields to produce another vector field (see Appendix B.7*). This means that when one changes coordinates, the components of R transform via some Jacobian factors implying that if R vanishes in one coordinate system, it also vanishes in any other coordinate system. In particular, the concept of a flat manifold (one with zero curvature such as the Euclidean spaces $\mathbb{R}^n$ with $g_{ij} = \delta_{ij}$) becomes independent of the choice of coordinates.

The components of the Riemann-Christoffel tensor $R^l{}_{kij}$ in a basis for vector fields $\{e_1, \cdots, e_n\}$ are defined via

$$R(e_i, e_j)e_k = \left([\boldsymbol{\nabla}_{e_i}, \boldsymbol{\nabla}_{e_j}] - \boldsymbol{\nabla}_{[e_i,e_j]}\right) e_k = R^l{}_{kij} e_l. \tag{B.66}$$

Thus, for any three vector fields u, v, w,

$$R(u,v)\, w = w^k\, u^i\, v^j R^l{}_{kij}\, e_l. \tag{B.67}$$

Let us specialize to a coordinate basis $e_i = \frac{\partial}{\partial x^i}$. Since coordinate vector fields commute ($[\partial_i, \partial_j] = 0$), the Riemann tensor simplifies to $R(\partial_i, \partial_j) = [\boldsymbol{\nabla}_i, \boldsymbol{\nabla}_j]$. We now wish to express its components in terms of the Christoffel symbols introduced in Appendix B.11*. From (B.57),

$$\begin{aligned}
(R(\partial_i,\partial_j)w)^l &= (\boldsymbol{\nabla}_i(\boldsymbol{\nabla}_j w))^l - (\boldsymbol{\nabla}_j(\boldsymbol{\nabla}_i w))^l \\
&= \partial_i(\boldsymbol{\nabla}_j w)^l + \Gamma^l_{ik}(\boldsymbol{\nabla}_j w)^k - (i \leftrightarrow j) \\
&= \partial_i(\partial_j w^l + \Gamma^l_{jk} w^k) + \Gamma^l_{ik}(\partial_j w^k + \Gamma^k_{jm} w^m) - (i \leftrightarrow j) \\
\Rightarrow \quad w^k R^l_{kij} &= \partial_i \partial_j w^l + \Gamma^l_{jk,i} w^k + \Gamma^l_{jk} \partial_i w^k + \Gamma^l_{ik} \partial_j w^k + \Gamma^l_{ik} \Gamma^k_{jm} w^m \\
&- \partial_j \partial_i w^l - \Gamma^l_{ik,j} w^k - \Gamma^l_{ik} \partial_j w^k - \Gamma^l_{jk} \partial_i w^k - \Gamma^l_{jk} \Gamma^k_{im} w^m.
\end{aligned} \tag{B.68}$$

As expected from the tensor character of R, all terms involving derivatives of w cancel out. Relabeling $m \leftrightarrow k$ in terms quadratic in Γ, we get

$$w^k R^l_{kij} = \left[\Gamma^l_{jk,i} + \Gamma^l_{im}\Gamma^m_{jk} - (i \leftrightarrow j)\right] w^k \tag{B.69}$$

with '$,i$' denoting ∂_i. Thus, the components of the $(1,3)$ Riemann tensor are

$$R^l{}_{kij} = \Gamma^l{}_{jk,i} - \Gamma^l{}_{ik,j} + \Gamma^m_{jk}\Gamma^l{}_{im} - \Gamma^m_{ik}\Gamma^l{}_{jm}. \tag{B.70}$$

By virtue of (B.59), they depend on the first two derivatives of the metric g_{ij} and its inverse g^{ij}.

Symmetries. $R^l{}_{kij}$ is clearly antisymmetric in the last two indices $R^l{}_{kij} = -R^l{}_{kji}$. Lowering l, we define a $(0,4)$ tensor $R_{mkij} = g_{ml} R^l{}_{kij} = g(R(e_i, e_j)e_k, e_m)$ and verify using (B.70) and (B.57) that R_{mkij} is antisymmetric in the first two indices and symmetric under exchange of the first pair of indices with the last pair (see Prob. B.30):

$$R_{mkij} = -R_{kmij} \quad \text{and} \quad R_{mkij} = R_{ijmk}. \tag{B.71}$$

---

[44] In particular, using $\boldsymbol{\nabla}_{fu} v = f \boldsymbol{\nabla}_u v$ and $\boldsymbol{\nabla}_u (fv) = u(f)v + f\boldsymbol{\nabla}_u v$, one finds that, $R(fu,v)w = fR(u,v)w$ and $R(u,v)(fw) = fR(u,v)w$ for any scalar function f.

The antisymmetry in the first pair is related to the behavior of a vector when parallel transported around a small parallelogram spanned by u, v. Since parallel transport preserves lengths and angles, such a vector can only undergo a rotation. The antisymmetry in question arises because infinitesimal rotations differ from the identity by an antisymmetric matrix, as shown in Eq. (B.99). The significance of the pair exchange symmetry will be clarified in the context of the geodesic deviation equation (B.84). In summary, the $(0, 4)$ Riemann tensor may be regarded as a real-valued multilinear map on four-tuples of vectors $R(X, Y, Z, W) = g(R(Z, W)Y, X)$ that is antisymmetric in both the first and last pairs and symmetric under their exchange. Thus, at each point $p \in M$, it defines a symmetric bilinear form on $\Lambda^2 T_p M$ (antisymmetrized tensor products of tangent vectors), which we may call the *curvature operator*. A special case, the 'curvature matrix' will appear in the geodesic deviation equation (B.83).

Ricci tensor and scalar. For some purposes, the $(1, 3)$ Riemann tensor has more information/components than we need, and it is useful to define its second rank and scalar contractions. The Ricci curvature is the symmetric $(0, 2)$ tensor defined as $\mathrm{Ric}_{kl} = R^i{}_{kil}$ while the scalar curvature or Ricci scalar is R (or S) $= g^{kl}\mathrm{Ric}_{kl}$.

Example. The Poincaré metric on the upper half-plane $U = \{(x, y) \in \mathbb{R}^2, \quad y > 0\}$ is $g_{ij} = \delta_{ij}/y^2$. The nontrivial Christoffel symbols are $\Gamma^y_{yy} = \Gamma^x_{xy} = \Gamma^x_{yx} = -\Gamma^y_{xx} = -1/y$ and the components of the Riemann tensor are

$$R^x{}_{yyx} = R^y{}_{xxy} = 1/y^2, \quad R^x{}_{xxy} = R^y{}_{yxy} = 0 \quad \text{and} \quad R_{yxxy} = 1/y^4. \tag{B.72}$$

The other components are either zero or follow from (anti)symmetry. In fact, there is only one linearly independent component of the Riemann tensor in two dimensions. The Poincaré metric has a negative definite Ricci tensor $\mathrm{Ric}_{ij} = -\delta_{ij}/y^2$ while the Ricci scalar is $R = g^{xx}\mathrm{Ric}_{xx} + g^{yy}\mathrm{Ric}_{yy} = -2$. We say that the Poincaré upper half-plane has constant negative curvature and call it the hyperbolic plane. Geodesics on U deviate exponentially fast. We will see why in Eq. (B.87).

Sectional curvature and Curvature biquadratic form. The information in the (1,3) Riemann tensor may be packaged in sectional curvatures. These are the curvatures associated to each tangent plane through any point p of M. Given a pair of tangent vectors u, v, the sectional curvature in the plane they span is defined as

$$\sec(u, v) = \frac{\mathscr{r}(u, v)}{\mathrm{Ar}(u, v)^2} = \frac{g(R(u, v)v, u)}{g(u, u)g(v, v) - g(u, v)g(v, u)}. \tag{B.73}$$

The numerator $\mathscr{r}(u, v)$ is called the curvature biquadratic form and the denominator is the square of the area ($|\boldsymbol{u} \times \boldsymbol{v}|^2$) of the parallelogram spanned by u and v. It can be shown that $\sec(u, v)$ does not depend on the choice of vectors that span a given plane (for instance, rescaling either u or v leaves $\sec(u, v)$ unchanged). What is more, the sectional curvature of the tangent plane at any point of a surface embedded in $\mathbb{R}^3$ reduces to its Gaussian curvature. For the upper half-plane, taking $u = \partial_x$ and $v = \partial_y$,

$$\sec(\partial_x, \partial_y) = -\frac{g(R(\partial_x, \partial_y)\partial_x, \partial_y)}{g(\partial_x, \partial_x)g(\partial_y, \partial_y) - g(\partial_x, \partial_y)^2} = -\frac{R^y{}_{xxy}\, g(\partial_y, \partial_y)}{1/y^4} = -1. \tag{B.74}$$

Furthermore, the sectional curvature of a 2-plane V_p is the Gaussian curvature of the totally geodesic surface tangent to V_p formed from geodesics passing through p and tangent to V.

B.12.2* Geodesic deviation and Riemannian curvature

Suppose $x(t)$ is a geodesic with affine parameter t, so that $\ddot{x}^i + \Gamma^i_{jk}\dot{x}^j\dot{x}^k = 0$. Let us look for a nearby geodesic $z^i = x^i + y^i$ where y^i are small. We impose the condition that z^i also solves the geodesic equation up to terms quadratic in y^i to get

$$\ddot{x}^i + \ddot{y}^i + \Gamma^i_{jk}(x+y)\,(\dot{x}^j + \dot{y}^j)(\dot{x}^k + \dot{y}^k) = 0. \tag{B.75}$$

Using $\Gamma^i_{jk}(x+y) = \Gamma^i_{jk}(x) + \Gamma^i_{jk,l}y^l + \mathcal{O}(y^2)$ and the symmetry of Γ, this becomes

$$\ddot{y}^i + 2\Gamma^i_{jk}\dot{x}^j\dot{y}^k + \Gamma^i_{jk,l}\dot{x}^j\dot{x}^k y^l = 0. \tag{B.76}$$

This is the geodesic deviation equation (GDE) for the time evolution of the separating vector y. It is also called the Jacobi equation and its solutions y are called Jacobi vector fields (defined along the geodesic $x(t)$). To find the Riemann tensor hidden inside (B.76), we wish to rewrite it in terms of covariant derivatives. To this end, we calculate the covariant derivative of the separating vector along geodesic $x(t)$:

$$(\boldsymbol{\nabla}_{\dot{x}} y)^i = \dot{x}^k\partial_k y^i + \Gamma^i_{\ jk}\dot{x}^j y^k = \dot{y}^i + \Gamma^i_{\ jk}\dot{x}^j y^k. \tag{B.77}$$

Our search for $\ddot{y}$ leads us to evaluate the second covariant derivative:

$$\begin{aligned}\left(\boldsymbol{\nabla}^2_{\dot{x}} y\right)^i &= \frac{d}{dt}\left(\boldsymbol{\nabla}_{\dot{x}} y\right)^i + \Gamma^i_{\ mn}\dot{x}^m(\boldsymbol{\nabla}_{\dot{x}} y)^n \\ &= \ddot{y}^i + \frac{d}{dt}\left(\Gamma^i_{\ jk}\dot{x}^j y^k\right) + \Gamma^i_{mn}\dot{x}^m\left(\dot{y}^n + \Gamma^n_{jk}\dot{x}^j y^k\right) \\ &= \ddot{y}^i + 2\Gamma^i_{\ jk}\dot{x}^j\dot{y}^k + \Gamma^i_{jk,l}\dot{x}^l\dot{x}^j y^k \\ &\quad -\Gamma^i_{jk}y^k\Gamma^j_{mn}\dot{x}^m\dot{x}^n + \Gamma^i_{mn}\Gamma^n_{jk}\dot{x}^j y^k\dot{x}^m.\end{aligned} \tag{B.78}$$

We used the geodesic equation in the last equality. Thus, the Jacobi equation becomes

$$(\boldsymbol{\nabla}^2_{\dot{x}} y)^i + \Gamma^i_{jk,l}\dot{x}^j\dot{x}^k y^l - \Gamma^i_{jk,l}\dot{x}^l\dot{x}^j y^k + \Gamma^i_{jk}\Gamma^j_{mn}\dot{x}^m\dot{x}^n y^k - \Gamma^i_{mn}\Gamma^n_{jk}\dot{x}^j y^k\dot{x}^m = 0. \tag{B.79}$$

After relabeling indices, we find that it may be written in terms of the Riemann tensor:

$$(\boldsymbol{\nabla}^2_{\dot{x}} y)^i = R^i_{\ jkl}\dot{x}^j\dot{x}^k y^l. \tag{B.80}$$

Using the definition $(R(u,v)w)^i = u^k v^l w^j R^i_{\ jkl}$, we get the Jacobi equation

$$\boldsymbol{\nabla}^2_{\dot{x}} y = R(\dot{x}, y)\dot{x} = -R(y, \dot{x})\dot{x}. \tag{B.81}$$

On a flat manifold, such as Euclidean space, $R^i_{\ jkl} = 0$ and the GDE in Cartesian coordinates becomes $\dot{x}^j\dot{x}^k\partial_j\partial_k y^i = \ddot{y}^i = 0$, with solution $y^i(t) = y^i(0) + \dot{y}^i(0)t$. So components of a Jacobi vector field grow linearly with time (if $\dot{y}^i(0) \neq 0$) or remain constant (if $\dot{y}^i(0) = 0$). These correspond to two straight lines starting nearby but in different directions or with parallel initial velocities.

Relating geodesic separation to sign of sectional curvature. To understand solutions of (B.81), it is convenient to expand the Jacobi vector field $y(t) = \sum_k c_k(t) e_k(t)$ in an orthonormal basis $\{e_1(t), e_2(t), \ldots, e_n(t)\}$ for $T_{x(t)}M$ that is parallel transported along the geodesic, i.e., $\boldsymbol{\nabla}_{\dot{x}} e_k = 0$. Then the Jacobi equation becomes

$$\ddot{c}_k e_k = -c_k R(e_k, \dot{x})\dot{x} \tag{B.82}$$

with a sum on k implied. Taking an inner product with e_j and using orthonormality $(e_j, e_k) = \delta_{jk}$, the GDE becomes $\ddot{c}_j(t) = -g(R(e_k, \dot{x})\dot{x}, e_j) c_k(t)$ or

$$\ddot{c}_j = -\sum\nolimits_k \mathcal{R}_{jk}(t) c_k \quad \text{where} \quad \mathcal{R}_{jk}(t) = g(e_j(t), R(e_k(t), \dot{x}(t))\dot{x}(t)). \tag{B.83}$$

So the components of the Jacobi field obey coupled linear ODEs with variable coefficients. The 'curvature matrix' $\mathcal{R}_{jk}(t)$ is a real symmetric matrix[45], so it can be diagonalized by a time-dependent orthogonal transformation to an orthonormal eigenbasis $\{\tilde{e}_1, \ldots, \tilde{e}_n\}$ where $\mathcal{R}_{jk}$ is diagonal with eigenvalues κ_j along the diagonal:

$$\tilde{\mathcal{R}}_{jk} = g(\tilde{e}_j, R(\tilde{e}_k, \dot{x})\dot{x}) = \kappa_j \delta_{jk}. \tag{B.85}$$

What is more, the eigenvalue κ_j is simply the curvature biquadratic form (B.73) in the plane spanned by the tangent $\dot{x}$ to the unperturbed geodesic and the eigenvector $\tilde{e}_j$:

$$\kappa_j = g(R(\tilde{e}_j, \dot{x})\dot{x}, \tilde{e}_j) = \mathscr{k}(\tilde{e}_j, \dot{x}) = (\text{Area}\langle \tilde{e}_j, \dot{x}\rangle)^2 \sec(\tilde{e}_j, \dot{x}). \tag{B.86}$$

The separating vector may also be expanded in the eigenbasis, $y = \sum_j \tilde{c}_j \tilde{e}_j$. The Jacobi equation for the components $\tilde{c}_j$ is decoupled:

$$\ddot{\tilde{c}}_j = -\kappa_j(t) \tilde{c}_j \quad \text{for} \quad j = 1, 2, \ldots, n. \tag{B.87}$$

Each is the equation for a linear oscillator (6.2) with a time-dependent squared frequency. However, both signs of κ_j are possible. Thus, we should expect the coefficients $\tilde{c}_j$ to oscillate when κ_j are positive and to grow exponentially for negative κ_j. Thus, at least for short times (till the linearized approximation breaks down), the behavior of neighboring geodesics is determined by the sign of the curvature biquadratic (or equivalently, the sign of the sectional curvature) in the plane spanned by the tangent to the original geodesic and the initial separating vector. Positive sectional curvatures lead to oscillatory behavior of nearby geodesics while negative sectional curvatures lead to exponential growth in separation.

---

[45] The curvature matrix $\mathcal{R}_{jk}(t) = R(e_j, \dot{x}, e_k, \dot{x})$ is symmetric for the same reason as the curvature operator is. In fact, from definition (B.67) and the index pair exchange symmetry of the (0,4) Riemann tensor (B.71),

$$\begin{aligned} \mathcal{R}_{ij} &= g(R(e_j, \dot{x})\dot{x}, e_i) = g_{kl}(R(e_j, \dot{x})\dot{x})^k (e_i)^l = g_{kl} R^k_{\ pmn} (e_j)^m \dot{x}^n \dot{x}^p (e_i)^l \\ &= R_{lpmn} (e_i)^l \dot{x}^p (e_j)^m \dot{x}^n = R_{mnlp} (e_i)^l \dot{x}^p (e_j)^m \dot{x}^n \\ &= R_{lpmn} (e_i)^m \dot{x}^n (e_j)^l \dot{x}^p = \mathcal{R}_{ji}. \end{aligned} \tag{B.84}$$

B.13* Groups, Lie groups and their Lie algebras

Definition. A group is a mathematical construct that, among other things, helps us express and work with symmetries. Groups occur in various parts of physics such as crystallography, atomic physics, relativity and particle physics [53, 119]. They help to recognize and organize patterns, but can also enter dynamical principles that constrain or determine the nature of forces. For instance, the angular distribution of possible locations of an electron in a hydrogen atom can be understood using the spherical symmetry of the electric potential felt by the electron. On the other hand, the strong nuclear force among quarks and gluons is determined by a 'gauge principle' based on a so-called color symmetry group. In mechanics, groups typically arise as families of symmetry transformations among states or configurations or solutions of the equations of a system. For example, rotations act on the possible locations of a planet in the Kepler problem while the $x \to -x$ reflection acts as a symmetry of an even harmonic oscillator potential $V(x) = \frac{1}{2}kx^2$ felt by a particle attached to a spring. However, it is advantageous to separate the algebraic concept of a group from its action on a space. Thus, we will begin by defining an 'abstract' group and later discuss how it may be realized via an action on an auxiliary space like the state space of a mechanical system. Precisely, a group G is a set of elements $g, h, k, \ldots$ among which a law of composition $G \times G \to G$ is defined: if $g, h \in G$, then their product or composition $gh \in G$. The product must satisfy the following properties. (i) It must be associative, i.e., $g(hk) = (gh)k$ for any $g, h, k \in G$. (ii) G must include an identity element e (sometimes denoted 1 or I) with $ge = eg = g$ for any $g \in G$. (iii) Every element g must have a two-sided inverse g^{-1}, i.e., $gg^{-1} = g^{-1}g = e$. Useful consequences are $(gh)^{-1} = h^{-1}g^{-1}$ and the cancellation law: if $gh = gk$ then $h = k$.

Cardinality, discrete and continuous groups. The number of elements $|G|$ in a group G is called its order or cardinality. A group of finite order is called a finite group. The 'trivial' group has just one element, the identity: $G = \{1\}$ with $1 \cdot 1 = 1$. The set $C_2 = \{1, -1\}$ under multiplication is a group of order two. While 1 is the identity, $(-1)(-1) = (-1)^2 = 1$. We say that -1 generates C_2 since -1 and $(-1)^2$ account for all the distinct elements. C_2 is called the cyclic group of order two. Notice that ± 1 are the two square-roots of unity. More generally, for $n = 1, 2, 3, \ldots$, we have the (multiplicative) cyclic group of order n consisting of the n^{th} roots of unity $\{1, e^{2\pi i/n}, e^{4\pi i/n}, \ldots, e^{2(n-1)\pi i/n}\}$. It is generated by $e^{2\pi i/n}$ and we write $C_n = \langle e^{2\pi i/n} \rangle$. For $n = 1, 2, 3, \ldots$, the set $\mathbb{Z}_n = \{0, 1, \cdots, n-1\}$ with composition given by addition modulo n (e.g., $2 + 3 \equiv 1 \pmod 4$) is also a cyclic group of order n. The identity element is 0 and 1 is its generator. Note that $1 + 1 + \cdots + 1$ (n summands) $= n1 \equiv 0 \pmod n$. We will soon see that $\mathbb{Z}_n$ and C_n are different presentations of the same group: up to 'isomorphism' there is just one cyclic group of a given order. Infinite groups could be discrete (like the additive group of integers $\mathbb{Z}$ or the infinite cyclic group) or continuous (like the multiplicative group of complex numbers of unit magnitude). The latter group is denoted $U(1)$ and its elements may be represented as $z(\theta) = e^{i\theta}$ for a real angle θ which is defined modulo 2π (see Fig. B.6). Composition is given by $z(\theta_1)z(\theta_2) = e^{i(\theta_1+\theta_2)} = z(\theta_1 + \theta_2)$.

Subgroup. A subset H of a group G is called a *subgroup* if it satisfies the group axioms with respect to the operations inherited from G [see Prob. B.33]. The identity subgroup $H = \{e\}$ and $H = G$ are subgroups of any group G. Examples: (i) $C_2 = \{\pm 1\}$ and more generally C_n are subgroups of $U(1)$. (ii) Given any element g of a group G, it generates a (cyclic) subgroup, namely the set of its powers $\langle g \rangle = \{g^0 = e, g, g^{-1}, g^2, g^{-2}, \cdots\}$. If there is a smallest positive integer n such that $g^n = e$, then $\langle g \rangle$ is essentially the same as (i.e., isomorphic to) a cyclic group of order n and otherwise it is an infinite cyclic group. (iii) Every finite group may be realized as a subgroup of a group of permutations (see Prob. B.37).

Group homomorphisms. Given a pair of groups, a map $\phi : G \to G'$ is called a *homomorphism* if it preserves products: $\phi(g_1 g_2) = \phi(g_1)\phi(g_2) \;\forall\; g_1, g_2 \in G$. If ϕ preserves products then (see Prob. B.34) ϕ maps the identity in G to that in G' and maps inverses to inverses: $\phi(g^{-1}) = \phi(g)^{-1}$. The homomorphic image $\phi(G) \subseteq G'$ is a subgroup of G'. A homomorphism $\phi : G \to G'$ is an isomorphism if it is bijective (1-1 and onto, and hence invertible). Two groups G and G' are *isomorphic* (denoted $G \cong G'$) if there is an isomorphism between them. Isomorphic groups are algebraically identical but could arise or be presented differently. E.g., C_n and $\mathbb{Z}_n$ are isomorphic, with the isomorphism mapping the generators to each other: $\phi(e^{2\pi i/n}) = 1$, so that $\phi(e^{2\pi i j/n}) = j$ for $j = 0, 1, \cdots, n-1$. The group of unimodular complex numbers $U(1)$ is isomorphic to that of 2×2 orthogonal matrices (real A with $A^t A = I$) with unit determinant ($SO(2)$). Composition is given by matrix multiplication. Its elements are $A(\theta) = (\cos\theta, \sin\theta| - \sin\theta, \cos\theta)$ for a real angle θ defined modulo 2π. The isomorphism maps $z = e^{i\theta}$ to $A(\theta)$. Verify that under matrix multiplication, $A(\theta_1)A(\theta_2) = A(\theta_1 + \theta_2)$.

Isomorphisms and automorphisms. An isomorphism ϕ from a group G to itself is called an *automorphism*. Every group has the identity or trivial automorphism defined by $\phi(g) = g$ for all $g \in G$. $C_2 = \{1, -1\}$ has no nontrivial automorphism since we cannot define $\phi(1) = -1$. Verify that C_3 has just one nontrivial automorphism given by $\phi(1) = 1, \phi(\omega) = \omega^2$ and $\phi(\omega^2) = \omega$ where $\omega = e^{2\pi i/3}$. Since an automorphism must preserve the algebraic structure, it must take a generator to another generator: we check that both ω and ω^2 are generators of C_3. $C_4 = \{1, i, -1, -i\}$ also has one nontrivial automorphism: it exchanges the two generators: $\phi(1) = 1$, $\phi(i) = -i$, $\phi(-1) = -1$ and $\phi(-i) = i$.

Conjugation and conjugacy classes. Given a group G, we say that $k \in G$ is conjugate to $h \in G$ if $k = ghg^{-1}$ for some[46] $g \in G$. Conjugation $\phi_g(h) = ghg^{-1}$ by a fixed element g defines an automorphism of G. It is called an *inner automorphism*. It is a homomorphism since $\phi_g(h_1 h_2) = g h_1 h_2 g^{-1} = g h_1 g^{-1} g h_2 g^{-1} = \phi_g(h_1)\phi_g(h_2)$. It is $1-1$ since $\phi_g(h_1) = \phi_g(h_2)$ implies $g h_1 g^{-1} = g h_2 g^{-1}$ whence $h_1 = h_2$. It is surjective since given any $k \in G$ we can always find an $h \in G$ such that $\phi_g(h) = k$, in fact $h = g^{-1} k g$. What is more, the inverse of ϕ_g is just $\phi_{g^{-1}}$.

The *conjugacy class* of h is the set $C_h = \{ghg^{-1} | g \in G\}$. The identity element is always in a conjugacy class by itself $C_e = \{e\}$. Conjugacy is an equivalence relation[47]. This implies G is a disjoint union of conjugacy classes.

---

[46] If g works, so do gh^n for $n \in \mathbb{Z}$ and more generally gg' for any g' that commutes with h.

Abelian and nonabelian groups. The nature of conjugation and conjugacy classes are related to the notion of a commutative group. We begin by defining the *group commutator* of a pair of elements as $[g,h] = ghg^{-1}h^{-1}$. The commutator measures the extent to which gh and hg differ. If gh and hg are the same, then $[g,h] = e$ and they are said to commute. A group is called *abelian* or *commutative* if $[g,h] = e$ or $gh = hg$ or $ghg^{-1} = h$ for all $g,h \in G$. Otherwise, it is nonabelian. Evidently, a group is abelian iff all conjugacy classes are singleton sets or equivalently, if every inner automorphism is the identity. Roughly, conjugacy classes get longer the more nonabelian a group is. Only the first 4 groups below are abelian.

Examples. There are many elementary examples of groups that arise in interesting ways, some of which we have met: (i) the multiplicative group $C_2 = \{1,-1\}$ consisting of the identity and reflection symmetry $x \to -x$ of an even potential $V(x)$ in one dimension as in Sect. 1.3*, (ii) the cyclic group C_5 of order 5, of rotational symmetries[48] of a regular pentagon (if one includes reflection symmetries, one obtains the dihedral group of order 10), (iii) the groups $\mathbb{R}^3$ and $\mathbb{R}$ of translations of 3d Euclidean space and time, (iv) the group $SO(2)$ of rotational symmetries of a circle or an axisymmetric (cylindrically symmetric) potential, (v) the group $SO(3)$ of proper rotations of 3d Euclidean space that came up in the context of Noether's theorem in Sect. 3.10, (vi) the group $O(3)$ of rotations and reflections of $\mathbb{R}^3$ (see Footnote 47 of Sect. 3.10), (vii) the Galilei group of Sect. 3.12 and (viii) the groups S_2 and S_3 of permutations of two and three objects encountered in Footnote 29 of Appendix B.6* and Footnote 33 of Appendix B.7*.

Lie groups. While examples (i), (ii) and (viii) are discrete groups (with finitely many elements), the rest are examples of continuous groups, where the group elements form continuous families and can be used to model continuous symmetries. Historically, discrete groups arose, in part, in modeling discrete symmetries of algebraic equations, while continuous groups arose via continuous symmetries of differential equations. Prominent among continuous groups are Lie groups, named after the Norwegian mathematician Sophus Lie. A Lie group is a group which is also a differentiable manifold, with the group operations of composition $(g,h) \mapsto gh$ and inversion $g \mapsto g^{-1}$ being smooth maps from $G \times G \to G$ and $G \to G$ (inversion must be a diffeomorphism). The dimension of a Lie group G is the dimension of the corresponding group manifold. Note that the Cartesian product $G \times G$ inherits a $2(\dim G)$-dimensional manifold structure from G upon using ordered pairs of charts and transition functions. The concept of smooth maps is as introduced in Appendix B.1.

---

[47] Conjugacy is reflexive: $h = ehe^{-1}$ (h is conjugate to h), symmetric: $h = g'kg'^{-1}$ where $g' = g^{-1}$ (h is conjugate to k if k is conjugate to h) and transitive: k conjugate to h and h conjugate to l implies k conjugate to l. A binary relation with these properties is called an equivalence relation. It ensures that conjugacy classes either coincide or do not overlap. For instance, transitivity implies that C_{h_1} and C_{h_2} cannot have a 'partial' overlap.

[48] Cyclic and dihedral groups are *point groups* in 2d. They are symmetries of regular polygons and molecules with a fixed point and are discrete subgroups of the orthogonal group. *Space groups* are symmetries of an infinite crystal and include discrete translations.

Matrix Lie groups. Natural examples of Lie groups are the matrix groups $GL_n(\mathbb{R})$ and $GL_n(\mathbb{C})$ of invertible $n \times n$ real and complex matrices with composition and inversion given by matrix multiplication and inversion (Nb. GL stands for general linear). For instance, $GL_n(\mathbb{R})$ is an n^2-dimensional submanifold (in fact, an open subset) of the space $\mathbb{R}^{n^2}$ of all $n \times n$ real matrices. Matrix multiplication and inversion may be shown to be smooth maps. Since matrix multiplication is generally noncommutative, these groups for $n > 1$ are nonabelian. Other examples of 'classical' Lie groups[49] such as the special linear, orthogonal, symplectic and unitary groups arise as closed subgroups of $GL_n(\mathbb{R})$ and $GL_n(\mathbb{C})$. The special linear groups $SL_n(\mathbb{R})$ and $SL_n(\mathbb{C})$ consist of invertible matrices with unit determinant. The orthogonal and special orthogonal groups $O(n)$ and $SO(n)$ consist of orthogonal matrices $(A^t A = I)$ in $GL_n(\mathbb{R})$ and $SL_n(\mathbb{R})$ respectively. Similarly, the unitary and special unitary groups $U(n)$ and $SU(n)$ consist of unitary matrices $(U^\dagger U = I)$ in $GL_n(\mathbb{C})$ and $SL_n(\mathbb{C})$. The symplectic group $Sp(2n, \mathbb{R})$ consists of $2n \times 2n$ matrices M that preserve the canonical symplectic structure: $M^t \omega M = \omega$ where $\omega = (0, -I|I, 0)$ and I is the $n \times n$ identity matrix (see Sect. 10.5 and Prob. 10.14). They are the linear canonical transformations of the phase space $\mathbb{R}^{2n}$. Later in this section, we will discuss some basic properties of Lie groups in the context of the orthogonal group. See [94] for more on continuous groups.

Transformation group acting on a set. In classical mechanics, groups often arise as families of (often symmetry) transformations of a space M such as a configuration or phase space or the space of solutions of equations of motion. For instance, the rotation group $SO(3)$ acts on the configuration space $\mathbb{R}^3$ of a particle in a spherically symmetric potential by rotating the radius vector about the force center: $\boldsymbol{r} \mapsto R\boldsymbol{r}$ for $R \in SO(3)$. Evidently, such a 'transformation group' is to be regarded as an action of an abstract group G on a set M. Precisely, an action of G on M is a map from $G \times M \to M$ taking $m \in M$ to $g \cdot m \in M$ such that $e \cdot m = m$ and $g \cdot (h \cdot m) = (gh) \cdot m$ for all $g, h \in G$ and $m \in M$. The set of points that a given point $m \in M$ can be mapped to, $\mathcal{O}_m = \{g \cdot m | g \in G\}$ is called the orbit of m under the action of G. The action is said to be *transitive* if every point of M can be mapped to every other point of M by the action of some group element. In other words, the action is transitive if M is the orbit of any of its points. The action of rotations on $\mathbb{R}^3$ is not transitive: for instance, the origin cannot be mapped to any other point by a rotation. On the other hand, translations act transitively on $\mathbb{R}^3$: any point can be translated to any other point.

Lie group as a homogeneous manifold. A manifold M (or even just a topological space or set) is homogeneous for a group G if it carries a transitive action of G. To be meaningful, one needs to specify the nature of the manifold M (topological, smooth or geometrically rigid like a Riemannian manifold) and the action of the group must respect that structure. Roughly, all points of a homogeneous manifold look locally the same. For example, the unit circle $x^2 + y^2 = 1$ on the plane is homogeneous under the action of the group $SO(2)$ of rotations about the z axis. The time axis $\mathbb{R}$ is homogeneous under the action of the group of time-translations $t \mapsto t + s$. Euclidean space $\mathbb{R}^3$ is homogeneous under the action of the group of space-translations $\boldsymbol{r} \mapsto$

---

[49] 'Classical' here is used to mean that these were among the first Lie groups to be studied.

$\boldsymbol{r} + \boldsymbol{s}$. The term *homogeneous* should ring a bell: recall the homogeneity of time and space from Sect. 3.12. By contrast, the rigid toroidal surface of an inflated tube of a car tyre is *not* homogeneous for the action of the group of rotations about the axle. This action is not transitive since it cannot change the distance of a point on the tyre from the axle. In fact, near a point on the inner rim, the tubular surface looks like a saddle or mountain pass while near a point on the outer rim, it looks like a hill, so neighborhoods of points do not all look the same. Though not a group[50], the round unit sphere S^2 is homogeneous for the rotation group in 3d as it carries a transitive action of the latter: any point can be rotated to any other point on S^2. An ellipsoid of revolution $E = \{x^2 + y^2 + 2z^2 = 1\}$ regarded as a rigid surface in $\mathbb{R}^3$ is not homogeneous under 3d rotations since they do not preserve E. Rotations about the z-axis act on the ellipsoid, though not transitively.

Any group is homogeneous under its own action: G acts on itself transitively via both left and right multiplication. We define the left action of G on itself via $L_g h = gh$ for any $g, h \in G$. The action is transitive since, given any $h, k \in G$, we have $L_{kh^{-1}} h = k$. The right action $R_g h = hg$ is similarly transitive. The right and left actions coincide if G is abelian. For a Lie group, L_g and R_g are diffeomorphisms of G. Thus, a Lie group G is a homogeneous manifold under the action of G.

Lie algebra of a Lie group. Among the points of G, the identity is distinguished by its simplicity. It makes sense to begin a detailed study of G by focusing on the linear neighborhood of the identity[51]. This leads to the idea of the Lie algebra $\underline{G}$, which, as a vector space, is the tangent space at the identity T_eG. Each tangent vector at the identity is a Lie algebra element. We may use left translations L_g (by all elements of G) to pushforward (B.40) any fixed tangent vector $u \in T_eG$ to obtain a 'left-invariant' vector field $L_{g*}u$ on G. Thus, for each $u \in \underline{G}$ we get an associated left-invariant vector field on G. Consequently, the Lie algebra may also be regarded as the space of left-invariant (or right-invariant) vector fields on G. The algebraic structure of the group endows T_eG (or the space of left-invariant vector fields) with the additional structure of a linear Poisson algebra[52], i.e., with a bilinear antisymmetric product or 'Lie bracket' satisfying the Jacobi identity (see Footnote 88 of Sect. 3.24*). In fact, the Lie bracket is simply the commutator of left-invariant vector fields (which is known to be antisymmetric and to satisfy the Jacobi identity, see Prob. B.7). For the Lie algebra of a matrix Lie group, the Lie bracket may be realized concretely in terms of the commutator of matrices, as we shall soon see in the context of the rotation group (B.102). In fact, we may write a group element in the infinitesimal neighborhood of the identity as $g = e^{su} \approx I + su + s^2u^2/2$ for a real s with $|s| \ll 1$. The matrix u (or su) is then an element of the Lie algebra. The group commutator $[g, h]$ of two such elements $g = e^{su}$ and $h = e^{tv}$ may be shown to be $[g, h] \approx I + st[u, v]$ (see Prob. B.46). Thus, the matrix commutator of Lie algebra elements is the first nontrivial approximation to the group commutator.

---

[50] Any Lie group has at least one nonvanishing vector field: the left-invariant vector field obtained by pushing forward a nonzero tangent vector at the identity. However, as noted in Fig. B.5b, S^2 does not admit a nonvanishing vector field.

[51] By homogeneity, the linear neighborhood T_gG of any other point $g \in G$ may be studied by left- or right-translating the tangent space at the identity via L_g or R_g. This idea is also used in studying the rotational dynamics of a rigid body (see Footnote 32 of Sect. 8.10).

[52] The Poisson tensor is linear in coordinates. In Sect. 10.6, we indicate how Lie brackets can arise from Poisson brackets in the context of infinitesimal canonical transformations.

Coset spaces. The idea of a group acting on itself is extremely useful and can be used to 'subdivide' a group. Given a subgroup H of G, we may consider all its left translates, i.e., the subsets $gH = \{gh | h \in H\}$ where g ranges over elements of G. The subsets gH are called left cosets of G by H. Note that distinct elements of G may produce the same coset. For instance, all elements $h_1, h_2, \ldots$ of H give rise to the same coset[53] $h_1 H = h_2 H = eH = H$. Moreover, all cosets have the same cardinality as H. In fact, the elements of the list gH are all distinct. Additionally, two cosets are either the same or disjoint: $g_1 H = g_2 H$ or $g_1 H \cap g_2 H = \{\}$. The former happens if $g_1 = g_2 h$ for some $h \in H$ and the latter happens if there is no such $h \in H$. Thus, a group is a disjoint union of (left) cosets[54]. The set of left cosets forms the left coset space denoted G/H and pronounced 'G mod H'. Similarly, the right translates Hg of the subgroup by elements of G leads to the right coset space, denoted $H \backslash G$. It is often convenient to pick an element from each coset and use it as a representative for the coset. For example, the even integers $2\mathbb{Z}$ form a subgroup of the additive group of integers $\mathbb{Z}$. There are only two cosets: the sets of even and odd integers: $2\mathbb{Z}$ and $2\mathbb{Z} + 1$ (left and right cosets coincide since addition is commutative). In this case, we could pick 0 and 1 as the two coset representatives.

Normal subgroup and quotient or factor group. In general, neither the space of left nor right cosets is a group. However, they acquire the structure of a group if H is a so-called normal subgroup of G. Precisely, N is a normal subgroup (denoted $N \lhd G$) if each left coset gN is also a right coset Ng for the same $g \in G$. Such an N is also called an invariant subgroup as it is one that is invariant under conjugation: $gNg^{-1} = N$ for any $g \in G$. It is then easy to see that the set of left (or right) cosets of G by N is a group with identity given by the coset $eN = N$. Indeed, the group multiplication and inversion (for left cosets) are given by

$$(gN)\,(g'N) = (gg')N \quad \text{and} \quad (gN)^{-1} = g^{-1}N \tag{B.88}$$

Here, we used the formulae: $gNg'N = gg'NN = gg'N$ and $(gN)^{-1} = N^{-1}g^{-1} = Ng^{-1} = g^{-1}N$ since $N = N^{-1}$ on account of it being closed under inverses. G/N is called the quotient group or factor group. Some elementary properties are worth noting. (i) Every subgroup of an abelian group is a normal subgroup. (ii) If G is finite, then the cardinality of the coset space G/H is $|G|/|H|$ (Lagrange's theorem). (iii) If N is an invariant Lie subgroup of the Lie group G, then the dimension of the coset space G/N is the difference between the dimensions of G and N. (iv) The kernel K (inverse image $\phi^{-1}(e')$ of the identity $e' \in G'$) of a group homomorphism $\phi : G \to G'$ is always a normal subgroup of G (see Prob. B.40) and the image $\phi(G)$ is isomorphic to G/K. (v) The center $Z(G)$ of a group G, consisting of elements that commute with all other elements, is an abelian normal subgroup. It is normal since every group element commutes with elements in the center: $Z(G)g = gZ(G)$.

---

[53] In formulae such as $h_1 H = h_2 H$ we mean that the two sets are the same, although the order of elements in the two lists may differ.

[54] (Left) cosets may be interpreted as equivalence classes. For any two elements of G, define the relation $g \sim g'$ if there is an $h \in H$ such that $gh = g'$. This relation is reflexive ($g \sim g$ since $ge = g$), symmetric ($g \sim g' \Rightarrow g' \sim g$ since $gh = g'$ implies $g'h^{-1} = g$) and transitive ($g \sim g'$ and $g' \sim g''$ implies $g \sim g''$ since $gh = g'$ and $g'h' = g''$ implies $ghh' = g''$) and therefore an equivalence relation. Evidently, the equivalence class of g is the left coset gH.

Commutator subgroup. The commutator subgroup $[G, G]$ consists of products of any number of group commutators $[h_1, h_2][h_3, h_4] \cdots$ for $h_i \in G$. Notably, the inverse of a commutator is a commutator: $[h, k]^{-1} = [k, h]$, so this is a subgroup. It is normal since the conjugate of a commutator is the commutator of conjugates. The quotient $G/[G, G]$ is an abelian group since we have factored out all commutators. More formally, $gh = [g, h]hg$ and $gh = hg[g^{-1}, h^{-1}]$. Thus, gh and hg lie in the same right (and left) coset so that the composition of cosets is commutative:

$$(g[G, G])(h[G, G]) = gh[G, G] = hg[G, G] = (h[G, G])(g[G, G]). \tag{B.89}$$

In fact, $[G, G]$ is the smallest invariant subgroup such that the factor group is abelian.

Simple and semisimple groups. A simple group G is one that does not have any normal subgroups other than G and $\{e\}$. Simple groups are like prime numbers, they do not admit any nontrivial factor groups and can serve as building blocks for other groups. The cyclic group C_p for prime p is simple as every nontrivial element is a generator. By contrast, $C_4 = \{\pm 1, \pm i\}$ is not simple: $C_2 = \{\pm 1\}$ is a normal subgroup. More generally, G is semisimple if G has no nontrivial abelian invariant subgroups. If G is simple, then it is automatically semisimple. A connected nonabelian Lie group is called simple if it does not have any proper connected normal Lie subgroups (it can have discrete normal subgroups). $SO(3)$, $SU(2)$ and $SL_2(\mathbb{R})$ are simple Lie groups while $SO(4)$ is semisimple but not simple. The unitary groups $U(n)$ and general linear groups $GL_n(\mathbb{R})$ for $n \geq 2$ are neither simple nor semisimple since multiples of the identity ($e^{i\theta} I$ for real θ and λI for nonzero real λ) form nontrivial abelian connected invariant Lie subgroups. In fact, $U(2)$ also admits $SU(2)$ as a normal subgroup.

We now introduce two ways in which we may combine a pair of groups to synthesize a larger one: the direct and semidirect products.

Direct product. Suppose H and N are a pair of groups with identity elements e_H and e_N. Then the Cartesian product $H \times N$ consisting of all ordered pairs (h, n) with $h \in H$ and $n \in N$ can be given the structure of a group called the direct product of H and N. The composition law is defined as $(h, n) \cdot (h', n') = (hh', nn')$ and $(h, n)^{-1} = (h^{-1}, n^{-1})$. The subgroups consisting of elements of the form (e_H, n) and (h, e_N) are isomorphic to N and H respectively. $H \times N$ and $N \times H$ are isomorphic groups. When the groups are abelian, one tends to use additive rather than multiplicative notation. For example, the group $\mathbb{R}^2$ of translations of the Euclidean plane is the direct product (or sum) of two copies of the group $\mathbb{R}$ of translations of the real line: $\mathbb{R}^2 = \mathbb{R} \times \mathbb{R}$.

$*$ **Semidirect product.** The semidirect product is a generalization of the direct product. Here, we suppose that we are given an action of H on N. More precisely, for each $h \in H$, we have an automorphism $\varphi_h : N \to N$ such that $\varphi_{h'} \varphi_h = \varphi_{h'h}$ and $\varphi_h^{-1} = \varphi_{h^{-1}}$. We may use this to define the composition law $(h, n) \cdot (h', n') =$

$(hh', n\varphi_h(n'))$. We verify in Prob. B.42 that $H \times N$ with this composition law is a group. It is called the semidirect product of H acting on N via φ and is denoted $H \ltimes N$. Evidently, the semidirect product reduces to the direct product if H acts trivially on N, i.e., $\varphi_h(n') = n'$ for all $h \in H$ and $n' \in N$. What is more, the set of elements (e_H, n) forms a normal subgroup of $H \ltimes N$ isomorphic to N. The Euclidean group is a semidirect product of 3d rotations acting on space translations. The Galilei and Poincaré groups are semidirect products (see (3.74) & Footnote 19 of Sect. 4.10*) of the group of rotations and boosts acting on space-time translations.

We now illustrate some of the concepts introduced so far in the context of the discrete permutation group and the continuous circle and orthogonal groups.

Permutation group. The permutation group S_n or symmetric group on n letters is the set of all permutations of n distinct objects, usually denoted $1, 2, \cdots, n$, with group multiplication given by composition of permutations. A permutation σ may be written in two-row notation as $\sigma = \left(\begin{smallmatrix} 1 & 2 & 3 & \cdots \\ \sigma(1) & \sigma(2) & \sigma(3) & \cdots \end{smallmatrix}\right)$. The group has order $n!$ since $\sigma(1)$ can be chosen in n ways followed by $\sigma(2)$ in $n-1$ ways and so on. A permutation may also be written as a product of disjoint cycles: its cycle decomposition. For $k = 0, 1, \ldots$, a $(k+1)$-cycle is of the form $(i\ \sigma(i)\ \sigma^2(i) \cdots \sigma^k(i))$ with $\sigma^{k+1}(i) = i$. For example, S_2 consists of 2 elements: the identity $\sigma = e$ [with $e(1) = 1, e(2) = 2$] and exchange transposition $\sigma = \tau$ [$\tau(1) = 2, \tau(2) = 1$] with $\tau^2 = e$. Thus,

$$e = \left(\begin{smallmatrix} 1 & 2 \\ 1 & 2 \end{smallmatrix}\right) = (1)(2) \quad \text{and} \quad \tau = \left(\begin{smallmatrix} 1 & 2 \\ 2 & 1 \end{smallmatrix}\right) = (12). \tag{B.90}$$

The group S_3 has 6 elements. The identity $\sigma(i) = i$ is denoted $(1)(2)(3)$. There are three pairwise transpositions[55] $(12)(3), (1)(23)$ and $(2)(31)$. Here, $(1)(23)$ means $\sigma(1) = 1, \sigma(2) = 3, \sigma(3) = 2$. There are also two cyclic permutations $(123) = (12)(23) = (13)(12)$ and $(132) = (12)(13)$ which have been written as products of pairwise exchanges composed from right to left. Here (132) means $\sigma(1) = 3, \sigma(3) = 2$ and $\sigma(2) = 1$. In the composition $\sigma = (12)(13)$, 3 is mapped to 1 which is then mapped to 2, so that $\sigma(3) = 2$. On the other hand, $\sigma(2) = 1$ and $\sigma(1) = 3$.

S_3 can be realized as the group of rigid motion *symmetries of an equilateral triangle* Δ with vertices labelled v_1, v_2, v_3, say counterclockwise, with horizontal base $v_1 v_2$ and apex v_3. The symmetries of Δ are counterclockwise rotations R_θ about the center by angles $\theta = 0, 2\pi/3, 4\pi/3$ and reflections about the perpendiculars through the vertices v_1, v_2 and v_3. The transformation group consisting of these 6 symmetries is called the *dihedral group* of order 6 and is isomorphic to S_3 via the following map. To R_0 we associate the identity element e. $R_{2\pi/3}$ is mapped to (123) since it takes $v_1 \to v_2$, $v_2 \to v_3$, $v_3 \to v_1$. Similarly, $R_{4\pi/3}$ corresponds to (132) as it takes $v_1 \to v_3$, $v_3 \to v_2$, $v_2 \to v_1$. In the same spirit, reflection through the perpendicular through v_1 is mapped to (23) and so on. Notice that the square of any reflection is the identity and that $R_{2\pi/3}^2 = R_{4\pi/3}$ while $R_{4\pi/3}^2 = R_{8\pi/3} = R_{2\pi/3}$. Correspondingly, the square of any transposition is the identity while $(123)^2 = (132)$ and $(132)^2 = (123)$. The 'multiplication table' of S_3 is displayed in Table. B.1. Evidently, it is a nonabelian group. In general, reflec-

---

[55] When clear from context, we suppress 1-cycles. So in S_3, (23) is short for $(1)(23)$.

$g\downarrow,\ h\rightarrow$	e	(12)	(23)	(31)	(123)	(132)
e	e	(12)	(23)	(31)	(123)	(132)
(12)	(12)	e	(123)	(132)	(23)	(31)
(23)	(23)	(132)	e	(123)	(31)	(12)
(31)	(31)	(123)	(132)	e	(12)	(23)
(123)	(123)	(31)	(12)	(23)	(132)	e
(132)	(132)	(23)	(31)	(12)	e	(123)

Table B.1: Multiplication table of gh for $g, h \in S_3$

tions do not commute $[(12)(23) = (123)$ while $(23)(12) = (132)]$ nor do rotations commute with reflections: $(123)(12) = (31)$ while $(12)(123) = (23)$.

By Lagrange's theorem, since the order of a subgroup must divide that of the group, S_3 can only have *subgroups* of order $1, 2, 3$ and 6. There are 4 nontrivial subgroups, each is cyclic and is generated by a transposition or cyclic permutation:

$$\{e, (12)\}, \quad \{e, (23)\}, \quad \{e, (31)\} \quad \text{and} \quad \{e, (123), (132)\}. \tag{B.91}$$

The first 3 are reflection symmetries while the fourth consists of rotations of Δ. Pairwise transpositions are the building blocks: any permutation can be expressed as a product of transpositions, although the expression is not unique. However, a permutation σ requires an even or odd number of transpositions to be expressed this way. Thus, we define the *sign (or signature or parity) of a permutation* $\operatorname{sgn}(\sigma)$ as ± 1 in the even and odd cases. The identity has sign $+1$ and any exchange has sign -1. For S_3, cyclic permutations have sign $+1$ as $(123) = (31)(12)$ and $(132) = (12)(31)$.

The sign of a permutation gives a homomorphism: $S_n \to C_2$. The kernel is the *alternating group* A_n of even permutations, a normal subgroup[56] of S_n. For $n = 3$, $A_3 = \{e, (123), (132)\}$ consists of rotational symmetries of Δ. It has 2 left cosets

$$\begin{aligned} & (12)A_3 = (23)A_3 = (31)A_3 = \{(12), (23), (31)\} \\ \text{and} \qquad & eA_3 = (123)A_3 = (132)A_3 = \{e, (123), (132)\} = A_3. \end{aligned} \tag{B.92}$$

As expected, the left cosets are also right cosets, i.e., $(12)A_3 = A_3(12)$, etc.

All members of a *conjugacy class* have cycle decompositions of the same structure. Cycle structure refers to the number of 1-cycles, 2-cycles, etc. Hence, we should expect S_3 to have three conjugacy classes: the identity, the transpositions and the cyclic permutations: $\{e\}$, $\{(12), (23), (31)\}$ and $\{(123), (132)\}$. The members of a conjugacy class must have the same parity. For instance, the conjugates of (12) are

$$\begin{aligned} (23)(12)(23)^{-1} &= (31), & (31)(12)(31)^{-1} &= (23), \\ (123)(12)(123)^{-1} &= (23) \quad \text{and} & (132)(12)(132)^{-1} &= (13). \end{aligned} \tag{B.93}$$

S_3 can be realized as a *semidirect product* $H \rtimes N$ of H acting on N, where H and N are cyclic groups of order 2 and 3. For instance, we take $H = \{e, (12)\}$ and $N = A_3$ regarded as subgroups of S_3 and consider the action of H on A_3 via conjugation: $\varphi_h(n') = hn'h^{-1}$. Thus, the semidirect product is

$$(h, n) \cdot (h', n') = (hh', nhn'h^{-1}). \tag{B.94}$$

---

[56] Conjugation by any element $(g\sigma g^{-1})$ cannot change the parity of σ, so A_n invariant.

The Cartesian product has six elements

$$(e,e),\ (e,(123)),\ (e,(132)),\ ((12),e),\ a=((12),(123)) \quad \& \quad b=((12),(132)). \tag{B.95}$$

The first 4 elements are identified with $e,(123),(132),(12) \in S_3$. If $a \leftrightarrow (31)$ and $b \leftrightarrow (23)$ then one finds that (B.94) agrees with the S_3 composition law. For instance,

$$((12),(123)) \cdot ((12),(123)) = ((12)^2, (123)(12)(123)(12)) = (e,(31)^2) = (e,e), \tag{B.96}$$

which agrees with $(31)^2 = e$ in S_3.

Circle group $U(1)$. Perhaps the easiest Lie group to understand is the group $U(1)$ of unimodular complex numbers $\{z \in \mathbb{C} | z^* z = 1\}$. As shown in Fig. B.6, the group elements lie on the unit circle in the complex plane, so the group is also called the circle group S^1. This establishes that it is a differentiable manifold. It is called $U(1)$ since it is also the set of 1×1 unitary matrices[57]. Any unimodular z may be expressed as $z = e^{i\theta}$ where θ is defined modulo 2π. The identity element is $z = 1$, corresponding to $\theta \equiv 0$ modulo 2π. The multiplication law is abelian $e^{i\theta_1} e^{i\theta_2} = e^{i(\theta_1+\theta_2)} = e^{i\theta_2} e^{i\theta_1}$. The inverse of $z = e^{i\theta}$ is the reciprocal $1/z = e^{-i\theta}$. Since $(\theta_1, \theta_2) \mapsto \theta_1 + \theta_2$ and $\theta \mapsto -\theta$ modulo 2π are smooth maps, $U(1)$ is a one-dimensional Lie group. It is compact (closed and bounded as a subset of the complex plane) and path connected though not simply connected. Its Lie algebra $\underline{U(1)}$ is the tangent space at $z = 1$, which is isomorphic to $\mathbb{R}$. $\underline{U(1)}$ can be taken to be the 1d vector space of imaginary numbers iy for $y \in \mathbb{R}$. A basis for the Lie algebra may be chosen as i. We notice that exponentiating a Lie algebra element such as πi gives us a group element $e^{\pi i} = \cos\pi + i \sin\pi = -1$. This map from Lie algebra to Lie group is called the exponential map. More generally, given a nonzero Lie algebra element (say i), exponentiating all its real multiples iy, we get a 1-parameter subgroup e^{iy}. In this case, the exponential map surjects onto the group but is many-to-one: $e^{iy} = e^{i(2n\pi+y)}$ for any $n \in \mathbb{Z}$. Since $U(1)$ is abelian, all its subgroups are also abelian, they are given by the cyclic groups C_n for $n = 1, 2, \cdots$. Here, $C_n = \{e^{2\pi i j/n} | j = 0, 1, 2, \cdots n-1\}$, so the elements of C_n lie at the vertices of a regular n-gon centered at the origin of the complex plane, with the identity as one of its vertices (see Prob. B.38 and Prob. B.39).

The orthogonal group O(3). The orthogonal group $G = O(3)$ consists of the set of 3×3 real orthogonal matrices, i.e., matrices A that satisfy $A^t A = I$ (see Prob. B.44 for examples). The generalization[58] to $n \times n$ orthogonal matrices for $n = 1, 2, 3, 4, \ldots$

---

[57] The unitary group $U(n)$ consists of $n \times n$ complex matrices with $U^\dagger U = I$ where $U^\dagger = (U^t)^*$. Equivalently, it consists of linear maps on an n-dimensional complex vector space that preserve a Hermitian positive-definite inner product (Footnote 3 of Sect. 10.3*). It is a real Lie group of dimension n^2: transition functions are smooth real (not complex) functions. In fact, $U(n)$ is the subgroup of elements $g \in O(2n)$ that preserve a complex structure: $g^t J g = J$. A complex structure J on a real vector space V is a linear map $J : V \to V$ with $J^2 = -I$.

[58] Alternatively, suppose V is an n dimensional real vector space with positive-definite inner product $\langle \cdot, \cdot \rangle$. Then $O(n)$ is the group of linear maps $A : V \to V$ that preserve the inner product $\langle Au, Av \rangle = \langle u, v \rangle$ for all $u, v \in V$ with product given by composition of maps. The definition is independent of the choice of V and inner product, it only depends on n.

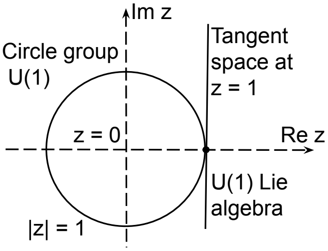

Figure B.6: The group $U(1)$ of unimodular complex numbers and its Lie algebra $\underline{U(1)} \cong \mathbb{R}$.

is called $O(n)$. The group composition law is associative matrix multiplication: note that $(AB)^t AB = B^t A^t AB = I$ if A and B are orthogonal. The identity element is the identity matrix while the inverse of A is simply its transpose A^t. It is a nonabelian group since $AB \neq BA$ in general for a pair of orthogonal matrices (see Prob. B.45). The orthogonal group is a matrix group, it is a subgroup of the general linear group of all invertible real 3×3 matrices. The orthogonal group is important as it is the group of rotations and reflections of 3d Euclidean space. It frequently arises as a group of symmetries (see Sect. 3.10) or as the configuration space (see Sect. 8.9) of a mechanical system. We will soon view $O(3)$ as a manifold. First, what is its dimension? The condition $A^t A = I$ implies that a 3×3 orthogonal matrix is one whose columns furnish an orthonormal basis $\{\boldsymbol{a}, \boldsymbol{b}, \boldsymbol{c}\}$ for $\mathbb{R}^3$ (see below). The first basis vector $\boldsymbol{a}$ is any unit vector. The latter are parametrized by points on the unit sphere $S^2 \subset \mathbb{R}^3$. Thus, 2 real parameters are needed to specify $\boldsymbol{a}$. Having picked $\boldsymbol{a}$, the second basis vector $\boldsymbol{b}$ can be any unit vector in the plane orthogonal to $\boldsymbol{a}$ and is specified by a point on the unit circle S^1 on this plane. Thus, one additional parameter is needed to specify $\boldsymbol{b}$. Having chosen $\boldsymbol{a}$ and $\boldsymbol{b}$, the third basis vector $\boldsymbol{c}$ must be perpendicular to both: $\boldsymbol{c} = \pm \boldsymbol{a} \times \boldsymbol{b}$. Thus, there is no additional continuous real parameter needed to specify $\boldsymbol{c}$. We conclude that $O(3)$ is a 3-parameter family of matrices. In fact, we may view it as a 3d submanifold of $\mathbb{R}^9$. Suppose we write A in terms of its columns,

$$A = \begin{pmatrix} \boldsymbol{a} & \boldsymbol{b} & \boldsymbol{c} \end{pmatrix} \quad \text{so that} \quad A^t = \begin{pmatrix} \boldsymbol{a}^t \\ \boldsymbol{b}^t \\ \boldsymbol{c}^t \end{pmatrix}. \tag{B.97}$$

The constraint $A^t A = I$, becomes 6 conditions on the 9 matrix elements of A:

$$\boldsymbol{a}^t\boldsymbol{a} - 1 = \boldsymbol{b}^t\boldsymbol{b} - 1 = \boldsymbol{c}^t\boldsymbol{c} - 1 = \boldsymbol{a}^t\boldsymbol{b} = \boldsymbol{b}^t\boldsymbol{c} = \boldsymbol{c}^t\boldsymbol{a} = 0. \tag{B.98}$$

Thus, $O(3)$ is the common zero locus of these six independent quadratic functions of nine real variables. Hence, we may view $O(3)$ as a 3d algebraic submanifold of $\mathbb{R}^9$. It is bounded since $\boldsymbol{a}, \boldsymbol{b}$ and $\boldsymbol{c}$ must each be a unit vector. It is closed[59] since it is the intersection of the inverse images of the closed one-element set $\{0\}$ under the continuous maps $\boldsymbol{a}^t\boldsymbol{a} - 1, \cdots, \boldsymbol{c}^t\boldsymbol{a}$ from $\mathbb{R}^9 \to \mathbb{R}$. Thus, $O(3)$ is a compact 3d manifold. However, it is not path connected. Taking the determinant of $A^tA = I$, we find $(\det A)^2 = 1$, so $\det A = \pm 1$. In Prob. B.44 we show that there are orthogonal matrices with either sign of determinant. Since the determinant cannot jump discontinuously from 1 to -1 along a continuous path, we conclude that $O(3)$ is disconnected. It has two connected components. The identity I lies in the connected component where $\det A = 1$ and comprises proper rotations of $\mathbb{R}^3$, as explained in Footnote 47 of Sect. 3.10. In fact, the connected component of the identity is a closed subgroup of $O(3)$ and is a Lie group in its own right, the special orthogonal group $SO(3)$ which is also the kernel of the determinant homomorphism from $O(3)$ to $C_2 = \{\pm 1\}$. The subgroup $SO(3)$ and its Lie algebra play a key role in our study of a rigid body in Chap. 8. The other component where $\det A = -1$ is not a subgroup as it is not closed under composition. It consists of so-called improper rotations and is a coset of $SO(3)$ by a reflection: product of a reflection and a proper rotation.

---

[59] For our purposes, a closed set C contained in Euclidean space is one that contains all its limit points with respect to the Euclidean distance function. The inverse image $f^{-1}(C)$ of a closed set under a continuous map f is closed. The intersection of a finite number of closed sets is closed. A closed and bounded subset of Euclidean space is called compact.

The orthogonal Lie algebra. The Lie algebra as a vector space is defined as the tangent space to the group at the identity. To identify the orthogonal Lie algebra $\underline{O(3)}$, we suppose $A \approx I + u$ and treat u to linear order. The orthogonality condition

$$(I + u^t)(I + u) \approx I \quad \text{becomes} \quad u + u^t = 0. \tag{B.99}$$

Thus, the Lie algebra of the orthogonal group consists of 3×3 real antisymmetric matrices[60]. A real linear combination of antisymmetric matrices $\alpha u + \beta v$ remains antisymmetric, so this is indeed a vector space. The entries above the diagonal are the only linearly independent entries of an antisymmetric matrix, so $\underline{O(3)}$ is a 3-dimensional real vector space isomorphic to $\mathbb{R}^3$. We say that $\underline{O(3)}$ is a 3-dimensional Lie algebra. It is no surprise that G and $\underline{G}$ have the same dimension. A convenient basis $\{e_1, e_2, e_3\}$ for $\underline{O(3)}$ is furnished by the matrices with ab-entries $(e_i)_{ab} = -\epsilon_{iab}$:

$$e_1 = -\begin{pmatrix} 0 & 0 & 0 \\ 0 & 0 & 1 \\ 0 & -1 & 0 \end{pmatrix}, \quad e_2 = -\begin{pmatrix} 0 & 0 & -1 \\ 0 & 0 & 0 \\ 1 & 0 & 0 \end{pmatrix} \quad \text{and} \quad e_3 = -\begin{pmatrix} 0 & 1 & 0 \\ -1 & 0 & 0 \\ 0 & 0 & 0 \end{pmatrix}. \tag{B.100}$$

This means any antisymmetric 3×3 matrix u may be expressed as $u = u^1 e_1 + u^2 e_2 + u^3 e_3$ where u^1, u^2, u^3 are real coefficients.

Exponential map. As with $U(1)$, given a nonzero Lie algebra element u, it determines a 1-parameter subgroup of the Lie group via the matrix exponential $u \mapsto A = e^{su}$ where $s \in \mathbb{R}$. Indeed, we verify that if u is antisymmetric, then A is orthogonal:

$$A^t = e^{su^t} = e^{-su} = A^{-1}. \tag{B.101}$$

More generally, by exponentiating[61] a linear combination $u^i e_i$ of basis elements, we obtain a three-parameter family of group elements: $e^{su^i e_i}$. All elements of the identity component of $O(3)$ [proper rotations, i.e., elements of $SO(3)$] may be obtained this way. However, improper rotations cannot be reached by exponentiating elements u of the Lie algebra, since $\det e^{su} = 1$ (see Prob. B.51). We could of course compose elements of $SO(3)$ by reflections to obtain the improper rotations. Thus, we see that the Lie algebra contains enough data to recover a finite neighborhood of the group identity. In favorable cases (e.g., compact connected groups such as $U(1)$ or $SO(3)$), the exponential map takes the Lie algebra surjectively onto the group.

---

[60] Since $SO(3)$ is the identity component of $O(3)$, they have the same Lie algebra.

[61] While the matrix exponential gives a map from the Lie algebra to the group for matrix groups, there is a more general way of defining the exponential map. Given an element of the Lie algebra $u \in T_eG$, it defines a left-invariant vector field X_u on G via the pushforward of u through the left-translation map to all points of G, $L_{g_*} : T_eG \to T_gG$. Now, consider the integral curve of X_u (with parameter s) that begins at the identity in the direction of u. This

Lie bracket and structure constants. As noted earlier, the group structure of a Lie group G endows the tangent vector space $\underline{G}$ at the group identity with a bilinear anti-symmetric product $\underline{G} \times \underline{G} \to \underline{G}$ called the Lie bracket, satisfying the Jacobi identity. For the Lie algebra of a matrix group, the Lie bracket is simply the commutator[62] of matrices (see Prob. B.46) and the Jacobi identity is automatically satisfied since it is a property of the matrix commutator (see Prob. B.47). For $\underline{O(3)}$, we verify (in Prob. B.48) that the Lie brackets among the basis elements in (B.100) is

$$[e_1, e_2] = e_3, \quad [e_2, e_3] = e_1 \quad \text{and} \quad [e_3, e_1] = e_2 \quad \text{or} \quad [e_i, e_j] = \epsilon_{ijk} e_k. \tag{B.102}$$

This Lie algebra should remind us of the cross products $\hat{x} \times \hat{y} = \hat{z}, \hat{y} \times \hat{z} = \hat{x}, \hat{z} \times \hat{x} = \hat{y}$ of the orthonormal basis vectors $\hat{x}, \hat{y}, \hat{z}$ of $\mathbb{R}^3$. In fact, $\underline{O(3)}$ is isomorphic[63] to the cross product Lie algebra of vectors in 3d Euclidean space $\mathbb{R}^3$, as we show in (11.68). The isomorphism takes vectors r_a to antisymmetric matrices via $u_{ab} = \epsilon_{abc} r_c$ and conversely $r_c = (1/2)\epsilon_{abc} u_{ab}$. In general, the Lie brackets among basis elements of a Lie algebra can be expressed as a linear combination of basis elements: $[e_i, e_j] = c_{ijk} e_k$. The coefficients c_{ijk} are called the structure constants of the Lie algebra (in the chosen basis). For $SO(3)$ or $O(3)$, the structure constants in the above basis are given by the components of the Levi-Civita symbol $c_{ijk} = \epsilon_{ijk}$.

Maurer-Cartan form. Given a matrix group G, we may define a distinguished $\underline{G}$-valued 1-form on it called the Maurer-Cartan form. It is given by the formula $\omega = g^{-1} dg$ which can be regarded as a matrix whose entries are 1-forms. Here, we regard g as a matrix whose entries g_{ij} are functions on the group at the point $g \in G$. Then dg is viewed as a 1-form on the group at g. Left translating by g^{-1} pulls this 1-form back to the identity. Thus, $g^{-1} dg$ is a Lie algebra-valued 1-form on the group. Though in a neighborhood of the identity, ω may be regarded as the exterior derivative of $\log g$ (defined via the logarithmic series for $\log(I + u)$), the latter is not a globally defined single-valued function on the group. So ω is not exact. In fact, in general it

---

is the solution of the system of 1st order ODEs $\dot{x} = X_u$ subject to the IC $x(0) = I$. The exponential map, by definition, maps u to the point $x(1) \in G$. The appearance of e^u in matrix groups is natural since the solution of this IVP in that case is $\exp(su)$.

[62] Note that while the commutator of matrices in $\underline{G}$ is an element of $\underline{G}$, the product of matrices in the Lie algebra of a matrix group is not regarded as an element of the Lie algebra. With reference to $\underline{O(3)}$, the product of antisymmetric matrices is not antisymmetric in general.

[63] The group $SU(2)$ of 2×2 unitary matrices with unit determinant also has a Lie algebra isomorphic to $\underline{O(3)}$. Indeed, the Lie brackets among $(1/2i)\times$ the Pauli matrices (B.107) [which furnish a basis for $\underline{SU(2)}$] are the same as those among e_1, e_2 and e_3.

is not closed either (see Prob. B.53). We will make use of the Maurer-Cartan form in working with the angular velocity of a rigid body (see Footnote 32 of Sect. 8.10).

B.14* Quaternions and the axis-angle representation of rotations

The Euler angles of Sect. 8.9 are not the only way of parametrizing rotations in three dimensions. The axis-angle representation of rotations (see Sect. 8.3) is another option, while Hamilton's quaternions provide a different approach, both of which we briefly introduce here. Additional background and references may be found in [71].

Quaternion algebra and norm. Quaternions $\mathbb{H}$ are a noncommutative generalization of the complex numbers $\mathbb{C}$. However, they share with $\mathbb{C}$ the properties of having an associative multiplication law that distributes over addition, admitting a compatible norm and permitting division by nonzero elements. While multiplication of complex numbers by complex numbers of unit magnitude effect rotations in the complex plane, conjugation of imaginary quaternions by unit quaternions will be seen to implement rotations in 3d. Recall that complex numbers $z = u + vi$ with $i^2 = -1$ may be viewed as ordered pairs (u, v) of real numbers. Quaternions $q = \alpha e + \beta i + \gamma j + \delta k$ may be viewed as ordered quadruples of real numbers $(\alpha, \beta, \gamma, \delta)$. While e (sometimes denoted 1) is the two-sided multiplicative identity, the other basis quaternions $\{i, j, k\}$ are postulated to satisfy the quaternion algebra

$$i^2 = j^2 = k^2 = -e, \quad ij = -ji = k, \quad jk = -kj = i \quad \text{and} \quad ki = -ik = j. \tag{B.103}$$

We also write $q = (\alpha, \boldsymbol{u})$ where $\boldsymbol{u} = (\beta, \gamma, \delta)$ and call α the scalar or real part of q and $\boldsymbol{u}$ the vector or imaginary part of q. Thus, the imaginary part of q is an ordinary vector $\boldsymbol{u} \in \mathbb{R}^3$ with Cartesian components (β, γ, δ). We may verify that the product of two quaternions $q = (\alpha, \boldsymbol{u})$ and $q' = (\alpha', \boldsymbol{u}')$ is the quaternion

$$qq' = (\alpha\alpha' - \boldsymbol{u} \cdot \boldsymbol{u}', \alpha\boldsymbol{u}' + \alpha'\boldsymbol{u} + \boldsymbol{u} \times \boldsymbol{u}'). \tag{B.104}$$

Thus, q and q' commute iff their vector parts are collinear. Every nonzero quaternion has a two-sided inverse given by the reciprocal $q^{-1} = (\alpha^2 + \boldsymbol{u}^2)^{-1}(\alpha, -\boldsymbol{u})$ where $\boldsymbol{u}^2 = \boldsymbol{u} \cdot \boldsymbol{u}$. As in $\mathbb{C}$, the conjugate of q is defined as $\bar{q} = \alpha e - \beta i - \gamma j - \delta k$. This allows us to define the scalar product of two quaternions as the real number

$$\langle q, q' \rangle = \Re(q\bar{q}') = \alpha\alpha' + \boldsymbol{u} \cdot \boldsymbol{u}' = \alpha\alpha' + \beta\beta' + \gamma\gamma' + \delta\delta'. \tag{B.105}$$

Notice that $\langle q, q' \rangle = \langle q', q \rangle$ is symmetric. The squared-norm of a quaternion

$$|q|^2 = \langle q, q \rangle = \Re(q\bar{q}) = \alpha^2 + \beta^2 + \gamma^2 + \delta^2 \tag{B.106}$$

is simply the square of the Euclidean length of the corresponding 4-tuple. The law of moduli $|qq'| = |q||q'|$ holds as a consequence of Euler's four-square identity[64].

---

[64] Euler's four-square identity (1748) states that $(\alpha^2+\beta^2+\gamma^2+\delta^2)(\alpha'^2+\beta'^2+\gamma'^2+\delta'^2) = (\alpha\alpha' - \beta\beta' - \gamma\gamma' - \delta\delta')^2 + (\alpha\beta' + \beta\alpha' + \gamma\delta' - \delta\gamma')^2 + (\alpha\gamma' - \beta\delta' + \gamma\alpha' + \delta\beta')^2 + (\alpha\delta' + \beta\gamma' - \gamma\beta' + \delta\alpha')^2$ for any pair of (say, real) 4-tuples $(\alpha, \beta, \gamma, \delta)$ and $(\alpha', \beta', \gamma', \delta')$. It may be verified by explicit computation and is a generalization of the Brahmagupta-Fibonacci 2-squares identity $(\alpha^2 + \beta^2)(\alpha'^2 + \beta'^2) = (\alpha\alpha' - \beta\beta')^2 + (\alpha\beta' + \beta\alpha')^2$. The latter ensures that $|zz'| = |z||z'|$ for any pair of complex numbers z, z'.

Unit quaternions and the group $SU(2)$. Unit quaternions are those with $|q| = 1$, which is the same as $\alpha^2 + \beta^2 + \gamma^2 + \delta^2 = 1$. Thus, unit quaternions parametrize the unit 3-sphere $S^3 \subset \mathbb{R}^4$. In fact, the set of unit quaternions may be identified with the group $SU(2)$ of 2×2 unitary matrices with unit determinant. To see this, we first note that quaternions may be represented by 2×2 complex matrices, which form the space denoted $M_2(\mathbb{C})$, equipped with the associative product given by matrix multiplication. In fact, we may obtain a homomorphism of associative algebras $F : \mathbb{H} \to M_2(\mathbb{C})$ by defining first for the basis elements

$$\begin{aligned} &F(e) = I, \quad F(i) = i\sigma_3, \quad F(j) = i\sigma_2 \text{ and } F(k) = i\sigma_1 \quad \text{where} \\ &\sigma_1 = \left(\begin{smallmatrix} 0 & 1 \\ 1 & 0 \end{smallmatrix}\right), \quad \sigma_2 = \left(\begin{smallmatrix} 0 & -i \\ i & 0 \end{smallmatrix}\right) \quad \text{and} \quad \sigma_3 = \left(\begin{smallmatrix} 1 & 0 \\ 0 & -1 \end{smallmatrix}\right) \end{aligned} \tag{B.107}$$

are the Pauli matrices. Hamilton's quaternion relations (B.103) are verified to be preserved by F, e.g., $F(i)F(i) = F(-e)$. Extending F linearly to $\mathbb{H}$ ($F(\lambda q + \mu q') = \lambda F(q) + \mu F(q')$ for any reals λ, μ), we get a 1-1 homomorphism of algebras

$$q \mapsto F(q) = \alpha I + i(\delta\sigma_1 + \gamma\sigma_2 + \beta\sigma_3) = \left(\begin{smallmatrix} \alpha+\beta i & \gamma+\delta i \\ -\gamma+\delta i & \alpha-\beta i \end{smallmatrix}\right). \tag{B.108}$$

The reciprocal of a nonzero quaternion is represented by the inverse matrix while the squared-norm $|q|^2$ is given by $\det F(q)$. Moreover, if q is a unit quaternion, one checks that $F(q)$ is a unitary matrix ($FF^\dagger = F^\dagger F = I$) with determinant one[65]. In fact, unit quaternions are mapped 1-1 by F onto the group $SU(2) \subset M_2(\mathbb{C})$.

Quaternions and rotations in 3d. The group $SO(3)$ of rotations of $\mathbb{R}^3$ is known [119] to be a 2:1 homomorphic image of $SU(2)$ [their Lie algebras are isomorphic (see Footnote 63 of Appendix B)]. Thus, it should not come as a surprise that unit quaternions can be used to describe rotations in 3d. To see how this is done, we first note that unit quaternions act on $\mathbb{H}$ by conjugation, taking $v \to v' = qvq^{-1}$. Next, we identify vectors $\boldsymbol{v}$ in 3d Euclidean space $\mathbb{R}^3$ with the imaginary quaternions $\Im\mathbb{H}$ by taking $v = (0, \boldsymbol{v})$. Moreover, one checks using (B.104) that if $v \in \Im\mathbb{H}$, then so is v'. Furthermore, by the law of moduli, $|v'| = |v|$ as $|q| = |q^{-1}| = 1$, so that conjugation by a unit quaternion takes an imaginary quaternion to another imaginary quaternion of the same length[66]. In more detail, if $v = (0, \boldsymbol{v})$ and $q = (\alpha, \boldsymbol{u})$ with $\alpha^2 + \boldsymbol{u} \cdot \boldsymbol{u} = 1$, then $q^{-1} = \bar{q} = (\alpha, -\boldsymbol{u})$ and some algebra using (B.104) allows us to show that

$$q(0, \boldsymbol{v})q^{-1} = (0, \boldsymbol{v}') \text{ where } \boldsymbol{v}' = R(q)\boldsymbol{v} = (\alpha^2 - \boldsymbol{u}^2)\boldsymbol{v} + 2\alpha(\boldsymbol{u} \times \boldsymbol{v}) + 2(\boldsymbol{u} \cdot \boldsymbol{v})\boldsymbol{u}. \tag{B.110}$$

---

[65] The entries of the $SU(2)$ matrix $F(q)$ are called Cayley-Klein parameters. They can be used in place of unit quaternions to parametrize rotations. They are expressible in terms of Euler angles (see p.155 of [45]):

$$\alpha + \beta i = e^{i(\psi+\phi)/2} \cos(\theta/2) \quad \text{and} \quad \gamma + \delta i = i e^{i(\psi-\phi)/2} \sin(\theta/2). \tag{B.109}$$

[66] In fact, conjugation by any nonzero quaternion takes an imaginary quaternion to another imaginary quaternion of the same length. In this case, the additional factor $1/(\alpha^2 + \boldsymbol{u}^2)$ appears on the RHS of (B.110). However, conjugation by two nonzero quaternions q and $\tilde{q} = \lambda q$ that differ by a rescaling by $\lambda \in \mathbb{R} \setminus \{0\}$, produce the same rotation of $\boldsymbol{v}$ since $\tilde{q}v\tilde{q}^{-1} = qvq^{-1}$. For this reason, we restrict to conjugation by unit quaternions.

Consequently, conjugation by a unit quaternion q is a norm-preserving linear transformation $R(q)$ of $\Im\mathbb{H}$. Thus, it must either be a proper or an improper rotation, i.e., $R^t R = I$ with $\det R = \pm 1$. To eliminate the possibility $\det R(q) = -1$, we note that the set of unit quaternions ($\cong S^3$) is path connected[67], so the continuous function $\det R(q)$ must be a constant[68]. It is easy to see that $\det R = 1$ when $q = e$ (see also Prob. B.55). Thus, conjugation by unit quaternions produce proper rotations of $\mathbb{R}^3$.

Axis-angle representation of rotation. One may wonder which rotation $R(q)$ corresponds to. It turns out that for the unit quaternion $q = (\alpha, \boldsymbol{u})$, $R(q)$ is the counterclockwise rotation about the axis $\hat{n} = \boldsymbol{u}/|\boldsymbol{u}|$ by an angle θ where $\alpha = \cos(\theta/2)$ (see Fig. 3.7). To show this and to better understand (B.110), let us write the rotation in terms of the axis $\hat{n}$ and angle θ (this is simply a change of variables to help recognize a rotation when we see one). The real and imaginary parts of the unit quaternion $q = (\alpha, \boldsymbol{u})$ are $\alpha = \cos(\theta/2)$ and $\boldsymbol{u} = \sin(\theta/2)\hat{n}$. Putting this in (B.110), we get

$$\boldsymbol{v}' = R(q)\boldsymbol{v} = \cos\theta\, \boldsymbol{v} + \sin\theta\, \hat{n} \times \boldsymbol{v} + 2\sin^2(\theta/2)(\hat{n}\cdot\boldsymbol{v})\,\hat{n}. \tag{B.111}$$

Let us first illustrate this through two examples. (i) Consider the case of infinitesimal angle $\theta \ll 1$. Then up to linear order in θ, $\boldsymbol{v}' \approx \boldsymbol{v} + \theta\, \hat{n} \times \boldsymbol{v}$. Comparing with (3.52), we recognize this as a counterclockwise rotation of $\boldsymbol{v}$ about $\hat{n}$ by infinitesimal angle θ. (ii) Next, suppose $\hat{n} = \hat{z}$ and $\boldsymbol{v} = \hat{x}$. Then $\hat{n}\cdot\boldsymbol{v} = 0$ and $\hat{n}\times\boldsymbol{v} = \hat{y}$. Consequently, $\boldsymbol{v}' = \cos\theta\,\hat{x} + \sin\theta\,\hat{y}$, which we immediately recognize as a rotation of $\hat{x}$ about $\hat{z}$ by counterclockwise angle θ.

More generally, we check that $\boldsymbol{v}'$ makes the same angle with $\hat{n}$ as $\boldsymbol{v}$ did:

$$\boldsymbol{v}'\cdot\hat{n} = \boldsymbol{v}\cdot\hat{n}(\cos\theta + 2\sin^2(\theta/2)) = \boldsymbol{v}\cdot\hat{n}. \tag{B.112}$$

Therefore, $\boldsymbol{v}'$ must lie on the cone swept by $\boldsymbol{v}$ about the axis $\hat{n}$. It is also straightforward to verify (as noted above, see also Prob. B.56) that $\boldsymbol{v}'\cdot\boldsymbol{v}' = \boldsymbol{v}\cdot\boldsymbol{v}$ so that $\boldsymbol{v}'$ has the same length as $\boldsymbol{v}$. To find the angle through which $\boldsymbol{v}$ has been rotated to obtain $\boldsymbol{v}'$ we must focus on the plane perpendicular to $\hat{n}$. From (B.111), note that

$$(\hat{n}\times\boldsymbol{v}')\cdot(\hat{n}\times\boldsymbol{v}) = \cos\theta\,(\hat{n}\times\boldsymbol{v})^2 \quad\Rightarrow\quad \frac{(\hat{n}\times\boldsymbol{v}')\cdot(\hat{n}\times\boldsymbol{v})}{|\hat{n}\times\boldsymbol{v}'||\hat{n}\times\boldsymbol{v}|} = \cos\theta \tag{B.113}$$

since $|\hat{n}\times\boldsymbol{v}'| = |\hat{n}\times\boldsymbol{v}|$ from (B.112). Combining, the component of $\boldsymbol{v}$ along $\hat{n}$ is unaltered while the one orthogonal to $\hat{n}$ is rotated by angle θ. Thus, we have shown that $R(q)\boldsymbol{v}$ is indeed a counterclockwise rotation of $\boldsymbol{v}$ by angle θ about $\hat{n}$. In particular, conjugation by the unit quaternion $q = (\cos(\theta/2), \sin(\theta/2)\hat{n})$ rotates any vector $\boldsymbol{v}$ (regarded as the imaginary part of a quaternion $v = (0, \boldsymbol{v})$) about the $\hat{n}$ axis counterclockwise by angle θ. This completes our brief discussion of the axis-angle representation of rotations and their connection to quaternions.

---

[67] The image of a path connected space under a continuous map is path connected. The punctured 4d Euclidean space $P = \mathbb{R}^4 \setminus \{0\}$ is path connected since any two points may be joined by a path consisting of two straight line segments. The continuous map $f(x) = x/||x||$ maps P onto $S^3 = \{x \in \mathbb{R}^4, ||x|| = 1\}$. Thus, S^3 is path connected.

[68] The function $\det R(q)$ is a polynomial in the components of $q = (\alpha, \boldsymbol{u})$ (see Prob. B.55), so it cannot jump between the values ± 1 on the path connected space of unit quaternions.

B.15 Problems

1. Consider the unit sphere S^2 embedded in $\mathbb{R}^3$: $x^2 + y^2 + z^2 = 1$. Let $N = (0, 0, 1)$ be the North pole of the sphere and consider the equatorial plane E defined by $z = 0$. Given any point $(x, y, z) \neq N$ on S^2, we define its **stereographic projection** to be the unique point $(X, Y) \in E$ through which the line joining N and P passes (see Fig. B.7). Describe how you might define the image of N under the stereographic projection using suitable limits. Express the coordinates (X, Y) of the stereographic projection of P in terms of x, y, z. The stereographic projection from the North pole provides a coordinate chart on $S^2 \backslash N$. Similarly, the stereographic projection from the South pole $S = (0, 0, -1)$ to the equatorial plane defines a coordinate chart on $S^2 \setminus S$. Find the coordinates (X', Y') of the point $P = (x, y, z) \in S^2$ of the stereographic projection from S. Find the transition function that expresses (X', Y') in terms of (X, Y) on the overlap $S^2 \setminus \{S, N\}$ between the two coordinate charts. Show that the transition function is smooth.

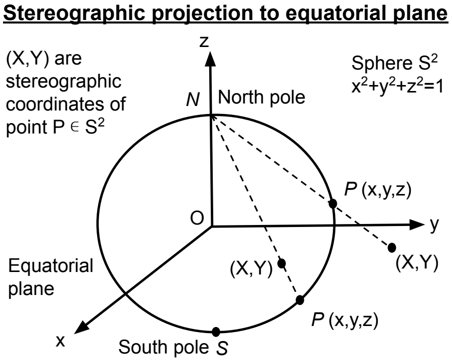
Stereographic projection to equatorial plane
z
(X,Y) are stereographic coordinates of point P ∈ S²
N
North pole
Sphere S²
x²+y²+z²=1
P (x,y,z)
O
y
(X,Y)
Equatorial plane
(X,Y)
P (x,y,z)
x
South pole S

Figure B.7: Stereographic coordinates (X, Y) of a point P on the sphere S^2 are given by the point of intersection with the equatorial plane of the line from the North pole through P.

2. Find the **Jacobian matrix** for the transformation from plane polar (r, ϕ) to Cartesian (x, y) coordinates on the punctured plane $[(x, y) \neq (0, 0)]$:

$$J = \frac{\partial(x, y)}{\partial(r, \phi)} = \begin{pmatrix} x_r & x_\phi \\ y_r & y_\phi \end{pmatrix}. \tag{B.114}$$

   Find $\det J$ and show that J is invertible on the punctured plane. Find J^{-1} and compare it with the Jacobian matrix for the inverse transformation.

3. **Diffeomorphism.** Find a smooth map (with smooth inverse) from the circle $x^2 + y^2 = 1$ to the circle $x^2 + y^2 = 2$ and also to the ellipse $x^2 + 2y^2 = 1$ and use these to show that the circles and ellipse are all diffeomorphic.

4. Find 2 **diffeomorphisms** ϕ between $(0, 1)$ and $\mathbb{R}$, using (a) a rational function and (b) a hyperbolic/trigonometric function. Explain why they are diffeomorphisms.

5. Consider the **vector field** on the **Euclidean plane** given by $v = y\frac{\partial}{\partial x} - x\frac{\partial}{\partial y}$. (a) Sketch the vector field on the x-y plane by displaying arrows. Which way does it

point at the origin? (b) Solve for the integral curve $(x(t), y(t))$ through the point $(x(0) = 1, y(0) = 0)$ and plot it. Compare with the previous sketch and comment on whether the arrows are tangent to the integral curve.

6. **Commutator.** Given 2 vector fields on a manifold which in local coordinates are given by $u = u^i \partial_i$ and $v = v^j \partial_j$, find $u(v(f))$ and $v(u(f))$ and show that they involve 2nd derivatives of f. Evaluate the difference $u(v(f)) - v(u(f))$ and confirm that it is the same as $[u, v]f$ where $[u, v]$ is the commutator defined in (B.8).
7. Use the formula for the commutator of vector fields in local coordinates to show that they satisfy the **Jacobi identity** $[u, [v, w]] + [w, [u, v]] + [v, [w, u]] = 0$.
8. (a) Show that the **Lie derivative** satisfies the Leibniz rule: $\mathcal{L}_u(fv) = (\mathcal{L}_u f)v + f\mathcal{L}_u v$ for a smooth function f and vector fields u, v. (b) Is $[fu, v] = f[u, v]$? What is $\mathcal{L}_{fu} v - f\mathcal{L}_u v$? Is the commutator linear over the space of functions?
9. **Wedge product.** Suppose f, g are smooth real-valued functions on 3d Euclidean space with Cartesian coordinates x, y, z. (a) Find the components of $df \wedge dg$ in the coordinate basis for 2-forms. (b) Compare with the components of $\boldsymbol{\nabla} f \times \boldsymbol{\nabla} g$ from vector calculus. (c) What is the geometric meaning of $\boldsymbol{\nabla} f \times \boldsymbol{\nabla} g$?
10. **Exterior derivative.** Consider the 1-form $\alpha = (x dx + y dy)/r^2$ on the punctured x-y plane $\mathbb{R}^2 \setminus (0, 0)$ where $r^2 = x^2 + y^2$. Show that the exterior derivative $d\alpha = 0$ (B.22). Thus, α is closed. Find a smooth function $f(x, y)$ on the punctured plane such that $\alpha = df$, thereby establishing that α is exact.

$*$11. **Multiply connected space.** An infinite cylinder $C = S^1 \times \mathbb{R}$ is connected but not simply connected. (a) Given a point $p \in C$, draw a closed curve that begins and ends at p that is homotopic to a point. (b) (b) Draw and describe a closed directed curve on C beginning and ending at p which cannot be continuously shrunk to p. (c) Classify all closed curves based at p into distinct homotopy classes (equivalence classes under continuous deformation) using an integer with a suitable name.

12. Suppose $A_\mu = (\phi, -\boldsymbol{A}) = (\phi, -A_x, -A_y, -A_z)$ are the Cartesian components of the **gauge potential 1-form** $A = A_\mu dx^\mu$ on 4d space-time with $x^\mu = (ct, x, y, z)$. Here ϕ and $\boldsymbol{A}$ are the scalar and vector potentials. Find the components of the field strength $F_{\mu\nu} = \partial_\mu A_\nu - \partial_\nu A_\mu$, arrange them in a 4×4 matrix and express them in terms of the electric and magnetic fields $\boldsymbol{E} = -\frac{1}{c}\partial_t \boldsymbol{A} - \boldsymbol{\nabla}\phi$ and $\boldsymbol{B} = \boldsymbol{\nabla} \times \boldsymbol{A}$.
13. Consider the 1-form on $\mathbb{R}^2$, $\omega(x, y) = y\, dx - x\, dy$. Since $d(df) = d^2 f = 0$, an 'integrability' condition for ω to be exact ($\omega = d\sigma$ for some σ) is that it be closed ($d\omega = 0$). On $\mathbb{R}^2$, $d\omega = 0$ is also sufficient for ω to be exact. Show that ω disobeys the **integrability condition**. Look for an integrating denominator $\tau(x, y)$ and function $\sigma(x, y)$ such that $\omega/\tau = d\sigma$ is exact on some open subset of $\mathbb{R}^2$. Comment on whether τ is unique. Remark: For a class of 1-forms ω associated to the infinitesimal heat added reversibly to a system, the 2nd law of thermodynamics guarantees the existence of an **integrating denominator** τ, which is the absolute temperature. σ is the entropy function on the thermodynamic state space.
14. Taking pressure p and volume V as independent variables for the internal energy U of a gas, use the 1st law of thermodynamics (see Appendix B.5*) to obtain

an expression for the **heat 1-form** ω [associated to the infinitesimal heat added reversibly to a fixed mass of a (not necessarily ideal) gas]. In some treatments, ω is denoted δQ or $đQ$. These are meant to convey that ω is *not* an exact differential.

15. **Euclidean volume form.** Suppose x^1, x^2, x^3 are Cartesian coordinates on $\mathbb{R}^3$ and ϵ_{ijk} is the Levi-Civita symbol. (a) Verify that $\Omega = \frac{1}{3!}\epsilon_{ijk} dx^i \wedge dx^j \wedge dx^k = dx^1 \wedge dx^2 \wedge dx^3$. (b) Transform this 3-form to spherical polar coordinates $x^1 = r\sin\theta\cos\phi$, $x^2 = r\sin\theta\sin\phi$, $x^3 = r\cos\theta$ and find the components of Ω in the new variables. (c) For a suitable function f, express the volume form as $\Omega = f(r,\theta,\phi) dr \wedge d\theta \wedge d\phi$ and compare f with the determinant of the Jacobian.

$*$16. **Determinant Levi-Civita formula.** Recall equation (B.36). (a) Write the analogous formula for 2×2 invertible matrices and ϵ_{ij} and verify that it is true. (b) For any 3×3 real matrix A, show that

$$\epsilon_{ijk} = \det A^{-1} A_i^l A_j^m A_k^n \, \epsilon_{lmn}. \tag{B.115}$$

17. **Pushforward and pullback.** Consider the smooth map $\phi : \mathbb{R} \to \mathbb{R}^2$ taking $x \mapsto (x, 0)$ in Cartesian coordinates. Find the pushforward $\phi_* v$ of the vector field $v = x\partial_x$ on $\mathbb{R}$. Find the pullbacks $\phi^*\alpha$ and $\phi^*\beta$ of the 1-forms $\alpha = dx$ and $\beta = dy$ on $\mathbb{R}^2$ as well as of the 2-form $\alpha \wedge \beta$. What about the pullback of any 2-form on $\mathbb{R}^2$? Repeat this problem for the map $\psi : \mathbb{R} \to \mathbb{R}^2$ taking $x \mapsto (0, x)$.

$*$18. **Poisson tensor.** Consider the Poisson manifold $\mathbb{R}^{2n}$ with canonical coordinates and momenta q^i, p_j for $1 \le i, j \le n$. Suppose $\xi^a(q,p)$ for $1 \le a \le 2n$ are a system of coordinates on (some open subset of) $\mathbb{R}^{2n}$ and define $r^{ab} = \{\xi^a, \xi^b\}$. If we make a change of variables $\xi^a \mapsto \eta^a$, then show that r^{ab} transform as components of a second rank contravariant tensor field. Hint: Use the definition (3.118) of the PB in terms of derivatives with respect to q^i and p_j.

19. Find the components h_{ab} ($h_{\theta\theta}, h_{\theta\varphi}, h_{\varphi\varphi}$ in polar coordinates θ, φ) of the **induced metric** on the unit sphere via the pullback (B.42) of the Euclidean metric on $\mathbb{R}^3$. Write down the 'square of the line element' $ds^2 = h_{ab} d\xi^a \otimes d\xi^b$ explicitly.

20. Consider the embedding $f : T^2 \to \mathbb{R}^3$ of the **2-torus** in $\mathbb{R}^3$ (with Cartesian coordinates) given by $(\theta, \varphi) \mapsto ((R + r\cos\theta)\cos\varphi, (R + r\cos\theta)\sin\varphi, r\sin\theta)$ where $R > r > 0$ are fixed. (a) Indicate the meanings of r, R, θ, φ by drawing a figure. (b) Find the pullback f^*g of the Euclidean metric $g_{ij} = \delta_{ij}$. (c) Find the corresponding Riemannian volume form on T^2.

$*$21. Suppose $(x(t), y(t), z(t))$ for $0 \le t \le 1$ is a space curve in 3d Euclidean space $\mathbb{R}^3$. Find a formula for its **length**. Suppose $(x(s,t), y(s,t), z(s,t))$ for $0 \le s, t \le 1)$ is a parametrized surface embedded in $\mathbb{R}^3$. Find a formula for its **surface area**.

$*$22. Suppose A is an $N \times N$ **matrix-valued 1-form** on $\mathbb{R}^2$ with coordinates x^0 and x^1. What this means is that when written as a linear combination of coordinate basis 1-forms dx^μ, the coefficients A_μ are $N \times N$ matrices. Viewed differently, A is a matrix, each of whose entries is a 1-form. In components, $A_b^a = (A_\mu)_b^a dx^\mu$ where $\mu = 0, 1$ and $a, b = 1, \ldots, N$ are matrix indices. We use up-down matrix indices since a matrix may be viewed as a (1,1) tensor. Now, we may construct an $N \times N$ matrix-valued 2-form via the wedge product $A \wedge A$. Show that $A \wedge A$ is given by

$$A \wedge A = [A_0, A_1] dx^0 \wedge dx^1, \quad \text{where} \quad [A_0, A_1] = A_0 A_1 - A_1 A_0. \tag{B.116}$$

∗23. Working on Euclidean space with Cartesian coordinates, show that **Gauss' divergence theorem and Stokes' theorem** are special cases of (B.55). See also [113].

24. Show that the **covariant derivative** of a vector field fv satisfies the **Leibniz rule** $\boldsymbol{\nabla}_i (f v^j) = (\partial_i f) v^j + f \boldsymbol{\nabla}_i v^j$ for any scalar function f.

∗25. **Christoffel symbols.** Establish (B.60) for the transformation of $\Gamma^i_{jk} v^k$ under a coordinate change $x \mapsto \tilde{x}$. Hint: Find $\tilde{\Gamma}^i_{jk}$ and $\tilde{v}^k$ separately. Show that

$$\tilde{\Gamma}^i_{jk} = \frac{\partial \tilde{x}^i}{\partial x^m} \frac{\partial x^p}{\partial \tilde{x}^j} \frac{\partial x^q}{\partial \tilde{x}^k} \Gamma^m_{pq} - \frac{\partial x^n}{\partial \tilde{x}^j} \frac{\partial^2 \tilde{x}^i}{\partial x^n \partial x^m} \frac{\partial x^m}{\partial \tilde{x}^k}. \tag{B.117}$$

To obtain this, begin with the formula for $\tilde{\Gamma}^i_{jk}$ in terms of $\tilde{x}$ derivatives of the $\tilde{g}$ metric and its inverse. For instance, the first term in this can be expressed as

$$\frac{1}{2} \tilde{g}^{il} \tilde{\partial}_j \tilde{g}_{lk} = \frac{1}{2} \frac{\partial \tilde{x}^i}{\partial x^m} \frac{\partial \tilde{x}^l}{\partial x^n} g^{mn} \tilde{\partial}_j \left(\frac{\partial x^o}{\partial \tilde{x}^l} \frac{\partial x^p}{\partial \tilde{x}_k} g_{op} \right). \tag{B.118}$$

Expand and add the other terms and exploit cancellations. Note that $\frac{\partial \tilde{x}^i}{\partial x^m} \frac{\partial x^m}{\partial \tilde{x}^k} = \delta^i_k$.

26. The **upper half plane** $U = \{(x, y) \in \mathbb{R}^2 | y > 0\}$ has the Poincaré metric $g = (dx \otimes dx + dy \otimes dy)/y^2$. (a) Find all the Christoffel symbols: Γ^x_{xx}, etc. (b) Show that the resulting geodesic equations are the pair of ODEs $y\ddot{x} - 2\dot{x}\dot{y} = 0$ and $y\ddot{y} + \dot{x}\dot{x} - \dot{y}\dot{y} = 0$ where dots denote derivatives with respect to an affine parameter t. (c) Establish that $p = \dot{x}/y^2$ and $H = (\dot{x}^2 + \dot{y}^2)/(2y^2)$ are conserved along geodesics. (d) Eliminate x and derive a self-contained ODE for y. (e) Solve for the geodesics when $p = 0$. Describe their shape in Euclidean language. How long (in t) does it take the geodesics to approach the x axis? (f) When p is not necessarily zero, show that the geodesic equations may be brought to a Newtonian form $\ddot{u} = -V'(u)$ where $y = e^u$. What is a potential $V(u)$? Interpret the answer.

27. Show that the **covariant derivative** satisfies $\partial_i (\phi_j v^j) = (\boldsymbol{\nabla}_i \phi_j) v^j + \phi_j \boldsymbol{\nabla}_i v^j$.

28. Show that the **metric tensor is covariantly constant** $\boldsymbol{\nabla}_i g_{jk} = 0$ if $\boldsymbol{\nabla}$ is the covariant derivative defined via the Christoffel symbols associated to the metric g_{jk}.

∗29. Suppose Γ^i_{jk} symmetric in the lower indices are a collection of **connection coefficients** that depend on a metric tensor g_{ij} and its first derivatives $\partial_i g_{jk}$. Suppose we are told that $\boldsymbol{\nabla}_i g_{jk} = \partial_i g_{jk} - \Gamma^l_{ij} g_{lk} - \Gamma^l_{ik} g_{jl} = 0$. By making a suitably general ansatz for Γ^i_{jk} try to fix it by requiring the covariant constancy of the metric.

∗30. Show that the **Riemann curvature** (B.65) behaves tensorially: (a) $R(fu, v)w = fR(u, v)w$ and (b) $R(u, v)(fw) = fR(u, v)w$ where f is any scalar function. Show that the components of the $(0, 4)$ Riemann tensor have the symmetries (c) $R_{mkij} = -R_{kmij}$ and (d) $R_{mkij} = R_{ijmk}$.

31. Consider the **round metric on the 2-sphere** $g = d\theta \otimes d\theta + \sin^2 \theta d\phi \otimes d\phi$. (a) Evaluate the Christoffel symbols. (b) Find the geodesic equation and compare with Prob. 3.17. (c) Find all components of the Riemann tensor. (d) Find the sectional curvature $K(\partial_\theta, \partial_\phi)$ and compare it with the Ricci scalar.

$*$32. Express the **geodesic deviation equation** $\ddot{\tilde{c}}_j = -\kappa_j(t)\tilde{c}_j$ (B.87) for the j^{th} component of a Jacobi vector field in first order form. Develop a series solution using the time evolution matrix of Sect. 13.4.2*.

33. (a) Show that H is a **subgroup** of G iff given $h, k \in H$, $hk^{-1} \in H$. (b) If H is a subgroup of G, then verify that $H_g = gHg^{-1}$ is also a subgroup, the 'conjugate subgroup' of H by the element g. H is normal if it is self-conjugate for every g.

34. **Group homomorphism.** Suppose a map between two groups $\phi : G \to G'$ preserves products: $\phi(gh) = \phi(g)\phi(h)$ for all $g, h \in G$. (a) Show that ϕ maps the identity in G to the identity in G' and maps inverses to inverses: $\phi(g^{-1}) = \phi(g)^{-1}$. (b) Also show that the homomorphic image $\phi(G) \subset G'$ is a subgroup of G'.

35. Find an **isomorphism** between (a) $U(1)$ and $SO(2)$ and (b) $(\mathbb{R}, +)$ and $(\mathbb{R}^+, \times)$.

36. Show that the group of 2×2 orthogonal matrices $O(2)$ is **nonabelian**.

37. Show that any group G of order n may be realized as a subgroup of the **permutation group** S_n. Hint. Use left multiplication L_g to associate with any element $g \in G$ a permutation of the group elements. Show that it is a homomorphism.

38. Identify the **quotients** $U(1)/C_n$ where C_n is the cyclic group of order $n \geq 1$.

39. Consider the abelian additive group of integers $\mathbb{Z}$. (a) For any integer n, show that the set $n\mathbb{Z}$ of integers divisible by n is a subgroup. (b) Find the cosets of $n\mathbb{Z}$ in $\mathbb{Z}$. (c) Argue that the quotient $\mathbb{Z}/n\mathbb{Z}$ is isomorphic to the **cyclic group** C_n.

40. The **kernel of a group homomorphism** $\phi : G \to G'$ is the set $\ker \phi = \phi^{-1}(e')$ of elements of G that are mapped to the identity $e' \in G'$. Show that $\ker \phi \lhd G$.

41. **Direct product.** (a) Find the composition law for $G = C_2 \times C_2$. Express it in terms of a multiplication table. (b) Is G isomorphic to the cyclic group C_4?

$*$42. Suppose $G = H \ltimes N$ is the **semidirect product** of the group H acting via φ on N. (a) Show that the composition law $(h, n) \cdot (h', n') = (hh', n\varphi_h(n'))$ is associative. (b) Show that the inverse of (h, n) is $(h^{-1}, \varphi_{h^{-1}}(n^{-1}))$. (c) Show that N may naturally be regarded as a normal subgroup of G in the sense that the set of elements (e_H, n) forms a normal subgroup of $H \ltimes N$ isomorphic to N.

$*$43. **Alternating group.** (a) Argue that the sign of a permutation in S_3 is well defined. (b) Show that A_3 is the commutator subgroup of S_3

44. Find these 3×3 **orthogonal matrices**, verify they satisfy $A^t A = I$ and find $\det A$. (a) A counterclockwise rotation by angle θ about the x, y and z axes. (b) A reflection in the xy, yz and zx planes. (c) A reflection through the origin.

45. Find a pair of 3×3 **orthogonal matrices** A and B that do not commute.

$*$46. Consider a matrix group G and its Lie algebra $\underline{G}$. The **Lie bracket or commutator** is the first approximation to the group commutator. Suppose $g = e^{su}$ and $h = e^{tv}$

are a pair of 1-parameter subgroups generated by the Lie algebra elements u and v. For small s and t, these are group elements in the vicinity of the group identity. Now, for g, h near the identity, the group commutator $[g, h] = ghg^{-1}h^{-1}$ can be expressed as the exponential of a Lie algebra element. Verify that

$$ghg^{-1}h^{-1} = e^{su}e^{tv}e^{-su}e^{-tv} = e^{st[u,v]+\mathcal{O}(st^2,s^2t)}. \tag{B.119}$$

We see the emergence of the Lie algebra commutator from the group commutator. Hint: Write $e^{su} \approx I + su + s^2u^2/2$, etc., and expand the LHS keeping terms up to second degree in s and t.

47. Show that the matrix commutator $[A, B] = AB - BA$ satisfies the **Jacobi identity**: $[A, [B, C]] + [C, [A, B]] + [B, [C, A]] = 0$ for any three square $n \times n$ matrices.

48. **Structure constants of $O(3)$.** Suppose we take e_1, e_2, e_3 (B.100) with matrix elements $(e_i)_{jk} = -\epsilon_{ijk}$ as a basis for $\underline{O(3)}$. Show that their commutators may be expressed as $[e_i, e_j] = \epsilon_{ijk}e_k$. Hint: Find the ab matrix element of either side.

49. Characterize the matrices that lie in the **Lie algebras** of the following matrix groups and use this to find the real dimensions of the corresponding Lie groups: (a) the real general linear group $GL_n(\mathbb{R})$, (b) the special linear group $SL_n(\mathbb{R})$ which is the subgroup with unit determinant (c) the orthogonal group $O(n)$, (d) $SO(n)$.

∗50. Relate the **structure constants of a Lie algebra** to the Poisson tensor of a Poisson algebra where the Poisson tensor r^{ij} is linear in the coordinates x^i.

51. Show that $\det e^u = 1$ if u is an **antisymmetric matrix**. Hint: $\det e^u = e^{\operatorname{tr} u}$. Establish this formula by going to the eigenbasis of u.

∗52. Consider the IVP $\dot{A} = [H, A(t)]$ for a dynamical matrix $A(t)$ where H is a fixed $n \times n$ matrix and $A(0)$ is given. This could be the Heisenberg EOM in quantum mechanics (Sect. 10.3∗). Show that the solution may be expressed via an exponential series and compare with (3.197):

$$A(t) = \exp(t\,\mathrm{ad}_H)A(0) \equiv A(0) + [tH, A(0)] + \frac{1}{2!}[tH, [tH, A(0)]] + \dots \tag{B.120}$$

∗53. Show that the exterior derivative of the **Maurer-Cartan form** $\omega = g^{-1}dg$ is given by $d\omega = -g^{-1}dg \wedge g^{-1}dg$.

54. The basis **quaternions** $1, i, j, k$ generate a group. Find its multiplication table.

∗55. **Conjugation by a unit quaternion.** Conjugation of an imaginary quaternion $(0, \boldsymbol{v})$ by a unit quaternion $q = (\alpha, \boldsymbol{u})$ results in the linear transformation $\boldsymbol{v}' = R(q)\boldsymbol{v} = (\alpha^2 - \boldsymbol{u}^2)\boldsymbol{v} + 2\alpha(\boldsymbol{u} \times \boldsymbol{v}) + 2(\boldsymbol{u} \cdot \boldsymbol{v})\boldsymbol{u}$. Show that $R(q)$ is the 3×3 matrix $R(q) = (\alpha^2 - \boldsymbol{u}^2)I - 2\alpha\tilde{u} + 2\boldsymbol{u}\boldsymbol{u}^t$ where $\tilde{u}$ is the matrix with entries $\tilde{u}_{ab} = \epsilon_{abc}u_c$. Write $R(q)$ explicitly as a 3×3 matrix and show that $\det R(q) = (\alpha^2 + \boldsymbol{u}^2)^3$.

56. **Axis-angle representation of a rotation.** Suppose $\boldsymbol{v}' = \cos\theta\, \boldsymbol{v} + \sin\theta\, \hat{n} \times \boldsymbol{v} + 2\sin^2(\theta/2)(\hat{n} \cdot \boldsymbol{v})\, \hat{n}$ where $\hat{n}$ is a unit vector. Show that $\boldsymbol{v}' \cdot \boldsymbol{v}' = \boldsymbol{v} \cdot \boldsymbol{v}$ and that $|\boldsymbol{v}' \times \hat{n}| = |\boldsymbol{v} \times \hat{n}|$. What is the significance of these results?

Supplementary reading

Some books that discuss topics related to those treated in this book are listed below. They include a wealth of material and problems that the reader may find useful.

1. Arnold V I, *Mathematical Methods of Classical Mechanics*, 2nd ed., Springer-Verlag (1989).
2. Calkin M G, *Lagrangian And Hamiltonian Mechanics*, World Scientific (1996).
3. Corben H C and Stehle P, *Classical Mechanics*, 2nd ed., John Wiley (1960); 2nd rev, ed., Dover (1994).
4. Esposito G, Marmo G and Sudarshan E C G, *From Classical to Quantum Mechanics*, Cambridge Univ. Press (2004).
5. Fetter A L and Walecka J D, *Theoretical Mechanics of Particles and Continua*, Dover (2003).
6. Fetter A L and Walecka J D, *Nonlinear Mechanics: A Supplement to Theoretical Mechanics of Particles and Continua*, Dover (2006).
7. Feynman R P, Leighton R and Sands M, *Feynman lectures on physics*, Vol. 1, Addison-Wesley (1966).
8. Feynman R P, Leighton R and Sands M, *The Feynman lectures on Physics* Vol. 2, Addison-Wesley (1964).
9. French A P, *Newtonian Mechanics*, MIT Introductory Physics Series, W W Norton (1971).
10. Gaspard P, *Chaos, Scattering and Statistical Mechanics*, Cambridge Univ. Press (1998).
11. Goldstein H, Poole C P and Safko J L, *Classical Mechanics*, 3rd ed., Pearson (2013).
12. Hand L N and Finch J D, *Analytical mechanics*, Cambridge Univ. Press (1998).
13. Jain S R, *Mechanics, Waves and Thermodynamics: An Example-Based Approach*, Cambridge Univ. Press (2016).
14. José J V and Saletan E J, *Classical Dynamics: A Contemporary Approach*, Cambridge Univ. Press (1998).
15. Kibble T W B and Berkshire F H, *Classical Mechanics*, 5th ed., Imperial College Press (2004).
16. Kittel C, Knight W D, Ruderman M A, *Mechanics*, Berkeley Physics Course, Vol. 1, McGraw-Hill (1965).

17. Kleppner D and Kolenkow R J, *An Introduction to Mechanics*, 2nd ed., Cambridge Univ. Press (2014).
18. Lanczos C, *The variational principles of mechanics*, 4th ed., Dover (1970).
19. Landau L D and Lifshitz E M, *Mechanics*, Vol. 1 of Course in Theoretical Physics, 3rd ed., Pergamon Press (1976).
20. Landau L D and Lifshitz E M, *Fluid Mechanics*, Vol. 6 of Course in Theoretical Physics, 2nd ed., Pergamon Press (1987).
21. Lowenstein J H, *Essentials of Hamiltonian Dynamics*, Cambridge Univ. Press (2012).
22. Mann P, *Lagrangian and Hamiltonian Dynamics*, Oxford Univ. Press (2018).
23. Matveev A N, *Mechanics and Theory of Relativity*, Mir Publishers (1989).
24. Morin D, *Introduction to Classical Mechanics: With Problems and Solutions*, Cambridge Univ. Press (2008).
25. Moulton F R, *An Introduction to Celestial Mechanics*, Macmillan (1914).
26. Ott E, *Chaos in Dynamical Systems*, 3rd ed., Cambridge Univ. Press (2002).
27. Percival I C and Richards D, *Introduction to Dynamics*, Cambridge Univ. Press (1982).
28. Rajeev S G, *Advanced Mechanics: From Euler's Determinism to Arnold's Chaos*, Oxford Univ. Press (2013).
29. Rajeev S G, *Fluid Mechanics, A Geometrical Point of View*, Oxford Univ. Press (2018).
30. Raychaudhuri A K, *Classical Mechanics: A Course of Lectures*, Oxford Univ. Press (1983).
31. Siegel C L and Moser J K, *Lectures on Celestial Mechanics*, Classics in Mathematics, Springer (1995).
32. Sommerfeld A, *Mechanics*, Academic Press (1964).
33. Sudarshan E C G and Mukunda N, *Classical Dynamics: A Modern Perspective*, Hindustan Book Agency (2015).
34. Symon K R, *Mechanics*, 3rd ed., Addison-Wesley (1971).
35. Synge J L and Griffith B A, *Principles of Mechanics*, McGraw-Hill (1942).
36. Thorne K S and Blandford R D, *Modern Classical Physics: Optics, Fluids, Plasmas, Elasticity, Relativity, and Statistical Physics*, Princeton Univ. Press (2017).
37. Tritton D J, *Physical Fluid Dynamics*, 2nd ed., Oxford Science Publications (1988).
38. Wells D A, *Schaum's Outline of Lagrangian Dynamics*, McGraw Hill (1967).
39. Whittaker E T, *A treatise on the analytical dynamics of particles & rigid bodies*, 2nd ed., Cambridge Univ. Press (1917).
40. Yourgrau W and Mandelstam S, *Variational Principles in Dynamics and Quantum Theory*, 3rd ed., Dover (2003).

References

[1] Abramowitz M and Stegun I A (Eds.), *Handbook of Mathematical Functions with Formulas, Graphs, and Mathematical Tables*, 9th printing, Dover (1972). 412

[2] Arnold V I, *Mathematical Methods of Classical Mechanics*, 2nd ed., Springer-Verlag (1989), p. 37, 245. 35, 131, 313, 352, 353, 460

[3] Arnold V I and Khesin B A, Topological methods in hydrodynamics, 2nd ed., Springer (2021). 558, 559, 644

[4] Ashcroft N W and Mermin N D, *Solid State Physics*, Brooks/Cole (1976). 403

[5] Asimov I, *Asimov's Biographical Encyclopedia of Science and Technology*, 2nd Rev. ed., Doubleday (1964). 41

[6] Babelon O, Bernard D and Talon M, *Introduction to classical integrable systems*, Cambridge University Press (2003). 357, 362

[7] Balachandran A P, Marmo G, Skagerstam B S and Stern A, *Classical topology and quantum states*, World Scientific (1991). 98

[8] Balakrishnan V, *Mathematical Physics with Applications, Problems and Solutions*, ANE Books (2020). xi, 214

[9] Balakrishnan V, Govindarajan S and Lakshmibala S, *The Central Force Problem in n Dimensions*, Resonance **25**(4), April 2020. 115

[10] Ball P, *Flow: Nature's Patterns, a tapestry in three parts*, Oxford Univ. Press, Oxford (2009). 531

[11] Batchelor G K, *An Introduction to Fluid Dynamics*, Cambridge Univ. Press (2000). 567, 569

[12] Bateman H, *Notes on a Differential Equation Which Occurs in the Two-Dimensional Motion of a Compressible Fluid and the Associated Variational Problems*, Proc. Roy. Soc. London Ser. A **125**, 598 (1929). 565

[13] Bodenmann S, *The 18th-century battle over lunar motion*, Physics Today, **63(1)**, 27 (2010). 26

[14] Born M, *Einstein's Theory of Relativity*, Rev. ed., Dover (2012). 150

[15] Born M and Wolf E, *Principles of Optics: Electromagnetic Theory of Propagation, Interference and Diffraction of Light*, Cambridge Univ. Press, 7th ed., (1999). 131, 137

[16] Cannon J R, *The one-dimensional heat equation*, Cambridge Univ. Press (2008). 520

[17] Cercignani C, *Ludwig Boltzmann: The Man Who Trusted Atoms*, Oxford Univ. Press (1998). 324

[18] Chapman S and Cowling T G, *The Mathematical Theory of Non-Uniform Gases*, 3rd ed., Cambridge Univ. Press (1970). 531

[19] Choudhuri A R, *The physics of Fluids and Plasmas: An introduction for astrophysicists*, Cambridge Univ. Press (1998). 531

[20] Coddington E A and Levinson N, *Theory of Ordinary Differential Equations*, McGraw-Hill (1955), p. 15. 182

[21] Corben H C and Stehle P, *Classical Mechanics*, 2$^{\text{nd}}$ ed., John Wiley (1960); 2$^{\text{nd}}$ rev, ed., Dover (1994). 229

[22] Coxeter H S M, *Introduction to Geometry*, Wiley (1969), p. 116. 30

[23] Davidson P A, *Turbulence: An introduction for scientists and engineers* , Oxford Univ. Press (2004). 532

[24] Dennery P and Krzywicki A, *Mathematics for Physicists*, Dover (1996). xi, 250, 494, 508

[25] Devaney R L, *A First Course In Chaotic Dynamical Systems: Theory and Experiment*, Perseus Books (1992). 479

[26] Devaney R L, *An Introduction To Chaotic Dynamical Systems*, Taylor and Francis (2003). 436

[27] Diacu F and Holmes P, *Celestial Encounters*, Princeton Univ. Press (1996). 296, 431

[28] Dirac P A M, *Classical Theory of Radiating Electrons*, Proc. R. Soc. London, Ser. A **167**, 148 (1938). 71

[29] Dirac P A M, *Lectures on Quantum Mechanics*, Dover (2001). 98

[30] Dirac P A M, *Methods in Theoretical Physics*, in *From a Life of Physics*, pp. 19–30, A Salam et. al., [International Symposium on Contemporary Physics, Trieste, Italy, 7-28 June, 1968], World Scientific (1989). 106

[31] Dorfman J R, *An Introduction to Chaos in Nonequilibrium Statistical Mechanics*, Cambridge Univ. Press (1999). 325

[32] Drazin P G and Johnson R S, *Solitons: an introduction*, Cambridge Univ. Press (1989). 10, 60, 357, 509

[33] Duarte P, *Plenty of elliptic islands for the standard family of area preserving maps*, Annales de l'Institut Henri Poincaré C, Analyse non linéaire, **11**(4), 359 (1994). 438

[34] Dunajski M, *Solitons, Instantons and Twistors*, Oxford Univ Press (2010). 509

[35] Einstein A, *Einstein's Essays in Science*, Dover (2009). 22

[36] Einstein A, *Investigations on the Theory of Brownian Movement*, Dover (1956). 525

[37] Feigenbaum M J, *Quantitative universality for a class of nonlinear transformations*, J. Stat. Phys., **19** (1), 25 (1978). 432, 442

[38] Fermi E, *Thermodynamics*, Sarat Book House (2007). 140, 555

[39] Fetter A L and Walecka J D, *Nonlinear Mechanics: A Supplement to Theoretical Mechanics of Particles and Continua*, Dover (2006). 431, 472

[40] Flaschka H, *The Toda lattice. II. Existence of integrals*, Phys. Rev. B**9**, 1924 (1974). 360

[41] Frisch U, *Turbulence: The Legacy of A. N. Kolmogorov* Cambridge Univ. Press (1995). 532

[42] Galilei G, *Dialogue Concerning the Two Chief World Systems*, (1632), Translated by Drake S, University of California Press, Berkeley (1953). 60, 85

[43] Gaspard P, *Chaos, Scattering and Statistical Mechanics*, Cambridge Univ. Press (1998). 452, 531

[44] Gleick J, *Chaos*, RHUK, (1997). 432

[45] Goldstein H, *Classical Mechanics*, 2nd ed., Addison-Wesley (1980). 663

[46] Goldstein H, Poole C P and Safko J L, *Classical Mechanics*, 3rd ed., Pearson (2013). 35

[47] Grad H, *Principles of the kinetic theory of gases*, in Flügge, S. (ed.), Encyclopedia of Physics, XII, Springer-Verlag, 205-294 (1958). 531

[48] Gradshteyn I S and Ryzhik I M, *Table of integrals, series and products*, 7th ed., Academic Press (2007). 237, 348, 412

[49] Griffiths D J, *Introduction to electrodynamics*, 4th ed., Pearson (2015). xi, 25, 112

[50] Griffiths D J, *Introduction to elementary particle physics*, 2nd Rev. ed., Wiley VCH (2008). 48

[51] Gutzwiller M C, *Chaos in Classical and Quantum mechanics*, Springer-Verlag (1990). 375

[52] Gutzwiller M C, *Moon-Earth-Sun: The oldest three-body problem*, Reviews of Modern Physics, **70**, 589 (1998). 342, 401, 402

[53] Hammermesh M, *Group theory and its application to physical problems*, Reprint Ed., Dover (2003). 649

[54] Hand L N and Finch J D, *Analytical mechanics*, Cambridge Univ. Press (1998). 250, 274

[55] Hartman P, *Ordinary Differential Equations*, Classics in applied mathematics **38**, 2nd ed., Society for Industrial and Applied Mathematicians (2002). 209

[56] Henon M, *Integrals of the Toda lattice*, Phys. Rev. B**9**, 1921 (1974). 360

[57] Hirsch M W, Smale S and Devaney R L, *Differential Equations, Dynamical Systems, and an Introduction to Chaos*, 3rd ed., Academic Press (2012). 190, 431, 454

[58] Huang K, *Quarks, Leptons and Gauge Fields*, 2nd ed., World Scientific (1992). 404

[59] Huang K, *Statistical Mechanics*, 2nd ed., John Wiley & Sons (1987). 324

[60] Huba J D, *NRL Plasma Formulary*, Naval Research Laboratory (2013). 577

[61] Ince E L, *Ordinary Differential Equations*, Dover (1978). 402

[62] Itzykson C and Zuber J-B, *Quantum Field Theory*, Dover (2006). 142

[63] Jeevitha T U and Das S, *A Pedagogical Relook at Bertrand's Theorem*, Resonance **24**(11), 1235-1251 (2019). 35

[64] John F, *Partial Differential Equations*, 3rd ed., Springer-Verlag (1978). 516, 517

[65] José J V and Saletan E J, *Classical Dynamics: A Contemporary Approach*, Cambridge Univ. Press (1998). 352, 454

[66] Khare A, *Chaos*, Physics Education, **10**, 30 (1993). 454

[67] Kibble T W B, *Geometrization of Quantum Mechanics*, Comm. Math. Phys., **65**, 189 (1979). 311

[68] Kleppner D and Kolenkow R J, *An Introduction to Mechanics*, 2nd ed., Cambridge Univ. Press (2014). 157, 289

[69] Kreyszig E, *Advanced Engineering Mathematics*, 10th ed., Wiley (2010). xi

[70] Krishnaswami G S and Phatak S S, *The Added Mass Effect and the Higgs Mechanism: How Accelerated Bodies and Elementary Particles Can Gain Inertia*, Resonance **25**(2), 191 (2020). 548

[71] Krishnaswami G S and Sachdev S, *Algebra and Geometry of Hamilton's Quaternions*, Resonance **21**(6), 529 (2016). xi, 662

[72] Krishnaswami G S and Senapati H, *An introduction to the classical three-body problem: From periodic solutions to instabilities and chaos*, Resonance, **24**(1), 87-114 (2019). xi, 26, 39, 49, 60, 133, 296, 319, 374, 431, 644

[73] Krishnaswami G S and Senapati H, *Classical three rotor problem: periodic solutions, stability and chaos*, Chaos, **29** (12), 123121 (2019). 417, 454, 457, 644

[74] Krishnaswami G S and Senapati H, *Ergodicity, mixing and recurrence in the three rotor problem*, Chaos, **30** (4), 043112 (2020). 457

[75] Krishnaswami G S and Vishnu T R, *Invariant tori, action-angle variables and phase space structure of the Rajeev-Ranken model*, J. Math. Phys. **60**, 082902 (2019). 353

[76] Krishnaswami G S and Vishnu T R, *The idea of a Lax pair - Part I: Conserved quantities for a dynamical system*, Resonance **25**(12), 1705 (2020). xi, 357, 405

[77] Krishnaswami G S and Vishnu T R, *The idea of a Lax pair - Part II: Continuum wave equations*, Resonance **26**(2), 257 (2021). xi, 359, 361, 362, 405, 509

[78] Krishnaswami G S and Yadav A, *Bifurcation cascade, self-similarity and duality in the 3-rotor problem*, Chaos, **33**, 083101 (2023). 417

[79] Kunze M and Spohn H, *Adiabatic Limit for the Maxwell-Lorentz Equations*, Ann. Henri Poincaré, **1**, 625 (2000). 71

[80] Lakshmanan M and Rajasekar S, *Nonlinear Dynamics: Integrability, Chaos and Patterns*, Springer-Verlag, Berlin (2003). 200, 427

[81] Lanczos C, *The variational principles of mechanics*, 4th ed., Dover (1970). 63, 70, 131

[82] Landau L, *The theory of superfluidity of helium II* Zh. Eksper. Teoret. Fiz. 11, 592 (1941) [English translation: J. Phys. USSR 5, 71 (1941)], reprinted in ter Haar D, *Collected papers of L D Landau*, Gordon and Breach Science Publishers, 301-330 (1965). 559

[83] Landau L D and Lifshitz E M, *Mechanics*, Vol. 1 of Course in Theoretical Physics, $3^{\rm rd}$ ed., Pergamon Press (1976). x, 8, 12, 32, 42, 106, 131, 213, 217, 218, 219, 277, 291, 413

[84] Landau L D and Lifshitz E M, *Classical Theory of Fields*, Vol. 2 of Course in Theoretical Physics, Butterworth-Heinemann (1982). 71

[85] Landau L D and Lifshitz E M, *Fluid Mechanics*, Vol. 6 of Course in Theoretical Physics, $2^{\rm nd}$ ed., Pergamon Press (1987). 571

[86] Lax P D, *Integrals of nonlinear equations of evolution and solitary waves*, Comm. Pure Appl. Math. **21**, 467 (1968). 357

[87] Lichtenberg A J and Lieberman M A, *Regular and Stochastic Motion*, Springer-Verlag (1983). 417, 431, 438, 454, 456, 460

[88] Lorenz E N, *Deterministic Nonperiodic Flow*, J. Atmos. Sci. **20**, 130 (1963). 431, 472, 491

[89] May R M, *Simple mathematical models with very complicated dynamics*, Nature **261**, 459 (1976). 432, 438

[90] McKean H and Moll V, Elliptic Curves: Function Theory, Geometry, Arithmetic, Cambridge Univ. Press (1999). 231

[91] Morrison P J and Greene J M, *Noncanonical Hamiltonian Density Formulation of Hydrodynamics and Ideal Magnetohydrodynamics*, Phys. Rev. Lett. **45**, 790 (1980), Erratum: **48**, 569 (1982). 559, 560

[92] Moulton F R, *An Introduction to Celestial Mechanics*, Macmillan (1914). 58

[93] Mukunda N, *Sir William Rowan Hamilton: Life, Achievements, Stature in Physics*, Resonance **21**(6), 493 (2016). 372

[94] Mukunda N and Chaturvedi S, *Continuous Groups for Physicists*, Cambridge Univ. Press (2022). 613, 652

[95] Nakahara M, *Geometry, Topology and Physics*, 2nd ed., Taylor & Francis, London (2003). 613

[96] Nakayama Y, *Visualized Flow: Fluid Motion in Basic and Engineering Situations Revealed by Flow Visualization*, Pergamon (1988) 531

[97] Nelson E, *Dynamical Theories of Brownian Motion*, 2nd ed., Princeton University Press (2001). 524

[98] Newton I, *The Principia*, A new translation by Cohen I B and Whitman A, University of California Press, Berkeley (1999). 25, 58

[99] Ott E, *Chaos in Dynamical Systems*, 3rd ed., Cambridge Univ. Press (2002). 352, 417, 432, 434, 438, 443, 445, 454, 460, 476, 477, 479

[100] Pathria R K and Beale P B, *Statistical Mechanics*, 3rd ed., Butterworth-Heinemann (2011). 421

[101] Perkins D H, *Introduction to High Energy Physics*, 4th ed., Cambridge Univ. Press (2000). 49

[102] Perrin J B, *Brownian Movement and Molecular Reality*, Translated by Soddy F, Dover (2013). 524, 525

[103] Pradhan T and Khare A V, *Plane Pendulum in Quantum Mechanics*, American Journal of Physics **41**, 59 (1973). 229

[104] Purcell E M and Morin D J, *Electricity and Magnetism*, 3rd ed., Cambridge Univ. Press (2013). 112

[105] Rai Choudhury A, The Physics of Fluids and Plasmas: An Introduction for Astrophysicists, Cambridge Univ. Press (1998). 324

[106] Rajeev S G, *Advanced Mechanics: From Euler's Determinism to Arnold's Chaos*, Oxford Univ. Press (2013). x, 132, 280, 296, 297, 319, 352, 371, 384, 460, 479, 644

[107] Rajeev S G, *Fluid Mechanics: A Geometrical Point of View*, Oxford Univ. Press (2018). 413, 558, 559, 644

[108] Rajeev S G, *Exact solution of the Landau-Lifshitz equations for a radiating charged particle in the Coulomb potential*, Ann. Phys. **323** 2654 (2008). 71

[109] Rohrlich F, *The self-force and radiation reaction*, Am. J. Phys. **68**, 1109 (2000). 71

[110] Rozanov Y A, *Probability Theory: A Concise Course*, Rev. English Edition, Translated and Edited by R. A. Silverman, Dover (1977). 529

[111] Saffman P G, *Vortex dynamics*, Cambridge Univ. Press (1992). 558

[112] Schoenberg M, *Vortex Motions of the Madelung Fluid*, Nuovo Cimento, **1**, 543 (1955). 578

[113] Schutz B F, *Geometrical methods of mathematical physics*, Cambridge Univ. Press (1980). 356, 613, 668

[114] Shankar R, *Principles of Quantum Mechanics*, 2nd ed., Plenum Press (1994). xi, 19, 113, 142, 367, 372, 404

[115] Shukla K S and Sarma K V, *Āryabhaṭīya of Āryabhaṭa*, Indian National Science Academy (1976). 85

[116] Siegel C L and Moser J K, *Lectures on Celestial Mechanics*, Classics in Mathematics, Springer (1995). 39, 352

[117] Sommerfeld A, *Mechanics*, Academic Press (1964). 63, 64, 68

[118] Sommerfeld A, *Thermodynamics and Statistical Mechanics*, Levant Books (2005). 555

[119] Sternberg S, *Group Theory and Physics*, Cambridge Univ. Press (1994). 649, 663

[120] Stone M and Goldbart P, *Mathematics for Physics: A Guided Tour for Graduate Students*, Cambridge Univ. Press (2009). xi, 613

[121] Strang G, *Introduction to Linear Algebra*, 5^{th} ed., Wellesley-Cambridge (2016). xi, 469

[122] Strogatz S H, *Nonlinear Dynamics and Chaos: With Applications to Physics, Biology, Chemistry, and Engineering*, 2nd ed., Taylor & Francis (2014). 173, 186, 190, 417, 444, 473, 476, 477

[123] Sudarshan E C G, Mukunda N and O'Raifeartaigh L, *Group theory of the Kepler problem*, Phys. Lett., **19**, 322 (1963). 115

[124] Sudarshan E C G and Mukunda N, *Classical Dynamics: A Modern Perspective*, Hindustan Book Agency (2015). x, 89, 98, 143, 565

[125] Symon K R, *Mechanics*, 3rd ed., Addison-Wesley (1971). 274, 296, 297

[126] Tabor M, *Chaos and Integrability in Nonlinear Dynamics: An Introduction*, Wiley-Interscience (1989). 417, 431, 454

[127] Thellung A, *On the hydrodynamics of non-viscous fluids and the theory of Helium II. Part II*, Physica **XIX**, 217 (1953). 565

[128] Thyagaraja A, *Recurrent motions in certain continuum dynamical systems*, Phys. Fluids **22**(11), 2093 (1979). 324

[129] Van Dyke M, *An album of fluid motion*, The Parabolic Press, Stanford, California (1988). 531, 571

[130] Verma H C, *Concepts of Physics*, Parts 1 and 2, Revised Reprint ed., Bharati Bhawan (2015). xi

[131] Weinberg S, *The Quantum Theory of Fields: Volume 1 Foundations*, Cambridge Univ. Press (2005). 98

[132] Whitham G B, *Linear and nonlinear waves*, Wiley (1974). 513

[133] Whittaker R T, *A Treatise on the analytical dynamics of Particles and Rigid Bodies*, 4th ed., Dover, New York (1944). 39, 106, 277, 296, 375

[134] Wolfram Research, Inc., *Mathematica*, Version 12.1, Champaign, IL (2020). 412

[135] Wybourne, B G, *Classical Groups for Physicists*, John Wiley and Sons (1974). 613

[136] Yoshida H, *A Type of Second Order Ordinary Differential Equations with Periodic Coefficients for which the Characteristic Exponents have Exact Expressions*, Celest. Mech., **32**, 73 (1984). 454

[137] Zakharov V E and Kuznetsov E A, *Hamiltonian formalism for nonlinear waves*, Physics-Uspekhi **40**(11), 1087 (1997). 564

[138] Zhang Y Z, *Special Relativity and its Experimental Foundations*, World Scientific (1997). 151

Index

abelian, 651, 655, 669
abscissa, 439, 590
acceleration, 2, 24, 41, 52, 59–61, 134, 157, 485, 542, 581, 587, 590, 592, 610
  centripetal, 24, 77, 588
  due to gravity, 13, 16, 64, 72, 193, 225, 290, 455, 489, 533, 543, 574
  four-vector, 168
accuracy, 431, 459
action, 75, 97, 100, 135, 136, 151, 168, 331, 347, 376
  at a distance, 420
  coordinate transformed, 105
  Euler-Maupertuis, 12, 19, 69, 76, 131, 133, 346, 377
  extremum, 139
  function of coordinates and time, 101
  functional, 365
  Hamilton-Lagrange, 69, 377
  multivalued, 347
  principle, 64, 69, 501, 566
  shift, 12, 19
  unit of, 349
  variable, 341, 348, 349, 353, 362, 363
adiabatic, 544
  flow, 566
  index, 534, 545, 574
  invariant, 350
  perturbation, 350
  process, 574, 575
    reversible, 534, 573
Aditya solar mission, 297
adjoint, Hermitian, 213
advection, 540, 542, 543, 546, 552, 565, 570
aerodynamics, 539
aerostatics, 533
affine
  parameter, 128, 647, 668
  transformation, 87, 128, 602
air, 574
algebra, 108
  associative, 309, 662
  commutative, 309, 620
  exterior, 635
  linear, 383
  noncommutative, 309
  of functions, 108
  of matrices, 108
algebraic equation, 369
  linear, 213
alpha particle, 42, 47
amplification, 218
amplitude, 3, 16, 196, 212, 217, 511
  slowly varying, 212
analytic
  continuation, 127
  real, 126, 595
angle, 581, 584, 587, 609
  azimuthal, 43
  between vectors, 132
  of deflection, 14
  of rotation, 246
  polar, 43, 611
  relative, 468, 471
  scattering, 44
  solid, 43
  variable, 341
angle-action variables, 75, 345, 347, 350–353, 355, 362, 366, 380, 415, 460, 469
  nonunique, 341, 346
angular
  acceleration, 294, 589, 593
    moment of, 293
  frequency, 33, 493, 505, 509, 510
  speed, 24, 296, 550, 576, 587, 592, 610
  velocity, 134, 246, 249, 291, 295, 361, 589
    Earth, 295
    matrix, 265
    vector, 248, 253, 286, 609
angular momentum, 20, 23, 52, 53, 66, 136, 253, 286, 361, 501, 581
  conservation, 29, 30, 32, 34, 45, 226, 253
    local, 557, 576
  current tensor, 557
  density, 557, 576
  fluid, 557
  flux, 557
  matrix, 361
  nonconservation, 226, 280
  origin, 557, 609
  phase space, 278
  Poisson algebra, 109, 121, 145, 277, 278, 287
  Poisson tensor, 123, 288
  relative, 29, 31, 38, 53, 113
  rigid body
    of center of mass, 253
    rotational, 254, 255
    square of, 558

    state space, 277
  rotation generator, 115, 318, 336, 340
  rotational, 253
  sphere, 272
  total, 29, 49, 253, 456, 466
annihilation
  e^+e^-, 49
  of fixed points, 418
annulus, 190, 274
ansatz, 211, 215, 219, 224, 488
antiderivative, 2, 556
antilinear, 309
aperiodic, 34, 326, 436
  orbit, 448
aphelion, 30, 32, 34
approximation, 531
arc length, 14, 99, 128–130, 133, 168, 240
  parametrization, 133
Archimedean solid, 252
area, 214, 279, 585, 667
  element, 279, 288, 312, 538, 628
    preservation, 335
  enclosed, 344
  form, 638
area-preserving map, 312, 325, 435, 479
areal speed, 23, 34, 515, 566
Arnold, Vladimir I, 352
Aryabhata, 85
ascending node, 262
aspect ratio, 473
associative, 143, 336, 603, 649, 669
astronomical unit, 22, 53
asymmetry, left-right, 571
asymptote, 43
asymptotic, 480
atlas, 614, 616
  oriented, 638
atmosphere, 472, 534, 573
atom, 47
  nuclear model, 42, 47
  plum pudding model, 47
atomic
  hypothesis, 525
  physics, 377
attractor, 222, 429, 432, 441, 445, 477, 480, 516
  diagram, 442
  global, 422
  periodic, 445
  strange, 191
automorphism, 650, 655
autonomous system, 106, 192, 234, 388, 481
auxiliary linear equations, 357
Avogadro's number, 322, 525
axial vector, 90, 550
axis, 609
  imaginary, 475
  of rotation, 246, 664
axisymmetric, 557
azimuthal, 591
  angle, 262, 593, 611
  component, 293
  velocity, 588, 592
  velocity field, 550, 576

backward difference, 478
ball, 640
barotropic relation, 545, 549, 556, 575
basin of attraction, 174, 188, 193, 222, 323, 422, 425, 450, 452, 481
basin of repulsion, 323, 452
basis, 392, 400, 448, 491, 519, 601, 621, 661
  change, 399, 416, 582, 603
  coordinate, 645, 667
  dependent, 567
  dual, 625
  independent, 567
  nonorthogonal, 260
  orthogonal, 449
  orthonormal, 449, 519, 581, 586, 648, 659
  position eigenstates, 518
  vector fields, 645
Bateman-Thellung Lagrangian, 565
BCH formula, 127
beam axis, 44
beats, 212, 223
Bergmann, Peter Gabriel, 98
Bernoulli
  Daniel, 531
  equation, 547
    unsteady, 547, 564, 565
  Jakob, 136
  Johann, 136
  principle, 546
  shift, 479
  specific energy, 547
  trials, 527
Bianchi identity, 123, 148, 288, 636, 637
bifurcation, 209, 222
  diagram, 418, 419, 421, 423, 430, 442
  fold, 418
  global, 430
  homoclinic, 430
  Hopf, 427
  interval, 442
  normal form, 418, 425
  of vector fields, 417
  period-doubling, 442
  pitchfork, 418, 420, 465
  points, 445
  saddle-loop, 430
  saddle-node, 193, 418
  transcritical, 420, 426
  turning point, 418
  two-dimensions, 425

- zero-eigenvalue, 427

bijective, 617, 650
bilinear form, 627
binary representation, 479
binomial
- distribution, 527
- series, 596

Birkhoff
- expansion, 341
- recurrence, 324

Black-Scholes equation, 513
Bloch
- Felix, 384
- theorem, 403
- waves, 402

block diagonal, 279
blowup, finite-time, 183, 194, 423, 573
body force, 542
- conservative, 534, 546, 558, 569
- per unit mass, 534
- per unit volume, 533, 566, 576

Bohr
- Niels, 151
- spectrum, 37

Bohr-Sommerfeld quantization, 12, 350
Boltzmann
- H-function, 324
- H-theorem, 324
- constant, 93, 516, 525, 555
- Ludwig, 324, 531
- transport equation, 324

Bonnet's theorem, 60
boost, 656
Born
- approximation, 47
- Max, 351
- series, 183

Bose-Einstein condensate, 579
bottleneck, 193, 233, 426, 430
bound
- state, 349
- trajectory, 5, 10, 13, 34, 115

boundary, 208, 640
- impenetrable, 544
- layer, 571
  - theory, 573
  - turbulent, 571
- of manifold, 640
- term, 70, 499
- value problem, 489

boundary conditions, 486, 515, 516, 543, 544
- decaying, 490, 556, 557, 579
- Dirichlet, 489, 493, 510, 515, 517, 529
- free, 503
- homogeneous, 491
- impenetrable, 567
- mixed, 489
- Neumann, 489, 515, 517, 529
- no-slip, 567, 568
- periodic, 359, 402, 436, 499, 504, 511, 556, 557
- Robin, 489

bounded, 275, 457
Boyle's law, 534
Brachistochrone problem, 69, 136, 381
Brahe, Tycho, 22
Brillouin zone, 403
Bromwich contour integral, 214
Brown, Robert, 523, 536
Brownian
- motion, 57, 513, 523, 535
- particle, 524, 530

Bruns, Heinrich, 296
Brusselator, 185
buckling of a card, 417
bulk modulus, 539
buoyancy, 473

calculus, 581
- fundamental theorem of, 101, 129, 223, 640
- variational, 55, 68, 136

caloric condition, 555, 575
canonical
- 1-form, 630, 636
- ensemble, 93
- formulation, charged particle, 111
- momentum, 113
- Poisson bracket, 108
- Poisson tensor, 630
- symplectic 2-form, 630

canonical transformation, 74, 92, 105, 115, 303, 310, 321, 335, 339, 353, 355, 370, 376, 380, 406, 435, 468
- 1-parameter family, 308, 310
- area preserving, 312
- composition, 317, 336, 338
- equations of, 345, 368
- exchange up to sign, 304, 331
- finite, 328, 332, 338, 345, 365, 479
- geometric nature, 320
- group of, 317, 336
- identity, 331, 372
- infinitesimal, 316, 320, 321, 335, 653
- infinitesimal generator, 316, 335, 336
- Lie algebra, 317
- linear, 315, 337, 338, 406, 652
- point, 334
- preserve Hamilton's equations, 304
- preserve Poisson brackets, 305
- preserve Poisson tensor, 315
- scaling, 334, 339
- succession of, 342
- symmetry, 319
- time evolution, 307, 317
- time-dependent, 367

Cantor
  Georg, 444
  set, 444
capacitor, 177, 192
Carathéodory, Constantin, 327
Carbonnelle, Father, 524
cardinality, 649, 654
carrying capacity, 419, 439
Cartesian
  components, 17, 610
  product, 227, 351, 389, 457, 651
cartography, 614
cascade, 442
Casimir, 124, 146, 148, 278, 288, 361, 558, 578
  level set, 279
causality, 55, 159, 161, 165, 216, 486
Cayley-Hamilton theorem, 606
Cayley-Klein parameters, 663
celestial
  hemisphere, 262
  mechanics, 239, 262, 464
cell phone, 614
center, 184, 189, 196, 201, 207, 209, 228, 235, 323, 325
  in conservative systems, 209
  nonlinear, 209, 236
  of group, 655
  of mass, 28, 29, 38, 49, 52, 160, 244–246, 280, 283–285, 297, 335, 337, 360, 402, 468
    angle, 468
    momentum, 248
    vector, 27
    velocity, 249
  of Poisson algebra, 278, 288
central
  force, 25, 35, 52
  potential, 23, 25, 34, 52, 81, 134, 374
centrifugal
  barrier, 31
  force, 293, 294, 296, 534
  potential energy, 294
centripetal acceleration, 24, 294, 593
chain rule, 52, 130, 223, 441
Chandler
  Seth Carlo, 270
  wobble, 257, 270
chaos, 191, 244, 296, 356, 366, 388, 431, 436, 451, 453, 454, 461, 481, 572
  global, 437, 456, 461, 480
  Hamiltonian, 431, 572
  onset of, 456
  transition to, 438, 454, 481
chaotic orbit, 433, 436, 438
Chapman, Sydney, 531
characteristic
  curves, 366, 379
  equation, 207, 321, 398, 474, 605, 606, 612
  polynomial, 415, 475, 605, 612
characteristics, 366
  equations for, 379
charge, 177, 499
  electric, 81, 168, 192
charged particle, 43, 293, 294
  coupling to EM field, 111
chart, 651
Chaudesaigues, 525
Chirikov
  Boris, 431, 456
  standard map, 434
choreography, 50
Christoffel
  Elwin Bruno, 641
  symbols, 128, 130, 148, 641, 645, 646, 668
chronometer, 16
circle, 30, 480, 615, 665
  osculating, 644
circular
  disk, 284
  functions, 230
  hoop, 72
  motion, 226, 581
    nonuniform, 588
    uniform, 24, 31, 466, 587, 610
circulation, 550, 552, 554, 599
Clairaut's theorem, 321, 496, 596, 611
Clairaut, Alexis, 26
clamp, 485, 486
classical limit, 142, 371
Clay Millennium Prize, 573
Clebsch
  Alfred, 563
  potentials, 559, 563, 578, 579
    barotropic flow, 563
  representation, 578
    adiabatic flow, 564
    gauge invariance, 578
    incompressible flow, 578
  variables, 563, 578
    Lagrangian, 564
clock, 16, 156
  atomic, 16
  synchronize, 149, 151
closed
  set, 275, 457, 659
  surface, 275
coarse-graining, 513
cobweb diagram, 439, 444, 480
codimension, 117
coefficient
  constant, 510
  matrix, 196, 198, 200, 206, 207, 209, 394, 404, 412
    determinant, 306
    trace, 416

periodic, 402
colatitude, 262
collision, 5, 38, 66, 160, 532
 elastic, 67, 135, 160
 inelastic, 54
 of cycles, 430
 of fixed points, 427
 of molecules, 532
 time, 39, 53, 54
 triple, 50
comet, 457
commensurate, 34, 211, 326, 351, 413
common ratio, 442
commutant, 114
commutation relations
 $\underline{SU(2)}$, 661
 Heisenberg, 310
 Landau, fluid, 559
commutative, 246, 583, 584, 651
commutator, 108, 147, 265, 310, 357, 358, 361, 363, 364, 561, 576, 578, 666
 group, 651, 655, 669
 iterated, 127
 of matrices, 661, 670
 subgroup, 655
 vector fields, 126, 621, 623, 644, 653
commute, 391, 396, 669
commuting flows, 356
compact, 191, 275, 457, 658, 659
compatibility conditions, 357, 359
completeness relation, 519
complex
 dynamics, 480
 function, 213
 numbers, 662
 structure, 658
 variable, 51, 380
component, 584, 586, 666
composition law, 649, 658, 669
compressibility, 539, 581
condensed matter, 245
conduction, 472
conductor, 574
cone, 260, 272, 664
 body, 269, 274
 space, 261, 269, 274, 286
configuration
 instantaneous, 57, 487
 space, 57, 75, 77, 105, 127, 245, 246, 304, 309, 333, 378, 389, 394, 414, 455, 490
  functions on, 309
  rigid body, 246, 262, 274
conformal, 132, 379
 factor, 132
conjugacy class, 650, 657
conjugate, 210, 662
 canonically, 342, 348
 momentum, 74, 76, 79, 92, 93, 101, 105, 135, 319, 341, 511
 variable, 544
conjugation, 604, 650, 654, 655, 657, 662, 663, 670
connected, 4
 component, 275, 619, 660
 multiply, 465, 620, 666
 path, 620, 658, 664
 simply, 465, 600, 620, 658
connection
 coefficients, 668
 Levi-Civita, 641
conservation laws, 26, 531
 global, 499
 local, 499, 501, 512, 515, 529, 531, 540, 558
conservative
 force, 2, 534, 598, 601
 system, 15, 188, 235, 323
conserved quantities, 66, 82, 83, 91, 92, 107–109, 116, 126, 209, 274, 278, 319, 342, 351, 353, 356, 358, 363, 366, 388, 393, 405, 435, 455, 456, 458, 459, 466, 512, 580, 668
 approximate, 460
 Euler top, 364
 explicitly time-dependent, 142
 in involution, 452
 independent, 37, 358, 364, 415
 infinitely many, 486
 Kepler problem, 113
 local, 362
 maximal set, 37
 Noether charge, 81, 500
 relations among, 37, 146
constant of motion, 81, 82, 84, 107
constrained extremization, 96
constraint, 63, 68, 71, 72, 96–98, 566
 equation, 544, 574
 holonomic, 56, 72, 243
 hypersurface, 96
 nonholonomic, 72, 99
 primary, 98, 99
 secondary, 99, 100
continuity equation, 540, 543, 549, 559
continuous map, 457
continuum
 limit, 528
 mechanics, 483, 532, 641
contour
 closed, 550, 598
 material, 553
contractible, 229, 471, 554, 620
contraction, 139, 287, 625
contravariant
 transformation, 622
 vector, 75
control parameter, 417, 418, 427, 428, 430, 453, 455, 473, 479

convection, 191, 474
  atmospheric, 431
  cells, 472
  rate of, 472
convergence, absolute, 241
convolution, 216, 609
coordinate
  -dependent, 626
  basis, 645, 667
  Cartesian, 51, 60, 76, 163, 230, 245, 287, 333, 370, 585, 611, 665
  center of mass, 52
  chart, 262, 613, 639, 665
  curvilinear, 59, 591
  cyclic, 75–77, 91, 99, 125, 136, 285, 303, 319, 341, 343, 345, 486, 504, 511
  cylindrical, 534, 550, 576
  elliptical, 374, 382
  functions, 66
  generalized, 69, 262, 303, 490, 501
  invariance, 104
  local, 615
  new, 367
  nonsingular change, 104
  old, 367, 369
  patch, 613, 614, 637
  plane polar, 30, 51, 60, 73, 76, 134, 194, 295, 296, 333, 374, 428, 511, 581, 590, 617, 665
  rectilinear, 73
  redundant, 285
  relative, 52
  singularity, 262
  spherical polar, 23, 31, 43, 52, 136, 262, 279, 288, 581, 593, 611
  transformation, 610, 616, 634, 641
    inverse, 616
  vector field, 645
Coriolis
  acceleration, 77, 294, 593
  force, 289, 290, 293–295, 297
  Gaspard-Gustave de, 293
corners, sharp, 618
correlation functions, 422
correspondence principle, 151, 161
coset, 669
  left, 654, 657
  representative, 654
  space, 654
cosines, law of, 609
cotangent
  bundle, 309, 389
  space, 75, 625, 626
  vector, 75
Coulomb potential, 544
countable, 443
coupling constant, 417, 434
covariance, 530
covariant
  constancy, 641, 643, 668
  derivative, 641, 647, 668
  tensor, 111
    second rank, 628
    transformation, 416
  vector, 75
  vector field, 625
covector, 75, 165, 624
  field, 625, 626
critical
  exponent, 39, 442
  point, 421
  slowing down, 421, 422, 440
  temperature, 422
cross
  product, 90, 91, 265, 312, 361, 581, 584, 609, 610, 661
  section
    differential, 43
    Mott, 48
    Rutherford, 42, 54
    total, 43, 54
crystal, 359
  lattice, 384, 403
  one-dimensional, 402
cube, 252, 415
  solid, 251
cubic
  curve, 618
  polynomial, 241, 282
Curie temperature, 422
curl, 90, 316, 550–552, 569, 578, 581, 599
current, 177, 499
  density, 512
curvature, 643
  biquadratic form, 646, 648
  Gaussian, 644
  matrix, 648
  operator, 646
  radius of, 644
  Ricci, 646
  sectional, 288, 646, 648
  tensor, 644
  zero, 359
curves, 99, 644, 667
  closed, 554, 666
  union of, 459
cycle, 185, 354
  decomposition, 656
  noncontractible, 354
cyclic group, 649, 651, 669
cycloid, 137, 242
cylinder, 227, 284, 557, 639, 666

d'Alembert
  Jean le Rond, 55, 63, 485, 488

principle, 63, 69, 71
d'Alembertian, 167
da Vinci, Leonardo, 531, 536, 550
damped oscillations, 6, 193, 428, 429
damping, 6, 88, 509
  coefficient, 6, 176, 201, 217, 221
  force, 525
Darboux
  coordinates, 121, 124
    barotropic flow, 564
  theorem, 124
de Broglie wavelength, 367
de Broglie, Louis, 377
de Groot, Jan Cornets, 41
de Moivre, Abraham, 529
decouple, 400
deficient matrix, 205, 208, 399, 605
deformable body, 243, 270
deformable medium, 149
deformation, continuous, 209, 352, 666
degenerate minima, 400
degrees of freedom, 1, 13, 28, 36, 56, 134, 143, 225, 274, 280, 296, 344, 388, 414, 416, 417, 455, 498, 532, 555, 572
  finite, 396
  infinite, 483, 486, 641
  one, 337, 342, 347, 383
  rotational, 246, 555
  translational, 245, 555
  two, 383
  vibrational, 555
Delaunay, Charles, 342
Delft, 41
dense, 356, 479, 480
density, 532, 533, 544
  electric charge, 544
  mass, 243, 509, 524, 540, 612
  probability, 525, 528
  stratified, 539
dependence, functional, 118, 415
derivation, 108, 622
  of an algebra, 108
derivative
  convective, 537
  covariant, 130, 641, 643, 668
  directional, 130, 622
  exterior, 355, 629, 630, 636, 641, 666, 670
    Leibniz rule, 636
    linearity, 636
    nilpotent, 636
  Fourier transform, 612
  functional, 502, 561, 577
  Lie, 576, 641, 666
  material, 537, 540, 542, 545, 553, 574
  operator, 519, 529
  partial, 581, 596, 641
  second, 62, 512, 666
  substantial, 537
  third, 62
  total, 537
  variational, 503
descending node, 262
detector, 43
determinant, 139, 207, 208, 278, 287, 306, 337, 451, 474, 604, 663, 667
deterministic, 431, 461
diagonalization, 220, 250, 363, 391, 394, 409, 414, 416, 582, 606, 612, 648
diffeomorphism, 617, 628, 633, 653, 665
  symplectic, 355
difference equation, 432, 478
  coupled nonlinear, 434
differentiable, 524, 611
differential, 595, 598
  exact, 102, 636
  imperfect, 102
  independent, 330
  of function, 581, 626
differential equation
  autonomous, 175, 477
  inhomogeneous linear, 211, 215, 220
  nonautonomous, 175
  ordinary, 2, 26, 91, 582
    coupled linear, 391
    linear, 213
    system of, 173, 535
  partial, 337, 488, 582
    linear system, 316, 338
    nonlinear, 532
differential form, 118, 146
  p-forms, 631
    space of, 635
  1-form, 595, 625, 643, 666
    action on vectors, 625
    matrix-valued, 667
  2-form, 628
    action on vectors, 629
    matrix-valued, 668
    space of, 629
  closed, 288, 355, 636, 666
  exact, 330, 575, 636, 666
  Lie algebra valued, 661
  space of, 635
  symplectic, 630
  volume, 123
diffusion, 461, 513, 531, 536
  constant, 525, 527, 528
  equation, 515, 523, 529, 530, 569
  heat, 472, 566
  momentum, 472
  velocity, 513, 566
  vorticity, 569
diffusivity, 515, 527, 529, 566
  thermal, 472, 528

dimension, 337, 601, 659, 670
  infinite, 336, 363, 518
dimensional
  analysis, 6, 14, 16, 17, 49, 140, 141, 163, 220, 336, 347, 362, 381, 393, 478, 515, 521, 529, 530, 571, 579, 580
  reduction, 175
dimensionless, 530, 570
dipole field, 187, 452
Dirac
  bra-ket notation, 141, 519
  delta, 214, 503, 520, 559, 582, 608
  Paul A M, 98, 106
Dirac-Bergmann theory of constraints, 98
direct
  problem, 8, 25, 60
  product, 669
  sum, 635
Dirichlet, Peter Gustav Lejeune, 489
disconnected, 4, 660
discontinuous, 530, 611
discrete group, 649
discrete-time dynamics, 452
discretization, 464, 478, 490
discriminant, 207, 241, 441, 474, 480
disk, 640
dispersion, 486, 506, 510
dispersion relation, 505, 509, 510, 512
  energy-momentum, 163, 167, 169
  linear, 490
displacement, 526
  field, 483
  fractional, 568
  infinitesimal, 63, 246, 581, 587
  vector, 13
  virtual, 63, 71
dissipation, 513, 570
  function, 204, 217, 222
  tensor, 205
dissipative process, 188, 189, 217, 322, 432, 451, 473, 513, 515
  driven, 472, 572
divergence, 7, 11, 167, 211, 217, 599
  covariant, 642
  exponential, 461
  integrable, 7, 18, 39
  logarithmic, 18, 229, 240
  nonintegrable, 54
  of series, 127
  of time period, 8, 430
  of vector field, 450, 474, 574, 581
  of velocity field, 538
  power-law, 229
  theorem, 514, 554, 557
dodecahedron, 252
domain of dependence, 497
dot product, 90, 584, 609
double pendulum, 387, 454, 481
  zero gravity, 467
double-valued, 470
double-well potential, 8, 272, 325
doubling map, 479
drag force, 571, 579
du Châtelet, Émilie, 3
dual vector space, 75, 625
Duffing equation, undamped, unforced, 236
dynamical
  information, 308
  system, 173, 432
    continuous-time, 432
    discrete-time, 432, 458, 476, 479
    Hamiltonian, 124
  variable, 66, 81, 106, 116, 122
dynamics, 278
  complex, 480
  regular, 352, 388, 435
  symbolic, 432
Dyson series, 183
Dzhanibekov
  effect, 273
  Vladimir, 273

Earth, 24, 64
  angular velocity, 295
  mass of, 25, 53
  precession, 257, 270
  radius of, 574
  rigid body, 270
  spin, 270
Earth-Moon-Sun system, 402
eccentricity, 24, 30, 33, 36, 53
  vector, 35
ecliptic plane, 22
eddies, 550
  recirculating, 572
  shedding, 571
  standing, 571
effective potential, 31, 34, 281
Ehrenfest, Paul, 349
eigenbasis, 398, 607, 612, 648, 670
eigendirection, 199
eigenfrequencies, 399
  imaginary, 400
eigenspace, 285, 359, 604
eigenvalue, 142, 196, 200, 207, 210, 219, 220, 222, 250, 283, 285, 309, 321, 357–359, 363, 384, 409, 414, 425, 428, 429, 447, 475, 479, 492, 512, 579, 582, 604, 605, 612, 648
  degenerate, 205, 251, 259
  distinct, 391
  Lax, 363
  multiplicity, 205
  nondegenerate, 359
  positive, 399

  problem, 252, 350, 358, 359, 363, 398, 399, 401, 492, 582, 604
eigenvectors, 205, 208, 219, 220, 250, 252, 359, 363, 384, 391, 399, 401, 414, 479, 492, 512, 567, 578, 582, 604, 605, 612
  generalized, 206, 416
  Lax, 363, 364
  linearly independent, 399, 606
eikonal, 371
  approximation, 367, 370, 371
  equation, 366, 371, 372
Einstein, Albert, 61, 150, 290, 525
Einstein-Smoluchowski relation, 525
elastic solid, 243, 483, 568
elastodynamic wave, 485
electric field, 112, 168, 170, 316, 544, 630, 666
electric potential, 112, 317
electromagnetic
  field, 98, 111, 168, 293, 366, 483, 501
  field tensor, 168, 170, 630, 666
  potentials, 112, 630, 666
  wave, 149, 485
electron, 42, 113, 384
electrostatics, 544
element of fluid, 542
elevator, 290, 292, 298
ellipse, 22, 29, 50, 53, 236, 272, 326, 342, 374, 428, 665
  arc length, 240
  area of, 34
  Cartesian form, 30
  concentric, 197, 351
  invariant, 353
  polar form, 30
  precessing, 34
  rotated, 30
ellipsoid, 475–477, 653
  oblate, 16, 270
  of inertia, 272
    semiaxes, 275
  triaxial, 368, 374
elliptic
  equation, 489, 509, 513
  functions, 16, 229, 375
    periodicity, 277
  integral, 374, 381, 382
    complete, 232–234, 237, 240–242, 277, 348, 349
    incomplete, 231, 234, 237, 240, 281, 348
    Legendre normal form, 231
  islands, 438
  modulus, 231, 233, 237, 241, 275, 287, 349
embedding, 458, 618, 644, 665
energy, 3, 17, 49, 78, 113, 223, 295, 343, 368, 455, 479, 532, 580
  absorbed, 224
  asymptotically high, 466
  center of mass, 53
  compressional, 555
  conservation, 17, 28–30, 32, 38, 63, 67, 107
    global, 510
    local, 486, 531, 556
  Coulomb, 46
  current density, 499, 556
  density, 499
    fluid, 556
  dissipated, 217
  double pendulum, 414
  eigenfunction, 376
  eigenvalue, 372
  ellipsoid, 272
  flux, 500, 556
  Helmholtz free, 140
  high, 456, 465, 467
  hypersurface, 456, 457
  internal, 102, 140, 514, 555, 666
    specific, 533
  kinetic, 67, 162, 268, 389, 456
    fluid, 555
  level set, 272
  levels, 349
  loss, 204
  low, 395, 455, 460
  monotonic, 6
  normal modes, 394
  of nutation, 281
  of spinning, 281
  pendulum, 15
  potential, 2, 179, 389
  relative, 28, 53
  relativistic, 162, 167
  rest, 162
  spectrum, 37
    rotational, 243
    vibrational, 243
  stretched string, 486, 498
  thermal, 555
  total, 28, 52, 360
Enskog, David, 531
enstrophy, 550, 552
enthalpy, 546, 573
  specific, 546, 556, 559, 575
  stagnation, 546
entropy, 102, 140, 515, 516, 534, 544, 573, 625, 666
  advection, 545
  advection equation, 560
  current, 545
  flux, 545
  global conservation, 545
  increase of, 324
  local conservation, 545
  production, 544
  specific, 533, 545, 548, 560, 575
    advection, 566

equation of motion, 73, 357
  first order, 564
  linearized, 383, 390, 582
equation of state, 531, 532, 534, 544, 545, 555, 564, 569, 624
equator, 296
equatorial plane, 262, 665
equilibration, 517
equilibrium, 3, 5
  approach to, 516
  distribution, 521
  hydrostatic, 533
  mechanical, 574
  stable, 13, 15, 195, 383, 390, 418, 581, 582
  state, 624
  static, 140, 195, 533
  thermal, 524, 532
  unstable, 13, 15, 228, 418
equipartition, 524, 555
equipotential, 534, 597
equivalence
  class, 666
  principle, 24, 41, 64, 289, 290
  relation, 651, 654
ergodic, 356
error
  margin, 396
  roundoff, 464
essential singularity, 371
ether, 149
Euclidean
  group, 656
  metric, 121
  plane, 643
  space, 57, 130, 414, 530, 583, 609, 613, 645, 667, 668
Euler
  3-body problem, 368, 382
  angles, 255, 261, 264, 265, 268, 274, 281, 285, 663
    conjugate momenta, 281, 286
    generalized velocities, 284
    singular, 264
  four-square identity, 662
  Leonhard, 50, 55, 244, 264, 270, 483, 531
  point, 297
  top, 142, 362, 364, 431, 558
  vector, 247, 256
Euler's equations
  barotropic flow, 553, 558, 559, 577
  ideal flow, 531
  incompressible flow, 561, 574
  inviscid fluid, 543, 549, 567
  Lagrangian, 578
  linearized, 549
  rigid body, 245, 267, 268, 275, 277, 286, 360, 558
    Hamiltonian formulation, 277
    Lax pair, 364
    static solutions, 272
    torque-free, 361
Euler-Fourier formulae, 494, 518
Euler-Lagrange equation, 70, 71, 97, 134, 136, 142, 170, 501
  for a field, 565
  rigid body, 256
Euler-Maupertuis principle, 12, 101, 131, 132
  fixed energy, 131
Eulerian variables, 483, 484
event, 55, 134, 153, 157, 159, 163, 169, 527
  past, future, 56
evolution equation, 27, 114
exact differential, 624, 637, 661
existence, failure of, 181
existence-uniqueness, 182
expectation value, 527
experiment, thought, 290
exponential, 456
  divergence, 446
  growth, 400, 447
  instability, 451
  map, 660, 669
  ordered, 404
  path-ordered, 404
  time-ordered, 127, 404
extremum
  constrained, 96, 97
  local, 96
  of action, 68
  of potential, 8, 69

factor group, 654, 655
factorization, 511
  multiplicative, 376
  of a rotation, 264
Fatou set, 480
Feigenbaum constant, 480
Feigenbaum, Mitchell, 431, 442
Fermat's principle, 131
Fermat, Pierre, 131
ferromagnet, 422
Feynman diagram, 48
Feynman path integral, 69, 142
field, 359, 483, 559, 623
  line, 535
  magnetic, 141
finite differences, 434, 478, 490, 512, 528
FitzGerald, George Francis, 150
fixed point, 174, 177, 191, 193, 196, 198, 221, 223, 227, 433, 477, 478
  annihilation, 418, 425
  asymptotically stable, 197, 198
  attractor, 174, 180, 188, 197, 202, 210, 323, 450
    global, 174
  center, 184, 201

  change in stability, 427
  classification, 207
  continuous family, 323
  elliptic, 196
  free, 190
  half-stable, 177, 418
  hyperbolic, 198
  isolated, 184, 209
  line of, 199, 201, 205, 208, 324, 420
  Lyapunov stable, 197
  neutrally stable, 199, 201
  nonisolated, 184, 208, 209
  nontrivial, 421, 423, 439, 445, 473, 475
  pair production, 418
  plane of, 208
  repeller, 174, 180, 181, 188, 197, 210, 323
  saddle, 198
  sink, 210
  source, 210
  spiral sink, 185
  spiral source, 185
  stability, 174, 479
    linear, 178, 193
    nonlinear, 480
  stable, 177
  stable node, 198
  star, 198
  symmetrical node, 198
  trivial, 439, 473
  unstable, 423, 429, 451
  X-point, 198
Fizeau, Hippolyte, 150
Flaschka variables, 360, 364
flat manifold, 647
Floquet exponents, 447
Floquet, Gaston, 384, 402
flow
  adiabatic, 544, 548, 556
  barotropic, 545, 551, 553, 558, 576
  commuting, 356
  compressible, 538, 539, 548, 569, 575
  creeping, 570
  detachment, 572
  dissipationless, 245, 531, 544
  energy, 555
  energy density, 556
  Eulerian description, 537
  gradient, 179, 189
  homentropic, 545–548, 556
  ideal, 531, 541, 543
  incompressible, 245, 323, 537, 539, 540, 549, 566, 568, 570, 575, 578
    constant density, 544, 560
  inviscid, 541, 542, 552
  irregular, 570
  kinetic energy, 555
  Lagrangian description, 537
  laminar, 417, 531, 535, 547, 568, 570
  of vector field, 623
  past a sphere, 570
  past cylinder, 571
  past obstacle, 570
  periodic in time, 571
  pipe, 568, 570
  planar, 550, 576
  Poiseuille, 568
  potential, 547, 550, 563
  potential energy, 564
  regular, 535, 570
  separation, 571
  shear, 550, 568
  steady, 174, 175, 535, 546, 568, 570, 571
  Stokes, 570
  symmetries of, 571
  time-reversed, 183
  turbulent, 417, 531, 570, 572
  unsteady, 547
  viscous, 531, 541, 543
  visualization, 535
  volume preserving, 451
fluctuations, 466
fluid, 243
  charged, 559
  element, 532, 533, 537, 539, 540
  flow, 531
  variables, 532
  viscous, 524
flux, 43, 499, 541, 552
  of angular momentum, 557
  of energy, 500, 556
  of momentum, 557
focus, 22, 29, 30, 43, 47, 51, 201, 297, 374
  common, 27
foliation, 275, 279, 351–353, 356, 460, 461
force, 2, 60, 135, 485, 649
  body, 533
  central, 25, 35, 52, 86, 611
  centrifugal, 289, 293
  complex, 224
  conservative, 2, 63, 71, 534
  constant, 195
  Coriolis, 293
  damping, 88, 525
  destabilizing, 234
  driving, 33, 212, 411, 570
  electrostatic, 46
  external, 61, 88, 254
  fictitious, 85, 289, 290, 292–294
  generalized, 389
  inertial, 63, 292
  internal, 254
  inverse-square, 24, 52
  linear restoring, 196, 210
  on string segment, 488

  periodic, 218
  restoring, 3, 386
  superposition of, 60
  surface, 533
    normal, 541
    tangential, 541
  time-dependent, 210
  velocity-dependent, 135, 294
form invariance, 306
Foucault's pendulum, 85, 293, 295
  precession, 295
four-covector, 165
four-divergence, 167
four-gradient, 167
four-momentum, 166
four-vector, 163, 164
  energy-momentum, 167
four-velocity, 166, 619
Fourier
  coefficients, 494, 510, 511, 518
  conjugate, 142
  integral, 213, 506
  inversion, 608
  Joseph, 484, 517, 531
  law, 513, 514, 529
  modes, 486, 506, 607
  series, 213, 486, 494, 504, 510, 518, 529
  space, 608
  synthesis, 211
  transform, 9, 48, 93, 142, 529, 582, 607, 612
fractal, 191, 432, 444
  set, 477
frame, 134, 135, 570
  accelerated, 59, 74, 289, 298
    uniformly, 289, 290
  body-fixed, 245, 258, 361
  comoving, 245, 249, 254, 255, 285
  corotating, 245, 297
  fixed, 245
  inertial, 58, 60, 61, 84, 134, 135, 150, 169, 245, 253, 289, 295, 298, 299
  lab, 135, 245, 247, 249, 285
  left-handed, 139, 586
  noninertial, 59, 85, 244, 255, 289, 296
  of fixed stars, 85
  principal axis, 250, 258, 361
  rest, 157, 161
  right-handed, 284, 586, 594, 611
  rotating, 293
  space, 245
  uniformly rotating, 294
free fall, 40, 273, 298
free particle, 2, 12, 58, 61, 62, 75, 80, 84, 85, 116, 127, 148, 223, 323, 326, 334, 336, 341, 368, 371, 374, 380, 387, 431
  in 1d, 135, 372
  in 2d, 377
  in 3d, 373, 378
free surface, 534
frequency, 14, 17, 218, 224, 295, 341, 351, 352, 390, 488, 648
  amplitude-dependent, 239
  angular, 196
  emission, absorption, 349
  natural, 211, 219
  resonant, 224
friction, 6, 41, 175, 217, 222, 283, 481
  fluid compression, 566
  Galilean boost, 88
  layers of fluid, 566
  sliding, 192, 471
Frobenius theorem, 356
full width at half maximum, 217, 224
function, monotonic, 477
functional, 376
  derivative, 502, 561
  of configuration space path, 100
  of phase space path, 102
  of velocity field, 561
fundamental matrix solution, 358, 363, 408, 412, 447, 520

Galilean
  boost, 74, 84–86, 153, 155, 292
    energy transformation, 299
  group, 88, 89
  invariance, 62, 85, 244, 255
    failure of, 88
  relativity, 60, 61, 85, 290
  transformations, 88, 140, 153, 159
Galilei, Galileo, 14, 16, 41, 55, 59, 60, 85, 150
Gamma function, 241
gas, 102, 322, 324, 514, 624
  Bose, 579
  calorically perfect, 575
  constant, 525
  diatomic, 555
  dilute, 567
  dynamics, 539
  ionized, 483
  monatomic, 555, 575
  polyatomic, 555
gauge, 578
  field, 98, 404
  potential, 168, 630, 666
  principle, 112
Gauss
  Carl Friedrich, 68, 644
  divergence theorem, 514, 538, 541, 574, 581, 600, 640, 668
  law, 544
Gaussian, 521, 528, 609
  curvature, 644
  elimination, 469

  Fourier transform, 612
  integral, 529
  propagators, 58
  pulse, 496
  wave packet, 506
Geiger, Hans, 42
generalized
  coordinate, 69
  momentum, 75
  velocity, 72, 75
generating series, 405
generator, 74, 316, 344, 376, 380
  finite canonical transformation, 328, 337, 340, 346, 365
  infinitesimal, 317, 318
  of a group, 649
  of first kind, 330, 339, 345, 346, 362, 380, 479
  of fourth kind, 332
  of second kind, 331, 337–339, 345, 347, 355, 367, 379
  of third kind, 332
genus, 476
geodesic, 128, 368, 374, 643, 644, 647
  deviation, 644
  deviation equation, 647
  equation, 128, 130, 148, 378, 379, 641, 647, 668
    reparametrized, 133
  instability, 288
  Jacobi-Maupertuis metric, 133
  null, 168
  time-like, 168, 170
  vector field, 643
geodynamos, 473
geometric sequence, 442
Gibbs, Josiah Willard, 582
Gimbal lock, 262
global attractor, 473
gold atoms, 42
golden mean, 438
Gouy, Louis Georges, 524
gradient, 52, 96, 167, 597, 601, 611
  flow, 179, 189, 194
  length scale, 367
  of a scalar, 316, 581
  vector field, 189, 194
Gram-Schmidt orthogonalization, 448
graph, 440
gravimeter, 16
gravitation, universal law of, 25
gravitational
  field, 289, 291, 298, 483, 567
  force, 13, 24, 280, 290
  mass, 290
  potential, 25
  potential energy, 456
  slingshot, 54
  wave, 485
gravity, 14, 98, 386, 473
  Probe B experiment, 245
  zero, 456
Green's function, 214, 223, 518, 544, 562, 582
Green's theorem, 600
Greene, John M, 438
group, 649
  $GL_n(\mathbb{C})$, 652
  $GL_n(\mathbb{R})$, 652, 655, 670
  $O(2)$, 669
  $O(3)$, 651, 658
  $O(n)$, 659, 670
  SL_2, 406, 655
  $SL_n(\mathbb{R})$, 652, 670
  $SO(2)$, 650, 669
  $SO(3)$, 245, 246, 262, 264, 265, 274, 285, 651, 655, 660, 663
  $SO(n)$, 670
  $SU(2)$, 655, 661, 663
  $SU(n)$, 652
  S^1, 658
  S_2, 651
  S_3, 651, 656
  S_n, 669
  $Sp(2n, \mathbb{R})$, 315, 652
  $U(1)$, 580, 649, 650, 658, 669
  $U(n)$, 652, 655, 658
  $\mathbb{Z}_2$, 422
  abelian, 669
  abstract, 649
  action, 652, 657
    transitive, 652
  alternating, 657
  automorphism, 301, 650
  canonical transformations, 317, 336
  center, 655
  commutator, 651
  continuous, 651
  cyclic, 649, 657, 669
  diffeomorphisms, 245
  dihedral, 651, 656
  discrete, 649, 651
  Euclidean, 656
  finite, 649
  Galilei, 651
    homogeneous, 89
    representation on space-time, 88
    semidirect product, 89, 656
  general linear, 659
  homomorphism, 650, 655, 669
  internal symmetries, 245
  left action, 653
  Lie, 89, 115, 651
  Lorentz, 164
  matrix, 337, 652, 660, 669
  nonabelian, 317, 336, 656, 659
  order, 649

  orthogonal, 81, 89, 139, 652
  permutation, 656
  Poincaré, 164, 656
  point, 651
  quotient, 654, 669
  right action, 653
  rotations and reflection, 659
  rotations in 2d, 653
  rotations in 3d, 262, 656
  semisimple, 655
  simple, 655
  special orthogonal, 81, 90
  symmetric, 628, 631
  symplectic, 315, 337, 652
  transformation, 652
  unitary, 652
group speed, 510
group velocity, 486, 506, 512
growth rate, 439
gyroscope, 244, 245

Hénon-Heiles system, 417, 432, 454
Hagen-Poiseuille equation, 569
Hall effect, 113
halo orbit, 297
Hamilton's
  characteristic function, 332, 345, 348, 372, 376, 377, 381
  equations, 91, 92, 99, 101, 103, 104, 106, 112, 125, 128, 131, 141, 143, 225, 226, 278, 302, 306, 310, 329, 335, 341, 352, 363, 368, 370, 478, 503, 510, 564, 577
    coordinate invariance, 104
    formal solution, 126
    variational principle, 102, 103
  optico-mechanical analogy, 370, 377
  principal function, 101, 332, 365, 367, 369, 372, 376, 380
  variational principle, 64, 68, 376
Hamilton, William Rowan, 55, 68, 372, 377, 662
Hamilton-Jacobi equation, 92, 101, 132, 332, 344, 365, 367, 371, 373, 377, 378, 380, 381, 454
  complete solution, 365, 368, 378
  incomplete solution, 368, 380
  time-dependent, 376
  time-independent, 345, 350, 381
  wavefronts, 379
Hamiltonian, 63, 64, 77, 91, 92, 112, 114, 115, 213, 339, 341, 378, 455, 457, 468
  adiabatic flow, 578
  barotropic flow, 559
  chaos, 431
  Clebsch variables, 564
  coordinate transformed, 105
  double pendulum, 414, 415
  dynamical system, 124
  flow, 174
  formulation, 308, 515
  hermiticity, 403
  incompressible flow, 561
  independent variables, 91
  infinitesimal generator, 317
  naive, 100
  new, 305, 329, 330, 335
  old, 305, 329
  operator, 198, 335
  quadratic, 310
  rigid body, 277
  rotating frame, 294
  stretched string, 503
  system, 388, 447, 451
  time-dependent, 92, 367, 404
  transformed, 367
  vector field, 125, 126, 173, 184, 188, 222, 227, 275, 451, 637
    linearization, 222, 323
  wave equation, 510
handle, 617
harmonic function, 516
harmonics, 493
Hartman-Grobman theorem, 209, 228, 236
heat, 102, 524, 624, 666
  added, 514, 624, 666
  capacity, 555, 573
  conduction, 483
  diffusion, 484, 513, 566
  equation, 489, 510, 515, 519, 528, 530, 566, 582
    boundary conditions, 515
    conservation form, 529
    dispersion, 509
    equilibrium state, 517
    fundamental solution, 520
    polynomial solutions, 530
    smoothing, 515, 516, 530
    uniqueness, 516, 520
  evolution operator, 519
  exchange, 544, 573, 574
  flux vector, 514, 517, 568
  kernel, 514, 518, 520, 521, 529
  specific, 529
  transfer, conductive/convective, 472, 473
  wave, 522
Heaviside step function, 515, 516
Heaviside, Oliver, 582
Heisenberg
  equation of motion, 93, 310, 363
  uncertainty principle, 65
  Werner, 349
helicity, 557, 569, 577, 578
  Casimir, 578
  density, 90, 557, 576, 577
  flow, 550
  local conservation law, 558
helix, 598, 610

Helmholtz
 decomposition, 561, 578, 599
 equation, 489, 509
 Hermann von, 551
 vortex theorem, 554
Hermitian matrix, 198, 220, 311, 359, 604
hermiticity, lack of, 403
herpolhode, 274
Hertz, Heinrich, 68, 72
Hessian, 95, 98, 331, 397, 402, 415
heteroclinic trajectory, 184
Hilbert space, 311, 335, 519
 complex, 309
 square-integrable functions, 309
Hill region, 132, 148, 298, 464, 481
Hill, George W, 401, 402, 464
homeomorphism, 209, 210, 236, 613, 617, 640
homoclinic
 bifurcation, 430
 phenomena, 296, 451
 points, 453
 tangency, 453
 tangle, 453
 trajectory, 184, 188, 236, 325, 430
homogeneity, time and space, 56, 62, 85, 88, 653
homogeneous
 background, 548
 equation, 33
 manifold, 652
homomorphism, 657, 663, 669
homothety, 50
homotopic, 620, 666
Hooke's law, 2, 3, 386, 492, 568
Hooke, Robert, 3
Hopf bifurcation, 427, 475
 subcritical, 429, 476
 supercritical, 428
horseshoe map, 431
Huygens' construction, 366
Huygens, Christiaan, 16, 242
hydrodynamics, 539, 556
hydrogen atom, 37, 351, 365, 370, 376
hydrostatics, 533, 542
hyperbola, 30, 47, 326, 374
hyperbolic
 equation, 488, 509, 513
 fixed point, 198, 209, 210
 functions, 287, 665
 plane, 646
hyperboloid, 167, 169, 643
hyperelliptic, 468
 integral, 238, 456, 469
  complete, 471
hypersurface, 116, 377, 388, 452, 455
 constraint, 96
 energy, 388, 415, 456, 457
 invariant, 388
hysteresis, 424, 430

icosahedron, 252
ideal gas, 532, 544, 545, 548, 555, 560, 564, 573–576
 potential energy, 555
identity element, 649, 653
ill-posed, 516
impact parameter, 38, 44, 457
improper rotations, 661
impulsive force, 214, 435, 582
inclusion map, 618
incommensurate, 244, 277, 326, 356, 386, 413, 455
independence
 functional, 116, 118, 388, 394
 linear, 116, 279, 609, 612
 statistical, 527
index, 400
 discrete, 243
 dummy, 75
 Greek, 163
 Latin, 163
 repeated, 75
induction, 358
inequality, saturated, 253
inertia, 1, 485
 ellipsoid, 271, 273
  semiaxes, 272
 law of, 58, 84
 metric, 288
 moment of, 49, 250, 280
 principal axes, 250, 284
  middle, 273
 principal moments, 244, 250–252, 265, 275, 284, 285, 361
 tensor, 249, 250, 253, 254, 258, 361
  circular disc, 284
  coin, 284
  cube, 251
  determinant, 284
  eigenvalues, 251, 259
  eigenvectors, 250
  rigid rotator, 284
  square plate, 284
  trace, 284
 term, 176
inertial
 coordinates, 152
 force, 63, 292, 570
 frame, 85, 150, 153, 159, 161, 163
 mass, 290
 observers, 151
infinite-dimensional, 69, 316, 317, 490, 558, 622
infinitesimal
 displacement, 246
 generator, 321, 337
 process, 624

  rotation, 246
  translation, 246
infinity, escape to, 431, 457
inhomogeneous, 642
initial
  conditions, 2, 19, 36, 65, 172, 211, 215, 274, 279, 374, 388, 393, 405, 478, 516, 522, 529, 590
    sensitivity to, 191, 356, 431, 433, 438, 442, 443, 456, 461, 477, 479, 480
  phase, 196
  state, 433
  value problem, 172, 182, 184, 200, 362, 370, 393, 404, 489, 496, 510, 511, 514, 515
  values, 308
injective, 602, 612
inner product, 364, 400, 490, 519
  Euclidean, 288, 391, 449
  Hermitian, 309, 311, 658
  indefinite, 164
  positive-definite, 309, 400, 658
instability, 212, 218, 244, 433
  chaotic, 461
  exponential, 451
  Kelvin-Helmholtz, 573
  Rayleigh-Taylor, 573
insulated, 515
integrability, 388, 486
  condition, 666
integrable, 431, 435, 455, 607, 624
  completely, 351, 366
  field theory, 405, 580
  Jacobi, 366
  Liouville, 342, 351, 366, 369, 375, 390, 455, 460, 466
  super, 366
  system, 60, 388, 390, 396, 456, 461
integral
  curve, 172, 192, 197, 227, 356, 535, 547, 554, 576, 622, 623, 643, 660
  equation, 183, 405
    linear, 9
    nonlinear, 8, 12
  invariant, 313, 558
  kernel, 9, 519
  transform, 10
integrating
  denominator, 624, 666
  factor, 2, 15, 17, 28, 52, 137, 395, 498, 624
integration, 18, 19
  by parts, 503, 566
  constant, 211, 346, 368
  numerical, 92, 459
  of forms, 639
intensity, 43
intensive variable, 539
interference, 507
interferometer, 150
interior, 640
internal energy, 514, 546, 573
  equation, 545, 575
  specific, 564
invariable plane, 274
invariance
  Galilean, 84
  of Hamiltonian, 319
  rotation, 44, 81, 501
  scale, 49
  space-translation, 28, 81, 486, 500, 501, 521, 526, 529
  time-translation, 215, 486, 501, 526
  translation, 9, 319
invariant
  set, 475
  subspace, 200, 206, 207
  surface, 475
  torus, 274, 351, 352
inverse
  function, 9, 369
  image, 275, 457, 659
  problem, 8, 22, 25, 60, 216
  scattering, 362
  two-sided, 143, 649, 662
  uniqueness, 143
involution, 96, 342, 351, 353, 357, 366, 375, 452
irrational, 351, 415, 479
irrotational, 547, 550, 571
isentropic, 546
Ising model, 422
islands of stability, 442
isobar, 534
isochronous, 8, 10, 16, 19, 196, 238, 239, 242
isometry, 164, 170, 315, 414, 628, 644
isomorphic, 602, 626, 650, 669
isomorphism, 165, 265, 364, 626, 656, 661, 669
isospectral, 358, 363, 364
isothermal, 548, 575
isotropic, 47
  fluid, 568, 579
  matrix, 567
  tensor, 567
isotropy, 53
  of space, 56, 62, 85, 88
iteration, 432, 439
  of a map, 433, 477, 479, 481

Jacobi
  Carl, 55, 131, 229, 374
  elliptic functions, 229, 234, 237, 241, 275, 287
    period, 277
  equation, 647
  identity, 109, 110, 122, 126, 143, 145–147, 287, 339, 561, 624, 636, 661, 666, 670
    in terms of Poisson tensor, 123
  integrable, 366

  integral, 296
  vector field, 647
  vectors, 49
Jacobi-Maupertuis metric, 132, 148, 379, 644
  inverse, 132
Jacobian, 100, 129, 633
  determinant, 104, 312, 632
  matrix, 104, 187, 209, 222, 235, 288, 315, 320, 336, 338, 354, 406, 427–429, 447, 474, 475, 479, 618, 622, 625, 630, 632, 665
    inverse, 622, 625, 630
James Webb telescope, 297
jerk vector, 610
Jordan
  basis, 409
  normal form, 206, 409, 415, 416, 606
    real, 410
Joule-Thomson experiment, 555
Julia set, 480
jumps, 424, 429
JWKB approximation, 367

Kapitza, Pyotr, 410
KdV equation, 486, 511
  Lax pair, 512
  linearized, 510
Kelvin's circulation theorem, 552, 554, 555
Kelvin, Lord (William Thomson), 551
Kepler
  constant, 22, 25, 34
  first law, 25
  Johannes, 22
  laws, 22, 52
  orbit, 50, 296
  second law, 34
  third law, 8, 24, 26, 34, 39, 296
Kepler problem, 50, 53, 116, 136, 242, 318, 326, 337, 339, 350, 351, 362, 366, 381, 431, 457
  canonical transformation, 339
  hidden symmetry, 115
  Poisson algebra, 113, 340
kernel, 278, 287, 602
  group homomorphism, 655, 657, 669
  heat, 529
  integral, 518, 529
  linear transformation, 104, 198, 206, 612
Killing vector field, 126
kinematics, 246, 278, 308, 590
kinetic energy, 3, 63, 133
  angular, 31
  matrix, 394
  mean, 524
  radial, 31
  rotational, 249, 361
  translational, 249, 524
kinetic theory of gases, 524, 531, 532, 555
Klein-Gordon field, 485
Kolmogorov, Andrey N, 352
Kolmogorov-Arnold-Moser theorem, 352, 388, 454, 461
Kovalevskaya, Sofya, 244
Kronecker delta, 503, 559, 579, 603

l'Hôpital, Guillaume de, 136
Lagrange
  Joseph-Louis, 50, 55
  multiplier, 55, 96–98, 100, 140, 142, 566
  point, 290, 297, 299
  theorem, 654, 657
Lagrange's equations, 68, 73, 99, 128, 370, 378, 389, 483
  coordinate invariance, 76, 104
  rigid rotator, 285
Lagrangian, 69, 72, 74, 97, 113, 129, 135, 291, 299, 333, 381, 389, 396, 413
  acceleration-dependent, 136
  Bateman-Thellung, 565, 578
  central potential, 81
  Clebsch variables, 564
  convexity, 94, 136, 141
  cubic in velocities, 138
  density, 143, 501
  description, 483
  effective, 97, 413
  explicitly time-dependent, 211, 292
  heavy top, 280
  invariant, 80
  invariant up to time derivative, 83
  inviscid flow, 564
  linear in velocities, 142, 565
  nonunique, 74, 135, 411
  quadratic approximation, 397, 411
  quadratic in velocities, 79, 127, 132
  rigid body, 255
  simple pendulum, 225
  singular, 98, 100
  stretched string, 143, 501
  transformed, 104, 335
  wave equation, 511
Lamb vector, 543, 566
laminar flow, 417, 473
Landau, Lev Davidovich, 559
Laplace
  equation, 489, 513, 516, 530
  Pierre-Simon, 529, 548
  transform, 213, 223
Laplace-Runge-Lenz vector, 29, 35, 53, 54, 113, 115, 146, 318, 339
Laplacian, 167, 511, 519, 529, 530, 544, 552, 562, 599
laser, 473
latitude, 296, 342, 593
lattice, 526
Laurent series, 611

Lax
  equation, 357–361, 363, 364, 512
  form, 356
  matrix, 358, 363, 364
  pair, 356, 359, 363, 486
    spectral parameter, 361
  Peter, 357
leaf, 356
least common multiple, 326, 386, 393
Leeuwenhoek, Antonie van, 524
left multiplication, 653
Legendre
  Adrien-Marie, 93
  normal form, 240, 382
  transform, 93, 98, 113, 140–144, 226, 332, 333, 335, 339, 362, 381, 503, 582
    inverse, 96
    multivalued, 95, 142
    partial, 95
Leibniz
  Gottfried Wilhelm, 7, 136
  rule, 110, 115, 122, 278, 288, 358, 503, 537, 540, 545, 556, 574, 576, 622, 642, 643, 666, 668
length, 667
length contraction, 157
level
  contours, 209, 298
  curve, 116, 196, 228, 236, 413, 435, 591, 596
    of energy, 467
  hypersurfaces, 274, 366, 415, 459
  set, 65, 116, 228, 272, 279
    common, 117, 274, 351, 353, 460
  surface, 475, 597
Levi-Civita
  connection, 641
  symbol, 91, 121, 145, 265, 287, 361, 364, 610, 632, 661, 667
  Tullio, 641
libration, 13, 229, 240, 297, 348, 410, 456, 469, 471
Lie algebra, 109, 115, 126, 624, 653, 658, 660, 663, 669, 670
  $\mathbb{R}^3$, 265
  canonical transformations, 317, 336
  cross product, 364, 661
  generator, 115
  Lorentz, 164
  of vector fields, 561
  orthogonal, 660
  so(3), 115, 265, 285, 364
  so(4), 115
  symplectic, 337
Lie bracket, 317, 336, 578, 653, 661, 669
  of vector fields, 561, 623
Lie derivative, 576, 622, 624, 641, 666
Lie dragging, 552
Lie group, 115, 126, 651, 670
  classical, 652
  homogeneous manifold, 653
  Lorentz, 164
Lie, Sophus, 651
light cone, 165, 497
light rays, 366
light signal, 153
light-like separation, 159, 165, 169
light-like vector, 165
limit cycle, 185, 189–191, 194, 222, 323, 427, 429, 430, 475
  creation/destruction, 430
  stable, 185, 428
  unstable, 476
limit point, 659
limit theorem, 529
Lindstedt, Anders, 239
Lindstedt-Poincaré method, 238
line
  element, 240, 667
  integral, 552, 598
  of fixed points, 199, 201
  of nodes, 262, 264, 266, 280
  spectra, 349
  vortex, 551
linear
  algebra, 383
  combination, 386, 393, 398, 601, 667
  equations
    auxiliary, 359
    coupled, 387
  independence, 398, 399, 581, 585, 601, 609
  space, 57
  superposition principle, 397
  transformation, 87, 154, 602, 612, 664
linear combination, 612
linearization, 633
linearized equations, 19, 390, 397, 447, 461, 512, 548, 549
Liouville
  1-form, 355
  integrable, 296, 357, 374, 452
  theorem, 320, 338, 406, 447, 451
  volume element, 275, 327
Liouville-Arnold theorem, 348, 351, 353
Lipschitz continuity, 182
liquid crystal, 568
lobe, 477
locus, 455
logarithmic series, 661
logistic
  difference equation, 432, 438
  differential equation, 419, 439
  map, 432, 438, 450, 480, 481
longitude, 262, 342
Lorentz
  boost, 159, 161, 169, 170
    composition, 164, 170

 covariant, 167
 force, 2, 168, 170, 293
 group, 164
 Hendrik Antoon, 150, 154
 invariant, 490
 scalar, 164
 transformation, 154, 155, 159, 164, 169
  composition, 164
Lorentzian, 217, 224
Lorenz
 Edward Norton, 191, 431, 472
 equations, 472
 map, 476
 oscillator, 417, 429, 432, 465, 472
 vector field, 476
Loschmidt's paradox, 324
Lotka-Volterra model, competitive, 174
Lyapunov
 Aleksandr, 196
 exponent, 404, 433, 446, 450, 461, 477, 481
  finite-time, 448
  largest, 448, 451, 481
  positive, 451
  vanishing, 450
 function, 179, 190, 194, 473, 475
 spectrum, 447, 449
  numerical, 448
 stability, 196
 time, 434

Möbius strip, 638
Mach number, 539, 549
Mach, Ernst, 149
macrostate, 516
magnetic
 dipole, 187
 field, 17, 90, 112, 140, 168, 170, 294, 299, 316, 422, 535, 540, 582, 630, 666
 flux, 552
magnetization, 422
magnetohydrodynamics, 559
Magnus series, 127
Mandelbrot set, 480
Mandelbrot, Benoit, 432
manifold, 319, 337, 377, 613, 614, 666
 connected, 619
 curved, 128
 differentiable, 55, 432, 616, 651
 disconnected, 619, 641
 flat, 645
 homogeneous, 652
 orientability, 637
 Riemannian, 129, 378, 639, 643
 simply connected, 619
 smooth, 122, 616, 618
 space-time, 163
 stable, 199, 220, 221, 451, 452
 symplectic, 637
 topological, 618
 unstable, 199, 221, 451–453
 with boundary, 640
 zero dimensional, 117
map, 432
 between manifolds, 617
 bilinear, skew-symmetric, 629
 continuous, 275, 659
 differentiable, 478
 invertible, 433
 iteration of, 433
 multilinear, 631
 smooth, 334, 617, 651, 665, 667
 twist, 438
Marsden, Ernest, 42
mass, 1, 14, 55, 85, 485
 conservation, 67
  local, 531
 current density, 541
 density, 243, 283, 485, 612
 distribution, 250
 flow rate, 569
 flux, 541
 gravitational, 24, 41, 64, 290, 298
 inertial, 24, 41, 59, 64, 290, 298
 matrix, 95, 127, 132, 148, 397
  free particle, 127
  position-dependent, 78, 141
 molar, 574
 molecular, 575
 of fluid, 540
 point, 283
 position-dependent, 135
 reduced, 27, 31
 relativistic, 161, 162, 167
 rest, 161–163
 time-dependent, 224
 total, 27
mass-shell, 167
mass-shell condition, 169
massless particle, 162, 163, 168
material element, 537, 539
Mathieu
 Émile, 383
 equation, 218, 383, 384, 402, 410, 411
 functions, 412
matrix, 582, 602, 622, 625
 antisymmetric, 287, 357, 363, 364, 395, 646, 660, 670
 deficient, 205, 220
 diagonal, 395
 elements, 397, 414, 518, 519, 670
 exponential, 219, 396, 404, 612, 660, 670
 group, 337, 659, 669, 670
 Hermitian, 391
 lower triangular, 490

  mechanics, 349
  nonsymmetric, 415
  positive-definite, 78, 396, 397
  positive-semidefinite, 249, 396, 414
  real symmetric, 78, 127, 220, 249, 250, 283, 363, 395, 401, 414, 415, 512, 607, 612, 648
  similar, 358
  symplectic, 337
  tridiagonal, 360, 492
  upper triangular, 205, 206
Maupertuis, Pierre Louis, 55
Maurer-Cartan form, 661, 670
maximum principle, 516, 523, 530
maximum, local, 400
Maxwell
  equations, 112, 149, 154, 366, 501, 582
  James Clerk, 149, 151
Maxwell-Boltzmann distribution, 324
May, Robert, 432
mean, 526
mean free path, 532
memoryless, 527
Mercury, perihelion precession, 26
meson, 485
metric tensor, 95, 126, 129, 288, 315, 378, 485, 618, 626, 627, 641, 643, 668
  conformal, 132, 379
  Euclidean, 121, 634
  indefinite, 163, 165
  induced, 449, 634, 667
  inverse, 128
  Lorentzian, 165, 628
  Minkowski, 164
  Poincaré, 668
  pseudo-Riemannian, 628
  Riemannian, 79, 127, 132, 414, 628
  signature, 165
Michelson, Albert, 149
Michelson-Morley experiment, 156
microstate, 516
Milne, Edward Arthur, 152
minimal coupling, 112
minimum, local, 400
Minkowski
  Hermann, 163
  metric, 164, 170
  space-time, 115, 163, 630
mixing, 436
mobility, 525
modulation, 212
module, 623, 635
moduli, law of, 663
modulo, 435, 479, 658
Moffat, Henry Keith, 558
mole, 575
molecular dynamics, 513, 531, 567
molecule, 243, 483, 524, 531, 532, 535, 555
  diatomic, 383, 413
    vibration, 386
moments, 526
momentum, 2, 248
  angular, 52, 82, 134, 389
    fluctuations, 466
  canonical, 113, 141, 293
  conjugate, 74, 76, 79, 92, 93, 99, 101, 105, 141, 143, 225, 285, 303, 378, 381, 389, 504, 511
  conservation, 67, 135, 161, 557
    local, 531, 557
  current tensor, 557, 576
  density, 557
  diffusion, 472
  equation, 557
  fluid, 557
  flux, 557
  generalized, 75, 303
  linear, 52, 53, 501
  longitudinal, 500
  mechanical, 113
  new, 367, 368, 377, 380
  Newtonian, 160
  old, 367, 369
  radial, 134
  relative, 27
  relativistic, 160, 161, 167
  rescaled, 434
  space, 380, 521, 607
  total, 28, 49, 360
  transferred, 47
  transverse, 500
monodromy matrix, 384, 405, 408, 412, 416, 432, 479
  eigenvectors, 401
  spectrum, 409
  trace, 416
Moon, 342
Moore, Chris, 50
Morley, Edward, 150
Moser, Jürgen, 352
multiplication table, 656
multiplicity, 605, 612
multivalued action, 347
multivalued function, 8

Navier, Claude-Louis, 531
Navier-Stokes equation, 531, 566
  compressible, 569, 579
  existence and regularity, 573
  incompressible, 579
  vorticity form, 570
network, cell phone, 614
Neumann, Carl, 489
Newcomb, Simon, 26, 270
Newton
  equations, 71, 85

    noninvariance of form, 76
  first law, 2, 58, 84, 127, 134, 135, 154, 168, 169
  gravitational constant, 16, 25
  Isaac, 25, 55, 58, 136, 370, 531, 548
  law of fluids, 568, 579
  law of gravity, 8, 25, 64
  laws of mechanics, 58, 484
  second law, 2, 14, 17, 25, 59, 61, 62, 68, 84, 92, 135, 168, 173, 175, 254, 289, 485, 488, 509, 531, 542, 668
    Galilean symmetry, 87
    inertialess limit, 175, 179
  third law, 25, 41, 65, 150, 255, 387
Newton-Lorentz equation, 111, 113, 141
nilpotent, 629, 636
node, 209, 323, 349
  asymptotically stable, 203
  degenerate, 202, 205, 207, 208, 210
  stable, 198, 201, 207, 426, 474
  symmetrical, 198, 200, 210
  unstable, 201, 207
Noether charge, 144, 338, 511
Noether's theorem, 28, 80, 82, 115, 140, 144, 319, 320, 466, 486, 501, 504, 511, 580
  converse, 320
  generalization, 83
nonabelian, 651, 652, 669
nonanalytic, 611
nonassociative, 609
nondegenerate, 279, 359
nondispersive, 486, 506, 510
nondynamical, 544
nonintegrable, 366
nonlinear, 469
  ODEs, 389
  saturation, 179, 192
  Schrödinger equation, 579
  vector field, 209
nonrelativistic
  limit, 160, 169
  mechanics, 56
  particle, 111
nontensorial, 642
norm, 164, 662
normal, 379
  form, 341
  matrix, 391, 607
  mode, 383–385, 387, 391, 392, 396, 399, 400, 413, 415, 455, 460, 485, 493, 518, 582
    energy, 393, 413, 415
    marginally unstable, 400
    periodic in time, 393
  plane, 644
  reaction, 192
  subgroup, 654, 656, 669
  vector, 96, 379, 476, 499, 538, 542, 557
nucleus, 42, 47
null
  geodesic, 168
  separated, 165
  space, 198, 205, 208, 278, 602
  vector, 165
nullclines, 187, 220
numerical experiments, 441
numerical solution, 464, 466, 481
nutation, 243, 281

O-point, 196, 228
observable, 66, 105, 173, 309, 363, 391
  algebra of, 620
  measurement of, 309
observation point, 484, 497
observer, 149
  accelerated, 290
  inertial, 152
  noninertial, 254
octahedron, 252
ODEs, 55, 366
  linear
    constant coefficients, 383
    coupled, 648
    homogeneous, 402
    periodic coefficients, 383
  nonlinear, 370
  uncoupled, 486
operator
  antisymmetric, 490
  creation-annihilation, 213
  curvature, 646
  negative-definite, 492
  symmetric, 491
optical path length, 131
optico-mechanical analogy, 365, 372
optics, 366, 371, 377
  geometrical, 372
orbit, 433
  aperiodic, 448
  bounded, 480
  chaotic, 433
  circular, 33, 402
  closed, 34, 185, 190
  diagram, 442
  elliptic, 33
  equation, 26, 32, 45, 382
  Hohmann transfer, 54
  hyperbolic, 32, 33, 43, 47
  lunar, 401
  minimum energy, 31
  of group action, 652
  parabolic, 32, 33
  period four, 441, 480
  period three, 441, 480
  period two, 441, 479–481
  periodic, 34, 191, 478

    - stability, 384
    - unstable, 480
  - quasiperiodic, 478, 480
  - straight line, 32
  - unbound, 32
  - under a map, 477
  - unstable, 441
- orbital plane, 35, 262
- ordinate, 590
- orientability, 275, 637
- orientation, 81, 89, 139, 246, 638, 641
- orthochronous, 155, 164
- orthogonal, 378, 391, 399, 612
  - group, 658
  - matrix, 220, 415, 607, 612, 669
  - transformation, 250, 391, 610, 648
- orthonormal, 51, 400
  - frame, 585
- oscillations, 185, 203, 225
  - damped, 6
  - driven, 411
  - driven damped, 217
  - forced, 210, 223
  - free, 195
  - harmonic, 196
  - in phase, 385
  - longitudinal, 485
  - out of phase, 386
  - parametric, 410, 411
  - radial, 32
  - small, 15, 196, 295, 383, 384, 390, 396, 455, 460, 548, 582
    - around periodic orbit, 383
  - stretched string, 143
  - transverse, 485
- oscillator
  - anharmonic, 3, 18, 209, 225, 234, 236, 454
    - exact solution, 237
  - coupled, linear, 397
  - coupled, nonlinear, 387
  - damped, 222
  - driven, 215, 223, 238
  - forced, 192, 224
  - harmonic, 3, 8, 10, 17, 18, 33, 80, 84, 140, 148, 195, 219, 220, 225, 234, 323, 325, 341, 342, 346, 349–351, 353, 357, 358, 362, 363, 380, 385, 431, 493, 648
    - aperiodically damped, 203
    - critically damped, 202, 204, 205, 222
    - damped, 201, 221, 322, 430
    - driven damped, 217, 224
    - energy, 196
    - energy level set, 116
    - Green function, 216
    - isotropic, 35
    - Lax matrix, 364
    - overdamped, 203, 221
    - phase portrait, 197
    - quantum, 213
    - trajectory, 220
    - underdamped, 202, 217
  - isotropic, 53, 148
  - Lorenz, 432
  - van der Pol, 185, 222
- osculating circle, 644
- outer product, 519
- overtones, 493

- pairing, 75, 624, 625
- Pantheon, 296
- parabola, 30, 207, 208, 471, 472, 535, 595
- parabolic equation, 489, 509, 513
- parabolic trajectory, 381
- paraboloid, 535
- parallel
  - axis theorem, 250, 280
  - translation, 585
  - transport, 130, 592, 643, 646, 648
- parallelepiped, 450
- parallelogram, 583, 585, 646
  - infinitesimal, 279, 646
- paramagnet, 422
- parameter, 218, 535
- parametric
  - oscillations, 218
  - resonance, 218, 224
- parity, 420, 435
- particle, 579, 609
  - charged, 140, 170
  - creation, 163
  - massless, 168
  - physics, 485, 558
  - subatomic, 245
  - test, 535
- particular solution, 33
- patch, 458
- path integral, 404
- pathlines, 535–537
- Pauli matrices, 194, 612, 661, 663
- Pauli, Wolfgang, 38
- PDE, 484
  - linear, 338, 485, 510, 513
  - nonlinear first order, 287, 365, 367
- pendulum, 432
  - bent, 472
  - compound, 13
  - coupled, 385, 413
  - cycloidal, 242
  - double, 387, 413, 432, 454, 467, 481
    - phase space, 389
    - small oscillations, 394, 414, 415
    - zero gravity, 456, 481
  - folded, 472
  - Foucault, 85, 295

  inverted, 411, 413
  Kapitza, 384, 410
    energy, 410
    instability, 413
    parametric resonance, 411
    small oscillations, 411
    stability, 411
  simple, 13, 19, 20, 72, 96, 209, 225, 348, 384, 434, 478, 479
    angle-action, 363
    driven damped, 481
    exact solution, 233
    Hamiltonian, 226
    inertialess damped, 180, 193
    Lagrangian, 225
    small oscillations, 363
    time period, 233, 240–242, 349
  spherical, 13
  triple, 414
pentagon, regular, 651
periapsis, 44
perihelion, 30, 32, 34, 35
period
  four, 480
  of revolution, 22
  three, 480
  two, 433
period-doubling, 442
periodic
  motion, 33, 34, 192, 236, 325
  orbit, 34, 433, 478, 479
    dense, 436, 443
    perturbation of, 401
  potential, 402
  solution, 447
    stability, 408
  trajectory, 347, 351, 431
permittivity, 37
permutation
  cyclic, 361, 656, 657
  group, 669
  sign, 657
perpendicular axis theorem, 253
Perrin, Jean, 525
perturbation, 341, 388, 573
  singular, 176, 567
  theory, 92, 238, 239, 461
    quantum mechanical, 239
  to periodic solution, 401
Pfaff, Johann Friedrich, 624
Pfaffian differential equation, 624
phase, 506
  difference, 53
  initial, 224
  path, 103, 376
  plane, 207, 434
  point, 342
  portrait, 66, 140, 174, 188, 192, 196, 207, 220, 228, 417, 430, 471
  shifts, 19
  slowly varying, 212
  space, 65, 105, 122, 172, 302, 311, 325, 351, 388, 417, 452, 456, 459, 461, 469, 474, 620, 652
    double pendulum, 457
    simple pendulum, 227
    topology, 225
    unbounded, 436
    volume conservation, 404
  speed, 506, 510
  trajectory, area enclosed, 344, 347
  transition, 417
    first order, 424
    second order, 421, 422, 440
  velocity, 486, 505, 512
photon, 17, 48, 162, 163
Picard iteration, 183, 194
Pisa, leaning tower, 41
pitchfork bifurcation, 418, 420, 427
  subcritical, 422, 427, 429, 430
  supercritical, 421, 427, 428, 474
pivot, 13, 225, 454
Planck's constant, 16, 58, 142, 151, 220, 365, 506
Planck, Max, 349
plane wave, 506, 509
plane, punctured, 620, 665
planetary motion, 22
planetary orbits, 29
plasma, 483
plasma confinement, 431
Plateau's problem, 69
Platonic solid, 252
Poincaré
  group, 164, 656
  Henri, 163, 176, 296, 327, 431, 458
  integral invariant, 313
  lemma, 601, 637
  metric, 646, 668
  recurrence theorem, 324, 327, 340
  return map, 432, 452, 458
  section, 452, 455, 458, 459, 467
  slice, 459
  surface, 388, 452, 456, 458, 481
Poincaré-Bendixon theorem, 190, 453, 454
Poincaré-Birkhoff theorem, 454, 461
Poincaré-Cartan integral invariant, 313
Poinsot construction, 273
Poinsot, Louis, 273
point
  charge, 49
  group, 651
  mass, 582, 612
  of observation, 535, 537
  particle, 23, 38, 379
  transformations, 302, 304, 331, 333, 334, 339

  - vortex, 551
- pointwise multiplication, 309
- Poiseuille flow, 568
- Poisson
  - algebra, 670
    - angular momentum, 109, 122, 287
    - barotropic flow, 558
    - canonical, 288
    - center, 124, 278, 288
    - closed, 115
    - degenerate, 124, 278
    - Kepler problem, 113, 115
    - linear, 115, 653
  - bivector field, 110, 288
  - bracket, 105, 106, 143–145, 310, 317, 336, 337, 339, 351, 370, 415, 504, 577, 627, 653
    - adiabatic compressible flow, 560
    - angular momentum, 121, 145, 146
    - antisymmetry, 107, 122
    - barotropic flow, 559, 577
    - basic, 108, 109, 303
    - bilinear, 122
    - canonical, 106, 108, 113, 121, 294, 299, 510, 560, 578
    - Clebsch variables, 563
    - equal-time, 308, 339
    - functionals of ρ, $\boldsymbol{v}$, 560
    - incompressible flow, 560, 577
    - inviscid flow, 559
    - iterated, 109, 126, 148
    - Jacobi identity, 122
    - Landau, 577
    - Leibniz rule, 107, 122
    - linearity, 107
    - Morrison-Greene, 560
    - noncanonical, 121, 277, 559, 563
    - polar coordinates, 144
    - unequal-time, 145, 308
  - commute, 107, 115, 278, 342, 345, 352, 353, 375, 455, 456, 466, 468, 558
  - equation, 48, 513, 544, 561
  - manifold, 122, 667
    - $\mathbb{R}^3$, 122, 124
    - $\mathbb{R}^{2n}$, 122
    - sphere, 125
    - symplectic leaves, 124, 279
  - Siméon Denis, 55
  - structure, 122
    - degenerate, 277
  - tensor, 109, 110, 121, 122, 143, 146, 148, 173, 278, 279, 311, 315, 627, 630, 636, 653, 667, 670
    - angular momentum, 287, 288
    - antisymmetric matrix, 110, 122
    - canonical, 109
    - contravariant second rank, 123
    - invertibility condition, 123
    - nondegenerate, 288
    - nonlinear, 122
  - theorem, 108, 115, 126
- polar angle, 262, 593
- polar plot, 54
- polar vector, 90, 550
- polarization, 485
- polhode, 273
- pollen grains, 523, 536
- polytropic exponent, 560, 578
- population, 439
  - dynamics, 419, 432
- position
  - coordinate, 586
  - eigenstates, 519
  - operator, 529
  - space, 522, 607
  - vector, 247, 248, 586, 592, 609
- positive-definite matrix, 142, 398
- positive-semidefinite matrix, 250, 283, 414
- potential, 2, 132, 367, 370, 415, 421, 430, 611, 668
  - attractive, 10
  - barrier, 235
  - body force, 546
  - central, 23, 25, 34, 52, 81, 134, 339
  - circularly symmetric, 374
  - Clebsch, 563
  - convex, 8
  - Coulomb, 12, 544
    - attractive, 47
    - repulsive, 43
  - decaying, 12
  - double-well, 140, 222, 234, 272
  - effective, 31, 34, 281, 296, 534
  - electrostatic, 544
  - energy, 2, 63, 179, 510
    - density, 556
    - matrix, 394
  - even, 8
  - external, 88
  - flow, 550, 563, 576
  - gravitational, 25, 31
  - integrable, 12
  - long-range, 12, 46
  - Mexican hat, 400
  - Newtonian, 12, 34, 43
  - nonunique, 8
  - periodic, 384, 402
  - quartic, 234, 374, 381, 422
  - repulsive, 10
  - Roche, 296
  - scalar, 112, 168, 561
  - scale invariant, 49
  - scattering, 12, 19
  - sech^2, 10, 18, 242
  - short-range, 47
  - spherically symmetric, 25
  - step, 4

  vector, 112, 141, 168, 293, 299, 540, 561
  velocity, 179, 550
  well, 235
    infinite, 349
  Yukawa, 47
power-law, 39, 522, 523
Poynting vector, 501
Prandtl number, 472
Prandtl, Ludwig, 573
precessing ellipse, 34
precession, 243, 258, 281
  back-and-forth, 283
  Foucault pendulum, 296
  lunar perigee, 26
  Mercury perihelion, 26
  monotonic, 282
pressure, 102, 140, 532, 533, 541, 543, 544, 547, 562, 567, 666
  atmospheric, 547
  gradient, 574
  mechanical, 569
  negative, 541
  thermodynamic, 569
primaries, 296
principal axes, 53, 244
principal axes of inertia, 250
principal moments of inertia, 250
Principia, Newton's, 58, 548
principle of virtual work, 64
probability, 526, 528
  amplitude, 17, 58
  conservation, 403
  density, 525–528, 530
  distribution, 526
  factorization, 527
  relative, 93
projectile, 381
projection, 581, 584, 586, 593, 602, 612
  divergence-free, 561, 562
propagator, 58
  free particle, Gaussian, 58
proper length, 157
proper time, 157, 161, 166, 168, 619
proton, 404
pseudoscalar, 90, 550
pseudotensor, 91
pseudovector, 90, 91, 550
pullback, 632, 667
puncture, 619
pushforward, 633, 653, 660, 667

quadratic form, 249, 283, 394
quadrature, 8, 32, 137, 176, 213, 231, 232, 281, 368, 381, 390, 456, 468, 469, 590
quadric surface, 272
quantization, 37, 349, 350
Quantum Electrodynamics, 48
quantum mechanics, 38, 69, 106, 142, 151, 198, 220, 308, 335, 363, 365, 370, 376, 377, 391, 402, 486, 559
  nonrelativistic, 47, 580
quantum number, 351
quark confinement, 404
quasiperiodic, 34, 211, 277, 325, 351, 356, 386, 392, 393, 415, 435, 438, 455, 460, 478
  trajectory, 431, 458
quaternions
  algebra, 662
  imaginary, 663, 670
  relations, 663
  unit, 663
quintic polynomial, 469

radar method, 151
radial, 591
  acceleration, 593
  component, 293
  coordinate, 592, 593, 611
  distance, 114
radian, 43, 587
radius of convergence, 127
radius of curvature, 644
random variable, 526, 530
  Bernoulli, 527
  binomial, 528
  continuous, 526
  independent, 527, 530
random walk, 513, 526, 530
rank, 279, 603, 612
  maximal, 618
rapidity, 160, 164, 169, 170
rate
  absorption, 217
  decay, 178, 179, 193, 201, 203, 222
  growth, 178, 179, 193, 201, 419
rational number, 479
rational ratio, 34, 393
ray optics, 93
Rayleigh number, 472
Rayleigh-Bénard convection, 472
RC circuit, 177
recurrence, 324, 326
recurrence time, 325, 328
reflection, 81, 89–91, 139, 246, 550, 651, 656, 660, 669
refractive index, 131
  inhomogeneous, 138, 366, 371
regular motion, 392, 431, 455, 481
regulator, 11
relation, functional, 116
relative variables, 27, 339
relativity
  Galilean, 59, 61, 62, 159
  general theory, 98, 245, 567

  principle of, 150, 167
  special theory, 56, 61, 150, 159
renormalization group, 442, 513
reparametrization, 100, 129, 168, 218, 224
resistance, 177, 541
resonance, 211, 212, 217, 218, 223, 239
  criterion for chaos, 431
  energies, 49
  overlap of, 456
  parametric, 218, 384, 411
resonant amplification, 218, 239
rest frame, 157
rest mass, 161, 168
restoring force, cubic, 234
restoring force, linear, 2, 386, 492, 494
reversible process, 573, 625, 666
Reynolds number, 570, 579
Reynolds similarity principle, 570
Reynolds, Osborne, 570
Riccati equation, 185
Ricci
  flow, 513
  Gregorio, 641
  scalar, 288, 646
  tensor, 646
Riemann
  Bernhard, 644
  curvature tensor, 288, 414, 644, 645, 647
    symmetries, 645
  surface, 476
Riemannian manifold, 378, 639, 643
right multiplication, 653
rigid body, 243, 360
  angular momentum, 253
    conservation, 257, 271
    sphere, 271
  angular orientation, 262
  angular velocity, 264, 265, 284
  anisotropic, 251, 270, 274, 275, 286
    Euler equations, 287
    force-free motion, 287
    stability, 287
  aperiodic motion, 273
  body-fixed frame, 261, 263
  center of mass, 283
  center of mass momentum, 267
  chalkboard duster, 273
  coin, 284
  collinear, 252
  comoving frame, 267
  configuration space, 246, 262, 274, 288
  corotating frame, 261
  corotating principal axis frame, 275
  coupling of rotation and translation, 268
  cuboid, 273
  dynamics, 291
  equations of motion, 255
  Euler equations, 267
  external force, 267
  external torque, 267, 273
  force-free motion, 257, 275, 285
  Hamiltonian, 277, 286
  inertial frame, 261
  infinitesimal rotation, 264
  kinetic energy, 249, 270, 277
  lab frame, 263, 267
  Lagrangian, 248, 255
  noncollinear, 246
  periodic motion, 273
  phase space, 274
  planar, 252
  principal axis frame, 267
  rotational angular momentum, 267
  rotational kinetic energy, 251, 265, 268
  spherical, 251
  square plate, 284
  stable motion, 272
  symmetric, 270
  tennis racquet, 273
  torque-free motion, 270
  unstable motion, 273
rigid motions, 312, 656
rigid rotator, 245, 252, 284
  angular momentum, 258
  body-fixed frame, 257
  configuration space, 246, 262, 285
  degrees of freedom, 246
  free motion, 257, 258
  inertia metric, 288
  lab frame, 257
  Lagrangian, 285
  principal axis frame, 257
  torque-free motion, 285
rigidity, 149, 541
ring, 623
ring of functions, 623, 635
Robin, Victor Gustave, 489
Roche effective potential, 290, 296, 299
Roche lobes, 298
Roche, Édouard Albert, 296
rosette, 34
rotation, 13, 85, 87, 229, 246, 263, 312, 456, 469, 472, 591, 646, 662, 663, 669
  angle, 246, 589
  axis of, 246
  axis-angle representation, 246, 662, 664, 670
  counterclockwise, 247, 656
  finite, 246, 338
  generated by angular momentum, 115, 318
  hyperbolic, 163, 164
  improper, 90, 246, 660
  infinitesimal, 82, 246, 258, 318, 340, 466
  local, 550
  matrix, 81, 87, 89, 247, 263, 265, 612

  number, 438
  proper, 90, 164, 246, 651, 660, 664
  uniform, 257, 471
rotational motion, 466
rotor, kicked, 432, 435
roughness, 432
Routh's criterion, 297
Routh, Edward, 297
Routh-Hurwitz criterion, 200
Routhian, 95
Rutherford, Ernest, 42

S-wave, 47
Sackur-Tetrode equation, 575
saddle, 643
saddle point, 198, 201, 207, 209, 210, 228, 235, 236, 323, 325, 400, 426, 474
saddle-loop bifurcation, 430
saddle-node bifurcation, 418, 423, 425
  infinite period, 430
  normal form, 418
  of cycles, 430
saw dust, 536
scalar, 37, 583
  curvature, 646
  field, 319, 533, 579, 581, 596, 611, 620
  function, 645
  Lorentz, 164
  potential, 501
  product, 581, 584
  pseudo, 90
  relation, 37
  triple product, 610
  true, 90
scaling, 334, 337, 602
scattering, 19, 42, 135
  amplitude, 19
    Born, 48
  angle, 44, 47, 54
  back, 44
  Coulomb, 42, 54
  elastic, 47
  forward, 44
  hadron-hadron, 49
  S-wave, 47
  trajectory, 10
Schrödinger
  eigenvalue problem, 372, 402, 416
  equation, 38, 64, 93, 183, 310, 349, 365, 370, 486, 514, 580
    nonlinear, 405, 579
    time-dependent, 198, 335, 370, 376, 506, 510
    time-independent, 350
  Erwin, 377
secular term, 239, 342
seismic wave, 485
self-adjoint operator, 309
self-intersections, 618
semiaxes, 342, 344
semiclassical, 12, 350, 365
  approximation, 370
  limit, 151, 376
semidirect product, 655, 657, 669
semimajor axis, 22, 30
semiminor axis, 30
separating vector, 647, 648
separation constant, 366, 372, 375, 492, 517
separation of variables, 7, 365, 366, 368, 372, 398, 454, 485, 491, 513, 517, 530
  additive, 376, 381
  multiplicative, 376
separatrix, 174, 225, 228, 234, 236, 242, 271, 273, 298, 325, 348, 435, 472
series, not convergent, 342
set, closed, 659
shadowing property, 464
shear, 541, 550
  flow, 568, 573
  viscosity, 566
  wave, 485
shift map, 479
sign, 657
signal, 56, 497
similarity
  mechanical, 39
  solution, 530
  transformation, 206, 220, 358, 363, 391, 392, 394, 400, 409, 415, 416, 604, 607, 612, 631
simultaneity, 55, 134
  relativity of, 152, 157
singleton set, 651
singlevalued, 8, 350
singular
  Lagrangian, 98
  perturbation, 176
  values, 448
sinusoidal forcing, 211
sleeping top, 283
Smale, Steven, 431
Smoluchowski, Marian, 525
smooth functions, 530, 595, 611, 620, 665, 666
  space of, 620
solar corona, 298
solar perturbations to Moon's orbit, 402
solenoidal, 540, 550, 561, 579
soliton, 60
solution
  general, homogeneous, 33, 211, 215, 217
  not in closed form, 390
  particular, 33, 211, 213, 215, 217, 224
  static, 66, 69
solvable, 366
sound waves, 149, 485, 539, 548, 575
source, 544

space group, 651
space of paths, 69
space-like separation, 159, 165, 169
space-like vector, 165
space-time, 485
  diagram, 152, 165, 168, 169, 497
  interval, 169
span, 356, 398, 601
special functions, 230
special relativity, 150
specific heat, 534, 575
  ratio, 545, 555
spectral
  decomposition, 200
  distribution, 217
  parameter, 361, 364
spectrum, 358, 384, 405, 408, 604
  expelled from, 549
  line, 349
speed, 100, 129, 587
  of light, 17, 48, 55, 56, 61, 111, 149, 151, 490
    constancy, 156
  of signals, 497
  of sound, 149, 539
    adiabatic, 549, 576
    isothermal, 575, 576
  of waves in string, 488
  terminal, 525
sphere, 262, 274, 279, 288, 458, 616, 617
  n-dimensional, 618
  great circle, 127
  not a group, 653
  orientability, 638
  particle on, 136, 381, 609
  Poisson manifold, 125
  Poisson tensor, 125
  round, 643
  round metric, 634, 667
  stereographic coordinates, 665
  symplectic tensor, 125, 288
  unit, 246, 659, 663
spherical ball, 251
spherical top, 285
  kinetic energy, 265
spikes, 242
spin, 422, 558
  axis, 285
spinning, 243, 550
spiral, 184, 209, 323
  sink, 185, 201, 207, 428, 429
  source, 185, 201, 207, 428, 429
spontaneous symmetry breaking, 401, 403, 418, 454, 465, 474, 571, 572
spring, 384, 413
  constant, 218, 384, 386
    matrix, 397, 415
    time-dependent, 224
  inertialess, 177
  nonlinear, 359
square, completing, 612
stability, 19, 432
  asymptotic, 478
  coefficient, 478
  exchange of, 419
  geodesic, 288
  index, 410, 412
  islands of, 438
  Lagrange points, 297
  linear, 178, 182, 474, 476
  Lyapunov, 196, 197, 221
  marginal, 210
  neutral, 196, 207
  periodic solution, 401, 408
  robust, 208, 210
  solar system, 431
  structural, 201
stagnation point, 174, 546
standard map, 431, 434, 435, 478, 479
star, 200, 208
state, 65, 122, 135
  pure, 309
  space, 65, 173, 432, 666
  vector, 403, 404
static, 367
static solution, 6, 174, 198, 396, 433
stationary phase approximation, 142, 506
stationary state, 371
statistical mechanics, 93
steady-state, 6, 217
steradian, 43
stereographic projection, 665
Stevin, Simon, 41
stochastic, 431, 513
stochasticity, transition to, 431
Stokes
  flow, 570, 571
  George Gabriel, 531, 550, 570
  theorem, 354, 550, 552, 581, 600, 601, 637, 640, 668
straight line, 130
strain, rate of, 568
  tensor, 568, 579
strange attractor, 477
streaklines, 535, 536, 572
stream function, 540, 552
streamlines, 535, 546, 547, 550, 570
stress
  compressional, 417
  deviatoric, 568, 579
  shear, 541
  tangential, 542, 543
  tensile, 541
  tensor, 541–543, 557, 567, 579
    deviatoric, 567, 568

    symmetry, 567
  viscous, 568
stretched string, 243, 483, 485, 510
  conservation laws, 499
  energy, 498
  Hamiltonian, 503
  Lagrangian, 501
  longitudinal momentum, 486, 500
  transverse momentum, 486, 500
  transverse vibrations, 486
string theory, 245
stroboscopic, 435, 477
structure constants, 661, 670
subalgebra, 356, 561
subgroup, 650, 657
  normal, 654, 657, 669
  one-parameter, 658, 660, 669
submanifold, 116, 356, 388, 449, 618, 659
  embedded, 618
  immersed, 618
subsonic, 539
subspace, 601, 612
sum rule, 450
Sun, 22
  mass of, 25, 53
superdiagonal, 416
superfluid Helium, 559
superintegrable, 37
superposition, 135, 326, 455, 495
  incommensurate, 386, 415, 459
  linear, 34, 60, 211, 213, 316, 399, 491, 506
supersonic, 539
superstable, 433
surface, 643
  element, 499, 538, 541
  force, 533, 543
    normal, 567
    tangential, 567
  integral, 543, 557, 639
  invariant, 476
symmetric group, 656, 669
symmetric top, 266, 277
  angular momentum, 269
    sphere, 285
  angular velocity, 269
  body-fixed frame, 259
  comoving frame, 259, 285
  ellipsoid of inertia, 285
  Euler's equations, 269, 285, 286
  free motion, 269
  heavy
    Lagrangian, 280
    locus of tip, 282
    nutation, 280
    nutation energy, 281
    precession, 280
    spinning, 280
  kinetic energy, 265
  precession, 260, 269
  precession rate, 260, 266
  principal axes, 266
  principal axis frame, 259
  rigid rotator limit, 286
  spherical top limit, 286
  spinning, 269
  spinning energy, 281
  spinning rate, 260, 266
  stability, 285
  subject to gravity, 280
  torque-free motion, 285
    Lagrangian, 286
symmetry, 244, 612, 649
  canonical transformation, 319
  circular, 381
  continuous, 192, 320, 414, 486, 651
  cyclic, 111, 275
  discrete, 192, 320, 420, 473, 474
  finite, 115
  generator, 320
  global, 580
  hidden, 113, 115
  infinitesimal, 80, 115, 126, 140, 319, 511
  left-right, 465, 571
  of equations of motion, 39, 80, 83, 84, 139
  of Lagrangian, 80, 139, 414
  of Stokes flow, 571
  parity, 421
  reflection, 236, 284, 473, 571
  rotation, 115, 281, 284, 581
  scaling, 39, 53, 337, 530
  space translation, 571
  spherical, 47
  spontaneous breaking, 403, 418, 465, 474, 571
  statistical restoration, 572
  three-fold, 252
symplectic
  diffeomorphism, 355
  form, 111, 123, 148, 173, 288, 311, 355, 630, 637, 638, 652
    antisymmetry, 111
    closed, 123, 636
    on S^2, 279
  gradient, 173
  group, 315, 337
  integrator, 92
  leaf, 124, 279, 288
  manifold, 123, 637
  matrix, 337
  structure, 123
  tensor, 123
    canonical, 337
  transformation
    linear, 315, 337
  vector space, 311

tangent, 524
  plane, 274, 335, 644, 646
  space, 59, 317, 384, 399, 621, 626, 653, 658, 660
  vector, 59, 100, 130, 379, 447, 621, 646
    angle between, 132
Taylor
  expansion, 126, 139, 211, 338, 390, 396, 419, 549, 581, 589, 594, 596, 611
  Geoffrey Ingram, 17, 572
  John Bryan, 434
  microscale, 572
temperature, 93, 102, 324, 422, 523, 529, 532, 544, 555, 625
  absolute, 140, 515, 524, 573, 666
  Centigrade, 515
  discontinuous, 516
  distribution, 514
  equilibrium, 516
  Fahrenheit, 515
  gradient, 568
    atmosphere, 574
  Kelvin, 515
tension, 13, 20, 97, 143, 298, 485, 495
  stretched string, 487, 509
tensor
  algebra, 400
  antisymmetric, 139, 287
  calculus, 55
  contravariant, 626, 633
    antisymmetric, 110, 287
    second rank, 626, 667
  covariant, 626, 633
    antisymmetric, 111, 631
    positive-definite, 400
    second rank, 395, 400, 627, 628
  density, 632
  fourth rank, 568, 579
  isotropic, 567
  mixed second rank, 395, 400, 630, 641
  product, 626
  rate of strain, 568
  symmetric, 78, 139, 287, 567
  type, 626
    $(0, 4)$, 645
    $(1, 1)$, 645
    $(1, 3)$, 645
    (p, q), 631
tent map, 443, 445, 480
tetrahedron, 243, 252, 415
thermal
  conductivity, 514, 515, 529
  diffusivity, 566
  equilibrium, 524
    global, 324, 532
    local, 532, 544, 555
  fluctuations, 422
  motion, 524, 535, 536
thermalization, 324
thermodynamics
  first law, 102, 140, 514, 546, 555, 565, 573, 575, 624, 666
  second law, 102, 140, 324, 565, 573, 575, 625, 666
  state space, 624
Thomson, Joseph John, 47
three-body problem, 26, 49, 53, 132, 239, 342, 431, 454
  choreography, 50
  Euler, 374
  Euler solutions, 50, 297
  figure-8 solution, 50
  Lagrange solutions, 50, 297
  planar, 50
  restricted, 290, 296, 299
three-rotor problem, 456
Tikhonov's theorem, 520
time
  arrow of, 155
  minimal, 137
  Newtonian, 131–133, 149
  nondimensional, 411
  proper, 157, 161
  reparametrization of, 148, 218, 224
time delay, 11, 19
  regularized, 11
time derivative, total, 330
time dilation, 156
time evolution, 310, 339, 358, 359, 367, 433
  backward, 192, 433, 516
  canonical transformations, 307
  Hamiltonian, 91
  infinitesimal, 107, 145
    canonical transformation, 317
  linearized, 448
  matrix, 384, 404, 405, 413, 447, 450, 451, 514
    composition law, 405
    reproducing property, 405
    unimodular, 406
  operator, 58, 518
  phase volume, 322
  via Poisson bracket, 106
time period, 5, 7, 18, 19, 53, 196, 217, 242, 344, 472, 493
  anharmonic oscillator, 237
  elliptic orbits, 34
  normal modes, 393, 413
  simple pendulum, 14, 229, 349
time series, 435
time step, 449
time-average, 436
time-dependence
  explicit, 78, 317, 322, 329
  implicit, 78
time-like
  curve, 166, 168

  geodesic, 168
  separation, 159, 165, 169
  vector, 165
time-ordered exponential, 406, 415, 447
time-reversal, 5, 7, 17, 451, 481, 513, 515
Toda chain, 364
Toda, Morikazu, 359
top
  anisotropic, 251, 287
    Euler equations, 270
    kinetic energy, 265
  heavy symmetric, 244, 280
  precession, 259
  sleeping, 283
  spherical, 251, 252
    free motion, 257
  spinning, 259
  symmetric, 251, 274
    axis, 269
    free motion, 259
  symmetry axis, 281
topological equivalence, 210, 617
topology, 225
  change, 456, 571
torque, 20, 66, 82, 193, 226, 456, 466, 585
  due to gravity, 280
  external, 253, 273, 481
  on rigid body, 256, 270
  origin, 609
torus, 275, 351, 389, 414, 436, 455, 457, 476, 557, 617, 619, 620, 653, 667
  n-dimensional, 354
  highly nonresonant, 352
  invariant, 274, 352, 353, 356, 388, 460, 461
  irrational windings, 191, 325
  resonant, 352
trace, 207, 208, 222, 604, 605
  of powers, 363
traceless matrix, 323, 357, 358, 403, 416, 447
trajectory, 59, 63, 101, 376, 378, 379, 388, 433, 524, 535, 586, 610
  bound, 10, 362
  chaotic, 477
  configuration space, 65, 377, 455
  existence, 135
  heteroclinic, 184
  homoclinic, 184
  irregular, 456
  nonunique, 136
  parabolic, 381
  periodic, 185, 456, 459
  phase space, 65, 227, 347
  quasiperiodic, 456
  shape of, 132
  trapped, 190
  unbound, 10
transcritical bifurcation, 420, 426
transformation
  affine, 87
  infinitesimal, 83
  invertible, 334
  laws, 395
  linear, 87
  similarity, 631
transients, 175, 217, 445, 481
transition
  function, 614, 616, 618, 638, 651, 658, 665
  libration to rotation, 465, 481
  matrix, 405
  order-chaos-order, 455, 456, 463, 466
  topological, 465
transitive group action, 652, 653
translation, 312, 652
  infinitesimal, 337
  space-time, 85, 86, 651
transpose, 263, 391, 604
transposition, 656
transversal, 459
trapped trajectory, 13, 190
trapping region, 190, 191
trapping surface, 476
traveling wave, 495
triangle
  equilateral, 50, 656
  inequality, 250, 253, 284
  isosceles, 510
triangular system, 20, 221, 469, 481
trident, 420
trigonometric
  functions, 231, 277, 393, 665
  series, 342
Trojan asteroid, 297
Tschirnhaus, Ehrenfried, 136
tunneling, 4
turbulence, 432, 568, 572
  decay of, 572
  fully-developed, 572
  length scales, 572
  transition to, 571, 572
turbulent, 473
  boundary layer, 571
  flow, 417, 572
  wake, 571, 572
turning point, 3, 4, 7, 8, 18, 32, 221, 236, 469
  bifurcation, 418
  radial, 38, 350, 362
twin paradox, 156
twist map, 438
two-body problem, 49
  gravitational, 86

unbound orbit, 14
unbounded phase space, 436
unbounded trajectory, 5, 32, 38

uncorrelated, 433, 456, 461
uncountable, 443
underdamped oscillator, time period, 202
underdetermined, 544
unimodal map, 438, 442, 480
unimodular, 404, 406, 658
unique solution, 182, 192, 405, 511, 516
uniqueness, 612, 666
  failure of, 181, 192, 611
unit
  circle, 659
  interval, 438
  quaternions, 670
unitary, 406
  matrix, 220, 604, 612, 661, 663
  transformation, 310, 391
    1-parameter family, 310
units, 439, 529
  CGS, 6
  CGS-Gaussian, 111
  Heaviside-Lorentz, 43, 501
  SI, 6, 37
universal, 39, 41, 442
  equation, 485, 486, 513
  gas constant, 525, 532
  law of gravitation, 22
universality, 432
unstable, 478
upper half-plane, 646

van der Pol equation, 222
van der Pol oscillator, 432
variable
  dependent, 135, 173
  independent, 140, 173, 488, 666
variance, 527, 530
variation of constants, 213
variational
  derivative, 503
  principle, 68, 144
    Euler-Maupertuis, 131
    phase space, 102, 328, 331, 332
vector, 582, 585
  axial, 90
  column, 601, 622
  contravariant, 75
  cotangent, 75
  covariant, 75
  displacement, 587
  identity, 543, 551, 575, 577, 629
  normal, 117
  polar, 90
  potential, 90, 142, 299, 316, 501, 540
  pseudo, 90
  relation, 37
  relative, 27
  row, 625
  space, 57, 397, 491, 519, 581, 584, 601, 623
    complex, 198
  tangent, 75, 265, 621
  true, 90
  unit, 51, 134, 585, 591
vector field, 55, 171, 173, 356, 432, 470, 473, 581, 597, 620, 621, 644, 667
  action on functions, 622
  autonomous, 175, 176, 184
  axial, 90
  bifurcations, 417, 430
  canonical, 147, 173, 356
  commutator, 126, 621, 666
  components, 621
  contravariant, 130, 622
  coordinate, 621
  coordinate basis, 288, 448
  curl-free, 316, 561, 599, 601
  discontinuous, 181, 192
  divergence-free, 316, 540, 561, 578, 599
  fixed point, 174
  gradient, 189
  Hamiltonian, 125, 126, 184, 188, 225, 234, 275, 451, 637
  Killing, 126
  left-invariant, 653, 660
  Lie algebra of, 561
  linear, 197, 207
  linearization, 187, 209
  Newtonian, 175
  nonautonomous, 175, 210
  noncoordinate basis, 621
  nonlinear, 175, 209
  nonvanishing, 275, 653
  on the circle, 180, 468, 470
  on the phase plane, 184
  one-dimensional, 175
  polar, 90
  quadratic, 418
  singlevalued, 180
  smooth, 622
  zeros, 174, 471
velocity, 532
  addition, 159, 169
  azimuthal, 52
  diffusion, 566
  generalized, 75, 142, 262, 264, 280, 390, 414
  gradient, 568
  initial, 13
  potential, 548, 550, 563
  radial, 52, 592
  translational, 291
  vector, 581, 587, 610
  vector field, 90, 533, 535, 544
    random, 572
viscosity, 551
  bulk, 566, 569

  - dynamic, 566
  - kinematic, 472, 525, 566
  - shear, 566, 567
  - volume, 566
- viscous fluid, 524
- viscous force, 570
- viscous medium, 177
- voltage, 177
- volume, 102, 538, 666
  - change in, 538
  - element, 320
  - flow rate, 569
  - form, 123, 638
    - Riemannian, 639
  - infinitesimal, 450, 474
  - integral, 543, 557, 639
  - of phase space, 325, 327
  - specific, 533
- von Kármán vortex street, 571
- vortex, 550, 571, 572
  - filament, 554
  - force, 543, 546, 547, 569, 578
  - line, 551, 554, 576
  - point, 551
  - ring, 551
  - sheet, 573
  - street, 571
  - stretching, 550
  - tube, 551, 554, 569
    - strength, 554
- vortices, staggered, 572
- vorticity, 90, 543, 550, 557, 563, 569, 576–579, 599
  - advection, 552
  - Clebsch variables, 563
  - diffusion, 569
  - evolution, 551, 558
    - viscous, 569
  - flux, 550, 552
  - frozen, 552, 554, 576
  - local conservation, 552, 576
  - moments of, 552
  - tensor, 568

- wake, turbulent, 572
- water wheels, 473
- wave
  - blast, 17
  - electromagnetic, 149
  - equation, 144, 167, 371, 485, 509, 510, 513, 575
    - conservation form, 500
    - conserved quantities, 505, 511
    - d'Alembert, 484, 488, 510, 549
    - d'Alembert solution, 495, 510
    - finite differences, 490
    - first order, 506, 510, 512
    - integrability, 486
    - uniqueness, 511
  - function, 58, 349, 365, 370, 372, 580
  - matter, 367
  - mechanics, 47, 377
  - nonlinear dispersive, 486
  - number, 488, 493, 505, 509, 510, 582
  - operator, 167, 495, 511
  - packet, 486, 506
  - plane, 350
  - propagating, 495
  - right- and left-moving, 486, 496, 505
  - small amplitude, 485
  - traveling, 486
  - vector, 506
- wave-particle duality, 379
- wavefronts, 156, 169, 366, 377–379, 506
- wavelength, 366, 493
  - de Broglie, 367
  - short, 370, 371
- wedge, 207, 221
- wedge product, 118, 146, 312, 628, 629, 635, 668
  - p-fold, 631
  - (anti)commutative, 635
  - antisymmetry, 629
  - three-fold, 631
- Weierstrass
  - differential equation, 241
  - elliptic function, 229, 241
  - Karl, 229
- Weyl, Hermann, 614
- Whitney, embedding, 618
- Whitney, Hassler, 614
- Whittaker's constant, 375, 382
- Wiener, Christian, 524
- Wilson loop, 404
- wind tunnel, 570
- WKB approximation, 367
- wobble, 243
- work, 2, 3, 62, 135, 162, 170, 256, 514, 581, 588, 598, 624
  - path-dependence, 62
  - path-independence, 600
  - virtual, 64, 71
- work-energy principle, 63, 162
- world line, 152, 166, 169, 619
- Wronskian, 412, 416

- X-point, 228

- Zermelo's paradox, 324
- zero
  - curvature, 359
  - gravity, 456, 467
  - locus, 659
  - mode, 387, 400, 505
- zeroth law of mechanics, 57, 523

This textbook is a self-contained treatment of classical mechanics that emphasizes its wider connections to other branches of physics, such as quantum mechanics, thermal physics, electromagnetism, optics, etc. While the mechanics of Galileo and Newton to that of Lagrange and Hamilton along with their applications form the core of the text, many modern developments have also been included. Special attention has been paid to pedagogy; thus the chapters have numerous explanatory remarks and examples, and are supplemented with problems. The sections of the book are arranged in a modular fashion to increase accessibility. This new text, with minimal prerequisites, is suited for beginning researchers as well as advanced undergraduates. At the same time, instructors and practicing physicists will find the treatment novel.

Govind Krishnaswami is a Professor of Physics at the Chennai Mathematical Institute, India, and is a recipient of the Apker Award and Marie Curie, EPSRC and Ramanujan Fellowships. His research in areas such as particle physics, nonlinear dynamics and fluid mechanics has often exploited ideas and tools from classical mechanics. He has taught a wide variety of subjects and is known for the clarity of his pedagogical articles in Resonance, a journal of science education.

ISBN 978-81-957829-9-4
9 788195 782994
www.hindbook.com